



XXth
Symposium
Neuroradiologicum

7-12 September 2014
ISTANBUL, TURKEY

LUTFI KIRDAR CONVENTION & EXHIBITION CENTER



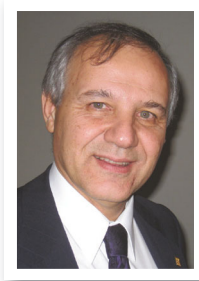
CONTENT	Page
WELCOME ADDRESS BY PROF. DR. E. TURGUT TALI	3
COMMITTEES	4
INTERNATIONAL ADVISORY COMMITTEE	5
LOCAL ORGANIZING COMMITTEE	8
SYMPOSIUM FACULTY	8
SYMPOSIUM MODERATORS	9
SYMPOSIUM NEURORADIOLOGICUM - PAST & FUTURE	10
GENERAL INFORMATION	11
SCIENTIFIC INFORMATION	15
ADMINISTRATIVE MEETINGS	17
SYMPOSIUM VENUE FLOOR PLANS	18
NEXT SYMPOSIUM; XXI st SYMPOSIUM NEURORADIOLOGICUM TAIWAN 2018	22
PROGRAM OVERVIEW	23
SCIENTIFIC PROGRAM	26
PLENARY SESSIONS ABSTRACTS	86
ORAL PRESENTATIONS ABSTRACTS	162
POSTER PRESENTATIONS ABSTRACTS	302
AUTHORS INDEX	466

This supplement was not sponsored by outside commercial interests. It was funded entirely by the publisher.

7-12 September 2014
ISTANBUL, TURKEY

LUTFI KIRDAR CONVENTION & EXHIBITION CENTER

XXth Symposium Neuroradiologicum



Dear Friends,

From the long-lost mists of time to current age of technology, humans tend to show an interminable desire for knowledge and problem-solving. Being devoted to this passion of discovering the causes and the results of the diseases, physicians had developed the radiology based on the basic principle of 'primum non nocere'.

It is intriguing if Roentgen were to dream that X-ray might be of use in the treatment of brain tumors or cerebral aneurysms when he discovered x-ray in 1895. Why did Hounsfield first develop computerized tomography for the purpose of brain imaging? His intuition might have directed him to the brain, the maestro of the body, to make the neuroradiology the locomotive force of the radiology realm.

In the following years neuroradiology has kept on being the leader of the field and pioneered the technological developments. The detailed anatomical images were first obtained for the brain but this was not enough; then came the visualization of tracts, fasciculi and even histopathologic images. The high field MR equipment was first designed to solve the mystery of brain. Physiological and biochemical information was first obtained in the brain.

Diffusion MRI made the moribund brain parenchyma shine. Perfusion MRI reveals the parenchymal supply not only in gray scale but also in color maps. It has become possible to 'read the minds' by functional MRI. Technical developments have not only brought new approaches to the diagnosis but also new and less invasive insight to the imaging-guided treatments. Radiofrequency and focused ultrasound have applications not only in movement disorders but also in brain tumors. Vertebral interventions, pain management and treatment of disc disease, and many more have become possible without open surgery.

In this symposium, we, the neuroradiologists, will enjoy ourselves in the discovery of the brain and spine with the neuroradiologic techniques. To include the newest developments into the current practice and to expand horizons, 450 scientists from 77 countries have worked hard on the program; the lecture topics, lecturers and the moderators were selected with meticulous care. All the topics are going to be covered by the well-known experts of the field. The program will be enhanced with additional 490 presentations.

During the symposium, we will work hard to illuminate the path of science all together.

I would like to express my most sincere appreciation to all who have and will contribute to this meeting. Lastly, I want to express my most sincere appreciation and gratitude to my family for their interminable support and patience.

On behalf of the entire committees, I welcome you all to Istanbul and wish this symposium to be fruitful for all of us.

E. Turgut Tali
President of the XXth Symposium Neuroradiologicum
Istanbul, September 8, 2014



COMMITTEES

PRESIDENT



E. Turgut Tali, Turkey

HONORARY PRESIDENT



Michael S. Huckman, USA

SYMPOSIUM SECRETARY



Naci Kocer, Turkey

INTERNATIONAL SCIENTIFIC COMMITTEE



A. James Barkovich
USA



Giuseppe Bonaldi
Italy



Saruhan Çekirge
Turkey



Mark Khangure
Australia



Laurie Loevner
USA

7-12 September 2014
ISTANBUL, TURKEY

LUTFI KIRDAR CONVENTION & EXHIBITION CENTER

XXth
Symposium
Neuroradiologicum



INTERNATIONAL ADVISORY COMMITTEE (*Surname Alphabetical*)

- Yasser Abbas, *Egypt*
Suzanne Abbas Mohd, *Bahrain*
Yosra Abdelzaher, *Egypt*
Fatma Abdulla Al -Mulhim, *Saudi Arabia*
Toshi Abe, *Japan*
Riadh Abid, *Tunisia*
Benjamin Adapon, *Philippines*
P. Henry Adapon, *Philippines*
Ademola Adeyekun, *Nigeria*
A. O. Adeyinka, *Nigeria*
Santa Adrian, *Romania*
Noriko Aida, *Japan*
Abdulkader Al Azzaz, *Saudi Arabia*
Mosleh Al Raddadi, *Saudi Arabia*
Jehad Al Watban, *Saudi Arabia*
Jamal AL Deen ALKoteesh, *UAE*
Aghiad AlKutoubi, *Lebanon*
Ibrahim Alorainy, *Saudi Arabia*
Sari Alsuhibani, *Saudi Arabia*
Abdulkarim Al Zabedi, *Yemen*
Vibeke Andrée Larsen, *Denmark*
John Andreou, *Greece*
Cosma Andreula, *Italy*
Aleksandr Antonenko, *Belarus*
Nicoletta Anzalone, *Italy*
Shigeki Aoki, *Japan*
Pablo Picasso Araújo Coimbra, *Brasil*
Maria Argyropoulou, *Greece*
Ankur Arora, *India*
Muhammad Azeemuddin, *Pakistan*
Søren Jacob Bakke, *Norway*
Danielle Baleriaux, *Belgium*
Nuria Bargallo, *Spain*
Alberto Beltramello, *Italy*
Mohamed Ben Hamouda, *Tunisia*
Khairiddine Ben Mahfoudh, *Tunisia*
Alejandro Berenstein, *USA*
Mauro Bergui, *Italy*
Sonia Bermudez, *Colombia*
Bruno Bernardi, *Italy*
Shahzad Bhatti, *Pakistan*
Alberto Bizzi, *Italy*
Edoardo Boccardi, *Italy*
Najat Boukhrissi, *Morocco*
William Bradley, *USA*
Beatriz Brea, *Spain*
Mircea Buruian, *Romania*
Sally Candy, *South Africa*
Nevia Caputo, *Italy*
Henrique Carrete Jr., *Brasil*
Fabiola Cartes Zumelzu, *Austria*
Katiuzka Casares, *Mexico*
Jan Casselmann, *Belgium*
Mauricio Castillo, *USA*
Germán Castillo Del Pozo, *Ecuador*
Claudio Campi Castro, *Brasil*
Edla Chadrycki, *Brasil*
Noureddine Chakir, *Morocco*
FengChi Chang, *Taiwan*
Rene Chapot, *Germany*
ChiJen CHEN, *Taiwan*
Jung-Eun Cheon, *South Korea*
Vincent Fook Hin Chong, *Singapore*
Gyoung-Ho Chung, *South Korea*
Elisa Ciceri, *Italy*
Claudia Cinnante, *Italy*
Christophe Cognard, *France*
Nadia Colombo, *Italy*
Carla Conceição, *Portugal*
Enrico Cotroneo, *Italy*
Alan Coulthard, *Australia*
Goge Damjanoski, *Macedonia*
Fatima Dashti, *Kuwait*
Tairkhan B.Dautov, *Rep. of Kazakhstan*
Philippe Demaerel, *Belgium*
Patricia Desmond, *Australia*
Orlando Diaz, *USA*
Stefanita Dima, *Romania*
Jorge Docampo, *Argentina*
M. Judith Donovan Post, *USA*
Didier Dormont, *France*
Antonios Drevelegas, *Greece*
Cyrine Drissi, *Tunisia*
Julia Duarte, *Portugal*
Paulina Due - Tonnessen, *Norway*
Yunis Efendiye, *Azerbaijan*
Adel Ibrahim Soliman Elbery, *UAE*
Joe El Khoury, *Lebanon*
Abdel Aziz El Nekeidy, *Egypt*
Ahmed Elsotouhy, *Qatar*
Eren Erdem, *USA*
Ulrike Ernemann, *Germany*
Birgit Ertl - Wagner, *Germany*
Marco Essig, *Germany*
Andrea Falini, *Italy*
Lázaro Luís Faria do Amaral, *Brasil*
Jens Fiehler, *Germany*
Kavous Firuznia, *Iran*
Allan Fox, *Canada*
Shailesh Gaikwad, *India*
Massimo Gallucci, *Italy*
Jose Maria Garcia Santos NR, *Spain*
Roberto Gasparotti, *Italy*
Jean-Yves Gauvrit, *France*
Hosein Ghanaati, *Iran*
Sayed Ahmed Ghoneim, *Egypt*
Wendell Gibby, *USA*
Nadine Girard, *France*
Dorit Goldsher, *Israel*
Lavier Gomes, *Australia*
Moshe Gomori, *Israel*
Ramon Gilberto Gonzales, *USA*
Nadia Gonzalez, *Argentina*
Eduardo González Toledo, *USA*
Bozena Góraj, *Denmark*
Augusto Goulão, *Portugal*
Athanasios Gouliamos, *Greece*
Mayank Goyal, *Canada*
WanYuo Guo, *Taiwan*
Rakesh Gupta, *India*
AK Gupta, *India*
Lotfi HaceinBey, *USA*
Marwan Haddad, *Lebanon*
Ahmed Halilah, *Jordan*
Sven Haller, *Switzerland*
Rashad Hassan Hamdi, *Egypt*
Nadia Hammami, *Tunisia*
Khalil Hamza, *Tunisia*
Ibtissem Hasni, *Tunisia*
Anton Hasso, *USA*
Victor Haughton, *USA*
Luc Van Den Hauwe, *Belgium*
J. Hendrikse, *The Netherlands*
John Hesselink, *USA*
Mohammed Hiari, *Jordan*
Takaaki Hosoya, *Japan*
Toshinori Hirai, *Japan*
Joshua Hirsch, *USA*
Chen Hoffmann, *Israel*
Emmanuel Houdart, *France*
Roula HouranyRizk, *Lebanon*
Stephan Hudak, *Hungary*
Thierry A. G. M. Huisman, *USA*
Murat Ibatullin, *Tataristan*
Mohammed Ismaiel, *Kuwait*
Haruo Isoda, *Japan*
Yasushi Ito, *Japan*
Rolf Jager, *UK*



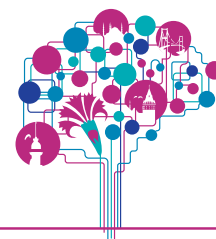
INTERNATIONAL ADVISORY COMMITTEE (*Surname Alphabetical*)

- Stipan Jankovic, *Croatia*
Ladislava Janouskova, *Czech Republic*
Pieter Janse van Rensburg, *South Africa*
Andja Jasovic, *Croatia*
Pyoung Jeon, *South Korea*
Mohamed Jiddane, *Marocco*
Blake Johnson, *USA*
Hussein Kamel, *Qatar*
Edward Kassel, *Canada*
Kazuhiro Katada, *Japan*
Tesfaye Kebede, *Africa*
Steven Kieffer, *USA*
Murphy Kieran, *Canada*
Tracy Kilborn, *South Africa*
Bum-Soo Kim, *South Korea*
Hyung-Jin Kim, *South Korea*
Mehmet Kocak, *USA*
Igor Kocijancic, *Slovenia*
Takao Kodama, *Japan*
Spyros Kollias, *Switzerland*
Yukunori Korogi, *Japan*
Korgun Koral, *USA*
Dusko Kozic, *Serbia*
Stéphane Kremer, *France*
Bodo Kress, *Germany, Brunei*
Timo Krings, *Canada*
M. Kruit, *The Netherlands*
Gaida Krūmina, *Latvia*
Walter Kucharczyk, *Canada*
Khalil Kurdi, *Saudi Arabia*
PingHong Lai, *Taiwan*
Hector Lambre, *Argentina*
Meng Law, *USA*
Seung-Koo Lee, *South Korea*
Stéphane Lehericy, *France*
Marco Leonardi, *Italy*
Youxiang Li, *China*
Uday Limaye, *India*
Sattam Lingawi, *Saudi Arabia*
HonMan Liu, *Taiwan*
Jianmin Liu, *China*
Sherman Lo, *Hong Kong*
Karl Olof Lövlblad, *Switzerland*
Milos Lucic, *Serbia*
Chao-Bao Luo, *Taiwan*
Ioana Lupescu, *Romania*
Martin G. Mack, *Germany*
Leonardo Macedo, *Brazil*
Masayuki Maeda, *Japan*
C. Majoie, *The Netherlands*
Tajuddin Malabarey, *Saudi Arabia*
Nadia Mama Larbi, *Tunisia*
Danny Mandell, *Canada*
Claude Manelfe, *France*
Luigi Manfrè, *Italy*
Salvatore Mangiafico, *Italy*
Asem Mansour, *Jordan*
Kenneth Maravilla, *USA*
Stefano Marcia, *Italy*
Joseph Masdeu, *USA*
John Mathis, *USA*
Jaime Medrano, *Panama*
Carolyn Meltzer, *USA*
Zulejha Merhemic, *Bosnia Herzegovina*
Fikri Meryem, *Morocco*
Mohamed Metkees, *Egypt*
Edward Michals, *USA*
Yukio Miki, *Japan*
David Mikulis, *Canada*
Zoran V. Milosevic, *Slovenia*
Svetlana Milosevic, *Serbia*
Mario Miranda, *Panama*
Yulia Mironova, *Ukraine*
NK Mishra, *India*
Peter Mitchell, *Australia*
Shigeru Miyachi, *Japan*
José Maria Modenesi Freitas, *Brasil*
Mohammed Mohammed, *Kuwait*
Norzaini Rose Mohd Zain, *Malaysia*
Asem Monsour, *Jordan*
Francisco José Mont 'Alverne, *Brasil*
Sergey P Morozov, *Russia*
Sobri Muda, *Malaysia*
Suresh Mukherji, *USA*
Mario Muto, *Italy*
David Nag, *UK*
Sonia Nagi, *Tunisia*
Jaishree Naidoo, *South Africa*
Ichiro Nakahara, *Japan*
Ech-cherif El Kettani Najwa, *Morocco*
Anis Nassar, *Lebanon*
Dragus Negru, *Romania*
Shigeru Nemoto, *Japan*
Senco Netkov, *Macedonia*
ShuHang NG, *Taiwan*
Luis Nombela Cano, *Portugal*
Teresa Nunes, *Portugal*
Sara Nuñez, *Colombia*
Pecaric Meglic Nuska, *Slovenia*
Paolo Nuzzi, *Italy*
Mojisola O Atalabi, *Nigeria*
Hiroshi Oba, *Japan*
Abdul Obadien, *Saudi Arabia*
Toshihide Ogawa, *Japan*
G. I. Ogbole, *Nigeria*
Olubunmi Ogunrin, *Nigeria*
Cecilia Okuma Ponce, *Chile*
Matthew F Omojola, *USA*
Orlando Ortiz, *USA*
David Ozteric, *Croatia*
Frank Pameijer, *The Netherlands*
Jacub Pandelaki, *Indonesia*
Adam Pany, *Malaysia*
Vasileios Papakostas, *Greece*
Paul M Parizel, *Belgium*
Goran Pavlisa, *Croatia*
Salvador Pedraza Gutiérrez, *Spain*
Gianni Pellicanò, *Italy*
Lachezar Penev, *Bulgaria*
Sladjana Petrovic, *Serbia*
Luiz Antônio Pezzi Portela, *Brasil*
Constantine Phatouros, *Australia*
Laurent Pierot, *France*
Patricia Orellana Pineda, *Chile*
Ronie Leo Piske, *Brasil*
Francesca Pizzini, *Italy*
Bogdan Popa, *Romania*
Sirintara Pongpech, *Thailand*
Igor Pronin, *Russia*
Branko Prstojevic, *Serbia*
Monther Qandeel, *Jordan*
Robert Quencer, *USA*
Ana Maria Quintero Corredor, *Colombia*
Perviz Quliyev, *Azerbaijan*
Elias Fouad Rabahi, *Brasil*
El Hassani Moulay Rachid, *Brasil*
Alireza Rasekhi, *Iran*
Tarek Rashad, *Egypt*
Umair Rashid Chaudhry, *Pakistan*
Fareeha Rauf, *Pakistan*
Raj Kumar Rauniyar, *Nepal*
Charles Raybaud, *Canada*
João Reis, *Portugal*
Luca Remonda, *Switzerland*
Wu Renhua, *China*
Frédéric Ricolfi, *France*
Andrea Righini, *Italy*

7-12 September 2014
ISTANBUL, TURKEY

LUTFI KIRDAR CONVENTION & EXHIBITION CENTER

XXth
Symposium
Neuroradiologicum



INTERNATIONAL ADVISORY COMMITTEE (*Surname Alphabetical*)

Carolyn Robson, *USA*
Rafael Rojas, *USA*
Carlos Romero, *Argentina*
Andrea Rossi, *Italy*
Alex Rovira, *Spain*
Howard Rowley, *USA*
Zoran Rumboldt, *USA*
Jordi Ruscalleda, *Spain*
Rustiadj, *Indonesia*
Niloufar Sadeghi, *Belgium*
Cindy Sadikin, *Indonesia*
Hirdesh Sahni, *India*
Nobuyuki Sakai, *Japan*
Osamu Sakai, *Japan*
Hosam Sakr, *Egypt*
Khaled Yacoub Salem, *Qatar*
Noriko Salomon, *USA*
Ugo Salvolini, *Italy*
Martin Sames, *Czech Republic*
M Ihab Sami Reda, *Egypt*
Pina Sanelli, *USA*
Kim Sang Joon, *South Korea*
Marek Sasiadek, *Poland*
Dawn Saunders, *UK*
Pamela Schaefer, *USA*
Bernhardt Schuknecht, *Switzerland*
Erin Schwartz, *USA*
Rasool Sedaghat, *Iran*
Tomaz Seruga, *Slovenia*
Fabiane Lorenzoni Sesti, *Brasil*
Dennis Shaw, *USA*
Ilan Shelef, *Israel*
Priyo Sidipratomo, *Indonesia*
Roger Siemund, *Sweden*
Tejinder Singh, *Australia*
Paramjeet Singh, *Qatar*
Roger Smith, *Canada*
Marion Smits, *The Netherlands*
Michael Soderman, *Sweden*
Laurent Spelle, *France*
Alessandra Splendiani, *Italy*
Marek Stajgis, *Poland*
Katarzyna Stanislawska, *Poland*
Claudio C. V. Staut, *Brasil*
S. Steens, *The Netherlands*
Dragan Stojanov, *Serbia*
Tatajana Stosic Opincal, *Serbia*
Luis Suazo, *Dominic Republic*
Gulpa Subasinghe, *Sri Lanka*
Stefan Sunaert, *Belgium*
Pia Sundgren, *Sweden*
Katarina Surlan Popovic, *Slovenia*
Valentyn Synitzin, *Russia*
Gordon Sze, *USA*
Istvan Szikora, *Hungary*
Waro Taki, *Japan*
Jean Tamraz, *Lebanon*
Toshiaki Taoka, *Japan*
Michael MuHuo TENG, *Taiwan*
Hitoshi Terada, *Japan*
Karel Terbrugge, *Canada*
Majda Thurnher, *Austria*
Laura Tisser, *Argentina*
Kalthoum Tlili-Graies, *Tunisia*
Carlos Torres, *Canada*
Carolina Tramontini, *Colombia*
Johannes Trenkler, *Austria*
Fabio Triulzi, *Italy*
Kazuhiro Tsuchiya, *Japan*
Patrick Turski, *USA*
Chrysa Tziakouri Shiakalli, *Cyprus*
Najam Uddin, *Pakistan*
Tanveer Ul haq, *Pakistan*
Andrzej Urbanik, *Poland*
Meher Ursekar, *India*
Sri Andreani Utomo, *Indonesia*
anton Valavanis, *Switzerland*
Jaap Valk, *The Netherlands*
M. Van Buchem, *The Netherlands*
R. Van den Berg, *The Netherlands*
Johan Van Goethem, *Belgium*
Leon Van Rensburg, *South Africa*
M. Van Walderveen, *The Netherlands*
Ritva Vanninen, *Finland*
Maria de Fátima Viana Vasco
Aragão, *Brasil*
Violeta Vasilevska
Nikodinovska, *Macedonia*
Leonardo Vedolin, *Brasil*
M. Vernooij, *The Netherlands*
Pedro Vilela, *Portugal*
Ruediger Von Kummer, *Germany*
Josef Vymazal, *Czech Republic*
Sherif Wahib, *Pakistan*
Jerzy Walecki, *Poland*
Isabel Wanke, *Germany*
Monika Warmuth-Metz, *Germany*
E.T. Wiggers-de Bruine,
The Netherlands
Nirmala Wijesinha, *Sri Lanka*
Robert Willinsky, *Canada*
Ho-Fai Wong, *Taiwan*
Kamran Yakubov, *Azerbaijan*
Kei Yamada, *Japan*
Ağakişi Yehyayev, *Azerbaijan*
Takashi Yoshiura, *Japan*
Tina Young Poussaint, *USA*
David Yousem, *USA*
Tarek Yousry, *UK*
Eugene Yu, *Canada*
Simon Yu, *Hong Kong*
William Yuh, *USA*
Martin Zauner, *Spain*
Kamil Zelenak, *Slovakia*
Robert A Zimmerman, *USA*
Giulio Zuccoli, *USA*



LOCAL ORGANIZING COMMITTEE CHAIRMAN



Civan Islak, Turkey

LOCAL ORGANIZING COMMITTEE (Surname Alphabetical)

Emel Ada, *Turkey*
Hüseyin Akan, *Turkey*
Oktay Algin, *Turkey*
Erkin Arıbal, *Turkey*
Feyyaz Baltacıoğlu, *Turkey*
Nail Bulakbaşı, *Turkey*
Mutlu Cihangiroğlu, *Turkey*
Abdulhakim Coşkun, *Turkey*
Unsal Coşkun, *Turkey*
Mehmet Cem Çallı, *Turkey*
Ercüment Çiftçi, *Turkey*
Yelda Özsunar, *Dayanır, Turkey*
Hasan Dinç, *Turkey*

H. Barış Diren, *Turkey*
Ahmet Candan Durak, *Turkey*
Canan Erzen, *Turkey*
Erhan Ilgıt, *Turkey*
Simay Kara, *Turkey*
Can Karaman, *Turkey*
Kader Karlıoğuz, *Turkey*
Osman Kızılkılıç, *Turkey*
Süleyman Men, *Turkey*
Özenç Minareci, *Turkey*
Burçe Özgen Mocan, *Turkey*
İsmail Oran, *Turkey*
Baran Önal, *Turkey*

Yusuf Öner, *Turkey*
Mustafa Özateş, *Turkey*
Hüseyin Özdemir, *Turkey*
Halil Öztürk, *Turkey*
Müfit Parlak, *Turkey*
Işıl Saatçi, *Turkey*
Kaya Saraç, *Turkey*
Ahmet Sarı, *Turkey*
Timur Sindel, *Turkey*
Utku Şenol, *Turkey*
Mustafa Taşar, *Turkey*
Murat Uçar, *Turkey*
Özkan Ünal, *Turkey*

SYMPOSIUM FACULTY (Surname Alphabetical)

Savvas Andronikou, *South Africa*
Nivedita Agarwal, *Italy*
Tommy Andersson, *Sweden*
Ethem Murat Arsava, *Turkey*
Jo Bhattacharya, *UK*
James Barkovich, *USA*
Minerva Becker, *Switzerland*
Alejandro Berenstein, *USA*
Alberto Beltramello, *Italy*
Juan Villa Blanca, *USA*
Giuseppe Bonaldi, *Italy*
Edoardo Boccardi, *Italy*
Jan Casselman, *Belgium*
Mauricio Castillo, *USA*
Alfredo Casasco, *Spain*
Saruhan Cekirge, *Turkey*
Roberta Cilio, *USA*
Kling Chong, *UK*
Vincent Chong, *Singapore*
Christoph Cognard, *France*
Patricia Desmond, *Australia*
Eren Erdem, *USA*
Adam Flanders, *USA*
Massimo Gallucci, *Italy*

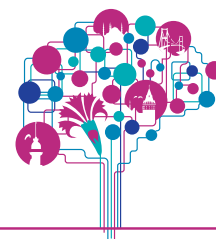
Afshin Gangi, *France*
Eloisa S. Gebrim, *USA*
P. Ellen Grant, *USA*
Rakesh Gupta, *India*
Renzo Guerrini, *Italy*
Wendel Gibby, *USA*
Wan-Yuo GUO, *Taiwan*
Anil Gholkar, *UK*
Johan Van Goethem, *Belgium*
Murat Hanci, *Turkey*
Sven Haller, *Switzerland*
Julie H. Harreld, *USA*
Hans Henkes, *Germany*
Thierry A.G. M. Huisman, *USA*
Civan Islak, *Turkey*
Mehmet Kocak, *USA*
Vasileios K. Katsaros, *Greece*
Timo Krings, *Canada*
Naci Kocer, *Turkey*
Marjo van der Knaap, *The Netherlands*
Yukunori Korogi, *Japan*
Rüdiger Von Kummer, *Germany*
Gregg Lawler, *USA*
Marco Leonardi, *Italy*

Philippe Demaerel Leuven, *Belgium*
Laurie Loevner, *USA*
Demetrius Lopes, *USA*
Leandro Tavares Lucato, *Brasil*
Pedro Lylyk, *Argentina*
Nina Mayr, *USA*
Luigi Manfre, *USA*
Stefano Marcia, *Italy*
Leonardo Macedo, *Brazil*
Ingeborg Krageloh-Mann, *Germany*
Monika Warmuth-Metz, *Germany*
Yukio Miki, *Japan*
Jacques Moret, *France*
Suresh Mukherji, *USA*
Kieran Murphy, *Canada*
Mario Muto, *Italy*
Yuko Ono, *Japan*
Hakan Oruçkaptan, *Turkey*
Anne Osborn, *USA*
Orlando Ortiz, *USA*
Burce Ozgen, *Turkey*
Paul Parizel, *Belgium*
Zoltan Patay, *USA*
Laurent Pierot, *France*

7-12 September 2014
ISTANBUL, TURKEY

LUTFI KIRDAR CONVENTION & EXHIBITION CENTER

XXth
Symposium
Neuroradiologicum



SYMPOSIUM FACULTY (*Surname Alphabetical*)

Charles Raybaud, *Canada*
Vijay Ramaswamy, *Canada*
Geir Ringstad, *Norway*
Carlo Romero, *Argentina*
Rafael Rojas, *USA*
Andrea Rossi, *Italy*
Alex Rovira, *Spain*
Daniel Roy, *Canada*
Andreas Righini, *Italy*
Zoran Rumboldt, *USA*

Isil Saatci, *Turkey*
Pia Sundgren, *Sweden*
Osamu Sakai, *USA*
Pamela Schaefer, *USA*
Marion Smits, *The Netherlands*
Laurent Spelle, *France*
Claudio Staut, *Brazil*
Gordon Sze, *USA*
Majda Thurnher, *Austria*
Tomoaki Terada, *Japan*

Toshiaki Taoka, *Japan*
Eduardo Gonzales Toledo, *USA*
Aquilla TURK, *USA*
Kei Yamada, *Japan*
Jian Yang, *China*
David Yousem, *USA*
Tarek Yousry, *UK*
William Yuh, *USA*
Giulio Zuccoli, *USA*

SYMPOSIUM MODERATORS (*Surname Alphabetical*)

Suzanne Abbas Mohd, *Bahrain*
German Abdo, *Ecuador*
Benjamin Adapon, *Phillippines*
Noriko Aida, *Japan*
Abdulkader Al Azzaz, *Saudi Arabia*
Jamal Al Kotes, *Abu Dhabi*
Jehad Al Watban, *Saudi Arabia*
Oktay Algin, *Turkey*
Alikhan Alikhanov, *Russia*
Pablo Araujo-Coimbra, *Brasil*
A. James Barkovich, *USA*
Mohamed Ben Hamouda, *Tunisia*
Giuseppe Bonaldi, *Italy*
Mircea Buruiian, *Romania*
Nick Bryan, *USA*
Nail Bulakbasi, *Turkey*
Cem Calli, *Turkey*
Katiuzaka Casares, *Mexico*
German Castillo A., *Ecuador*
Umair Rashid Chaudry, *Pakistan*
Sandy Chen, *Taiwan*
Jacques Chiras, *France*
Elisa Ciceri, *Italy*
Sossio Cirillo, *Italy*
Abdulhakim Coskun, *Turkey*
Saruhan Çekirge, *Turkey*
Maria de Fatima Viane Vasco Aragao, *Brasil*
Jurate Dementaviciene, *Lithuania*
Baris Diren, *Turkey*
Paulina Due Tonnessen, *Norway*
Sarmite Dzelzitis, *Latvia*
Ahmed El Belgati, *Kuwait*
Ahmed Elsotouhy, *Qatar*
Franz Fellner, *Austria*
Kavous Firuzna, *Iran*
Olof Flodmark, *Sweden*
Matthew Folorunso Omojola, *USA*
Allan Fox, *Canada*
Bassem Georgy, *USA*

Nadine Girard, *France*
Dorith Goldsher, *Israel*
Bozena Goraj, *The Netherlands*
Gang Guo, *China*
Athanasios Gouliamos, *Greece*
Lotfi Hacein-Bey, *USA*
Ahmed Halilah, *Jordan*
John Hesselink, *USA*
Roula Hourany, *Lebanon*
Francis Hui, *Singapore*
Thiery A.G.M. Huisman, *USA*
Murat Ibatullin, *Tataristan*
Dong Ik Kim, *South Korea*
Erhan Ilgit, *Turkey*
Izlem Izbudak, *USA*
Soren Jacob Bakke, *Sweden*
Eva Jacobsen, *Norway*
Mohamed Jidane, *Marocco*
Sang Joon Kim, *Korea*
Hussein Kamel, *Qatar*
Kazuhiro Katada, *Japan*
Mark Khangure, *Australia*
Tracy Kilborn, *South Africa*
Osman Kizilkilic, *Turkey*
Naci Kocer, *Turkey*
Gaida Krumina, *Latvia*
Raj Kumar Rauniyar, *Nepal*
Rudiger Von Kummer, *Germany*
Hon-Man Liu, *Taiwan*
Sherman Lo, *HongKong*
Lauire Loevner, *USA*
Seamus Looby, *Ireland*
Alfonso Lozano, *Colombia*
Milos Lucic, *Serbia*
Lazaro Luis Fariado Amaral, *Brasil*
Karl-Olof Lövlblad, *Switzerland*
Masayuki Maeda, *Japan*
Charles Majoie, *The Netherlands*
Irfan Mamoon, *Saudi Arabia*
Ljubo Markovic, *Denmark*

Jamie Medrano Lin, *Panama*
Zulejha Merhemic, *Bosnia Herzegovina*
Ozenc Minareci, *Turkey*
Angel Mironov, *USA*
Yulia Mironova, *Ukraine*
Nalini Kant Mishra, *India*
Peter Mitchell, *Australia*
Norzaini Rose Mohd Zain, *Malaysia*
Sobri Muda, *Malaysia*
Shigeru Nemoto, *Japan*
Cecilia Okuma Ponce, *Chile*
Baran Onal, *Turkey*
Yusuf Oner, *Turkey*
Patricia Orellana, *Chile*
Orlando Ortiz, *USA*
Anne G. Osborn, *USA*
Yelda Ozsunar, *Turkey*
Özkan Özsarlak, *Belgium*
M. Halil Öztürk, *Turkey*
Adam Pany, *Malaysia*
Vasileios Papakostas, *Greece*
Matilda Papathanasiou, *Greece*
Zoltan Patay, *USA*
Goran Pavlisa, *Croatia*
Hans Kristian Pedersen, *Norway*
Lachezar Penev, *Bulgaria*
Igor Pronin, *Russia*
Luca Remonda, *Switzerland*
Diana Rodriguez, *USA*
Andrea Rossi, *Italy*
Howard Rowley, *USA*
Gabor Rudas, *Hungary*
Niloufar Sadeghi, *Belgium*
Cindy Sadikin, *Indonesia*
Michael Sage, *USA*
Bernhard Schuknecht, *Switzerland*
Cagin Senturk, *USA*
Ilan Shelef, *Israel*



XXth Symposium Neuroradiologicum

7-12 September 2014
ISTANBUL, TURKEY

LUTFI KIRDAR CONVENTION & EXHIBITION CENTER

SYMPOSIUM MODERATORS (*Surname Alphabetical*)

Roger Siemund, *Sweden*

Lars Stenberg, *Sweden*

Peter Stoeter, *Dominican Republic*

Tatjana Stosic Opincal, *Serbia*

Stephen Stuckey, *Australia*

Katarina Surlan Popovic, *Slovenia*

Emin Turgut Tali, *Turkey*

Aylin Tekes, *USA*

Kalthoum Tlili-Graies, *Tunisia*

Carolina Tramontini, *Colombia*

Brian Tress, *Australia*

Agnieszka Trojanowska, *Poland*

Charles Truwit, *USA*

Sri Andreani Utomo, *Indonesia*

Luc Van Den Hauwe, *Belgium*

Ritva Vanninen, *Finland*

Leon VanRensburg, *South Africa*

Pedro Vilela, *Portugal*

Francisca T. Wiggers-DeBruine,

The Netherlands

Nirmala Wijesinha, *Sri Lanka*

Ho-Fai Wong, *Taiwan*

Ren-hua Wu, *China*

David Yousem, *USA*

Wan Yuo Guo, *Taiwan*

Kamil Zelenak, *Slovakia*

Dora Zlatarova, *Bulgaria*

Giulio Zuccoli, *USA*

SYMPOSIUM NEURORADIOLOGICUM - PAST & FUTURE

I	Antwerp	1939	Rudolph Thienpont
II	Rotterdam	1949	George Ziedses des Plantes
III	Stockholm	1952	Erik Lindgren
IV	London	1955	James W.D. Bull
V	Brussels	1957	Donald L. McRea
VI	Rome	1961	Giovanni Ruggiero
VII	New York	1964	Juan Taveras
VIII	Paris	1967	Herman Fischgold
IX	Göteborg	1970	Ingmar G. Wikbom
X	Punta del Este	1974	Nestor Azambuja
XI	Wiesbaden	1978	Sigurd Wende
XII	Washington	1982	Giovanni Di Chiro
XIII	Stockholm	1986	Torgny Greitz
XIV	London	1990	George Du Boulay
XV	Kumamoto	1994	Mutsumasa Takahashi
XVI	Philadelphia	1998	Sadek K. Hilal
XVII	Paris	2002	Luc Picard
XVIII	Sydney	2006	Michael Sage
XIX	Bologna	2010	Marco Leonardi
XX	Istanbul	2014	E. Turgut Tali
XXI	Taiwan	2018	Wan-Yuo GUO

7-12 September 2014
ISTANBUL, TURKEY

LUTFI KIRDAR CONVENTION & EXHIBITION CENTER

XXth Symposium Neuroradiologicum



GENERAL INFORMATION

Venue:

LUTFI KIRDAR INTERNATIONAL CONVENTION & EXHIBITION CENTER

Harbiye, 34267, Istanbul - Turkey

Tel: +90 212 373 1100

www.icec.org

Onsite Secretariat & Registration Opening Hours:

Sunday, 7 September	: 14.00 - 20.00
Monday, 8 September	: 07.30 - 20.00
Tuesday, 9 September	: 07.30 - 19.00
Wednesday, 10 September	: 07.30 - 19.00
Thursday, 11 September	: 07.30 - 19.00
Friday, 12 September	: 07.30 - 19.00

CME- Continuing Education Credits:

XXth Symposium Neuroradiologicum is accredited by the European Accreditation Council for Continuing Medical Education (EACCME) to provide the following CME activity for medical specialists. The EACCME is an institution of the European Union of Medical Specialists (UEMS), www.uems.net

XXth Symposium Neuroradiologicum was granted 30 European CME credits (ECMEC) by the European Accreditation Council for Continuing Medical Education (EACCME).

European Accreditation

European Accreditation is granted by the EACCME in order to allow participants who attend the above-mentioned activity to validate their credits in their own country.

American Medical Association (AMA)

Through an agreement between the European Union of Medical Specialists and the American Medical Association, physicians may convert EACCME credits to an equivalent number of AMA PRA Category 1 Credits™. Information on the process to convert **EACCME credit to AMA credit** can be found at www.ama-assn.org/go/internationalcme.

Royal College of Physicians and Surgeons of Canada

Live educational activities, occurring outside of Canada, recognized by the UEMS-EACCME for ECMEC credits are deemed to be Accredited Group Learning Activities (Section 1) as defined by the Maintenance of Certification Program of The Royal College of Physicians and Surgeons of Canada.

EACCME credits

Each medical specialist should claim only those hours of credit that he/she actually spent in the educational activity. The EACCME credit system is based on 1 ECMEC per hour with a maximum of 3 ECMECs for half a day and 6 ECMECs for a full-day event.

Certificate of Attendance

The certificate of attendance will be distributed to all participants, please ask the Secretariat.



GENERAL INFORMATION

Social Program

Opening Ceremony: Monday, 8 September 2014, 17:00 – 19:00 at Anadolu Auditorium

Welcome Reception will be held in the Main foyer of the Symposium venue, all attendees are invited to join the reception.

Farewell Dinner: Thursday, 11 September 2014, 20:00 – 23.30 Portaxe, Baltalimani

Farewell Dinner will be held on Thursday, 11 September 2014, between 20:00 – 23.30 in Portaxe, Baltalimani on Bosphorus. You may get farewell dinner tickets from the registration desk.

USEFUL INFORMATION AND CONTACTS

ARRIVAL IN ISTANBUL

Istanbul has two international airports; Istanbul Ataturk Airport and Sabiha Gökçen International Airport. Mostly the Ataturk Airport is used by major airlines as it is in the European side of Istanbul. The congress venue is in the European side close to Taksim Square.

Ataturk International Airport is located 20 km from Taksim Square (city centre):

“Symposium Welcome Desk” will be in the main hall of the Exit Area of the International Terminal of Atatürk Airport during the Symposium.

By Taxi: A taxi from the Atatürk Airport to the Taksim Square costs between 17€ to 20€. The trip takes between 35 and 65 minutes depending on stream of traffic. Please note: The taxi rates are same all day and night long.

By Shuttles Buses: Shuttle Buses called “Havas” travel between Ataturk Airport and Taksim Square every 30 minutes. It takes approximately 45 and 75 minutes depending on stream of traffic. The ticket costs 5 €.

By Public Buses: The Bus 96T travel between Ataturk Airport and Taksim Square every 50 minutes. It takes approximately 60 and 90 minutes depending on stream of traffic. The ticket costs 1 €.

Note: The Public Buses are available between 07:00 - 21:00 hours.

Sabiha Gökçen International Airport is located on the Anatolian shore of Istanbul and 50 km from Taksim Square (city center):

By Taxi: A taxi from the airport to the Taksim Square costs between ~50 €. The trip takes between 50 and 90 minutes depending on stream of traffic.

By Shuttles Buses: Shuttle Buses called “Havatas” travel between Sabiha Gokcen International Airport and Taksim Square every 1 hour. It takes approximately 70 and 90 minutes depending on stream of traffic. The ticket costs 6 €.

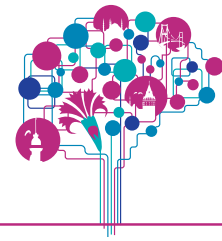
By Public Buses: The Bus E-3 travel between Ataturk Airport and 4.Levent Subway Station. It takes approximately 100 and 120 minutes depending on stream of traffic. The ticket costs 2,5 €.

Note: The Public Buses are available between 02:00 - 23:00 hours.

7-12 September 2014
ISTANBUL, TURKEY

LUTFI KIRDAR CONVENTION & EXHIBITION CENTER

XXth Symposium Neuroradiologicum



GENERAL INFORMATION

CITY TRANSPORT

Many modes of transportation are available in and around Istanbul. Please visit: <http://www.turkeytravelplanner.com> for more information.

TIME ZONE

Turkey is two hours ahead of Greenwich Mean Time (GMT) and seven hours ahead of Eastern Standard Time (EST).

ELECTRICITY

General Household electric power is 220 volts, 50 Hz. Plugs are generally standard continental European type. British and USA appliances need an adaptor.

CURRENCY

The local currency is Turkish Lira (TL). The exchange rate changes daily. Foreign currency can be exchanged at the airport, banks, hotels and exchange offices.

CREDIT CARDS; All major credit cards (Visa, Mastercard, American Express) are accepted by almost every shop, restaurant, hotel, etc.

BANKS

Bank business hours are from Monday to Friday, 09.00-17.00. Banks are closed on Saturday, Sunday and Public Holidays. All banks have almost similar exchange rates. Exchange offices are open seven days a week and approximately 16 hours a day.

POSTAL SERVICES

Hotels often provide basic postal services. Post offices are open daily except Saturday, Sunday and public holidays.

TELECOMMUNICATION

Turkey is one of the most advanced countries in the world in the fields of telecommunications and publishing. Istanbul, in particular, possesses a highly advanced telecommunication infrastructure.

DINING OUT

Istanbul is a culinary delight no matter what your budget. From simple workers' eateries and sidewalk cafes to posh culinary palaces with liveried waiters, Turkish cuisine is good and the value-for-money unbeatable. A typical Turkish dish generally consists of lamb, mutton, and veal with a variety of vegetables. Pilaf, all kinds of pastry, bulgur, haricot beans, mezes with rich olive oil, and vegetables are also common side dishes. Meatballs, shish kebab, and doner kebab are also classic dishes. Because of its coastal location, fish is also popular although it is usually cooked simply, such as grilled, or fried with olive oil and freshly squeezed lemon juice. Istanbul is the commercial and cultural centre of Turkey; and there are restaurants of many nationalities such as Korean, Russian, Italian, and Chinese. American-style fast-food outlets are becoming more popular, but for a quick snack it is more appropriate to fill up at the plethora of tiny takeaways offering kebabs and snacks. It is easy to sample good quality regional cuisine in typical small restaurants, usually at low cost, especially in the commercial and business areas.

DRIVING LICENCE

International driving licenses are recognized throughout Turkey. Car rental firms ask for a valid national license.



XXth Symposium Neuroradiologicum

7-12 September 2014
ISTANBUL, TURKEY

LUTFI KIRDAR CONVENTION & EXHIBITION CENTER

GENERAL INFORMATION

TIPPING

Service charges are included in the cost of all goods and services. Although it is not mandatory, a small tip is customary for good service. As a guideline, add about 10% to the total bill when paying cash.

VAT

The value-added tax, here called KDV, is 18%. Hotels typically combine it with a service charge of 10% to 15%, and restaurants usually add a 15% service charge.

Value-added tax is nearly always included in quoted prices. Certain shops are authorized to refund the tax (ask).

Special assistance

If you need special assistance and for emergency please contact with secretariat.

Please contact;

Mr. Soykan Guler: Mobile Phone: +90 533 581 3071

CONTACTS

PRESIDENT

E. Turgut TALI, MD

Professor and Director
Section of Neuroradiology,
Department of Radiology
Gazi University
School of Medicine Besevler,
Ankara 06510 TURKEY
P: +90 312 212 4040
F: +90 312 212 4040
E: turgut.tali@gazi.edu.tr
ettali@yahoo.com

SYMPOSIUM SECRETARY

Naci KOCER, MD

Professor
Department of Radiology,
Division of Neuroradiology
Istanbul University
Cerrahpasa Medical Faculty
Koca M. Pasa Cad. No: 124
Cerrahpasa, Istanbul 34300
TURKEY
P: +90 212 414 3000-22727
E: nkocer@istanbul.edu.tr

SYMPOSIUM ORGANIZER



Gayrettepe Mah. Yıldız Posta Cad.
Akın Sitesi 1. Blok No: 6 Kat: 1 D: 3
34349 Beşiktaş - Istanbul / TURKEY
P: +90 212 347 63 00
F: +90 212 347 63 63

SYMPOSIUM ORGANIZING SECRETARY



Serap Tantekin

Gayrettepe Mah. Yıldız Posta Cad.
Akın Sitesi 1. Blok No: 6 Kat: 1 D:
334349 Beşiktaş - Istanbul / TURKEY
P: +90 212 347 63 00
Mobile: +90 530 147 13 89
E: info@wfns2014.com

7-12 September 2014
ISTANBUL, TURKEY

LUTFI KIRDAR CONVENTION & EXHIBITION CENTER

XXth
Symposium
Neuroradiologicum



SCIENTIFIC INFORMATION

WFNRS 2014 ORAL PRESENTATION GUIDELINES

DISCLOSURE:

IN COMPLIANCE WITH EACCME REQUIREMENTS ALL SPEAKERS ARE REQUESTED TO INCLUDE A SLIDE DISCLOSING CONFLICTS OF INTEREST AT THE BEGINNING OF THEIR PRESENTATION

PRESENTATION FORMAT:

Format for PowerPoint Presentations: The accepted formats are PowerPoint 2010 and previous versions.

Font size of your Presentation

Try to remember when preparing your PowerPoint slides, that the font size should be large enough so that when projected it can be seen from the rear of the session hall.

Orientation of your Presentation (Page Set-up)

Please remember that your PowerPoint slide presentation should be prepared in a Landscape format and NOT Portrait. If using a PowerPoint (or any other computer) presentation, please note you need to bring it on a CD, a DVD or on a "disk on key" Memory stick (using the USB port in the computer) and load it on one of the congress' computers in the Speakers' Ready Room, at least 4 hour before the start of the session.

You may supply your own laptop computer as a back-up. If combining video films with PowerPoint, please make sure to check it in the session hall where your lecture is taking place during a coffee or lunch break prior to your session, at least 30 minutes before the start of the session - even after checking it in the Speakers' Ready Room.

Please note that the Congress computers in the session halls are being supplied with Office 2010.

IMPORTANT NOTE FOR MACINTOSH USERS

In order to use MAC presentations on a PC compatible computer please note that you need to prepare it according to the instructions below, before bringing it to the Speakers' Ready Room:

Use a common font, such as Arial, Times New Roman, Verdana etc. (special fonts might be changed to a default font on a PowerPoint based PC).

Insert pictures as JPG files (and not TIF, PNG or PICT - these images will not be visible on a PowerPoint based PC).

Use a common movie format, such as AVI, MPG and WMV (MOV files from QuickTime will not be visible on a PowerPoint based PC).

Please note that VHS Video projection, 35 mm slide projection and Overhead projection (projection of transparencies) will not be available.

WHEN YOU ARRIVE AT THE CONGRESS:

All presenters must register at the registration desk on arrival and check in at the speaker's preview room. Please check the program to confirm the date and time of your presentation. Speakers must report to the Speakers' Preview Room at least 2 hours before their session.

You may review your PowerPoint presentation in this room: Please pass your presentation CD/DVD or memory stick to the dedicated technician who will then upload the presentation and check for viruses (We can read PowerPoint 2010 and earlier versions. Any embedded movies or sound files should also be included on the disc or stick as separate files, for back-up purposes).

Please; assemble in your session room at least 10 minutes before the beginning of the session.

Ensure that you sit near the front of the room with easy access to the right hand side of the stage.

Ensure that you keep to the time allocated to you, as it will cause disruption to sessions if you run over your allotted time.



SCIENTIFIC INFORMATION

Timing of Oral Presentations: 8 minutes

Additional Information

Security: Speakers are required to provide identification in order to submit their presentation as well as to access it in the Speaker Ready Room. Recording devices such as cameras are not permitted in the Speaker Ready Room. All presentation files are deleted at the end of the conference, unless permission has been granted to the conference association to retain the presentation files.

WFNRS 2014 POSTER PRESENTATION GUIDELINES

Acceptable Electronic Exhibit File Formats: PowerPoint 2010 (PC) PowerPoint 2007 (PC) PowerPoint 2003 (PC) PowerPoint XP (PC) PowerPoint 2011 (Mac) PowerPoint 2008 (Mac) PowerPoint 2004 (Mac) PowerPoint 2001 (Mac), PDE, Flash is NOT supported.

Presentation Style

- Organize material in logical order, with all images and text supporting the central premise of the exhibit in a concise manner. Text and images should complement and reinforce one another. Although animations may be used, they should be kept to a minimum. Presentations should be user-friendly, visually attractive, and fast-paced (the learner should be able to view the entire exhibit in 4 minutes or less).

Slide Requirements

- Presentations must flow sequentially from beginning to end.
 - Keep slides simple and easy to read.
 - The first slide should identify the title, authors and institution.
 - The second slide should include the disclosure statement.
 - The third slide should clearly state the goals and objectives of the exhibit as well as the target audience. (Multiple slides may be used as necessary).
 - The last slide should contain author contact information.
 - Each slide should be proofread for factual, grammatical, and spelling errors. Exhibits including errors will need to be revised and may not qualify for an award.
 - The maximum number of slides per presentation is 25 slides.
 - No videos should be added to the presentation.
 - Slides should NOT include layered images or sliding images that cover other images or text.
- During the exhibit setup, DATA WILL BE LOST if this guideline is not followed.
- JavaScript pop-ups are not allowed.

Screen Resolutions and Dimensions

- Exhibits will be displayed on a monitor with a screen resolution of 1280 x 1024 (4:3) pixels.

Commercial Promotion

- All exhibits should serve an educational or scientific purpose and must not promote commercial organizations or products.

Patient Confidentiality

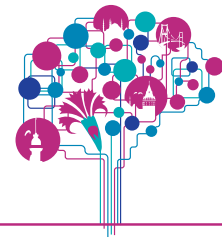
It is the responsibility of all program presenters to ensure that any use or disclosure of patient information is appropriate for the activity and in accordance with all applicable codes of ethics, policies and federal and state laws. Exhibitors are encouraged to review their obligations under any applicable privacy law prior to submission of an exhibit. Please be sure that patient information is not stored on the notes page layout in PowerPoint or in image file names.

Timing of Poster Presentations: 4 minutes

7-12 September 2014
ISTANBUL, TURKEY

LUTFI KIRDAR CONVENTION & EXHIBITION CENTER

XXth
Symposium
Neuroradiologicum



ADMINISTRATIVE MEETINGS

ESNR - EBNR European Diploma in Neuroradiology Final Examinations

Date : 07 September 2014, Sunday

Time / Location : 09:00 – 19:00 / TBD

ESNR Honorary Membership & Diploma Ceremony

Date : 09 September 2014, Tuesday

Time / Location: 17.15-19.00 / Anadolu Auditorium

ESNR Institutional Members Council Meeting

Date : 09 September 2014, Tuesday

Time / Location: 11.00-12.30 / Dolmabahce C

ESNR & Symposium Awards Ceremony

Date : 10 September 2014, Wednesday

Time / Location: 13.30 -15.00 / Anadolu Auditorium

ESNR Executive Committee Meeting

Date : 11 September 2014, Thursday

Time / Location: 08.30-10.30 / Levent 2

ESNR GENERAL ASSEMBLY

Date : 12 September 2014, Friday

Time / Location: 13.30 -15.00 / HALIC

WFNRS Executive Committee Meeting

Date : 8 September 2014, Monday

Time / Location: 13.30 / Levent 2

WFNRS GENERAL ASSEMBLY

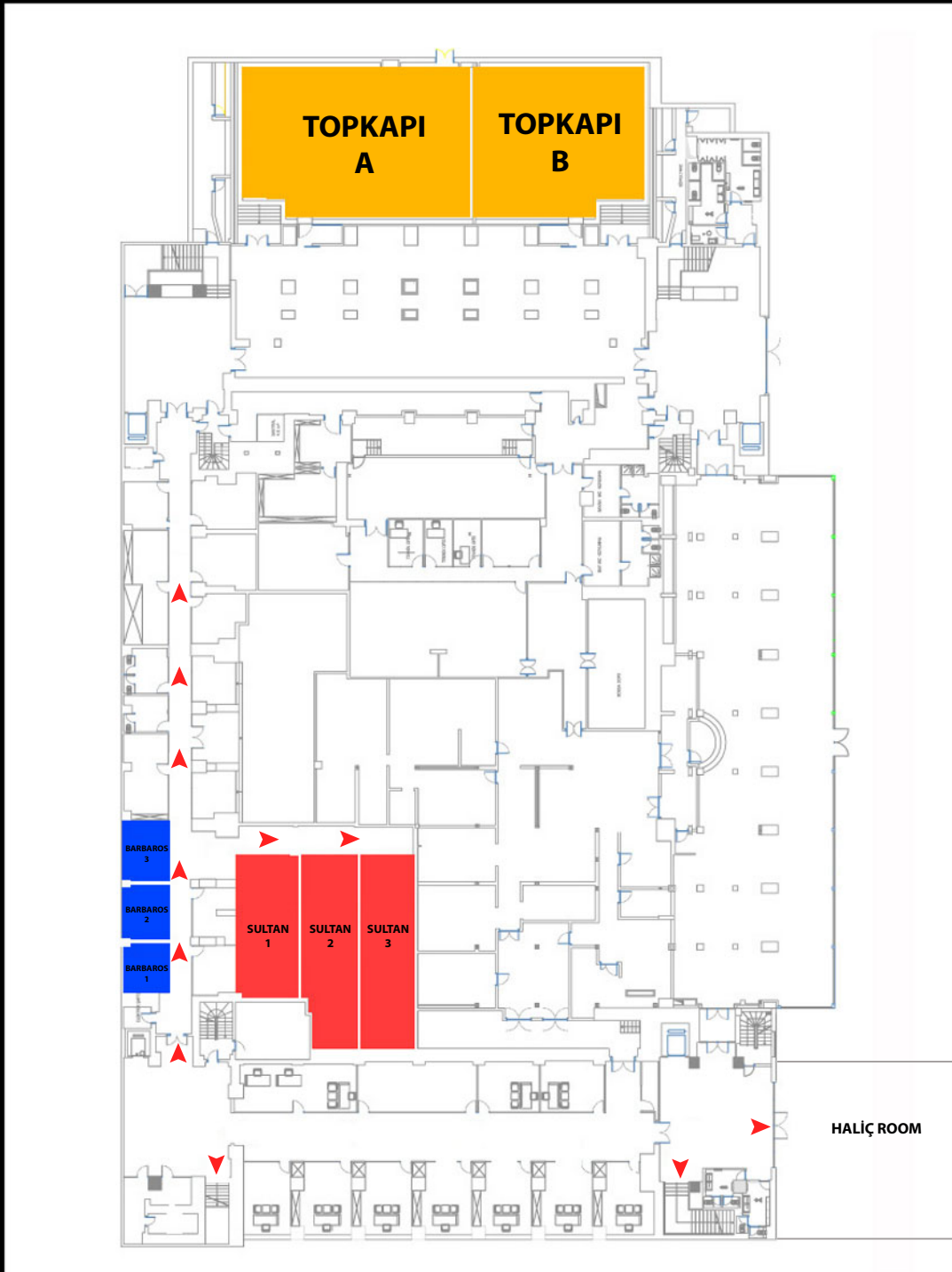
Date : 8 September 2014, Monday

Time / Location: 12.00 / HALIC



SYMPOSIUM VENUE FLOOR PLANS

LOWER LEVEL



7-12 September 2014
ISTANBUL, TURKEY

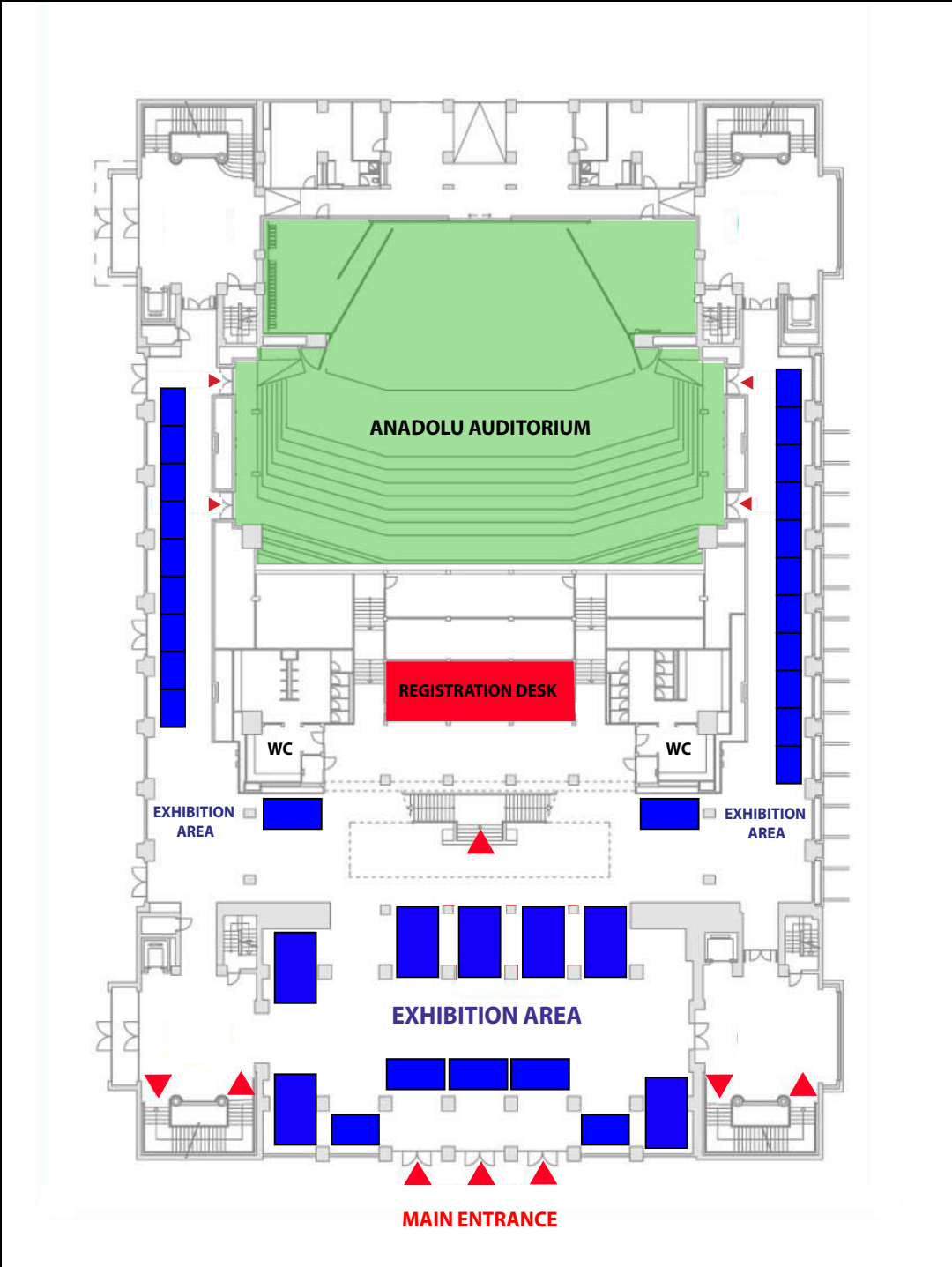
LUTFI KIRDAR CONVENTION & EXHIBITION CENTER

XXth Symposium Neuroradiologicum



SYMPOSIUM VENUE FLOOR PLANS

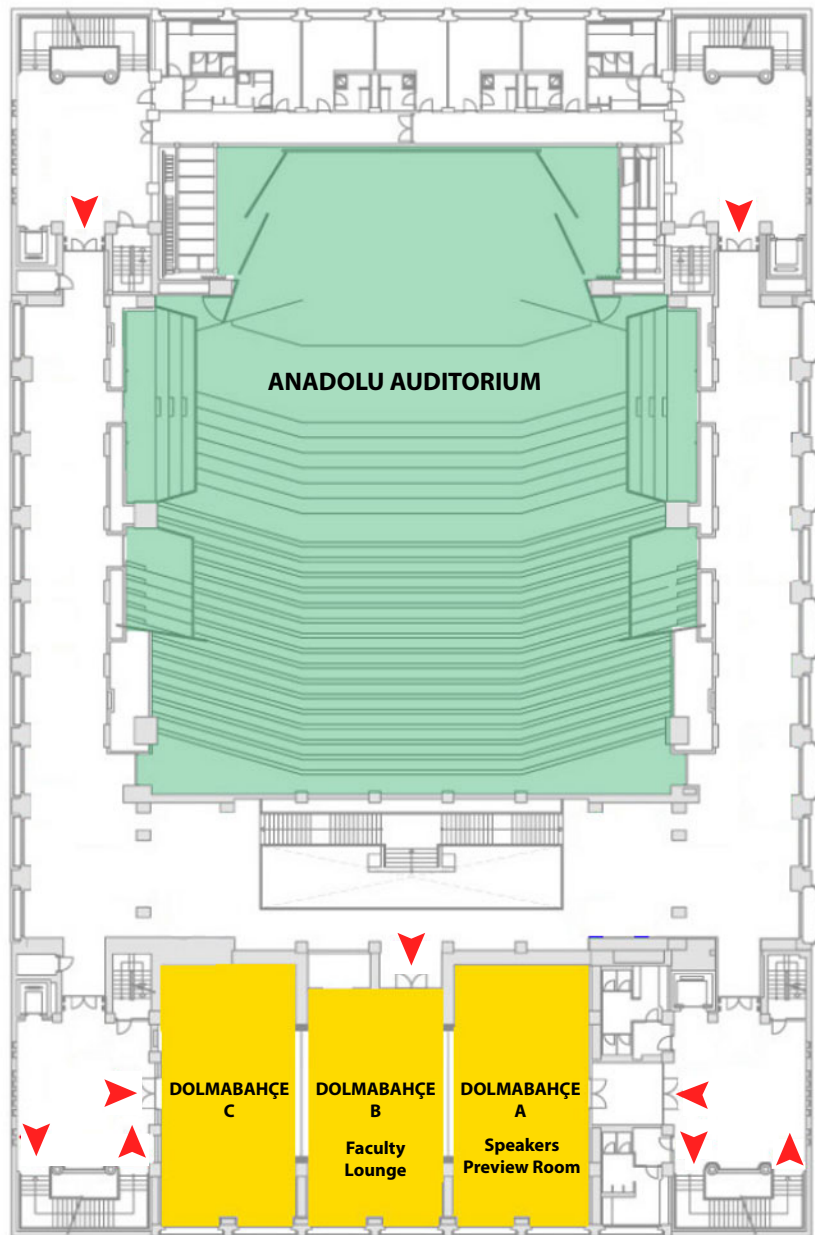
GROUND LEVEL





SYMPOSIUM VENUE FLOOR PLANS

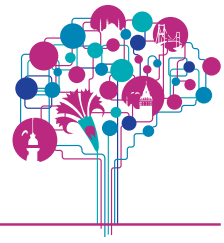
LEVEL - 1



7-12 September 2014
ISTANBUL, TURKEY

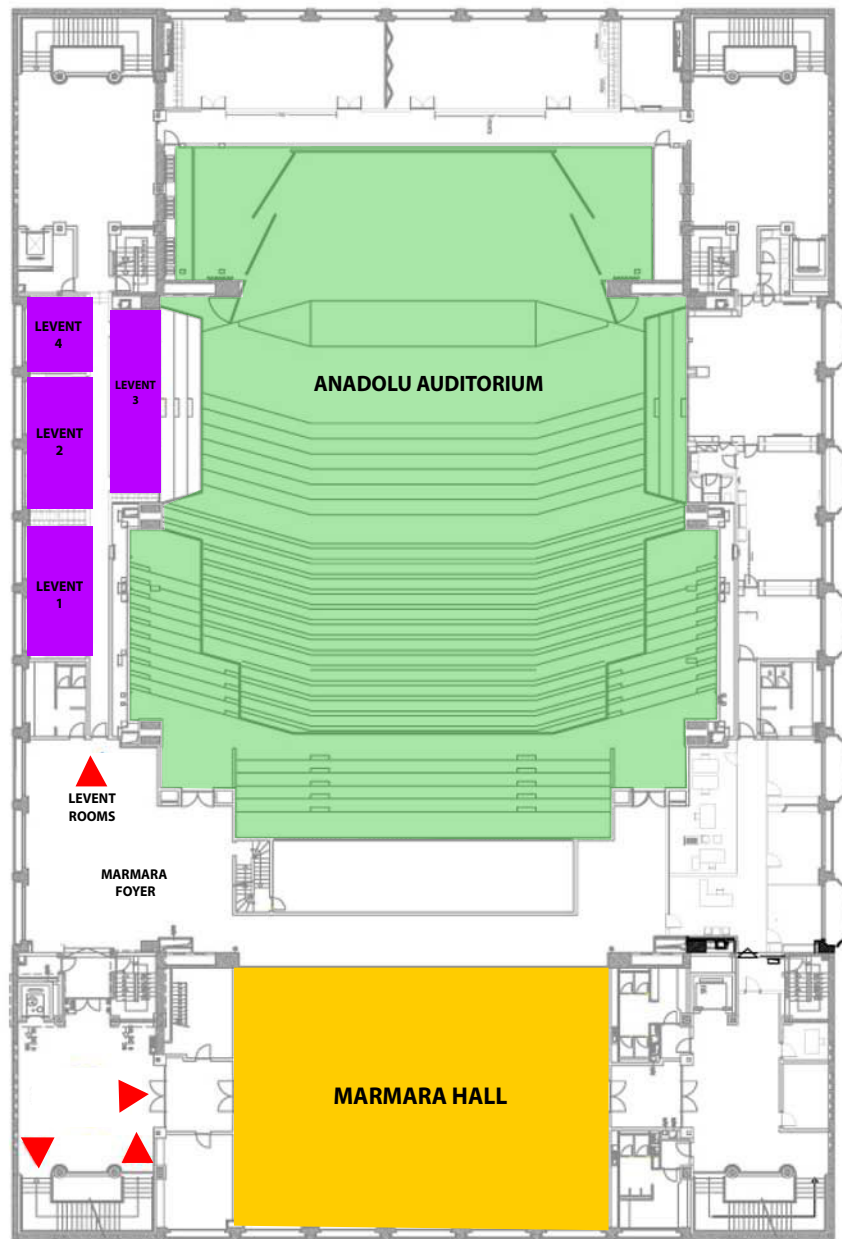
LUTFI KIRDAR CONVENTION & EXHIBITION CENTER

XXth
Symposium
Neuroradiologicum



SYMPOSIUM VENUE FLOOR PLANS

LEVEL - 2





**NEXT SYMPOSIUM; XXIst SYMPOSIUM NEURORADIOLOGICUM
TAIWAN 2018**



Dear Honorable Delegates,

Our warmest greetings from Taipei!

The upcoming XXI Symposium Neuroradiologicum will grace springtime Taipei, Taiwan, at the International Convention Center, between March 19-24, 2018. It is hosted by Neuroradiological Society of Taiwan, and co-hosted by Japanese Society of Neuroradiology, Korean Society of Neuroradiology, and Head & Neck Radiology

The theme of the upcoming symposium, "One World, One Family," illustrates our belief that the event in Taipei will be a game-changer: since the first assembly in Belgium 1939, only a handful of events were hosted outside the European continent. But with Taipei - one of Asia's most enchanting capital cities - organizing the XXI Symposium, you can anticipate stimulating sessions, hands-on workshops, speeches by acclaimed national and international speakers, and an exciting itinerary of social events.

Further, neuroradiologicum has an abiding tradition of recognizing that excellence in this specialty could only progress with concerted effort of sharing perspectives, the latest findings, and cutting-edge technologies that cover all aspects of the specialty; thus the chosen theme: "One World, One Family," to underpin the spirit of the symposium in Taipei.

Now, our sincerest welcome to all of you to Taipei, a city that makes sense all that is contrastive yet wonderful: here, you can expect the world's most advanced metro systems, and cultural marvels that date back thousands of years ago; what is more, you will be blown away by Taipei's jaw-dropping culinary diversity, where food is considered a religion. The city is also home to some of Asia's most tourism-worthy destinations; along your travels, you can sample Taipei citizens' hospitality that international bloggers rave about.

Finally, our greatest appreciation is for the encouragement of the neuroradiological communities worldwide. Your support has given Taiwan a strong foothold in the international Neuroradiological medical profession; your participation, therefore, will be key to the success of XXI Symposium Neuroradiologicum.

We look forward to seeing you in Taipei!

Symposium President

Professor Wan-Yuo, GUO, M.D., Ph.D.

Symposium Vice-Presidents

Professor Yukunori KOROGI, M.D., Ph.D. (Japan)

Professor Sang-Joon KIM, M.D., Ph.D. (Korea)

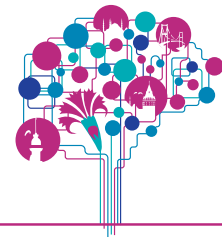
Professor Sandy CY CHEN, M.D. (Taiwan)

Professor Ho-Fai WONG, M.D. (Taiwan)

7-12 September 2014
ISTANBUL, TURKEY

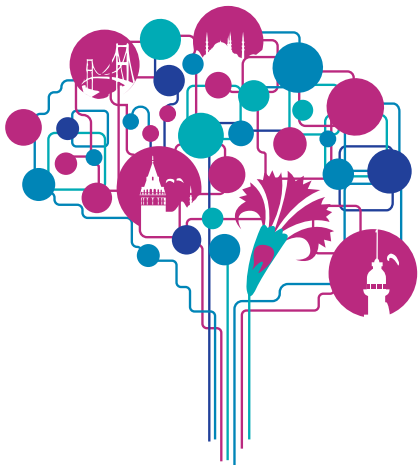
LUTFI KIRDAR CONVENTION & EXHIBITION CENTER

XXth
Symposium
Neuroradiologicum



PROGRAM OVERVIEW

		XXth SYMPOSIUM NEURORADIOLOGIUM - PROGRAM OVERVIEW																	
		08 September 2014, Monday			09 September 2014, Tuesday			10 September 2014, Wednesday			11 September 2014, Thursday			12 September 2014, Friday					
07 September 2014	ESNR European Diploma in Neuroradiology Examination																		
08.30-10.30	STROKE Basic Pathophysiology of Stroke and MIMICS	Head & Neck Tumors MARMARA HALL			Developmental Delay ANADOLU AUDITORIUM			Disc Disease and Management MARMARA HALL			Spine & Spine Interventional NR MARMARA HALL			Spine Interventional NR MARMARA HALL			Intravascular Interventional NR MARMARA HALL		
10.30-11.00		Coffee Break			Coffee Break			Coffee Break			Coffee Break			Coffee Break					
11.00-12.30	Diagnosis of Acute Stroke	Obit and Paramasal sinuses TOPKAPI A+B			ESNR Institutional Consil Meeting DOLMABAHCEC			Fetal and Neonatal imaging ANADOLU AUDITORIUM			Spine Tumors & Treatment MARMARA HALL			Minimally Invasive Intervention and Innovation MARMARA HALL			Presentations & Discussion on Controversial Approaches & Controversies in Endovascular Anaysym Treatment MARMARA HALL		
12.30-13.30		Lunch			Lunch			Lunch			Lunch			Lunch					
13.30-14.30	Stroke Management on Imaging Findings	Neck, Lymph node and plexuses TOPKAPI A+B			Malformations and Epilepsy ANADOLU AUDITORIUM			Spine Tumors & Treatment MARMARA HALL			Infection/Inflammatory/ Degenerative Diseases of the Spine MARMARA HALL			Endovascular Treatment of Acute Stroke: The Past, Present and Future MARMARA HALL			Endovascular Treatment of Spinal Vascular Malformations MARMARA HALL		
13.30-15.00		Coffee Break			Coffee Break			Coffee Break			Coffee Break			Coffee Break					
15.00-15.30	Hemorrhage	Temporal Bone & Cranial nerves TOPKAPI A+B			Pediatric Sedation and Trauma ANADOLU AUDITORIUM			Augmentation MARMARA HALL			ESNR & Symposium Awards Ceremony ANADOLU AUDITORIUM			Vascular Disease in Children TOPKAPI A+B			CNS Infections ANADOLU		
15.30-17.00		Coffee Break			Coffee Break			Coffee Break			Coffee Break			Coffee Break					
17.00-17.15		Opening Ceremony ANADOLU AUDITORIUM			ESNR Honorary Membership & Diploma Ceremony ANADOLU AUDITORIUM			Parallel Scientific Paper Presentations			Parallel Scientific Paper Presentations			Parallel Scientific Paper Presentations			Parallel Scientific Paper Presentations		
17.15-19.00																			



XXth
Symposium
Neuroradiologicum

SCIENTIFIC PROGRAM



SCIENTIFIC PROGRAM

Monday, September 8, 2014

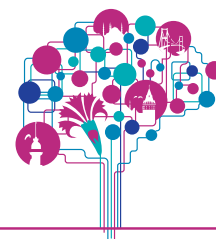
STROKE	Marmara Hall
08:30 - 10:30	Basic Pathophysiology of Ischemic Stroke and Mimics
Moderators	: E. Turgut Tali, Turkey, Nick Bryan, USA
	Hemodynamic Reserve Concept Clinical Implications and Assessment
	<i>Ethem Murat Arsava</i>
	<i>Hacettepe University Neurology Ankara, Turkey</i>
	Pathophysiology of Cerebral Ischemia and Recovery Mechanism of Neuronal Damage
	<i>Patricia Desmond</i>
	<i>Royal Melbourne Hospital, University of Melbourne Radiology Melbourne, Australia</i>
	Controversies in Perfusion Weighted Imaging; Mismatch Concept and Salvageable Brain Tissue
	<i>Kei Yamada</i>
	<i>Kyoto Prefectural University of Medicine Radiology Kyoto, Japan</i>
	Stroke Mimics and Venous Stroke
	<i>William T.C. Yuh</i>
	<i>University of Washington Radiology Seattle, USA</i>
	O001- Acute-onset Migrainous Aura Mimicking Acute Stroke: MR perfusion imaging features
	<i>Franz Fellner¹, Christine Fellner¹, Gerhard Haitchi¹, Milan Vosko², Maximilian Ziernhöld¹</i>
	<i>AKH Linz Radiology Linz, Austria¹ AKH Linz Neurology, Austria²</i>

HEAD & NECK	Topkapı AB Hall
08:30 - 10:30	Head & Neck Tumors
Moderators	: Laure Loevner, USA, Bernhardt Schuknecht, Switzerland
	Orbits and Globe
	<i>Suresh Mukherji</i>
	<i>Michigan State University, USA</i>
	Cranial Nerves of the Orbit 3, 4 And 6
	<i>J. W. Casselman^{1,2,3}</i>
	<i>Department of Radiology AZ St-Jan Brugge AV, Brugge, Belgium¹</i>
	<i>University of Ghent, Gent, Belgium²</i>
	<i>Department of Radiology⁴ & Otorhinolaryngology⁵ St- Augustinus, Wilrijk, Belgium³</i>
	Anatomy and Pathology of the Temporal Bone
	<i>Burce Ozgen</i>
	<i>Hacettepe University, Turkey</i>
	Anatomy of the Auditory Pathways
	<i>Jan W. Casselman^{1,2,3}</i>
	<i>Department of Radiology AZ St-Jan Brugge AV, Brugge, Belgium¹</i>
	<i>University of Ghent, Gent, Belgium²</i>
	<i>Department of Radiology⁴ & Otorhinolaryngology⁵ St- Augustinus, Wilrijk, Belgium³</i>

7-12 September 2014
ISTANBUL, TURKEY

LUTFI KIRDAR CONVENTION & EXHIBITION CENTER

XXth
Symposium
Neuroradiologicum



SCIENTIFIC PROGRAM

O002-The Relationship Between The Race And Gender And Pattern Of Isolated Orbital Fractures

Merve Gursoy ¹, Roxana Rivera-Michlig ², David M. Yousem ¹, Lukasz S. Babiarz ¹, Michael P. Grant ²

The Johns Hopkins Medical Institutions The Russell H. Morgan Department of Radiology and Radiological Sciences ¹, The Johns Hopkins Medical Institutions Division of Oculoplastics Surgery, Wilmer Eye Institute ²

10:30 - 11:00 COFFEE BREAK

STROKE

Marmara Hall

11:00 - 12:30

Diagnosis of Acute Stroke

Moderators : Howard Rowley, USA, Soren Jacob Bakke, Norway

Imaging of ischemic parenchyma in hyperacute stage of ischemic stroke

Zoran Rumboldt

University of Rijeka School of Medicine, Croatia

Imaging of Ischemic Penumbra Methods for Assessing Ischemic Penumbra in Experimental and Clinical Models

Patricia Desmond

Royal Melbourne Hospital, University of Melbourne Radiology Melbourne, Australia

MRI of Cerebral blood flow, reactivity and beyond (ASL MRI of cerebral blood flow, BOLD and ASL measurements of cerebrovascular reactivity, Beyond CBF: oxygen extraction fraction and cerebral blood volume)

Pamela Schaefer

Harvard University, Massachusetts General Hospital, Boston, USA

O003-Based Magnetic Resonance Imaging Reveals Relative Oxygen Extraction Fraction Changes in Patients with Hyperacute Stroke

Alexandra S. Gersing ¹, Monika Ankenbrank ¹, Benedikt J. Schwaiger ¹, Vivien Toth ¹, Silke Wunderlich ², Claus Zimmer ¹, Christine Preibisch ¹

Technical University Munich, Klinikum rechts der Isar Neuroradiology Munich-Germany ¹

Technical University Munich, Klinikum rechts der Isar Neurology -Germany ²

HEAD & NECK

Topkapı AB Hall

11:00 - 12:30

Orbit and Paranasal Sinuses

Moderators : Agnieszka Trojanowska, Poland, Leon Janse Van Rensburg, South Africa

Anatomy and pathology of the oral cavity and oropharynx

Suresh Mukherji

Michigan State University, USA

Modern imaging of non-neoplastic salivary gland diseases

Minerva Becker

Geneva University Hospital, Switzerland

Thyroid nodules and parathyroid imaging

Laurie Loevner

University of Pennsylvania, USA

12:30 - 13:30 LUNCH BREAK



SCIENTIFIC PROGRAM

13.00-14.00 Poster Presentations

Adult NR 1 Moderator: Nick Bryan, USA

SULTAN 1

EP001-Neuroimaging Findings in Alcohol Related Encephalopathies; What Radiologists Need to Know?
Hye Jin Baek, Hong Dae Kim, Choong Ki Eun

EP002-Encephalitis with Restricted Diffusion and Absent T2W Flair Changes
Hilwati Hashim, Norzaini Rose Mohd Zain, Shanti Viswanathan

EP003-Cranial MR Imaging Findings of Wolfram (DIDMOAD) Syndrome a Case Report
Rahsan Gocmen, Ezgi Guler

EP004-Neuroimaging Findings of a Case with Primary Leptomeningeal Melanomatosis
Rahsan Gocmen, Nazire Pinar Acer, Ahmet Cagkan Inkaya, Asli Kurne

EP005-Hyper IgE Syndrome Initially Presenting with Progressive Multifocal Leukoencephalopathy
Rahsan Gocmen, Nazire Pinar Acar, Nergis Agayeva, Asli Kurne

EP006-Pseudohypoxic Brain Swelling after Intracranial Electrode Placement an Extremely Rare Complication
Rahsan Gocmen, Mehmet Akif Topcuoglu, Irsel Tezer, Burcak Bilginer, Serap Saygi

EP007-Pyogenic Brain Abscesses Necrotic Glioblastomas and Necrotic Metastatic Brain Tumors Discrimination with Susceptibility Weighted Imaging
Ping-Hong Lai, Jui-Hsun Fu, Tzu-Chao Chuang, Hsiao-Wen Chung, Hing-Chiu Chang, Huey-Shyan Lin, Po-Chin Wang, Shuo-Hsiu Hsu, Huay-Ben Pan

EP008-Venous Hypertension with Intracranial Hemorrhagic Complication
Clayton Chi-Chang Chen, Fong Y Tsai, Chi-Jen Chen, Kwo-Whei Lee

EP009-Cerebral Venous Drainage Variants Pathology and Impact on the Diagnosis of Headache
Diana Quiñones Tapia, Carlota Andreu Arasa, Juan Viaño

EP010-Additional Value of 3D FLAIR in Relation to T2 weighted Images in the Evaluation of the Optic Pathway in Patients with Sellar Suprasellar Tumors
Mika Kitajima, Toshinori Hirai, Shigetoshi Yano, Yoshinori Shigematsu, Yasuhiko Iryo, Minako Azuma, Machiko Tateishi, Yasuyuki Yamashita

EP011-Possible Compensatory Plasticity of Anterior Thalamic Nucleus to Memory Impairment in Normal Pressure Hydrocephalus Patients Manifested As Increased Anisotropy and Fiber Density
Cheng-Yu Chen, Shih-Wei Chiang, Hsiao-Wen Chung, Ping-Huei Tsai, Hua-Shan Liu, Yi-Hsiu Hsiao, Chao-Ying Wang, Ming-Chung Chou, Hung-Wen Kao, Fong Y Tsai

EP012-Brain Gliomas' Peritumoral Normal Appearing White Matter Evaluation with 3 Tesla MR Spectroscopy
Italo Aprile, Giulia Belardinelli, Marco Muti, Antonio Di Renzo, Paola Fiaschini, Nicolò Haznedari, Nevia Caputo

EP013-Symptomatic Pontine Capillary Telangiectasia Which Is Diagnosed by Susceptibility Weighted Imaging
Murat Asik, Pinar Beyaz, Furkan Ertem, Suleyman Dikici, Zehra Isik Hasiloglu

EP014-Innumerable Cerebral Hemorrhages in Influenza Associated Encephalitis a Case Report
Ji-Ye Lee, *Su Ok Seong*

EP015-Clinical Applications of Neuroimaging with Susceptibility Weighted Imaging
Hyunkoo Kang

7-12 September 2014
ISTANBUL, TURKEY

LUTFI KIRDAR CONVENTION & EXHIBITION CENTER

XXth
Symposium
Neuroradiologicum



SCIENTIFIC PROGRAM

Adult NR 2

Moderator: Sandy Chen, Taiwan

SULTAN 1

EP016-The Diagnostic Value of Postcontrast Susceptibility Weighted Imaging in the Assessment of Intracranial Brain Neoplasm at 3T

Hyunkoo Kang

EP017-Applications of Dual Energy CT in Neuroimaging

Vrushali Bachhav, Abhijit Patil, Mehmet Kocak, Sharon Byrd

EP018-Radiological Findings of Oligodendroglial Tumors Retrospective Analysis of a Single Institution Experience

Yoshiyasu Hiratsuka, Keiichi Kikuchi, Shirou Ooue, Teruhito Mochizuki

EP019-Title Two Stage Voxel based Parametric Response of the Apparent Diffusion Coefficient for Predicting the Subsequent Tumor Progression Pattern in Patients with Glioblastoma Comparison with Single Stage Measurement

Ra Gyoung Yoon, Ho Sung Kim, Dae Yoon Kim, Seung Chai Jung, Myeong Ju Goh, Sang Joon Kim

EP020-Radiological Features of Intracranial Germinoma

Keiichi Kikuchi, Yoshiyasu Hiratsuka, Shiro Ohue, Teruhito Mochizuki

EP021-Radiographic Features with Pathological Correlation in Cerebral Amyloid Inflammatory Vasculopathy A Case Report

Maria Pia Pappalardo, Paolo Arculeo, A Lo Bello, Giuseppe Craparo, Simona Arculeo, Paola Marchese, Cesare Gagliardo, Massimo Midiri

EP022-Epstein Barr Virus associated Primary Central Nervous System Lymphomas in Immunocompetent Patients Showed Characteristic MR images Mimicking Glioblastoma 4 Cases Reports and Review of The Literature.

Yusuke Uchiyama, Ayako Yoshida, Norimitsu Tanaka, Yasuo Sugita, Kiyohiko Sakata, Toshi Abe

EP023-Doubt on the Association between Transient Global Amnesia and Intracranial Venous Reflux Based on the Time of Flight MR Angiography

Eunhee Kim, Dong Hoon Lee, Hyung Suk Seo

EP024-Attenuation and Heterogeneity of Cerebral Gliomas on Unenhanced CT: A Relationship with Tumor Grade Indicates Bioamarker Potential

Karoline Skogen, Balaji Ganeshan, Kenneth Miles, Johan Baptist Dormagen, Anselm Schulz, Eirik Helseth, Andres Alonso

EP025-CD8 Encephalopathy in HIV: A Case Report with Clinical CSF and MRI and Histological Findings

Sally Candy, Kathleen Bateman, Shikar Mothila

EP026-Central Nervous System Involvement by Multiple Myeloma a Pictorial Essay

Arian Lasocki, Shane Gangatharan, Francesco Gaillard, Simon Harrison

EP027-Distinguishing Clinico Radiological Features in Patients with Central Nervous System Tumefactive White Matter Lesions

Xuling Lin, Kevin Tan, Lishya Liauw, Aung Soe Tin, Weiling E Soon, Yin Shih Zhu Yiin, Boon-Ping Toe, Hwei-Yee Lee, Wai-Yung Yu



SCIENTIFIC PROGRAM

EP028-”D.M.T.E.S” Useful Categorization of Variable Diseases Involving Splenium of the Corpus Callosum
In Kyu Yu, Youn Joo Lee, Chang June Song, Jin Young Kim

EP029-Intracerebral Hemorrhagic Mass Manifesting As Initially Spontaneous Hemorrhage
In kyuu Yu, Youn Joo Lee, Chang June Song, Seung Hwan Baek

EP030-Various high DWI SI Lesions Mimicking Acute Cerebral Infarction (ACI)
In Kyu Yu, Youn Joo Lee, Hee Kyung Kim

Adult NR 3

Moderator: Ritva Vanninen, Finland

SULTAN 2

EP031-Levothyroxine as Potential Cause of Osmotic Demyelination Syndrome

Gordana Milenkovic, Biljana Georgievski-Brkic, Aleksandra Terzic-Beljakovic, Ljubinko Milenkovic, Marjana Vukicevic

EP032-Correlation between Magnetic Resonance Angiography and Transcranial Doppler Sonography
Gordana Milenkovic, Biljana Georgievski-Brkic, Veljko Maksic, Ljubinko Milenkovic, Tatjana Ducic-Jaramaz

EP033- Neuroimaging in Posterior Reversible Encephalopathy Syndrome

Adriana Ojeda, Paola Acevedo, Maria Belen Nallino, Ana Maria Uriarte

EP034- Comparison of Cerebral Blood Flow on Perfusion MRI by Using Arterial Spin Labeling and Dynamic Susceptibility Contrast in Brain Tumors

Arisa Ohara, Kazuhiro Tsuchiya, Miho Gomyo, Hidekatsu Tateishi, Toshiaki Nitatori

EP035- Intracranial Plaque Imaging by High resolution 2D Imaging at 3T

Miho Gomyo, Kazuhiro Tsuchiya, Arisa Ohara, Hidekatsu Tateishi, Isao Miyazaki, Toshiaki Nitatori

EP036- Bilateral Thalamic Lesions a Pictorial Review

Anil Ozgür, Kaan Esen, Hakan Kalegasi, Arda Yilmaz, Engin Kara, Altan Yildiz

EP037- Immunotherapy Related Neurological Complications Ipilimumab induced Hypophysitis

Pachymeningitis and Other Immune related Neurological Complications

Judith Gadde, Alberto Iaia

EP038- Evaluation of Cerebrospinal Fluid Dynamics Using Time Spatial Labeling Inversion Pulse Technique for Endoscopic Third Ventriculostomy in Hydrocephalic Patients

Kayoko Abe, Kazufumi Suzuki, Yuko Ono, Yasuo Aihara, Yoshikazu Okada, Shuji Sakai

EP039- Susceptibility Weighted Magnetic Resonance Imaging Evaluation of Familial Cerebral Cavernous Angiomas

Haci Taner Bulut, Mehmet Akif Sarica, Ali Haydar Baykan

EP040- Radiation Necrosis Imaging Spectrum and Practical Approach

Ankush Patel, Uresh Patel

EP041- Congenital Dolichoectasia of Cerebral Arteries; a Comprehensive Review of Cases

Mustafa Gok, Celal Cinar, Halil Bozkaya, Ismail Oran

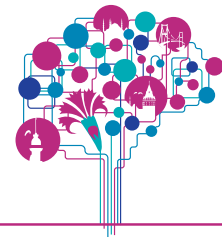
EP042- Sometimes a Meningioma Isn't Just a Meningioma

Mariana Diogo, João Jacinto, Isabel Fragata, *Carla Conceição*, Manuela Mafra, Luís Cerqueira, João Reis

7-12 September 2014
ISTANBUL, TURKEY

LUTFI KIRDAR CONVENTION & EXHIBITION CENTER

XXth
Symposium
Neuroradiologicum



SCIENTIFIC PROGRAM

EP043- Focal Radiological Changes Due To Status Epilepticus (SE), Report of Two Cases

Luciana León Cejas, Julieta Quiroga Narvaez, Pablo Bonardo, Julieta Mazziotti, Carlos Rugilo, Juan Chomont, Beatriz Afonso, Ricardo Reisin, Manuel Fernandez Pardal

EP044- Evaluation of Multiple System Atrophy Cerebellar Type with the Use of MR Imaging and Perfusion Spect
Fuminori Miyoshi, Yoshiko Kanasaki, Yuki Shinohara, Shinya Fujii, Toshihide Ogawa

EP045- Reversible Posterior Encephalopathy Syndrome (PRES), Report of Our Experience in 19 Patients

Luciana León Cejas, Julieta Quiroga Narvaez, Pablo Bonardo, Julieta Mazziotti, Carlos Rugilo, Juan Chomont, Diego Miñarro, Emanuel Silva, Ricardo Reisin, Manuel Fernandez Pardal, Pablo Young, Laura Bongiovani

Adult NR 4

Moderator: Howard Rowley, USA

SULTAN 2

EP046- Cortical Blindness after Coronariography. A Case Report

Ingeborg Lopez, Rodrigo Riveros, Roberto Marileo, Cecilia Okuma, Aaron Vidal, Rodrigo Rivera, J. Gabriel Sordo, Lautaro Badilla

EP047- Corpus Callosum Involvement in Anti Aquaporin 4 Disease. Case Report

Ingeborg Lopez, Roberto Marileo, Cecilia Okuma, Sabrina Oporto, Aaron Vidal, Rodrigo Rivera, J. Gabriel Sordo, Lautaro Badilla

EP048- Linear Scleroderma with Neurologic Involvement Two Case Reports

Ingeborg Lopez, Roberto Marileo, Rodrigo Riveros, Cecilia Okuma, Aaron Vidal, Rodrigo Rivera, J. Gabriel Sordo, Claudia Tissera, Lautaro Badilla

EP049- Prefrontal Cortex Phylogeny Development and Pathological Conditions. Pictorial Essay

Rosana Salvatico, Hector Lambre, Cecilia Rollan, Gabriela de Pino, Carlos Romero

EP050- Vascular Signs Its Meaning and Importance in the Diagnosis of Brain Head and Neck Pathology

Rosana Salvatico, Hector Lambre, Rosana Ceratto, Angel Ferrario, Pedro Lylyk

EP051- Autoimmune Limbic Encephalitis Caused by Ovarian Neoplasms Reports of Two Cases and Literature Review

Yao-Liang Chen, Ho-Fai Wong

EP052- Resting State Neural Network in Monolateral and Bilateral Tinnitus

Ji Hye Jang, Chang-Woo Ryu, Geon-Ho Jahng, Eui Jong Kim, Woo Suk Choi

EP053- MR Imaging In Relation To Phylogenetic Anatomy of the Cerebellum in Spinocerebellar Ataxia from Conventional MRI to Diffusion Imaging

Kanako Sato, Koji Kamagata, Ryuji Sakakibara, Hitoshi Terada, Shigeki Aoki

EP054- Three Cases of Progressive Multifocal Leukoencephalopathy with Specific Involvement of Pyramidal Tract an Important Differential Consideration

Kouhei Kamiya, Ryusuke Irie, Harushi Mori, Akira Kunimatsu, Masaaki Hori, Noriko Sato, Shigeki Aoki, Kuni Ohtomo

EP055- Preoperative Diagnosis of Suprasellar Papillary Craniopharyngioma and Germ Cell Tumors of Adult Patients

Han-Jui Lee, Feng-Chi Chang, Hsiu-Mei Wu, Alex S. C. Hung, Chih-Chun Wu, Wan-Yuo Guo

EP056- Susceptibility Weighted Imaging Improves the Accuracy of Brain MRI to Differentiate between Parkinson's Disease and Atypical Parkinsonism

Frederick Meijer, Bram Fasen, Bastiaan Bloem, Bozena Goraj



SCIENTIFIC PROGRAM

EP057- Panencephalopathic Type of Crutzfeldt Jacob Disease in Indian Subpopulation Case report
N K Mishra, A Garg, L Joseph, S B Gaikwad

EP058- Predisposing Factors in Posterior Circulation Infarcts a Vascular Morphological Assessment
Gökçen Coban, Bilal Egemen Cifci, Erkan Yıldırım, Ahmet Muhteşem Ağıldere

EP059- Demyelinating Patterns associated to Primary CNS Lymphoma
Antonio Mas-Bonet, Maria J Picado-Valles, Apolonia Moll-Servera, Carmen Gassent-Balaguer, Nestor Calvo-Rado, Ines Barcelo, Mariano Del-Valle, Salvador Miralbes-Celma

EP060- Transient Homonymous Hemianopia Caused by Cerebral Venous Sinus Thrombosis
Gökçen Coban, Aylin Karalezli, Bahriye Horasanli, Nilüfer Yesilirmak

STROKE

Marmara Hall

13:30 - 15:00

Stroke Management on Imaging Findings

Moderators

: Allan Fox, Canada, Charles Majoie, The Netherlands

Revisit Diagnosis and Treatment of Acute Stroke: Myth and Truth

William T.C. Yuh

University of Washington Radiology Seattle, USA

CT and MRI Strategies to Guide Reperfusion Therapies

Rüdiger von Kummer

University Hospital Neuroradiology Dresden, Germany

Hemorrhagic Transformation and Reperfusion Hemorrhage Clinical and Radiological Predictors and Prognosis

Rüdiger von Kummer

University Hospital Neuroradiology Dresden, Germany

O004-Structural and Functional Correlation in Normal and Abnormal White Matter in the CARDIA Cohort

Harsha Battapady¹, Ilya Nasrallah¹, Guray Erus¹, Alex Smith¹, Lenore Launer², David Jacobs³, Pamela Schreiner³, Kiang Liu⁴, Beth Lewis⁵, Christos Davatzikos¹, *Nick Bryan*¹
Univ. Pennsylvania Radiology -United States¹ NIH NIA -United States² Univ. Minnesota Epidemiology -United States³ Northwestern Univ. Medicine -United States⁴ Univ. Alabama Medicine -United States⁵

HEAD & NECK

Topkapı AB Hall

13:30 - 15:00

Neck: Lymph node and plexuses

Moderators

: Katarina Surlan Popovic, Slovenia, Ahmed El Beltagi, Kuwait

Imaging of sinonasal tumors and aggressive inflammation

Laurie Loevner

University of Pennsylvania, USA

PET/CT and PET/MRI in Head and Neck Oncology

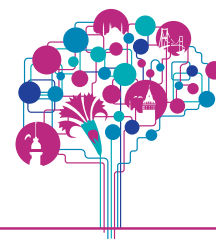
Minerva Becker

Geneva University Hospital, Switzerland

7-12 September 2014
ISTANBUL, TURKEY

LUTFI KIRDAR CONVENTION & EXHIBITION CENTER

XXth
Symposium
Neuroradiologicum



SCIENTIFIC PROGRAM

Imaging laryngeal and hypopharyngeal cancer

Eloise S. Gebrim

University of Sao Paulo, Brazil

O005-Optimization of Double Inversion Recovery Contrast for Brachial Plexus Imaging of the Neck

Mariah H. Bashir¹, Kwan-Jin Jung¹, Robert J. Bert¹

Univ. of Louisville Radiology Louisville-USA¹

15:00 - 15:30 COFFEE BREAK

STROKE

Marmara Hall

15:30 - 17:00

Hemorrhage

Moderators : Hussein Kamel, Qatar, Peter Mitchell, Australia

Intracerebral Hemorrhage: A Review

Mauricio Castillo

The University of North Carolina at Chapel Hill, USA

Acute Subarachnoid Hemorrhage: A Review

Mauricio Castillo

The University of North Carolina at Chapel Hill, USA

Assessing the Recovery from Stroke Using Advanced MR Imaging Techniques

Kei Yamada

Kyoto Prefectural University of Medicine Radiology Kyoto, Japan

Physiology of the Blood Clotting System and Its Pharmaceutical Modulation

Ethem Murat Arsava

Hacettepe University Neurology Ankara, Turkey

HEAD & NECK

Topkapı AB Hall

15:30 - 17:00

Temporal Bone & Cranial nerves

Moderators : Franz Fellner, Austria, Nail Bulakbasi, Turkey

Imaging of the Jaw: Benign and Malignant Lesions

Osamu Sakai

Boston University School of Medicine Radiology Boston, USA

Inflammatory and Malignant Nodes

Vincent Chong

National University Hospital Diagnostic Radiology Singapore, Singapore

Imaging of perineural spread in head and neck tumors

Eloise S. Gebrim

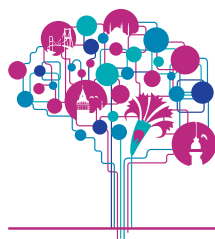
University of Sao Paulo, Brazil

BREAK

17:00 - 17:15

OPENING CEREMONY 17:15 - 19:00

ANADOLU AUDITORIUM



SCIENTIFIC PROGRAM

Tuesday, September 9, 2014

PEDIATRIC DIAGNOSTIC NR

Anadolu Auditorium

08:30 - 10:30

Developmental Delay

Moderators

: A. James Barkovich, USA, Goran Pavlisa, Croatia

**Types of developmental delay; Clinical Evaluation of the Developmentally Delayed Child:
What the Child Neurologist needs from the Neuroradiologist**

Ingeborg Krageloh-Mann

University children's Hospital, Germany

Imaging of the Developmentally Delayed Child: Metabolic Disorders

Marjo S. van der Knaap

Department of Child Neurology, VU University Medical Center, Amsterdam, The Netherlands

Imaging of the Developmentally Delayed Child Structural Abnormalities

Charles Raybaud

Hospital for Sick Children, Toronto-Canada

**O006-MRI Findings in Patients with Developmental Delay with Correlation with Clinical
Presentation**

Ahmed Elsotouhy¹, Walid Mubarak¹, Jehan Alrayahi¹, Mohamed Alberawi¹, Hazar Taban¹,
Hussein Kamel¹

*HMC Radiology Doha, Qatar*¹

SPINE & SPINE INTERVENTIONAL NR

Marmara Hall

08:30 - 10:30

Disc Disease and Management

Moderators

: Giuseppe Bonaldi, Italy, Orlando Ortiz, USA

Imaging of disc disease (herniation and DDD) and nomenclature

Adam Flanders

Thomas Jefferson University Hospital, USA

Disc: when is it painful, when should be treated?

Giuseppe Bonaldi

Osp. Giovanni XXIII, Bergamo Neuroradiology, Italy

Automated Lumbar Percutaneous Discectomy

Wendell A. Gibby

*Adjunct Professor of Radiology, University of California San Diego
CEO - Novard Corporation, USA*

Percutaneous disk injections; a review.

Mario Muto

Cardarelli Hospital, Italy

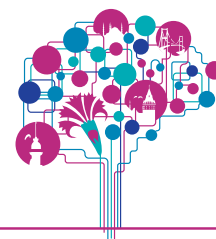
10:30 - 11:00

COFFEE BREAK

7-12 September 2014
ISTANBUL, TURKEY

LUTFI KIRDAR CONVENTION & EXHIBITION CENTER

XXth
Symposium
Neuroradiologicum



SCIENTIFIC PROGRAM

PEDIATRIC DIAGNOSTIC NR		Anadolu Auditorium
11:00 - 12:30	Fetal and Neonatal Imaging	
Moderators	: Charles Truwit, USA, Tracy Kilborn, South Africa	
	Neonatal Encephalopathy: Clinical, Neurophysiological and Imaging aspects	
	<i>Roberta Cilio¹, P. Ellen Grant²</i>	
	<i>University of California San Francisco, USA¹, Harvard Medical School, USA²</i>	
	State of the Art Imaging of Fetal Brain, Head, Neck and Spine	
	<i>Andrea Righini</i>	
	<i>Radiology and Neuroradiology Department, Children's Hospital V. Buzzi, Milan, Italy</i>	
	Using Two Compartment White Matter Model of Diffusion Kurtosis Imaging to Reveal the Diffuse Excessive High Signal Intensity (DEHSI) in Preterm Neonates	
	<i>Jian Yang</i>	
	<i>The First Affiliated Hospital, Xi'an Jiaotong University, Radiology Department, Xi'an, China</i>	
	O007-Fetal Brain Morphology After in Utero Repair of Open Neural Tube Defects	
	<i>Christin Nasiadko¹, Ianina Scheer¹, Martin Meuli², Ueli Moehrlen², Nicole Ochsenbein³</i>	
	<i>Kinderspital Zuerich Radiology Zuerich-Switzerland¹, Kinderspital Zuerich Surgery²</i>	
	<i>Universitätsklinikum Zuerich Obstetrics³</i>	
SPINE & SPINE INTERVENTIONAL NR		Marmara Hall
11:00 - 12:30	Spine Tumors & Treatment	
Moderators	: Suzanne Abbas Mohd, Bahrain, Umair Rashid Chaudhry, Pakistan	
	Focal and Diffuse Bone Marrow Diseases, in Particular Neuroradiologic Expression of Different Haematologic Pathologies and Expected Changes during Their Treatment and Infiltrative Vertebral Marrow Changes	
	<i>Claudio C. V. Staut</i>	
	<i>Brazilian Society of Neuroradiology, Brazil</i>	
	Advanced imaging of vertebral tumors and tumor-like conditions including Nuclear Medicine	
	<i>Carlos Romero</i>	
	<i>FLENI-Neurological Children Disease Foundation, Argentina</i>	
	Advanced imaging of Spinal Cord tumors and mimics	
	<i>Majda Thurnher</i>	
	<i>Medical University Vienna, Austria</i>	
	O008-Targeted Radiofrequency Ablation (t RFA) of Malignant Spine Lesions before Cement Augmentation; Early Clinical Outcome	
	<i>Mark Georgy¹, Melinda Reyes², Jennifer Padwal³, Bassem Georgy⁴</i>	
	<i>University of California San Diego Public Health San Diego-United States 1 Point Loma Nazarene</i>	
	<i>University Chemistry-Biology -United States² University of California, San Diego Medical School</i>	
	<i>-United States³ University of California, San Diego Radiology, USA⁴</i>	
12:30 - 13:30	LUNCH BREAK	



SCIENTIFIC PROGRAM

13.00-14.00 **Poster Presentations**

Head and Neck 1 **Moderator: Stephen Stuckey, Australia** **SULTAN 1**

EP061- IgG4 Related Disease in Head and Neck CT Findings

Dong Woo Park, Mi Mi Kim, Young Jun Lee, Choong Ki Park, Hyun Koo Kang

EP062- Long Term Ultrasonographic Findings of Face and Neck US after Injection of Facial Filler the Role of Artifact on US

JiHwa Ryu, Choong Ki Eun, Kwang Hwi Lee, Hong Dae Kim

EP063- The Role of Parathyroid Hormone Assay on Fine Needle Aspiration Washouts and Ultrasonographic Findings in Nonfunctional Parathyroid Cysts

JiHwa Ryu, Choong Ki Eun, Kwang Hwi Lee, Hong Dae Kim

EP064- Three Dimensional Brain Tumor Rendering in Magnetic Resonance Imaging with Use of Open Source Software VR Render

LA Shih, C.R. Lu, K.-C Liu, H.S Wu, C.Y Wei

EP065- Small Lesions Involving Scalp and Skull in Pediatric Age

Jeong Hyun Yoo

EP066- Detectability and Anatomical Correlation of Middle Ear Cholesteatoma Using Fused Thin Slice Non Echo Planar Imaging Diffusion Weighted Image (FTS nEPID)

Masafumi Kanoto, Yoshihiro Konno, Takaaki Hosoya, Fumika Watarai, Yukio Sugai, Tomoo Watanabe, Seiji Kakehata

EP067- An in vivo MRI Study of cuprizone Induced Demyelination of C57BL/6 Mouse at 7.0T

Tingting Nie, Yanlong Jia, Gen Yan, Renhua Wu

EP068- Imaging Features of Orbital Neoplasm Developed in Pediatrics

Jeong Hyun Yoo

EP069- Imaging Characteristics of Intraorbital and Circumorbital Lesion a Pictorial Review

Ayako Yoshida, Yusuke Uchiyama, Norimitsu Tanaka, Toshi Abe

EP070- Imaging Spectrums of Common Dental Disease Encountered on Facial Bone CT What the Radiologist Needs to Know

JeeYoung Kim, SooAh Im

EP071- Shear Wave Elastography for the Evaluation of Diffuse Thyroid Gland Pathology Preliminary Results

See-Sung Choi, Se-Jeong Jeon

EP072- Review of Orbital Trauma

Warinthorn Phuttharak, Patanaree Luanratanakorn, Vallop Laopaiboon

EP073- Imaging Spectrum of Orbital Pathologies at the Lacrimal Fossa

Warinthorn Phuttharak, Pattanaree Luanratanakorn, Laopaiboon Vallop

7-12 September 2014
ISTANBUL, TURKEY

LUTFI KIRDAR CONVENTION & EXHIBITION CENTER

XXth
Symposium
Neuroradiologicum



SCIENTIFIC PROGRAM

EP074- Facial Nerve Imaging and Pathology
Warinthorn Phuttharak, John Hesselink

EP075- Evaluation of Predictive Value of Diffusion Weighted MRI Parameters for Early Response to Chemotherapy of Recurrence Laryngeal Carcinoma
Jelena Mihailovic, Vesna Vukovic

Head and Neck 2

Moderator: Gabor Rudas, Hungary

SULTAN 1

EP076- A Case Report of Congenital Dacryocystocele in Neonate MRI Findings

Kenichi Suzuki, Masaaki Hori, Eiichi Kohta, Hideaki Suzuki, Masahiro Kobayashi, Junichi Kodera, Keiko Matsumoto, Sunao Mizumura, Nobuyuki Shiraga

EP077- Diffusion Tensor and Resting State Connectivity Mapping in Deep Brain Stimulation Patients at Very Low RF Power A Feasibility Study

Subhendra N Sarkar, Michael D Fox, David B Hackney, Ludy C Shih, Fernando A Barrios, Ron L Alterman, Efsthios Papavassiliou, Rafael R Rojas

EP078- Diagnosis and Treatment Outcome in Orbital Extra Ocular Muscle and Retro Bulbar Optic Nerve Cysticercosis

Raj Kumar Rauniyar, Mukesh Kumar Gupta, Kalim Ahmed, AK Pant

EP079- Histogram Analysis of Dynamic Contrast Enhanced MR Imaging for Distinguishing between Squamous Cell Carcinomas and Malignant Lymphoma of the Oropharynx

Jinna Kim, Mina Park, Yoon Seong Choi, Sung Jun Ahn, Seung-Koo Lee

EP080- Application of Dynamic Contrast Enhanced MR Imaging in Head and Neck Squamous Cell Carcinoma A Correlation study of DCE Parameters with Clinicopathologic Characteristics by Histogram Analysis

Jinna Kim, Mina Park, Seung-Koo Lee, Meng Law, Mark Shiroishi

EP081- Comparisons of Contrast Enhancement on Inner Ear among Patients with Unilateral Otologic Symptoms in 3D FLAIR MR Images at 10 minutes and 4 Hour after Gadolinium Injection

Dong Woo Park, Tae Yoon Kim, Chung Ki Park, Young Jun Lee, Ji Young Lee

EP082- CT and MR Imaging in Evaluation of Uncommon Sinonasal Malignancies

Saida Jerbi Omezzine, Radhouane Hamdi, Nouha Turki, Maher Dhifallah, Nabil Driss, Hassine Hamza

EP083- Primary Malignant Mucosal Melanoma of Nasopharynx an Unusual Cause of Unilateral Hearing Loss
Tümey Bekci, Kerim Aslan, Hediye Pınar Günbey, Lütfi İncesu

EP084- Pictorial Review of Sinonasal Malignancies

Patrick Tze Hern Teo

EP085- Solitary Fibrous Tumor of the Nasal Cavity a Case Report

Yukihiko Ogihara, Minoru Morikawa, Ninpei Yamaguchi, Haruo Takahashi, Sadanori Akita, Akiyoshi Hirano, Naoe Kinoshita, Junya Fukuoka, Masataka Uetani

EP086- CT and MR Findings of the Intraosseous Lipoma of the Sphenoid Bone

Yeliz Pekcevik, Ilker Burak Arslan, Yildiz Arslan



SCIENTIFIC PROGRAM

EP087- False Positivity of Diffusion Weighted Imaging for Revealing Squamous Cell Carcinoma of the Palatine Tonsil

Yeliz Pekcevik, Ibrahim Cukurova, İlker Burak Arslan

EP088- Two Cases of Clival Chordomas with Atypical Clinical and Radiological Presentation

Ilaria Desideri, Mario Sabato, Ilaria Pesaresi, Roberta Doria, Michele Puglioli, Raffaele Nunziata, Carlo Bartolozzi, Mirco Cosottini

EP089- Comparing Radiological Tumor Density and Volume Measurement with Pathological Tumor Stroma Proportion and Volume Measurement; and the Relationship with Prognosis in Patients with Laryngeal Carcinoma

Eren Ozer, Emel Ada, Mehtat Unlu, Hasan Oğuz Cetinayak, Sulen Sarioglu, Ahmet Omer Ikiz

EP090- DCE MRI vs DWI in Nasopharyngeal Carcinoma at 3T: Initial Report

Atilla Kokurcan, Ali Yusuf Öner, Ramazan Yildiz, Mustafa Karaca

Stroke

Moderator: **Lotfi Haccin-Bey, USA**

SULTAN 2

EP091- Perfusion CT and Early Thrombolytic Therapy Outcome Our Experiences

Stipan Jankovic, Ante Buča, Kreimir Kolić, Kreimir Dolić, Sanja Lovrić-Kojundžić

EP092- Changes in Gray and White Matter Detected on CT Cerebral Perfusion in Patients with Unilateral Cerebral Arterial Stenosis

Michael Mu Huo Teng Teng, Yi Hsuan Kao, Chung Jung Lin, Feng Chi Chang, Wan Yuo Guo

EP093- SWI and DWI Features and Follow Up Imaging Findings of A Case with Cerebral Fat Embolism

Rahsan Gocmen, Nazire Pinar Acar, Ethem Murat Arsava, Mehmet Akif Topcuoglu

EP094- The Risk of Aneurysmal Re Bleeding During CT Angiography in Patients with Acute Subarachnoid Hemorrhage

Naoki Ishige, Hirokazu Tanno, Hiroaki Ozaki, Yoshihiko Fuse, Kobayashi Masayoshi

EP095- Blood Brain Barrier Disruption and Related Brain Metabolic Changes after Ischemia Onset in Rats an in vivo CE MRI and 1H MRS study at 7.0 T

Gen Yan, Zhuozhi Dai, Kuan Geng, Yinghua Xuan, Renhua Wu

EP096- Application of Dual energy CT in The Diagnosis of Acute Ischemic Stroke

Ming-Tsung Chuang, Yi-Sheng Liu, Ching-Wen Chen, Ming-ching Ou, Hong-Ming Tsai

EP097- Clinical Outcomes of Manual Aspiration Thrombectomy for Acute Ischemic Stroke Refractory to Stent Based Thrombectomy

Woong Yoon, Seul Kee Kim, Heoung Keun Kang

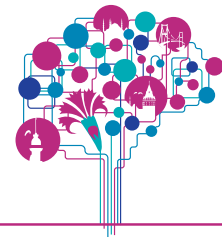
EP098- Emergent Intracranial Angioplasty with or without Stenting for Underlying Atherosclerosis in Patients with Acute Ischemic Stroke

Woong Yoon, Seul Kee Kim, Heoung Keun Kang

7-12 September 2014
ISTANBUL, TURKEY

LUTFI KIRDAR CONVENTION & EXHIBITION CENTER

XXth
Symposium
Neuroradiologicum



SCIENTIFIC PROGRAM

EP100- Is Intravenous Thrombolysis an Adequate Choice for Patients with Acute Large Arterial Infarctions with Hyperdense Artery Sign (Red Thrombus)

Kuei-Hong Kuo, Yi-Ju Pan, Yen-Jun Lai

EP101- Can It Be Detected Lipid Rich Necrotic Core in Carotid Atheroma in vivo By Using Carotid Diffusion Weighted Magnetic Resonance Imaging

Gyung Ho Chung, Hyo Sung Kwak, Seung Bae Hwang, Gong Yong Jin, Young Min Han

EP102- Improved Detection of Hyperdense MCA Sign by Sagittal Reformations ROI Analysis

Tomoya Nakatsuka, Rumiko Kasai, Shusuke Kasuya, Noriko Kitamura, Masayuki Odashima, Tsutomu Inaoka, Hitoshi Terada

EP103- Cerebral Venous Thrombosis Presenting As Bilateral Subdural Hematomas

Biljana Georgievski Brkic, Magdalena Radovic Stefanovic, Gordana Milenkovic, Tatjana Ducic Jaramaz Petar Nikic Svetlana Djokovic

EP104- The Effect of Cilostazol against the Cerebral Artery Restenosis by Percutaneous Transluminal Cranial Balloon Angioplasty (PTCBA)

Yoshinori Aoyagi, Takahisa Mori, Tomonori Iwata, Yuichi Miyazaki, Shigen Kasakura, Yuhei Tanno

EP105- Clinical Usefulness of Multishot Diffusion Weighted Sequence (RESOLVE) For the Diagnosis of Acute Infarction at the Brainstem and Posterior Fossa Comparison of Single Shot Echo Planar Diffusion Weighted Sequence

JeeYoung Kim, SooAh Im, Kook-jin Ahn, Yohan Son

EP106- Longitudinal Imaging of [C] PBR28 Uptake in Neuroinflammation Following Focal Cortical Stroke Model in SD Rat

Miklós Tóth, Philip Little, Fabian Arnberg, Jan Mulder, Halldin Christer, Balázs Gulyás, Staffan Holmin

EP107- The Usefulness of Diffusion Weighted Fluid Attenuated Inversion Recovery Imaging in the Diagnostics And Timing Of Stroke

Grzegorz Witkowski, Agnieszka Piliszek, Halina Sienkiewicz-Jarosz, Agnieszka Skierczynska, Renata Poniatowska, Malgorzata Dorobek, Anna Filipek-Glisczynska, Danuta Ryglewicz, Jerzy Walecki

EP108- Imaging the Dynamics of Glucose Metabolism in Experimental Ischemic Stroke

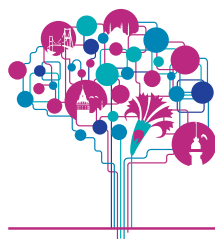
Fabian Arnberg, Jonas Grafström, Johan Lundberg, Sahar Nikkhou-Aski, Philip Little, Li Lu, Michael Söderman, Sharon Stone-Elander, Staffan Holmin

EP109- Bridging Intravenous and Intra Arterial Thrombolysis for Acute Ischemic Stroke Experience in Surabaya Indonesia

Cindy Sadikin, Hartono Yudi Sarastika, Ardhiana Kasaba, Agustinus Iskandar, Yanna Saelan

EP110- Time of Flight Brain MRA in Predicting Severe Carotid Stenosis

Hsueh Han Wang, Feng Chi Chang



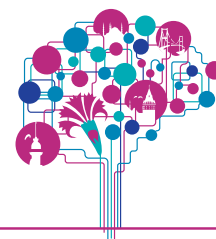
SCIENTIFIC PROGRAM

-
- Adult NR 5** **Moderator: John Hesselink, USA** **SULTAN 2**
- EP111- High Resolution MR Angiography Versus DSA in Diagnosis of Skull Base Meningiomas
Evgeny Shults, Igor Pronin, Aram Tonoyan, Ludmila Fadeeva, Valery Kornienko
- EP112- Magnetic Resonance Appearance of Brain in Snake Bite Patients Resonating The Venomous Findings
N Khandelwal, Chirag K Ahuja, Vivek Gupta, Sameer Vyas, Ajay Kumar, Ashish Bhalla
- EP113- Altered Magnetization Transfer Ratio as a marker of Subclinical Cerebral Oedema in patients of Minimal Hepatic Encephalopathy
Rahul Rai, Rk Dhiman, *N Khandelwal*, Chirag K Ahuja, Naveen Kalra, Y Chawla, Ajay Duseja
- EP114- Diffuse Leucoencephalopathy in a Patient with Rapid Cognitive Decline Consider Lymphomatosis Cerebri
Luc van den Hauwe, Gunther De Temmerman, Stephanie Smet, Stef Meers, Koen Goedseels, Christine Langenaeken, Joris Beck, Peter Bracke
- EP115- Too Late for a Pilocytic Astrocytoma
João Jacinto, Mariana Diogo, Isabel Fragata, *Carla Conceição*, Manuela Mafra, João Reis
- EP116- What You See Is Not What You Get...
João Jacinto, Mariana Diogo, Isabel Fragata, *Carla Conceição*, Manuela Mafra, João Reis
- EP117- MR Features of Infections Affecting Basal Ganglia and Thalami
Ritu Kakkar, Sameer Soneji, Shrinivas Desai
- EP118- MRI Features of Japanese Encephalitis
Ritu Kakkar, Sameer Soneji, Shrinivas Desai
- EP119- Assessment of Deep and Cortical Gray Matter Involvement via DTI and Correlation with Volumetric Analysis in MS Patients
Isa Cam, Hande Bickin, Yonca Anik, Bahattin Ozkul, Ali Demirci, Serdar Caglayangil
- EP120- The Neuroanatomic Knowledge Helping in the Differential Diagnosis of Lesions of the Brain Stem
Lázaro Luís Faria do Amaral, Ricardo Tavares Daher, Anderson Benine Belizia, Victor Hugo Rocha Marussi, Saulo Pimenta Lacerda
- EP121- Isolated Restricted Diffusion of the Splenium Associated with Anorexia Nervosa A Case Report
Yasemin Kayadibi, Amalya Zeynalova, Elmar Bayraktarov, Evrim Ozmen, Zehra Isik Hasiloglu
- EP122- The Role of Heavily T2-weighted 3D MR Myelography in the Evaluation of CSF Leakage
Chang June Song, In Ho Lee, Da Mi Kim, Si Sung Choi, In Kyu Yu
- EP123- Cerebellar Liponeurocytoma Case Report and Literature Review
Pablo Picasso de Araújo Coimbra, Bruno Braga Penha da Silva, Eduardo Sousa Frota de Almeida, Idalia Luzia Fortaleza Chaves Martins, Cleto Dantas Nogueira, Paula Galvão de Andrade, Luciana Vieira Farias, Ylana Mayra de Almeida Silveira, Diego Silva Vasconcelos Alves, Kelnner Portela Luz, Walimir Leite Pontes Filho
- EP124- Pictorial Review of the Neuroradiology of Thrombotic Thrombocytopenic Purpura
Fiona Chatterjee, Ayokunle Ogungbemi, Rolf Jager, Harpreet Hyare
- EP125- Toxoplasmic Myelitis as the Initial Presentation of Aids
Fernando Travassos, Joyce Benevides, Rosivalda Teixeira, Pedro Braga-Neto, Francisco José Mont, *Pablo Coimbra*

7-12 September 2014
ISTANBUL, TURKEY

LUTFI KIRDAR CONVENTION & EXHIBITION CENTER

XXth
Symposium
Neuroradiologicum



SCIENTIFIC PROGRAM

PEDIATRIC DIAGNOSTIC NR		Anadolu Auditorium
13:30 - 15:00	Malformations and Epilepsy	
Moderators	: Nadine Girard, France, Vasileios Papakostas, Greece	
	Pathophysiology of Epilepsy	
	<u>Renzo Guerrini</u>	
	<i>University of Florence, Children's Hospital A. Meyer, Italy</i>	
	Imaging New Onset Seizures (infection, drugs, channelopathies)	
	<u>A. James Barkovich</u>	
	<i>University of California, San Francisco, USA</i>	
	Imaging Findings in Epilepsy (Lesions Drug Effects Seizure Effects)	
	<u>Charles Raybaud</u>	
	<i>Hospital for Sick Children, Toronto-Canada</i>	
	New Concepts in Brain Malformations	
	<u>A. James Barkovich</u>	
	<i>University of California, San Francisco, USA</i>	
	O009-Pediatric Epilepsy Diagnostic yield of MRI	
	<u>Roula Hourani</u> ¹ , Adeb Oweidat ¹ , Ahmad Beydoun ² , Wassim Nasreddine ²	
	<i>American University of Beirut Diagnostic Radiology Beirut-Lebanon 1 American University of Beirut Neurology, Lebanon²</i>	
<hr/>		
SPINE & SPINE INTERVENTIONAL NR		Marmara Hall
13:30 - 15:00	Spine Tumors & Treatment	
Moderators	: Zulejha Merhemic, Bosnia Herzegovina, Athanasios Gouliamos, Greece	
	Hot and cold tumor therapies	
	<u>Afshin Gangi</u>	
	<i>Hopitaux Universitaires de Strasbourg, France</i>	
	Vertebral angiomas – when and how to treat	
	<u>Kieran Murphy</u>	
	<i>University of Toronto, Canada</i>	
	CT-Guided Autonomic Nerve Blocks	
	<u>Wendell A. Gibby</u>	
	<i>Adjunct Professor of Radiology, University of California San Diego</i>	
	<i>CEO – Novard Corporation, USA</i>	
	O010-Rare Extramedullary Intradural Tumors in Children and Adolescent	
	<u>Andja Jasovic</u> ¹ , Sharoona Dowlut ¹ , Tejas Goora ¹	
	<i>Apollo Bramwell Hospital Diagnostic Radiology Rose Hills, Mauritius¹</i>	
<hr/>		
15:00 - 15:30	COFFEE BREAK	



SCIENTIFIC PROGRAM

PEDIATRIC DIAGNOSTIC NR	Anadolu Auditorium
15:30 - 17:00	Pediatric Sedation and Trauma
Moderators	: Zoltan Patay, USA, Gaida Krumina, Latvia
	Effects of Anesthesia on Anatomic and Quantitative Pediatric Neuroimaging
	<u>Julie H. Harreld</u>
	<i>St. Jude Children Radiological Sciences Memphis, USA</i>
	Anesthesia in Pediatric Neuroimaging Imaging Effects Physiology and Alternatives
	<u>Julie H. Harreld</u>
	<i>St. Jude Children Radiological Sciences Memphis, USA</i>
	Imaging of Central Nervous System Injuries in Non Accidental Trauma
	<u>Thierry A.G.M. Huisman</u>
	<i>Johns Hopkins Hospital Pediatric Radiology Baltimore, USA</i>
	Modern Neuroimaging of Traumatic Brain Injury
	<u>Paul Parizel</u>
	<i>Antwerp University Hospital, Belgium</i>

SPINE & SPINE INTERVENTIONAL NR	Marmara Hall
15:30 - 17:00	Augmentation
Moderators	: Bassem Georgy, USA, Cem Calli, Turkey
	Review of literature and update on trials (i.e., NEJM trials vs Rest of the World)
	<u>Kieran Murphy</u>
	<i>University of Toronto, Canada</i>
	Advanced vertebral augmentation
	<u>Eren Erdem</u>
	<i>University of Arkansas for Medical Sciences, Little Rock, USA</i>
	Posterior Arch and Extravertebral Augmentation
	<u>Luigi Manfre</u>
	<i>Minimal Invasive Spine Dept – Cannizzaro Hpt – Catania, Italy</i>
	O011-Vertebral Augmentation with Titanium T6 Endoprosthesis a Preliminary Experience
	<u>Emanuele Piras</u> ¹ , Stefano Marini ¹ , Stefano Marcia ¹
	<i>ASL 8 U.O.C. Radiologia - P.O. SS. Trinità Cagliari, Italy</i> ¹

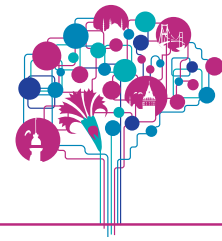
17:00 - 17:15	BREAK
----------------------	--------------

17:15 - 19:00	PARALLEL SCIENTIFIC PAPER PRESENTATIONS (Stroke 1)
Moderators:	Ahmed Elstouhy, Qatar, Hans Kristian Pedersen, Norway
	Marmara Hall
O035- Leptomeningeal Enhancement on Magnetic Resonance Imaging as a Predictor of Hemodynamic Insufficiency	
	<u>Hyung Suk Seo</u> , Doran Hong, Young Hen Lee
O036- Predicting the Reversibility of Cytotoxic Edema in PRES by Using Diffusion Kurtosis Imaging (DKI)	
	<u>Gang Guo</u> , Yonggui Yang, Fang Chen, Zhongping Zhang
O037- CT Perfusion as Imaging Predictor of Clinical Outcome in Acute Ischemic Stroke	
	<u>Biljana Georgievski-Brkic</u> , Dusko Kozic, Jelena Ostojic, Magdalena Radovic-Stefanovic, Marjana Vukicevic, Aleksandra Terzic-Beljakovic, Gordana Milenkovic

7-12 September 2014
ISTANBUL, TURKEY

LUTFI KIRDAR CONVENTION & EXHIBITION CENTER

XXth
Symposium
Neuroradiologicum



SCIENTIFIC PROGRAM

O038- Effects of Arterial Choice for the Arterial Input Function on Perfusion Parameters in Isolated Posterior Circulation

Monique Meyer, Eric Munoz, *Robert Bert*

O039- Quantitative Measurement of Regional Cerebral Blood Flow Using DSC MRI with the BookEnd Method Practical Performance in Clinical Routine

Arnold Koehl, Gert Reiter, Christian Nasel

O040- Superselective pcASL –a Novel MRI Method for Individual Characterization of Intracerebral Perfusion
V. Toth, M. Helle, C. Zimmer, H.H. Eckstein, C. Preibisch

O041- Remission of Diffusion Lesions in Acute Stroke MR Imaging. A Follow Up Study with 176 Consecutive Patients

Franz Fellner, Christine Fellner, Alexandra Barthol, Kaveh Akbari, Daniel Flöry

O042- CTP; is it Essential or Just an Additional Tool before Thrombolysis in Patients Presenting with Acute Stroke

Hussein Kamel, Mohamed Alkaphoury, Ahmed Own, Naveed Akhtar, Saadat Kamran, Ahmed El Sotouhy

O043- Ct Perfusion and Angiographic Assessment of Pial Reperfusion in Acute Ischemic Stroke the CAPRI Study

Arturo Consoli, Tommy Andersson, Luca Verganti, Stefano Vallone, Andrea Zini, Enrico Fainardi, Andrea Saletti, Alfonso Cerase, Daniele Romano, Sandra Bracco, Svetlana Lorenzano, Salvatore Mangiafico

O044- An Automated Method for Segmentation of Brain Infarcts

Guray Erus, Ann Peiffer, Lenore Launer, Sigurdur Sigurdsson, Christos Davatzikos, *Nick Bryan*, Manoj Tanwar

17:15 - 19:00 PARALLEL SCIENTIFIC PAPER PRESENTATIONS (Stroke 2)

Moderator: Norzaini Rose Mohd Zain, Malaysia, Matthew Folorunso Omojola, USA Dolmabahce C Hall

O045- Carotid Elongation Does not Affect Angiographic Results of Mechanical Thrombectomy in Acute Stroke

Umut Yilmaz, Ruben Mühl-Benninghaus, Andreas Simgen, Wolfgang Reith, Heiko Körner

O046- Carotid Stent Related Hypoperfusion Artifact in Arterial Spin Labeling Perfusion Study

Chi Jen Chen, David Yen Ting Chen, Ying Chi Tseng

O047- Intermediate Catheters Reduce the Length of Mechanical Thrombectomy Procedures in Acute Basilar Artery Occlusions

Ruben Mühl-Benninghaus, Heiko Körner, Andreas Simgen, Wolfgang Reith, Umut Yilmaz

O049- Implementation of Neurointerventional Treatment in Acute Stroke Patients with Large Vessel Occlusions in Norway

Kathinka D. Kurz, Lars Fjetland, Frode Johannessen, Martin W. Kurz

O050- Mechanical Thrombectomy in Egyptian Acute Ischemic Stroke Patients Initial Experience Using Catch + Device
Ossama Mansour, Tamer Ibrahim



SCIENTIFIC PROGRAM

O051- Evaluation of Clot Burden Score in Acute Ischemic Stroke Patients Treated With Thrombolysis
Ahmad Sobri Muda, Hilwati Hashim, Shahizon Azura Mukari, Mohd Redzuan Ismail, Sarah Yaziz, Syazarina S Osman

O052- Craniectomy Reduced Mortality and Improved GOS among Large MCA Infarction Patients with Middle Line Shifting More than 0 mm.

Yueh-Hsun Lu, Michael MH Teng, Chan-Ming Yang, Feng-Chi Chang, Wang-Yuo Guo

O053- Medullary Arteries of the Cerebrum the Basis for a New Classification of Ischemia Infarction
Shoki Takahashi, Shunji Mugikura, Toshiaki Akashi, Takaki Murata, Yumiko Kato, Yasuko Tatewaki

O054- Role of CT Scans in Predicting Malignant Course of Middle Cerebral Artery Stroke

Saadat Kamran, Naveed Akhtar, Hussain Kamel, Ahmed El Sotouhy, Ahmed Own, Sohail Al Rukun, Ashfaq Shuaib

17:15 - 19:00 PARALLEL SCIENTIFIC PAPER PRESENTATIONS (Head and Neck 1)

Moderators: Luc van den Hauwe, Belgium, Yulia Mironova, Ukraine

Topkapı A Hall

O055- Imaging and Disease Spectrum in Ocular and Orbital Lesions in Eastern Nepal

Raj Kumar Rauniyar, Mukesh Kumar Gupta, Kalim Ahmed, Ashok Pant

O056- ECG Gated CT Angiography of Intracranial Aneurysms (broken and not) Using 320 Row Detector CT Scanner Identification of Higher Risk Aneurysms and Rupture Site before Surgery

Federico D Orazio, Aldo Victor Giordano, Sergio Carducci, Alessandra Splendiani, Massimo Gallucci

O057- Prevalence and Risk of Malignancy in Incidental Thyroid Nodules on Low Dose Screening Chest CT A Retrospective Study

Hyobin Seo, Ji-Hoon Kim, Kwang Nam Jin, Ji Sang Park, Koungh Mi Kang, Eun Kyung Lee

O058- Ultrasound Based Risk Stratification for Malignancy in Thyroid Nodules Four tiered Categorization System

Hyobin Seo, Dong Gyu Na, Ji Hoon Kim, Ji Won Yoon, Kyung Won Kim

O059- Dynamic Contrast Enhanced MR Imaging of Neck Lymph Nodes Predicts Neck Control in Oropharyngeal or Hypopharyngeal Squamous Cell Carcinoma Treated with Chemoradiotherapy

Shu Hang Ng, Ho Fai Wong, Yao Liang Chen, Jiun Jie Wang, Chi Wah Yeh

O060- Optimization of Double Inversion Recovery Contrast for Squamous Cell Carcinoma of the Neck

Mariah H. Bashir, Kwan Jin Jung, Robert J. Bert

O061- Feasibility of Cone Beam Computed Tomography Dacryocystography by Direct Catheterisation of the Lacrimal Drainage System

Chiara Mabilia, Zsuzsanna Valyi, Luisa Divano

O062- MR Imaging Features of Pharyngeal Tuberculosis a hint of Discrimination from Pharyngeal Malignancy

Aleum Lee

O063- Loss of Reflex Tearing after Maxillary Orthognathic Surgery

Aleum Lee

O064- Skull Base Re Ossification after Endovascular Treatment of Intracranial Vascular Lesions

Amel Azizi, Elisa Pomero, Katia Gete, Michel Runge, Alessandra Biondi

7-12 September 2014
ISTANBUL, TURKEY

LUTFI KIRDAR CONVENTION & EXHIBITION CENTER

XXth
Symposium
Neuroradiologicum



SCIENTIFIC PROGRAM

O065- Diffusivity of Extraocular Muscles in Patients with Thyroid Associated Ophthalmopathy Comparison with Conventional MRI

Akio Hiwatashi, Osamu Togao, Koji Yamashita, Kazufumi Kikuchi, Hiroshi Honda

17:15 - 19:00 PARALLEL SCIENTIFIC PAPER PRESENTATIONS (Head and Neck 2)

Moderators: Raj Kumar Rauniyar, Nepal, Pedro Vilela, Portugal **Topkapı B Hall**

O066- Differential Diagnosis of Inflammatory Pseudotumor and Carcinoma of the Nasopharynx Value of Conventional T2 Weighted Image based on the Lesion Conspicuity

Hye Na Jung, Hyung-Jin Kim, Yi-Kyung Kim, Mina Song, Jihoon Cha, Sung Tae Kim

O067- Head and Neck Paragangliomas and the Jugular Vein

Emanuele Orru, Merve Gursoy, Philippe Gailloud, Ari M Blitz, John P Carey, Alessandro Olivi, David M Yousem

O068- The Role of Diffusion Weighted Magnetic Resonance Imaging in Differentiation of Parotid Gland Masses With Histopathological Correlation

Yasemin Karaman, Anil Ozgur, Demir Apaydin, Cengiz Ozcan, Rabia Arpacı, Meltem Nass Duce

O069- Hypoglossal Canal Invasion by Glomus Jugulare Tumors Clinico Radiological Correlation

Merve Gursoy, Emanuele Orru, Ari M. Blitz, John P. Carey, Alessandro Olivi, David M. Yousem

O070- Diffusion Weighted MR Imaging in Lymph Node Metastases of Squamous Cell Carcinoma

Yeliz Pekcevik, Ibrahim Cukurova, Ilker Burak Arslan

O071- Anaplastic Thyroid Carcinoma What Radiologists Need to Know in an Unfamiliar Entity in Lethal Neoplasm

Aleum Lee

O072- An Exploratory Pilot Study into the Correlation of MRI Perfusion Diffusion Parameters and 18F FDG PET Metabolic Parameters in Primary Head and Neck Cancer

Jin Wook Choi, Miran Han, Sun Yong Kim

O073- Oropharyngeal Squamous Cell Carcinomas; Can Imaging Findings Predict HPV Status

Sandeep Bhuta, Louise Van Camp, Tim Ireland

O074- Hypopharyngeal Cancer Preoperative Imaging and Pathological Staging Correlation.

Yueh-hsun Lu, Jiing-Feng Lirng, Chan-Ming Yang, Feng-Chi Chang, Wang-Yuo Guo

O075- Cine CT Guided Biopsy of Clival Uncommon Tumors

Hector Lambre, Rosana Salvatico, Pedro Lylyk

O076- Differentiation of Inflammatory Pseudotumor from Lymphoma in the Head and Neck the Usefulness of Dynamic Contrast Enhanced and Diffusion Weighted MR Imaging

Yi-Kyung Kim, Hyung-Jin Kim, Jihoon Cha, Ji Young Lee, Mina Song, Sung Tae Kim

O077- The Pattern of Enhancement of Basal Cell Adenoma and Myoepithelioma of the Parotid Gland at Two Phase CT Comparison with Warthin Tumor

Yi-Kyung Kim, Hyung-Jin Kim, Ji Young Lee, Jihoon Cha, Sung Tae Kim, Mina Song



SCIENTIFIC PROGRAM

17:15 - 19:00 PARALLEL SCIENTIFIC PAPER PRESENTATIONS (Pediatric NR)

Moderators: **Aylin Tekes, USA, Roula Hourany, Lebanon**

Halic Hall

O078- Utility of 1H MRS in the Diagnosis and Disease Monitoring for Pediatric CNS Disorders

Noriko Aida, Moyoko Tomiyasu, Kumiko Nozawa, Yuta Fujii, Mikako Enokizono, Takayuki Obata, Sumimasa Yamashita

O079- Frontomethaphyseal Dysplasia Radiology Findings and DDX

Yunus Afandiyev

O080- Diffusion Tensor Imaging Based Assessment of White Matter Tracts in Very Preterm Neonates

Julia Pavaine, Julia Young, Benjamin Morgan, Charles Raybaud, Manohar Shroff, Margot Taylor

O081- Ischemia a Potential Cause for Pineal Cyst Development

Evrin Ozmen, Yasemin Kayadibi, Betul Derinkuyu, Cesur Samanci, Havva Akmaz Unlu, Tulin Hakan Demirkan, Zehra Isil Hasiloglu, Ibrahim Adaletli, Sebu Kurugoglu

O082- The Value of Prenatal Brain MRI in the Management of Congenital Cytomegalovirus Infection

Amelia Fernández-Zubillaga, Aranzazu Royo, Cristina Utrilla, María de la Calle, Roberto Rodríguez, Gonzalo Garzón

O083- Echo Planar Diffusion Weighted MRI and High Resolution CT in the Study of Pediatric Cholesteatoma. A Comparative Study

Angel Sanchez-Montanez, Juan Pablo Salazar, Felix Pumarola, Ignacio Delgado, Elida Vazquez

O084- Radiological and Clinical Manifestations of Megalencephaly Capillary Malformation (MCM) Syndrome

Angel Sanchez-Montanez, Ignacio Delgado, Susana Boronat, Paola Cano, Elida Vazquez

O085- Pictorial Review of Suprasellar Tumors the Importance of the Signal Intensity of the Neurohypophysis on T1 to Narrow the Differential Diagnosis

M. De Fatima Vasco Aragao, Lucas Vasco Aragao, Marcelo Moraes Valenca, Maria Lucia Lima Soares

O086- Lymphocytic Hypophysitis in Children How the Magnetic Resonance Imaging may Support the Diagnosis

Chiara Carducci, Paola Cambiaso, Lorenzo Figà Talamanca, Stefania Galassi, Bruno Bernardi

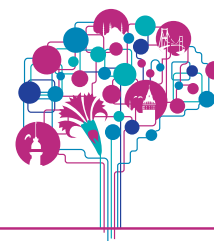
17:15 - 19:00 ESNR Honorary Membership & Diploma Ceremony

Anadolu Auditorium

7-12 September 2014
ISTANBUL, TURKEY

LUTFI KIRDAR CONVENTION & EXHIBITION CENTER

XXth
Symposium
Neuroradiologicum



SCIENTIFIC PROGRAM

Wednesday, September 10, 2014

PEDIATRIC DIAGNOSTIC NR

Anadolu Auditorium

08:30 - 10:30 **New Concepts of Pediatric Brain Tumors**

Moderators : Bozena Goraj, The Netherlands, Noriko Aida, Japan

New concepts of tumorigenesis in children

Vijay Ramaswamy

Hospital for Sick Children, Canada

New concept 2: Medulloblastoma revisited

Zoltan Patay

St. Jude Children's Research Hospital, Memphis, USA

Clinical Evaluation and Staging of Paediatric Brain Tumours

Monika Warmuth-Metz

University Hospital Würzburg Neuroradiology, Würzburg, Germany

Side effects of Pediatric Brain Tumor Therapy

Zoltan Patay

St. Jude Children's Research Hospital, Memphis, USA

O012-Reorganization of the Visual Pathways after Early Age Tumor Removal Assessed By Functional Magnetic Resonance Imaging and Fiber Tractography

G. Aghakhanyan¹, F. Tinelli², K. Mikellidou³, F. Frijia⁴, R. Arrighi⁵, V. Greco⁶, R. Canapicchi⁴, M.C. Morrone³, D. Montanaro⁴

*Scuola Superiore Sant Anna, Institute of Life Sciences, Pisa, Italy*¹ *Stella Maris Scientific Institute, Pisa, Italy*² *University of Pisa, Department of Translational Research on New Technologies in Medicine and Surgery, Pisa, Italy*³ *Fondazione CNR/Regione Toscana G. Monasterio, U.O.s Neuroradiologia, Pisa -Italy*⁴ *University of Florence, Department of Neuroscience, Psychology, Pharmacology and Child Health, Florence, Italy*⁵ *CNR-Instituto Nazionale di Ottica, Florence, Italy*⁶

SPINE & SPINE INTERVENTIONAL NR

Marmara Hall

08:30 - 10:30 **Basic Biomechanics and Spine Trauma**

Moderators : Dorith Goldsher, Israel, Milos Lucic, Serbia

Lumbar Sacral Pelvic Biomechanics and Sagittal Balance

Massimo Gallucci

University of L'Aquila DISCAB L'Aquila, Italy

Dynamic evaluation of spine instability

Murat Hanci

Istanbul University, Turkey

Spinal cord injury

Gordon Sze

Yale University School of Medicine, USA

Spinal trauma

Paul Parizel

Antwerp University Hospital, Belgium



SCIENTIFIC PROGRAM

O013-Vertebral Body Stenting and Cement Augmentation to Restore Structural Stability in Extreme Spinal Osteolysis

*Alessandro Cianfoni*¹, Eytan Raz¹, Daniele Romano¹, Michael Reinert², Gianfranco Pesce³, Giuseppe Bonaldi⁴

*Neurocenter of Southern Switzerland Neuroradiology Lugano, Switzerland*¹ *Neurocenter of Southern Switzerland Neurosurgery, Switzerland*² *IOSI Radiation Oncology, Switzerland*³ *Osp. Giovanni XXIII, Bergamo Neuroradiology, Italy*⁴

10:30 - 11:30 COFFEE BREAK

10.30-11.30 Poster Presentations

Vascular Interventional NR 1

Moderator: Elisa Ciceri, Italy

SULTAN 1

EP126- Endovascular Treatment of Carotid Stenosis an Experience in the Single Center Trial

Daehyun Hwang, Wooyoung You

EP127- Quantitative Cerebral Angiography Evaluate Cerebral Venous Circulation with Aneurysmal Rupture

Kwo-Whei Lee, Fong Y Tsai, Wei-Liang Chen, Chi-Kuang Liu, Chen-Ling Kuo

EP128- Results of Endovascular Treatment for Unruptured Intracranial Aneurysms (UIA) Single Center Experience

Svetlana Milosevic Medenica

EP129- Covered Stent Placement for Emergency Reconstruction of Ruptured Carotid Artery during or after Transsphenoidal Surgery

Byung Moon Kim, Pyoung Jeon, Dong Joon Kim, Dong Ik Kim

EP130- Retrieval of Dislodged Coil with Stent Retriever

Mustafa Gok, Celal Cinar, Halil Bozkaya, Ismail Oran

EP131- Onyx in Brain Arteriovenous Malformation Embolisation: Experience in a Malaysian Tertiary Referral Center

Hilwati Hashim, A. Sobri Muda, Aida Abdul Aziz, Zuhanis Abdul Hamid

EP132- Evaluation of Contrast Enhanced MR Angiography and Time OF Flight MR Angiography at 3Tesla in Previously Coiled Intracranial Aneurysms

Anshu Mahajan, *N Khandelwal*, Vivek Gupta, Ajay Kumar, SK Gupta

EP133- Endovascular Treatment of 88 Anterior Communicating Artery Aneurysms. Overall Perioperative Results

Yon Kwon Ihn, Won Sang Jung, Yoon Joon Hwang

EP134- Shunted Pouches of Cavernous Sinus Dural AVFs Evaluation by 3DRotational Angiography

Hiro Kiyosue, Shuichi Tanoue, Ryuichi Shimada, Hiromu Mori

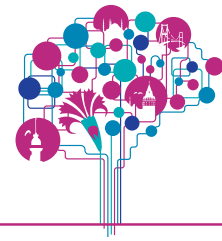
EP135- Clinical Results of Carotid Artery Revascularization as Carotid Artery Stenting for First Line Treatment Single Center Experience in Japan

Ichiro Nakahara, Haruka Miyata, Tsuyoshi Ohta, Shoji Matsumoto, Ryota Ishibashi, Masanori Gomi, Masato Saka, Takuya Okada, Hidehisa Nishi, Kazutaka Sonoda, Junpei Koge, Sadayoshi Watanabe, Izumi Nagata

7-12 September 2014
ISTANBUL, TURKEY

LUTFI KIRDAR CONVENTION & EXHIBITION CENTER

XXth
Symposium
Neuroradiologicum



SCIENTIFIC PROGRAM

EP136- Endovascular Treatment of Vertebro Vertebral Fistula (VVF) in A Patient with Neurofibromatosis Type 1 (NF1) Present with Right Sided Neck Mass and Pulsatile Tinnitus A Case Experience in Ramathibodi Hospital
Pakorn Jiarakongmun, Ekkachat Chanthanaphak, Thanaboon Worakijthamrongchai, Sirintara Pongpech

EP137- Acute Tonsillar Herniation in Malignant Cranial Dural Arteriovenous Fistula Rapid Recovery Following Transvenous Fiber Coil Embolization A Case Report
Ekachat Chanthanaphak, Pakorn Jiarakongmun, Thanaboon Worakijthamrongchai, Sirintara Pongpech

EP138- Treatment of Bizzare Shaped Wide Necked MCA Aneurysms with Penumbra Coils 400 without Supporting Devices Report of 4 Cases and Review of Literature
Svetlana Milosevic Medenica

Vascular Interventional NR 2 Moderator: Mark Khangure, Australia SULTAN 1

EP139- Endovascular Treatment of Travamtic Vertebral Artery Arteriovenous Fistula and Pseudoaneurysm
Isa Cam, Ercüment Ciftci, Sevtap Gumustas, Halil Ibrahim Ada, Ahmet Yalniz, Bayram Yildirim, Tugce Agirlar

EP141- Coil Embolization of Cavernous Sinus Dural Arteriovenous Fistula via Direct Puncture of Superior Ophthalmic Vein after Surgical Exposure of the Vein
Kostas Lagios, Ioannis Ntountas, Theodoros Bazinas, Michalis Mantatzis

EP142- Endovascular Treatment of Giant Extracranial Vertebral Aneurysms With Neurofibromatosis Type 1 A Report of 3 Cases
Pao-Sheng Yen, Chun-Han Liao

EP143- Intracranial Aneurysms Treated by Flow – Diverting Stents Results of Long – Term Follow – up with Contrast – Enhanced MR – Angiography
Maximilian Patzig, Lorenz Ertl, Robert Forbrig, Hartmut Brückmann, Gunther Fesl

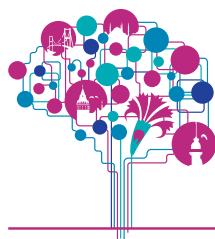
EP144- Contrast Enhanced Angiographic Cone Beam CT (CBCT) Practical Usage in Neurointervention Cases
Ahmad Sobri Muda, Nik Azuan Nik Ismail, Zahiah Mohamed, Mohd Redzuan Ismail, Rozman Zakaria, Yazmin Yaacob, Ainul Syahrilfazli Jaafar

EP145- Subacute Recanalization of Parent Artery after Internal Trapping of Ruptured Dissecting Aneurysms Does Not Lead to rebleeding a Report of 3 Cases
Yasuhiro Takeichi

EP146- Mechanical Coil Insertion System
Noriaki Matsubara, Shigeru Miyachi, Kenichi Haraguchi, Yoshitaka Nagano, Hiroyuki Yamada, N Marui, Akihito Sano, Hideo Fujimoto, Takashi Izumi, Toshihiko Wakabayashi

EP147- Morbidity Associated with Endovascular Treatment of Complex Intracranial Aneurysms with Self Expanding Stents vs Flow Diverters
Bernardo Lander, García María Berenice, Alonso Arturo, Alvarado Mariangela, López Stefania, Viso René

EP148- Transverse –Sigmoid Sinus Dural Arteriovenous Fistula Presenting With Recurrent Transient Ischaemic Attack a Technical Case Report
Marlina Ramli, Khairul Azmi Abdul Kadir, Hilwati Hashim



SCIENTIFIC PROGRAM

EP149- The Rate of Restenosis in Carotid Artery Stents and Late Follow up Results
Rahime Sezer, Ahmet Peker, Emrah Çağlar, Elif Peker, Umman Sanlıdilek

EP150- Efficacy and Limitations of Transarterial Acrylic Glue Embolization for Intracranial Dural Arteriovenous Fistulas
Naoko Miyamoto, Isao Naito

EP151-Transvenous Embolization of Cavernous Sinus Dural Arteriovenous Fistula via Angiographic Occlusive Inferior Petrous Sinus
Chao-Bao Luo, Michael MH Teng, Feng-Chi Chang, Wan-Yuo Guo, Chung-Jung Lin

Adult NR 6

Moderator: Sossio Cirillo, Italy

SULTAN 2

EP152- Visual Deficits and Pituitary Adenomas, the Myth of Bitemporal Hemianopia
In Ho Lee, Fabiana Tavares, Elcin Zan, Ari Blitz, Neil Miller, Michael Boland, David Yousem

EP153- Importance Neuroimaging and Clinical Neurophysiological Methods in Diagnosis and Treatment Vestibulocochlear Syndrome
N.S. Alekseeva, M.V. Krotenkova, A.A. Baev, J.V. Bukovskaya, T.A. Popova, V.V. Gnezditsky, M.S. Semenov, O.V. Korepina

EP154- CT Angiography after Carotid Artery Stenting Assessment of the Utility of Adaptive Statistical Iterative Reconstruction and Model Based Iterative Reconstruction
Keita Kuya, Yuki Shinohara, Makoto Sakamoto, Shinya Fujii, Toshio Kaminou, Takashi Watanabe, Toshihide Ogawa

EP155-Correlation of Volume Transfer Coefficient K Trans and R CBV with High and Low Grade Gliomas
Laura Barletta, Maurizio Bergamino, Luca Roccatagliata, Lucio Castellan

EP156-The Role Of Diffusion And Perfusion Weighted Magnetic Resonance Imaging In Distinguishing Glioblastoma on The Background Of Multiple Sclerosis Lesions Case Report
Radoslav Georgiev, Boyan Balev, Marianna Novakova, Deyan Dzhenkov, Deyan Handzhiev

EP157- MRI Findings in the Diagnosis of Central Nervous System Vasculitis
Saida Jerbi Omezzine, Radhouane Hamdi, Samia Younes, Kalthoum Tlili Graeiss, Hassine Hamza

EP158-Extensive Brain Lesions Cystic Necrotic Areas and Poor Outcome in Neuromyelitis Optica
Gunes Orman, Scott Newsome, Yeliz Pekcevik, In Ho Lee, Maureen Mealy, Michael Levy, Izlem Izbudak

EP159- Bilateral Hypoplasia of the Internal Carotid Artery a Case Report
Kaan Esen, Anil Ozgur, Hakan Kalegasi, Engin Kara, Arda Yilmaz

WITHDRAWN

EP161- Multimodal Imaging in Primary Central Nervous System Lymphomas with Typical and Atypical MR Imaging Features
Youngjin Heo, Sang Joon Kim, Ho Sung Kim, Choong Gon Choi, Seung Chai Jung



SCIENTIFIC PROGRAM

WITHDRAWN

EP163- MRI Aspects in Hyperacute Ischemic Stroke Series of Cases of Peculiar Diffusion Weighted Images (DWI) and Apparent Diffusion Coefficient (ADC) Evolution

Tatiana Goyanna Lyra, Daniel de Souza Delgado, Luis Filipe de Sousa Godoy, Marcos Fernando de Lima Docema, Maria da Graca Martin

EP164- Diabetic Striatopathy in a Patient with Hemiballismus

Anil Ozgür, Kaan Esen, Hakan Kalegasi, Arda Yilmaz, Engin Kara

EP165- Intravoxel Incoherent Motion MR Imaging Principles and Clinical Applications

Hee Mang Yoon, Chong Hyun Suh, Jin Seong Lee, Young Ah Cho, Ah Young Jung, Chong Hyun Yoon

EP166- Evaluation of the Posterior Cingulate Region with FDG PET and Advanced MR Techniques in Patients with Amnesic MCI, Comparison of the Methods

Anna Zimny, Joanna Bladowska, Adam Macioszek, Elzbieta Trypka, Renata Wojtynska, Jerzy Leszek, Marek Sasiadek

Adult Nr 7

Moderator: Kazuhiro Katada, Japan

SULTAN 2

EP167- Sellar Chondrosarcoma without Bone Involvement a Case Report

Roberto Marileo, Ingeborg Lopez, Rodrigo Riveros, Cecilia Okuma, Aaron Vidal, Rodrigo Rivera, J.Gabriel Sordo, Lautaro Badilla

EP168-18FDG PET MR Coregistration as a Method for Localization of Epileptogenic Zone in Drug resistant Epilepsy

Dora Zlatareva, Krassimir Minkin, Irena Kostadinova, Petya Dimova, Marin Penkov

EP169- Neurocysticercosis an Important Differential Diagnosis

Pablo Picasso de Araújo Coimbra, Rafael Costa Lima Maia, Tiago Silva Holanda Ferreira, Daniel Gurgel Fernandes Tavora, Eliseu Becco Neto, Jackson Augusto Gondim Oliveira, Stelio da Conceição Araújo Filho, Francisco Ramos Júnior, Edson Lopes Júnior

EP170- Giant Aneurysm of Middle Cerebral Artery with the Size of 6 X 7 cm

Pablo Picasso de Araújo Coimbra, Rafael Costa Lima Maia, Tiago Silva Holanda Ferreira, Daniel Gurgel Fernandes Tavora, Eliseu Becco Neto, Francisco Ramos Júnior, Stelio da Conceição Araújo Filho, Edson Lopes Júnior

EP171- Usefulness of MR Spectroscopy with an Elevated Peak at 3.56 PPM in Differentiation between Hemangiopericytoma Solitary Fibrous Tumor and Meningioma

Minoru Morikawa, Reiko Ideguchi, Hideki Ishimaru, Yukihiro Ogihara, Takayuki Matsuo, Kensaku Kamata, Naoe Kinoshita, Mikako Enokizono, Masataka Uetani

EP172- Late CO Poisoning

Annapaola Bocchio, Davide Machado, Alessandra Pozzato, Teodoro Meloni, Enrico Visetti

EP173- A Case of Cerebellar Glioblastoma in A Young Adult

Annapaola Bocchio, Davide Machado, Anna Rosano, Francesca Nebiolo, Teodoro Meloni



SCIENTIFIC PROGRAM

WITHDRAWN

EP175- Role of MRI in Diagnostic Long Standing Overt Ventriculomegaly as a Cause Of Secundar Amenorrhoea
Vesna Vukovic, Jelena Mihailovic

EP176- Intraventricular Tumors Typical Imaging Findings on CT and MRI
Kevin Van Looveren, Luc van den Hauwe, Maxim R. Parizel, Thomas Van Thielen, Frank De Belder, Caroline Venstermans, Johan W. Van Goethem, Martin Lammens, Paul M. Parizel

EP177- Neuroimaging of Intracranial Extra Axial Non Meningiomatic Tumors Multimodal MRI Findings
Ben Abdallah Amel, Mama Nadia, Berrich Amira, Arifa Nadia, Iyadh Ksira, Yacoubi, Mohamed Taher, Tlili Kalthoum

EP178- MR Findings of Limbic Encephalitis Herpes Simplex Virus versus Autoimmune Encephalitis
Li Li, Shunji Mugikura, Takaki Murata, Yumiko Kato, Yasuko Tatewaki, Daddy Mata Mbemba, Keiichi Jingu, Shoki Takahashi

EP179- Diffusion Weighted Imaging with a b=3000 Improves the Detection of the Lesion Edge and Core in Progressive Multifocal Leucoencephalopathy (PML)
Claudia Godi, Enrico De Vita, Lewis Haddow, Indran Davagnanam, Hans Rolf Jäger

EP180- Contrast Perfusion Weighted MR Imaging OF Intracranial Tumors
Kamel Walha, Amir Abdallah, Aymen Arous, Leila Mchirgui, Cyrine Drissi, Rym Sebai, Nadia Hammami, Sonia Nagi, Hafedh Jemel, Mohamed Ben Hamouda

EP181- Trigeminal Neuralgia Associated with Persistente Primitive Trigeminal Artery Report of 3 Cases
Marcelo Moraes Valenca, M. de Fatima Vasco Aragao, Maria Lucia Lima Soares

PEDIATRIC DIAGNOSTIC NR

Anadolu Auditorium

11:00 - 12:30 **Scoliosis / Pediatric Back Pain**
Moderators : Alikhan Alikhanov, Russia, Abdulhakim Coskun, Turkey
Types and Causes Back Pain in Children
Andrea Rossi
G. Gaslini Children's Hospital, Italy

Imaging of the Child with Acute Back Pain
Thierry A.G.M. Huisman
Johns Hopkins Pediatric Radiology Baltimore, USA

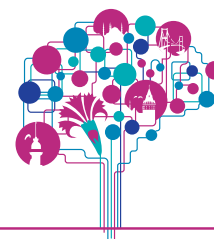
Imaging the scoliotic spine with MRI
Andrea Rossi
G. Gaslini Children's Hospital, Italy

O014-Pediatric Spinal Cord Diffusion Changes in Craniocervical Junction Malformations
Gunes Orman¹, Ximin Li², Carol B. Thompson², Thierry A. G. M. Huisman¹, Izlem Izbudak¹
*Johns Hopkins School of Medicine Radiology/Pediatric Neuroradiology Baltimore-United States*¹
*Hopkins Bloomberg School of Public Health Biostatistics*²

7-12 September 2014
ISTANBUL, TURKEY

LUTFI KIRDAR CONVENTION & EXHIBITION CENTER

XXth
Symposium
Neuroradiologicum



SCIENTIFIC PROGRAM

SPINE & SPINE INTERVENTIONAL NR

Marmara Hall

11:00 - 12:30 **Minimally Invasive Intervention and Innovation**

Moderators : Bassem Georgy, USA, Kazuhiro Tsuchiya, Japan

New Trends in Percutaneous Rigid Spine Fixation

Luigi Manfre

Minimal Invasive Spine Dept. Cannizzaro Hpt. Catania, Italy

Percutaneous dynamic spine fixation and interspinous spacers

Giuseppe Bonaldi

Osp. Giovanni XXIII, Bergamo Neuroradiology, Italy

Role of Radiologists in Neuromodulation procedures (spinal cord stimulations)

Gregory J. Lawler

Neuroimaging and Interventional Spine Services, Ridgefield, USA

O015-Transoral Route for the Percutaneous Vertebroplasty of C1 Lesions

Frédéric Clarençon¹, Evelyne Cormier¹, Raphaël Bonaccorsi², Hugues Pascal-Mousselard²,

Jacques Chiras¹

*Pitié-Salpêtrière Hospital Interventional Neuroradiology France¹ Pitié-Salpêtrière Hospital
Orthopedic Surgery, France²*

12:30 - 13:30 **LUNCH BREAK**

13:30 - 14:30 **ESNR & Symposium Awards Ceremony**

Anadolu Auditorium

PEDIATRIC DIAGNOSTIC NR

Topkapı AB Hall

13:30 - 15:00 **Vascular Disease in Children**

Moderators : Giulio Zuccoli, USA, Francisca T. Wiggers-DeBruine, The Netherlands

Imaging Strategies in Arterial and Venous Pediatric Stroke Conventional and Advanced

Kling Chong

Great Ormond Street Hospital for Children Radiology London, UK

Vascular malformation syndromes

Timo Krings

Toronto Western Hospital, Canada

Intracranial Sinovenous Thrombosis in Childhood Thrombosis and Beyond

Kling Chong

Great Ormond Street Hospital for Children Radiology London, UK

O016-Diagnostic Imaging Evaluation of Ischaemic Stroke in Children Twelve Years Experience

Eva Kovacs¹, Peter Barsi², Gyorgy Balazs³, Gyorgy Varallyay², Gabor Rudas², Zoltan

Harkanyi¹, Judit Moser⁴, Beata Rosdy⁴, Katalin Kollar⁴

Heim Pal Childrens' Hospital Radiology Budapest-Hungary¹ Semmelweis University MR

Research Center -Hungary² Semmelweis University Department of Cardiovascular Surgery

-Hungary³ Heim Pal Childrens' Hospital Neurology -Hungary⁴



SCIENTIFIC PROGRAM

SPINE & SPINE INTERVENTIONAL NR

Marmara Hall

13:30 - 15:00 **Infectious, Inflammatory, Degenerative Diseases of the Spine**

Moderators : Igor Pronin, Russia, Jamal Al Den Al Kotes, Abu Dhabi

Inflammatory Arthritis and Degenerative Disease

Johan Van Goethem

University Hospital Antwerp Radiology Edegem, Belgium

Update on spinal infections and mimics

Gordon Sze

Yale University School of Medicine, USA

Role of biopsies

Orlando Ortiz

Winthrop-University Hospital, USA

O017-Imaging Features of Spinal Fractures in Ankylosing Spondylitis

Ivana Zupetic 1, Vera Ersek-Rakic 2, Dina Miklic 1, Martina Salaj 1, Ljubica Luetic-Cavor 1, Petra Margetic 1

Clinical Hospital Center "Sestre milosrdnice" Diagnostic Radiology Department Clinic for Traumatology Zagreb Zagreb-Croatia 1 Clinical Hospital Center "Sestre milosrdnice" Diagnostic Radiology Department, University Clinic for Traumatology Zagreb 2

COFFEE BREAK 15:00 - 15:30

PEDIATRIC DIAGNOSTIC NR

Topkapı AB Hall

15:30 - 17:00 **Pediatric CNS infections**

Moderators : Katiuzaka Casares, Mexico, Pablo Araujo-Coimbra, Brazil

CNS Infection: TB and HIV

Savvas Andronikou

Department of Radiology, Faculty of Health Sciences, University of Cape Town, South Africa

Neuroimaging in Viral and Autoimmune Childhood Encephalitis

Philippe Demaerel

University Hospital KU Leuven Radiology Leuven, Belgium

Childhood Cysticercosis and other Parasitic Disorders of the Pediatric CNS

Leandro Tavares Lucato

Hospital das Clínicas, Faculdade de Medicina, Universidade de São Paulo Radiology São Paulo-Brazil

O018-Infectious and Post Infectious Meningo Encephalitis Pictorial Review

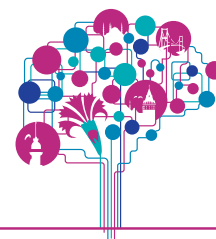
*Mouna Laadhari 1, Nadia Mama ¹, Amira Berriche ¹, Nadia Arifa ¹, Houda Ajmi ², Samia Tilouch ³, *Kalthoum Tlili 1**

Sahloul University Hospital Radiology Department -Tunisia 1 Sahloul University Hospital Paediatric Department -Tunisia ² Farhat hached University Hospital Paediatric Department -Tunisia ³

7-12 September 2014
ISTANBUL, TURKEY

LUTFI KIRDAR CONVENTION & EXHIBITION CENTER

XXth
Symposium
Neuroradiologicum



SCIENTIFIC PROGRAM

SPINE & SPINE INTERVENTIONAL NR

Marmara Hall

15:30 - 17:00

Pain Management Interventions

Moderators : Dora Zlatareva, Bulgaria, Jacques Chiras, France

Injections and complications.

Eren Erdem

University of Arkansas for Medical Sciences, Little Rock, USA

RF Treatments in Spine

Stefano Marcia

Ss Trinita Radiology Cagliari, Italy

Sacro-iliac joint treatments (including radiofrequency neurolysis)

Orlando Ortiz

Winthrop-University Hospital, USA

O019-CT Guided Infiltrative Therapies of the Sacro Iliac Joints Long Term Evaluation of Efficacy on Wide Population

*Federico D Orazio*¹, Lorenzo Gregori¹, Aldo Victor Giordano², Sergio Carducci²,

Alessandra Splendiani³, Massimo Gallucci³

*Ospedale San Salvatore L'Aquila, U.O. Neuroradiologia e Radiologia Interventistica Scuola di Specializzazione in Radiodiagnostica, Università degli Studi di L'Aquila L'Aquila, Italy*¹ *Ospedale San Salvatore L'Aquila, U.O. Neuroradiologia e Radiologia Interventistica U.O. Neuroradiologia e Radiologia Interventistica, Italy*² *Università degli Studi di L'Aquila, U.O. Neuroradiologia e Radiologia Interventistica Dipartimento Scienze Cliniche Applicate e Biotecnologie, Italy*³

15:30 - 17:00

NEURORADIOLOGY

Dolmabahce C Hall

Moderators : Olof Flodmark, Sweden, Michael Sage, Australia

Past, Today & Future of Neuroradiology

Marco Leonardi

Bologna University, IRCCS Neuological Research Hospital, Italy

17:00 - 17:15 BREAK

17:15 - 19:00 PARALLEL SCIENTIFIC PAPER PRESENTATIONS (Spine)

Moderators: Mohamed Ben Hamouda, Tunisia, Kavous Firuzna, Iran Marmara Hall

O087- Intracardiac Cement Migration after Percutaneous Vertebroplasty Incidence and Risk Factors
Sarah Fadili, Frédéric Clarencon, Evelyne Cormier, Lise Le Jean, *Jacques Chiras*

O088- Spinal Extradural Arteriovenous Fistulas

Hui-Ling Hsu, David Yen-Ting Chen, Ying-Chi Tseng, Chi-Jen Chen

O089- Lumbar Spinal Cord fMRI During Electrical Stimulation of Anterolateral Leg

Yanlong Jia, Zhiwei Shen, Tingting Nie, Tao Zhang, *Renhua Wu*

O090- Diffusional Kurtosis Imaging Using a Rician Noise Removal Evaluation of Compressed Spinal Cords in Vivo
Masaaki Hori, Koji Kamagata, Mariko Yoshida, Kouhei Kamiya, Michimasa Suzuki, Ryusuke Irie, Akira Nishikori, Yutaka Ozaki, Atsushi Nakanishi, Kanako Sato, Yuko Adachi, Miyoko Takayama, Kouhei Tsuruta, Shigeki Aoki



SCIENTIFIC PROGRAM

O091- Post Radiation Spine Imaging Findings

Ozlem Alkan, Senay Demir, Cem Onal, Nalan Yazici, Ayse Erbay

O092- Imaging Findings in Posterior Elements as a cause of Low Back Pain

Juan Ovalle

O093- Success Story of Ozonucleolysis in Disc Lesions in Pakistan

Umair Rashid Chaudhry

O094- Adhesive Arachnoiditis in Post Operative Lumbar Spine

Violeta Vasilevska Nikodinovska, Ulrike Szeimies, Axel Stabler

O095- Vascular Manifestations of Cervical Spine Trauma on CTA A Retrospective Institutional Experience

Vivek Sindhvani, Monika Arya

O096- Quantitative MRI in Hypokalaemic Periodic Paralysis Reveals Age Dependent Fat Infiltration of Lower Limb Muscles

Elham Rawah, Jasper M Morrow, Christopher DJ Sinclair, Matthew RB Evans, Sachit Shah, Mary M Reilly, Michael Hanna, John S Thornton, Tarek A Yousry

O097- MRI Quantifies Lumbosacral Nerve Root Hypertrophy in Chronic Inflammatory Demyelinating Polyradiculoneuropathy

Sachit Shah, Jasper M Morrow, Christopher DJ Sinclair, Matthew RB Evans, Michael G Hanna, Michael P Lunn, Mary M Reilly, John S Thornton, Tarek A Yousry

17:15 - 19:00

PARALLEL SCIENTIFIC PAPER PRESENTATIONS (Adult NR 1)

Moderators: Ilan Shelef, Israel, Nirmala Wijesinha, Sri Lanka

Dolmabahce C Hall

O098- Fast Quantitative Magnetization Transfer Imaging in 3D in Primary Brain Tumors and Metastases Is There a Correlation with PWI and DWI

Meritxell Garcia, Monika Gloor, Oliver Bieri, Ernst-Wilhelm Radue, Johanna M. Lieb, Dominik Cordier, Christoph Stippich

O099- Incidence and Prognostic Significance of Non Enhancing Cortical FLAIR Hyperintensity in Glioblastoma

Arian Lasocki, Francesco Gaillard, Mark Tacey, Katharine Drummond, Stephen Stuckey

O100- Multifocal and Multicentric Glioblastoma Improved Characterisation with FLAIR Imaging and Prognostic Implications.

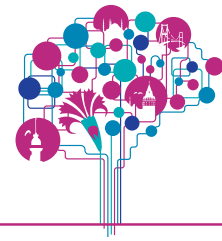
Arian Lasocki, Francesco Gaillard, Mark Tacey, Katharine Drummond, Stephen Stuckey

O101- Incidence and Imaging Follow up of Lesions Consistent with a Low Grade Glioma Distant from a Histologically Proven Glioblastoma

Arian Lasocki, Francesco Gaillard, Mark Tacey, Katharine Drummond, Stephen Stuckey

O102- Diagnostic Accuracy and Reproducibility of Intravoxel Incoherent Motion MR Imaging for Differentiating Among Glioblastoma Metastasis and Lymphoma

Myeong Ju Goh, Ho Sung Kim, Choong-Gon Choi, Sang Joon Kim



SCIENTIFIC PROGRAM

O103- Utility of Multiparametric Voxel by Voxel Tumor Clustering Using Permeability and Apparent Diffusion Coefficient for Differentiating Recurrent Glioblastoma from Radiation Necrosis

Ji Eun Park, Ho Sung Kim, Choong Gon Choi, Sang Joon Kim

O104- Added Value of Intravoxel Incoherent Motion Imaging in Patients with Recurrent Glioblastoma Comparison with Contrast enhanced Perfusion MR Imaging

Gil-Sun Hong, Ho Sung Kim, Choong Gon Choi, Sang Joon Kim

O105- Title Added Value of Intravoxel Incoherent Motion MR Imaging to Contrast enhanced Perfusion MR Imaging for Predicting Recurrent Metastatic Brain Tumor Following Gamma Knife Radiosurgery

Dae Yoon Kim, Ho Sung Kim, Ra Gyoung Yoon, Choong Gon Choi, Sang Joon Kim

O106- Atypical Imaging Features of Primary Central Nervous System Lymphoma Mimicking Glioblastoma in Non AIDS Patients Utility of Intravoxel Incoherent Motion MR Imaging

Ji Eun Park, Ho Sung Kim, Choong Gon Choi, Sang Joon Kim

O107- Prognostic Value of Combined Visualization of ADC Diffusion Maps and CBV Perfusion Maps in Patients with Newly Diagnosed Glioblastoma

Katerina Deike, Benedikt Wiestler, Markus Graf, Martin Bendszus, *Alexander Radbruch*

O108- Diagnostic Accuracy and Reproducibility of Amide Proton Transfer Imaging for Characterization of Solid and Necrotic Portions of Glioma Experimental and Clinical Studies

Ho Sung Kim, Choong Gon Choi, Sang Joon Kim

17:15 - 19:00 PARALLEL SCIENTIFIC PAPER PRESENTATIONS (Research & Neuroradiological Sciences 1)

Moderators: Jurate Dementaviciene, Lithuania, Mircea Buruian, Romania Topkapı A Hall

O109- Efficacy of CT Guided Percutaneous Intralesional Bleomycin Injection for the Treatment of Orbital Low Flow Vascular Malformations and Hemangiomas

Ho Fai Wong, TY Chen, MC Wu, *Nancy Duarte*

O110- Evaluation of the Effect on Surgical Decision Making of the Intra Operative Display of the Optic Radiation during Temporal Lobe Epilepsy Surgery

A. Kenji Yamamoto, Laura Mancini, Mark J. White, Anna Miserocchi, Andrew McEvoy, Pankaj Daga, Gavin P. Winston, John S. Duncan, Tarek A. Yousry

O111- Peri Lesional Changes in Diffusion Tensor Imaging (DTI) parameters after Gamma Knife Stereotactic Radiosurgery

Herwin Speckter, José Bido, Giancarlo Hernandez, Diones Rivera, *Luis Suazo*, Santiago Valenzuela, Bernd Foerster, Eddy Perez-Then, Jairo Oviedo, Peter Stoeter

O113- Degeneration and Plasticity of the Optic Pathway in Alström Syndrome

Valentina Citton, Jan Marshall, Angela Favaro, Baglione Alessandro, Pietro Maffei, Paolo Meneguzzo, Luca Wies, Francesco Bona, Annalena Venneri, Renzo Manara

O114- Functional Connectivity and Cerebral Networks in Crucial Intracerebral Regions are Affected in Patients with Systemic Lupus Erymatous (SLE)

Jessika Nystedt, Olof Strandberg, Andreas Jönsen, Åsa Lilja, Anders Bengtsson, Petra Nilsson, Peter Mannfolk, Pia Sundgren



SCIENTIFIC PROGRAM

O115- Structural Covariance Networks of Striatum Subdivision in Patients with Parkinson's Disease
Wei-Che Lin, Kun-Hsien Chou, Pei-Lin Lee, Ching-Po Lin, Hsiu-Ling Chen, Cheng-Hsien Lu

O116- Maximizing the Extent of Resection and Survival Benefit of Patients in Glioblastoma Surgery High Field iMRI Versus Conventional and 5 ALA Assisted Surgery
Sotirios Bisdas, Constantin Roder, Marcos Soares Tatagiba, Ulrike Ernemann, Vasileios K. Katsaros

O117- Protocol Combining Advanced and Functional MRI with Neuropsychological Evaluation for Patient Tailored Therapy Decision and Treatment of Brain Masses
Vasileios K. Katsaros, Sotirios Bisdas, Evangelia Liouta, Agapi Alexandra Katsarou, Laurent Hermoye, George Stranjalis

O118- Resting State fMRI as a Tool in the Preoperative Intraoperative and Postoperative Functional Assessment of Patients with Brain Masses
Vasileios K. Katsaros, Evangelia Liouta, Constantin Roder, Edyta Charyasz, Uwe Klose, Marco Soares Tatagiba, Sotirios Bisdas

O119- Diffusion Kurtosis Imaging in Glioma Grading
Vasileios K. Katsaros, Yiannis Spandonis, Sotirios Bisdas, George Stranjalis

O120- Practice and Pitfalls of Contrast Enhanced T2 FLAIR in Neuroradiology
Howard Rowley

O121- Manganese Enhanced Magnetic Resonance Imaging of the Chronic Manganese Toxicity in the Edaravone and Oxitosin Treated Rats
Melda Apaydin, Oytun Erbas, Vedat Evren, Cem Calli, Dilek Taskiran

17:15 - 19:00 PARALLEL SCIENTIFIC PAPER PRESENTATIONS (Research & Neuroradiological Sciences 2)

Moderators: Carolina Tramontini, Colombia, Özkan Özsarlak, Belgium

Topkapı B Hall

O122- Absolute quantification of brain metabolite concentration of prefrontal lobe and hippocampus of healthy youth around taking Codeine Hydrochloride using 1H-MRS and LCModel
Hailong Lan, Yeyu Xiao, Renhua Wu

O123- Substantia Alba Demyelination and Brain Metabolite Alteration in Cognitive Impairment Patients
Meilian Wu, Hailong Lan, Yeyu Xiao, Renhua Wu

O124- Grey Matter Alterations in Patients with Pantothenate Kinase Associated Neurodegeneration (PKAN)
Rea Rodriguez-Raecke, Pedro Roa-Sanchez, Herwin Speckter, Rafael Fermin-Delgado, Eddy Perez-Then, Jairo Oviedo, Luis Suazo, Peter Stoeter

O125- Brain Magnetic Resonance pH Imaging MRS and CEST
Renhua Wu, Zhuozhi Dai, Zhiwei Shen

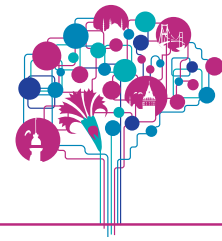
O126- Brain Anatomical Substrates of Mirror Movements in Kallmann Syndrome
Alessandro Salvalaggio, R Manara, V Citton, V Palumbo, A D'Errico, E Elefante, E Cantone, G Ottaviano, E Napoli, G Coppola, F Di Salle, S Rizzati, E De Carlo, NA Greggio, G Bonanni, AA Sinisi, A Favaro

O127- The Shades of White Distinction between Edema and Gliosis with Quantitative Water Mapping
Omid Nikoubashman, Ann Maria Oros-Peusquens, Carolin Weiß, Martin Wiesmann, John Shah

7-12 September 2014
ISTANBUL, TURKEY

LUTFI KIRDAR CONVENTION & EXHIBITION CENTER

XXth
Symposium
Neuroradiologicum



SCIENTIFIC PROGRAM

O128- Preliminary Results Of Tissue Contrast Optimization Of The Brainstem Using Phase Difference Enhanced (PADRE) Post Processing of 3D Gradient Echo (GE) Images at 1.5T.

Nandor Pinter, Joseph Fritz, Thomas Perkins, Laszlo Mechtler

O129- Isolated Congenital Superior Oblique Paresis a High Resolution MRI Phenotype Study

Indran Davagnanam, Annegret Dahlmann-Noor, Jane Sowden, John Thornton, Tarek Yousry

O130- Ex vivo Demonstration of the Fourth Cranial Nerve Nucleus on High Resolution 3T 7T and 9.4T MRI

Indran Davagnanam, John Thornton, Penny Gowland, Tarek Yousry

O131- The Utility of Gadoterate Meglumine Enhanced MRI in Adult and Pediatric Patients with Central Nervous System Lesions (SENTIO study)

Raphaelle Souillard

O132- Correlating the Structural Impairment of Hippocampus with Cognitive Disorders in Parkinson's Disease a 3T MRI Voxel Based Morphometry and Diffusion Tensor Imaging Study on 80 Patients

Bruno Law-ye, Clémentine Vignon, Pierre Berroir, Marie Vidailhet, Lydia Yahya-Cherif, Stéphane Lehericy

O133- Optimal Concentration of Gadolinium based Contrast Agent on Contrast Enhanced MR Imaging Sequences in Phantoms.

Jae Kyun Kim, Seung Tae Woo, Jun Soo Byun, Woong Jae Lee, Bon Chul Ha

O234- Cortical Reorganization of Pain Processing in Patients with Chronic Pelvic Pain Syndrome

Christian Weisstanner, Livio Mordasini, George N Thalmann, Christian Rummel, Rajeev K Verma, Eugenio Abela, Peter Jüni, Andrea Federspiel, Thomas M Kessler, Roland Wiest

O233- Meta Analytical Comparison of Voxel Based Morphometry Studies in Migraine

Hsu-Huei Weng, Yuan-Hsiung Tsai, Chih-Feng Chen, Jiann-Der Lee, Shuu-Jiun Wang, Chun-Yuh Yang



SCIENTIFIC PROGRAM

Thursday, September 11, 2014

ADULT DIAGNOSTIC NR

Anadolu Auditorium

08:30 - 10:30

CNS TUMORS 1

Moderators : Mark Khangure, Australia, Alfonso Lozano, Colombia
Genomic Mapping of Brain Tumors.

Anne G. Osborn

University of Utah School of Medicine, USA

From Diagnosis to Response Assessment in brain tumors.

Mehmet Kocak

Rush University Medical Center, USA

Timing of Follow up Examinations What to Expect to See; Application of Advanced Imaging Tools in Response Assessment and Standardization of Reports and Potential Pitfalls

Rafael Rojas

Beth Israel Deaconess Medical Center, Harvard Medical School Radiology, Section Neuroradiology Boston, USA

When an image that looks like a tumor: Brain tumoral like-lesions.

Mehmet Kocak

Rush University Medical Center, USA

O020-Brain Gliomas Correlation between Diffusion Kurtosis Imaging and Tumor Malignancy

Aram Tonoyan 1, Farida Grinberg 2, Ezequiel Farrher 2, Igor Pronin 1, Ivan Maximov 2

Lyudmila Shishkina 1, Evgeniy Shults 1, David Pitskhelauri 1, Valeriy Kornienko 1

Burdenko Neurosurgery Institute Neuroradiology Moscow-Russia 1 Forschungszentrum Juelich GmbH Institute of Neuroscience and Medicine – 4 -Germany 2

ADULT DIAGNOSTIC NR

Topkapı AB Hall

08:30 - 10:30

Advanced Techniques

Moderators : Masayuki Maeda, Japan, Luca Remonda, Switzerland

Quantitative Imaging: Imaging Biomarker for Brain Disorder

Toshiaki Taoka

Nara Medical University Radiology Kashihara, Japan

Multimodal Neuroimaging

Marion Smits

Erasmus MC Radiology Rotterdam, The Netherlands

Diffusion Tensor Image for Monitoring Treatment Effects

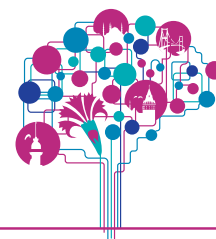
Toshiaki Taoka

Nara Medical University Radiology Kashihara, Japan

Functional MRI BOLD and Beyond

Marion Smits

Erasmus MC Radiology Rotterdam, The Netherlands



SCIENTIFIC PROGRAM

O021-Microstructural Effects of a Neuro Modulating Drug Evaluated by Diffusion Tensor Magnetic Resonance Imaging in Mice

*Karl Egger*¹, Philipp Janz¹, Mate Doebroessy¹, Markus Obmann¹, Thomas Bienert¹, Marco Reisert¹, Carola Haas¹, Horst Urbach¹, Laura Harsan¹, Dominik von Elverfeldt¹

*University Medical Center Freiburg Department of Neuroradiology Freiburg-Germany*¹

INTRAVASCULAR INTERVENTIONAL NR

Marmara Hall

08:30 - 10:30 **Long Term Results of Advanced Endovascular Aneurysm Treatment Techniques Developed During the Recent Decade**

Moderators : Naci Kocer, Turkey, Saruhan Cekirge, Turkey

Long term results of single stent assisted coiling: view from a large experience and recent literature

Demetrius Lopes

RUSH University, USA

Long term results of dual stent assisted coiling: view from a large experience and recent literature

Saruhan Cekirge

Bayindir Hospital and KORU Hospital, Turkey

Long term results of extraaneurysmal Flow diversion/modification: view from a large experience and recent literature

Pedro Lylyk

ENERI-Clinica La Sagrada Familia, Argentina

Long term results of intraaneurysmal Flow diversion/modification: view from a large experience and recent literature.

Laurent Pierot

CHU Reims, France

What has been the progress in treating giant aneurysm with flow diversion/modification: Long term results, problems and solutions

Naci Kocer

Istanbul University, Turkey

Current status of the clinical trials on aneurysm endovascular treatment

Anil Gholkar,

Newcastle Upon Tyne Hospitals, NHS Trust, UK

10:30 - 11:00 COFFEE BREAK

ADULT DIAGNOSTIC NR

Anadolu Auditorium

11:00 - 12:30 **CNS TUMORS 2**

Moderator : Nalini Kant Mishra, India, Niloufar Sadeghi, Belgium

Ultra-High Field MR of Brain Tumors and Potential Therapeutic Applications

Nina A. Mayr

Univ. of Washington Radiation Oncology Seattle, USA

Image guided Radiation Therapy and post Radiation Therapy imaging

Nina A. Mayr

Univ. of Washington Radiation Oncology Seattle, USA



SCIENTIFIC PROGRAM

Magnetic Resonance Metabolic Imaging in Oncology

*A. Beltramello**, L. Nicoli*, G. Cabrini**, F.B. Pizzini*, MC. Dehecchi**, C. Ghimenton**, A. Eccher**, G. Caliarì*, G.K. Ricciardi*.

Dept of Pathology & Diagnostics, Units of Neuroradiology and Molecular Pathology**,
University Hospital Verona, Italy*

O022-The Prognostic Value of Dynamic Susceptibility Contrast Enhanced Perfusion and Diffusion Tensor MR Imaging in Patients with Glioblastomas

Gokcen Coban 1, Suyash Mohan ², Feride Kural ¹, Sumei Wang ², Donald M. ORourke ³
Harish Poptani ²

Baskent University Medical School Radiology Department Konya-Turkey 1 University of Pennsylvania, Philadelphia Radiology Department -United States 2 University of Pennsylvania, Philadelphia Neurosurgery Department, USA ³

ADULT DIAGNOSTIC NR

Topkapı AB Hall

11:00 - 12:30

Advanced Techniques

Moderators

: Paulina Due Tonnessen, Norway, Roger Siemund, Sweden

Real-time fMRI neurofeedback: Progress and challenges

Sven Haller

University Hospitals of Geneva and Faculty of Medicine of the University of Geneva, Switzerland

Deep brain stimulation and imaging

Hakan Oruckaptan

Liv Hospital, Istanbul, Turkey

Advanced Functional Imaging of the Brain

Wendell A. Gibby

Adjunct Professor of Radiology, University of California San Diego

CEO – Novard Corporation, USA

O023-Juxtacortical Lesion of Multiple Sclerosis Assessment of Gray Matter Involvement with Phase Difference Enhanced Imaging (PADRE)

Koichiro Futatsuya ¹, Shingo Kakeda ¹, Issei Ueda ¹, Keita Watanabe ¹, Junji Moriya ¹, Yu Murakami ¹, Satoru Ide ¹, Atsushi Ogasawara ¹, Norihiro Ohnari ¹, Kazumasa Okada ², Tetsuya Yoneda ³, Yukunori Korogi ¹

University of Occupational and Environmental Health School of Medicine Radiology Kitakyushu-shi-Japan ¹ University of Occupational and Environmental Health School of Medicine Neurology -Japan ² Faculty of Life Sciences, Kumamoto University Medical Physics in Advanced Biomedical Sciences, Japan ³

INTRAVASCULAR INTERVENTIONAL NR

Marmara Hall

11:00 - 12:30

Presentations & Discussion on Controversial Approaches & Controversies in Endovascular Aneurysm Treatment

Moderators

: Kamil Zelenak, Slovakia, Karl-Olof Lövblad, Switzerland

The use Flow Divertors in the endovascular treatment of complex MCA bifurcation aneurysms: Follow-up results

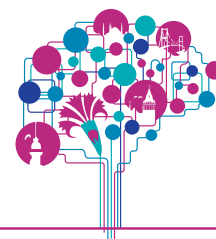
Isil Saatci

KORU Hospital, Turkey

7-12 September 2014
ISTANBUL, TURKEY

LUTFI KIRDAR CONVENTION & EXHIBITION CENTER

XXth
Symposium
Neuroradiologicum



SCIENTIFIC PROGRAM

The use of Flow Divertors in the endovascular treatment of aneurysms with an important branch arising from the aneurysm sac: Long term follow up results

Eduardo Boccardi

Hospital Niguarda, Italy

O024-Cerebral Aneurysm Treatment with Flow Re Direction Endoluminal Device (FRED): Initial Experience with Short and Mid Term Follow up Results

*Burak Kocak*¹, Muzaffer Saglam², Cigdem Akyol Beyoglu³, Osman Kizilkilic¹, Civan Islak¹, Naci Kocer¹

*Cerrahpasa Medical Faculty Department of Radiology Istanbul-Turkey*¹ *GATA Haydarpasa Teaching Hospital Department of Radiology -Turkey*² *Cerrahpasa Medical Faculty Department of Anesthesiology and Reanimation, Turkey*³

12:30 - 13:30 LUNCH BREAK

13.00-14.00 Poster Presentations

Spine

Moderator: Angel Mironov, USA

SULTAN 1

EP182- Follow up MR Findings of Spinal Meningioma after Stereotactic Radiotherapy

Yoon Joon Hwang, Byung Hoon Lee, Yon Kwon Ihn

EP183- Langerhans Cell Histiocytosis (LCH) of the Lumbal Spine during Pregnancy

Felicia Pilar Gunadi, Farhan Anwary, Rista D Soetikno

EP184- A Rare Servical Intradural Extramedullary Melanocytoma Case Report

Amalya Zeynalova, Yasemin Kayadibi, Elmar Bayraktarov, Evrim Ozmen, Zehra Isik Hasiloglu

EP185- Vertebrobasilar Territory Stroke Syndromes and Imaging Findings

Juan Ovalle

EP186- Spinal Cord Glioblastoma Multiforme in a Patient with Down syndrome

Pablo Picasso de Araújo Coimbra, Rafael Costa Lima Maia, Tiago Silva Holanda Ferreira, Daniel Gurgel Fernandes Tavora, Wellington Barros Oliveira de Moura, André Soldati Antônio, Stelio da Conceição Araújo Filho, Edson Lopes Júnior

EP187- Intraspinal Subdural or Epidural Hygroma in Cases of Intracranial Hypotension. Which One is Correct Diagnosis

Izumi Anno

EP188- Interventional Neuroradiology C Spine Procedures

Francesco Massari, Giuseppe Bonaldi, Alessandro Cianfoni

Pediatric NR 1

Moderator: Thierry A.G.M. Huisman, USA

SULTAN 1

EP189- Factors Correlating Outcome in Congenital Muscular Torticollis a Single Center Study

JiHwa Ryu, Choongki Eun, KwangHwi Lee, HongDae Kim

EP190- Neuroimaging Findings of Twin Sisters with Incontinentia Pigmenti Who Presented With Recurrent Encephalopathy Attacks

Rahsan Gocmen, Bahadir Konuskan, Dilek Yalnizoglu, Kader Karli Oguz



SCIENTIFIC PROGRAM

EP191- Imaging of Intracranial Lipomas

Jeong Hyun Yoo

EP192- Foetal MRI Correlation between Antenatal Ultrasound Antenatal MRI and Post natal Imaging the Cape Town Experience

Arthur Daire, Savvas Andronikou, Sally Candy

EP193- Value of Diffusion Weighted Imaging in Neonatal Hypoglycemia

Fuldem Donmez, Muhtesem Agildere

EP194- Traumatic Craniocervical Junction Ligamentous Injuries and Epidural Retroclival Hematoma

Bilal Egemen Çifçi, Gökçen Çoban, Mahmut Gökdemir, Enes Duman

EP195- Metabolic Disorders Presenting in Neonatal Period

Ritu Kakkar, Sameer Soneji, Shrinivas Desai

EP196- Magnetic Resonance Fiber Tracking In a Neonate with Hemimegalencephaly

Laura Scariolla, Thomas Re, Emi Takahashi, Stefania Galassi, Lorenzo Figà Talamanca, Carlo Cosimo Quattrocchi, Bruno Bernardi, Daniela Longo

EP197- “Papillary Glandular Sign” in Large Suprasellar Pilocytic Astrocytomas

Manzoor Ahmed, Anwar Ul Haq, Essam Alshail, Mohammad Dogar, Joyce Mbekeani

EP198- Congenital Adrenal Hyperplasia and Brain Magnetic Resonance Imaging Abnormalities

Saida Jerbi Omezzine, Radhouane Hamdi, Samia Younes, Maher Dhifallah, Hassine Hamza

EP199- Dynamic Susceptibility Weighted Contrast Enhanced Perfusion MRI Analysis of Pediatric Intracranial Tumors in the Posterior Foss

Augusto Elias Mamere, Leonir Terezinha Feltrin, Renata Mendes Lacerda Fava

EP200- A Unique Combination of Dyke Davidoff Masson Syndrome and Down Syndrome Diffusion Tensor Tractography Findings

Kerim Aslan, Tumay Bekci, Hediye Pinar Gunbey, Lutfi Incesu, Meltem Ceyhan Bilgici

EP201- A Missed Diagnosis Acute Encephalopathy with Biphasic Seizures and Late Reduced Diffusion

Tümay Bekci, Kerim Aslan, Cenk Şecaattin Onaral, Engin Yosma

Pediatric NR 2

Moderator: Andrea Rossi, Italy

SULTAN 2

EP202- Paraneoplastic Disease. Tumor Ovaries Manifesting As Encephalomyelitis

Jurkiewicz Elzbieta, Nowak Katarzyna, Malczyk Katarzyna, Kotulska Katarzyna, Borkowska Julita

EP203- Pineal Region Germinal Neoplasia with Adenocarcinoma Transformation

Roberto Marileo, Ingeborg Lopez, Rodrigo Riveros, Cecilia Okuma, Aaron Vidal, Rodrigo Rivera, J. Gabriel Sordo, Claudia Tissera, Lautaro Badilla

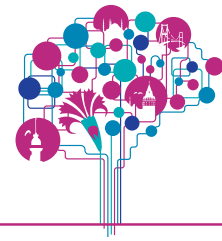
EP204- MRI Findings in Children with Open Spinal Dysraphism Don't Forget to Look at the Brain

Dora Zlatareva, Assen Tzekov, Arash Rastgou

7-12 September 2014
ISTANBUL, TURKEY

LUTFI KIRDAR CONVENTION & EXHIBITION CENTER

XXth
Symposium
Neuroradiologicum



SCIENTIFIC PROGRAM

EP205- Ruptured Intracranial Mycotic Aneurysm in Young Children a Case Report

Mohd Rizal Abu Bakar, Rohsila Mohamad, Rohaizan Yunus

EP206- Pediatric Cerebral Arteriovenous Malformations (AVMs)

Angel Sanchez-Montanez, Alvaro Cortes, Ignacio Delgado, Fuat Arikan, Elida Vazquez

EP207- Morphologic Change of The Pituitary Gland on MR in Children with Idiopathic Central Precocious Puberty

Hee Mang Yoon, Jae-Yeon Hwang, Hye-Kyung Yoon, Sae Rom Chung, Young Ah Cho, Jin Seong Lee, Ah Young Jung, Chong Hyun Yoon

EP208- Posterior Fossa Tumors in Childhood Radiologic Findings and Pathologic Correlation

Faten Bouzayen, Nadia Mama, Mehdi Gaha, Aymen Ben Tebra, Hedi Krifa, Med Tahar Yacoubi,

Kalthoum Tlili

EP209- Imaging of Neuronal Tumors of the Central Nervous System Radiologic Pathologic Correlations

Mouna Laadhari, Nadia Mama, Amel Ben Abdallah, Khaled Kadri, Nadia Arifa, Iadh Ksira, Med Taher

Yacoubi, Kalthoum Tlili

EP210- Diencephalic–Mesencephalic Junction Dysplasia on Fetal MRI

Mariasavina Severino, Domenico Tortora, Mariya Malova, Rodica Mardari, Alessandro Parodi, Dario Paladini, Luca Ramenghi, Andrea Rossi

EP211- Bandlike Calcification With Simplified Gyration and Polymicrogyria – A Rare Disease With Typical Imaging Findings

Tiago Rodrigues, Catarina Magalhães, Gabriela Soares, Inês Carilho, Luís Botelho, Pedro Pinto

EP212- Gobbi's Syndrome

Ariana Jacinto, Pablo Picasso, Carlos Macedo, Alvaro Menezes

EP213- Pediatric Small Bowel Transplant Brain Imaging Findings

Matthew Folorunso Omojola, Diana Florescu, Steven Johnson, Fang Qiu, Matthew L White

EP214- Carotid Blowout Syndrome Endovascular Management by Stenting & Embolization

Jaime Tisnado

EP260- **Susceptibility Weighted MR Sequences Technical Insights and Clinical Applications Focusing on Inflammatory and Infectious Diseases of the CNS**

Leandro Tavares Lucato, Livia M. T. Scianni Moraes, Jeanette Janaina Jaber Lucato,

Germana Titoneli Vieira, Claudia Costa Leite

Adult NR 8

Moderator: Ho-Fai Wong, Taiwan

SULTAN 2

EP215- Time Domain Frequency Decomposition and Filtering of Multiphase Low Dose CT Perfusion Datasets for High Quality Structural Image Reconstruction

Luke Gerke

EP216- 3D Surface Rendered PET CT in Suspected Osteomyelitis Post Cranioplasty and Infected Myocutaneous Flaps Post Craniofacial Reconstructive Surgery

Shanker Raja, Yasser Orz, Yaser AlJadhaj, Sharad George, Sven Larsson



SCIENTIFIC PROGRAM

EP217- MR ADC Histogram Moments Percentiles and Distances in Management of Choroid Plexus Tumors and Correlation with Histopathology and Ki 67

Shanker Raja, Sharad George, Sadeq AlDandan, Abdullah AlRashed, Sven Larsson, Ahmed Lary

EP218- Can Multiparametric MRI Reliably Differentiate Choroid Plexus Tumors?

Abdullah AlRashed, Larrson Sven, Sadeq Al-Dandan, Abdulazeez Akintokun, Amhed Larry, Shanker Raja

EP219- Cases of PML in Natalizumab after 10 Treatments CHU Tlemcen Algeria

Djaouad Bouchenak Khelladi, Salim Allal

EP220- Eccentric Target Signs in Cerebral Toxoplasmosis, the Use of 3D MPRAGE for Lesion Characterization
Zaharuddin Haron, Norzaini Rose Mohd Zain, Ahmad Sobri Muda, Syazarina Syaris Osman, Shahizon Azura Mohamed Mukari

EP221- Gemistocystic Astrocytoma with Anaplastic Transformation, the Use of MR Perfusion in Disease Monitoring

Shahizon Azura Mohamed Mukari, Zaharuddin Haron, Ahmad Sobri Muda, Syazarina Syaris Osman, Norzaini Rose Mohd Zain

EP222- Secondary Neuronal Degeneration Caused by Remote Intracranial Lesions MR Imaging Findings

Ha Hun Song, Young-Joo Kim

EP223- Neurological Manifestations of End Stage Renal Disease MRI Findings

Young-Joo Kim, Ha Hun Song

EP224- Multimodal Imaging in Brain Death Assesment

Roberto Marileo, Ingeborg Lopez, Rodrigo Riveros, Cecilia Okuma, Rodrigo Rivera, Aaron Vidal, Juan Sordo, Lautaro Badilla

EP225- Brain MRI Follow Up After Twenty Years in a Series of Systemic Lupus Erythematosus (SLE) Patients

Maria Teresa Peltz, Simona Secci

EP226- High Resolution Diffusion Weighted Imaging and MR Perfusion with Arterial Spin Labeling (ASL) in Patient with Transient Global Amnesia (TGA) Another Brick Supporting Vasculopathic Pathogenesis.

Maria Teresa Peltz, Simona Secci, Grazia Bitti, Maurizio Melis

EP227- Emergency Magnetic Resonance Imaging (MRI) in Neurological Diseases

Melda Apaydm, Ö. Tuğçe Kalaycı, Fazil Gelal

EP228- Significance of Prominent Hypointense Signals in Draining Veins Adjacent To Areas of Cerebral Infarction on Susceptibility Weighted Imaging

Kookjin Ahn, Jinhee Jang, Hyunseok Choi, Solyung Jung, Bumsoo Kim

EP229- Hematoma Shape Hematoma Size GCS Score and ICH Score which Predict the 30 Day Mortality Better for ICH

Chun-Jung Juan, Chih-Wei Wang, Yi-Jui Liu, Hsian-He Hsu

EP230- A Case of Thrombosed Vertebral Artery Aneurysm with Brain Stem Compression and Infarction

Atila Kokurcan, Emrah Yilmaz, Suna Örs, M.Koray Akkan, Serap Gültekin

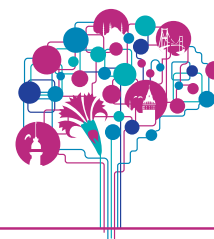
EP261-Double Inversion Recovery Cervical Cord Imaging at 3T: Is It Better For Multiple Sclerosis Lesion Detection?

Chian Aun Chang, Abigail Chong, Ronil Chandra, Kenneth Chuah, Cathy Soufan, Deepa Rajendran, Ernie Butler, Stephen Stuckey

7-12 September 2014
ISTANBUL, TURKEY

LUTFI KIRDAR CONVENTION & EXHIBITION CENTER

XXth
Symposium
Neuroradiologicum



SCIENTIFIC PROGRAM

ADULT DIAGNOSTIC NR	Anadolu Auditorium
13:30 - 15:00	CNS Infections
Moderators	: Lazaro Luis Fariado Amaral, Brazil, Kalthoum Tlili-Graies, Tunisia
	Highlight the Diverse Neuroimaging Features of Various Tropical and Subtropical Endemic Infectious Diseases
	<i>Rakesh K. Gupta</i>
	<i>Fortis Memorial Research Institute Radiology & Imaging Gurgaon, India</i>
	Diseases or Conditions More Common in Different Regions of the World
	<i>Yukunori Korogi</i>
	<i>University of Occupational & Environmental Health Radiology Kitakyushu, Japan</i>
	Discussion and Diagnosis of Dys-immune Encephalitis
	<i>Rakesh K. Gupta</i>
	<i>Fortis Memorial Research Institute Radiology & Imaging Gurgaon, India</i>
	O025-Assessment of Early Cerebral Damage in The Course Of HIV and HCV Infection Using Perfusion MR Imaging Is the Hepatitis C Virus More Dangerous for the Brain
	<i>Joanna Bladowska</i> ¹ , <i>Anna Zimny</i> ¹ , <i>Brygida Knysz</i> ² , <i>Anna Koltowska</i> ¹ , <i>Krzysztof Malyszczak</i> ³ , <i>Pawel Szewczyk</i> ¹ , <i>Jacek Gasiorowski</i> ² , <i>Michal Furdal</i> ⁴ , <i>Marek Sasiadek</i> ¹
	<i>Wroclaw Medical University Department of General Radiology, Interventional Radiology and Neuroradiology Wroclaw-Poland</i> ¹ <i>Wroclaw Medical University Department of Infectious Diseases, Liver Diseases and Acquired Immune Deficiency -Poland</i> ² <i>Wroclaw Medical University Department of Psychiatry -Poland</i> ³ <i>Regional Specialistic Hospital Department of Cardiology, Poland</i> ⁴
	ADULT DIAGNOSTIC NR
	Topkapı AB Hall
13:30 - 15:00	Advanced Imaging
Moderators	: Irfan Mamoon, Saudi Arabia, Brian Tress, Australia
	What to expect from MR Spectroscopy
	<i>Marco Leonardi</i>
	<i>Bologna University, IRCCS Neuological Research Hospital, Italy</i>
	C arm CT and Quantitative DSA
	<i>Wan-Yuo Guo</i>
	<i>Taipei Veterans General Hospital Radiology Taipei-Taiwan</i>
	Angioscopy
	<i>Timo Krings</i>
	<i>Toronto Western Hospital, Canada</i>
	O026-Usefulness of Acute Stroke Imaging with Wide Area Detector CT Before Endovascular Reperfusion Therapy in the Anterior Cerebral Circulation
	<i>Takahisa Mori</i> ¹ , <i>Tomonori Iwata</i> ¹ , <i>Yuhei Tanno</i> ¹ , <i>Shigen Kasakura</i> ¹ , <i>Yoshinori Aoyagi</i> ¹ , <i>Kazuhiro Yoshioka</i> ¹
	<i>Shonan Kamakura General Hospital Stroke Center Stroke Treatment Kamakura, Japan</i> ¹



SCIENTIFIC PROGRAM

INTRAVASCULAR INTERVENTIONAL NR

Marmara Hall

13:30 - 15:00 **Endovascular Treatment of Acute Stroke. The Past, Present and Future**
Moderators : Ljubo Markovic, Denmark, Rudiger Von Kummer, Germany
Summary of completed studies on endovascular acute stroke treatment
Aquilla Turk
Medical University of South Carolina, USA

Summary of Ongoing Studies on Endovascular Acute Stroke Treatment
Tommy Andersson
Karolinska Hospital Neuroradiology Stockholm, Sweden

What Would Be the Future of Acute Stroke Treatment
Ethem Murat Arsava
Hacettepe University Neurology Ankara, Turkey

O027-The pREset Retriever for Endovascular Treatment of Stroke after MCA Occlusion Safety and Clinical Outcome
*Benedikt Jakob Schwaiger*¹, Fabian Kober¹, Alexandra Sophia Gersing¹, Holger Poppert², Claus Zimmer¹, Sascha Prothmann¹
*Klinikum rechts der Isar der TU Muenchen Neuroradiology Muenchen-Germany*¹ *Klinikum rechts der Isar der TU Muenchen Neurology -Germany*²

15:00 - 15:30 COFFEE BREAK

ADULT DIAGNOSTIC NR

Anadolu Auditorium

15:30 - 17:00 **Cerebro Spinal Fluid**
Moderators : German Abdo, Ecuador, Oktay Algin, Turkey
Hydrocephalus (part 1: etiology and diagnosis)
Geir Ringstad
Oslo University Hospital - Rikshospitalet, Norway

Hydrocephalus Part 2 (Evaluation of Treatment Options and Follow up)
Yukunori Korogi
University of Occupational & Environmental Health Radiology Kitakyushu, Japan

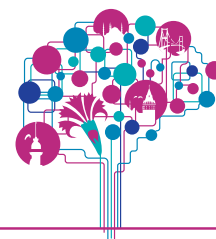
Other CSF disorders (except hydrocephalus)
Geir Ringstad
Oslo University Hospital - Rikshospitalet, Norway

Quantitative CSF Flow Analysis in Chiari Malformation
Wendell A. Gibby
Adjunct Professor of Radiology, University of California San Diego
CEO - Novard Corporation, USA

7-12 September 2014
ISTANBUL, TURKEY

LUTFI KIRDAR CONVENTION & EXHIBITION CENTER

XXth
Symposium
Neuroradiologicum



SCIENTIFIC PROGRAM

ADULT DIAGNOSTIC NR

Topkapı AB Hall

15:30 - 17:00

Telemedicine Architecture

Advantages and challenges in Telemedicine. For example: The setup of a Neuroscience Rehab Center at Jerudong Park Medical Center in Brunei Darussalam

Moderators : Datin Uta Meyding-Lamade, Germany, Bodo Kress, Germany

Opening remarks

Bodo Kress

Head of Department of diagnostic and interventional Neuroradiology, Krankenhaus, Frankfurt, Germany and Head of Department of Neuroradiology, Jerudong Park Medical Center, Jerudong, Brunei Darussalam

From 0 to 100: Setup of a Neuroscience Rehab center

Datin Uta Meyding-Lamade

Head of Department of Neurology, Krankenhaus Nordwest, Frankfurt, Germany and Head and CEO of The Brunei Neuroscience and Rehabilitation Center, Jerudong Park Medical Center, Jerudong, Brunei Darussalam

It is simple, we will do it via the internet. Challenges in network and infrastructure

Mattes Papendieck

CEO Meytec Telemedicine Systems, Werneheuchen, Germany

24/7 Neuroradiology over a distance of 12000 km

Bodo Kress

Head of Department of diagnostic and interventional Neuroradiology, Krankenhaus, Frankfurt, Germany and Head of Department of Neuroradiology, Jerudong Park Medical Center, Jerudong, Brunei Darussalam

The specialist on site. Role of the radiographer in a teleneuroradiological concept

Varghese Paulouse

Chief Radiographer, Department of diagnostic imaging, Jerudong Park Medical Center, Jerudong, Brunei Darussalam

Video-conference: Looking abroad, ward round over the distance

Datin Uta Meyding-Lamade

Head of Department of Neurology, Krankenhaus Nordwest, Frankfurt, Germany and Head and CEO of The Brunei Neuroscience and Rehabilitation Center, Jerudong Park Medical Center, Jerudong, Brunei Darussalam

Video conference: Global classroom. Interactive teleteaching of students

Bodo Kress

Head of Department of diagnostic and interventional Neuroradiology, Krankenhaus, Frankfurt, Germany and Head of Department of Neuroradiology, Jerudong Park Medical Center, Jerudong, Brunei Darussalam

Discussion and Closing remarks

Bodo Kress, Germany



SCIENTIFIC PROGRAM

INTRAVASCULAR INTERVENTIONAL NR

Marmara Hall

15:30 - 17:00 **Controversies on Supraaortic Revascularization in 2014**

Moderators : Hon-Man Liu, Taiwan, Erhan Ilgit, Turkey

Intracranial stenting: Dead or Alive? Need another trial?

Hans Henkes

Klinikum Stuttgart / Klinik Für Neuroradiologie, Germany

Revascularization of non-acute total ICA occlusions: What is real indication?

Tomoaki Terada

Showa University Fujigaoka Hospital, Japan

How Far Can We Go with Medical Treatment Neurologist View

Ethem Murat Arsava

Hacettepe University Neurology Ankara-Turkey

O028-Bail Out Intracranial Stenting with After Unsuccessful Thrombectomy

Nicola Limbucci 1, Leonardo Renieri 1, Nappini Sergio 1, Arturo Consoli 1, Andrea Rosi 1, Salvatore Mangiafico 1

Careggi University Hospital, Florence Interventional Neuroradiology Firenze-Italy 1

17:00 - 17:15 BREAK

17:15 - 19:00 PARALLEL SCIENTIFIC PAPER PRESENTATIONS (Adult NR 2)

Moderators: Jaime Medrano Lin, Panama, Gang Guo, China

Marmara Hall

O134- Dynamic Susceptibility Contrast enhanced (DSC) MR based Perfusion Imaging to Differentiate Recurrence from Stable Disease in Brain Gliomas

Niloufar Sadeghi, Jean Christophe Lebrun, Julie Absil, Thierry Metens, Serge Goldman

O135- Preoperative Evaluation of Brain Tumors Added Value of 320 Section Dynamic Volume CT to Standard 3T MR Images

Toshinori Hirai, Yasuhiko Iryo, Hideo Nakamura , Mika Kitajima , Eri Hayashida , Minako Azuma , Seitara Oda , Daisuke Utsunomiya , Yoshinori Shigematsu , Yasuyuki Yamashita

O136- Diagnostic Utility of Dynamic Susceptibility weighted Contrast enhanced Perfusion MR Imaging for the Peritumoral Region in Differentiating Glioblastomas from Solitary Brain Metastases.

Andres Server, Tone E.D. Orheim, Bjørn A. Graff, Roger Josefsen

O137- Which is the Best Advanced MR Imaging Protocol for Predicting Recurrent Metastatic Brain Tumor following Gamma knife Radiosurgery Focused on Perfusion Method

Won Jung Chung, Ho Sung Kim, Choong Gon Choi, Sang Joon Kim, Seung Chai Jung

O138- Optimized Combination of MR Imaging Modalities for Predicting Recurrent Glioblastoma Study of Diagnostic Accuracy and Reproducibility

Chong Hyun Suh, Ho Sung Kim, Seung Chai Jung, Chung Gon Choi, Sang Jun Kim

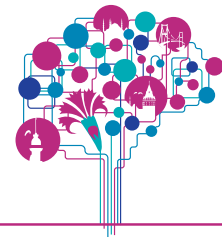
O139- Differentiation of True Progression from Pseudoprogression in Glioblastoma Patients Treated with Radiation Therapy and Concomitant Temozolomide Application of Subependymal Enhancement Pattern and Diffusion weighted Imaging

Roh-Eul Yoo, Seung Hong Choi

7-12 September 2014
ISTANBUL, TURKEY

LUTFI KIRDAR CONVENTION & EXHIBITION CENTER

XXth
Symposium
Neuroradiologicum



SCIENTIFIC PROGRAM

O140- Astrocytoma with TP53 Molecular Mutation and Its MRI Characteristics

M. de Fatima Vasco Aragao, Meng Law, Girish Fatterpekar, Bradley Delman, Ana Bader, Mary Fowkes, Thomas Naidich, Marcelo Moraes Valenca

O141- Are There Differences between Macrocyclic Gadolinium Contrast Agents for Brain Tumor Imaging Results of a Multicenter Intra Individual Crossover Comparison of Gadobutrol with Gadoteridol (The TRUTH study)

Cesare Colosimo, Ken Maravilla, Sefano Bastianello, Eva Bueltmann, Toshinori Hirai, Tiziano Frattini, Martin Smith, Manuela Vaneckova, Mayank Goyal, Joseph Baima, Robert Babel, Tomasz Drózdź

O142- Expert Witnesses Neuroradiologists' Perspectives in America

David Yousem, Nara Pereira, Kelly Yousem, Jonathan Lewin

O143- Error in Neuroradiology an Analysis of Reports in the Radiology Events Register (RaER)

Catherine Mandel, Jane Grimm, Tim Schultz

17:15 - 19:00 PARALLEL SCIENTIFIC PAPER PRESENTATIONS (Adult NR 3)

Moderators: Ahmed Halilah, Jordan, Lachezar Penev, Bulgaria

Dolmabahce C Hall

O144- High Signal Intensity Abnormalities Evaluated by 3D Fluid Attenuated Inversion Recovery Imaging Adjacent to Developmental Venous Anomalies Identified by Susceptibility Weighted Imaging at 3T

Maki Umino, Masayuki Maeda, Nobuyoshi Matsushima, Keita Matsuura, Hajime Sakuma

O145- Analysis of Hyperdense Sign on Non Contrast CT for Diagnosing Cerebral Venous Thrombosis

Sohail Zaheer, Raphael Glikstein, Satya Patro, Nicholas Seppala, Nikolai Steffenhagen, Daniela Iancu

O146- Leukoaraiosis and Microbleeds in Alzheimers Disease in Australian Population; Is There a Link and Does It Influence Cognition?

Sandeep Bhuta, Charlie Hsu, Rhondda Jones, Margaret Bilska

O147- Stripe Sign of Precentral Gyri in Amyotrophic Lateral Sclerosis a Novel Finding on Phase Difference Enhanced Imaging

Shingo Kakeda, Tetsuya Yoneda, Mari Miyata, Satoru Ide, Yasuhiro Hiai, Koichiro Futatsuya, Keita Watanabe, Yu Murakami, Atsushi Ogasawara, Junji Moriya, Yukunori Korogi

O148- Progressive Cerebellar Atrophy in Course of Hypertrophic Olivary Degeneration

Angel Mironov

O149- Diffuse Hypoperfusion in Normal Appearing White Matter (NAWM) and Deep Gray Matter (DGM) Regions in Patients with Neuropsychiatric Systemic Lupus Erythematosus (NPSLE)

Efrosin Papadaki, Antonios Fanouriakis, Eleytherios Kavroulakis, Georgios Bertsiyas, Prodromos Sidiropoulos, Dimitrios Boumpas, Apostolos Karantanas

O150- Subcortical Calcification on CT as Diagnostic Sign of Transverse sigmoid Dural Arteriovenous Fistula With Cortical Venous Reflux

Shunji Mugikura, Takahiro Metoki, Takaki Murata, Noriko Kurihara, Yasushi Matsumoto, Masayuki Ezura, Shoki Takahashi

O151- Longitudinal MRI Study of the Spinal Cord in Lamin B1 Autosomal Dominant Leukodystrophy Do the First Symptoms Come from the Spinal Cord

Johannes Finnsson, Jimmy Sundblom, Atle Melberg, Raili Raininko

O152- Hyperintense Dentate Nuclei on T1 Weighted MRI

Mehmet Emin Adin, David Mark Yousem, Lawrence Kleinberg



SCIENTIFIC PROGRAM

O153- MR Perfusion Abnormalities in Organophosphorus Poisoning and Correlation with Spect and Neurocognitive Testing Abnormalities

Kovilapu Uday Bhanu, N Khandelwal, Sameer Vyas, Ashish Bhalla, Br Mittal

O154- Atrophy, Focal Spinal Cord Lesions and Alterations of Diffusion Tensor Imaging (DTI) Parameters in Asymptomatic Virus Carriers and Patients Suffering from Human T-Lymphotropic Virus Type 1 (HLTV1) Associated Myelopathy Tropical/Spastic Paraparesis (HAM TSP)

Caroline Cubbison, Massiel Gonzalez-Reinoso, Carlos Vilchez, Eddy Perez-Then, Pedro Roa, Bernd Foerster, Jairo Oviedo, Luis Suazo, Peter Stoeter

O211- Clinical Implementation of Physiological Quantitative MRI; Conclusions from a Survey of UK Neuroradiology Units

Adam Waldman, Stephen Price, Abigail Evans

17:15 - 19:00 PARALLEL SCIENTIFIC PAPER PRESENTATIONS (Vascular Interventional 1)

Moderators: Abdulkader Al Azzaz, Saudi Arabia, Peter Stoeter, Dominican Republic Topkapı A Hall

O155- Treatment of Multiple Intracranial Aneurysms with One Stage Coiling

Byung Moon Kim, Pyoung Jeon, Dong Joon Kim, Dong Ik Kim

O156- Endovascular Treatment of Ruptured Blister Like Aneurysms with Special Reference to the Flow Diverting Strategies

Mustafa Gok, Celal Cinar, Halil Bozkaya, Ismail Oran

O157- Factors Associated with Complications and Recanalization of Embolized Pericallosal Artery Aneurysms

Goran Pavlisa, David Ozretic, Marko Rados

O158- Treatment of Elastase Induced Aneurysms in New Zealand White Rabbits with a New Flow Diverting Device the Derivo Embolization Device

Andreas Simgen, Desiree Ley, Umut Yilmaz, Ruben Mühl-Benninghaus, Körner Heiko, Yoo-Jin Kim, Bruno Scheller, Andreas Müller, Wolfgang Reith

O159- GREAT- a Randomised Aneurysm Trial Procedural Safety and Core Lab Assessed Angiographic Baseline Results

Christian A. Taschner, René Chapot, Vincent Costalat, Jerome Berge, Patrick Courtheoux, Alessandra Biondi, Laurent Pierot, Rafael Blanc, Ansgar Berlis, Horst Urbach, Hervé Brunel, Betty Jean, Sophie Gallas, Xavier Barreau, Krzysztof Kadziolka, Jean Gabrillargues, Samer El Shikh, Hubert Desal, Jens Fiehler, Alain Bonafé

O160- An Analysis of Intraoperative Adverse Events for Interventional Therapy of Intracranial Aneurysms Based on Ruptured Status

Sundeep Mangla, Yaseen Karim, Ahmed Eldib

O161- MoyaMoya Disease

Kirankumar Dyawarkonda

O162- Endovascular Working Channel Through the Wall of Small Vessels to the Extra Vascular space in CNS Liver and Heart

Johan Lundberg, Stefan Jonsson, Staffan Holmin

O163- Posterior Circulation Dissecting Aneurysms review of 87 Cases from a Single Center

N K Mishra, Chetan Ravi, L Joseph, S B Gaikwad

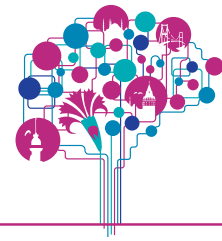
O164- Ruptured Basilar Artery Perforator Aneurysms Outcome in 5 Cases

Robert Forbrig, Lorenz Ertl, Maximilian Patzig, Christian Brem, Hartmut Brückmann, Gunther Fesl

7-12 September 2014
ISTANBUL, TURKEY

LUTFI KIRDAR CONVENTION & EXHIBITION CENTER

XXth
Symposium
Neuroradiologicum



SCIENTIFIC PROGRAM

O165- The Wee (Within 24 Hours) Aneurysm Endovascular Coiling After Subarachnoid Hemorrhage Single Center Experience

Ossama Mansour, Abdelrahman A.

O166- Virtual Stenting of Intracranial Aneurysm for Stent Alone Treatment by Using Computational Fluid Dynamics Analysis

Dae Chul Suh, HyungBin Yu, Yunsun Song

17:15 - 19:00 PARALLEL SCIENTIFIC PAPER PRESENTATIONS (Vascular Interventional 2)

Moderators: Ozenc Minareci, Turkey, Francis Hui, Singapore

Topkapı B Hall

O167- Diameter and Length Change of Carotid Stent after Deployment in a Small Case Series

Te-Chang Wu, Yu-Kun Tsui, Chien-Jen Lin

O168- Cervical Artery Stenting Prior to Intracranial Thrombectomy in Endovascular Treatment of Acute Stroke does not Impair Clinical Outcome at 90 Days

Wiebke Kurre, Marta Aguilar-Pérez, Sebastian Fischer, Elisabeth Schmid, Hansjörg Bänzner, Hans Henkes

O169- Endovascular Management of Carotid Blowout Syndrome in Patients of Head and Neck Cancers

Feng-Chi Chang, Chao-Bao Luo, Wan-Yuo Guo, Michael Mu Huo Teng, Jiing-Feng Lin, Chung-Jung Lin

O170-Traumatic Carotid Cavernous Fistula Single Balloon Treatment Experience

Prijo Sidipratomo, Jacub Pandelaki

O171- Safety and Long Term Efficacy of Flow Diversion versus Standard Coiling in the Treatment of Unruptured Carotid Ophthalmic Aneurysms a Retrospective Analysis

Federico Di Maria, Silvia Pistocchi, Frédéric Clarençon, Raphael Blanc, Eimad Shotar, Bruno Bartolini, Jacques Chiras, Hocine Redjem, Nader Sourour, Michel Piotin

O172- ECA Stenting in Cerebrovascular Insufficiency Indications Efficacy and Durability Single Clinical Experience

Ossama Mansour, Mohamed Megahed

O173- Endovascular Treatment of Rupture Internal Carotid Artery Pseudoaneurysm After Radiotherapy for Head and Neck Tumor Long Term Follow Up

Sherman Lo, WL Poon, YL Cheung, CM Chan, KW Tang, PH Wong

O174- Utility of Flat Detector PBV Source Images in Diagnosing Intracranial Arterial Stenosis

Sheng-Che Hung, Chung-Jung Lin, Wan-Yuo Guo, Chao-Bao Luo, Feng-Chi Chang

O175- Intracranial Angioplasty and Stenting for Symptomatic Stenotic Atherosclerotic Disease the KFMC Experience

Sultan AlQahtani, Fahmi Alsenani, Hussam abo-shaer, Ayman Hamad

O176- Stent Assisted Coiling Using the Acandis Acclino Device and Short Term Follow up

Heiko Koerner, Wolfgang Reith, Andreas Simgen, Ruben Muehl-Benninhaus, Umut Yilmaz

O177- Endovascular Intervention for Galenic Venous Malformation and Dilatation. Therapeutic Decision and Genetic Analysis

Yuo Iizuka, Yoshiaki Tsutsumi, Yoshifumi Konishi



SCIENTIFIC PROGRAM

17:15 - 19:00 PARALLEL SCIENTIFIC PAPER PRESENTATIONS (Vascular Interventional 3)

Moderators: Baran Onal, Turkey, Sobri Muda, Malaysia **Halic Hall**

O178- Hybrid Y Configured Dual Stent Assisted Coil Embolization in the Treatment of Wide Necked Bifurcation Aneurysms

Erol Akgul, Tugsan Balli, Erol Aksungur

O179- Endovascular Treatment of Complex Cerebral Large and Giant Aneurysms Using A Telescopic Combination of the Leo and Silk Stents

Vania Anagnostakou, Muzaffer Saglam , Mujgan Orman , Osman Kizilkilic , Civan Islak , Naci Kocer

O180- Endovascular Coil Embolization for Distal Posterior Cerebral Artery (PCA) Aneurysm

Masaru Hirohata, Kimihiko Orito, Yukihiro Nakamura, Motohiro Morioka

O181- High Mesh Density Low Permeability Flow Diverter in the Treatment of Intracranial Aneurysms a Prospective Non randomized Multicenter Clinical Trial

Ajay K Wakhloo, Christian A. Taschner, Pedro Lylyk, Joost de Vries, Javier Lundquist, Alessandra Biondi, Marius Hartmann, Istvan Szikora, Laurent Pierot, Sakai Nobuyuki, Imamura Hirotooshi, Nader Sourour, Ian Rennie, Martin Skalej, Oliver Beuing, Alain Bonafé, Francisco Mery, Francis Turjman, Patrick Brouwer, Edoardo Boccardi, Luca Valvassori, Shahram Derakhshani, Marc Litzenberg, Mathew Gounis

O182- Stent and Balloon Assisted Coiling of Ruptured Cerebral Aneurysms in the Acute Stage

Kirill Orlov, Vadim Berestov, Alex Krivoshapkin, Dmitry Kislitsin, Timur Shayakhmetov, Anton Gorbatikh, Pavel Seleznev

O183- MCA Aneurysms Coiling without Assisted Technique Our Experience

Umair Rashid Chaudhry

O184- Y-Stent Assisted Coiling of Bifurcation Aneurysms with Open Cell Stents

Nicola Limbucci, Leonardo Renieri, Sergio Nappini, Arturo Consoli, Andrea Rosi, Salvatore Mangiafico

O185- Y-Stent Technique for Endovascular Treatment of Wide Neck Bifurcation Cerebral Aneurysms

Kamil Zeleňák

O187- Long term follow up in Intracranial Aneurysms Treated Using the Surpass Flow Diverter Stent

Alessandra Biondi, Elisa Pomerio, Florence Descourvierer, Arnaud Flores, Clara Prud'homme, Eviane Farah, Françoise Cattin

O188- Flow Diverter Stenting in Intracranial Aneurysms Previously Treated with a Regular Stent Should We Do It

Alessandra Biondi, Elisa Pomerio, Arnaud Flores, Katia Gete, Clara Prud'homme, Eviane Farah, Françoise Cattin

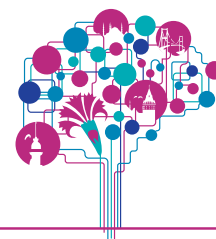
O189- Safety and Efficacy of a New Device for the Treatment of Wide Neck Bifurcation Aneurysms (pCONus) – Preliminary Experience

Marta Aguilar-Pérez, Wiebke Kurre, Oliver Ganslandt, Hansjörg Bätzner, Hans Henkes

7-12 September 2014
ISTANBUL, TURKEY

LUTFI KIRDAR CONVENTION & EXHIBITION CENTER

XXth
Symposium
Neuroradiologicum



SCIENTIFIC PROGRAM

Friday, September 12, 2014

ADULT DIAGNOSTIC NR

Anadolu Auditorium

08:30 - 10:30 **Multiple Sclerosis 1**

Moderators : Tatjana Stosic Opincal, Serbia, Benjamin Adapon, Philippines

Neuroradiological manifestations of novel treatments

Tarek A. Yoursy

UCL Institute of Neurology / National Hospital for Neurology & Neurosurgery, UK

Susceptibility-Weighted MR Imaging in Multiple Sclerosis

Alex Rovira

Hospital Universitari Vall d'Hebron Barcelona, Spain

MRI Monitoring in MS Treatment Efficacy and Safety

Yukio Miki

Osaka City University Diagnostic and Interventional Radiology Osaka, Japan

ADULT DIAGNOSTIC NR

Topkapı AB Hall

08:30 - 10:30 **Advanced Techniques**

Moderators : Cecilia Okuma Ponce, Chile, Lars Stenberg, Sweden

Imaging biomarkers in Neuroradiology

Pia Sundgren

Lund University, Sweden

Exciting and challenging in ultra-high field MR

Juan Villa Blanca

UCLA David Geffen School of Medicine, USA

Role of SWI in CNS Disorders

Giulio Zuccoli

Children's Hospital of Pittsburgh of Upmc, USA

O030-Correlative Assessment of Tumor Microcirculation Using Contrast Enhanced Perfusion MRI and Intravoxel Incoherent Motion Diffusion Weighted MRI Is there a Link between Them

Vasileios K. Katsaros¹, Christian Braun², Jens Schittenhelm³, Tze Hern Teo⁴, Choon Hua Thng⁴, Tong San Koh⁵, Sotirios Bisdas⁶

University of Athens of MRI and Neuroradiology Athens-Greece¹ University of Tübingen Department of Neurology -Germany² University of Tübingen Department of Neuropathology -Germany³ National Cancer Center Department of Oncologic Imaging -Singapore⁴ Duke-NUS Graduate Medical School Center for Quantitative Medicine -Singapore⁵ University of Tübingen Department of Neuroradiology -Germany⁶

INTRAVASCULAR INTERVENTIONAL NR

Marmara Hall

08:30 - 10:30 **Endovascular Cerebral Pial AVM Treatment in 2014**

Moderators : Eva Jacobsen, Norway, Cagin Senturk, USA

Transvenous intranidal AVM treatment: When and How?

Jacques Moret

Beaujon University Hospital, France



SCIENTIFIC PROGRAM

O031-Predictive Factors for Neurological Outcome after an Intracerebral Hematoma Secondary to BAVM Rupture

Eimad Shotar¹, Frédéric Clarençon¹, Nader Sourour¹, Federico Di Maria¹, Mathieu Debare², Vincent Degos², Aurélien Nouet³, Chiheb Zeghal², Jacques Chiras¹
*Pitié-Salpêtrière Hospital, Université Paris VI University Department of Interventional Neuroradiology Paris, France*¹ *Pitié-Salpêtrière Hospital, Université Paris VI University, Neuro Intensive Care Unit, France*² *Pitié-Salpêtrière Hospital Université Paris VI University, Department of Neurosurgery, France*³

COFFEE BREAK 10:30 - 11:00

ADULT DIAGNOSTIC NR

Anadolu Auditorium

11:00 - 12:30 **Multiple Sclerosis 2**

Moderators : Renhua Wu, China, Patricia Orellana, Chile

MR Imaging in the Radiologically Isolated Syndrome

Alex Rovira

Hospital Universitari Vall d'Hebron Barcelona, Spain

Imaging of grey matter pathology in Multiple Sclerosis.

Tarek A. Yoursy

UCL Institute of Neurology / National Hospital for Neurology & Neurosurgery, UK

Use of brain and spinal cord MRI for differential diagnosis

Majda Thurnher

Medical University Vienna, Austria

O032-Neuromyelitis Optica Neuromyelitis Optica Spectrum Disorder with Brain Abnormalities as Initial Presentation Imaging Characteristics and Clinical Correlation Preliminary Study

In Ho Lee¹, Scott Newsome², Gunes Orman¹, Michael Levy², Yeliz Pekcevik¹,

Maureen Mealy², Izlem Izbudak¹

*The Johns Hopkins Medical Institutions RADIOLOGY Baltimore-United States*¹ *The Johns Hopkins Medical Institutions NEUROLOGY -USA*²

ADULT DIAGNOSTIC NR

Topkapı AB Hall

11:00 - 12:30 **Intraoperative neurosurgical imaging**

Moderators : Sarmite Dzelzitis, Latvia, Murat Ibatullin, Tataristan

Intra Operative Neurosurgical Imaging: What Information is Necessary from Imaging?

Vasileios K. Katsaros

University of Athens Department of MRI Athens-Greece

On Line Imaging (Dedicated Low Field Open Systems) vs Step Wise Imaging (Modified Conventional High Field Systems)

Yuko Ono

Tokyo Women's Medical University Diagnostic Imaging and Nuclear Medicine Shinjuku-ku-Japan

Neurosurgical Experience from Open Craniotomies and Transsphenoidal Approaches

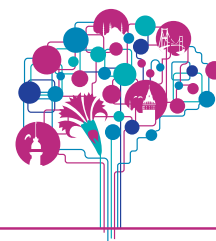
Yuko Ono

Tokyo Women's Medical University Diagnostic Imaging and Nuclear Medicine Shinjuku-ku-Japan

7-12 September 2014
ISTANBUL, TURKEY

LUTFI KIRDAR CONVENTION & EXHIBITION CENTER

XXth
Symposium
Neuroradiologicum



SCIENTIFIC PROGRAM

INTRAVASCULAR INTERVENTIONAL NR

Marmara Hall

11:00 - 12:30 **Endovascular Dural AVF Treatment in 2014**

Moderators : German Castillo, Ecuador, Shigeru Nemoto, Japan

How did Onyx and MMA approach change the treatment indications in recent years?

Christoph Cognard

Hopital Purpan, France

When should transvenous treatment be used?

Laurent Spelle

Beaujon Hospital - Paris Diderot University, France

How Can I Decrease the Rate of Complication in Dural AVF Management

Daniel Roy

CHUM Notre-Dame Hospital Radiology Montreal, Canada

12:30 - 13:30 **LUNCH BREAK**

13.00-14.00 **Poster Presentations**

Neurological Sciences

Moderator: Wan Yuo Guo, Taiwan

SULTAN 1

EP231- Default Mode Network Functional Connectivity in Middle Aged Cognitively Intact APOE ϵ 4 Carriers
Chi Tseng, David Yen-Ting Chen, Chi-Jen Chen

EP232- Neurochemistry in Hypomyelination Model Mouse Depicted on MR Spectroscopy

Jun-ichi Takanashi, Nobuhiro Nitta, Hitoshi Terada, A. James Barkovich, Hiroko Tada, Ichio Aoki

EP233- Clinical of Study of Chemical Exchange Saturation Transfer MRI on Brain Metastases at 1.5 Tesla

Yonggui Yang, Zhiwei Shen, Zhongping Zhang, Fang Chen, Gang Guo, Renhua Wu

EP234- Brain Metabolic Alterations of Patients with Diabetic Hypertension: A 2D-1H Proton Magnetic Resonance Spectroscopic Imaging Study

Zhen Cao, Bi Di Ye, Zhi Wei Shen, Ren Hua Wu, Ye Yu Xiao

EP235- **A Potential Method for Imaging GABA in vivo Using Chemical Exchange Saturation Transfer**

Tao Zhang, Zhuozhi Dai, Yanlong Jia, Renhua Wu

EP236- Brain Metabolism in HIV infection a 7T Proton Magnetic Resonance Spectroscopy Study

Mona Mohamed, Peter Barker, Richard Skolasky, Ned Sacktor

EP237- Acute Effect of Methadone Maintenance Dose on Cerebral Blood Flow in Heroin Users under Methadone Maintenance Treatment

Hsiu-Ling Chen, Pei-Chin Chen, Chien-Chih Chen, Meng-Chang Tsai, Wei-Che Lin

EP238- Investigating Neuronal Metabolic Characterization in Peritumoral Area of Brain Glioma using 1H MRS at 7T

Meizhi Yi, Yan Gen, Guishan Zhang, Tao Zhang, Renhua Wu

EP239- Fetal Magnetic Resonance Imaging in the Pathology of the Central Nervous System

Mercedes Serra, Maria Sol Toronchik, Cecila Rollan, Hernan Chaves, Gabriela De Pino, Adolfo Etchegaray, Claudia Cejas, Carlos Romero



SCIENTIFIC PROGRAM

EP240- Posterior Fossa Malformations Characteristic Findings on MRI
Gabriela Michelin, M. Sol Toronchik, M. Mercedes Serra, Carlos Romero

EP241- Brain Intrinsic Resting State Functional Connectivity Modulation Induced by Mental Effort in Multiple Sclerosis Patients with Fatigue
Emanuele Pravata, Carlo Sestieri, Massimo Caulo, Chiara Zecca, Alessandro Cianfoni, Claudio Gobbi

EP242- Resting State fMRI in Assessing Changes of DMN Activation Pattern in Neurodegenerative Diseases
Evgeniia Seliverstova, Yury Seliverstov, Rodion Konovalov, Marina Krotenkova, Sergey Illarioshkin

EP243- FLT-PET/CT in Restaging Primary AND Metastatic Brain Lesions
Alexandra Nikaki, Panagiotis Georgoulis, Vassiliki Filippi, Ioannis Tsougos, Fani Vlachou, Dimitrios Kechagias, Theodoros Pipikos, Roxani Efthymiadou, Vassilios Prassopoulos, Ioannis Andreou

EP244- Volumetric Analysis of Atrophy in Alzheimer's disease and Mild Cognitive Impairment
Berrin Cavusoglu, Emel Ada, Derya Durusu Emek Savas, Gorsev Yener

Research

Moderator: **Diana Rodriguez, USA**

SULTAN 2

EP245- Vascular Occlusion Effects of Endovascular Radiofrequency Wire Electrode on Rabbit Renal Artery Comparison with PVA Embolization
Daehyun Hwang, wooyoung You

EP246- Preliminary Analysis of Chemical Exchange Saturation Transfer (CEST) Images and Z Spectrum of Different Metabolism Models
Yonggui Yang, Zhiwei Shen, Fang Chen, Zhongping Zhang, Xiaojin Xu, Gang Guo, Renhua Wu

EP247- Non Invasive Detection of 2 Hydroxyglutarat in Patients with IDH Mutated Glioma via MR Spectroscopy in a Clinical Setting
Thomas Huber, Christine Preibisch, Jan Bauer, Tobias Boeck-Behrens, Changho Choi, Claus Zimmer

EP248- MR Morphometry of Hippocampus in MDD Patients and Healthy Volunteers
MR-morphometry of hippocampus in MDD patients and Ananyeva N.

EP249- The Diagnostic and Grading Value of Diffusion Tensor Imaging in Patients with Carpal Tunnel Syndrome
Haci Taner Bulut, Adem Yildirim, Burcu Ekmekci, H. Pınar Gunbey

EP250- Tracking of Gd DTPA Labeled Mesenchymal Stem Cells by 7T MRI
Kuan Geng, Yanlong Jia, Tingting Nie, Renhua Wu

EP251- Quantitative MRI for the Evaluation of Active MS Lesions without Gadolinium Based Contrast Agent
Ida Blystad, Irene Håkansson, Anders Tisell, Jan Ernerudh, Örjan Smedby, Peter Lundberg, Elna-Marie Larsson

EP252- The Usefulness of Auditory Brain Stem Response Monitoring on Preoperative Embolization for Hypervascular Skull Base Tumors in Patients with Hearing depression
Miki Hioki, Takao Hashimoto, Yujirou Tanaka, Hirofumi Okada, Daisuke Watanabe, Michihiro Kohno

7-12 September 2014
ISTANBUL, TURKEY

LUTFI KIRDAR CONVENTION & EXHIBITION CENTER

XXth
Symposium
Neuroradiologicum



SCIENTIFIC PROGRAM

EP253- Fabry Disease Brain MRI Findings in Adults and Children

Pfister Pablo, Serra Mercedes, Toronchik Maria Sol, Chaves Hernan , Rollan Cecilia, Yañez Paulina,
Romero Carlos, Reisin Ricardo

EP254- Highly Reconstructed MRI T2 Map by Optimized Principal Component Coefficient Algorithm Based on Compressed Sensing at 7.0 Tesla

Guishan Zhang, Gang Xiao, Zhiwei Shen, Renhua Wu

EP255- Hippocampal Disease Most Prevalent Pathological Conditions at Our Institution

Estefania Triñanes, Pablo Martin Pfister, Cecilia Rollan, Hernan Chaves, Paulina Yañez, Carlos Romero

EP256- Diagnostic Value of Magnetic Resonance Imaging (MRI) and Apparent Diffusion Coefficient (ADC) in Determination of Grading of Astrocytomas

Reyhan Eddy, Rahmad Mulyadi, Tiara Anindhita, Hartono Tjahjadi, Trevino Pakasi

EP257- Effect of a Mediterranean Diet Intervention on 3T MRI-Monitored Carotid Plaque Progression and Vulnerability. A Sub-Study of the PREDIMED Trial

Núria Bargalló-Alabart, Aleix Sala-Vila , Rosa Gilabert , Edwin-Saúl Romero-Mamani, Ramón Estruch , Emilio Ros

EP258- Effects of Selegiline on Lesion Size and Rat Endothelial Cell Adhesion Molecule (RECA) Expression in a Rat Stroke Model

Nandor Pinter, Sandor Nardai , Zoltan Nagy

EP259- Lexicographic Analysis of Neuroradiologic Reports for Identification of Key Concepts and Relationships between Them

Luke Gerke, Bradley Delman

EP262- Evaluation of Corticospinal Tract Radiation Exposure by Implementation of Tractography in Gamma Knife Treatment Planning of Cerebral AVMs

Giuseppe Kenneth Ricciardi, Roberto Foroni, Antonio Nicolato, Michele Longhi, Pasquale Mirtuono, Francesca Benedetta Pizzini, Alberto Beltramello

13:30 - 15:00 ESNR General Assembly

Halic Hall

ADULT DIAGNOSTIC NR

Anadolu Auditorium

13:30 - 15:00

Degenerative Brain

Moderators

: Izlem Izbudak, USA, Maria de Fatima Viane Vasco Aragao, Brazil

Principles of classification analyses in mild cognitive impairment (MCI) and Alzheimer disease.

Sven Haller

Department of Imaging and Medical Informatics, University Hospitals of Geneva and Faculty of Medicine of the University of Geneva, Switzerland

Imaging in Dementia: Role of MRI.

Leonardo Macedo

ALLIAR - CEDIMAGEM - UFJF, Brazil

Movement disorders

Leonardo Macedo

ALLIAR - CEDIMAGEM - UFJF, Brazil



SCIENTIFIC PROGRAM

O033-Voxel based Analysis of Quantitative Susceptibility Data in Subjects with CN MCI and AD

Ji Hye Jang 1, Hye Soo Koo 2, Chang-Woo Ryu 2, Yi Wang 3, Geon-Ho Jahng 4, Eui Jong Kim 1, Woo Suk Choi 1

Kyung Hee University Hospital Radiology Seoul-Korea, South 1 Kyung Hee University Hospital at Gangdong Radiology -Korea, South 2 Weill Cornell Medical College Radiology -United States 3 Kyung Hee University Hospital at Gangdong Radiology, Korea, South 4

ADULT DIAGNOSTIC NR

Topkapı AB Hall

13:30 - 15:00

Legal and Socioeconomic

Moderators : David Yousem, USA, Sherman Lo, HongKong

International Practice Standards With Respect To Legal / Ethical Issues

For Malpractice, Incidental Findings on Research Scans, Financial Implications across National Healthcare Systems

David Yousem

Associate Dean of Professional Development, Johns Hopkins School of Medicine, USA

How to Add, Measure, Proof and Showcase the Value of Neuroradiology

David Yousem

Associate Dean of Professional Development, Johns Hopkins School of Medicine, USA

Forensic Neuroradiology: Cognitive Changes in Brain Trauma and Changes in Criminal Brains

Eduardo Gonzalez-Toledo

LSU School of Medicine, USA

INTRAVASCULAR INTERVENTIONAL NR

Marmara Hall

13:30 - 15:00

Endovascular Treatment of Spinal Vascular Malformations

Moderators : Dong Ik Kim, South Korea, Halil Öztürk, Turkey

Anatomical and angioarchitectural tricks for the succesful endovascular treatment of spinal AVMs and the impact of intraoperative flat panel CTA for treatment planning

Civan Islak

Istanbul University, Turkey

Treatmentof spinal pial vascular malformations: When to treat and not to treat

Alfredo Casasco

Ntra Sra del Rosario Hospital, Spain

COFFEE BREAK 15:00 - 15:30

ADULT DIAGNOSTIC NR

Anadolu Auditorium

15:30 - 17:00

Psychiatric Diseases

Moderators : Sang Joon Kim, South Korea, Seamus Looby, Ireland

Advanced Neuroimaging in Psychiatry

Nivedita Agarwal

Santa Maria del Carmine Hospital, Italy

Neuroimaging in Psychiatry: Depression, Schizophrenia and Bipolar

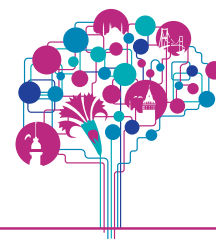
Eduardo Gonzales Toledo

LSU School of Medicine, USA

7-12 September 2014
ISTANBUL, TURKEY

LUTFI KIRDAR CONVENTION & EXHIBITION CENTER

XXth Symposium Neuroradiologicum



SCIENTIFIC PROGRAM

Advanced Neuroimaging in Anxiety and PTSD

Nivedita Agarwal

Santa Maria del Carmine Hospital, Italy

ADULT DIAGNOSTIC NR

Topkapı AB Hall

15:30 - 17:00

Case Discussion

Moderator

: Anne G. Osborn, USA

Anne G. Osborn, USA

Majda Thurnher, Austria

Mauricio Castillo, USA

Paul Parizel, Belgium

INTRAVASCULAR INTERVENTIONAL NR

Marmara Hall

15:30 - 17:00

Pediatric Neurovascular interventions

Moderators

: Cindy Sadikin, Indonesia, Jihad Al Watban, Saudi Arabia

Interventional treatment of pediatric venous and lymphatic malformation

Alejandro Berenstein

Mount Sinai Healthcare System, USA

Endovascular treatment of GVA malformations: Tricks for the success,

Jo Bhattacharya, UK

O034-Paediatric Intracranial Aneurysms Approach and Treatment

*Anne Jutta Schmitt*¹, Adam Rennie², Fergus Robertson², Stefan Brew², Vijeya Ganesan³,

Sanjay Bhate³, Owase Jeelani⁴, Kristian Aquilina⁴

University College London Hospital Radiology London-United Kingdom *1 National Hospital of Neurology and Neurosurgery, Great Ormond Street Hospital Neuroradiology -United Kingdom*

2 Great Ormond Street Hospital Neurology -United Kingdom *3 Great Ormond Street Hospital Neurosurgery -* *4*

17:00 - 17:30 Closing Ceremony

Anadolu Auditorium

17:30 - 19:00 PARALLEL SCIENTIFIC PAPER PRESENTATIONS (Adult NR 4)

Moderators: Baris Diren, Turkey, Sri Andreani Utomo, Indonesia

Marmara Hall

O190- Cerebral Ischemia Detected with Diffusion Weighted MR Imaging After Filter Protected Stenting of High Grade Symptomatic Carotid Artery Stenoses

Ender Uysal, *Ömer Naci Tabakcı*, Deniz Türkyılmaz Mut, Dilek Necioglu Orken, Muzaffer Basak

O191- Clinical Study of Chemical Exchange Saturation Transfer MRI on Cerebral Infarction at 1.5 Tesla

Yonggui Yang, Zhiwei Shen, Xiaojin Xu, Fang Chen, Zhongping Zhang, Gang Guo, Renhua Wu

O192-Limbic-Auditory Interactions of Tinnitus; Evaluation with Diffusion Tensor Imaging

Hediye Pinar Gunbey, Emre Gunbey, Kerim Aslan, Taner Bulut, Asude Unal, Lutfi Incesu



SCIENTIFIC PROGRAM

O193- Utility of DWI-FLAIR mismatch in early stroke in identifying time window to guide management: A study of 32 patients

Ritu Kakkar, Sameer Soneji, Shrinivas Desai

O195- A Five Year Period of Evolution In MR-MRA Imaging Follow-Up Of Large And Giant Intracranial Aneurysms Treated With Pipeline Embolization Device

Carolina Parada, Jorge Chudyk, Hector Lambre, Pedro Lylyk

O196- Can MRI Diagnose Occult Hairline Skull Fractures Better Than CT in Craniocerebral Trauma

Vivek Sindhvani, Monika Arya

O197- The Time Dependent Occurrence Analysis of Intracranial Aneurysm Rupture in North of Sweden and In Czech Republic (6 Years Analysis of Dates Clusters)

Jiri Neuwirth, Frantisek Charvat, Ivana Kralova

O198- Dynamic CT Angiography for the Evaluation of Shunting Vascular Malformation of Brain and Spine

Federico D Orazio, Aldo Victor Giordano, Sergio Carducci, Alessandra Splendiani, Massimo Gallucci

O199- Lesions of the Foramen of Monro Region One Year's Differential Diagnosis

Mariana Diogo, João Jacinto, Isabel Fragata, Carla Conceição, Manuela Mafra, Luís Cerqueira, João Reis

O200- Dural Venous Sinus Morphology in Idiopathic Intracranial Hypertension

Indran Davagnanam, Clare Fraser, Gordon Plant

17:30 - 19:00 PARALLEL SCIENTIFIC PAPER PRESENTATIONS (Adult NR 5)

Moderators: Yelda Ozsunar, Turkey, Matilda Papathanasiou, Greece

Dolmabahce C Hall

O201- International Differences in Neuroradiology Training

Tanja Schneider, David Yousem

O202- MRI Findings in Spinal Tuberculosis in an Endemic Country

Jureerat Thammaroj, Amnat Kitkhumdee, Kittisak Sawanyawisuth, Prathana Chowchun, Kayoon Promon

O203- Susceptibility Weighted Imaging in Parenchymal Neurosyphilis a New Radiological Hallmark

Ilaria Pesaresi, Mario Sabato, Ilaria Desideri, Melania Guida, Michele Puglioli, Mirco Cosottini,

Carlo Bartolozzi

O204- Differentiation of Infective from Neoplastic Rim Enhancing Brain Lesions Using T2 Relaxometry

Hanafiah Mohammad, Shahizon Azura Mohamed Mukari, Norzaini Rose Mohd Zain, Ahmad Sobri Muda, Syazarina Osman

O205- A Typical CNS Tuberculosis

Abdulkader Alazzaz, Fatima Alattas, Abubaker Shadha

O206- NSSaFe Study Observational Study on the Incidence of Nephrogenic Systemic Fibrosis (NSF) In Renal Impaired Patients Following Gadoteric Acid Administration

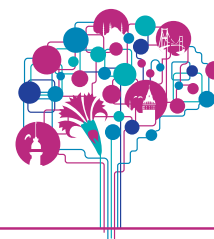
Bruno Beomonte Zobel

O207- The Utility of Gadoterate Meglumine Enhanced MRI in Adult and Pediatric Patients with Central Nervous System Lesions (SENTIO study)

7-12 September 2014
ISTANBUL, TURKEY

LUTFI KIRDAR CONVENTION & EXHIBITION CENTER

XXth
Symposium
Neuroradiologicum



SCIENTIFIC PROGRAM

Raphaelle Souillard-Scemama, Olivier Naggara, Philippe Page, Johan Pallud, Jean François Meder, Catherine Oppenheim

O208- Resting State fMRI Assessment of Language Networks in Epilepsy Patients: A Progress Report
Ali Murat Koc, Ali Yusuf Oner , Melike Guryıldırım, Halil Özer, E. Turgut Tali

O209- Is the Wyler Grade of Hippocampal Sclerosis Reflected on MRI
Horst Urbach, Ralf Schwarzwald, Hans-Jürgen Huppertz, Albert Becker, Jan Wagner, Henriette Tschampa

O210- Fusion of Preoperative MRI and Postoperative CT Images for the Evaluation of Electrode Position in STN DBS
Isabelle Barnaure , Pierre Pollak, Shahan Momjian, Julien Bally, Karl-Olof Lovblad, Colette Boex, Pierre Burkhard, Maria-Isabel Vargas

17:30 - 19:00 PARALLEL SCIENTIFIC PAPER PRESENTATIONS (Vascular Interventional 4)

Moderators: Osman Kizilkilic, Turkey, Adam Pany, Malaysia

Topkapı A Hall

O212- Vascular Injuries after Cranio Spinal Surgery Endovascular Perspective
Mustafa Gok, Celal Cinar, Halil Bozkaya, Ismail Oran

O213- Comparison between Computed Tomography Angiography (CTA) Magnetic Resonance Angiography (MRA) and 2d 3d Rotational Digital Subtraction Angiography (DSA) in the Follow Up of Intracranial Aneurysms Treated by Endovascular Coiling
Chirag K Ahuja, N Khandelwal, Ajay Kumar, Paramjeet Singh, Sn Mathuria, Vivek Gupta

O214- Double Solitaire Mechanical Thrombectomy in Acute Stroke Effective Escalating Strategy for Large Artery Occlusions Refractory to Single Stent retriever Treatment
Stephan Meckel, Vojtech Sychra, Christoph Strassila, Christian A Taschner, Mathias Reinhard, Horst Urbach, Joachim Klisch

O215- Successful Intra Arterial Reperfusion Therapy Improves Clinical Outcomes in Acute Stroke Secondary to Large Vessel Occlusions – TICI Based Analysis
Sundeep Mangla, Raghu Loganathan, Moh Paul, Victor Teresita, Kanna Balavenkatesh, Schori Melissa

O216- Endovascular Cooling Catheter System for Selective Cerebral Hypothermia in Acute Stroke Therapy an Animal Feasibility Study
Stephan Meckel , Andreas Keuler, Lynn Boos, Mukesch Shah, Förster Katharina, Niesen Wolf-Dirk, Giorgio Cattaneo, Martin Schumacher

O217- Transbrachial Approach as a First Access Route for Neurointervention
Takahisa Mori, Tomonori Iwata , Yuhei Tanno , Shigen Kasakura , Yoshinori Aoyagi , Kazuhiro Yoshioka

O218- Balloon Guide Catheter in Complex Mechanical Thrombectomy Procedures of Acute Anterior Circulation Stroke Beyond Proximal Occlusion and Flow Reversal
Theo Demerath, Samer Elshikh, Andreas Keuler, Horst Urbach, Stephan Meckel



SCIENTIFIC PROGRAM

O219- Predictive Value of Neurophysiological Monitoring During Endovascular Mechanical Thrombectomy
Kornelia Kreiser, Ehab Shiban, Silke Wunderlich, Florian Ringel, Claus Zimmer

O220- Pre Surgical Embolization of Nasopharyngeal Angiofibroma a Pakistani Experience
Shahzad Karim Bhatti, Umair Rashid Chaudhry

O221- 3D Vascular Model is Valuable in Neurointervention
Shigeru Nemoto

O222- Preoperative Embolization of Juvenile Nasopharyngeal Angiofibroma: A 2 Years Retrospective Study in Indonesian Public hospital
Prijo Sidipratomo, Indrati Suroyo, Eppy Buchory

O223- Behavioral Difference between NBCA and Onyx for Embolization of Brain Arteriovenous Malformations under Flow Control with ED Coils
Takuya Nakazawa, Atsusi Tsuji, Toshihiro Yokoi, Kenichi Tsuji, Yayoi Yoshimura, Kenji Takagi, Junya Jito, Naoki Nitta, Tadateru Fukami, Kazuhiko Nozaki

17:30 - 19:00 PARALLEL SCIENTIFIC PAPER PRESENTATIONS (Research & Neuroradiological Sciences 3)

Moderators: Yusuf Oner, Turkey, Mohamed Jidane, Morocco

Topkapı B Hall

O224- To Bleed or not to Bleed Prospective Hemorrhage Rates of Cerebral Cavernomas
Omid Nikoubashman, Federico Di Rocco, Michel Zerah, Kshitij Mankad, Martin Wiesmann

O225- Acute Ischemic Stroke in Non Human Primates a Validation Study Using Near Infrared Spectroscopic Tomography for Cerebral Monitoring of Stroke and Intracranial Hemorrhage
Sundeeep Mangla, Frank Barone, Tigran Gevorgyan, Harry Graber, Douglas Pfeil, Yong Xu, Jenny Libien, Jean Charchafli, John Kral, Randall Barbour, Daniel Lee

O226- A Novel 3 Dimensional Voxel based Analysis of Focal Cerebral Ischemia in Rats
Sang-Hoon Cha, Kyung Sik Yi, Chi-Hoon Choi, Hong Jun Lee, Jinwoo Hwang, Sang Rae Lee, Youngjeon Lee

O227- Prognostic Value of Blood Flow Measurements Using Arterial Spin Labeling in Gliomas
Julia Furtner, *Vasileios K. Katsaros*, Benjamin Bender, Christian Braun Braun, Jens Schittenhelm, Marco Skardelly, Sotirios Bisdas

O228- Resting State Network Based Characterization of Epilepsy Related fMRI Activation Patters
Lajos Rudolf Kozák, Louis André van Graan, Umair Javid Chaudhary, Ádám Szabó, Louis Lemieux

O229- Longitudinal Deactivation Changes in Patients with Relapsing remitting Multiple Sclerosis
Sofya Kulikova, Anastasiya Peresedova, Vasiliy Bryukhov, Elena Kremneva, Marina Krotenkova, Igor Zavalishin

O230- Altered Default Mode Network Functional Connectivity in Alzheimer's disease and Its Relation with CSF Biomarkers
Arzu Ceylan Has, Ozlem Celebi, Andac Uzdogan, Filiz Akbiyik, Bulent Elibol, Esen Saka, Kader Karli Oguz

O231- Optimization of Conditional Probabilities of a Bayesian Expert System for Neuroradiology Differential Diagnosis

Ilya Nasrallah, Manoj Tanwar, Suyash Mohan, Harold Kundel, Edward Herskovits, *Nick Bryan*

O232- Effect of MR Imaging Parameter Changes on Fractional Anisotropy Value Differs between the Gray and White Matter of Human Brain

Sang Joon Kim, Young Jun Choi, Choong Gon Choi, Geon-Ho Jahng



XXth
Symposium
Neuroradiologicum

**PLENARY SESSIONS
ABSTRACTS**



PLENARY SESSIONS ABSTRACTS

Monday, September 8, 2014

STROKE

Marmara Hall

**08:30 - 10:30 Basic Pathophysiology of ischemic Stroke and Mimics
Hemodynamic Reserve Concept Clinical Implications and Assessment**

Ethem Murat Arsava

Hacettepe University Neurology Ankara, Turkey

The cerebral blood flow and oxygen supply are kept at steady state levels in a wide range of physiological conditions in order to maintain a continuous supply of energy to the cerebral tissue. One of the mechanisms that contribute to cerebral hemodynamic reserve is the cerebrovascular autoregulatory response, which is characterized by vasodilatation in cerebral arteries in response to decreases in cerebral blood flow. Another mechanism that is triggered in the setting of compromised blood flow is increased oxygen extraction from the systemic circulation. Both of these mechanisms, vasodilatation and increased oxygen fraction, help cerebral tissues to maintain their viability during an acute ischemic insult or chronic cerebral ischemia. Patients with compromised hemodynamic reserve constitute the group of patients who are at risk for future ischemic events. Proper identification of these patients with various methods like perfusion studies, collateral imaging or transcranial Doppler ultrasound, might provide an opportunity for timely administration of certain therapeutic measures.

Pathophysiology of Cerebral Ischemia and Recovery Mechanism of Neuronal Damage

Patricia Desmond

Royal Melbourne Hospital, University of Melbourne Radiology Melbourne, Australia

PURPOSE: To review the underlying pathophysiology of cerebral ischemia and explore recovery mechanisms of neuronal damage

METHODS: Review of past and current literature.

RESULTS: During the initial few hours of vascular occlusion, different metabolic functions breakdown at varying CBF levels. At declining flow rates in both global and focal models of ischemia, protein synthesis is first inhibited in neurons, followed by anaerobic glycolysis, the release of neurotransmitters, impaired energy metabolism, and finally membrane depolarization. Mechanisms that give rise to ischemic cell death occur via three major mediators: unregulated increases of intracellular Ca²⁺ concentration, tissue acidosis, nitric oxide and free radical production. In the early phases of ischemia, the injury is compromised by waves of spreading depression that further compromise regional CBF. In the minutes, hours, days after this initial ischemic insult, brain injury is modulated by: inflammatory processes, the induction of immediate early genes (some of these genes are thought to contribute to cellular destruction, whereas others may mediate protective processes), free radicals, and later by apoptotic mechanisms.

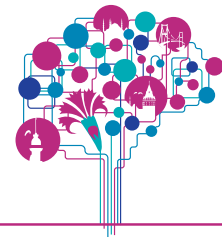
CONCLUSION: The complexity of processes in cerebral ischemia means that there are many potential therapeutic targets that may aid in neuronal recovery.

Controversies in Perfusion Weighted Imaging: Mismatch Concept and Salvageable Brain Tissue

Kei Yamada

Kyoto Prefectural University of Medicine Radiology Kyoto, Japan

Perfusion weighted imaging (PWI) is one of the innovations in the field of stroke imaging. It is, however, still controversial whether it should be used in a routine clinical setting. This is because the patient selection based on PWI is not supported by the results from randomized controlled trials. For instance, the Desmoteplase in Acute Ischemic Stroke Trial (DIAS) II used mismatch concept for patient selection, and ended in negative results [1].



PLENARY SESSIONS ABSTRACTS

More recently, the Mechanical Retrieval and Recanalization of Stroke Clots Using Embolectomy (MR RESCUE) trial failed to show a benefit with a penumbra based patient selection, by either MR or CT perfusion imaging [2].

Besides the diffusion-perfusion mismatch concept, there are a few alternative methods proposed to be beneficial in identifying those who may benefit from reperfusion therapy, which include MRA-DWI mismatch and the clinical-diffusion mismatch. Among those alternatives, it has been implied recently that the MRA-DWI mismatch could be promising [3].

Another area of active research using PWI is the prediction of the tissue fate. Based on the research on primates, it has been suggested that regional cerebral blood flow (rCBF) decrease below 23 ml/100 g/min will lead to electric failure [4]. If rCBF decreases to a further degree or when this condition persists for a long period of time, membrane failure will take place and will lead to irreversible damage. This CBF level has been confirmed to be applicable to humans, using PET, SPECT, and Xe-CT. Whether this concept is also applicable to PWI is another topic that would be dealt in this review [5, 6].

REFERENCES

1. Hacke W et al. Lancet Neurol. 2009; 8: 141-150.
2. Kidwell CS et al. N Engl J Med. 2013; 368: 914-923.
3. Mishra NK et al. Stroke. 2014; 45: 1369-1374.
4. Jones TH et al. J Neurosurg. 1981; 54: 773-782.
5. Akazawa K, Yamada K et al. Neuroradiology. 2008; 50: 939-945.
6. Qiao Y et al. Stroke. 2014; 45: 1355-1362.

Stroke Mimics and Venous Stroke

William T. C. Yuh

Univ. of Washington Radiology Seattle, United States

The primary pathophysiology of venous stroke and associated brain parenchyma are quite different than that of ischemic stroke, although clinically it may be challenge particularly in older patients who may not be able to give clear history or patients wake up with stroke. While acute ischemic stroke is caused by insufficiency of the arterial supply, venous stroke is primarily due to insufficiency in the venous drainage. Therefore the main damage from the arterial vs. venous stroke is different: ischemic infarction vs. hemorrhage respectively. The ischemic component of the venous stroke is only a secondary cause from the venous of congestion, tends to be small and likely occurs in the later stage of the venous occlusion.

Because the underlying pathophysiology is different than the arterial stroke, the imaging characteristics and treatment strategy are usually different than those of the arterial stroke. Venous stroke tends to have no or minimal vasogenic edema (from BBB breakdown) or DWI (from ischemia) abnormality, and not to follow the arterial vascular territory. With the underlying venous congestion, venous stroke may be associated with interstitial edema (increase interstitial fluid flow from venous structure to ventricles), hydrocephalus and massive brain swelling without significant hyperintensity on the T2-weighted or FLAIR images. Because the insult to the brain is not mainly from acute ischemic event, at least initially, the therapeutic window for the venous stroke is usually much longer up to days and weeks, instead of hours as in the acute ischemic stroke.



PLENARY SESSIONS ABSTRACTS

0001-Acute Onset Migrainous Aura Mimicking Acute Stroke MR Perfusion Imaging Features

Franz Fellner ¹, Christine Fellner ¹, Gerhard Haitchi ¹, Milan Vosko ², Maximilian Ziernhöld ¹
AKH Linz Radiology Linz-Austria ¹ AKH Linz Neurology, Austria ²

PURPOSE: In a very limited number of cases, acute migrainous aura may present clinically as acute brain infarction. Since these patients increasingly undergo stroke MR, the aim of this study was to evaluate patterns of MR perfusion abnormalities in acute migrainous aura. **MATERIALS AND METHODS:** In a retrospective analysis, 1850 MR studies performed for the suspicion of acute brain infarction were analyzed for patients suffering from acute migrainous aura and not from stroke (clinically and imaging based). All patients were examined clinically by two neurologists and underwent a stroke MR protocol including perfusion weighted imaging. Two radiologists reviewed perfusion maps visually and quantitative for presence, vascular territory and grade of perfusion abnormality.

RESULTS: Among 1850 MR studies, 20 (1.08%) patients were found who received acute migrainous aura as the final diagnosis after complete clinical and imaging workup.

Hypoperfusion was found in 14 of 20 patients (70%) with delayed rMTT and TTP and decreased rCBV and rCBF, not confined to a single vascular territory. Bilateral hypoperfusion was seen in 3/14 cases, in 11/14 cases hypoperfusion with a posterior predominance was found. TTP and rMTT were the best maps to depict perfusion changes at visual assessment, but also rCBF maps demonstrated significant hypoperfusion at quantitative analysis. In all patients, clinical and imaging follow up was negative for stroke.

CONCLUSIONS: Acute migrainous aura is a rare, but important differential diagnosis among patients referred for MR under the suspicion of acute brain infarction. Characteristic perfusion abnormalities can be seen in the majority of cases.

HEAD & NECK –

Topkapı AB Hall

08:30 - 10:30 Head & Neck Tumors

Orbits and Globe

Suresh Mukherji

Michigan State University, USA

Cranial Nerves of the Orbit 3, 4 And 6

J. W. Casselman^{1,2,3}

Department of Radiology AZ St-Jan Brugge AV, Brugge, Belgium¹

University of Ghent, Gent, Belgium²

Department of Radiology⁴ & Otorhinolaryngology⁵ St- Augustinus, Wilrijk, Belgium³

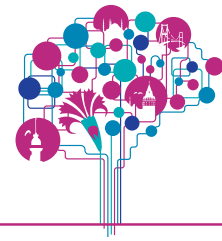
The oculomotor (III), trochlear (IV) and abducent (VI) nerves supply motor fibers to the extraocular muscles of the globe and levator muscle of the eyelid. The third nerve also supplies parasympathetic pupillomotor fibers to the ciliary ganglion. Lesions of the oculomotor nerves can affect their nucleus, fascicular segment, cisternal segment, cavernous segment or their course in the orbital apex.

The MR technique must be adapted to each of these anatomic locations. The nucleus and fascicular segment are best seen on selective axial T2/PD TSE or m FFE/Medic/Merge images and diffusion weighted images. The cisternal segment should be examined using axial heavily T2-weighted submillimetric images (e.g. FIESTA, 3D-TSE, DRIVE, b-FFE) and coronal Gd-enhanced T1-weighted images.

The latter are also suited to study the cavernous segment. The orbital apex region is best evaluated on coronal Gd-enhanced T1-weighted images with Fat Saturation (e.g. Dixon sequence).

The nerve palsy can be isolated but frequently adjacent involved structures cause additional neurologic deficits. These additional symptoms are helpful in the localization of the lesion.

Many lesions can affect the oculomotor nerves but unfortunately imaging can remain negative (e.g. diabetic & hypertensive ocular motor nerve dysfunction). Infarctions, aneurysms, fistulas, neurovascular conflicts,



PLENARY SESSIONS ABSTRACTS

trauma, schwannomas, cavernous hemangiomas, skull base tumors, lymphoma, leukemia, leptomeningeal carcinomatosis, meningiomas, pituitary tumors, inflammatory (e.g. multiple sclerosis, lupus, Behçet, ophthalmoplegic migraine, Tolosa-Hunt) and infectious diseases (e.g. rhombencephalitis, Lyme disease, herpes zoster, fungal infection, cavernous sinus thrombosis) etc. are some of the most frequent causes and will be discussed and illustrated.

Anatomy and pathology of the temporal bone

Burce Ozgen

Hacettepe University, Turkey

Anatomy of the Auditory Pathways

Jan W. Casselman^{1,2,3}

Department of Radiology AZ St-Jan Brugge AV, Brugge, Belgium¹

University of Ghent, Ghent, Belgium²

Department of Radiology⁴ & Otorhinolaryngology⁵ St- Augustinus, Wilrijk, Belgium³

The Central Auditory System (CAS) starts in the inner ear in the organ of Corti. The sensory hairy cells of the auditory pathway are located in the organ of Corti in the scala media. The bipolar first order neurons of the sensory auditory pathway are located in the spiral ganglia. Dendrites from the bipolar neurons carry afferent information from the sensory hairy cells in the organ of Corti to the cell bodies. Axons of the bipolar neurons continue in the internal auditory canal (IAC) where they join the vestibular nerves to form the VIIIth nerve, and divide in an anterior and posterior group to respectively reach the anterior and posterior cochlear nuclei. Heavily T2-weighted submillimetric MR images are needed to evaluate this anatomy in the inner ear, IAC and cerebellopontine angle although Gd-enhanced T1-weighted or FLAIR images are necessary to understand how the blood-labyrinth barrier works. The cochlear nuclei give rise to the trapezoid body which crosses the brainstem and then continues rostrally in the lateral part of the pons as the lateral lemniscus. The cochlear nuclei, together with the superior olivary complex and the nuclei of the lateral lemniscus, constitute the rhombencephalic part of the CAS. Today the non myelinated cochlear nuclei and myelinated lateral lemniscus can be visualised on high resolution multi-echo gradient-echo images. The lateral lemniscus then ascends towards the inferior colliculus which is the mesencephalic centre of the CAS. The brachium of the inferior colliculus connects the inferior colliculus with the ipsilateral medial geniculate body which is the auditory diencephalic nucleus. The auditory radiation starts at the medial geniculate body and reaches the telencephalic centres in the superior temporal cortex: the transverse gyrus of Heschl or primary auditory cortex and the planum temporale. There is also an efferent descending auditory pathway which has an inhibitory and corrective function. The above anatomy and associated function will be discussed in more detail as well as the imaging techniques that allow to visualise this anatomy. Special attention will go to “anatomy” related pathology or how the anatomy explains pathology development and location.

O002-The Relationship Between Race and Gender and Pattern of Isolated Orbital Fractures

Merve Gursoy ¹, Roxana Rivera-Michlig ², *David M. Yousem* ¹, Lukasz S. Babiarz ¹, Michael P. Grant ²

The Johns Hopkins Medical Institutions The Russell H. Morgan Department of Radiology and Radiological Sciences ¹ *The Johns Hopkins Medical Institutions Division of Oculoplastics Surgery, Wilmer Eye Institute* ²

OBJECTIVE: To determine the location of orbital floor fractures in relation to the infraorbital canal and to assess the fracture patterns by race and gender.

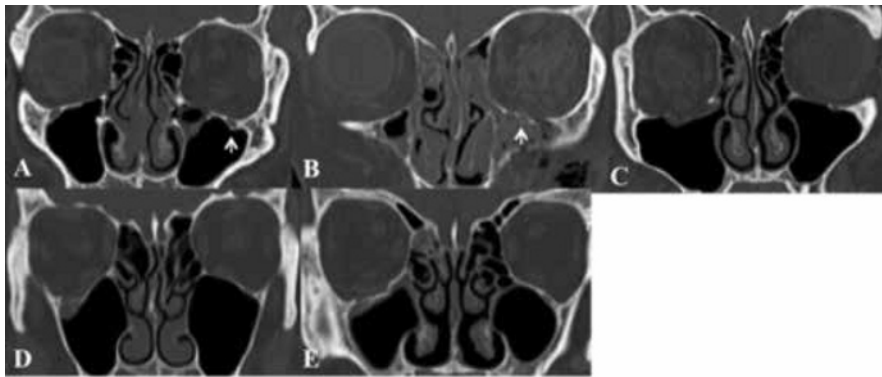
MATERIALS and METHODS: CT scans of patients of different ages, gender, and races with unilateral isolated orbital floor fractures were retrospectively reviewed. The extensions of orbital floor fractures were divided into five groups (Fig. 1): type 1 – orbital floor medial to the infraorbital canal without canal involvement; type 2 – orbital floor lateral to the infraorbital canal without canal involvement; type 3 – orbital floor medial to the infraorbital



PLENARY SESSIONS ABSTRACTS

canal with canal involvement; type 4 – orbital floor lateral to the infraorbital canal with canal involvement; and type 5 – orbital floor medial and lateral to the infraorbital canal with canal involvement. Coincidental medial and lateral orbital wall fractures were also noted. The reviewers were blinded to the demographic information. RESULTS: 50 Caucasian males, Caucasian females, African-American males, and African-American females (mean age of 45.3 years, range: 18-92 years, standard deviation: 18.2) were studied. Type 3 orbital floor fracture was most common in all four subgroups. Isolated orbital floor fractures were the most common in Caucasians (67/100; 67%) and fractures involving the floor and medial wall were most common in African-Americans (52/100; 52%). The presence of an associated medial wall fracture was significantly higher in African-Americans than Caucasians ($p=0.009$).

CONCLUSION: In conclusion, based on our analysis, most isolated orbital floor fractures, regardless of race and gender, involve the orbital floor medial to the IOC and extend to involve the IOC canal proper. The pattern of isolated orbital floor fractures with regard to the IOC did not vary by race or gender. However, African-Americans are more likely to have an associated medial wall fracture, and this is especially true of African-American women. These variations in fracture patterns may provide insight into the biomechanics of the internal buttress of the orbit, and be noteworthy when fracture repair is contemplated.



STROKE

Marmara Hall

11:00 - 12:30 **Diagnosis of Acute Stroke**

Imaging of ischemic parenchyma in hyperacute stage of ischemic stroke.

Zoran Rumboldt

University of Rijeka School of Medicine, Croatia

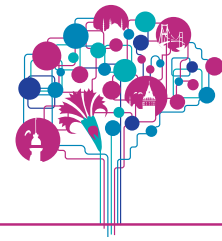
Imaging of Ischemic Penumbra Methods for Assessing Ischemic Penumbra in Experimental and Clinical Models

Patricia Desmond

Royal Melbourne Hospital, University of Melbourne Radiology Melbourne, Australia

PURPOSE: The purpose of this review is to describe neuroimaging modalities capable of identifying ischemic penumbra. The ischemic penumbra is defined as perfused brain tissue that is at a level of perfusion within the thresholds of functional impairment and morphological integrity and which has the capacity to recover if perfusion is improved. It exists, even for a short period of time in the center of ischemia, from which irreversible necrosis propagates to the neighboring tissues over time. METHODS: Current penumbral imaging methods include PET, MR and CT.

RESULTS: The penumbra has become the focus of intense imaging research because accurate detection of this 'tissue at risk' could be used to identify patients who would benefit most from acute treatment. PET is considered to be the gold standard for CBF quantification with tissue viability assessed in terms of maintained



PLENARY SESSIONS ABSTRACTS

rates of cerebral oxygen metabolism. MR diffusion and perfusion-weighted imaging has been used to translate the imaging concept of penumbra to one of diffusion

(DWI)-perfusion mismatch. This conceptual framework of penumbra is not absolute and controversies remain regarding whether DWI can correctly identify infarct core and whether perfusion-weighted imaging accurately identifies tissue at risk outside the DWI lesion. CT correlates of MR DWI perfusion mismatch have been developed and implemented on modern CT scanners. Many problems exist regarding consensus over definitions of penumbra and how post-processing of particularly perfusion data should be optimally performed. It may be that a combination of neuroimaging modalities that include biomarkers of blood flow, metabolism and blood brain barrier breakdown along with molecular imaging markers of cell injury are needed to more clearly delineate irreversibly damaged and potentially salvageable tissue in the penumbra.

CONCLUSION: The mismatch concept is a simplification of the concept of core and penumbra and lacks pathophysiological specificity. However, stroke MRI is the best clinical approximation to the tissue at risk and remains the best performing diagnostic tool for clinical research and therapy. Despite theoretical and real limitations, imaging of the ischemic penumbra remains an area of great clinical interest and active research. Further imaging developments may aid in delivering a more accurate picture of the ischemic penumbra.

MRI of Cerebral blood flow, reactivity and beyond (ASL MRI of cerebral blood flow, BOLD and ASL measurements of cerebrovascular reactivity, Beyond CBF: oxygen extraction fraction and cerebral blood volume

Pamela Schaefer

Harvard University, Massachusetts General Hospital, Boston, USA

O003-Based Magnetic Resonance Imaging Reveals Relative Oxygen Extraction Fraction Changes in Patients with Hyperacute Stroke

*Alexandra S. Gersing*¹, *Monika Ankenbrank*¹, *Benedikt J. Schwaiger*¹, *Vivien Toth*¹, *Silke Wunderlich*², *Claus Zimmer*¹, *Christine Preibisch*¹

Technical University Munich, Klinikum rechts der Isar Neuroradiology Munich, Germany ¹ *Technical University Munich, Klinikum rechts der Isar Neurology, Germany* ²

PURPOSE: Hypoxia plays an important role for the outcome in cerebral ischemia. Recently, a new method based on the quantitative blood-oxygenation-level dependent (BOLD) effect and independent measurement of T₂, T₂^{*} and cerebral blood volume (CBV) was proposed for qualitative mapping of the relative oxygen extraction fraction (rOEF). In this study, we applied this BOLD-based method for assessment of rOEF in patients with stroke or severe arterial stenosis. Purpose of this study was to evaluate whether rOEF maps are an improved predictor for penumbra estimation, compared to the established method of the apparent diffusion coefficient (ADC) and time to peak (TTP) mismatch.

MATERIALS AND METHODS: Thirty-six patients (63 ± 16 years old; 14 males) with suspected ischemia or severe carotid artery stenosis were examined with a 3 T scanner. Quantitative

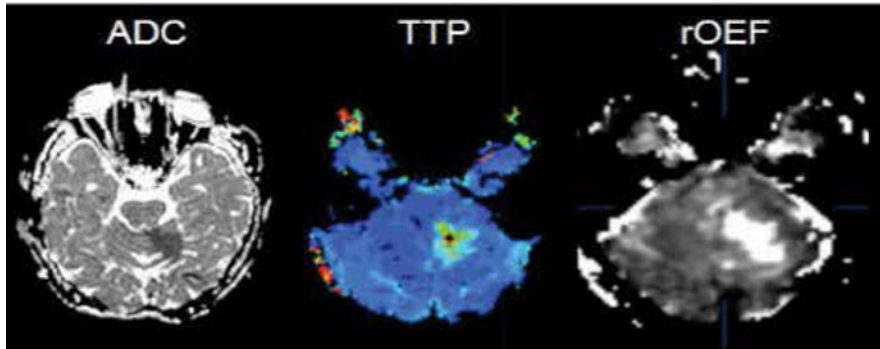
measurements of T₂ multi-echo GRASE and T₂^{*} multi-GE were performed with a measurement time of 3.5 minutes. Cerebral blood volume was derived from the routine DSC PWI. For assessment of hypoxic areas, $rOEF = R2' / (c \cdot rCBV)$ was calculated with $R2' = (1/T2^*) - (1/T2)$, relative rCBV and $c = 4.3 \cdot \pi \cdot \Delta = 317 \text{ Hz}$ at 3 T. Relative OEF maps were compared with FLAIR, ADC, TTP and CBV maps and correlated with the clinical outcome in order to evaluate its prognostic value for patient selection regarding therapy.

RESULTS: Twenty-three patients (15 with acute, 3 with subacute ischemia and 5 with severe arterial stenosis) showed areas of prolonged TTP (> 4s) and/or diffusion restriction. On the lesion side in areas with prolonged TTP without diffusion restriction, rOEF presented a signal intensity increase from 0.59 ± 0.19 to 1.44 ± 0.85 ($p=0.077$). In regions with diffusion restriction this effect was less pronounced (1.03 ± 0.62 , $p=0.082$). Relative OEF lesion was associated with TTP lesion in size and location (Figure). Prolonged TTP values correlated with rOEF value increase ($r=0.50$, $p<0.05$). Regional CBV reduction correlated with rOEF value increase ($r=0.54$, $p=0.046$).



PLENARY SESSIONS ABSTRACTS

CONCLUSIONS: In stroke patients, rOEF measurements were able to detect ischemic areas as well as differences between ischemic core and surrounding tissue. Relative OEF values correlate with perfusion prolongation. These results underline the assumption that areas with increased rOEF outside the ischemic core represent tissue with potentially reversible metabolic and functional impairment.



HEAD & NECK

Topkapı AB Hall

11:00 - 12:30 **Orbit and Paranasal Sinuses**
Anatomy and pathology of the oral cavity and oropharynx
Suresh Mukherji
Michigan State University, USA

Modern imaging of non-neoplastic salivary gland diseases
Minerva Becker
Geneva University Hospital, Switzerland

Thyroid nodules and parathyroid imaging
Laurie Loevner
University of Pennsylvania, USA

STROKE

Marmara Hall

13:30 - 15:00 **Stroke Management on Imaging Findings**
Revisit Diagnosis and Treatment of Acute Stroke: Myth and Truth
William TC. Yuh
Univ. of Washington Radiology Seattle, United States

The gold standards for managing acute stroke has been very much the same for decades and traditionally based upon the ischemic duration, size of the ischemia (NIHSS or size of abnormal imaging) and risk factors (age, HTN, DM, etc.). With the introduction of t-PA, and advancement in stroke imaging, and endovascular/mechanical reperfusion device/technique, there are promising hopes to further improve outcomes of acute stroke. However, controversial remains including the standard inclusion criteria in triaging acute stroke therapy. Furthermore, recent JNEM article reported that mechanical recanalization did not provide better outcome than those by IV t-PA. This talk will revisit the current stroke imaging protocols and the decades' old standards for the management of acute stroke patients. These include using DWI/PI mismatching for the assessment of ischemic Penumbra and triaging of stroke treatment based upon the fixed 3-6 hours' therapeutic window. Furthermore, the current concept of "Time is Brain" and its urgency to salvage penumbra may overshadow the principle of "Do no Harm" to avoid hemorrhagic complication.



PLENARY SESSIONS ABSTRACTS

Not until we can reliably determine the ischemic tissue being alive (viability) or salvageable (reversibility) immediately before triaging a proper therapeutic option, current approach in treating acute stroke may not be personalized and its treatment outcome including the hemorrhagic complication may seem to be a statistical games. This presentation will provide an overview of the functional imaging modalities, including ultra-high field MRI (7 and 8 T), and their potential integration into therapy paradigms for the treatment of acute ischemic stroke.

CT and MRI Strategies to Guide Reperfusion Therapies

Rüdiger von Kummer

University Hospital Neuroradiology Dresden, Germany

BACKGROUND: The rationale of reperfusion therapies is the enhancement of perfusion through ischemic, but still viable brain tissue. This paper will discuss imaging strategies with impact on acute stroke therapy and clinical outcome.

METHOD: Review of CT and MRI strategies.

RESULTS: Randomized prospective studies that have tested the effect of different imaging strategies for a proven effective ischemic stroke treatment are missing. In theory, reperfusion therapy is clinically effective in patients with arterial obstruction and functionally relevant brain ischemia, if the treatment can recanalize the artery and enhances blood supply to ischemic brain tissue that is not yet damaged and able to regain neuronal function. This means that brain imaging should provide the following information: Type and site(s) of arterial obstruction(s), volume and degree of perfusion deficit, capacity of collateral blood flow, and volume of ischemic damage (infarction). This information is provided by either CT or MRI in combination with CT angiography (CTA) and CT perfusion imaging (CTP) or with MR angiography (MRA) and MR perfusion imaging (MRP).

DISCUSSION: The assessment of arterial obstruction often allows the diagnosis of underlying arterial disease and thus secondary prophylaxis. Moreover, it allows an estimate of the extent of perfusion deficit and collateral capacity and can thus be used as a surrogate for CTP or MRP. Thin slice CT detects thrombi with high accuracy. Non-enhanced CT is highly specific for ionic edema and thus for the first stage of infarction. Diffusion weighted MRI (DWI) is sensitive for cytotoxic edema that may develop into infarction, but can recover with early reperfusion. DWI is highly supportive to early recognize the pattern of brain ischemia and thus to diagnose its cause. Tenecteplase have been shown to be effective in acute stroke patients selected by CT, CTA and CTP. Trials with Desmoteplase are ongoing in patients selected by CT/CTA or DWI/MRA only. The near future will show whether imaging information is superior to the surrogate marker "time" in identifying patients who will benefit from reperfusion therapies.

Hemorrhagic Transformation and Reperfusion Hemorrhage Clinical and Radiological Predictors and Prognosis

Rüdiger von Kummer

University Hospital Neuroradiology Dresden, Germany

BACKGROUND: Hemorrhagic transformation of ischemic brain tissue and brain hemorrhage after arterial recanalization may cause disability and death that may be avoided by a better understanding of causes and conditions.

METHODS: Review of the available literature.

RESULTS: Hemorrhagic transformation (HT) of ischemic brain tissue is the final consequence of ischemic blood-brain-barrier breakdown visible in all ischemic infarctions under microscope. The degree and extent of ischemia as hyperglycemia facilitate macroscopic HT that can be categorized into hemorrhagic infarctions (HI) and parenchymal hematoma (PH) each graded in to 1 (minor) and 2 (major). PH2 is thus defined as a dense clot covering > than 1/3 of the infarction and causing mass effect. It is often associated with neurological deterioration in contrast to the other HT categories. Symptomatic intracranial hemorrhage (SICH) is defined as



PLENARY SESSIONS ABSTRACTS

a HT causing neurological deterioration by more than 3 points on the NIH stroke score scale. Brain hemorrhage after arterial recanalization event without thrombolysis is best explained by arterial hypertension affecting brain territories with impaired blood flow autoregulation.

DISCUSSION: The diagnosis of SICH requires brain imaging in case of neurological deterioration after ischemic stroke and a careful judgment whether brain hemorrhage, brain edema or infarct expansion were causing neurological deterioration. Patients need careful arterial blood pressure monitoring after arterial recanalization. Lowering of arterial blood pressure may avoid hyperperfusion syndrome and brain hemorrhage.

O004-Structural and Functional Correlation in Normal and Abnormal White Matter in the CARDIA Cohort

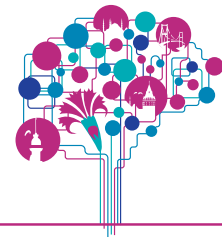
Harsha Battapady ¹, Ilya Nasrallah ¹, Guray Erus ¹, Alex Smith ¹, Lenore Launer ², David Jacobs ³, Pamela Schreiner ³, Kiang Liu ⁴, Beth Lewis ⁵, Christos Davatzikos ¹, Nick Bryan ¹
Univ. Pennsylvania Radiology -United States 1 NIH NIA -United States 2 Univ. Minnesota Epidemiology -United States 3 Northwestern Univ. Medicine -United States 4 Univ. Alabama Medicine, United States 5

INTRODUCTION: MRI is used to detect cerebral white matter hyperintensities (WMH) or leukoaraiosis. WMH are associated with cognitive decline, future infarction and depression. The etiology is unclear; however we hypothesize that cardiovascular risk factors result in alterations of cerebral blood flow (CBF) and vascular reactivity (VR), causing tissue damage, demyelination, and gliosis. These are thought to disrupt neural connectivity, resulting in clinical deterioration. Our purpose is to investigate how CBF, VR and diffusion measurements are affected by the occurrence of WMH, compared to their values on Normal Appearing White Matter (NAWM).

MATERIAL & METHODS: The CARDIA trial is a multicenter study which has followed initially healthy and young patients for over 25 years. 3D T1, FLAIR (FL) and T2, pseudo-continuous arterial spin label (pCASL), diffusion tensor imaging (DTI) and breath-hold fMRI were acquired for 463 participants of the CARDIA cohort. WMH and NAWM were segmented from T1, T2 and FL images fully-automatically using image processing tools. Fractional anisotropy (FA) and Trace (TR) maps from DTI and CBF maps from pCASL were calculated using standard processes. Percent signal-change in BOLD fMRI between breath-hold and rest was calculated as a measure of VR. Mean signal values for WMH and NAWM regions were separately extracted for each image map and were used for statistical analysis by paired t-test.

RESULTS: Significant differences were found in CBF, FA and TR between WMH and NAWM regions. CBF was higher in NAWM than in WMH (28.2 ± 6.75 vs. 21.6 ± 8.76 mm³/100gms/min $p < 0.00001$). FA was higher in NAWM than in WMH (0.39 ± 0.020 vs. 0.30 ± 0.050 , $p < 0.00001$). TR was lower in NAWM than in WMH (0.0023 ± 0.00008 vs. 0.0036 ± 0.0007 , $p < 0.00001$). VR did not exhibit significant differences between WMH and NAWM (0.673 ± 0.458 vs. 0.679 ± 0.496 , $p > 0.05$).

DISCUSSION: WMH simultaneously demonstrates decreased perfusion, decreased FA, and increased TR compared to NAWM. These are compatible with the vascular injury hypothesis. Evaluation of longitudinal change in this cohort may allow evaluation of whether the presence of DTI or CBF abnormalities predicts subsequent development of WMH.



PLENARY SESSIONS ABSTRACTS

HEAD & NECK

Topkapı AB Hall

13:30 - 15:00 Neck: Lymph node and plexuses

Imaging of sinonasal tumors and aggressive inflammation

Laurie Loevner

University of Pennsylvania, USA

PET/CT and PET/MRI in Head and Neck Oncology

Minerva Becker

Geneva University Hospital, Switzerland

Imaging laryngeal and hypopharyngeal cancer

Eloise S. Gebrim

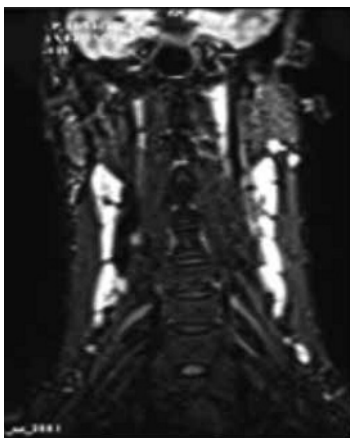
University of Sao Paulo, Brasil

O005-Optimization of Double Inversion Recovery Contrast for Brachial Plexus Imaging of the Neck

Mariah H. Bashir¹, Kwan-Jin Jung¹, Robert J. Bert¹

*Univ. of Louisville Radiology Louisville, USA*¹

INTRODUCTION. Short Tau Inversion Recovery (STIR) and fat saturated T1-weighted (FST1) imaging sequences are used for brachial plexus imaging. Problems with FST1 result from heterogeneous fat suppression. STIR sequences are sensitive to nerve sheath water content and are not typically useful post contrast. We hypothesized that Double Inversion Recovery (DIR) might negate these problems for pre or post contrast imaging of the brachial plexus and began its evaluation. **METHODS.** The formula for DIR ($tia = tib - t1csf * \log(0.5 * (1 - (1 - \exp(-tib/t1csf))) / \exp(-tib/t1csf))$) was placed within commercial mathematical software (Matlab, v.2013b) to determine the inversion times that might be used for brachial plexus imaging. A table of target tissues with known T1 values was created for the independent variables. The long inversion time (T1a) was calculated to null water, using the established T1 (4163msec). The input T1 for calculating the output short TI (T1b) was varied from fat (371msec) to striated muscle (898msec). Compared TI values of the non-nulled tissue (fat or muscle) and nerve (T1=1083) estimated contrast. A commercial MRI system (3T, MAGNETOM Skyra, Siemens Healthcare USA, Malvern, PA) and 3D-DIR sequence (SPACE, Siemens Healthcare USA, Malvern, PA) tested the results. Scan time was targeted as 6 min. and TR and TE were adjusted empirically (maintaining general T2 contrast). Two trained neuroradiologists and an MR physicist evaluated images for anatomic definition and nerve conspicuity. **RESULTS.** The attached image was obtained with the following parameters: slice thickness 1.4mm/TR=5000ms/TE=202ms/T1a2200ms/T1b=300/NSA/Echotrain=193/bandwidth=870Hz/FA=120o/PE steps=213). Contrast



ratios are: 5.4 nerve/fat, 2.0 nerve/muscle. Fat interposed between nerve and muscle dominated considerations in optimizing nerve conspicuity. Retaining some signal in boundary tissue helped maintain anatomic information.

CONCLUSIONS. DIR is a promising technique for brachial plexus imaging, with potential for pre and post contrast assessment of nerve inflammation. Advantages are homogeneous fat suppression and potential Gadolinium contrast sensitivity. We are continuing optimization with complex modeling and clinical testing.



PLENARY SESSIONS ABSTRACTS

STROKE

Marmara Hall

15:30 - 17:00 Hemorrhage

Intracerebral Hemorrhage: A Review

Mauricio Castillo

The University of North Carolina at Chapel Hill, USA

ICH is more common in men, African, Asian and those with high alcohol intake and hypertension. Most non-lobar bleeds occur in the deep brain and are related to hypertension with the most common sites being the putamen and thalamus. Lobar hematomas tend to be related to amyloidosis particularly in the elderly. Genetic risks for ICH exist in hypertension, amyloidosis, cavernomas, HHT, CADASIL, and some collagen vascular diseases. Microbleeds are an important marker of ICH risk. Hypertensive ICH is related to lipohyalinosis of small arteries and occurs in 3 stages: initial bleed, expansion, and edema development. Hematomas are not static and experience significant changes early on leading to the disruption of the BBB, local coagulopathies, ischemia, and inflammation. Hematomas harboring a spot sign expand eccentrically while those without it expand from their center. Amyloidosis involves the leptomeningeal arteries in the posterior brain due to their delamination and subsequent rupture. Amyloidosis results in 3 types of bleeds: SAH and superficial siderosis, microbleeds, and larger hematomas. These patients have a 15% x year risk of rebleeding and recovery tends to be poor. Despite advances in diagnosis surgical treatment leads to only a modest improvement in outcome.

Acute Subarachnoid Hemorrhage: A Review

Mauricio Castillo

The University of North Carolina at Chapel Hill, USA

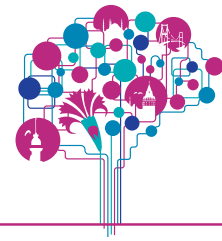
One can think of SAH as a continuing spectrum from diffuse (95%) to localized (5%). The most common causes of diffuse SAH are trauma and aneurysm ruptures. SAH had been classified predominantly using the clinical Hunt and Hess scale and the imaging-based Fisher scale with higher grades having worse outcomes. Blood gets into the SA space via different mechanisms. Factors leading to aneurysm rupture include intraluminal flow dynamics, biology and genetics of walls, and influences of the peri-aneurysmal environment. In trauma, SAH is caused by ruptured or dissected arteries and/or veins and venous thrombosis. Amyloid is an important cause of convexity SAH in the elderly as is venous thrombosis. Venous rupture nearly always occurs at the bridging level and may be due to ischemia of the already weak vein walls. Other entities leading to SAH which will be discussed are: PRES, vasculitis, AVM, AVE, septic aneurysms, tumors, and cavernomas. There are 2 types of benign and focal SAH: perimesencephalic and quadrigeminal but SAH at the perimedullary cisterns carries a poor prognosis and is generally due to vertebral artery injury. For the diagnosis of SAH, a negative CT and CTA offer a positive predictive value equal to that of negative lumbar puncture. The utility of SWI and FLAIR will be addressed. SAH continues to have a poor outcome and those that survive have significant psychological issues. We are starting to identify some genetic factors that lead to a better prognosis and some that lead to a worse one. Life style changes in women make them especially at risk for SAH nowadays.

Assessing the Recovery from Stroke Using Advanced MR Imaging Techniques

Kei Yamada

Kyoto Prefectural University of Medicine Radiology Kyoto, Japan

The advent of new MR imaging technique, such as diffusion-tensor imaging (DTI) had substantial impact on the diagnosis of stroke, and it has now become one of the essential research/clinical tools in this field. Water molecules will preferentially diffuse in a direction parallel to the axon's longitudinal axis but is relatively restricted in the perpendicular axis. This phenomenon can be represented mathematically by the diffusion tensor. The tensors of cerebral white matter can be reconstructed to track three-dimensional macroscopic fiber orientation. This technique is known as tractography. Translation of the longest axis of the tensor (v1) into neural trajectories can be achieved by various algorithms [1, 2].



PLENARY SESSIONS ABSTRACTS

As a clinical tool, this technique primarily targets the intracranial space occupying lesions, i.e. brain tumors and vascular malformations [3-4], but has been also utilized for other conditions, including stroke [5-7]. This method was initially used to identify the spatial relationship between the lesion and vital fiber tracts of the brain. It was later shown that there is in fact correlation between the degree of tract involvement and the clinical symptoms as well as the clinical outcome [6].

REFERENCES

1. Mori S et al. *Ann Neurol* 1999; 45: 265-9
2. Conturo TE et al. *Proc Natl Acad Sci USA* 1999;96:10422-10427
3. Nimsy C et al. *Neuroimage*. 2006; 30: 1219-29.
4. Yamada K et al. *Radiology* 2003; 227: 295-301
5. Kunimatsu A et al. *Neuroradiology* 2003; 45: 532-5
6. Konishi J, Yamada K et al. *Neurology*. 2005;64: 108-13.
7. Sakai K, Yamada K et al. *J Neurol Neurosurg Psychiatry* 2009; 80: 986-90

Physiology of the Blood Clotting System and Its Pharmaceutical Modulation

Ethem Murat Arsava

Hacettepe University Neurology Ankara, Turkey

Platelets and coagulation cascade constitute the two key elements of hemostasis in the human body. Despite their fundamental role for normal physiology, the pharmacological modulation of these systems is highly critical in terms of stroke management. Platelet aggregation and activation can be downregulated via inhibition of the thromboxane pathway (e.g. aspirin), ADP pathway (e.g. clopidogrel) or GPIIb-IIIa receptors (e.g. tirofiban). On the other hand, pharmaceuticals like warfarin and heparin target the coagulation cascade. Warfarin inhibits the synthesis of coagulation factors (II, VII, IX, X) in the liver, while heparin, via its interaction with antithrombin, inhibits coagulation factors that are already present in the systemic circulation. New oral anticoagulants, which have been developed as alternatives to warfarin and do not require routine monitoring, exert their anticoagulant effects either by inhibiting factor X (e.g. abixaban, rivaroxaban, edoxaban) or factor II (e.g. dabigatran).

HEAD & NECK

Topkapı AB Hall

15:30 - 17:00 Temporal Bone & Cranial nerves

Imaging of the Jaw Benign and Malignant Lesions

Osamu Sakai

Boston University School of Medicine Radiology Boston, United States

The jaw consists of the maxilla and mandible, and is very unique as it has teeth in addition to the osseous structure. Jaw lesions develop from both odontogenic and nonodontogenic origins and have varying degrees of destructive potential, many of them being histologically benign. To establish a reasonable differential diagnosis, it is very important to differentiate odontogenic lesions from non-odontogenic lesions, mostly based on the relationship between the lesion and teeth, although it is not always easy. In this lecture, the basic imaging approach to lesions of the mandible and maxilla, as well as characteristic imaging features of these various lesions will be discussed. Common odontogenic cystic lesions include periapical (radicular) and dentigerous (follicular) cysts, and common benign odontogenic tumors represent a broad spectrum of lesions, such as odontomas, keratocystic odontogenic tumors, ameloblastomas, odontogenic myxomas, and adenomatoid odontogenic tumors. Further, malignant odontogenic tumors, although not very common, include malignant ameloblastoma, ameloblastic carcinoma, and other rarer tumors.



PLENARY SESSIONS ABSTRACTS

Common benign nonodontogenic lesions include various fibro-osseous lesions such as periapical cemental dysplasia, ossifying fibromas, and fibrous dysplasia. Malignant nonodontogenic tumors that often involve the jaw include squamous cell carcinomas, osteosarcomas, metastatic tumors, and lymphoma. In addition, vascular lesions such as hemangiomas and arteriovenous malformations may develop in the jaw, further expanding the differential diagnosis. Because lesions of the jaw have a wide range of pathologic features yet similar imaging appearances, familiarity with embryologic characteristics and secondary findings is very important. Patient age at manifestation, prevalence, location within the mandible or maxilla, cystic or solid appearance, border contour, and effect of the lesion on adjacent structures are all considerations in making the diagnosis. Despite this information, however, many lesions are impossible to differentiate without biopsy. In such cases, defining the degree of malignant potential is very helpful. Although imaging will not always provide a specific diagnosis, it should help narrow the differential diagnosis, thereby helping to guide patient treatment. In addition to conventional imaging modalities such as radiographs and CT, utilization of advanced imaging such as MRI and PET will be discussed.

Inflammatory and Malignant Nodes

Vincent Chong

National University Hospital Diagnostic Radiology Singapore, Singapore

The incidence rate of metastases of unknown primary (MUP) is about 2%. Neck nodes account for 10% of these cases. The criteria for the diagnosis of cervical nodal MUP include: no history of previous malignancy; no history of symptoms related to malignancy; no clinical or laboratory evidence of malignancy; and one or more nodes proven by histology or cytology to have malignant tissue. Most primaries are located in the nasopharynx, pyriform sinus, tongue base, and tonsils. Nodal metastasis is the single most important prognostic factor in SCCa of the head and neck. The 5-year adjusted survival in patients with no nodal metastasis is 86%. In patients with metastases the survival is reduced to 63%. In addition, nodal metastases with extracapsular spread further reduce the survival rate to 30%. The level of nodal metastasis correlates significantly with distant metastasis. In patients with supraclavicular lymphadenopathy, the incidence of distant metastasis is 52%. The existing criteria for diagnosing nodal metastasis have serious shortcomings. The most commonly adopted measurement for nodal enlargement is 10 mm. However, 50% of nodes harbouring malignant cells measure less than 5 mm and 25% of nodes with extracapsular spread measures less than 10 mm. In addition, 20% of enlarged nodes are found to be hyperplastic harbouring no malignant cells. In clinical practice therefore, tumours with more than 20% probability of occult nodal metastasis warrant elective node dissection. PET CT has contributed to the evaluation of sub centimetre metastases in the selection of patients for elective neck dissection.

TB lymphadenitis is most commonly seen in the posterior triangle and supraclavicular fossa. The nodes may appear discrete, matted or as confluent masses. Necrosis is encountered in more than 50% of the nodes. Kikuchi-Fujimoto disease (KFD) and Kimura Disease (KD) should be considered in the differential diagnosis of inflammatory nodes. Kikuchi-Fujimoto disease (KFD) is a benign self-limited lymphadenopathy. KD typically shows blood eosinophilia with well-defined nodular masses and plaque-like infiltrative masses usually adjacent to the major salivary glands. The parotid gland is most commonly affected followed by the submandibular gland. More than half of the cases have associated lymphadenopathy.

Ima Perineural spread in head and neck tumors

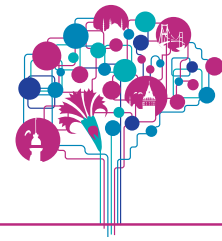
Eloise S. Gebrim

University of Sao Paulo, Brasil

7-12 September 2014
ISTANBUL, TURKEY

LUTFI KIRDAR CONVENTION & EXHIBITION CENTER

XXth
Symposium
Neuroradiologicum



PLENARY SESSIONS ABSTRACTS

OPENING CEREMONY 17:15 - 19:00 ANADOLU AUDITORIUM

Tuesday, September 9, 2014

PEDIATRIC DIAGNOSTIC NR

Anadolu Auditorium

08:30 - 10:30 Developmental Delay

Types of developmental delay; Clinical Evaluation of the Developmentally Delayed Child: What the Child Neurologist needs from the Neuroradiologist.

Ingeborg Krageloh-Mann

University children's Hospital, Germany

Imaging of the Developmentally Delayed Child: Metabolic Disorders

Marjo S. van der Knaap

Department of Child Neurology, VU University Medical Center, Amsterdam, The Netherlands

PURPOSE: The complex structural and functional topography of the brain is reflected in complex patterns of selective vulnerability of brain structures to various adverse influences. These patterns of selective vulnerability can be visualized by MRI and form the basis of the MRI interpretation process called "MRI pattern recognition". Different inborn metabolic defects are associated with highly consistent patterns of MRI abnormalities. Apparently specific structures and parts of structures have an individual vulnerability for specific metabolites and defects. The purpose of the lecture is to illustrate MRI pattern recognition in metabolic disorders in children. **METHODS:** We have consistently studied MRI patterns in metabolic disorders in children in the past 25 years, using a growing database of presently over 3000 cases.

RESULTS: We have defined the MRI patterns for many known (1) and unclassified metabolic disorders (2). The latter has resulted in the definition of multiple novel disorders, including megalencephalic leukoencephalopathy with subcortical cysts (MLC), vanishing white matter disease (VWM), hypomyelination with atrophy of the basal ganglia and cerebellum (HABC), leukoencephalopathy with brainstem and spinal cord involvement and lactate elevation (LBSL), hypomyelination with brainstem and spinal cord involvement and leg spasticity (HBSL), leukoencephalopathy with thalamus and brainstem involvement and lactate elevation (LTBL), and leukoencephalopathies related to a defect in polyol metabolism, a chloride channel ClC-2 defect or mitochondrial alanyl tRNA synthetase defect. Using genetic linkage analysis and now whole exome sequencing, we have identified the genetic defect for all disorders mentioned.

CONCLUSIONS: The MRI phenotypes associated with individual genetic defects have proven to be homogeneous and consistent, allowing an MRI-based diagnosis for these disorders. The basis of the selective vulnerability of individual structures and parts of structures for specific adverse influences is not understood. Insight into the mechanisms behind the MRI phenotypes would greatly enhance our understanding of the pathophysiology of the diseases.

(1) Van der Knaap MS, Valk J. Magnetic Resonance of myelination and myelin disorders. Springer, Heidelberg, 2005.

(2) Van der Knaap MS, Breiter SN, Naidu S, Hart AAM, Valk J. Defining and categorizing leukoencephalopathies of unknown origin: MR imaging approach. *Radiology* 1999; 213: 121-133

Imaging of the Developmentally Delayed Child Structural Abnormalities

Charles Raybaud

Hospital for Sick Children, Toronto, Canada

The term of developmental delay (DD) describes many different conditions which all result in a child not reaching its developmental milestones. It is used in children below 5 years, while mental retardation is used in older children. DD may affect the motor function, language, cognition, social interaction and management



PLENARY SESSIONS ABSTRACTS

of daily activities. It is characteristically static, in contrast with the progressive deterioration that is typically observed in inborn errors of metabolism. Epilepsy, cerebral palsy and autism may be associated. Assessment of DD includes evaluation of chromosomal or genetic disorders (family history, specific features), developmental history (perinatal HIE, stroke, infection, hypothyroidism, TORCH, fetal intoxication, previous oncological treatments), and features suggestive of structural brain abnormality (epilepsy, cerebral palsy, cranial deformity). MR (rather than CT) is also part of it. Given the wide range of possible pathologies, there is no specific imaging protocol: brain size and morphology (including hindbrain), the maturation milestones and any evidence of remote injury should be appropriately investigated.

In a significant number of cases, one of several recognizable patterns may be encountered. Some are related to previous brain injury: TORCH (microcephaly, poor myelination, calcification); HIE of the premature (PVL, periventricular hypomyelination, periventricular porencephaly), or term (deep rolandic gliosis, atrophy of basal ganglia, chronic stroke) neonate. A malformation may be identified: holoprosencephalies (especially lobar and interhemispheric variant), midline defects (commissural agenesis, septo-optic dysplasia), malformations of cortical development, heterotopia, malformations of the hindbrain such as Joubert-related syndrome. Specific images of a neuroectodermal syndrome may be demonstrated (TSC, NF1, macrencephalies).

Other less specific abnormalities are observed in DD patients more than in the general population: mild diffuse atrophy, poor myelination, diffuse prominence of the VR spaces are not much contributive but persistent midline cava, ventriculomegaly with prominent occipital horns and squaring of the lateral ventricular angles, a drooping and prominent callosal splenium, or a poor development of the anterior temporal lobes are more suggestive of a developmental problem. MRS is usually non-contributive, except in the specific instance of a child with severe language delay when it may show the lack of normal Creatine peak specific of an inborn disorder of Creatine metabolism.

O006-MRI Findings in Patients with Developmental Delay with Correlation with Clinical Presentation

Ahmed Elsotouhy, Walid Mubarak, Jehan Alrayahi, Mohamed Alberawi, Hazar Taban,

Hussein Kamel

HMC Radiology Doha, Qatar

PURPOSE: Developmental delay is a frequent clinical presentation referred for MRI evaluation. It is frequently of unknown etiology and with limited options in terms of long term management. In this retrospective study, we sought to determine the efficiency of MRI of the brain in depicting abnormalities in patients with developmental delay.

MATERIALS AND METHODS: MRI studies of 219 pediatric patients, older than 1 year of age presenting with developmental delay, with or without neurological abnormalities, was performed. Findings were reported by an attending neuroradiologist.

RESULTS: Out of 219 children (mean age, 3.8 years; range, 1.0–11.0 years) referred for investigation of developmental delay, 53 patients (24.2%) had isolated developmental delay and 166 patients (75.8%) had developmental delay with an associated neurological abnormality. Neurological abnormalities included 23 with seizures, 64 with hypotonia and 39 with microcephaly and or dysmorphic features.

Normal MRI findings were noted in 45 out of 53 patients with isolated developmental delay (85%). Normal MRI findings were noted in 46 out of 166 patients with associated neurological abnormalities (28%).

Radiological abnormalities were noted in 8 out of 53 patients with isolated developmental delay (15%) of patients. While radiological abnormalities were found in 120 out of 166 patients with an associated neurological abnormality (72%).

Of the 120 patients with neurological abnormality, 7 out of 19 patients with seizure (36.8%), 29 out of 60 patients with hypotonia (48.3%) and 20 out of 35 patients with microcephaly and dysmorphic



PLENARY SESSIONS ABSTRACTS

feature (57%) were reported as having a radiological abnormality respectively. All 6 patients who had more than one neurological abnormality (100 %) were found to have an abnormal MRI. CONCLUSIONS: A large percentage (84%) of patients with isolated developmental delay had no abnormal radiological findings in their MRI examinations. In contrast, 72 % of patients with developmental delay and an associated neurological abnormality were found to have abnormal MRI findings and 100 % of patients with more than one type of neurological abnormality had abnormal radiological findings.

We conclude that the presence of associated neurological abnormalities in patients presenting with developmental delay makes a good indication for MRI examination of the brain. Patients with isolated developmental delay are less likely to benefit from MRI.

SPINE & SPINE INTERVENTIONAL NR

Marmara Hall

08:30 - 10:30 Disc Disease and Management

Imaging of disc disease (herniation and DDD) and nomenclature.

Adam Flanders

Thomas Jefferson University Hospital, USA

Disc: when is it painful, when should be treated?

Giuseppe Bonaldi

Osp. Giovanni XXIII, Bergamo Neuroradiology, Italy

Automated Lumbar Percutaneous Discectomy

Wendell A. Gibby

Adjunct Professor of Radiology, University of California San Diego, CEO – Novard Corporation, USA

In 1984 Dr. Gary Onik, a UCSF radiology resident, invented a novel procedure for decompressing spinal disc herniations. Combining device miniaturization with a highly efficient vacuum-assisted guillotine disc aspiration unit and easy insertion kit created a revolutionary new treatment for contained disc herniations. Once out of the hands of its inventor, the procedure had a somewhat tempestuous career. In early years, radiologists lacked the experience and temperament necessary to perform interventional spine procedures. This led to the deployment of this procedure by

neurosurgeons and orthopedic surgeons whose training and skills were more suited to an open surgical approach where the herniation could be seen and directly removed. The critical skills of patient selection which required a synthesis not just of clinical information, but appearance on MRI and discographic findings to predict whether the herniation was contained, were in short supply.

The theory behind the procedure was fairly simple. Think of a contained disc herniation as a radial tire with a bad bulge. Let some of the air (disc) out, and the bulge recedes, eliminating radial forces on annular nerve fibers as well as direct compression of nerve roots. The procedure, because of its low morbidity, was soon tried on a wide range of patients. Unfortunately, a large majority of patients with spinal degenerative disease are not candidates. First, the disc must be soft and hydrophilic to be removed and cause a measurable decrease in intradiscal pressure. Secondly, there must not be complicating factors such as spinal canal stenosis, ligamentum flavum hypertrophy, significant facet arthritis, disc fragments, etc.

The purpose of this talk is to discuss a 27-year history of performing these procedures including a prospective study looking at discography as one of the predictors for success, morphology of discs both before and after the procedure on high resolution MRI scanning, and various fundamental predictive indices to allow for patient selection that optimize outcome.



PLENARY SESSIONS ABSTRACTS

The epidemic of open back surgery in the U.S.A. and other westernized countries has exposed many people to needless complications and condemned them to lives of chronic failed back syndrome with unrelenting pain and disability. Used judiciously with proper patient selection, this procedure can be an intermediate, minimally invasive approach that achieves excellent results without risks inherent with open surgery. In addition to assisting the practitioner in selecting the appropriate patients for this, a number of tricks of the trade to perform this procedure more effectively, especially in tough to reach places such as the L5-S1 level with a high iliac crest, will be shown. In addition, other useful tips such as pre-surgical disc hydration, intradiscal antibiotics, appropriate postoperative physical therapy, etc., will be discussed.

Familiarity with this technique may spur the development of other image-guided minimally invasive surgical procedures that can diminish morbidity and improve outcomes for degenerative disease of the spine alongside other pain management techniques used by radiologists today.

Spinal Intervention Neuroradiology

Key Words: Percutaneous Discectomy, ALPD, Herniated Disc,

Percutaneous disk injections; a review.

Mario Muto

Cardarelli Hospital, Napoli, Italy

PEDIATRIC DIAGNOSTIC NR

Anadolu Auditorium

11:00 - 12:30 **Fetal and Neonatal Imaging**

Neonatal Encephalopathy: Clinical, Neurophysiological and Imaging aspects

Roberta Cilio¹, P. Ellen Grant²

University of California San Francisco, USA¹, Harvard Medical School, USA²

State of the Art Imaging of Fetal Brain, Head, Neck and Spine.

Andrea Righini

Radiology and Neuroradiology Department, Children's Hospital V. Buzzi, Milan, Italy

State of the art expert Ultrasound is able to diagnose the vast majority of cerebral, spine, and head-neck anomalies; however, in the last decade prenatal MR imaging has proven to provide additional and valuable information in selected clinical fetal abnormal conditions.

Brain: focal cortical plate and sub-plate malformations can be depicted even at a very early stage (before 24 week gestation); ischemic lesions are detectable by Diffusion MR in the acute phase, as remarkable advance of prenatal imaging; complex malformations of midline inter-hemispheric structures are better characterized by MR; rare brain-stem dysmorphisms can be detected by MR, whether associated or not with cerebellar malformations.

Head-Neck: in ocular globe anomalies detection, such as in optic nerve head coloboma case, or inner ear malformations (i.e cystic labyrinth), MR is by far more accurate than Ultrasound; in the diagnosis of upper airway malformative obstruction (i.e. CHAOS syndrome) MR is very valuable, allowing treatment planning.

Spine: spinal content, the cord in particular, can be assessed by MR in cases with Ultrasound ascertained bone dysraphism; so for example, the degree of cord derangement in dyastematomyelia or close dysraphism cases (i.e. myelocystocele maque') can be better assessed.

Future advanced clinical applications of prenatal MR on CNS are foreseeable on the basis of current research results: DTI evaluation of intrauterine brain normal and abnormal development; automatic 3D segmentation of brain structure, comparing data from the proband case with ones of an average fetal brain template; fast H1 spectroscopy studies, monitoring brain metabolites profile overtime (i.e. in growth restriction).

Two types of substantial limitations currently affect prenatal MR imaging: 1) technical ones, since for example the image spatial resolution of most of cases is still not better than 1 mm², so to result much worse than one of postnatal imaging; 2) clinical: since for example the prognostic meaning of many of the newer and more subtle MR findings is not clear.



PLENARY SESSIONS ABSTRACTS

Using Two Compartment White Matter Model of Diffusion Kurtosis Imaging to Reveal the Diffuse Excessive High Signal Intensity (DEHSI) in Preterm Neonates

Jian Yang

The First Affiliated Hospital, Xi'an Jiaotong University, Radiology Department, Xi'an, China

PURPOSE: The diffuse excessive high signal intensity (DEHSI) is extremely common in preterm infants on near-term images. It is still under debate about whether it represents a true white matter (WM) abnormality or just the relative immature in WM. The aim of this study was exploring the water diffusivity in DEHSI regions based on the two-compartment WM Diffusion Kurtosis Imaging (DKI) model.

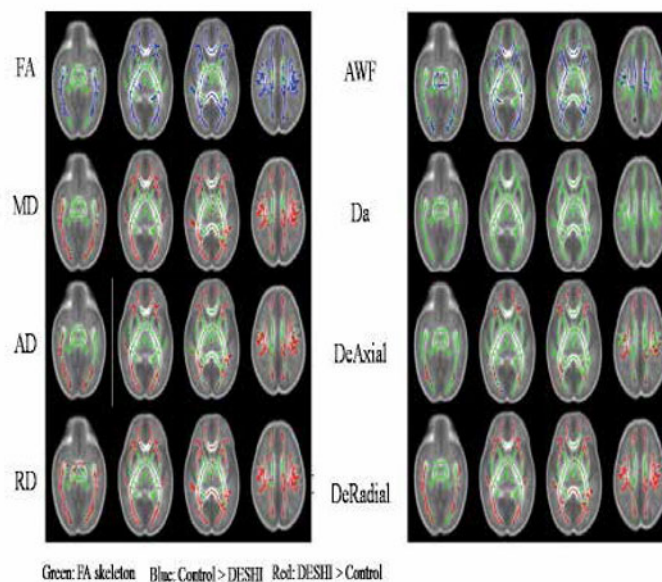
METHODS: 21 preterm neonates with DEHSI and 21 normal controls (matched with gestational age (GA), postmenstrual age at MR scan (PMA) and birth weights (BW)) who underwent MRI at term-equivalent age were enrolled. Conventional MRI and DKI were performed on a 3T scanner (GE, Signa HDxt). DKI protocols were: 18 directions, b value=0,1000, 2000, 2500 s/mm²[SUP]2[/SUP],

TR/TE=8000/120ms, slice thickness= 4 mm without gap, field of view = 180mm×180mm, matrix = 256×256. All DKI data were processed using a custom-written program in MATLAB. ROIs were chosen in centrum semiovale, anterior and posterior periventricular WMs at the level of the body of lateral cerebral ventricle. The difference of all diffusion parameters between DEHSI and control group were analyzed by paired-sample t test. Tract-based spatial statistics (TBSS) analysis was performed to assess differences of all diffusion parameters between DEHSI and control group.

RESULTS: Compared with control group, FA, axonal water fraction (AWF) of above WM regions in DEHSI group were significantly decreased (Fig.1), while mean diffusivity (MD), axial diffusivity (AD), radial diffusivity (RD), axial extra-axonal space diffusivity (De//), radial extra-axonal space diffusivity (DeII) were significantly increased (Fig.1). Mean kurtosis (MK), axial kurtosis (AK), radial kurtosis (RK), intra-axonal diffusivity (Da) (see Fig.1) showed no significant difference between two groups.

CONCLUSION: Based on the two-compartment diffusion model, this study demonstrated that the diffusion changes in DEHSI were mainly due to the increased water and/or enlarged space in extra-axonal space, rather than injuries to axons or the process of myelination.

Fig.1 All diffusion parameters of two-compartment WM DKI model between DEHSI and control neonates: TBSS results





PLENARY SESSIONS ABSTRACTS

O007-Fetal Brain Morphology After in Utero Repair of Open Neural Tube Defects

*Christin Nasiadko*¹, Ianina Scheer¹, Martin Meuli², Ueli Moehrlen², Nicole Ochsenbein³
Kinderspital Zuerich Radiology Zuerich, Switzerland ¹ *Kinderspital Zuerich Surgery* ² *Universitätsspital Zuerich Obstetrics, Switzerland* ³

BACKGROUND: Various neuroanatomical abnormalities, including Chiari type II are seen in children with open neural tube defects. Since the randomized MOMS-Trial, fetal surgery has become a new therapy in selected cases of spina bifida. While clinical outcome has been investigated, there is only sparse information on postoperative morphology. Aim of our study was to compare associated abnormalities before and after fetal surgery, as well as assess morphometric changes of the posterior fossa. **METHOD:** Retrospective review of pre- and postoperative fetal MRI of 9 children who underwent in-utero repair of the open neural tube defects. Between December 2010 and December 2013 a total of 18 MR-studies were performed. Ventricular width, width of the external CSF spaces, tonsillar / cerebellar displacement, cerebellar length, posterior fossa area and associated hydrocephalus, heterotopia or aqueductal stenosis were evaluated.

RESULTS: Preoperative findings were Chiari type II in all cases and heterotopia in one case. After in-utero closure of the spinal defect the hindbrain herniation was reversed in all cases within 4 weeks. In 7/9 individuals (78%) aqueductal stenosis was unmasked in the postoperative studies. Ventricular width decreased in 1/9 case (11%), was stable in 1/9 case (11%) and increased in the other 7/9 cases (78%). The preoperatively diagnosed heterotopia was confirmed postoperatively and newly detected in 3/9 other cases (33%). The spinal defect was completely closed in all cases. **CONCLUSION:** Fetal MRI 4 weeks after in-utero repair of the open neural tube defect shows reversal of hindbrain herniation and of other Chiari type II associated changes.

SPINE & SPINE INTERVENTIONAL NR

Marmara Hall

11:00 - 12:30 Spine Tumors & Treatment

Focal and Diffuse Bone Marrow Diseases, in Particular Neuroradiologic Expression of Different Haematologic Pathologies and Expected Changes during Their Treatment and Infiltrative Vertebral Marrow Changes

Claudio C. V. Staut

Brazilian Society of Neuroradiology, Brazil

With its exquisite contrast resolution and ability to differentiate hematopoietic and fatty marrow, MRI is an important technique for evaluating the bone marrow noninvasively.

The following lecturer reviews the techniques of bone marrow MRI, normal anatomic and physiologic variants, and the MRI findings in common focal and diffuse haematologic marrow disorders with special focus on treatment effects.

MR imaging findings of the marrow after radiation therapy and chemotherapy will be described.

Also a brief discussion on new techniques to evaluate bone marrow.

Advanced imaging of vertebral tumors and tumor-like conditions including Nuclear Medicine

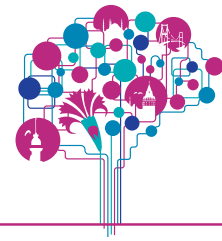
Carlos Romero

FLENI-Neurological Children Disease Foundation, Argentina

Advanced imaging of Spinal Cord tumors and mimics

Majda Thurnher

Medical University Vienna, Austria



PLENARY SESSIONS ABSTRACTS

O008-Targeted Radiofrequency Ablation (tRFA) of Malignant Spine Lesions before Cement Augmentation; Early Clinical Outcome

*Mark Georgy*¹, *Melinda Reyes*², *Jennifer Padwal*³, *Bassem Georgy*⁴

*University of California San Diego Public Health San Diego-United States*¹ *Point Loma Nazarene University Chemistry-Biology -United States*² *University of California, San Diego Medical School -United States*³ *University of California, San Diego Radiology, United States*⁴

Report early clinical outcome of t-RFA followed by cement augmentation in malignant lesions of the spine using a novel bipolar RF ablation system, purpose built for minimally invasive procedures in the axial skeleton. MATERIALS AND METHODS: 51 spinal lytic lesions in 34 patients with different malignant etiologies were included after IRB approval. Primary diagnosis includes; 11 cases of myeloma, 9 cases of breast cancer, 6 cases of lung cancer, 5 cases of lymphomas and one case of each pancreatic, renal and neuroendocrine tumors. The STAR Tumor Ablation System is a bipolar device that contain two thermocouples (TC) positioned at 10 and 20 mm from center of the ablation zone to permit real-time monitoring of the ablation zone. RF warmed cement augmentation via the same guiding cannula was performed after lesion ablation.

RESULTS: All procedures were performed safely with no complications or thermal injury. Ablation time ranged from 1.5-6 minutes. Maximum recorded temperature was 65 °C at the distal TC and 50 °C at the proximal TC (10 and 20 mm from the center of the ablation zone, respectively). TCs on the electrode were used to confirm re-establishment of core temperature prior to cement augmentation. Post procedure CT showed no significant cement leakage. Average VAS scores dropped from 7.8 pre-procedure to 3.6, 2-4 weeks post-procedure. Average ODQ scores improved from 26.5 to 15.7, 2-4 weeks post-procedure. Decreased tumor volume and decreased metabolic activity was confirmed by MRI and PET scan, respectively.

CONCLUSION: Targeted RF Ablation followed by RF warmed high viscosity cement augmentation was performed successfully in this series of malignant spinal lesions. Improvement in pain and functional status was noted in all patients. The STAR Tumor Ablation System is a robust, articulating, navigational osteotome, containing an extensible electrode that permitted minimally invasive access to all lesions, regardless of location. Proximal and distal TCs allowed accurate monitoring of the temperature inside the vertebral body to avoid complications of nearby vital structures. Targeted delivery of high viscosity cement following ablation via the same guiding cannula provided vertebral stability.

PEDIATRIC DIAGNOSTIC NR

Anadolu Auditorium

13:30 - 15:00 Malformations and Epilepsy

Pathophysiology of Epilepsy

Renzo Guerrini

University of Florence, Children's Hospital A. Meyer, Italy

Imaging New Onset Seizures (infection, drugs, channelopathies)

A. James Barkovich

University of California, San Francisco, USA

Imaging Findings in Epilepsy (Lesions Drug Effects Seizure Effects)

Charles Raybaud

Hospital for Sick Children, Toronto, Canada

Epilepsy is a chronic neurological disease characterized by the occurrence of recurrent unprovoked seizures. The mechanism responsible for the seizures may be functional (typically disorder of neurotransmission) or structural. Functional ("idiopathic") epilepsies may usually be recognized clinically and electrographically, and do not typically deserve radiological investigations. Structural epilepsies in children tend to be more severe;



PLENARY SESSIONS ABSTRACTS

as they are related to a structural abnormality of the brain, they may be associated with diverse neurocognitive or neurological deficits (e.g developmental delay, cerebral palsy). They also tend to become refractory with time, so that a surgical approach is considered to remove or isolate the causal lesion and its associated epileptogenic network. The radiological diagnosis now rests upon MR imaging, possibly oriented and complemented by functional studies such as MEG, PET or SPECT. Because the imaging features of the lesion may be subtle, the MR study must be rigorous, using the best available equipment: 3T magnet, high definition coils, high definition T1 (MPRAGE/SPGR), T2 and FLAIR (2-3mm slices) in multiple planes.

Any chronic lesion of the brain may be epileptogenic, notably the early destructive lesions associated with the development of an abnormal circuitry (early stroke, infection, trauma), and obviously any developmental disorder of the cortex. These comprise the focal cortical dysplasia, with the related conditions of hemimegalencephaly and syndromic tuberous sclerosis complex; the epilepsy-associated cortical-based tumors (mostly ganglioglioma, DNET and pleomorphic xantho-astrocytomas); hypothalamic hamartomas; vascular disorders such as Stürge Weber or meningio-angiomas; chronic inflammatory conditions like Rasmussen's encephalitis. Although true hippocampal sclerosis is observed in children, it is not as common an indication of epilepsy surgery as it is in adults. Other disorders may be associated with epilepsy but are generally not amenable to surgery, either developmental (malformations of cortical development and gray matter heterotopia, major brain malformation such as holoprosencephaly or commissural agenesis) or inflammatory (FIRES). Finally imaging is important also to evaluate the effects of the seizures on the brain, and the unwanted effects of the treatments.

New Concepts in Brain Malformations

A. James Barkovich

University of California, San Francisco, USA

O009-Pediatric Epilepsy Diagnostic yield of MRI

Roula Hourani¹, Adeb Oweidat¹, Ahmad Beydoun², Wassim Nasreddine²

*American University of Beirut Diagnostic Radiology Beirut-Lebanon*¹

*American University of Beirut Neurology, Lebanon*²

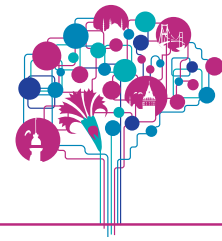
OBJECTIVE: To evaluate pediatric patients with newly diagnosed epilepsy, determine the usefulness of EEG and MRI in stratifying epilepsy syndromes, and to test the hypothesis that those tests will significantly increase the yield over clinical evaluation (history and physical examination) alone.

METHODS: This is a multicenter cohort study from across Lebanon. Eligible patients included all patients between the age of 6 months and 18 years of age, with a single unprovoked seizure or with newly diagnosed epilepsy (two or more unprovoked seizures). This study entailed a detailed neurological examinations, sleep deprived 3 hours video-EEG study, an epilepsy protocol MRI. The MRIs were classified as "normal", "abnormal and epileptogenic", or "abnormal and non-epileptogenic" based on previously published criteria.

Patients known to have pseudoseizures, severe psychiatric illness, provoked seizures, and/or take substance abuse will be excluded from the study.

RESULTS: A total of 755 children were included. These consisted of 502 children with two or more unprovoked seizures (mean age = 7.9 years (range (6 months -17 years), M/F = 281/221) and 253 children with a single unprovoked seizure (mean age = 9 years (range (6 months -17 years), M/F =163/90). In patients with two or more unprovoked seizures, 453 patients already underwent an epilepsy protocol MRI. 152 (34.9%) children had an epileptogenic lesion on the MRI. In patients with a single unprovoked seizure, 207 patients already underwent an epilepsy protocol MRI. 60 (29%) children had an epileptogenic lesion on the MRI.

There was a trend towards more frequent epileptogenic lesion in patients with two or more unprovoked seizures compared to those with a single seizure that did not reach statistical significance (p = 0.13). The types of epileptogenic lesion were MCD, gliosis, stroke, vascular, MTS, tumoral and infection 55.4%, 16.2%, 14.9%, 5.4%, 4.1%, 2.7% and 1.4% respectively.



PLENARY SESSIONS ABSTRACTS

CONCLUSION: A high percentage of patients with newly diagnosed epilepsy who undergo a dedicated epilepsy MRI protocol were found to have an epileptogenic lesion. This underscores the importance of obtaining a high quality MRI interpreted by an expert especially in patients with newly diagnosed localization related epilepsy.

SPINE & SPINE INTERVENTIONAL NR

Marmara Hall

13:30 - 15:00 Spine Tumors & Treatment

Hot and Cold Tumor therapies

Afshin Gangi

Hopitaux Universitaires de Strasbourg, France

Vertebral angiomas – when and how to treat

Kieran Murphy

University of Toronto, Canada

CT-Guided Autonomic Nerve Blocks

Wendell A. Gibby

Adjunct Professor of Radiology, University of California San Diego, CEO – Novard Corporation, USA

The human body is endowed with two distinct nervous systems. When pain conditions are considered, we almost reflexively think of the somatic nervous system. This, of course, provides pain fibers, proprioception, and highly localized dermatomal pain localization. The pain fibers travel from skin, joints and bone to the dorsal root ganglia of the spine, thence through the dorsal columns of the spinal cord and register in pain centers within deeper brain structures. If you smash your thumb with a hammer, this is the pain system that tells you it hurts.

However, there is a second, important and more primitive nervous system, which is our autonomic nervous system. In this case, the afferent sympathetic neurons synapse at various ganglia in the body. Rather than being located in the spinal cord or along the central neural axis, these are paraspinal in location. These include ganglia such as the stellate, splanchnic, celiac, lumbar, and sacral plexus ganglia. The hallmark of this system is its innervation of visceral organs. The pain characteristically is less well localized and tends to refer to a generalize area rather than to a specific dermatome or

somatome. This nervous system is extremely important in pathologic states of pain; especially in states of malignancy or chronic inflammation. In addition, the autonomic nervous system is intimately involved in cardiac contractility and sympathetic tone of blood vessels, the vasoconstriction of smooth muscles, as well as visceral organ pain sensation. When dysfunctional, the autonomic nervous system can exist in a state of extreme sensitivity that can create pathologic regional pain complexes, reflex sympathetic dystrophy (RSD), ventricular dysrhythmias, phantom extremity pain, and in some cases, post-traumatic sympathetically induced cerebral and/or pulmonary edema.

The advent of computerized tomography has allowed a facile window to access the autonomic nervous system in order to treat states of pain induced by diffuse visceral disease such as malignancy, as well as dysfunctional states creating self-perpetuating cycles of autonomic nervous system dysfunction such as RSD. With CT guidance, one can readily access various sympathetic ganglia including the stellate ganglia at the base of the neck, the splanchnic nerves near the crura of the hemi diaphragm, the celiac plexus in the upper abdomen, and the lumbar and sacral plexi in the paraspinal

regions of the abdomen and pelvis respectively. Regional blocks with anesthetics and local corticosteroid injections are not without potential complications. The unique anatomy, pathophysiology, indications and complications of sympathetic nerve blocks will be presented with a fairly simple how-to approach easily accessible by any neuroradiologist under CT guidance. In addition, longer term sympathetic plexus block with neurolysis utilizing ethanol ablation will be presented and discussed.



PLENARY SESSIONS ABSTRACTS

Spinal Interventional Neuroradiology

Key Words: spinal nerve blocks, CT, sympathetic plexus block, autonomic nervous system

O010-Rare Extramedullary Intradural Tumors in Children and Adolescent

Andja Jasovic, Sharoona Dowlut, Tejas Goora

Apollo Bramwell Hospital Diagnostic radiology Rose Hills-Mauritius

Intradural extramedullary neoplasms are uncommon in pediatric and adolescent population and have a limited differential diagnosis. Knowledge of specific imaging characteristics in correlation with patho-histological findings of intradural extramedullary neoplasms helps to further narrow the differential diagnosis and plan of the therapy. MRI is the modality of choice to fully characterize these masses, and the appearance will vary depending on the histology, and is thus discussed as part of individual articles. The key benefits of MRI over other modalities, is the ability to clearly define the relationship of the mass to the cord and to identify secondary lesions.

We are presenting three cases of different extramedullary tumors at the level of the thoracic spine. First case is a 9 yr female with myxoid neurofibroma in the spinal canal at the level of L3 successfully operated in our clinic. Second is a 16yr male with thoracic dumbbell tumor with PH of PNET obtained on CT guided biopsy. Cases of PNET have been increasingly reported in recent years but there are still very few reports of PNET originating in the spinal cord. Third case is a 17 yr male with extradural mass compression at the level D8/D10. We present clinical findings and compare imaging features with possible differential diagnoses on these ages and localizations.

Rare tumors in children and adolescents represent unmet therapeutic needs, as no treatment algorithm and schemes are established for many of them. Presenting rare cases can give more data for farther retrospective studies.

PEDIATRIC DIAGNOSTIC NR

Anadolu Auditorium

15:30 - 17:00 Pediatric Sedation and Trauma

Effects of Anesthesia on Anatomic and Quantitative Pediatric Neuroimaging

Julie H. Harreld

St. Jude Children Radiological Sciences Memphis, United States

Anesthesia in Pediatric Neuroimaging Imaging Effects Physiology and Alternatives

Julie Harreld

St. Jude Children Radiological Sciences Memphis, United States

RATIONALE: Most young children, and many older children and adults, require anesthesia or sedation to undergo MRI due to fear or inability to remain still for the duration of the scan. Though consideration is given to the risks of anesthesia when making decisions regarding whether to sedate or not, these risks are generally considered fairly short-term, including potential for respiratory depression and emergence delirium. However, emerging research suggests that anesthesia may have long-term effects on working memory in adults, and on cognitive development in children receiving anesthesia even just once in early childhood. In our research, we have found that propofol, a commonly-used anesthetic in the pediatric setting, causes decreased cerebral blood flow and compensatory increases in cerebral blood volume, which manifests as increased vascular signal in the sulci on FLAIR imaging. The appearance is identical to the asymmetric vascular FLAIR signal seen in the sulci of patients with Moyamoya disease (the "ivy sign"), which directly correlates with neurologic symptoms and resolves following revascularization and recovery from the chronic hypoperfusion state induced by intracranial vascular stenoses. The physiologic effects of anesthesia and supplemental oxygen on cerebral perfusion,



PLENARY SESSIONS ABSTRACTS

neurovascular coupling and blood oxygen levels are evident on MRI sequences including perfusion, SWI, FLAIR and BOLD/functional MRI, and may be confusing or potentially misinterpreted as disease. Further, these changes may point to mechanisms potentially underlying memory and cognitive deficits associated with anesthesia. As neuroradiologists, we are uniquely positioned to interpret these imaging changes and drive forward the understanding of the long-term effects of anesthetics on neurophysiology and cognition.

OUTLINE: In this session, we will review:

- Indications for anesthesia in diagnostic imaging
- Common anesthetics used for pediatric imaging, including mechanisms and risk profiles
- How anesthesia affects clinical imaging sequences like FLAIR and SWI, and why
- How anesthesia affects fMRI and quantitative MR perfusion measures through effects on cerebral metabolism, blood flow and neurovascular coupling
- Emerging research on the short and long-term effects of anesthesia on memory and cognition, including proposed mechanisms and how they relate to imaging
- Alternatives to anesthesia in diagnostic imaging including behavioral and technical modifications.

Imaging of Central Nervous System Injuries in Non Accidental Trauma

Thierry A.G.M. Huisman

Johns Hopkins Hospital Pediatric Radiology Baltimore, United States

It is estimated that 6% to 10% of young children brought to the emergency department (ED) with traumatic injury are victims of non-accidental injury. The population-based estimate of inflicted traumatic brain injury (TBI) in children less than 1 year of age leading to hospitalization in an intensive care setting is 30 per 100.000 children yearly. The median age for inflicted TBI is approximately 2–4 months of age. Apart from being the most common cause of traumatic death in the first 2 years of life, non-accidental head injury is responsible for significant neurological morbidity. Non-accidental injury should be suspected when there is a discrepancy between the trauma history and encountered imaging findings, if there are hemorrhages of different age, if there are unusual findings, when retinal hemorrhages are present, or if the child has evidence of overall poor care. Clinical presentation may be subtle and include various degrees of decreased levels of consciousness, irritability, respiratory distress, poor feeding, and seizures. The radiologist should alert the clinician if there is the slightest suspicion of non-accidental injury to prevent additional injury on follow up. Patterns of non-accidental traumatic injury to the central nervous system varies with age. In the current presentation we will discuss the typical imaging findings suggestive of non-accidental trauma for the various age groups as well as several mimickers of trauma.

Modern Neuroimaging of Traumatic Brain Injury

Paul Parizel

Antwerp University Hospital, Belgium

SPINE & SPINE INTERVENTINAL NR

Marmara Hall

15:30 - 17:00 Augmentation

Review of literature and update on trials (i.e., NEJM trials vs Rest of the World)

Kieran Murphy

University of Toronto, Canada

Advanced vertebral augmentation.

Eren Erdem

University of Arkansas for Medical Sciences, Little Rock, USA

Posterior Arch and Extravertebral Augmentation

Luigi Manfredi

Minimal Invasive Spine Dept. Cannizzaro Hpt., Catania, Italy



PLENARY SESSIONS ABSTRACTS

The posterior arch and the spinous processes/laminae complex can be involved in several disease. In case of severe arthrosic and/or osteoporosis contact of spinous processes related to disc degeneration can generate local chronic pain, resistant to chemical (steroid infiltration) or physical (radioablation) therapy. Moreover, osteoporosis can be responsible for laminae remodeling in patients treated with interspinous devices (ISD) because of symptomatic spinal canal stenosis. We evaluate the possibility to perform cementoplasty of the spinous processes (spinoplasty - SP) in patients affected by posterior arch painful edema and tumors.

Percutaneous application of interspinous process spacers (IPS) has become a powerful technique resolving symptoms in patients affected by foraminal or lumbar canal stenosis. However, 3% to 6% of failure has been described in the literature, generally related to osteoporotic bone and laminae remodeling, reducing the space between the posterior arches and restoring the symptoms. We evaluate the possibility to strengthen the posterior arch by performing PMMA augmentation before introducing a second IPS.

Finally, we evaluate the possibility to use PMMA in case of extravertebral – paraspinal lesions.

All the patients with painful spinous process edema were evaluated using CT and MRI, revealing abnormal signal intensity inside the posterior arch. In patients candidate to ISD treatment, severe spinal canal stenosis with normal appearance of the posterior arch were appreciated. SP was performed using a CT-guided technique, 13G needles and 1 to 3cc of PMMA per level.

As a result, patients affected by painful spinous processes edema became painless in 24 hours after SP and no complication was detected at 1 week-3 months follow-up controls. Patients undergone prophylactic SP before ISD implant had no recurrence of pre-op symptoms nor laminae remodeling at 3, 6 and 12 months control.

Conclusion: Vertebroplasty of the posterior arch using CT-guided PMMA injection seems to be a powerful technique in those patients who need posterior arch augmentation.

- David H. Kim and Todd J. Albert. **Interspinous** Process Spacers J. Am. Acad. Orthop. Surg., April 2007; 15: 200 - 207
- Ryan D. Murtagh, Robert M. Quencer, Antonio E. Castellvi, and James J. Yue
- New Techniques in Lumbar Spinal Instrumentation: What the Radiologist Needs to Know
- Radiology, August 2011; 260: 317 - 330.

O011-Vertebral Augmentation with Titanium T6 Endoprosthesis a Preliminary Experience

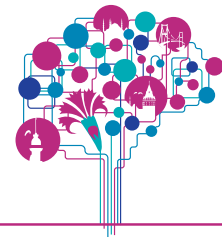
*Emanuele Piras, Stefano Marini, Stefano Marcia
ASL 8 U.O.C. Radiologia - P.O. SS. Trinità Cagliari, Italy*

PURPOSE: The aim of this study was to evaluate the effectiveness of a titanium vertebral augmentation system in the treatment of painful vertebral compressive fractures.

MATERIALS and METHODS: Twenty-one consecutive patients (6 male, 15 female, average age: 74,9) with painful vertebral compressive fractures underwent titanium vertebral augmentation system procedure. Patients had been previously evaluated with clinical examination and X-Ray, CTs and MRI-T2wSTIR. All the procedures were executed with local anaesthesia and bilateral approach under digital fluoroscopic guidance. A total of 23 vertebrae were treated. Clinical evaluation, assessment of pain by means of a 11-points visual analogue scale (VAS, 0-10) and of functions by means of the Oswestry disability scale (ODI 0-100%) was performed at baseline and at one month after the procedure. Height restoration by mean of volume calculation with CTs was made before and after the procedure, as well as the Cobb angle.

RESULTS: We have obtained a progressive reduction of the pain in all the patients (Av. VAS pre: 8.3, post 2.7, difference: 5.6), an improvement of function (ODI baseline: 56%, at 1M: 24%, difference: 32%) a good restoring of the height (Av. h pre: 11.3mm, post: 16.7mm, difference: 5.4mm), and a good increasing of the volume of the vertebral bodies (Av. V pre: 13.74cm³, post: 22.42cm³, difference: 8.68cm³). The Cobb angle increased 3.6°. No major complications arose, neither device migration was noted.

CONCLUSION: From our preliminary studies the implant of vertebral augmentation with titanium t6-endoprosthesis resulted to be safe and effective in the treatment of painful VCF providing pain relief and anatomical restoration.



PLENARY SESSIONS ABSTRACTS

Wednesday, September 10, 2014

PEDIATRIC DIAGNOSTIC NR

Anadolu Auditorium

08:30 - 10:30 **New Concepts of Pediatric Brain Tumors**

New concepts of tumorigenesis in children

Vijay Ramaswamy

Hospital for Sick Children, Canada

New concept 2: Medulloblastoma revisited

Zoltan Patay

St. Jude Children's Research Hospital, USA

Clinical Evaluation and Staging of Paediatric Brain Tumours

Monika Warmuth-Metz

Universityhospital Würzburg Neuroradiology, Würzburg, Germany

Central review of pathology has been accepted for a long time for brain tumour studies. Since the publications by Deutsch et al. (1996) and Packer et al. (2006) it has been clarified that also local staging of imaging in medulloblastoma trials bears a considerable danger of incorrect stratification into the various risk groups. This leads to over- or undertreatment and should be avoided

For the German HIT (brain tumour)-studies a reference institution has been established since 1991. Meanwhile the imaging examinations of all German brain tumour trials are centrally reviewed and about 7.000 cases of various brain tumours have been collected in a database since 2000.

One advantage offered by a central review is to collect a large number of various and rare tumours and tumour like lesions to improve the knowledge on possibly specific imaging characteristics. The central review establishes the best possible way to exclude individually varying results of staging examinations by different (neuro) radiologists. As the methods and terminology of response assessment as well as frequent but not directly tumour related findings during and after treatment are not well known among the (neuro) radiological community a standardized response evaluation for trials is necessary. The discrepancy rate between local and central evaluation in our database reaches about 25%. Major reasons for discrepancies are the correct identification of the presence or absence of a meningeal dissemination.

The central review also assures a quality control of the imaging and the adherence to a basic standard e.g of MRI examinations in times of a wide variety of sequences.

The European section of the SIOP (Société Internationale d'Oncology Pédiatrique) is running multinational European trials especially for rare entities and therefore the European reference radiologists have formed an imaging group discussing and harmonizing the protocols and evaluation procedures across Europe. An important aim is to introduce various scientific questions based on multimodal imaging into future protocols.

Side effects of Pediatric Brain Tumor Therapy

Zoltan Patay

St. Jude Children's Research Hosopital, USA



PLENARY SESSIONS ABSTRACTS

O012-Reorganization of the Visual Pathways after Early Age Tumor Removal Assessed By Functional Magnetic Resonance Imaging and Fiber Tractography

G. Aghakhanyan ¹, F. Tinelli ², K. Mikellidou ³, F. Frijia ⁴, R. Arrighi ⁵, V. Greco ⁶, R. Canapicchi ⁴, M.C. Morrone ³, D. Montanaro ⁴

Scuola Superiore Sant Anna, Institute of Life Sciences, Pisa, Italy 1 Stella Maris Scientific Institute, Pisa, Italy 2 University of Pisa, Department of Translational Research on New Technologies in Medicine and Surgery, Pisa, Italy 3 Fondazione CNR/Regione Toscana G. Monasterio, U.O.s Neuroradiologia, Pisa, Italy 4 University of Florence, Department of Neuroscience, Psychology, Pharmacology and Child Health, Florence, Italy 5 CNR-Istituto Nazionale di Ottica, Florence, Italy 6

PURPOSE: To evaluate the visual pathways of a seven-year-old child, following surgical removal of a right hemisphere parieto-temporo-occipital giant cell ventricular papilloma at four months of age, using functional magnetic resonance imaging (fMRI) and diffusion tensor imaging (DTI) tractography. The patient has normal vision on the right visual field and preserved vision in the central 15° of the left visual field.

METHODS: The patient underwent diagnostic brain imaging investigation under propofol sedation with a GE 3T scanner (Excite HDx, GE Medical Systems, Milwaukee, WI). A purpose-built MRI-compatible visual projector ($\pm 40^\circ$ binocular visual field) allowed visual cortex mapping with a high-luminance flash stimulus (0.5Hz). The upper, lower, right and left visual quadrants were identified using moving dots within four circular sectors. Stimulation was monocular with the left eyelid fixed-open. DTI was acquired using an EPI single-shot spin-echo sequence with 32 directions. Visual pathways were mapped with a probabilistic fiber-tracking algorithm implicated in FDT (FMRIB's Diffusion Toolbox). Primary visual cortex (V1) and middle temporal (MT) visual area were manually demarcated using fMRI activation maps. Optic radiation was delineated by tracking fibers from the lateral geniculate nucleus (LGN) to V1. Further reciprocal anatomical connections were established between the LGN and the superior colliculus (SC), and striate-extrastriate cortical regions.

RESULTS: BOLD signals in response to flash stimulation were bilaterally identified with reduced activation in the right V1. The right MT was dislocated in the anterior direction due to the post-surgical cavity. In this lesioned hemisphere, multi-point tractography analysis revealed very few and sparse optic fibers to V1, but an increased structural connectivity between the LGN, MT and V1. Moreover, interconnected pathways were revealed between right and left SC to the left V1. There were no analogous pathways from left to right SC and the right V1.

CONCLUSIONS: Activity in the lesioned hemisphere was observed, which did not arise from the optical radiations on the same side. On the basis of tractography analysis, we propose two different mechanisms of the functional and structural reorganization in the visual pathways: one, via the right LGN mediated by the right MT projecting to the right V1; the other, via the right SC routing to the left SC, projecting to the left V1.

SPINE & SPINE INTERVENTINAL NR

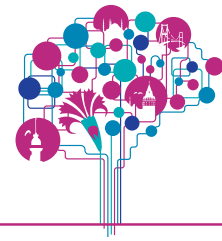
Marmara Hall

08:30 - 10:30 Basic Biomechanics and Spine Trauma

Lumbar Sacral Pelvic Biomechanics and Sagittal Balance

*Massimo Gallucci, Federico D'Orazio, Luca Sacchetti, Lorenzo Gregori
University of L'Aquila DISCAB L'Aquila, Italy*

The biomechanics related to lumbosacral spine are more popular and better known from therapists than those related to sacrum and pelvis. Sacral-pelvic compartments are however very often compromised and underestimated. To effectively understand the concept of lumbar-sacral-iliac dysfunction it is necessary to know the concepts of "form closure" and "force closure". The first is realized at the level sacro-iliac due to the friction present between the articular surfaces, obtained by the effect of (a) perfect complementarity between ridges



PLENARY SESSIONS ABSTRACTS

(sacral slope) and trenches (pelvic side) facing each other on the articular surface; (b) different composition of the opposing surfaces (articular cartilage on the sacral side and fibrocartilage on the iliac); (c) almost perfectly vertical spatial orientation of the articular surfaces; (d) action of intrinsic and extrinsic ligaments. The “force closure” contributes to the dynamic stabilization of joint, creating at this level an additional force of closure of the articular chain of the pelvis. Three distinct systems participate, namely: (a) Passive (capsule, ligaments); (b) Active (stabilizing muscles); (c) Control (purely neurological).

For each category of dysfunction we can distinguish: (a) Postural dysfunction: observed as a result of an alteration in length or in the pattern of muscle activation; (b) Hypomobility dysfunction: arises as a result of microtrauma, degenerative or inflammatory processes that cause joint stiffness or malposition; (c) Instability dysfunction: derives from the impairment of one or more elements contributing to determine the form and / or force closure. Accurate clinical and radiological evaluations of lumbar-sacral-pelvic stability are mandatory before approaching the patient with correct therapy. In such direction, dynamic and axial loaded radiological exams reveal a certain role, like, i.e., up-right MRI or axial loaded and prone/supine CT. Once established the correct diagnostic protocol, the role of interventional techniques can finally be determined (pharmacological or RF pain blocks, pedicular screws, sacro-iliac screws) and provide better results.

Dynamic evaluation of spine instability

Murat Hanci

Istanbul University, Turkey

Spinal cord injury

Gordon Sze

Yale University School of Medicine, USA

Spinal trauma

Paul Parizel

Antwerp University Hospital, Belgium

O013-Vertebral Body Stenting and Cement Augmentation to Restore Structural Stability in Extreme Spinal Osteolysis

Alessandro Cianfoni¹, Eytan Raz¹, Daniele Romano¹, Michael Reinert², Gianfranco Pesce³,
Giuseppe Bonaldi⁴

*Neurocenter of Southern Switzerland Neuroradiology Lugano, Switzerland*¹ *Neurocenter of Southern Switzerland Neurosurgery, Switzerland*² *IOSI Radiation Oncology, Switzerland*³ *Osp. Giovanni XXIII, Bergamo Neuroradiology, Italy*⁴

PURPOSE: Vertebral augmentation (VA) can be used in neoplastic vertebral lesions for pain-palliation and/or stabilization of collapsed or at-risk-of-collapse vertebral bodies (VB). Osteolysis widely involving cortical margins of the VB pose a risk of cement leakage and can ultimately limit the amount of cement that can be injected, resulting in insufficient stabilization.

We report preliminary experience in palliative pain and stabilization treatment of extreme lytic neoplastic vertebral lesions with percutaneous vertebral body stents (VBS) and cement. **MATERIALS AND METHODS:** Retrospective assessment of technical and clinical results of 10 consecutive VA performed with VBS implants and cement in 10 patients with a metastatic extensive lytic lesion of a thoracic or lumbar VB. Aim of the VA was pain-palliation and/or stabilization in painful and/or fractured and/or at-risk-of-collapse vertebral lesions. Patients were 6 F and 4 M, age range 42-78 year. Vertebral lesions were metastases of solid tumors, with lytic changes involving extensively the posterior wall and/or antero-lateral wall, and or disc-plates cortical bone, as shown by pre-procedure CT. All procedures were performed under fluoroscopic-guidance; in two cases fluoroscopy was combined with CT-guidance. Technical results were assessed through



PLENARY SESSIONS ABSTRACTS

intra-operative images, immediate post-procedure CT, and one-month post-procedure spine radiographs. Clinical results were assessed by reviewing clinical charts of standard one-week and one-month follow-up. RESULTS: Six lumbar and 4 thoracic levels were treated. Three patients had no significant pain and were treated exclusively for stabilization purposes; three patients of those presenting with back pain, were treated during the same procedure also at other vertebral levels, solely with cement augmentation. Procedures were uneventful in all cases. One epidural cement leak occurred, with no clinical consequence. The procedure was deemed technically successful in providing structural stability to the target VB by VBS implant and cement filling in all cases. Patients with pain reported VAS decrease from average 7.5 pre-procedure to 6.0 at one week and 3.5 at one month. No VBS implant mobilization nor further or newly developed VB collapse was noted at one-month spine radiographs. CONCLUSIONS: The use of VBS can act as a primary structural implant that restores structural stability of the VB, and can help contain injected cement, allowing with increased safety and efficacy the percutaneous VA of extreme VB osteolysis.

PEDIATRIC DIAGNOSTIC NR

Anadolu Auditorium

11:00 - 12:30 Scoliosis / Pediatric Back Pain

Types and Causes Back Pain in Children

Andrea Rossi

G. Gaslini Children's Hospital, Italy

Imaging of the Child with Acute Back Pain

Thierry A.G.M. Huisman

Johns Hopkins Pediatric Radiology, Baltimore, United States

Acute back pain in children should always be taken seriously. The etiology of acute back pain is diverse and will in many cases primarily include trauma. However, if there is no adequate trauma history various other etiologies should be considered or ruled out including infectious diseases (e.g. spondylodiscitis or myelitis), tumor (primary or secondary) including osseous tumors, spinal cord tumors, subarachnoid seeding from an intracranial neoplasm, osseous malformations, intradural or intraspinal hemorrhages from an intraspinal vascular malformation, hydromyelia/hydrosyringomyelia due to a spinal cord tumor or focal obstruction including Chiari 1 malformation. In addition, especially in young children symptoms may be misleading and back pain may also result from various pathologies that are primarily occurring outside of the vertebral column or spinal canal/cord like e.g. renal pathologies including tumors, obstruction or stones as well as various paravertebral neoplasms or infections that affect the paraspinal nervous system. A dedicated, high end neuroimaging is essential to correctly identify and characterize the reason for the acute back pain. Depending on the age and suspected pathology ultrasound, computer tomography, magnetic resonance imaging or nuclear medicine studies should be considered. In the current review we will discuss common and less common pathologies that may be encountered in children with acute back pain.

Imaging the scoliotic spine with MRI

Andrea Rossi

G. Gaslini Children's Hospital, Italy



PLENARY SESSIONS ABSTRACTS

O014-Pediatric Spinal Cord Diffusion Changes in Craniocervical Junction Malformations

*Gunes Orman*¹, Ximin Li², Carol B. Thompson², Thierry A. G. M. Huisman¹, Izlem Izbudak¹

*Johns Hopkins School of Medicine Radiology/Pediatric Neuroradiology Baltimore, USA*¹ *Johns Hopkins Bloomberg School of Public Health Biostatistics Baltimore, USA*²

PURPOSE: It is well-known that acquiring high quality diffusion tensor imaging (DTI) of the spinal cord (SC) is challenging due to multiple reasons (e.g. small cord size, eddy currents, bone/CSF/air interfaces). But, previous studies showed that DTI provides valuable quantitative information to detect abnormalities in normal appearing SC on conventional MRI.

Cranio-cervical junction malformations (CCJM) may cause compression on SC. We hypothesize that DTI might be used to show early microstructural changes in CCJM.

MATERIALS AND METHODS: Pediatric cervical SC (CSC) DTI studies of patients with CCJM were prospectively acquired. Region of interests (ROI) were placed manually on the sagittal plane DTI at 7 consecutive intervertebral disc levels. Fractional anisotropy (FA) and mean diffusivity (MD) values were obtained for each level. FA and MD values were compared with our previous normal pediatric CSC DTI database.

RESULTS: A total of 9 DTI studies were included in the study. The mean age of the children was 5.13 (between 0.17 and 9) years. (Females=6).

The patients were comprised of 4 groups. Group 1: Chiari 1 malformation without craniocervical decompression (3 patients). Group 2: Chiari 1 malformation with craniocervical decompression (3 patients). Group 3: Chiari 2 malformation (2 patients with myelomeningocele repair and ventriculoperitoneal shunt placement). Group 4: Achondroplasia (1 patient, history of suboccipital craniectomy and cervicomedullary decompression). FA values were lower than controls at all levels in all patients, except 1 patient with normal FA values at the first 5 levels. In the groups 1 and 4; the FA values were more prominently lower at the first two CSC levels. Similarly, MD values were higher in all patients, except the same patient who had normal MD values at the first 5 levels in group 2. On conventional MRI hydromyelia was present in 4 patients, .

CONCLUSION: Our preliminary data showed that pediatric SC DTI is feasible in CCJM. FA and MD values were significantly abnormal at the craniocervical junction where T2 signal of the cord was normal. Further studies are needed to elaborate the microstructural changes in CCJM and might be used in the future for early detection and management before hydromyelia develops.

SPINE & SPINE INTERVENTIONAL NR

Marmara Hall

11:00 - 12:30 **Minimally Invasive Intervention and Innovation**

New Trends in Percutaneous Rigid Spine Fixation

Luigi Manfredi

Minimal Invasive Spine Dept. Cannizzaro Hpt. Catania, Italy

Degenerative lumbar spine instability is one of the most frequent cause of low back pain, and frequently patient are overexposed to chronic use of steroid to obtain pain sedation. There are typical CT & MRI signs suggestive of chronic facet disease, but the best test to confirm the FJS (Facet Joint Syndrome) is definitely a CT-guided injection of Lidocaine at the level of zygo-apophyseal nerves.

Facet radiofrequency ablation is generally used to treat these patients, although 20% approximately of treated patients do not manage to obtain pain relief after, and something new must be done in these RF resistant patients.

The Sacro-iliac joint (SIJ) is the largest, strongest and best protected joint in human body, as a complex system of ligaments (Anterior Sacroiliac, Interosseus, Sacrospinous and sacrotuberosus) and muscles (gluteus maximus,piriformis and biceps femoris) concur to stabilize the joint. Nevertheless, several condition can occur in generating SIJ instability. In women SIJ ligaments are weaker than in males, to be prepared to the necessary sacral mobility for delivery: consequently, post-partum SIJ instability can occur, as for patients affected by degenerative arthritic disease. Moreover, posterior interbody fixation (PIF) significantly increases sacro-iliac



PLENARY SESSIONS ABSTRACTS

stress, and 75% of patients underwent PIF treatment suffer from SIJ in 5 years. Innervation of SIJ is complex, as the posterior surface of the joint receive collaterals from L3 to S4 dorsal rami. Consequently, SIJ instability is responsible for pain referred non only at the local area of inflammation, but frequent irradiated to lower limbs, overlaying other common causes of radicular pain. The average mechanical threshold to activate SIJ nociceptor is 70g, as compared to facet joint (6g) and lower lumbar disc (241g): consequently pain sensitivity of the SIJ is definitely higher than disc sensitivity. Despite several Authors claim the SIJ instability being the cause of 5 to 25% of all low back pain (LBP) the diagnosis and treatment of SIJ instability is frequently underestimated.

Despite more aggressive surgery has been proposed to solve the problem as posterior interbody fixation with screws and bars, we adopted recently introduced new CT-guided techniques for transpedicular and/or pure intervertebral facet fixation using a couple of microscrews with or without percutaneous bars.

Conventional open-surgery with sacroiliac fixation (SF) has been performed for a long time with good results in term of pain control: recently, however, new “one-step” fixation procedures has been proposed. We describe a new technique to be adopted in patients affected by painful SIJ instability treated with fully SF CT-guided technique in simple analog-sedation.

REFERENCES:

1. Okuda S. et al. Surgical Outcomes of Posterior Lumbar Interbody Fusion in Elderly Patients. *Surgical Technique J Bone Joint Surg Am.* 2007;89:310-320.
2. Su BW, Cha TD, Kim PD. An anatomic and radiographic study of lumbar facets relevant to percutaneous transfacet fixation. *Spine* 2009 May 15;34(11).
3. Milchteim C, Yu WD, Ho A. Anatomical parameters of subaxial percutaneous transfacet screw fixation based on the analysis of 50 computed tomography scans: Clinical article. *J Neurosurg Spine.* 2012 Jun;16(6):573-8.
4. Voyadzis JM, Anaizi AN. Minimally invasive lumbar transfacet screw fixation in the lateral decubitus position after extreme lateral interbody fusion: a technique and feasibility study. *J Spinal Disord Tech.* 2013 Apr;26(2):98-106.
5. Amoretti N, Amoretti ME, Hovorka I, Percutaneous facet screw fixation of lumbar spine with CT and fluoroscopic guidance: a feasibility study. *Radiology.* 2013 Aug;268(2):548-55.
6. Bernard TN, Cassidy JD. The sacroiliac syndrome. Pathophysiology, diagnosis and management. In: Frymoyer JW, ed. *The adult spine*
7. Murata Y, Takahashi K, Yamagata M, et al. Sensory innervation of the sacroiliac joint in rats. *Spine* 2000;16:2015-9
8. Grob KR, Neuhuber WL, Kissling RO. Innervation of the sacroiliac joint in humans. *Z Rheumatol* 1995;54:117-22
9. Ikeda R. Innervation of the sacroiliac joint: macroscopic and histological studies. *J Nippon Med Sch* 1991;58:587-96
10. Fortin JD, Kissling RO, O'Connor BL, Vilensky JA. Sacroiliac joint innervation and pain. *Am J Orthop* 1999;28:68-90
11. Yamashita T, Cavanaugh JM, El-Bohy AA, et al. Mechanosensitive afferent units in the lumbar facet joint. *J Bone Joint Surg (Am)* 1990;72:865-70
12. Yamashita T, Minaki Y, Oota, et al. Mechanosensitive afferent units in the lumbar intervertebral disc and adjacent muscle. *Spine* 1993;18:2252-6
13. Minaki Y, Yamashita T, Ishii S. An electrophysiological study on the mechanoreceptors in the lumbar spine and adjacent tissues. *Neurol Orthop* 1996;20:23-35

Percutaneous dynamic spine fixation and interspinous spacers.

Giuseppe Bonaldi

Osp. Giovanni XXIII, Bergamo Neuroradiology, Italy



PLENARY SESSIONS ABSTRACTS

Role of Radiologists in Neuromodulation procedures (spinal cord stimulations)

Gregory Lawler

Neuroimaging and Interventional Spine Services, Ridgefield, USA

O015-Transoral Route for the Percutaneous Vertebroplasty of C1 Lesions

Frédéric Clarençon ¹, Evelyne Cormier ¹, Raphaël Bonaccorsi ², Hugues Pascal-Mousellard ², *Jacques Chiras* ¹
Pitié-Salpêtrière Hospital Interventional Neuroradiology -France ¹ *Pitié-Salpêtrière Hospital Orthopedic Surgery, France* ²

OBJECTIVE: To present our experience in 5 consecutive patients treated by percutaneous vertebroplasty (PV) via a transoral route for tumor lesions of the lateral mass of C1. **MATERIALS and METHODS:** From February 2012 to August 2013, 5 consecutive patients (4 males, 1 female, mean age = 73 y) underwent PV via a transoral route for tumor lesions of the lateral mass of C1. Three patients had osteolytic metastases from various neoplasms (pancreas, bladder, lung), one patient had a multiple myeloma and the remaining patient had a biopsy proven aggressive haemangioma of C1. All these lesions were osteolytic and were located on the left lateral mass of C1. All the procedures were performed under general anaesthesia; the posterior aspect of the pharynx was exposed by means of a Boyle-Davis mouth gag. A 11G bone needle was positioned under fluoroscopic guidance. The satisfactory positioning of the bone needle was controlled on CT-scan. In average, 1.5 mL of PMMA bone cement were injected under fluoroscopic guidance. In 4/5 cases, a balloon protection was inflated in the V3 segment of the ipsilateral vertebral artery during the cement injection. **Complications (major/minor) were systematically collected; effectiveness in terms of pain relief was evaluated on visual analogue scale (VAS) at 1 month.**

RESULTS: No complication occurred. No intra-canal or venous leakage was observed. No infectious complication was reported. Analgesic effect was reported at one month follow-up, with a mean VAS decrease of 6.5 ± 4.3 .

In one case (aggressive haemangioma) a slight increasing of the lesion's size was observed on MRI follow-up, that remained stable on further imaging follow-ups. No local recurrence was observed for metastatic lesions.

CONCLUSION: PV of the lateral mass of C1 via a transoral route is a safe and effective technique.

PEDIATRIC DIAGNOSTIC NR

Topkapı AB Hall

13:30 - 15:00 **Vascular Disease in Children**

Imaging Strategies in Arterial and Venous Pediatric Stroke Conventional and Advanced

Kling Chong

Great Ormond Street Hospital for Children Radiology, London, UK

- Stroke is a clinical diagnosis, but radiology is required for the initial diagnosis and on subsequent follow-up.
- Peer reviewed evidence-based clinical guidelines for the diagnosis and management of Stroke in Childhood have been published 1. Diagnostic definitions and imaging recommendations from the International Pediatric Stroke Study Group (IPSS) are available⁵
- The risk factors and variety of underlying pathologies & aetiologies are very different from adult stroke. A large proportion have multiple pathologies and risk factors that act synergistically to result in stroke. Diagnostic imaging strategies need to be tailored accordingly.
- For the acute diagnosis of arterial ischaemic stroke in childhood, cross-sectional brain imaging is mandatory. Brain MRI should be undertaken as soon as possible, with CT as an acceptable initial alternative, if MRI is not available in the first 48 hrs.



PLENARY SESSIONS ABSTRACTS

- Supportive investigations for cause of stroke, and for use with the diagnostic definitions of disease subtypes, include imaging of the entire intra- and extra-cranial cerebral vasculature and echocardiography. This should be undertaken within 48 hours of presentation of arterial ischaemic stroke.
- The use of thrombolytic agents in children is considered experimental and not recommended unless part of an ongoing study. However, diagnostic imaging is used to guide the use of aspirin, anticoagulation and other therapeutic interventions.

REFERENCES:

1. Management of stroke in infants and children: a scientific statement from a special writing group of the American Heart Association Stroke Council and the Council of Cardiovascular Disease in the Young. Roach ES, Golomb M, Adams R et al. *Stroke* 39, 2644-2691 (2008)1.
2. Investigation of risk factors in children with arterial ischaemic stroke. Ganesan V, Pregler M, McShane, et al, *Annals of Neurology* 53:167-173 (2003)
3. Conventional cerebral angiography in children with ischaemic stroke. Ganesan V, Savvy L, Chong WK, et al, *Pediatric Neurology* 20: 38-42 (1999)
4. Knowledge of Consequences: Understanding Stroke in Children. Roach ES, deVeber GA & Kirkham FJ. *J Child Neurol* 15: 277-278 (May 2000)
5. Toward the definition of cerebral arteriopathies of childhood. Sébire G, Fullerton H, Riou E & deVeber G. *Curr Opin Pediatr* 16:617-622; (2004)
6. Toward a Consensus-Based Classification of Childhood Arterial Ischemic Stroke. Bernard TJ, Manco-Johnson MJ, Lo W, et al. *Stroke* 43:371-377; (2012)

Vascular malformation syndromes

Timo Krings

Toronto Western Hospital, Canada

Intracranial Sinovenous Thrombosis in Childhood Thrombosis and Beyond

Kling Chong

Great Ormond Street Hospital for Children Radiology, London, UK

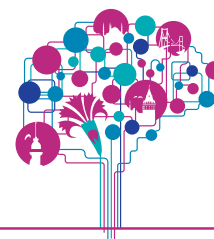
Pediatric cerebral venous sinus thrombosis is rare and considered often underdiagnosed. Neuroradiologists should be aware of the non-specific clinical presentation of headache and seizures. Imaging options include CT, CTV, MR, MRV and for those in infancy, ultrasound. Radiological features may be subtle and there are diagnostic pitfalls. The aim of diagnosis is to guide management which may range from supportive measures such as managing fluid balance and intracranial pressure, to specific interventions such as anticoagulation to prevent clot propagation, thrombolysis, thrombectomy and other endovascular therapies. There is debate on whether cases with sepsis should be treated differently.

Recommendations for imaging and therapy are mostly extrapolated from adult data. There is a need for more pediatric studies.

Clinical guidelines on endovascular therapy in this age group have been published (Class IIb; Level of Evidence C). These indicate that endovascular therapy may be considered in selected subjects with clinical progression despite achieving therapeutic levels of anticoagulation.

REFERENCES:

1. Antithrombotic Treatment in Neonatal Cerebral Sinovenous Thrombosis: Results of the International Pediatric Stroke Study. Jordan LC, Rafay MF, Smith SE et al, *J Pediatr*. 2010 May ; 156(5): 704-710.
2. Cerebral sinovenous thrombosis in pediatric practice. Hedlund GL. *Pediatr Radiol* (2013) 43:173-188
3. Potential pitfalls in imaging of paediatric cerebral sinovenous thrombosis. Bracken J, Barnacle A, Ditchfield M. *Pediatr Radiol*. 2013 Jan;43(2):219-31.
4. Cerebral sinovenous thrombosis in children: diagnosis and treatment. Jackson BF1, Porcher FK, Zapton DT, Losek JD. *Pediatr Emerg Care*. 2011 Sep;27(9):874-80



PLENARY SESSIONS ABSTRACTS

5. Diagnosis and Management of Cerebral Venous Thrombosis: A Statement for Healthcare Professionals From the American Heart Association/American Stroke Association; Spasonick et al on behalf of the American Heart Association Stroke Council and the Council on Epidemiology and Prevention : AHA/ASA Scientific Statement Stroke. 2011; 42: 1158-1192

O016-Diagnostic Imaging Evaluation of Ischaemic Stroke in Children Twelve Years Experience

*Eva Kovacs*¹, Peter Barsi², Gyorgy Balazs³, Gyorgy Varallyay², Gabor Rudas², Zoltan Harkanyi¹, Judit Moser⁴, Beata Rosdy⁴, Katalin Kollar⁴

*Heim Pal Childrens' Hospital Radiology Budapest-Hungary*¹ *Semmelweis University MR Research Center -Hungary*² *Semmelweis University Department of Cardiovascular Surgery -Hungary*³ *Heim Pal Childrens' Hospital Neurology -Hungary*⁴

PURPOSE: Arterial ischaemic stroke (AIS) is significantly less common in children than in adults and the time elapsed from onset of symptoms to diagnosis is generally longer. We present our observations concerning the diagnostic imaging evaluation of AIS in children based on cases treated in our hospital, in order to make recommendations to improve diagnosis and treatment.

MATERIALS AND METHODS: A retrospective chart and image review of 32 patients treated with the diagnosis of AIS in a tertiary pediatric hospital between 2002-2014 was made. Data from 22 patients whose initial imaging study and at least one follow up examination was available were summarized.

RESULTS: Of 22 patients 17 were male, the average age was 7.3 years. 17 patients were initially examined by CT, only eight of these examinations were evaluated positive on the first reading. However, on the second reading additional three positive studies were found. 13 children presented with sudden onset of symptoms, seven of them had imaging evaluation within six hours (all underwent CT), which was rated positive in only two cases. Following a negative CT scan, only one patient had an emergency MRI within six hours. As a result of a positive CT scan one child underwent selective thrombolysis, while the administration of systemic therapy (antiaggregation and anticoagulation) was based on positive MRI results in 20 cases, on positive CT result in one case. When alterations were detectable on CT, they were visible on non-enhanced CT scans already. Blood vessel evaluation was done by MRA in all but two cases.

CONCLUSION: In our experience urgent imaging evaluation of children with sudden onset of focal neurological symptoms was carried out mainly with CT. The majority of patients underwent an emergency non-enhanced CT scan. For further evaluation and follow up MRI/MRA examination was done. In light of therapeutic options revision of the current practice is necessary.

SPINE & SPINE INTERVENTINAL NR

Marmara Hall

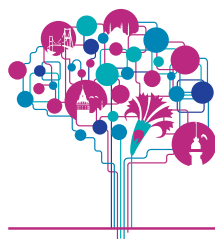
13:30 - 15:00 Infection/inflammatory/Degenerative Diseases of the Spine

Inflammatory Arthritis and Degenerative Disease

Johan Van Goethem, Luc van den Hauwe, Caroline Venstermans, Frank De Belder, Paul Parizel
University Hospital Antwerp Radiology Edegem-Belgium

Spondylarthritis is a general term for inflammatory arthritis of the spine. Several disease entities fall under this description and the most important ones are listed below:

- spondylarthritis
- o seronegative spondylarthropathies prv/spine 0.2%...1%
- o rheumatoid arthritis prv/spine 0.3%...0.8%
- o SAPHO (synovitis, acne, pustulosis, hyperostosis, osteitis)
- CRMO (chronic recurrent multifocal osteomyelitis) prv/spine 0.04%
- PPHS (pustulo-psoriatic hyperostotic spondylarthritis)
- o metabolic deposition diseases:



PLENARY SESSIONS ABSTRACTS

- gout (urate crystal) prv/spine 0.05%...0.1%
- CPPD - pseudogout (Ca pyrophosphate) prv/spine 0.3%
- o juvenile idiopathic arthritis (juvenile RA, juvenile AS, Still's, ...) prv/children/spine 0.005...0.1%
- o calcific longus colli tendinitis, hemodialysis, OPLL, ...

Each pathology is listed with its prevalence in the spine. Of these, the group of the seronegative spondylarthropathies is the most important one. Within this disease group, 5 entities are recognized:

- ankylosing spondylitis
- psoriatic arthritis
- enteropathic spondylarthropathy
- reactive arthritis
- undifferentiated

All of these diseases have common features including chronic inflammation of cartilaginous joints, entheses and synovia, no rheumatoid factor, both axial and appendicular skeleton are affected and there is an onset in young adults and a genetic predisposition. Moreover there is a genetic factor and these diseases are often associated with HLA B27, being positive in 95% of patients with ankylosing spondylitis. Clinically these patients may present with back (neck) pain, morning stiffness, pathologic fractures, fatigue and fever associated with chronic inflammation.

The radiographic hallmarks of seronegative spondylarthropathies are:

- inflammation (erosions), repair (sclerosis) and ossification/ankylosis
- bilateral sacroiliitis
- vertebral corner lesions (Romanus)
- syndesmophytes (outer annulus)

The diagnosis of a seronegative spondylarthropathy is made clinically and may be confirmed by imaging. To make the diagnosis either imaging positive for sacroiliitis + 1 SpA feature or HLA-B27 + 2 SpA features are needed. The SpA features include inflammatory back pain, arthritis, enthesitis (heel), uveitis, dactylitis and psoriasis. Although plain films are still widely used MRI is more sensitive in detecting spondylarthropathies. Changes are most obvious at the sacro-iliac joints but also the vertebral column may exhibit typical imaging features.

Update on spinal infections and mimics

Gordon Sze

Yale University School of Medicine, USA

Role of biopsies.

Orlando Ortiz

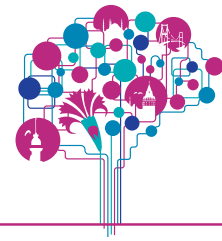
Winthrop-University Hospital, USA

O017-Imaging Features of Spinal Fractures in Ankylosing Spondylitis

*Ivana Zupetic*¹, Vera Ersek-Rakic², Dina Miklic¹, Martina Salaj¹, Ljubica Luetic-Cavor¹,
Petra Margetic¹

*Clinical Hospital Center "Sestre milosrdnice" Diagnostic Radiology department Clinic for traumatology Zagreb
Zagreb-Croatia 1 Clinical Hospital Center "Sestre milosrdnice" Diagnostic Radiology department, University
Clinic for traumatology Zagreb, Croatia*²

PURPOSE: Fractures of the spine in patients with ankylosing spondylitis (AS) may be a result of minor trauma and lead to severe neurological deficits. They are difficult to detect on plain radiographs, specially transverse spinal fractures. CT or/and MRI are often required for diagnosis. The purpose of our investigation was to characterize spinal fractures and determine the value of different imaging modalities in AS.



PLENARY SESSIONS ABSTRACTS

MATERIALS AND METHODS: In a six-year period (from 2008 to 2014) 18 patients were admitted to our hospital with fractures of ankylosing spine. In all cases conventional radiographs were the first imaging choice followed by CT and/or MR. We carefully reviewed clinical histories and imaging presentations. **RESULTS:** In 18 patients with ankylosing spine and fractures, the lower cervical spine was affected in 9 patients, thoracic spine in 4, and lumbar spine in 5 patients. The fall was the immediate cause of the fracture in most of the cases.

Seven patients had contusion of the medulla, one patient had traumatic cervical disc herniation, and in three patients intradural extramedullary hematoma was found.

All imaging modalities; radiographs, CT and MRI was obtained in 7 patients. In 5 patients conventional radiographs and CT was done and 6 patients diagnosed with conventional radiographs and MR.

CONCLUSION: The diagnosis of transverse spinal fractures in patients with ankylosing spondylitis may be difficult on conventional films.

Fractures of the vertebral body and posterior elements was better seen on CT scan. MR is advantageous due to its ability to demonstrate signal abnormalities of the posterior elements, (interspinous or supraspinous ligaments) and contiguous soft tissue structures, spinal canal, and spinal cord, which combined with disk and vertebral body abnormalities, play a major role for accurate diagnosis of this type of fracture.

PEDIATRIC DIAGNOSTIC NR

Topkapı AB Hall

15:30 - 17:00 **Pediatric CNS infections**

CNS Infection: TB and HIV

Savvas Andronikou

Department of Radiology, Faculty of Health Sciences, University of Cape Town, South Africa

The Western Cape of South Africa has the highest per capita prevalence of TB in the world. There are also 5.5 million people living with HIV in SA. To put this in perspective, the South African population with AIDS is greater than general population of Swaziland, Botswana and Lesotho combined. Africa which has only 10% of world's population has 90% of the **paediatric** HIV cases and only 36% children with HIV received ARV's (in 2007). Both TB and HIV can manifest in the CNS, and imaging plays a vital role in diagnosis, detecting complications, prognosis and monitoring of treatment.

TB meningitis causes inflammation in the meninges and cisterns. In turn, this causes inflammation of vessels with infarction, inflammation of the adjacent parenchyma with necrosis and obstruction of CSF flow resulting in hydrocephalus. The classic imaging pattern of TBM is a triad of basal enhancement, infarction and hydrocephalus.

HIV encephalopathy, on the other hand, results in shrinkage of the brain as a result of atrophy and disturbed integrity of white matter while the dampened immune response results in more infections of the CNS.

This presentation will demonstrate the classic imaging findings of TB meningitis and HIV encephalopathy.

It will also demonstrate less well-known features of TB such as millitary meningeal nodules, borderzone necrosis, missing posterior pituitary bright spot and the advantages of imaging with MRI.

In addition the presentation will demonstrate classic appearances of HIV encephalopathy as well as ways of demonstrating white matter disease and atrophy using objective measures, from DTI and post processing of the corpus callosum, respectively.

Lastly the presentation will demonstrate examples of TBM in patients who are HIV infected to show the pitfalls of diagnosing TBM when there is immunosuppression. Co-infection of the CNS with HIV and TB produces some paradoxical imaging appearances. The immune suppression masks the inflammatory markers of TBM on MRI resulting in less basal enhancement with unusual distributions, less hydrocephalus and less basal ganglia infarction with hemispheric infarcts of HIV vasculitis predominating.



PLENARY SESSIONS ABSTRACTS

Bibliography:

1. Andronikou S, Smith B, Hatherhill M, Douis H, Wilmshurst J. Definitive neuroradiological diagnostic features of tuberculous meningitis in children. *Pediatr Radiol.* 2004 Nov;34(11):876-85
2. Przybojewski S, Andronikou S, Wilmshurst J. Objective CT criteria to determine the presence of abnormal basal enhancement in children with suspected tuberculous meningitis. *Pediatr Radiol.* 2006 Jul;36(7):687-96
3. Andronikou S, Smith B, Hatherhill M, Douis H, Wilmshurst J. Definitive neuroradiological diagnostic features of tuberculous meningitis in children. *Pediatr Radiol.* 2004 Nov;34(11):876-85
4. Pienaar M, Andronikou S, van Toorn R. *Childs Nerv Syst.* 2009 Aug;25(8):941-7
5. Andronikou S, Wilmshurst J, Hatherill M, VanToorn R. Distribution of brain infarction in children with tuberculous meningitis and correlation with outcome score at 6 months. *Pediatr Radiol.* 2006 Dec;36(12):1289-94
6. Janse van Rensburg P, Andronikou S, van Toorn R, Pienaar M. Magnetic resonance imaging of miliary tuberculosis of the central nervous system in children with tuberculous meningitis. *Pediatr Radiol.* 2008 Dec;38(12):1306-13
7. Dekker G, Andronikou S, van Toorn R, Scheepers S, Brandt A, Ackermann C. MRI findings in children with tuberculous meningitis: a comparison of HIV-infected and non-infected patients. *Childs Nerv Syst.* 2011 Apr 15.
8. Ackermann C, **Andronikou S**, Laughton B, Kidd M, Dobbels E, Innes S, van Toorn R, Cotton M. White Matter Signal Abnormalities in Children with suspected HIV-Related Neurologic Disease on Early Combination Antiretroviral Therapy. *Pediatr Infect Dis J.* 2014 Mar 3. [Epub ahead of print]
9. **Andronikou S**, van Toorn R, Boerhout E. MR imaging of the posterior hypophysis in children with tuberculous meningitis. *Eur Radiol.* 2009 Sep;19(9):2249-54. Epub 2009 Apr 28. PubMed PMID: 19399504.
10. George R, **Andronikou S**, du Plessis J, du Plessis AM, Van Toorn R, Maydell A. Central nervous system manifestations of HIV infection in children. *Pediatr Radiol.* 2009 Jun;39(6):575-85. Epub 2009 Mar 10. Review. PubMed PMID: 19277636.
11. Omar N, **Andronikou S**, van Toorn R, Pienaar M. Diffusion-weighted magnetic resonance imaging of borderzone necrosis in paediatric tuberculous meningitis. *J Med Imaging Radiat Oncol* 2011;55:563-70 (Winner of Academic Day Poster)

Neuroimaging in Viral and Autoimmune Childhood Encephalitis

Philippe Demaerel

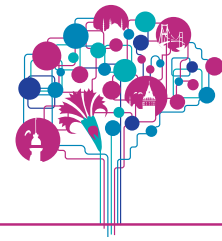
University Hospital KU Leuven Radiology Leuven, Belgium

PURPOSE: Review the imaging findings in viral and autoimmune encephalitis in childhood.
MATERIALS AND METHODS: retrospective analysis of imaging findings in children with viral or autoimmune encephalitis between 2009 and 2014.

RESULTS: systemic inflammatory disorders with a dysregulation of the immune system as well as systemic autoimmune disorders characterized by autoantibodies and impaired T cell immunity were analyzed. These include a large variety of diseases among them multiple sclerosis (MS), acute disseminating encephalomyelitis (ADEM), autoantibody related encephalitis, Behçet disease, juvenile idiopathic arthritis, Rasmussen encephalitis, Guillain-Barré syndrome,...

Particular attention was paid to the relevant clinical observations and to the role of imaging in reaching a diagnosis. The distribution of the lesions and the differences/similarities with the imaging findings in adults will be discussed. The differential diagnosis but also the relationship between ADEM and MS and between ADEM and Guillain-Barré will be demonstrated.

CONCLUSION: Neuroimaging plays an important role in the diagnosis of viral and autoimmune encephalitis because the clinical findings often remain non specific at presentation.



PLENARY SESSIONS ABSTRACTS

Childhood Cysticercosis and other Parasitic Disorders of the Pediatric CNS

Leandro Tavares Lucato

Hospital das Clínicas, Faculdade de Medicina, Universidade de São Paulo Radiology São Paulo-Brazil

0018-Infectious and Post Infectious Meningo Encephalitis Pictural Review

Mouna Laadhari¹, Nadia Mama¹, Amira Berriche¹, Nadia Arifa¹, Houda Ajmi², Samia

Tilouch³, *Kalthoum Tlili*¹

Sahloul University Hospital Radiology Department -Tunisia *1 Sahloul University Hospital Paediatric Department -Tunisia* *2 Farhat hached University Hospital Paediatric Department, Tunisia* ³

PURPOSE: To discuss neuro imaging findings with the emphasis on MR imaging, including diffusion weighted imaging (DWI) of infectious and postinfectious brain lesions in immunocompetent patients. To assess the features of bacterial, viral, fungal and parasitic brain infections on conventional and advanced imaging techniques.

MATERIALS AND METHODS: We retrospectively reviewed the medical records and MR images of patients treated for encephalitis over the period of 8 years (2005-2013).

The diagnosis of infectious encephalitis was based on the detection of specific viral antigen or serologic markers in Cerebral Spinal Fluid (CSF). Conventional MR sequences were obtained in all patients with MR Spectroscopy (MRS) in 18 cases.

RESULTS: Viral infections include: herpes simplex virus (HSV) encephalitis (n=5), rubella (n=3), enteroviruses (n=1) and West Nile virus (WNV) (n=5). Bacterial encephalitis include tuberculosis (n=5) and lyme disease (n=1). Imaging revealed characteristic distribution: temporal involvement in HSV, thalamic in WNV, sub cortical white matter and basal ganglia involvement in Rubella encephalitis. Thirty seven cases (20 boys and 17 girls) of ADEM were reported. Lesions with abnormal signal changes were found predominantly in the sub cortical white matter of frontal and parietal lobes. Corpus callosum involvement was noted in 9 cases and cortical gray matter involvement in 8 whereas deep gray matter involvement was noted in 17 cases.

CONCLUSIONS: Two major types of encephalitis are exhibited: direct infectious process involving the central nervous system (CNS), and noninfectious encephalitis/encephalopathy mainly caused by an autoimmune-mediated mechanism. Viruses are the most common causes of infectious encephalitis. Post infectious encephalitis predominantly affect children and include essentially the ADEM. Differentiating infectious from noninfectious CNS involvement is essential because the treatment and outcome are different. Although the confirmation of the diagnosis often requires the detection of specific viral antigens or serologic markers in CSF, MR imaging provides many clues for the specific diagnosis based on the characteristic lesions distribution. DWI is particularly helpful both for early detection of infectious processes and for their differentiation from other diseases. MRS and MR perfusion may provide additional information in selected cases.

SPINE & SPINE INTERVENTIONAL NR

Marmara Hall

15:30 - 17:00 Pain Management Interventions

Injections and complications

Eren Erdem

University of Arkansas for Medical Sciences, Little Rock, USA

RF Treatments in Spine

Stefano Marcia

Ss Trinita Radiology Cagliari, Italy

RF treatments in spine involve percutaneous procedures for the treatment of degenerative disease and percutaneous tumour ablation.



PLENARY SESSIONS ABSTRACTS

Among degenerative pathologies, RF procedures are performed on facet disease or degenerative disc disease. Facet joint treatments consist of Radiofrequency Neurotomy (RFN) for the treatment of pain due to facet joint syndrome.

RFN consists of thermal ablation of medial branch of dorsal rami of spinal nerves, in order to interrupt nerve conduction using an electrode needle positioned under CT or fluoroscopic guidance connected to a dedicated RF generator. The procedure is performed in day-surgery with local anaesthesia. Main indication is low back pain due to facet joint syndrome resistant to conservative (medical and physical) therapy.

While Lumbar RFN has documented efficacy (1B+) in reducing chronic back pain in patients with facet joint syndrome, cervical RFN has fair evidence and thoracic RFN has limited evidence. The procedures can be repeated when symptoms return. Complication rates are very low. The RF treatment for contained disc herniations, also called disc nucleoplasty or coablation, consists of ablation and coagulation of the nucleus pulposus through a bipolar electrode-needle introduced by percutaneous approach using CT or fluoroscopy, in order to reduce the intradiscal pressure in the nucleus pulposus. The procedure is performed in day-surgery with local anaesthesia.

Main indication is contained disc herniation confirmed by MRI with back pain, sciatica or crural pain that limits activity for at least 6 weeks duration, with no significant improvement after conservative therapy.

Discitis is the most common complication of percutaneous disc decompression techniques occurring in up to 0.24% per patient.

Although many studies suggest a positive outcome, the indicated evidence for Disc Nucleoplasty is still to be considered fair.

Recently intradiscal radiofrequency pulsed application has been used to treat discogenic pain. Pulsed radiofrequency treatment (PRF) has been reported to induce changes in the pain conduction when applied close to a nerve.

However, randomized studies are needed to confirm these observations.

RF is also used to treat spine tumours as a palliative technique in order to prolong the survival, improve functions and relieve pain. RF ablation can also be combined with vertebroplasty.

Sacro-iliac joint treatments (including radiofrequency neurolysis)

Orlando Ortiz

Winthrop-University Hospital, USA

O019-CT Guided Infiltrative Therapies of the Sacro Iliac Joints Long Term Evaluation of Efficacy on Wide Population

*Federico D Orazio*¹, Lorenzo Gregori¹, Aldo Victor Giordano², Sergio Carducci²,

Alessandra Splendiani³, Massimo Gallucci³

Ospedale San Salvatore L Aquila, U.O. Neuroradiologia e Radiologia Interventistica Scuola di Specializzazione in Radiodiagnostica, Università degli Studi di L Aquila L Aquila-Italy ¹ *Ospedale San Salvatore L Aquila, U.O. Neuroradiologia e Radiologia Interventistica U.O. Neuroradiologia e Radiologia Interventistica -Italy* ² *Università degli Studi di L Aquila, U.O. Neuroradiologia e Radiologia Interventistica Dipartimento Scienze Cliniche Applicate e Biotecnologie -Italy* ³

PURPOSE: To evaluate long-term efficacy of CT-guided sacroiliac joint (SIJ) injections in the management of painful articular dysfunction.

MATERIALS AND METHODS: In the period between January 2008 and December 2012 794 patients undergone SIJ injections after a painful articular dysfunction was assessed by using CT and MR imaging of hip together with clinical examination. All patients answered the Oswestry Disability Index questionnaire before treatment and were re-evaluated with the same method three weeks and two months after treatment. All patients had Oswestry Disability Index scoring >40% ("severe disability"); the treatment was judged as effective



PLENARY SESSIONS ABSTRACTS

when, at the follow-up visit, Disability Index (D.I) scored <20% and a second treatment was again practiced when it scored between 20 and 40%. The treatment consisted in the injection of a mixture of corticosteroids, local anesthetics and O2-O3 in the joint space performed under CT guidance.

RESULTS: 794 patients [mean age 60, 17 years - 587 men (73,92%) and 207 women (26,07%)] undergone SIJ injection. At three weeks evaluation 383 patients (48,2%) reached D.I.<20% (Group A - effective treatment); all the remaining 411 patients obtained a D.I. between 20-40% (Group B - mild efficacy) and were retreated. Among them, 197 patients (40,1%) kept D.I. values not significantly lower three weeks after, and the treatment was discontinued. At two months follow-up visit 297 patients (37,4%) kept D.I. values <20%(effective treatment), 284 (35,7%) had a D.I. between 20 and 40%, showing late increase of symptoms, with values lower than those measured at first clinical evaluation and 213 (26,8%) did not show a durable reduction of their D.I.

CONCLUSION: The clinical value of CT-guided infiltration of anti-inflammatory drugs and local anesthetics is to identify, at a time, the origin of the pain until then supposed coming from the SIJ and to achieve an almost immediate benefit to the patient, which could be made as a result of lower doses of drugs taken by systemic route. Although this benefit is demonstrated reduced over time, the technique, performed by trained personnel, does not expose patients to any significant risk of major complications, and can be easily repeated to recurrence of symptoms if there is no alternative strategy to treat it.

15:30 - 17:00 Neuroradiology: Past, Today & Future **Dolmabahce C Hall**

Marco Leonardi
Bologna University, IRCCS Neurological Research Hospital, Italy



PLENARY SESSIONS ABSTRACTS

Thursday, September 11, 2014

ADULT DIAGNOSTIC NR

Anadolu Auditorium

08:30 - 10:30 CNS TUMORS 1

Genomic Mapping of Brain Tumors.

Anne G. Osborn

University of Utah School of Medicine, USA

From Diagnosis to Response Assessment in brain tumors.

Mehmet Kocak

Rush University Medical Center, USA

Timing of Follow up Examinations What to Expect to See; Application of Advanced Imaging Tools in Response Assessment and Standardization of Reports and Potential Pitfalls

Rafael Rojas

Beth Israel Deaconess Medical Center, Harvard Medical School Radiology, Section of Neuroradiology, Boston, USA

In this presentation we will review the importance of time management, how to monitor and what to expect to observe in the different MRI patterns of post treated primary brain tumors. We will review the advantages and disadvantages of advanced neuroimaging techniques such as DTI, MRI spectroscopy, functional MRI, and how we can apply these concepts in the standardization of reports. With the current diagnostic imaging technology, we can detect early changes by contrast enhancement MR imaging, just after or during treatment that may mimic early tumor progression. These changes can be induced by a variety of nontumoral processes, such as postsurgical changes, treatment-related inflammation, ischemia, and sub-acute radiation effects. Therefore, contrast-enhanced MR imaging should be used within the first 36 to 48 hours after surgery to identify residual tumor in the postsurgical bed, and no later than 72 hours after surgery, to avoid confusion with nontumoral inflammation. Additionally, the neuroradiologist should be familiar with the changes induced by radiation therapy, and with the concepts of tumoral progression and tumoral pseudo-response, which often simulate disease worsening, and remarkably both appear to be associated with short term improvement patient outcome.

When an image that looks like a tumor: Brain tumoral like-lesions.

Mehmet Kocak

Rush University Medical Center, USA

O020-Brain Gliomas Correlation between Diffusion Kurtosis Imaging and Tumor Malignancy

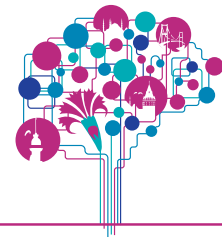
*Aram Tonoyan*¹, *Farida Grinberg*², *Ezequiel Farrher*², *Igor Pronin*¹, *Ivan Maximov*²

*Lyudmila Shishkina*¹, *Evgeniy Shults*¹, *David Pitskhelauri*¹, *Valeriy Kornienko*¹

Burdenko Neurosurgery Institute Neuroradiology Moscow-Russia *1 Forschungszentrum Juelich GmbH Institute of Neuroscience and Medicine, Germany*²

PURPOSE: Diffusion kurtosis imaging (DKI) has been introduced as an advanced extension of diffusion tensor imaging (DTI). DKI characterizes the diffusion deviation degree from the Gaussian model. The goal of this study is to assess the diagnostic efficacy of DKI in grading among grade I-II gliomas, grade III gliomas and glioblastomas.

MATERIALS AND METHODS: 39 patients with cerebral gliomas underwent imaging with a 3-T MR scanner. A spin-echo EPI sequence was used to acquire DKI using b values of 0, 1000 and 2500 s/mm² and 60 gradient directions. Absolute and normalized to the contralateral NAWM values of the diffusion tensor (DT) parameters (mean diffusivity (MD), axial diffusivity (AD), radial diffusivity (RD), fractional anisotropy (FA), relative anisotropy (RA)) and the DK parameters (mean kurtosis (MK), axial kurtosis (AK), radial kurtosis (RK),



PLENARY SESSIONS ABSTRACTS

kurtosis anisotropy (KA)) of tumors were compared in the most malignant solid parts (in accordance with maximal MK) of 16 grade-I-II gliomas, 11 grade-III gliomas and 12 grade-IV gliomas ($P < 0.05$ significance level, Mann-Whitney test). All patients were operated within 2 weeks after MRI, and the data of our study were confirmed by morphological and immunohistochemical analysis.

RESULTS: Absolute and normalized values of MK, AK, RK, KA, FA, RA were significantly higher in HGG (grade III-IV) and absolute and normalized values of MD, AD, RD were significantly lower in HGG, compared with LGG (grade I-II).

Absolute and normalized values of MK, AK, RK, were significantly higher in grade-III gliomas and absolute and normalized values of MD, AD, RD were significantly lower in grade-III gliomas, compared with LGG (grade-I-II).

Absolute and normalized values of MK, AK, RK, KA, were significantly higher in grade-IV gliomas and absolute and normalized values of MD, AD, RD were significantly lower in grade-IV gliomas, compared with grade-III gliomas.

CONCLUSIONS: DKI demonstrated a promising potential to differentiate among glioma grades and provided added value in comparison with conventional DTI.

ADULT DIAGNOSTIC NR (PARALLEL SESSION 1)

Topkapı AB Hall

08:30 - 10:30 **Advanced Techniques**

Quantitative Imaging: Imaging Biomarker for Brain Disorder

Toshiaki Taoka

Nara Medical University Radiology Kashihara, Japan

As well as morphological image, functional images using MRS, diffusion images including diffusion tensor images or other methods become increasingly important in the diagnosis and the treatment monitor of the disease. The quantitative information obtained by these imaging methods are used as imaging biomarker in these days. The term biomarker has been defined as "A characteristic that is objectively measured and evaluated as an indicator of normal biologic processes, pathogenic processes, or pharmacologic responses to a therapeutic intervention" by the United States Food and Drug (FDA). Biological information obtained from the image is regarded as biomarkers broadly, and this concept has been applied to medical treatment or drug discovery.

The imaging biomarkers have the advantage that the quantitative information as well as qualitative information can be obtained minimally invasive or non-invasive manner.

Relaxation time (T1, T2), which is fundamental parameter of magnetic resonance is also used as imaging biomarker. The development of functional imaging method by MRI has developed variety of imaging biomarkers. Diffusion images including diffusion weighted images, diffusion tensor images and non-Gaussian diffusion images (q-space image, diffusion kurtosis image) provide information of the water movement in the tissues. Information of the brain perfusion can be obtained by dynamic contrast enhanced perfusion method or arterial spin labelling method. Information of the chemical component in the tissue can be measured by MR spectroscopy.

These imaging biomarker can be used in the clinical practice in that they can assist the diagnosis by conventional morphological approach by providing objective information. In addition the information provided these imaging biomarker can be applied for the follow up study in which comparison of objective data is necessary.



PLENARY SESSIONS ABSTRACTS

Multimodal Neuroimaging

Marion Smits

Erasmus MC Radiology Rotterdam, The Netherlands

Although there is a wide variety of techniques available to study the brain's structure and function, these techniques are generally used in isolation. Integration of different modalities, however, has several important benefits. For studying brain function for instance, the integration of electro-encephalography (EEG) with functional magnetic resonance imaging (fMRI) allows for taking advantage of each of the techniques' strong points: EEG's superior temporal resolution to fMRI is combined with fMRI's superior spatial resolution to EEG. Furthermore, techniques can be integrated to combine the study of functional and structural imaging techniques, such as fMRI and diffusion tensor imaging (DTI) respectively.

The increasing availability of computer aided diagnostic and support systems makes multimodal neuroimaging feasible. Again, instead of assessing imaging features in isolation, imaging features may be combined to increase diagnostic accuracy. Such imaging features may be derived from MRI, computed tomography (CT), but also from functional imaging modalities such as positron emission tomography (PET). The integration of such systems (MRI/CT-PET) facilitates multimodal imaging by acquiring features simultaneously.

Diffusion Tensor Image for Monitoring Treatment Effects

Toshiaki Taoka

Nara Medical University Radiology Kashihara, Japan

Although there is various category and mechanism of the disease, the role of imaging is quite important in the diagnosis and the treatment monitor of the disease. In the clinical practice, diffusion weighted images has been widely used as one of the important imaging technique which provide useful information in a short imaging time. Although cerebral infarction is the major clinical application of diffusion image, there are diseases in which the information of diffusion is important including inflammatory diseases, neoplastic diseases and diseases with edematous changes. Diffusion tensor image is the method to evaluate anisotropic motion of water molecules which is modulated by the random movement of water molecules within tissue.

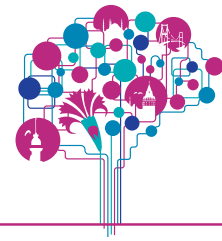
Increased diffusivity and decreased diffusion anisotropy are pointed out in various white matter degenerative brain disorders and changes in diffusion tensor parameters may reflect the extent of degenerative axonal and/or myelin loss of white matter tract. In that sense, treatment monitor of demyelinating disease is one of good application of diffusion tensor imaging. By using diffusion tensor images, serial changes of demyelinating lesions can be assessed due to the ability to visualize and quantify pathological changes in demyelinating lesions and normal-appearing brain tissue over time. As for brain tumor, large number of studies has been reported in pre-surgical grading or planning, in addition, there are also attempts to monitor treatment effect including monitoring effect of radiation therapy and chemotherapy or changes in the normal appearing brain. Degenerative diseases including Alzheimer disease are also shows alterations of the water diffusion in the brain tissue, thus information of the water diffusion in the tissue can help monitoring treatment effects. Widespread of the MR imager with ability of diffusion tensor measurement will facilitate further development of the usage of diffusion tensor image for monitoring treatment of the brain disorder.

Functional MRI BOLD and Beyond

Marion Smits

Erasmus MC Radiology Rotterdam, The Netherlands

Functional MR imaging (fMRI) is used extensively in the research arena to study an infinite number of questions regarding the brain's function and structure under normal conditions, as well as with neurological and psychiatric disease. The clinical use of these techniques, on the other hand, is by comparison fairly limited. The current main indication is the presurgical assessment of the relationship between the brain tissue to be resected



PLENARY SESSIONS ABSTRACTS

and functionally eloquent brain tissue. In the context of brain tumour surgery, the aim is maximum tumour resection, while at the same time avoiding functional deficit. With tumour localisation in or near presumed eloquent brain areas, such as the motor or language areas, additional fMRI may be advantageous to guide the neurosurgical approach, shorten surgery duration and obtain prognostic information prior to surgery. fMRI is used to localise eloquent cortex, which is particularly useful when normal anatomy is obscured by tumour mass effect or in cases of cortical plasticity.

The most commonly used fMRI technique is based on the blood oxygenation level dependent (BOLD) contrast. The BOLD contrast depends on multiple effects, not only the blood oxygenation, but also changes in the cerebral blood flow and blood volume. This renders the contrast difficult to interpret, not quantifiable, and sensitive to variability due to both external and physiological factors. Several alternatives exist, but are less commonly used. Functional imaging with arterial spin labeling (functional ASL) has the advantage of providing a quantitative measure of cerebral blood flow, potentially rendering it more suited for longitudinal and multicentre studies. Both BOLD and ASL come with limitations inherent to the underlying technique which are of particular importance when used in a clinical context. These can mainly be attributed to violation of the assumption of neurovascular coupling underlying both BOLD fMRI and functional ASL. The objectives are to learn about:

1. common clinical applications of fMRI;
2. the techniques underlying fMRI, such as BOLD and ASL.
3. limitations of fMRI, related to the underlying imaging techniques.

O021-Microstructural Effects of a Neuro Modulating Drug Evaluated by Diffusion Tensor Magnetic Resonance Imaging in Mice

*Karl Egger*¹, Philipp Janz¹, Mate Doebroessy¹, Markus Obmann¹, Thomas Bienert¹, Marco Reisert¹, Carola Haas¹, Horst Urbach¹, Laura Harsan¹, Dominik von Elverfeldt¹
*University Medical Center Freiburg Department of Neuroradiology Freiburg-Germany*¹

PURPOSE: In a recently published diffusion tensor magnet resonance imaging (DT-MRI) study with Friedreichs ataxia patients we showed significant correlations of specific diffusion parameters with clinical scores and significant changes in diffusion parameters in white matter structures after administration of human recombinant erythropoietin (EPO). We concluded that DT-MRI may serve as a biomarker for disease progression and is able to detect microstructural changes due to neuro-modulating therapies. There is evidence that EPO promotes adult hippocampal neurogenesis and neuronal differentiation.

Aim of the present study was to reproduce cerebral diffusion parameter changes after EPO administration in mice and correlate the DT-MRI findings with hippocampus related behavioral and microstructural changes.

MATERIALS AND METHODS: In vivo mouse brain DT-MRI was performed using a 7T Bruker Biospin animal scanner (Bruker, Ettlingen, Germany). In total 12 C57BL/6N mice (2 groups with 6 mice each) were scanned before and after intraperitoneal injections of erythropoietin or saline (control group) every other day for a period of 2 weeks. Additional bromodeoxyuridine (BrdU) injections were performed in both groups to detect cell proliferation. Immediately after the follow-up scans all mice underwent behavioral testing using the Water-Maze test to probe working and spatial memory and spatial navigation, functions that are considered to be hippocampus dependent. After sacrifice histologic evaluation was performed in neuro-proliferative areas of the hippocampal formation, e. g. the subgranular zone (SGZ).

RESULTS: Regarding the hippocampal area DT-MRI after EPO administration revealed significant changes in specific diffusion parameters as decreased trace, as well as decreased axial and radial diffusivity in comparison to the control group ($p < 0.05$). The EPO-treated mice also showed significant differences in cell proliferation when compared to the saline-treated control group (see image), correlating with diffusion parameter findings. Finally, the behavioral testing revealed a clear trend to better cognitive performance of the EPO-treated mice.

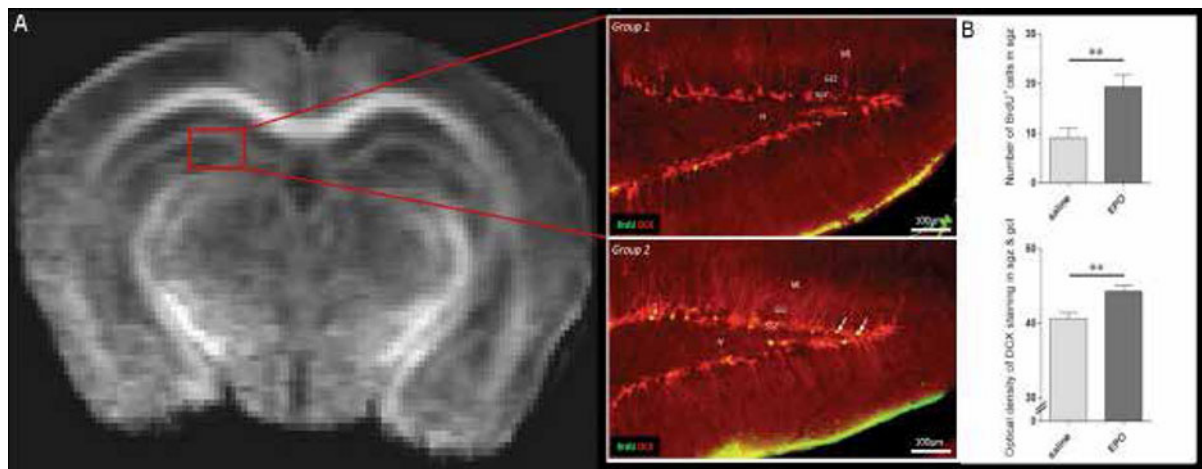


PLENARY SESSIONS ABSTRACTS

CONCLUSION: This proof of concept study showed for the first time that DT-MRI is able to detect histologically proven microstructural changes due to a neuro-modulating drug therapy. Therefore, our results confirm the hypothesis that DT-MRI is able to serve as a reliable, non-invasive biomarker for monitoring microstructural therapy effects.

Image

DTI-MRI of a mouse-brain (A) with corresponding histological ROI within the dentate gyrus (Group1 - saline and Group2 - EPO-treated) showing significant differences in cell proliferation (B).



INTRAVASCULAR INTERVENTIONAL NR

Marmara Hall

08:30 - 10:30 Long Term Results of Advanced Endovascular Aneurysm Treatment Techniques Developed During the Recent Decade

Long term results of single stent assisted coiling: view from a large experience and recent literature

Demetrius Lopes

RUSH University, USA

Long term results of dual stent assisted coiling: view from a large experience and recent literature

Saruhan Cekirge

Bayindir Hospital and KORU Hospital, Ankara, Turkey

Long term results of extraaneurysmal Flow diversion/modification: view from a large experience and recent literature

Pedro Lylyk

ENERI-Clinica La Sagrada Familia, Argentina

Long term results of intraaneurysmal Flow diversion/modification: view from a large experience and recent literature.

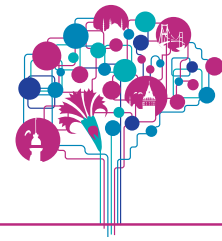
Laurent Pierot

CHU Reims, France

What has been the progress in treating giant aneurysms with flow diversion/modification: Long term results, problems and solutions

Naci Kocer

Istanbul University, Turkey



PLENARY SESSIONS ABSTRACTS

Current status of the clinical trials on aneurysm endovascular treatment

Anil Gholkar

Newcastle Upon Tyne Hospitals, NHS Trust, UK

ADULT DIAGNOSTIC NR

Anadolu Auditorium

11:00 - 12:30 CNS TUMORS 2

Ultra-High Field MR of Brain Tumors and Potential Therapeutic Applications

Nina A. Mayr

Univ. of Washington Radiation Oncology Seattle, United States

With the rapid advances of magnetic resonance imaging (MRI) technologies, many of the critical problems experienced with ultra-high-field (UHF) MRI have either been resolved or improved so that various disease entities and pathophysiologies can be investigated in the clinical setting. Based on the preliminary clinical data, new 'excitation waves' induced by UHF MRI have triggered 'multiecho resonances' throughout the medical and scientific community, as well as among manufacturers, owing to the potential of this technology in research and patient care. However, there are also criticisms of UHF MRI regarding its biophysiological limitations, unsolved technical and safety issues, and cost-effectiveness. While the debate continues over whether UHF MRI is a useful 'new tool for the child', technical improvements and the expansion of clinical applications of the technology continue.

This presentation will review the challenges, opportunities, preliminary clinical results, and limitations of UHF MRI for clinical applications in humans. The potential application for radiation therapy treatment planning and dose delivery will be discussed.

Image guided Radiation Therapy and post Radiation Therapy imaging

Nina A. Mayr

Univ. of Washington Radiation Oncology Seattle, United States

With the rapid advancement in radiation therapy technologies, high-precision delivery of radiation for brain lesions has become a widely available tool in the treatment of CNS tumors, including single- and multi-fraction delivery, such as Gamma knife radiosurgery and fractionated stereotactic radiation therapy (SRT). In addition, new radiation modalities, such as proton and particle therapy, are being explored for CNS tumors. Similarly such technologies increasingly enable high-precision treatment delivery in skull base and head and neck region that allow better protection of normal tissue and thereby radiation dose escalation to the tumor for better tumor control. The choice of imaging modalities and the use of imaging in radiation therapy planning require different paradigms than imaging for diagnostic purposes, and are areas of continued investigation.

This presentation will give an overview of imaging modalities in CNS tumors and their integration into the radiation therapy planning process and cancer surveillance. Current and novel radiation treatment modalities for brain tumors will be reviewed. Novel applications of imaging as early outcome predictor and biomarkers of response will be discussed. Pitfalls and future directions will be reviewed.



PLENARY SESSIONS ABSTRACTS

Magnetic Resonance Metabolic Imaging in Oncology

A. Beltramello¹, L. Nicoli¹, G. Cabrini², F.B. Pizzini¹, MC. Dehecchi², C. Ghimenton², A. Eccher², G. Caliarì¹, G.K. Ricciardi¹

Dept of Pathology & Diagnostics, Units of Neuroradiology¹ and Molecular Pathology², University Hospital Verona, Italy

The WHO classification of brain tumors established in 2007, which is presently considered the key reference for clinical classification and treatment, does not completely take into account the molecular status of these tumors. According to molecular biology, gliomas can be further classified into distinct molecular subgroups with different patterns of age, localisation, response to therapy and outcome, so that molecular marker status now can be used in order to guide clinical decision, at least in subtypes of gliomas. Current neuro-imaging can be expanded in order to discover, together with conventional and advanced parameters, radiogenomic determinants adequate to be indicative (proxy) of the molecular status of an individual brain tumor, enhancing diagnostic and therapeutic possibilities. Single marker approaches involve mainly three molecular markers that are assessed routinely by molecular biology techniques because of their diagnostic, prognostic or predictive value: MGMT methylation, 1p19q codeletions and IDH mutational status.

MGMT methylation: gliomas with methylated MGMT have reduced ability to repair the DNA damages induced by chemotherapeutic alkylating agents, so that they are associated with significant increase in response to therapy and overall survival. Conventional MRI proxy to MGMT methylation status are the absence of peri-tumoral edema and tumoral contrast enhancement (while ring tumoral enhancement is associated to unmethylated MGMT); on the other hand, diffusivity, according to many authors, is the advanced MRI parameter proxy to MGMT methylation status (min ADC; mean ADC).

IDH mutations: gliomas carrying IDH mutations have reduced amount of ATP content with decreased cell replication, leading to increase in overall survival. Most grade II and III gliomas share IDH mutations, which carry a better prognosis than do IDH-wild type gliomas of the same histological grade. Conventional MRI proxy to IDH mutations are the absence of peri-tumoral edema, non-contrast enhancement and frontal lobe localization; high concentration of 2HG (hydroxyglutarate) in the tumor cells, as a consequence of IDH mutations, is the advanced MRI parameter that can be measured by MR spectroscopy.

1p19q-codeletions: gliomas with 1p19q-codeletions are strongly associated with oligodendroglial histology and better outcome, due to a less aggressive natural course and higher sensibility to radio- or chemotherapy: typically 1p19q-codeleted tumors have IDH mutations. Conventional MRI proxy to 1p19q-codeletions are the same as for IDH mutations while a specific advanced MRI parameter has not yet found at the moment.

According to Weller (Lancet 2013) single marker profiling might only be a transient diagnostic standard, which could soon be replaced at reasonable cost by tumor genome-wide molecular profiling techniques: advanced MRI techniques have to be continuously implemented in order to keep more and more in touch with molecular biology techniques.

O022-The Prognostic Value of Dynamic Susceptibility Contrast Enhanced Perfusion and Diffusion Tensor MR Imaging in Patients with Glioblastomas

Gokcen Coban¹, Suyash Mohan², Feride Kural¹, Sumei Wang², Donald M. O'Rourke³, Harish Poptani²

Baskent University Medical School Radiology Department Konya-Turkey¹ University of Pennsylvania, Philadelphia Radiology Department -United States² University of Pennsylvania, Philadelphia Neurosurgery Department, United States³

PURPOSE: Our aim is to assess the utility of relative cerebral blood volume (rCBV) and mean diffusivity (MD) measurements in predicting survival for patients with glioblastomas before surgery.

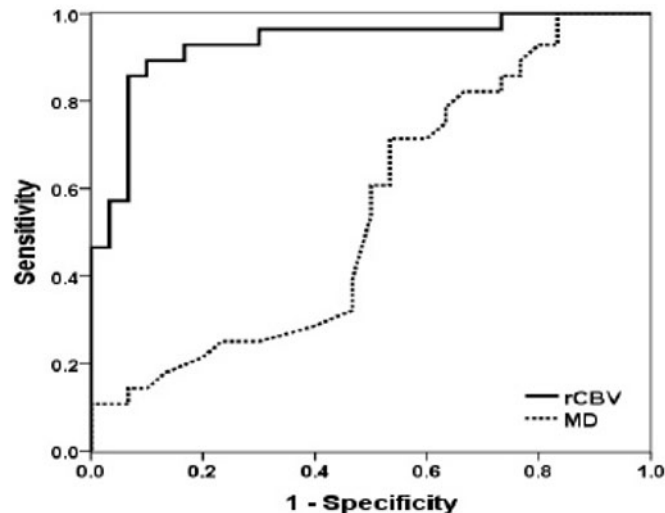
MATERIALS AND METHODS: Between June 2006 to December 2013, 58 patients (32 men and



PLENARY SESSIONS ABSTRACTS

26 women; mean age 62.7 years; age range 22-89 years) with a pathologically proven glioblastomas were included in the study. Patients divided into two groups depending on overall survival time as long survival (> 15 months) and short survival (<15 months). All patients underwent MRI including dynamic susceptibility contrast-enhanced perfusion (DSC) and diffusion tensor MR imaging before surgery. After the surgery, all the patients were treated with chemotherapy and radiation therapy.. RESULTS: The rCBV values of patients with short survival were significantly higher compared with those of long survival ($p < 0.05$). MD measurement didn't reach any significant difference. Kaplan-Meier survival curves demonstrated that glioblastomas with low rCBV (< 5.79) have a median survival time of 23 ± 3.4 months, whereas glioblastomas with high rCBV (> 5.79) have a median survival time of 5 ± 1.9 months. There was a significant difference between high rCBV and low rCBV groups ($p < 0.001$). For the MD measurement, glioblastomas with low MD ($< 8.35 \times 10^{-4} \text{mm}^2/\text{s}$) have a median survival time of 14 ± 2.0 months, whereas glioblastomas with high MD ($> 8.35 \times 10^{-4} \text{mm}^2/\text{s}$) have a median survival time of 18 ± 1.4 months. There was no significant difference (Table 1). CONCLUSION: Our results brought a new perspective that rCBV may be a predictor for overall survival in high grade gliomas. The study may have a strong prognostic impact and might help in individual treatment planning.

Table 1: Receiver operative characteristic (ROC) curves of maximum relative cerebral blood volume (rCBV) and mean diffusivity (MD) from the enhancing part of the tumor. rCBV is the best predictor for patient survival with area under the curve of 0.93 and cut-off value of 5.79.



ADULT DIAGNOSTIC NR (PARALLEL SESSION 1) Topkapı AB Hall

11:00 - 12:30 Advanced Techniques

Real-time fMRI neurofeedback: Progress and challenges.

Sven Haller

University Hospitals of Geneva and Faculty of Medicine of the University of Geneva, Switzerland

Deep brain stimulation and imaging.

Hakan Oruckaptan

Liv Hospital, Istanbul, Turkey

Advanced Functional Imaging of the Brain

Wendell A. Gibby

Adjunct Professor of Radiology, University of California San Diego, CEO – Novard Corporation, USA



PLENARY SESSIONS ABSTRACTS

Functional imaging (fMRI) interrogates the brain and measures brain functions in real time. For many years we have monitored simple physiologic processes such as cerebral cortical activation with finger tapping to localize the motor cortex prior to surgical intervention. However, fMRI can be used to test many complex cerebral functions if appropriate paradigms are created. The basis of fMRI is increased oxygen consumption in localized cortical regions during brain activation with selective tasks. The resulting physiologic response causes an inflow of oxygenated hemoglobin, altering capillary micromagnetic environment, and creating less susceptibility-induced signal loss. fMRI is a very sensitive tool to evaluate the brain, detecting serious functional problems even when structural imaging is normal.

However, the ability to extract meaningful and reproducible information from functional imaging of the brain requires at least three critical components:

1. An appropriate paradigm created to tease out specific brain activation from all other areas; e.g., how to test long-term memory without allowing patients to fudge and utilize alternative short-term memory processes.
2. Adequate controls are essential. The activation of the brain is predicated upon a physiologic response to brain oxygenation which varies significantly based upon age and perfusion status. Furthermore, there are documented differences between males and females (for example, language). Not all areas of activation are equally important in a particular paradigm; e.g. activation of the hippocampal formations is a vital clue in long-term memory evaluation. While the superior parietal lobule may activate, it is less relevant. Far too many studies are case reports of a few patients compared against a handful of graduate students which neither fulfill the criteria for appropriate controls, nor are present in sufficient numbers to exclude the ever present biological variability found in human brains.
3. The technology needed to evaluate fMRI has to undergo a profound evolution in ease of use, simplicity, speed, and lack of operator-induced prejudice (thresholding). The images are inherently noisy with data that is at the signal-to-noise limit for imaging. Optimization of the model against which statistics are generated must be done to account for perfusion status. Providing motion correction to thousands of images in three dimensions, and interfacing multiple acquisitions improves signal-to-noise and data quality. Lastly, there must be a better paradigm for displaying all of this information in a more relevant, easier-to-read format.

We've had 12 years of experience with advanced functional imaging. Working with Novarad Corporation, we have developed sophisticated technologies for "push button" functional imaging tools that allow for rapid acquisition, processing of data, statistical analysis of normal versus abnormal control sets, a vastly superior methodology to reduce motion artifacts, a dynamic model used to perform statistical tests, and a much improved paradigm for presenting this data. This lecture will provide a clear, step-by-step approach to fMRI and its interpretation.

Adult Diagnostic Neuroradiology

Key Words: Functional MRI, FMRI, Functional Imaging

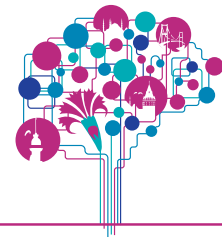
O023-Juxtacortical Lesion of Multiple Sclerosis Assessment of Gray Matter Involvement with Phase Difference Enhanced Imaging (PADRE)

*Koichiro Futatsuya*¹, *Shingo Kakeda*¹, *Issei Ueda*¹, *Keita Watanabe*¹, *Junji Moriya*¹, *Yu Murakami*¹, *Satoru Ide*¹, *Atsushi Ogasawara*¹, *Norihiro Ohnari*¹, *Kazumasa Okada*², *Tetsuya Yoneda*³, *Yukunori Korogi*¹

*University of Occupational and Environmental Health School of Medicine Radiology Kitakyushu-shi-Japan*¹

*University of Occupational and Environmental Health School of Medicine Neurology -Japan*² *Faculty of Life*

*Sciences, Kumamoto University Medical Physics in Advanced Biomedical Sciences -Japan*³



PLENARY SESSIONS ABSTRACTS

BACKGROUND and PURPOSE: In multiple sclerosis (MS), a juxtacortical lesion at the border between the gray matter (GM) and subcortical white matter (WM) may often involve the GM. Although the plaque burden within GM seems correlated with neurologic impairment in MS patients, it may be difficult to identify the GM involvement of juxtacortical lesions with conventional MRI alone. A recently developed, phase-weighted MR imaging technique “Phase Difference Enhanced Imaging (PADRE)” can delineate the GM and WM clearly due to the difference in myelin concentration. Our purpose is to evaluate whether PADRE is useful for the detection of GM involvement in the juxtacortical lesion of MS.

MATERIALS AND METHODS: Thirteen MS patients underwent PADRE in addition to routine MR imaging including a 3D FLAIR. One neuroradiologist reviewed the conventional MR images of the 13 patients and selected 58 juxtacortical lesions in 6 patients. Two other neuroradiologists participated as observers. At the first reading session, the conventional MR images were shown, and the radiologists classified the 58 MS lesions into five patterns as follows: a lesion involving (a) U-fiber alone, (b) GM alone, (c) GM and U-fibers (d) U-fiber and deep WM, and (e) GM, U-fiber, and deep WM. At the second reading session, the radiologist reviewed the PADRE images as well as the conventional MR images, and reevaluated the classification of the MS lesions. The kappa value for interobserver agreement was also evaluated.

RESULTS: At the first reading session, 58 MS lesions were classified as follows; (a): 27 lesions (46.6%), (b): 1 (1.7%), (c): 20 (34.5%), (d): 9 (15.5%), and (e): 1 (1.7%). Therefore, a total of 22 lesions (38%) were judged as involving the GM. At the second reading session, the classification was changed in 18 lesions (31%); all 18 lesions were judged (a) or (d) (=GM involvement -) at the first reading, and (b) or (e) (GM involvement +) at the second reading (Figure). Therefore, 40 lesions (69 %) involved the GM on PADRE. For the classification of MS lesions, the kappa value was 0.558 for the first reading session and 0.857 for the second reading session.

CONCLUSIONS: Juxtacortical lesions often involve the GM, and PADRE is useful for detection of the GM involvement of the juxtacortical lesions.

Figure

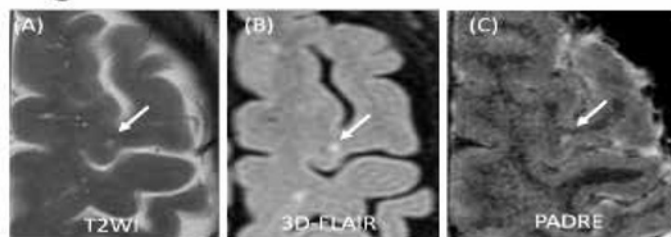


Figure caption An example of a small juxtacortical lesion which also involves the GM. At the first reading session, two neuroradiologists judged the small lesion as not involving the GM; they could not say convincingly that the lesion involved the GM because of almost no contrasts between the GM and subcortical WM on T2WI (A) and 3D FLAIR (B). At the second reading session with PADRE image (C), however, they judged the lesion as involving the GM. Because PADRE offers very clear contrast between the GM and subcortical WM, even a subtle involvement of the GM might be easily identified.



PLENARY SESSIONS ABSTRACTS

INTRAVASCULAR INTERVENTIONAL NR

Marmara Hall

11:00 - 12:30 Presentations & Discussion on Controversial Approaches & Controversies in Endovascular Aneurysm Treatment

The use Flow Divertors in the endovascular treatment of complex MCA bifurcation aneurysms: Follow-up results

Isil Saatci

KORU Hospital, Ankara, Turkey

The use of Flow Divertors in the endovascular treatment of aneurysms with an important branch arising from the aneurysm sac: Long term follow up results

Eduardo Boccardi

Hospital Niguarda, Italy

O024-Cerebral Aneurysm Treatment with Flow Re Direction Endoluminal Device (FRED) Initial Experience with Short and Mid Term Follow up Results

Burak Kocak¹, Muzaffer Saglam², Cigdem Akyol Beyoglu³, Osman Kizilkilic¹, Civan Islak¹, Naci Kocer¹

Cerrahpasa Medical Faculty Department of Radiology Istanbul-Turkey¹ GATA Haydarpasa Teaching Hospital Department of Radiology -Turkey² Cerrahpasa Medical Faculty Department of Anesthesiology and Reanimation -Turkey³

PURPOSE: Flow diverter (FD) stents are relatively new devices in treatment of complex cerebral aneurysms. Flow re-direction endoluminal device (FRED; Microvention inc.) has been in clinical use since 2012. Our aim was to report our initial single-center FRED experience with short and mid-term results. **MATERIALS AND METHOD:** Between February 2012 and 2014, forty-seven patients with 53 aneurysms were treated with FRED. Clinical and radiological data of the patients were retrospectively reviewed. **RESULTS:** All of the procedures were performed successfully. In 51 aneurysms, single FRED was used without any additional device or material. Nonetheless, in two cases, the aneurysms were occluded with coils in the same session. During follow-up period, changes in stent morphology occurred in 6 patients. Mortality and permanent morbidity rates were 2% and 0%, respectively. The complete occlusion rates were 42% at 0-1 month, 72% at 2-3 months, 82% at 4-6 months, and 93% at 7-12 months.

CONCLUSION: Considering our experience with the increasing number of the patients treated with FRED, it seems that this new device has an ability to serve in treatment of cerebral aneurysms with its different design and technical advantages. It has nearly similar occlusion rates in short and mid-term compared to the results of other FD studies and meta-analyses. However, those results are in absolute need of mid and long-term follow-up results of multi-center large series.

ADULT DIAGNOSTIC NR

Anadolu Auditorium

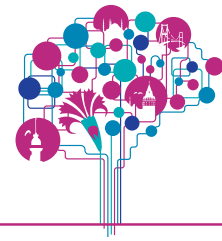
13:30 - 15:00 CNS Infections

Highlight the Diverse Neuroimaging Features of Various Tropical and Subtropical Endemic Infectious Diseases

Rakesh K. Gupta

Fortis Memorial Research Institute Radiology & Imaging Gurgaon, India

Central nervous system (CNS) infections are treatable life threatening conditions; however require prompt diagnosis and initiation of specific treatment for better outcome. A wide variety of viruses, bacteria, fungi and parasites can cause central nervous system (CNS) infection in humans. Clinical signs and symptoms of such CNS infections are mainly nonspecific, preventing early clinical diagnosis. Infections of the brain can be divided into those that predominantly affect the meninges of the brain



PLENARY SESSIONS ABSTRACTS

(meningitis), and those that affect the brain parenchyma itself (encephalitis). Frank abscess formation within the parenchyma or involvement of the coverings of the brain (empyema) can also occur. Analysis of cerebrospinal fluid (CSF), biopsy, and laboratory examination remain the gold standard to identify the infectious agent in the CNS. Neuroimaging plays a crucial role in the diagnosis and therapeutic decision making, as laboratory confirmation may take days to reach a definitive diagnosis. MRI is the modality of choice as it is more sensitive and specific for detection of both parenchymal and meningeal abnormalities. Advanced MRI tools further help in improving the specificity of a diagnosis. Key neuroimaging features of the commonly encountered CNS infections will be discussed in this presentation.

Diseases or Conditions More Common in Different Regions of the World

Yukunori Korogi

University of Occupational & Environmental Health Radiology Kitakyushu, Japan

CNS infections are caused by a broad range of pathogenic agents. Imaging findings are often nonspecific; a careful history and appropriate clinical/laboratory investigations are necessary for accurate diagnosis and appropriate treatment. In this lecture, I will cover the topics other than tropical and subtropical endemic infectious diseases as well as disimmune encephalitis; that is, acquired pyogenic infections such as meningitis and brain abscess as well as acquired viral infections such as herpes simplex encephalitis.

Meningitis is an acute or chronic inflammatory infiltrate of meninges and CSF. Many different infectious agents can cause meningitis; most cases are caused by acute pyogenic (bacterial) infection. The basal cisterns and subarachnoid spaces are most commonly involved by meningitis, followed by the cerebral convexity sulci. Imaging should be used in conjunction with appropriate clinical and laboratory evaluation. Hyperintensity in the subarachnoid cisterns and superficial sulci on FLAIR is a typical but nonspecific finding of meningitis. DWI may be helpful in meningitis, as the purulent subarachnoid space exudates usually show restriction. Bacterial meningitis enhances intensely and uniformly on postcontrast T1WI. A curvilinear pattern that follows the gyri and sulci is common. Contrast-enhanced FLAIR scans may be helpful in detecting subtle cases.

Herpes simplex encephalitis is hemorrhagic, necrotizing central nervous system infection by herpes simplex virus, and most common cause of sporadic fatal encephalitis. Disease typically caused by reactivation of virus in immunocompetent patients, and HSV relatively uncommon in HIV (+) population. Most cases show fever, focal neurological deficits, significant alteration in level of consciousness, psychiatric symptoms, and cognitive defects. Herpes simplex encephalitis has a notable affinity for the limbic system. The anterior and medial temporal lobes, insular cortex, subfrontal area, and cingulate gyri are most frequently affected. Bilateral but asymmetric disease is typical. Extratemporal, extralimbic involvement occurs but is more common in children compared to adults. The basal ganglia are usually spared. MR is the imaging procedure of choice. T2WI/FLAIR demonstrates cortical/subcortical hyperintensity with relative sparing of the underlying white matter. DWI is also sensitive for detecting the signal changes.

Discussion and Diagnosis of Dys-immune Encephalitis

Rakesh K. Gupta

Fortis Memorial Research Institute Radiology & Imaging Gurgaon, India

Encephalitis, defined as inflammation of the brain tissue, is a common medical emergency. Early diagnosis and appropriate treatment are of paramount importance to ensure good outcome. In absence of infectious etiology, other diagnoses must be considered promptly. Autoimmune or dysimmune encephalitis associated with neural autoantibodies or dysregulated immune responses are being increasingly recognized as important and potentially reversible non-infectious causes of an encephalitic syndrome.¹

Initially, this type of encephalitis was considered a paraneoplastic phenomenon, typically associated with a number of tumors and many of the antibodies (abs) targeted against intracellular antigens (such as hu, cV2/cRMP5 and Ma2). Patients with these antibodies and associated tumors are unlikely to respond to immunotherapy



PLENARY SESSIONS ABSTRACTS

and have in general a poorer prognosis.^{2,3} More recently described antibodies are directed against cell surface molecules and ion channels in particular. By contrast to those with paraneoplastic encephalitis, patients with antibodies against surface antigens often have no underlying tumor and respond well to immunotherapy.^{4,5} Despite a growing knowledge of dysimmune encephalitis, this area remains poorly understood. Importantly, it is often a treatable neurologic condition and hence its consideration and recognition is of great importance. The intention of this presentation is to raise awareness and discuss imaging features of dysimmune encephalitis.

1. Wingfield T, McHugh C, Vas A, et al. Autoimmune encephalitis: a case series and comprehensive review of the literature QJM 2011 104 921–31.
2. Dalmau J, Rosenfeld MR. Paraneoplastic syndromes of the CNS, Lancet Neurol, 2008;7:327–40.
3. Vincent A. immunology of disorders of neuromuscular transmission, Acta Neurol Scand Suppl, 2006;113:1–7.
4. Zuliani I, Graus F, Giometto B, et al., central nervous system neuronal surface antibody associated syndromes: review and guidelines for recognition, J Neurol Neurosurg Psychiatry, 2012;83:638–45.

Vincent A, Bien CG, irani SR, Waters P, autoantibodies associated with diseases of the CNS: new developments and future challenges, Lancet Neurol, 2011;10:759–72.

O025-Assessment of Early Cerebral Damage in The Course Of HIV and HCV Infection Using Perfusion MR Imaging Is the Hepatitis C Virus More Dangerous for the Brain

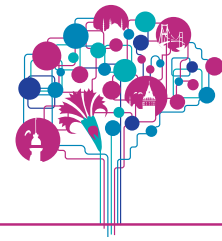
*Joanna Bladowska*¹, Anna Zimny¹, Brygida Knysz², Anna Koltowska¹, Krzysztof Malyszczak³, Pawel Szewczyk¹, Jacek Gasiorowski², Michal Furdal⁴, Marek Sasiadek¹

*Wroclaw Medical University Department of General Radiology, Interventional Radiology and Neuroradiology Wroclaw-Poland*¹ *Wroclaw Medical University Department of Infectious Diseases, Liver Diseases and Acquired Immune Deficiency -Poland*² *Wroclaw Medical University Department of Psychiatry -Poland*³ *Regional Specialistic Hospital Department of Cardiology -Poland*⁴

PURPOSE: The aim of the study was to evaluate early disturbances in cerebral microcirculation using magnetic resonance (MR) perfusion-weighted imaging (PWI) in asymptomatic HIV-1-positive and HCV-positive patients as well as to assess the correlation between perfusion-weighted imaging (PWI) measurements and the clinical data.

MATERIALS AND METHODS: Fifty-six patients: 17 HIV-1-positive non-treated, 18 HIV-1-positive treated with combination antiretroviral therapy (cART), 7 HIV-1/HCV-positive non-treated, 14 HCV-positive before antiviral therapy and 18 control subjects were enrolled in the study. PWI was performed with a 1.5T MR unit using the dynamic susceptibility contrast (DSC) method. Cerebral blood volume (CBV) measurements relative to the cerebellum (rCBV) were evaluated in the posterior cingulate region (PCG), basal ganglia (BG), temporoparietal (TPC) and frontal cortices (FC), as well as in white matter of frontoparietal areas. Correlations of rCBV values with immunologic data, liver histology activity index (HAI) as well as the cognitive tests results were analysed. Analysis of variance followed by the post hoc Tukey LSD test was used for statistical evaluation (significant $p < 0.05$). Additionally, we applied the Bonferroni correction (significant $p < 0.0055$).

RESULTS: Significantly lower rCBV values ($p < 0.05$) were found in the right TPC and left FC as well as in PCG in all HIV-1-positive and HCV-positive patients compared to controls. HIV-1-positive cART treated and HIV-1/HCV-positive patients demonstrated lower rCBV values in the right FC and the left TPC, while HCV-positive subjects revealed lower rCBV values in the left TPC regions. We found significantly increased rCBV values in BG in HCV-positive patients compared to controls as well as to all HIV-1-positive subjects. There were significant correlations between rCBV values in the temporoparietal and frontal cortices, basal ganglia region and the cognitive tests results. We did not observe any significant correlations between rCBV values and CD4 T cell count or HAI score. According to the Bonferroni correction only HCV subjects showed significant changes of rCBV values ($p < 0.0055$).



PLENARY SESSIONS ABSTRACTS

CONCLUSION: PWI examination enables the assessment of HIV-related as well as HCV-related early cerebral dysfunction in asymptomatic subjects. HCV-infected patients seem to reveal the most pronounced perfusion changes. Hyperperfusion in basal ganglia may be an indicator of brain inflammation in HCV patients.

ADULT DIAGNOSTIC NR (PARALLEL SESSION 1) Topkapı AB Hall

13:30 - 15:00 Advanced Imaging

What to expect from MR Spectroscopy

Marco Leonardi

Bologna University, IRCCS Neuological Research Hospital, Italy

C arm CT and Quantitative DSA

Wan-Yuo Guo

Taipei Veterans General Hospital Radiology Taipei, Taiwan

Flat-detector digital subtractive angiography (FD-DSA, cone-beam CT or C-arm CT) becomes a standard reference imaging in neurovascular disorders. Compared with multi-detector CT or conventional imaging intensifier DSA, FD-DSA provides: wider scanning coverage, better scanning efficacy, higher spatial resolution and lower radiation dose. The advantages enable FD-DSA for one-stop imaging that saves patient transportation, provides in-room real-time hemodynamics availability during interventional procedures and more importantly therapeutic guidance for various neurovascular disorders. Nowadays, measurement of cerebral perfusion, namely cerebral blood volume (CBV), cerebral blood flow (CBF) and circulation times, using FD-DSA is becoming feasibly available in clinical setting. In addition, recent development of time resolved 3D-DSA, so-called 4D-DSA, further extends the application of FD-DSA. The spatial and temporal resolutions provided by 4D-DSA exceed that of CT angiography and MR angiography. It will empower C-arm CT one more step further toward the era of "one-stop Imaging" by enriching the hemodynamics obtained from DSA. The presentation covers the contents of quantification of cerebral hemodynamics ranging from diagnostic to intra-interventional procedures and post-therapeutic evaluation. The diseases categories included: carotid arterial occlusive diseases, dural arteriovenous fistula with/without sinus disorders, cerebral arteriovenous malformation, post-hemorrhagic arterial spasm and moyamoya disease. The treatments employed for this patient cohort included re-vascularization and de-vascularization procedures, namely, extracranial and intracranial carotid artery stenting, intra-arterial thrombectomy/thrombolysis, EC-IC bypass, microsurgery, radiosurgery, embolization and/or their combinations. The application is also further extended to patients with various types of aortic dissection/aneurysm. C-arm CT provides imaging guidance for combining stent-graft with hybrid cervical de-branching of thoracic endovascular aortic repair and allows evaluation of peri-therapeutic brain hemodynamics in one-stop.

The improvement of imaging technology in DSA (high efficacy flat detector with high spatial resolution and improving contrast resolution) allows us to quantitatively study cerebral hemodynamics of patients with neurovascular disorders by using only FD-DSA. It will definitely change the scenario of our future imaging practice in neurovascular disorders.

Angioscopy

Timo Krings

Toronto Western Hospital, Canada



PLENARY SESSIONS ABSTRACTS

O026-Usefulness of Acute Stroke Imaging with Wide Area Detector CT Before Endovascular Reperfusion Therapy in the Anterior Cerebral Circulation

Takahisa Mori, Tomonori Iwata, Yuhei Tanno, Shigen Kasakura, Yoshinori Aoyagi, Kazuhiro Yoshioka
Shonan Kamakura General Hospital Stroke Center Stroke Treatment Kamakura, Japan

BACKGROUND and PURPOSE: The wide area detector CT (ADCT) enables volume scanning (VS) for the whole brain and can provide whole brain CT perfusion (CTP) and dynamic vascular analysis (3D/4D-CTA) in one examination. Whole brain 4D-CTA can dynamically display the affected cerebral artery, other cerebral arteries and intracranial arterial communication like digital subtraction angiography (DSA). Therefore, 4D-CTA may allow us to perform reperfusion therapy directly to the target vessel without diagnostic whole brain angiography. The aim of this study was to investigate the usefulness of ADCT before endovascular reperfusion therapy in the anterior cerebral circulation (ACC). **MATERIALS AND METHOD:** Included in our retrospective analysis were patients 1) who were transferred to our institution from November 2010 to November 2013, 2) who underwent ADCT (Aquilion ONE, Toshiba) before endovascular reperfusion therapy (ERT) and 3) who underwent ERT for the affected artery in the ACC within 8 hours of the onset. Acute imaging protocol for stroke diagnosis and reperfusion therapy consists of pre-contrast CT and subsequent MRI set (DWI, MRA, T2WI, T2*WI) and subsequently helical 3D-CTA from the aorta to the distal neck arteries and whole brain VS for 3D-, 4D-CTA and CTP. Each volume consisted of 160 images of 1-mm thickness with z-axis coverage of 16-cm. Evaluated were onset-to-puncture time (OPT), door-to-puncture time (DPT) and successful ERT. Successful ERT was defined as TICI of 2b or 3.

RESULTS: During the study period, 17 patients matched to our inclusive criteria. Aorticercival 3D-CTA helped endovascular therapists to decide which approach was suitable to patients, transfemoral or transbrachial. Intracranial 4D-CTA gave them useful information to perform a direct access to the target artery without diagnostic whole brain angiography. Median OPT and DPT were 3.5 and 2.1 hours, respectively. Successful ERT rate was 76% (14/17).

CONCLUSION: Our acute stroke imaging protocol using ADCT can rapidly provide endovascular therapists with useful information just before ERT in acute stroke setting.

INTRAVASCULAR INTERVENTIONAL NR

Marmara Hall

13:30 - 15:00 Endovascular Treatment of Acute Stroke. The Past, Present and Future

Summary of completed studies on endovascular acute stroke treatment

Aquilla Turk

Medical University of South Carolina, USA

Summary of Ongoing Studies on Endovascular Acute Stroke Treatment

Tommy Andersson

Karolinska Hospital Neuroradiology Stockholm, Sweden

PURPOSE: In the March 2013 issue of the New England Journal of Medicine, three articles were published, all claiming that intra-arterial treatment (IAT) for acute ischemic stroke was not superior to intravenous thrombolysis. Since then, there has been an urge to perform new studies, preferably randomized controlled ones, and consequently there are many on-going at the moment. However, these studies all suffer from some common, conceptual problems. These problems as well as reported interim results will be analysed and discussed.

MATERIALS AND METHODS: The protocols from some of the larger studies were analysed as well as reported problems and published interim results.



PLENARY SESSIONS ABSTRACTS

RESULTS: All studies suffer from three major problems:

1. Non-consecutive enrolment
2. Difficulties in achieving consent
3. Difficulties in standardizing the endovascular procedure

CONCLUSIONS: Because of the large, conceptual problems that these on-going studies face, the validity of the future results are jeopardized, i.e. not reflecting the truth. In addition, even a for endovascular treatment positive result may be dangerous in the long run as it allows also small centres to perform IAT with a consequent increase in complication rate.

What Would Be the Future of Acute Stroke Treatment

Ethem Murat Arsava

Hacettepe University Neurology Ankara, Turkey

Despite the proven efficacy of intravenous thrombolysis, only a minority of patients can actually benefit from the therapy in the real world setting. Issues with timely diagnosis of acute ischemic stroke is one of the critical barriers in administration of thrombolytic therapies. The implementation of care systems with dedicated stroke units and emergency departments equipped with state-of-the-art technologies like specialized stroke ambulances will increase the widespread applicability of the treatment in the near future. Furthermore, the use of newer generation thrombolytic agents like tenecteplase or reteplase, which are considered to have a better safety profile compared to tissue plasminogen activator, might help in optimizing the benefit obtained from intravenous thrombolysis. Although recently published trials of intra-arterial thrombolysis were not able to establish their superiority in comparison to standard care, there is a certain sub-group of patients that have a high potential for benefit from intra-arterial thrombolysis. Development of clinical and imaging algorithms that will accurately identify such patients would be critical in optimizing patient selection. The future of acute stroke management will however not only consist of therapies aiming recanalization and reperfusion, but will also include neuroprotective strategies that will make use of hypothermia, targeted drug delivery systems and nanomedicine.

O027-The pREset Retriever for Endovascular Treatment of Stroke after MCA Occlusion Safety and Clinical Outcome

*Benedikt Jakob Schwaiger*¹, Fabian Kober¹, Alexandra Sophia Gersing¹, Holger Poppert², Claus Zimmer¹, Sascha Prothmann¹

*Klinikum rechts der Isar der TU Muenchen Neuroradiology Muenchen-Germany*¹ *Klinikum rechts der Isar der TU Muenchen Neurology -Germany*²

PURPOSE: Endovascular mechanical thrombectomy (MT) is a promising therapeutic option in acute ischemic stroke (AIS) after large vessel occlusion. Purpose was to analyze safety and efficacy of the pREset device, a new stent retriever system for MT.

MATERIALS AND METHODS: Retrospectively, 48 consecutive patients (24 female; age 71.0±11.9) treated for acute MCA occlusion using the pREset device solely or in combination with other MT devices, were identified. Therapy decision was based on CT+CTA performed at admission. Recanalization success was evaluated by TICI score and a CT was performed 24 hours after intervention, for detection of complications. MCA anatomy was assessed in angiograms. Clinical performance was evaluated with NIHSS at admission and discharge, and functional outcome was measured using mRS at discharge and follow-up. RESULTS: In 32 patients (66.7%) MT was performed using pREset solely, while in the remaining patients multiple devices were used. 34 patients (65.4%) additionally received IV rtPA. Successful recanalization (TICI 2b/3) was achieved in 29 patients (90.6%) using pREset solely, while the rate of successful recanalization was significantly lower (n=10, 62.5%; p<0.05) after a significantly longer procedural time (45.0±28.1 versus 73±43.2 minutes;



PLENARY SESSIONS ABSTRACTS

$p < 0.05$) if multiple devices were used. Overall rate of TICI2b/3 was 81.3% ($n=39$). The rate of procedure-related complications was 8.3% ($n=1$ for vasospasm, perforation, dissection and thrombus dispersion, respectively). SAH was detected in 4 patients (8.3%), and intracranial hemorrhage in 7 patients (14.6%). None of those events was associated with a clinical deterioration. There was a highly significant influence of MCA curvature on recanalization success ($p < 0.005$). No significant influence of IV rtPA on recanalization rates or clinical outcome was detected.

TICI2b/3 was associated with significantly better NIHSS scores and a favorable clinical outcome (mRS 0–2) at discharge ($p < 0.05$). Also, the 90-day mortality was significantly lower in patients with TICI 2b/3 ($p < 0.005$).
CONCLUSION: This study showed a high recanalization rate and low complication rate in patients treated with the pREset, especially when treated with this device solely. Clinical outcome was significantly better after successful recanalization. This strongly suggests that MT with pREset is an adequate therapy for AIS induced by MCA occlusion. Vessel anatomy, i.e. MCA curvature, is a significant determining factor for recanalization success.

ADULT DIAGNOSTIC NR

Anadolu Auditorium

15:30 - 17:00 CSF

Hydrocephalus (part 1: etiology and diagnosis)

Geir Ringstad

Oslo University Hospital - Rikshospitalet, Norway

Hydrocephalus Part 2 (Evaluation of Treatment Options and Follow up)

Yukunori Korogi

University of Occupational & Environmental Health Radiology Kitakyushu, Japan

Hydrocephalus is disorders of CSF production, circulation, and/or absorption; it is relatively common in the elderly and a potentially treatable cause of encephalopathy. There are no currently accepted evidence-based guidelines for either the diagnosis or treatment of normal pressure hydrocephalus (NPH). NPH is characterized by ventriculomegaly with normal CSF pressure and altered CSF hydrodynamics. Idiopathic NPH (iNPH) is distinguished from secondary NPH. The nature and severity of symptoms as well as the disease course vary in NPH. Impaired gait is the typical initial symptoms. The classic triad of dementia, gait disturbance, and urinary incontinence is present in a minority of patients. While gait disturbances are seen in most cases, not all patients exhibit impaired cognition. Recently, a condition of DESH (disproportionately enlarged subarachnoid-space hydrocephalus) has been gradually recognized. The DESH concept may be useful for differentiation from age-related brain atrophy; in DESH, the ventricle system and the Sylvian fissure are widely dilated, while the sulci at the high convexity are “disproportionately” tight. Localized CSF “pool” (localized enlarged sulcus) seems also characteristic of DESH. As treatment options of NPH, some patients initially respond dramatically to ventricular shunting. The favorable response to shunting varies from one-third to two-third of patients according to clinical diagnosis such as “possible” NPH or “probable” NPH. Long-term outcome is more problematic. While early gait improvement is common, only one-third of patients experience continued improvement three years after shunting. Cognition and urinary incontinence are even less responsive. The iNPH may include DESH and non-DESH; it is reported that about 90% of the DESH patients with gait disturbance will response to the shunt operation.

AVIM (Asymptomatic ventriculomegaly with features of idiopathic normal pressure hydrocephalus on MRI) is asymptomatic DESH whose brain MRI findings resemble to iNPH; about one fourth of the patients of AVIM may eventually develop gait disturbance and dementia during 4-8 years follow up. In this lecture, focusing on NPH, I briefly review the syndrome and summarize the spectrum of imaging findings that may suggest the evaluation of treatment options and follow-up in hydrocephalus.

7-12 September 2014
ISTANBUL, TURKEY

LUTFI KIRDAR CONVENTION & EXHIBITION CENTER

XXth
Symposium
Neuroradiologicum



PLENARY SESSIONS ABSTRACTS

Other CSF disorders (except hydrocephalus)

Geir Ringstad

Oslo University Hospital - Rikshospitalet, Norway

Quantitative CSF Flow Analysis in Chiari Malformation

Wendell A. Gibby

Adjunct Professor of Radiology, University of California San Diego, CEO – Novard Corporation, USA

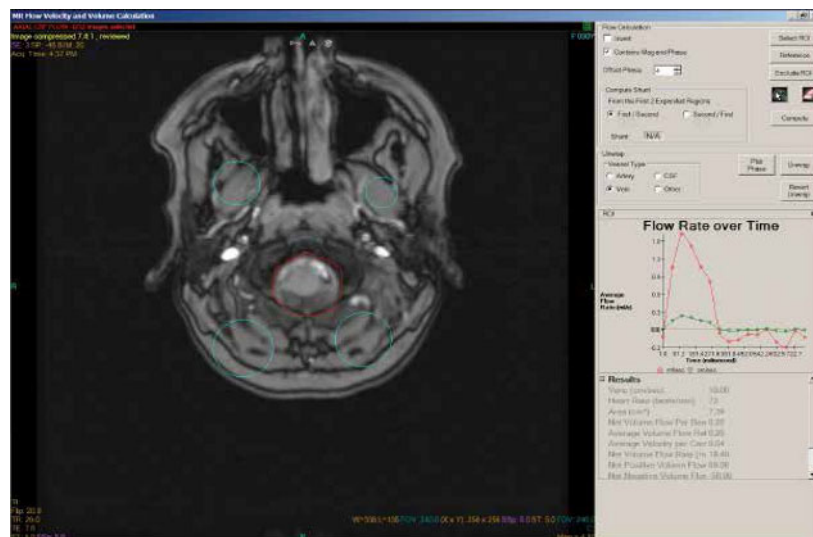
PURPOSE: Chiari malformations are reported in pathologic studies at a rate of 1/1000. However, the advent of MRI has revealed it is much more common - about 1/100. Diagnosis is made by measuring cerebellar tonsils protruding through foramen magnum a distance of 5 mm or more. This is a somewhat arbitrary measurement. Chiari malformations are significant because of what they cause; headaches, and in some cases syringomyelia of the spinal cord. This study utilized flow imaging to evaluate cerebral spinal fluid (CSF)

dynamics and better predict patients with a significant Chiari malformation. In the past we have had to “eyeball” this. Many cerebellar tonsils extend more than 5 mm and yet the foramen magnum is not “tight.” Some extend less and are very symptomatic. The advent of phase contrast imaging with MR has given us a noninvasive way to study CSF flow through the foramen magnum. However, this has also been fraught with subjectivity. One typically looks at the sloshing of fluid through the foramen on flow studies and tries to determine based on experience whether the flow is appropriate.

MATERIALS AND METHODS: We have developed a new CSF flow analysis system on standard Windows computers that allows the selection of measurement location, calculation of the area of interest, peak and average flow velocities (both positive and negative), net flow volumes, and exclude unwanted arterial flow. Subjectively we selected ten Chiari malformations demonstrating little CSF space on axial T2W images through the foramen magnum.

RESULTS: We have successfully applied this to ten Chiari malformation patients as a proof of concept, and have noted an increase in the peak velocity of flow in patients with “tight” foramen magnum. Flow is usually absent dorsally and increased in velocity ventrally. We have noted patterns of flow that are more common with Chiari patients.

CONCLUSION: CINE phase contrast flow velocity measurements through the foramen magnum may allow us to distinguish in a more quantitative way significant Chiari malformations by measuring peak velocities. We would like to offer this technology to interested research centers for a multi-institutional study of Chiari patients and CSF flow.





PLENARY SESSIONS ABSTRACTS

ADULT DIAGNOSTIC NR (PARALLEL SESSION 1) Topkapı AB Hall

15:30 - 17:00 Telemedicine architecture session (*Parallel Session*)

Advantages and challenges in Telemedicine. For example: The setup of a Neuroscience Rehab Center at Jerudong Park Medical Center in Brunei Darussalam

Opening remarks

Bodo Kress

Head of Department of diagnostic and interventional Neuroradiology, Krankenhaus, Frankfurt, Germany and Head of Department of Neuroradiology, Jerudong Park Medical Center, Jerudong, Brunei Darussalam

From 0 to 100: Setup of a Neuroscience Rehab center

Datin Uta Meyding-Lamade

Head of Department of Neurology, Krankenhaus Nordwest, Frankfurt, Germany and Head and CEO of The Brunei Neuroscience and Rehabilitation Center, Jerudong Park Medical Center, Jerudong, Brunei Darussalam

It is simple, we will do it via the internet. Challenges in network and infrastructure

Mattes Papendieck

CEO Meytec Telemedicine Systems, Werneheuchen, Germany

24/7 Neuroradiology over a distance of 12000 km

Bodo Kress

Head of Department of diagnostic and interventional Neuroradiology, Krankenhaus, Frankfurt, Germany and Head of Department of Neuroradiology, Jerudong Park Medical Center, Jerudong, Brunei Darussalam

The specialist on site. Role of the radiographer in a teleneuroradiological concept

Varghese Paulouse

Chief Radiographer, Department of diagnostic imaging, Jerudong Park Medical Center, Jerudong, Brunei Darussalam

Video-conference: Looking abroad, ward round over the distance

Datin Uta Meyding-Lamade

Head of Department of Neurology, Krankenhaus Nordwest, Frankfurt, Germany and Head and CEO of The Brunei Neuroscience and Rehabilitation Center, Jerudong Park Medical Center, Jerudong, Brunei Darussalam

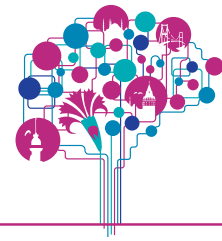
Video conference: Global classroom. Interactive teleteaching of students

Bodo Kress

Head of Department of diagnostic and interventional Neuroradiology, Krankenhaus, Frankfurt, Germany and Head of Department of Neuroradiology, Jerudong Park Medical Center, Jerudong, Brunei Darussalam

Discussion and Closing remarks

Bodo Kress, Germany



PLENARY SESSIONS ABSTRACTS

INTRAVASCULAR INTERVENTIONAL NR **Marmara Hall**

15:30 - 17:00 Controversies on Supraaortic Revascularization in 2014

Intracranial stenting: Dead or Alive? Need another trial?

Hans Henkes

Klinikum Stuttgart / Klinik Für Neuroradiologie, Germany

Revascularization of non-acute total ICA occlusions: What is real indication?

Tomoaki Terada

Showa University Fujigaoka Hospital, Japan

How Far Can We Go with Medical Treatment Neurologist View

Ethem Murat Arsava

Hacettepe University Neurology Ankara, Turkey

The demonstration of carotid artery revascularization as an effective therapeutic approach in patients with moderate to severe symptomatic carotid artery stenosis is considered as one of the milestones in secondary prevention of stroke. This was later followed by the use revascularization therapies, either by surgical or endovascular means, for the treatment of similar conditions like asymptomatic carotid artery stenosis, carotid artery occlusion or intracranial stenosis. Most of the trials that tested the efficacy of revascularization therapies over medical therapy were performed in an era where aggressive medical management was not part of the standard of care.

The implementation of modern medical therapy strategies that include tight blood pressure control, aggressive blood glucose and lipid management, monitoring for life style changes, has led to a substantial decrease in the incidence of primary and recurrent strokes, and therefore a reduction in the benefit that might be potentially obtained from revascularization performed on top of medical therapies.

O028-Bail Out Intracranial Stenting with After Unsuccessful Thrombectomy

Nicola Limbucci, Leonardo Renieri, Nappini Sergio, Arturo Consoli, Andrea Rosi, Salvatore Mangiafico
Careggi University Hospital, Florence Interventional Neuroradiology Firenze, Italy

PURPOSE: The most common endovascular intervention for acute ischemic stroke is thrombectomy, while intracranial acute stenting is not routinely performed. In case of unsuccessful recanalization after thrombectomy, stenting can be performed as a bail-out procedure to achieve vessel patency. We report our experience of bail-out stenting for severe stroke after unsuccessful thrombectomy.

MATERIALS AND METHODS: Among all thrombectomies performed in our institution from Jan 2008 to Dec 2013 (180 cases) we selected all patients treated by bail-out permanent stenting. 24 consecutive patients were selected (mean age 67.4; 13M 12F). The stent was deployed after failed thrombectomy only if the target artery was fully or partially patent with the stent on site. Tirofiban ev bolus (weight-dependent) was administered, followed by 6-12 hours infusion; double anti platelet therapy was started after 12-24 hours. We evaluated recanalization time, recanalization rate, hemorrhage rate and clinical outcome by means of 3 months mRS.

RESULTS: Stroke involved the the basilar artery in 5 cases (20.8%) and the anterior circulation in 19 cases (79.2%; 5 carotid syphon and 14 M1 occlusions); in 5 patients, concomitant extracranial carotid occlusion was observed.



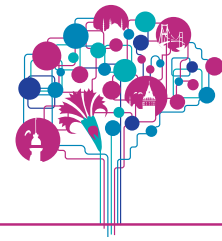
PLENARY SESSIONS ABSTRACTS

Mean NIHSS at admission was 20.1. Mean onset to start of treatment time was 264 minutes. Mean door-to-recanalization time was 380 minutes. Devices used for thrombectomy were: Solitaire (50%), Revive (16.7%), Trevo (12.5%), Enterprise (12.5%), Phenox (4.2%), Merci (4.2%). The mean number of thrombectomy attempts was 2.9. In 10 patients adjunctive intrarterial urokinase was administered (mean 300000IU). In 21 patients Tirofiban was administered after stenting.

Intracranial stenting was performed with: Solitaire (79.2%), Enterprise (16.7%), Neuroform (4.2%). No intraprocedural complications occurred. Four patients underwent extracranial carotid stenting. Good recanalization (TICI 2b-3) rate was 62.5%. Symptomatic intracranial hemorrhage rate was 4.2%.

Good clinical outcome rate was 37.5%. Three months mortality was 16.7%.

CONCLUSIONS: In our experience, permanent bail-out stenting allowed a good recanalization rate and acceptable clinical results in patients that had not been recanalized by conventional treatments. We believe that bail-out stenting is a safe adjunctive technique that improves clinical outcome in a subgroup of patients who presumably would have a very poor outcome due to persistent major vessel occlusion. It is likely that a faster recanalization time would improve clinical results.



PLENARY SESSIONS ABSTRACTS

Friday, September 12, 2014

ADULT DIAGNOSTIC NR

Anadolu Auditorium

08:30 - 10:30 **Multiple Sclerosis 1**

Neuroradiological manifestations of novel treatments

Tarek A. Yoursy

UCL Institute of Neurology / National Hospital for Neurology & Neurosurgery, UK

Susceptibility-Weighted MR Imaging in Multiple Sclerosis

Àlex Rovira

Hospital Universitari Vall d'Hebron Barcelona, Spain

Although based on its high sensitivity MR imaging has become the key diagnostic tool in the diagnosis of MS, many imaging findings seen in MS patients are not specific for the disease. The 2010 McDonald criteria have become more liberal over time possibly leading to the undesirable situation of MS overdiagnosis (Solomon et al. Neurology 2010). Therefore, disease differentiation is a key issue in this context. The perivenular distribution pattern and increase iron deposition in MS lesions has been a target to address this issue particularly when MR systems operating at higher magnetic field strengths ($\geq 3T$) are used (Sinnecker T et al. Neurology 2012; Wuerfel J et al. Mult Scler 2012, Tallantyre et al. Neurology 2008; Tallantyre et al. Invest Radiol 2009, Tallantyre et al. Neurology 2011; Hammond KE et al. Ann Neurol 2008; Haacke et al, JMRI 2009).

A rather new sequence, susceptibility weighted imaging (SWI) described by Haacke in 2004 (Haacke et al. MRM 2004), which combines magnitude and phase images, has shown high sensitivity for detecting iron in the form of hemosiderin or ferritin within brain tissue and small veins due to their paramagnetic properties. This technique has added value for these purposes particularly when co-registered and mixed to standard pulse sequences such as T2-FLAIR coining the term FLAIR* (Sati P, et al. Radiology. 2012; Grabner et al. JMRI 2011). Recent experience with the implementation of SWI at 3.0T/7.0T in MS has shown that most focal chronic, and some acute, demyelinating lesions can be depicted as areas of low signal intensity likely representing iron deposition (Haacke et al. JMRI 2009; Hammond KE et al., Ann Neurol 2008; Absinta et al. Ann Neurol 2013; Hagemeyer et al. JMRI 2012; Bian et al. MSJ 2012), and that a substantial proportion (higher than 40%) of MS lesions shows a central vein (Sinnecker T et al. Neurology 2012; Tallantyre et al. Neurology 2008; Tallantyre et al. Invest Radiol 2009; Kau Eur Radiol 2013; Luo et al. MSJ 2013; Wuerfel et al. MSJ 2012). Future studies will have to demonstrate whether the incorporation of these imaging findings will further improve the specificity of MRI in the diagnosis of MS.

MRI Monitoring in MS Treatment Efficacy and Safety

Yukio Miki

Osaka City University Diagnostic and Interventional Radiology Osaka, Japan

MR imaging has been established as the most important tool for diagnosing multiple sclerosis (MS). Furthermore, this modality is increasingly being used to monitor disease activity, disease progression and therapeutic effects, and is therefore now recognized as an "imaging biomarker" for MS (1). T2-lesion volume is one of the MR measurements most frequently used in clinical trials (2-4). Several studies have shown that T2-lesion volume has no significant correlation with disabilities at the time of MR examination (5-8). Possible reasons for this discrepancy may include: 1) presence of brain atrophy; 2) presence of spinal cord lesions; 3) heterogeneity of T2-lesions; and 4) presence of microscopic lesions in normal-appearing white matter. However, T2-lesion volume has been reported to correlate significantly with later (>5 years) disabilities (8, 9).



PLENARY SESSIONS ABSTRACTS

Another frequently used MR measurement is the count of gadolinium-enhancing lesions (4). Enhancing lesion number/volume is considered to represent disease activity, thus this measurement is also frequently used to evaluate drug efficacy in clinical trials (10).

Other MR measurements used for clinical trials include measurement of brain atrophy, measurement of T1-blackhole volume, magnetization transfer ratio histograms, and MR spectroscopy (4, 11). Diffusion-weighted MR imaging is also used for quantitative analysis of MS. The apparent diffusion coefficient and fractional anisotropy are both reportedly decreased in MS lesions (12). Diffusion kurtosis of normal-appearing white matter has been reported to be decreased in MS patients (13). In addition, diffusion-weighted thermometry has revealed decreased brain temperatures in MS patients, potentially representing decreased brain metabolism (14).

MR imaging is also useful for diagnosing the side effects of drugs. Recently, it has been reported that MS patients treated with natalizumab may develop progressive multifocal leukoencephalopathy (PML)(15). MR imaging is useful for diagnosing natalizumab-associated PML and the related immune reconstitution inflammatory syndrome.

REFERENCES:

1. Filippi, et al. *JMRI* 2010;31:770-88
2. Jacobs, et al. *NEJM* 2000;343:898-904
3. Saida, et al. *Neurology* 2005;64:621-30
4. Lovblad, et al. *AJNR* 2010;31:983-9
5. Miki, et al. *Radiology* 1999;213:395-9
6. Kremenutzky, et al. *Brain* 2006;129:584-94
7. Filippi, et al. *JNeuroimaging* 2007;17Suppl1:3S-9S
8. Fisniku, et al. *Brain* 2008;131:808-17
9. Filippi, et al. *Neurology* 1994;44:635-41
10. Saida, et al. *MultScler* 2012;18:1782-90
11. van Buchem, et al. *Neurology* 1998;50:1609-17
12. Tievsky, et al. *AJNR* 1999;20:1491-9
13. Yoshida, et al. *JpnJRadiol* 2013;31:50-5
14. Sai, et al. *JMRI* [epub ahead of print]
15. Bloomgren, et al. *NEJM* 2012;366:1870-80

ADULT DIAGNOSTIC NR (PARALLEL SESSION 2) Topkapı AB Hall

08:30 - 10:30 Advanced Techniques

Imaging biomarkers in Neuroradiology

Pia Sundgren

Lund University, Sweden

Exciting and challenging in ultra-high field MR.

Juan Villa Blanca

UCLA David Geffen School of Medicine, USA

Role of SWI in CNS Disorders

Giulio Zuccoli

Children's Hospital of Pittsburgh of Upmc, USA



PLENARY SESSIONS ABSTRACTS

O030-Correlative Assessment of Tumor Microcirculation Using Contrast Enhanced Perfusion MRI and Intravoxel Incoherent Motion Diffusion

Weighted MRI Is there a Link between Them

*Vasileios K. Katsaros*¹, Christian Braun², Jens Schittenhelm³, Tze Hern Teo⁴, Choon Hua Thng⁴, Tong San Koh⁵, Sotirios Bisdas⁶

University of Athens of MRI and Neuroradiology Athens-Greece ¹ *University of Tübingen Department of Neurology -Germany* ² *University of Tübingen Department of Neuropathology -Germany* ³ *National Cancer Center Department of Oncologic Imaging -Singapore* ⁴ *Duke-NUS Graduate Medical School Center for Quantitative Medicine -Singapore* ⁵ *University of Tübingen Department of Neuroradiology -Germany* ⁶

Purpose of this study was to correlate intravoxel incoherent motion (IVIM) imaging with classical perfusion-weighted MRI metrics in human gliomas.

Parametric images for slow diffusion coefficient (D), fast diffusion coefficient (D*), and fractional perfusion-related volume (f) in 20 patients with high-grade gliomas were generated. Maps of Fp (plasma flow), vp (vascular plasma volume), PS (permeability surface-area product), ve (extravascular, extracellular volume), E (extraction ratio), ke (influx ratio into the interstitium), and tc (vascular transit time) from dynamic contrast-enhanced (DCE) and dynamic susceptibility (DSC) contrast-enhanced MRI were generated. A region-of-interest (ROI) analysis on the contralateral healthy white matter and on the tumor areas was performed and the extracted parameter values were tested for any significant differences among tumor grades or any correlations. Only f could be significantly correlated to DCE-derived vp and tc in healthy brain tissue. Concerning the tumor regions, Fp was significantly positively correlated with D* and inversely correlated with f in DSC measurements. The D*, f, and $f \times D^*$ values in the WHO grade III gliomas were non significantly different than in the grade IV gliomas. Trend to significant negative correlations between f and PS as well as between $f \times D^*$ and ke in DCE experiments.

Presumably due to different theoretical background, tracer properties and modeling of the tumor vasculature in the IVIM theory, there is no clearly evident link between D*, f and DSC- and DCE-derived metrics.

INTRAVASCULAR INTERVENTIONAL NR Marmara Hall

08:30 - 10:30 Endovascular Cerebral Pial AVM Treatment in 2014

Transvenous intranidal AVM treatment: When and How?

Jacques Moret

Beaujon University Hospital, France

O031-Predictive Factors for Neurological Outcome after an Intracerebral Hematoma Secondary to BAVM Rupture

*Eimad Shotar*¹, Frédéric Clarençon¹, Nader Sourour¹, Federico Di Maria¹, Mathieu Debare², Vincent Degos², Aurélien Nouet³, Chiheb Zeghal², Jacques Chiras¹

Pitié-Salpêtrière Hospital. Université Paris VI University. Department of Interventional Neuroradiology Paris-France ¹ *Pitié-Salpêtrière Hospital. Université Paris VI University. Neuro Intensive Care Unit. -France* ² *Pitié-Salpêtrière Hospital. Université Paris VI University. Department of Neurosurgery. -France* ³

OBJECTIVE: To identify predictive factors for long-term neurological outcome after an intracerebral hematoma (ICH) secondary to brain arteriovenous malformation (bAVM) rupture. **MATERIALS AND METHODS:** Retrospective analysis of a prospective single center cohort of 55 consecutive patients (27 females, 28 males, mean age = 40.8±15y) admitted to neurosurgical intensive care unit after ICH secondary to bAVM rupture between January 2005 and December 2010. Neurological outcome was evaluated with the modified Rankin Scale (mRS) (mean delay of 36.3±21.1 months).



PLENARY SESSIONS ABSTRACTS

Predictive factors tested were demographic, clinical, biological and radiological data at admission. RESULTS: Twenty-five patients (45.5%) had favorable long-term neurological outcome (mRS \leq 2) while 30 patients (54.5%) had unfavorable outcome (mRS $>$ 3). Twelve patients (21.8%) died in intensive care unit and two patients deceased during the follow-up period from a new hemorrhagic episode at 16 and 23 months, respectively.

Predictive factors for poor neurological outcome were: advanced age ($p=0.0033$), past history of blood hypertension ($p=0.0057$), high systolic blood pressure at admission ($p=0.040$), initial elevated glycemia ($p=0.012$), initial high score on Glasgow coma scale ($p=0.0041$), ICH volume ($p=0.018$), midline shift ($p=0.0070$), associated intraventricular hemorrhage ($p=0.048$) and initial high S100 protein serum level ($p=0.00016$).

CONCLUSION: ICH secondary to BAVM rupture is associated with high morbidity and mortality rates. Our study found numerous demographic, clinical, biological and imaging predictive factors at admission for poor neurological outcome.

ADULT DIAGNOSTIC NR

Anadolu Auditorium

11:00 - 12:30 Multiple Sclerosis 2

MR Imaging in the Radiologically Isolated Syndrome

Alex Rovira

Hospital Universitari Vall d'Hebron Barcelona, Spain

The term subclinical lesions suggestive of MS is already known by both post-mortem studies showing the presence of typical lesions of MS in autopsies of patients who had never developed symptoms, as in brain MRI studies performed in relatives of patients with the disease. However, with the increasing use of MRI is becoming more common to discover incidental brain white matter abnormalities. These findings may be from non-specific, or have some morphological characteristics and geographical distribution highly suggestive of a demyelinating disease. The term "radiologically isolated syndrome" (RIS) was introduced by Okuda in 2009 to describe those asymptomatic patients with radiographic abnormalities highly suggestive of multiple sclerosis (MS). Sometimes these lesions may even meet the MRI criteria for dissemination in space, which are currently used to predict future development or conversion to MS in patients presenting a clinically isolated syndrome (CIS). However, we must not forget that these radiological criteria should be applied only when the patient had experienced any clinical manifestations suggestive of a demyelinating disease. Therefore, what happens in those patients in whom we found highly suggestive lesions but have never had symptoms? Due to lack of knowledge about the natural history or evolution of this new syndrome, clinical and therapeutic management of these patients is not well established, nor is the risk of conversion to MS. Recent data, however, indicates that the presence of gadolinium-enhancing, cervical cord and cortical lesions significantly increase the risk of conversion to CIS or MS. All these data have improved the characterization of RIS subjects and in our understanding of risk factors for initial symptom development.

REFERENCES:

- Okuda DT, et al. Incidental MRI anomalies suggestive of multiple sclerosis: the radiologically isolated syndrome. *Neurology*, 2009; 72: 800-5.
- Okuda DT, et al. Asymptomatic spinal cord lesions predict disease progression in radiologically isolated syndrome. *Neurology*, 2011; 76: 686-92.
- Lebrun C., et al. Unexpected multiple sclerosis: follow-up of 30 patients with magnetic resonance imaging and clinical conversion profile. *J Neurol Neurosurg Psychiatry*, 2008; 79:195-8.
- Granberg T., et al. Radiologically isolated syndrome-incidental magnetic resonance imaging findings suggestive of multiple sclerosis, a systematic review. *Multiple Sclerosis Journal* 2013; 19:271-80



PLENARY SESSIONS ABSTRACTS

Imaging of grey matter pathology in Multiple Sclerosis.

Tarek A. Yoursy

UCL Institute of Neurology / National Hospital for Neurology & Neurosurgery, UK

Use of brain and spinal cord MRI for differential diagnosis

Majda Thurnher

Medical University Vienna, Austria

O032-Neuromyelitis Optica Neuromyelitis Optica Spectrum Disorder with Brain Abnormalities as Initial Presentation Imaging Characteristics and Clinical Correlation Preliminary Study

In Ho Lee¹, Scott Newsome², Gunes Orman¹, Michael Levy², Yeliz Pekcevik¹,

Maureen Mealy², *Izlem Izbudak*¹

*The Johns Hopkins Medical Institutions RADIOLOGY Baltimore-United States*¹ *The Johns Hopkins Medical Institutions Neurology, USA*²

Neuromyelitis optica or neuromyelitis optica spectrum disorder (NMO/NMOSD) usually present with optic neuritis (ON) or transverse myelitis (TM). The brain abnormalities as initial presentation are uncommon, recently recognized and not widely understood. When patients initially present with brain symptoms, NMO/NMOSD is not within the differential diagnoses of either clinicians or radiologists. Therefore the accurate diagnosis and treatment of these patients are delayed. We sought to assess the imaging and clinical characteristics of NMO/NMOSD with brain symptoms as initial manifestation. We retrospectively reviewed the imaging findings and medical records of 125 patients diagnosed as NMO/NMOSD between 2001 and 2014. We evaluated the initial clinical presentation, presence of relapse, and presence of serum NMO IgG antibody. The lesion location, signal intensities on T1, T2 weighted, and FLAIR images, diffusion characteristics on DWI/ADC maps and enhancement pattern after contrast administration were evaluated on brain MRI. Of 125 patients with NMO/NMOSD, a total of 18 patients (F: M=15:3, age range: 8-86 years) with brain symptoms as initial presentation was enrolled in our study. Nausea or vomiting were the most common symptoms (n=10), followed by hiccup, diplopia, severe headache, syncope, slurred speech, and etc. 6/18 patients (33.3%) initially presented with only brain symptoms while 12 (66.7%) presented with brain symptoms associated with TM or ON. 16/18 patients showed multiphasic course after the initial attack regardless of TM or ON or brain symptoms. Serum NMO IgG Ab was positive in 13 patients. All patients underwent brain MRI and 13 MRI were available for review. The brain stem (n= 9/13) was the most common lesion location followed by periventricular or subcortical white matter (n= 3/13). All lesions showed high signal intensity on T2W and FLAIR images and iso to low signal intensity relative to the white matter on T1WI. Focal restricted diffusion was noted in only one lesion in the medulla while facilitated diffusion was noted in the remainder of brain stem lesions and periventricular white matter lesions. There was focal or partial enhancement in medullary (n=3), pontine (n=1) and periventricular white matter lesions (n=1). NMO/NMOSD may initially present with brain symptoms, which are well correlated with brain lesions in our study. Therefore, radiologists should keep NMO/NMOSD in differential diagnoses particularly when there are lesions in the brain stem associated with nausea or vomiting.



PLENARY SESSIONS ABSTRACTS

ADULT DIAGNOSTIC NR (PARALLEL SESSION 2) Topkapı AB Hall

11:00 - 12:30 Intraoperative neurosurgical imaging

Intra Operative Neurosurgical Imaging: What Information is Necessary from Imaging

*Vasileios K. Katsaros*¹, Sotirios Bisdas², George Stranjalis³

*University of Athens Department of MRI Athens-Greece*¹ *University of Tübingen Department of Neuroradiology -Germany*² *University of Athens Department of Neurosurgery -Greece*³

Radiological images have been used as a guide in neurosurgery for decades. Soon after their introduction by Röntgen, surgeons took advantage of this new form of information to better plan and perform surgical procedures. In 1918 a stereotactic frame designed for human use was built. However, it was not until 30 years later that this device was rediscovered. In 1947 the technique of stereotaxy was further developed and involved the use of a three-dimensional Cartesian coordinate system for the human brain.

Image guided neurosurgery (IGNS) systems have been and still are developed using pre-operative anatomical images, including CT, MRI, and DSA, as a navigational guide.

In addition to anatomical information, neuro-navigational systems may integrate functional information in the form of PET, MR spectroscopy, perfusion imaging, fiber tractography (FT) and fMRI to expand the information content used.

Recent trends in neurosurgery show that IGNS is increasingly applied in brain tumors, by using preoperative 3D data that are mostly acquired from MRI. In IGNS, the accuracy of the navigation system is a prerequisite for the safe and precise tumor resection, which may be impaired by the "brain shift" after craniotomy and ongoing tumor resection. Intraoperative CT but mostly MRI (iMRI) can solve this problem by acquiring intraoperative image data-sets, and the continuous updating of the navigation system.

Further indications for iMRI in tumor surgery include resection control by 3D-T1 after the intravenous administration of Gadolinium chelates or 3D FLAIR and perfusion MRI (in combination with 5-ALA) and the early detection and/or confirmation of complications, such as ischemia (diffusion and perfusion MRI) or hemorrhage [gradient echo T2* or Susceptibility Weighted Imaging (SWI)]. iMRI is an alternative to stereotaxy for guided biopsies when the pre-operative work-up fails to establish a diagnosis.

Besides brain tumors other common indications of intraoperative neuroimaging monitoring, mostly by means of iMRI, include the transsphenoidal resection of pituitary adenomas / suprasellar tumors and intractable epilepsy.

Less frequent applications of iMRI are intracranial cyst drainage, abscess evacuation, deep brain modulator placement in Parkinson's disease and/or movement disorders, surgery of vascular malformations or vascular by-pass surgery (i.e. in Moya-Moya disease), and microvascular decompression using MRA in high-field systems, shunt placement in hydrocephalus in combination with US, and recently spinal surgery.

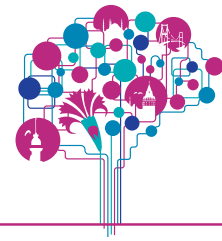
On Line Imaging (Dedicated Low Field Open Systems) vs Step Wise Imaging (Modified Conventional High Field Systems)

*Yuko Ono*¹, Yoshihiro Muragaki², Takashi Maruyama³, Manabu Tamura², Kosaku Amano³, Kayoko Abe¹, Shuji Sakai¹, Yoshikazu Okada³

*Tokyo Women's Medical University Diagnostic Imaging and Nuclear Medicine Shinjuku-ku-Japan*¹ *Tokyo Women's Medical University Advanced Biomedical Engineering & Science, Faculty of Advanced Techno-Surgery*² *-Japan*² *Tokyo Women's Medical University Neurosurgery -Japan*³

PURPOSE: Evaluation of usefulness of low field intraoperative MRI (iMRI) to reduce risk of neurosurgery, comparing with preoperative high field MRI (pMRI).

MATERIALS AND METHODS: Open iMRI at 0.3 or 0.4T was set in the small operating theater with suitable and movable table for operating procedure and MR study. 1247 cases of iMRI were performed from 2000 to



PLENARY SESSIONS ABSTRACTS

2013. iT1WI and iT2WI were performed by 3mm thickness with 230mm FOV, 256x160 matrix and 1 excitation, reconstruction images of 1.5mm thickness. Imaging time was about 4 minutes for each. The all devices and medical instruments and electric wires were changed into diamagnetic and 5 gauss line was limited in 2.5 meters in diameter. pMRI was generally performed by 1.5 or 3.0T with 3-7mm thickness, by T1WI, T2WI, FLAIR, Gd-T1WI in axial, coronal and sagittal slices. DWI, DTI and/or functional (f)MRI were also performed in necessary and capable cases. The pMRI was adjusted to the first iMRI after craniotomy considering brain shift for the most suitable operative maneuver for the lesion. Functional brain mapping by cortical stimulation as sensory and motor evoked potentials was confirmed during surgery and compared with activated area on fMRI and iMRI. Awake craniotomy was done for lesions close to the verbal areas, when the patients were cooperative. iMRI was performed just after craniotomy, repeated 1 to 3 times during operative procedure as required.

RESULTS: Low field open MR apparatus was convenient for setting in the limited area and safe for maintaining patient's positioning and careful observation during examination. Low S/N ratio due to low field MRI was overcome using noise reduction filter and suitable sequences. iMRI presented brain shift due to craniotomy, suction of CSF and/or partial resection of the tumor, respectively.

CONCLUSION: Detail information about the lesion by pMRI was important to obtain anatomical and characteristic findings and relation between the lesions and the eloquent areas. iMRI and direct cortical stimulation for functional brain mapping were important to reduce surgical risk and reach the goal of extended tumor removal for better outcome, confirming extension of the lesions and its relation to the eloquent areas with brain shift due to operative procedure.

Neurosurgical Experience from Open Craniotomies and Transsphenoidal Approaches

*Yuko Ono*¹, *Yoshihiro Muragaki*², *Takashi Maruyama*³, *Manabu Tamura*², *Kosaku Amano*³, *Kayoko Abe*¹, *Shuji Sakai*¹, *Yoshikazu Okada*³

*Tokyo Women's Medical University Diagnostic Imaging and Nuclear Medicine Shinjuku-ku-Japan*¹ *Tokyo Women's Medical University Advanced Biomedical Engineering & Science, Faculty of Advanced Techno-Surgery -Japan*² *Tokyo Women's Medical University Neurosurgery -Japan*³

PURPOSE: Evaluation of intraoperative (i)MRI for neurosurgery of the gliomas, meningiomas, pituitary tumors and others, reviewing results of them comparing with previous neurosurgery. MATERIALS AND METHODS: iMRI was performed for 1000 cases of gliomas, 57 cavernous malformations, 32 pituitary adenomas, 28 functional brain surgery for epilepsy, 26 metastatic tumors, 25 meningiomas, and 79 other tumors and vascular lesions. The verbal area was confirmed by preoperative fMRI and/or Wada test. Preoperative (p)MRI and first iMRI were fused or carefully compared to preserve the eloquent areas of the brain, considering brain shift after craniotomy. Cases with gliomas, the eloquent areas were always confirmed by somatosensory and motor evoked potentials during surgical procedure, or confirmed speech ability under awake craniotomy. For the pituitary tumors, surgical procedure with iMRI and high quality endoscopic findings was compared for precise tumor removal avoiding surgical risks. Degree of tumor removal and outcome of the patients were compared with previous results and advantage of neurosurgery with iMRI was discussed.

RESULTS: In the total cases of the gliomas in Grade (G) 2-4, resection rate was 92.3±0.7% by general anesthesia and 86.3±1.1% by awake craniotomy. 5-year-survival of 347 patients in G2/G3 operated using iMRI was 87.3% versus 88.2% of 21 cases in G2/G3 without iMRI. 2-year-survival for 170 patients in G4 operated with iMRI was 44.3 % and mean survival time of them was 21.9 months versus 34.6 % and 11.7 months in 26 patients in G4 operated before without iMRI. The pituitary microadenomas were clearly differentiated from the normal pituitary tissue by the high quality endoscope. iMRI was useful for the macroadenomas with lobulation or invasion into the cavernous sinuses or posterior ethmoid sinuses. Detail information by pMRI and high quality endoscopic findings during surgical procedure were also satisfactory for operative procedure in the most macroadenomas. iMRI was tried to use for the meningiomas, metastases, functional surgery for epilepsy and the vascular lesions, but there was no evident advantage for these benign lesions, considering time loss for iMRI.

CONCLUSION: iMRI is greatly helpful for extended resection of the malignant tumors preserving the eloquent areas and better outcome.



PLENARY SESSIONS ABSTRACTS

INTRAVASCULAR INTERVENTIONAL NR Marmara Hall

11:00 - 12:30 Endovascular Dural AVF Treatment in 2014

How did Onyx and MMA approach change the treatment indications in recent years?

Christoph Cognard

Hopital Purpan, France

When should transvenous treatment be used ?

Laurent Spelle

Beaujon Hospital - Paris Diderot University, France

How Can I Decrease the Rate of Complication in Dural AVF Management

Daniel Roy

CHUM Notre-Dame Hospital Radiology Montreal, Canada

PURPOSE: To discuss the clinical, anatomical and technical aspects of the endovascular management of intracranial dural AVF those contribute to reduce the rate of complication.

MATERIALS AND METHODS: Retrospective review of intracranial dural AVFs where endovascular treatment was contemplated at our institution since 2002. Clinical presentation, anatomical location and type according to Cognard's classification were noted. Endovascular strategy, anatomical and clinical results as well as complications are reported. Factors related to complications are discussed.

RESULTS: we retrieved 166 dural fistulas in 160 patients. Most patients presented with ocular symptoms (47), tinnitus (43) or haemorrhage (39). Some involvement of pial veins(type 2a+b,2b,3,4 or 5) was present in 103 fistulas. Endovascular treatment was attempted in 136 fistulas. Trans venous approach was used in 54 cases, mainly for cavernous sinus lesions. Arterial approach was performed solely in 70 cases or combined with venous approach in 11 DAVFs. After endovascular treatment, complete anatomical cure was obtained in 116 cases and reduction of flow with clinical cure in 9. In 8 patients cure was obtained by surgery after endovascular attempt. Three fistulas remained untreated. Permanent neurological complications occurred in 5 patients: 1 death from haemorrhage, 2 from cranial nerve ischemia, 1 from venous infarction and 1 pulmonary emboli. One patient suffered transient symptoms from venous compromise. Transient VIth nerve palsy was frequent after trans venous embolization of cavernous sinus DAVFs.

CONCLUSION: Reduction of complication rate in the endovascular treatment of dural AVFS requires appropriate patient selection, thorough understanding of the anatomy and appropriate selection of approaches and material.

ADULT DIAGNOSTIC NR

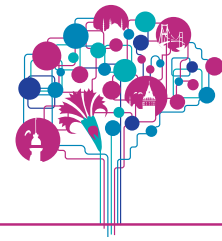
ANADOLU AUDITORIUM

13:30 - 15:00 Degenerative Brain

Caffeine in the Elderly and MCI

*Sven Haller*¹, Cristelle Rodriguez², Dominik Moser¹, Simona Toma², Jeremy Hofmeister², Indrit Sinanaj², Dimitri Van De Ville³, Panteleimon Giannakopoulos², Karl-Olof Lovblad¹

Department of Imaging and Medical Informatics, University Hospitals of Geneva and Faculty of Medicine of the University of Geneva, Switzerland Department of Imaging and Medical Informatics, University Hospitals of Geneva and Faculty of Medicine of the University of Geneva, Switzerland Commugny-Switzerland¹ Department of Mental Health and Psychiatry, University Hospitals of Geneva and Faculty of Medicine of the University of Geneva, Switzerland Department of Mental Health and Psychiatry, University Hospitals of Geneva and Faculty of Medicine of the University of Geneva, Switzerland -Switzerland² Department of Radiology and Medical Informatics, University of Geneva, Switzerland⁴ Institute of Bioengineering, Ecole Polytechnique Fédérale de Laus Department of Radiology and Medical Informatics, University of Geneva, Switzerland⁴ Institute of Bioengineering, Ecole Polytechnique Fédérale de Laus -Switzerland³



PLENARY SESSIONS ABSTRACTS

BACKGROUND: Recent epidemiologic data suggests a positive effect of caffeine in neurodegeneration, notably mild cognitive impairment (MCI) and Alzheimer Dementia. Using functional magnetic resonance imaging, we assessed working memory performance, functional connectivity and baseline perfusion in healthy elderly controls and MCI participants. **MATERIALS AND METHODS:** Two related prospective, placebo-controlled crossover design studies included 24 healthy elderly individuals (mean age 68.8 ± 4.0 years) and 17 MCI (mean age 70.7 ± 4.6 years) performing a 2-back working memory task in fMRI. Analyses include complimentary assessment of task-related activations (general linear model, GLM), functional connectivity (tensorial independent component analysis, TICA), and baseline perfusion (arterial spin labeling, ASL)

RESULTS: Despite a reduction in whole-brain global perfusion (25.5%, $p > 0.001$ in HC and 29.9%, $p > 0.001$ in MCI), caffeine enhanced task-related GLM activation in a distributed network most pronounced in the bilateral striatum and to a lesser degree in the right middle and inferior frontal gyrus, bilateral insula, left superior and inferior parietal lobule as well as in the cerebellum bilaterally. Functional connectivity was significantly enhanced (+8.2%) in caffeine versus placebo in a task-relevant network including the pre-frontal cortex, the supplementary motor area, the ventral premotor cortex and the parietal cortex as well as the occipital cortex (visual stimuli) and basal ganglia in HC. The inverse comparison of placebo versus caffeine had no significant difference. In MCI, caffeine resulted in an increased activation in parietal regions yet decreased activation in frontal regions as compared to HC. The VBM and TBSS analyses excluded potentially confounding differences in grey matter density and white matter microstructure between MCI and HC.

CONCLUSIONS: The present findings suggest that acute caffeine intake enhances working memory-related brain activation as well as functional connectivity of BOLD fMRI in elderly individuals and more pronounced in MCI. The high caffeine-related activation in the striatum can be attributed to the high local concentration of adenosine receptors. The current results on caffeine will also be discussed with respect to recent investigations illustrating a beneficial effect of chocolate on early stages of dementia.

Imaging in Dementia: Role of MRI.

Leonardo Macedo

ALLIAR - CEDIMAGEM - UFJF, Brasil

Movement disorders

Leonardo Macedo

ALLIAR - CEDIMAGEM - UFJF, Brasil

O033-Voxel based Analysis of Quantitative Susceptibility Data in Subjects with CN, MCI and AD

*Ji Hye Jang*¹, Hye Soo Koo², Chang-Woo Ryu², Yi Wang³, Geon-Ho Jahng⁴, Eui Jong

Kim¹, Woo Suk Choi¹

*Kyung Hee University Hospital Radiology Seoul-Korea, South*¹ *Kyung Hee University Hospital at Gangdong Radiology -Korea, South*² *Weill Cornell Medical College Radiology -United States*³ *Kyung Hee University Hopital at Gangdong Radiology -Korea, South*⁴

PURPOSE: To investigate quantitative susceptibility in three groups of subjects with cognitive normal (CN), mild cognitive impairments (MCI) and Alzheimer's disease (AD). Because AD is expected to have the most iron plaques, we expected that the AD brains would produce the least signals in comparison to the CN and MCI brains.

MATERIALS AND METHODS: Subjects of 20 CN, 21 MCI, and 21 AD participated after informed consent. A fully first-order flow-compensated three-dimensional (3D) gradient echo sequence ran to obtain magnitude and phase images, which were later used to produce final quantitative susceptibility mapping (QSM). Furthermore, 3D T1-weighted images were acquired for the brain tissue segmentation, image registration, and masking-out of non-brain tissues, including CSF and vessels. The QSM images were produced by implementing the Morphology



PLENARY SESSIONS ABSTRACTS

Enabled Dipole Inversion (MEDI) method. After the QSM images were smoothed using isotropic 4 mm Gaussian kernel, the differences of QSM data among the three groups were investigated by performing a voxel-based statistical analysis using a one-way analysis of variance (ANOVA) test with subject age and gender as covariates. RESULTS: QSM values would decrease from CN to MCI and to AD. Compared with MCI subjects, QSM values in CN subjects were high in the left superior frontal gyrus and the left superior temporal gyrus. The lower signals were also found in the left superior frontal gyrus and the left superior temporal gyrus. Compared with the AD group, the QSM values in CN subjects were high in the left parahippocampal gyrus and the left inferior frontal gyrus, but low in the right cingulate gyrus. Compared with AD patients, QSM values in MCI subjects were high in the right superior temporal and the left superior temporal, but low in the left middle frontal gyrus. CONCLUSION: We were able to identify the brain regions in which the susceptibility changes occurred among the different groups. More differences were found when CN and AD groups were compared than when CN and MCI groups were compared.

ADULT DIAGNOSTIC NR (PARALLEL SESSION 2) Topkapı AB Hall

13:30 - 15:00 Legal and Socioeconomic

International Practice Standards With Respect To Legal / Ethical Issues

For Malpractice, Incidental Findings on Research Scans, Financial Implications across National Healthcare Systems

David M. Yousem

Associate Dean of Professional Development, Johns Hopkins School of Medicine, USA

The degree to which neuroradiologists are subject to medicolegal scrutiny varies widely across the globe. While some countries accept malpractice litigation as an unwelcome, but necessary part of the practice of medicine, in others suits against physicians are not part of the culture. This talk will emphasize the experience of two sentinel nations, the United States and the host country of Turkey, set against the results of a worldwide survey of experience in medical malpractice as it relates to neuroradiologists. The incidence of malpractice suits, expense entailed, results of court rulings, and attitudes towards the judicial system and expert witnesses will be explored. The ethics of reading research scans for the finding of incidental lesions will also be explored with reference to international and local standards. The issues of the time, cost, benefits, and disadvantages for these readings will be debated.

How to Add, Measure, Proof and Showcase the Value of Neuroradiology

David M. Yousem

Associate Dean of Professional Development, Johns Hopkins School of Medicine, USA

A panel discussion of how one might increase favorable public attitudes towards neuroradiologists will be presented. The value of diagnostic and interventional neuroradiology will be assessed in situations such as early stroke interventions, brain tumor assessments in and outside the operating rooms, low back pain, and myelopathy by experts in the field.

Forensic Neuroradiology: Cognitive Changes in Brain Trauma and Changes in Criminal Brains

Eduardo Gonzalez-Toledo

LSU School of Medicine, USA

Depression, behavioral changes, cognitive impairment, insomnia are some of the consequences of brain trauma. In some patients it means the loss of a job, the way to social isolation. Neuroradiology can be of great help to discover the cause of the patient's problems and also to document the brain lesions for legal claims.

Computed tomography, a good tool in the acute setting is not very useful to detect subtle lesions after months or years after trauma.



PLENARY SESSIONS ABSTRACTS

Magnetic resonance is the modality of choice. Even standard magnetic resonance may look as normal if we don't use specific sequences and appropriate analysis of the brain.

In our practice we have a "forensic protocol" that can shed light on the brain of a person having a trauma 5 years ago, as some of the changes are permanent as permanent the disabilities can be.

The basic protocol consist of a 3D, T1 weighted sequence in order to reconstruct the cortex. Cortical integrity can be assessed with software providing cortical thickness information. In normal patients we will have specific thickness according to the location: occipital cortex should be thinner than the frontal dorsal cortex. However, in pathological circumstances, there is a change in cortex condition in color maps of cortical thickness. Susceptibility weighted image shows hemosiderin deposits as hypointense foci. This is due to the presence of iron, generally stored in the microglia and persist for years.

Diffusion tensor imaging can reconstruct the white matter tracts, some of them classically reported as damaged in brain trauma: cingulum, genu of the corpus callosum. The measurement of fractional anisotropy gives an objective value for easier evaluation.

Resting state fMRI is a functional examination requiring 5 minutes of a patient lying at rest when acquiring the sequence. We can produce maps with the connections between selected areas but also the comparison of the patient's connectivity with a normal database, providing information about areas of hyper or hypoconnectivity. In criminals, finding a lesion, specially in brain areas related to the limbic system may introduce the concept of antisocial personality disorder. The presence of a brain lesion explaining the criminal behavior is twofold useful: avoids the capital punishment but is conditioning the perpetrator release to a psychiatric counseling and treatment, protecting the society. More common lesions involve the frontal orbital cortex (BA11), anterior and posterior cingulum, amygdala, temporal basal lateral cortex.

INTRAVASCULAR INTERVENTIONAL NR

Marmara Hall

13:30 - 15:00 Endovascular Treatment of Spinal Vascular Malformations

Anatomical and angioarchitectural tricks for the succesful endovascular treatment of spinal AVMs and the impact of intraoperative flat panel CTA for treatment planning

Civan Islak

Istanbul University, Turkey

Treatment of spinal pial vascular malformations: When to treat and not to treat

Alfredo Casasco

Ntra Sra del Rosario Hospital, Spain

ADULT DIAGNOSTIC NR

ANADOLU AUDITORIUM

15:30 - 17:00 **Psychiatric Diseases**

Advanced Neuroimaging in Psychiatry

Nivedita Agarwal

Santa Maria del Carmine Hospital, Italy

Neuroimaging in Psychiatry: Depression, Schizophrenia and Bipolar

Eduardo Gonzales Toledo

LSU School of Medicine, USA

Like in epilepsy, in some psychiatric patients we can recognize some structural patterns and in some others we don't. The later will be easier to treat, because the most probable cause would be metabolic at the level of neurotransmitters. This is also the main reason to study the patients with neuroradiological methods.



PLENARY SESSIONS ABSTRACTS

Computed tomography can provide some information, like dominance, signs of depression, patterns for schizophrenia, vascular lesions, post-traumatic lesions, neoplasms.

However, the modality of choice is magnetic resonance. Our protocol includes a 3D T1WI, axial and coronal T2WI, 3D FLAIR, 3D susceptibility weighted image, diffusion tensor imaging (DTI). Magnetic resonance spectroscopy and resting state functional MRI (rsfMRI) are added in some patients to optimize diagnosis.

Morphological and functional patterns will be shown illustrating depression with lesions in the limbic prefrontal area, in the dominant hemisphere, in the basal lateral polar temporal. Schizophrenics with morphological changes in temporal lobes, collateral sulcus, dorsolateral prefrontal cortex. Bipolar disorder and schizophrenia share reduced FA in the anterior limb of the internal capsule, anterior thalamic radiation and in the region of the uncinate fasciculus. Bipolar patients have lower FA values in superior longitudinal fasciculus and corpus callosum than schizophrenics.

Patients with morphological changes in brain have more severe forms and are more refractory to medication.

Advanced Neuroimaging in Anxiety and PTSD

Nivedita Agarwal

Santa Maria del Carmine Hospital, Italy

ADULT DIAGNOSTIC NR (PARALLEL SESSION 2)

Topkapı AB Hall

15:30 - 17:00 Case Discussion

Anne Osborn, USA, Majda Thurnher, Austria, Mauricio Castillo, USA, Paul Parizel, Belgium

INTRAVASCULAR INTERVENTIONAL NR

Marmara Hall

15:30 - 17:00 **Pediatric Neurovascular interventions**

Interventional treatment of pediatric venous and lymphatic malformation

Alejandro Berenstein

Mount Sinai Healthcare System, USA

Endovascular treatment of GVA malformations: Tricks for the success,

Jo Bhattacharya

UK

O034-Paediatric Intracranial Aneurysms Approach and Treatment

Anne Jutta Schmitt¹, Adam Rennie², Fergus Robertson², Stefan Brew², Vijeya Ganesan³,

Sanjay Bhate³, Owase Jeelani⁴, Kristian Aquilina⁴

*University College London Hospital Radiology London-United Kingdom*¹ *National Hospital of Neurology and Neurosurgery, Great Ormond Street Hospital Neuroradiology -United Kingdom*² *Great Ormond Street Hospital Neurology -United Kingdom*³ *Great Ormond Street Hospital Neurosurgery* –⁴

PURPOSE: Paediatric intracranial aneurysm show major differences in etiology, risk factors and morphology when compared to aneurysms seen in the adult population.

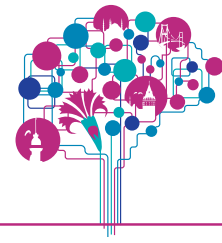
MATERIALS AND METHODS: A retrospective case and imaging review was performed for all paediatric aneurysm patients (≤ 18 years) presenting to our institution between 2005-2013. The aim of our study was to further characterise the different types of aneurysms and their treatment.

RESULTS: A total of 19 paediatric patients were treated for 21 aneurysms during the study period. The mean age at presentation was 8.9 years (range: 0.1 – 16.2 years) with a female to male ratio of 1:1.2. In 66.6% of patients computed tomography imaging revealed subarachnoid haemorrhage with an average Fisher grade of 3.6. 62% of the aneurysms were located within the anterior circulation.

7-12 September 2014
ISTANBUL, TURKEY

LUTFI KIRDAR CONVENTION & EXHIBITION CENTER

XXth
Symposium
Neuroradiologicum



PLENARY SESSIONS ABSTRACTS

Depending on their morphology, we further divided the aneurysms in categories: Seven of the 21 aneurysms were saccular, four fusiform, three traumatic and three dissections. One aneurysm was due to immunodeficiency, one was a mycotic aneurysm and one showed segmental ectasia. One further aneurysm demonstrated as an ectatic vessel with no segmental distribution. Underlying conditions that we recorded were HIV, aortic stenosis with infective endocarditis, Noonan syndrome with pulmonary stenosis and PHACES syndrome.

16 of the 21 aneurysms were treated endovascularly, 3 of those with flow diverting stents. 2 aneurysms were treated surgically and 3 patients with 3 aneurysms did not receive interventional or surgical treatment. 2 patients died due to the severity of their pre-operative condition, but we achieved good outcome in the remaining patients.

CONCLUSIONS: Pediatric intracranial aneurysms are uncommon as compared to in adult patients. The pathomechanism, underlying systemic diseases and vessel wall factors need to be considered to determine the best therapeutic approach.

17:00 - 17:30 Closing Ceremony

Anadolu Auditorium



XXth
Symposium
Neuroradiologicum

**ORAL PRESENTATIONS
ABSTRACTS**



ORAL PRESENTATIONS ABSTRACTS

Tuesday, September 9, 2014

PARALLEL SCIENTIFIC PAPER PRESENTATIONS

(Stroke 1) 17:15 - 19:00

Marmara Hall

O035-Leptomeningeal Enhancement on Magnetic Resonance Imaging as a Predictor of Hemodynamic Insufficiency

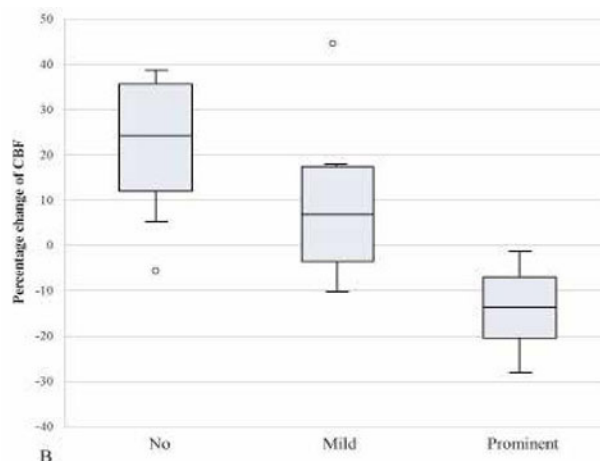
*Hyung Suk Seo*¹, Doran Hong², Young Hen Lee²

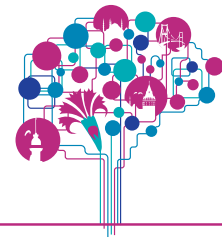
*Korea University Ansan Hospital Radiology Ansan-si-Korea, South*¹ *Korea Univerisy Ansan Hospital Radiology -Korea, South*²

PURPOSE: Increased leptomeningeal enhancement on MRI is considered as a sign of leptomeningeal collateral flow in cerebrovascular stenosis or occlusion, but a conclusion has yet to be reached concerning the hemodynamic contribution through leptomeningeal collaterals. This study aimed to evaluate the value of increased leptomeningeal enhancement on MRI in relation to relative cerebral blood flow (rCBF) and cerebrovascular reserve using acetazolamide-challenged perfusion CT. **METHODS:** A retrospective analysis was performed using 31 patients (M:F = 18:13; mean age, 55.9 years; range 26-79 years) with internal carotid artery (ICA) or proximal middle cerebral artery (MCA) occlusive disease without collateral flow through the circle of Willis, who underwent enhanced T1-weighted 3T MRI and acetazolamide-challenged perfusion CT. They were graded into 3 groups according to the degree of increased leptomeningeal enhancement according to the contralateral normal cerebral hemispheres on enhancing axial T1WI. The rCBF and percentage change of CBF before and after acetazolamide infusion reflecting cerebrovascular reserve was obtained in the ipsilateral MCA territory except for infarction. The rCBF and percentage change of CBF were compared among the 3 groups using ANOVA.

RESULTS: Patients with prominent leptomeningeal enhancement (n=11) had a -13.7% mean percentage change of CBF. The patients with mild (n=11) and no increased enhancement (n=9) showed a 6.9% and 23.8% change, respectively. The degree of leptomeningeal enhancement was significantly reverse-correlated with percentage change of CBF (p=0.000, Figure), whereas the rCBFs were not significantly different.

CONCLUSIONS: Prominent leptomeningeal enhancement on MRI indicates decreased cerebrovascular reserve in patients with ICA or proximal MCA occlusion. It could suggest that increased enhancement of the leptomeninges on MRI is related to decreased leptomeningeal flow or hemodynamic insufficiency of the primary collaterals. Consequently, the degree of leptomeningeal enhancement indicates impaired hemodynamics in ischemic stroke patients.





ORAL PRESENTATIONS ABSTRACTS

O036-Predicting the Reversibility of Cytotoxic Edema in PRES by Using Diffusion Kurtosis Imaging (DKI)

*Gang Guo*¹, Yonggui Yang¹, Fang Chen¹, Zhongping Zhang²

*The 2nd Hospital of Xiamen Radiology Xiamen-China 1 GE Healthcare*²

PURPOSE: Conventional diffusion MR imaging has been widely used for detecting the cytotoxic edema in the brain diseases. However, there have been some limitations in estimating the reversibility of cytotoxic edema by conventional DWI. Diffusion kurtosis imaging is an advanced diffusion MRI method that yields additional information to conventional DWI and may improve characterization of tissue microstructure. The goal of this study is to elucidate the possible prediction of reversibility underlying cytotoxic edema using these new diffusion kurtosis imaging metrics.

METHODS and MATERIALS: We performed a retrospective review of both DTI and DKI metrics data of 9 lesions within cytotoxic edema in a patient with severe posterior reversible encephalopathy syndrome(PRES). The correlations between the volumetric changes before and after treatment with both initial DTI and DKI metrics were statistically analyzed.

RESULTS: There were the significant correlations between initial DKI metrics and changes of the volume within cytotoxic edema before and after treatment (MK: correlation 0.791, $p=0.011$; Ka: correlation 0.805, $p=0.009$; Kr: correlation 0.732, $p=0.025$, respectively). While comparing with the corresponding regions of the healthy subject, the relative increase of MK and Ka values before treatment were significant correlation with volumetric changes within these lesions (MK: correlation 0.802, $p=0.009$; Ka: correlation 0.855, $p=0.003$). There were no correlation between initial DTI metrics (as well as DTI metrics) and the volumetric changes of these lesions.

CONCLUSIONS: As additional data to conventional DWI, DKI could stratify heterogeneous DWI lesions, improving characterization of tissue injury, and potentially predict the salvageable lesion within DWI deficits.

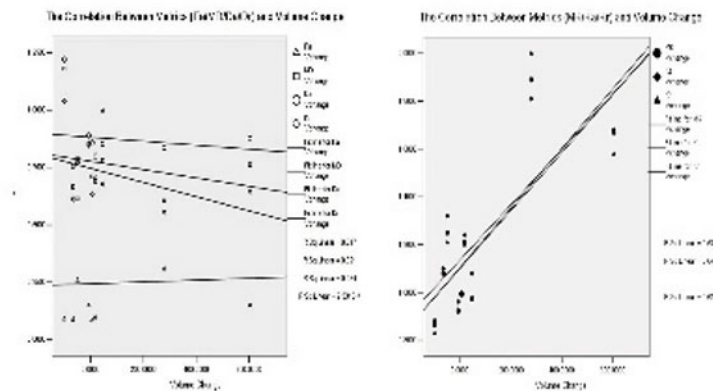


Fig. legend

The correlation between initial DTI metrics and DKI metrics with volumetric changes pre- and post-treatment of the cytotoxic edema lesions. There were significant correlation between DKI metrics with the volumetric changes pre- and post-treatment of the cytotoxic edema lesions (b); there were no significant correlation for DTI metrics.



ORAL PRESENTATIONS ABSTRACTS

O037-CT Perfusion as Imaging Predictor of Clinical Outcome in Acute Ischemic Stroke

*Biljana Georgievski-Brkic*¹, Dusko Kozic², Jelena Ostojic³, Magdalena Radovic-Stefanovic

⁴, Marjana Vukicevic⁵, Aleksandra Terzic-Beljakovic¹, Gordana Milenkovic¹

*Stroke hospital "Sveti Sava" Radiology Belgrade-Serbia*¹ *Institution for Oncology Vojvodina Radiology -Serbia*²

*Clinical center Novi Sad Radiology -Serbia*³ *Clinical center Bezanijska kosa Radiology -Serbia*⁴ *Stroke hospital "Sveti Sava" Neurology -Serbia*⁵

PURPOSE: The purpose of this study is to determine the prognostic accuracy of perfusion computed tomography (CTP) in acute stroke patients.

METHODS: We retrospectively analyzed 97 patients presenting with middle cerebral artery (MCA) stroke within the first 6 hours after symptom onset, in Stroke hospital "Sveti Sava" in Belgrade, from March 2009 to March 2014. All patients on admission underwent non contrast CT of brain (NNCT), CT angiography (CTA) and CTP covering 20 mm of brain (four slices of 5mm). 74 patients were treated with intravenous tissue plasminogen activator (rtPA) and 23 patients were not treated with rtPA. We performed 24 hours follow up NNCT. The size of infarct core (CBV) and the size of the penumbra (CBF/CBV mismatch) on CTP, the final infarct size on follow-up NNCT and percent of preserving predicting penumbra (PPPP) were measured. Those measurements represented radiological parameters. We also evaluated each patient's clinical condition, defined by the National Institutes of Health Stroke Scale (NIHSS), in emergency room at admittance and assessed on 30 days later. We correlated radiological, clinical parameters and time period after symptom onset.

RESULTS: There was highly significant correlation between PPPP and NIHSS ($r = 0.59$, $P < 0.001$), significant correlation between CBV and NIHSS ($r = -0.32$, $P < 0.01$), while there was no correlation between time period after symptom onset and NIHSS ($r = -0.07$, $P = 0.51$). There was highly significant correlation between CBV and mortality ($r = 0.46$, $P < 0.001$) and significant correlation between PPPP and mortality ($r = -0.33$, $P < 0.01$). Mortality had no correlation with time period after symptom onset ($r = 0.13$, $P = 0.19$). Results of linear regression indicated, that the PPPP contributed to prediction of NIHSS three times as much then CBV parameter alone.

CONCLUSION: Time period after symptom onset cannot reflect the outcome, but CTP has potential as surrogate marker of stroke severity. The PPPP is the most important predictor of the NIHSS improvement and CBV is the most important predictor of mortality.

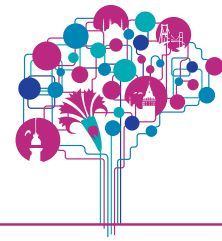
O038-Effects of Arterial Choice for the Arterial Input Function on Perfusion Parameters in Isolated Posterior Circulation

Monique Meyer¹, Eric Munoz¹, *Robert Bert*¹

*University of Louisville Radiology Louisville-United States*¹

PURPOSE: CT perfusion imaging is an important tool stroke assessment. Anomalies have been revealed, questioning the assumptions made in the underlying model used for analysis of cerebral blood flow (CBF). One anomaly occurs in the occipital lobes when the blood supply isolated. An important question is whether this anomaly represents a true physiologic decrease in CBF or oversimplification in the model. Low velocities in the vertebral arteries can contribute to timing delays in the arrival of contrast. We hypothesized that replacing the anterior circulation (ACirc) arterial input function (AIF) with an AIF from the posterior circulation (PCirc) might partially correct the anomalous decrease in Time to Peak (TTP) and Mean Transit Time (MTP) calculated by commercial software in such isolated systems.

METHODS: Perfusion studies were reviewed and excluded cases with acute stroke, arterial dissection and high grade stenosis. Cases were then separated into those with and without bilateral isolated posterior circulations. Ten cases were chosen for evaluation. All studies were processed utilizing commercial software. Circulation was classified as bilaterally isolated when bilateral posterior communicating arteries were less than 1mm and P1 segments were >3mm. Mean attenuation vs. time curve data points were collected from the standard ACirc



ORAL PRESENTATIONS ABSTRACTS

arterial input function. ROIs of identical areas were placed in the isolated PCirc and comparable ACirc. Both ROI values for mean TTP and MTT were recorded. The raw data was then reprocessed using a PCirc AIF and values of TTP and MTT reprocessed. The new PCirc values were recorded and subtracted from respective ACirc values from the initial processing.

RESULTS: Mean PCirc values for TTP and MTT for the 10 subjects were 8.78s and 3.40s (ranges: TTP=7.58-13.35, MTT=3.01-3.72) using the standard ACirc AIF. Mean ACirc values were 7.76s and 3.35s (ranges: 6.85-9.61, 3.01-3.7). Percent differences for TTP and MTT were 13.1% & 1.5%. Mean PCirc values after reprocessing with a PCirc AIF were TTP=7.92, MTT=3.32. Percent ACirc-PCirc fell to TTP=2%, MTT=0.9%.

CONCLUSIONS: Isolated posterior circulation can result in both visually detectable and numerically measurable differences in TTP and MTT comparing PCirc vs ACirc in patients, this was correctable by using a local AIF.

O039-Quantitative Measurement of Regional Cerebral Blood Flow Using DSC MRI with the BookEnd Method Practical Performance in Clinical Routine

*Arnold Koehler*¹, Gert Reiter², Christian Nasel¹

*Karl Landsteiner University - University Clinic Tulln Department of Radiology Tulln-Austria*¹ *Siemens AG Healthcare Sector -Austria*²

BACKGROUND: The assessment of cerebral perfusion using dynamic susceptibility contrast-magnetic resonance imaging (DSC-MRI) lacks a reliable quantification providing just one unambiguous result for a given measurement. Recently the BookEnd (BK-E)-method, that uses the T1w-signal for normalizing the T2*-signal of DSC-MRI, was reported to allow a reliable quantification of regional cerebral blood flow (rCBF). The practicability of this promising method in comparison to established perfusion assessment was investigated in this study.

METHOD: Patients (n=32), which were examined due to TIA that did not result in DWI-positive focal lesions, were included. DSC-MRI was performed using two different protocols optimized for the BK-E-method. Firstly, a sequence, comparable to earlier BK-E-reports (FOV=220mm; TR=1100ms; TE=35ms; matrix=128x128; slice thickness: 6mm; slices=13; repeats=50) was used (group1). Secondly, a sequence optimized for temporal and spatial resolution was engaged (FOV=220mm; TR=1030ms; TE=16ms; matrix= 102x88; slice thickness: 6mm; slices= 20; repeats=50) in order to reach an adequate full brain coverage with a high signal sampling rate (group2).

Using the BK-E- and standard singular value decomposition (SVD) method rCBF-maps were generated in all cases. Furthermore, standardized time-to-peak (stdTTP) maps, which provide an unambiguous quantitative hemodynamic measure of cerebral perfusion, were computed. Additionally, rCBF-maps derived from an optimized pulsed arterial spin labeling (PASL) sequence of the same examination were available. Finally, all perfusion-maps were coregistered and grey (GM) and white matter (WM) perfusion was assessed on a voxel-by-voxel basis.

RESULTS: Global GM-rCBF was 122.1 (BK-E), 255.1 (uncor.SVD) and 53.6 (PASL) [mean; unit:ml/100g/min] in group 1 (n=15). In group 2 (n=17) global GM-rCBF was 147.0 (BK-E), 224.1 (uncor.SVD) and 47.0 (PASL) [mean;unit:ml/100g/min]. GM-mean-stdTTP was 2.2sec (group1) and 2.3sec (group2), respectively. In WM a global rCBF of 96.1 (BK-E), 115.3 (uncor.SVD) and 32.9 (PASL) was found in group 1 [mean;unit:ml/100g/min]. In group 2 global WM-rCBF was 72.8 (BK-E), 86.1 (uncor.SVD) and 30.6 (PASL) [mean;unit:ml/100g/min]. WM-mean stdTTP was 2.6sec (group 1) and 2.7sec (group 2).

CONCLUSION: A relative overestimation of absolute rCBF in WM is suggested using the BK-E method, which could have implications on measurements in acute stroke. An influence from spatial resolution, which was different for the two groups, is considerable. The uncorrected SVD-approach, which provided relative rCBF only, appeared more stable. Different levels of perfusion between the groups, on the other hand, as a source of the found inconsistencies, can be ruled out, because stdTTP and PASL independently showed comparable, regular perfusion states in both groups.



ORAL PRESENTATIONS ABSTRACTS

O040-Superselective pcASL; a Novel MRI Method for Individual Characterization of Intracerebral Perfusion

*V. Toth*¹, M. Helle², C. Zimmer¹, H.H. Eckstein³, C. Preibisch¹

Klinikum rechts der Isar Neuroradiology Munich-Germany ¹ *Philips GmbH -Germany* ² *Klinikum rechts der Isar Vascular Surgery -Germany* ³

INTRODUCTION: Superselective pseudocontinuous arterial spin labeling (pcASL) is a novel ASL approach, where a circular spin labeling spot enables targeted specific vessel labeling even in difficult anatomical situations with elongated vessels. 1, 2 Thus, non-invasive imaging of altered perfusion

territories is possible in patients with cerebrovascular stenooclusive disease. Patients with multiple extracranial stenoses and cerebral infarcts often present a diagnostic conundrum with a difficulty to determine the currently symptomatic vessel. The unique possibility of pcASL to overlay selective perfusion maps on diffusion weighted images helps answering the question of infarct origin.

MATERIALS AND METHODS: 40 patients with previously diagnosed multiple extracranial stenoses and TIAs of unclear origin were examined in a Philips Achieva 3.0T MR. In addition to standard clinical protocol (FLAIR, DWI, T2*w and TOF MRA), superselective pcASL was performed with labeling of 3-6 extracranial arteries. In 10 cases, additional contrast enhanced perfusion with bolus tracking (DSC) was performed. Comparison of two post-processing softwares (Philips iViewBOLD and Brainlab BOLD Analysis) was performed in 10 cases. In 3 cases, MRI results were correlated with DSA reports. Volumetry was performed in Brainlab iPlanCranial 3.0 (Brainlab, Feldkirchen, Germany).

RESULTS: Overall, the labeling of 3 vessels provided satisfactory diagnostic information with an additional imaging time of 7:15 minutes. Technical performance was robust. Online evaluation with the iViewBOLD software was reliable and reproducible. Correlation with DSA showed absolute accordance. Comparing DSC TTP and global pcASL, normally perfused regions were overlapping with a non-significant difference ($p=0.01$). Percentage of perfusion volumes per vessel correlated significantly with stenosis grade ($r=0.6$, $p<0.05$). DWI lesions could be assorted to a specific perfusion territory in all cases.

DISCUSSION: The novel superselective pcASL method for non-invasive selective perfusion territory imaging is a robust tool in the neuroradiology of cerebrovascular stenooclusive disease with influence on clinical decisions. Validation with cDSA and contrast enhanced perfusion measurements is robust. Further studies may highlight pathophysiological insights in chronic cerebrovascular disease.

O041-Remission of Diffusion Lesions in Acute Stroke MR Imaging. A Follow Up Study with 176 Consecutive Patients

*Franz Fellner*¹, Christine Fellner¹, Alexandra Barthol¹, Kaveh Akbari¹, Daniel Flöry¹

AKH Linz Radiology Linz-Austria ¹

PURPOSE: The mismatch concept in stroke MR is based on the assumption that diffusion weighted imaging indicates infarct core representing irreversibly damaged tissue. However, this thesis has not yet been proven in a large patient cohort with adequate MR follow-up. Thus, the aim of this study was to analyze temporal evolution of restricted diffusion at follow up MR within 24 hours.

MATERIALS AND METHODS: 176 consecutive stroke patients (within 12 months) demonstrating restricted diffusion at initial MR examination were evaluated. Extension of diffusion restriction was judged both on initial MR as well as on follow-up after 24 hours. Changes in lesion extension were assessed by two radiologists independently, as well as overall image quality (4-tier scale).

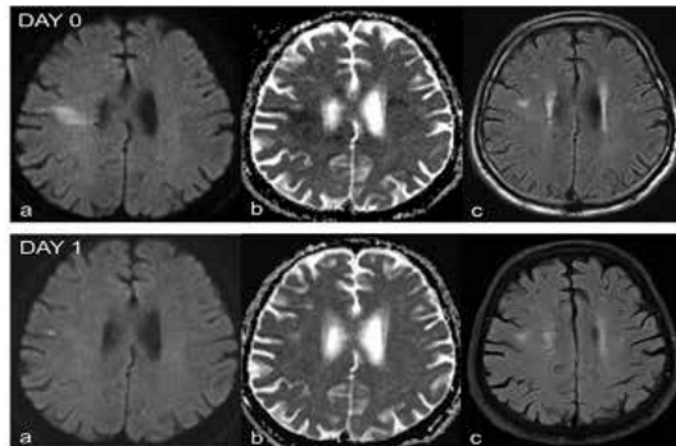
RESULTS: Extension of lesions with restricted diffusion at follow up MR was identical to the initial scan in 104/176 (59,1%) and increased in 66/176 (37,5%). The lesions was decreased (meaning partial involution of the lesion) in 6/176 (3,4%) and completely resolved in none of the patients (0%) Mean rating of image quality was 2.1 for initial MRI and 2.3 for follow-up. That means, in 96.6% the initial lesion with restricted diffusion proved to be the infarction core indeed, whereas in 3.4% partial resolution was seen.



ORAL PRESENTATIONS ABSTRACTS

In none of the patients the initial lesion did resolve completely.

CONCLUSIONS: Our findings prove the existing assumption that diffusion restriction represents infarct core, which may remain unchanged or increase in volume over time, indicating an accuracy of almost 97%. Partial or complete resolution of diffusion-restriction is extremely rare.



O042-CTP; is it Essential or Just an Additional Tool before Thrombolysis in Patients Presenting with Acute Stroke

*Hussein Kamel*¹, Mohamed Alkaphoury¹, Ahmed Own¹, Naveed Akhtar², Saadat Kamran², Ahmed ElSotouhy¹

*Hamad Medical Corporation Radiology Doha-Qatar*¹ *Hamad Medical Corporation Neurology-Qatar*²

AIM of the WORK: to evaluate the impact of the addition of CT Perfusion (CTP) to plain CT evaluation, before the initiation of intravenous thrombolysis in patients presenting with acute stroke. MATERIALS AND METHODS: CT scan examinations of all patients who presented for CT evaluation during the period from April 16/2013 till March 15/2014, with the clinical diagnosis of acute stroke and within the appropriate time frame for initiation of thrombolysis were reviewed. Patients who were excluded from thrombolysis based on plain CT findings, e.g. due to the presence of hemorrhage, established stroke, etc. were excluded. Of the remaining patients, designated for thrombolysis, only patients in whom CTP and CT angiography (CTA) were performed after plain CT examination were included in our study.

In a retrospective review, the findings on plain CT, CTP and CTA were reviewed separately by two Neuroradiologists, experienced in stroke imaging. Patients were labelled as suitable for thrombolysis or not based on the plain CT scan alone. Then CTP images were reviewed using a similar approach, to evaluate what was the impact of the addition of CTP to plain CT. Results of CTA are separately analyzed outside the present study.

RESULTS: 238 patients presented for CT scan evaluation. Out of these, 61 patients who did not have a contraindication for thrombolysis on the plain CT and who have had the three modalities (CT, CTP and CTA) performed were identified.

Based on review of plain CT alone, 50 patients were designated for thrombolysis. After review of the CTP, 36 patients were excluded and only 14 patients were found to be suitable for thrombolysis. CONCLUSION: In our population, CTP was an essential tool in the decision making before the initiation of thrombolysis in patients presenting with acute stroke. Findings in this study relate to our population and our local circumstances when the study was performed. Never the less, it highlights the importance of the use of CTP, in absence of a contra indication. CTA was felt to be redundant in presence of a normal CTP.



ORAL PRESENTATIONS ABSTRACTS

O043-Ct Perfusion and Angiographic Assessment of Pial Reperfusion in Acute Ischemic Stroke the CAPRI Study

*Arturo Consoli*¹, Tommy Andersson², Luca Verganti³, Stefano Vallone³, Andrea Zini⁴, Enrico Fainardi⁵, Andrea Saletti⁵, Alfonso Cerase⁶, Daniele Romano⁶, Sandra Bracco⁶, Svetlana Lorenzano⁷, Salvatore Mangiafico¹

*Careggi University Hospital Interventional Neuroradiology Unit Florence-Italy*¹ *Karolinska Institutet Department of Clinical Neuroscience -Sweden*² *Baggiovara Hospital, Modena Department of Neuroradiology -Italy*³ *Baggiovara Hospital, Modena Department of Neurology -Italy*⁴ *Sant Department of Neuroradiology -Italy*⁵ *Le Scotte Hospital, Siena Department of Neuroradiology -Italy*⁶ *Sapienza University Hospital, Rome Department of Neuroscience -Italy*⁷

BACKGROUND AND PURPOSE: Recanalization is not the only factor that may determine a favorable outcome in patients with acute ischemic stroke. The role of collaterals is still debated and not yet fully understood. The aim of this international, multicentric, retrospective study was to evaluate the correlation between CT-Perfusion maps and collateral circulation evaluated with a novel angiographic score, the Careggi Collateral Score (CCS). **MATERIALS AND METHODS:** 103 patients (M:F=52:51, mean age 65.9) with anterior circulation stroke and a documented major artery occlusion (complete MCA, ICA, ICA + M1), imaged with Non Contrast CT (NCCT), CT-Angiography (CT-A) and CT-Perfusion and successively subjected to DSA evaluation and endovascular treatment in 4 experienced centers from January 2010 to June 2012 were included within the analysis. Two core labs evaluated CT data (ASPECT score on NCCT, CBV and MTT maps, Clot Burden Score on CT-A were assessed) and other two core labs evaluated the angiographic ones (site of occlusion, CCS score and TICI score); all the core labs evaluated the images blinded to the clinical data. NIHSS score at baseline, after 24 hours and at the discharge and data about main vascular risk factors were collected. Onset-Time-to-Treatment, time of intervention, time of reperfusion were calculated. mRS 0-2 after 3 months was considered as favorable clinical outcome. **RESULTS:** Median baseline NIHSS was 16 and 38.6% of the patients received IV t-PA. 79% of the patients were treated with thrombectomy, 12% with IA t-PA alone and 9% with rescue therapy. The occlusion site was proximal M1 in 38.6%, distal M1 in 36.6 and ICA +-M1 in 24.8%, 78% of the patients had good collaterals according to CCS. mRS0-2 was achieved in 47.6% and TICI 2b-3 in 64.1%. Good collateral circulation was correlated to baseline and 24 hours NIHSS ($p=0.031$), favorable outcome after 3 months ($p=0.002$), lower death rate ($p=0.006$) and with perfusional parameters (particularly the mismatch calculated as MTT-CBV ASPECTS; $p=0.032$).

CONCLUSIONS: CT-Perfusion and angiographic findings may be correlated regarding the evaluation of the ischemic penumbra and might be considered together for patient selection. However, a prospective study with a larger number of patients would provide more solid results.

O044-An Automated Method for Segmentation of Brain Infarcts

Guray Erus¹, Ann Peiffer², Lenore Launer³, Sigurdur Sigurdsson⁴, Christos Davatzikos¹,
Nick Bryan I, Manoj Tanwar¹

*Univ. Pennsylvania Radiology -United States*¹ *Bowman Gray School of Medicine Epidemiology -United States*²
*NIH NIA -United States*³ *NIH AGES -United States*⁴

PURPOSE: Many clinical studies investigating cerebrovascular disease require detection and quantification of infarcts, which is a tedious task to perform manually. We propose an automated infarct segmentation method that combines intensity information with the spatial information within a rule-based framework to accurately segment both cortical and sub-cortical infarcts.

MATERIALS AND METHODS: The proposed framework consists of three main components: (i) segmentation of hyper-intense lesions and necrosis, (ii) detection of sub-cortical infarcts based on a set of adjacency rules, and (iii) detection of cortical infarcts based on location.



ORAL PRESENTATIONS ABSTRACTS

A computer-assisted segmentation method (WMLS) is used for segmenting hyper-intense lesions. The method uses a combination of image analysis and pattern classification in order to characterize lesions, based on local features extracted from multi-parametric Magnetic Resonance Imaging (MRI)

sequences. Image intensities from multiple MR acquisition protocols, after co-registration, are used to form a voxelwise feature vector that helps to discriminate lesion from various normal tissue image profiles. To detect necrosis, the T1 scan of a subject is first segmented into 3 tissue types, white matter (WM), grey matter (GM) and cerebrospinal fluid (CSF) using the AdpkMean algorithm. The ventricular and cortical CSF are eliminated through template warping using the Hammer algorithm and image morphology. The hyperintensity and necrosis masks are combined together using image morphology techniques for subcortical-infarct detection. Cortical infarcts were detected based on spatial location, using a cortex mask obtained by warping predefined regions of interest (ROIs) on a template image to the subject space. RESULTS: The method (M) is validated on MRI scans of 50 subjects from the AGES study with infarct counts in 10 different anatomical regions (4 lobes and basal ganglia) manually extracted by two independently trained raters. Kappa scores are calculated between each pair of raters. The method obtained scores comparable to intra-rater agreement both for sub-cortical (kR1, R2=0.48, kM, R1=0.34, kM, R2=0.49) and cortical infarcts (kR1, R2=0.74, kM, R1=0.53, kM, R2=0.65).

CONCLUSIONS: We present a fully automated infarct segmentation method with performance comparable to intra-rater agreement. Such a method is specifically useful in population studies not only for its practical advantage in application, but also for reproducibility of the final segmentations.

PARALLEL SCIENTIFIC PAPER PRESENTATIONS

(Stroke 2) 17:15 - 19:00

Dolmabahce C Hall

O045-Carotid Elongation Does Not Affect Angiographic Results of Mechanical Thrombectomy in Acute Stroke

*Umut Yilmaz*¹, Ruben Mühl-Benninghaus¹, Andreas Simgen¹, Wolfgang Reith¹, Heiko Körner¹

*Saarland University Hospital Department of Neuroradiology Homburg-Germany*¹

PURPOSE: New techniques have substantially raised recanalization rates of mechanical thrombectomy in acute ischemic stroke in the last few years with initial prospective trials reporting good neurological outcome in up to 58% of the cases. However some recent highly disputed reports questioning the benefit of endovascular therapy have boosted the discussion about the importance of patient-selection. The purpose of this study was to investigate whether an elongation of the carotid artery affects the angiographic outcome of the recanalization procedure in MCA-occlusions.

MATERIALS AND METHODS: The data of 54 patients with occlusions of the M1-segment who underwent mechanical thrombectomy was included. The lengths of the carotid arteries were measured using preinterventional CT-angiograms. To take individual patient height into account these lengths were divided by the length of the spine from the tip of the dens to the bottom of the th3 vertebral body (referred to as CS-Ratio). Angiographic results were scored according to the mTICI-score.

RESULTS: Recanalization with mTICI $\geq 2b$ was achieved in 83.3%. The mean CS-Ratio was 1.32 ± 0.13 . There was a significant correlation between the CS-Ratio and the age of the patients. There were no significant differences in the CS-Ratios of occlusions that were successfully recanalized and those that were not. Neither were there significant correlations of the CS-Ratio and the length of procedure or the number of deployments of the stent retrievers.

CONCLUSIONS: In this retrospective analysis we report that carotid elongation does not affect angiographic results of mechanical thrombectomy in acute stroke.



ORAL PRESENTATIONS ABSTRACTS

O046-Carotid Stent Related Hypoperfusion Artifact in Arterial Spin Labeling Perfusion Study

*Chi-Jen Chen*¹, David Yen-Ting Chen¹, Ying-Chi Tseng¹

*Suang-Ho Hospital/Taipei Medical University Department of Medical Imaging New Taipei City-Taiwan*¹

PURPOSE: Arterial spin labeling (ASL) technique for detecting cerebral perfusion is increasingly used in many clinical institutes worldwide because it has the advantage of devoid of the use of contrast agent. The study aimed to elucidate the causes of cerebral hypoperfusion measured by ASL on the stenting side after carotid artery stenting (CAS).

MATERIALS and METHODS: Consecutive patients with symptomatic internal carotid artery stenosis receiving CAS at our hospital were included in the study. CBF was measured by pseudocontinuous ASL on a 3-Tesla MRI scanner on the day before, one day after and three days after the procedure. Changes of the cerebral hemodynamic after CAS were assessed.

RESULTS: 22 patients were included. 17 patients had increased or stationary CBF after CAS. 5 patients had significantly reduced CBF on the stenting side after CAS (20.2%, 20.1%, 43.2%, 27.2%, and 34.0% decrease compared to the pre-stenting CBF, $P = 0.025$) while CBF increased on the contralateral side. No carotid stent thrombosis developed in the five patients. High stent position was noticed above the C2 body in the five patients. After tagging plane adjustment to avoid tagging on the stent, no more cerebral hypoperfusion were noticed.

CONCLUSION: When using ASL to monitor post-stenting CBF, the stent may cause artifact that leads to a low CBF in the territory of the stented vessel. We suggest add a MRA to identify the stent position and adjust the tagging plane to avoid the stent-related artifact in this condition.

O047-Intermediate Catheters Reduce the Length of Mechanical Thrombectomy Procedures in Acute Basilar Artery Occlusions

*Ruben Mühl-Benninghaus*¹, Heiko Körner¹, Andreas Simgen¹, Wolfgang Reith¹, Umut Yilmaz¹

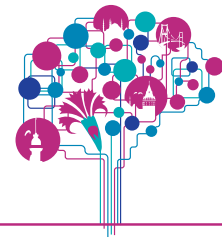
*Saarland University Hospital Department of Neuroradiology Homburg-Germany*¹

BACKGROUND and PURPOSE: In the last years technical developments have substantially raised recanalization rates of endovascular treatments of intracerebral artery occlusions in acute ischemic stroke. By using these new techniques several prospective trials have reported recanalization rates with $\text{TICI} \geq 2\text{b}$ from 69 to 79% as well as good neurological outcome ($\text{mRS} \leq 2$ at 90 days) in 55 to 58% of the cases. The degree of the recanalization and the length of the procedure are factors known to influence the clinical outcome of patients treated endovascularly. Yet still little is known about factors influencing the angiographic results of thrombectomy procedures. The purpose of this study was to investigate whether the use of intermediate catheters affects the angiographic outcomes of mechanical thrombectomy procedures in acute basilar artery occlusions.

MATERIALS and METHODS: 47 consecutive patients with acute BA-occlusions who underwent endovascular treatment with stent retrievers in our department were retrospectively identified. We analyzed the angiographic data regarding the use of intermediate catheters, the lengths of the procedures, the number of deployments of the stent retrievers, the angiographic results and the site of access to the basilar artery.

RESULTS: The mean length of the mechanical thrombectomy procedures was 63.5 ± 39.5 min with 2.2 ± 1.4 stent retriever deployments. Procedures were performed via the right vertebral artery in 24 cases (51%). Recanalization with $\text{mTICI} \geq 2\text{b}$ was achieved in 74.5%. Intermediate catheters were used in 13 cases. The mean length of the procedures was significantly shorter when intermediate catheters were used (44.8 ± 27.6 min vs. 70.7 ± 41.4 min, $P = .043$). There were no significant differences in the number of deployments or in the final mTICI -scores.

CONCLUSIONS: In this retrospective analysis we report that the use of intermediate catheters significantly reduces the length of mechanical thrombectomy procedures in acute basilar artery occlusions.=



ORAL PRESENTATIONS ABSTRACTS

O049-Implementation of Neurointerventional Treatment in Acute Stroke Patients with Large Vessel Occlusions in Norway

*Kathinka D. Kurz*¹, Lars Fjetland¹, Frode Johannessen¹, Martin W. Kurz²

*Stavanger University Hospital Department of Radiology Stavanger-Norway*¹ *Stavanger University Hospital*

*Department of Neurology -Norway*²

PURPOSE: Neurointerventional treatment in acute stroke patients with large vessel occlusions is controversially discussed. Efficacy of a neurointerventional approach is yet not proven and procedural techniques are in continuous development. Yet, most important the neurointerventional procedures are traditionally conducted by neurointerventional radiologists. However, there are too few of such sub-specialists to provide a well covering service in Norway. Therefore we have at the Stavanger University Hospital developed a close cooperation between diagnostic neuroradiologists and general interventional radiologists ("The Stavanger model") and thereby established a neurointerventional treatment. We will discuss the pivotal role of the diagnostic neuroradiologist in the Stavanger model. Additionally we present the safety and efficacy of our approach and compare the results achieved to those of previous reports from centers with specialized interventional neuroradiologists.

MATERIALS AND METHODS: A total of 86 patients with acute ischemic stroke due to large-vessel occlusion were treated with either intra-arterial thrombolysis or mechanical thrombectomy. Patients were consecutively included in a prospective follow up study. Radiological outcome was estimated by measuring the established revascularization due to the Thrombolysis in Myocardial Infarction (TIMI) score. Bleeding complications were assessed according to the ECASS 2 criteria. Clinical outcomes were measured using the National Institutes of Health Stroke Scale scale (NIHSS). Long term outcome was measured using the modified Rankin scale at 90 days (mRS). The principles of the Stavanger model will be outlined.

RESULTS: Mean patient age was 67.4 (range 31 – 92); the average NIHSS at hospital admission was 17 (range 2 – 36). Successful recanalization was achieved in 81.4 % of the patients. Procedure-related complications occurred in 15.1 % of the patients, and 10.6 % had a symptomatic intracerebral hemorrhage. Patients who were successfully recanalized had a significantly better neurologic improvement postinterventionally (NIHSS 6.4 vs -2.8, $p < 0.001$), a significantly better outcome at 90 days (mRS 2.7 vs 5.1, $p < 0.01$), and a reduced mortality (20% vs 50%, $p = 0.01$).

CONCLUSION: Our results show that diagnostic neuroradiologists can establish and maintain a neurointerventional treatment for acute stroke patients in close cooperation with general interventional radiologist. The obtained radiological results and patient outcomes are in line with the published results in the literature achieved by interventional neuroradiologists. Patients with successful recanalization profit clinically.

O050-Mechanical Thrombectomy in Egyptian Acute Ischemic Stroke Patients Initial Experience Using Catch + Device

*Ossama Mansour*¹, Tamer Ibrahim²

*Alexandria University Neurology & Neuroradiology Alexandria-Egypt*¹ *Alexandria University Neurosurgery*

*Egypt*²

BACKGROUND and PURPOSE: Mechanical thrombectomy presents today a promising alternative to traditional stroke therapies. Our aim with this study was to evaluate the safety and efficacy of mechanical thrombectomy using the Catch plus device in the treatment of acute stroke and report the angiographic results and clinical outcomes.

MATERIALS AND METHODS: We performed an analysis of 13 consecutive patients with ischemic stroke treated with the Catch plus stent retriever device at our center. Thirteen patients were treated with the device: Anterior circulation occlusion was identified in 69 % of patients (n = 9, 6 with M1 middle cerebral artery, 2 patients with carotid terminus and one patient with C7 internal carotid occlusions) versus vertebrobasilar occlusion (n = 4 with Basilar artery occlusion). Four (30.8%) patients received an additional treatment to aid revascularization, in the form of thrombus vaccination via the microcatheter while 5 (38.5%) patients received



ORAL PRESENTATIONS ABSTRACTS

preprocedural bridging IV dose with rtPA (mean dose of 35 mg).

RESULTS: The mean age was 56.8 years (range, 28-81 years; 53.8% females). The median NIHSS score at presentation was 16 (range, 11-26). The mean symptom-to-procedure start time was 342 minutes (range, 180-590 minutes). Recanalization (TIMI grade 2-3 flow) was achieved in 12/13 (92%). Four patients developed asymptomatic hemorrhagic transformation (30.7%); one patient (7.7%) had serial focal seizures secondary to hemorrhagic transformation. Procedural complications occurred in 3 patients without clinical consequences: 1 clot fragmentations and 2 vasospasms. The mean follow up period was 60.7 days (range, 25-160 days). Thirty-day mortality was 7.7%; good 30-day functional outcome (mRS, s 2) was achieved by 69.2% (9/13). The median NIHSS score at discharge was 5 (range, 4-26) with median reduction of NIHSS score by 7 points improvement. **CONCLUSIONS:** In our retrospective case series, the Catch+ device appears effective in achieving recanalization and improving 30-day outcome in patients with acute ischemic stroke.

O051-Evaluation of Clot Burden Score in Acute Ischemic Stroke Patients Treated With Thrombolysis

*Ahmad Sobri Muda*¹, Hilwati Hashim², Shahizon Azura Mukari¹, Mohd Redzuan Ismail¹,

Sarah Yaziz¹, Syazarina S Osman¹

*Universiti Kebangsaan Malaysia Medical Center Radiology Bandar Tun Razak-Malaysia*¹ *Universiti Teknologi Mara Radiology -Malaysia*²

OBJECTIVE: To evaluate the clot burden score (CBS) in acute ischaemic stroke (AIS) patients treated with thrombolysis.

MATERIALS AND METHODS: Retrospective review of AIS patients treated with thrombolysis in Universiti Kebangsaan Malaysia Medical Centre (UKMMC) from January 2011 to January 2013. The CBS is calculated by two neuroradiologists using the CTA images of the perfusion scan (CTP and CTA) done before thrombolysis. Patients outcome was assessed at 3 months follow up using Modified Rankin Scale (MRS).

RESULT: Results are still being tabulated and analysed. It will be ready in time for the symposium.

CONCLUSION: We postulate that a low CBS is associated with a poor outcome.

O052-Craniectomy Reduced Mortality and Improved GOS among Large MCA Infarction Patients with Middle Line Shifting More than 10 mm.

*Yueh-Hsun Lu*¹, Michael MH Teng², Chan-Ming Yang¹, Feng-Chi Chang³, Wang-Yuo Guo³

*Taipei City Hospital Zhong-Xing branch Radiology Taipei-Taiwan*¹ *Cheng Hsin Hospital Radiology -Taiwan*²

*Taipei Veterans General Hospital Radiology -Taiwan*³

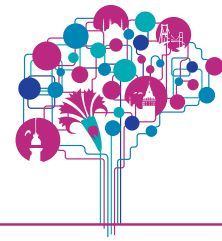
PURPOSE: Large middle cerebral artery infarction could cause mass effect and life threatening. Decompressive craniectomy may increase survival rate but the indication is still controversial.

MATERIALS and METHODS: There were 350 patients were diagnosed as MCA infarction by brain CT and brain MRI due to hemiparesis or hemiplegia in our hospital from 2004 to 2010. Midline shift was observed in 40 patients. Among them, 1 patient died with septic shock and the 2 patients suffer from bilateral MCA infarction, were excluded. We retrospectively reviewed the charts, operative findings, and images of remaining 37 patients.

RESULT: Overall, 15 patients had a midline shift less than 10mm (average 5.2 mm). No operation was done (average infarction volume 58.33%) and no mortality is noted in this group. The average Glasgow outcome scale is 3.88.

Another 22 patients was found to have midline shift more than 1cm, 13 patients received craniectomy (group A) and 9 received conservative treatment (B). The average age between these A and B is 57.44+/- 14.11 versus 84.88+/- 5.16 (p < 0.001). The average midline shift length is 15.68 +/- 2.63 mm versus 17.68 +/- 3.16 mm (p = 0.77). The infarction volume is 433.76 +/- 68.73 ml versus 425.64 +/- 58.79 ml (p = 0.42). Preoperative coma scale is 8.67+/- 2.03 versus 8.22 +/- 2.94 (p = 0.38). Except the significant difference of age, no significant difference is noted at gender, milline shift length, infarction volume and preoperative coma scale.

The mortality rate is significantly lower in group A (0/13, 0%) than that (7/9, 78%) of groups B (p < 0.001). The



ORAL PRESENTATIONS ABSTRACTS

average Glasgow outcome scale (GOS) is also significant higher in group A (3.56 +/- 0.70) than group B. (1.22 +/- 0.41, $p < 0.01$).

CONCLUSION: Decompressive craniectomy can reduce mortality and improve GOS among patients with more than 10mm midline shifting in our series. This simple index may need further prospective and large scale study, but can be used as a practical index for decision making.

O053-Medullary Arteries of the Cerebrum the Basis for a New Classification of Ischemia Infarction

*Shoki Takahashi*¹, Shunji Mugikura¹, Toshiaki Akashi², Takaki Murata¹, Yumiko Kato¹, Yasuko Tatewaki¹

Tohoku University Hospital Radiology Sendai-Japan ¹ *Nara Medical University Radiology -Japan* ²

BACKGROUND and PURPOSE: Medullary arteries of the cerebrum supply nearly entire cerebral white matter. Ischemic cerebral lesions/ infarcts are usually discussed from the viewpoint of large arteries only, but rarely of medullary arteries. This study is to elucidate and discuss clinical significance of medullary artery circulation in the pathomechanism of ischemic lesions.

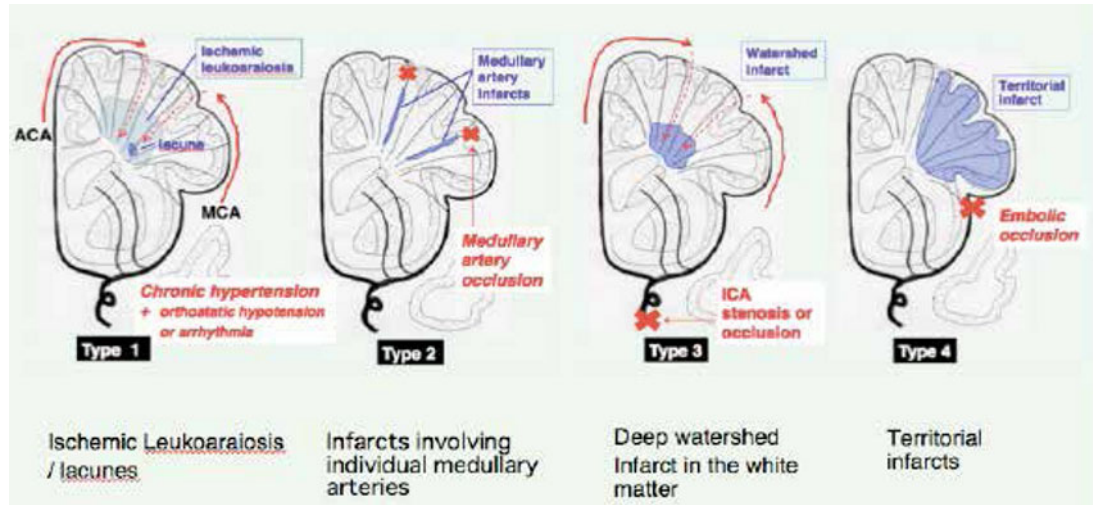
MATERIALS AND METHODS: A) We examined the course and distribution of medullary arteries by observing cadaveric microangiograms, and by tracing dilated perivascular spaces along medullary arteries on clinical MR images. Concurrently, we also referred to the previous literature to reconfirm the anatomy of the medullary arteries. B) We attempted classification of ischemic cerebral injuries/ infarcts in the light of medullary artery circulation.

RESULTS: A) Medullary arteries arise at right angles from pial arteries, run perpendicularly through the cortical layers, and enter the white matter to reach paraventricular region. They are very thin (100 to 200 μm) and long (20 to 50 mm), each providing blood supply to a cylindrically-shaped unit. B) Apart from the basal perforator lesions, ischemic cerebral injuries/ infarcts were classified into four types, which could be exemplified by clinically common MR findings in daily practice: 1) Ischemic leukoaraiosis, or incompletely infarcted lesions of the white matter often associated with lacunar infarcts; 2) Infarcts involving individual medullary arteries, typically presenting with infarcts of linear/ cylindrical distribution extending from the pial surface toward ventricular wall or punctate lesions in the white matter; 3) Deep watershed infarcts, which are usually caused by hemodynamic mechanism in cases with hypoperfusion, e.g., cervical carotid stenosis/ occlusion; 4) Territorial infarcts or ordinary cortical infarcts that are caused by truncal or pial artery occlusion, atheromatous or embolic, involving both cortical gray and underlying white matter supplied by medullary arteries.

CONCLUSION: Recognizing the anatomic characteristics of the medullary arteries and their presumed circulation pattern would facilitate to understand the mechanism of various patterns of ischemic cerebral lesions.



ORAL PRESENTATIONS ABSTRACTS



O054-Role of CT Scans in Predicting Malignant Course of Middle Cerebral Artery Stroke

Saadat Kamran¹, Naveed Akhtar¹, Hussain Kamel², Ahmed El Sotouhy², Ahmed Owen², Sohail Al Rukun³, Ashfaq Shuaib¹

Hamad General hospital Neuroscience Doha-Qatar¹ Hamad General hospital Radiology -Qatar² Rashid Hospital Neurology -United Arab Emirates³

BACKGROUND: Decompressive hemicraniotomy (DH is recommended in patients <60 years within 48 hours of stroke. Volume of stroke on diffusion imaging has been used as a marker of malignant course of stroke.

MATERIALS AND METHODS: A retrospective review of DH in MCA done including demographic, clinical (risk factors, NIHSS, GCS, signs of herniation, time to herniation time to surgery), radiological variables (infarct volumes calculated by (A.B.C/2) method, vascular territory involved, subfalcine, uncal herniation, vascular occlusion). Markers of cerebral atrophy (CA) measured by semiautomated method. CA markers were frontal horn ratio (FHR) frontal horn horizontal length/ transverse skull diameter (TSD), Intercaudate ratio (ICR)-intercaudate distance at foramen Monroe /TSD, mid lateral ventricle ratio (MLR)-mid lateral ventricle horizontal/TSD, third ventricle ratio TVR)-mid third ventricle/TSD.

RESULTS: 250 CT scans of 110 patients, 86 men and 24 women, mean age 46.85 p<0.44, 64 right and 46-left hemispheres. Mean arrival time 4.5 hours, mean GCS 12.4 p<0.079. Mean time (MT) to 1st CT 7.06 hours (St. d 8.60), mean infarct volume (MIV) 1st 117.96cm³(range 0-420.21) p<0.55, MT 2nd CT 42.69 hours (St.d 33.39), MIV 2nd 330.48(40-750) p<0.026, MT3rd CT (n=33) 78.98 (st.d 63.90), MVI3rd 377.51 (131.80-650) p<0.99. MCA stroke alone p<0.07, additional to MCA (ACA, PCA, ACA+PCA) on 1st CT p<0.65, additional to MCA (ACA, PCA, ACA+PCA) on 2nd CT p<0.002. Herniation signs p<0.84, mean herniation time p<0.148, uncal p<0.163, subfalcine herniation p<0.870. Progression of stroke volume over time p<0.99,vascular occlusion p<0.44, type of vessel occluded (ICA) p<0.034.

Mean FHR 0.2909 (range 0.0999-.6000), association with, time to herniation p<0.24, signs herniation p<0.56, coma p<0.723, additional infarct p<0.03, time of surgery p<0.50, mRS 3 month p<0.009 (inversely). ICR 0.1218 (0.0395-0.4000) infarct volume p<0.046, sign of herniation p<0.72, time of herniation p<0.28, mRS p<0.029 (inversely). MLR 0.2139 (0.0741-0.5066) herniation time p<0.66, infarct vol p<0.04, time to surgery p<0.50, mRS p<0.012 (inversely). TVR 0.0522(0.000-0.3906) herniation time p<0.76, herniation sign p<0.86, time to surgery<0.56, mRS p<0.043 (inversely).



ORAL PRESENTATIONS ABSTRACTS

CONCLUSION: The second CT, area of stroke additional to MCA, and internal carotid artery occlusion predicted a malignant course of the MCA stroke. CA markers did not predict malignant progression but were inversely related to clinical outcome.

PARALLEL SCIENTIFIC PAPER PRESENTATIONS

(Head and Neck 1) 17:15 - 19:00

Topkapı A Hall

O055-Imaging and Disease Spectrum in Ocular and Orbital Lesions in Eastern Nepal

*Raj Kumar Rauniyar*¹, Mukesh Kumar Gupta², Kalim Ahmed², Ashok Pant¹

*B.P.Koirala Institute of Health Sciences Radio-diagnosis and Imaging Dharan-Nepal*¹ *B.P.Koirala Institute of Health Sciences Radiodiagnosis and Imaging -Nepal*²

PURPOSE: Ocular and orbital lesions are common in this part of Nepal and most of them presents with proptosis associated with other symptoms. These cases required radiological evaluation for early diagnosis and to know the extent of involvement. This study was carried out to analyze the spectrum of diseases, which manifested as proptosis in eastern Nepal. Role of Imaging modalities and early diagnosis is emphasized.

MATERIALS AND METHODS: All the patients referred to our department for the evaluation of proptosis either by plain radiography, ultrasonography (US), Computed Tomography (CT) and Magnetic resonance Imaging (MRI) over the period of three years were included in the study. Diagnosis was made on the basis of Imaging features, Fine needle aspiration cytology (FNAC) and histopathological examination of operative specimens where ever surgery was performed.

RESULTS: There were 212 eyes with proptosis (including due to acute trauma), which underwent Imaging evaluation Ocular and orbital tumors were most common cause of proptosis accounting for 34.25% of cases followed by pseudotumour and infection 21.15%. Other lesions were Parasitic infestation 7.30%,Paranasal lesions spreading to orbit 17.20%,Trauma and foreign body 6.60% and miscellaneous 13.50%

CONCLUSION: Many of the cases of proptosis in this part of Nepal were neglected presenting late in advanced stage of disease requiring extensive surgery. This calls for awareness and early Imaging evaluation of the cases of proptosis and prompt management. CT Scan was the most effective Imaging modalities in the diagnosis, however MRI was better for vascular, hemorrhagic and orbital apex pathologies. There was little role of plain Radiography in the diagnosis.

O056-ECG Gated CT Angiography of Intracranial Aneurysms (broken and not) Using 320 Row Detector CT Scanner Identification of Higher Risk Aneurysms and Rupture Site before Surgery

*Federico D Orazio*¹, Aldo Victor Giordano², Sergio Carducci², Alessandra Splendiani³,

Massimo Gallucci⁴

*Scuola di Specializzazione in Radiodiagnostica, Università degli studi di L Aquila U.O. Neuroradiologia e Radiologia Interventistica L'Aquila-Italy*¹ *Ospedale San Salvatore L Aquila U.O. Neuroradiologia e Radiologia Interventistica -Italy*² *Università degli Studi di L Aquila Neuroradiologia, Dipartimento Scienze Cliniche Applicate e Biotecnologie -Italy*³ *Università degli Studi di L Aquila Neuroradiologia, Dipartimento Scienze Cliniche Applicate e Biotecnologie -Italy*⁴

PURPOSE: To evaluate diagnostic potentials of ECG-gated CT angiography (CTA) of intracranial aneurysms

MATERIALS AND METHODS: In the period between January 2012 and December 2013, 70 ECG-gated CTA were performed using a 320 row detector CT scanner, in as many patients with cerebral aneurysms both broken and not. Scan protocol was designed as follows: first scan without contrast media: FOV=160mm/120KV/300mA/ Rot.Time=0,35s/Collimation=0,5mm; second scan, with contrast superimposable on the first to obtain



ORAL PRESENTATIONS ABSTRACTS

further bone subtraction, had duration of one heart beat between an R-R interval. The subtracted volume was reconstructed with a step interval of 5%, obtaining 20 volumes per each contrast scan. An MPR and 3D rendering of the aneurysms could then be observed in motion during the whole RR interval. The sites where abnormal/not synchronized movement of the aneurysmal wall were found, then were compared with its intra-operative observation during neurosurgical treatment which was filmed.

RESULTS: Among the aneurysms studied, 40 belonged to the anterior circulation and 10 to the posterior one. We found abnormal or not synchronized movement in part of the aneurysmal wall in 15% of the unbroken intracranial aneurysms; similar findings were found in about 45% of the broken aneurysms studied in emergency before surgical treatment, and in that case it always matched with the cleavage site highlighted during surgery.

CONCLUSION: ECG-gated CTA is a promising add to the study of intracranial aneurysms. It can help in identifying a subpopulation of intracranial aneurysms with higher risk of rupture or directly demonstrate the site of rupture before surgical treatment. This information can be useful when planning both endovascular and/or a surgical treatment of intracranial aneurysms both broken and not.

O057-Prevalence and Risk of Malignancy in Incidental Thyroid Nodules on Low Dose Screening Chest CT A Retrospective Study

*Hyobin Seo*¹, Ji-Hoon Kim², Kwang Nam Jin³, Ji Sang Park⁴, Koung Mi Kang², Eun Kyung Lee⁵

*Gangnam center, Seoul National University Hospital Healthcare system Radiology Seoul-Korea, South*¹ *Seoul National University College of Medicine, Seoul National University Hospital Radiology -Korea, South*² *SMG-SNU Boramae medical center Radiology -Korea, South*³ *Soonchunhyang University Bucheon Hospital Radiology -Korea, South*⁴ *Dongguk University Ilsan Hospital Radiology -Korea, South*⁵

PURPOSE: After the result of the National Lung Screening Trial (NLST), the use of low-dose chest CT (LDCT) for lung cancer screening is expected to increase. The purpose of this study is to define the prevalence and malignancy rate of incidental thyroid nodules (ITNs) and to find the suspicious features for a malignant thyroid nodule in patients with LDCT for lung cancer screening. **MATERIALS and METHODS:** LDCT in high risk of lung cancer was performed in 2767 consecutive patients from January 2004 to May 2013. Among them, 2288 patient had thyroid US within six months from LDCT scans. Two radiologists retrospectively evaluated ITNs on LDCT and US. Prevalence, malignant risk and suspicious CT features including multiplicity, size, attenuation and calcification of ITNS were assessed and compared to histopathologic results from biopsy or surgery. Student t test, χ^2 test and interobserver agreement were used for statistical analysis.

RESULT: The prevalence of ITNs on LDCT was 5.7% (157 patients). Among these nodules, calcifications were demonstrated in 57 patients (36.3%). Interobserver agreement was good in interpreting calcifications ($K = 0.687$). The malignancy rate was 2.2% (3/135) in ITNs on LDCT. The average size of the ITNs on CT was 13.5mm (1.9mm to 41.4mm). Between CT nodule positive and negative groups, the proportion of female patients (6.4% vs 2.1%), thyroid nodule prevalence on US (98.5% vs 51.5%), nodule multiplicity on US (73.8% vs 53.6%), largest size of the nodule (14.4 ± 8.3 mm vs 6 ± 3.8 mm), the proportion of suspicious nodules (71.3% vs 16.6%), proportion of biopsied nodules (40.7% vs 6.6%) and malignancy risk (2.2% vs 0.4%) were significantly different ($P \leq 0.03$). In comparison of cytologic benign or neoplastic nodules, only calcification was significantly suspicious feature suggesting neoplasm on LDCT (34.8% vs 83.3%, $P = 0.034$). Nodule attenuation except calcification was not significantly associated neoplastic nodule (51.9 ± 19.8 vs 54.6 ± 34.8 , $P = 0.792$). **CONCLUSION:** The prevalence of ITNs on LDCT was 5.7% and most of ITNs were benign. Only calcification was significantly associated with neoplastic nodules in ITNs. Nodule attenuated except calcification was not associated with thyroid neoplasm.



ORAL PRESENTATIONS ABSTRACTS

O058-Ultrasound Based Risk Stratification for Malignancy in Thyroid Nodules Four Tiered Categorization System

*Hyobin Seo*¹, Dong Gyu Na², Ji-Hoon Kim³, Ji Won Yoon⁴, Kyung Won Kim⁴

*Gangnam center, Seoul National University Hospital Healthcare system Radiology Seoul-Korea, South*¹

*Human Medical Imaging and Intervention Center Radiology -Korea, South*² *Seoul National University College of Medicine, Seoul National University Hospital Radiology -Korea, South*³ *Gangnam center, Seoul National University Hospital Healthcare system Endocrinology -Korea, South*⁴

PURPOSE: The purpose of this study was to retrospectively stratify the malignancy risk of thyroid nodules based on ultrasound (US) patterns.

MATERIALS and METHODS: US-guided FNA was performed in 1357 consecutive patients. A total of 1058 nodules with final diagnoses (238 malignant nodules and 820 benign nodules) were included for this study. Two thyroid radiologists retrospectively evaluated US characteristics of thyroid nodules. Malignancy risk of each nodule was analyzed according to US features with an emphasis on nodule echogenicity, and it was stratified into 4 tier-categories. A χ^2 test was used for statistical analysis. **RESULT:** The malignancy rate was 5.9% (30/507) in isoechoic nodules, 18.2% (2/11) in hyperechoic nodules, 35.6% (158/444) in hypoechoic nodules, and 50.0% (48/96) in markedly hypoechoic nodules. In multivariate analysis, isoechogenicity, indistinct margin, and non-solid internal content were predictive of benign nodules ($P < 0.01$), while hypoechogenicity, markedly hypoechogenicity, spiculated/microlobulated margin, solid content, taller-than-wide shape, microcalcification, and macrocalcification were predictive of malignancy ($P < 0.05$). Although presence of any malignant US feature (spiculated/microlobulated margin, taller-than-wide shape, microcalcification, and macrocalcification) were significantly associated with malignancy in hypoechoic or markedly hypoechoic nodules (malignancy risk; 48.0% and 60.7%, respectively), any malignant US feature was not associated with malignancy in isoechoic nodules (malignancy risk; 14%). Thyroid nodules could be classified into 4 categories according to the malignancy risk; benign (category 1, cyst, nodule with comet-tail artifact, spongiform appearance, risk 0%), probably benign (category 2, isoechoic nodule without any calcification, risk $\leq 5\%$), indeterminate (category 3, risk > 5 and $< 50\%$) including category 3A (low risk, isoechoic nodule with any calcification or hyperechoic nodule), category 3B (high risk, markedly hypoechoic or hypoechoic nodule without any malignant US feature), and suspicious malignancy (category 4, markedly hypoechoic or hypoechoic nodule with at least one of malignant US features, risk $> 50\%$).

CONCLUSION: The malignancy risk of thyroid nodules could be stratified into 4 tiers by combination of nodule echogenicity and malignant US features. Our US based 4-tier categorization system will be useful for predicting the risk of malignancy and management decision in thyroid nodules.

O059-Dynamic Contrast Enhanced MR Imaging of Neck Lymph Nodes Predicts Neck Control in Oropharyngeal or Hypopharyngeal Squamous Cell Carcinoma Treated with Chemoradiotherapy

*Shu-Hang Ng*¹, Ho-Fai Wong¹, Yao-Liang Chen¹, Jiun-Jie Wang², Chi-Wah Yeh³

*Chang Gung Memorial Hospital Diagnostic Radiology Kueishan-Taiwan*¹ *Chang Gung University Medical*

*Imaging and Radiological Sciences -Taiwan*² *Chang Gung Memorial Hospital Diagnostic Radiology -Taiwan*³

PURPOSE: We prospectively investigated the ability of pharmacokinetic parameters derived from pretreatment dynamic contrast-enhanced perfusion MR imaging (DCE-PWI) and diffusion-weighted MR imaging (DWI) of neck lymph node in predicting the neck control of oropharyngeal or hypopharyngeal squamous cell carcinoma (OHSCC) patients treated with chemoradiation.

MATERIALS AND METHODS: Between November, 2009 and August, 2013, patients with untreated OHSCC scheduled for chemoradiation were eligible for this study. DCE-PWI and DWI were performed in addition to conventional MRI. The relationship of neck control with the following clinical and imaging variables was analyzed: the hemoglobin level, N-stage, primary tumor location, gross volume of neck metastatic nodes,



ORAL PRESENTATIONS ABSTRACTS

maximum standardized uptake value, metabolic tumor volume and total lesion glycolysis on FDG PET/CT, transfer constant (Ktrans), volume of blood plasma and volume of extracellular extravascular space (Ve) on DCE-PWI, and apparent diffusion coefficient on DWI of the neck metastatic nodes. The patients were also divided into a neck control group and a neck failure group, and their clinical and imaging parameters were compared.

RESULTS: There were 69 patients (37 with oropharynx SCC and 32 with hypopharynx SCC) with successful pretreatment DCE-PWI and DWI available for analysis. After a median follow-up of 17 months, 25 (36.2%) participants had neck failure, whereas the remaining 44 (63.8%) patients achieved neck control. Logistic Regression analysis revealed that only the Ktrans and Ve values were significantly associated with 2-year neck control (P = 0.02, P = 0.001 respectively). When the neck control and neck failure groups were compared, significant differences were observed in Ktrans and the Ve (P = 0.02 and P = 0.001, respectively).

CONCLUSION: In OHSCC patients treated with chemoradiation, pretreatment Ktrans and Ve derived from DCE-PWI of neck lymph nodes were the predictors of neck control, while all the DWI and PET parameters were not.

O060-Optimization of Double Inversion Recovery Contrast for Squamous Cell Carcinoma of the Neck

Mariah H. Bashir¹, Kwan-Jin Jung¹, *Robert J. Bert*¹

*Univ. of Louisville Radiology Louisville-United States*¹

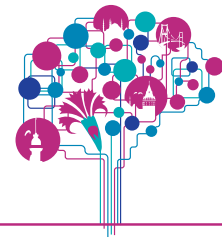
INTRODUCTION: Double Inversion Recovery (DIR) can null both water and another tissue component (fat, muscle, etc) and might better define tumor boundaries than T2 TSE or STIR for oral-pharyngeal squamous cell carcinoma (OPSCCa). We are testing DIR for this purpose.

MATERIALS AND METHODS: The palatine tonsils were chosen as a surrogate for OPSCCa. The formula for DIR ($tia = tib - t1csf * \log(0.5 * (1 - (1 - \exp(-tib/t1csf))) / \exp(-tib/t1csf))$) was developed within commercial software (Matlab, version 2013b) to determine the short inversion times that might optimize tonsillar/OPSCCa imaging. A table of target tissues with known T1 values was created for the formula independent variables. The long inversion time (TIa) was calculated to null water, using the established water T1 value (4163msec) to reduce free water signal. The input T1 for calculating the output (short) TI (TIb) was varied from fat (371msec) to striated muscle (898msec). Comparing TI values of non-nulled tissues (fat, muscle, tonsil) provided contrast estimates. A 3D DIR commercial sequence (3T MAGNETOM Skyra, Siemens Healthcare USA, Malvern, PA) then tested these parameters. Scan time was limited to 6 min. and TR, TE adjusted empirically for T2 contrast.

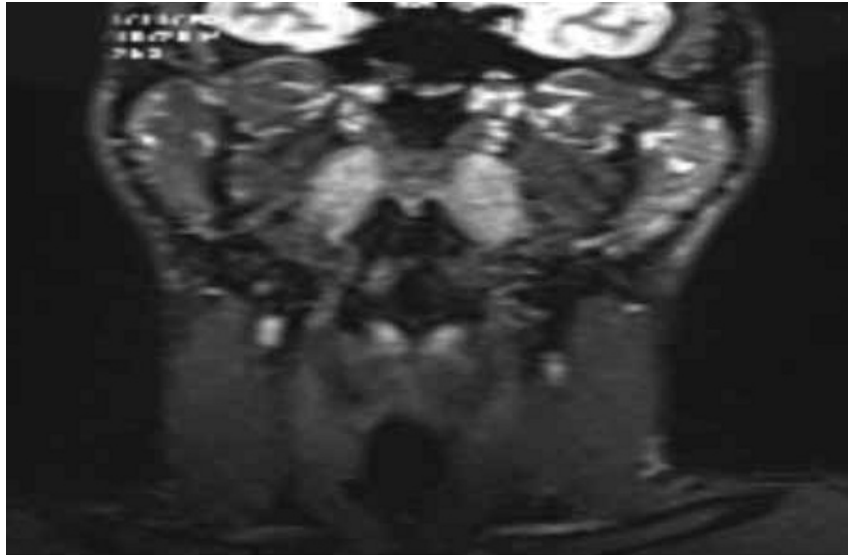
Images were visually inspected by two trained neuroradiologists and an MR physicist for overall utility. **RESULTS:** Preliminary image with the following parameters is shown: (slice thickness = 1.4mm/TR = 5000ms/TE = 202ms/TIa = 3300ms/TIb = 300ms/NSA = 2/Echotrain = 193/bandwidth = 870/FA = 120.

Resulting signal ratios: 10.1 tonsil/fat, 2.76 tonsil/muscle, 3.74 LN/muscle, 13.65 LN/fat. Tonsils are surrounded by muscle, so contrast might be further adjusted for more muscle suppression. Some signal in boundary tissues was preferred for maintaining anatomic positional information.

CONCLUSIONS: DIR shows promise for visualizing OPSCCa, providing excellent tumor definition, reduction in fat signal, fewer artifacts than fat suppression techniques and less edema than STIR or TSE for defining tumor boundaries. Optimizing contrast between tissues with DIR is complex and requires both computational and subjective considerations. We are pursuing more complex modeling, and sequence testing on patients with and without contrast. An update will be provided at the conference.



ORAL PRESENTATIONS ABSTRACTS



O061-Feasibility of Cone Beam Computed Tomography Dacryocystography by Direct Catheterisation of the Lacrimal Drainage System

*Chiara Mabilia*¹, *Zsuzsanna Valyi*², *Luisa Divano*¹

*CHU Brugmann Radiology Brussels-Belgium*¹ *CHU Brugmann Ophthalmology -Belgium*²

PURPOSE: Imaging of the lacrimal system is usually performed by computed tomography dacryocystography (CT-DCG), a technique which combines slice acquisition with contrast filling of the lacrimal drainage system. Cone-Beam Computed Tomography (CBCT) is a relatively new technique, widely used for dental and maxillofacial imaging. It provides high resolution multiplanar images and allows excellent spatial resolution with a relatively low dose of irradiation.

We describe this technique on a NewTom 5G Cone-Beam system to perform CBCT-DCG, in order to assess its feasibility in the evaluation of the lacrimal drainage system.

MATERIALS AND METHODS: In 14 patients with persistent epiphora, we performed CBCT-DCG to assess the patency or the presence of stenosis of the lacrimal drainage system and to determine the level and the etiology of the stenosis. Following a plain acquisition, DCG is performed by catheterization. Manual injection of about 5 ml of diluted water-soluble iodinated contrast (1:1 dilution) is realized. The injection of contrast is stopped when the patient tastes the solution, draining from the nose into the pharynx, which usually occurs within seconds. The injection is also stopped in case of high resistance during injection. The study is performed with the patient supine; acquisition is realized from the roof of the orbit to the hard palate. The data acquired are reformatted into axial, coronal and sagittal planes. In a patient with persistent epiphora and previous surgery and radiotherapy of the right maxillary sinus, CBCT-DCG showed a distal post-radiation stenosis of the lacrimal duct, with lack of contrast drainage into the pharynx (see image).

RESULTS: CB-DCG is indicated in investigating patients with epiphora when the clinical examination suggests a mechanical obstruction. Progression of the contrast medium and the environmental structures are assessed in order to detect congenital or acquired stenosis and to clearly define its level, with the aim to plan treatment.

CONCLUSION: CB-DCG has the potential to become the method of choice in the evaluation of lacrimal drainage system pathology because of its reduced radiation exposure.

This exam allows a very good assessment of the anatomic and pathologic conditions of the lacrimal drainage system and helps in the presurgical planning.



ORAL PRESENTATIONS ABSTRACTS



O062-MR Imaging Features of Pharyngeal Tuberculosis a hint of Discrimination from Pharyngeal Malignancy

*Aleum Lee*¹

*Soonchunhyang University Hospital, Bucheon Radiology Bucheonsi-Korea, South*¹

PURPOSE: To present the MR imaging features of pharyngeal tuberculosis: rare and often mimicking malignancy. And we investigated which MR imaging finding is useful to discriminating from malignancy for reducing unnecessary invasive endoscopic biopsy

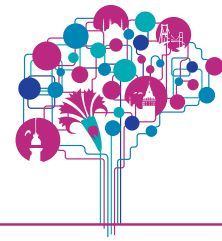
MATERIALS AND METHODS: We investigated MR images of 18 patients (F:M =15:3; age range, 24~75) among 20 consecutive patients with histopathologically proven nasopharyngeal tuberculosis (NP-TB) during 12 years (from January 2002 to February 2013). Two patients had a history of

concurrent nasopharyngeal carcinoma (NPC) were excluded. MR images of all patients were retrospectively reviewed. The extent, shape, and signal intensity of the nasopharyngeal lesions were analyzed in a consensus by two neuroradiologists. The pattern of MR imaging were analyzed into 3 groups by mucosal lesion identified: intact mucosa (I), a discrete polypoid mass in the adenoids (II), and infiltrative thickening of the NP wall (III)

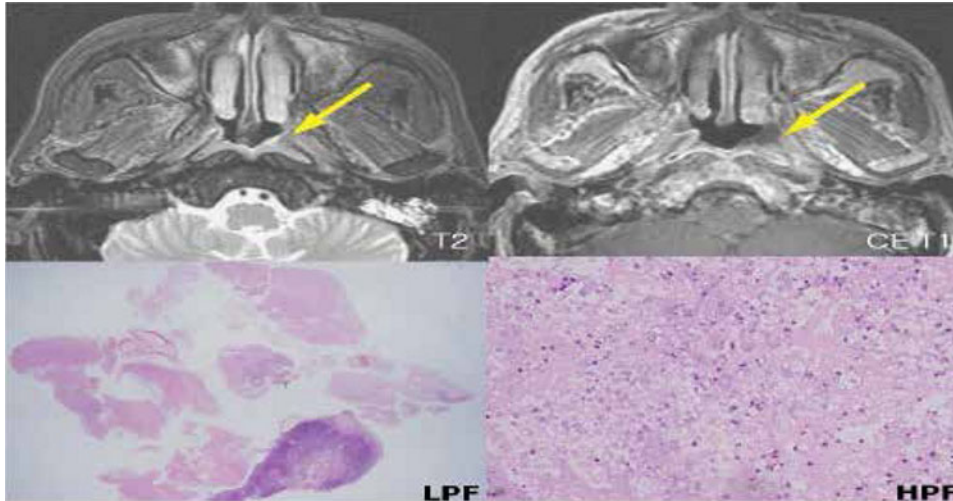
RESULTS: The shape of the NP mucosa was intact mucosa (I) in 4 (22.2%), a discrete polypoid mass in 2 (11.1%) and infiltrative wall thickening (III) in 12 (66.7%) patients. The lesions of NP-TB confined within the pharyngeal mucosal space in 14 (77.7%) and extended to the skull base in 4 (22.2%) patients. Only two cases of TB has revealed extension outside the walls of the nasopharynx, and no case of TB has revealed deep extension into the parapharyngeal fat, nasal cavity, oropharynx, skull base, or cranium.

All lesions of NP-TB showed intermediate T1, T2 SI and strong enhancement. Characteristically, all lesions had irregular surfaces and T2 bright signal intensity mucosal lesions, considered as ulceration on clinico-radiological correlation. Pulmonary tuberculosis was identified by an abnormal chest radiograph in 8 of 18 cases (44.4%). The most common presenting symptom was cervical lymphadenopathy in 10 (55.5%) patients. There were also mastoid effusion in 6 (33.3%), the denervation atrophy of the 12th cranial nerve in one case on MR images.

CONCLUSIONS: The differential diagnosis of NP-TB from carcinoma is difficult. In polypoid mass pattern, usually lesions are confined to nasopharyngeal mucosa and in infiltrative wall thickening pattern, ulcerative mucosal lesion with linear T2 bright SI are common. These MR features may be helpful for differentiating NP-TB from malignancy.



ORAL PRESENTATIONS ABSTRACTS



O063-Loss of Reflex Tearing after Maxillary Orthognathic Surgery

*Aleum Lee*¹

*Soonchunhyang University Hospital, Bucheon Radiology Bucheonsi-Korea, South*¹

BACKGROUND: Few reports have described the ophthalmic complications that occur after maxillary orthognathic surgery. Since cases of decreased reflex tearing after maxillary orthognathic surgery are extremely rare, we describe 2 cases of loss of reflex tearing after maxillary orthognathic surgery. **Case presentation:** The patients who were 18-year-old and 32-year-old Asian women suffered from unilateral dryness and irritation caused by maxillary orthognathic surgery. In both patients, Schirmer's test (II) showed reduced reflex tearing in 1 eye. Computed tomography showed that the pterygoid plate had been fractured in both patients.

CONCLUSIONS: The location of the pterygopalatine ganglion and its associated fibers in the pterygopalatine fossa may be injured during Le Fort osteotomy.

O064-Skull Base Re Ossification after Endovascular Treatment of Intracranial Vascular Lesions

*Amel Azizi*¹, *Elisa Pomerio*¹, *Katia Gete*¹, *Michel Runge*², *Alessandra Biondi*¹

*Besançon University Hospital Neuroradiology and Endovascular Therapy Besançon-France*¹ *Besançon University Hospital Musculoskeletal Radiology -France*²

PURPOSE: Cataclysmic epistaxis is a rare but potentially fatal complication in giant/large (G/L) intracranial aneurysms. Most of the lesions are located in the carotid siphon. This complication occurs secondary to erosion of the adjacent sphenoid wall and rupture of the aneurysm sac in the sinus. In case of bone erosion, ENT procedures can also be responsible for aneurysm rupture. The purpose of our study was to evaluate the re-ossification of the skull base on CT follow-up after endovascular treatment of G/L intracranial aneurysms. To our knowledge, these findings have never been previously reported. **MATERIALS AND METHODS:** Thirty-two out of 62 patients (25 females-7 males; mean age: 54 years) treated for a G/L intracranial aneurysm presented an erosion of the skull base related to the contiguous aneurysm. The bone erosion was evaluated on pre-treatment CT scan. Twelve out of the 32 patients were treated by occlusion of the parent artery, 8 by coils (with stent-assisted coil placement in 2) and 12 patients with a flow diverter stent. 22/32 patients had a CT follow-up within a time period of 6 -12 months, 4/32 are still under evaluation, 3/32 underwent only MR studies and 3/32 were lost at follow-up. Presence of a re-ossification of bone structure was systematically assessed. The timing



ORAL PRESENTATIONS ABSTRACTS

of the re-ossification was evaluated in relation to the date of the interventional procedure and the CT findings
RESULTS: On angiographic follow-up, all the patients presented exclusion or a significant shrinkage of the aneurysm. Densification of the sinus bone adjacent to the aneurysm sac, corresponding to a re-ossification of the sphenoid sinus wall, was observed at CT in 22/32 patients after aneurysm treatment independently of the endovascular technique used. Statistical analysis of the results is still in progress. CONCLUSION: In most of cases re-ossification of the previously eroded skull base is observed at 1 year CT imaging follow-up after endovascular treatment of intracranial aneurysms. Persistent bone erosion is correlated to persistent aneurysm patency and pulsatility.

O065-Diffusivity of Extraocular Muscles in Patients with Thyroid Associated Ophthalmopathy Comparison with Conventional MRI

*Akio Hiwatashi*¹, *Osamu Togao*¹, *Koji Yamashita*¹, *Kazufumi Kikuchi*¹, *Hiroshi Honda*¹
*Kyushu University Clinical Radiology Fukuoka-Japan*¹

PURPOSE: Three-dimensional (3D) turbo field echo with diffusion-sensitized driven-equilibrium (DSDE-TFE) preparation obtains diffusion-weighted images with higher spatial resolution and less susceptibility artifacts compared to echo planar imaging. The purpose of this study was to evaluate feasibility of DSDE-TFE to evaluate extraocular muscles in patients with Basedow's ophthalmopathy. MATERIALS AND METHODS: This retrospective study was approved by our institutional review boards, and written informed consent was waived. 23 patients with thyroid associated ophthalmopathy (17 females and 6 males; age range 26–83 year old; median 57 year) were studied. All patients underwent MR imaging with a 3.0-T system with an 8-channel head coil. For DSDE-TFE, motion probing gradients were conducted at one direction with b-values of 0 and 500 s/mm²[SUP]2[/SUP]. The other imaging parameters were as follows: TR/TE = 6.2/3.0 ms, FA = 10°, ETL = 75, FOV = 240 mm, voxel size = 1.5×1.5×1.5 mm³, NEX = 2, and acquisition time = 5 min 22 s. Additionally, T1WI, fat suppressed T2WI, and fat suppressed postcontrast T1WI were also obtained. The apparent diffusion coefficients (ADCs) of extraocular muscles were measured on coronal reformatted images. Signal intensity on T1WI, fat suppressed T2WI, and postcontrast T1WI compared to normal-appearing white matter, and cross sectional areas of the muscles also measured. Clinical activity score (CAS) was also evaluated. Statistical analyses were performed with Pearson correlation coefficients, linear regression analysis and Mann-Whitney U test. A p-value less than 0.05 was considered significant.

RESULTS: Extraocular muscles were clearly visualized on DSDE-TFE. On DSDE-TFE, the average ADCs of the extraocular muscles in each orbit ranged from 1.30 ×10³ mm²/s to 3.22×10⁻³ mm²/s (mean ± SD; 2.23 ± 0.42×10⁻³mm²/s). There were statistically significant correlation between ADC with size of the muscles (r = 0.58, p < 0.001). There were no statistically significant correlation with ADC and signal intensity on conventional MRI and CAS.

CONCLUSION: With its insensitivity to field inhomogeneity and high spatial resolution, the 3D DSDE-TFE technique enabled us to assess diffusivity in extraocular muscles of thyroid associated ophthalmopathy.

PARALLEL SCIENTIFIC PAPER PRESENTATIONS

(Head and Neck 2) 17:15 - 19:00

Topkapı B Hall

O066-Differential Diagnosis of Inflammatory Pseudotumor and Carcinoma of the Nasopharynx Value of Conventional T2 Weighed Image based on the Lesion Conspicuity

*Hye Na Jung*¹, *Hyung-Jin Kim*¹, *Yi-Kyung Kim*¹, *Mina Song*¹, *Jihoon Cha*¹, *Sung Tae Kim*¹
*Samsung Medical Center, Sungkyunkwan University School of Medicine Radiology Seoul-Korea, South*¹

PURPOSE: It is difficult to distinguish nasopharyngeal inflammatory pseudotumor (NIPT) from nasopharyngeal carcinoma (NPC) on MR imaging, because both lesions can infiltrate the adjacent structures. In our practice, conventional T2-weighted image (WI) helps make differentiation between these



ORAL PRESENTATIONS ABSTRACTS

two conditions, because NIPT tends to become smaller on T2-WI than on T1-WI, compared to NPC. The purpose of this study is to evaluate the value of conventional T2-weighted imaging for the differentiation between NIPT and NPC.

MATERIALS AND METHODS: We retrospectively reviewed MR imaging findings of 14 patients with histologically proved IPTs from January 1997 to December 2012. MR imaging of 18 patients with NPCs in T4 stage between January 2006 and December 2012 were also evaluated. All subjects underwent MRI of the nasopharynx before treatment. We measured the area of the lesion by placing the largest possible polygonal region of interest within the lesion, which was seen to be the largest on axial contrast enhanced (CE) T1-WI, and obtained the area on CET1-WI (ACET1). The areas of the lesion on T1- and T2-WIs (AT1 and AT2, respectively) were measured on the corresponding images in the same manner. From measurement, we calculated T1 and T2 area ratios (ARs), which were determined as AT1/ACET1 and AT2/ACET1, respectively. We compared T1 and T2 ARs between NIPTs and NPCs using a Mann-Whitney test for statistical analysis.

RESULTS: The values of T2 AR were 0.50 ± 0.22 mm² for IPTs and 0.89 ± 0.14 mm² for NPCs, respectively, which was statistically significant between the two groups ($P < .001$). In contrast, the values of T1 AR were 1.14 ± 0.34 mm² for IPTs and 0.98 ± 0.14 mm² for NPCs, which was statistically insignificant between the two groups ($P = .15$).

CONCLUSIONS: Compared to NPC, NIPT seems to become smaller in area on T2-WI than on T1-WI with and without contrast enhancement. The lesion conspicuity on T2-WI may be useful to differentiate between NIPT and NPC.

O067-Head and Neck Paragangliomas and the Jugular Vein

Emanuele Orru 1, Merve GURSOY 1, Philippe Gailloud 2, Ari M Blitz 1, John P Carey 3, Alessandro Olivi 4, *David M Yousem 1*

Johns Hopkins Medical Institution Neuroradiology -United States 1 Johns Hopkins Medical Institution Interventional Neuroradiology -United States 2 Johns Hopkins Medical Institution Otolaryngology -United States 3 Johns Hopkins Medical Institution Neurosurgery -United States 4

BACKGROUND and PURPOSE: Head and neck paragangliomas are tumors that show a variable tendency to invade the jugular vein. The aim of this study was to assess the rate of jugular vein invasion by these tumors and to determine if this feature is specific only for glomus jugulare tumors. The accuracy of CT, MRI and DSA in detecting this feature was compared.

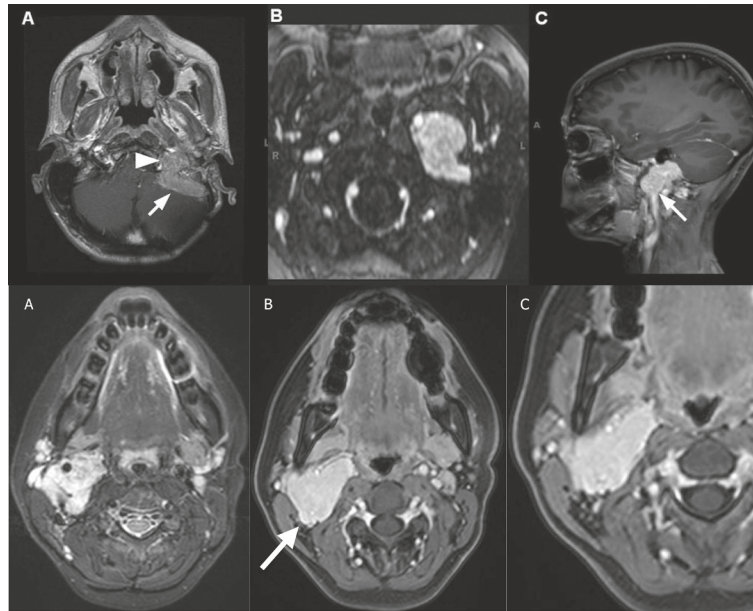
MATERIALS and METHODS: The neuroradiology studies of patients who underwent surgical resection for pathology proven head and neck paragangliomas in the past 5 years were retrospectively evaluated for signs of jugular vein invasion. Imaging findings were compared with the surgical reports for definitive proof of vessel invasion. Data were processed to determine the rate of jugular vein invasion by the different subtypes of tumors and the specificity, sensitivity and accuracy of each modality in predicting such invasion.

RESULTS: Twenty-four tumors were found in 22 patients. Eleven (45.8%) were glomus jugulare, 8 (33.3%) were carotid body tumors, 5 (20.8%) were glomus vagale. Jugular vein invasion was surgically proven in 100% of glomus jugulare, 60% (3/5) of the glomus vagales and 25% (2/8) of the carotid body tumors. Accuracy rates for MRI (92.3%), CT (92.3%) and DSA (94.1%) in detecting the feature were comparable.

CONCLUSIONS: Jugular vein invasion is characteristic of glomus jugulare tumors, but can be present to a lesser extent in glomus vagale and carotid body tumors, and is not specific to glomus jugulares. All the currently available imaging modalities show high accuracy in detecting tumoral invasion of the vein.



ORAL PRESENTATIONS ABSTRACTS



O068-The Role of Diffusion Weighted Magnetic Resonance Imaging in Differentiation of Parotid Gland Masses With Histopathological Correlation

Yasemin Karaman¹, *Anil Ozgur*², Demir Apaydin², Cengiz Ozcan³, Rabia Arpacı⁴, Meltem Nass Duce²
*Antalya Education and Research Hospital Radiology -Turkey*¹ *Mersin University Radiology Mersin-Turkey*²
*Mersin University Otorhinolaryngology -Turkey*³ *Mersin University Pathology -Turkey*⁴

PURPOSE: The aim of this study is to assess the diagnostic efficacy of magnetic resonance diffusion-weighted imaging (DWI) in the characterization of parotid gland tumors.

MATERIALS AND METHODS: Thirty-six patients, who were referred our department with a prediagnosis of parotid mass between 2011 March-2012 March, were included in the study. A total of 41 lesions were analyzed with magnetic resonance imaging (MRI). On DWI, the images were obtained with using three different b values (100, 500 and 1000 sec/mm²). Apparent diffusion coefficient (ADC) maps were created for each group. Mean ADC values were calculated, according to the histopathologic subtypes. The final diagnosis was made by fine-needle aspiration cytology (FNAC) after MRI/DWI or by histopathologic examination performed after surgery. Mean ADC values of benign lesions-malignant lesions, pleomorphic adenoma-Warthin's tumor, pleomorphic adenoma-malignant lesions and Warthin's tumor-malignant lesions were compared.

RESULTS: Among 41 lesions, 32 were benign, 9 were malignant. The most common benign and malignant tumor was pleomorphic adenoma and lymphoma, respectively. While the highest ADC value belonged to hemangioma (3.127×10^{-3} mm²/sec) and pleomorphic adenoma (1.876×10^{-3} mm²/sec), the lowest ADC value belonged to lipoma (0.183×10^{-3} mm²/sec) and lymphoma (0.714×10^{-3} mm²/sec). For comparisons, ADC values obtained with b=500 were used. The mean ADC value of benign lesions was significantly higher than malignant lesions (p=0.004). The mean ADC values of pleomorphic adenoma were significantly higher than Warthin's tumor (p=0.001) and malignant tumors (p=0.001). According to ROC curve analysis, pleomorphic adenoma and Warthin's tumor were distinguished from each other with a 1.5×10^{-3} mm²/sec cut-off point, 84% sensitivity and 93.7% specificity; pleomorphic adenoma and malignant lesions were distinguished from each other with a 1.6×10^{-3} mm²/sec cut-off point, 100% sensitivity and 81.25% specificity. Because the mean ADC values were matched, Warthin's tumor and malignant tumors could not be distinguished.

CONCLUSIONS: The distinction can be made between pleomorphic adenoma-Warthin tumor and pleomorphic adenoma-malignant tumors by using DAC; but DAG is not efficient in the differentiation of Warthin's tumor and malignant tumors. DWI may be a beneficial tool in the lesion characterization, but it is necessary to use DWI in combination with conventional MRI for more accurate results.



ORAL PRESENTATIONS ABSTRACTS

O069-Hypoglossal Canal Invasion by Glomus Jugulare Tumors Clinico Radiological Correlation

Merve Gursoy¹, Emanuele Orru¹, Ari M. Blitz¹, John P. Carey², Alessandro Olivi³, *David M. Yousem*¹

*The Johns Hopkins Medical Institution Division of Neuroradiology, The Russell H. Morgan Department of Radiology and Radiological Science*¹ *The Johns Hopkins Medical Institution Department of Otolaryngology, Head and neck Surgery*² *The Johns Hopkins Medical Institution Department of Neurosurgery*³

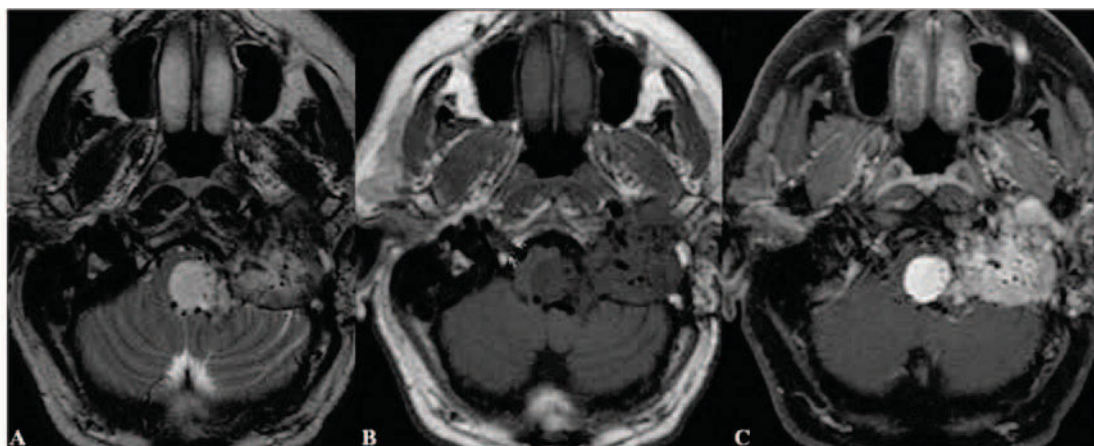
PURPOSE: The aim of this retrospective study is to assess the rate at which glomus jugulare (GJ) tumors invade the hypoglossal canal (HC) and to correlate CT and MRI findings with the clinical evidence of cranial nerve (CN) XII dysfunction.

MATERIALS AND METHODS: Thirty-one patients with a diagnosis of GJ evaluated in the past five years were identified via a radiology information system keyword search. The neuroradiological studies (CT, MRI) and medical data including history, symptoms, and clinical features of all patients with GJs were analyzed. CT and MRI imaging modalities were reviewed by an attending neuroradiologist blinded to the clinical findings for characteristics of the GJ, looking specifically for HC invasion. The HC was said to be invaded when neoplastic tissue spread beyond a wall of the HC, directly invaded it (Fig. 1) or expanded (Fig. 2) or destroyed the canal walls. The specificity, sensitivity and accuracy of each modality in correlating imaging features and clinical findings of hypoglossal nerve involvement were determined.

RESULTS: Thirty-one GJ tumors were identified. Imaging studies identified HC involvement in 22 tumors (71.0%). Thirteen of 31 patients (41.9%) had clinically evident CN XII dysfunction symptoms. All thirteen patients showed HC invasion by imaging but there were an additional 9 GJ tumors, which demonstrated HC invasion by imaging without CN XII symptoms (i.e. imaging false positive). The false positives were defined as imaging positive, clinical negative. Accuracy rates for MRI 76.7% (23/30) and CT 78.6% (11/14) in predicting such dysfunction were comparable.

CONCLUSION: Imaging findings of invasion on MRI and CT correlate well (76.7-78.5%) with clinical findings of hypoglossal nerve dysfunction. This pathway of spread must be carefully addressed at the time of surgery for eradication of the tumor as well as to ensure that inadvertent intraoperative damage to the hypoglossal nerve does not occur. Furthermore, relying just on clinical symptoms to suggest whether or not the hypoglossal canal is invaded at imaging is not reliable.

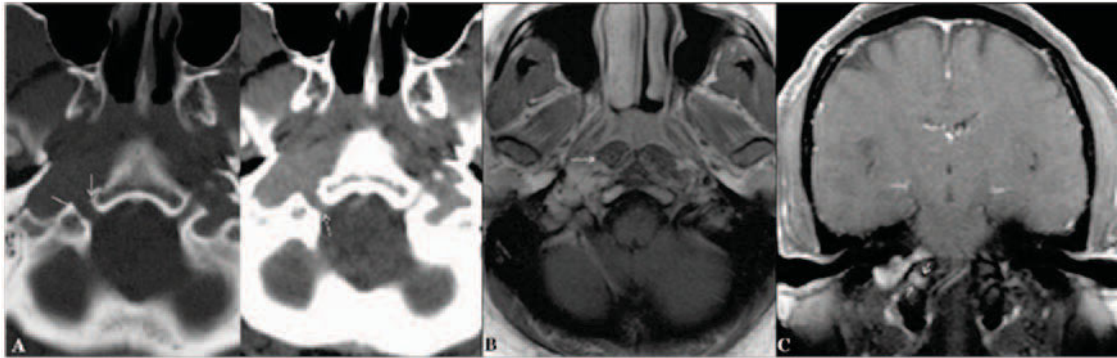
Figure 1





ORAL PRESENTATIONS ABSTRACTS

Figure 2



O070-Diffusion Weighted MR Imaging in Lymph Node Metastases of Squamous Cell Carcinoma

*Yeliz Pekcevik*¹, Ibrahim Cukurova², Ilker Burak Arslan²

*Izmir Tepecik Training and Research Hospital Radiology Izmir-Turkey*¹ *Izmir Tepecik Training and Research Hospital Head and Neck Surgery -Turkey*²

PURPOSE: We aim to compare apparent diffusion coefficient (ADC) values of nodal metastases in head and neck squamous cell carcinoma (SCC).

MATERIALS AND METHODS: Ethics committee approval and informed consent were obtained. Patients with nodal metastases underwent 1.5-T MR imaging, including diffusion weighted echo planar imaging performed with b values of 0 and 1000 s/mm². ADC values of the histologically proven nodal metastases (1 cm or greater in short-axis diameter) of head and neck SCC retrospectively evaluated. A region of interest was drawn around the malignant node on ADC maps. Mean ADC values were compared using Kruskal-Wallis test. Receiver operating characteristic analysis was employed to investigate whether ADC-based differentiation is possible among squamous cell carcinomas depends on their histologic characteristics.

RESULTS: Twenty-seven patients (24 men, three women; mean age, 60.7 years) with 42 nodes underwent imaging. Mean ADC values for nodal metastases of the nasopharyngeal carcinoma (n:15), oropharyngeal carcinoma (n:12), laryngeal carcinoma (n:10) and hypopharyngeal carcinoma (n:5) were $(0.710 \pm 0.160$ [standard deviation] $\times 10^{-3}$ mm²/s, $(0.960 \pm 0.190) \times 10^{-3}$ mm²/s, $(0.900 \pm 0.250) \times 10^{-3}$ mm²/s, and $(1.060 \pm 0.150) \times 10^{-3}$ mm²/s, respectively. Significant differences were found between the nasopharyngeal and other SCC metastases. There were no significant differences among the other groups. By selecting 0.850×10^{-3} mm²/s as an ADC threshold value, we can differentiate nasopharyngeal carcinoma metastases from other carcinomas metastases with sensitivity of 80% and specificity of 85% (area under the curve, 0.890).

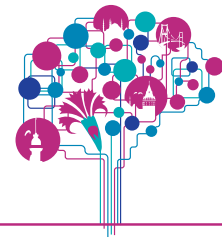
CONCLUSION: The present study demonstrates that ADC values of the nodal metastases in head and neck SCCs are similar other than the nasopharyngeal carcinoma. Diffusion weighted imaging may help distinguish nasopharyngeal carcinoma metastases from other SCC metastases.

O071-Anaplastic Thyroid Carcinoma What Radiologists Need to Know in an Unfamiliar Entity in Lethal Neoplasm

*Aleum Lee*¹

*Soonchunhyang University Bucheon Radiology Bucheonsi-Korea, South*¹

PURPOSE: Anaplastic thyroid carcinoma (ATC) is a rare disease, but leading cause of thyroid cancer mortality. There have been few large studies of ATC and imaging finding is not well known. The purpose of this study was to identify characteristic features of the ATC on ultrasound (US) and computed tomography (CT) images and to establish the US and CT criteria for differentiating ATC from other thyroid masses.



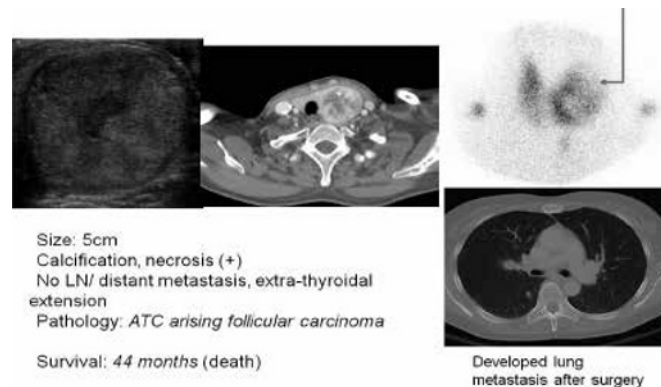
ORAL PRESENTATIONS ABSTRACTS

To determine the features that would serve as a useful predictor of prognosis of ATC. MATERIALS AND METHODS: We reviewed imaging and medical records of 50 patients diagnosed with ATC from May 1994 to March 2013 at two university hospitals.

The US and CT images were analyzed according to the following parameters: size, margin (well defined or ill defined), composition (cystic, mixed, or solid), mean attenuation value on CT, ratio of attenuation of the mass to that of the adjacent muscle (M/m attenuation ratio) on CT, echogenicity on US, presence of necrosis or calcification (stippled or nodular) of the thyroid mass; and tumor-spreading patterns including the presence of surrounding normal thyroid tissue in the involved lobe, involvement of the contralateral thyroid lobe, extension into the adjacent structures, and cervical lymphadenopathy. The following clinical data were collected: sex, age of the patient, treatment, pathologic subgroup (pure ATC, ATC arising from papillary carcinoma, and focal anaplastic change), and the survival duration. Diagnosis of ATC was confirmed by histopathological examination in 38 patients and cytopathological examination in 12. Statistical analysis was performed using univariate/multivariate analysis and Kaplan–Meier survival curve.

RESULTS: The mean age of the patients at diagnosis was 69 years. ATC appeared as a large mass (average size: 4.3 cm) accompanied by necrosis in 32 cases (64.0%), calcification in 41 (82.0%), direct invasion into the adjacent organs in 37 (74.0%), and cervical LN metastasis in 33 (66.0%). The median overall survival was 6.5 months (95% confidence interval, 6.0–8.6). Multi-variant analysis identified the patient's age ($p = 0.004$), tumor size ($p = 0.011$), LN metastasis ($p = 0.001$), and pure ATC on pathology ($p = 0.016$) as significant predictors of poor prognosis.

CONCLUSION: Radiologists should be familiar with the clinical manifestations, characteristic imaging findings, and their prognostic factors for appropriate diagnosis of ATC.



O072-An Exploratory Pilot Study into the Correlation of MRI Perfusion Diffusion Parameters and 18F FDG PET Metabolic Parameters in Primary Head and Neck Cancer

*Jin Wook Choi*¹, Miran Han¹, Sun Yong Kim¹
*Ajou Medical Center Radiology Suwon-Korea, South*¹

PURPOSE: Microcirculation, cellularity and glucose metabolism may have relationship or affect each other in the same tumor. The understanding of their relationship could contribute to the field of oncologic imaging such as tumor characterization, guidance for treatment planning, early prediction of treatment responses and evaluation of treatment outcome. In this study, we investigated the relationships between tumor metabolism determined by 18FDG positron emission tomography, tumor microcirculation determined by dynamic contrast enhanced MRI, and tumor cellularity determined by diffusion MRI in patients with primary head and neck cancer.

MATERIALS AND METHODS: We included 14 patients (13 men, 1 women; mean age, 62.64 years \pm 13.79 [SD]) with histopathologically proven head and neck cancer, who underwent DCE-MRI, DWI (b values; 0 and



ORAL PRESENTATIONS ABSTRACTS

1000 seconds/mm²) and 18FDG PET before treatment. The mean time interval between MRI and 18FDG PET/CT was 3.5 days (range: 0~14 days). The perfusion parameters (K_{trans} , K_{ep} , V_e , V_p , AUC) from DCE-MRI and apparent diffusion coefficient (Mean ADC [ADC_{mean}] and minimum ADC [ADC_{min}]) values from DWI were evaluated within the manually

placed polygonal region of interest plotted around the main tumor on every image slice. Necrotic area and large feeding vessels are excluded from ROI. Maximum SUV (SUV_{max}) was measured for the entire tumor region of interest. Mean SUV (SUV_{mean}) and total lesion glycolysis (TLG = SUV_{mean} x tumor volume) were calculated with the margin thresholds as 40%. Data normality was tested by the Kolmogorov-Smirnov test. Comparisons were made by using Pearson correlation.

RESULTS: Averaged values of DCE-MRI, DWI and 18FDG PET parameters are summarized in Table 1. Significant correlations were shown between K_{trans} and TLG ($r=0.609$), V_e and TLG ($r=0.575$), AUC and TLG ($r=0.635$), ADC_{min} and TLG ($r=-0.604$), and ADC_{mean} and V_p ($r=0.541$).
CONCLUSION: This study demonstrated the correlation between tumor microcirculation, cellularity and glucose metabolism using DCE-MRI, DWI and FDG-PET which based on different mechanism. This relationship is complex and each diagnostic technique may provide complementary information for the tumor biology.

Table 1. The averaged values of DCE-MRI, DWI and ¹⁸F₂FDG PET parameters in the tumor sites

Quantitative parameters	Averaged value
K_{trans} (min ⁻¹)	1.26 ± 0.63
K_{ep} (min ⁻¹)	3.59 ± 1.25
V_e	0.45 ± 0.25
V_p	0.12 ± 0.03
AUC	0.39 ± 0.15
ADC _{mean} (x10 ⁻³ mm ² /s)	0.88 ± 0.18
ADC _{min} (x10 ⁻³ mm ² /s)	0.31 ± 0.20
SUV _{max}	12.18 ± 3.74
SUV _{mean}	6.72 ± 1.29
TLG (g)	124.5 ± 126.7

Data are expressed as mean ± standard deviation

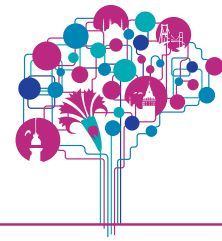
O073-Oropharyngeal Squamous Cell Carcinomas; Can Imaging Findings Predict HPV Status

Sandeep Bhuta¹, Louise Van Camp², Tim Ireland³

Gold Coast University Hospital, School of Medicine, Griffith University Medical Imaging Gold Coast-Australia¹

Gold Coast University Hospital Medical Imaging -Australia², Gold Coast University Hospital Biomedical Technology -Australia³

PURPOSE: To describe imaging characteristics of the primary tumor and metastatic neck lymphadenopathy in oropharyngeal cancers and to assess its utility in predicting HPV status of the patient.
MATERIALS AND METHODS: Retrospective review of patients (from February 2012 to 2014) with Oropharyngeal cancer referred to specialist head and neck clinic and confirmed p16 status was performed. Pretreatment staging CT were reviewed by sub specialty trained Head and Neck Radiologist and Fellow. Imaging protocol consisted of post contrast CT and MRI of neck on a 128 slice CT and 1.5/3.0 T MR Systems. Abnormal lymph nodes were assessed for size, shape, number. Node features like smooth or irregular enhancement, low density cystic nature, Hounsfield Unit (HU) value were noted. Primary was assessed for HU value and enhancement characteristics. Correlation was made between the clinical and imaging features of HPV positive and negative tumours.



ORAL PRESENTATIONS ABSTRACTS

RESULTS: 77 patients were included in the study. The youngest patient (33Y) was in the HPV+ group and the oldest (88Y) was HPV-. The majority of cases were males (16 F and 61 M). Patients with HPV+ had smaller primary tumours and lymph nodes were large (mean 21.5mm p value 0.03) bilateral, homogeneous, and cystic (mean 30HU, p value 0.001) with smooth thin well defined wall and rim enhancement. HPV -ve primaries were large (mean 35.8mm p value 0.03) with no significant difference in HU value between two groups. HPV - nodes were unilateral and smaller with necrosis and higher HU (mean 54.6HU p value 0.001)

CONCLUSION: Imaging features of p16 positive metastatic neck nodes (Intranodal cystic change) from oropharyngeal primaries are unique and characteristic. This finding enables to differentiate HPV + or - nodes and may predict the patients p16 status based on Imaging. This radiologic signature can be used as an adjunct to existing molecular tests and needs larger studies for establishing specific imaging criteria.

O074-Hypopharyngeal Cancer Preoperative Imaging and Pathological Staging Correlation.

*Yueh-hsun Lu*¹, Jiing-Feng Lirng², Chan-Ming Yang¹, Feng-Chi Chang², Wang-Yuo Guo²

*Taipei City Hospital Zhong-Xing Branch Radiology Taipei-Taiwan*¹ *Taipei Veterans General Hospital Radiology -Taiwan*²

INTRODUCTION: Hypopharyngeal cancer is more common in eastern than western world. The incidence in Taiwan is also high. It may be related to betel nuts and smoking. We compared pretreatment imaging staging and final pathological staging and study for the differences.

MATERIALS AND METHODS: From 2008 to 2014, there were 351 patients diagnosed as hypopharyngeal cancer by endoscopic biopsy or surgical resection. Pretreatment image studies included CT, MRI or both studies. 153 cases had received surgical resection and are included. Among these patients, 107 cases receive contrast enhanced (CE) CT study and 46 cases receive CE MRI study. The pretreatment original tumor invasion area and lymph nodes involvement were recorded and compared with final operation pathological staging.

RESULTS: 143 cases are male (93.5%). The final pathological diagnosis of original tumor involvement in CT and MRI is T1 and in situ: 8 and 2, T2: 23 and 6, T3: 28 and 9, T4: 48 and 29; lymph nodes is N0: 28 and 6, N1: 25 and 11, N2: 52 and 27, N3: 4 and 2. The overall correct diagnostic rate of T is higher in MRI group (42/46, 91.30%) then CT group (79/104, 75.96%) (p < 0.01). Underestimation is the most common mismatch cause in original tumor invasion. Failure to detect invasion of thyroid cartilage is the main cause of underestimation of staging. In evaluation of nodal involvement, the correct diagnostic rate in CT is 75.96% (79/104) and 82.60% (38/46) in MRI (p = 0.17). These cases with small sized lymph nodes less than 1cm caused mismatch of image diagnosis and final pathology in staging of lymph nodes.

CONCLUSION: CT and MRI both are important tools for establishing the extent of the primary tumor and the extent of cervical and retropharyngeal lymph nodes metastasis. MRI is superior to CT in evaluation of focal tissue invasion. Correct pretreatment staging can help the precise treatment planning.

O075-Cine CT Guided Biopsy of Clival Uncommon Tumors

*Hector Lambre*¹, Rosana Salvatico¹, Pedro Lylyk²

*ENERI Radiology Buenos Aires-Argentina*¹ *ENERI Neurosurgery -Argentina*²

PURPOSE: To show the utility and safety of freehand Cine CT-guided biopsy of the clivus.

MATERIALS AND METHODS: Three patients were studied with 64 detectors CT helical scans and 1,5 T and 3 T MRI with and without gadolinium.

An 11G and 15G Jamshidi needle were introduced thru nasal cavity and thru the mandibular window using Cine CT-guidance.

RESULTS: Three patients were studied for headaches and facial neuralgia and CT scans were performed followed by MRI. Similar findings were obtained in all patientes as pterygopalatine fossa involvement, para-



ORAL PRESENTATIONS ABSTRACTS

pharyngeal space obliteration and clivus sclerosis.

Once discarded another organ involvement a CT-guided biopsy was conducted.

In one case we use trans-nasal approach and on the other two we use the mandibular sigmoid notch window. Important headaches were seen in the three cases after the procedure but were controlled with non-steroid analgesics.

The first case was an inflammatory pseudotumor of the parapharyngeal space invading the clivus of a 36 y/o woman.

The second case was a primary B cell lymphoma of the clivus on a 65 y/o woman and the third case turned out to be squamous cell carcinoma from the pharynx infiltrating the clivus.

DISCUSSION: Nasopharyngeal carcinoma is the most common primary lesion to involve the skull base, they spread primary by infiltrating the neighboring regions rather than by expansion. The most common clival infiltration from this tumor is a destructive lesion, sclerosis has been described in the past but it is also been found as a bone reaction.

The most common symptoms from clival involvement are orbito-frontal headaches, visual disturbances, ophthalmoplegia and ptosis. Cranial nerves are affected next, usually III, IV, V y VI. The principal cranial nerve involved is the fifth producing numbness and facial pain and the second nerve affected is the sixth causing diplopia.

The MR images give much more information because of the better contrast resolution and sensitivity for soft tissue lesions and bone involvement, the use of contrast can depict clearly muscular infiltration and peri-neural spread.

CONCLUSION: Clival tumors are relatively rare and sometimes appear as solitary and non-characteristic lesions therefore Cine CT-guided biopsy should be considered as a safe and very useful tool for a prompt diagnosis.

O076-Differentiation of Inflammatory Pseudotumor from Lymphoma in the Head and Neck the Usefulness of Dynamic Contrast Enhanced and Diffusion Weighted MR Imaging

*Yi-Kyung Kim*¹, Hyung-Jin Kim¹, Jihoon Cha¹, Ji Young Lee¹, Mina Song¹, Sung Tae Kim¹

Samsung Medical Center, Sungkyunkwan Universtiy School of Medicine Radiology Seoul-Korea, South¹

PURPOSE: The aim of this study was to differentiate inflammatory pseudotumor from lymphoma in the head and neck region by using dynamic contrast enhanced MRI (DCE-MRI) and diffusion-weighted imaging (DWI).

MATERIALS AND METHODS: DCE-MRI and DWI were performed in 22 patients with inflammatory pseudotumor and 10 patients with lymphoma. DCE-MRI parameters (K_{trans}, k_{ep}, v_e, and v_p) and minimum ADC values were compared between two groups. Histogram analysis was conducted to obtain the mean, 25%, 50%, 75% and 95% percentile values of DCE parameters. The diagnostic performances of each parameters were evaluated with ROC curve analysis.

RESULTS: ADC (inflammatory pseudotumor, $0.826 \pm 0.266 \times 10^{-3}$ mm²/sec; lymphoma, $0.433 \pm 0.083 \times 10^{-3}$ mm²/sec), k_{ep} (inflammatory pseudotumor, 0.115 ± 0.073 min⁻¹; lymphoma, 0.170 ± 0.089 min⁻¹), v_e (inflammatory pseudotumor, 0.153 ± 0.062 ; lymphoma, 0.097 ± 0.040) and v_p (inflammatory pseudotumor, 0.027 ± 0.012 ; lymphoma, 0.015 ± 0.012) were significantly different between inflammatory pseudotumor and lymphoma (P<0.001, 0.03, 0.01, 0.03, respectively). On the histogram analysis, 95% percentile of v_e and 50% percentile of k_{ep} showed the most significant difference between groups (both P=0.007). On the ROC curve analysis, ADC (AUC=0.946), 95% percentile of v_e (AUC=0.796) and 50% percentile of k_{ep} (AUC=0.796) showed high accuracy. ADC < 0.52×10^{-3} mm²/sec (90.0% sensitivity, 90.9% specificity), 95% percentile of v_e < 0.17 (90.0% sensitivity, 68.2% specificity) and 50% percentile of k_{ep} > 0.107 (80.0% sensitivity, 81.8% specificity) optimally helped distinguish lymphoma from inflammatory pseudotumor. CONCLUSION: DCE-MRI and DWI were useful to differentiate inflammatory pseudotumor from lymphoma in the head and neck region.

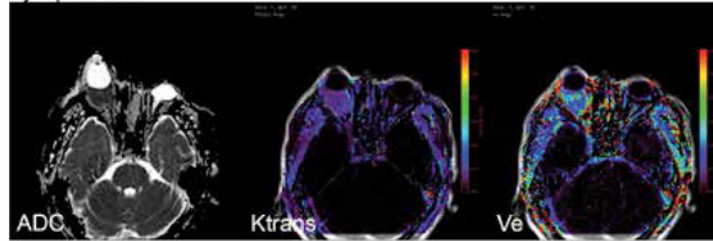


ORAL PRESENTATIONS ABSTRACTS

Inflammatory pseudotumor



Lymphoma



O077-The Pattern of Enhancement of Basal Cell Adenoma and Myoepithelioma of the Parotid Gland at Two Phase CT Comparison with Warthin Tumor

Yi-Kyung Kim¹, Hyung-Jin Kim¹, Ji Young Lee¹, Jihoon Cha¹, Sung Tae Kim¹, Mina Song¹
*Samsung Medical Center, Sungkyunkwan University School of Medicine Radiology Seoul-Korea, South*¹

PURPOSE: Early washout is reported to be a characteristic pattern of enhancement of Warthin tumors (WTs) at two-phase CT. However, our experience is that basal cell adenomas (BCAs) and myoepitheliomas (MEs) also frequently demonstrate the similar pattern of enhancement like WT. The purpose of this study was to verify the enhancement pattern in these tumors at two phase CT. **MATERIALS AND METHODS:** From 2003 to 2013, we retrospectively evaluated two-phase CT examinations of histologically proved BCAs (n=19; 5 men, 14 women; mean age, 62 years) and MEs (n=10; 3 men, 7 women; mean age, 56 years) arising in the parotid gland. CT scans were obtained at early and delayed phases with scanning delays of 40 and 120 seconds, respectively. For comparison, we also assessed two-phase CT scans obtained in patients with histologically proved WT (n=20; 19 men, 1 women; mean age, 55 years). For the qualitative analysis, visual assessment was performed by two radiologists in consensus. For the quantitative analysis, we measured the attenuation values on early and delayed CT scans by placing the largest possible circular region of interest within the same position of the solid component of the tumors. We calculated HU_{early}/HU_{delay} which represents the ratio of the attenuation value at delayed phase scanning to that at early phase scanning. The relative ratio of the attenuation value which was determined by the following equation, $HU_{early}-HU_{delay}/HU_{early}$, was also calculated. Statistical analysis was performed using analysis of variance with post hoc test.

RESULTS: Visually, a washout pattern of enhancement at delayed phase was seen in 14 of 19 BCAs (74%), 7 of 10 MEs (70%), and 20 of 20 WT (100%). The mean HU_{early} and HU_{delay} of BCAs, MEs, and WT were 114.6 and 83.5, 139.8 and 100.2, and 106.4 and 70.8, respectively. No statistical significance was found either in the ratios of the attenuation value or in the relative ratios of the attenuation value among three groups of tumors.

CONCLUSIONS: Most of BCAs and MEs of the parotid gland show a washout pattern of



ORAL PRESENTATIONS ABSTRACTS

enhancement at two-phase CT. The pattern of enhancement of these tumors is similar to that of WTs, which may result in difficulty making the correct preoperative diagnosis on CT scans.

PARALLEL SCIENTIFIC PAPER PRESENTATIONS

(Pediatric NR) 17:15 - 19:00

Halic Hall

O078-Utility of 1H MRS in the Diagnosis and Disease Monitoring for Pediatric CNS Disorders

Noriko Aida¹, Moyoko Tomiyasu², Kumiko Nozawa¹, Yuta Fujii¹, Mikako Enokizono¹
Takayuki Obata², Sumimasa Yamashita³

Kanagawa Children Radiology Yokohama-Japan *1 National Institute of Radiological Sciences Research Center for Charged Particle Therapy -Japan* *2 Kanagawa Children Neurology -Japan* *3*

PURPOSE: To review and illustrate the usefulness of 1H-MRS in the diagnosis and disease monitoring of various pediatric CNS disorders, which were difficult to obtain only at routine MRI. **MATERIALS AND METHODS:** MRI and 1H-MRS were performed on 3T and 1.5T clinical scanners (MAGNETOM Verio and Avanto; Siemens, Erlangen, Germany). The spectra were acquired using single voxel, PRESS sequence with water presaturation with TE/TR 30/5000 and 4 to 32 number of excitations. The acquisition time including simming scan estimated about 5 minutes in each. Spectral data processing including signal quantification was performed using LCModel.

RESULTS: We could make diagnoses of two cases of Creatine transporter deficiency from characteristic spectrum, deficient creatine peaks, and Sojgren-Larsen disease from large elevation of 1.3 ppm lipid peak although these 3 patients had no MRI abnormalities. Quantification of brain metabolites using LCModel revealed abnormal elevation of GABA in an encephalopathic infant leading to the diagnosis of the third reported case of GABA transaminase deficiency in the world. A peak of 0.9 ppm meaning the elevation of branched amino acids confirmed the diagnosis of Maple syrup urine disease in an encephalopathic neonate with brain stem and thalamic restricted diffusion. In addition to the MR findings of cerebellar atrophy and lenticular calcification, reduced choline and myo-inositol peaks leads the diagnosis of Folate transporter deficiency in two siblings. In the latter 3 disorders, changes of their spectral abnormalities well-reflected disease condition from the treatments. Elevation of myo-inositol in the brain stem helped us to diagnose a girl with failure to thrive as the early stage of juvenile Alexander disease. In various mitochondrial disorders (several types of Leigh syndrome, stroke attack of MELAS, Leukoencephalopathy with brainstem and spinal cord involvement and lactate elevation), interesting changes and distribution of elevated lactate peaks which reflected disease conditions were observed. MRSs revealed serial and pathological changes of the metabolites and were helpful in the differential diagnosis of various white matter diseases including X-linked adrenoleukodystrophy, Metachromatic leukodystrophy, Alexander disease, Hypomyelination with atrophy of the basal ganglia and cerebellum, Vanishing white matter disease, and Pelizaeus Merzbacher disease and PMD like diseases.

CONCLUSION: 1H-MRS is a powerful tool not only for the diagnosis but also disease monitoring in pediatric CNS disorders.

O079-Frontometaphyseal Dysplasia Radiology Findings and DDX

Yunus Afandiyev¹

Tusi Imaging Center Radiology Baku-Azerbaijan *1*

Frontometaphyseal dysplasia - X linked recessive congenital syndrome. About 50 cases were reported in literature up to 2009 (known as Gorlin- Cohen and Gorlin-Holt syndromes). We report a familial case of this syndrome in Azerbaijan (father- daughter): Pathognomonic "Mephistophelean face" appearance found in 16 year-old female. About 30 radiologically evident anomalies were found during observation and were documented. CT reveals a malformation of skull base – large foramen magnum, hypoplastic occipital bones,



ORAL PRESENTATIONS ABSTRACTS

hypertrophy of outer and inner lamina and others. Specific calvarial hyperostosis was found. Absence of mastoid bones and anodontia accompanied by skeletal abnormalities - elongation of phalanges, deformities of clavicles and widened scapulae. Genu valgum and tibia recurvatum were found. US diagnosed kidney and uterine congenital abnormalities. The differential diagnosis with diffuse idiopathic hyperostosis, marble bone disease, calvarial bone dysplasia and different systemic craniostenoses as well as and Pyle disease has been provided using the craniofacial X-ray images, MR/CT findings. Various associated neuroradiological and somatic abnormalities, were found and described in the case report. Systemic radiologic approach and assessment are offered for evaluation and differential diagnosis of frontometaphyseal dysplasia syndrome in this oral presentation.

O080-Diffusion Tensor Imaging Based Assessment of White Matter Tracts in Very Preterm Neonates

*Julia Pavaine*¹, Julia Young², Benjamin Morgan², Charles Raybaud¹, Manohar Shroff³, Margot Taylor³
*Hospital for Sick Children, University of Toronto. Diagnostic Imaging Toronto-Canada*¹ *Hospital for Sick Children Diagnostic Imaging -Canada*² *Hospital for Sick Children, University of Toronto Diagnostic Imaging -Canada*³

PURPOSE: In the very preterm brain, white matter is selectively vulnerable to injury as a consequence of germinal matrix/intra-periventricular hemorrhages (GMH/IVH) and punctate lesions, which can result in sensori-motor impairments, and may impact later cognitive outcomes. We assessed white matter development in very preterm (VPT) neonates using diffusion tensor imaging (DTI), targeting two high-risk areas: the posterior limb of the internal capsule (PLIC) and optic radiation (OR). **MATERIALS AND METHODS:** DTI data (15 directions, $b=700\text{m/s}^2$) were obtained from 91 VPT neonates within two weeks of birth, 28.8 weeks mean gestational age (GA), using a 1.5T GE MR system. DTI data were non-linearly registered onto a cohort-generated template created using high-resolution T2 volumes acquired for each subject (Lerch et al., 2011). Bilateral PLIC and OR tracts were manually traced onto the template and transformed back to each infant's scan to obtain subject-specific regions of interest (ROIs). Mean fractional anisotropy (FA) values were then calculated within each ROI for each subject. Infants were grouped for presence and severity of GMH and white matter injury (Miller et al., 2003) into three groups: no injury, mild/moderate injury, and severe injury. Linear regressions were performed between GA and FA for each tract. Analyses of covariance were performed between groups and FA, while controlling for sex and GA.

RESULTS: FA was highly associated with GA at scan bilaterally in the PLIC ($p<0.001$ for both) and left and right optic radiation ($p=0.004$ and $p=0.025$, respectively). Thirty-seven neonates experienced mild/moderate injury and 13 had severe injury. Analyses revealed a significant difference between groups in the left PLIC ($F(2,86)=5.414$, $p=0.006$). Post-hoc tests confirmed that this effect was driven by the severely injured group having the lowest FA compared to those with no injury and mild/moderate injury ($F(1,50)=11.035$, $p=0.002$ and $F(1,46)=5.829$, $p=0.020$, respectively). No other significant results between groups were found in the right PLIC or bilateral optic radiation. **CONCLUSIONS:** DTI data provide better understanding of the VPT brain's response to injury. Severe injury demonstrated the lowest FA in the left PLIC, affecting descending motor pathways. In contrast, the OR was unaffected by injury shortly after birth, which may be evidence for a protracted response to injury compared to the PLIC.

O081-Ischemia a Potential Cause for Pineal Cyst Development

*Evrin Ozmen*¹, Yasemin Kayadibi¹, Betul Derinkuyu², Cesur Samanci¹, Havva Akmaz Unlu², Tulin Hakan Demirkan², Zehra Isil Hasioglu¹, Ibrahim Adaletli¹, Sebuhan Kurugoglu¹
*Istanbul University Cerrahpasa Medical Faculty Radiology Istanbul-Turkey*¹ *Ankara Pediatric And Pediatric Hematology Oncology Training And Research Hospital Radiology -Turkey*²

PURPOSE: Pineal cysts are common incidental findings at magnetic resonance (MR) examinations especially after the improvement of imaging techniques. The etiology of pineal cyst development is still not clear. Herein we investigated whether there is an association between ischemia and pineal cyst prevalence.



ORAL PRESENTATIONS ABSTRACTS

MATERIALS AND METHODS: The magnetic resonance images and clinical data of 201 patients with periventricular leukomalacia (110 female, 91 male; between the age of 0-18 years with the mean age of 7.15 years) and 1295 patients (690 female, 605 male; between the age of 0-18 years with the mean age of 7.7 years) who did not have any evidence of periventricular leukomalacia were evaluated by two radiologists independently. Differences between patients who had periventricular leukomalacia and controls were examined by using Pearson chi square test for the presence or absence of pineal cyst. A p value less than 0.05 was considered as statistically significant.

RESULTS: Pineal cysts were detected in 32.34% (65/201) of study patients while those were detected only in 6.49% (84/1295) of control group ($p < 0.001$). The patients with periventricular leukomalacia were more likely to have pineal cyst (Odds ratio 6.74 with 95% confidence interval between 4.66 and 9.74). There was substantial agreement between two radiologists in terms of the existence of pineal cysts on magnetic resonance images.

CONCLUSION: Pineal cysts are the most common benign lesions of pineal gland and usually detected incidentally at routine MR examinations. Physiological degeneration or necrotic change following ischemic degeneration of intrapineal glial plate are suggested theories for pineal cyst development. We found that the prevalence of pineal cysts increased in patients with hypoxic ischemic encephalopathy when compared with normal population. Age and sex of the patients did not affect pineal cyst prevalence. We suggest that an ischemic process may have a role in the etiopathogenesis of pineal cyst development

O082-The Value of Prenatal Brain MRI in the Management of Congenital Cytomegalovirus Infection

*Amelia Fernández-Zubillaga*¹, Aranzazu Royo¹, Cristina Utrilla¹, María de la Calle², Roberto Rodríguez², Gonzalo Garzón¹

Hospital Universitario La Paz Radiology Madrid-Spain¹ Hospital Universitario La Paz Obstetrics -²

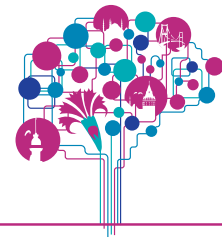
PURPOSE: Congenital cytomegalovirus (CMV) infection can lead to severe neurological sequelae. The goal of this study was to evaluate the potential to predict the risk of symptomatic neonatal infection of fetal magnetic resonance imaging (MRI) in comparison to prenatal neuro-ultrasound (US). Our secondary goal was to compare the prenatal findings and the neurological symptoms at 18 months of age.

MATERIALS AND METHODS: We reviewed the abnormal findings in prenatal brain MRI and US in 10 cases of congenital CMV infection (confirmed positive polymerase chain reaction in amniotic fluid) referred to our institution in the years 2011 to 2013. Both imaging techniques were performed between gestational weeks 24 and 32. Fetal MRI examinations were performed in a General Electric, 1,5 Tesla, Signa MRI suite. US examinations were performed with a General Electric Voluson system equipped with 3D software. The prenatal findings were compared with findings from postnatal transfontanelar US examination and clinical follow-up at 18 months.

RESULTS: US showed CNS abnormalities in 3 (30%) cases: cerebellar hypoplasia (1), ventriculomegaly (2), microcephaly (2), periventricular calcifications (2), enlarged cisterna magna (1) and ventricular sinechiae (1); 7 cases had a normal US. Five (50%) fetuses exhibited CNS

abnormalities on MRI: cerebellar hypoplasia (4), ventriculomegaly (3), altered neuronal migration (3), enlarged cisterna magna (3), microcephaly (2), periventricular calcifications (2), cortical anomalies (3), white matter anomalies (4), temporal lobe lesions (2) and ventricular sinechiae (1), and 5 had no anomalies. In 2 (20%) of the cases with normal US, MRI found anomalies (unilateral ventriculomegaly and cerebellar hypoplasia, confirmed at postnatal MRI). US and MRI were normal in 4 (40%) of cases. Of the 5 fetuses with findings in prenatal MR, 1 died in the neonatal period, 1 had severe neurological symptoms, 2 had mild neurological symptoms and 1 was asymptomatic at 18 months follow-up.

CONCLUSIONS: 1. Prenatal MRI provides additional information to that obtained with US, such as cerebellar hypoplasia, neuronal migration delay and gyration anomalies. Both techniques should be offered in congenital CMV cases. 2. Although the small size of our series does not allow us to draw statistically significant conclusions, our study suggests that fetal brain MRI increases the positive predictive value of US in the diagnosis of symptomatic neonatal infection.



ORAL PRESENTATIONS ABSTRACTS

O083-Echo Planar Diffusion Weighted MRI and High Resolution CT in the Study of Pediatric Cholesteatoma. A Comparative Study

*Angel Sanchez-Montanez*¹, Juan Pablo Salazar², Felix Pumarola³, Ignacio Delgado¹, Elida Vazquez¹
*University Hospital Vall d'Hebron Pediatric Neuroradiology Barcelona-Spain*¹ *University Hospital Vall d'Hebron Radiology*²
*University Hospital Vall d'Hebron ENT Surgery*³

PURPOSE: -To evaluate the use of Echo-Planar DWI in the diagnosis of cholesteatoma in pediatric population.
- To compare results and imaging findings with High-Resolution CT (HRCT) with bone window.

MATERIALS AND METHODS: Retrospective review of pediatric cases with echo-planar DWI (1.5 and 3T) for cholesteatoma evaluation, from January 2011 to March 2013.

A review of the ENT medical history was carried out, analysing imaging findings and radiological reports of cases evaluated by pediatric neuroradiologist with the corresponding pathology reports.

Correlation between imaging findings on DWI with HRCT was done.

RESULTS: 32 cases were identified between 4 and 17 year-old. DWI depicted a positive result for cholesteatoma in 17 of these 32 cases, while 15 were negative. Out of these 17 children with cholesteatoma by DWI, 8 were positive according to the pathology report and 8 according to ENT surgeon. There was only one case with positive DWI and negative pathology report.

19 cases (59,4%) had been evaluated with both high-resolution CT and DWI for cholesteatoma, while 13 cases were studied using DWI without HRCT.

5 of 10 patients (50%) with positive results for cholesteatoma on DWI had also positive results in HRCT, while 4 of 9 cases with negative DWI (44 %) had also negative HRCT. In general, the concordance between CT and DWI was 52,6%. 17 patients had DWI and pathology report. Among them 94,1% were both positive. There was one case (5,8%) with cholesteatoma by DWI but negative pathology result; therefore sensitivity was 100 % and the PPV 94%.

HRCT only identified 5 of 10 positive cases by pathology, therefore its sensitivity was 50% with 5 false negative results.

CONCLUSIONS: DWI-MRI is a fundamental tool in cholesteatoma diagnosis; however, it is still a complementary diagnostic imaging option. The overall concordance between DWI AND HRCT in this study was 52,6%.

Cholesteatoma might be present even without bone erosion, which is one of the key findings on HRCT. This shows the importance of using DWI independently of HRCT results.

We have demonstrated in this study that DWI could be used for the initial diagnosis and follow-up of cholesteatoma, reducing radiation exposure.

O084-Radiological and Clinical Manifestations of Megalencephaly Capillary Malformation (MCM) Syndrome

*Angel Sanchez-Montanez*¹, Ignacio Delgado¹, Susana Boronat², Paola Cano³, Elida Vazquez¹
*University Hospital Vall d'Hebron Pediatric Neuroradiology Barcelona-Spain*¹ *University Hospital Vall d'Hebron Pediatric Neurology -Spain*² *University Hospital Vall d'Hebron Neurosurgery -Spain*³

PURPOSE: Megalencephaly-Capillary Malformation (M-CM) is a syndrome of unknown etiology whose main clinical symptoms are megalencephaly and capillary malformations, which frequently occur in the philtrum, upper lip and nose, also found in limbs and trunk. Other features include

neonatal hypotonia, developmental delay, hydrocephalus, overgrowth, polydactyly, body asymmetry and connective tissue disorders. The most valuable neuroimaging findings include white matter lesions, cerebral asymmetry, ventriculomegaly, cerebellar tonsillar herniation, cortical dysplasia and polymicrogyria. The pathogenesis of hydrocephalus and herniation is attributed to a combination of several factors, being the initial event a cerebellar rapid growth difficulting and distorting the dynamics of cerebrospinal fluid. To this date approximately 130 cases have been reported. The aim of this paper is to review the radiological findings of five patients with MCM recently studied in our institution, conducting a review of the literature.

MATERIALS AND METHODS: We reviewed the medical records of five patients with M-CM from 2005



ORAL PRESENTATIONS ABSTRACTS

to the current date in our institution. We describe their clinical and radiological findings, particularly MRI, comparing with those described in the literature.

RESULTS: The most common radiological findings in the five patients diagnosed with M-CM were tonsillar descent (5 / 5), ventriculomegaly (5 / 5), white matter lesions (4 / 5), dilated Virchow-Robin spaces (3 / 5), and abnormalities of venous sinuses and / or intracranial veins (3 / 5), findings consistent with those previously described. The most frequent clinical manifestations in our series were macrocephaly (5 / 5), developmental delay (4 / 5), overgrowth (5 / 5) and cutaneous manifestations such as midline facial nevus flammeus (5 / 5).

CONCLUSIONS: The recognition of typical imaging findings of M-CM is very important, especially in order to an early management of ventriculomegaly.

O085-Pictorial Review of Suprasellar Tumors the Importance of the Signal Intensity of the Neurohypophysis on T1 to Narrow the Differential Diagnosis

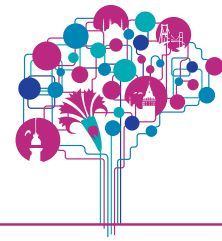
*M. De Fatima Vasco Aragao*¹, Lucas Vasco Aragao², Marcelo Moraes Valenca³, Maria Lucia Lima Soares⁴
*Multimagem; Universidade Mauricio De Nassau Radiology Recife-Brazil*¹ *Escola Pernambucana De Medicina -Brazil*² *Universidade Federal De Pernambuco Pos-Graduação Em Neuropsiquiatria, Neurocirurgia E Distúrbio Do Comportamento -Brazil*³ *Faculdade De Medicina Da Universidade Federal De Alagoas Radiology*⁴

PURPOSE: The role of the neuroradiologist goes beyond detecting and localizing the tumor, assessing its relationship with the surrounding structures, and knowing if there is hydrocephalus and potential intracranial hypertension. A more precise diagnostic hypothesis to predict prognosis and to assist in the treatment planning is mandatory. However, formulating diagnostic hypotheses is a complex intellectual process, difficult to be decomposed into parts. The aim of this paper is to make a practical review, emphasizing the main clinical (e.g. age) and the radiological features of the most frequent suprasellar tumors, particularly evaluating the signal intensity of the neurohypophysis as a tool in the differential diagnosis.

MATERIALS AND METHODS: This pictorial essay revises suprasellar masses from our institution. The suprasellar tumors were first classified according to incidence age in pediatric and adults. Distinguishing CT and/or MRI features are discussed for each neoplastic type. In addition, to make the differential diagnosis, we emphasize the importance of assessing whether the neurohypophysis shows normal signal intensity (hyperintense in T1) or not, and also the intensity of the intra and suprasellar mass lesion, mainly on T2.

RESULTS: In children, the most frequent tumors are: chiasmic hypothalamus glioma (pilocytic astrocytoma and pilomixóide astrocytoma), germinoma, histiocytosis and craniopharyngioma. In adults they are: pituitary adenoma, meningioma and craniopharyngioma. A differential diagnosis will also be made with non-neoplastic suprasellar lesions: lymphocytic hypophysitis, tuberculosis, hamartoma of the tuber cinereum, Rathke's cleft cyst, arachnoid, epidermoid and dermoid cysts and aneurysm. Regarding the signal intensity in children, the pilocytic astrocytoma is hyperintense on T2, and the neurohypophysis is normally hyperintense on T1. The opposite happens with histiocytosis and germinoma which are hypointense or isointense on T2 and show absence of normal hyperintensity of the neurohypophysis on T1. These features are also found in lymphocytic hypophysitis.

CONCLUSION: In suprasellar tumors, the analysis continues to rely on the most fundamental criteria. These are clinical data (especially age) and features of the tumor in conventional images. It is also very important to observe the neurohypophysis signal intensity on T1.



ORAL PRESENTATIONS ABSTRACTS

O086-Lymphocytic Hypophysitis in Children How the Magnetic Resonance Imaging may Support the Diagnosis

*Chiara Carducci*¹, Paola Cambiaso², Lorenzo Figà Talamanca¹, Stefania Galassi¹, Bruno Bernardi¹
*Children's Hospital "Bambino Gesù" Neuroradiology Unit Rome-Italy*¹ *Children's Hospital "Bambino Gesù"*
*Endocrinology and Diabetology Unit -Italy*²

PURPOSE: Lymphocytic hypophysitis (LH) in children is a rare condition. Magnetic Resonance Imaging (MRI) is known to be useful in diagnosis of germinoma and Langerhans Cell Histiocytosis (LCH) of pituitary region, showing similar clinical and MRI findings. We analyzed clinical data and MRI findings to identify how the MRI may help the challenging diagnosis of LH.

MATERIALS AND METHODS: This retrospective study, conducted in a Children's Hospital (January 2002 to March 2014), includes eleven patients (M/F: 7/4, age range: 3 to 11 yrs) presenting CDI, disappearance of the posterior hypophysis (PH) bright spot. Clinical evaluation every 3 months (first year), every 6 months thereafter; MRI follow up every 4 to 6 months for 2 years, yearly for 3 years. Serial testing of germ cells tumor markers (all patients) were negative (negative result did not exclude a germinoma). In all cases skeletal study or scintigraphy was performed (negative). In all cases final diagnosis of LH was confirmed by clinical and MRI evolution.

RESULTS: Eleven patients: Clinical onset with isolated central diabetes insipidus (CDI); initial MRI findings often not allowed definitive differential diagnosis from germinoma or LCH. MRI onset: Lack of PH bright spot (11/11 patients), pituitary stalk thickening (PST) (8/11) with anterior pituitary gland (APG) increasing size (4/8), borderline PST with quite normal pituitary gland size (1/11), stalk thin with APG small (2/11). First MRI of last two patients: the oldest studies in our series, performed after weeks from clinical onset. 2/4 patients showing PST and large APG presented contrast enhancement including a large area of the infundibular region. During clinical follow-up: CDI remained isolated in 6/11; in 4/11 there was also defect of GH, in 3 of these also central hypothyroidism and hypogonadism. Follow up of 1/11 was lost. MRI outcome: size reduction of all PTS cases (8/8), normalization in size of borderline stalk case, stable appearance in 2/11 with first MRI showing stalk thin and small APG.

CONCLUSIONS: Absence of bright spot PH is confirmed as CDI MRI finding. Reduction of pituitary stalk in the MRI follow-up, associated with the clinical outcome, seems to represent an important MRI sign of LH normal evolution. Other important signs: reduction of the enlarged adenohypophysis, progressive disappearance of abnormal infundibular enhancement. MRI is able to identify abnormalities of the hypothalamic/pituitary region often associated with CDI. Moreover, our study confirms the importance of close MRI follow up in challenging differential diagnosis of LH versus germinoma/LCH and a well defined MRI followup



ORAL PRESENTATIONS ABSTRACTS

Wednesday, September 10, 2014

PARALLEL SCIENTIFIC PAPER PRESENTATIONS

(Spine) 17:15 - 19:00

Marmara Hall

O087-Intracardiac Cement Migration after Percutaneous Vertebroplasty Incidence and Risk Factors

Sarah Fadili ¹, Frédéric Clarencon ¹, Evelyne Cormier ¹, Lise Le Jean ², *Jacques Chiras* ¹

Pitié-Salpêtrière Hospital Interventional Neuroradiology -France ¹ *Pitié-Salpêtrière Hospital Anesthesiology -France* ²

OBJECTIVE: To evaluate the incidence of intracardiac cement embolism during percutaneous vertebroplasty (PV).

MATERIALS AND METHODS: Single-center retrospective analysis of 1512 consecutive patients (996 females, 516 males; mean age = 68 y) who underwent 1855 PV with PMMA cement for thoracic and/or lumbar vertebral compression fracture (VCF) (tumor lesion: 45.5%, osteoporosis: 33.7%, trauma: 10%, other: 10.8%).

A chest imaging (plain X-ray and/or CT-scan) was performed when a venous leakage was suspected by the operator during the procedure.

The rate of cement cardiac migration (CCM) was evaluated. Age, sex, operator's experience, lesion type (tumor, osteoporosis, trauma), sub-type of tumor lesions (blastic, osteolytic or mixed) were evaluated as risk factors for CCM. Clinical consequences of CCM were evaluated in post-procedure and at 1-month follow-up.

RESULTS: In 65.4 % post-PV chest imaging was available. Seventy-one patients (4.7%) had CCM during the 1855 procedures. These CCMs were isolated in 14% of the cases and associated with lung cement embolism in 86% of the cases.

The rate of CCM was independent from age, sex, operator's experience, lesion type, tumor lesions' sub-type. Five patients (7%) with CCM had symptoms potentially related to this complication: one cardio-respiratory arrest, that immediately recovered and without any clinical consequence, one pericardial effusion, and 3 cases of transitory dyspnea without further consequence. All these patients had an associated lung cement migration.

CONCLUSION: CCM during PMMA PV are not exceptional (4.7% the cases) but are asymptomatic in most cases (93%).

O088-Spinal Extradural Arteriovenous Fistulas

Hui-Ling Hsu ¹, David Yen-Ting Chen ¹, Ying-Chi Tseng ¹, Chi-Jen Chen ¹

Shuang-Ho Hospital/Taipei Medical University Department of Medical Imaging New Taipei City-Taiwan ¹

PURPOSE: Spinal extradural arteriovenous fistulas (AVFs) are rare conditions. They are characterized by the presence of an arteriovenous communication, localized to the paraspinal soft tissues and the epidural venous plexus. The author aims to introduce these rare conditions with case demonstration.

METHODS: The author exhibit 4 cases of extradural AVFs to demonstrate the spectrum of the disease. Clinical findings, diagnostic evaluation, treatment and outcome are discussed.

FINDING: Two cases of spinal extradural AVFs have extradural fistulous locations (both at L3 level) and large epidural venous lakes with intradural venous drainage. They presented with progressive myelopathy. Transarterial embolization (TAE) with N-butyl cyanoacrylate (NBCA) was performed to occlude the fistula and the venous lake in both cases successfully. Regression of cord edema was noted and the symptoms were relieved in one patient and improved in another. The third case presents with cervical radiculomyelopathy. Angiography revealed an extradural AVF at T12 level with epidural venous drainage but without intradural venous drainage. TAE with NBCA was performed to occlude the fistula successfully. The symptoms completely resolved. The fourth case was an incidental finding. An extradural AVFs at cervical level was noted without intradural venous drainage or mass effect on surround tissue. No treatment was needed.



ORAL PRESENTATIONS ABSTRACTS

CONCLUSION: Spinal extradural AVFs are rare malformations which differ from dural AV fistulae in many ways. Careful differentiation and evaluation with selective spinal angiography was important before the treatment to be performed.

O089-Lumbar Spinal Cord fMRI During Electrical Stimulation of Anterolateral Leg

Yanlong Jia ¹, Zhiwei Shen ¹, Tingting Nie ¹, Tao Zhang ¹, *Renhua Wu* ¹

2nd Affiliated Hospital, Shantou University Medical Department of Medical Imaging -China ¹

PURPOSE: To determine the feasibility and reproducibility of lumbar spinal cord functional magnetic resonance imaging by electrical stimulation of anterolateral leg and to detect the possible characteristics of lumbar spinal cord fMRI activated areas and signal intensity changes. **MATERIALS and METHODS:** All studies were performed at GE1.5T Signa MR, using an eight-channel abdomen coil for RF pulse transmitting and receiving. The skin on the anterolateral leg (L5 sensory dermatome) of twelve volunteers, which have no neurological disease, were stimulated by a electrical stimulator (intermittent pulse, frequency 20HZ) in this study using a single-shot fast spin echo sequence to detect fMRI activation based on SEEP effect. Block design was used as activation patterns, such as R1-S1-R2-S2-R3-S3-R4. The imaging data were analyzed with SPM8 and generated t test images ($p < 0.05$, cluster activation pixels > 0).

RESULT: Spinal fMRI activation was found in the lumbar spinal cord in all volunteers (12/12), in addition to a volunteer movement out of the statistics. In the sagittal fMRI, activations were mainly located in L1 (9/11), T12 (11/11), T11 (9/11) vertebral level. In the axial fMRI, activations were mainly located in the simulative ipsilateral dorsal horn and slight activation were also been found in ventral horn and the contra-lateral dorsal area. The activation signal intensity changes varied widely ranging from 0.3% to 2.0%, among subjects.

CONCLUSION: It is feasible to study the lumbar spinal cord fMRI based on SEEP effect using the 1.5T MR and a repetitive activation distribution ranged from L1 to T11 was detected in this study. However, further research is needed to prove the accuracy of activation and eliminate the false activations surround the spinal cord causing by CSF pulsation.

O090-Diffusional Kurtosis Imaging Using a Rician Noise Removal Evaluation of Compressed Spinal Cords in Vivo

Masaaki Hori ¹, Koji Kamagata ¹, Mariko Yoshida ¹, Kouhei Kamiya ¹, Michimasa Suzuki ¹, Ryusuke Irie ¹, Akira Nishikori ¹, Yutaka Ozaki ², Atsushi Nakanishi ³, Kanako Sato ¹, Yuko

Adachi ¹, Miyoko Takayama ¹, Kouhei Tsuruta ¹, Shigeki Aoki ¹

Juntendo University School of Medicine Radiology Tokyo-Japan ¹ *Juntendo University Nerima Hospital Radiology*

² Juntendo University Shizuoka Hospital Radiology ³

PURPOSE: The purpose of this study is to investigate the efficacy of the Rician noise removal for the calculation of diffusion metrics for spinal cords compressed by non-malignant intra-spinal canal mass lesions in vivo.

METHODS: Five patients with non-malignant intra-spinal canal mass lesions were enrolled in this study (three women and two men, mean age 49.8 y). Pathologies were one granuloma and four benign tumors. Diffusional kurtosis (DK) image data were acquired with a 3-T MR scanner. Imaging parameters were as follows: repetition time/echo time, 6996/73 (ms/ms); number of signals acquired, one; section thickness, 3 mm; 30 sections; field of view, 80 x 80 mm²; matrix, 64 x 64 (128 x 128 reconstructed); imaging time, approximately 7 min; six b values (0, 400, 800, 1200, 1600, and 2000

s/mm²) with diffusion encoding in 6 directions for every b value. Diffusion metric maps were calculated by using the free software dTV II FZR_x (Image Computing and Analysis Laboratory, Department of Radiology, The University of Tokyo Hospital, Japan). Apparent diffusion coefficient (ADC), fractional anisotropy (FA), lambda L1, L2, and L3 were calculated based on a conventional monoexponential model using b=0 and 800 s/mm² data. Mean DK values were calculated from all the b-value data. ADC, FA, L1, L2, L3, and DK of the spinal cord white matter compressed by mass lesion were measured by tract-specific



ORAL PRESENTATIONS ABSTRACTS

analysis with or without the Rician noise removal. Statistical evaluations were performed by using IBM SPSS Statistics software (version 19.0; SPSS, Chicago, IL) using the paired t-test with Bonferroni correction.

RESULTS: DK of the patients' compressed spinal cords decreased significantly with the Rician noise removal (0.42 ± 0.17 , mean \pm SD, dimensionless), compared with DK without the Rician noise removal (0.86 ± 0.10) ($P=0.0044$). Although there was no statistically significant difference, FA, ADC, and L1 tended to increase with the Rician noise removal. While compressed but not destroyed neural tract bundles showed decreased DK and increased FA, the results of diffusion metrics with the Rician noise removal were judged to be more accurate.

CONCLUSIONS: For accurate evaluation of microstructural changes in the spinal cord in vivo, use of the Rician noise removal is recommended for analysis, in particular for DK.

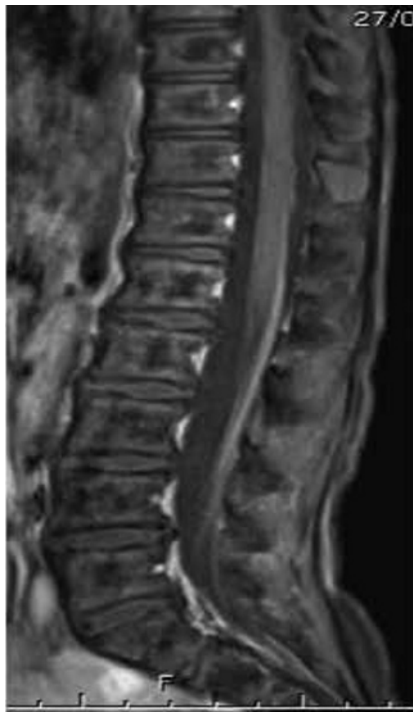
O091-Post Radiation Spine Imaging Findings

*Ozlem Alkan*¹, *Senay Demir*¹, *Cem Onal*², *Nalan Yazici*³, *Ayşe Erbay*³

*Baskent University Radiology Adana-Turkey*¹ *Baskent University Radiation Oncology -Turkey*² *Baskent University Pediatric Oncology -Turkey*³

PURPOSE: Our aim is to evaluate the MR findings after craniospinal irradiation therapy of 21 patients retrospectively.

METHODS: Twenty-one patients, 13 males and 8 females with an average age of 11 (5 to 25) were retrospectively



evaluated. Seventeen patients had medulloblastoma, 1 had anaplastic ependymoma, 1 had atypical rhabdoid-teratoid tumor, 1 had PNET and 1 had non-Hodgkin lymphoma. Nine of 21 patients (42%) had spinal leptomeningeal metastases. All patients received a total dose of 36 Gy spinal irradiation. MR scans of the spine were reviewed for the changes due to radiotherapy at vertebrae, spinal cord and nerve roots.

RESULTS: All patients had homogeneous or heterogeneous fatty degeneration in the bone marrow. Three patients (14%) had multiple compression fractures. Five patients (23%) had marked enhancement of lumbar posterior nerve roots. Six patients (29%) had marked enhancement of the cauda equine (Figure 1). Three patients (14%) had diffuse spinal cord atrophy. One patient (4%) had focal spinal cord atrophy. Two patients (9%) had focal myelomalacia of the spinal cord.

CONCLUSIONS: Radiation induced changes in the spine include fatty degeneration of bone marrow, osteopenia, myelopathy and, lumbosacral radiculopathy. The MR appearance after radiation is that of increased signal intensity of the bone marrow of the vertebral bodies. Radiation-induced osteopenia causes compression fractures of the vertebrae. Enhancement of lumbar posterior nerve roots and cauda equine can be seen after radiation therapy.

Knowing about the radiologic appearances of radiation-induced changes may prevent misinterpretations.



ORAL PRESENTATIONS ABSTRACTS

O092-Imaging Findings in Posterior Elements as a Cause of Low Back Pain

*Juan Ovalle*¹

*High diagnostic technology - Cedica Diagnostic Imaging Ibagué-Colombia*¹

PURPOSE: The main objective of this work is schematically illustrated in MR studies the findings associated with lumbar pain caused in the posterior elements. Facet synovitis, facet osteoarthritis, stress injuries of the pars interarticularis, changes in the flavum ligament, hypervascularity, transitional segments, edema or interspinous interspinous ligament will be illustrated in a didactic way through cases.

MATERIALS AND METHODS: Chronic back pain is a common cause of morbidity and disability. Radiologists often tend to focus on the anterior and middle column when interpreting imaging studies, forgetting the posterior elements as a cause of pain. Different methods have proven effective in demonstrating or locate the cause of pain, gamagraphic studies, computed tomography, with and with out contrast MR and PET-FDG. With RM we have a great help with the liquid-sensitive sequences such as STIR, T2 fat-saturated, T1 with fat saturation and administration of intravenous contrast medium.

CONCLUSION: Posterior elements have been implicated as common and important cause of axial back pain. The radiologists must understand and interpret the imaging findings as a cause of pain originating in the posterior elements. The facet joints, pars interarticularis, ligamentum flavum, the interspinous ligament, the spinous processes can be evaluated efficiently and sensitive STIR sequences, Fat Sat T2, and gadolinium T1 Fat Sat showing edema, inflammatory involvement of the articular capsule, hypervascularization such reactive process.

O093-Success Story of Ozonucleolysis in Disc Lesions in Pakistan

*Umair Rashid*¹

*PGMI Neuro Radiology Lahore-Pakistan*¹

BACKGROUND AND PURPOSE: Direct injection of Oxygen-Ozone in to the discs has proved to be the effective alternative for surgery in patients with disc herniation in many countries around the world. We report our experience with ozonucleolysis with patients effected by lower backache, sciatica and pain cervical region (Brachalgia) due to disc herniation including post operative recurrence or disc prolapse

MATERIALS AND METHODS: Eleven Thousand & Two Hundred patients were treated with single to multiple sessions of Oxygen Ozone therapy. All the patients had CT or MRI evidence of annulus tear/ disc prolapse with clinical signs of nerve root compression. The procedure was performed under angio fluoroscopy using 22/23 G spinal needle with out any form of anesthesia. All the patients received intra discal injection of Oxygen Ozone mixture with and without periganglionic infiltration at a ozone concentration 30 Ugm/ml. Among these patients 7000 were males and 4200 were females between the age of 20-80 years. Therapeutic out come was assessed 5 months after treatment by using modified MacNab method.

RESULTS: A satisfactory therapeutic outcome was obtained. 55% of the patients showed complete recovery with resolution of symptoms. 20% of the patients complained of occasional episodic pain and with no limitation of occupational activity. 15% of cases showed insufficient improvement. 5% of cases had insufficient improvement and went for surgery. 10% of cases never turned up after the first visit.

CONCLUSION: Intradiscal with and without periganglionic injection of Ozone for herniated discs has revolutionized percutaneous approach to nerve root diseases making it safer, cheaper and easier to repeat than treatments currently use in Pakistan.



ORAL PRESENTATIONS ABSTRACTS

O094-Adhesive Arachnoiditis in Post Operative Lumbar Sine

*Violeta Vasilevska Nikodinovska*¹, Ulrike Szeimies², Axel Stabler²

*University Surgical Clinic "St.Naum Ohridski"-Skopje Radiology Skopje-Macedonia*¹ *Radiologie-muenchen-harlaching Radiology -Germany*²

PURPOSE: The purpose of this retrospective study was to assess the frequency of magnetic resonance imaging (MRI) signs of postoperative adhesive lumbar arachnoiditis.

MATERIALS AND METHODS: In this retrospective study, 63 patients previously operated on for lumbar disc herniation as well as re-operated due to persistent pain or recurrence of the symptoms were investigated. Axial T2-weighted images (1.5 and 3 T, slice thickness 1mm, eight-channel phased array coil) of three standard levels L3/4, L4/5 and L5/S1 for presence of adhesive arachnoiditis (AA) were evaluated. Centrally clumped or peripheral adherent roots on MR images were graded as mild, moderate and severe adhesions. There were 24 man and 39 women, (mean age 64.8 years, range 40-89). Of 63 patients, 53% had only one operation, mean 13.3 years ago and 44% had two or more operations on the lumbar spine, mean 17.3 years from the first operation.

RESULTS: Of 63 patients at level L3/4 36 patients (57%) have no MR signs for adhesive arachnoiditis (AA). 18 patients (28.5%) have mild AA, only 3 pts have severe adhesions. At level L4/5 most of the cases (65%), have mild (33.3%) and moderate (31.7%) MRI signs for AA. Seven cases have severe adhesions. The situation was different at level L5/S1 where 55.6% (35pts) of the cases have severe MRI signs for AA. At this level mild AA have 14 pts (22.2%), in 8 cases AA was absent.

CONCLUSIONS: Adhesive lumbar arachnoiditis is essentially unrecognized disease. Arachnoiditis does occur after extradural lumbar surgery. Clinical diagnosis is hard to achieve, using MRI, is evidence for the diagnosis obtainable.

O095-Vascular Manifestations of Cervical Spine Trauma on CTA A Retrospective Institutional Experience

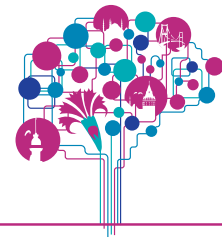
*Vivek Sindhvani*¹, Monika Arya² *University of Missouri Radiology Columbia-United States*¹ *University of Missouri Internal Medicine -United States*²

PURPOSE: Although vertebral artery injury (VAI) is the commonest vascular manifestation in patients with cervical trauma, there are gamut of other vascular injuries that warrant timely management before symptoms of cerebrovascular insufficiency develop. Computed Tomographic Angiography (CTA) provides extremely rapid, highly sophisticated and minimally invasive assessment of the head and neck vasculature in patients with cervical trauma and has brought it to the forefront in management of patients with suspected vascular injury.

MATERIALS AND METHODS: A retrospective review of patients who underwent CTA based on a combination of clinical assessment and CT cervical spine findings between January 2012 and December 2013 following cervical trauma was performed to determine the frequency and type of vascular injuries in these patients and to further determine their association with cervical (type and location) as well as skull base fractures.

RESULTS: 133 total patients underwent CTA based on clinical and CT findings. 65 patients (49%) had cervical or skull base fractures, of which 12 (18%) had VAI (Grade I-IV), 3 (5%) had venous sinus thrombosis and 1 had thyrocervical trunk injury with extravasation. Of the 68 patients who did not have a demonstrable fracture, 2 patients had VAI and 3 patients had internal carotid artery dissection. Of total 133 total patients 22 (17%) had some kind of vascular injury. Commonest vertebral artery injury was Grade IV as per (Biffel et al) grading system.

CONCLUSIONS: Threshold for performing CTA in patients with cervical (foramen transversarium, articular facet, C1-C3 subluxations) and/or skull base fractures should be low and an astute physician should not underestimate the chances of a vascular injury even in the absence of cervical fractures. There are varied vascular manifestations; the commonest being Grade IV vertebral artery injury. CTA is the frontrunner in evaluating vascular injury in patients with cervical spine trauma.



ORAL PRESENTATIONS ABSTRACTS

O096-Quantitative MRI in Hypokalaemic Periodic Paralysis Reveals Age Dependent Fat Infiltration of Lower Limb Muscles

Elham Rawah ¹, Jasper M Morrow ², Christopher DJ Sinclair ¹, Matthew RB Evans ², Sachit Shah ¹, Mary M Reilly ², Michael Hanna ², John S Thornton ¹, Tarek A Yousry ¹

UCL, Institute of Neurology, London Neuroradiological Academic Unit. London-United Kingdom 1 UCL, Institute of Neurology, London MRC Centre for Neuromuscular Diseases. -United Kingdom ²

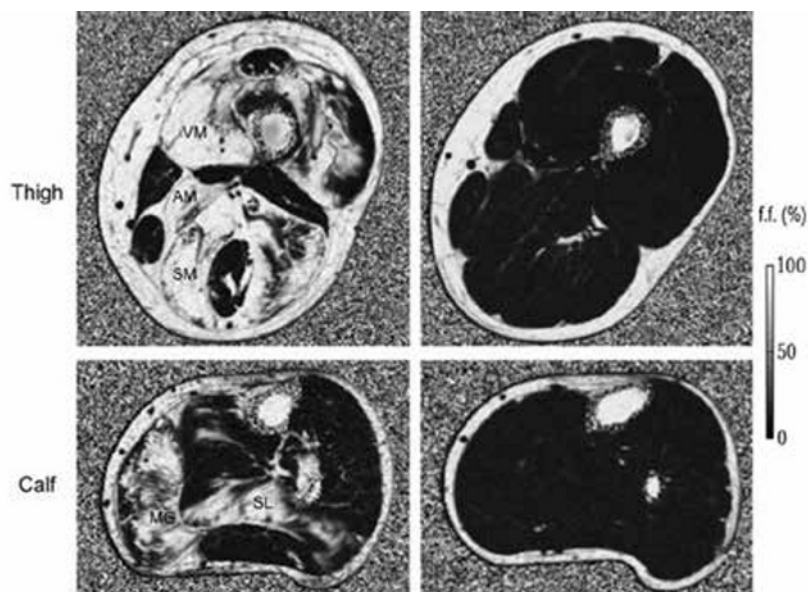
PURPOSE: Hypokalaemic periodic paralysis (HypoPP) is a muscle channelopathy characterised by recurrent paralytic attacks. Over time, a proportion of patients also develop fixed weakness resulting in significant disability. A previous study has qualitatively demonstrated fatty infiltration in HypoPP patients with permanent muscle weakness, but this has not yet been quantified. The aim of this study was to quantify fat infiltration in lower limb muscles of patients with HypoPP using MRI, as this may provide an objective method of monitoring disease progression.

MATERIALS AND METHODS: Lower limb muscle MRI was performed at 3T in 12 patients with HypoPP (9M/3F, age 42±12y) and 12 healthy controls (9M/3F, age 41±10y). Muscle fat infiltration was quantified using percentage voxel fat fraction obtained by 3-point Dixon fat-water decomposition. Thigh and calf muscles were analysed using whole muscle regions of interest drawn by an observer blinded to diagnosis on a single axial slice.

RESULTS: Mean muscle fat fraction was significantly increased in patients compared with controls at both thigh (patients: 10.2±15.4%; controls 1.5±0.5%) and calf (8.3±10.5%; 1.7±0.6%) level. Muscle involvement was variable with greatest mean fat infiltration in adductor magnus (17.8%) and vastus medialis (14.7%) in the thigh and in medial gastrocnemius (15.9%) in the calf. Overall fat fraction correlated with age in patients ($\rho=0.76$, $p<0.01$) but not in controls ($\rho=0.17$, $p=0.6$). The age-severity relationship appeared dichotomous with normal fat fraction in patients younger than 40 (1.8±1.2%), but significantly increased in patients older than 40 (15.5±14.2%). Example thigh and calf fat fraction maps for a male patient aged 53, and a male patient aged 23 are shown in figures 1a) and 1b).

CONCLUSIONS: Quantitative MRI reveals clear evidence of muscle selective fat infiltration in HypoPP patients aged over 40. This suggests a potential window for treatment before this age where effective therapy may prevent irreversible muscle damage.

1a) Male aged 53y. 1b) Male aged 23y.





ORAL PRESENTATIONS ABSTRACTS

O097-MRI Quantifies Lumbosacral Nerve Root Hypertrophy in Chronic Inflammatory Demyelinating Polyradiculoneuropathy

*Sachit Shah*¹, Jasper M Morrow², Christopher DJ Sinclair¹, Matthew RB Evans², Michael G Hanna², Michael P Lunn², Mary M Reilly², John S Thornton¹, Tarek A Yousry¹

*UCL Institute of Neurology, Neuroradiological Academic Unit, London-United Kingdom*¹ *UCL Institute of Neurology, MRC Centre for Neuromuscular Diseases, -United Kingdom*²

PURPOSE: Chronic inflammatory demyelinating polyradiculoneuropathy (CIDP) is a treatable, immune-mediated condition characterised by progressive or relapsing motor and sensory deficits in all four limbs. The diagnosis is based on a combination of clinical, neurophysiological and supportive criteria, but can often be challenging. Consensus guidelines include hypertrophy of lumbosacral nerve roots on MRI as a supportive criterion, although the evidence for this has not been fully validated. Our aim was to quantify nerve root diameter and cross-sectional area in the lumbosacral region in patients with CIDP versus healthy controls using MRI.

MATERIALS AND METHODS: MRI of the lumbosacral plexus was performed at 3T in 10 patients with CIDP (7M/3F, age 52 ± 15y) and 10 healthy controls (7M/3F, age 50 ± 11y), using a 3D T1-weighted gradient echo sequence (1mm isotropic resolution). Orthogonal diameter and cross-sectional area of the lumbosacral nerve roots (L1 to S2) were measured at three defined points along their course (intraforaminal, at the foraminal outlet and extraforaminal) by an observer blinded to the diagnosis.

RESULTS: Mean diameter of the lumbosacral nerve roots was significantly increased in patients (6.9 ± 1.9mm; 95% CI 5.4-8.4) compared to controls (5.0 ± 0.9mm; 95% CI 4.1-5.9) (p<0.05). A corresponding increase was also shown in mean cross-sectional area (patients 47.1 ± 26.4mm², 95% CI 26.0-68.2; controls 27.1 ± 8.8mm², 95% CI 18.5-35.7). The degree of involvement within the patient group was most marked at the L5 and S1 levels, and varied along the course of the nerve root; the greatest difference in mean diameter was shown in the extraforaminal portion of the L5 nerve roots (patients 9.4mm; controls 5.0mm; p<0.01). A threshold upper nerve root diameter of 6.0mm at the L5 level distinguished between patients and controls with a sensitivity of 83% and a specificity of 92%.

CONCLUSION: MRI quantification of lumbosacral nerve root dimensions reveals significant hypertrophy in patients with CIDP, with the extraforaminal portions of the L5 and S1 nerve roots particularly affected. This provides supportive evidence for continued inclusion of lumbosacral nerve root hypertrophy on MRI in the diagnostic criteria for CIDP.

PARALLEL SCIENTIFIC PAPER PRESENTATIONS

(Adult NR 1) 17:15 - 19:00

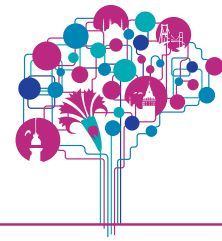
Dolmabahce C Hall

O098-Fast Quantitative Magnetization Transfer Imaging in 3D in Primary Brain Tumors and Metastases Is There a Correlation with PWI and DWI

*Meritxell Garcia*¹, Monika Gloor², Oliver Bieri², Ernst-Wilhelm Radue³, Johanna M. Lieb¹, Dominik Cordier⁴, Christoph Stippich¹

*Clinic for Radiology & Nuclear Medicine, University of Basel Hospital Division of Diagnostic & Interventional Neuroradiology Basel-Switzerland*¹ *Clinic for Radiology & Nuclear Medicine, University of Basel Hospital Division of Radiological Physics -Switzerland*² *University of Basel Hospital Medical Imaging Analysis Center -Switzerland*³ *University of Basel Hospital Department of Neurosurgery -Switzerland*⁴

PURPOSE: The additive information of magnetization transfer (MT)-imaging to conventional MRI in brain tumors has been assessed in a previous work. Its diagnostic benefit however, is still undetermined. This study analyses whether MT-imaging provides additive information to DWI and PWI in brain tumors. The hypothesis is that MT-estimates do neither correlate with ADC nor with PWI-parameters, which would strengthen their diagnostic value.



ORAL PRESENTATIONS ABSTRACTS

MATERIALS AND METHODS: MT-imaging, DWI, and PWI of 24 patients with primary brain neoplasms and metastases were analysed. Whole-brain MT-data in 3D with balanced steady-state free precession (bSSFP) were acquired in 9 minutes. MT-analysis included magnetization transfer ratio (MTR) and quantitative MT-parameters (qMT): Relaxation times (T1, T2), exchange rate (kf), and macromolecular content (F). Six regions of interest (ROIs) were chosen: Contrast enhancing (T1w-CE) and non-contrast enhancing (T1w-non-CE) on T1w, proximal (T2w-pSI) and distal hyperintensity (T2w-dSI on T2w) on T2w, and two references in normal appearing tissue (white matter, thalamus). MT-values were correlated with PWI (CBF, CBV) and ADC. **RESULTS:** In the references MT-parameters did not correlate with ADC or PWI-values. MT- and PWI-parameters showed no correlation for the tumors. Compared to PWI, MT-values in tumors showed lower data dispersion and differed significantly from the references, whereby the different tumors tended to arrange in groups: In the T1w-CE, T1w-non-CE, and T2w-pSI ROIs MT-values of glial tumors were more remote from the references than MT-values of metastases. ADC correlated with all MT-estimates in GBMs, and with kf in mixed glial tumors (Table 1).

CONCLUSIONS: Correlation between ADC and MT-estimates in glial tumors may result from tissue distortion. The considerable correlation between ADC- and MT-parameters in glial tumors only, and the missing correlation between PWI and MT-parameters strengthen our hypothesis that MT-imaging has to be considered an additive technique for diagnostic brain tumor imaging evaluation. One benefit is the lack of need of contrast. The use of MT-imaging however, has still to be assessed in larger studies.

r	T1 [ms]	T2 [ms]	MTR [%]	kf [s ⁻¹]	F [%]
ADC GBM	0.78	0.77	-0.55	-0.68	-0.72
ADC mixed glial tumors	0.57	0.73	-0.20	-0.53	-0.43
ADC meningiomas	0.68	0.49	0.00	-0.45	0,14
ADC metastases	0.39	0.71	-0.18	-0.36	-0.08

Correlation between ADC and MT-parameters for the different pathologies

O099-Incidence and Prognostic Significance of Non Enhancing Cortical FLAIR Hyperintensity in Glioblastoma

*Arian Lasocki*¹, Francesco Gaillard², Mark Tacey³, Katharine Drummond⁴, Stephen Stuckey⁵

*Radiology -Australia*² *Melbourne EpiCentre -Australia*³ *The Royal Melbourne Hospital Neurosurgery -Australia*⁴ *Monash Health Diagnostic Imaging -Australia*⁵

PURPOSE: To determine the incidence and prognostic implications of non-enhancing cortical FLAIR (fluid attenuated inversion recovery) hyperintensity in histologically-proven glioblastomas. **MATERIALS AND METHODS:** Institutional Human Research Ethics Committee approval was obtained. Patients with a new diagnosis of glioblastoma between September 2007 and December 2010 were identified. Only patients with at least FLAIR and post-contrast T1-weighted sequences were included. Pre-operative Magnetic Resonance Imaging studies were reviewed together by two readers to determine whether there was evidence of non-enhancing cortical signal abnormality, based primarily on the FLAIR sequence. It was graded as either 'negative', 'minor' (a thin rim around enhancing tumour) or 'more extensive'. Patient survival was then compared between groups, correcting for age, sex, performance status, axial measurements of the largest enhancing lesion and location (deep, periventricular or peripheral).

RESULTS: 151 patients met the inclusion criteria. 77 patients (51%) had evidence of non-enhancing cortical signal abnormality - minor in 37 of these patients (median survival 220 days) and more extensive in 40 (median survival 310 days). The 74 patients without non-enhancing cortical signal abnormality had a median survival of 261 days. On multivariate analysis, there was no significant difference in survival between the three groups (p=0.109 comparing 'negative' and 'minor'; p=0.399 comparing 'negative' and 'more extensive'). The only



ORAL PRESENTATIONS ABSTRACTS

significant differences in survival were when assessing only patients with peripherally-located enhancing lesions, when the presence of non-enhancing cortical signal abnormality was associated with worse survival (hazard ratio=3.4, $p=0.003$ for 'minor'; HR=2.3, $p=0.038$ for 'more extensive').

CONCLUSIONS: Non-enhancing cortical signal abnormality is common in glioblastoma, occurring in about half of cases. In general, its presence does not alter survival, and factors such as the location of the tumour are more important prognostic indicators. Assessing only peripheral lesions, however, non-enhancing cortical signal abnormality is associated with a worse prognosis. This may reflect a greater volume of tumour remaining after resection or outside the radiotherapy field, increasing the rate of recurrence.

O100-Multifocal and Multicentric Glioblastoma Improved Characterisation with FLAIR Imaging and Prognostic Implications.

*Arian Lasocki*¹, Francesco Gaillard², Mark Tacey³, Katharine Drummond⁴, Stephen Stuckey⁵
*Peter MacCallum Cancer Centre Cancer Imaging East Melbourne-Australia*¹ *The Royal Melbourne Hospital Radiology -Australia*² *Melbourne EpiCentre -Australia*³ *The Royal Melbourne Hospital Neurosurgery -Australia*⁴ *Monash Health Diagnostic Imaging -Australia*⁵

PURPOSE: To determine the incidence and significance of multiple enhancing lesions in histologically-proven glioblastomas.

MATERIALS AND METHODS: Institutional Human Research Ethics Committee approval was obtained. Patients with a new diagnosis of glioblastoma between September 2007 and December 2010 were identified. Pre-operative Magnetic Resonance Imaging (MRI) studies were reviewed to determine whether or not there was more than one enhancing lesion and, if present, whether there was evidence on imaging of a communication between lesions (multifocal) or not (multicentric). The presence of a communication was predominantly determined using the fluid attenuated inversion recovery (FLAIR) sequence. Patient survival was then compared between groups, correcting for age, sex, performance status, axial measurements of the largest enhancing lesion and location (deep, periventricular or peripheral).

RESULTS: 55 of 167 patients (33%) had more than one discrete enhancing lesion. In the majority (49 of 55, or 89%), there was evidence of a communication between all lesions, ie. a multifocal glioblastoma. The communication was parenchymal (along white and/or grey matter, including the corpus callosum) in 45 of these, subependymal in three cases and leptomeningeal in one case. There was no convincing imaging communication in six patients, consistent with a multicentric glioblastoma. Patients demonstrating multiple enhancing lesions had a median survival of 183 days, compared to 304 days for patients without multiple lesions. There was no difference in survival on multivariate analysis, however ($p=0.747$). A deep location was predictive of worse survival ($p<0.001$ compared to a peripheral location; $p=0.008$ compared to a periventricular location), and was more common in patients with multiple lesions (35 of 55, or 64%) compared to those without (38 of 112, or 34%).

CONCLUSIONS: The presence of multiple enhancing lesions in glioblastoma is relatively common, occurring in about one-third of cases, and hence the possibility of a multifocal glioblastoma is important to consider pre-operatively. Modern MR imaging, in particular FLAIR, shows that the majority are multifocal glioblastomas, with true multicentricity being rare. Patients with multiple enhancing lesions have a worse prognosis, but this is not necessarily due to multiplicity per se; rather, it is likely related to greater dissemination of disease and more frequent involvement of deep structures.



ORAL PRESENTATIONS ABSTRACTS

O101-Incidence and Imaging Follow up of Lesions Consistent with a Low Grade Glioma Distant from a Histologically Proven Glioblastoma

*Arian Lasocki*¹, Francesco Gaillard², Mark Tacey³, Katharine Drummond⁴, Stephen Stuckey⁵

*Peter MacCallum Cancer Centre Cancer Imaging East Melbourne-Australia*¹ *The Royal Melbourne Hospital Radiology -Australia*² *Melbourne EpiCentre -Australia*³ *The Royal Melbourne Hospital Neurosurgery -Australia*⁴ *Monash Health Diagnostic Imaging -Australia*⁵

PURPOSE: To determine the incidence of additional lesions consistent with low grade glioma in patients with a new diagnosis of glioblastoma, with subsequent imaging follow-up.

MATERIALS AND METHODS: Institutional Human Research Ethics Committee approval was obtained. Patients with a new diagnosis of glioblastoma between September 2007 and December 2010 were identified. Only patients with at least FLAIR (fluid attenuated inversion recovery) and post-contrast sequences were included. Pre-operative Magnetic Resonance Imaging (MRI) studies were reviewed together by two readers to determine whether there were lesions with imaging appearances consistent with a low grade glioma separate from the dominant tumour (ie. multicentric lesions on imaging). This was based primarily on the FLAIR sequence, with the diagnosis being made on the presence of cortical signal hyperintensity and mass effect, without post-contrast enhancement.

RESULTS: 9 of 151 patients (6%) had lesions consistent on imaging with a low grade glioma separate from the dominant tumour. Their median survival was 183 days, compared to 264 days for patients without this feature. This worse survival was statistically significant on multivariate analysis ($p=0.024$). There was a high incidence of multiple enhancing lesions separate from the focus of low grade tumour, occurring in 5 of these 9 patients. Excluding studies performed immediately post-operatively, follow-up MRIs were performed in three patients. In all three, these additional areas of tumour developed enhancement and evidence of necrosis within one year, and became confluent on FLAIR with the dominant lesion. In a fourth patient, a further separate lesion had developed evidence of necrosis in the 22-day interval between the full diagnostic study and the limited post-contrast study performed for stereotaxis.

CONCLUSIONS: The presence of a low grade glioma separate from the dominant lesion is an uncommon finding in glioblastoma, but likely to be useful in making the preoperative diagnosis of a glioma over other differentials. It is a poor prognostic feature. These lesions appear to de-differentiate much faster than expected for a low grade glioma and are thus likely to represent more advanced lesions than their appearances suggest. Confluence with the dominant lesion developing with time suggests that some are in fact connected at diagnosis, despite the communication not being visible with MRI.

O102-Diagnostic Accuracy and Reproducibility of Intravoxel Incoherent Motion MR Imaging for Differentiating Among Glioblastoma Metastasis and Lymphoma

*Myeong Ju Goh*¹, Ho Sung Kim², Choong-Gon Choi², Sang Joon Kim²

*Jeju National University Hospital Radiology Seoul-Korea, South 1 Asan Medical Center Radiology -Korea, South*²

PURPOSE: Intravoxel Incoherent Motion (IVIM) MR imaging can provide noncontrast acquisition of both diffusion and perfusion parameters. Our objective was to determine the diagnostic accuracy of IVIM-derived perfusion (f) and diffusion (D) parameters for differentiating among glioblastoma, metastasis, and PCNSL.

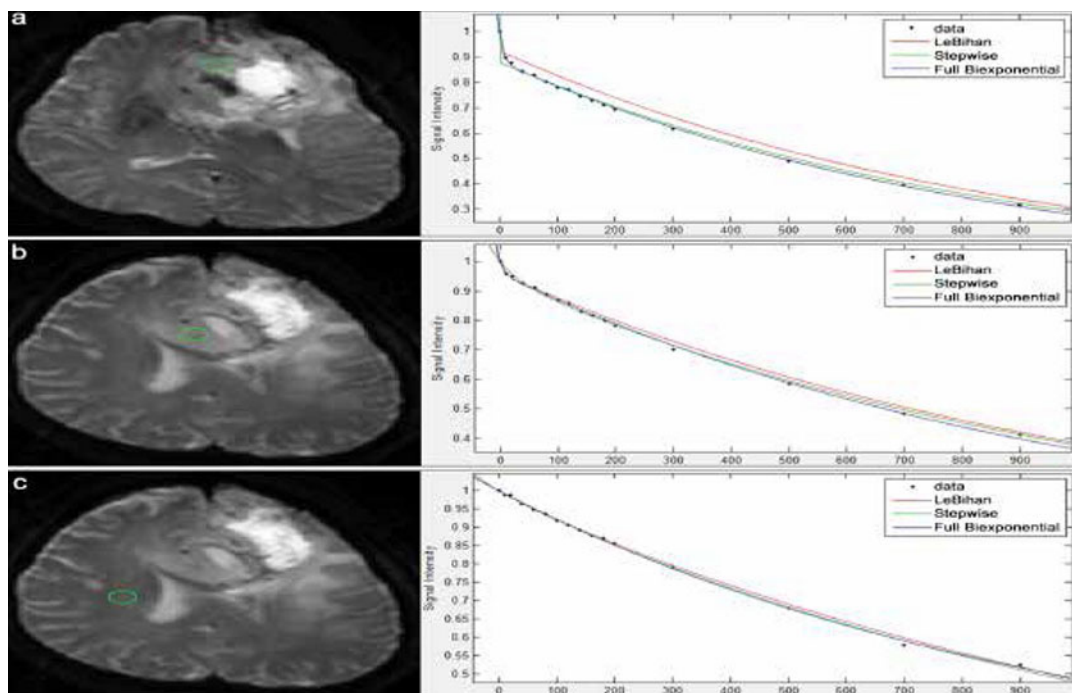
MATERIALS AND METHODS: 128 patients who had pathologically confirmed glioblastoma (n=55), metastasis (n=31), or PCNSL (n=42) prior to any treatment were enrolled. Two neuroradiologists independently calculated maximum f (f_{max}) and minimum D (D_{min}). The differences of f_{max} and D_{min} among the three tumor pathologies were determined by one-way ANOVA with multiple comparisons. A corresponding nCBV and ADC were used for validation of the f and D using partial correlation analysis, respectively.



ORAL PRESENTATIONS ABSTRACTS

RESULTS: The mean fmax was significantly higher in the glioblastoma group (0.103 ± 0.017 for reader 1; 0.109 ± 0.024 for reader 2) and the metastasis group (0.105 ± 0.022 for reader 1; 0.107 ± 0.026 for reader 2) than in the PCNSL group (0.025 ± 0.014 for reader 1; 0.023 ± 0.012 for reader 2) ($P < .001$ for each), respectively. The mean Dmin did not significantly differ among the three groups. The correlation between f and corresponding nCBV was highest in the glioblastoma group and the correlation between D and corresponding ADC was highest in the PCNSL group.

CONCLUSION: IVIM-derived f significantly differs between hypervascular and hypovascular tumors and correlates best with nCBV in the hypervascular brain tumor. D correlates best with ADC in the hypovascular brain tumor



O103-Utility of Multiparametric Voxel by Voxel Tumor Clustering Using Permeability and Apparent Diffusion Coefficient for Differentiating Recurrent Glioblastoma from Radiation Necrosis

*Ji Eun Park*¹, Ho Sung Kim¹, Choong Gon Choi¹, Sang Joon Kim¹
Asan Medical Center Radiology Seoul -Korea, South¹

PURPOSE: To determine if enlarging contrast-enhancing lesion (CEL) with similar tumor microenvironment (TM) in patients with posttreatment glioblastoma, could be labeled by clustering methods and assess if the volume fraction of identified clusters is different between recurrent glioblastoma (RGM) and radiation necrosis (RN).

MATERIALS AND METHODS: 84 study patients with pathologically proven RGM (n = 50) or RN (n = 34) treated with chemoradiotherapy (CCRT) underwent conventional, dynamic contrast-enhanced (DCE), and diffusion-weighted MR imagings. Initial area under the curve at 60sec (IAUC60) and apparent diffusion coefficient (ADC) values were estimated voxel by voxel from the DCE and DWI MR images. Enlarging CELs with similar TM were identified by k-means clustering of the IAUC60 and ADC over all patients. The volume fraction of each cluster was used to evaluate the prognostic value of the clusters. The sensitivities and specificities of clustering multiparametric analyses were compared with those of univariate analysis.



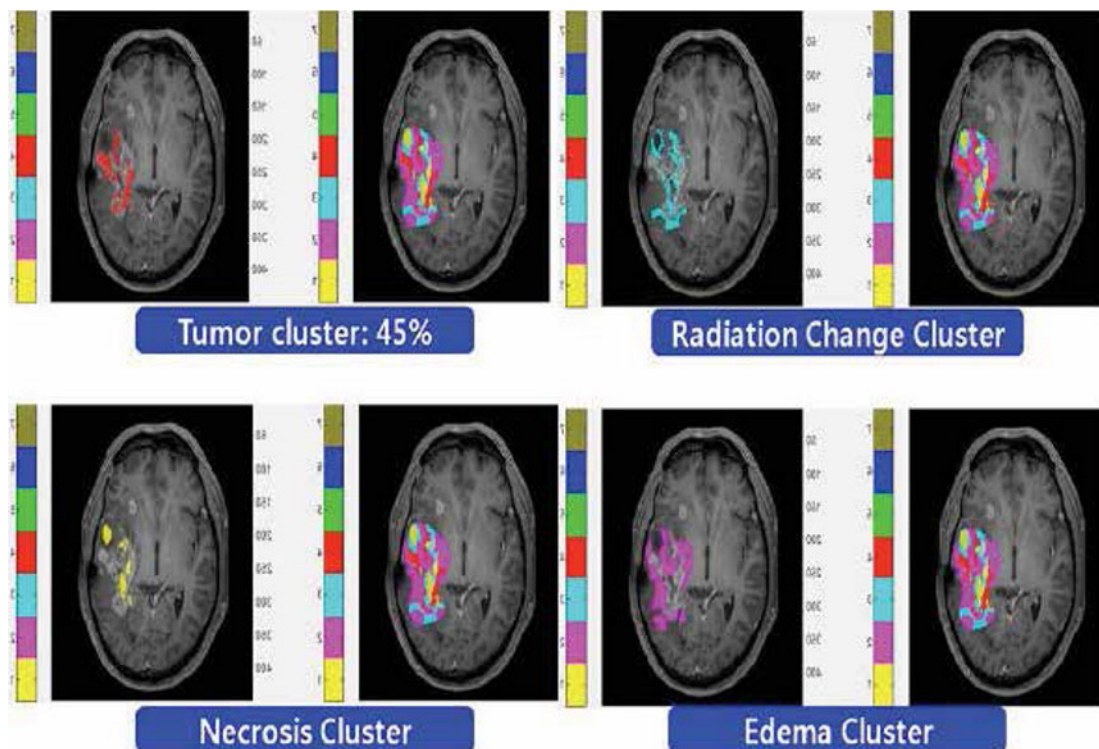
ORAL PRESENTATIONS ABSTRACTS

RESULTS: Three clusters (permeability-ADC codominant, permeability-dominant, nondominant) provided a sufficient reduction of the cluster variance to label different TM. The mean cluster volume fractions of permeability-ADC codominant, permeability-dominant, and nondominant cluster were 42%, 38% and 20% for the RGM group and 12%, 39% and 49% for the RN group. The permeability-ADC codominant cluster was most significantly associated with RGM. Multiparametric k-means clustering led to markedly improvement of differentiation over univariate analyses, with a maximum sensitivity and specificity in the range of 80-90% for the diagnosis of RGM using the clustering (CE-T1, IAUC60, ADC).

CONCLUSION: Intra-CEL regions showing similar TM properties could successfully be labeled in three distinct clusters and the volume fraction of permeability-ADC codominant cluster was most significantly associated with RGM.

Fig 1. 52-year-old male with enlarging contrast-enhancing lesion 45 weeks after CCRT shows 45% of tumor cluster, suggesting predominant recurrent glioblastoma.

Fig 2. 47-year-old female with enlarging contrast-enhancing lesion 39 weeks after CCRT shows 12% of tumor cluster, suggesting predominant radiation necrosis.





ORAL PRESENTATIONS ABSTRACTS

O104-Added Value of Intravoxel Incoherent Motion Imaging in Patients with Recurrent Glioblastoma Comparison with Contrast enhanced Perfusion MR Imaging

*Gil-Sun Hong*¹, Ho Sung Kim², Choong Gon Choi², Sang Joon Kim²

*Asan medical center Radiology Seoul-Korea, South*¹ *Asan medical center Radiology -Korea, South*²

PURPOSE: To evaluate the diagnostic accuracy of intravoxel incoherent motion (IVIM)-derived perfusion (f) and diffusion (D) parameters in relation to dynamic susceptibility contrast (DSC) perfusion MR imaging for differentiating recurrent glioblastoma (RGM) from radiation necrosis (RN). **MATERIALS AND METHODS:** This retrospective study was approved by our institutional review board, with the requirement for informed patient consent waived. Sixty-five consecutive patients with pathologically confirmed RGM (n=37, 56.9%) or RN (n=28, 43.1%) were assessed using conventional, DSC, and IVIM MR imaging. 90 percentile histogram cutoff of normalized cerebral blood volume (nCBV90) and f (f90) and 10 percentile cutoff of apparent diffusion coefficient (ADC10) and D (D10) were calculated. Conventional MR imaging (CI) enhancement pattern, nCBV90, ADC10, f90, and D10 were included in multivariate models to predict a diagnosis of RGM versus RN.

RESULTS: f90 was significantly different between the RGM (mean, 0.101 ± 0.016 [standard deviation]) and RN (mean, 0.021 ± 0.010) ($P < .001$). Adding f90 and D10 to the CI significantly improved the area under the receiver operating characteristic curve (AUC) from 0.652 to 0.979. Adding nCBV90 resulted in AUC improvement from 0.892 to 0.932. The mean f90 was significantly higher in the RGM group (0.101 ± 0.016) than in the RN group (0.021 ± 0.010) ($p < 0.0001$). The mean D10 was significantly lower in the RGM group (0.101 ± 0.016) than in the RN group ($P = 0.190$). ROC curve analyses showed f90 to be an excellent predictor for differentiating RGM from RN, with a sensitivity of 95.2% and a specificity of 89.7%.

CONCLUSION: IVIM MR imaging can provide an added value to contrast-enhanced perfusion MR imaging for predicting RGM.

O105-Title Added Value of Intravoxel Incoherent Motion MR Imaging to Contrast enhanced Perfusion MR Imaging for Predicting Recurrent Metastatic Brain Tumor Following Gamma Knife Radiosurgery

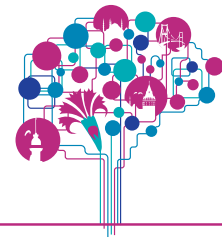
*Dae Yoon Kim*¹, Ho Sung Kim², Ra Gyoung Yoon², Choong Gon Choi², Sang Joon Kim²

*Bundang Jesaeng hospital Radiology Seongnam-si-Korea, South*¹ *Asan Medical Center Radiology -Korea, South*²

PURPOSE: The purpose of this study was to determine the added value of intravoxel incoherent motion MR Imaging (IVIM)-derived perfusion (f) and diffusion (D) parameters to contrast-enhanced perfusion MR imaging for predicting recurrent metastatic brain tumor following gamma knife radiosurgery (GKRS).

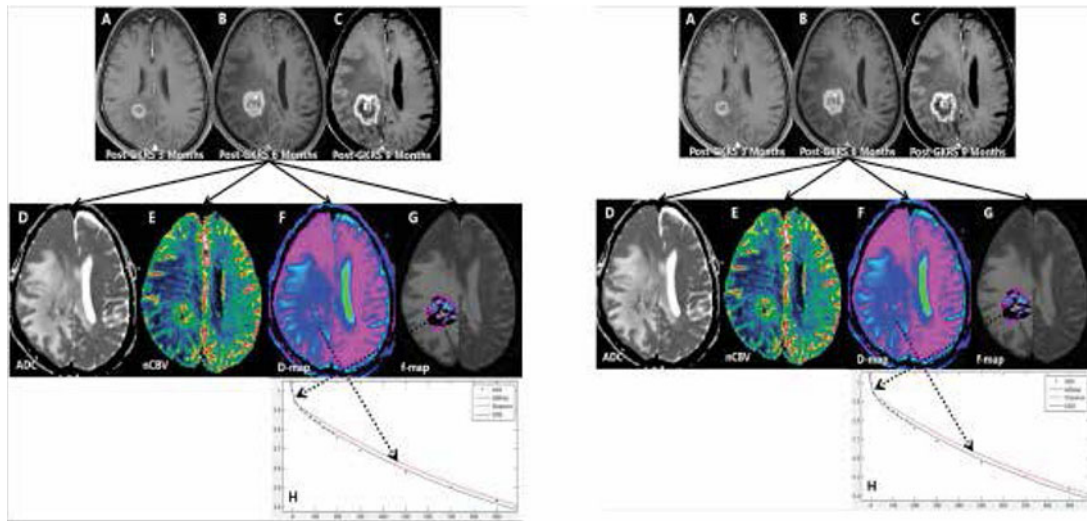
MATERIALS AND METHODS: 125 consecutive patients with metastatic brain tumor treated with GKRS, were assessed using IVIM and dynamic susceptibility contrast (DSC) perfusion MR imagings. Two readers independently calculated the 90th and 10th percentile histogram cutoffs for f (f90), normalized cerebral blood volume (nCBV90), and D (D10), respectively. Areas under the receiver operating characteristic (AUC) curve, leave-one-out cross validation, and intraclass correlation coefficient (ICC) were assessed.

RESULTS: With the combination of f90 and D10 used as a discriminative index, the sensitivity and specificity for differentiation were 82.5% and 92.9% for reader 1 and 85.7% and 94.5% for reader 2, respectively. With the nCBV90 used as a discriminative index, the sensitivity and specificity were 75.5% and 92.7% for reader 1 and 79.1% and 94.2% for reader 2, respectively. Using leave-one-out cross validation, adding IVIM to nCBV90 significantly improved the cross validated accuracy from 84.2% to 92.5% for reader 1 and from 86.5% to 93.9% for reader 2, respectively. The ICCs between readers were higher for perfusion parameters (ICC range, 0.82-0.90) than for diffusion parameters (ICC range, 0.69-0.77).



ORAL PRESENTATIONS ABSTRACTS

CONCLUSION: IVIM MR imaging can provide an added value to contrast-enhanced perfusion MR imaging for predicting recurrent metastatic brain tumor following GKRS



O106-Atypical Imaging Features of Primary Central Nervous System Lymphoma Mimicking Glioblastoma in Non AIDS Patients Utility of Intravoxel Incoherent Motion MR Imaging

*Ji Eun Park*¹, Ho Sung Kim¹, Choong Gon Choi¹, Sang Joon Kim¹
*Asan Medical Center Radiology Seoul-Korea, South*¹

PURPOSE: To determine the utility of intravoxel incoherent motion (IVIM)-derived perfusion and diffusion parameters for differentiating atypical primary central nervous system lymphoma (PCNSL) from glioblastoma in non-AIDS patients.

MATERIALS AND METHODS: Our institutional review board approved this retrospective study and waived the informed consent requirement. Sixty patients with pathologically confirmed atypical PCNSLs (n=19) or glioblastomas (n=41) were assessed using maximum f (fmax) and minimum D (Dmin) derived from IVIM.

Two readers independently calculated IVIM parameters as well as maximum normalized cerebral blood volume (nCBV) and minimum apparent diffusion coefficient (ADC). Leave-one-out cross-validation and intraclass correlation coefficient (ICC) were assessed to determine reliability and reproducibility of the parameters, respectively.

RESULTS: Mean fmax was significantly higher in the glioblastoma group than in the atypical PCNSL group (reader 1: 0.101 ± 0.016 [standard deviation] vs 0.021 ± 0.010 , $P < .001$; reader 2: 0.107 ± 0.024 vs 0.027 ± 0.015 , $P < .001$). Mean Dmin did not significantly differ between the two groups ($P = .202$ for reader 1; $P = .091$ for reader 2). Using the fmax as a discriminative index, the sensitivity and specificity were 89.5% and 95.1% for reader 1 and 84.2% and 95.1% for reader 2, respectively. There was a significant positive correlation between fmax and the corresponding nCBV ($r = 0.68$, $P < .001$). The ICC between readers was highest for measurement of fmax (ICC = 0.92).

CONCLUSION: IVIM imaging can be used as a noninvasive imaging method to differentiate malignant brain tumors showing similar conventional MR imaging features.

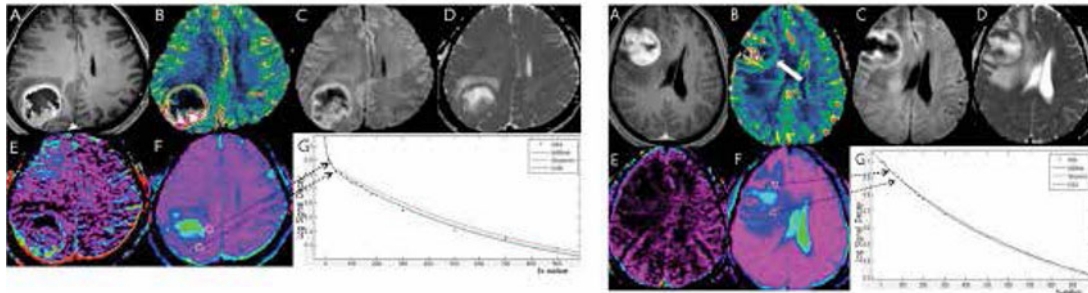
Figure 1. Glioblastoma. A, contrast-enhanced T1-weighted image. B, Normalized CBV. C, DWI.



ORAL PRESENTATIONS ABSTRACTS

D, ADC map. E, F-map. and F, D-map. G, Log signal intensity decay as a function of different b values is definitely biexponential in the contrast-enhancing lesion.

Figure 2. Atypical primary CNS lymphoma. A, CET1. B, Normalized CBV. C, DWI. D, ADC map. E, F-map. and F, D-map. G, Log signal intensity decay as a function of different b values is monoexponential in the contrast-enhancing lesion.



O107-Prognostic Value of Combined Visualization of ADC Diffusion Maps and CBV Perfusion Maps in Patients with Newly Diagnosed Glioblastoma

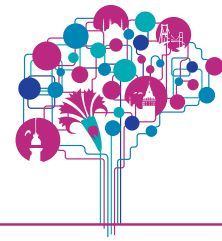
Katerina Deike¹, Benedikt Wiestler², Markus Graf³, Martin Bendszus¹, Alexander Radbruch¹
*University of Heidelberg Neuroradiology -Germany*¹ *university of Heidelberg Neurooncology -Germany*² *German Cancer Research Center (DKFZ) Radiology -Germany*³

PURPOSE: Decreased apparent diffusion coefficient (ADC) values on diffusion weighted imaging (DWI) and increased relative cerebral blood volume (rCBV) on dynamic susceptibility contrast enhanced perfusion (DSC) have been reported to identify areas of increased malignancy in glioblastoma. Here we investigated if a combined visualization of both imaging techniques can identify prognosis-related growth patterns.

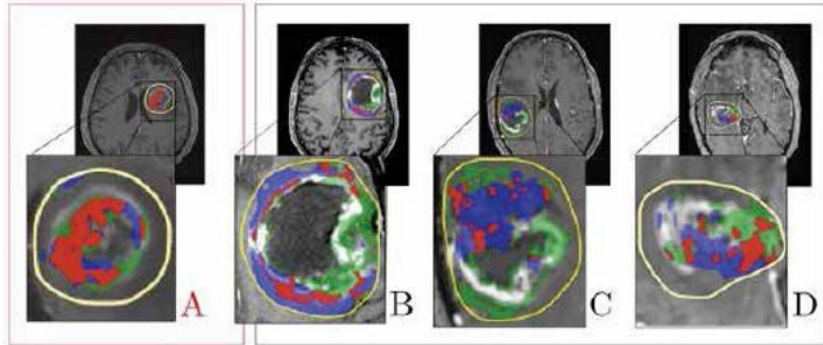
MATERIALS AND METHODS: Sixty-five subsequent treated patients presenting ring-enhancing glioblastoma on T1-w-imaging were examined with DWI and DSC perfusion prior to surgery (contrast agent: gadoteric acid; Dotarem). ADC and CBV maps were coregistered on the T1-w image and a ROI was manually delineated encompassing the enhancing lesion. Within this ROI thresholds of CBV and ADC were visualized: Pixels with ADC < the 30th percentile (ADC_{min}), pixels with CBV > the 70th percentile (CBV_{max}) and the corresponding intersection (intersection_{rel}) were automatically calculated and visualized.

Initially, all neoplasia with a mean intersection_{rel} more than the upper quartile (Q3) of the normally distributed mean intersection_{rel} of all patients were subsumed to the first growth pattern termed big intersection (BI, figure 1A). Subsequently, the remaining tumors were ascribed to growth patterns depending on the pictorial representation of ADC_{min}, CBV_{max} and their intersection_{rel}. **RESULTS:** Log-rank test exposed a significantly longer overall survival (OS) of BI (n=16 patients) compared to noneBI (n=49 patients; p=0.0057). Thirtyone, 4 and 14 patients of noneBI group were classified as predominant ADC- (figure 1B), CBV- (figure 1C) and mixed growth group (figure 1D). Comparing CBV-, BI- and mixed group to the reference group ADC multivariate Cox model revealed hazard ratio of 0.1, 0.24 and 0.33 (p-values: 0.03, 0.0005 and 0.004).

CONCLUSION: Our study provides evidence that the combination of diffusion- and perfusion-imaging allows visualization of different glioblastoma growth patterns which enable a statement about biological behavior of glioblastoma and about OS.



ORAL PRESENTATIONS ABSTRACTS



O108-Diagnostic Accuracy and Reproducibility of Amide Proton Transfer Imaging for Characterization of Solid and Necrotic Portions of Glioma Experimental and Clinical Studies

*Ho Sung Kim*¹, Choong Gon Choi¹, Sang Joon Kim¹
*Asan Medical Center Radiology Seoul-Korea, South*¹

PURPOSE: To determine the diagnostic accuracy and reproducibility of amide proton transfer (APT) imaging for characterization of solid and necrotic portions of glioma.

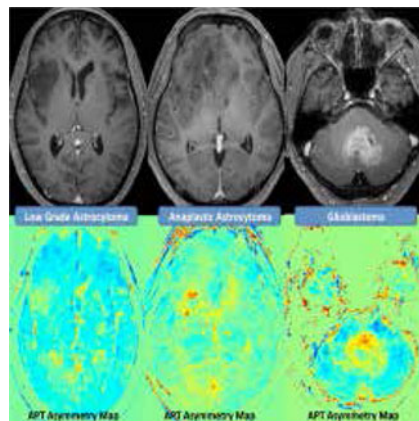
MATERIALS AND METHODS: This retrospective study was approved by our institutional review board, with the requirement for informed patient consent waived. Forty-two patients with pathologically proven gliomas were enrolled in this study. APT signals on the calculated APT asymmetry map at the offset of 3.5 ppm were measured on solid portions (APT_{solid}) and within necrotic or cystic portions (APT_{necrosis_cyst}) using 'hot-spot' method. The diagnostic performance of APT imaging was determined by one-way ANOVA with multiple comparisons and leave-one-out

cross validation. Interreader agreement was assessed by using intraclass correlation coefficient (ICC).

RESULTS: APT_{solid} can significantly differentiate among low grade glioma, anaplastic glioma and glioblastoma (0.059 ± 0.017 vs 0.037 ± 0.012 vs 0.0015 ± 0.009 ; $P = .005 - .031$ for multiple comparisons). APT_{necrosis_cyst} was significantly higher in low grade glioma than in high grade glioma (0.032 ± 0.014 vs 0.0016 ± 0.011 ; $P = .009$).

For 27 patients showing necrosis or cyst within tumors, APT_{necrosis_cyst} was significantly different between low grade glioma and glioblastoma. By using leave-one-out cross validation, a sensitivity and a specificity of the APT_{solid} for differentiating between low-grade and high-grade (anaplastic glioma and glioblastoma) gliomas were 95.7% and 92.4%, respectively. The ICCs for APT_{solid} and APT_{necrosis_cyst} were 0.87 and 0.83, respectively.

CONCLUSION: APT_{solid} provides superior diagnostic accuracy for differentiating between anaplastic glioma and glioblastoma than nCBV, with an excellent interobserver agreement.





ORAL PRESENTATIONS ABSTRACTS

PARALLEL SCIENTIFIC PAPER PRESENTATIONS

(Research & Neuroradiological Sciences 1) 17:15 - 19:00

Topkapı A Hall

O109-Efficacy of CT Guided Percutaneous Intralesional Bleomycin Injection for the Treatment of Orbital Low Flow Vascular Malformations and Hemangiomas

Ho Fai Wong ¹, TY Chen ¹, MC Wu ¹, *Nancy Duarte* ¹
CGMH linkou Neuroradiology -Taiwan ¹

BACKGROUND AND PURPOSE: The treatment of orbital vascular malformations remains a challenge and bleomycin used in percutaneous sclerosing therapy is an effective option in some reported cases. However, the intralesional bleomycin injection (IBI) is not exactly if lesion is not superficial or retrobulbar in location. We introduce a technique for percutaneous IBI under CT guidance. Direct confirmation the injection of the bleomycin within the lesion and the definite distribution of the bleomycin.

MATERIALS AND METHODS: From 2008 to 2013, 17 patients with low flow orbital malformations and hemangiomas were treated with CT guide IBI. All patients were follow-up with images and clinically.

RESULTS: All patients had significant improvement in their gross appearance and regression of the lesion size. The patients were followed by CT scan after four weeks of the injection. Some patients were necessary two or three sessions. No procedure-related complications and no recurrence observed.

CONCLUSIONS: The CT guide percutaneous bleomycin injection is an effective and safe technique used for the treatment of the low flow orbital vascular malformation and hemangioma with a low incidence of complications.

O110-Evaluation of the Effect on Surgical Decision Making of the Intra Operative Display of the Optic Radiation during Temporal Lobe Epilepsy Surgery

A. Kenji Yamamoto ¹, Laura Mancini ², Mark J. White ², Anna Miserocchi ³, Andrew McEvoy ³, Pankaj Daga ⁴, Gavin P. Winston ⁵, John S. Duncan ⁵, Tarek A. Yousry ¹

UCL Institute of Neurology Neuroradiological Academic Unit London-United Kingdom ¹ *National Hospital for Neurology and Neurosurgery Lysholm Department of Neuroradiology -United Kingdom* ² *National Hospital for Neurology and Neurosurgery Department of Neurosurgery -United Kingdom* ³ *UCL Centre for Medical Image Computing -United Kingdom* ⁴ *UCL Institute of Neurology Department of Clinical and Experimental Epilepsy -United Kingdom* ⁵

PURPOSE: Temporal lobe resection (TLR) for temporal lobe epilepsy is an effective treatment. The main complication of surgery is a visual field defect (VFD) due to damage to the optic radiation (OR). The benefit of OR diffusion tensor imaging tractography (DTIT) in surgical planning is established. The intra-operative display of the OR is being increasingly used, however its benefit in influencing surgical decision making is challenging to quantify. The primary surgical outcome, the reduction in seizure frequency, may be insensitive to directly attribute this to the intra-operative display of DTIT. We attempt to quantify the real-time changes in surgical decision making with the presentation of the OR peri-operatively and intra-operatively.

MATERIALS AND METHODS: 8 patients were imaged pre-operatively at 3T. The trajectory to the temporal horn of the lateral ventricle was planned before surgery by the neurosurgeon using iPlan (BrainLAB) on structural MRI alone. The OR was overlaid, and the neurosurgeon asked whether the trajectory would change. In 4 patients, the neurosurgeon indicated the most posterior extent where they would resect the temporal pole, without the OR overlaid on the operating microscope. Following resection of the temporal pole (during which time the OR was overlaid), the distance from the resection margin to the OR was measured using intra-operative MRI. Post-operative VFDs were measured.



ORAL PRESENTATIONS ABSTRACTS

RESULTS: In all cases the planned trajectory to the temporal horn was not changed when the OR was available however, the entry point to the ventricle always differed from planned (median=8.1mm, range=2.9-12.6mm). In 4 cases, both the planned and final distances from the resection margin to the OR were calculated. In 3, the final resection margin was further from the OR than planned, the values were +2.1mm (23.7% post-op VFD), +4mm (no post-op VFD) , +13.8mm (no post-op VFD) (where + indicates a real surgical cavity further from the OR than planned). In the remaining case the final resection was marginally closer by -0.7mm (14.5% post-op VFD).

CONCLUSION: This pilot study aims to quantify the immediate changes to the surgical approach with the intra-operative display of the OR. The results suggest that it has a protective role during TLR and the methodology described could be used in a larger series of TLR and neuro-oncology surgical cases.

O111-Peri Lesional Changes in Diffusion Tensor Imaging (DTI) parameters after Gamma Knife Stereotactic Radiosurgery

Herwin Speckter¹, José Bido¹, Giancarlo Hernandez¹, Diones Rivera¹, *Luis Suazo*¹, Santiago Valenzuela¹, Bernd Foerster², Eddy Perez-Then³, Jairo Oviedo⁴, Peter Stoeter¹

CEDIMAT Gamma Knife Dominicano -Dominican Republic ¹ *Philips Healthcare Customer Support -Brazil* ²
CEDIMAT Dep. of Science -Dominican Republic ³ *CEDIMAT Dep. of Radiology -Dominican Republic* ⁴

PURPOSE: In Gamma Knife stereotactic radiosurgery (GKSRS), it is generally assumed that due to the steep decline of the radiation gradient, the peri-lesional tissue can be spared from radiation damage. However, longitudinal studies using advanced Magnetic Resonance Imaging (MRI) techniques to look for such microstructural lesions outside the target are rare and present contradictive results (Ravn S et al., *Acta Oncol.* 2013;52:1314-1319; Chang Z et al. *Technol Cancer Res Treat.* 2014;13:21-28). The present investigation was performed in non-infiltrating lesions like meningiomas or vascular malformations and looked especially for alterations of otherwise normal-appearing peri-lesional brain tissue after GKR.

MATERIALS AND METHODS: In 43 patients with various brain lesions, MRI including DTI (3T Achieva, Philips) was performed before and 5 – 20 months after GKRSRS and change of parameters was measured in peri-lesional areas, in relation to the radiation dose applied.

RESULTS: Alterations of Mean Diffusivity (MD) and Radial Diffusivity (RD) were more pronounced inside the lesion, but did not exceed 5.5% on average. Outside the lesion, there was an increase of MD of 2.5 % and of RD of 3.6 % in the 15-10 Gy isodose volume and an increase of 2.1% and 3.1% for both parameters in the 10-5 Gy isodose volume. Fractional Anisotropy (FA) showed a reduction of 1.7% and 1.8 % in the corresponding volumes and a reduction of 1.4% within the lesion.

CONCLUSION: In contrast to the reports mentioned above, we saw only mild changes of DTI parameters in normal brain tissue surrounding the lesions, which partially may have been induced by the radiation itself and partially be due to other effects. Thus, our study underlines the relative safety of this form of treatment, if meticulous conformal planning keeps collateral radiation as low as possible.



ORAL PRESENTATIONS ABSTRACTS

O113-Degeneration and Plasticity of the Optic Pathway in Alström Syndrome

*Valentina Citton*¹, Jan Marshall², Angela Favaro³, Baglione Alessandro³, Pietro Maffei⁴, Paolo Meneguzzo³, Luca Wies⁵, Francesco Bona⁶, Annalena Venneri⁵, Renzo Manara
IRCCS San Camillo Hospital Neuroradiology Lido of Venice-Italy¹ Bar Harbour Jackson Laboratory -United States
² University of Padua Neurosciences -Italy³ University of Padua Medicine -Italy⁴ IRCCS San Camillo Hospital
Neurosciences -Italy⁵ University of Padua Neuroradiology -Italy⁶ University of Salerno Neuroradiology -Italy⁷

BACKGROUND AND PURPOSE: Alström Syndrome (AS) is a rare inherited ciliopathy featured by early progressive cone-rod dystrophy leading to early blindness. A previous MRI study disclosed unexpected concomitant brain changes, mainly involving the occipital regions. The present multimodality MRI study investigates the functional and structural changes of the optic pathway in AS aiming to provide insights into the underlying pathogenic mechanisms.

MATERIALS AND METHODS: Eleven genetically proven AS patients (mean-age 23 years; range: 6–45, 5 females) and nineteen age- and gender-matched controls underwent brain MRI: the study protocol included conventional sequences, resting state functional MRI and diffusion tensor imaging.

RESULTS: The evaluation of the occipital regions showed in AS patients i) diffuse white matter density decrease while grey matter density decrease spared the occipital poles (voxel-based morphometry), ii) diffuse fractional anisotropy decrease and radial diffusivity increase while mean and axial diffusivity were normal (tract based spatial statistics), iii) reduced connectivity in the medial visual network strikingly sparing the occipital poles (independent component analysis). Placing seeds in both the occipital poles, the seed-based analysis revealed significantly increased connectivity in AS patients towards the anterior portion of the left insula (right and left seeds) and towards the left frontal operculum, inferior and middle frontal gyri and the medial portion of both thalami (left seed).
CONCLUSION: The protean occipital brain changes in AS patients likely reflect the coexistence of diffuse primary myelin derangement, anterograde transsynaptic degeneration and complex cortical reorganization differently involving the anterior and posterior visual cortex.

O114-Functional Connectivity and Cerebral Networks in Crucial Intracerebral Regions are Affected in Patients with Systemic Lupus

Erymatous (SLE)

*Jessika Nystedt*¹, Olof Strandberg², Andreas Jönsen³, Åsa Lilja⁴, Anders Bengtsson⁵, Petra Nilsson⁶, Peter Mannfolk⁷, Pia Sundgren¹

Department of Clinical Sciences, University of Lund Division of Diagnostic Radiology Lund-Sweden¹ Faculty of Science, University of Lund Medical Radiation Physics, Lund -Sweden² Department of Clinical Sciences, University of Lund Section for Rheumatology, Lund -Sweden³ Center for Primary Health Care Research, University of Lund Center for Primary Health Care Research -Sweden⁴ Department of Clinical Sciences, University of Lund Section for Rheumatology -Sweden⁵ Department of Clinical Sciences, University of Lund Department of Neurology -Sweden⁶ Faculty of Science, University of Lund Medical Radiation Physics -Sweden⁷

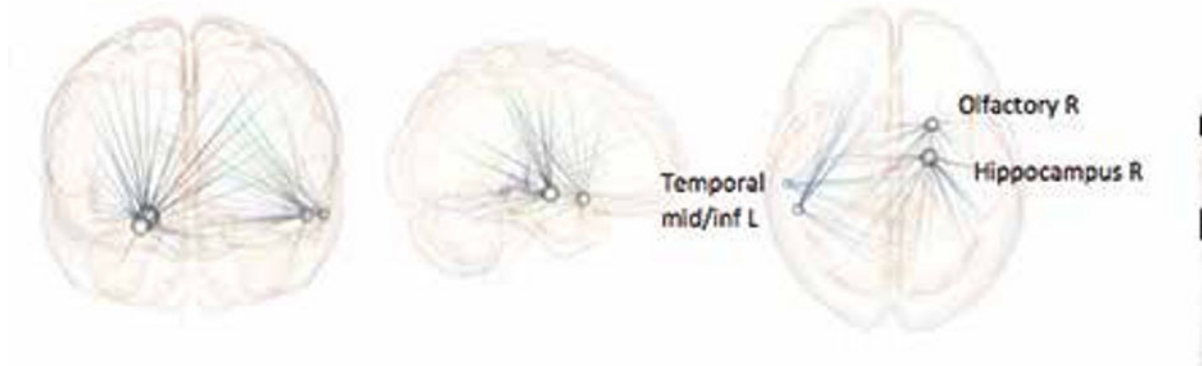
PURPOSE: In a pilot resting state fMRI (rs-fMRI) study investigate if SLE patients with cognitive impairment but without NP complications showed signs of altered functional connectivity, in comparison to SLE patients without cognitive impairment.

MATERIALS AND METHODS: 10 female patients (age 18-52, mean 37,6 years) diagnosed with SLE, without obvious clinical or subjective signs of cognitive dysfunction, underwent the Central Nervous System Vital Signs (CNSVS) cognitive test [1]. Patients with decline in more than one cognitive domain were categorized as cognitive impaired.

To address potential changes in brain function we used rs-fMRI to compare regional connectivity in SLE patients, with (n=5) or without cognitive impairment (n=5).



ORAL PRESENTATIONS ABSTRACTS



A gradient-echo EPI pulse sequence was used (TR/TE=1850/30 ms, in-plane resolution=3x3 mm², slice thickness=3 mm, 256 volumes). Preprocessing included realignment, slice timing correction, smoothing with 6 mm isotropic Gaussian kernel and normalization to standard MNI space using FMRIB Software Library (FSL).

Confounding signals were regressed out of the data (cerebrospinal fluid, white matter, motion parameters). Connectivity analysis was performed for each subject (pairwise correlation between time courses averaged over 840 regions-of-interest) and subsequent group comparisons were made using Permutation tests. RESULTS: No differences in age, Montgomery-Åsberg's Depression Scale (MADRS-S), Hospital Anxiety and Depression Scale (HAD) or Flinders Fatigue Scale (FSS) were found between the groups. Decreased connectivity was found in brain regions essential for working memory, executive function and cognitive flexibility such as hippocampus and anterior gyri cinguli in cognitive impaired SLE patients compared with those that were not cognitively impaired.

CONCLUSION: Rs-fMRI might be a promising tool in identifying early signs of cognitive impairment in SLE patients. Functional connectivity and cerebral networks in crucial intracerebral regions might be affected and detectable with f-MRI in patients with SLE, even before subjective or clinical signs associated with cognitive failure or other neuropsychological symptoms occur. 1. Reliability and Validity of a Computerized Cognitive Neuro-Cognitive Test Battery CNS- Vital Signs. C. Thomas Gualtieri et al.

O115-Structural Covariance Networks of Striatum Subdivision in Patients with Parkinson's Disease

*Wei-Che Lin*¹, Kun-Hsien Chou², Pei-Lin Lee³, Ching-Po Lin⁴, Hsiu-Ling Chen¹, Cheng-Hsien Lu⁵
*Kaohsiung Chang Gung Memorial Hospital and Chang Gung University College of Medicine Department of Diagnostic Radiology Kaohsiung-Taiwan*¹ *National Yang-Ming University Brain Research Center -Taiwan*² *National Yang-Ming University Department of Biomedical Imaging and Radiological Sciences -Taiwan*³ *National Yang-Ming University Institute of Neuroscience -Taiwan*⁴ *Kaohsiung Chang Gung Memorial Hospital and Chang Gung University College of Medicine Department of Neurology -Taiwan*⁵

PURPOSE: Parkinson's disease (PD) is a neurodegenerative disorder associated with the striatum. Previous studies indicated that subdivisions of the striatum with distinct functional connectivity profiles contribute to different pathogeneses in PD. Segregated structural covariance (SC) pattern between the striatum and neocortex remain unknown in PD. The purpose of this study is to map and compare the subregional striatal SC network organization between healthy controls and PD patients and to investigate their association with the disease severity.

MATERIALS AND METHODS: Forty-eight PD (21 men and 27 women, mean age 61.7 ± 11.3 years) and 30 age and sex matched healthy controls (16 men and 14 women, mean ages 59.1 ± 5.9 years) were enrolled.

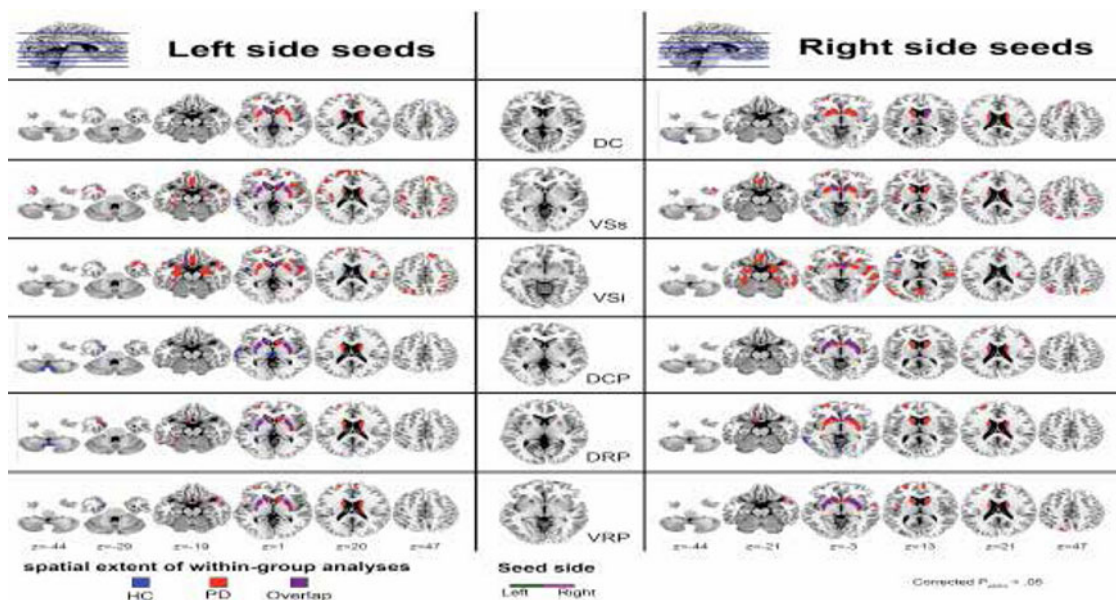


ORAL PRESENTATIONS ABSTRACTS

The striatal SC network was statistically inferred by correlating the mean gray matter volume of six striatal subdivisions (including the bilateral dorsal caudate, superior ventral striatum, inferior ventral striatum, dorsal caudal putamen, dorsal rostral putamen, and ventral rostral putamen) with the entire neocortical gray matter volume in voxel-wise manner. Regional differences in SC patterns of the striatal subdivisions between groups were tested. We further investigated the association between regional GM volume and clinical evaluation (including UPDRS, HY-stage, and SE-ADL) within the patient group.

RESULTS: The PD patients revealed marked atrophy in the striatum, cerebellum and extra-striatum neocortices. As predicted, segregated striatal SC network patterns were observed in both groups. This suggests that in PD, pathological processes occurring in the striatum affect the same striato-cortical networks that co-vary with the striatum in healthy brains (Fig). The PD patients further demonstrated atypical striatal SC patterns between the caudate, parahippocampus temporal cortices and cerebellum, which corresponded to dopaminergic associated network. The areas with significant group differences in SC were further associated with disease severity.

CONCLUSIONS: Our findings support previous studies indicating that PD is associated with altered striato-cortical networks, and suggest that structural changes in the striatum may result in a cascade of alterations in multiple neocortices.

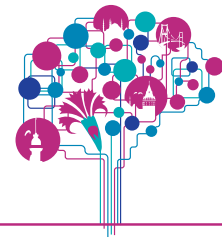


O116-Maximizing the Extent of Resection and Survival Benefit of Patients in Glioblastoma Surgery High Field iMRI Versus Conventional and 5 ALA Assisted Surgery

Sotirios Bisdas¹, Constantin Roder², Marcos Soares Tatagiba², Ulrike Ernemann¹, Vasileios K. Katsaros³
University of Tübingen Department of Neuroradiology -Germany¹ University of Tübingen Department of Neurosurgery -Germany² University of Athens Department of MRI Athens-Greece³

AIMS: A safe total resection followed by adjuvant chemoradiotherapy should be the primary goal in the treatment of glioblastomas (GBMs) to enable patients the longest survival possible. 5-aminolevulinic acid (5-ALA)- and intraoperative MRI (iMRI)-assisted surgery, have been shown in prospective randomized trials to significantly improve the extent of resection (EOR) and subsequently survival of patients with GBMs. No direct comparison of surgical results between both techniques has been published to date. We analyzed the additional value of iMRI in glioblastoma surgery compared to conventional surgery with and without 5-ALA.

MATERIALS AND METHODS: Residual tumor volumes, clinical parameters and 6-month progression-free survival (6M-PFS) rates after GBM resection were analyzed retrospectively for 117 patients after conventional,



ORAL PRESENTATIONS ABSTRACTS

5-ALA and iMRI-assisted surgery.

RESULTS: Mean residual tumor volume (range) after iMRI-assisted surgery [0.5 (0.0-4.7) cm³] was significantly smaller compared to the residual tumor volume after 5-ALA-guided surgery [1.9 (0.0-13.2) cm³; $p = .022$], which again was significantly smaller than in conventional white-light surgery [4.7 (0.0-30.6) cm³; $p = .007$]. Total resections were significantly more common in iMRI- (74%) than in 5-ALA-assisted (46%, $p = .05$) or white-light surgery (13%, $p = .03$). Improvement of the EOR by using iMRI was safely achievable as peri- and postoperative morbidities were comparable between cohorts. Total resections increased 6M-PFS from 32% to 45%.

CONCLUSIONS: Analysis of residual tumor volumes, total resections and neurological outcomes demonstrate that iMRI may be significantly superior to 5-ALA and white-light surgery for glioblastomas at comparable peri- and postoperative morbidities. Longer 6M-PFS was observed in patients with total resections.

O117-Protocol Combining Advanced and Functional MRI with Neuropsychological Evaluation for Patient Tailored Therapy Decision and Treatment of Brain Masses

*Vasileios K. Katsaros*¹, Sotirios Bisdas², Evangelia Liouta³, Agapi-Alexandra Katsarou¹, Laurent Hermoye⁴, George Stranjalis³

*University of Athens Department of MRI Athens-Greece*¹ *University of Tübingen Department of Neuroradiology -Germany*² *University of Athens Department of Neurosurgery -Greece*³ *Imagilys -Belgium*⁴

PURPOSE: To evaluate a combined neuroimaging and neuropsychological protocol for treatment decision, presurgical planning, imaging-guided surgery and treatment monitoring of brain masses. **MATERIALS & METHODS:** From September 2011 until today, 333 patients (392 examinations) with brain masses were evaluated pre-surgically as well as post-surgically (59 patients). Our protocol included neuropsychological tests (frontal executive and visuospatial functions, language, motor, memory, emotion and behavior), structural MRI, SWI, task-based fMRI, diffusion and perfusion MRI, as well as spectroscopy on a 1.5T magnet before surgery as well as 3 and 12 months after surgery, following radio- and/or chemotherapy treatment. The fMRI paradigms (motor mapping, tactile, language, visual, Stroop, memory and cognitive tasks) were selected according to the

neuropsychological evaluation results. The acquired and post-processed data from structural, functional and advanced (DTI, MR spectroscopy, and perfusion) MRI were used for differential diagnosis and treatment decision. In case of surgical approach (biopsy, ablative or gross total excision), the necessary data was transferred to a neuronavigation system for imaging-guided surgery. In all cases undergone surgical resection, histopathologic results were available.

RESULTS: 75 patients were excluded from the study due to inadequate cooperation and motion artifacts, which resulted in poor image quality. The remaining 258 patients included 35 cases with low-grade gliomas, 87 high-grade gliomas, 2 DNET, 10 lymphomas, 57 meningiomas, 8 cavernomas/ arteriovenous malformations, 3 developmental venous anomaly, 3 PNET, 45 metastases, 2 colloid cysts, 2 epidermoids, 3 inflammation and 1 post-infectious angitis. Based on a previously published algorithm for brain tumors we were able to establish the correct diagnosis in 249/258 patients (96,5%). In 172/258 patients (67%) the combination of neuropsychological and neuroimaging evaluation showed that gross total excision was possible, thus we proceeded with surgery instead of biopsy. The imaging-guided surgery in 151/172 (87.7%) of the patients achieved gross total excision, especially in the groups of low-grade gliomas and meningiomas.

CONCLUSION: The combined protocol of advanced MR techniques and fMRI with neuropsychological evaluation demonstrated clinical feasibility, high diagnostic accuracy, and allowed on an individual base decision and planning of the treatment regimen in patients with brain masses.



ORAL PRESENTATIONS ABSTRACTS

O118-Resting State fMRI as a Tool in the Preoperative Intraoperative and Postoperative Functional Assessment of Patients with Brain Masses

*Vasileios K. Katsaros*¹, Evangelia Liouta², Constantin Roder³, Edyta Charyasz⁴, Uwe Klose⁴, Marco Soares Tatagiba³, Sotirios Bisdas⁴

*University of Athens Department of MRI Athens-Greece*¹ *University of Athens Department of Neurosurgery -Greece*² *University of Tübingen Department of Neurosurgery -Germany*³ *University of Tübingen Department of Neuroradiology -Germany*⁴

PURPOSE: Resting-state functional MRI (fMRI) has emerged as an important method for assessing neural networks, enabling extensive connectivity analyses between multiple brain regions. This method might provide important results in patient with brain masses preoperative, in an intraoperative setting of high-field intraoperative MR scanner, as well as postoperative. The aim of this study was to investigate the feasibility to perform resting state fMRI for the functional assessment of patients with brain masses.

MATERIALS AND METHODS: 67 patients were evaluated preoperative, 20 patients referred for a surgical resection of intracranial masses received total intravenous anesthesia with propofol 2 % and fentanyl and 23 patients were examine postoperative, by 1.5 MR Scanners. The intraoperative MR scanner is placed in an operating room with an adapted operating table (IMRIS, Nuernberg, Germany). Three-dimensional anatomical T1-, T2-weighted images and 3D-FLAIR for co-registration were acquired prior to the EPI measurements (TR 2 s, TE 50 ms, resolution 3,4*3,4*3,4 mm³, 220 repetitions).

Single-subject independent component (IC) analysis was performed with the GIFT toolbox (MIALAB, Mind research Network) using previously described methods and algorithms. Smoothed data were decomposed into 41 components. The components were assigned to published resting-state networks (RSN) components as far as possible.

RESULTS: In all patients, up to 12 from the 28 published RSN components could be identified, including auditory network (IC 17), sensorimotor networks (IC 07, 23, 24), default-mode networks (IC 25, 50, 53), attentional networks (IC 52, 55, 71, 72, 60) and visual networks (IC 46, 64, 67) . No reduction of the RSN intensity in comparison to subjects in resting wakefulness was found in the anesthetized patients.

CONCLUSIONS: Our results show that resting-state fMRI measurements can be performed for functional assessment of patients with brain masses preoperative, even when they are anesthetized, by intraoperative high-field MRI system, as well as postoperative, allowing us an objective evaluation of non-cooperative tumor cases.

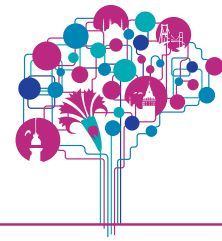
O119-Diffusion Kurtosis Imaging in Glioma Grading

*Vasileios K. Katsaros*¹, Yiannis Spandonis², Sotirios Bisdas³, George Stranjalis⁴

*University of Athens Department of MRI and Neuroradiology Athens-Greece*¹ *Philips Clinical Neuroscience -Greece*² *University of Tübingen Department of Neuroradiology -Germany*³ *University of Athens Department of Neurosurgery -Greece*⁴

PURPOSE: To evaluate Diffusion Kurtosis Imaging (DKI) in differentiating low from high grade gliomas.

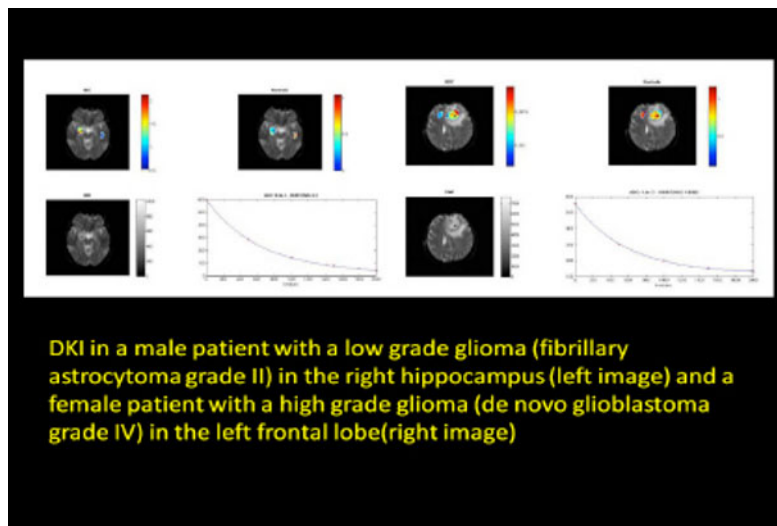
MATERIALS AND METHODS: Nineteen patients (11 female, 8 male) with histopathologically confirmed gliomas were included. Group A comprised 6 patients with low grade gliomas (all grade II) while group B comprised 13 patients (3 grade III and 10 grade IV). Diffusion Kurtosis Imaging (DKI) was applied in all patients, using five b-values (0, 500, 1000, 1500, 2000) in a 1.5T magnet, accomplishing the protocol used for brain masses evaluation. ADC maps and Kurtosis (K) maps were created. The maximum K ("hot spot method" - Kmax) and corresponding ADC were calculated for both groups. Average Kmax and corresponding ADC were calculated (Fig. 1 and 2). These data were compared among the tumor grades by using the Mann-Whitney test as well as to calculate sensitivity, specificity, PPV, NPV and the area under the curve of receiver operating characteristics (AUROC).



ORAL PRESENTATIONS ABSTRACTS

RESULTS: Average K max was 0.26 (± 0.09) and 0.83 (± 0.28) and Average corresponding ADC was 2.33 (± 0.77) and 1.13 (± 0.36) $\times 10^{-3}$ mm²/sec for low grade and high grade gliomas, respectively. Average MK values differed significantly between low and high grade gliomas ($p \leq 0.003$). With a Kmax threshold value of 0.44 sensitivity, specificity, PPV and NPV were 84.6%, 100%, 100% and 75%, respectively, resulting in AUROC of 0.923 to discriminate low from high grade gliomas.

CONCLUSIONS: Diffusion Kurtosis Imaging analysis is an accurate method for the differentiation between low and high grade gliomas.



O120-Practice and Pitfalls of Contrast Enhanced T2 FLAIR in

Neuroradiology

Howard Rowley¹

Univ. Wisconsin Radiology Madison-United States¹

PURPOSE: To describe applications, pitfalls, and protocol implementation tips for post-contrast T2 FLAIR in routine clinical practice and volunteer MRI protocols.

MATERIALS AND METHODS: Over the past 15 years our group has performed over 25,000 clinical and research volunteer brain MR exams using post contrast T2 FLAIR. Studies have been done at 0.7T, 1.5T, and 3T using 2D and 3D techniques on several commercial magnets. Over time we have modified our overall protocols and discovered practical tips and pitfalls to be aware of when using this sequence.

RESULTS: Post-contrast T2 FLAIR has become a routine sequence for all contrast-enhanced brain exams for a variety of reasons: 1) By moving this sequence into the first post contrast position of the protocol, and replacing one of the previously acquired post-contrast T1 series, we save about 5 minutes per brain exam. 2) Since we usually perform this series first after injection, this inserts a 3-5 minute delay before the post-contrast T1 is obtained, improving T1 enhancement. 3) This is the most sensitive sequence for the detection of leptomeningeal diseases (e.g. meningitis). 4) Contrast enhancement is seen on T2 FLAIR for the majority of intra-axial lesions, particularly those with long T2's, making it a useful composite image for common conditions (e.g. tumors, MS). 5) When implemented as a 3D FLAIR, this provides another important option for treatment planning, surgical navigation, and multi-modality fusion. Pitfalls and pointers are: 1) A pre-contrast T2 FLAIR is not needed. 2) This must always be used in conjunction with T1 post contrast series; some lesions (e.g. extra-axial or T2 short lesions) are not well seen. 3) The choroid plexus, slow-flowing venous structures, pial angiomas, and embryologic meningeal remnants are bright on this sequence and should not be mistaken for pathology. 4) For pituitary exams or protocols requiring early imaging or dynamic gadolinium injection, the T2 FLAIR can be placed later in the protocol without compromise.



ORAL PRESENTATIONS ABSTRACTS

CONCLUSIONS: Post-contrast T2 FLAIR offers the advantages of shorter protocols, increased sensitivity to meningeal diseases, improved T1 contrast performance, and produces a valuable composite image. It must be used in conjunction with standard post contrast T1 series and with knowledge of normal anatomical variants and pitfalls unique to this sequence.

O121-Manganese Enhanced Magnetic Resonance Imaging of the Chronic Manganese Toxicity in the Edaravone and Oxytocin Treated Rats

*Melda Apaydin*¹, Oytun Erbas², Vedat Evren³, Cem Callı⁴, Dilek Taskiran³

*KÇU IAEA Radiology Izmir-Turkey*¹ *Tokat University Physiology -Turkey*² *Ege University Physiology Turkey*³ *Ege University Radiology*⁴

PURPOSE: Manganese (Mn) is an essential mineral for producing energy from the nutrients by digesting the protein synthesized in the body. In constant fatigue, memory problems, infertility, weight loss, especially in children and infants with growth retardation symptoms are seen. In our study, chronic Mn poisoning in rats are investigated with the neuroprotective activity of Oxytocin, Edaravon, saline. **MATERIALS AND METHODS:** 220-250 gr., 30 female Sprague-Dwaley retrieved experiment rat. Rats (n = 20), exposed a period of one month to obtain chronic Mn toxicity. A group of rats is a control group (n = 10) received saline. While the first group (n = 10) treated with Edaravon, the other group (n = 10) is treated with Oxytocin for neuroprotection. All the groups and sham animals were imaged pre and post Mn with MRI (3T MRI scanner (Siemens Magnetom Verio, Germany).

RESULTS: The histopathology results showed Edaravon was the most neuroprotective agent. But Manganese enhanced (Mn) MRI with neuroprotective agents did not show any imaging difference.

CONCLUSION: Cellular biology to be Mn for metal, is an potential contrast agent for magnetic resonance imaging (MRI). MnMRG provides anatomical and physiological knowledge such as the neural circuits in the brain especially in the animal disease models. However, toxicity and neurological diseases caused by excess Mn. In this study, the neuroprotective effect of Edaravone has confirmed in histopathology. In the future Mn with some neuroprotective agents can be given for effective neuroimaging studies.

PARALLEL SCIENTIFIC PAPER PRESENTATIONS

(Research & Neuroradiological Sciences 2) 17:15 - 19:00

Topkapı B Hall

O122-Absolute Quantification of Brain Metabolite Concentration of Prefrontal Lobe and Hippocampus of Healthy Youth around taking Codeine Hydrochloride Using 1H MRS and LCModel

Hailong Lan¹, *Yeyu Xiao*¹, Renhua Wu¹

*Medical Imaging Department of The 2nd Affiliated Hospital of the Medical College of Shantou University Medical Imaging Department of The 2nd Affiliated Hospital of the Medical College of Shantou University -China*¹

PURPOSE: To offer experimental data reference for the further study of codeine habituation. **MATERIALS AND METHODS:** Twenty right-handed healthy youth were included (10 males, 10 females, mean age 24.9±1.9 years). MRS data were collected by GE 1.5T MR scanner, using point resolved spectroscopy (PRESS) sequence (TE/TR 30 ms/3000 ms). The regions of interest (ROI) were located over the bilateral prefrontal lobes and hippocampus, size of ROI was 2 cm × 2 cm × 2 cm. The data of spectra were post-processed by LCModel software and the concentrations of metabolites were ultimately measurement. The metabolite concentration of each people was analyzed by paired-samples t test of spss19.0.

RESULT: Before taking codeine phosphate, the concentration of NAA in left prefrontal lobe was higher than that in the same-sided hippocampus. After taking codeine phosphate, GPC increased in the left prefrontal lobe while Ins declined.



ORAL PRESENTATIONS ABSTRACTS

CONCLUSION: Codeine Phosphate can change the metabolites' concentrations alternations of the left prefrontal lobes. It is considered that the concentrations of GPC and Ins are related with the drug-dependent.

O123-Substantia Alba Demyelination and Brain Metabolite Alteration in Cognitive Impairment Patients

Meilian Wu ¹, Hailong Lan ¹, Yeyu Xiao ¹, Renhua Wu ¹

Medical Imaging Department of The 2nd Affiliated Hospital of the Medical College of Shantou University Medical Imaging Department of The 2nd Affiliated Hospital of the Medical College of Shantou University -China ¹

OBJECTIVE: Voxel-Based Morphometry (VBM) and magnetic resonance spectroscopy (MRS) were used to investigate the correlation between substantia alba demyelination and brain metabolites alteration of bilateral frontal lobe in cognitive impairment (CI) patients.

METHODS: This study was carried out in the 2nd Affiliated Hospital of Shantou University Medical College, Shantou, China between July 2013 and December 2013. 25 patients with CI in different levels according to the results of neuropsychological test and 15 healthy control subjects with normal neuropsychological test and without obvious substantia alba demyelination were enrolled in this study. The patients with CI were classified into two groups: CI with substantia alba demyelination group (n=11, Group A) and CI without substantia alba demyelination group (n=14, Group B). The MR study was performed on a 1.5T GE Signa HDX scanner. MRI imaging including axial

T1WI, T2WI, T2Flair and 3D-fsPGR were obtained for each subject. Single-voxels 1H spectra were acquired using point resolved selective spectroscopy sequence localized in bilateral frontal lobe. VBM analysis were performed after 3D-fsPGR scanning of each subject, recording the sizes of substantia alba demyelination, exploring the correlation between substantia alba demyelination and CI levels. Software Linear Combination of Model was used to quantitatively analyze the results of bilateral frontal lobe spectrum and measure the absolute concentration of N-acetylaspartate compound (NAA), creatine compound (Cr), choline-containing compounds (Cho), myo-Inositol (MI) and other metabolites, and relative concentration of NAA/Cr, Cho/Cr, MI/Cr, NAA/MI and other metabolites in bilateral frontal lobe in centrum semiovale levels. The correlation between the concentrations of the metabolites and the CI scores, the size alteration of substantia alba demyelination and the concentrations alteration of brain metabolites were investigated. Two sample t-test, one-way analysis of variance and Spearman analysis were used to analyze the measurement data.

RESULTS: In CI patients with substantia alba demyelination, wider substantia alba demyelination correlated with more severe cognitive impairment. MI concentration of Group A in right frontal lobe and Group B in bilateral frontal lobe were higher than normal control Group. mI/Cr of Group A in right frontal lobe was higher than normal control Group. Cr concentration and Cho/Cr rate between group did not reach statistical significance. NAA/MI of Group A and B were lower than normal control Group, and Group A < Group B. The cognitive impairment scores were negatively correlated with the size of substantia alba demyelination.

CONCLUSIONS: CI is closely related with substantia alba demyelination and decreased NAA/MI ratio, this indicated that they should share the same etiological factor. The neuronal loss and/or functional impairment of CI patients with substantia alba demyelination are more severe than that without substantia alba demyelination



ORAL PRESENTATIONS ABSTRACTS

O124-Grey Matter Alterations in Patients with Pantothenate Kinase Associated Neurodegeneration (PKAN)

Rea Rodriguez-Raecke ¹, Pedro Roa-Sanchez ², Herwin Speckter ³, Rafael Fermin-Delgado ³,
Eddy Perez-Then ⁴, Jairo Oviedo ³, Luis Suazo ², *Peter Stoeter* ³

Medizinische Hochschule Hannover Dep. of Neurology -Germany ¹ *CEDIMAT Dep. of Neurology and Neurosurgery -Dominican Republic* ² *CEDIMAT Dep. of Radiology -Dominican Republic* ³ *CEDIMAT Dep. of Science -Dominican Republic* ⁴

PURPOSE: Pantothenate Kinase Associated Neurodegeneration (PKAN) is a rare heritable disease marked by dystonia. In contrast to the well-known “Eye-of-the tiger” sign affecting the globus pallidus, little is known about other deviations of brain morphology, especially about grey matter changes.

MATERIALS AND METHODS: We investigated 29 patients with PKAN and 29 age-matched healthy controls using Magnetic Resonance Imaging (3T Achieva, Philips) and Voxel-Based Morphometry. Clinical symptoms were quantified according to the Burke-Fahn-Marsden scale.

RESULTS: As compared to controls, children with PKAN presented increased grey matter density in the putamen and nucleus caudatus and adults with PKAN presented increased grey matter density in the ventral part of the anterior cingulate cortex (Fig. 1). A multiregression analysis with dystonia score as predictor showed grey matter reduction in the cerebellum, posterior cingulate cortex, superior parietal lobule, pars triangularis and small frontal and temporal areas and an analysis with age as predictor showed grey matter decreases in the putamen, nucleus caudatus, supplementary motor area and anterior cingulated cortex.

CONCLUSIONS: The grey matter increases may be regarded as a secondary phenomenon compensating the increased activity of the motor system due to a reduced inhibitory output of the globus pallidus. With increasing age, the grey matter reduction of cortical midline structures however might contribute to the progression of dystonic symptoms due to loss of this compensatory control.

O125-Brain Magnetic Resonance pH Imaging MRS and CEST

Renhua Wu ¹, Zhuozhi Dai ¹, Zhiwei Shen ¹

Shantou University Medical Imaging Shantou-China ¹

An important advantage of magnetic resonance technology is its ability to non-invasively measure brain structure, function, and biochemistry. Despite much progress on anatomical imaging, clinically practical methods for functional and biochemical assessments are still under development. Our aim is to solve the key issue of theory impeding clinical utilization together and develop practical techniques for the noninvasive measurement of whole brain pH for use in the assessment of a range of diseases and conditions including schizophrenia, brain tumors, stroke, and others.

A very important biochemical property that has been known to be altered in many pathological states is tissue acid-base balance. Compared with normal tissue, extracellular pH (pHe) is normally lower in tumors, and intracellular pH (pHi) is often higher, as measured using microelectrodes. However, this method is invasive and not optimal for monitoring extracellular pH variables. Intracellular pH (pHi) and extracellular pH (pHe) are regulated in a dynamic steady state by protons entering and leaving cellular space, by the removal of waste products such as lactate, and the effect of internal buffer mechanisms such as HCO₃⁻ and CO₂ and reduced perfusion.

Recently, a diverse set of pH indicators has been described. Some of them show the character of pH-dependent chemical shift and others show the pH-dependent magnetization transfer as well as the pH-dependent relaxation, as seen in our initial work at Shantou University on pH MRI.



ORAL PRESENTATIONS ABSTRACTS

Non-invasive brain pH measurements have routinely relied on P-31 magnetic resonance (MR) spectroscopy techniques which require additional MR hardware, take too long to be clinically useful, and provide very limited spatial resolution. In recent years, other non-invasive methods to measure regional pH have been developed. These methods based on MR imaging (MRI) or MR spectroscopy (MRS) are used to measure intra- or extracellular pH either in vitro or in vivo. A promising technique is the chemical exchange saturation transfer (CEST).

O126-Brain Anatomical Substrates of Mirror Movements in Kallmann Syndrome

*Alessandro Salvalaggio*¹, R Manara², V Citton³, V Palumbo⁴, A D'Errico⁴, E Elefante⁴, E Cantone⁴, G Ottaviano⁵, E Napoli⁶, G Coppola⁴, F Di Salle², S Rizzati⁵, E De Carlo⁵, NA Greggio⁵, G Bonanni⁵, AA Sinisi⁴, A Favaro⁵

*University of Padova Neuroscience Padova-Italy*¹ *University of Salerno*² *IRCSS S.Camillo, Venezia*³

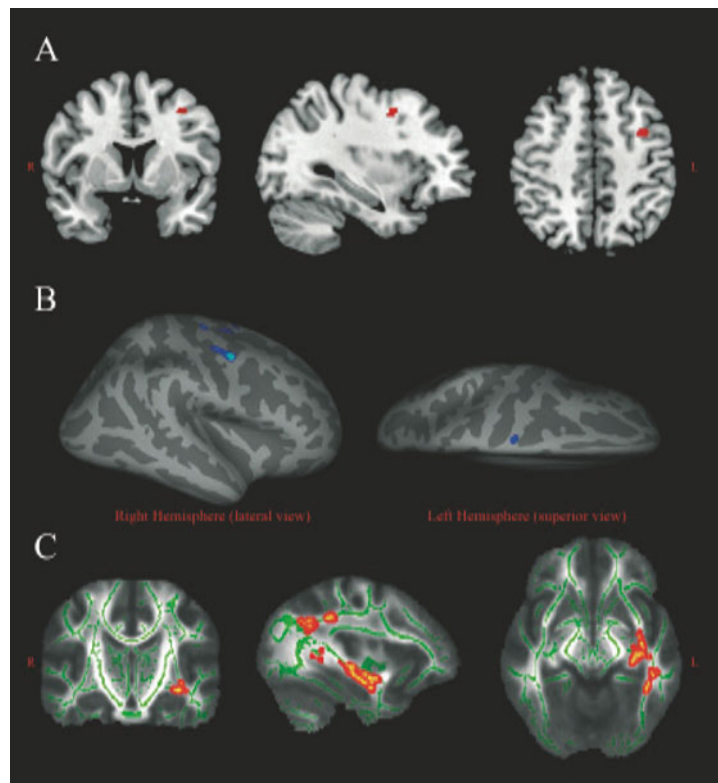
*University "Federico II" of Napoli*⁴ *University of Padova*⁵ *Medicanova diagnostic center, Battipaglia (SA)*⁶

PURPOSE: The aim of the present study was to investigate brain anatomical substrates of mirror movements in Kallmann syndrome by means of a panel of quantitative MRI analyses. Among male patients affected with Kallmann syndrome (a genetically determined disease due to defective neural migration leading to hypogonadotropic hypogonadism and hypo/anosmia) about 40% present with the peculiar phenomenon of mirror movements (involuntary movements mirroring contralateral voluntary hand movements). Several pathogenic hypotheses have been proposed, but the ultimate neurological mechanisms are still elusive.

MATERIALS AND METHODS: Forty-nine male Kallmann syndrome patients (mean-age 29.9 years; range: 15-55) underwent brain MRI (Achieva 1.5T, Philips). The study protocol included 3D-T1, FLAIR and diffusion tensor imaging (32 non-collinear gradient encoding directions; b-value = 800 s/mm²). Voxel based morphometry, sulcation, curvature and cortical thickness analyses and tract based spatial statistics were performed using SPM8, Freesurfer and FSL. All patients underwent a complete physical and neurological examination including the evaluation of mirror movements (according to Woods and Teuber criteria).

RESULTS: Kallmann syndrome patients presenting with mirror movements (16/49, 32%) displayed the following brain changes: 1) increased gray matter density in the depth of the left precentral sulcus behind the middle frontal gyrus; 2) decreased cortical thickness in the precentral gyrus bilaterally, in the depth of right precentral sulcus and in the posterior portion of the right superior frontal gyrus; 3) decreased FA in the left hemisphere involving the temporal lobe and peritrigonal white matter. No differences were shown by cortical curvature and sulcation analyses.

CONCLUSIONS: The composite array of brain changes observed in Kallmann syndrome patients with mirror movements likely represents the anatomical-structural underpinnings leading to the peculiar derangement of the complex circuitry committed to unilateral hand voluntary movements.





ORAL PRESENTATIONS ABSTRACTS

O127-The Shades of White Distinction between Edema and Gliosis with Quantitative Water Mapping

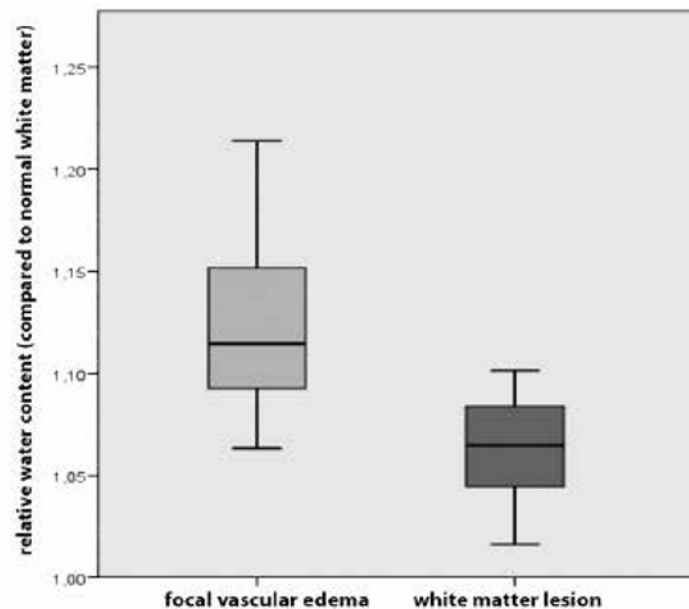
*Omid Nikoubashman*¹, Ann Maria Oros-Peusquens², Carolin Weiß³, Martin Wiesmann¹, John Shah²
University Hospital Aachen Neuroradiology Aachen-Germany ¹ *Forschungszentrum Jülich INM4 -Germany* ²
University Hospital Cologne Neurosurgery -Germany ³

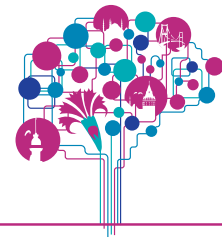
PURPOSE: Preliminary study to evaluate the value of quantitative water mapping in the differential diagnosis of white matter lesions (WML).

MATERIALS AND METHODS: We measured the absolute cerebral water content via quantitative magnet resonance imaging (MRI) using a previously published long TR-method (scan time: 7 minutes). We calculated the relative water content of a given region of interest relative to normal white matter. We then compared the water content of supposedly gliotic T2 (-FLAIR) hyperintense WML to areas with vascular white matter edema caused by focal mass effect.

RESULTS: Overall, we analyzed 6 elderly patients with WML and/or cerebral edema. Mean relative water content of supposedly gliotic WML was 1.06, ranging from 1.02 to 1.10 (median: 1.06; standard deviation: 0.03). Mean relative water content of areas with vascular edema was 1.13, ranging from 1.06 to 1.21 (median: 1.11; standard deviation: 0.05). Water content of gliotic and edematous areas differed significantly ($p < 0.001$, Student's t test). According to receiver operating characteristic analysis, values greater than 1.10 are likely to represent edema with a sensitivity and specificity of 75% and 100%, respectively (area under the curve = 0.891; $p < 0.001$).

CONCLUSIONS: Although the current study is based on a small sample, our findings suggest that an increase of white matter water content greater than 10% is likely to correspond to edema and that it may be possible to reliably distinguish gliotic from edematous areas in the white matter using quantitative MRI.





ORAL PRESENTATIONS ABSTRACTS

O128-Preliminary Results Of Tissue Contrast Optimization Of The Brainstem Using Phase Difference Enhanced (PADRE) Post Processing of 3D Gradient Echo (GE) Images at 1.5T.

*Nandor Pinter*¹, Joseph Fritz¹, Thomas Perkins², Laszlo Mechtler³

*Dent Neurologic Institute Department of Neuroimaging Amherst-United States*¹ *Philips Healthcare -United States*² *Dent Neurologic Institute -United States*³

PURPOSE: To create enhanced tissue contrast for brainstem structures by post processing routine and high resolution 1.5T 3D GE datasets with PADRE.

MATERIALS AND METHODS: 3D GE scans were acquired on seven volunteers (4 males, 3 females, mean age: 34.5years) using a 1.5T Philips Intera scanner. Scan parameters were TR:44 ms, TE:38ms, flip angle:30°. Spatial resolution was 1x1x2mm for standard resolution scans (SR) of the whole brain and 0.4x0.4x1.4mm for high resolution (HR) scans of midbrain, pons and adjacent structures. Data was reconstructed with standard PADRE parameters optimized for vessel visualization (VO) and a new set of parameters (PP) optimized by our group for enhancing tissue contrast. Contrast between structures was calculated for magnitude and both versions of PADRE images. Visual assessment was performed by a radiologist.

RESULTS: Contrast of red nucleus and substantia nigra was the highest with PP when compared to magnitude (M) and VO images on both SR and HR scans.

On HR images PP was able to differentiate pars compacta and pars reticulata of substantia nigra, the crural fibers and pallidal-nigral pathway (fascicula nigrale). Red nucleus was heterogeneous. Other structures were clearly visualized as well, likely representing the spinothalamic tract, medial lemniscus, the caudal part of corticopontine fibers and the pontocerebellar fibers in the lower midbrain and upper pons.

CONCLUSION: By selectively changing the phase differences we were able to enhance tissue contrast on both SR and HR images when compared to standard susceptibility weighted imaging (SWI) reconstructions. The combination of HR image acquisition with optimized PADRE settings was able to create a more detailed map of the brainstem at 1.5T than routine clinical scans or conventional SWI reconstructions.

O129-Isolated Congenital Superior Oblique Paresis a High Resolution MRI Phenotype Study

*Indran Davagnanam*¹, Annegret Dahlmann-Noor², Jane Sowden³, John Thornton⁴, Tarek Yousry⁴

*UCL Institute of Neurology Brain Repair & Rehabilitation London-United Kingdom*¹ *UCL Institute of Ophthalmology Ocular Biology and Therapeutics -United Kingdom*² *UCL Institute of Child Health Developmental Biology and Genetics -United Kingdom*³ *University College London Hospitals Lysholm Department of Neuroradiology -United Kingdom*⁴

PURPOSE: Isolated congenital superior oblique paresis (CSOP) is the commonest congenital cranial nerve palsy. Magnetic resonance imaging (MRI) studies have either demonstrated SO hypoplasia or fourth cranial nerve (CN-IV) absence in 73%-100% of individuals with CSOP. We develop a high-resolution imaging protocol to both visualise and correlate the cisternal segment of CN-IV with quantitative SO cross-sectional areas in individuals with CSOP and age-matched controls.

MATERIALS AND METHODS: Ten adult CSOP and 11 controls underwent a standardised 3-Tesla MRI high-resolution imaging protocol of the extra-ocular muscles (EOM); coronal T1-W SE 2mm sections, AT: 4min 15s and coronal STIR 2mm sections, AT: 6min 3s and cisternal segment of CN-IV; CISS 0.35mm isotropic sections, AT: 9min 39s.

All images were reviewed by an experienced neuroradiologist blinded to diagnosis. A region of interest (ROI) was semi-automatically applied to each maximal EOM cross-sectional area in the coronal plane. CISS images were analysed using on MPRs to visualise the cisternal segment of CN-IV in 3 orthogonal planes, recording presence and laterality.

RESULTS: Full MRI datasets are available for 7 CSOP and 13 controls (mean age: 38 ±12.2 and 34.65 ±10.8 years). Cisternal CN-IV was visualised in all controls, and was unilaterally absent in 3 and thinner in 1/7 CSOP.



ORAL PRESENTATIONS ABSTRACTS

Clinical CSOP and particularly MRI CN-IV abnormality were associated with reduced ipsilateral SO mean cross-sectional area (MCSA) and increased SO MCSA variability, reflected in greater SD (table 1).

CONCLUSION: Patients with clinical CSOP demonstrate absent CNIV, reduced SO maximal cross-sectional areas but increased variability compared to healthy controls.

Table 1. MRI findings in controls and patients with CSOP

All measurements in mm ²	Healthy Controls (n=13)	Clinical CSOP with abnormality of CN-IV (n=4)	MRI findings all CSOP (n=7), incl. one bilateral case
Mean maximal cross-sectional area of SO	23.1 (SD 2.7) Range: 19.1 - 28.5	Ipsilateral SO 14.5 (SD 6.5) Contralateral SO 29 (SD 6)	Affected SO 19.7 (SD 7.3) Non-affected SO 28.6 (SD 5.6)
Mean inter-orbital difference in SO maximal cross sectional area	2.7 (SD 2.1)	14.7 (SD 3)	11 (SD 3)

O130-Ex vivo Demonstration of the Fourth Cranial Nerve Nucleus on High Resolution 3T 7T and 9.4T MRI

*Indran Davagnanam*¹, John Thornton², Penny Gowland³, Tarek Youstry²

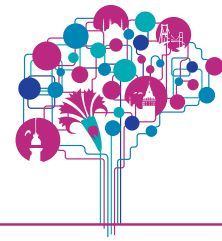
*UCL Institute of Neurology Brain Repair & rehabilitation Unit London -United Kingdom*¹ *University College London Hospitals Lysholm Department of Neuroradiology -United Kingdom*² *University of Nottingham Sir Peter Mansfield Magnetic Resonance Imaging Unit -United Kingdom*³

PURPOSE: Demonstration of the detailed cytoarchitectural anatomy of the brain stem is currently achieved through histo-pathological sectioning and staining. Experimental high-resolution ex-vivo 9.4-Tesla MRI imaging has been able to demonstrate the anatomy of these structures. The smallest of these structures is the fourth cranial nerve nucleus (CN-IV) which may be involved in inherited conditions. We aim to demonstrate and accurately localise CN-IV in ex-vivo brainstem specimens on 3T and 7T clinical MRI, correlating these with ultrahigh resolution 9.4T MRI.

MATERIALS AND METHODS: A whole ex-vivo brainstem specimen sectioned from the mesencephalon at the level of the red nuclei to the mid-Pons was scanned on clinical 3T, 7T and non clinical 9.4T MRI units. The imaging protocol at:

1. Siemens Trio 3T: 3D Proton-density weighted gradient echo 0.8-mm isotropic resolution/2 averages, TR/TE=19/5.58ms, AT: 2x17min
2. Philips Achieva 7T: 2D Proton-density weighted gradient echo 0.5-mm in-plane resolution, TR/TE=500/16ms, AT: 3hr15min.
3. VNMR5 Varian 9.4T: Fast spin echo multislice sequence: TR/TE=3500/35ms, 100x100µm in-plane resolution, 0.5mm slice thickness AT:6hr30min

RESULTS: One whole midbrain and upper pontine ex-vivo specimen was imaged on 3T, 7T and 9.4T MRI units. Two further half ex-vivo specimens have been obtained and are scheduled to be similarly imaged. Of the completed scans, there is clear visualisation of CN-IV, located as paired structures just dorsal to the medial longitudinal fasciculi at the level of the decussation of the superior cerebellar peduncle fibres (Figure 1) at all 3 field strengths. The intra-parenchymal course of the fourth nerve fasciculi, decussation at the superior medullary velum and proximal cisternal segments of the fourth cranial nerve were clearly demonstrated on 7T and 9.4T.



ORAL PRESENTATIONS ABSTRACTS

CONCLUSIONS: Demonstration of the smallest of the cranial nerve nuclei is possible on 3T and 7T clinical MRI units. This may provide valuable novel insights into inherited and acquired congenital cranial nerve nuclei pathologies such as congenital superior oblique palsy.

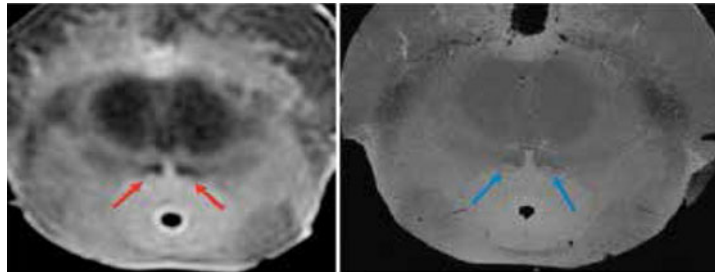


Figure 1: Ex-vivo 4th cranial nucleus at 3T (red arrows) and 9.4T (blue arrows)

O131-The Utility of Gadoterate Meglumine Enhanced MRI in Adult and Pediatric Patients with Central Nervous System Lesions (SENTIO study)

*Raphaelle Souillard*¹

*Centre hospitalier Sainte Anne Radiology Paris-France*¹

PURPOSE: To demonstrate superiority of gadoterate meglumine-enhanced MRI over unenhanced images for visualization of brain and spinal lesions in adults and children.

MATERIALS AND METHODS: Multicenter, randomized, double-blind, fixed-sequence [unenhanced T1 & T2 MRI followed by either gadoterate meglumine (Dotarem, 0.1 mmol/kg) or gadopentetate dimeglumine (Magnevist, 0.1 mmol/kg) T1-enhanced MRI], study. Pediatric patients (aged ≥ 2 years) were assigned to the gadoterate meglumine group only. MR images of all patients were read by one on-site radiologist and three off-site blinded independent readers.

The primary endpoint was lesion visualization with gadoterate meglumine enhanced MRI comparing unenhanced images in up to five of the largest lesions utilizing three co-primary endpoints: border delineation, internal morphology and degree of contrast enhancement.

Main secondary criteria were evaluated on-site for lesion visualization and both on-site and off-site for: level of diagnostic confidence, image quality, signal intensity, number of lesions, and comparison of gadoterate meglumine and gadopentetate dimeglumine for diagnostic efficacy. Clinical safety was assessed through the reporting of adverse events (AEs), injection site intolerance reactions, changes in vital signs, electrocardiogram recordings and laboratory measures.

RESULTS: A total of 402 patients were evaluable: 364 adults (245 gadoterate meglumine, 119 gadopentetate dimeglumine) and 38 children.

The primary endpoint was significantly superior ($p < 0.001$) as well as for all three co-primary endpoints for all independent readers when comparing enhanced images to unenhanced images.

No statistically significant differences between gadoterate meglumine and gadopentetate dimeglumine were observed for all 3 co-primary variables for the 3 independent readers.

Analysis of pediatric group for all 3 independent readers, showed that mean scores for each of the three co-primary endpoints were higher for “enhanced” compared to “unenhanced” images. Both contrast agents were well tolerated. Related AEs were reported in 3.8% adult gadoterate meglumine and in 7.7% gadopentetate dimeglumine patients. The most common AEs were injection site pain, headache and nausea. No related serious AEs occurred.

CONCLUSION: Gadoterate meglumine significantly improved lesion visualization over unenhanced MRI alone for CNS lesions and provided a good general safety profile in both adults and children.



ORAL PRESENTATIONS ABSTRACTS

O132-Correlating the Structural Impairment of Hippocampus with Cognitive Disorders in Parkinson's Disease a 3T MRI Voxel Based Morphometry and Diffusion Tensor Imaging Study on 80 Patients

*Bruno Law-ye*¹, Clémentine Vignon², Pierre Berroir², Marie Vidailhet³, Lydia Yahya-Cherif², Stéphane Lehericy⁴

*Pitié-Salpêtrière Neuroradiology Paris-France*¹ *ICM- Pitié-Salpêtrière CENIR -France*² *Pitié-Salpêtrière Neurology -France*³ *Pitié-Salpêtrière Neuroradiology, CENIR -France*⁴

PURPOSE: Parkinson's disease is the second most common neurodegenerative disease. Apart from motor symptoms, cognitive disorders are often seen and are among the most frequent non-motor aspects of the disease. These troubles mostly include attentional and executive disorders but also memory disorders.

Our goals were to assess the structural impairment of hippocampus in Parkinson's disease (PD), by means of voxel-based morphometry and diffusion tensor imaging (DTI) in 3 Tesla MRI and to determine its relation to mild cognitive impairment (MCI) in PD.

MATERIALS AND METHODS: Our study population was composed of 55 parkinsonian patients (PD) and 25 healthy volunteers (HV), included prospectively between April 2010 and September 2012. The diagnosis of idiopathic Parkinson disease was assessed by expert neurologists in our center before their inclusion and all patients were tested by a neuropsychologist. The PD patients were divided into two groups: patients with mild cognitive impairment (MCI, n = 23) and without MCI (non MCI, n = 32). All patients underwent brain MRI (3 Tesla, Trio TIM 32 channels, Siemens) including 3DT1 MP-RAGE, 3D T2* and diffusion tensor imaging. The hippocampus were segmented automatically by Freesurfer® software. Hippocampal segmentations in 6 patients (7,5%) needed manual corrections. Pre-treatments of the T1 and DTI images were performed using FSL® non-linear image registration tool. The images were then analyzed with voxel-based-morphometry and DTI, providing us the data for hippocampal volumes, fractional anisotropy (FA) and mean diffusivity (MD)

RESULTS: Hippocampal MD was significantly increased in PD patients vs HV (0.8496 vs 0.8217 mm²/s; p= 0.01).

MD was significantly increased in MCI PD patients when compared with non-MCI PD patients (0.8564 vs 0.8450 mm²/s; p=0.03).

We did not find a significant difference of hippocampal volume in PD vs HV.

There was however a trend toward a decreased volume in MCI vs non-MCI patients (4057,2 vs 4214,1 cubic millimeters; p= 0.11)

There was no significant modification of FA in PD vs HV or MCI vs non-MCI.

CONCLUSION: Hippocampal MD was significantly increased in PD patients compared with healthy volunteers, underlining the specific impairment of this structure in Parkinson's disease. Moreover, within the PD group, MD was significantly increased in the MCI vs the non-MCI. These results seem to indicate that hippocampal MD could be a specific and reliable biomarker for Parkinson's disease cognitive disorders.

O133-Optimal Concentration of Gadolinium based Contrast Agent on Contrast Enhanced MR Imaging Sequences in Phantoms.

*Jae Kyun Kim*¹, Seung Tae Woo², Jun Soo Byun¹, Woong Jae Lee¹, Bon Chul Ha¹

*Chung-Ang University Hospital Radiology Seoul-Korea, South*¹ *Bayer HealthCare Radiology & Interventional -Korea, South*²

PURPOSE: The purpose of this study was to find optimal concentration of gadolinium-based contrast agent (GBCA) showing the maximum signal intensity on common contrast enhanced magnetic resonance (MR) imaging sequences.



ORAL PRESENTATIONS ABSTRACTS

MATERIALS AND METHODS: Approval by the institutional review board was not required because our study was in vitro and patients were not involved. Spin echo (SE) T1-weighted, 3D Fast low angle shot (FLASH) and T2 fluid attenuated inversion recovery (FLAIR) sequences were performed in phantoms at 1.5 and 3.0 T. We evaluated various concentrations of gadolinium-based contrast agent on each three MR imaging sequences. Gadobutrol, the most commonly used GBCA in our practice, was imaged at thirty two dilutions on each three MR imaging sequences: 0.0125, 0.025, 0.05, 0.1, 0.2, 0.3, 0.4, 0.5, 0.6, 0.7, 0.8, 0.9, 1, 2, 3, 4, 5, 6, 7, 8, 9, 10, 20, 30, 40, 50, 60, 70, 80, 90, 100, 200 mmol/L. Oil and served as controls.

RESULTS: Peak signal intensities were obtained at 1, 5 and 0.4 mmol/L of gadolinium on SE T1 (repetition time (TR): 500, echo time (TE): 9.8, flip angle (FA): 90), 3D turbo FLASH (TR: 5.26, TE: 1.8, FA: 10) and T2 FLAIR sequences (TR: 9000, TE: 80, FA: 90, inversion time (TI): 2500) at 1.5T. At 3.0 T, peak signal intensities were also obtained at 1, 5 and 0.4 mmol/L of gadolinium on SE T1 (TR: 550, TE: 10, FA: 90), 3D turbo field echo (TFE) T1 (TR: 7.65, TE: 3.68, FA: 8) and T2 FLAIR sequences (TR: 9000, TE: 120, FA: 90, TI: 2500).

CONCLUSIONS: The maximum signal intensity was obtained with lower gadolinium concentration on T2 FLAIR sequence compared with T1 sequences at both 1.5 T and 3.0 T. Optimal concentration of GBCA on SE T1 sequence was lower than that on 3D FLASH T1 sequence at both 1.5 T and 3.0 T. Because concentration of gadolinium in patient's blood vessels decreases with time, it is appropriate to conduct 3D FLASH T1 first, SE T1 next and T2 FLAIR lastly.

O234-Cortical Reorganization of Pain Processing in Patients with Chronic Pelvic Pain Syndrome

*Christian Weisstanner*¹, Livio Mordasini², George N Thalmann³, Christian Rummel⁴, Rajeev K Verma⁴, Eugenio Abela⁵, Peter Jüni⁶, Andrea Federspiel⁷, Thomas M Kessler⁸, Roland Wiest⁴
Support Center for Advanced Neuroimaging (SCAN), University Institute of Diagnostic and Interventional Neuroradiology, Inselspital, University of Bern Departement of Radiology, Neuroradiology and Nuclearmedicine Bern-Switzerland¹ Clinic for Urology, St. Gallen Hospital, St. Gallen, Switzerland -Switzerland² Department of Urology, Inselspital, University of Bern, Bern,Switzerlande -Switzerland³ Support Center for Advanced Neuroimaging (SCAN), University Institute of Diagnostic and Interventional Neuroradiology, Inselspital, University of Bern -Switzerland⁴ Department of Neurology, Inselspital, University of Bern, Bern, Switzerland -Switzerland⁵ Clinical Trial Unit, University of Bern, Bern, Switzerland -Switzerland⁶ Department of Psychiatric Neurophysiology, University Hospital of Psychiatry and University of Bern, Bern, Switzerland -Switzerland⁷ Neuro-Urology, Spinal Cord Injury Center & Research, University of Zürich, Balgrist University Hospital, Zürich, Switzerland -Switzerland⁸

PURPOSE: Chronic pelvic pain syndrome (CPPS) impairs the life of millions of people worldwide and is a serious economic burden for every health care system. Many CPPS patients are refractory and therapies that influence central pain processing pathways have not been in regular use up to now. Recently, sono-electromagnetic therapy was introduced as a non-invasive neuromodulative option for treating CPPS. The goal of this study was to longitudinally investigate the effect of sono-electro-magnetic therapy for CPPS on cortical reorganization and modulation of regional cerebral blood flow in a prospective study.

MATERIALS AND METHODS: In a randomized, placebo-controlled, double-blind single center trial, men with CPPS were randomly assigned to treatment for 12 weeks with either sono-electromagnetic or placebo therapy. We assessed longitudinal relative gray matter volume (rGMV) changes associated with verum versus placebo therapy using voxel-based morphometry. We further investigated longitudinal cortical perfusion changes using pseudocontinuous arterial spin labeling (pCASL). **RESULTS:** After 12 weeks of treatment, significant longitudinal increases of cortical cerebral blood flow (CBF) were detected in the somatosensory cortex in patients with verum therapy and CBF was up-regulated in the left prefrontal cortex in the placebo group. Treatment responders revealed a CBF down-regulation in the prefrontal cortex (PFC) and anterior cingular cortex (ACC), a CBF up-regulation in the DLPFC and an increase of rGMV in the Ncl. accumbens (Nac). In nonresponders, CBF up-regulation in the hippocampus was found (all p<0.001 unc.).



ORAL PRESENTATIONS ABSTRACTS

CONCLUSIONS: Decreased perfusion in the ACC and PFC associated with rGMV increase in the Nac suggests a central neuromodulation effect related to plasticity in the mesolimbic dopaminergic pathway associated with reduced emotional pain processing in CPPS patients. Similar effects of verum vs. placebo therapy implicate an individual anticipation of an analgesic effect and open a path for central modulating therapy strategies in CPPS. **Funding:** This study has been supported by the Inselspital, Bern University Hospital.

O233-Meta Analytical Comparison of Voxel Based Morphometry Studies in Migraine

*Hsu-Huei Weng¹, Yuan-Hsiung Tsai¹, Chih-Feng Chen¹, Jiann-Der Lee², Shuu-Jiun Wang³, Chun-Yuh Yang⁴
Chang Gung Memorial Hospital at Chiayi, Chang Gung University College of Medicine Dept. of Diagnostic Radiology Chiayi County-Taiwan 1 Chang Gung Memorial Hospital at Chiayi, Chang Gung University College of Medicine Department of Neurology -Taiwan 2 Taipei-Veterans General Hospital, Taipei The Neurological Institute -Taiwan 3 College of Health Sciences, Kaohsiung Medical University, Kaohsiung Faculty of Public Health - 4*

PURPOSE: Voxel-based morphometry (VBM) has been widely used to detect structural differences in the density or volume of gray matter. Neuroimaging meta-analysis methods are available recently. The authors reviewed the literature on use of VBM in imaging migraine studies to identify specific structural differences in patients with migraine, compared with healthy subjects. The authors looked for consistently reported results of regional differences in gray matter in migraine.

MATERIALS AND METHODS: The authors used PUBMED to retrieve articles published from January 2000 to January 2014. The authors included all VBM researches evaluating patients with migraine using GingerALE procedure to analyze significant differences reported in all VBM studies of

migraine patients and compared the findings of studies to index gray matter differences. **RESULTS:** People with migraine had regional gray matter reduction in both sides of precentral and medial frontal gyri and right middle frontal gyrus.

CONCLUSIONS: Gray matter reductions in migraine patients occur in bilateral precentral and medial frontal and right middle frontal regions, which may be related to the pain processing abnormalities seen in this patient population.



ORAL PRESENTATIONS ABSTRACTS

Thursday, September 11, 2014

PARALLEL SCIENTIFIC PAPER PRESENTATIONS

(Adult NR 2) 17:15 - 19:00

Marmara Hall

O134-Dynamic Susceptibility Contrast enhanced (DSC) MR based Perfusion Imaging to Differentiate Recurrence from Stable Disease in Brain Gliomas

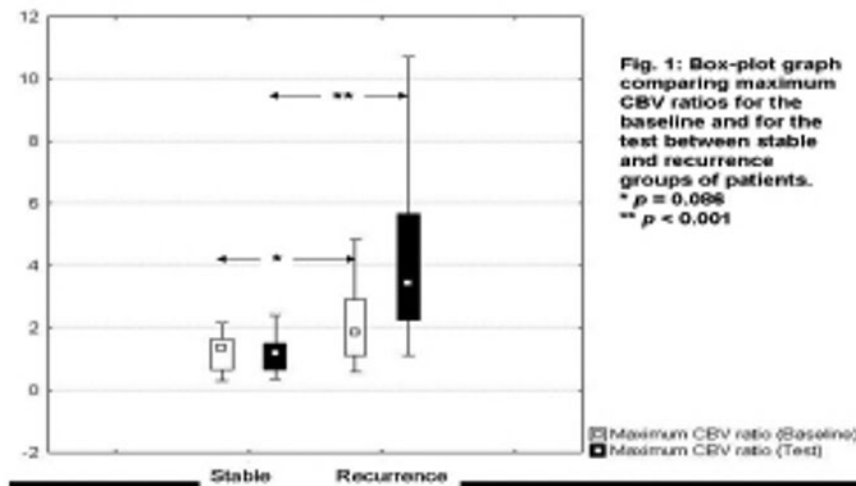
*Niloufar Sadeghi*¹, Jean Christophe Lebrun¹, Julie Absil¹, Thierry Metens¹, Serge Goldman²
*Erasm Hospital-ULB Radiology Brussels-Belgium*¹ *Erasm Hospital-ULB Nuclear Medecine -Belgium*²

PURPOSE: To evaluate Dynamic Susceptibility Contrast-enhanced (DSC) MR-based perfusion imaging for early detection of tumor progression or tumor recurrence during glioma follow-up

MATERIALS AND METHODS: This retrospective study included 38 patients aged between 17 and 59 (mean: 38 ± 9) with histologically proven brain gliomas who were followed-up by MR-imaging. All patients had at least two consecutive MR studies including Dynamic Susceptibility Contrast-enhanced perfusion imaging during their follow-up. The first MR study was considered as the baseline and the second MR study as the test. Morphologic MR images were co-registered with perfusion maps, therefore Cerebral Blood Volume (CBV) ratios could be measured in the lesion areas defined by T2/FLAIR and/or T1 with contrast signal abnormality. Maximum CBV ratios have been recorded for further analysis. All patients were followed for at least 6 months after the second MR study (test). Maximum CBV ratios were compared between patients with stable disease and those with recurrence. Receiver operating characteristic curve for maximum CBV ratios was generated for the differentiation between recurrent and stable disease.

RESULTS: Among the 38 patients included, 26 patients had low grade gliomas and 12 patients had high grade gliomas. Sixteen patients showed recurrence based on clinical and/or histological follow-up, whereas 22 patients remained stable. The time interval between the two MR examinations including DSC sequence was 8.55 ± 7.29 months. On the test MR study, maximum CBV ratios were statistically higher in the recurrence group compared to the stable group ($p < 0.001$), whereas on the baseline MR study, there was no significant difference of CBV ratios between the two groups ($p = 0.086$) (Figure 1). The cut-off of 1.45 of maximum CBV ratio showed the best accuracy in

distinguishing between recurrence and stable disease (sensitivity:100%; specificity:73.9%).
CONCLUSION: DSC perfusion MR may be helpful for early detection of recurrence during the follow-up of brain gliomas.





ORAL PRESENTATIONS ABSTRACTS

O135-Preoperative Evaluation of Brain Tumors Added Value of 320

Section Dynamic Volume CT to Standard 3T MR Images

*Toshinori Hirai*¹, Yasuhiko Iryo¹, Hideo Nakamura², Mika Kitajima¹, Eri Hayashida¹, Minako Azuma¹, Seitaro Oda¹, Daisuke Utsunomiya¹, Yoshinori Shigematsu¹, Yasuyuki Yamashita¹

*Kumamoto University Diagnostic Radiology Kumamoto-Japan*¹ *Kumamoto University Neurosurgery -Japan*²

PURPOSE: The purpose of this study was to assess whether 320-section dynamic volume CT (DVCT) images add value to the standard 3T MR images in the preoperative evaluation of brain tumors. **MATERIALS AND METHODS:** Fifteen patients (5 men, 10 women; age 28-78 years, mean 58 years) with brain tumors underwent a 320-section DVCT scan in addition to the preoperative MR protocol study. The tumors included glioblastoma in 5 patients, meningioma in 4, oligodendroglioma in 3, and hemangiopericytoma and ependymoma in 1 each. CT images obtained from the dynamic volume scan included pre- and post-contrast CT, 3D CT angiography (CTA), 4D CTA, 3D CT venography (CTV), and perfusion CT. The preoperative MR imaging sequences included T1-, T2-, diffusion-weighted, FLAIR, post contrast T1-weighted images, MR angiography and perfusion imaging. Two radiologists independently evaluated the CT and MR imaging studies. One radiologist measured relative cerebral blood volume (rCBV) in the tumor and contralateral brain on CT and MR perfusion. Referring neurosurgeons were questioned as to whether the information gained from the 320-section DVCT, as compared to the 3T MR images, was useful for surgical treatment.

RESULTS: The DVCT was superior to 3T MRI for visualization of arterial feeders in 3/15 tumors (20%), for delineation of venous structures in 12 (80%), and for understanding the relationship of the tumor to adjacent arteries and venous structures in 6 (40%). The average standardized rCBV value was 12.5 ± 2.30 for MR perfusion and 8.7 ± 2.68 for CT perfusion. There was a good correlation in standardized rCBV values between CT and MR perfusion ($r = 0.88$, $p < 0.001$). In 10/15 (67%) patients who underwent surgery, the additional information obtained using 320-section CT was useful for surgical treatment, especially for hypervascular tumors.

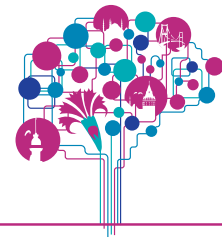
CONCLUSION: 320-section DVCT images are a useful supplement to 3T MRI for preoperative evaluation of brain tumors.

O136-Diagnostic Utility of Dynamic Susceptibility weighted Contrast enhanced Perfusion MR Imaging for the Peritumoral Region in Differentiating Glioblastomas from Solitary Brain Metastases.

*Andres Server*¹, Tone E.D. Orheim², Bjørn A. Graff³, Roger Josefsen⁴

*Oslo University Hospital Section of Neuroradiology, Department of Radiology and Nuclear medicine Oslo-Norway*¹ *Oslo University Hospital Interventional Centre -Norway*² *Vestre Viken Hospital Trust -Norway*³ *Oslo University Hospital Department of Neurosurgery -Norway*⁴

PURPOSE: Differentiation of glioblastomas and solitary brain metastases is an important clinical problem because the treatment strategy can differ significantly. The purpose of this study was to investigate the value of dynamic susceptibility-weighted contrast-enhanced perfusion MR imaging (DSC-MRI) in differentiating glioblastomas from solitary brain metastases in peritumoral regions. **MATERIALS AND METHODS:** A prospective study of 61 patients (40 GBMs and 21 metastases) was performed at 3T using DSC-MRI. Normalized rCBV and rCBF from tumoral (rCBVt, rCBFt), peri-enhancing region (rCBVe, rCBFe) and by dividing the value in the tumor by the value in the peri-enhancing region (rCBVt/e, rCBFt/e) were calculated. Statistical comparisons of data sets were performed with the use of Student's t test or by the Mann-Whitney rank sum test ($p < .05$). Receiver operating characteristic (ROC) curve analysis was performed for each of the variables. Sensitivity, specificity, positive predictive value (PPV), and negative predictive value (NPV) as well as accuracy were reported for the optimal thresholds.



ORAL PRESENTATIONS ABSTRACTS

RESULTS: The rCBVe and rCBFe were significantly greater in GBMs compared with those of metastases. The optimal cutoff value for differentiating GBM from metastasis was 0.80 which implies a sensitivity of 95%, a specificity of 92%, a PPV of 86%, and a NPV of 97% for rCBVe ratio. **CONCLUSION:** Our results support the hypothesis that DSC-MRI can detect infiltration of tumor cells in the peri-enhancing region. rCBVe, rCBVt/e and rCBFe, rCBFt/e from the peri-enhancing regions of the tumor can improve diagnostic performance in differentiating glioblastomas from solitary brain metastases.

O137-Which is the Best Advanced MR Imaging Protocol for Predicting Recurrent Metastatic Brain Tumor following Gamma Knife Radiosurgery Focused on Perfusion Method

*Won Jung Chung*¹, Ho Sung Kim², Choong Gon Choi², Sang Joon Kim², Seung Chai Jung²

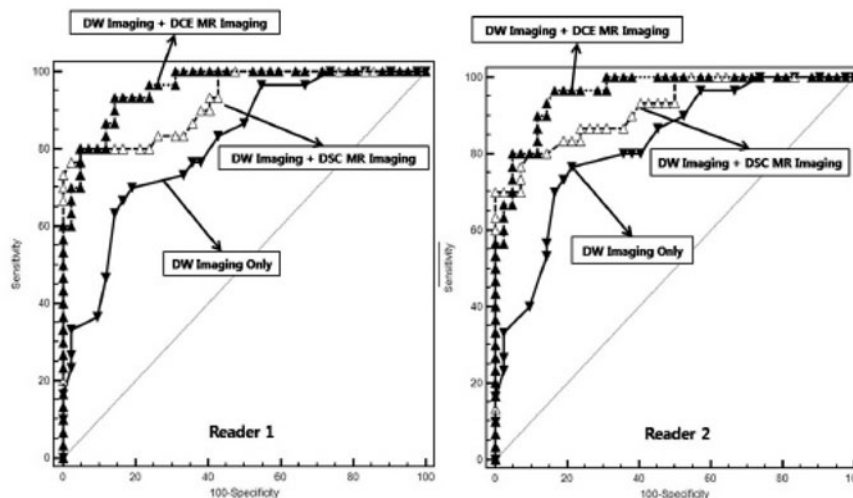
*Asan Medical Center Radiology of Health Screening and Promotion Center Seoul-Korea, South*¹ *Asan Medical Center Radiology and Research Institute of Radiology -Korea, South*²

PURPOSE: High spatial resolution of dynamic contrast-enhanced (DCE) MR imaging allows characterization of heterogenous tumor microenvironment. Our purpose was to determine which is the best advanced MR imaging protocol, focused on additional MR perfusion method, for predicting recurrent metastatic brain tumor following gamma-knife radiosurgery (GKRS).

MATERIALS AND METHODS: 72 consecutive patients with post-GKRS metastatic brain tumor, were enrolled. Two readers independently calculated the percentile histogram cutoffs for normalized cerebral blood volume (nCBV) from dynamic susceptibility contrast (DSC) imaging and initial area under the time signal-intensity curve (IAUC) from DCE imaging, respectively. Area under the receiver operating characteristic curve (AUC) and interreader agreement were assessed.

RESULTS: For differentiating tumor recurrence (TR) from treatment-related effect (TE), adding DCE imaging to diffusion-weighted imaging (DWI) significantly improved AUC from 0.814 to 0.951 for reader 1 and from 0.822 to 0.962 for reader 2, respectively. There was no significant difference of AUC between the combination of DWI with DSC imaging and the combination of DWI with DCE imaging for both readers. With the combination of DWI and DCE imaging, the sensitivity and specificity were 93.3% and 85.7% for reader 1 and 96.7% and 85.7% for reader 2, respectively. The intraclass correlation coefficient (ICC) between readers was highest for calculation of the 90th percentile histogram cutoffs for IAUC (ICC, 0.87).

CONCLUSIONS: Adding perfusion MR imaging to DWI significantly improves the prediction of recurrent metastatic tumor, however, the diagnostic performance is not affected by selection of either DSC or DCE MR perfusion method.





ORAL PRESENTATIONS ABSTRACTS

O138-Optimized Combination of MR Imaging Modalities for Predicting Recurrent Glioblastoma Study of Diagnostic Accuracy and Reproducibility

*Chong Hyun Suh*¹, Ho Sung Kim¹, Seung Chai Jung¹, Chung Gon Choi¹, Sang Jun Kim¹
*Asan Medical Center Radiology Seoul-Korea, South*¹

PURPOSE: To compare the added value of dynamic contrast-enhanced (DCE) MR imaging with that of dynamic susceptibility contrast-enhanced (DSC) MR imaging to the combination of contrast-enhanced T1-weighted imaging (CE-T1WI) and diffusion-weighted imaging (DWI) for predicting recurrent glioblastoma.

MATERIALS AND METHODS: This retrospective study was approved by our institutional review board, with the requirement for informed patient consent waived. CE-T1WI, DWI, DSC and DCE MR imagings in 87 patients with pathologically proven recurrent glioblastoma (n=50) or radiation necrosis (n=37), were retrospectively reviewed. Histogram cutoffs of quantitative parametric values were calculated from DWI, DSC and DCE MR imagings, respectively. An area under the receiver operating characteristic curve (AUC) and interreader agreement were assessed.

RESULTS: For predicting recurrent glioblastoma, adding DCE imaging to the combination of CE-T1WI and DWI significantly improved AUC from 0.833 to 0.972 for reader 1 and from 0.816 to 0.955 for reader 2, respectively. Adding DSC imaging also significantly improved AUC (0.935 for reader 1 and 0.938 for reader 2). However, there was no significant difference of AUC between the combination of CE-T1WI, DWI and DSC imaging and the combination of CE-T1WI, DWI and DCE imaging for both readers. The interreader agreement was highest for the combination of CE-T1WI, DWI and DCE imaging (k = 0.79) and lowest for the CE-T1WI and DWI (k = 0.67).

CONCLUSION: Adding perfusion MR imaging to the combination of CE-T1WI and DWI significantly improves the prediction of recurrent glioblastoma, however, selection of perfusion MR method does not affect the diagnostic performance.

Table 1. Comparison of the Area under the Receiver-Operating Characteristic Curve of MR Imaging Protocol

MR Imaging Protocol and Comparison	Reader 1			Reader 2		
	AUC	95% CI	P Value	AUC	95% CI	P Value
MR Imaging Protocol						
CE-T1WI + DWI	0.84	0.78, 0.89		0.81	0.74, 0.86	
CE-T1WI + DWI + DSC	0.95	0.91, 0.98		0.93	0.89, 0.97	
CE-T1WI + DWI + DCE	0.96	0.92, 0.99		0.97	0.93, 0.99	
Comparison						
CE-T1WI + DWI vs CE-T1WI + DWI + DSC			<.001			.002
CE-T1WI + DWI vs CE-T1WI + DWI + DCE			<.001			<.001
CE-T1WI + DWI + DSC vs CE-T1WI + DWI + DCE			.68			.22

Note.— CI = confidence interval.



ORAL PRESENTATIONS ABSTRACTS

Figure 1: Images obtained in a 57-year-old man with pathologically proven recurrent glioblastoma..

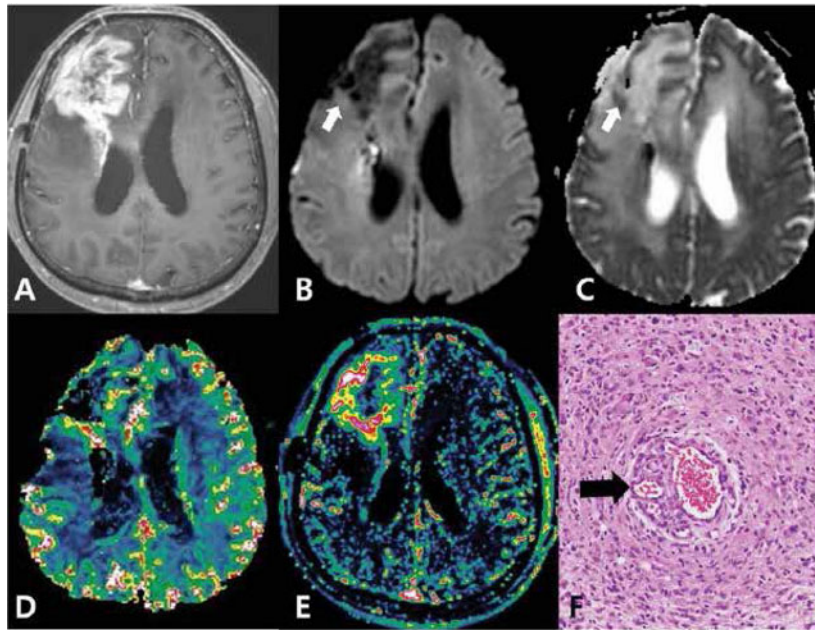
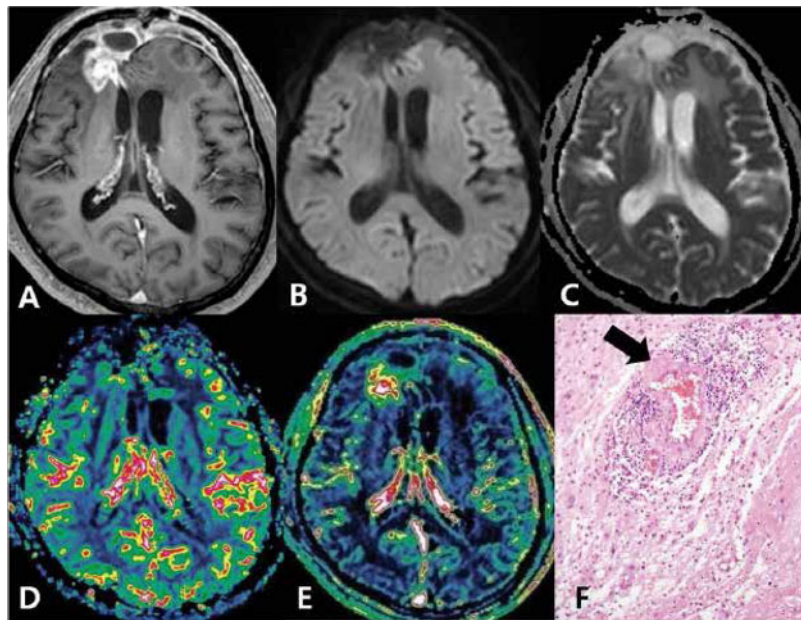


Figure 2: Images obtained in a 52-year-old woman with pathologically proven radiation necrosis.





ORAL PRESENTATIONS ABSTRACTS

O139-Differentiation of True Progression from Pseudoprogression in Glioblastoma Patients Treated with Radiation Therapy and Concomitant Temozolomide Application of Subependymal Enhancement Pattern and Diffusion weighted Imaging

*Roh-Eul Yoo*¹, Seung Hong Choi¹

*SNUH Radiology Seoul-Korea, South*¹

PURPOSE: To explore the predictive value of the subependymal enhancement pattern and diffusion-weighted imaging for differentiation of true progression from pseudoprogression in glioblastoma (GBM) treated with radiation therapy and concomitant Temozolomide (TMZ).

MATERIALS AND METHODS: Conventional magnetic resonance (MR) images, including contrast enhanced T1-weighted MR images, and diffusion-weighted images ($b = 1000 \text{ sec/mm}^2$) obtained within two months of concurrent chemotherapy and radiation therapy (CCRT) completion were retrospectively reviewed. Forty-two GBM patients with newly developed or enlarged enhancing lesions were identified and classified into true progression and pseudoprogression groups based on follow-up MR imaging after adjuvant TMZ. Subependymal enhancement was analyzed in terms of 1) the presence or absence, 2) location (ventricular or leptomeningeal), and 3) pattern (local or distant with respect to enhancing lesions). Cumulative apparent diffusion coefficient (ADC) histograms were constructed to determine the fifth percentile points.

RESULTS: Subependymal enhancement was significantly more common in the true progression group ($n = 24$) than in the pseudoprogression group ($n = 18$) (79.2% [19 of 24] vs. 44.4% [8 of 18], $P = .027$). Specifically, distant subependymal enhancement was found to be predictive for true progression ($P = .042$). There was no significant difference in the frequency of local subependymal enhancement between the two groups ($P = 1.000$). The fifth percentile of the cumulative ADC histogram was significantly lower in the true progression group than in the pseudoprogression group ($P = .014$). Multiple logistic regression analyses showed that both distant subependymal enhancement and the fifth percentile of the cumulative ADC histogram were independent factors associated with true progression ($P = .025$ and $P = .016$, respectively). Sensitivity and specificity for diagnosis of true progression were 83.3% and 66.7% using both factors.

CONCLUSION: Both distant subependymal enhancement and the fifth percentile of the cumulative ADC histogram were significant independent factors predictive of true progression. **Clinical Relevance:** Distant subependymal enhancement and ADC values of enhancing lesions are independent factors predictive of true progression and both need to be considered to improve the diagnostic accuracy.

O140-Astrocytoma with TP53 Molecular Mutation and Its MRI Characteristics

*M. de Fatima Vasco Aragao*¹, Meng Law², Girish Fatterpekar³, Bradley Delman⁴, Ana Bader⁴, Mary Fowkes⁵, Thomas Naidich⁴, Marcelo Moraes Valenca⁶

*Multimagem; Universidade Mauricio de Nassau Radiology Recife-Brazil*¹ *USC University Hospital Radiology -United States*² *New York University Langone Medical Center Radiology -United States*³ *Mount Sinai School of Medicine, NY Radiology -United States*⁴ *Mount Sinai School of Medicine, NY Pathology -United States*⁵ *Federal University of Pernambuco, Neurosurgery -Brazil*⁶

PURPOSE: The TP53 gene is the most significant gene for cancer suppression. It is found in 59% of low-grade astrocytomas, in 53% of anaplastic astrocytomas, and in 65% of secondary GBMs. In primary GBMs, only 28% are found to harbor the TP53 mutation. To date, only genetic analysis of surgical specimens allows molecular subtyping. A noninvasive radiographic predictor of TP53 mutation in astrocytoma subtypes would be of value in the preoperative assessment to predict its biological features and prognosis. The purpose is to determine the MRI findings associated with TP53 mutation in astrocytomas.



ORAL PRESENTATIONS ABSTRACTS

MATERIALS AND METHODS: We reviewed 54 preoperative MRIs patients with astrocytomas tested for TP53. Tumors were classified using WHO criteria as grades II, III, or IV. Detectable nuclear immunohistochemical staining was recorded as positive (TP53+) and non-detectable stain was recorded as negative (TP53-). MRI included T1 pre- and post-contrast, T2 and FLAIR. Scans were reviewed for: (a) presence and type of enhancement; (b) presence of necrosis and (c) presence of edema. Chi-square test was used.

RESULTS: 11 (20.4%) were grade II; 18 (33.3%) were grade III, and 25 (46.3%) were grade IV. TP53 mutation was present (TP53+) in 3/11 (27%) of grade II, 14/18 (78%) of grade III and 13/25 (52%) of grade IV. The TP53+ was more prevalent in grade III/IV (27/43, 63%) than in grade II (3/11, 27%) ($p=0.0344$). Among all cases, TP53+ was present in 30/54 (55.6%) patients. Of the 30 TP53+ tumors, 3 (10%) were grade II, 14 (46.7%) were grade III, and 13 (43.3%) were grade IV. Enhancement was present in 28/30 (93.3%) TP53+ astrocytomas versus 18/24 (75.0%) TP53- astrocytomas ($p=0.0595$) and statistical trend was observed. The heterogeneous type of enhancement was significantly more frequent in the TP53+ astrocytomas [14/30 (47%) versus 5/24 (21%), $p=0.0482$]. The edema was more frequent in the TP53+ group (83% vs. 63%, $p=0.0826$) with statistical trend. The presence of necrosis was similar between TP53- and TP53+ groups (57% vs. 58%).

CONCLUSION: The frequency of TP53+ mutations was much lower in Grade II astrocytomas than in higher grade tumors. The astrocytomas with a TP53 mutation more frequently present the heterogeneous enhancement. Although without statistical differences the TP53+ astrocytomas seem to present more edema. No differences were found regarding the presence of necrosis.

O141-Are There Differences between Macrocytic Gadolinium Contrast Agents for Brain Tumor Imaging Results of a Multicenter Intra Individual Crossover Comparison of Gadobutrol with Gadoteridol (The TRUTH study)

*Cesare Colosimo*¹, Ken Maravilla², Sefano Bastianello³, Eva Bueltmann⁴, Toshinori Hirai⁵, Tiziano Frattini⁶, Martin Smith⁷, Manuela Vaneckova⁸, Mayank Goyal⁹, Joseph Baima¹⁰, Robert Babbel¹¹, Tomasz Drózdź¹²
Policlinico "Agostino Gemelli" Istituto di Radiologia Roma-Italy ¹*University of Washington MR Research Laboratory -United States* ²*University of Pavia Neuroradiology Department -Italy* ³*Oberartzin Institut fur Diagnostische und Interventionelle Neuroradiologie Hochschule Hannover Department of neuroradiology -Germany* ⁴*Kumamoto University Department of Diagnostic Radiology -Japan* ⁵*Ospedale Valduce Diagnostica per Immagini -Italy* ⁶*Beth Israel Deaconess Medical Center Department of Radiology -United States* ⁷*General Faculty Hospital Department of Magnetic Resonance -Czech Republic* ⁸*Seaman Family MR Centre Department of Radiology -Canada* ⁹*Clinical Radiologists, S.C. Department of Radiology -United States* ¹⁰*Samaritan Health Services - IRB Department of Radiology -United States* ¹¹*Samodzielny Publiczny Zakład Świątokrzyskie Centrum Onkologii -Poland* ¹²

PURPOSE: Gadobutrol (Gadovist/Gadavist) and gadoteridol (ProHance) differ only in that a hydroxypropyl group on the gadoteridol molecule is replaced by a trihydroxybutyl group on the gadobutrol molecule and that gadobutrol is formulated at a 1M concentration compared to 0.5M for gadoteridol. We sought to determine whether these differences impact morphologic contrast-enhanced MRI of brain tumors using a multicenter intra-individual crossover study design.

MATERIALS AND METHODS: 229 adult patients with suspected or known brain tumors underwent two identical MRI exams at 1.5T, one with gadoteridol and the other with gadobutrol both at a dose of 0.1 mmol/kg bodyweight. The agents were injected in randomized order separated by 3-14 days. Imaging sequences and post-injection acquisition timing were identical for the two exams (T1wSE and high-resolution T1wGRE sequences at 3-7 min post-dose). Three blinded readers evaluated images qualitatively for diagnostic information (lesion extent, delineation, morphology, enhancement, global preference) and quantitatively in terms of pre- to post-dose changes in % lesion enhancement, contrast-to-noise ratio (CNR) and lesion-to-background ratio (LBR). Accuracy for the MR diagnosis of brain disease was assessed using the final clinical on-site diagnosis as reference standard. Data were analyzed using the Wilcoxon signed rank test, McNemar test and Mixed model.



ORAL PRESENTATIONS ABSTRACTS

RESULTS: 209 patients successfully underwent both examinations. Eleven patients were excluded because of protocol violations leaving 198 in the per-protocol analysis population. None of the three readers noted any differences between the two agents in terms of lesion extent, lesion delineation, lesion internal morphology, lesion enhancement, or global preference (p values from 0.687 to 1.00). A total of 444 lesions were confirmed at the on-site final diagnosis. Lesion detection rates ranged from 78.4-87.6% for gadoteridol and from 73.2-84.9% for gadobutrol, without significant differences between agents. Inter-reader agreement for lesion detection was noted for 74.1% and 73.0% of patients for gadoteridol and gadobutrol, respectively. No significant differences were demonstrated in terms of quantitative parameters.

CONCLUSIONS: Our findings indicate that gadoteridol and gadobutrol at 0.1 mmol/kg bodyweight provide similar qualitative and quantitative diagnostic information for the visualization and diagnosis of brain lesions. Assessment by three fully blinded neuroradiologists revealed clear equivalence between the agents.

O142-Expert Witnesses Neuroradiologists' Perspectives in America

*David Yousem*¹, Nara Pereira¹, Kelly Yousem⁴, Jonathan Lewin¹

*Johns Hopkins Radiology Owings Mills-United States*¹

PURPOSE: Physician malpractice expert witnesses may testify on behalf of physicians or patients. We sought to assess the experience of neuroradiologists as expert witnesses and their attitudes about such testimony.

MATERIALS AND METHODS: A survey was distributed to the 4357 email addresses of the membership of the ASNR with questions about expert witnesses.

RESULTS: 912 of 4357 answered at least one of the questions in the survey. 43.6% (373/856) of ASNR respondents had experience as expert witnesses. Of those neuroradiologists over 50 years of age, 70.6% (245/347) had served as an expert witness. 33% (36/108) of women and 44% (309/697) of men had served as experts. A higher percentage of interventional neuroradiologists (54.1%, 33/61) had served as expert witnesses than diagnostic (44.5%, 292/656) neuroradiologists. Most offer to testify on behalf of both plaintiffs and defendant physicians (229/332; 69.0%). Women (84.4%, 27/32) are more willing to testify for both plaintiff and defendants than men (67.7%, 197/291). Some do not testify/review cases on behalf of a plaintiff mostly because they do not think that physicians should testify against other physicians, even if negligence is present (31/144; 21.5%). This was the most common reason not to be an expert witness for a plaintiff at all age groups.

CONCLUSIONS: Of neuroradiologists answering the survey, nearly half (43.6%) have served as expert witnesses. Most serve for both plaintiffs and defendants, but some (21.5%) feel that physicians should never testify against colleagues on behalf of the plaintiff, even if the plaintiff's case is meritorious.

O143-Error in Neuroradiology an Analysis of Reports in the Radiology Events Register (RaER)

*Catherine Mandel*¹, Jane Grimm², Tim Schultz³

*Peter MacCallum Cancer Centre Cancer Imaging East Melbourne-Australia*¹ *The Royal Australian and New Zealand College of Radiologists -Australia*² *Australian Patient Safety Foundation -Australia*³

PURPOSE: Error is common in healthcare. Understanding when and how things can go wrong is important if safety is to be improved.

MATERIALS AND METHODS: The RaER database was searched for events related to neuroradiology. The reports were extracted, checked for relevance and classified according to principle incident type.

RESULTS: From a total of 2787 classified reports, 122 were retrieved. After review there were 85 separate incidents related to neuroradiology.

The majority (about three quarters) was reported by medical practitioners. The others were from State Health Department, Medical Indemnity and Radiation Regulator databases and from cases collected during research studies.



ORAL PRESENTATIONS ABSTRACTS

Over half the incidents both started and were detected during the decision to image or during clinical decision-making. Errors related to wrong patient (7), wrong test (12) and unnecessary repeat tests (6) could be mitigated by the application of robust checking procedures, such as "time out"¹ and careful vetting of referrals for clinical justification.

Diagnostic errors due to missed diagnosis (18), misdiagnosis (4), delayed diagnosis (4) and procedural complications (8) could be mitigated by attention to training, continuing professional development, staffing and human factors such as fatigue, ambient environment, interruptions and distractions. Communication was a factor in 25% of cases.

Issues related to scheduling, patient care, allergic reaction and a miscellany of other causes accounted for the rest. Many of these can be addressed by looking at systems issues.

CONCLUSION: Patient safety incidents are common in healthcare. Common causes include failure of communication, diagnostic error and incorrect studies. Whilst most do not result in harm, knowing what can or does go wrong is fundamental to improving healthcare.

REFERENCES: 1. World Health Organization (nd) Safe Surgery Saves Lives - The Second Global Patient Safety Challenge. (Accessed at <http://www.who.int/patientsafety/safesurgery/en/>.)

PARALLEL SCIENTIFIC PAPER PRESENTATIONS

(Adult NR 3) 17:15 - 19:00

Dolmabahce C Hall

O144-High Signal Intensity Abnormalities Evaluated by 3D Fluid Attenuated Inversion Recovery Imaging Adjacent to Developmental Venous Anomalies Identified by Susceptibility Weighted Imaging at 3 T

*Maki Umino*¹, Masayuki Maeda¹, Nobuyoshi Matsushima², Keita Matsuura³, Hajime Sakuma²
Mie University School of Medicine Radiology Tsu, Mie-Japan *1 School of Medicine Radiology -Japan* *2 Suzuka Kaisei Hospital Neurology -Japan* ³

PURPOSE: To evaluate brain parenchymal high-signal-intensity abnormalities adjacent to developmental venous anomalies (DVAs) identified by susceptibility-weighted imaging (SWI) at 3 T. **MATERIALS AND METHODS:** One hundred and thirty patients with 137 DVAs identified by SWI were retrospectively studied. 3D fluid-attenuated inversion recovery (FLAIR) images were reviewed for parenchymal high-signal-intensity abnormalities adjacent to DVAs and SWI images were reviewed for hypointense foci (microhemorrhages or cavernous malformations) adjacent to DVAs. Patient age, the degree of underlying white matter disease, DVA location (supratentorial or infratentorial), and the presence or absence of hypointense foci were compared across DVAs with and without adjacent high-signal-intensity abnormalities. The correlation between patient age and the size of any high-signal-intensity abnormality was analyzed using linear regression. **RESULTS:** Forty-two of 137 DVAs (30.7%) had adjacent high-signal-intensity abnormalities. An adjusted prevalence rate of 18/71 (25.4%) was obtained by excluding patients with considerable underlying white matter disease. DVA location was associated with the presence of high-signal-intensity abnormalities ($p < 0.05$). High-signal-intensity abnormalities were more frequent in DVAs in supratentorial regions than in DVAs in infratentorial regions. Patient age, the degree of underlying white matter disease, and the presence of hypointense foci were not associated with the presence of high-signal-intensity abnormalities. There was a significant correlation between patient age and the size of high-signal-intensity abnormalities ($p < 0.01$). **CONCLUSIONS:** 3D FLAIR imaging permits detection of small high-signal-intensity abnormalities associated with DVAs. The size of DVA-associated high-signal-intensity abnormalities increased with patient age.



ORAL PRESENTATIONS ABSTRACTS

O145-Analysis of Hyperdense Sign on Non Contrast CT for Diagnosing Cerebral Venous Thrombosis

Sohail Zaheer ¹, Raphael Glikstein ¹, Satya Patro ¹, Nicholas Seppala ¹, Nikolai Steffenhagen ², *Daniela Iancu* ¹
University of Ottawa Neuroradiology Section -Canada ¹ *University of Ottawa Neurology Section -Canada* ²

PURPOSE: Timely diagnosis of cerebral venous thrombosis (CVT) is essential. Non-contrast CT (NCCT) is the initial investigation of choice, where the occluded sinus appears hyperdense. The purpose of this study was to assess the value of hyperdense sign and attenuation ratios in diagnosing CVT on NCCT.

MATERIALS AND METHODS: Using a case control retrospective study we evaluated 19 patients with acute CVT and 20 control patients without CVT. Final diagnosis of CVT was confirmed or ruled out with CT/MR venogram for all the patients. Three blinded readers (junior resident, fellow and staff neuroradiologist) evaluated the initial NCCT for hyperdense sign first using only axial slices, then axial, coronal and sagittal reformats, and finally using region of interest (ROI) attenuation measurements. In addition to absolute values, attenuation ratios were measured to better differentiate thrombosed from non-thrombosed sinuses. These ratios were measured as follows: target sinus/lowest attenuation sinus, target sinus/basilar artery, target sinus/internal carotid artery, target sinus/non-haemorrhagic temporal lobe, and target sinus/non-haemorrhagic frontal lobe. **RESULTS:** Overall, the hyperdense sign was found to be: on axial slices only: 61.4% sensitive (95% CI 51.8%-70.2%), 96.8% specific (95% CI 95.7%-97.6%), and 94.1% accurate (95% CI 92.9%-95.2%), with the addition of coronal and sagittal reformats: 64.9% sensitive (95% CI 55.3%-73.4%), 98.8% specific (95% CI 98.0%-99.2%), and 96.2% accurate (95% CI 95.2%-97.1%), and with absolute attenuation measurement: 62.3% sensitive (95% CI 52.7%-71.1%), 98.7% specific (95% CI 97.9%-99.2%), and 96.0% accurate (95% CI 94.9%-96.9%).

There was statistically significant difference in average attenuation between acutely thrombosed sinuses (68.6HU, 95% CI 65.3-71.9) and non-thrombosed sinuses (52.1HU, 95% CI 50.7-53.5). 61HU was the optimal cut-off for diagnosis of CVT with 84.4% sensitivity and 89.6% specificity.

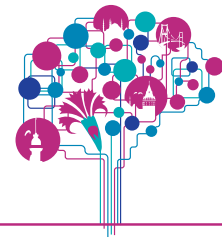
Among the above proposed attenuation ratios, the target sinus/lowest attenuation sinus ratio was most useful in differentiating acutely thrombosed sinuses from non-thrombosed sinuses. For thrombosed sinuses the average ratio was 1.43 (95% CI 1.36-1.51), while for non-thrombosed sinuses it was 1.06 (95% CI 1.05-1.08). Optimal cut-off of 1.29 led to sensitivity of 87.5% and specificity of 96.0%. **CONCLUSIONS:** Subjective assessment of hyperdense sign on NCCT to diagnose CVT has rather low sensitivity (61.4%-64.9%). Use of objective thresholds for absolute attenuation (> 61HU) and attenuation ratio of the suspected sinus/normal appearing sinus (> 1.29) improves sensitivity to 84.4% and 87.5% respectively.

O146-Leukoaraiosis and Microbleeds in Alzheimers Disease in Australian Population; Is There a Link and Does It Influence Cognition?

Sandeep Bhuta ¹, Charlie Hsu ², Rhondda Jones ³, Margaret Bilska ⁴
Gold Coast University Hospital, School of Medicine, Griffith University Medical Imaging Gold Coast-Australia ¹
Gold Coast University Hospital Medical Imaging -Australia ² *James Cook University Statistics -Australia* ³
Gold Coast University Hospital Medicine -Australia ⁴

PURPOSE: The aim of the study was to determine the incidence and distribution of lobar microbleeds in patients with Alzheimer disease (AD) and mild cognitive impairment (MCI) and to assess its association with Leukoaraiosis and its effect on cognition.

MATERIALS AND METHODS: Patients with presumed clinical diagnosis of AD and MCI (n=38) referred from Specialist Dementia Clinic were included and healthy age matched controls (n=26) were used. Retrospective review of MRI was performed by two independent readers (CC-TH and SB). Location and number of microbleeds as lobar or basal ganglia was discerned with SWI and phase sequences. Leukoaraiosis was rated on T2-weighted images using a modified Age-Related White Matter Changes Rating Scale (ARWMC). Mini mental score examination



ORAL PRESENTATIONS ABSTRACTS

(MMSE) was used as an index to assess patients cognitive status. Data was modelled as negative binomial regression. SPlus 8.2 (Tibco Software) or R 3.0.1 (R Foundation for Statistical Computing) was used for analysis. RESULTS: The average number of microbleeds was 4.7 times higher in the AD and MCI group versus the control group ($p = 0.043$) Microbleeds increased progressively with age in the 70+ age group ($p = 0.010$) at a rate of 11% per year. There was occipital predominance of lobar microbleeds in AD and MCI compared to control group ($p = 0.007$). Basal ganglia microbleeds were less frequent with no significant difference between groups. Increase in modified ARWMC scores was associated with higher number of lobar microbleeds from score 0 to 2 but not between score 2 to 3. There was no consistent relationship between number of lobar microbleeds and MMSE in the AD and MCI group, similarly no consistent relationship was seen with Superficial Siderosis (SS) and AD although sample size of SS was small.

CONCLUSION: AD and MCI patients have higher incidence and number of microbleeds with an occipital predominance compared to normal controls implying vasculopathy in AD and possible vascular pathway for neuronal damage and neurodegeneration. Numerical value of lobar microbleeds is not a reliable marker of cognition (MMSE) and its relationship is inconsistent. A larger patient cohort may be required to elucidate the complexity of microbleeds in AD and MCI patients.

O147-Stripe Sign of Precentral Gyri in Amyotrophic Lateral Sclerosis a Novel Finding on Phase Difference Enhanced Imaging

*Shingo Kakeda*¹, Tetsuya Yoneda², Mari Miyata¹, Satoru Ide¹, Yasuhiro Hiai², Koichiro Futatsuya¹, Keita Watanabe¹, Yu Murakami¹, Atsushi Ogasawara¹, Junji Moriya¹, Yukunori Korogi¹

*University of Occupational and Environmental Health Radiology Kitakyushu -Japan*¹ *Faculty of Life Medical Physics in Advanced Biomedical Sciences -Japan*²

BACKGROUND and PURPOSE: In the patients with amyotrophic lateral sclerosis (ALS), the MR signal alterations in the precentral gyrus on T2WI, such as low signal-intensity (SI) of the grey matter (GM) or high SI of the subcortical white matter (WM), have been reported; however, these findings are not specific to ALS. A recently developed, phase-weighted MR imaging technique "Phase Difference Enhanced Imaging (PADRE)" can delineate the GM and WM very clearly due to the difference in myelin concentration. Our purpose is to evaluate the SI of the precentral gyri in the ALS

patients in comparison with healthy subjects by using PADRE.

MATERIALS AND METHODS: Five patients with ALS and 20 healthy volunteers were enrolled in this study. Axial images were acquired with 3T MR system. The PADRE images consisted of a three-dimensional 3D multiecho spoiled gradient-echo sampling. For the precentral gyri, two neuroradiologists compared the SI of the GM with the subcortical WM on PADRE images and divided into 3 grades: hyperintense, isointense, or hypointense. We also evaluated susceptibility-weighted imaging (SWI)-like images with the same manner.

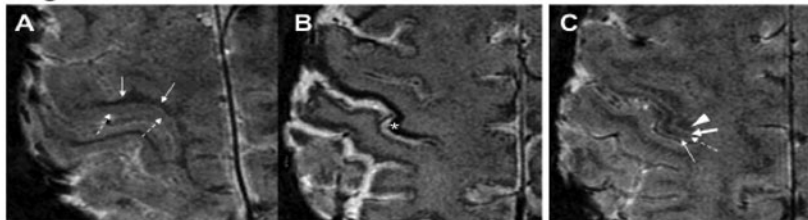
RESULTS: On PADRE, the GM of the precentral gyrus was hyperintense to the subcortical WM in all 20 healthy volunteers (Figure, A), and hypointense in all 5 patients with ALS. On the SWI-like images, the GM of the precentral gyrus was hypointense for all the healthy volunteers and the patients (Figure, B). Furthermore, in ALS patients, four layers, high, low, high, and low SI from the pial surface of the precentral gyri, were seen on PADRE images (Figure, C), which seemed to correspond to the superficial GM, deeper GM, superficial subcortical WM, and deeper subcortical WM,

respectively (stripe sign). The stripe sign was not observed on the SWI-like images in any ALS patients. CONCLUSIONS: In ALS patients PADRE images showed the four layers in the precentral gyri, which might reflect the iron deposition in a part of the GM and the reduced concentration of myelin in the superficial subcortical WM. The assessment of the precentral gyri with PADRE may be useful for the diagnoses of ALS.



ORAL PRESENTATIONS ABSTRACTS

Figure



Comparison of the SI of the right precentral gyrus. (A) PADRE image of a healthy volunteer. The GM (dotted arrows) is hyperintense to the subcortical WM (arrows). (B) SWI-like image of an ALS patient. The GM is totally hypointense (asterisk). (C) PADRE image of the same patient as above. Four layers, high SI (arrow), low SI (dotted arrow), high SI (large arrow), and low SI (arrowhead), are clearly seen, which seems to correspond to the superficial GM, deeper GM, superficial subcortical WM, and deeper subcortical WM from the pial surface, respectively.

O148-Progressive Cerebellar Atrophy in Course of Hypertrophic Olivary Degeneration

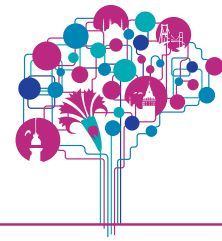
Angel Mironov¹

Creighton University Medical Center Radiology Omaha-United States¹

PURPOSE: It is well acknowledge that the primary (ischemia, hemorrhage, mass, trauma) or secondary (surgical treatment) injury of the dentato-rubro-olivary pathway may generate an unique pathological & imaging condition representing the phenomenon of hypertrophic olivary degeneration (HOD). The purpose is to present two cases with classical acquired features of HOD associated with progressive cerebellar atrophy in the very late period. The progressive global cerebellar atrophy has been not considered previous in the definition of the HOD.

MATERIALS AND METHODS: The first patient (50 year-old male) suffered symptomatic pontine hemorrhage due to cavernoma. He was followed up for up to 10 years after surgery. The second patient (32 year-old female) had history of systemic lupus erythematosus (SLE) and developed vasculitis with lacunar insults of the brain stem. The patient was followed up to 5 year after the first onset. The patients were evaluated by imaging studies. **RESULTS:** The first case was found to have 10 months after surgery for pontine cavernoma an abnormal T2 symmetrical signal in the olives of medulla oblongata bilateral. Later the patient developed progressive diplopia, numbness, poor coordination, dysarthria and intractable tremor. Repeated imaging in the following ten years progressive general cerebellar atrophy. The second case suffered SLE and developed ischemic lesions of pons and thalamus. Repeated MRI revealed abnormal T2 hyperintensity of olives involving the entire medulla oblongata. Follow-ups in coming years showed persistent abnormal T2 signal of olives, shrinking of the superior medulla, and impressive progressive atrophy of pons and cerebellum.

The chronological development of HOD in both cases showed initial T2 abnormality 10 months / 3 weeks after ictus, with persistent increased T2 signal and mild olivary hypertrophy for 3 years / 4 years following by continued signal decrease and olivary shrinking & impressive cerebellar atrophy. **CONCLUSION:** The progressive involvement of the cerebellum in our cases may suggest similarities with the primary autosomal - inherited cerebelloolivary degeneration of Holmes. The evolution of the acquired HOD may suggest that the primary injury of dentato-rubro-olivary pathway may have either the same impact on the cerebellum, or the injury of the dento-rubro-olivary pathway may be suitable for generation of acquired olivopontocerebellar degeneration.



ORAL PRESENTATIONS ABSTRACTS

O149-Diffuse Hypoperfusion in Normal Appearing White Matter (NAWM) and Deep Gray Matter (DGM) Regions in Patients with Neuropsychiatric Systemic Lupus Erythematosus (NPSLE)

*Efrosin Papadaki*¹, Antonios Fanouriakis², Eleytherios Kavroulakis¹, Georgios Bertias², Prodromos Sidiropoulos², Dimitrios Boumpas², Apostolos Karantanis¹

*University Hospital Of Heraklion Radiology Heraklion-Greece*¹ *University Hospital Of Heraklion Rheumatology -Greece*²

INTRODUCTION AND PURPOSE: PET and SPECT studies revealed hypometabolism and hypoperfusion in NAWM and DGM regions in NPSLE patients, but have limited anatomic resolution and high-radiation dose. The DSC-MRI technique is widely used for the detection of hemodynamic changes in CNS diseases, but its application in NPSLE is still very limited.

To investigate possible hemodynamic impairment in NPSLE patients, using DSC-MRI.

MATERIALS AND METHODS: Brain MRI studies were performed to 30 NPSLE patients (NPSLE), 30 SLE patients without CNS involvement (SLE-CON) and 25 normal volunteers (NRM). DSC-MRI technique was applied and regional cerebral blood volume (CBV), cerebral blood flow (CBF), and mean transit time (MTT) values were estimated in 20 regions of interest (ROIs), placed in NAWM and DGM structures bilaterally. The regional CBV, CBF, and MTT values were normalized to the respective values of the cerebellar dentate nuclei for each patient. Group differences on normalized perfusion values were assessed using one-way ANOVAs, separately for each ROI and evaluated at Bonferroni-adjusted $\alpha = 0.05/20$ (ROIs) = 0.0025.

RESULTS: NPSLE patients had lower CBF values and higher MTT values than NRM, across all 20 ROIs, but higher CBV values only in NAWM. Compared to SLE-CON, NPSLE patients had lower CBF values in DGM and higher MTT values in NAWM and DGM. Lower CBF values in NPSLE patients, as compared to SLE-CON, reached significance in periventricular NAWM and semioval center. There was no significant difference in CBF, CBV, and MTT values between SLE-CON and NRM.

CONCLUSIONS: NPSLE patients are characterized by significant hypoperfusion in DGM compared to SLE-CON patients and NRM, and hypoperfusion in NAWM compared to NRM. There is no significant hemodynamic differences between SEL- control patients and NRM.

O150-Subcortical Calcification on CT as Diagnostic Sign of Transverse sigmoid Dural Arteriovenous Fistula With Cortical Venous Reflux

*Shunji Mugikura*¹, Takahiro Metoki¹, Takaki Murata¹, Noriko Kurihara², Yasushi Matsumoto³, Masayuki Ezura⁴, Shoki Takahashi¹

*Tohoku University, Graduate School of Medicine Diagnostic Radiology Sendai-Japan*¹ *Sendai Medical Center Radiology -Japan*² *Kohnan Hosp Neuroendovascular Therapy -Japan*³ *Sendai Medical Center Neurosurgery -Japan*⁴

BACKGROUND AND PURPOSE: The annual mortality rate of the patients who had dural arteriovenous fistula (dAVF) with cortical venous reflux (CVR) is high without treatment (10.4%), and early diagnosis is desirable. Diagnosis of dAVF is often difficult when the symptoms are chronic or nonspecific one such as tinnitus, headache, dizziness, dementia and so on other than characteristical ocular symptoms or acute symptoms accompanied with intracranial hemorrhage or infarction. Our purpose is to determine the prevalence of subcortical calcifications on CT in patients with dAVF and show its role as the diagnostic sign of dAVF.

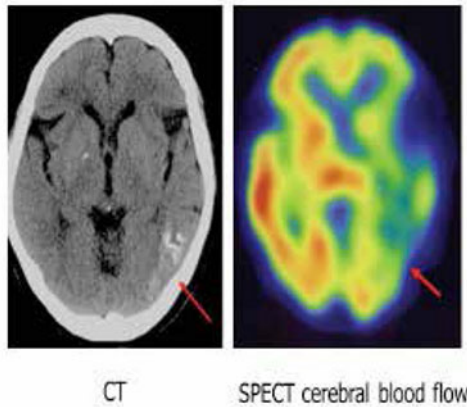
MATERIALS AND METHODS: In 119 consecutive patients diagnosed with dAVF by the cerebral angiographic findings, we Review for Prevalence of subcortical calcifications on CT, Diagnostic symptoms, Shunting point of dAVF and Presence of CVR on angiograms.

RESULTS: Subcortical calcification: 10 of 119 cases (8.4%). All ten cases with Intraparenchymal calcification had shunting at the Transverse and/or Sigmoid (TS) sinus. All 10 cases with subcortical calcification had CVR. All Subcortical calcification was found in the posterior part of the hemisphere with shunting. Curvilinear calcification at the cortico-medullary junction at the bottom of cerebral sulci.



ORAL PRESENTATIONS ABSTRACTS

CONCLUSIONS: Subcortical calcification on CT is a sign of TS-dAVF with CVR specifically in patients who present chronic or non-specific symptoms. Subcortical calcifications found in TS-dAVF could be caused by venous congestion due to long-lasting CVR without being noticed or diagnosed.



O151-Longitudinal MRI Study of the Spinal Cord in Lamin B1 Autosomal Dominant Leukodystrophy Do the First Symptoms Come from the Spinal Cord

Johannes Finnsson ¹, Jimmy Sundblom ², Atle Melberg ², *Raili Raininko* ¹
Uppsala University Radiology -Sweden ¹ Uppsala University Neurology -Sweden ²

PURPOSE: Lamin B1 autosomal dominant leukodystrophy (ADLD), also known as adult-onset ADLD with autonomic symptoms, is caused by a duplication of the LMNB1 gene. Patients present in the fourth to sixth decade with autonomic symptoms and later develop symptoms from the pyramidal and cerebellar tracts. MR abnormalities have been described in the brain and spinal cord. We relate MRI findings in the spinal cord to clinical symptoms.

MATERIALS AND METHODS: 14 subjects (6 females, 8 males) from two families with proven genetic linkage to the disease were examined with MRI of the spinal cord, 9 subjects were examined at least twice. All but one also underwent brain MRI. The age at the first examination was 34-70 years and follow-up times (MRI and neurology) were 1-10 years (median 5 years). Two subjects were asymptomatic, the rest had mild to severe symptoms when recruited to the study. In addition to visual evaluation, measurements of sagittal and coronal diameters as well as cross-sectional areas were obtained on spinal MRI.

RESULTS: All subjects, even the asymptomatic, exhibited severe spinal cord atrophy. The typical finding was a high white matter (WM) T2 signal intensity in the entire spinal cord. Only in two subjects some sparing of WM could be seen. One of them only had one examination. The other one was asymptomatic during a 6-year follow-up but the entire spinal WM was hyperintense in the second examination. On follow-up, we found progress of atrophy in three patients, who also manifested clinical deterioration. Four more patients exhibited increased symptomatology although no radiological progress was perceptible, but measurement precision of small objects is limited on MRI. All subjects showed abnormalities on brain MRI but, in contrast to the severely affected spinal cord, they were mild in asymptomatic subjects. All symptomatic subjects had urinary problems and variable other autonomic symptoms. Motor symptoms started months or years later and involved first the legs (spastic paraplegia), then the arms.

CONCLUSION: The entire spinal cord WM is severely affected in lamin B1 ADLD, even in asymptomatic subjects with genetic linkage to the disease. The first symptoms resemble those in myelopathy. We hypothesize that the first affected part of the CNS in lamin B1 ADLD may be the spinal cord.



ORAL PRESENTATIONS ABSTRACTS

O152-Hyperintense Dentate Nuclei on T1 Weighted MRI

*Mehmet Emin Adin*¹, David Mark Yousem¹, Lawrence Kleinberg²

*Johns Hopkins University The Russell H. Morgan Department of Radiology & Radiological Science, Division of Neuroradiology baltimore-United States*¹ *Johns Hopkins University The Department of Radiation Oncology and Molecular Sciences-United States*²

PURPOSE: We retrospectively reviewed records of patients with history of brain irradiation to detect an association between T1W hyperintense dentate nuclei and various variables including but not limited to number of contrast enhanced MRI scans, site, dose and technique of radiotherapy, and brain tumor histology. **MATERIALS AND METHODS:** We retrospectively reviewed the medical records of 709 consecutive patients who were treated with brain irradiation at Johns Hopkins Medical institution between June 1995 and January 2010. Clinical notes, discharge summaries, operative notes, radiological studies, and radiation therapy summaries were reviewed. We also reviewed prior studies performed at outside institutions, when available. Radiological interpretation by two independent radiologists was performed blinded to the clinical diagnosis and treatment protocol. A decision of hyperintense dentate nucleus was made based on the qualitative comparison of signal intensity of middle cerebellar peduncle and dentate nucleus on T1 weighted MR images. CT studies of patients with bright dentate nuclei on pre-contrast T1 weighted MR images were also reviewed (n=54)

RESULTS: Of 184 (83 females, 101 males) subjects who underwent 2677 MRI studies (mean: 14.55, range: 1-60) following IV gadolinium administration, 103 patients showed hyperintense dentate nuclei on T1W MRI images. Mean follow up time was 62.5 months (median: 48, standard deviation: 58.7) regardless of dentate nucleus intensity. Our preliminary statistical analysis suggests significant relationship between total numbers of contrast enhanced MRI studies and dentate nuclei hyperintensity. Radiation dose and site, field strength of the scanner histology of underlying tumor did not have a significant association with appearance of T1W bright dentate nuclei. **CONCLUSION:** Repeated performance of gadolinium-enhanced studies may contribute to a bright appearance of dentate nuclei on unenhanced T1 weighted MR images

O153-MR Perfusion Abnormalities in Organophosphorus Poisoning and Correlation with Spect and Neurocognitive Testing Abnormalities

Kovilapu Uday Bhanu¹, *N Khandelwal*¹, Sameer Vyas¹, Ashish Bhalla², Br Mittal³

*Pgimer Radiodiagnosis -India*¹ *Pgimer Internal Medicine -India*² *Pgimer Nuclear Medicine -India*³

INTRODUCTION AND PURPOSE: Acute organophosphate (OP) pesticide poisonings cause substantial morbidity and mortality worldwide. Generally, acute OPP occurs following ingestion with suicidal intent and occasionally following accidental exposure to aerosol during agricultural spraying. Many imaging modalities, like computerized tomography (CT), MRI, and single photon emission computed tomography (SPECT) of the brain, have been used to quantitate the acute insult caused to the brain following acute Organophosphorus poisoning. The purpose of this study was to correlate MR Perfusion and SPECT in patients of Acute Organophosphorus poisoning.

MATERIALS AND METHODS: In this prospective study 20 patients were included who ingested Organophosphorus compound. All the patients underwent BRAIN SPECT acquisition and MRI BRAIN on 1.5/3T MR system. Neurocognitive tests were performed for all patients.

RESULTS: Based on visual analysis a total 7 patients showed perfusion defects. Based on the cut off values of nL:C ratios the total perfusion defects were 29. On the basis of equal misclassification rates various cut off values for all the areas were obtained at different sensitivity and specificity. On MR perfusion based on the cut off values of nCBV ratios and nCBF ratios the total number of patients showing perfusion defects was 6 and 8 respectively. The total number perfusion defects were 29 and 45 respectively. There was significant difference of the nCBV ratios and nCBF ratios seen between the control group (n=20) and positive patients group (n=6 and n=8 respectively) with (p value > 0.05).



ORAL PRESENTATIONS ABSTRACTS

All the defects seen on SPECT are well appreciated on nCBF maps (MRI perfusion) suggestive of 100% correlation. CONCLUSION: Our study, which has been carried out within first week of poisoning has revealed various hypoperfused defects in brain on SPECT and MR perfusion study. Significant correlation of SPECT and MR perfusion hypo perfusion defects were seen, with higher number of perfusion defects on MR perfusion.

O154-Atrophy Focal Spinal Cord Lesions and Alterations of Diffusion Tensor Imaging (DTI) Parameters in Asymptomatic Virus Carriers and Patients Suffering from Human T Lymphotropic Virus Type 1 (HTLV 1) Associated Myelopathy Tropical Spastic Paraparesis (HAM TSP)

*Caroline Cubbison*¹, Massiel Gonzalez-Reinoso¹, Carlos Vilchez¹, Eddy Perez-Then², Pedro Roa³, Bernd Foerster⁴, Jairo Oviedo¹, Luis Suazo⁵, Peter Stoeter¹

*CEDIMAT Dep. of Radiology Santo Domingo-Dominican Republic*¹ *CEDIMAT Dep. of Science -Dominican Republic*² *CEDIMAT Dep. of Neurology -Dominican Republic*³ *Philips Healthcare Customer Support -Brazil*⁴ *CEDIMAT Dep. of Neurosurgery -Dominican Republic*⁵

PURPOSE: In HAM/TSP, spinal cord atrophy is a well-known finding in Magnetic Resonance Imaging (MRI). But in contrast to histological reports, focal lesions of the spinal cord have only been described in MRI reports in exceptional acute cases. Here, we looked for such focal lesions and for alterations of DTI parameters of the long fiber tracts in the usual case of a long-standing and slowly progressive disease.

MATERIALS AND METHODS: We examined 11 symptomatic patients, 11 sero-positive, but asymptomatic HTLV-1 carriers and 18 sero-negative volunteers (3T Achieva, Philips). Sagittal and transversal T2 weighted images were visually assessed for focal cord lesions. The spinal cord cross sectional area and the segmental cord volume were measured at all levels. High-resolution DTI (1.8x1.8x1.8 mm) was performed in sagittal planes from the bregma down to the cervical spine. For tractography and calculation of Fractional Anisotropy (FA) and Mean Diffusivity (MD) we used manufacturer-provided software.

RESULTS: Two thirds of patients showed focal lesions affecting the antero-lateral columns and in two cases also the dorsal columns were affected. Compared to volunteers, there was a significant spinal cord atrophy and a reduction of FA (-43% and -7%, p<0.001). Carriers (as compared to controls) did not show significant atrophy or focal lesions and only a mild FA reduction (-3%) of their ventral tracts just below the level of significance.

CONCLUSIONS: In addition to severe spinal cord atrophy and reduction of FA of long fiber tracts, we also found focal spinal cord lesions on high-resolution MRI also in chronic HAM/TSP patients thus confirming previous histological reports. Asymptomatic virus carriers did not show focal lesions or atrophy. However, their mild (although not significant) FA reduction could be an indication of spinal cord involvement, but without clinical manifestation.

O211-Clinical Implementation of Physiological Quantitative MRI; Conclusions from a Survey of UK Neuroradiology Units

*Adam Waldman*¹, Stephen Price², Abigail Evans³ *Imperial College, London Imaging London-United Kingdom*¹ *Cambridge University Neurosurgery -United Kingdom*² *University College London Clinical trials Unit -United Kingdom*³

PURPOSE: Although quantitative and physiological MRI biomarkers add value in neurooncology, particularly low grade glioma (LGG) management, clinical implementation remains limited. To understand this better, we undertook a survey of current practice in UK neuroradiology units.

MATERIALS AND METHODS: An online survey from British Society of Neuroradiologists membership included questions on: MRI platform (manufacturer/field strength), structural protocols, frequency of surveillance imaging, volumetric growth rates analysis, perfusion (DSC-MRI, DCE-MRI,



ORAL PRESENTATIONS ABSTRACTS

ASL), MRS (single voxel, multivoxel), diffusion (ADC) and other methods such as PET. Data were gathered on processing and analysis platforms and personnel performing processing (radiologist, radiographer, imaging scientist). Use of different physiological MRI methods in research and clinical applications were also compared, and factors limiting implementation of physiological methods (imaging and radiologist time; equipment; evidence, perception and understanding of clinical value; physics support/involvement). RESULTS: Responses were received from 21/31 neuroscience centres undertaking neurooncology imaging, using 32 1.5T and 18 3T systems. Imaging protocol, policy and intervals for LGG varied; approximately 50% imaged 6 monthly, depending on resection status and other stratifiers. 10% used volume measurements for growth rates. 57% performed DSC-perfusion at presentation, follow up or both, although only 30% used the method routinely. >50% analysed rCBV maps qualitatively or semiquantitatively, and 30% co-registered them with structural datasets. All used manufacturers software/workstations, although 10% also used other platforms for processing. 30% used MRS routinely, and 50% in selected cases. <20% of centres performed DCE-MRI or ASL. 80% felt that physics/imaging science support limited quantitative MRI use; 50% reported minimal or no support for acquisition or processing optimisation. Ranked limitations to implementation reported were protocol and radiologist time, lack of proper biomarker validation, MRI system/workstation access/capability and radiologist/clinician perception of utility.

DISCUSSION: The majority of centres use some physiological imaging in neurooncology, although bias towards these is likely in survey responders. Specific research projects appear supported, although clinical implementation remains highly variable. Processing time appears to be a major limitation, and there was also a reluctance to dedicate limited resources to partly validated methods.

CONCLUSIONS: Better multisite validation of imaging biomarkers, more streamlined acquisition, processing and analysis protocols, dedicated radiologist or technical time and clinician education are needed to improve rational implementation of physiological MRI in clinical neuro-oncology and other neurological conditions

PARALLEL SCIENTIFIC PAPER PRESENTATIONS

(Vascular Interventional 1) 17:15 - 19:00

Topkapı A Hall

O155-Treatment of Multiple Intracranial Aneurysms with One Stage Coiling

*Byung Moon Kim*¹, Pyoung Jeon², Dong Joon Kim¹, Dong Ik Kim¹

*Severance Hospital, Yonsei University College of Medicine Radiology Seoul-Korea, South*¹ *Samsung Medical Center, Sungkyunkwan University School of Medicine Radiology -Korea, South*²

BACKGROUND AND PURPOSE: The aim of this study was to evaluate the safety and effectiveness of one-stage coiling for multiple intracranial aneurysms.

MATERIALS AND METHODS: All patients who underwent one-stage coiling for two or more aneurysms were identified from a prospectively registered neurointerventional database over 10 years. The patient characteristics and clinical and angiographic outcomes at discharge and follow-up were retrospectively evaluated.

RESULTS: A total of 167 patients (M:F=30:137; mean age, 58 years) with multiple aneurysms (a total of 418 aneurysms; mean, 2.5 aneurysms/patient) underwent attempted one-stage coiling for two or more aneurysms (a total of 359 aneurysms; mean, 2.1 aneurysms/patient). In 131 patients (78.4%), all detected aneurysms were treated with coiling only. Treatment-related morbidity and mortality at discharge were 1.8% and 0.6% per patient, respectively. Of the 132 patients without subarachnoid hemorrhage, favorable outcomes (mRS, 0–2) at discharge were 129 (97.7%), and of the 35 patients with SAH, 27 (77.1%) had favorable outcomes at discharge. Of the 162 patients (97%) for whom clinical follow-up was available (mean, 35.8 months), 154 patients (95.1%) had favorable outcomes. Immediate post-treatment angiography showed complete occlusion in 186 (51.8%) patients, neck remnants in 134 (37.3%), sac remnants in 33 (9.2%), and failure in 6 (1.7%). Of the 262 (73.9%) aneurysms that underwent follow-up imaging (mean, 24.8 months), 244 (93.1%) showed a stable or improved state, with 12 (4.6%) minor and 6 (2.3%) major recurrences.



ORAL PRESENTATIONS ABSTRACTS

CONCLUSIONS: One-stage coiling of multiple aneurysms seemed to be safe and effective, with low morbidity and mortality.

O156-Endovascular Treatment of Ruptured Blister Like Aneurysms with Special Reference to the Flow Diverting Strategies

*Mustafa Gok*¹, Celal Cinar², Halil Bozkaya², Ismail Oran²

*Kafkas University Hospital, Kars Radiology Izmir-Turkey*¹ *Ege University Hospital, Izmir Interventional Radiology -Turkey*²

PURPOSE Blister-like aneurysm (BA) is a rare type of intracranial aneurysm that is difficult to treat both surgically and endovascularly with high morbidity and mortality rates. The current literature knowledge describing the surgical and endovascular treatment of this type of aneurysm offers no clear consensus on the optimal treatment. The aim of this study was to present clinical and angiographic results of BAs treated endovascularly by using predominantly flow diverting strategies. **MATERIALS AND METHODS:** Sixteen ruptured BAs in 16 consecutive patients (2 men and 14 women; mean age 46.5 years, range 22–67 years) were treated using predominantly endovascular methods during the last 6 year period. Initial clinical and radiological findings, treatment results, clinical and angiographic outcomes, and follow-up were retrospectively evaluated. Treatment modalities were organized as paying special attention to endovascular reconstruction with the flow diverting strategies using stents. (Table)

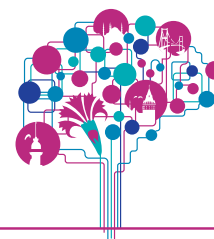
RESULTS: Control angiographies were available in 15 of 16 patients, in which there were 14 aneurysm occlusion, and one aneurysm filling treated later by wrapping. Clinical outcome was good in 11, fair in 4, and bad in 1 patient.

As the flow diversion, a novel perspective for aneurysm, carries inherent slow-acting progressive occlusion effect under dual antiaggregating drugs, ruptured BAs rise a fair for interventionalist as their fragile structure prone to rupture perioperatively.

CONCLUSION: Our series showed that endovascular reconstructive treatment of ruptured BAs by using flow-diverting strategies is technically challenging but can be done with acceptable clinical and good radiological midterm results.



Table: Summary of patient and treatment characteristic, and clinical and angiographic outcome of 16 ruptured BAs.



ORAL PRESENTATIONS ABSTRACTS

No/ Age/ Sex	Time to Primary Treatment	Primary Treatment	Loading Type	Complications	Follow-up Results (Months)	mRS
1/47/F	9 days	Single stent (Leo plus)	NG tube	Acute stent thrombosis	Patent aneurysm (6)	0
2/39/M	16 days	Telescopic stent (Leo plus)	POL 8 hours before	None	Exitus at 25th day	6
3/55/F	9 days	Single stent (Leo plus)	NG tube	Acute MCA M1 thrombosis	PAO (12)	3
4/22/F	60 days	Telescopic stent (Leo plus)	POL 8 hours before	None	Aneurysm occlusion (6)	0
5/49/F	45 days	Telescopic stent (Leo plus)	POL 8 hours before	None	Aneurysm occlusion (6)	0
6/49/F	7 days	Telescopic stent (Leo plus)	POL 8 hours before	None	Aneurysm occlusion (6)	2
7/67/F	18 days	Telescopic stent (Leo plus)	POL 8 hours before	None	Aneurysm occlusion (6)	3
8/50/F	15 days	Flow-diverting stent (Pipeline)	POL 8 hours before	None	Aneurysm occlusion (6)	1
9/38/M	60 days	Flow-diverting stent (Pipeline)	POL 8 hours before	None	Aneurysm occlusion (12)	0
10/47/F	26 days	Telescopic flow-diverting stent (Pipeline)	POL 8 hours before	None	Aneurysm occlusion (3)	4
11/48/F	14 days	PAO with balloon	POL 8 hours before	None	PAO (3)	1
12/33/F	10 days	Telescopic flow-diverting stent (Pipeline)	POL 8 hours before	None	Aneurysm occlusion (3)	2
13/48/F	20 days	Flow-diverting stent (Pipeline)	POL 8 hours before	None	Aneurysm occlusion (6)	0
14/48/F	35 days	Flow-diverting stent (Pipeline)	POL 6 hours before	Insufficient stent expansion	Aneurysm occlusion (3)	3
15/55/F	20 days	Flow-diverting stent (Pipeline)	POL 8 hours before	None	Aneurysm occlusion (6)	0
16/49/F	13 days	Flow-diverting stent (Pipeline)	POL 8 hours before	Pericallosal infraction	Aneurysm occlusion (2)	1

Note: NG; Nasogastric, POL; Peroral loading

O157-Factors Associated with Complications and Recanalization of Embolized Pericallosal Artery Aneurysms

*Goran Pavlisa*¹, David Ozretic¹, Marko Rados¹

*University Hospital Center Zagreb Clinical Institute of Radiology Zagreb-Croatia*¹

PURPOSE: We present a series of 28 patients who underwent endovascular treatment due to a pericallosal artery aneurysm. To our knowledge, this is the largest such series of patients reported so far. The distal location and generally small size of these aneurysms makes them difficult for both surgical and endovascular treatment. Our aim was to define the risk factors for recanalization and complications of treatment.

MATERIALS AND METHODS: In this single-center retrospective study we investigated the relationship between the rate of complications and aneurysm recanalization against the anatomical, technical, clinical factors and demographic features. Statistical analysis was performed by Mann-Whitney test, correlation-contingency test and simple regression, using StatView 5.0 software.

RESULTS: Symptomatic peri-procedural complications occurred in 11% of patients. Aneurysm recanalization was encountered in 29% and in 18% it was considered significant to warrant a second interventional procedure. Statistically significant correlation, with $p < 0,05$, was found between complications and stent implantation. Recanalization was significantly correlated to initial incomplete occlusion, branch incorporation and anatomical variations. It was also more often found in female patients (no male patients experienced aneurysm recanalization), and associated with wide neck of the aneurysm, but with no statistical significance.

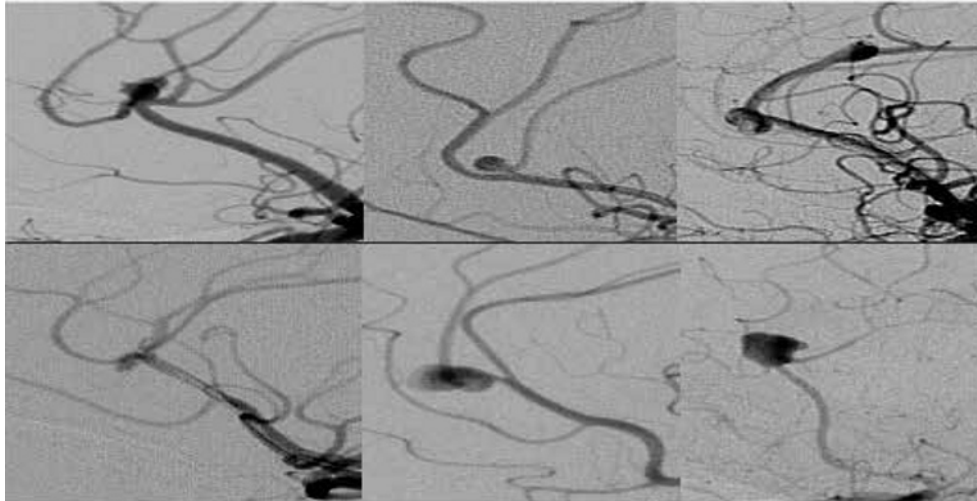
CONCLUSIONS: Pericallosal aneurysms in our study were morphologically and anatomically very heterogenous. Relatively large aneurysms, with incorporated arterial branches and angulation of pericallosal artery were associated with a higher risk of recanalization.

Figure legend

Digital subtraction angiography showing highly variable anatomy of pericallosal artery aneurysms.



ORAL PRESENTATIONS ABSTRACTS



158-Treatment of Elastase Induced Aneurysms in New Zealand White Rabbits with a New Flow Diverting Device the Derivo Embolization Device

Andreas Simgen ¹, Desiree Ley ¹, Umut Yilmaz ¹, Ruben Mühl-Benninghaus ², Körner Heiko

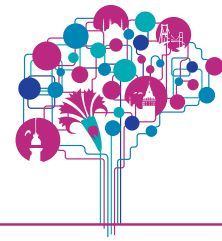
¹, Yoo-Jin Kim ³, Bruno Scheller ⁴, Andreas Müller ⁵, Wolfgang Reith ¹

Saarland University Hospital, Homburg/Saar, Germany *Neuroradiology Homburg-Germany* ¹ *Saarland University Hospital, Homburg/Saar, Germany* *Saarland University Hospital, Homburg/Saar, Germany* *Neuroradiology -Germany* ² *Saarland University Hospital, Homburg/Saar, Germany* *Pathology -Germany* ³ *Saarland University Hospital, Homburg/Saar, Germany* *Cardiology -Germany* ⁴ *Saarland University Hospital, Homburg/Saar, Germany* *Radiology -Germany* ⁵

INTRODUCTION: In the past years flow diverters have provided a promising alternative to treat complex intracranial aneurysms. We report about the preclinical performance of the Derivo® embolization device (Acandis GmbH, Pforzheim, Germany) in the treatment of elastase-induced aneurysms. **MATERIALS AND METHODS:** The Derivo® is a braided self-expanding stent composed of nitinol. The device was implanted across the necks of 17 elastase-induced aneurysms in New Zealand white rabbits. Additional devices were implanted in the abdominal aorta covering the origin of branch arteries. Angiographic follow-ups were performed immediately after placement of the device, after 3 months (n=8) and 6 months (n=9). After explantation the devices underwent micro-CT and MR-imaging (9.4 Tesla) before being histologically examined.

RESULTS: Aneurysm occlusion rates were noted as Grade I in 1 (6%), Grade III in 1 (6%), and Grade IV in 15 (88%) of 17 aneurysms respectively, indicating a complete or near- complete occlusion of 94% under double antiplatelet therapy. Navigation and positioning was feasible in all cases without deployment failures or stent migration. Radiopaque markers at both ends provided good visibility. Distal device occlusions were found in 3 cases and led to one grade I occlusion after 3 months. Distal device occlusions were caused by an extremely undersized vessel diameter in the distal subclavian artery and better understood after micro-CT and MR-imaging. No case of branch artery occlusion was seen. Intimal proliferation and diameter stenosis were moderate.

CONCLUSION: The Derivo® is a bio- and hemocompatible flow diverter which provides excellent occlusion of elastase-induced aneurysms, while preserving branch arteries.



ORAL PRESENTATIONS ABSTRACTS

O159-GREAT a Randomised Aneurysm Trial Procedural Safety and Core Lab Assessed Angiographic Baseline Results

*Christian A. Taschner*¹, René Chapot², Vincent Costalat³, Jerome Berge⁴, Patrick Courtheoux⁵, Alessandra Biondi⁶, Laurent Pierot⁷, Rafael Blanc⁸, Ansgar Berlis⁹, Horst Urbach¹, Hervé Brunel¹⁰, Betty Jean¹¹, Sophie Gallas¹², Xavier Barreau⁴, Krzysztof Kadziolka¹³, Jean Gabrillargues¹¹, Samer El Shikh¹, Hubert Desal¹⁴, Jens Fiehler¹⁵, Alain Bonafé³
*University Hospital Freiburg Neuroradiology Freiburg-Germany*¹ *Krupp Krankenhaus Essen Neuroradiology -Germany*² *University Hospital Montpellier Neuroradiology -France*³ *University Hospital Bordeaux Neuroradiology -France*⁴ *University Hospital Caen Neuroradiology -France*⁵ *University Hospital Besançon Neuroradiology -France*⁶ *University Hospital Reims Neuroradiology -France*⁷ *Fondation Rothschild, Paris Neuroradiology -France*⁸ *Klinikum Augsburg Neuroradiology -Germany*⁹ *University Hospital Marseille Neuroradiology -France*¹⁰ *University Hospital Clermont-Ferrand Neuroradiology -France*¹¹ *University Hospital Créteil, Paris Neuroradiology -France*¹² *University Hospital Reims Neuroradiology -France*¹³ *University Hospital Nantes Neuroradiology -France*¹⁴ *University Hospital Hamburg Neuroradiology -Germany*¹⁵

BACKGROUND and PURPOSE: To clinically evaluate the safety and efficacy of Hydrosoft coils (Microvention, Aliso Viejo, Ca) for the treatment of intracranial aneurysms

MATERIALS and METHODS: This randomised, controlled multicenter trial was conducted in 15 centres in France and 6 centres in Germany. Both ruptured and unruptured aneurysms were included. Patients were randomized between March 2010 and February 2014 to the Hydrosoft or control arms in a block design stratified by rupture status. Any bare platinum coils were allowed in the control arm, and assist devices could be used as clinically required. Clinical data was collected prospectively into a web-based database designed for this purpose. Angiographic data was reviewed by an independent core-lab. **RESULTS:** Five hundred and three patients were recruited. We will report on baseline characteristics of patients included, aneurysm presentation, the coiling procedure, and the immediate clinical outcome. In addition we will present the angiographic baseline results with respect to the Raymond classification as determined by the independent core-lab.

CONCLUSION: The present study collects data necessary to help in medical decision making. Within the controlled environment of this randomized, prospective trial safety characteristics as well as the ability to provide stable aneurysm occlusion are being compared between the Hydrosoft coil and standard platinum coils.

O160-An Analysis of Intraoperative Adverse Events for Interventional Therapy of Intracranial Aneurysms Based on Ruptured Status

*Sundeep Mangla*¹, Yaseen Karim², Ahmed Eldib²
*SUNY Downstate Health Science Center Radiology, Neurology, Neurosurgery, Brooklyn-United States*¹ *SUNY Downstate Health Science Center Radiology -United States*²

INTRODUCTION AND PURPOSE: Interventional therapy has become the primary treatment modality for cerebral aneurysms in most cerebrovascular centers. We analyzed our single operator experience including primary success, retreatment rates, use of adjunct devices, and adverse events with respect to presentation, unruptured cerebral aneurysms (UIAs) vs. SAH/ICH associated aneurysms (SAHa).

MATERIALS AND METHODS: We performed a retrospective review of clinical records and imaging of a prospectively maintained database of aneurysm therapies performed from 3/01/04 to 6/30/13. Data gathered included presentation (SAHa/UIA), primary success of treatment, retreatment, adjunct devices (stents/balloons), intra-operative adverse events (embolic/hemorrhagic), and immediate clinical outcome (<24 hours). **RESULTS:** A total of 131 aneurysms were treated in 107 patients in 123 operations (66 UIA and 65 SAHa). Treatment was successfully achieved in 124/131 (94.7%), and 9/131 (6.9%) represented retreatments or staged operations. Stents were employed in 15/131 (11.5%), and Balloon remodeling in 47/131 (35.9%). In the SAHa



ORAL PRESENTATIONS ABSTRACTS

group, we experienced 7 (10.8%) intraoperative perforations of the aneurysm with no neurologic deficit/change, disabling stroke, or death in 2(3.1%), 2(3.1%), 3(4.6%) patients respectively. Embolic events (including coil migration) were experienced in 2(3.0%) operations: 1(1.5%) with no deficit, 1(1.5%) disabling stroke, 0 deaths. In the SAHa group, overall intraoperative mortality (<24hrs) was experienced in 3(4.6%), with disabling stroke in 3(4.6%). In the UIAs, we experienced 2(3.0%) intraoperative perforations of the aneurysm with no neurologic deficit/change, disabling stroke, or death in 2(3.0%), 0(0%), 0(0%) patients respectively. Embolic events (including coil migration) were experienced in 3(4.5%) operations: 1(1.5%) with no deficit, 2(3.0%) disabling stroke, 0 deaths. In the UIAs group, overall intraoperative mortality was 0 with disabling stroke in 2(3.0%).

CONCLUSION: Cerebral Aneurysms presenting with SAH/ICH are at significantly higher risk of experiencing aneurysm perforation when compared with UIAs. Embolic event rates are similar between the groups. Overall intra-operative disabling morbidity and mortality rates for aneurysm therapy are higher with ruptured presentation (9.2%) vs. (3.0%).

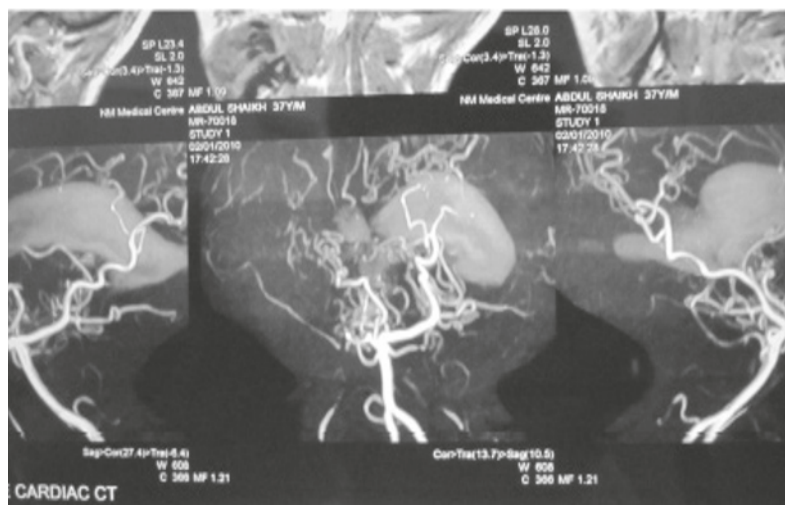
Adverse Event	Ruptured (n=65)	Unruptured (n=66)
SAH - no deficit	2 (3.1%)	2 (3.0%)
SAH - stroke	2 (3.1%)	0 (0%)
SAH - death	3 (4.6%)	0 (0%)
Emboli/coil - no deficit	1 (1.5%)	1 (1.5%)
Emboli/coil - stroke	1 (1.5%)	2 (3.0%)
Emboli/coil - death	0 (0%)	0 (0%)

O161-MoyaMoya Disease

*Kirankumar Dyawarkonda*¹

*K.B.Bandra Bhabha Hospital Crititcal care Medicine Mumbai-India*¹

The moya moya disease is a very rare condition affecting internal carotid arteries, occurring more commonly in children but also found in adults.the symptoms range from TIA's to stroke in children to intracerebral bleed in adults. We here report a case history of a middle aged man who presented with signs and symptoms of intra cerebral haemorrhage on DSA , the pt, had unilateral stenosed internal carotid artery with multiple plial collaterals. This case report suggests that the Moya Moya disease should be included in possible causes of intracerebral hemorrhage especially in young adults which rare in young and elderly people.





ORAL PRESENTATIONS ABSTRACTS

O162-Endovascular Working Channel Through the Wall of Small Vessels to the Extra Vascular space in CNS Liver and Heart

*Johan Lundberg*¹, Stefan Jonsson², Staffan Holmin¹

*Karolinska Institutet Clinical Neuroscience Stockholm-Sweden*¹ *Royal Institute of Technology Materials Sciences -Sweden*²

PURPOSE: For local treatment administration significant risks are attributed to creating parenchymal access in some places in the body, e.g. the central nervous system (CNS), pancreas and thoracic cavity. Endovascular intervention has been confined to work within the vascular tree. We have now developed an endovascular prototype catheter to create a working channel through the vessel wall: the trans-vessel wall technique. This technique includes detaching the distal tip through the vessel wall at the end of the procedure, thereby preventing hemorrhage. In summary, we have during the development used the technique to create access to the abdominal cavity, the axillary pit and to transplant insulin-producing cells to the pancreas. We are currently adapting the technique for use in the CNS, liver and heart.

MATERIALS AND METHODS: With clinical angiography- and catheter-systems we performed interventions in Macaque CNS and swine heart and liver and long term follow up interventions in swine external carotid artery (ECA), and pancreas. Stenosis formation was assessed with angiography and biocompatibility of the detached distal tip with histology. Cone-beam computed tomography (CBCT) was also used to evaluate the intervention and at follow up.

RESULTS: The trans-vessel wall prototype is fully integrated with clinical neuro-endovascular catheters and angiography equipment. We observed neither acute bleedings during establishment of the working channel nor thrombosis nor embolization after detachment of the distal tip. We can administer substances.

Angiography and CBCT showed vessels without stenosis and the detached distal tips outside the contrast stream one year after implantation; the vast majority of implants has probably had overgrowth of endothelium and then they become dislodged out of the bloodstream during the rebuilding of the vasculature architecture. Thereafter, the implants have become encapsulated with fibrin not thicker than 200 µm with a very limited inflammatory response. The vessels had normal histological appearances. This indicates that the trans-vessel wall technique is not comparable with stent placement and its ability to induce restenosis.

CONCLUSIONS: This study clearly shows that the trans-vessel wall technique is safe and that it is applicable to also the CNS, the liver and the heart, thereby opening new venues for extravascular work with endovascular methods. This technique might be applicable to cell therapy, viral transfections of gliomas, injection of nanoparticles and growth factors or cytological sampling.

O163-Posterior Circulation Dissecting Aneurysms review of 87 Cases from a Single Center

*N K Mishra*¹, Chetan Ravi¹, L Joseph¹, S B Gaikwad¹

*Neurosciences Center, All India Institute Of Medical Sciences Neuroradiology New Delhi-India*¹

PURPOSE: Review epidemiology, clinical profile & management outcome of patients with posterior circulation dissecting aneurysms.

MATERIALS AND METHODS: Data on demographics, clinical presentation, neurological deficits at presentation, treatment modality instituted (endovascular/surgical or conservative therapy) and its' outcome upon discharge and on follow up were extracted from medical records for the period January 2007 to August 2013 and analyzed.

RESULTS: Eighty seven patients (M:F=57:30, mean age=41.2 yrs) were diagnosed with posterior circulation dissecting aneurysms accounting for 5.96% of 1459 patients with intracranial aneurysms who underwent DSA during the study period.

The most common location of the dissecting aneurysms was posterior cerebral artery (26~29.88%) followed by vertebral artery (24~27.58%). Sixty-nine (79.31%) patients presented with subarachnoid hemorrhage, eleven



ORAL PRESENTATIONS ABSTRACTS

with mass effect symptoms and seven with ischemic symptoms. Endovascular treatment was instituted in 45 cases and surgery in 10 cases. 32 cases were conservatively managed. Twenty out of 87 were lost to follow up and were omitted from further analysis. Mean duration of follow up in the rest 62 was 22.6 months. In the conservatively managed group of 22 patients, spontaneous complete thrombosis was seen in 6(27.2%) while 7(31.8%) died. In embolization group, mortality was seen in 2 out of 36 patients while the rest are doing well. One of 9 patients who underwent surgical treatment died.

CONCLUSION: Endovascular or surgical intervention in posterior circulation dissecting aneurysms results in better outcome compared to conservative treatment. Spontaneous thrombosis is frequent but an unpredictable phenomenon as observed in our study (10.4%) with no definite angiographic features to indicate such an outcome. In view of fairly significant mortality and recurrent haemorrhage in patients treated conservatively, active intervention wherever possible is justified in reducing the risk of recurrent haemorrhage and mortality thereof.

O164-Ruptured Basilar Artery Perforator Aneurysms Outcome in 5 Cases

*Robert Forbrig*¹, Lorenz Ertl¹, Maximilian Patzig¹, Christian Brem¹, Hartmut Brückmann¹, Gunther Fesl¹

*Medical Center Großhadern Neuroradiology Munich-Germany*¹

INTRODUCTION AND PURPOSE: Basilar artery (BA) perforator aneurysms may lead to severe subarachnoid hemorrhage (SAH). In a case of acute ruptured aneurysm there is some uncertainty concerning the therapeutic management. In most cases conservative management is carried out, because 1) the approach to the anatomic site for coiling or clipping is challenging and 2) flow diverter stenting is hazardous due to required antiplatelet therapy and the efficacy of this therapeutic approach is still uncertain.

MATERIALS AND METHODS: 5 patients (3 male; median age 71) who presented with a ruptured BA perforator aneurysm between 2007 and 2013, were analyzed retrospectively. In detail, CT-, DSA and MR-imaging data, the treatment regimen, the clinical course and the long-term patient outcome were evaluated.

RESULTS: Four patients presented with SAH Fisher IV, one patient with SAH Fisher III. The WFNS score was I in two cases and V in three cases. Four patients received conservative therapy. In one case the parent vessel was an angioma feeder and was embolized. Each patient developed an ischemic perforator stroke in the area of the aneurysm. Three patients showed cerebral vasospasms with consecutive ischemic ACA/MCA stroke in one case. One patient suffered from circumscribed re-SAH in the area of the aneurysm 20 days after the first bleeding. After 6 months, this patient showed severe hemiparesis and dysarthria leading to a median Rankin scale (MRS) of 5. In the other patients, MRS was 1 (two cases) and 0 (two cases). Mean follow-up time was 34 months (range, 6 - 78 months). **CONCLUSION:** Despite severe SAH and high morbidity, the long term patient outcome was remarkably good in most cases. In only one patient a circumscribed re-SAH occurred. Conservative management of ruptured BA perforator aneurysms seems to be an acceptable treatment regimen.

O165-The Wee (Within 24 Hours) Aneurysm Endovascular Coiling After Subarachnoid Hemorrhage Single Center Experience

*Ossama Mansour*¹, Abdelrahman A²

*Alexandria University Neurology & Neuroradiology Alexandria-Egypt*¹ *Alexandria University Neurology -Egypt*²

BACKGROUND AND PURPOSE: The timing of definitive aneurysm treatment (coiling or clipping) in acute aneurysm subarachnoid hemorrhage was a subject of contro-versy. Although most neurointerventionalist agreed on early aneurysm treatment (within the first 72 hours), whether wee aneurysm coiling (within the first 24 hours) was beneficial remained debatable.

We aimed to investigate whether wee aneurysm coiling is associated with better neurological outcome.



ORAL PRESENTATIONS ABSTRACTS

MATERIALS AND METHODS: retrospectively we reviewed our data , where Two-hundred and seventy-six patients had

Hemorrhage onset time and aneurysm coiling time available for analysis. All patient records were analyzed to extract relative data.

RESULTS: For the 97 poor-grade (World Federation of Neurological Surgeons grading scale 4 to 5) patients, there was a significant association between Short Form-36 mental scores and the wee aneurysm coiling (50 ± 10 vs. 46 ± 10 , $P = 0.019$) and a trend toward association between the wee aneurysms coiling and favorable neurological outcome (odds ratio 2.4 [95% confidence interval 1.0 to 6.0], $P = 0.062$). A reduction in clinical rebleeding (12% vs. 22%, $P = 0.168$) was observed in patients undergoing a wee aneurysm coiling.

CONCLUSIONS: Aneurysm treatment performed within the 24-hour window may be associated with a better outcome and halve the clinical rebleeding risk in poor-grade aneurysmal subarachnoid hemorrhage patients.

O166-Virtual Stenting of Intracranial Aneurysm for Stent Alone Treatment by Using Computational Fluid Dynamics Analysis

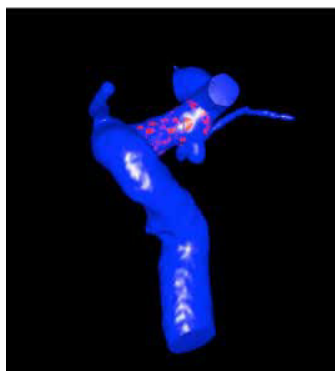
*Dae Chul SUH*¹, HyungBin Yu², Yunsun Song³

*Asan Medical Center Radiology Seoul-Korea, South*¹ *Siemens Healthcare -Korea, South*² *Asan Medical Center Radiology -Korea, South*³

PURPOSE: To access hemodynamic effect of stent-alone treatment in cerebral aneurysm with virtual stenting models by using newly developed computational fluid dynamics (CFD) analysis
METHODS AND MATERIALS: 3D DSA images of four aneurysms were obtained before and after stent-alone treatment. Using the CFD platform V2 (Siemens, Erlangen Germany) a geometric mesh model of the aneurysm was created by manually selecting the region of interest of the obtained vessel tree and locating the inlet and outlets. The platform provided simulation of virtual stent deployment on the cerebral mesh models by using streamlines, wall shear stress and flow vectors. For the computation of the flow in the cerebral vessels, the Newtonian fluid model was applied to the blood properties with pre-specified density and viscosity. The Navier-Stroke equations were used as the basic principles of numerically solving the conversation of mass and momentum under appropriate boundary conditions.

RESULTS: CFD simulation after virtual stenting corresponded to the follow-up result after stent-alone treatment and predicted disappearance of aneurysms in two and shrinkage of aneurysms in two after the treatment, and thus resulted in good correlation between the prediction of virtual stenting and the actual result of post-treatment of the aneurysms.

CONCLUSION: CFD analysis by using virtual stenting of CFD platform V2 is a reliable tool for the prediction of the destiny of the aneurysms after stent placement. Virtual stenting by using computational fluid dynamics can predict the effect of stent placement on aneurysm and is recommended when consideration of stent-alone treatment for intractable aneurysm.





ORAL PRESENTATIONS ABSTRACTS

PARALLEL SCIENTIFIC PAPER PRESENTATIONS

(Vascular Interventional 2) 17:15 - 19:00

Topkapı B Hall

O167-Diameter and Length Change of Carotid Stent after Deployment in a Small Case Series

*Te-Chang Wu*¹, Yu-Kun Tsui¹, Chien-Jen Lin¹

*Chi-Mei Medical Center Radiology Tainan-Taiwan*¹

PURPOSE: To evaluate the carotid stent diameter/ length change after stent deployment.
MATERIALS AND METHODS: In the past five years, six symptomatic patients (all males; mean age: 64.3 years-old) received two carotid stenting procedures, five of which had bilateral significant carotid stenosis (i.e. symptomatic stenosis>60% or asymptomatic stenosis>80%) and one of which had significant intrastent restenosis. The most narrowed diameter (ND) and whole stent length (WL) of first deployed stent in the initial and second procedures were record.

RESULTS: In these six patients, the mean interval between two carotid stenting procedures was 128 days (53-272 days). Two patients had thick calcified plaque (TCP). The average of increased ND ratio in all six patients, four patients without TCP and two patients with TCP were 23.33%, 32.35% and 5.3% respectively. The average of decreased WL ratio in all patients, four non-TCP patients and two TCP patients were 8.67%, 9.77% and 6.45% respectively.

CONCLUSION: Because of the inertial radial force of carotid stent, carotid stent will keep diameter increment (up to 32.35%) and length shortening (up to 9.77%) after deployment.

O168-Cervical Artery Stenting Prior to Intracranial Thrombectomy in Endovascular Treatment of Acute Stroke does not Impair Clinical Outcome at 90 Days

*Wiebke Kurre*¹, Marta Aguilar-Pérez¹, Sebastian Fischer¹, Elisabeth Schmid², Hansjörg

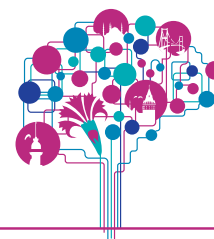
Bäzner², Hans Henkes¹

*Klinikum Stuttgart Neuroradiology Stuttgart-Germany*¹ *Klinikum Stuttgart Neurology -Germany*²

BACKGROUND AND PURPOSE: Cervical artery stenting has to be performed in some acute stroke cases to access intracranial embolic vessel occlusions. We aimed to assess whether cervical artery stenting adds an additional risk and impairs clinical outcome.

MATERIALS AND METHODS: Patients treated for an intracranial embolic vessel occlusion with the pREset retriever between August 2011 and June 2013 (n=249) were divided into two groups depending on the necessity to place a cervical stent. Patients receiving intracranial stents were excluded. We tested for imbalances between the two groups taking into account gender, age, NIHSS, atrial fibrillation (AF), diabetes, hyperlipidaemia, hypertension (HT), coronary heart disease, peripheral artery disease, the proportion of patients with unknown time window, the proportion of patients receiving intravenous thrombolysis, location of occlusion, recanalization rate, duration of treatment, parenchymal haemorrhage (PH), subarachnoid haemorrhage (SAH) and clinical outcome at 90 days applying the dichotomized mRS approach (0-2 vs. 3-6). The same parameters were tested as predictors for clinical outcome and significant predictors for outcome together with stenting vs. no stenting were included in a logistic regression model to control for confounders.

RESULTS: Patients requiring an extracranial stent were significantly younger, predominantly male and more frequently active smokers. The incidence of AF was lower. Treatment duration was significantly longer with cervical stenting. The frequency of PH, SAH and poor clinical outcome did not differ between patients with and without cervical stenting (Table 1). Univariable analysis revealed AF, diabetes, HT, unknown time window, PH, older age and a higher NIHSS as risk factors for poor clinical outcome. In a logistic regression model including all of the above and stenting vs. no stenting only diabetes (p=0.05, OR 2.14, 95% CI 1.00-4.56), unknown time window (p=0.026, OR 2.39, 95% CI 1.11-5.14), older age (p=0.004, OR 1.06, 95% CI 1.02-1.10), higher NIHSS



ORAL PRESENTATIONS ABSTRACTS

($p=0.000$, OR 1.15, 95% CI 1.10-1.21) and PH ($p=0.001$, 13.96, 95% CI 2.87-67.84) remained as independent risk factors for poor clinical outcome.

CONCLUSION: Cervical artery stenting in the setting of acute stroke does not increase the risk for poor clinical outcome at 90 days.

O169-Endovascular Management of Carotid Blowout Syndrome in Patients of Head and Neck Cancers

*Feng-Chi Chang*¹, Chao-Bao Luo¹, Wan-Yuo Guo¹, Michael Mu Huo Teng¹, Jiing-Feng Lirng¹, Chung-Jung Lin¹

Taipei Veterans General Hospital & National Yang Ming University, School of Medicine Radiology Taipei Taiwan¹

PURPOSE: To retrospectively evaluate the factors related to the outcomes of endovascular management in patients with head-and-neck cancers (HNC) associated with carotid blowout syndrome (CBS).

MATERIALS AND METHODS: Between 2000 and 2013, 96 patients with HNC with CBS underwent endovascular therapy. According to the location of the pathological lesions, the 40 patients located in the branches of external carotid artery was group 1 and the 56 patients located in the trunk of carotid artery was group 2. The group 2 was further divided into 2 subgroups by the way of management: group 2A was treated with deconstructive management by embolization and group 2B was treated with reconstructive management with stent-graft placement. The patients of group 1 was treated with deconstructive management. Fisher's exact test was used to examine demographic features, clinical and angiographic severities, and clinical and imaging findings as predictors of endovascular management outcomes.

RESULTS: Technical success and immediate hemostasis were achieved in all patients. Technical complications were encountered in 19 patients (19.7%), including 1 patient of group 1 (2.5%), 9 patients of group 2A (23.7%), 9 patients of group 2B (50%) ($P=0.0001$). Rebleeding occurred in 26 patients (27.1%), including 14 patients of group 1 (35%), 5 patients of group 2A (13.2%), 7 patients of group 2B (38.9%) ($P=0.0435$). Hemostatic period (months) of all patients was 8.1 ± 34.7 (0.01-80), including the group 1, 2A & 2B as 10.9 ± 18.8 , 7.59 ± 14.6 , 2.9 ± 3.0 ($P=0.2736$). Significantly worse technical complication, hemostatic outcome and survival in the 47 patients of acute CBS than the 49 patients of impending and threatened CBS were found (table).

CONCLUSION: Poor technical and hemostatic outcome was noted in the patients with reconstructive management of the carotid artery and those with advanced clinical severity of CBS. The lesion located in the external carotid artery was associated with high rebleeding. We suggest applying early intervention and deconstructive endovascular management in patients of HNC with CBS.

Table . Clinical severity and outcome of 96 patients of CBS accepted endovascular treatment

Variable	Threatened/ Impending CBS (n=49)	Acute CBS (n=47)	P
Technical			
Immediate Hemostasis	49(100%)	47(100%)	1
Complication	4(8.2%)	15(31.9%)	0.0035
Hemostatic			
Rebleeding	8(16.3%)	18(38.3%)	0.0155
Hemostatic period (mon)	11.0±19.7	5.1±8.6	0.0216
Survival			
Survival time (mon)	11.5±19.6	9.0±19.1	0.0709



ORAL PRESENTATIONS ABSTRACTS

O170-Traumatic Carotid Cavernous Fistula Single Balloon Treatment Experience

*Prijo Sidipratomo*¹, Jacub Pandelaki¹

*University of Indonesia Radiology Jakarta-Indonesia*¹

BACKGROUND AND PURPOSE: Traumatic Carotid Cavernous Fistula is quiet common in Jakarta Indonesia due to traffic accident. Endovascular techniques are the methods of choice for the treatment of patients with carotid cavernous fistulas we report our experience from single center in Ciptomangunkusumo Hospital Jakarta Indonesia a tertiary hospital, using single detachable ballon due to limitation of health insurance finances.

MATERIALS AND METHODS: We report in retrospective view our data base from January 2012 until Desember 2013 all the case of traumatic carotis cavernous fistula treated with detachable balloon. We found 11 cases were treated by using single detachable balloon. We followed the case until 6 month pos embolization.

RESULTS: All 11 cases the fistula were obliterated. There were no recurrent case and mayor complication.

CONCLUSION: In this series due to limitation of insurance finance we could obliterated all the fistula with single detachable balloon. We concluded embolization with this technique is save.

O171-Safety and Long Term Efficacy of Flow Diversion versus Standard Coiling in the Treatment of Unruptured Carotido Ophthalmic Aneurysms a Retrospective Analysis

*Federico Di Maria*¹, Silvia Pistocchi², Frédéric Clarençon¹, Raphael Blanc², Eimad Shotar¹, Bruno Bartolini², Jacques Chiras¹, Hocine Redjem², Nader Sourour¹, Michel Piotin²

*GH Pitié Salpêtrière Neuroradiology Paris-France*¹ *Fondation Ophtalmologique Rothschild Neuroradiology -France*²

PURPOSE: Carotido-ophthalmic aneurysms (COA) are prone to recanalisation after endovascular treatment. Flow diversion (FD) has emerged as a promising option, its goal being a stable aneurysm occlusion on the long term. We compared angiographic outcome and complication rates in two groups of patients treated at our institutions either by standard coiling (SC) or FD over 7 years.

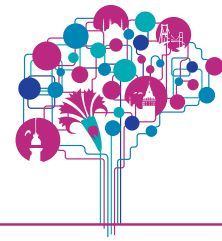
MATERIALS AND METHODS: From February 2006 to December 2013, 161 unruptured COA's subdivided into two consecutive cohorts, were treated endovascularly in 136 patients. Sixtyseven COA's were treated by SC in 61 patients. Balloon-assisted technique was employed in 41 cases, stent-assistance in 26. Flow diverters were used in 94 previously untreated aneurysms (75 patients). Additional coiling was performed in 25 cases. Clinical, angiographic results and complication rates were retrospectively analysed. Imaging follow-up (FU) was carried out by 3DTOF MRA and DSA at 6 months at 12 months respectively, then MRA yearly.

RESULTS: No procedure-related deaths and no aneurysmal bleeding occurred. Four thromboembolic events (6.6%), leading to permanent morbidity in 1 case (1.6%) occurred in the SC group. Two delayed homolateral intra-parenchimal hemorrhages (2.6%), 2 optic nerve compressions and 2 thromboembolic events were observed in the FD group (7,4% complication rate), resulting in 4,2% permanent morbidity. No statistically significant difference was found between complication (p=0.9) and morbidity rates (p=0.6).

Partial recanalisation was observed on latest FU after 1 year (mean 65.3+/-27.1 months) in 23/43 (53.5%) COA's treated by SC (11 neck remnants and 12 residual sacs), leading to re-treatment in 11 (25.6%, 16.4% of the total). Of the 17 aneurysms coiled by stent-assisted technique, 7 had recanalised at latest FU (41.2%).

In the FD group (mean FU 37.2+/- 25.4 months), 53.8% of all COA's were occluded within 6 months, 72.2% within 12 months, 85.3% on latest FU. No aneurysmal recanalisation was observed after thrombosis had occurred. Retreatment rate was 2.1% (2 aneurysms still patent at 24 months, requiring a second FD).

The difference between recanalisation rates was significant (p=0.0005), even when discarding neck remnants (p=0.009).



ORAL PRESENTATIONS ABSTRACTS

CONCLUSION: In this subset of aneurysms, our retrospective analysis shows better stability of occlusion after use of FD compared to SC, without significant difference in permanent morbidity. Flow diversion might increase the rate of long-lasting occlusion in COA's. Larger samples and long-term follow-up will better assess complication rates and treatment efficacy.

O172-ECA Stenting in Cerebrovascular Insufficiency Indications Efficacy and Durability Single Clinical Experience

*Ossama Mansour*¹, Mohamed Megahed²

Alexandria University Neurology & Neuroradiology Alexandria-Egypt¹ Alexandria University Critical Care Medicine -Egypt²

BACKGROUND AND PURPOSE: The external carotid artery (ECA) anastomoses in many distal territories supplied by the internal carotid artery (ICA) and is an important source of collateral circulation to the brain. In patients with symptomatic stenosis of the ICA, an ipsilateral stenosed ECA may precipitate additional sequelae such as transient ischemic attacks (TIAs), stroke, and ophthalmologic disturbances.

To examine the effectiveness of ECA stenting in treating cerebrovascular insufficiency due to symptomatic stunned cerebral state (e.g. in ipsilateral ICA occlusion, severe ipsilateral stenosis with contralateral ICAO etc.).

MATERIALS AND METHODS: we retrospectively reviewed patient databases in our center to identify all individuals who underwent ECA stenting Between June 2003 and June 2008. For all discovered cases, a common submission form to collect relevant demographic information, clinical data, procedural details, and follow up data were collected by mail- questionnaire follow-up sheet for further analysis.

RESULTS: 15 patients with stented 15 external carotid stenoses were identified for our cohort. The mean age of the selected patients (10 men, 5 women) was 67 years (range, 47-82 years). The indications for treatment were ECA stenoses according to the North American Symptomatic Carotid Endarterectomy Trial (NASCET) criteria. 6 symptomatic lesions, based on the "protection therapy" concept was treated, while we treated 9 symptomatic lesions that had the rationale based on the "augmentation therapy". Presenting symptoms included signs of transient ischemic attack, stroke, and amaurosis fugax. During follow up period with a median follow-up time of 22 months (range, 5-85 months; mean, 29 months), ECA stenting was associated with preservation of neurological status in 10 patients and resolution of symptoms in 5 patients. Symptomatic in-stent restenosis did not occur within any patient during the follow-up course.

CONCLUSION: ECA stenting in symptomatic ipsilateral ICA disease could be a potentially effective strategy to preserve neurological function and to relieve ischemic symptoms. a larger study could elucidate the true indications of this management strategy.

O173-Endovascular Treatment of Rupture Internal Carotid Artery Pseudoaneurysm After Radiotherapy for Head and Neck Tumor Long

Term Follow Up

*Sherman Lo*¹, WL Poon¹, YL Cheung¹, CM Chan¹, KW Tang¹, PH Wong²

Queen Elizabeth Hospital Radiology Kowloon-Hong Kong¹ Queen Elizabeth Hospital Neurosurgery -Hong Kong²

PURPOSE: This study evaluate the long-term outcome and effectiveness of two different types of endovascular treatments: 1) Coil entrapment of parent artery v.s. 2) stenting of the diseased artery.

MATERIALS AND METHODS: From a prospective data repository, 25 consecutive patients with 26 radiation-induced ICA pseudoaneurysms that ruptured and treated between October 1999 and February 2014, were retrieved. Hospital records, angiographic findings, intraprocedural, 30 days postop, and long term clinical outcome and complications were analyzed, with subsequent clinical and radiological imaging follow-up.

RESULTS: During the 15 years study period, 25 patients (22 male; age range 33-78 years) with head and neck radiotherapy, presented with rupture ICA pseudoaneurysms and were treated by endovascular means in our



ORAL PRESENTATIONS ABSTRACTS

hospital. The average time interval for pseudoaneurysm development after completion of radiotherapy was 11 years (range 2-19 years). Most pseudoaneurysms were arising from petrous segment of ICA (44%), followed by cervical segment (36%) and lacerum segment (20%). Therapeutic coil entrapment of the affected internal carotid artery was performed in 5 patients, and stenting of the diseased artery (with or without coils obliteration of pseudoaneurysm) was performed in 20 patients. Immediate hemostasis was achieved in all patients. 20 (80%) patients were discharged successfully from hospital, 18 patients (72%) without any major neurological defects (mRS <2). There were total seven complications encountered within 30 days after the procedure. Two patients rebleed during hospitalization and five patients encountered cerebral infarctions. Three complications (2 rebleed and 1 cerebral infarct) occurred in stenting group; whereas, four complications (4 cerebral infarct) occurred in coil entrapment group. Five mortalities (20%) happened within 30 days postop, three (60%) occurred in coil entrapment group and two (11%) in stenting group. The result of this study showed statistical significant differences in complication rates ($p=0.01$) and mortality ($p=0.04$) between coil entrapment group versus stenting group in treating ruptured postradiotherapy related ICA pseudoaneurysm. 30 days, 1 year and 3 years post-treatment mortality rates in coil entrapment v.s. stenting group were 60% v.s. 10% ($p=0.04$), 80% v.s. 60% ($p>0.05$), and 80% v.s. 85% ($p>0.05$) respectively. CONCLUSION: Both endovascular treatments, coil entrapment and stenting of diseased vessels, achieved effective immediate haemostasis and obliteration of the pseudoaneurysms. Stenting of pseudoaneurysms were shown to have a favorable immediate post-op and 30 days post-op outcomes.

O174-Utility of Flat Detector PBV Source Images in Diagnosing Intracranial Arterial Stenosis

*Sheng-Che Hung*¹, Chung-Jung Lin¹, Wan-Yuo Guo¹, Chao-Bao Luo¹, Feng-Chi Chang¹
*Taipei Veterans General Hospital Radiology Taipei-Taiwan*¹

PURPOSE: Parenchymal blood volume imaging (PBV) can provide cerebral blood volume values in the angiosuite and can be used for monitoring cerebral hemodynamic information without patient transfer. The aim of this study was to evaluate the reliability of PBV source images for detection of intracranial stenosis.

MATERIALS and METHODS: Eleven DSA exams of 11 patients were retrospectively evaluated. The axial, coronal, and sagittal MIP reformation of the source images were evaluated by two blind observers, and the final results were compared with DSA as the reference standard.

RESULTS: The intraclass correlation between two raters were excellent (ICC = 0.876). The sensitivity was 86.6% and specificity was 62% for detecting intracranial stenosis compared with DSA.

CONCLUSION: Besides the CBV information, the reconstructed source images of PBV can also be useful for evaluating intracranial arterial steno-occlusive changes.

O175-Intracranial Angioplasty and Stenting for Symptomatic Stenotic Atherosclerotic Disease the KFMC Experience

*Sultan AlQahtani*¹, Fahmi Alsenani², Hussam abo-shaer¹, Ayman Hamad²

*King Fahad Medical City Interventional & Diagnostic Neuroradiology Department Riyadh-Saudi Arabia*¹ *King Fahad Medical City Stroke Neurology Department -Saudi Arabia*²

BACKGROUND AND PURPOSE: Since the 1990s, angioplasty and stent placement for symptomatic stenosis of the supra-aortic vessels has proven to be an effective and safe modality of treatment, especially in patients presenting with strokes, transient ischemic attacks, or other related syndromes. The success rates of endovascular stent placement and angioplasty have shown high technical and clinical success rates, with low complications. Yet, complications related to balloon infiltration and stent fixation such as embolic formation or re-stenosis remains of a huge concern among clinicians.

To share King Fahad Medical City's experience over the past 4 years in treating recurrent symptomatic intracranial stenosis using angioplasty and stenting in addition to medical therapy.

MATERIALS AND METHOD: From 2010 to 2013, the charts of 52 patients presented to King Fahad Medical



ORAL PRESENTATIONS ABSTRACTS

City (KFMC) with symptomatic intracranial stenotic symptoms were reviewed and analyzed retrospectively. All patients were treated with angioplasty and stent placement. They all went through the same process in which they were all admitted a day before the procedure and discharged one day after the procedure from the stroke unit. All patients were under general anesthesia during the procedure and were all extubated immediately afterwards.

RESULTS: 52 patients were treated with the same procedure. No complications were noted except for a single case in which a non-disabling pontine infarct occurred 8 hours after treatment of a severe mid basilar stenosis with a calcified plaque; there were no periprocedural deaths in our series. All patients benefited from the procedure and had relief of their symptoms.

CONCLUSION: Based on our experience, we believe that intracranial angioplasty and stenting for symptomatic intracranial stenosis is considered safe and effective procedure, with a morbidity of less than 2% and a mortality of less than 1%.

O176-Stent Assisted Coiling Using the Acandis Acclino Device and Short Term Follow up

Heiko Koerner¹, Wolfgang Reith¹, Andreas Simgen¹, Ruben Muehl-Benninhaus¹, Umut Yilmaz¹
*Saarland University Hospital Neuroradiology -Germany*¹

INTRODUCTION AND PURPOSE: Stent assisted coiling is a feasible method for the treatment of wide-neck cerebral aneurysms. We report our experience with stent assisted coiling of wide-neck aneurysms using the Acandis® Acclino® Device, which is a self-expanding nitinol stent.

MATERIALS AND METHODS: We retrospectively analyzed our cases of stent assisted coilings of unruptured aneurysms using the Acandis® Acclino® stent. We looked into patient outcome, aneurysm occlusion rates and complication rates after the intervention and the first follow up after 3-6 months.

RESULTS: Stent deployment was possible in all 33 cases. In one case, the microcatheter could not be advanced into the aneurysm to perform the coiling. Stent assisted coiling was successful in the remaining 32 cases with a class 1 or class 2 occlusion rate (=complete occlusion or neck remnant) of 93% after 6 months. Procedural complications occurred in two cases (6%)

CONCLUSION: Stent assisted coiling using the Acandis® Acclino® device is a feasible and safe method for the treatment of wide-neck aneurysms.

O177-Endovascular Intervention for Galenic Venous Malformation and Dilatation. Therapeutic Decision and Genetic Analysis

Yuo Iizuka¹, Yoshiaki Tsutsumi², Yoshifumi Konishi³
*Ohashi Medical Center, Toho University Neuroradiology, Stroke Center Meguro-Ku-Japan*¹ *National Center For Child And Development Radiology* - ² *Kyorin University Neurosurgery* - ³

PURPOSE: We present our clinical experience in diagnosis and treatment of Galenic venous malformation and dilatation (GVM &GVD), with an emphasis on morphological classification, symptomatic algorithm, endovascular strategies, factors affecting treatment, and the preliminary report of genetic analysis.

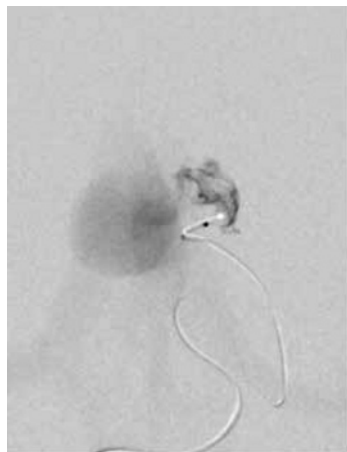
MATERIALS AND METHODS: From 1995 to 2014, 40 Galenic venous malformation and dilatation experienced. Angioarchitecture, imaging findings, clinical symptoms of them were analyzed.

RESULTS: In our series, eighteen out of 27 patients (67.5%) were successfully treated and half of them developed neurologically normal on follow-up after embolization. In this same group of treated patients, four of the 27 (14.8%) showed improvement, but demonstrated permanent neurological disability. The mortality rate in our series was 18.5% (five out of 27 patients). Eight patients closed short life around birth without treatment. Five patients follow without treatment. There are two mutation (endglin & RASA1) confirmed by genetic analysis.

CONCLUSION: Endovascular intervention should be indicated even if in GVM with severe congestive heart failure, pulmonary hypertension. Diffusion weighted images of fetus brain and superior vena cava pressure by Doppler are useful for therapeutic decision-making.



ORAL PRESENTATIONS ABSTRACTS



PARALLEL SCIENTIFIC PAPER PRESENTATIONS (Vascular Interventional 3) 17:15 - 19:00

Halic Hall

O178-Hybrid, Y-Configured Dual Stent Assisted Coil Embolization in the Treatment of Wide Necked Bifurcation Aneurysms

*Erol Akgul*¹, Tugsan Balli¹, Erol Aksungur¹

*Medical Faculty, Cukurova University Radiology Adana-Turkey*¹

PURPOSE: Stent-assisted coil embolization is widely used in the treatment of wide-necked cerebral aneurysms. In Y-stenting, stabilization of the first stent may be problematic as in some cases it migrates during second stent insertion. In this report, we evaluate the safety and effectiveness of the technique and present the longterm results of hybrid, Y-configured, dual stent-assisted coil embolization in the treatment of wide-necked bifurcation aneurysms.

MATERIALS and METHODS: We retrospectively evaluated the patients treated endovascularly due to cerebral aneurysms. Twenty patients treated with hybrid Y-stent-assisted coil embolization were enrolled in the study. In hybrid stenting, an open-cell intracranial stent (Neuroform) was used as a first stent to prevent its migration. A closed-cell stent (Enterprise or Acclino) was used as a second stent and the aneurysm was embolized with coils through the stent struts.

RESULTS: In the study, 14 of 20 patients were females and six were males. Their ages were between 16 and 82 (mean: 52). In all patients, hybrid Y-stenting and coil embolization were accomplished successfully. No stent migration occurred. Clinically neither symptomatic neurologic complication nor death was seen.

Of 20 wide-necked bifurcation aneurysms, nine were at the basilar tip, while eight were at the middle cerebral and three at the anterior cerebral arteries. One of the patients had a subarachnoid hemorrhage. Hybrid Y-stenting and coil embolization were performed in recanalized aneurysms previously treated with coil embolization in three patients and with surgery in one. The other 16 patients had not previously been treated. The mean angiographic follow-up was 24 months (6-52 months). No recanalization was seen in the patients.

CONCLUSION: Hybrid, Y-configured, dual stent-assisted coil embolization is a safe and effective method in the treatment of wide-necked bifurcation aneurysms to prevent stent migration and aneurysm recanalization, and is a viable alternative to microsurgery.



ORAL PRESENTATIONS ABSTRACTS

O179-Endovascular Treatment of Complex Cerebral Large and Giant Aneurysms Using A Telescopic Combination of the Leo and Silk Stents

*Vania Anagnostakou*¹, Muzaffer Saglam², Mujgan Orman¹, Osman Kizilkilic¹, Civan Islak¹, Naci Kocer¹
*Istanbul University, Cerrahpasa Medical Faculty Radiology, Division of Neuroradiology Istanbul-Turkey*¹
*GATA Haydarpasa Teaching Hospital Radiology -Turkey*²

PURPOSE: We propose the combined use of the Leo and Silk stents for the treatment of complex large and giant aneurysms. We report the advantages and technical aspects of this technique, and present immediate technical success along with the post treatment short and midterm imaging and clinical results.

MATERIALS AND METHODS: Our study included 23 patients with 25 intracranial aneurysms and mean age of 47.2 years. Seventeen aneurysms were found in the anterior circulation and 8 in the posterior circulation. Fifteen were saccular and 10 were fusiform. Mean aneurysm size was 20,6mm. From the 25 aneurysms in total, 8 were giant (≥ 25 mm), 5 were very large (≥ 20 mm), 6 were large (≥ 15 mm) and the remaining 6 were smaller (≤ 15 mm). Mean neck diameter of saccular aneurysms was 9,2mm, and for fusiforms mean length of aneurysmatic vessel segment was 15,6mm. All patients received a combined treatment with Leo and Silk stents in a telescopic fashion.

RESULTS: All patients received a combined treatment with Leo and Silk stents in a telescopic fashion. Immediate technical success was achieved in all patients. In 7 patients intra-procedural and/or acute procedure related complications were encountered. Mean angiographic follow-up period was 16 months with a range of 2 months to 3 years. Up to now 75% aneurysms are occluded, 20% show a small neck remnant and 5% continues to fill. Overall procedure related mortality and morbidity were 8,7% each. During follow-up period no side-branch occlusions were observed. Before treatment mRs was 0 in 18 patients, 1 in 3p, 3 in 1p, 2 in 1p. After treatment mRs was 0 in 18 patients, 1 in 1p, 3 in 1p, 2 in 1p and 6 in 2p.

CONCLUSION: The telescopic combination of braided FD stents for the treatment of intracranial large and giant aneurysms proved to be a usefulness technique in complex anatomical sites. This combination enables us to reconstruct the diseased arterial segment using long Leo stent as a scaffold and consequently to increase the flow diverting effect by positioning inside the less porous but with less radial force shorter Silk stent. With this novel endovascular technique, clinical and morphological findings are quite promising.

O180-Endovascular Coil Embolization for Distal Posterior Cerebral Artery (PCA) Aneurysm

*Masaru Hirohata*¹, Kimihiko Orito¹, Yukihiro Nakamura¹, Motohiro Morioka¹
*Kurume University Neurosurgery Kurume-Japan*¹

PURPOSE: Aneurysms of the posterior cerebral artery (PCA) are rare. Endovascular embolization of PCA aneurysms has evolved rapidly because surgery of PCA aneurysms is technically challenging. The purpose of this study was to report the clinical presentation, endovascular treatment, and outcome of PCA aneurysms.

MATERIALS AND METHODS: From 1998 to 2013, we treated 19 patients (F:M = 9:4, Age: 37-78 years, mean: 58.7) with PCA aneurysms. Thirteen patients presented with subarachnoid hemorrhage (SAH), one presented with a symptomatic temporal lobe seizure and the remaining five were asymptomatic.

Sixteen aneurysms were located on the P2 segment and another three aneurysms were located on the P3 segment of the PCA

RESULTS: Sixteen aneurysms were treated with aneurysm embolization, two with embolization of the aneurysm and the parent PCA and another with proximal PCA occlusion. Five aneurysms were treated with balloon remodeling technique and another was treated with the double catheter technique. Angiography indicated that seven of the ten aneurysms treated with aneurysm embolization were complete and there was a small neck remnant in three. One patient treated for aneurysm and a parent PCA showed temporal lobe infarction and one patient suffered from a small thalamic infarction due to delayed occlusion of PCA 7 months after treatment.

CONCLUSION: PCA territory has a rich anatomical collateral supply from choroidal arteries, anterior or middle cerebral artery, so PCA area relatively resistant to ischemia. Some authors mentioned that the parent



ORAL PRESENTATIONS ABSTRACTS

artery occlusion in the P2 segment was safe. However ischemic complication may occur (as our 2 cases). Therefore, aneurysm embolization sparing parent PCA flow should be selected for PCA aneurysm.

O181-High Mesh Density Low Permeability Flow Diverter in the Treatment of Intracranial Aneurysms a Prospective Non randomized Multicenter Clinical Trial

Ajay K Wakhloo¹, *Christian A. Taschner*², Pedro Lylyk³, Joost de Vries⁴, Javier Lundquist³, Alessandra Biondi⁵, Marius Hartmann⁶, Istvan Szikora⁷, Laurent Pierot⁸, Sakai Nobuyuki⁹, Imamura Hirotooshi⁹, Nader Sourour¹⁰, Ian Rennie¹¹, Martin Skalej¹², Oliver Beuing¹²,

Alain Bonafé¹³, Francisco Mery¹⁴, Francis Turjman¹⁵, Patrick Brouwer¹⁶, Edoardo Boccardi

¹⁷, Luca Valvassori¹⁷, Shahram Derakhshani¹⁸, Marc Litzenberg¹⁹, Mathew Gounis²⁰

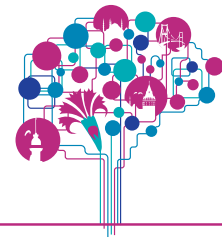
University of Massachusetts Medical School Radiology -United States ¹ *University Hospital Freiburg Neuroradiology Freiburg-Germany* ² *ENERI, Buenos Aires Neurosurgery -Argentina* ³, *Radboud University Nijmegen Medical Center Neurosurgery -The Netherlands* ⁴ *University Hospital of Besançon Neuroradiology -France* ⁵ *Helios Hospital, Berlin Neuroradiology -Germany* ⁶ *National Institute of Neurosciences, Budapest Neuroradiology -Hungary* ⁷ *University Hospital of Reims Neuroradiology -France* ⁸ *Kobe City Medical Center General Hospital, Kobe Neurosurgery -Japan* ⁹ *Hôpital Pitié-Salpêtrière, Paris Neuroradiology -France* ¹⁰ *The Royal Hospitals, Belfast Neuroradiology -United Kingdom* ¹¹ *Universitätsklinikum Magdeburg Neuroradiology -Germany* ¹² *Hôpital Guy de Chauillac, Montpellier Neuroradiology -France* ¹³ *Universidad Católica de Chile, Santiago Neurosurgery -Chile* ¹⁴ *Hôpital Neurologique, Lyon Neuroradiology -France* ¹⁵ *Erasmus University Medical Center, Rotterdam Neuroradiology -The Netherlands* ¹⁶ *Niguarda Ca' Granda Hospital, Milan Neuroradiology -Italy* ¹⁷ *Queen's University Hospital, London Neuroradiology -United Kingdom* ¹⁸ *Stryker Neurovascular, Fremont, CA -United States* ¹⁹ *University of Massachusetts Medical School New England Center for Stroke Research -United States* ²⁰

BACKGROUND AND PURPOSE: We present preliminary clinical and angiographic results of intracranial aneurysm (IA) treatment with a high mesh density, low permeability flow diverter (FD) obtained in a prospective, multicenter, non-randomized, single-arm trial.

MATERIALS AND METHODS: Surpass FDs (Stryker Neurovascular, Fremont, CA, USA) were implanted in 165 patients with 190 IAs of the anterior and posterior circulation at 24 centers. Primary efficacy endpoint was percentage of aneurysms with 100% occlusion on 6-month DSA. Primary safety endpoint was death and major stroke through follow-up period of minimum 6 months.

RESULTS: Successful FD delivery was achieved in 161 patients with 186 aneurysms (98%); number of devices used per aneurysm was 1.05. Clinical follow-up (mean, 11 months) of 150 patients (93.2%) showed primary safety endpoint occurred in 11 subjects. Procedure-related permanent neurological morbidity and mortality was 4.3% and 2.5%, respectively. For the subgroup with posterior circulation aneurysm, permanent neurological morbidity and mortality was 7.4% and, 11.1% respectively. Periprocedural ischemic stroke <31 days, SAH < 8 days, and IPH < 8 days were encountered in 3%, 2.5% and 2.5% of subjects respectively. No ischemic strokes > 30 days or SAH > 7 days were seen; one patient presented with IPH at 2 weeks. Perforator stroke and new onset or worsening of cranial nerve deficit was observed in 1.2% and 2.5% of subjects respectively. Follow-up angiographies were available in 158 (86.8%) aneurysms (mean, 11 months) and showed 100% occlusion in 119 aneurysms (75%).

CONCLUSIONS: Our clinical and angiographic outcome data show a high rate of aneurysm occlusion and acceptable safety for treatment of intracranial aneurysms with a high mesh density flow diverter.



ORAL PRESENTATIONS ABSTRACTS

O182-Stent and Balloon Assisted Coiling of Ruptured Cerebral Aneurysms in the Acute Stage

*Kirill Orlov*¹, Vadim Berestov¹, Alex Krivoschapkin¹, Dmitry Kislitsin¹, Timur

Shayakhmetov¹, Anton Gorbatikh¹, Pavel Seleznev¹

*Novosibirsk Research Institute of Circulation Pathology Neurosurgery Department Novosibirsk-Russia*¹

PURPOSE: To evaluate the results of the balloon and stent assisted coiling of cerebral aneurysms in the acute period of subarachnoid hemorrhage.

MATERIALS AND METHODS: In the department of neurosurgery of the Novosibirsk Research Institute of Circulation Pathology in the period from January 2011 to December 2013 73 patients with 97 cerebral aneurysms underwent endovascular treatment in the acute period of subarachnoid hemorrhage: 17 patients had multiple aneurysms (from 2 up to 5). 46 (63%) patients were female, 27 (37%) were male, mean age - 47 years (from 20 to 78 years).

The most frequent location of aneurysms in our series was ICA - 39 (40.2%), less frequently aneurysms were located at the ACA - 25 (25.8%) and MCA bifurcation - 17 (17.5%), posterior circulation aneurysm location occurred in 12 cases (12.4%) .

RESULTS: Operations were performed within the period of 19 days (with average being 7 days) after the rupture, immediately after admission. In acute period totally 86 aneurysms were occluded (up to 4 simultaneously), four aneurysms were embolized lately in posthemorrhagic period. 7 aneurysms due to the small size and low risk of rupture were not treated.

Coils as a single embolic material were used for 53 aneurysms (61.6%), assisting techniques were used for 33 aneurysms (38,4%): 25 aneurysms (29.1%) required balloon-assistance, 8 aneurysms (9.3%) were closed with stent-assistance methods.

Transvenous introduction of eptifibatide (Integrilin) scheme followed by oral antiplatelet therapy (aspirin and clopidogrel) after wake up has been used for stent-assistance in the acute period. Intraoperative complications were observed in 10 cases: 9 were hemorrhagic (aneurysm perforation), 1 - ischemic (vasospastic stroke). In our series of stent-assisted coiling during acute SAH perioperative complications were not reported. Balloon-assisted techniques were accompanied by 4 hemorrhagic complications due to intraoperative aneurysm rupture.

CONCLUSION: Balloon-assisted embolization of cerebral aneurysms in the acute stage of rupture allows for greater packing density of the coils in the aneurysmal sac and minimizes risk of the aneurysm perforation.

Use of intracranial stents during acute intracranial hemorrhage allows to achieve good results in embolization of complex aneurysms with wide neck without the increase of the overall surgical risk.

O183-MCA Aneurysms Coiling without Assisted Technique Our Experience

*Umair Rashid*¹

*PGMI Neuro Radiology Lahore-Pakistan*¹ *Neuroradiology Department, PGMI, Lahore General Hospital, Lahore*

PURPOSE: To assess risk of delayed coiling of the MCA aneurysms without assisted technique.

MATERIALS AND METHODS: This study was conducted from July 2010 to February 2014 at the Department of Neuroradiology, Post Graduate Medical Institute, Lahore General Hospital, Lahore. A total of 50 patients with cerebral aneurysms at the level of MCA were included in this study of both genders. **RESULTS:** Out of 50 patients, there were 20(40%) males and 30 (60%) female patients.

Their age ranged from 22 - 65 years. The maximum numbers of patients were in their fifth and sixth decade of life. In our study successful coiling was done in all patients with minimal recurrence/recanalization of cerebral aneurysms at MCA.

CONCLUSION: Conventional coiling in MCA aneurysms in delayed circumstances appears equally better alternative to coiling with assistant techniques.



ORAL PRESENTATIONS ABSTRACTS

O184-Y Stent Assisted Coiling of Bifurcation Aneurysms with Open Cell Stents

*Nicola Limbucci*¹, Leonardo Renieri¹, Sergio Nappini¹, Arturo Consoli¹, Andrea Rosi¹, Salvatore Mangiafico¹
*Careggi University Hospital, Florence Interventional Neuroradiology Firenze-Italy*¹

PURPOSE: Despite evolution of endovascular techniques, coiling of wide neck bifurcation aneurysms is still challenging. Y-stent assisted coiling has been reported as an effective technique for such complex cases, however many technical variation of this procedure do exist. We report our experience in Y-stent assisted coiling of bifurcation aneurysms using open cells stents.

MATERIALS AND METHODS: Fourty-four consecutive patients with wide-neck bifurcation aneurysms were included in this series; technical failure occurred in 5 cases (11.4%) so the planned Y-stent assisted coiling procedure was performed in 39 patients. Aneurysm site was: 18 middle cerebral artery, 10 anterior communicating artery, 9 basilar tip, 2 internal carotid artery tip.

Our standard technique involved deployment of the first open cell stent in the most angulated bifurcation branch, then deployment of another open cell stent in the other branch crossing the interstices of the first stent. The aneurysm was coiled after jailing of the microcatheter or catheterization of the stents. All procedures were performed under double antiplatelet therapy. Periodical clinical and angiographic follow-up was performed.

RESULTS: Among 39 Y-sent assisted coiling procedures, 2 procedural complications occurred (5.1%). Both complications were aneurysm perforation: one patient had minor disability (mRS 1) and one patient died (mortality 2.6%). No delayed ischemic stroke occurred; one patient experienced transitory ischemic attack after early antiplatelet discontinuation. Mean angiographic follow-up time was 18 months. Complete immediate occlusion was obtained in 92.3% on patients. At follow-up no recanalization occurred in fully occluded aneurysms.

One remnant regrowth at follow-up and was recoiled achieving complete occlusion. No significant in-stent stenosis occurred.

CONCLUSIONS: Y-stent assisted coiling of bifurcation aneurysms appears a safe and effective technique, with high post-procedure occlusion rate and low recanalization rate at follow-up. The complication rate is reasonably low, considering that treatment of bifurcation aneurysms is very challenging or sometimes unfeasible with other techniques. Closed cells stents can be safely used for Y-stenting, indeed they offer the advantage of easier catheterization, delivery and deploying into distal and tortuous vessel than open cell stents. Aneurysm occlusion appears very stable over time, we guess

that this is likely to depend on flow diverting effect of crossing stents.

O185-Y Stent Technique for Endovascular Treatment of Wide Neck Bifurcation Cerebral Aneurysms

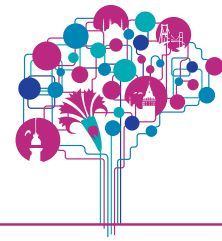
*Kamil Zeleňák*¹
*University Hospital, Martin Department of Radiology Martin-Slovakia*¹

PURPOSE: To evaluate periprocedural complication of Y-stent technique for endovascular treatment of wide-neck bifurcation cerebral aneurysms.

MATERIALS AND METHODS: From December 2011 to June 2013 13 patients (2 male and 11 female) with average age 57,8 year (33-81) (8 patients with ruptured aneurysm and 5 patients with unruptured aneurysm) were treated by usage Y-stent technique for wide-neck bifurcation cerebral aneurysm. Location of aneurysms was as follows: AcomA: 3 patients, MCA: 4 patients, ICA: 1 patient, basilar tip: 4 patients, PcomA: 1 patient.

RESULTS: There was no periprocedural rupture and one perioperative thrombembolic event.

CONCLUSION: The reconstruction by using Y-stent technique can be used successfully in selected patients with wide-neck bifurcation cerebral aneurysms.



ORAL PRESENTATIONS ABSTRACTS

O187-Long term follow up in Intracranial Aneurysms Treated Using the Surpass Flow Diverter Stent

*Alessandra Biondi*¹, Elisa Pomero¹, Florence Descourvierer¹, Arnaud Flores¹, Clara Prud'homme¹, Eviane Farah², Françoise Cattin¹

*Besancon University Hospital Neuroradiology and Endovascular Therapy Besancon-France*¹ *Besancon University Hospital Anesthesiology -France*²

PURPOSE: The Surpass Flow Diverter Stent is a self-expandable braided device preloaded in a microcatheter delivery system. This flow diverter stent is made by a cobalt chromium mesh with 12 platinum tungsten wires of the same diameter. Our purpose was to evaluate long term clinical and angiographic results in a series of patients with intracranial aneurysms treated using the Surpass Flow Diverter Stent.

MATERIALS AND METHODS: Twenty-five patients (20 females, 5 males, mean age: 52 years) with 30 aneurysm treated by the 29 Surpass Flow Diverter Stent were included in the study. Seventeen aneurysms were unruptured, 2 ruptured and 11 residual/recurrent. 75 % of patients suffered from a previous SAH, multiple aneurysms and/or familiar history of SAH.

RESULTS: No clinical permanent complications were observed after the procedure. One patient died at 5 days after the procedure due to the aneurysm bleeding. Occlusion rate immediate after the procedure and at follow-up will be reported and discussed. Aneurysm rate occlusion was 60.5% at 3 months follow-up and 90.1% at 1 year. MR findings suggesting silent embolisms were similar to those observed using other Flow Diverter or regular Stents.

CONCLUSIONS: The results confirm that the use of the SurpassFlow Diverter Stent is an effective and relatively safe technique in some configurations of intracranial aneurysms. The angiographic follow-up is promising. However, more experience and long-term follow up are needed in order to define precisely the indications of the Flow Diverter stents.

O188-Flow Diverter Stenting in Intracranial Aneurysms Previously Treated with a Regular Stent Should We Do It

*Alessandra Biondi*¹, Elisa Pomero¹, Arnaud Flores¹, Katia Gete¹, Clara Prud'homme¹, Eviane Farah², Françoise Cattin¹

*Besancon University Hospital Neuroradiology and Endovascular Therapy Besancon-France*¹ *Besancon University Hospital Anesthesiology -France*²

PURPOSE: To evaluate clinical and angiographic results and long term follow up in a series of patients with a recanalized intracranial aneurysm previously treated using a regular stent.

MATERIALS AND METHODS: Nine patients with a recanalized intracranial aneurysms treated by a regular stent and coils (1 neuroform stent in three patients, 1 enterprise stent in three patients, 2 enterprise stents in two patients and 1 Leo stent in one patient) were included in the study. Flow diverter stents were Pipeline stent (ev3 company) in six cases and Surpass stents in three. DynaCt or XperCT was used in all cases in order to evaluate correct deployment of the stent.

RESULTS: Flow diverter stent deployment failed in one case and was very challenging in two. No clinical complications were observed immediately after the procedure and at follow up. All patients underwent long term angiographic and MR follow-up studies. Complete occlusion was observed in six of eight patients in whom the procedure was successful.

CONCLUSIONS: Flow diverter stenting in aneurysms previously treated with a regular stent remains a challenging procedure and should be reserved in selected cases. The evaluation of the full deployment of the previous stent could be difficult, however this information is crucial in order to plan a correct indication for flow diverter stenting.



ORAL PRESENTATIONS ABSTRACTS

O189-Safety and Efficacy of a New Device for the Treatment of Wide Neck Bifurcation Aneurysms (pCONus) – Preliminary Experience

*Marta Aguilar-Pérez*¹, *Wiebke Kurre*¹, *Oliver Ganslandt*², *Hansjörg Bänzner*³, *Hans Henkes*¹

*Klinikum Stuttgart Neuroradiology Stuttgart-Germany*¹ *Klinikum Stuttgart Neurosurgery -Germany*² *Klinikum Stuttgart Neurology -Germany*³

PURPOSE: Wide neck bifurcation aneurysms (WNBA) are considered to belong to the subgroup of aneurysms with increased difficulty and risks. Balloon- and stent-remodeling are known techniques for their treatment. pCONus is a self-expanding, completely retrievable, electrolytically detachable device with a proximal shaft, 4 distal petals and a nylon cross in the distal end of the shaft. The device is made to bridge the orifice of WNBA in order to allow better control of the coil occlusion. It combines elements of “waffle cone” stent deployment and the no longer available TriSpan Device. Our purpose was to evaluate the safety and efficacy of this device for the treatment of WNBA

MATERIALS AND METHODS: 46 consecutive patients underwent endovascular treatment of WNBA using pCONus between February, 2012 and February, 2014. Target vessels included the anterior circulation in 37 (80.4%) and the posterior circulation in 9 (19.6%). 12 patients were treated in the setting of acute subarachnoid hemorrhage (26.1%).

RESULTS: Neither technical failure nor rupture was encountered. Acute thrombi formation was observed in only one patient (2.2%), which resolved after administration a body weight adapted bolus dose of eptifibatid (Integrilin). After the initial procedure, total occlusion was achieved in 18 (39.1%) patients and a neck remnant was evident in 15 (32.6%). Follow-up angiography was available in 29 patients and demonstrated complete occlusion in 15 (51.7%). Evident coil compaction requiring re-treatment was observed in six patients. pCONus also assisted re-coiling.

CONCLUSION: pCONus allows controlled coil occlusion of WNBA, both ruptured and unruptured. Major complications are rare.



ORAL PRESENTATIONS ABSTRACTS

Friday, September 12, 2014

PARALLEL SCIENTIFIC PAPER PRESENTATIONS

(Adult NR 4) 17:15 - 19:00

Marmara Hall

O190-Cerebral Ischemia Detected with Diffusion Weighted MR Imaging After Filter Protected Stenting of High Grade Symptomatic Carotid Artery Stenoses

Ender Uysal ¹, Omer Naci Tabakci ¹, Deniz Turkyilmaz Mut ¹, Dilek Necioglu Orken ²,
Muzaffer Basak ¹

*Sisli Etfal Training and Research Hospital Radiology -Turkey 1 Sisli Etfal Training and Research Hospital
Neurology -Turkey ²*

INTRODUCTION AND PURPOSE: We aimed to evaluate possible cerebral embolies , their localization and quantity during the carotid artery stenting procedure by using DWI MR imaging, **MATERIALS AND METHODS:**68 patients with symptomatic and severe carotid artery stenosis who referred to our clinic for filter protected carotid artery stenting procedure were included in this study. The WI images with a standard B value of 1000, were taken 24 hours before and after the CAS procedure and evaluated retrospectively at work station by two separate radiologists according to the quantity, size and localization of the acute ischemic lesions with consensus. Size measurement were done regarding the largest diameter of the lesions and localization of the lesions were classified as ipsilateral and contralateral.

RESULTS: CAS procedure failed in 4 out of 72 patients due to anatomical difficulties in one, inability passing through the critical stenosis in another and presence of intraluminal thrombosis in remaining two patients. The procedure was successfully performed in the remaining 68 patients. None of the patients developed major stroke and the overall mortality of the procedure was zero. Acute ischemic lesions (AIL) were present in 10 out of 68 patients on post -stent DW MRI. AILs in 8 out of 10 patients were located ipsilaterally; one patient had AILs on the contralateral side whereas the other one had on both hemispheres. All the lesions seen on the ipsilateral hemisphere were with embolic character of less than 3 mm size and counted less than 10 in number. However, DWI MRI of one patient showed lesions on both hemispheres; the contralateral lesion with hemodynamic character bigger than 10 mm and distributed in the ACA-MCA watershed zone.

CONCLUSION: In this study 14% of the patients suffering from severe symptomatic carotid stenosis and treated with filter protected CAS procedure had AILs presented on post- stent DW MRI. Although the filter protection may not always prevent cerebral embolies, all patients with an embolic event had a subclinical course. It can be suggested that CAS related ischemic lesions could be decreased by thorough study of the plaque nature and appropriate selection of the patients before the procedure.

O191-Clinical Study of Chemical Exchange Saturation Transfer MRI on Cerebral Infarction at 1.5 Tesla

Yongui Yang ¹, Zhiwei Shen ², Xiaojin Xu ³, Fang Chen ³, Zhongping Zhang ⁴, Gang Guo ³,
Renhua Wu ⁵

*The 2nd Hospital of Xiamen Radiology Xiamen-China ¹ The 2nd Affiliated Hospital, Shantou University Medical
College - ² The 2nd Hospital of Xiamen - ³ GE healthcare - ⁴ The 2nd Affiliated Hospital, Shantou University - ⁵*

PURPOSE: to investigate the feasibility of CEST on the patients with cerebral infarction at a widely used 1.5T clinical MRI scanner.

MATERIALS AND METHODS: In this study, total nine patients comprising of 3 with hyperacute cerebral infarction, 3 with acute cerebral infarction and 3 with subacute cerebral infarction were enrolled and imaged with CEST, z-spectrum and conventional fluid-attenuated inversion recovery (FLAIR) sequence on a 1.5T clinical whole body MR scanner (Signa HDe, GE Healthcare) before



ORAL PRESENTATIONS ABSTRACTS

the symptom onset, within 24 hours and after 1 week, respectively. Concretely, the CEST scan was performed with TR=60ms, TE=minimum available, flip angle=35°, acquisition matrix=128×128,FOV=20cm. All the infarctions were scanned at two radio frequency (RF) offset of ±224Hz (±3.5ppm) relative to the water. A control image with no saturation pulse applied was also acquired. To increase the signal-to-noise (SNR) ratio, the saturated CEST images and the control image were averaged 8 times. Fat saturation was applied. The amide proton transfer (APT) images were calculated as magnetic transfer ratio (MTR) asymmetry at 3.5ppm.

The z-spectrum (normalized signal intensities with respect to unsaturated) was acquired from an offset range of +255Hz to -255Hz with an interval of 10 Hz, and was fitted by a 12th order polynomial for per pixel. All the patients also underwent diffusion-weighted imaging (DWI) and perfusion-weighted imaging (PWI), both of which are increasingly used in acute stroke.

RESULTS: The infarction lesions showed hypoperfusion on the PWI images, hyperintense on the FLAIR and DWI images. Similarly, the saturated images (Figure 1a and 1b) also demonstrated different intensity levels between the lesion and normal tissue. The infarction lesions appeared hypointense on the APT image as shown in Figure. 1c and the size of lesion agreed well with that of the DWI image (Figure 1d). In addition, the zones of lesions and edema on the APT image showed different levels of hypointensity.

CONCLUSION: CEST may offer a specific and sensitive method to characterize cerebral infarction, especially in evaluating the presence of salvageable tissue which is functionally impaired and at risk of infarction, i.e. ischemic penumbra, and thus provide complementary information to DWI and PWI.

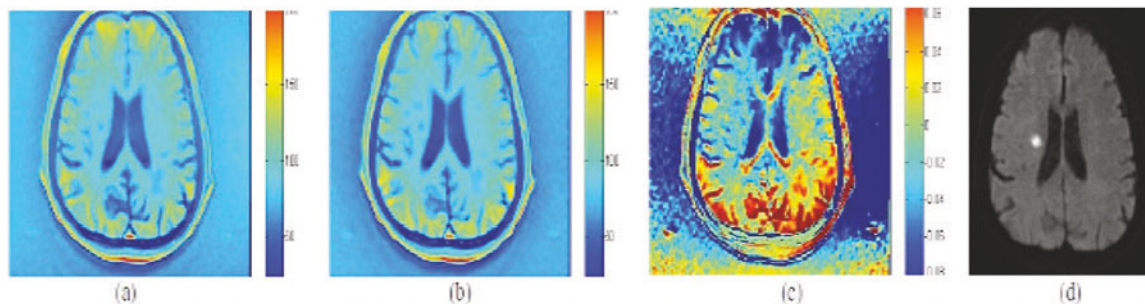


Figure 1. Representative MR images of a brain infarction at 1.5T: saturated image at 224Hz (a), saturated image at -224Hz (b), the APT image(c), the DWI image(d).

O192- Limbic-Auditory Interactions of Tinnitus ; Evaluation with Diffusion Tensor Imaging

*Hediye Pinar Gunbey¹, Emre Gunbey², Kerim Aslan¹, Taner Bulut³, Asude Unal⁴, Lutfi Incesu¹.
Ondokuz Mayıs University, Department of Radiology, Samsun, Turkey¹, Ondokuz Mayıs University,
Department of Otolaryngology, Samsun, Turkey², Adiyaman University, Department of Radiology, Adiyaman,
Turkey³, Samsun Training and Research Hospital, Department of Otolaryngology, Samsun, Turkey⁴*

PURPOSE: Tinnitus is defined as an imaginary subjective perception in the absence of an external sound. The obvious effects of tinnitus on quality of life affects the development of treatment pathophysiological models. Convergent evidence proposes that tinnitus perception includes auditory, attentional and emotinal components. The aim of this study is to investigate the talamic , auditory and limbic interactions associated with tinnitus related distress by diffusion tensor imaging (DTI).



ORAL PRESENTATIONS ABSTRACTS

Methods: A total of 30 tinnitus patients 15 with and 15 without hearing loss and 15 age-sex matched healthy controls underwent an audiologic examination as well as an MRI protocol including structural and DTI sequences. All participants completed Tinnitus Handicap Inventory (THI) and Visual Analog Scales (VAS) related with tinnitus distress. The mean FA and ADC values were obtained for auditory cortex (AC), inferior colliculus (IC), lateral lemniscus (LL), medial geniculate body (MGB), thalamic red nucleus (TRN), corpus callosum genu-splenium, amygdala (AMG), hippocampus (HIP), parahippocampus (PHIP) and prefrontal cortex (PFC).

RESULTS: The IC, MGB, TRN, AMG showed FA decrement and ADC increment in tinnitus patients according to healthy controls ($p < 0,05$). The LL FA values decreased significantly ($p = 0,030$) only in tinnitus patients with hearing loss. Bilateral hippocampal FA decreased ($p < 0,01$) and bilateral parahippocampal ADC increased ($p < 0,01$) significantly in tinnitus patients. In correlation analysis with audiologic findings, the hearing loss showed negative correlation with FA values and positive correlation with ADC values of contralateral IC and LL. As hearing loss increased the ADC values of ipsilateral AC increased positively ($r = 0,363$, $p = 0,007$). Independently from tinnitus side, the FA values of right MGB related negatively with hearing loss (R- $r = -0,320$; L- $r = -0,326$). In correlation with THI and VAS scores, a negative relation found between the FA values of AMG and THI total (THI-S), emotional (THI-ES) and catastrophic (THI-CS) subscale scores. Hippocampal FA values showed negative correlation with THI functional (THI-FS)/ THI-CS subscales, sleep-VAS and attention deficiency (AD) VAS scores. Additionally bilateral ADC values of PHIP and PFC significantly correlated with AD- VAS scores.

CONCLUSION: In conclusion to our knowledge this is the first DTI study to investigate the grey matter structures related to tinnitus perception. In the present study, the significant correlation of FA and ADC with clinical parameters suggests that DTI can provide helpful information for tinnitus. Magnifying the microstructures DTI can help to evaluate three faces of tinnitus nature: hearing, emotion and attention.

O193-Utility of DWI FLAIR Mismatch in Early Stroke in Identifying Time Window to Guide Management a Study of 32 Patients

*Ritu Kakkar*¹, Sameer Soneji 1, Shrinivas Desai ¹
*Jaslok Hospital CT and MRI Mumbai-India*¹

PURPOSE: To analyze whether a mismatch in detection of an acute ischaemic lesion between diffusion-weighted images (DWI) and fluid-attenuated inversion recovery (FLAIR) i.e. DWI-FLAIR mismatch can be used to detect patients within the recommended time window for treatment.

MATERIALS AND METHODS: 32 patients (M:F=3:1) with clinically diagnosed acute stroke (<6 hours duration) underwent MRI. DWI and FLAIR images were obtained and visibility of acute ischaemic lesions was judged. Statistical analysis was done to calculate the sensitivity, specificity, positive predictive and negative predictive values.

RESULTS: 31 out of 32 patients had lesions detectable on DWI of which 24 were not seen on FLAIR. 7 patients showed mild FLAIR hyperintensity. DWI-FLAIR mismatch had a sensitivity of 77%, specificity of 100%, positive predictive value of 75% and negative predictive value of 25%.

CONCLUSION: Patients of acute stroke with an detectable acute ischaemic lesion showing DWI-FLAIR mismatch are likely to be within a time window for which thrombolysis is safe and effective.



ORAL PRESENTATIONS ABSTRACTS

O195-A Five Year Period Of Evolution In MR MRA Imaging Follow Up Of Large And Giant Intracranial Aneurysms Treated With Pipeline Embolization Device

*Carolina Parada*¹, Jorge Chudyk², Hector Lambre¹, Pedro Lylyk²

ENERI Radiology CABA-Argentina ¹ *ENERI Interventional Neuroradiology -Argentina* ²

PURPOSE: Long term follow-up evaluation of large and giant intracranial aneurysms treated with PED using a non-invasive diagnostic technique such MR-MRA have not been reported. We report our experience in the evolution of these challenging aneurysms after their treatment with PED.

MATERIALS AND METHODS: From 570 large and giant aneurysms treated with PED between 2009 and 2013 a total of 92 were selected with the following criteria: 1) large and giant intracranial aneurysms treated with PED and 2) MR-MRA imaging follow up. The imaging examinations were performed with 3T magnet (Achieva Philips Healthcare, Best, the Netherlands) and included FLAIR, T1, T2, MR angiography and T1 postgadolinium sequences. **RESULTS:** 76% aneurysms were located at the anterior circulation being 58% supraclinoid, 26% carotid cavernous and 16% distal to the Circle of Willis. The remaining 24% were located at the posterior circulation with 64% at the basilar trunk and 36% at the vertebral arteries.

The predominant morphology was the sacular form with 63% followed by the dissecting form with 25% and the fusiform form with 12%. It was also the sacular aneurysm the predominant form of occlusion with 59%.

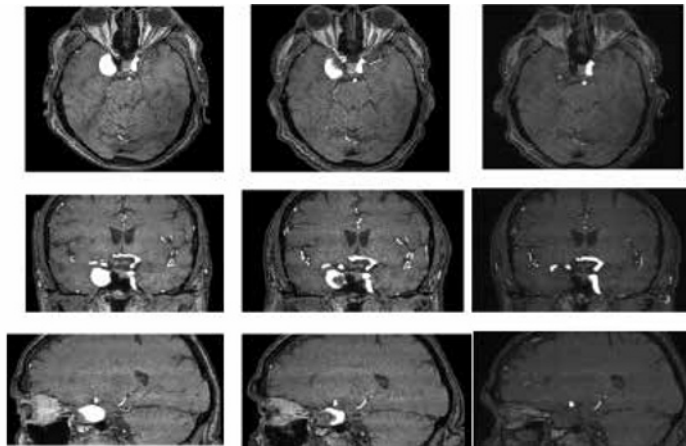
The MRA showed complete occlusion in 66% having most of them occluded in a six month period after treatment with predominance of the supraclinoid aneurysms with 79%. 34% showed signs of residual neck or sac.

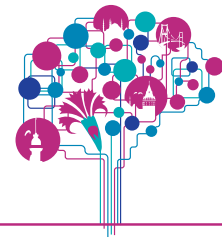
The MRA also showed shrinking or total regression of the aneurysm sac in 60% being the majority supraclinoid aneurysms with 40%.

32% of the aneurysms treated remain without changes in size, although 41% were also treated with Coils and appeared exclude from circulation. 8% showed an increase of size with predominance of the anterior circulation with 80%.

We analyze the parenchymal environment of the aneurysms having 79% with no alterations and 21% with surrounding edema that show resolution after treatment. The postgadolinium T1 sequences showed enhancement of the aneurysm sac in 31% of the 66% occluded finding that could be related to complete endothelialization.

CONCLUSION: Our data provide good correlation to DSA results supporting the use of MR imaging as an effective non-invasive diagnostic tool that should be considered for follow up as it provides excellent spatial resolution, imaging quality and rather better rates of morbidity –morbidity.





ORAL PRESENTATIONS ABSTRACTS

O196-Can MRI Diagnose Occult Hairline Skull Fractures Better Than CT in Craniocerebral Trauma

*Vivek Sindhwani*¹, *Monika Arya*²

University of Missouri Radiology Columbia-United States ¹ *University of Missouri Internal Medicine -United States* ²

PURPOSE: We conduct this study to evaluate if MRI can diagnose occult/hairline fractures better than CT in patients with Craniocerebral trauma. We report on clinical impact and benefits.

MATERIALS AND METHODS: Retrospective review of data between November 2011 to November 2013 on patients who underwent both CT & MRI following craniocerebral trauma and had reported calvarial fractures was performed to look for fractures reported on MRI but were either missed or called suspicious on CT scan. Fracture line was best demonstrated as linear T2/FLAIR high signal

across the diploic space and bony cortex on MRI. We also looked for additional trauma related findings in this subset of patients and compared CT and MRI. MR images were obtained as per standard trauma protocol on 1.5 T MRI (Seimens Avanto, Aera & Symphony). CT images were obtained as per standard trauma protocol on 64 slice Seimens (Definition & Definition AS) and 16 slice Seimens Symphony.

RESULTS: 43 patients demonstrated calvarial fractures, among the ones who underwent both CT and MRI following craniocerebral trauma. 5 (11%) had occult/hairline, undisplaced calvarial fractures (2 parietal, 1 temporal and 2 occipital) that were missed on initial CT scans. 3 of these missed fractures were retrospectively seen on CT but 2 of them were not well appreciated. MRI failed to accurately demonstrate 3 skull base fractures. In this subset of patients MRI was far superior in demonstrating thin subdural (SDH) and subtle subarachnoid hemorrhages (SAH) (best seen on FLAIR sequence), brainstem injuries, cortical contusions and findings suggesting diffuse axonal injury.

CONCLUSION: MRI proved to be more sensitive than CT in detecting hairline/occult calvarial fractures in certain locations. However, MRI failed to be as sensitive and accurate for skull base fractures. MRI proved to be more sensitive in diagnosing brainstem injury, subtle SAH, thin SDH, Diffuse axonal injury and small cortical contusions.

O197-The Time Dependent Occurrence Analysis of Intracranial Aneurysm Rupture in North of Sweden and In Czech Republic (6 Years Analysis of Dates Clusters)

*Jiri Neuwirth*¹, *Frantisek Charvat*², *Ivana Kralova*³

*NUS Radiology Praha*⁶-*Sweden*¹ *UVN Radiology -Czech Republic*² *NUS Intensive care Unit -Sweden*³

INTRODUCTION AND PURPOSE: Knowledge of the temporal pattern of the occurrence of subarachnoid hemorrhage (SAH) may provide the insight into triggering factors and lead to the development of new preventive strategies for this devastating disorder. Previous studies have yielded inconsistent and/or inconclusive results on week and seasonal variations in the occurrence of SAH in various countries. Different hypotheses have been described in literature. The mentioned triggers are: seasonal periodicity, diurnal periodicity, barometric pressure – absolute level or delta changes in time, stormy weather, moon phase or physical activity.

The purpose of the present study was to determine whether there is a particular diurnal, circaseptan (weekly), or circannual (monthly, seasonal) pattern in the occurrence of SAH and whether these temporal variations of SAH occurrence in one of populations are different from those in other populations.

MATERIALS AND METHODS: Our study compared two geographical regions and the occurrence of SAH in time during several years. The minimal time resolution was one day. The date of occurrence was set to the day of SAH finding on CT. Only confirmed aneurysmatic source of SAH by the CT angiography or conventional angiography were included in our data sets.



ORAL PRESENTATIONS ABSTRACTS

RESULTS: The two series of 266 (SW) resp. 320 (CZ) subarachnoid hemorrhages (SAH) of aneurysmatic origin in 72 months were analysed. All intervals (in days) between successive events were calculated within SW and CZ series. All intervals (in days) between successive events were calculated within SW and CZ series. Interval between events (days) N Mean Median SD Minimum Maximum 25.percentile 75.percentile SW 266 7,71 6 7,62 0 43 2 11 CZ 320 6,77 5 6,45 0 46 2 9,75 The maximal peak - interval 1day (new event occurred next day) 14% (count 45) was observed in CZ series. The corresponding days - the second day from 2 successive days with event were detected in the CZ series and the weekend days were identified. On Wednesday and Thursday 2 successive events were more often observed than on other weekdays. The difference is significant $p=0,039$.

Another analysis was done to confirm or to exclude the month - seasonal prevalence and trends. Spearman's correlation between month order and seasonal adjusted month's is not significant in both series CZ ($p=0,67$), SW ($p=0,46$).

CONCLUSION: There was not found any seasonal prevalence of this long series of SAH in the European regions and no correlation of the time dependent curve. The only significant time pattern in both series was seen in circaseptan rhythm.

O198-Dynamic CT Angiography for the Evaluation of Shunting Vascular Malformation of Brain and Spine

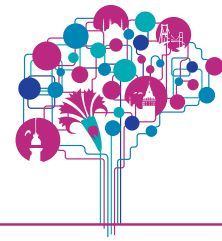
*Federico D Orazio*¹, Aldo Victor Giordano², Sergio Carducci², Alessandra Splendiani³, Massimo Gallucci³
U.O. Neuroradiologia e Radiologia Interventistica Scuola di Specializzazione in Radiodiagnostica, Università degli Studi di L Aquila L Aquila-Italy¹ Ospedale San Salvatore L Aquila U.O. Neuroradiologia e Radiologia Interventistica -Italy² Università degli Studi di L Aquila Neuroradiologia, Dipartimento Scienze Cliniche Applicate e Biotecnologie -Italy³

PURPOSE: To evaluate the effectiveness of 4D CT angiography for the assessment of brain and spinal vascular shunting malformations in comparison with DSA

MATERIALS AND METHODS: In the period between June and December 2013, 13 intracranial and 2 spinal 4D CTA examinations were performed in 15 patients. A 320 rowdetector CT scanner was used; it allowed volumetric, continuous (cine) scans with the following parameters:

FOV=160mm/80KV/300mA/Rotation Time=0,35s/Tot Scan time=15s/Collimation=0,5mm. After obtaining informed consent, we performed 4D CTA. All patients studied with 4D CTA undergone a DSA study within 48 hours from CT. Subsequently, all DSA and 4D CTA studies were anonymized and independently evaluated by 2 different neuroradiologists, by using a standardized scoring sheet. **RESULTS:** All 4D CTA studies confirmed the presence of a shunting vascular malformation of the brain (11 AVM, 2 dFAV) and spine (2 dFAV) and were judged suitable for assessing the architecture of vascular lesions observed in terms of classification according to the SpetzlerMartin grade scale (brain AVM) and to the Cognard classification (dFAV). Because of the 4D CTA high spatial and temporal resolution we could correctly evaluate both with DSA and 4D CTA the presence of the vascular malformations, their position, the size of the nidus, the number and types of arterial feeders observed, the pattern of venous drainage (i.e. superficial and/or deep) allowing to plan a further endovascular treatment when technically achievable.

CONCLUSION: 4D CTA demonstrated to be a powerful new diagnostic tool to investigate the hemodynamics of vascular shunting lesions both in brain and spine. We believe that using 4D CTA can be useful in the diagnostic set up of these kind of vascular lesions, and could reduce, in the future, the use of DSA only for therapeutic purposes.



ORAL PRESENTATIONS ABSTRACTS

O199-Lesions of the Foramen of Monro Region One Year's Differential Diagnosis

Mariana Diogo ¹, João Jacinto ¹, Isabel Fragata ¹, *Carla Conceição* ¹, Manuela Mafra ², Luís Cerqueira ¹, João Reis ¹

CHLC Neuroradiology -Portugal ¹ CHLC Neuropathology -Portugal ²

INTRODUCTION and PURPOSE: Space occupying lesions of the foramen of Monro (FoM) region include an array of both benign and malignant entities, often offering a diagnostic challenge. Some of these demand immediate surgical treatment, while others can be classified as “leave-me-alone” entities. Imaging plays a preponderant role in this distinction.

The purpose of this exhibit is to review the differential diagnosis of FoM masses through a series of illustrative clinical cases in order to help fellow radiologists improve their diagnostic accuracy and broaden their differential diagnosis list.

MATERIALS AND METHODS: We present a series of illustrative clinical cases collected from our institution's neuroradiology imaging archive during the year of 2013. A short clinical introduction of each case is presented, with illustrative Computer tomography (CT) and Magnetic resonance (MR) images for each case. Diagnosis presented include colloid cysts of the third ventricle, high and low grade gliomas of the septum pellucidum (SP), and SP cyst. Typical CT and MR imaging characteristics are described for each pathology, as well as imaging pitfalls. Complications of FoM lesions are also presented.

RESULTS /CONCLUSIONS: Although most lesions of the FoM region are benign and diagnosed as incidental findings, they might present as life-threatening acute hydrocephalus. Tumoral lesions are mostly symptomatic at presentation and surgical resection, when possible, is the treatment of choice. Distinguishing them from leave-me-alone lesions is crucial to the radiologist in order to help with the diagnostic and therapeutical approach and avoid unnecessary interventions.

O200-Dural Venous Sinus Morphology in Idiopathic Intracranial Hypertension

Indran Davagnanam ¹, Clare Fraser ², Gordon Plant ³

The National Hospital for Neurology & Neurosurgery Lysholm Department of Neuroradiology London-United Kingdom ¹ *Sydney Eye Hospital Department of Neuro-ophthalmology & Strabismus -Australia* ² *The National Hospital for Neurology & Neurosurgery Department of Neuro-Ophthalmology -United Kingdom* ³

PURPOSE: Dural venous sinus stenosis is reported in the majority of patients with idiopathic intracranial hypertension (IIH). However, much controversy surrounds the causal relationship between narrowing and IIH pathogenesis. We aimed to examine the comparative dural venous sinus anatomy in patients with IIH and a control population using contrast enhanced computed tomography timed for the venous phase (CTV).

MATERIALS AND METHODS: Diagnosis of IIH was made by a neuro-ophthalmologist based on the Dandy criteria. Control patients were those undergoing CT scanning for ophthalmic assessment. Two trained observers blinded to patient diagnosis objectively reviewed the CTV scans for differences in gross morphology and alternate venous outflow channels. Transverse sinuses (TS) were assessed using an established scoring system (Farb Score) for stenosis.

Direct measurements of the sinus and bony groove taken at points of maximum and minimum cross sectional area. Measurements were taken at the narrowest and widest points along the TS for venous sinus and bony groove height (cranio-caudal) and width (anterior-posterior). The ratio of venous sinus to bony groove (sinus/groove) was compared between patients and controls.

RESULTS: Thirty IIH patients and 60 controls were included. 97% of IIH patients and 5% control patients had bilateral distal dural venous sinus stenosis (> 50% narrowing), and the degree of stenosis was correlated with LP opening pressure, $p=0.006$ $\rho=-0.35$. The stenoses seen in IIH patients are relatively smaller than the widest point in the sinus and their adjacent bony grooves compared to controls, $p<0.001$. A narrowing in the proximal two thirds of the sinus and large arachnoid granulations were more common in controls. Alternative venous drainage channels were more prominent and a split torcular was more common in IIH patients.



ORAL PRESENTATIONS ABSTRACTS

CONCLUSIONS: Comparison of venous system anatomy showed significant differences beyond the established presence or absence of TS stenosis. The increased degree of narrowing relative to the maximum diameter of the TS in IIH patients suggests secondary compression from elevated CSF pressure. Bony groove disparity also reinforces that the venous narrowing is non-developmental.

PARALLEL SCIENTIFIC PAPER PRESENTATIONS

(Adult NR 5) 17:15 - 19:00

Dolmabahce C Hall

O201-International Differences in Neuroradiology Training

*Tanja Schneider*¹, David Yousem¹

*The Johns Hopkins University Neuroradiology Baltimore-United States*¹

PURPOSE: To better understand foreign neuroradiology training program parameters and compare them to a representative US program.

MATERIALS AND METHODS: By means of an email based questionnaire, radiologists across the globe were surveyed regarding the training formats for neuroradiology at their institutions. The number of trainees and attendings, length of program, information about case logs, teaching schedules and national examinations were collected for 40 countries and the USA spanning all 5 continents. **RESULTS:** Fifteen of 41 countries (36.6%) do not provide fellowship training in neuroradiology. Others have formal post-residency curriculums (n = 26/41, 63.4%). Compared to a typical US

program, many programs have fewer fellows in diagnostic and interventional neuroradiology (USA: 11, other countries: ≤ 8) and fewer lectures (USA: daily), but the duration of fellowship training is almost equal (1-2 years).

CONCLUSION: There is a wide variety in terms of fellowship offerings, program sizes and teaching quantity for neuroradiology across the continents. The US neuroradiology program is highly specialized, more structured and demanding.

O202-MRI Findings in Spinal Tuberculosis in an Endemic Country

*Jureerat Thammaroj*¹, Amnat Kitkhuamdee⁵, Kittisak Sawanyawisuth⁵, Prathana Chowchun⁵, Kayoon Promon⁵

*Khon Kaen Radiology Khon Kaen-Thailand*¹

PURPOSE: Spinal tuberculosis accounts for 50% of skeletal tuberculosis. MRI is a helpful tool for spinal tuberculosis. MR findings in spinal tuberculosis, however, may have several different patterns.

MATERIALS AND METHODS: The MR imaging features of spinal tuberculosis and classification as usual and unusual findings are reported. The MR images in 52 proven spinal tuberculosis patients in Srinagarind Hospital from 1996 to 2005 were retrospectively reviewed.

RESULTS: There were five characteristics of unusual manifestations included multiple skip lesions, vertebral body involvement, lamina and spinous process involvement, single vertebral collapse, and intramedullary tuberculoma. The skip lesion of spinal tuberculosis was the only distribution pattern significantly identified as being an unusual characteristic by multiple logistic regression.

CONCLUSION: The most common unusual pattern of spinal tuberculosis is skip lesions (11.5%). The distribution of this pattern is statistically significant as an important MR imaging feature for defining unusual spinal tuberculosis.



ORAL PRESENTATIONS ABSTRACTS

O203-Susceptibility Weighted Imaging in Parenchymal Neurosyphilis a New Radiological Hallmark

Ilaria Pesaresi¹, *Mario Sabato*², Ilaria Desideri², Melania Guida³, Michele Puglioli¹, Mirco Cosottini², Carlo Bartolozzi²

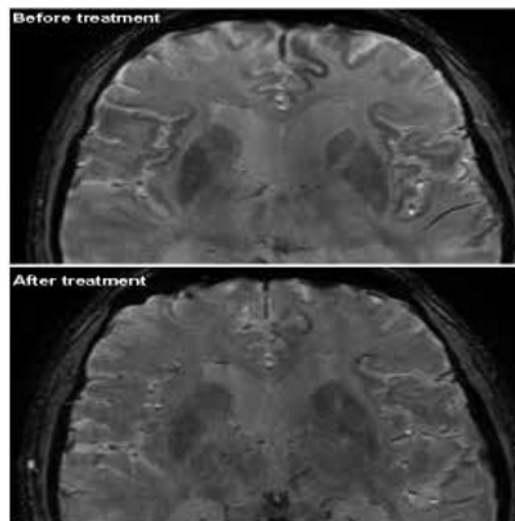
AOU Pisa Unit of Neuroradiology -Italy¹ University of Pisa Department of Translational Research and New Technologies in Medicine and Surgery Pisa-Italy² University of Pisa Department of Neurology -Italy³

PURPOSE: General Paresis (GP) is a late form of parenchymal Neurosyphilis, manifesting as dementia or neuropsychiatric disorder decades after the primary infection by *Treponema Pallidum*. We describe and interpret radiological findings in GP, focusing on Susceptibility Weighted Imaging (SWI). This is the first study in which SWI are used in the evaluation of Neurosyphilis.

MATERIALS AND METHODS: We studied three patients with General Paresis, all males and immunocompetent, admitted for cognitive impairment. The diagnosis of Neurosyphilis was formulated on the basis of serological tests and Cerebrospinal Fluid (CSF) analysis. The patients were treated with penicillin G 24 million units/day for 6-21 days. A 3 Tesla Magnetic Resonance examination including Susceptibility Weighted ANgiography (SWAN) sequence was performed before and after the instauration of penicillin therapy.

RESULTS: Conventional sequences showed diffuse brain atrophy, particularly affecting the frontal and temporal lobes. In two of three patients, mesial-temporal hyperintensity was observed in T2-weighted sequences. SWI revealed cortical hypointensity, mainly distributed in the deep cortical layers. After the instauration of penicillin therapy, the patients had clinical improvement. Follow-up MR examination demonstrated the partial reversibility of cortical hypointensity on SWI sequence.

CONCLUSIONS: According with previous pathological examinations on patients with Neurosyphilis, it is possible that these alterations are expression of cellular infiltrates and iron deposits. The distribution in the deepest cortical layers supports the hypothesis that they could be due to the activation of the microglia. This pattern, never signaled before in other infectious disease of the Central Nervous System, could be a radiological hallmark of parenchymal Neurosyphilis.





ORAL PRESENTATIONS ABSTRACTS

O204-Differentiation of Infective from Neoplastic Rim Enhancing Brain Lesions Using T2 Relaxometry

Hanafiah Mohammad¹, Shahizon Azura Mohamed Mukari², *Norzaini Rose Mohd Zain*³, Ahmad Sobri Muda², Syazarina Osman²

*Universiti Teknologi MARA Medical Imaging Unit -Malaysia*¹ *Universiti Kebangsaan Malaysia Medical Centre Department of Radiology Kuala Lumpur-Malaysia*² *Hospital Kuala Lumpur Department of Diagnostic Imaging -Malaysia*³

BACKGROUND AND PURPOSE: Characterizing a ring enhancing brain lesion remains a challenge and conventional MRI sequences may not be adequate, particularly if the clinical presentation is not obvious. MR T2 relaxometry allows quantitative measurement of T2 relaxation of brain pathology, which is affected by relative proportion of protein and water as well as cellular density. The aim of our study was to determine whether or not ring enhancing brain lesions of infective origin can be differentiated from neoplasm using MR T2 relaxometry sequence. We hypothesized that T2 relaxometry can differentiate between the two.

MATERIAL AND METHODS: Axial view T2 maps were generated by using a 15-ECHO T2 relaxometry with acquisition time of 5.4 minutes on 3-T Verio Siemens MRI machine. T2 relaxation times were measured in the central core of 31 ring enhancing lesions from 23 patients. (13 female, 18 male, age range 12-73 years old). The T2 relaxation times of tumour versus infective lesions were analysed. **RESULTS:** The mean T2 relaxation time of infective abscesses was 194.6msec (range 89.5-498.7msec; SD 144.8) and that of tumour was 1207.3 msec (range 147.8-1350.2msec ; SD 1077.3). Between group analyses showed the mean value of T2 relaxation time of the tumour group is significantly different and greater than that of the infective group (p 0.011).

CONCLUSION: Our data showed that T2 relaxometry is a potential quantitative MR technique that can differentiate infective from neoplastic rim enhancing brain lesions. It may serve as a useful research tool as an adjunct MR technique in an attempt to diagnose a rim enhancing brain lesion.

O205-A Typical CNS Tuberculosis

*Abdulkader Alazzaz*¹, Fatima Alattas³, Abubaker Shadha³
*King Fahad Hospital In Madinah Radiology Madinah-Saudi Arabia*¹

BACKGROUND AND PURPOSE:

Our objective was to evaluate the uncommon CT and MR features of CNS TB in order to make a definite diagnosis, Discuss their pathogenesis, diagnosis, and treatment, Highlight the awareness to know the atypical TB pattern that help in early diagnosis and management & prevent fatal complication.

Still tuberculosis is significant public health concern & its prevalence is markedly increased in recent years, approximately 5 to 10% of cases of TB have CNS involvement.

This article presents the range of atypical manifestations of tuberculosis (TB) of the craniospinal axis which is including rare location, unusual pattern with some rare complication as well as concurrence of two or more rare finding in same patient.

MATERIALS AND METHODS: We provide group of cases with rare location like pineal gland, suprasellar cistern & pituitary stalk involvement, An abscess formation is uncommon complication as a solely lesion in 3 of our patient & one case is with concurrent with all different tuberculomas stages. big pachymeningeal masses are illustrated in four cases as well as two cases mimicking intra axial tumor. We also illustrated a rare TB complication on brain vasculatur e.g ruptured cerebral mycotic aneurysm. Involvement of vertebral column is common in tuberculosis but intra & extramedullary tuberculoma are rare as well as tuberculous myelitis.



ORAL PRESENTATIONS ABSTRACTS

CONCLUSION: Generally all these atypical manifestation of TB can mimic other disease like malignency or demylinating disease. Its complication on brain vascular is fatal & increase the mortality & the delay in the diagnosis of inta axial & intra/extra medullary involvement will also increase the morbidity. So awareness of the atypical TB pattern help in early diagnosis and management.

O206-NSsaFe Study Observational Study on The Incidence Of Nephrogenic Systemic Fibrosis (NSF) In Renal Impaired Patients Following Gadoteric Acid Administration

*Bruno Beomonte Zobel*¹

*"Campus Bio-Medico" University Diagnostic Imaging Department Rome-Italy*¹

PURPOSE: To prospectively estimate the incidence of NSF in patients with moderate to severe renal impairment after administration of gadoteric acid.

MATERIALS AND METHODS: A worldwide observational post-marketing study is being conducted to collect safety data in 1,000 patients (adults and children), with moderate to severe and end-stage renal impairment, scheduled to undergo a routine contrast-enhanced Magnetic Resonance Imaging (MRI) examination using gadoteric acid (DOTAREM®). Risk factors at inclusion, indications for MRI and occurrence of adverse events are recorded for each patient. Three follow-up visits are performed between 3 and 27 months after contrast-enhanced MRI in order to detect any occurrence of NSF.

RESULTS: As of February 6, 2014, the cut-off date for the interim safety analysis, the study included 351 patients (mean age: 69.9 years (range: 21-92); male, 62.4%). Mean eGFR at inclusion was 36.1 ml/min/1.73m² (range: 4.0-59.1) including 65.2% of moderate, 16.5% of severe, 15.4% of end stage renal insufficiency or dialysis and 2.8% of kidney transplanted patients. Central Nervous System MRI examinations accounted for nearly 29%. The first follow-up visit (between 3 and 12 months after MRI) was done for 178 patients, the second follow-up visit (between 13 and 21 months after MRI) was done for 87 patients and the third follow-up visit (between 22 and 27 months after MRI) was done for 28 patients. Only 2 patients (0.6%) had adverse events and none were related to gadoteric acid. No cases of NSF were reported.

CONCLUSIONS: This interim safety analysis confirmed the very good safety profile of gadoteric acid in renal impaired patients.

O207-The Utility of Gadoterate Meglumine Enhanced MRI in Adult and Pediatric Patients with Central Nervous System Lesions (SENTIO study)

*Raphaelle Souillard-Scemama*¹, Olivier Naggara¹, Philippe Page², Johan Pallud², Jean

Francois Meder¹, Catherine Oppenheim¹

*CHSA Neuroradiology PARIS-France*¹ *CHSA Neurosurgery -France*²

PURPOSE: To demonstrate superiority of gadoterate meglumine-enhanced MRI over unenhanced images for visualization of brain and spinal lesions (including tumor, vascular, inflammatory or infectious diseases) in adults and children.

MATERIALS AND METHODS: Multicenter, randomized, double-blind, fixed-sequence [unenhanced T1 & T2 MRI followed by either gadoterate meglumine (Dotarem, 0.1 mmol/kg) or gadopentetate dimeglumine (Magnevist, 0.1 mmol/kg) T1-enhanced MRI], active comparator study (SENTIO study). Pediatric patients (aged ≥2 years) were assigned to the gadoterate meglumine group only. MR images of all patients were read by three off-site blinded independent readers. All patients were also evaluated by one on-site radiologist.

The primary endpoint was lesion visualization with gadoterate meglumine enhanced MRI comparing unenhanced images in up to five of the largest lesions utilizing three co-primary endpoints: border delineation, internal morphology and degree of contrast enhancement. For each of the 3 endpoints, a score was computed by summing all lesion scores for a given patient.



ORAL PRESENTATIONS ABSTRACTS

Each co-primary endpoint was then analyzed using a multiple regression model.

Main secondary criteria were evaluated on-site for lesion visualization and both on-site and off-site for: level of diagnostic confidence, image quality, signal intensity, number of lesions, and comparison of gadoterate meglumine and gadopentetate dimeglumine for diagnostic efficacy. Clinical safety was assessed through the reporting of adverse events (AEs), injection site intolerance reactions, changes in vital signs, electrocardiogram recordings and laboratory measures.

RESULTS: A total of 402 patients were evaluable: 364 adults (245 gadoterate meglumine, 119 gadopentetate dimeglumine) and 38 children.

The primary endpoint (lesion visualization post gadoterate meglumine enhanced MRI) was significantly superior ($p < 0.001$) as well as for all three co-primary endpoints for all independent readers when comparing enhanced images to unenhanced images (Table 1). This superiority of gadoterate meglumine enhanced imaging was also confirmed in analysis of evaluations by on-site evaluators. No statistically significant differences between gadoterate meglumine and gadopentetate dimeglumine were observed for all 3 co-primary variables for the 3 independent readers.

Analysis of pediatric group for all 3 independent readers, showed mean scores for each of the three co-primary endpoints were higher for “enhanced” compared to “unenhanced” images.

Both contrast agents were well tolerated. Related AEs were reported in 3.8% adult gadoterate meglumine and in 7.7% gadopentetate dimeglumine patients. The most common AEs were injection site pain, headache.

O208-Resting State fMRI Assessment of Language Networks in Epilepsy Patients A Progress Report

*Ali Murat Koc*¹, Ali Yusuf Oner¹, Melike Guryildirim¹, Halil Ozer¹, E. Turgut Tali¹

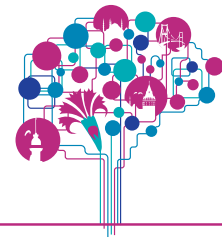
*Gazi University School of Medicine Radiology Ankara-Turkey*¹

PURPOSE: Preoperative language network assessment through task - based functional MRI has been widely used in epilepsy patients. Using resting-state fMRI to define language networks, especially motor and sensory language areas (Wernicke & Broca) is an alternative technique. The purpose of this paper is to compare conventional task-based functional MRI and “task free” resting state fMRI results on refractory temporal lobe epilepsy (TLE) patients at 3T.

MATERIALS AND METHODS: An institutional review board approval was obtained for this study. A total of 25 refractory TLE patients, referred for presurgical evaluation were included in this study. First a “task free” resting state data then the “task-based” functional MRI data via two language tasks were acquired on a 3T scanner. T1 and T2W images on axial and coronal planes are then acquired to define the extend of epileptogenic region. Data driven from “task-based” and resting state fMRI were processed with Brain Voyager (QX 2.2, Brain Innovation). Following evaluation of the language network related signals and their distance to the epileptic regions, Region of Interest (ROI), Voxel and lateralization index (LI) analysis were performed. Dice coefficient analysis was used for spatial comparison of this two methods regarding Wernicke and Broca areas of language networks. Finally t-test of dice coefficients and ANOVA analysis of mean voxel numbers were done to assess statistical analysis of spatial comparison.

RESULTS: Language network signals in the context of Wernicke and Broca areas were successfully defined on all patients with both fMRI techniques. Distance of these areas to the epileptogenic zones obtained with both techniques were comparable. Activation signals recorded with both methods showed good spatial correlation.

CONCLUSION: Resting state fMRI can be used as a promising alternative to conventional “task-based” fMRI. This new technique can be recommended in neurologically and/or visually impaired patients. Resting state fMRI for preoperative workup of language networks in TLE patients is a promising technique which is expected to extend the spectrum of patient profiles and to ease their evaluation.



ORAL PRESENTATIONS ABSTRACTS

O209-Is the Wyler Grade of Hippocampal Sclerosis Reflected on MRI

*Horst Urbach*¹, Ralf Schwarzwald², Hans-Jürgen Huppertz³, Albert Becker⁴, Jan Wagner⁵, Henriette Tschampa⁶

*Medical Center University Freiburg Neuroradiology Freiburg-Germany*¹ *University Freiburg Neuroradiology -Germany*² *Swiss Epilepsy Center -Switzerland*³ *Medical Center University Bonn Neuropathology -Germany*⁴ *Medical Center University Bonn Epileptology -Germany*⁵ *Medical Center University Bonn Radiology -Germany*⁶

BACKGROUND & PURPOSE: To relate hippocampal volume and signal intensity to Wyler grading of HS.

MATERIALS AND METHODS: Of 100 consecutive patients with drug-resistant temporal lobe epilepsy and HS as histopathological diagnosis 32 patients had undergone high resolution 3 Tesla MRI and anatomically well preserved hippocampi following selective amygdalo-hippocampectomy. Hippocampal volume on 3D T1-weighted gradient echo and signal intensity on FLAIR TSE sequences were automatically determined using Freesurfer and SPM tools and related to Wyler grading. Seizure outcome following epilepsy surgery was determined according to Engel and ILAE after one year. **RESULTS:** Histopathological evaluation revealed four Wyler grade II, 19 Wyler grade III, and 9 Wyler grade IV HS. Hippocampal volumes on 3D T1-gradient echo images were 3.075 +- 0.32 ml for Wyler Grade II, 2.189 +-0.58 ml for Wyler grade III, 2.62 +- 0.43 ml for Wyler grade IV, and 3.081 +-0,39 ml for the contralateral, non-operated side HS (t-test p < 0.05). Normalized FLAIR signal intensities were 1263, 1273, 1260 and 1228, respectively (t-test p < 0.05). Visual analysis of Wyler grade II HS revealed no clear abnormalities. Two of 4 (50%) Wyler grade II, 16/19 (84%) Wyler grade III, and 6/9 Wyler grade IV patients were seizure-free one year following surgery.

CONCLUSION: In patients with Wyler grade II HS hippocampal volume can be normal while normalized FLAIR signal intensity is in the range of Wyler grade III and IV signal intensities. Quantitative FLAIR signal analysis is thus helpful in patients with mild HS.

O210-Fusion of Preoperative MRI and Postoperative CT Images for the Evaluation of Electrode Position in STN DBS

*Isabelle Barnaure*¹, Pierre Pollak², Shahan Momjian³, Julien Bally², Karl-Olof Lovblad¹, Colette Boex², Pierre Burkhard², Maria-Isabel Vargas¹

*Hôpitaux Universitaires de Genève Service de Neuroradiologie Geneva-Switzerland*¹ *Hôpitaux Universitaires de Genève Service de Neurologie -Switzerland*² *Hôpitaux Universitaires de Genève Service de Neurochirurgie -Switzerland*³

PURPOSE: Imaging has an essential role in the evaluation of correct positioning of electrodes implanted for deep brain stimulation (DBS). Although MRI offers superior anatomic visualization of target sites, there are safety concerns in patients with implanted material; imaging guidelines are inconsistent and vary. The fusion of postoperative CT with preoperative MRI images can be an alternative for the assessment of electrode positioning. The purpose of this study was to assess the accuracy of measurements realized on fused images (acquired without a stereotactic frame) using a manufacturer-provided software

MATERIALS AND METHODS: Data from 23 Parkinson's disease patients who underwent bilateral electrode placement for subthalamic nucleus (STN) DBS were acquired. Preoperative high-resolution T2-weighted sequences at 3T and postoperative CT series were fused using a commercially available software (Integrated Registration, AW, GE Healthcare). Electrode tip position was measured on the obtained images in three planes (in relation to the midline or AC-PC line respectively and to each other) and assessed in relation to measurements realized on postoperative 3D T1-images acquired at 1.5T. **RESULTS:** Preliminary results showed mean differences in electrode tip position between measurements on fused images and postoperative MRI of 0.1mm (distance to the midline measured in an axial plane) to 1mm (distance to AC-PC line in a sagittal plane).

CONCLUSION: Fusion of CT and MRI images provides a safe and fast technique for postoperative assessment of electrode position in DBS.



ORAL PRESENTATIONS ABSTRACTS

PARALLEL SCIENTIFIC PAPER PRESENTATIONS

(Vascular Interventional 4) 17:15 - 19:00

Topkapı A Hall

O212-Vascular Injuries after Cranio Spinal Surgery Endovascular Perspective

*Mustafa Gok*¹, Celal Cinar², Halil Bozkaya², Ismail Oran²

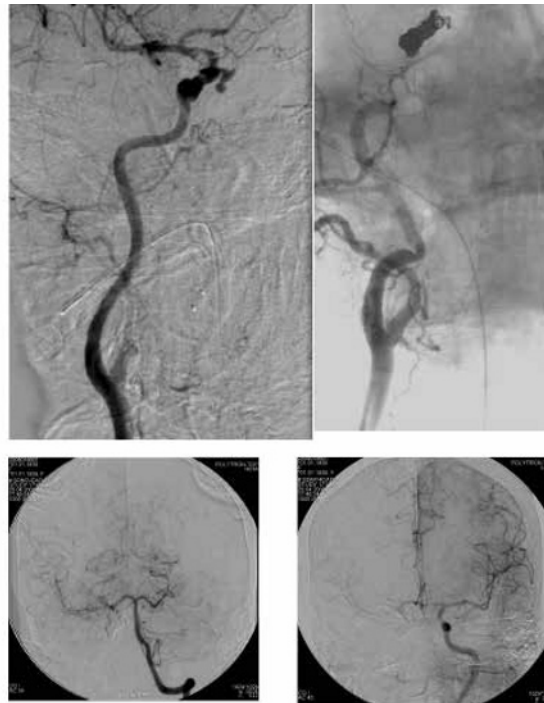
*Kafkas University Hospital, Kars Radiology Izmir-Turkey*¹ *Ege University Hospital, Izmir Interventional Radiology -Turkey*²

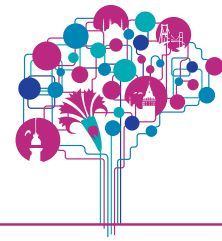
PURPOSE: Vascular complications during cranio-spinal surgery are fortunately few in number. We retrospectively reviewed all vascular injuries encountered after cranio-spinal surgery that were diagnosed during the last 15 years in our institution.

MATERIALS AND METHODS: We retrospectively analyzed 25 patients who had vascular injuries during cranial, spinal and skull base surgeries. All patients were diagnosed as associated vascular injuries by means of catheter angiography. All patients were suspicious for vascular injury after initial radiological (CT, MRI, Doppler US) and clinical work-up.

RESULTS: Three patients were asymptomatic, while the remaining 22 had some symptoms related to vascular injury at the time of admission. Vascular injuries were 10 internal carotid artery injury (after transsphenoidal surgery), 5 iliac arteriovenous fistula (after lumbar disc operation), 4 vertebral artery injury (one skull-base surgery, three spinal tumor surgery), 3 internal carotid artery injury (after skull base surgery), 1 subclavian artery injury (during ventriculoperitoneal shunt operation), 2 intradural distal internal carotid artery aneurysm (after sphenoid wing meningioma operation). The possibility of vascular lesion should be kept in mind after cranio-spinal surgery.

CONCLUSION: Endovascular therapy allows to eliminate majority of these potentially dangerous lesions with good long-term clinical follow-up.





ORAL PRESENTATIONS ABSTRACTS

O213-Comparison between Computed Tomography Angiography (CTA) Magnetic Resonance Angiography (MRA) and 2d 3d Rotational Digital Subtraction Angiography (DSA) in the Follow Up of Intracranial Aneurysms Treated by Endovascular Coiling

Chirag K Ahuja¹, *N Khandelwal*¹, Ajay Kumar¹, Paramjeet Singh¹, Sn Mathuria², Vivek Gupta¹

*Pgimer Radiodiagnosis -India*¹ *Pgimer Neurosurgery -India*²

BACKGROUND and PURPOSE: Endovascularly coiled intracranial aneurysms show higher chances of recanalization and warrant regular follow-up. Digital subtraction angiography (DSA) is the standard follow-up imaging procedure but carries a small but significant risk of complications. We compare non-invasive modalities namely computed tomography angiography (CTA), magnetic resonance angiography (MRA-3DTOF) with 2D and 3D rotational DSA in the post-op evaluation of such patients.

MATERIALS AND METHODS: After obtaining institute ethical clearance, ten random patients were enrolled who had undergone endovascular coiling with/without balloon assistance over the last 1 year. All were subjected to CTA (16/64 slice scanner), MRA-3DTOF (3T scanner), 2D and 3DDSA (biplane DSA machine) according to standard acquisition protocols. Appropriate multiplanar reconstructions were made in MIP, VRT and SSD formats and blinded evaluation of all modalities was performed in these patients. Artifact characterization was done and the remnant/recanalized aneurysms were categorized according to the Raymond classification.

RESULTS: Ten ruptured aneurysms were coiled and imaged after a mean duration of 96 days (30-365 days). All imaging were done within 7 days of each other for best comparisons. The mean native aneurysm size was 8.67 mm (3mm-26 mm). Confident evaluation could be done in 100% cases on MRA, 2DDSA and 3DDSA while 30% (3/10) on CTA due to extensive streak artefacts in the latter. 4/10 recanalizations were detected- 1 neck remnant (Raymond Class 2) and 3 sac remnants (class 3). The mean recanalized aneurysm size was 2.0625±0.82104 mm, 2.4286±1.30475 mm and 2.8750±1.8424 mm on 2DDSA, 3DDSA and MRA respectively. The 3 recanalizations on CTA were of originally small aneurysms (<4 mm).

CONCLUSIONS: MRA is an excellent non-invasive modality to detect remnant/recanalized aneurysms in coiled patients and can replace DSA in long term follow-up. CTA can be useful in small aneurysms when MRA is not feasible but should always be followed by DSA in doubtful cases.

O214-Double Solitaire Mechanical Thrombectomy in Acute Stroke Effective Escalating Strategy for Large Artery Occlusions Refractory to Single Stentriever Treatment

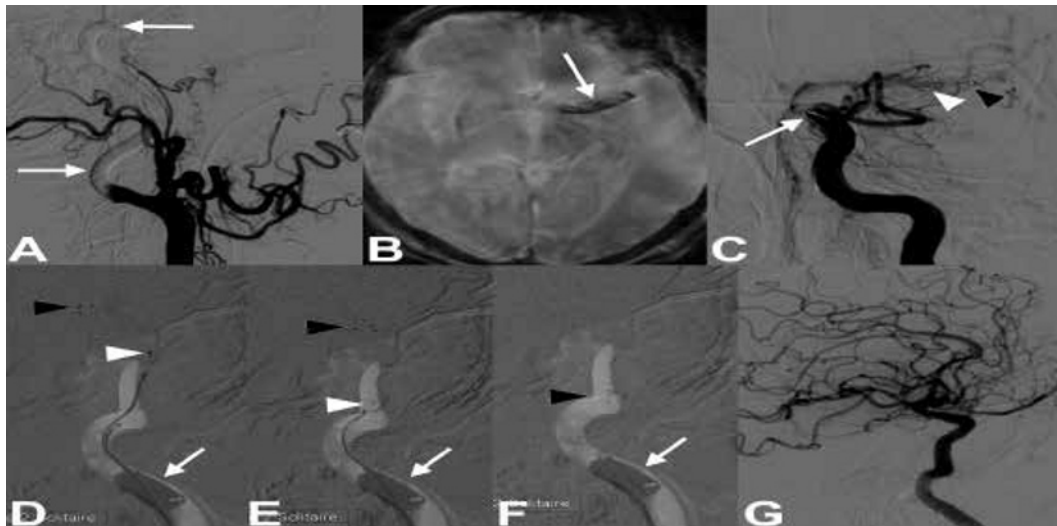
*Stephan Meckel*¹, Vojtech Sychra², Christoph Strassila², Christian A Taschner¹, Mathias Reinhard³, Horst Urbach¹, Joachim Klisch²

*University Hospital Freiburg Neuroradiology Freiburg-Germany*¹ *HELIOS Hospital Erfurt Institute of Diagnostic and Interventional Radiology and Neuroradiology -Germany*² *University Hospital Freiburg Neurology -Germany*³

PURPOSE: Mechanical thrombectomy (MT) using a single Solitaire stent retriever (SR) system has demonstrated high efficacy for recanalization of large cerebral artery occlusions in acute stroke. We aimed to evaluate the feasibility, safety, and efficacy of a novel double SR technique as an escalating treatment for proximal anterior circulation occlusions that are refractory to single stent retriever MT. **MATERIALS AND METHODS:** All patients treated with the double SR technique using the Solitaire system for acute stroke with refractory large artery occlusions, that were located in the anterior circulation, were retrospectively selected from two large neurointerventional centres. Time to recanalization, Angiographic outcome (TICI), additional treatments, complications, and clinical outcome at 3 months were assessed.

ORAL PRESENTATIONS ABSTRACTS

RESULTS: 9 patients (median NIHSS 17, mean age, 69.1 years) were treated with double Solitaire SR MT technique for refractory large artery occlusions. Occlusions were located in the MCA M1 segment (n=4), and in terminal ICA (n=5, [B]Figure[/B]) including two ICA tandem occlusions. Prior single SR MT was performed in 8/9 patients (mean # passes; 2.6). Double Solitaire SR technique was feasible in all procedures (mean # passes, 1.2). In 1 patient, additional single SR MT after double Solitaire SR MT was performed. Other additional treatments included proximal ICA stenting (n=2), intracranial balloon angioplasty (n=1), and intraarterial eptifibatid (n=1). Recanalization of target vessel (TICI 2b/3) was achieved in 88.9% (8/9). Mean time from start to final recanalization was 60.5 minutes (range, 38-100). Procedure related complications occurred in 11.1% (1/9, arterial rupture). At 90 days, overall mortality was 22.2% (2/9) and good clinical outcome (mRS 0-2) was 55.6% (5/9). **CONCLUSIONS:** Double Solitaire SR technique for MT treatment of acute stroke MT is as a feasible and relatively fast escalation strategy for proximal anterior circulation occlusions that are refractory to standard single SR. In this small series, a low complication rate and high rate of target vessel recanalization was demonstrated.



O215-Successful Intra Arterial Reperfusion Therapy Improves Clinical Outcomes in Acute Stroke Secondary to Large Vessel Occlusions – TICI Based Analysis

*Sundeep Mangla*¹, Raghu Loganathan², Moh Paul³, Victor Teresita⁴, Kanna Balavenkatesh⁴, Schori Melissa⁵
SUNY Downstate Health Science Center Radiology, Neurology, Neurosurgery, Brooklyn-United States¹ Lincoln Medical Center Internal Medicine and Critical Care -United States² Lincoln Medical Center Radiology -United States³ Lincoln Medical Center Internal Medicine -United States⁴ Lincoln Medical Center Internal Medicine -United States⁵

PURPOSE: Our study analyzed our experience utilizing currently available intra-arterial reperfusion strategies, technical success at achieving reperfusion, and its effects on clinical outcomes at discharge.

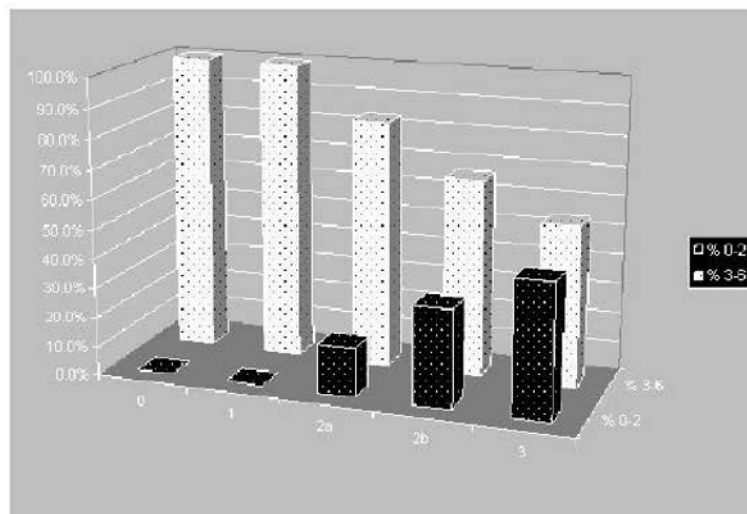


ORAL PRESENTATIONS ABSTRACTS

MATERIALS AND METHODS: We performed an IRB approved retrospective review of a prospectively maintained clinical database of patients receiving intra-arterial reperfusion therapy at Lincoln Medical Center from 9/1/2009 – 1/31/2013. 47 consecutive patients triaged with CTA/CTP imaging for large vessel occlusions within 8 hours of symptom onset underwent intra-arterial therapy (IA alone (25/47 – 54.2%), or IV followed by IA (22/47 – 46.8%)) based on the presence of a large vessel occlusion, independent of perfusion imaging parameters. Combinations of therapies were employed, primarily mechanical thrombectomy with the Penumbra aspiration system (42/47 – 89.4%), secondarily MERCI device (8/47 – 17.0%), with low dose (1-10 mg) IA tPA (16/47 – 34.0%). Clinical imaging (CT, DSA, and MRI), and clinical outcomes (NIHSS, mRS) were reviewed thru discharge. Angiographic outcomes were graded based on Thrombolysis In Cerebral Ischemia system (TICI). RESULTS: TICI 0, 1, 2a, 2b, 3 was achieved in 5 (10.6%), 1 (2.1%), 12 (25.5%), 18 (38.3%), 11

(23.4%) patients respectively. Favorable mRS outcome at discharge (0-2) was positively associated with higher grades of TICI reperfusion (mRS), TICI 0 (0/5 – 0%); 1 (0/1 – 0%); 2a (2/12 – 16.7%); 2b (6/18 – 33.3%); 3 (5/11 – 45.5%) (Figure). 21/47 (44.7%) patients experienced an 8 point or greater improvement in NIHSS at discharge, overall 13/47 (27.7%) achieved mRS (0-2) at discharge, with 5/47 (10.6%) mortality and symptomatic intracranial hemorrhage in 4/47 (8.5%).

CONCLUSION: Our experience with IAT suggests that significant clinical improvement can be experienced in prolonged therapeutic windows (< 8 hours), however, the threshold for reperfusion to achieve favorable clinical outcome may be higher than previously thought (TICI 2b or greater). A significant percentage of patients may still suffer significant functional brain injury despite reperfusion.



O216-Endovascular Cooling Catheter System for Selective Cerebral Hypothermia in Acute Stroke Therapy an Animal Feasibility Study

Stephan Meckel¹, Andreas Keuler¹, Lynn Boos¹, Mukesh Shah², Förster Katharina³, Niesen Wolf-Dirk⁴, Giorgio Cattaneo⁵, Martin Schumacher¹

University Hospital Freiburg Neuroradiology Freiburg-Germany¹ University Hospital Freiburg Neurosurgery Germany² University Hospital Freiburg University Heart Center -Germany³ University Hospital Freiburg Neurology -Germany⁴ Acandis GmbH & Co. KG, Pforzheim -Germany⁵

PURPOSE: In acute ischemic stroke, mild hypothermia after recanalization therapy has been shown to reduce complications and lead to improved clinical outcomes. Hitherto, systemic hypothermia has been induced by endovascular venous cooling, cold saline infusion, or surface cooling devices. Selective cerebral hypothermia



ORAL PRESENTATIONS ABSTRACTS

applied prior and/or during endovascular stroke recanalization procedures may decrease systemic side-effects of cooling and enable early neuroprotection in the critical phase of reperfusion of ischemic brain. In this study, we aimed to establish an animal model for and assess the feasibility of the Acandis intracarotid cooling catheter system.

MATERIALS AND METHODS: This study included 10 adult large animals (1 house pig; 9 sheep) and was performed under general anesthesia. Temperature probes were introduced into the frontal and temporal brain cortex bilaterally by neurosurgical burr hole craniotomies. Femoral vessels were surgically prepared and a temperature probe was inserted into the inferior vena cava (IVC). Via transfemoral endovascular access the cooling catheter system was introduced successively in both common carotid arteries (CCA). Selective intracarotid blood cooling was applied with cooling fluid in a closed loop and without direct blood contact. Systemic (IVC and nasal) temperatures and local cortical brain temperatures were measured simultaneously during cooling (maximum duration, 1 hour) and rewarming phases. CCA diameters and flow were measured angiographically and by Doppler ultrasound, respectively, during cooling. The correct positioning of brain temperature probes was verified by CT.

RESULTS: The porcine model was not suitable due to small CCA luminal diameters. In the sheep model, the CCA diameter was between 6.3-8mm with good flow conditions under cooling through the catheter system (flow acceleration in CCA compatible with moderate stenosis measured by Doppler ultrasound). Maximum cerebral cooling in the ipsilateral temporal cortex was -2.8°C . Maximum cooling in the contralateral cerebral cortex was -1.7°C , and maximum systemic cooling (IVC) was -1.4°C .

CONCLUSIONS: The sheep represents a good animal model to test the Acandis intracarotid cooling catheter system with CCA diameters compatible to humans. Selective mild hypothermia was achieved within the ipsilateral cerebral hemisphere. The systemic cooling effect was considerably lower compared to the ipsilateral brain. Further studies are required to demonstrate the therapeutic benefit of selective cerebral cooling in an animal stroke model.

Sponsored by Federal Ministry of Education and Research, Germany (BMBF grant 13GW0015B)

O217-Transbrachial Approach as a First Access Route for Neurointervention

*Takahisa Mori*¹, Tomonori Iwata¹, Yuhei Tanno¹, Shigen Kasakura¹, Yoshinori Aoyagi¹, Kazuhiro Yoshioka¹
*Shonan Kamakura General Hospital Stroke Treatment Stroke Treatment Kamakura-Japan*¹

INTRODUCTION AND PURPOSE: Transfemoral approach for neuroendovascular treatment is widely used but sometimes limited by aortic or peripheral arterial conditions. The purpose of our study was to investigate the feasibility and safety of transbrachial procedures using the sheath-guide specifically designed for transbrachial cannulation into the carotid artery.

MATERIALS AND METHODS: Included for analysis were patients who underwent transbrachial neurointervention from January 2012 to December 2013. We used the particular sheath-guides with two types of distal length; 1: 1) MSK-guide 7.5x90; 6Fr (2.24 mm, 0.088 inch) (ID: internal diameter) guiding sheath with 7.5cm-distal part and 90 cm in length 2) MSK-guide 7.5x70; 6Fr (ID) guiding sheath with 7.5cm-distal part and 70 cm in length 2: MSK-guide 15x90(3D); It is designated for transbrachial direct cannulation into the internal carotid artery (ICA) and for fitting to the anatomical feature of the ICA. MSK-guide (Medikit Co.Ltd., Tokyo, Japan)

RESULTS: During the period, 293 procedures were done. Among them, 207 were elective and 86 emergent. MSK-guide were used in 155 of 207 elective cases and in 49 of 86 emergent cases. All transbrachial procedures were successful. Transbrachial procedures didn't depend on anatomical features of the abdominal aorta and/or peripheral arteries. Transbrachial procedures didn't depend on vascular diseases of the abdominal aorta and/or peripheral arteries. The MSK-guide provided good support-force.



ORAL PRESENTATIONS ABSTRACTS

CONCLUSION: Transbrachial neurointervention was feasible and safe by using the MSK-guide sheath specifically designated for transbrachial cannulation into the carotid arteries. Routine transbrachial approach can open the door for patients and neuroendovascular physicians.

O218-Balloon Guide Catheter in Complex Mechanical Thrombectomy Procedures of Acute Anterior Circulation Stroke Beyond Proximal Occlusion and Flow Reversal

Theo Demerath¹, Samer Elshikh¹, Andreas Keuler¹, Horst Urbach¹, *Stephan Meckel*¹
*University Hospital Freiburg Neuroradiology -Germany*¹

PURPOSE: In acute ischemic stroke related to large cerebral artery occlusions, mechanical thrombectomy (MT) using stent retriever (SR) devices allows for safe and efficient recanalization treatment. Balloon guide catheters (BGC) are often used for flow arrest/reversal during SR retraction to avoid distal clot embolization. In the majority of MT procedures, fast and complete recanalization of the occluded vessel is possible. However, the complexity of MT may be increased due to upstream ICA stenosis requiring stenting, or extremely tortuous proximal vasculature. Here, we present the use of a BGC to overcome various technical problems in complex MT.

MATERIALS AND METHODS: This retrospective technical case series included all patients that were treated with MT for large cerebral artery occlusions where a BCG was utilized to manage technical problems related to difficult vascular access or access/placement of stents in addition to its standard use of temporary carotid occlusion and flow reversal during SR retrieval. The technical details of this particular use of a BCG were described and illustrated by images/movies. Procedure-related complications, clinical (mRS) and angiographic (TICI) outcome were evaluated.

RESULTS: Seven patients (mean age, 75.3 years; 46-90 years) with acute anterior circulation strokes (mean NIHSS, 13.2; range 9-16) due to MCA M1 occlusion (n=2); terminal ICA (ICAT) occlusion (n=1), tandem ICA occlusion (n=2), high-grade ICA stenosis with MCA M1 occlusion (n=1), and proximal ICA occlusion with non-occlusive ICAT emboli (n=1) were treated. A temporarily inflated BCG enabled rapidly a difficult coaxial passage of microcatheter/distal access catheter (DAC) system through a placed stent (n= 3), a difficult introduction of stent delivery system through a high-grade ICA stenosis (n=1), and proximal anchorage for difficult distal access with microcatheter (n=2) or DAC (n=1) due to arterial tortuosity with catheter push-back. No direct procedure-related complications were observed. Complete recanalization of occluded target vessel (TICI 2b/3) was achieved in 6/7 cases. 3/6 cases had good clinical outcome (mRS 0-2) at discharge (1 patient is still hospitalized). **CONCLUSIONS:** Temporary inflation of BCG is a safe, fast and helpful tool for proximal anchorage/stabilization in case of difficult access for ICA stenting, passage of placed ICA stent with microcatheter/ DAC, or distal catheterization during complex MT procedures for anterior cerebral artery occlusion stroke.

O219-Predictive Value of Neurophysiological Monitoring During Endovascular Mechanical Thrombectomy

*Kornelia Kreiser*¹, Ehab Shiban², Silke Wunderlich³, Florian Ringel², Claus Zimmer¹

*Klinikum rechts der Isar, TU München Neuroradiology München-Germany*¹ *Klinikum rechts der Isar, TU München Neurosurgery -Germany*² *Klinikum rechts der Isar, TU München Neurology -Germany*³

INTRODUCTION AND PURPOSE: In comprehensive stroke centers Mechanical Thrombectomy (MTE) is a common therapy in occlusions of large vessels with high recanalization rates. A substantial number of these patients are treated under general anaesthesia (GA). So far, there is no possibility to get any feedback about the neurological status and possible recovery of the impaired brain functions during the procedure. Neurophysiological monitoring (NPM) is a well-established method in (neuro)vascular surgery. It allows to get real time informations about affected brain functions.



ORAL PRESENTATIONS ABSTRACTS

The aim of this study was to evaluate the benefit of NPM during MTE regarding the real time-information and the predictive value for the long-term outcome.

MATERIALS AND METHODS: We performed NPM during MTE of strokes in the anterior and posterior circulation. NPM included motor and somatosensory evoked potentials (MEPs/SSEPs) before, immediately after opening of the occluded vessel and in short intervals until the end of GA. The neurological status was assessed before treatment, the day after, seven and 90 days after the treatment including NIHSS and mRS.

RESULTS: 20 patients were examined. There were 9, 7 and 4 patients with occlusion of the medial cerebral artery, internal carotid artery and basilar artery, respectively. MEPs were evaluable in 19 (95%), SSEPs in 13 (65%) cases. Successful reperfusion was achieved in 16 cases (TICI 2b or 3). MEPs sensitivity and specificity were 90.9% and 87.5% respectively. SSEPs sensitivity and specificity were 71.4% and 83.3%, respectively. An immediate response of MEPs to the mechanical opening of the occluded vessel was significantly correlated both with a better short term ($p=0,03$) and a better long term outcome ($p=0,03$).

CONCLUSION: MEPs and SSEPs are safe and feasible methods of real time monitoring of reperfusion success with respect to functional outcome during MTE for acute ischemic stroke. MEPs have higher rates of sensitivity and specificity than SSEPs and seem better suited in a setting in which a rapid setup is crucial. NPM during MTE appears to show the clinical long term success immediately.

REFERENCES: Yeon JY, Seo DW. Transcranial motor evoked potential monitoring during the surgical clipping of unruptured intracranial aneurysms. *J Neurol Sci.* 2010 Jun 15;293(1-2):29-34.
Hacke W, Zeumer H. Monitoring of hemispheric or brainstem functions with neurophysiologic methods during interventional neuroradiology. *AJNR* 1983 May-June;

O220-Pre Surgical Embolization of Nasopharyngeal Angiofibroma a Pakistani Experience

*Shahzad Karim Bhatti*¹, Umair Rashid¹

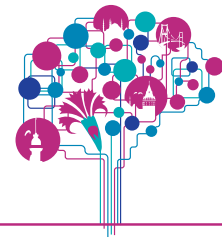
*Lahore General Hospital Neuroradiology Lahore-Pakistan*¹

PURPOSE: Juvenile nasopharyngeal angiofibroma is a benign highly vascular tumor affecting young adolescent boys, originating from the posterolateral wall of the nasal cavity. Study is done to evaluate the pre surgical embolization of nasopharyngeal angiofibroma in order to reduce blood loss and intra operative time during surgery.

MATERIALS AND METHOD: All patients went through internal and external carotid angiography with superselective angiography of vessel supplying the tumor Pre surgical embolization of 30 patients done with spongostone in angiography suit of Neuroradiology department, Lahore General Hospital, Lahore, Pakistan with ages ranging from 12 to 18 years males from January 2011 to December 2013. All the patients underwent surgery within 24 hours of embolization.

RESULTS: Out of 30 patients, Internal maxillary artery was supplying 20 patients, while 6 were supplied by accessory meningeal and 4 had blood supply from ascending pharyngeal artery. Pre surgical embolization with Spongostone proved significant reduction in intra operative blood loss and reduced surgical resection time.

CONCLUSION: Pre surgical embolization appears to be the treatment of choice as it significantly reduces intraoperative blood loss minimizing the need of blood transfusion, shortens intra operative time and makes resection easier.



ORAL PRESENTATIONS ABSTRACTS

O221-3D Vascular Model is Valuable in Neurointervention

*Shigeru Nemoto*¹

*Tokyo Medical and Dental University Endovascular Surgery Tokyo-Japan*¹

PURPOSE: 3D imaging is valuable in diagnostic neuroradiology and neurointervention. In coiling of the aneurysm, shaping of the microcatheter is a key to successful catheterization of the aneurysm. With 3D printer a 3D vascular aneurysm model is made according to the dicom data. Usefulness of this vascular model in coil embolization of cerebral aneurysm is examined.

MATERIALS AND METHODS: An aneurysm vascular model is made of ABS resin with 3D printer according to dicom data of cerebral aneurysm. A microcatheter is shaped as same as this aneurysm vascular model. Microcatheter is navigated into the aneurysm and coils were inserted into the aneurysm. Results were compared with and without vascular model.

RESULTS: Catheter shaping according to the vascular model leads to easy navigation into the aneurysm and to stable catheterization during coil insertion.

CONCLUSION: Catheter shaping according to the 3D vascular model is valuable in coil embolization of the aneurysm not only for beginners but also for experts. 3D vascular model is an extremely useful device in neurointervention of the cerebral aneurysms.

O222-Preoperative Embolization of Juvenile Nasopharyngeal Angiofibroma A 2 Years Retrospective Study in Indonesian Public hospital

*Prijo Sidipratomo*¹, Indrati Suroyo¹, Eppy Buchory²

*University of Indonesia Radiology Jakarta-Indonesia*¹ *Univerity of Pajajaran Bandung Radiology*²

PURPOSE: Juvenile nasopharyngeal angiofibroma is a pathologically benign yet locally aggressive and destructive vascular lesion of head and neck region typically affecting adolescent boys. The purpose of this report is to explain the role of super-selective embolization of JNAs prior to surgical resection.

MATERIALS AND METHODS: we review a 2 years retrospective cases from January 2012 until December 2013 in top referral hospital in Indonesia. We used coaxial system technique and gelfoam as a main embolic material. Embolization was done three days prior of surgery.

RESULT: There were 24 cases received preoperative embolization and almost no blood transfusion needed during surgery.

CONCLUSION: Preoperative embolization of Juvenile Nasopharyngeal angiofibroma is an effective tool to reduce the blood loss during surgery. Gelfoam is an effective embolic material.

O223-Behavioral Difference between NBCA and Onyx for Embolization of Brain Arteriovenous Malformations under Flow Control with ED Coils

*Takuya Nakazawa*¹, Atsusi Tsuji¹, Toshihiro Yokoi¹, Kenichi Tsuji¹, Yayoi Yoshimura¹,

Kenji Takagi¹, Junya jito¹, Naoki Nitta¹, Tadateru Fukami¹, Kazuhiko Nozaki¹

*Shiga University of medical science Neurosurgery Otsu-Japan*¹

PURPOSE: The treatment of brain arteriovenous malformations (AVMs) is still challenging. Although microsurgical resection of an AVM provides immediate cure, this treatment modality has considerable risk of morbidity and mortality. The combined risks of multimodality therapy were emphasized, but meta-analysis could not provide reliable estimate. In our institute, microsurgical resection for anatomically accessible AVM, especially with ruptured presentation, was preferred and appropriate presurgical embolization was considered that it made identification of feeding artery and the nidus excision easier at the nidus excision.



ORAL PRESENTATIONS ABSTRACTS

Therefore, it is important that embolic procedure should be performed with low morbidity risk. However, AVMs sometimes possess high-flow shunts or extremely short distance feeder to draining vein. In these anatomical situations, migration of liquid embolic agent to the venous side can occur easily and may result in devastating hemorrhage. To prevent the migration of embolic materials, we often performed flow control by coils before injecting embolic material. In this report, behavioral difference between n-butyl cyanoacrylate (NBCA) and Onyx (Covidien, Irvine, Calif) and effectiveness of flow control by ED coils (Kaneka Medix Co., Osaka, Japan) for liquid embolization of AVMs are presented.

MATERIALS AND METHODS: From 2011, nine patients with brain AVMs were embolized with NBCA or Onyx presurgically under flow control by placing ED coils through Marathon Flow Directed MicroCatheter (Covidien, Irvine, Calif) in feeding artery just proximal to nidus.

RESULTS: ED coils have so flexible delivery wire enough to place coils through Marathon catheter, even if which was navigated to long tortuous feeding artery. In all patients, delivery of ED coil to intended place was succeeded. In 5 patients embolized with NBCA, NBCA was trapped near the coils. In contrast Onyx penetrated beyond coils and reached more distal into the nidus than NBCA. Only one patient had persistent minimal neurological deficit due to embolization.

CONCLUSIONS: Adjuvant presurgical embolization of AVMs under flow control with ED coils results in a low risk rate. Flow control by ED coils is easy in delivery to the tortuous feeding artery and effective in control of liquid embolic materials. Onyx tends to reach more distal beyond ED coils than NBCA.

PARALLEL SCIENTIFIC PAPER PRESENTATIONS

(Research & Neuroradiological Sciences 3) 17:15 - 19:00

Topkapı B Hall

O224-To Bleed or not to Bleed Prospective Hemorrhage Rates of Cerebral Cavernomas

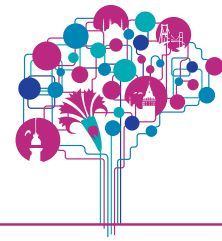
*Omid Nikoubashman*¹, Federico Di Rocco², Michel Zerah³, Kshitij Mankad⁴, Martin Wiesmann¹

*University Hospital, Aachen Neuroradiology Aachen-Germany*¹ *Hôpital Necker Enfants Malades, Paris Neurosurgery -France*² *Hôpital Necker Enfants Malades Paris Neurosurgery -France*³ *Great Ormond Street Hospital, London Neuroradiology -United Kingdom*⁴

PURPOSE: To provide a morphologic classification of cerebral cavernous hemangiomas reflecting their prospective hemorrhage rate.

MATERIALS AND METHODS: We categorized 355 cerebral cavernomas of 70 patients according to their morphological appearance in magnet resonance imaging (MRI) using the Zabramski classification. We performed multivariate hemorrhage risk analyses and calculated prospective hemorrhage rates based on survival analyses for all lesions with a radiological observation period greater than 180 days.

RESULTS: Considering all 355 cavernomas, there were 199 MRI examinations with 1558 distinct observations during a cumulative observation period of 1094.2 lesion-years. Considering 255 cavernomas with an observation period greater than 180 days, there were 1398 distinct observations with a mean observation period of 4.2 lesion-years. Mean hemorrhage rate of all 355 lesions was 4.5% per lesion-year. The presence of (sub)acute blood degradation products was the strongest indicator for an increased hemorrhage risk ($p < 0.001$): mean annual hemorrhage rate and mean hemorrhage free interval for lesions with and without signs of (sub)acute blood degradation products were 23.4% (literature: 4.5%-60%) and 22.6 months and 3.4% (literature: 0%-6%) and 27.9 months, respectively. Dot-sized lesions, clearly visible in T2* and not or barely visible in T1 and T2 sequences, had a mean annual hemorrhage rate of 1.3% and a mean hemorrhage free interval of 37.8 months. Neither cavernoma size (Log rank test: $p = 0.299$), nor infratentorial lesion localization (Log rank test: $p = 0.540$) had a significant impact on hemorrhage rate.



ORAL PRESENTATIONS ABSTRACTS

CONCLUSIONS: Our findings imply a tripartite classification that is not only morphologic but corresponds to prospective hemorrhage risks: 1) lesions with signs of (sub)acute blood degradation products bear the highest hemorrhage risk and may be associated with acute or subacute clinical symptoms. 2) Lesions without signs of (sub)acute blood degradation products bear an intermediate hemorrhagic risk but may be symptomatic in the context of seizures. 3) Dot-sized lesions bear the lowest hemorrhage rate and appear to be asymptomatic unless they are hemorrhagic.

O225-Acute Ischemic Stroke in Non Human Primates a Validation Study Using Near Infrared Spectroscopic Tomography for Cerebral Monitoring of Stroke and Intracranial Hemorrhage

*Sundeeep Mangla*¹, Frank Barone², Tigran Gevorgyan³, Harry Graber⁴, Douglas Pfeil⁵,
Yong Xu⁴, Jenny Libien⁴, Jean Charchafli⁶, John Kral², Randall Barbour⁴, Daniel Lee³

*SUNY Downstate Health Science Center Radiology, Neurology, Neurosurgery, Brooklyn-United States*¹ *SUNY Downstate Health Science Center Neurology -United States*² *SUNY Downstate Health Science Center Surgery -United States*³ *SUNY Downstate Health Science Center Pathology -United States*⁴ *SUNY Downstate Health Science Center Surgery, Pathology -United States*⁵ *SUNY Downstate Health Science Center and Yale University Anesthesiology -United States*⁶

INTRODUCTION AND PURPOSE: Near-infrared spectroscopic (NIRS) tomography is an evolving and exciting portable technology for continuous cerebral monitoring in critical care and operative procedures. We developed and validated an endovascular acute ischemic stroke non-human primate (NHP) model with NIRS monitoring of acute cerebral ischemic and hemorrhagic events in real-time. **MATERIALS AND METHODS:** During stroke induced by unilateral microcatheter occlusion of the middle cerebral artery, we used a NIRS imager with a 270 source-detector channel array for cerebral monitoring of anesthetized Bonnet Macaques. We performed experiments in 5 Macaques using 3 hours of reversible unilateral occlusion of the middle cerebral artery (MCA) to induce ischemia/stroke, with continuous recordings of total hemoglobin (Hbtotal) levels and hemoglobin saturation (HbsO₂) from each channel comparing pre/post events and bilateral hemisphere measurements. NIRS data were also used to construct three-dimensional tomographic functional images of the scalp and brain. Comparative analyses were performed for pre- and post-stroke events within and between cerebral hemispheres. We also performed immediate post-stroke CT Perfusion, MRI, and post-mortem brain histopathology to confirm ischemic and hemorrhagic stroke injury.

RESULTS: Ischemia was achieved in 5/5 animals as confirmed by CT Perfusion and/or MRI Diffusion Imaging and Pathology at autopsy. After refinements in the NIRS monitoring protocol during the first 3 experiments, successful recordings were obtained in the last 2 subjects. Inadvertent vessel perforation in one case allowed us to study subarachnoid hemorrhage. NIRS tomography findings correlated with histopathology, CT, and MRI during acute cerebral ischemia and

subarachnoid hemorrhage in these 2 subjects. Significant localized decreases in Hbtotal resulting from contrast boluses mimicking transient ischemia were noted (19 injections: statistically significant left-right differences in 15 [79%] cases [$p < 0.0001$]; inter-hemispheric differences had expected directionality in 18 of 19 [94.7%] cases). Regional verapamil injections increased Hbtotal levels on the ipsilateral side ($p = 2 \times 10^{-8}$), whereas diffuse subarachnoid hemorrhage produced bilaterally increased Hbtotal compared to baseline levels ($p = 0.0001$). Following microcatheter-induced cerebral ischemia, Hbtotal levels fell in the region corresponding to the occluded artery, compared to the same region in the contralateral cerebral hemisphere ($p < 0.0001$).

CONCLUSIONS: NIRS tomography accurately captured both cerebral ischemia and hemorrhage in real time demonstrating its potential.



ORAL PRESENTATIONS ABSTRACTS

O226-A Novel 3 Dimensional Voxel based Analysis of Focal Cerebral Ischemia in Rats

*Sang-Hoon Cha*¹, Kyung Sik Yi¹, Chi-Hoon Choi², Hong Jun Lee³, Jinwoo Hwang⁴, Sang Rae Lee⁵, Youngjeon Lee⁵

*Chungbuk National University Hospital Radiology Cheongju-Korea, South*¹ *National Medical Center Radiology -Korea, South*² *Chung-Ang University Medical Research Institute -Korea, South*³ *Philips Healthcare Clinical Science -Korea, South*⁴ *Korea Research Institute of Bioscience and Biotechnology National Primate Research Center -Korea, South*⁵

PURPOSE: For the translational research of focal cerebral ischemia, rat middle cerebral artery occlusion (MCAO) models with more homogenous in nature are absolutely needed. To evaluate and establish more homogenous focal cerebral ischemia models, a novel 3 dimension (3D) voxel-based analysis was invented. This is to present our observation of experimental stroke in rats.

MATERIALS AND METHODS: Rats were subject to middle cerebral artery occlusion (MCAO) using the suture technique. Immediately after occlusion, the animals were placed into an MRI scanner (3.0 T) and diffusion weighted imaging (DWI) was repeated every 10 minutes. Immediately after each MR scan, DWI and apparent diffusion coefficient (ADC) maps were evaluated to determine whether successful MCA territorial infarction was obtained by two neuroradiologists. Five rats were followed with repeated DWI for 50 minutes (Group 1) and 4 rats for 100 minutes (Group 2). Percentage of hemispheric lesion volume (%HLV) and ADC value (ADC) were evaluated for quantitative analysis of ADC-derived lesion characteristics using 3D volume analysis. 3D lesions were segmented by ITKsnap (<http://www.itksnap.org/pmwiki/pmwiki.php>) with automatic thresholding method using AFNI software package (<http://afni.nimh.nih.gov/afni/>).

RESULTS: Successful MCA territorial infarction was induced in nine rats (9/32, 28.1%) and they showed MCA territorial infarction at the first DWI 10 minutes after MCAO. 3D voxel-based analyses showed that all ADC-derived lesion volumes did not change during the MRI follow-up period in two groups (mean %HLV of group 1 = 24.5±7.1%; group 2 = 24.9±7.3%). ADC values of the ischemic lesions showed no temporal changes during the DWI observation (mean ADC of group 1 = 467±29×10⁻⁶ mm²/sec; group 2 = 475±33×10⁻⁶ mm²/sec).

CONCLUSION: Applying prospective diffusion MRI and 3D voxel-based analysis, we observed and evaluated experimental brain infarctions with more homogenous MR characteristics.

O227-Prognostic Value of Blood Flow Measurements Using Arterial Spin Labeling in Gliomas

Julia Furtner¹, *Vasileios K. Katsaros*², Benjamin Bender³, Christian Braun Braun⁴, Jens Schittenhelm⁵, Marco Skardelly⁶, Sotirios Bisdas³

*Medical University of Vienna Department of Biomedical Imaging und Image-guided Therapy -Austria*¹ *University of Athens Department of Neuroradiology Athens-Greece*² *University of Tübingen Department of Neuroradiology -Germany*³ *University of Tübingen Department of Neurology -Germany*⁴ *University of Tübingen Department of Neuropathology -Germany*⁵ *University of Tübingen Department of Neurosurgery -Germany*⁶

PURPOSE: The period of progression free survival (PFS) within the same histopathological glioma grades may have high variability, mainly without a known cause. The purpose of this study was to reveal the predictive value of quantified tumor blood flow (TBF) values obtained by arterial spin labeling (ASL) for PFS in patients with histopathologically proven astrocytomas independent of WHO grade.

MATERIALS AND METHODS: Twenty-four patients with untreated gliomas underwent tumor perfusion quantification by means of pulsed ASL in 3T. The clinical history of the patients was retrospectively extracted from the local database. Receiver operating characteristic curves were used to define an optimal cut-off value of maximum TBF (mTBF) values for subgrouping in low-perfused and high-perfused gliomas. Kaplan-Meier curves and Cox proportional hazard regression model were used to determine the predictive value of mTBF for PFS.



ORAL PRESENTATIONS ABSTRACTS

RESULTS: An optimal mTBF cut-off value of 182 ml/100g/min (sensitivity = 83%, specificity = 100%) was determined. Patients with low-perfused gliomas had significantly longer PFS compared to patients with high-perfused gliomas ($p=0.0012$) independent of the WHO glioma grade.

CONCLUSION: Quantified mTBF values obtained by ASL offer a new and totally non-invasive marker, significantly surrogating the histopathological WHO grading, to predict the PFS in patients with gliomas.

O228-Resting State Network Based Characterization of Epilepsy Related fMRI Activation Patters

*Lajos Rudolf Kozák*¹, Louis André van Graan², Umair Javaid Chaudhary³, Ádám Szabó¹, Louis Lemieux²

*Semmelweis University MR Research Center Budapest-Hungary*¹ *UCL Institute of Neurology Department of Clinical and Experimental Epilepsy -United Kingdom*² *Epilepsy Society MRI Unit -United Kingdom*³

INTRODUCTION AND PURPOSE: Functional MRI activations are usually described in relation to macrostructural¹ or microstructural² brain anatomy. However, in epilepsy a functionally derived framework may be more appropriate for describing discharge related activation/deactivation patterns² given the connections between activations and seizure semiology^{3,4,5}. Based on the correspondence of resting state and task-based fMRI maps^{6,7} We aimed to develop an atlasing tool based on resting state networks (RSNs) for the interpretation of epilepsy related BOLD responses.

MATERIALS AND METHODS: Our RSN_Atlasing extension of SPM

(<http://www.fil.ion.ucl.ac.uk/spm/>) is based on publicly available RSN maps^{6,7} thresholded and transformed to MNI space. It provides an extensible framework for processing activation maps; the output includes RSN-wise activation extent, overlap and activation/deactivation measures, etc. Validation was done (A) on resting-state fMRI data of 15 healthy volunteers processed with

MELODIC (<http://fsl.fmrib.ox.ac.uk/>); and (B) on SPM{F}-maps corresponding to early, established and late ictal phases, and interictal discharges on 6 frontal lobe, 4 focal reflex, 2 temporal lobe, and 2 parietal lobe epilepsy patients from a previous study³.

RESULTS: RSN activation maps of volunteers showed good correspondence with atlas maps (median RSN involvement >75% for RSN1, RSN2, RSN4, RSN6, RSN7 and RSN10), nevertheless there was pronounced overlap between the visual networks and splitting of the DMN and the executive control network. RSN Atlasing yielded individual characterisation of seizure-related activation maps spatially (proportion of activated voxels) and temporally (changes in maps during the ictal phases). Our results confirmed significant engagement of a growing number of RSNs through seizure evolution from the early ictal (i.e. onset), to ictal 'established' and late ictal phases, gradually involving more RSNs, with the overall proportion of activation being similar across the patients.

CONCLUSION: Our tool provides a fast, standardised and objective quantitative comparative approach for characterizing epilepsy related activation patterns in a functional framework based on RSN engagement. The suggested framework is not restricted to epilepsies; it can be used for activation studies, and it may also allow for objective assessment of network attenuations by pharmacological intervention.

REFERENCES

1. Tzourio-Mazoyer, N. (2002), *NeuroImage*, 15(1):273-289.
2. Eickhoff, S.B. (2005), *NeuroImage*, 25(4):1325-1335.
3. Chaudhary, U.J. (2012), *Brain*, 135(12):3645-63.
4. Thornton, R.C. (2012), *Neuroimage* 53:196-205.
5. Tyvaert, L. (2008), *Brain*, 131:2042-2060.
6. Smith, S.M. (2009), *PNAS*, 106(31):13040-5.
7. Laird, A.R. (2011), *J Cogn Neurosci*, 23(12):4022-37.



ORAL PRESENTATIONS ABSTRACTS

O229-Longitudinal Deactivation Changes in Patients with Relapsing Remitting Multiple Sclerosis

*Sofya Kulikova*¹, Anastasiya Peresedova², Vasiliy Bryukhov¹, Elena Kremneva¹, Marina Krotenkova¹, Igor Zavalishin²

*Research Center of Neurology RAMS Neuroradiology Moscow-Russia*¹ *Research Center of Neurology RAMS Neurology -Russia*²

PURPOSE: to investigate deactivation changes in relapsing-remitting multiple sclerosis (RRMS) patients during the relapse and in the follow-up.

MATERIALS and METHODS: data were acquired from 15 RRMS patients (5 men, 10 women, all right-handed, aged 19-42) during the relapse also characterized by unilateral light hand palsy, in three and twelve months after it. All patients underwent full neurological examination including nine-hole peg test (NHPT) and MRI on 1.5 T scanner including fMRI sequence. FMRI was performed using simple movement block paradigm of flexion and extension of II-V fingers with 1Hz frequency for both hands. FMRI post-processing analysis was performed using SPM8. 12 healthy subjects entered the control group and underwent the same MRI examination.

RESULTS: FMRI data analysis in the control group showed deactivation in the ipsilateral sensorimotor cortex (iSM1) and several other areas that form so-called default mode network and decrease their activity during task performance. Deactivation analysis in RRMS patients during the relapse showed absence of deactivation in the iSM1 during both palsy and non-palsy hand movement. In three months all patients experienced subjective clinical recovery of hand function, but according to NHPT performance fine motor skills of the former palsy hand were still damaged. Deactivation analysis showed small deactivation area in the iSM1 during both former palsy and non-palsy hand movement. In twelve months NHPT showed full fine motor skills recovery in all patients. FMRI data analysis showed iSM1 deactivation comparable with the control group during both former palsy and non-palsy hand movement.

CONCLUSION: RRMS relapse is characterized by iSM1 deactivation decrease, which recover over time together with the hand function, being a temporary phenomenon probably due to compensatory recruitment, transcallosal fibers damage or increased cortical excitability because of inflammation. ISM1 deactivation recovery could be a sign of improvement of movement specificity control that was impaired due to an acute damage during the relapse.

This study was supported by President's Grant No.MK-3052.2014.7

O230-Altered Default Mode Network Functional Connectivity in Alzheimer's Disease and Its Relation with CSF Biomarkers

*Arzu Ceylan Has*¹, Ozlem Celebi², Andac Uzdogan³, Filiz Akbiyik³, Bulent Elibol², Esen Saka², Kader Karli Oguz⁴

*Bilkent University National Magnetic Resonance Research Center (UMRAM) ANKARA-Turkey*¹ *Hacettepe University Department of Neurology -Turkey*² *Hacettepe University Department of Biochemistry -Turkey*³ *Hacettepe University Department of Radiology -Turkey*⁴

PURPOSE: To investigate functional connectivity (FC) of ventral and dorsal parts of posterior cingulate cortex (PCC) and other default-mode-network (DMN) structures separately in Alzheimer's Disease (AD) by resting state functional MRI (RS-fMRI) and determine if there's a correlation with CSF biomarkers.

MATERIALS and METHODS: RS-fMRI and 3D T1-weighted structural images of fifteen patients with mild to moderate AD and 10 age-matched healthy controls were obtained in a 3.0 T scanner (Trio, Tim, Siemens, Germany) along with detailed neuropsychological evaluation.



ORAL PRESENTATIONS ABSTRACTS

Following preprocessing of the data using SPM8 (<http://www.fil.ion.ucl.ac.uk/spm/software/spm8/>) and normalization to the Atlas of MNI, we performed independent component analysis on FSL (<http://fsl.fmrib.ox.ac.uk/fsl/fslwiki/>) and obtained group maps for AD and healthy controls. Analysis of FC of low-frequency BOLD fluctuations was carried out with the “conn”

(www.nitrc.org/projects/conn) toolbox. We examined connectivity patterns separately for seven different seed regions-of-interest (ROIs) of 6mm-radius in expected DMN nodes. Correlation coefficient images between PCC/subunits and DMN nodes were z-transformed, with one-sample t-test examining within group connectivity (voxelwise threshold of $p < 0.005$).

We determined CSF A β 1-42, t-tau, p-tau levels using ELISA (Innotest, Innogenetics, Ghent, Belgium).

RESULTS: Mini-mental state examination (MMSE) scores of AD and controls were 18.1 (standard deviation (sd): 8.6) and 27.5 (sd: 2.4), respectively ($p < 0.05$). Neuropsychological test scores of episodic memory, semantic memory, executive and visuospatial functions were worse in AD ($p < 0.05$).

In AD group, we found diminished FC of ventral PCC and the both medial temporal lobes; and the absence of FC of dorsal PCC and medial temporal lobes. In contrast, connectivity of dorsal PCC and inferior parietal lobules, and ventral PCC and medial prefrontal cortex increased.

CSF level of A β 1-42 was highly correlated with the functional connectivity of PCC (dorsal and ventral) and retrosplenial cortex on the right side.

CONCLUSIONS: We showed impairment of DMN FC in AD and differential alteration of FC of dorsal and ventral subcomponents of PCC and the other parts of the DMN. Furthermore, presence of correlation between FC of PCC - retrosplenial cortex and A β 1-42 levels; and absence of correlation between tau biomarkers and FC of any of the DMN structures are in accordance with the known pathologic observations of early involvement of PCC with A β deposition in AD.

O231-Optimization of Conditional Probabilities of a Bayesian Expert System for Neuroradiology Differential Diagnosis

Ilya Nasrallah¹, Manoj Tanwar¹, Suyash Mohan¹, Harold Kundel¹, Edward Herskovits²,

*Nick Bryan*¹

*Univ. Pennsylvania Radiology -United States*¹ *Univ. Maryland Radiology -United States*²

PURPOSE: We developed a Bayesian network expert system (BES) model for Neuroradiology differential diagnosis (DDx). This network integrates reader-extracted data from brain MRIs using pre-defined conditional probabilities (CPs) to output posterior probabilities for eleven diseases and normal. In this study, we test the hypothesis that models based upon consensus agreement of neuroradiologists (M1P2) or derived from data extracted from cases (M1P3) would show improved performance, as compared to a model based on a single expert's CPs (M1P1).

MATERIALS AND METHODS: Three readers (resident, neuroradiology fellow and attending) extracted KFs and generated Rad-DDx from 101 cases: 6 of each disease and 35 normals. Modified Delphi method was used for expert consensus CP modification (M1P2). For the data driven model (M1P3), CPs were calculated from the KFs extracted by the readers. BES network structure was identical for all models.

Reader extracted KFs were run through each BES model to generate DDx and evaluated by complete and partial receiver operating curve (ROC) analysis. Area under the curve (AUC) was compared between Model DDxs and Rad-DDx.

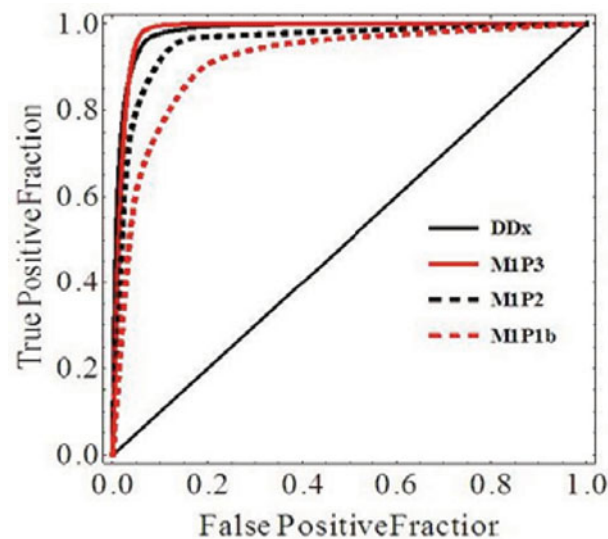
RESULTS: The figure shows mean ROC curves. Rad-DDx and M1P3 had the highest AUC while M1P1 had the lowest. Compared to Rad-DDx, M1P1 showed significant difference ($p = 0.01$) while M1P2 and M1P3 did not. Partial curve analysis between false positive fractions 0-0.2 showed significant difference between M1P2 and M1P1 ($P = 0.025$) and between M1P3 and M1P1 ($p < 0.01$) while M1P2 and M1P3 did not differ.



ORAL PRESENTATIONS ABSTRACTS

CONCLUSION: A BES using CPs based on expert consensus and radiologists' extracted KFs resulted in improved performance of a prototype differential diagnosis system for neuroradiology. After optimization, this BES performed comparably to radiologists. This pilot study is now being expanded to a complete neuroradiology module with 120 diseases.

Figure: Mean ROC curves for the reader-DDx and the three BES models.



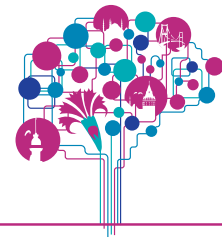
O232-Effect of MR Imaging Parameter Changes on Fractional Anisotropy Value Differs between the Gray and White Matter of Human Brain

*Sang Joon Kim*¹, Young Jun Choi¹, Choong Gon Choi¹, Geon-Ho Jahng²

*Asan Medical Center, University of Ulsan Radiology Seoul -Korea, South*¹ *East-West Neomedical Center, Kyung Hee University College of Medicine Radiology -Korea, South*²

PURPOSE: To investigate the effects of MR imaging parameter changes on the fractional anisotropy (FA) of diffusion tensor imaging (DTI) in the gray and white matter of human brain. MATERIALS AND METHODS: This study was approved by the institutional review board and informed consent was obtained from all subjects. To evaluate effects of MR imaging parameters of DTI, 4 DTI scan parameters were tested changing parameter one-at-a-time and stepwise incremental fashion: five different sensitivity-encoded (SENSE) factors; five different echo time (TE) values; six different b-values; and three different set of number of diffusion gradient directions (NDGD). Total 20 healthy adult volunteers were scanned; 5 persons per each parameter. Regions-of-interest were defined in the thalami and corpus callosum. The relationships between alterations in FA values and MR imaging parameters were evaluated using Spearman's correlation analysis. We also evaluated the difference of FA value between the thalami and corpus callosum using student t-test.

RESULTS: The FA values demonstrated positive correlation with SENSE factors ($r_2=0.667$, $P<0.001$) and TE ($r_2=0.788$, $P<0.001$), and negative correlation with NDGD ($r_2=-0.794$, $P<0.001$) in the thalami, while in the corpus callosum FA value showed positive correlation only with SENSE factors ($r_2=0.412$, $P=0.041$). The mean FA values in the corpus callosum and thalami were 0.590 ± 0.058 and 0.376 ± 0.020 respectively, with statistically significant difference.



ORAL PRESENTATIONS ABSTRACTS

CONCLUSIONS: The FA values demonstrated correlation with SENSE factors, TE, and NDGD while no correlation with b-values. The responses of FA values were different between the corpus callosum and the thalami. Therefore, attention to the choice of imaging parameters should be required in applying DTI to clinical studies.

Table. Correlations of MR scan parameter variations with fractional anisotropy (FA) values

	Corpus callosum		Thalami	
	rho	p-value	rho	p-value
SENSE	0.412	0.041	0.667	0.000
TE	0.345	0.091	0.788	0.000
b value	-0.186	0.325	-0.357	0.052
NDGD	-0.397	0.143	-0.794	0.000

SENSE=sensitivity-encoding,

TE= echo time,

NDGD= number of diffusion-gradient directions



XXth
Symposium
Neuroradiologicum

**POSTER PRESENTATIONS
ABSTRACTS**



POSTER PRESENTATIONS ABSTRACTS

Monday, September 8, 2014

Poster Presentations

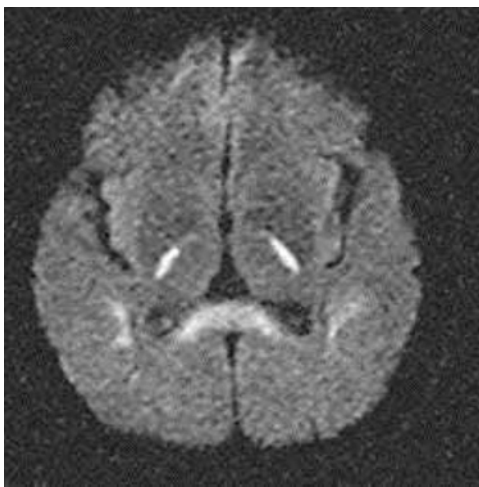
13.00-14.00

Adult NR 1

EP001-Neuroimaging Findings in Alcohol Related Encephalopathies; What Radiologists Need to Know?

*Hye Jin Baek*¹, Hong Dae Kim¹, Choong Ki Eun¹

*Inje University College of Medicine, Haeundae Paik hospital Radiology Busan-Korea, South*¹



Alcohol is one of the most commonly abused substances and alcohol-related brain changes have a broad-spectrum of CNS disorders. This pictorial review will provide an overview of neuroimaging

findings of direct and indirect alcohol-related toxic effects. We will illustrate the cases of alcohol-related brain changes including brain atrophy, osmotic myelinolysis, Marchiafava-Bignami disease, Wernicke encephalopathy, hepatic encephalopathy, and alcohol withdrawal syndrome. Brain atrophy can be reversible if alcohol abuse is stopped. In contrast, some kinds of alcohol-induced encephalopathies can lead to fatal clinical course, thus an early diagnosis is important for immediate initiation of an appropriate therapy such as thiamine supplementation. However, in daily practice, clinical findings are often nonspecific, so the radiologist plays an important role in the detection of alcohol abuse and its related clinical conditions.

Therefore, this review provides the important neuroimaging findings associated with alcohol consumption, and it can be crucial in helping to make diagnoses and appropriate treatment.

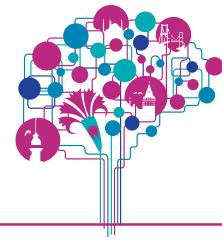
EP002-Encephalitis with Restricted Diffusion and Absent T2W Flair Changes

*Hilwati Hashim*¹, Norzaini Rose Mohd Zain², Shanti Viswanathan³

*Universiti Teknologi Mara Radiology Sg. Buloh-Malaysia*¹ *Hospital Kuala Lumpur Radiology -Malaysia*²

*Hospital Kuala Lumpur Neurology -Malaysia*³

Herpes simplex encephalitis can show early restricted diffusion, sometimes preceding FLAIR abnormalities. We described a case of a 52 year old male with complaints of haemoptysis and haematemesis who then developed 2 episodes of generalized tonic clonic seizures while being treated in Emergency Department. Non-contrasted CT brain showed cerebral atrophy. Lumbar puncture showed a slightly raised protein but is otherwise non conclusive. Electroencephalogram showed severe encephalopathy. For cerebral protection, he was intubated and subsequently referred for MRI. His MRI showed restricted diffusion seen in the splenium of corpus callosum and bilateral white matter of parieto-occipital region. However, there is no corresponding T1W, T2W or FLAIR abnormalities seen. There was also no haemorrhage seen. No parenchymal or leptomeningeal enhancement were noted. Correlating with the clinical status and his EEG findings, a diagnosis of encephalitis was suggested. The patient was diagnosed with viral encephalitis and treated with acyclovir to which he responded. This case exemplifies the advantage of diffusion sequence in helping to make a diagnosis, particularly when there is no abnormality seen in other sequences.



POSTER PRESENTATIONS ABSTRACTS

EP003-Cranial MR Imaging Findings of Wolfram (DIDMOAD) Syndrome a Case Report

*Rahsan Gocmen*¹, Ezgi Guler¹

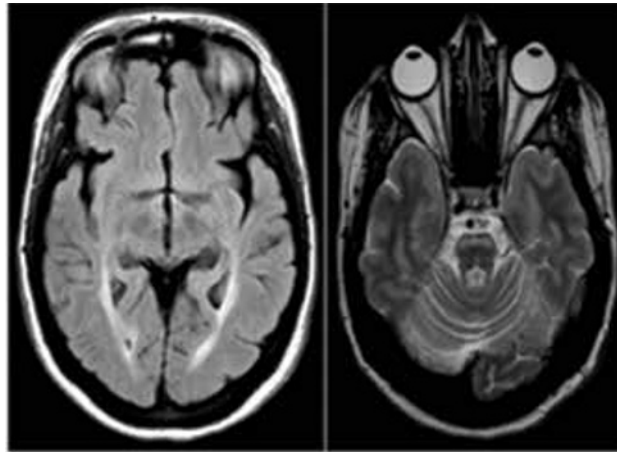
*Hacettepe University Department of Radiology Ankara-Turkey*¹

PURPOSE: Wolfram syndrome, which was first described in 1938, is a rare autosomal recessive disorder. The syndrome features diabetes insipidus (DI), diabetes mellitus (DM), optic atrophy (OA), and deafness. DIDMOAD is a commonly accepted acronym for this disorder. Neuroimaging findings of this rare syndrome have been described in the literature with a limited number of cases. Our aim is to report cranial magnetic resonance (MR) imaging findings in a patient with complete clinical manifestations of Wolfram syndrome, presenting significant MR imaging abnormalities.

CASE REPORT: Our case was a 31-year-old female who was previously diagnosed with Wolfram syndrome. At the age of 5 years, she was diagnosed with type 1 diabetes mellitus. Hypothyroidism was developed 15 years ago. She suffered from progressive visual loss and optic atrophy for the past 12 years. She developed progressive hearing loss 3 years ago.

IMAGING FINDINGS: Abdominal sonography revealed findings in accordance with neurogenic bladder and bilateral hydronephrosis. Cranial MR imaging findings included thinning of bilateral optic nerves, absence of the neurohypophyseal 'bright signal' on T1 weighted images, atrophy of cerebrum, cerebellum, and brainstem. Atrophy was predominantly seen in cerebellum and brainstem. High signal intensity on T2 weighted images was demonstrated in pons and bilateral peritrigonal areas/optic tracts.

SUMMARY AND CONCLUSION: The diagnosis of Wolfram syndrome is primarily based on clinical findings. However, interpretation of imaging findings is essential. Radiologists should be familiar with MR imaging and clinical findings of this rare syndrome.



EP004-Neuroimaging Findings of a Case with Primary Leptomeningeal Melanomatosis

*Rahsan Gocmen*¹, Nazire Pinar Acer², Ahmet Cagkan Inkaya³, Asli Kurne²

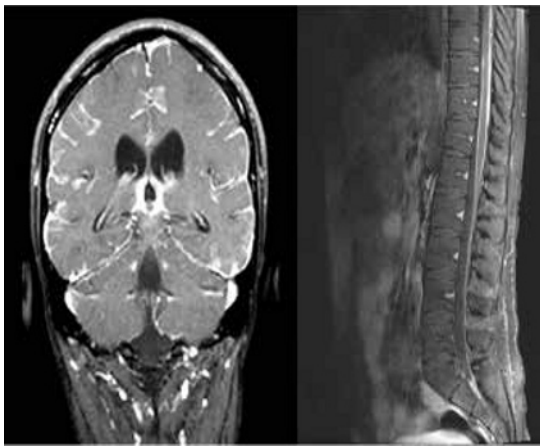
Hacettepe University Department of Radiology Ankara-Turkey ¹ *Hacettepe University Department of Neurology -Turkey* ² *Hacettepe University Department of Infectious Diseases -Turkey* ³

PURPOSE: Primary leptomeningeal melanomatosis (PLM) is a very rare and aggressive form of intracranial melanoma. We present imaging findings, treatment, and ten months follow-up of a patient with the histopathologically proven of PLM.



POSTER PRESENTATIONS ABSTRACTS

CASE REPORT: 22-year-old male patient was admitted with nausea, vomiting and fever. He had no significant medical history. Neurological examination was normal except mild sleepiness. There was no neck stiffness. Cerebrospinal fluid (CSF) sampling showed high opening pressure and elevated protein levels. Atypical cells were seen the CSF cytology indicating a possible epithelial neoplasia. Brain biopsy was performed and during surgery, the dark brown and black colour changes on the leptomeninges were noticed. The biopsy material showed dense cellular infiltration in the leptomeninges, into Virchow-Robin spaces, and superficially, and within the brain substance, composed mainly of melanocytes, positive by immunohistochemistry for melanocytic markers, Human Melanoma Black 45 (HMB45), Melan-A and S100. Histopathological evaluation was reported as leptomeningeal malignant melanoma. On systemic screening, no primary focus was found. Patient was discharged with temozolamid treatment and radiotherapy started.



IMAGING FINDINGS: Brain magnetic resonance imaging (MRI) showed leptomeningeal thickening and contrast enhancement. T1W images before contrast material administration showed diffuse T1 shortening along the spinal leptomeninges. Spinal MRI showed diffuse leptomeningeal thickening and contrast enhancement and leptomeningeal increase signal intensity on precontrast T1W along spinal cord. **SUMMARY AND CONCLUSION:** Despite having a better prognosis than secondary malignant melanoma, PLM is still a rare and aggressive disease. Radiological differential diagnosis includes infectious and inflammatory diseases. T1 shortening on the precontrast T1W images is an important clue in the diagnosis of PLM.

EP005-Hyper IgE Syndrome Initially Presenting with Progressive Multifocal Leukoencephalopathy

*Rahsan Gocmen*¹, Nazire Pinar Acar², Nergis Agayeva², Asli Kurne²
*Hacettepe University Department of Radiology Ankara-Turkey*¹ *Hacettepe University Department of Neurology -Turkey*²

PURPOSE: We present, an HIV seronegative 23-year-old patient with an extremely rare inherited immunodeficiency disease, hyper IgE syndrome (Job's syndrome) who developed progressive multifocal leukoencephalopathy (PML) and lymphoma. To our knowledge, this is the second time that PML has been reported to occur in association with hyper IgE syndrome.

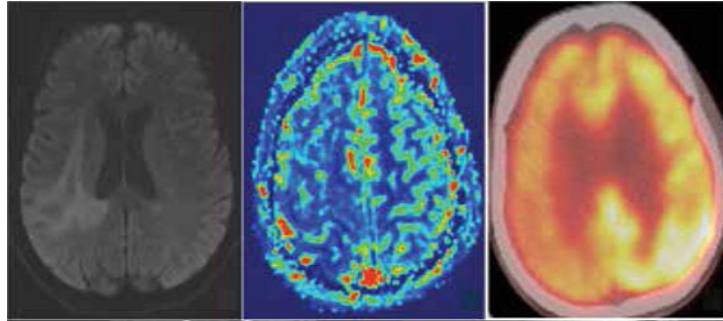
CASE REPORT: A 23-year-old male was admitted to the hospital with weakness on his left side. In early childhood, he was hospitalized for recurrent sinopulmonary infections. He had suffered from measles infection, recurrent dermatitis and molluscum contagiosum since early childhood. Besides he experienced labial herpes simplex virus infection at least two times in a year. His parents were first degree cousins. One of his five siblings died because of meningitis at the age of five. Serum IgE value was 854 UI/mL (0-87 UI/ml).

IMAGING FINDING: Brain MR imaging showed diffuse hyperintense subcortical white matter lesion involving the right parietal and frontal lobe, with a relative sparing of cortex and periventricular white matter. There was no enhancement of the lesion on T1W image after gadolinium injection. Isotropic DWI showed a hypointense center and well-defined hyperintense rim. MR spectroscopy revealed a decreased NAA and increased Cho, and a lactate peak. MR perfusion study showed mixed-changes. A radiological diagnosis of PML was considered most likely. The chest CT scan revealed parenchymal mass as well as pneumatocele and parenchymal consolidation in the left lung. On PET-CT study observed a decreased FDG uptake consisted with hypometabolism in the brain lesion whereas the lung lesions demonstrate increased FDG uptake. The lung mass was surgically resected



POSTER PRESENTATIONS ABSTRACTS

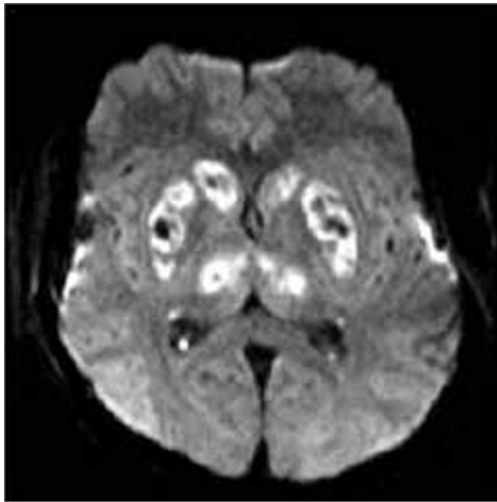
histologically reported as diffuse large b-cell lymphoma. He was treated with intravenous IVIg and cidofovir for 6 months. His symptoms did not improve and he continued to deteriorate and died 6 months after diagnosis. CONCLUSION: PML typically occurs in the setting of severe acquired cellular immunodeficiency, but it also may rarely accompany occult inherited and mild immunodeficiency syndromes such as HIES. Clinicians should be aware that PML can occur as first considerable clue of overlooked HIES in adulthood.



EP006-Pseudohypoxic Brain Swelling after Intracranial Electrode Placement an Extremely Rare Complication

*Rahsan Gocmen*¹, Mehmet Akif Topcuoglu², Irsel Tezer², Burcak Bilginer³, Serap Saygi²

Hacettepe University Department of Radiology Ankara-Turkey *1 Hacettepe University Department of Neurology -Turkey* *2 Hacettepe University Department of Neurosurgery -Turkey*³



PURPOSE: Pseudohypoxic brain swelling (PHBS) is a newly defined clinico-radiologic entity that occur after otherwise uneventful cranial surgery. PHBS is characterized clinically by unexpected neurologic deterioration, generalized seizures, brainstem dysfunction and even comatose condition. Its pathophysiology remains not well defined. The purpose of this presentation is to describe of magnetic resonance (MR) imaging findings in a case with PHBS occurring after intracranial electrode placement.

CASE REPORT AND IMAGING FINDINGS: A 32-year-old female patient suffered from epilepsy was assessed for epilepsy surgery. No remarkable findings in MR imaging. Interictal and ictal scalp EEGs were uninformative. The patient underwent a craniotomy for subdural electrode placement. Surgery was uneventful. Following the operation, she did not awaken, underwent generalized seizures and the patient's Glasgow coma scale decreased 4/15 within a few hours. Cranial MR performed 6th hour after the operation

and revealed mild caudal displacement of the cerebellar tonsils, increased signal in the bilateral basal ganglia, thalami, and diffuse cerebellar cortical swelling on T2-weighted (W) images. A diffusion-W images and ADC map showed vasogenic edema associated with some degree cytotoxic edema. Susceptibility-W images reveal foci of hemorrhagic transformation in the area of lesions. MR venography showed no venous thrombosis. MR perfusion indicated low perfusion in the area of lesions. Her symptoms gradually improved. Follow-up MR showed largely resolution of signal abnormalities on the postoperative 13th day. She was discharged with complete resolution of symptoms 30 days after operation.

SUMMARY AND CONCLUSION: PBHS as potential fatal complication should be kept in mind in unawaken or patients with unexpected neurological deterioration following uneventful cranial surgery. It should be distinguished from global brain hypoxi due to similar imaging findings.



POSTER PRESENTATIONS ABSTRACTS

EP007-Pyogenic Brain Abscesses Necrotic Glioblastomas and Necrotic Metastatic Brain Tumors Discrimination with Susceptibility Weighted Imaging

*Ping-Hong Lai*¹, Jui-Hsun Fu¹, Tzu-Chao Chuang², Hsiao-Wen Chung³, Hing-Chiu Chang⁴, Huey-Shyan Lin⁵, Po-Chin Wang⁶, Shuo-Hsiu Hsu⁶, Huay-Ben Pan⁶

*Kaohsiung Veterans General Hospital Department of Radiology Kaohsiung-Taiwan*¹ *National Sun Yat-Sen University, Kaohsiung, Taiwan Department of Electrical Engineering -Taiwan*² *National Taiwan University, Taipei, Taiwan Department of Electrical Engineering -Taiwan*³ *School of Medicine at Duke University Brain Imaging and Analysis Center -Taiwan*⁴ *School of Nursing, Fooyin University, Kaohsiung, Taiwan Program of Health-Business Administration -Taiwan*⁵ *Kaohsiung Veterans General Hospital Department of Radiology -Taiwan*⁶

PURPOSE: Brain abscess can simulate intracranial necrotic glioblastomas multiforme (GBM) and necrotic metastasis (Meta) in MRI appearance. Susceptibility-weighted imaging (SWI) is a high-resolution, three-dimensional, fully velocity-compensated gradient-echo sequence that uses both magnitude and phase data.

The purpose of this study was to investigate the discrimination of abscess and necrotic tumors at SWI.

MATERIALS and METHODS: SWI was performed in 21 patients with pyogenic brain abscesses, 21 patients with rim-enhancing glioblastomas, 23 patients with rim-enhancing metastases at 1.5 Tesla. Three observers assessed independently the intralesional susceptibility signal (ILSS), and analyzed with qualitative (QL) and semi-quantitative (SQ) methods. Logistic regression models were used to distinguish between any two diseases. After receiver operating characteristic (ROC) analysis, area under ROC curve was compared between two different methods in any two diseases. **RESULTS:** In qualitative analysis, ILSSs were seen in 12 (57.14%) of 21 abscesses, in 20 (95.24%) of 21 glioblastomas, and in 16 (69.57%) of 23 metastases. In semi-quantitative analysis, a low degree of ILSS (ILSS grade 0 and 1, 85.72%) was in the majority of abscesses and a high degree of ILSS (ILSS grade 3, 76.19%) was in the majority of glioblastomas. ILSS was relatively evenly spread across the four ILSS categories of metastatic group. SQ model was significantly better than QL model in distinguishing abscess from glioblastoma ($P < .001$). A derived ILSS cut-off grade of 1 or less was quantified as having a sensitivity of 85.7%, specificity of 85.7%, accuracy of 88.1%, PPV of 90.0%, and NPV of 86.4% in distinguishing the abscess from glioblastoma.

CONCLUSION: A high-grade ILSS may help distinguish glioblastomas from abscesses and solitary metastatic brain tumors. The lack of ILSS or low-grade ILSS can be a more specific sign in the imaging diagnosis of abscesses.

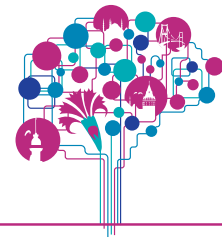
EP008-Venous Hypertension with Intracranial Hemorrhagic Complication

*Clayton Chi-Chang Chen*¹, Fong Y Tsai², Chi-Jen Chen³, Kwo-Whei Lee⁴

*Taichung Veterans General Hospital Department of Radiology Taichung-Taiwan*¹ *University California Irvine Medical Center -United States*² *Taipei Medical University Imaging Research Center -Taiwan*³ *Chang-Hua Christian Hospital Department of Radiology -Taiwan*⁴

PURPOSE: Endovascular procedures have been widely used to restore cerebral circulation for stroke. Hemorrhagic complication may in some occasions after therapeutic procedures. The purpose is to evaluate the venous hypertensive complication may be relating to cerebral venous impairment.

MATERIALS AND METHODS: Retrospectively reviewed 317 consecutive patients from two and half years. Among of those patients, 54 patients had received endovascular procedures with stent and thrombolysis to treat ischemic stroke. Male:female=34:24; age range from 15 to 89 with average 56.2 years. **RESULT:** Among those 54 patients, 14 patients suffered various degree of complication from venous hypertension all of those 14 patients had impaired abnormal drainage with ipsilateral transverse sinus. 6 of those fatal hemorrhagic patients had atresia of ipsilateral transverse sinus. Those non-fatal patients had hypoplasia transverse sinus without atresia.



POSTER PRESENTATIONS ABSTRACTS

CONCLUSION: Abnormal venous transverse sinus which may impair cerebral venous drainage and lead to venous hypertension with hyperperfusion. fatal hemorrhagic complication may occur with atresia of ipsilateral transverse sinus.

EP009-Cerebral Venous Drainage Variants Pathology and Impact on the Diagnosis of Headache

*Diana Quiñones Tapia*¹, Carlota Andreu Arasa¹, Juan Viaño¹
*Hospital NS del Rosario Neuroradiology Madrid-Spain*¹

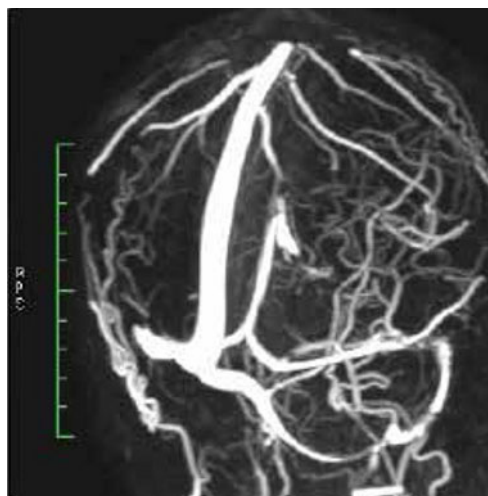
PURPOSE: Nowadays submillimeter resolution in CT and MR permit direct visualization of small intracranial venous vessels. Non-invasive angiographic techniques with or without contrast give us further information of intracranial veins, allowing more detail in venous structure definition. We can evaluate venous anatomy, venous drainage distribution, collaterals and intravascular content. This information may have relevant clinical implications in the study of headache, tinnitus, trauma, and many other pathologies.

METHODS: Retrospective review of MRI and CT cases with the diagnosis of “cerebral venous pathology” or “venous variants” from the last 2 years in a MRI and CT diagnostic Unit. Selected examples of different entities were obtained to cover varied venous pathologies in a pictorial review.

RESULTS: Normal venous content is fluid blood, but slow flow or intravascular clot can give abnormal MRI signal. Arachnoid granulations are normal structures which may be inside the venous sinuses, but in some cases they may obstruct venous drainage and are associated with thrombosis. Venous morphology and size gives us the clue to the differential diagnosis of intracranial hypertension and hypotension.

Acute and chronic venous thrombosis have different imaging patterns. Venous collaterals develop easier in children and in chronic venous obstruction, while they are sparse in acute venous thrombosis. Intracranial dural sinuses are not symmetric, and venous drainage variants are frequent. These anatomic variants may be related to tinnitus, and site of hemorrhagic complications associated with venous thrombosis. Developmental venous anomalies may be associated with cavernomas and bleed.

CONCLUSIONS: Cerebral venous imaging requires conventional CT and MRI as well as angiographic techniques. The observation of venous structures in detail and venous drainage patterns can give us the clue in the diagnosis of intracranial hypertension or hypotension, many headaches and thrombotic disease.





POSTER PRESENTATIONS ABSTRACTS

EP010-Additional Value of 3D FLAIR in Relation to T2 weighted Images in the Evaluation of the Optic Pathway in Patients with Sellar Suprasellar Tumors

*Mika Kitajima*¹, Toshinori Hirai¹, Shigetoshi Yano², Yoshinori Shigematsu¹, Yasuhiko Iryo¹, Minako Azuma¹, Machiko Tateishi¹, Yasuyuki Yamashita¹
*Kumamoto University Diagnostic Radiology Kumamoto-Japan*¹ *Kumamoto University Neurosurgery -Japan*²

PURPOSE: To evaluate whether 3D-FLAIR at 3T is useful for assessing the anterior optic pathway (OP) in patients with large sellar-suprasellar tumors.

METHODS: Forty-three patients with sellar-suprasellar tumors (24 pituitary adenomas, 12 craniopharyngiomas, 4 Rathke's cleft cysts, 2 germ cell tumors, and 1 dermoid cyst) underwent 3T-MRI. Two neuroradiologists independently reviewed T2WI, pre- and post-contrast 3D-FLAIR images. Using a 4-point grading system, they determined whether 3D-FLAIR yielded additional information to T2WI on abnormal OP hyperintensity and on the anatomical relationship between the lesion and the OP. Another neuroradiologist evaluated the incidence and distribution of OP hyperintensity on 3D-FLAIR. Qualitative assessments were statistically analyzed with the Wilcoxon signed-rank test and the level of interobserver agreement with the kappa coefficient. The distribution of OP hyperintensity was compared in patients with pituitary adenomas and craniopharyngiomas using the χ^2 [SUP]2/[SUP]-test. **RESULTS:** 3D-FLAIR yielded additional information to T2WI for the depiction of abnormal OP hyperintensity in 69.8% of patients, and in 87.5% for the anatomical relationship. Significantly more information was provided by non-contrast than contrast-enhanced 3D-FLAIR for the depiction of abnormal OP hyperintensity ($p = 0.008$). For the anatomical relationship, there was no statistically significant difference. Interobserver agreement was very good ($kappa = 0.81$) for the depiction of OP hyperintensity and good ($kappa = 0.70$) for the anatomical relationship. The incidence of OP hyperintensity was 69.8%. Although the hyperintensity distribution varied with the histologic tumor type, optic tract hyperintensity was statistically more frequent in patients with craniopharyngiomas than pituitary adenomas ($p = 0.001$).

CONCLUSIONS: 3T 3D-FLAIR provides additional information to T2WI for the assessment of the anterior OP in patients with sellar-suprasellar tumors. The administration of contrast material is not useful for assessing OP signal changes.

EP011-Possible Compensatory Plasticity of Anterior Thalamic Nucleus to Memory Impairment in Normal Pressure Hydrocephalus Patients Manifested As Increased Anisotropy and Fiber Density

*Cheng-Yu Chen*¹, Shih-Wei Chiang², Hsiao-Wen Chung², Ping-Huei Tsai¹, Hua-Shan Liu¹, Yi-Hsiu Hsiao³, Chao-Ying Wang⁴, Ming-Chung Chou⁵, Hung-Wen Kao⁶, Fong Y Tsai³
*Taipei Medical University Hospital Department of Medical Imaging Taipei City-Taiwan*¹ *National Taiwan University Graduate Institute of Biomedical Electronics and Bioinformatics -Taiwan*² *Taipei Medical University Imaging Research Center -Taiwan*³ *National Defense Medical Center Department and Graduate Institute of Biology and Anatomy -Taiwan*⁴ *Kaohsiung Medical University Department of Medical Imaging and Radiological Sciences -Taiwan*⁵ *Tri-Service General Hospital Department of Radiology -Taiwan*⁶

PURPOSE: We aim to examine the diffusion tensor parametric behavior of anterior thalamic nucleus in response to memory changes in normal pressure hydrocephalus.

METHOD: 10 NPH patients and 10 normal controls were enrolled in this study. NPH patients were diagnosed according to Japanese guidelines for management of idiopathic NPH. Memory were evaluated on the Chinese version of Wechsler Memory Scale and Rey Complex Figure Test. DTI was performed on a 1.5T using single-shot echo-planar imaging technique with parameters as follows: TR=10000ms; TE=85.3ms; diffusion directions=15; FOV=240; matrix size=128×128. Fiber-tracking was performed based on probabilistic streamlines method to identify the region of AN. Tract density of AN and Tensor parametrics for each subject was calculated by averaging measurements from both hemispheres. **RESULT:** In verbal memory test, NPH patients had average 35% decrease in immediate memory and 44 %



POSTER PRESENTATIONS ABSTRACTS

decrease in delayed memory while non-verbal test means showed less than 5% of normal score. Significant increase in FA, q and fiber density in NPH patients were shown as compared to control. In short, the FA increase seems to be dominated by the increase of q, considering the relative stable of L. The increase of fiber density is twice than that of the control. There was no significant difference of the tensor metrics, including λ_1 , λ_2 , λ_3 , MD, and L, between NPH patients and the control.

CONCLUSION: In conclusion, alternations of diffusion tensor metrics can be measured in thalamic nucleus responsible for memory in NPH patient, which have potential clinical implications for responses monitoring at microstructure level in NPH patients under treatment.

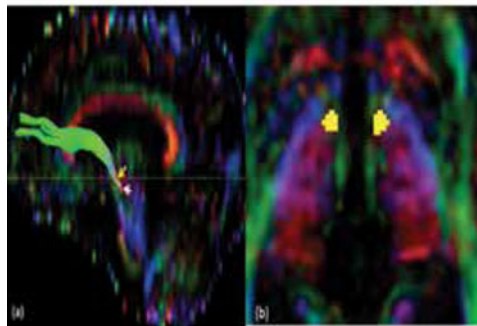


Fig1 (a) Fiber tracking based on probabilistic streamline. White arrow indicates mammillary body and yellow arrow indicates anterior nucleus of thalamus. A horizontal line shows the axial plane in figure 1(b) where the tensor metrics of AN (yellow regions) were calculated.

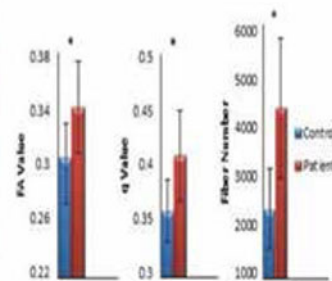


Fig. 2 Significant increase in FA, q value and fiber numbers in AN of NPH patient as compared to the control subjects.

EP012-Brain Gliomas' Peritumoral Normal Appearing White Matter

Evaluation with 3 Tesla MR Spectroscopy

*Italo Aprile*¹, Giulia Belardinelli¹, Marco Muti², Antonio Di Renzo¹, Paola Fiaschini¹, Nicolò Haznedari¹, Nevia Caputo¹

*Neuroradiology Diagnostic Imaging Terni-Italy*¹ *Medical Physics Oncologic Radiotherapy -Italy*²

The gliomas' margins are undefined with morphological T2-weighted magnetic resonance (MR) sequences. In our study peritumoral normal appearing white matter (NAWM) was analyzed with spectroscopy in 55 gliomas. The first goal was to exactly identify tumors' margins. The second goal was to characterize glioblastomas. The third goal was to find out which is the first abnormality detectable with MR in the early stages of gliomas' growth. Fifty-five patients, all with histologically verified brain gliomas were studied (33 glioblastomas, 10 anaplastic gliomas and 12 low grade gliomas). A 3 Tesla equipment was used and, in addition to the morphological study also with Gadolinium, a spectroscopic Chemical Shift sequence with intermediate TE (135 ms) was acquired. By means the normal contralateral white matter the quantitative data were normalized. How many and what types of gliomas NAWM abnormalities, detectable with spectroscopy, were evaluated. Both NAA and Cho were evaluated and we have considered their values as pathological if they were different from the normal ones by at least 15%. Then the average Cho/NAA ratio of peritumoral NAWM was calculated for each of the 3 histological types performing the comparison with statistical methods (t-test).

In 33/55 cases NAWM abnormalities were founded. They were 28/33 glioblastomas and 5/10 anaplastic gliomas. Out of 28 positive glioblastomas in 16 patients NAA reduction was showed while in the other 12 cases also Cho increase was detected. Instead, in all 5 positive anaplastic gliomas only NAA reduction was present, while Cho was always normal. The mean glioblastomas' peritumoral Cho/NAA value was 1.20 whereas that of anaplastic gliomas was 0.76 (statistically significant difference, $p < 0.05$). The mean value of anaplastic gliomas and low grade ones taken together was 0.71 (significant difference with glioblastomas, $p < 0.05$).

Thus we have shown that often in high grade gliomas neoplastic tissue outside the area of signal alteration T2 is present. This finding is common in glioblastomas (84% of cases) and may help to characterize it. Finally,



POSTER PRESENTATIONS ABSTRACTS

we have shown that there may be changes in the white matter, detectable by spectroscopy, before they appear changes in the T2 signal.

So brain gliomas' study with spectroscopy should also be extended to NAWM for the surgery and radiotherapy's planning.

EP013-Symptomatic Pontine Capillary Telangiectasia Which Is Diagnosed by Susceptibility Weighted Imaging

*Murat Asik*¹, Pinar Beyaz¹, Furkan Ertem², Suleyman Dikici¹, Zehra Isik Hasiloglu³

*Istanbul University Cerrahpasa Medical School Department of Radiology Istanbul-Turkey*¹ *Istanbul University Istanbul Medical School -Turkey*² *Istanbul University Cerrahpasa Medical School Division of Neuroradiology, Department of Radiology -Turkey*³

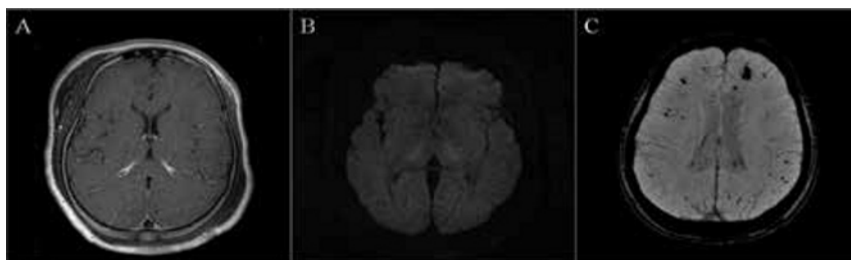
Capillary telangiectasias rarely cause symptoms and are commonly discovered incidentally on neuroimaging. Unlike other vascular malformations which are easily detected in conventional magnetic resonance (MR) imaging or catheter angiograms, capillary telangiectasias cannot be easily recognized. On T1-weighted and T2-weighted MR images capillary telangiectasias are not detectable but they show faintly enhancement on post contrast T1-weighted images. Specific MR imaging sequence is used diagnosis of capillary telangiectasias because capillary telangiectasias are small vascular malformations and do not show characteristic signal on conventional MR imaging. Susceptibility-Weighted Imaging (SWI) is a useful and specific MR imaging sequence for small vascular malformations which show marked signal loss on SWI. We report a case of isolated symptomatic capillary telangiectasia which was diagnosed by SWI.

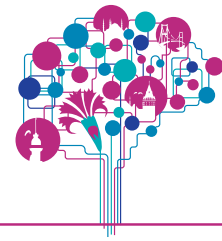
EP014-Innumerable Cerebral Hemorrhages in Influenza Associated Encephalitis a Case Report

Ji-Ye Lee 1, *Su Ok Seong* 1

Myongji Hospital Radiology -Korea, South 1

We describe a rare case of influenza A- and B-associated meningoencephalitis with countless scattered micro- and macrohemorrhagic lesions of both cerebral hemispheres. A 19-year-old type I diabetic lady presented fever and upper respiratory symptoms followed by respiratory distress and disturbance of consciousness. Magnetic Resonance Imaging (MRI) on the 10th day of her illness showed diffuse leptomeningeal enhancement along both cerebral hemispheres (figure A) and restricted diffusion at both thalami on diffusion-weighted image (figure B), suggesting meningoencephalitis and a few hemorrhagic lesions in both frontal subcortical white matter. The influenza A and B virus were found on nasopharyngeal swab and CSF (cerebrospinal fluid) study revealed the findings of viral meningitis. The follow-up MRI in a month of her illness showed innumerable variable sized hemorrhagic foci along both cerebral hemispheres both on T2-weighted gradient-echo images and on susceptibility-weighted images (figure C). There have been a few case reports to describe hemorrhagic lesions associated with influenza, but this is the first report to demonstrate innumerable hemorrhagic lesions of the white matter of both cerebral hemispheres in a patient with influenza encephalitis caused by both influenza A and B.





POSTER PRESENTATIONS ABSTRACTS

EP015-Clinical Applications of Neuroimaging with Susceptibility Weighted Imaging

*Hyunkoo Kang*¹

*Seoul Veterans Hospital Department of Radiology Seoul-Korea, South*¹

PURPOSE: Susceptibility weighted image (SWI) is three-dimensional (3D), spoiled gradient-echo sequence that provide a high sensitivity for the detection of blood degradation products, calcifications, and iron deposits. This pictorial review is aimed at illustrating and discussing its main clinical applications. **METHODS:** After obtaining local ethics committee approval, we retrospectively reviewed the brain MR images of a total of 200 patients underwent MR examinations that included SWI on a 3 tesla (T) MR imager. Among the 200 patients, 80 showed developmental venous anomaly (DVA), 22 showed cavernous malformation, 12 showed calcifications in various pathological conditions, 15 showed susceptibility vessel sign, 52 showed brain tumors, 6 showed microbleeds, 2 showed diffuse axonal injury (DAI), 3 showed arteriovenous malformation (AVM), 5 showed dural arteriovenous fistula (AVF), 1 showed moyamoya disease, and 2 showed parkinson's disease (Table 1).

RESULTS: SWI is very useful in developmental venous anomaly and cavernous malformation, in characterising brain tumors and degenerative diseases of the brain, in detecting cerebral microbleeds and in recognizing calcifications in various pathological conditions. The phase images are especially useful in differentiating between paramagnetic susceptibility effects of blood and diamagnetic effects of calcium. SWI can also be used to evaluate changes in iron content in neurodegenerative disorders and to predict stroke evolution.

CONCLUSION: SWI is useful in differentiating and characterising diverse brain disorders.

Adult NR 2

EP016-The Diagnostic Value of Postcontrast Susceptibility Weighted Imaging in the Assessment of Intracranial Brain Neoplasm at 3T

*Hyunkoo Kang*¹

*Seoul Veterans Hospital Department of Radiology Seoul-Korea, South*¹

PURPOSE: The aim of this study is to estimate the diagnostic value of postcontrast susceptibility-weighted imaging (SWI) in the assessment of intracranial brain neoplasm at 3 tesla (T).

METHODS: Twenty-seven intracranial brain neoplasm patients (11 with meningiomas, 13 with metastases; and three with glioblastomas) were enrolled in this study. They underwent examinations that included SWI and postcontrast SWI in addition to conventional magnetic resonance (MR) sequences on a 3T MR imager. Two radiologists consensually rated the visibility of the tumor margins, the visibility of the internal architecture of the tumors on pre, and postcontrast T1 weighted images (T1WI), and, pre and postcontrast SWIs, and the grade of intratumoral susceptibility signals (ITSS) on SWI and postcontrast SWI.

RESULTS: The postcontrast T1WI and postcontrast SWI were statistically superior to the T1WI and SWI with regard to the visibility of the tumor margins. The pre, and postcontrast SWIs were statistically superior to the T1WI, and the postcontrast SWI was statistically equivalent to the postcontrast T1WI with regard to the visibility of the internal architecture of the tumors ($p < 0.0083$, Wilcoxon signed rank test, pairwise comparison with Bonferroni correction)(Fig. 1)(Table 1). Although the postcontrast SWI was unable to distinguish between glioblastomas and solitary metastatic tumors, differentiation was achieved between glioblastomas and meningiomas, as well as between solitary metastatic tumors and meningiomas ($p < 0.0167$, Kruskal-Wallis test with Dunn procedure) using the ITSS score and the visibility of the internal architecture score.

DISCUSSION: A paramagnetic contrast medium may influence SWI data due to T2 shortening and additional signal loss. However, our results showed that postcontrast SWI clearly visualized the characteristics and the



POSTER PRESENTATION ABSTRACTS

architecture of brain neoplasms with good delineation of the tumor margins. Postcontrast SWI showed both ITSS that was not visible with conventional MR sequences and contrast enhancement that was visible with conventional MR sequences.

CONCLUSION: Postcontrast SWI clearly visualized the internal architecture and tumor margins of brain neoplasms. ITSS and contrast enhancement can be assessed in postcontrast SWI.

Table 1. Statistical analysis of the mean score of the grading of the visibility of tumor margins and the internal architecture of tumors ($p < 0.0083$, Wilcoxon signed rank test, pairwise comparison with Bonferroni correction).

	Visibility of tumor margin		Internal architecture of tumor	
	*p-value		p-value	
T1 vs T1E	0.0000	T1 < T1E	0.0000	T1 < T1E
T1 vs SWI	0.2044	**N/S	0.0000	T1 < SWI
T1 vs SWIE	0.0380	N/S	0.0000	T1 < SWIE
T1E vs SWI	0.0000	T1E < SWI	0.5536	N/S
T1E vs SWIE	0.1305	N/S	0.1554	N/S
SWI vs SWIE	0.0001	SWI < SWIE	0.4076	N/S

Postcontrast T1WI : T1E, Postcontrast SWI : SWIE, *Reference value < 0.0083, **N/S: No statistical difference

The diagnostic value of postcontrast susceptibility-weighted imaging in the assessment of intracranial brain neoplasm at 3T

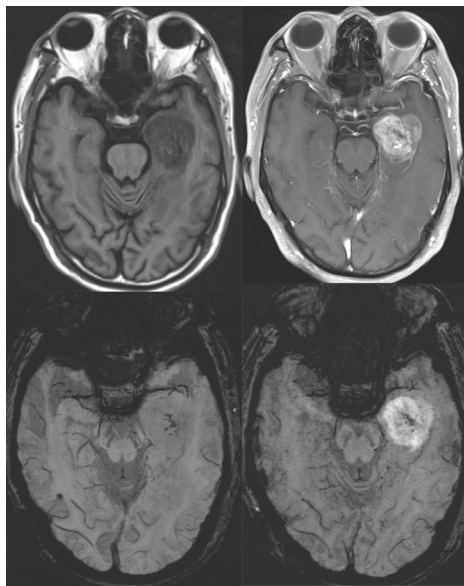


Figure 1: Glioblastoma. A: T1 precontrast. The lesion is barely visible with poor degree tumor margin delineation (arrow). B: Postcontrast T1 shows intratumoral heterogeneity (arrow). Strong enhancement sharply delineates the margins of the lesion (excellent degree). C: SWI precontrast. Grade 2 ITSS indicates 6-10 dot-like or linear low intensity structures (arrow head). D: Postcontrast SWI shows the internal structure and the margins of the lesion more clearly than noncontrast SWI (arrow).



POSTER PRESENTATIONS ABSTRACTS

EP017-Applications of Dual Energy CT in Neuroimaging

*Vrushali Bachhav*¹, Abhijit Patil¹, Mehmet Kocak¹, Sharon Byrd²

*Rush university medical center Neuroradiology CHICAGO-United States*¹ *Rush university and medical center Neuroradiology -United States*²

INTRODUCTION: Dual energy CT is a recent advance in CT technology, which allows for rapid acquisition of datasets at two different energies. Current dual energy CT scanners offer improved temporal resolution which may be helpful in CT angiography and increased photon flux, which may be helpful in imaging obese patients. Dual-energy CT provides information about how materials behave at different energies, provides capability to generate virtual unenhanced datasets and improves detection of iodine-containing substances on low-energy images. This leads to improved tissue characterization and analyses of chemical composition of materials.

APPROACH and METHODS: In this exhibit we will demonstrate the neuroradiologic applications of dual energy CT for various pathologies in the head, neck and spine using demonstrative examples wherever relevant. In addition the physics of dual energy scanners will also be discussed in this exhibit.

DISCUSSION: Neuroradiological applications of Dual energy CT include differentiation of tumor bleeding from pure ICH, differentiation of hemorrhage from contrast staining in patients post vascular intervention, better quantification of carotid stenosis with removal of hard plaques from the vessels, bone removal on head and neck CT angiography and improved characterization of thyroid nodules. In addition metal artifact reduction by dual energy CT using monoenergetic extrapolation may be helpful in patients with spinal instrumentation including CT myelography.

CONCLUSION: Dual energy CT capabilities are promising for improved detection and characterization of lesions in the head, neck and spine and for evaluation of vascular structures. Further research is needed to validate these applications before their use becomes widespread. Reductions in radiation dose are possible if the need for true unenhanced datasets is eliminated and if low tube currents are used, radiation doses delivered in dual-energy CT are similar to those used in single-energy CT.

EP018-Radiological Findings of Oligodendroglial Tumors Retrospective

Analysis of a Single Institution Experience

*Yoshiyasu Hiratsuka*¹, Keiichi Kikuchi¹, Shirou Ooue², Teruhito Mochizuki¹

*Ehime University School of Medicine Department of Radiology Toon-Japan*¹ *Ehime University School of Medicine Department of Neurosurgery -Japan*²

PURPOSE: The tumors with oligodendroglioma component are extended to several pathological types and grades of WHO classification. Pretherapeutic determination of tumor grade is clinically important, but it is still challenging. The purpose of this study was to review the radiological findings of tumors including MRI, CT, and PET, and to assess the image characteristics depending on their malignancy.

MATERIALS and METHODS: Twenty-eight patients (18-75 y.o. mean 48.6 y.o. 15 male and 13 female) with the tumor including oligodendroglioma component were subjected, who have been pathologically proved after surgical resection from March 2009 to December 2013. The types of tumors were: oligodendroglioma and oligoastrocytoma classified as WHO grade II, anaplastic oligodendroglioma and anaplastic oligoastrocytoma as WHO grade III, and glioblastoma with oligodendroglioma component as WHO grade IV. All cases underwent CT and MRI including DWI, FLAIR, SWI and Gd-enhanced T1WI. Furthermore, MR spectroscopy, Perfusion MRI and PET-CT (FDG and methionine) were performed for about two-thirds of patients. We reviewed retrospectively and assessed the characteristics of images.

RESULTS: In 28 cases, 9 cases were grade II, 14 cases were grade III, and 5 cases were grade IV.

Locations of tumors were frontal or lateral lobe in 23 cases, and these tumors were mainly localized on the cortex to subcortical parenchyma. Other locations were brainstem/cerebellum in 3 cases, white matter of the parietal lobe and septum pellucidum in 1 case, respectively.



POSTER PRESENTATIONS ABSTRACTS

The small calcifications were observed in 7 cases on CT, but not shown in the grade IV tumors. In MRI, the low signal area on SWI to indicate bleedings was observed in 7 cases (4 in grade IV and 3 in grade III). Similarly, the necrotic change on Gd-T1WI was shown in 8 cases (4 in grade IV and III, respectively). Neither finding was shown in grade II tumors. On PET examination, FDG uptake of tumors was decreased and methionine uptake was increased generally. The difference between WHO grading and the uptake pattern was not significant. CONCLUSIONS: It is still difficult to distinguish these tumors, but it is suggested to be helpful for the accurate evaluation of tumors by proper combination of the image characteristics obtained from several radiological examinations.

EP019-Title Two Stage Voxel based Parametric Response of the Apparent Diffusion Coefficient for Predicting the Subsequent Tumor Progression Pattern in Patients with Glioblastoma Comparison with Single Stage Measurement

Ra Gyoung Yoon ¹, Ho Sung Kim ¹, *Dae Yoon Kim* ², Seung Chai Jung ¹, Myeong Ju Goh ³, Sang Joon Kim ¹
Asan Medical Center Radiology Seoul-Korea, South 1 Bundang Jesaeng hospital Radiology -Korea, South ² Jeju National University Hospital Radiology ³

PURPOSE: To determine the diagnostic accuracy and reproducibility of the apparent diffusion coefficient (ADC) parametric response (ADCPR) for predicting the subsequent tumor progression pattern, compared with single stage ADC measurement in patients with glioblastoma.

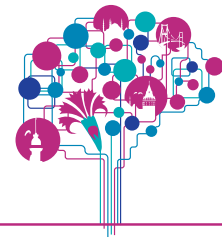
METHODS: Twenty patients with glioblastoma who received concurrent chemoradiotherapy, after which they demonstrated an enlarged, contrast-enhancing lesion during the routine follow-up study performed with three-month interval, were enrolled in this study. ADCPR, a two stage voxel-by-voxel parametric response parameter, was calculated from serial ADC maps acquired before and at the time an enlarged, contrast-enhancing lesion first appeared. Two stage ADCPR and single stage ADC histogram measurements (10 percentile cutoff value of ADC, ADC10) were compared as potential predictors of subsequent tumor progression at three, six, and nine months following the imaging study. The progression-free period was determined using the Cox proportional hazard ratio.

RESULTS: The percentage decrease of ADCPR was significantly higher in the tumor progression group than in the stable group at the three- and six-month follow-up studies, although it did not differ significantly between the two groups at the nine-month follow-up study. There was no significant difference of ADC10 between the two groups seen on the three-, six- and nine-month follow-up studies. The inter-reader agreement was higher for calculating the two stage ADCPR than for the single-stage ADC10 (intraclass correlation coefficient, 0.98 versus 0.81, respectively).

CONCLUSIONS: Two stages ADCPR can be a superior potential imaging biomarker to single stage ADC measurement for determining subsequent three- and six-month tumor progression in patients with glioblastoma.

Table. Differences in the Imaging Parameters between Tumor Progression and Stable Groups.

	Reader 1		ADCPR		Reader 2		ADCPR	
	Progression	Stable	Progression	Stable	Progression	Stable	Progression	Stable
3 Months								
Median	1.02	0.99	26.4	8.2	1.02	0.99	27.1	10.8
P-value	0.4118		0.0138		0.3321		0.0440	
AUC	0.612		0.837		0.633		0.776	
Cutoff	1.00		8.3		1.00		20.4	
6 Months								
Median	1.03	0.99	26.4	5.7	1.02	0.99	27.1	9.3
P-value	0.6698		0.0028		0.5224		0.0157	
AUC	0.556		0.889		0.583		0.815	
Cutoff	1.00		8.3		1.00		20.4	
9 Months								
Median	1.00	1.00	15.9	8.3	0.99	1.00	14.6	10.5
P-value	0.5224		0.0756		0.7762		0.1356	
AUC	0.597		0.766		0.532		0.753	
Cutoff	1.1		3.04		1.0		19.74	



POSTER PRESENTATIONS ABSTRACTS

EP020-Radiological Features of Intracranial Germinoma

*Keiichi Kikuchi*¹, Yoshiyasu Hiratsuka¹, Shiro Ohue², Teruhito Mochizuki¹

*Ehime University School of Medicine Radiology Toon-Japan*¹ *Ehime University School of Medicine Neurosurgery -Japan*²

PURPOSE: We investigate the radiological image spectrum of intracranial pure germinoma and discuss the image characteristics. We will also present the other pathologies which have mimic image findings with germinoma.

METHODS: We recruited 23 pure germinoma patients (15 male, 8 female, aged 7-53 years, mean age 18.9 years) from our patient records. 19 cases had pathologically proven on resected surgical specimen, and 4 cases were diagnosed by clinical and image findings. We reviewed CT and MRI referred to patients records.

RESULTS: Locations were in pineal body: 6, suprasellar: 7, double midline (pineal and suprasellar): 5, basal ganglia: 3, basal ganglia to brain parenchyma: 2. Dissemination to ventricles were evident in 4. Optic nerve involvement was demonstrated in one suprasellar case. Clinical symptoms were diabetes insipidus: 11, headache/nausea: 8, visual disturbances: 5, hemiparesis: 3, general fatigue: 3, memory disturbance: 1, dizziness: 1. CT findings were high density to brain parenchyma in 19. In 2 cases of basal ganglia germinoma demonstrated atrophy in basal ganglia and thalamus. Small calcifications were observed in 8 cases dominantly in peripheral.

In MRI, signal intensities of solid compartment were iso intensity to white matter in T1WI and T2WI both. Cyst formations were observed in 15. In one large brain parenchymal germinoma case, multiple large cyst with mass effect was observed. Contrast enhancement was observed in all cases except 2 basal ganglia cases. Enhancement pattern is relatively strong and homogenous.

DWI was obtained in 16, high intensity to brain parenchyma was observed in 6, iso intensity was in 8. In 2 cases, image quality of DWI was deteriorated due to susceptibility artifact from the skull base.

CONCLUSIONS: Intracranial germinomas arise in or near the midline of the brain between 10 and 25 years old. Diabetes insipidus is the most frequent clinical symptom. Although the pineal and suprasellar lesions are preferred sites, small numbers of intracranial germinomas arise in thalamus, basal ganglia and brain parenchyma. Germinomas are usually high density in CT and isointense with cortex on all MRI sequences. Relatively strong enhancements are found in contrast enhanced MRI.

Cyst formation is also frequent image findings in various sizes.

EP021-Radiographic Features with Pathological Correlation in Cerebral Amyloid Inflammatory Vasculopathy A Case Report

*Maria Pia Pappalardo*¹, Paolo Arculeo¹, A Lo Bello¹, Giuseppe Craparo¹, Simona Arculeo², Paola Marchese², Cesare Gagliardo², Massimo Midiri²

*A.R.N.A.S. Civico- Di Cristina-Benfratelli Neuroradiology and Interventional Unit Palermo-Italy*¹ *Section of Radiological Sciences Department of Medical and Forensic Biopathology and Biotechnologies University of Palermo -Italy*²

We present the case of a 62-year-old woman, with normal blood pressure, presented at time of admission in April 2012, with mild cognitive impairment, motor aphasia, mental confusion and language disorders. At CT, the patient was found to have supratentorial hypodense cortical-subcortical lesion in the left temporo-occipital region (Fig.1). MR study (1.5T scanner) with acquisition of scans in the axial, sagittal, and coronal projections, Spin-Echo (SE) sequences with T1 and T2 weighted images, showed cerebral swollen WM lesions, with heterogeneous high signal intensity on the T2-weighted and FLAIR sequences (Fig.2-3), hypointense signal on T1 weighted sequences, without restriction in DWI/ADC, disposed in the bilateral occipital and left temporal regions, with an extension to the gray/WM interface (corticomedullary junction). They had low perfusion, and after the administration of contrast material, we did not observe contrast enhancement, which meant that the blood-brain barrier had remained intact. No suggestion for hemorrhagic lesions was present in



POSTER PRESENTATIONS ABSTRACTS

SE T1 or T2 weighted images. Follow-up CT and MRI investigations 10 months later, showed increase in size of described WM alterations on the FLAIR and coronal T2-weighted sequences (Fig.4-5) and only Gradient Echo (GE) images demonstrated multiple, scattered microhemorrhages (<5mm), with cortical-subcortical lobar distribution, due to haemosiderin deposits and compatible with the diagnosis of CAA (Fig.6). CT and MRI images showed characteristic patterns of CAA, where cortico-subcortical microhemorrhages may be associated with inflammatory alterations. The

microhemorrhages are typically cortical or subcortical, with sparing of the basal ganglia that are, preferentially involved in hypertensive hemorrhages of arteriosclerotic patients [1]. The MRI findings described of T2-hyperintense WM lesions, pathogenetically linked to a disorder often characterized by and cortical-subcortical microbleeds, may be sufficient for the diagnosis of CAA-ri [1].

EP022-Epstein Barr Virus associated Primary Central Nervous System Lymphomas in Immunocompetent Patients Showed Characteristic MR images Mimicking Glioblastoma 4 Cases Reports and Review of The Literature.

*Yusuke Uchiyama*¹, Ayako Yoshida¹, Norimitsu Tanaka¹, Yasuo Sugita², Kiyohiko Sakata³, Toshi Abe¹
*Kurume University School of Medicine Radiology Kurume-Japan*¹ *Kurume University School of Medicine Pathology -Japan*² *Kurume University School of Medicine Neurosurgery -Japan*³

PURPOSE: Epstein-Barr virus (EBV) is associated with several malignant diseases. EBV has been implicated in the pathogenesis of primary central nervous system (PCNS) lymphomas in immunocompetent hosts. Simultaneously, it is known that EBV-positive PCNS lymphomas indicated poor prognosis, compared to EBV-negative PCNS lymphomas. To report four cases of EBV-positive PCNS lymphomas that showed characteristic findings on MR images.

METHODS: From November 2007 to November 2009, we identified patients with isolated EBV positive PCNS lymphoma through a search of the histopathology database in our institute and affiliated hospitals; medical and radiological data were analyzed. Immunophenotype, in situ hybridization analysis of EBV-encoded small nuclear early region (EBER) and immunoglobulin rearrangement studies were performed on the pathological specimens.

RESULTS: Four patients with EBV-positive CNS lymphomas who ranged in age from 56 to 80 years old (mean: 71.7 years, male:female=3:1) underwent surgery in the study period. All patients examined for human immunodeficiency virus (HIV) were serologically negative, and analysis of their life style provided no clinical evidence of HIV infection. Two cases of tumor sites were cerebral hemispheres, and others were cerebellar hemispheres. All cases formed relatively large mass formations with marked perifocal edema, and showed strong and irregular enhancement mimicking glioblastomas by contrast-enhanced MR studies. In addition, all histological features of tumors showed extensive necrosis correspond to poor enhanced areas on MR images.

CONCLUSIONS: These cases and review of literature indicated it might be EBV-positive PCNS lymphomas resembling glioblastomas in appearance on MR findings, and might be usefulness for strategy of the therapy.

EP023-Doubt on the Association between Transient Global Amnesia and Intracranial Venous Reflux Based on the Time of Flight MR Angiography

*Eunhee Kim*¹, Dong Hoon Lee², Hyung Suk Seo³
*Seoul National University Bundang Hospital Radiology Seongnam-si, Gyeonggi-do-Korea, South*¹ *Seoul Medical Center Radiology -Korea, South*² *Korea University Ansan Hospital Radiology -Korea, South*³

PURPOSE: There has been debated on an association between transient global amnesia (TGA) and jugular venous reflux (JVR). Intracranial JVR can be assessed by intracranial time of flight (TOF) MR angiography (MRA), and is known to be influenced by intrathoracic pressure. Intrathoracic pressures of subjects might



POSTER PRESENTATIONS ABSTRACTS

be altered under certain circumstances, so both emergency room (ER)-visitors and health promotion center (HPC)-visitors were selected as controls to compare with prevalence of JVR in TGA-patients.

METHODS: 167 patients with TGA, and 167 age- and sex-matched ER visitors and HPC visitors were enrolled, respectively. All had performed brain MRI and MRA using a 3T MR system. Intracranial JVR was defined as abnormal venous signals in the inferior petrosal, sigmoid, and/or transverse sinuses on intracranial TOF MRA. Presence and sidedness (left or right) of intracranial JVR was assessed in TGA-patients, ER-visitors, and HPC-visitors.

RESULTS: The mean age of the 167 patients with TGA was 61 ± 8.8 years (range 33–83 years), and female were 108 (64.7%). Intracranial JVR on intracranial TOF MRA was seen 7(4.2%) patients with TGA, 8(4.8%) in ER-visitors and 3(1.8%) in HPC-visitors, respectively. There were no statistical significances in prevalence and sidedness of JVR among three groups ($p=0.298$ and $p= 0.632$, respectively).

CONCLUSION: TGA patients showed a low prevalence of JVR on intracranial TOF MRA, and no statistical difference was found in comparing with that of control groups. This study threw a question to a hypothesis that intracranial venous congestion due to jugular venous reflux is highly associated with pathophysiology of TGA. Figure: A 72-years-old female with TGA. High resolution diffusion-weighted image with $b=2000$ shows a small high signal lesion (arrow) at the right hippocampal head, suggesting TGA lesion (A). Abnormal venous signal in the inferior petrosal sinus (arrow head) due to JVR is seen on the intracranial TOF MRA (B).

Figure A

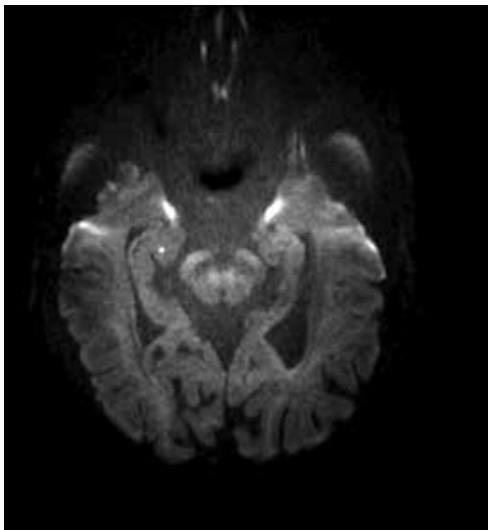
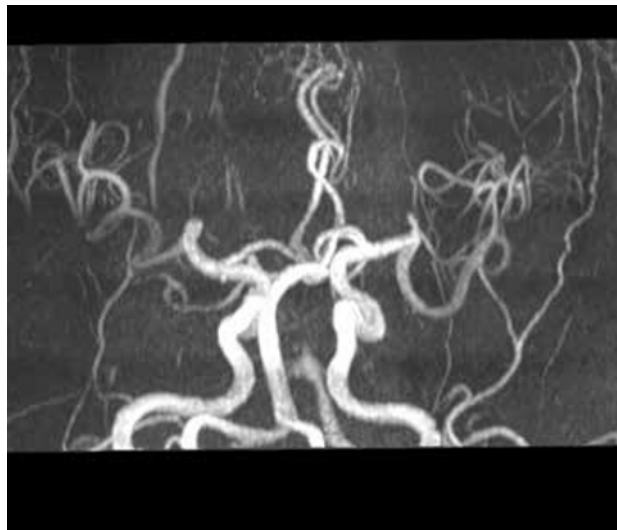


Figure B



EP024-Attenuation and Heterogeneity of Cerebral Gliomas on Unenhanced CT A Relationship with Tumor Grade Indicates Bioamrker Potential

*Karoline Skogen*¹, Balaji Ganeshan², Kenneth Miles², Johan Baptist Dormagen¹, Anselm Schulz¹, Eirik Helseth³, Andres Alonso¹

*Oslo University Hospital Radiology Oslo-Norway*¹ *University College London Nuclear medicine -United Kingdom*² *Oslo University Hospital Neurosurgery -Norway*³

PURPOSE: Tumor necrosis and collagen are recognized histological features of high grade glioma that may relate to disease progression. As these tissue features are associated with lower and higher attenuation values on unenhanced CT respectively, we hypothesised that high-grade (HGG) and low-grade (LGG) gliomas would exhibit differences in tumor attenuation and heterogeneity on non-contrast CT.

METHODS: The study comprised CT images from 72 and 16 patients with histologically confirmed HGG and

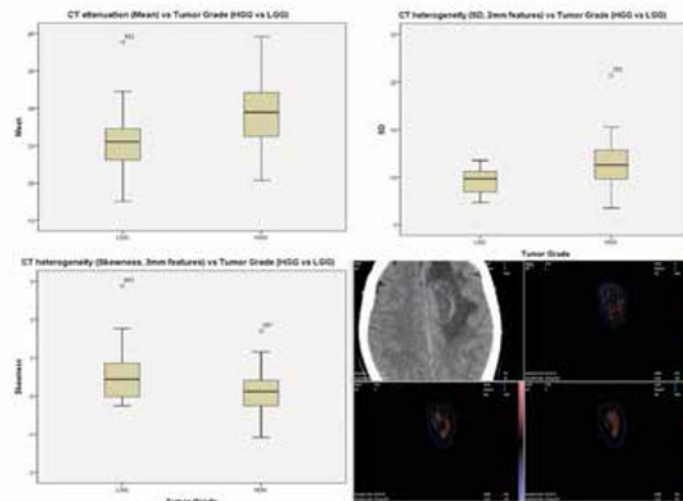


POSTER PRESENTATIONS ABSTRACTS

LGG respectively, imaged prior to surgical intervention (resection or biopsy). Mean attenuation values were obtained from each tumor. The heterogeneity of CT attenuation values was assessed using histogram analysis before and after Laplacian of Gaussian (LoG) filtration which highlighted image features of a specified size between 2mm and 6mm radius. Histogram characteristics comprised standard deviation (SD) reflecting the frequency and attenuation differences of image features highlighted by filtration, and skewness indicating the relative preponderance of bright or dark image features highlighted.

RESULTS: HGG exhibited higher mean attenuation values (29.46 vs 25.52, $p=0.005$). HGG were also more heterogeneous especially for image features of 2mm radius as shown by SD (11.28 vs 9.84, $p=0.005$). LoG filtration highlighted darker features in HGG as shown by lower skewness e.g. for image features of 3mm radius (0.12 vs 0.44, $p=0.018$).

CONCLUSION: The differences in attenuation and heterogeneity are consistent with greater levels of collagen and necrosis in HGG. Given the prognostic significance of these tissue features, and their prospects as therapeutic targets, attenuation and heterogeneity measures on unenhanced CT have the potential to act as biomarkers for patients with glioma.



EP025-CD8 Encephalopathy in HIV: A Case Report with Clinical CSF and MRI and Histological Findings

*Sally Candy*¹, Kathleen Bateman², Shikar Mothila²

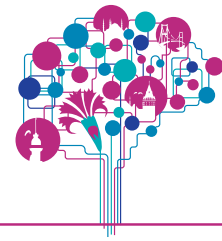
Groote Schuur Hospital Radiology Cape Town-South Africa 1 Groote Schuur Hospital Neurology -²

PURPOSE: To describe the clinical, imaging and histological characteristics of CD8 encephalopathy in an HIV positive patient.

METHODS: 45 year old female with CD4 of 167 who had defaulted ARVs 3 months prior, presented with a 2 week history of headache and confusion. On examination she had profound psychomotor retardation and perseveration but no focal deficit or cranial nerve abnormality with a MMSE score of 21/30 and MOCA of 12.

FINDINGS: CT head showed bilateral nonenhancing diffuse periventricular, right temporal and posterior fossa white matter low density. MRI confirmed a similar distribution of FLAIR

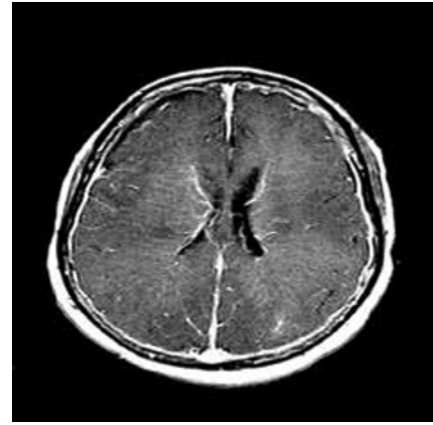
hyperintensity and low signal on T1WI. Post Gadolinium there was streaky perivenular enhancement parallel to the ventricular surface, diffuse dural enhancement and a small right frontal low signal subdural collection. Blood CD8 count was 2286 with CD4:8 ratio of 0.14:1. CSF culture was negative for JC,EB,HS virus, cryptococcus and TB. CSF protein was initially 0.81 rising to 1.92 with normal glucose, <10 lymphocytes and no



POSTER PRESENTATIONS ABSTRACTS

polymorphonuclear cells. Brain biopsy revealed diffuse perivascular infiltration by CD8 lymphocytes with absence of multinucleated giant cells and no demyelination. The patient has had a minimal response to high dose steroids.

CONCLUSION: Leucoencephalopathy is common in both PML and HIV encephalopathy but has been only recently attributed to CD8 encephalopathy. This case report serves to raise awareness of this devastating but potentially treatable cause for acute onset encephalopathy in HIV positive patients.



EP026-Central Nervous System Involvement by Multiple Myeloma a Pictorial Essay

*Arian Lasocki*¹, Shane Gangatharan², Francesco Gaillard³, Simon Harrison²

Peter MacCallum Cancer Centre Cancer Imaging East Melbourne-Australia ¹ *Peter MacCallum Cancer Centre Haematology & Medical Oncology -Australia* ² *The Royal Melbourne Hospital Radiology -Australia* ³

PURPOSE: To illustrate the various imaging manifestations of central nervous system involvement by multiple myeloma.

METHODS: Patients with evidence of central nervous system (CNS) involvement by multiple myeloma were identified at The Peter MacCallum Cancer Centre and The Royal Melbourne Hospital based on a diagnosis of meningeal myelomatosis (defined as the presence of plasma cells in the cerebrospinal fluid) and/or neuroimaging consistent with the diagnosis. Imaging was reviewed by a consultant Radiologist at each site.

FINDINGS: The most common manifestation of CNS involvement described is osseous plasmacytomas of the skull or vertebrae with secondary dural involvement. Leptomeningeal myelomatosis can also occur, while parenchymal infiltration is rare. Imaging may also reveal additional extramedullary plasmacytomas, for example within the subcutaneous soft tissues of the scalp or to the orbit. Imaging of each of these manifestations is presented, with clinical correlation.

CONCLUSIONS: CNS involvement is a very rare manifestation of multiple myeloma with a dismal prognosis. In recent times, the overall survival of patients with multiple myeloma has significantly improved due to novel therapies. CNS involvement is occurring later in the course of disease, but its incidence appears to be increasing, possibly related to these novel therapies altering the natural history of disease through changes in the tumour microenvironment. It has a wide spectrum of imaging appearance and can mimic other conditions.

EP027-Distinguishing Clinico Radiological Features in Patients with, Central Nervous System Tumefactive White Matter Lesions

Xuling Lin¹, Kevin Tan¹, Lishya Liauw², Aung Soe Tin³, Weiling E Soon⁴, Yin Shih Zhu Yiin², Boon-Ping Toe², Hwei-Yee Lee⁵, *Wai-Yung Yu*²

National Neuroscience Institute Neurology -Singapore ¹ *National Neuroscience Institute Neuroradiology -Singapore* ² *Eastern Health Alliance Health Services Research -Singapore* ³ *National University of Singapore Yong Loo Lin School of Medicine -Singapore* ⁴ *Tan Tock Seng Hospital Pathology -Singapore* ⁵

PURPOSE: Currently, there is limited data to guide clinicians in differentiating DD from CNS tumours. The purpose of this study is to determine the clinical and radiological features that differentiates demyelinating diseases (DD) from lymphoma and gliomas, in patients with central



POSTER PRESENTATIONS ABSTRACTS

nervous system (CNS) tumefactive white matter lesions (WML).

METHODS: We retrospectively reviewed all patients with tumefactive lesions and histologically-proven or clinically-diagnosed DD, CNS lymphoma or glioma at our tertiary centre from 1999 to 2012. We recorded demographic, clinical, laboratory and radiological data. Two neuroradiologists blinded to the final diagnoses rated MRI scans at presentation. We analysed results using logistic regression.

RESULTS: 141 patients were analysed: DD (14), glioma (84) and lymphoma (43). Patients with DD were younger and more often female (mean age 43.9 years; female 78.6%), compared with glioma (49; 39.3%) and lymphoma (58.8; 37.2%).

DD were more commonly associated with positive anti-nuclear antibody, rheumatoid factor and cerebrospinal fluid (CSF) oligoclonal bands (45.5%; 33.3%; 20.0%) compared to glioma (10.0%; 0.0%; 0.0%) and lymphoma (20.0%; 0.0%; 0.0%). Presenting symptoms did not distinguish between diagnoses.

WML were smaller in DD compared to glioma and lymphoma (46.7mm vs 66.9mm vs 70.5mm). WML were more often periventricular in DD (78.6%) and lymphoma (86.0%) compared to glioma (36.9%); and discrete in DD (42.9%) compared to lymphoma (18.6%) and glioma (17.9%). More DD WML had no peripheral rim enhancement (72.9%) compared to glioma (32.9%) and lymphoma (9.3%); when present, rim enhancement was more often incomplete (DD 75.0%; glioma 30.9%; lymphoma 20.5%). Moderate-severe mass effect was seen in glioma (53.5%) and lymphoma (52.6%) but not DD (0.0%).

CONCLUSIONS: Tumefactive DD WML tend to be smaller, discrete, periventricular with less peripheral rim enhancement and mass effect. Laboratory tests but not presenting symptoms may also aid in distinguishing DD from CNS tumours.

Identifying distinguishing clinical and radiological features will guide management and avoid invasive biopsy.

EP028-”D.M.T.E.S” Useful Categorization of Variable Diseases Involving Splenium of the Corpus Callosum

*In Kyu Yu*¹, Youn Joo Lee¹, Chang June Song², Jin Young Kim¹

*Eulji University Hospital Radiology Daejeon-Korea, South*¹ *Chungnam National University Hospital Radiology -Korea, South*²

PURPOSE: Splenium of the corpus callosum (SCC) is one of the most common area of various diseases involved. If, systematic categorization of various diseases of SCC is established, differential diagnosis will be more easier. Our aim of this exhibit is to suggest useful categorization of SCC diseases and to show various imaging features of that lesions, frequently encountered in practice.

CONTENT ORGANIZATION: We will present many cases of patients with SCC lesions shown on MRI (including conventional MR sequences and DWI), clinically or pathologically confirmed. And we categorized these heterogeneous SCC lesions into 5 groups according to the first letter of their

causes, so called “D.M.T.E.S.”: D - Drugs (antiepileptics, antiemetics), Demyelinating disease (multiple sclerosis), M - Metabolic etiology (vitamin B12 deficiency, hypo & hypernatremia, hypoglycemia), T - Toxic, Trauma (diffuse axonal injury), E - Encephalopathy or Encephalitis (MERS, ADEM, PRES), and S - Seizure, Stroke.

SUMMARY: It may be very useful for summarizing, differential diagnosis in heterogeneous diseases, involving the SCC in actual clinical practice, to use categorization called “D.M.T.E.S.”



POSTER PRESENTATIONS ABSTRACTS

EP029-Intracerebral Hemorrhagic Mass Manifesting As Initially Spontaneous Hemorrhage

*In kyu Yu*¹, Youn Joo Lee¹, Chang June Song², Seung Hwan Baek¹

*Eulji University Hospital Radiology Daejeon-Korea, South*¹ *Chungnam National University Hospital Radiology -Korea, South*²

PURPOSE: Intracerebral mass occasionally manifest as intracerebral hemorrhage, which must be differentiated from spontaneous intracerebral hemorrhage caused by common cause such as hypertensive cerebrovascular disease, and vascular malformation. The aim of this exhibit is to present various brain masses, initially manifesting as acute intracerebral hemorrhage and suggesting differentiating clue in hemorrhagic mass.

CONTENT ORGANIZATION: We retrospectively reviewed clinical findings, and CT, MR images in the patients with acute intracerebral hemorrhage. Among them, we selected pathologically confirmed brain masses with hemorrhage and classified them according to the location, intra-axial and extra-axial lesions. The intra-axial lesions include glioblastoma multiforme, Primitive neuroectodermal tumor(PNET), pleomorphic xanthoastrocytoma(PXA), Pilocytic astrocytoma, Hemangioblastoma, Cavernous malformation, and hemorrhagic metastasis(lung cancer, melanoma, choriocarcinoma, RCC). The extra-axial lesions include acoustic schwannoma, hemangiopericytoma, and meningioma. We will also present the differentiated imaging clues between the hemorrhagic mass and pure ICH.

CONCLUSION: There are many causes in spontaneous intracerebral hemorrhage, but hemorrhage from intracerebral masses are rare. Tumor bleeding has distinguishing imaging features from other pure ICH on CT & MR images. For this reason, It is important to interpret acute intracerebral hemorrhage, whether or not underlying hemorrhagic mass.

EP030-Various high DWI SI Lesions Mimicking Acute Cerebral Infarction (ACI)

*In Kyu Yu*¹, Youn Joo Lee¹, Hee Kyung Kim¹

*Eulji University Hospital Radiology Daejeon-Korea, South*¹

PURPOSE: To present spectrum of various disease causing high SI on DWI, mimicking ACI and explain differentiating image clues from ACI.

CONTENT ORGANIZATION: We will present high DWI SI lesions mimicking acute cerebral infarction (ACI) into six categories; hemorrhage (subacute hemorrhage, chronic hemorrhage, cortical laminar necrosis, DAI), Acute encephalitis (HSE, Japanese encephalitis, Enteroviral meningoencephalitis, AIDS ecephalopathy, Creutzfeldt-Jakob disease), Acute demyelinating disease or vasculitis(acute multiple sclerosis Vasculitis with anti-phospholipid antibody syndrome), acute metabolic or toxic encephalopathy (Hypoglycemic, Hyperglycemic encephalopathy, Acute, delayed CO intoxication, Hypoxic-ischemic encephalopathy, Acute ODMS, Wernicke encephalopathy, Uremic encephalopathy Toxic encephalopathy), benign or malign mass lesion (Abscess, epidermoid cyst, malign. tumor) and others (acute Wallerian degeneration, seizure related hemispheric change).

CONCLUSION: There are many high DWI lesions mimicking ACI, including subacute or chronic hemorrhage, acute encephalitis, demyelinating ds., metabolic or toxic encephalopathy, mass lesions and others. It is practically useful in differential diagnosis for high DWI lesions, mimicking ACI, using categories of the high DWI lesions.



POSTER PRESENTATIONS ABSTRACTS

Adult NR 3

EP031-Levothyroxine as Potential Cause of Osmotic Demyelination Syndrome

*Gordana Milenkovic*¹, Biljana Georgievski-Brkic², Aleksandra Terzic-Beljakovic¹, Ljubinko Milenkovic³, Marjana Vukicevic⁴

*Stroke hospital Sveti Sava Radiology Belgrade-Serbia*¹ *Stroke hospital Sveti Sava Radiology -Serbia*² *Policlinic IN MEDIC Ultrasonography -Serbia*³ *Stroke hospital Sveti Sava Neurology -Serbia*⁴

INTRODUCTION: Osmotic demyelination syndrome, formerly called “central pontine myelinolysis” and/or “extrapontine myelinolysis” belongs to the group of metabolic brain diseases. Essentially, there is an acute demyelination caused by rapid shifts in serum osmolality. Etiology: heterogeneous disorders with osmotic stress, most common due to iatrogenic correction of hyponatremia, less there is osmotic derangement with azotemia, hyperglycemia, hypokalemia, ketoacidosis.

PURPOSE: Proving that Magnetic Resonance Imaging (MRI) is highly sensitive method for the diagnosis of osmotic demyelination syndrome.

METHODS: MRI were done on GE machine, type SIGNA, 1,5 T, using T1W/SE, T2W/frFSE, T2/FLAIR, T2*GE and 3D TOF sequences, with DWI and ADC map and postcontrast MT/T1 in axial plane. We also have done MR spectroscopy at the control MRI.

CASE REPORT: A 43-years old woman has a history of thyrotoxicosis and daily thyrosuppressive therapy. Somehow, she made a mistake and instead of this drug, she bought levothyroxine in a pharmacy.

After a short time she began to feel bad, and nine days before hospitalization suddenly emerged global aphasia. She was transported in our hospital from another institution. In emergency department neurologist found that baseline vital signs were normal. Neurological status: Right central facial paresis and global aphasia. Mental status: Valid. Blood laboratories findings: normal, except reduced ultrasensitive TSH and elevated fT4.

RESULTS: MRI findings: For the most part of pons, central bilaterally, we have find symmetric, confluent T2/FLAIR hyperintensity, mildly hyperintense on DWI, with no postcontrast enhancement. We suspected central pontine myelinolysis and demanded MRI with MR spectroscopy after three months, with adequate therapy of hyperthyroidism (Thyrosol) in the meantime. Then, we found the regression of MRI findings, hyperintensity in pons is lower than initially. MR spectroscopy indicated that overall biochemical profile corresponds with chronic demyelization.

With thyrosuppressive therapy, there has been a significant improvement in speech, with residual mild motor dysphasia.

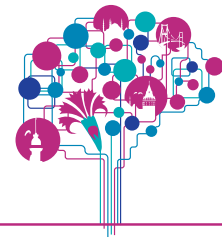
CONCLUSION: We present the patient with MRI findings of osmotic demyelination syndrome, which is most likely caused by iatrogenic hyperthyroidism.

EP032-Correlation between Magnetic Resonance Angiography and Transcranial Doppler Sonography

*Gordana Milenkovic*¹, Biljana Georgievski-Brkic¹, Veljko Maksic¹, Ljubinko Milenkovic², Tatjana Ducic-Jaramaz³

*Stroke hospital Sveti Sava Radiology Belgrade-Serbia*¹ *Policlinic IN MEDIC Ultrasonography -Serbia*² *Stroke hospital Sveti Sava Neurology -Serbia*³

INTRODUCTION: Magnetic Resonance Angiography (MRA) and Transcranial Doppler Sonography (TCD) are noninvasive methods for evaluation blood vessels of the Circle of Willis, which are of great importance for the diagnosis of cerebrovascular diseases. Special Hospital Sveti Sava in Belgrade specializes for modern methods of the diagnosis and treatment of these diseases. Because of that, MR angiography is a mandatory part of standard Magnetic Resonance Imaging protocol for the brain examination. Also, each patient in our hospital is examined by TCD.



POSTER PRESENTATIONS ABSTRACTS

PURPOSE: Both methods, MRA and TCD, have advantages and disadvantages. With correlation, we increase the reliability and validity of examinations.

METHODS: In order to determinate the degree of correlation between MRI and TCD we have performed small series of 50 patients with atherosclerotic changes on blood vessels of the brain. This pathological changes were diagnosed by MRA, which is done on GE machine, type Sygna, 1,5T, using 3D TOF sequence. After that, each patient has done TCD, on one of three machines: DWL-HP LE; RIMED and SPENSER. 23 patients (46%) were male and 27 (54%) female. The average age was 51,7 years (27.y.-79.y.).

RESULTS: In 27 patients (54%) MRA showed atherosclerotic changes (significant stenosis, subocclusion, occlusion) of the anterior segment of the Circle of Willis (ICA, MCA), and 23 patients (46%) have changes of the posterior segment (VAA, BA, PCA). 29 patients (58%) had an acute or subacute ischemia of the brain. Analysis of the obtained data showed that correlation in group with atherosclerotic changes at blood vessels of anterior segment Circle of Willis is 77,77% and 69,56% in patients with changes of posterior segment.

CONCLUSION: We found that correlation between MRA and TCD is 73,66%, so we can say that MRA and TCD are complementary methods for reliable evaluation of blood vessels of the brain, with high degree of correlation.

EP033-Neuroimaging in Posterior Reversible Encephalopathy Syndrome

*Adriana Ojeda*¹, Paola Acevedo⁴, Maria Belen Nallino⁴, Ana Maria Uriarte⁴
*Fundacion J.R. Villavicencio Neuroradiology ROSARIO-Argentina*¹

PURPOSE: Posterior reversible encephalopathy syndrome (PRES) is a clinical and radiological syndrome caused by various heterogeneous medical conditions: hypertensive encephalopathy, citotoxic and immunosuppressive therapy and autoinmunes diseases. Our aim is to report our experience in ten patients with PRES and to highlight the value of MRI findings in the diagnosis and prognosis of this disease.

MATERIAL AND METHODS: From January 2009 until December 2013, 10 patients with diagnosis of PRES have undergone high-field MRI exams in our service. Clinical and imaging findings were retrospectively analysed.

RESULTS: 8 patients were women and 2 were males with a mean age of 30 years.

Characteristic imaging findings in all of them included vasogenic edema. Three of them had citotoxic edema lesions in MR diffusion weighted imaging sequence (DWI). Both posterior and anterior circulation territories were involved in 80 % of patients with predilection for posterior areas. 20 % showed only posterior compromise. Regarding the causes, 5 patients had neurotoxicity, two

hypertensive encephalopathy, one postpartum angiopathy and two a combination of risk factors such as autoinmune diseases, hypertension and infections.

CONCLUSION: PRES is an increasingly recognized clinicoradiological syndrome associated with multiple clinical and toxic disorders. As neuroradiological findings are often characteristic, they may be the first clue to diagnosis. The prompt recognition of MRI findings has important therapeutic and prognostic implications because the reversibility of the clinical and radiological abnormalities is contingent on early treatment. MRI diffusion weighted sequences provides not only a powerful means for PRES diagnosis but also a wealth of prognostic information for the patient.



POSTER PRESENTATIONS ABSTRACTS

EP034-Comparison of Cerebral Blood Flow on Perfusion MRI by Using Arterial Spin Labeling and Dynamic Susceptibility Contrast in Brain Tumors

*Arisa Ohara*¹, Kazuhiro Tsuchiya², Miho Gomyo¹, Hidekatsu Tateishi¹, Toshiaki Nitatori¹
*Kyorin university faculty of medicine Department of Radiology Mitaka-Japan*¹ *Tokyo Teishin Hospital Department of Radiology -Japan*²

PURPOSE: Arterial spin labeling (ASL) is a technique that can visualize cerebral blood flow (CBF) by electromagnetically labeling the arterial flow. To clarify the difference between ASL and dynamic susceptibility contrast (DSC) perfusion imaging that is an established technique in the diagnosis of brain tumors, we carried out a comparative study of the two methods.

METHODS: In 28 preoperative cases, we visually compared perfusion maps and divided them into three patterns as follows: (1) ASL was greater than DSC, (2) both were almost equal, and (3) ASL was less than DSC. Then we drew a region of interest (ROI) in three areas with signal increase within tumor in ASL and DSC. We calculated their mean value respectively. Another ROI was placed in one area in the contralateral reference brain on ASL and DSC. A mean value of an ROI of tumor divided by that of ROI of contralateral reference brain was defined as an "ASL and DSC ratio". Their lesions

of the study group included glioblastoma with oligodendroglioma component (7 cases), glioblastoma (5 cases), meningioma (3 cases), lymphoma (3 cases), metastasis (2 cases), oligodendroglioma (2 cases), and others (6 cases).

RESULTS: In 21 of the 28 cases, CBF by the two methods were equivalent. In 5 cases, CBF by ASL was less than that of by DSC, while the former was greater in the remaining 2 cases. In lesions with intense or moderate enhancement on postcontrast T1WI, the mean value of ASL was almost equal to or greater than DSC. In cases whose mean value of ASL was smaller than that of DSC, lesions showed moderate, poor, or no enhancement on postcontrast T1WI.

CONCLUSION: As cases showing less CBF on ASL than on DSC tended to show minor contrast enhancement, ASL seems to be less sensitive than DSC in cases of tumor with a mild degree of blood-brain-barrier disruption.

EP035-Intracranial Plaque Imaging by High resolution 2D Imaging at 3T

*Miho Gomyo*¹, Kazuhiro Tsuchiya², Arisa Ohara¹, Hidekatsu Tateishi¹, Isao Miyazaki³, Toshiaki Nitatori⁴

*Kyorin University Faculty of Medicine Department of Radiology Mitaka-Japan*¹ *Tokyo Teishin Hospital Department of Radiology -Japan*² *Kyorin University Hospital Section of Radilology -Japan*³ *Kyorin University Faculty of Medicine Department of Radilology -Japan*⁴

PURPOSE: Lacunar infarcts are often caused by stenosis of the parent artery due to atheromatous plaque formation. Branch atheromatous disease (BAD) is another important cause of lacunar infarcts caused by a plaque that encroaches on the orifice of the perforating artery. Recent studies have reported that high-resolution MR imaging can be used to assess the morphology of intracranial artery vessels. The purpose of this study was to assess the value of intracranial plaque imaging by high-resolution 2D imaging at 3T in identifying the causative lesion of lacunar infarcts developed in the territory of perforating arteries of the middle cerebral artery (MCA).

MATERIALS AND METHODS: Our study group comprised 6 patients (age range: 68-78 years; 3 males and 3 females) with M1 stenosis or clinically diagnosed BAD who underwent MR imaging during a 6-month period. They included 1 patient after embolic M1 occlusion followed by revascularization, 2 patients with BAD and 3 with M1 stenosis or obstruction. Intracranial plaque imaging was performed on a 3T MR scanner (Vantage Titan 3T; Toshiba Medical Systems) in a plane perpendicular to the long axis of M1 using a fast dual spin-echo sequence employing following parameters: repetition time, 3000 ms; echo times, 18/90 ms; pixel size, 0.4x0.4 mm; slice thickness, 2 mm, field of view, 10 cm; and number of excitations, 1.



POSTER PRESENTATIONS ABSTRACTS

RESULTS: In the patient after M1 revascularization, an isointense nodular lesion was found occupying the M1 lumen and was considered to be a chronic clot. Two patients with BAD showed a crescent-shaped plaque that showed isointensity. In the remaining 3 patients, thickening of the M1 wall were depicted as a ring-shaped abnormal signal.

CONCLUSION: Our plaque imaging by high-resolution 2D imaging enables detailed evaluation of the state of vascular lumen responsible for lacunar infarcts in the MCA territory.

EP036-Bilateral Thalamic Lesions a Pictorial Review

Anil Ozgür¹, Kaan Esen¹, Hakan Kalegasi², Arda Yilmaz², Engin Kara¹, Altan Yildiz¹

Mersin University Department of Radiology Mersin-Turkey¹ Mersin University Department of Neurology -Turkey²

PURPOSE: The purpose of this exhibit is to discuss imaging features of bilateral thalamic lesions and diagnostic approach.

METHODS: We reviewed the pathologies which involve bilateral thalamus and classified them as primum neoplasm, metabolic and toxic disorders, demyelinating disorders, infection and vascular occlusion.

RESULTS: We will present pathologies including bilateral thalamic glioma, Wernicke encephalopathy, osmotic myelinolysis, Fahr disease, Wilson disease, Leigh disease, multiple sclerosis, acute demyelinating encephalomyelitis (ADEM), Cruetzfeldt-Jacob disease, infarct of Percheron artery, deep venous thrombosis and hypotensive cerebral infarct.

CONCLUSIONS: Bithalamic lesions have a limited differential diagnosis. Clinical history and associated neuroimaging findings are relatively helpful in guiding appropriate diagnosis in the presence of bilateral thalamic lesions.

EP037-Immunotherapy Related Neurological Complications Ipilimumab induced Hypophysitis Pachymeningitis and Other Immune related Neurological Complications

Judith Gadde¹, Alberto Iaia¹

Christiana Care Health System Diagnostic Radiology Newark-United States¹

PURPOSE: 1. To review the human monoclonal antibody ipilimumab, its mechanism of action and its clinical use in patients with metastatic melanoma.

2. To review rare immune-related neurological complications associated with the use of ipilimumab, discuss their clinical presentation, treatment and patient prognosis.

3. To illustrate the MR imaging features of immune-related neurological complications of ipilimumab, with emphasis on hypophysitis and pachymeningitis.

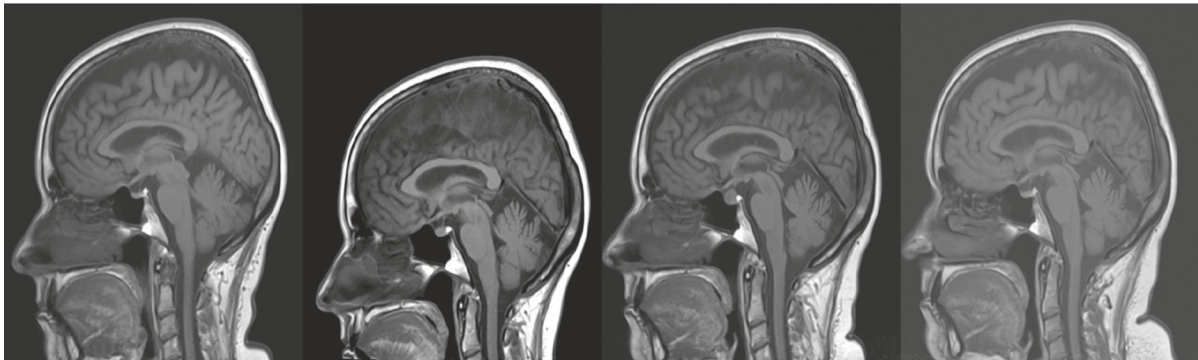
METHODS: Gadolinium enhanced MRI of the sella turcica was performed at our institution in patients prior to initiation of ipilimumab therapy, at the time of development of hypophysitis and pachymeningitis and following discontinuation of ipilimumab therapy. The majority of the illustrations are from two patients with documented ipilimumab-induced hypophysitis, one of which also demonstrated associated pachymeningitis. Additional images included in the poster are of three cases seen at a different institution.

RESULTS: MR imaging findings of hypophysitis and pachymeningitis secondary to ipilimumab therapy are illustrated, with description of the patients' clinical symptoms and review of their endocrinologic data confirming hypophysitis. A remarkable increase in size of the hypophysis is observed following two doses of ipilimumab. Upon cessation of therapy, the hypophysis decreases rapidly in size. Remarkable atrophy in our patients' hypophysis correlates with clinical evidence of hypopituitarism requiring hormone replacement therapy. Pachymeningeal thickening and enhancement in one patient resolved completely after cessation of ipilimumab therapy. Additional neurological complications associated with ipilimumab are illustrated, with images and clinical vignettes documenting these entities. **CONCLUSIONS:** Ipilimumab is a human monoclonal



POSTER PRESENTATION ABSTRACTS

antibody used for treatment of metastatic melanoma. It inhibits the suppressive effects of cytotoxic T-lymphocyte antigen 4 expression and potentiates the body's immune response against tumors. This immunosuppression can lead to several autoimmune disorders. Neurological complications include autoimmune hypophysitis and pachymeningitis, disorders that are reversible with cessation of ipilimumab therapy. Neuroradiologists should be familiar with the MR imaging appearance of these complications as recognition can lead to prompt treatment and better patient outcome.



EP038-Evaluation of Cerebrospinal Fluid Dynamics Using Time Spatial Labeling Inversion Pulse Technique for Endoscopic Third Ventriculostomy in Hydrocephalic Patients

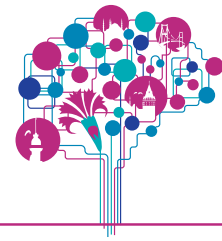
*Kayoko Abe*¹, Kazufumi Suzuki¹, Yuko Ono¹, Yasuo Aihara², Yoshikazu Okada², Shuji Sakai¹
*Tokyo Women's Medical University Diagnostic Imaging and Nuclear Medicine Tokyo-Japan*¹ *Tokyo Women's Medical University Neurosurgery - Japan*²

PURPOSE: The purpose of this study is to evaluate cerebrospinal fluid (CSF) dynamics at sites of endoscopic third ventriculostomy (ETV) using time-spatial labeling inversion pulse (time-SLIP) technique by 3 Tesla magnetic resonance imaging (MRI).

MATERIALS AND METHODS: 18 hydrocephalic patients (5 female and 13 male, age from 4 months to 83 years) performed ETV were included; 9 cases with malignant tumors, 2 cases with infant subependymal hemorrhage, 2 cases with congenital hydrocephalus, 2 cases with ependymitis, 2 cases with benign aqueductal stenosis or obstruction, 1 case with craniosynostosis. CSF imaging using time SLIP technique, a method with labeled CSF as internal tracer by selective inversion-recovery pulse is set to be depicted upward and downward CSF flow at the ETV sites. Time-SLIP examination was performed just after ETV or in chronic stage, for visualization of CSF flow at the ETV sites.

RESULT: Upward and downward pulsatile CSF flow was clearly observed at the ETV sites in 16 cases, presented improved hydrocephalus and did not need further treatment, except for one with the disseminated tumors presented no CSF flow and led to further ventriculoperitoneal (VP) shunt due to progressive hydrocephalus. The other 4 cases presented no CSF flow at the ETV site. One of them underwent ETV and a VP shunt at the same time. The other patient underwent a VP shunt after ETV because of progressive external hydrocephalus and CSF flow at the ETV site was clearly observed before VP-shunt. In the other case, CSF flow was not detected in the early study after ETV, but detected in the repeated study 3 weeks after ETV. In the last case, ETV was performed because of a tumor in the pineal region, which was disappeared after chemotherapy.

CONCLUSION: CSF imaging using time-SLIP technique is sensitive to detect kinetic change of CSF hydrodynamics at ETV sites and capable to predict for the therapeutic effect after ETV and VP shunt.



POSTER PRESENTATIONS ABSTRACTS

EP039-Susceptibility Weighted Magnetic Resonance Imaging Evaluation of Familial Cerebral Cavernous Angiomas

*Haci Taner Bulut*¹, Mehmet Akif Sarica¹, Ali Haydar Baykan¹

*Medical Faculty of Adiyaman University Radiology Adiyaman -Turkey*¹

PURPOSE: We investigated the imaging features of Cavernous angioma (CA) lesions and the diagnostic value of Susceptibility-weighted imaging (SWI) compared with T2*-weighted gradient echo (GRE) sequences in patients with the familial form of the disease.

MATERIALS AND METHODS: We retrospectively evaluated 19 familial CA patients (8 men, 11 women; mean age, 36 years). T1-weighted, T2-weighted, T2*-weighted GRE, and SWI sequences were performed to all patients. The numbers of CA lesions seen on T2*-weighted GRE and SWI sequences were analyzed. The correlations between the numbers of lesions on both sequences with age were evaluated. CA lesions were classified according to the classification of Zabramski et al. **RESULTS:** The number of lesions was higher on than on T2*-weighted GRE ($P < .001$). There was a significant strong correlation between the age of the patients and number of lesions in the cohort on T2*-weighted GRE ($r = 0.81$, $P < 0.001$) and SWI ($r = 0.85$, $P < 0.001$) sequences. Approximately 44% of the CA lesions which were detected only by SWI, could not be categorized according to the classification of Zabramski et al.

CONCLUSIONS: The sensitivity of SWI for determining the number of CA lesions in patients with the familial form of the disease is significantly higher than that of T2*-weighted GRE. This study indicated that the Zabramski classification is insufficient to identify all CA lesions, and a new type should be defined to represent lesions that are seen on SWI but not on T2*-weighted GRE

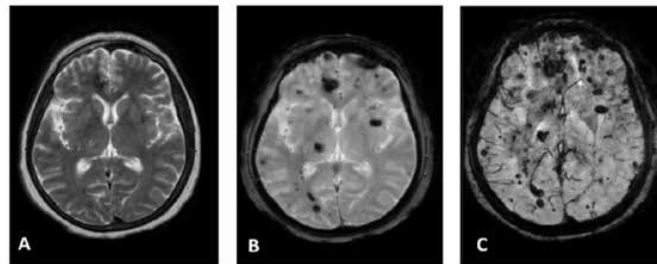


Figure . A, Axial T2-weighted image shows three foci of low signal intensity on the right frontal, occipital and left basal ganglia regions. **B,** T2*-weighted GRE image demonstrates multiple foci of low signal intensity on the both cerebral hemisphere regions (type IV). **C,** SWI shows a higher number of lesions and confirms the presence of larger lesions, which are not seen on the T2*-weighted GRE image

EP040-Radiation Necrosis Imaging Spectrum and Practical Approach

*Ankush Patel*¹, Uresh Patel²

*Royal College of Surgeons Faculty of Medicine Dublin-Ireland*¹ *Seattle Radiologists Neuroradiology -United States*²

Despite the best efforts of the neuroradiology community, the holy grail of distinguishing radiation related brain necrosis from tumor recurrence and/or tumor progression as well as treatment related pseudo-response and pseudo-progression remains elusive. While there is no fail safe imaging methodology to distinguish between these processes; having the ability to do so is of vital importance in the management and survival of these patients. It is, often the clinical course, a brain biopsy, or imaging over a lengthy follow-up interval that enables the distinction of recurrent tumor from radiation necrosis, not the specific imaging itself.

The armamentarium available to neuroradiologists includes gadolinium enhanced MRI, MR Diffusion, MR Perfusion, MR Spectroscopy and PET-CT. Interpretation cannot be performed in a vacuum; clinical information such as tumor type and grade, treatment history including time course, radiation dose and radiation dosimetry maps are of vital importance to the radiologist in making an assessment. We will demonstrate helpful imaging features and give a practical approach to the analysis of cases. A retrospective analysis using the keyword "radiation necrosis" revealed 370 neuroimaging studies between



POSTER PRESENTATIONS ABSTRACTS

March 2003 and February 2014. 312 (84%) were MRI scans of the brain and 58 (16%) were PET-CT. All MRI scans were performed with contrast. Dynamic perfusion data available in 259 scans. DTI in 201 scans Spectroscopy was performed in 125 scans.

EP041-Congenital Dolichoectasia of Cerebral Arteries; a Comprehensive Review of Cases

*Mustafa Gok*¹, Celal Cinar², Halil Bozkaya², Ismail Oran²

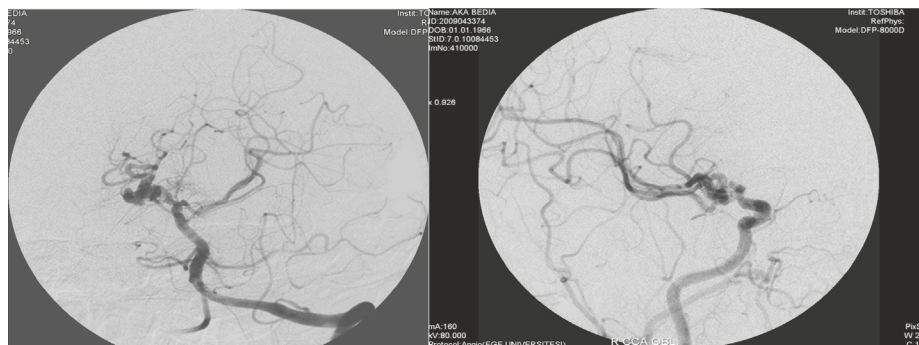
*Kafkas University Hospital, Kars Radiology Izmir-Turkey*¹ *Ege University Hospital, Izmir Interventional Radiology -Turkey*²

Dolichoectasia, which is elongation and fusiform dilatation of the intracranial vessels, has an incidence of 0.06–5.8%. Several types of dolichoectasia are distinguished—atherosclerotic and congenital types—the latter seen in younger patients without atherosclerosis or other known causes of cerebral aneurysms. A third type, resulting from dissection, can present with a dolichoectatic appearance. Atherosclerotic dolichoectasia is the more common type and the age at onset is usually greater than 40 years with a male predominance. The congenital type is more rare and generally found in people younger than 40 years, with a female predominance.

We performed a retrospective and prospective analysis of the angiographies performed in our department between 1998 and 2014 (16 years). All cases were studied with digital subtraction angiography (DSA), some studies were complemented with magnetic resonance angiography (MRA) and computed tomography angiography (CTA).

We found 7 cases with dolichoectasia of cerebral arteries. All of these cases were under age 40 and female so we consider them as congenital dolichoectasia. The main clinical presentation of those cases was headache.

Because there are not many studies in the literature about congenital dolichoectasia, management of these patients are not clear.



EP042-Sometimes a Meningioma Isn't Just a Meningioma

Mariana Diogo¹, João Jacinto¹, Isabel Fragata¹, *Carla Conceição*¹, Manuela Mafra², Luís Cerqueira¹, João Reis¹
*CHLC Neuroradiology -Portugal*¹ *CHLC Neuropathology -Portugal*²

INTRODUCTION AND PURPOSE: Although it is not uncommon for multiple tumors to arise within the same patient, tumor-to-tumor metastasis is a rare entity. In the intracranial compartment, meningioma is the most common host tumor, with breast and lung carcinomas being the most common primary sites. The purpose of this exhibit is to report and illustrate 4 cases of tumor-to-meningioma metastasis, with 4 different primary donors: endometrial, breast, prostate and lung carcinomas.

METHODS: We retrospectively reviewed all intracranial meningiomas histologically diagnosed in our centre that had pre-surgical imaging, from January 1st 2012 to December 31st 2013. Secondary deposits in meningiomas were identified and characterized. Computer tomography (CT) and magnetic resonance (MR) findings were studied and are presented here to illustrate this rare pathology.

RESULTS: A total of 139 intracranial meningiomas were identified. Of those 4 (2,88%) had secondary deposits from extracranial donor tumors. All presented as an imaging diagnostic challenge: in the neuroradiology reports the 1st diagnostic hypothesis was meningioma (with invasive/atypical characteristics), followed by secondary dural deposits. All patients presented with neurological symptoms at time of intracranial imaging. CT/MR studies showed extra-axial lesions all with marked associated parenchymal oedema; two showed blurring of the dural/parenchymal margins, suggesting invasion. The 4 meningiomas had heterogeneous signal in all sequences, with inhomogeneous enhancement. Rare calcifications were identified.



POSTER PRESENTATIONS ABSTRACTS

CONCLUSIONS: Meningiomas are a common, vastly described, intracranial tumor. In rare cases they serve as hosts for metastasis arising from extracranial malignancy. We describe 4 cases and review its imaging and clinical characteristics. Although both entities are rare, it is our belief that meningiomas with atypical or aggressive imaging characteristics in a patient with a previously known primary tumor should raise the suspicion of intratumor metastasis.

EP043-Focal Radiological Changes Due To Status Epilepticus (SE), Report of Two Cases

*Luciana León Cejas*¹, Julieta Quiroga Narvaez¹, Pablo Bonardo¹, Julieta Mazziotti¹, Carlos Rugilo², Juan Chomont², Beatriz Afonso², Ricardo Reisin¹, Manuel Fernandez Pardal¹
British Hospital Neurology Buenos Aires-Argentina ¹ *British Hospital Neuroradiology -Argentina* ²

INTRODUCTION: The incidence of reversible transient periictal MRI abnormalities is still unknown (ranging from 0.007 to 29.4%). The majority of these changes have a focal, unilateral and cortical pattern. Less frequently they have a subcortical component, with either mass effect or affecting structures anatomically distant from the seizure focus. These phenomenon have been related to local hyperperfusion induced by seizure activity and have been reported in DWI, FLAIR and MRI angiography (MRA).

OBJECTIVE: To report 2 patients with MRI changes associated with SE.

CASE REPORT 1: A 73 year old man with a history of angioimmunoblastic non Hodgkin lymphoma, was admitted to our hospital because of impairment of consciousness, visual hallucinations and left bilateral periorbital and perioral myoclonic movements. On examination he presented left arm ataxia, hemisensory loss, hemianopia and left anosognosia. Brain MRI showed increased signal intensity on T2- WI, FLAIR and DWI images in the cortical right occipital lobe and the ipsilateral pulvinar nucleus. MRA revealed increased flow in the distal branches of the right posterior cerebral artery (PCA) and prominent leptomeningeal vessels. Tc 99m ECD – SPECT indicated right

frontoparietooccipital hyperperfusion. EEG: temporal partial right SE. After treatment the patient remitted the myoclonic movements but persisted with neurological deficit. MRA 2 months later showed complete resolution.

CASE REPORT 2: A 61 year old woman with a history of breast cancer with metastasis in the right cerebellar hemisphere and left parietal lobe. After the removal of the cerebellar mass she developed right hemiparesis and persistent tonic-clonic movements on the right side. EEG: showed temporal partial left SE. Her brain MRI revealed in addition to the known enhancing cortical lesion in the left parietal lobe; a new left fronto parietal cortical hyperintensity with increased signal in the ipsilateral pulvinar nucleus .The SE resolved after treatment.

Follow-up MRI 10 days later showed resolution of the new cortical and pulvinar images

CONCLUSION: The SE is an electro- clinical syndrome that can be associated with transient radiological changes. These images are reversible in the majority of patients however they could persist associated with neurological deficits.

EP044-Evaluation of Multiple System Atrophy Cerebellar Type with the Use of MR Imaging and Perfusion Spect

*Fuminori Miyoshi*¹, Yoshiko Kanasaki², Yuki Shinohara¹, Shinya Fujii¹, Toshihide Ogawa¹ *Tottori University Radiology Yonago-Japan* ¹ *Matsue city hospital Radiology -Japan* ²

BACKGROUNDS AND PURPOSE: We have sometimes encountered the cases which show asymmetrical MR imaging findings. Our purpose is to assess the frequency and significance of asymmetrical MR imaging and 99mTc-ECD SPECT findings of cerebellum, MCP, and pons in patients with MSA-C. We also compared laterality of image findings and cerebellar symptoms.



POSTER PRESENTATIONS ABSTRACTS

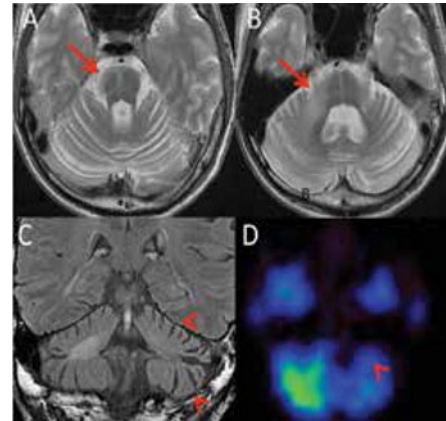
MATERIALS AND METHODS: We retrospectively reviewed 28 patients with MSA-C who underwent MR imaging and 99mTc-ECD SPECT. We evaluated atrophy, signal change on T2-weighted images, laterality of atrophy on MR imaging, and the perfusion change in the brain with or without laterality on 99mTc-ECD SPECT. We also compared between the latest MR imaging and SPECT findings and between the latest images and the past images.

RESULTS: Laterality was identified in 64%, 61%, and 21% of cerebellum, MCP, and pons, respectively on MR imaging and in 71% of cerebellum on SPECT.

Comparison between the latest MR imaging and SPECT findings showed laterality of cerebellar/MCP atrophy on MR imaging and decreased cerebellar perfusion on SPECT was matched in 57% of the cases and mismatched in 11% of the cases.

Comparison between the latest images and the past images on MR imaging and SPECT showed same laterality in 43% of the cases and laterality of cerebellar/MCP atrophy and decreased cerebellar perfusion was matched in 13% of the cases among mismatched group.

CONCLUSIONS: Asymmetrical changes were observed in 68% of the MSA-C patients on MR imaging and SPECT. It is necessary to consider MSA-C as differential diagnosis when we encounter asymmetrical changes.



EP045-Reversible Posterior Encephalopathy Syndrome (PRES), Report of Our Experience in 19 Patients

*Luciana León Cejas*¹, Julieta Quiroga Narvaez¹, Pablo Bonardo¹, Julieta Mazziotti¹, Carlos Rugilo², Juan Chomont², Diego Miñarro¹, Emanuel Silva³, Ricardo Reisin¹, Manuel Fernandez Pardal¹, Pablo Young⁴, Laura Bongiovani⁴

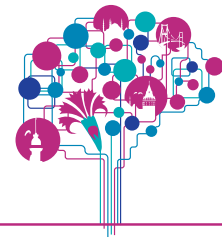
*British Hospital Neurology Buenos Aires-Argentina*¹ *British Hospital Neuroradiology -Argentina*² *Madariaga Hospital Neurology -Argentina*³ *British Hospital Internal Medicine -Argentina*⁴

PRES is a clinical and radiological syndrome not clearly understood. Classic neuroimaging features consist of reversible posterior vasogenic subcortical edema. It has been commonly associated with different comorbid medical conditions. Atypical presentations such as hemorrhages, unilateral, brainstem, basal ganglia, cortical lesions or frontal involvement have been also described. PRES rarely could be recurrent and though is typically reversible lesions can progress to ischemic infarct. **OBJECTIVE:** To report our experience and to describe atypical features in PRES.

MATERIAL AND METHODS: We retrospectively analyzed 19 patients with clinical and neuroimaging features consistent with PRES at British Hospital Bs As. The diagnosis was confirmed with brain TC scan and /or brain MRI.

RESULTS: 12 females and 7 males with a mean age of 35 years were included (range 15 to 74). Presenting symptoms were: seizures (42%), headache (36%), coma (36%), altered mental changes (26%) and bilateral blindness (10%). Comorbid conditions: chemotherapy and immunosuppression in 8 patients, eclampsia in 4 patients, hemodialysis in 2 patients and hypertensive emergency in 5 patients. We found high blood pressure ($\geq 140/90$ mmhg) at presentation in 17 of 19 patients (mean peak blood pressure 169/95 mmhg), 8 patients persisted hypertensive at 48 hours after admission.

Eighteen patients had brain MRI while only in a patient the diagnosis was confirmed with CT scan. Imaging findings showed lesions in: frontal and parietoccipital lobes 10 patients; cerebellar hemispheres cortical



POSTER PRESENTATIONS ABSTRACTS

involment 1 patient; basal ganglia 1 patient. Three patients had hemorrhagic lesions, subarachnoid hemorrhage 1 patient and intracerebral hemorrhage 2 patients with platelet count below 50.000 in the last two patients. Two patients had recurrent PRES. The MRI showed permanent injury in 4 patients.

The morbidity and mortality was 42% (4 patients had chronic epilepsy and 4 patients died).
CONCLUSION: Up to 78% of our patients had an atypical presentation, so the medical team must think in PRES even when the involment are not typically reversible and confined to posterior and subcortical region. The majority of our patients were hipertensive at admission and 35% of them had hemorrhage and/or permanent lesion. Poor prognosis was associated to hemorrhagic presentation, recurrence and residual lesion in the follow up.

Adult NR 4

EP046-Cortical Blindness after Coronariography A Case Report

*Ingeborg Lopez*¹, Rodrigo Riveros¹, Roberto Marileo¹, Cecilia Okuma¹, Aaron Vidal¹,
Rodrigo Rivera¹, J. Gabriel Sordo¹, Lautaro Badilla¹
*Instituto de Neurocirugia Dr. Alfonso Asenjo Neuroradiology Santiago-Chile*¹

INTRODUCTION: Cortical blindness after angiographic procedures is a rare complication described in 1970. Most of the published reports have been associated with neuroangiographic procedures. The etiology is unknown, and spontaneous recovery is reported from a few hours to 4 days.

CASE REPORT: A 58 years old man was admitted with acute coronary syndrome, requiring primary stent angioplasty. After angioplasty, he suffered of bilateral amaurosis associated with headache and decreased level of consciousness. Contrast enhanced brain CT showed abnormal enhancement in both occipital lobes. Brain MRI excluded acute ischemic or hemorrhagic lesions. Perfusion MRI showed increased relative brain blood volume in both occipital lobes, without changes in brain blood flow nor time. The patient had complete visual recovery after 4 days. Control perfusion MRI performed showed normalization of relative brain blood volume.

CONCLUSION: We report a clinical case with cortical blindness post coronariography and perfusion disturbances contemporary to clincial syndrome; it may help to understand the pathophysiology of this rare angiographic complication.

EP047-Corpus Callosum Involvement in Anti Aquaporin 4 Disease Case Report

*Ingeborg Lopez*¹, Roberto Marileo¹, Cecilia Okuma¹, Sabrina Oporto², Aaron Vidal¹,
Rodrigo Rivera¹, J. Gabriel Sordo¹, Lautaro Badilla¹
*Instituto de Neurocirugia Dr. Alfonso Asenjo Neuroradiology Santiago-Chile*¹ *Hospital Salvador Neurology -Chile*²

INTRODUCTION: The discover of autoantibody against aquaporin-4 has broadened neuromyelitis optica (NMO) spectrum disorder. Inclusion of the autoantibody testing in the recently revised diagnostic criteria for NMO led to the distinction of this disorder from other autoimmune CNS diseases. NMO non typical brain lesions have been identified in the hypothalamus, corpus callosum, brainstem and periventricular area.

CASE REPORT: We report a healthy 21 years old man, who developed headache associated with left hemiparesis. Brain magnetic resonance (MRI) showed corpus callosum`s splenium involvement, spinal MRI was normal. Cerebrospinal fluid analysis was normal, oligoclonal band and antiaquaporin-4 were positive. After two years patient remains without significant changes in the imaging findings.

CONCLUSION: We report a case with corpus callosum involvement with anti-aquaporin-4 autoantibodies positive. The presence corpus callosum involvement with autoantibody against aquaporin-4 suggest aquaporin-4 disease spectrum confirming the heterogeneity in the expression of this disorder.



POSTER PRESENTATIONS ABSTRACTS

EP048-Linear Scleroderma with Neurologic Involvement Two Case Reports

*Ingeborg Lopez*¹, Roberto Marileo¹, Rodrigo Riveros¹, Cecilia Okuma¹, Aaron Vidal¹, Rodrigo Rivera¹, J. Gabriel Sordo¹, Claudia Tissera², Lautaro Badilla¹

Instituto de Neurocirugia Dr. Alfonso Asenjo Neuroradiology Santiago-Chile *1 Instituto de Neurocirugia Dr. Alfonso Asenjo Pathology -Chile*²

INTRODUCTION: Scleroderma is a rare disease of unknown etiology, characterized by thickening and hardening of skin due to increased collagen production. Linear scleroderma in “coup de sabre” is characterized by a linear frontoparietal scleroderma. This type of scleroderma has been associated with neurological symptoms such as epilepsy, pyramidal syndrome and ocular abnormalities; brain MRI usually shows parenchymal lesions ipsilateral to skin abnormalities.

CASE REPORTS: We report two patients with diagnosed lineal scleroderma in “coupe de sabre”: a 73 year old woman with headache and 10 years old boy with seizures, dysarthria and paresthesias. Both brain MRI showed extensive brain abnormalities at the same side of skin lesion. A stereotactic biopsy was performed to the second patient; it showed vascular abnormalities.

CONCLUSION: Neurologic abnormalities are frequently found in patients with scleroderma. Here we report two clinical cases with MRI evidence of neurologic and neurovascular involvement, one of them with pathologic confirmation.

EP049-Prefrontal Cortex Phylogeny Development and Pathological Conditions; Pictorial Essay

*Rosana Salvatico*¹, Hector Lambre¹, Cecilia Rollan¹, Gabriela de Pino¹, Carlos Romero¹
*FLENI Neuroradiology CABA-Argentina*¹

PURPOSE:

- To review phylogeny, ontogeny and embryological development of the prefrontal cortex.
- To describe its functions and its relation to behavior, emotion and memory.
- To exemplify the most frequent pathology.

METHODS: We analysed retrospectively 627 patients in our database, with pathology in the frontal lobe, between May 2010 and February 2014, which were studied with brain Multislice Computed Tomography (MSCT), 3/1.5 Teslas Magnetic Resonance (MR) and angioMR.

RESULTS: Congenital or acquired pathologies were found in the prefrontal cortex in 238 cases (143 males/ 95 females; mean age: 41 y/o) such as infarctions, primary and secondary tumors, hemorrhages, contusions, traumatic and postoperative sequelae, cortical dysplasia, metabolic, inflammatory, infectious and degenerative conditions. Table 1

CONCLUSIONS: Knowledge of the broad spectrum of diseases that can affect the prefrontal cortex is key, since this area is deeply linked to behavior, emotion and memory.

RESULTS	PATIENTS	%
INFARCTIONS	20	8,40
HEMORRHAGE	10	4,20
PRIMARY TUMORS	26	10,92
SECONDARY TUMORS	41	17,27
CONTUSIONS	19	7,98
TRAUMATIC SEQUELAE	14	5,88



POSTER PRESENTATIONS ABSTRACTS

POSTOPERATIVE SEQUELAE	13	5,46
CORTICAL DYSPLASIA	25	10,50
INFECTION	14	5,88
INFLAMMATION	22	9,24
DEGENERATIVE DISEASES	25	10,50
METABOLIC DISEASES	9	3,77
TOTAL	238	100

EP050-Vascular Signs Its Meaning and Importance in the Diagnosis of Brain Head and Neck Pathology

*Rosana Salvatico*¹, Hector Lambre¹, Rosana Ceratto¹, Angel Ferrario¹, Pedro Lylyk¹
*ENERI Neuroradiology CABA-Argentina*¹

PURPOSE:

-To report the most frequent signs in brain, head and neck vascular pathology

-To describe the pathophysiological meaning and importance of these signs in the early diagnosis.

METHODS: We analysed retrospectively 886 patients in our database, suffering from brain, head and neck vascular pathology, between March 2011 and February 2014, which were studied with brain Multislice Computed Tomography (MSCT), 3 Teslas Magnetic Resonance (MR), angiMR and Digital Subtraction Angiography (DSA)

RESULTS: We found vascular signs in 318 cases (195 males/ 123 females; mean age:48 y/o) with acute or chronic conditions such as infarctions, dissections, obstructions, bleedings, aneurysms, tumors, inflammatory diseases (vasculitis) and other congenital or acquired pathologies (Moya-Moya, development venous malformation). Table 1

CONCLUSIONS: Knowledge of main features and meaning of vascular signs contributes to the early and accurate diagnosis of many brain, head and neck conditions.

RESULTS	PATIENTS	%
INFARCTIONS	139	43,7
OBSTRUCTIONS	48	15,1
BLEEDINGS	26	8,2
ANEURYSMS	43	13,5
DISSECTIONS	25	7,9
TUMORS	17	5,3
INFLAMMATION	6	1,9
OTHER	14	4,4
TOTAL	318	100



POSTER PRESENTATIONS ABSTRACTS

EP051-Autoimmune Limbic Encephalitis Caused by Ovarian Neoplasms

Reports of Two Cases and Literature Review

*Yao-Liang Chen*¹, Ho-Fai Wong²

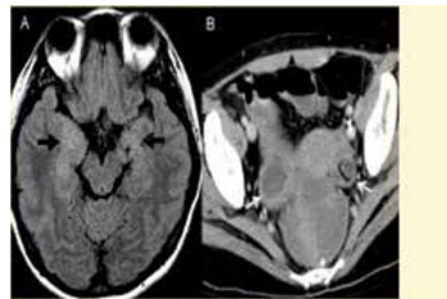
*Chang Gung Memorial Hospital, Keelung; Chang Gung University Radiology Taoyuan -Taiwan*¹ *Chang Gung Memorial Hospital, Linkou; Chang Gung University Medical and Intervention -Taiwan*²

PURPOSE: To demonstrate two patients with ovarian neoplasms contributing to autoimmune limbic encephalitis mimicking herpes encephalitis clinically and on imagings.

MATERIAL AND METHODS: Both women were 30 years of ages, one healthy woman without recordable medical history and another one with pregnancy of 11-week gestational age. The healthy one suffered from commoncold-like symptoms for 5 days with low-grade fever, followed by generalized tonic-clonic seizure, confusion and rapid deterioration into comatose status. Brain MR disclosed swelling over bilateral limbic systems. She was referred to our institute and right ovarian cyst was found. Anti-NMDA receptor antibody was proven by serology under impression of autoimmune limbic encephalitis. Right ovarian mature cystic teratoma was proven thereafter. She gradually recovered with steroid pulse therapy and plasmapheresis. However, the pregnant woman with history of bilateral ovarian endometriomas underwent laparoscopic enucleation and ovarian hyperstimulation syndrome caused by infertility treatment. She suffered from memory loss for 5 days, followed by low-grade fever and similar clinical courses and imaging presentations as that of the healthy one. Anti-AMPA receptor antibody was titrated in serum. Then steroid pulse therapy and plasmapheresis was applied.

RESULTS: The healthy one recovered to independent walking with neurological sequel at nine-month follow-up. Although same treatment was applied to the pregnant women, comatose status persisted as no further ovarian intervention.

CONCLUSION: Autoimmune limbic encephalitis is rare disease and initially mimicking herpes encephalitis clinically and on imaging. Gynecological and autoimmune profile surveys are crucial for young female patients if imaging presentation of limbic encephalitis.



A. Brain MRI disclosed hyperintensity on bilateral hippocampi and amygdalae (black arrows) on FLAIR image, more swelling on the right.
B. Enhanced axial CT showed bilateral ovarian neoplasms (white arrows), the right one with well-demarcated cystic content and the left one with fatty content and a calcified spot. Histology proved right ovarian endometriosis and left ovarian mature cystic teratoma.

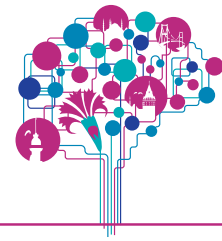
EP052-Resting State Neural Network in Monolateral and Bilateral Tinnitus

*Ji Hye Jang*¹, Chang-Woo Ryu², Geon-Ho Jahng², Eui Jong Kim¹, Woo Suk Choi¹

*Kyung Hee University Hospital Radiology Seoul-Korea, South*¹ *Kyung Hee University Hospital at Gangdong Radiology -Korea, South*²

PURPOSE: Most of investigation about the neuronal activity in tinnitus was the fMRI with task-base paradigm by using auditory or somatic modulation. However, few studies have investigated the neuronal activity of resting state in tinnitus. The objective of this study is identify the difference of resting state networks between patients with tinnitus and matching healthy control by using resting state fMRI.

METHODS: Total 73 age-matched subjects consisting of 18 left-sided tinnitus, 16 right-sided right tinnitus, 19 bilateral tinnitus, and 20 healthy controls underwent resting state fMRI scan. Using previously defined regions-of-interest, we computed the connectivity in default mode and auditory network, and the resting state network was compared by group independent component analysis. **Results:** In default mode network, tinnitus groups had connectivity in anterior cingulate, bilateral inferior frontal, prefrontal gyri, and motor sensory area was found to be increased in tinnitus. Group of bilateral tinnitus had increased area at bilateral angular gyri and caudate nucleus compared with monolateral tinnitus and



POSTER PRESENTATIONS ABSTRACTS

healthy control. Comparison of the auditory network of resting state indicate reduced functional connectivity of auditory network and increased functioning in additional brain region including prefrontal, and middle temporal regions. Bilateral tinnitus group showed greater activation in bilateral superior frontal gyrus and lower activation in bilateral superior temporal gyrus than monolateral tinnitus groups.

DISCUSSION: These results suggested that the chronic tinnitus may be related to aberrant functioning of the default mode network. Alteration of default mode and auditory network between monolateral and bilateral tinnitus imply that the monolateral and bilateral tinnitus may have different mechanism.

CONCLUSION: Our research suggested that resting state fMRI would be useful to lateralize tinnitus and analyze the mechanism of the tinnitus without task-base paradigm.

EP053-MR Imaging In Relation To Phylogenetic Anatomy of the Cerebellum in Spinocerebellar Ataxia from Conventional MRI to Diffusion

Imaging

*Kanako Sato*¹, Koji Kamagata¹, Ryuji Sakakibara², Hitoshi Terada², Shigeki Aoki¹

*Juntendo University School of Medicine Department of Radiology Tokyo-Japan*¹ *Toho University Sakura Medical Center Department of Radiology -Japan*²

PURPOSE: Spinocerebellar ataxia (SCA) is a progressive autosomal inherited disease that results in ataxia due to degeneration of the cerebellum, the brainstem, and the spine. Volumetric and diffusional changes are helpful in the differential diagnosis of ataxia including spinocerebellar degeneration (SCD) such as multiple system atrophy and cortical cerebellar atrophy. The cerebellum has three regions derived from different phylogenetic origins (Figure 1). Site-specific degeneration patterns of the cerebellum in relation to phylogenetic origins are thought to be related to symptoms.

The purpose of this presentation is to review clinical presentations and imaging findings in relation to phylogenetic anatomy of the cerebellum among different types of SCA and SCD. To investigate diffusional changes, we performed analyses of diffusion tensor imaging (DTI) and diffusional kurtosis imaging (DKI) in patients with SCA type 6 (SCA6).

METHODS: We reviewed the followings: (1) Pathogeneses of SCA (2) Conventional MRI and volumetric MRI findings among different types of SCA and SCD (3) Advanced diffusion imaging including our analyses of DTI and DKI. We performed tract-specific analysis for all of the cerebellar peduncles and ROI analysis for the cerebellar white matter in patients with SCA6. ROIs were set depending on phylogenetic origins. Fractional anisotropy (FA), apparent diffusion coefficient (ADC), and mean kurtosis (MK) are compared between two groups.

RESULTS: Significant increase of ADC and significant decrease of MK are observed in both the middle cerebellar peduncle (MCP) and inferior cerebellar peduncle (ICP) in patients with SCA6. There was no significant change in FA and in the superior cerebellar peduncle (SCP). ROI study showed significant decrease of FA and MK only in mid part of the cerebellum.

CONCLUSION: This review would improve understanding of MR imaging in relation to phylogenetic anatomy of the cerebellum in SCA. Our findings implied the usefulness of ADC and MK, and degeneration in relation to phylogenetic origins in patients with SCA6.



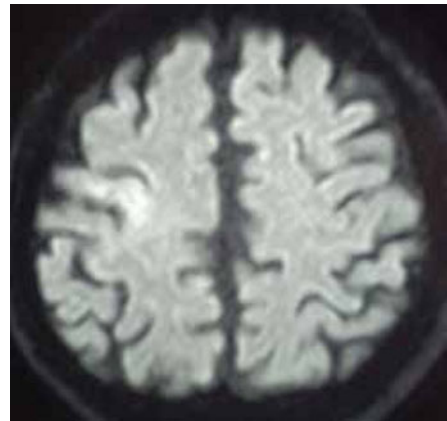
POSTER PRESENTATIONS ABSTRACTS

EP054-Three Cases of Progressive Multifocal Leukoencephalopathy with Specific Involvement of Pyramidal Tract an Important Differential Consideration

*Kouhei Kamiya*¹, Ryusuke Irie², Harushi Mori¹, Akira Kunimatsu¹, Masaaki Hori², Noriko Sato³, Shigeki Aoki², Kuni Ohtomo¹

*The University of Tokyo Graduate School of Medicine Department of Radiology Tokyo-Japan*¹ *Juntendo Graduate School of Medicine Department of Radiology -Japan*² *National Center Hospital of Neurology and Psychiatry Department of Radiology -Japan*³

Progressive multifocal leukoencephalopathy (PML) is a demyelinating disease caused by reactivation of JC virus in immuno-compromised patients. We report three cases of PML, which showed unique, selective involvement of the pyramidal tract. Each patient presented with subacute onset progressive hemiplegia, and showed exacerbation of the symptom over several months. At the initial hospital visit, MRI demonstrated hyper-intense lesion on T2WI and DWI limited in the subcortical white matter of the unilateral pre-central gyrus. The lesion expanded, over a few months, along the pyramidal tract reaching into the internal capsule. As the lesion increased, a typical peripheral DWI hyper-intense pattern became obvious. PML commonly shows multifocal lesions located predominantly in subcortical areas on MRI, and discrete involvement of the pyramidal tract is rare. To date, a few sporadic case reports have described PML with predominant affection of the pyramidal tract. In some cases, the initial MRI findings somewhat resembled with Wallerian degeneration following cortical stroke. All cases presented with progressive hemiparesis as the first clinical sign, as in our cases. PML with selective involvement of pyramidal tract should be recognized as a differential diagnosis of subacute progressive hemiparesis especially in immuno-compromised hosts, even when the initial MRI findings is very limited in the unilateral pre-central gyrus.



EP055-Preoperative Diagnosis of Suprasellar Papillary Craniopharyngioma and Germ Cell Tumors of Adult Patients

*Han-Jui Lee*¹, Feng-Chi Chang¹, Hsiu-Mei Wu¹, Alex S. C. Hung¹, Chih-Chun Wu¹, Wan-Yuo Guo¹
*Taipei Veterans General Hospital Department of Radiology Taipei-Taiwan*¹

PURPOSE: Suprasellar papillary craniopharyngiomas (PCP) and germ cell tumors (GCT) share some imaging and clinical manifestations but have different treatment modality and outcome. We sought to compare their clinical and imaging findings to get the accurate pretherapeutic diagnosis, for making an appropriate treatment modality and improving the outcome.

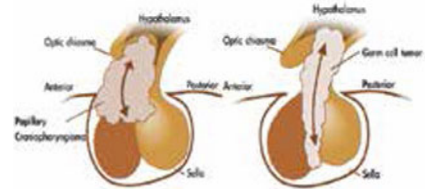
METHODS: We retrospectively enrolled clinically and/or pathologically diagnosed suprasellar PCP (n=18, male/female= 13/5) and GCT (n=17, male/female=13/4) in adult patients of our institute from 2003 to 2013. Both MR and clinical findings were retrieved from hospital PACS and HIS systems for reviewing and comparison. All quantitative measurement were made by standard tool equipped in the hospital PACS and qualitative assessment of lesional characters were made based on consensus of the authors (HJ and FC).

RESULTS: Clinical findings of PCP vs GCT: age [years, (46 ± 14) vs (23 ± 7), p< 0.0001] and diabetes insipidus [2/18 (11%) vs 11/17 (65%), p=0.001]; MR findings of PCP vs GCT: pituitary stalk thickening (1.6 ± 0.4mm vs 5.4 ± 4.2mm, p<0.0001), vertical infundibular extension [1/18 (6%) vs 16/17 (94%), p<0.0001], sagittal dumbbell shape [17/18 (94%) vs 1/17 (6%), p<0.0001], diffusion restriction [1/17 (6%) vs 8/12 (67%), p=0.0009].



POSTER PRESENTATIONS ABSTRACTS

CONCLUSIONS: Younger age, diabetes insipidus, MR characters of restriction diffusion and vertical infundibular extension favor GCT. Dumbbell shape gives clue to PCP. According to the anatomical involvement, subfrontal surgical approach for PCP and trans-ventricular surgical approach combined with irradiation for GCT are suggested to improve the outcome.



EP056-Susceptibility Weighted Imaging Improves the Accuracy of Brain MRI to Differentiate between Parkinson's Disease and Atypical Parkinsonism

Frederick Meijer ¹, Bram Fasen ¹, Bastiaan Bloem ², *Bozena Goraj* ¹

Radboud University Nijmegen Medical Centre Radiology and Nuclear medicine -The Netherlands ¹ *Radboud University Nijmegen Medical Centre Neurology -The Netherlands* ²

OBJECTIVE: Differentiating between Parkinson's disease (PD) and atypical parkinsonism (AP) is challenging, especially in early disease stages. Conventional brain MRI has high specificity for AP, though sensitivity is limited. As PD and the various forms of AP can demonstrate abnormal mineralization in different brain structures, susceptibility weighted imaging (SWI) could possibly improve the diagnostic accuracy of brain MRI.

The goal of our study is to evaluate whether SWI is of added value to conventional 3 Tesla brain MRI in differentiating between PD and the various forms of neurodegenerative AP in early stage parkinsonism.

MATERIAL and METHODS: In this prospective observational cohort study, 65 patients presenting with parkinsonism but with initial uncertain diagnosis had a 3 Tesla brain MRI, consisting of conventional and SWI sequences. In addition, 13 age- and sex- matched healthy controls were scanned. Probable diagnoses could be made in 56 patients after mean clinical follow-up of 24.8 months. Performance of brain MRI was evaluated in 38 patients diagnosed with PD and 18 patients diagnosed with AP (12 MSA-P, 3 PSP and 3 LBD). The SWI sequences were analyzed by a ROI method. Mean SWI signal intensity of different brain structures was calculated for each diagnosis and one-way ANOVA, corrected for multiple comparisons with a Bonferroni correction, was performed to analyze differences between the groups. ROC analyses were performed to evaluate the ability of conventional brain MRI as well as conventional brain MRI combined with selected SWI measures to differentiate between PD and AP.

RESULTS: Mean SWI signal intensity of the putamen was significantly lower for MSA-P for both sides and the anterior and posterior parts ($p < 0.001$), in comparison to the other diseases as well as healthy controls. The SWI sequence improved the diagnostic accuracy of brain MRI to identify MSA-P (AUC 0.78 -> 0.87). In addition, the diagnosis of AP as a group was increased by putaminal SWI measures (AUC 0.80->0.91). The trade-off between sensitivity and specificity can be influenced by choosing an optimal threshold.

CONCLUSIONS: SWI improves the diagnostic accuracy of brain MRI in differentiating between PD and AP by identifying increased putaminal susceptibility in MSA-P. The diagnostic accuracy for both conventional brain MRI and SWI depends on defining and validating imaging criteria.



POSTER PRESENTATIONS ABSTRACTS

EP057-Panencephalopathic Type of Crutzfeldt Jacob Disease in Indian Subpopulation Case report

*N K Mishra*¹, A Garg¹, L Joseph¹, S B Gaikwad¹

Neurosciences Center, All India Institute Of Medical Sciences Neuroradiology New Delhi-India 1

INTRODUCTION: Crutzfeldt Jacob disease is most common prion disease. Panencephalopathic type of CJD characterized by extensive involvement of white matter & grey matter is rare variety reported mostly in Japanese population.

CASE REPORT: A 69-year-old female presented with 5-months history of rapid onset cognitive decline & myoclonus. Initial CT & MRI evaluation of patient showed presence of diffuse cerebral atrophy along with presence of T2 hyperintensity in bilateral posterior periventricular white matter with no diffusion restriction. Subsequent MRI done 4 months later revealed extension of periventricular hyperintensities to bilateral caudate nuclei and basal ganglia and diffusion restriction in. Diffusion restriction was also seen in bilateral frontal & parietal cortices (cortical ribbon sign). EEG showed characteristic periodical spikes.

DISCUSSION: Creutzfeldt–Jakob Disease (CJD) is a rare, progressive and invariably fatal neurodegenerative disease characterized by specific histopathological features. Of the four subtypes of CJD described, the commonest is sporadic CJD (sCJD)³.

White matter lesions are rare in cases of CJD & are considered to be secondary to gray matter lesions. Mizutani et al described 8 cases of CJD with primary white matter involvement & termed Panencephalopathic CJD. Until now most cases of Panencephalopathic CJD are reported in Japanese population with few cases in European population⁴. To our knowledge this is first instance in Indian subpopulation with predominant white matter involvement.

Matsusue et al studied serial MRI & histologic changes of 6 biopsy proved pCJD cases and found that cerebral white matter lesions are primary changes of the disease. Histological features of lesions show severe loss of myelin & axons associated with spongiform changes or tissue rarefaction & proliferation of gemistocytic astrocytes⁴.

Our case initially had involvement of white matter with no imaging involvement of gray matter. On serial follow up MRI white matter changes progressed with involvement of gray matter structures suggesting involvement of white matter in primary manner in this variety of CJD.

CONCLUSION: This case illustrates that CJD with primary involvement of cerebral white matter can also occur in Indian subpopulation & physicians need to be aware of the same to allow for early diagnosis and management.

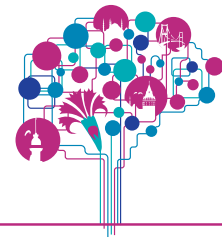
EP058-Predisposing Factors in Posterior Circulation Infarcts a Vascular Morphological Assessment

*Gökçen Çoban*¹, Bilal Egemen Çifçi¹, Erkan Yıldırım¹, Ahmet Muhteşem Ağıldere¹

Baskent University Medical School Radiology Department Konya-Turkey¹

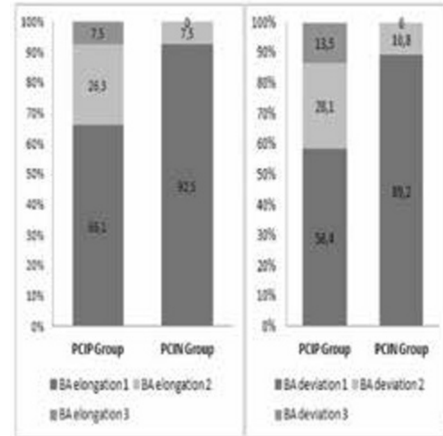
OBJECT: The relationship between vertebrobasilar artery dolichoectasia and ischemic symptoms is not completely understood. Previous studies have reported that risk of ischemic symptom development is high in patients with basilar artery (BA) aneurysm, and tortuous and elongated arteries lead to cranial nerve palsies. Our study assessed the effect of shape, diameter, elongation and deviation criteria of BA, convergence angle and diameter variations of vertebral arteries (VA), and concurrent chronic diseases on posterior circulation infarcts. Method: The study included patients who underwent brain and diffusion MRI examination with suspected cerebrovascular accident (CVA) and were diagnosed with posterior circulation infarct between January 2010 and May 2013.

Patients with a cardiac pathology with a possible causal relationship with infarct, and those with carotid, vertebral, or basilar artery stenosis or occlusion detected at DSA, CT angiography, or MR angiography were excluded from the study. VA and BA diameter, right and left VA angles at the level of bifurcation, and BA elongation, deviation, and shape of BA were assessed in a total of 306 patients (120 infarct negative control



POSTER PRESENTATIONS ABSTRACTS

group and 186 infarct positive patient group). Ischemic lesions in the posterior circulation were classified according to their anatomical location and vascular perfusion areas. Combined effects of all possible risk factors for infarct were assessed with multivariate logistic regression analysis. RESULTS: Age ($p=0,749$) and sex ($p=0,070$) was homogenous among the control and patient groups. No significant difference was noted between the control and patient groups with respect to BA diameter ($p=0,676$). The most effective risk factors for posterior circulation infarcts were as follows: a BA elongation of 2 or 3, a BA transverse location of 2 or 3, an increase in left VA angle, and history of hypertension (HT), hypercholesterolemia, and diabetes mellitus (DM). Discussion: Mortality and morbidity is high in patients with ischemic lesions in posterior circulation. Timely detection and treatment of at-risk patients may be life-saving. Reporting marked morphological BA and VA variations detected at routine brain MR examinations will aid in selection of patients with chronic diseases which are at risk. Figure 1: The ratio of subjects with the BA elongation (right) and BA deviation (left) according to infarct negative control group (PCIN) and infarct positive



P059-Demyelinating Patterns associated to Primary CNS Lymphoma

*Antonio Mas-Bonet*¹, Maria J Picado-Valles², Apolonia Moll-Servera¹, Carmen Gassent

Balaguer³, Nestor Calvo-Rado³, Ines Barcelo⁴, Mariano Del-Valle⁴, Salvador Miralbes Celma⁴

*Hospital Son Espases NeuroRadiology Palma de Mallorca-Spain*¹ *Hospital Son Espases NeuroRadiology -Spain*²

*Hospital Son Espases Radiology -Spain*³ *Hospital Son Espases Neurology -Spain*⁴

PURPOSE: Demyelination could be an ancillary finding associated to Primary Central Nervous System Lymphoma (PCNSL), in some cases it is very difficult to differentiate from Tumefactive Demyelinating Lesions. Our purpose is to describe the demyelinating patterns associated to PCNSL in basis of MRI findings.

METHODS: We reviewed retrospectively the pre and post-operative MRI of 20 patients with proved PCNSL from the last six years. The studies were performed on GE Magnets 1,5T and 3 T. In all the cases we obtained spectroscopy (MRS). 8 patients had demyelination.

RESULTS: 8 patients were included. All were histologically diagnosed as diffuse large B cell lymphomas (CD20+) and all presented a variable degree of T-cells infiltrates (CD4+ or CD8). The 8 cases had prominent areas of demyelination 6 present on preoperative MRI and 2 on follow up. In 7 cases we had histologic evidence of demyelination on biopsy (rarefaction of white matter, myelin loss, gliosis and axonal loss). In two cases the demyelination developed after biopsy (one case pre-treatment and in the other case after treatment).

We found three main patterns of demyelination: a) Focal associated to the main lesion, b) Multifocal mostly in two or three different areas and c) Diffuse white matter demyelination.

CONCLUSIONS: The association of areas of focal demyelination in the different patterns described with enhancing lesion should suggest the diagnosis of lymphoma. It may be difficult to differentiate these demyelinating patterns from Tumefactive demyelinating lesions. Diffuse demyelinating patterns had worse prognosis. In some cases the diffuse patterns appeared progressively after biopsy.



POSTER PRESENTATIONS ABSTRACTS

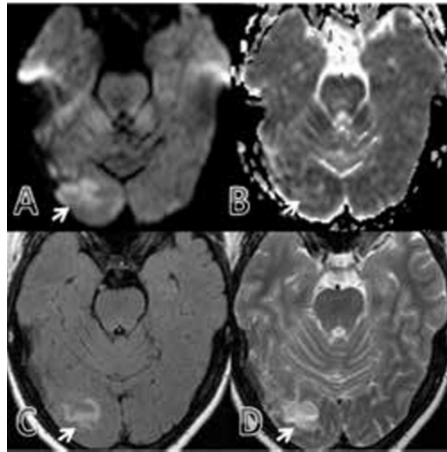
EP060-Transient Homonymous Hemianopia Caused by Cerebral Venous Sinus Thrombosis

*Gökçen Çoban*¹, Aylin Karalezli², Bahriye Horasanlı³, Nilüfer Yeşilirmak²

*Baskent University Medical School Radiology Department Konya-Turkey*¹ *Baskent University Medical School Ophthalmology Department -Turkey*² *Baskent University Medical School Neurology Department -Turkey*³

Venous thromboembolism is still a major health problem around the world, although it is often clinically silent and undiagnosed especially in younger women. Underlying conditions that may cause cerebral venous sinus thrombosis (CVST) are various and the etiology is unknown in such cases. Combined oestrogen-progestin oral contraceptives have been associated with an increased risk of venous thromboembolism. There are only a few case series homonymous hemianopia with CVST hemianopia caused by CVST due to using oral contraceptive and diagnosed with MRI in a 24 year old woman. Her symptoms are rapidly improved and the visual field defect had fully resolved with oral anticoagulation treatment in a week. Homonymous hemianopia is an uncommon vision problem and our case highlights the importance of imaging techniques to resolve unexpected clinical findings.

Figure 1: Diffusion-weighted MR image b-1000 (a) and ADC map (b) shows the ischemic lesion in the right occipital lobe (white arrows). Axial (c) FLAIR image (TR/TE: 6000/100; TI: 2000) and axial (d) T2-weighted turbo spin echo (TSE) image (TR/TE, 4500/100) shows an increased signal intensity in the subcortical white matter in the right occipital lobe (white arrows) due to a rare form of stroke by the thrombosis of the right transvers sinus.





POSTER PRESENTATIONS ABSTRACTS

Tuesday, September 9, 2014

Poster Presentations

13.00-14.00

Head and Neck 1

EP061-IgG4 Related Disease in Head and Neck CT Findings

*Dong Woo Park*¹, *Mi Mi Kim*¹, *Young Jun Lee*¹, *Choong Ki Park*¹, *Hyun Koo Kang*²

*Hanyang University College of Medicine Radiology Guri-si-Korea, South 1 Seoul Veterans Hospital Radiology Korea, South*²

PURPOSE: Immunoglobulin G4 (IgG4)-related disease is recently established benign disease, which is characterized by infiltration of IgG4-positive plasma cells and lymphocytes with surrounding fibrosis, and good response to steroid therapy. We evaluate CT imaging features of IgG4-related disease in the head and neck.

METHODS: A total of 7 patients with histopathologically confirmed IgG4-related disease in the head and neck were included, who were 4 men and 3 women with mean age, 52 years; age range, 32-73 years. Imaging findings were retrospectively evaluated, particularly focusing location, laterality, shape, margin, internal architecture, attenuation on precontrast CT images and enhancement pattern.

RESULTS: The lesions, presented as either enlarged glands (n=7) or focal nodule (n=1) were distributed in the submandibular gland (n=5), lacrimal gland (n=2) and nasopal area (n=1). One patient had both a lacrimal and submandibular gland lesion simultaneously. Most of lesions show diffuse and globular glandular enlargement, well-defined margin, homogenous internal architecture, hypo- or iso-attenuation on precontrast CT images and well enhancement. All lacrimal gland lesions were bilateral, while submandibular gland lesions were either unilateral or bilateral. **CONCLUSIONS:** IgG4-related disease is a multisystemic disease that may also involves head and neck, while the submandibular and lacrimal glands are a predilection for this disease in our cases. IgG4-related disease should be included in the differential diagnosis when the enlargement of these glands with some key image features presents.

EP062-Long Term Ultrasonographic Findings of Face and Neck US after Injection of Facial Filler the Role of Artifact on US

*JiHwa Ryu*¹, *ChoongKi Eun*¹, *KwangHwi Lee*¹, *HongDae Kim*¹

Haeundae Paik Hospital radiology Busan-Korea, South

PURPOSE: To evaluate ultrasonographic findings on face (injected site) and neck (non-injected site) after the injection of facial filler with long term follow-up period.

MATERIALS AND METHODS: Forty three consecutive patients with the history of previous injection of facial filler were enrolled in single institution from 2010 to 2013. All patients were females and mean age was 62.7 years old (range: 46-76). Mean follow-up period after injection of facial filler was 16.1-years (range: 2-30), and mean number of injection of facial filler was 1.72 (range: 1-5). We investigated US examinations for abnormal findings in injected site on face and the presence of abnormal lymph node (LN) in non-injected site on neck in all patients.

RESULTS: All patients revealed multiple small unilocular cysts with reverberating artifact and snowstorm appearance with strong posterior acoustic shadow in subcutaneous fat of both buccal spaces or forehead on face US. On neck US, 29 (67.4%) patients revealed abnormal cervical LNs which were mainly located in bilateral level 1 and 2, as follows; globally hyper-echoic LNs with posterior hyper-echoic trail in 12 (27.9%) patients, enlarged LNs with multiple hyper-echoic foci in 4 (9.3%) patients, coexistence of two patterns in 13 (30.2%) patients. Remaining 14 (32.6%) patients revealed unremarkable findings on US.

CONCLUSION: US findings after injection of facial filler were multiple small cysts and snowstorm appearance on face and enlarged LNs with hyper-echoic change on neck. Artifact on US can influence on differentiating other diseases arising head and neck.



POSTER PRESENTATIONS ABSTRACTS

EP063-The Role of Parathyroid Hormone Assay on Fine Needle Aspiration Washouts and Ultrasonographic Findings in Nonfunctional Parathyroid Cysts

*JiHwa Ryu*¹, ChoongKi Eun¹, KwangHwi Lee¹, HongDae Kim¹
*Haeundae Paik Hospital radiology Busan-Korea, South*¹

PURPOSE: To analyze parathyroid hormone (PTH) assay on fine needle aspiration (FNA) washouts and ultrasonographic (US) findings in nonfunctional parathyroid cyst (NPC) MATERIALS AND METHODS: We retrospectively reviewed 16 cases in two institutions. All NPCs were confirmed by clear aspirated fluid without blood contamination and elevation of PTH level on FNA washouts. We evaluated clinical features (gender, age, clinical symptom, serum PTH, serum calcium) and analyzed intra-cystic fluid (volume, nature, washout PTH, and cytology). We regarded that the specific US findings of NPC were concave contour, wrinkle sign and tear drop in cystic wall. We evaluated the change in size of post-aspirated NPC in follow-up US.

RESULTS: The patients were female-prevalent (M:F= 3:13, mean age: 54.7 years, range: 30 – 79). Fourteen patients had no clinical symptom. Serum PTH and serum calcium were within normal range. Mean PTH level on FNA washouts was 801.9pg/ml (range: 23-5000). Mean size of NPC was 2.6cm (range: 0.7-6.5). NPC was revealed on left side in 14 patients and infra-thyroidal area in 15 patients.

Thirteen patients had at least one specific finding on US. In 10 of 11 patients underwent cytology, cytologic results revealed non-diagnostic. In 7 patients who had follow-up US, all NPCs had regrowth. **CONCLUSION:** PTH on FNA washouts is essential to diagnose NPC, although it has variable range. The specific US findings of NPC are concave contour, wrinkle and tear drop sign of cystic wall.

EP064-Three Dimensional Brain Tumor Rendering in Magnetic Resonance Imaging with Use of Open Source Software VR Render

*L.-A Shih*¹, C.-R. Lu², K.-C Liu², H.-S Wu², C.-Y Wei¹

*Chang Bing Show Cwan Memorial Hospital Neurology Taichung city-Taiwan 1 Asian Institute of Telesurgery (IRCAD-Taiwan) Medical Image Research Department -Taiwan*²

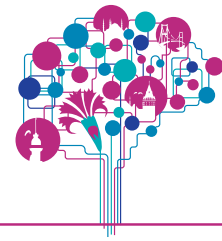
BACKGROUND: Three-dimensional rendering of brain images is more frequently applied in clinical evaluation due to improving computer technology.

OBJECTIVE: Three-dimensional structure of brain tumor was rendered from magnetic resonance imaging by using the software VR Render.

PATIENTS AND METHODS: Two patients who presented with unusual headache and rapidly altered mental status. They were found to have suspected brain tumor with image from 1.5 Tesla magnetic resonance brain scan with contrast. (SENSE-NV_8 coil, Achieva, Philips and 8HRBRAIN coil, EXCITE III, GE) We used three-dimensional virtual model to build three-dimensional image from 0.7-mm images of the brain magnetic resonance imaging. These images were processed with open-source software (VR-Render). Visualization of multiplanar magnetic resonance images was done at first. We then applied color contrast to each layer of tissue and highlighted all the anatomical details precisely.

RESULTS: The tumor morphology was reconstructed successfully in these two patients with the use of the software, VR Render. Information about the tumor includes its shape, size, and cerebral edema it made and vessels it involved, The severity of ventricle compression was also available. Accurate tumor localization was performed using anatomical landmarks and fiducial markers position.

CONCLUSION: Reconstruction of magnetic resonance imaging images provides us information about diagnosis and further treatment in neurosurgery. Three-dimensional rendering of image from brain tumor is still challenging because of variability of size, shape and location of the brain tumor. It's first trial to adapt neurological images on the software VR Render. More studies were needed for improving image precision, establishing standard protocol and being integrated into augmented reality in neurosurgery.



POSTER PRESENTATIONS ABSTRACTS

EP065-Small Lesions Involving Scalp and Skull in Pediatric Age

*Jeong Hyun Yoo*¹

*Ewha womans Univ Mokdong Hospital Radiology Seoul-Korea, South*¹

PURPOSE: 1.To illustrate various lesions involving scalp and skull in the pediatric age. 2.To learn characteristic radiologic findings involving scalp and skull lesions in pediatrics. 3.To provide the teaching points for the accurate differential diagnosis.

METHOD: We retrospectively reviewed CT and MR images of many diseases involving scalp and skull in the pediatric age. We tried to use most cases were proven by surgery. And we tried to show many cases if the same disease had the different sites (eg. skull or scalp or both of them involvements) or different disease state (simple or complicated or combined other disease).

RESULTS: There are various lesions involving scalp and skull in the pediatric age. These lesions range from the congenital lesions such as dermoid and epidermoid, vascular lesions such as hemangioma or vascular malformation, benign and malignant tumors including primary and secondary lesions such as Langerhans cell histiocytosis, metastasis from neuroblastoma, and others including bone lesions such as osteoma, cephalhematoma, etc... Those lesions can be located in the scalp only, or calvarium or both of them. It is often difficult to provide correct diagnosis and requires characterizing these lesions for the differential diagnosis.

CONCLUSION: There are various lesions involving scalp and skull in pediatric age. This review can provide basic knowledge and differential diagnostic points using the CT and MR images.

EP066-Detectability and Anatomical Correlation of Middle Ear Cholesteatoma Using Fused Thin Slice Non Echo Planar Imaging Diffusion Weighted Image (FTS-nEPID)

*Masafumi Kanoto*¹, Yoshihiro Konno¹, Takaaki Hosoya¹, Fumika Watarai¹, Yukio Sugai¹,

Tomoo Watanabe², Seiji Kakehata²

*Yamagata University Faculty of Medicine Dept. of Diagnostic Radiology Yamagata-Japan*¹ *Yamagata*

*University Faculty of Medicine Dept. of Otolaryngology Head and Neck Surgery -Japan*²

PURPOSE: Middle ear cholesteatomas show high intensity on diffusion weighted images (DWIs). DWI can distinguish cholesteatomas from granulation and fluid collection. However, images of the middle ear are unclear in a normal DWI with echo planar imaging (EPI) because they are

susceptibility to artifacts. We performed fused thin slice non EPI DWI and MR cisternography (FTS-nEPID) for cholesteatoma patients to increase the detectability of FTS-nEPID for cholesteatoma.

METHODS: The subjects are 70 consecutive patients who underwent FTS-nEPID as a preoperative study. Otorhinolaryngologists performed the operation. We anatomically classified the middle ear into four portions (attic, tympanic cavity, mastoid antrum and mastoid cell). An experienced radiologist evaluated the images for cholesteatoma and assessed the anatomical invasive range in four portions using only FTS-nEPID. We classified large cholesteatomas that invaded in more than three portions

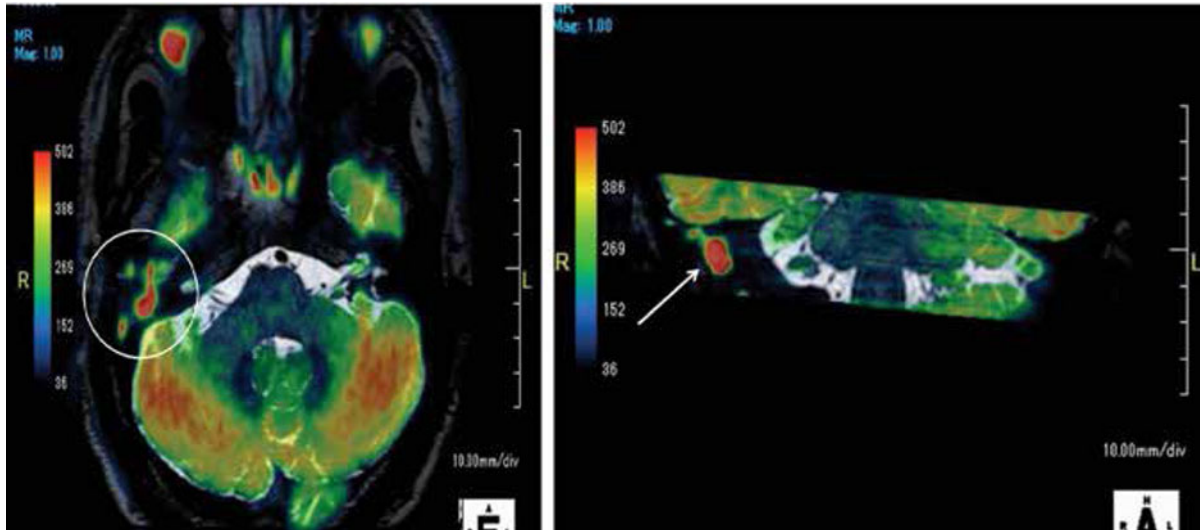
and small ones invaded in less than two portions based on the results obtained from surgery, and calculated the sensitivity, specificity, positive predictive value (PPV) and negative predictive value (NPV).

RESULTS: For large cholesteatomas where the patient has an existing diagnosis, a radiologist could identify cholesteatomas in all cases. In anatomical evaluation, the sensitivity, specificity, PPV and NPV were 51%, 57%, 88%, and 18%, respectively. For small cholesteatomas with an existing diagnosis, the sensitivity, specificity, PPV and NPV were 59%, 78%, 92%, and 30%, respectively. In anatomical evaluation, the sensitivity, specificity, PPV and NPV were 40%, 85%, 60%, and 71%, respectively.

CONCLUSIONS: FTS-nEPID is useful for detecting large and small cholesteatomas. However, further research is needed for anatomical evaluation because there were many false negative results.



POSTER PRESENTATIONS ABSTRACTS



EP067-An in vivo MRI Study of cuprizone Induced Demyelination of C57BL/6 Mouse at 7.0T

Tingting Nie¹, Yanlong Jia¹, Gen Yan¹, *Renhua Wu*¹

The Second Affiliated Hospital, Shantou University Medical College Department Of Radiology -China¹

OBJECTIVE: Cuprizone (CPZ)-induced demyelination of C57BL/6 mouse model was widely recognized and used to explore multiple sclerosis (MS)-like brain lesions. In this study, we assessed MS-like brain lesions using T2-weighted imaging and diffusion tensor imaging (DTI).

METHODS: C57BL/6 mice were scanned with a 7.0 T MRI scanner (Agilent, USA) respectively after four weeks 0.2% CPZ-containing diet and regular chow diet using fsems (TR/TE=2000ms/48ms) and fsemsdw_ dual (TR/TE=2000ms/36ms, b=1000 s/mm² = 14.65 ms) sequences. Then we calculated the normalized T2 signal intensity (a ratio of T2 signal intensity of corresponding region and ventricle) and measured fractional anisotropy (FA) value, axial diffusivity and radial diffusivity of each region. Regions of interest included cerebral cortex (CTX), caudate putamen (CP), hippocampus (HP) and thalamus (TH).

RESULTS: Compared with controls, obvious increased normalized T2 signal intensities were observed in CTX (p<0.01), HP (p<0.01) and CP (p<0.01), which was mild in TH (p=0.119). Reduced FA values were evident in areas of CTX (p=0.01), HP (p<0.05) and CP (p<0.05), which was also mild in TH (p=0.136). In the regions of reduced FA, an increase in radial diffusivity (p<0.05) and a less pronounced decrease of axial diffusivity (p=0.256) were found.

CONCLUSIONS: DTI is sensitive to detecting cuprizone-induced demyelination of C57BL/6 mouse, reflecting tissue structure. Our results also indicate that the decreases of FA may more likely due to increased radial diffusivity. The data provide further support for white matter abnormalities particularly contributing to MS-like brain lesions in CPZ-fed mice.



POSTER PRESENTATIONS ABSTRACTS

EP068-Imaging Features of Orbital Neoplasm Developed in Pediatrics

*Jeong Hyun Yoo*¹

*Mokdong Hospital Radiology Seoul-Korea, South*¹

PURPOSE: A wide spectrum of benign and malignant neoplasms can arise in the pediatric orbit. Imaging plays an important role in the diagnosis and management by depicting the lesion and its extent. The purpose of this study is to illustrate the imaging features of various orbital neoplasms encountered in pediatrics.

METHODS: We retrospectively reviewed our imaging record and collected representative cases of pediatric orbital neoplasm. We categorized orbital diseases based on their tissue of origin into tumors of mesenchymal origin, neural origin tumors, and vascular malformations or tumors, and we added congenital orbital masses. We try to illustrate the best imaging features of the various diseases with the review of teaching points.

RESULTS: The mesenchymal origin tumors were included rhabdomyosarcoma, Langerhans cell histiocytosis, leukemia and lymphoma. Neural origin tumors of orbit were included retinoblastoma, optic nerve glioma, meningioma, schwannoma, neurofibroma and neuroblastoma.

Vascular masses were included capillary hemangioma, orbital lymphangioma, orbital varix, cavernous hemangioma, arteriovenous malformation, carotid cavernous fistula, vascular mass related with syndrome such as PHACE syndrome, choroid angioma in the Sturge-Weber syndrome.

Congenital orbital masses were dermoid and epidermoid, lipoma, coloboma, persistent primary hyperplastic vitreous (PHPV), coats disease, congenital cyst, cephalocele.

CONCLUSION: Imaging plays an important role in the diagnosis and management of wide range of pediatric orbital diseases.

EP069-Imaging Characteristics of Intraorbital and Circumorbital Lesion a Pictorial Review

*Ayako Yoshida*¹, Yusuke Uchiyama¹, Norimitsu Tanaka¹, Toshi Abe¹

*Kurume University School of medicine Radiology Kurume-Japan*¹

PURPOSE: The purpose of this educational exhibit is: 1) to review various radiographic manifestations of intraorbital and circumorbital lesions by utilizing computed tomography (CT) and magnetic resonance (MR) imaging, 2) to discuss characteristic imaging features that can help differential diagnosis to these lesions.

METHODS: This retrospective case review of clinically and pathologically proved orbital lesions has been accumulated over 5-year time period at our institution. Imaging studies (CT and MR imaging) was performed, and illustrate the findings and complement the succinct review of various diseases within the orbit and circumorbital regions. Examples discussed include, but are not limited to, the following: infection, neoplasm, inflammation and vascular anomalies.

RESULTS: The following types of intraorbital lesions are included in this review: abscess, adenoid cystic carcinoma, inflammatory pseudotumor, dermoid cysts, hemangioma, orbital varix, orbital lymphoproliferative disease, nerve sheath meningioma, and IgG4-related sclerosing disease.

CONCLUSIONS: A wide spectrum of orbital and circumorbital lesions is seen, and multimodality imaging approach plays a crucial role in the diagnosis and management of these entities. Some lesions have characteristic imaging findings. Through illustrative case examples, we can help to differential diagnosis for these lesions.



POSTER PRESENTATIONS ABSTRACTS

EP070-Imaging Spectrums of Common Dental Disease Encountered on Facial Bone CT What the Radiologist Needs to Know

*JeeYoung Kim*¹, *SooAh Im*²

*Yeouido St. Mary Radiology Seoul-Korea, South*¹ *Seoul St. Mary Radiology -Korea, South*²

To illustrate the CT findings of common dental disease encountered on facial bone CT. Dental disease is common clinical problem and frequently encountered on facial bone CT. However, the radiologist are frequently skip the mention about dental lesion in the report of facial bone CT. We review the normal anatomy of the jaw and address definition and describe the CT imaging features of common dental disease such as cyst, tumor, tumor-like conditions, and some inflammatory condition.

In this exhibition, we described the imaging findings of common dental disease encountered on facial bone CT. The knowledge of these finding is helpful for differential diagnosis of dental disease.

EP071-Shear Wave Elastography for the Evaluation of Diffuse Thyroid Gland Pathology Preliminary Results

*See-Sung Choi*¹, *Se-Jeong Jeon*¹

*Wonkwang University Hospital Radiology Iksan-Korea, South*¹

PURPOSE: To assess whether shear wave elastography can differentiate normal from pathological thyroid parenchyma.

METHODS: We evaluated 34 subjects (mean age 39.7 ± 15.3 years, 19 women and 15 men): 15/34 were control group (normal thyroid function), and 19/34 were disease group. In disease group, 15 (78.9%) patients had Graves' disease, 3(15.8%) had Hashimoto's thyroiditis (diagnosed by specific tests), 1 (5.3%) had diffuse thyroid goiter. In all patients, 2 to 4 elastographic measurements were made in the both thyroid lobes, using a 4-9 MHz linear probe. Median values were calculated for thyroid stiffness and expressed in kPa.

RESULTS: Thyroid stiffness (TS) assessed by means of shear wave in healthy subjects (20.83 ± 4.98 kPa) was significantly lower than in diffuse thyroid disease (37.13 ± 30.21 kPa) ($P = 0.006$).

CONCLUSION: Shear wave seems to be a useful method for the assessment of diffuse thyroid gland pathology. Also, we expect that shear wave elastography can seem to evaluate for effect of treatment and can use by tool for follow up in patients who have diffuse thyroid disease.

EP072-Review of Orbital Trauma

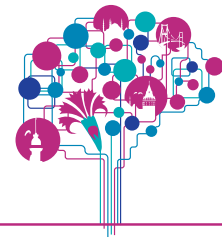
*Warinthorn Phuttharak*¹, *Patanaree Luanratanakorn*², *Vallop Laopaiboon*¹

*Khon Kaen University Radiology Khon Kaen-Thailand*¹ *Khon Kaen University Ophthalmology -Thailand*²

PURPOSE: 1) To provide an overview of orbital trauma imaging
2) To review and illustrate common CT findings in orbital trauma
3) Discuss clinical relevance of the imaging findings and potential treatment options

METHODS: We retrospectively reviewed all CT studies of patients with orbital trauma presenting during the past 5 years at our institution.

FINDINGS/DISCUSSION: The presentation will be a pictorial essay format covering the following details : 1) Brief review of orbital anatomy; 2) CT findings of orbital trauma such as fractures, extraocular muscle entrapment, globe injury, orbital hemorrhage, orbital emphysema, lens dislocation; 3) Review of potential complications associated with orbital trauma; 4) Discussion of clinical relevance and potential treatment options



POSTER PRESENTATIONS ABSTRACTS

CONCLUSION: CT scan has come to play a major role in the orbital examination of acute trauma patients. After review this educational presentation, readers should have an understanding of 1) Orbital anatomy ;2)CT findings in orbital trauma and potential complications; 3) Clinical relevance of imaging findings and treatment options.

EP073-Imaging Spectrum of Orbital Pathologies at the Lacrimal Fossa

*Warinthorn Phuttharak*¹, Pattanaree Luanratanakorn², Laopaiboon Vallop¹

*Khon Kaen University Radiology Khon Kaen -Thailand*¹ *Khon Kaen University Ophthalmology -Thailand*²

PURPOSE: 1) To review and illustrate CT,MRI findings in common orbital pathologies at the lacrimal fossa
2)To differential diagnosis of these various pathologies
3)Discuss clinical relevance and potential treatment options

METHODS: We retrospectively reviewed all CT,MRI studies of patients with lacrimal fossa pathologies presenting during the past 5 years at our institution.

FINDINGS/DISCUSSION: The presentation will be a pictorial essay format covering the following details : 1) Brief review of the lacrimal fossa anatomy; 2) CT,MRI findings of common pathologies at the lacrimal fossa ; 3) Review key imaging findings to aid in the differential diagnosis of these various pathologies ; 4) Discussion of clinical relevance and potential treatment options

CONCLUSION: Many different pathological entities arise from the lacrimal fossa and each of them requires a different treatment approach, the radiological characterization of each lesion is crucial. CT and MRI have come to play an important role in the patients with orbital pathologies at the lacrimal fossa. After review this educational presentation, readers should have an understanding of 1) Lacrimal fossa anatomy ; 2) CT and MRI findings in common pathologies at the lacrimal fossa; 3) The differential diagnosis of these various pathologies; 4) Clinical relevance and treatment options.

EP074-Facial Nerve Imaging and Pathology

*Warinthorn Phuttharak*¹, John Hesselink²

*Khon Kaen University Radiology Khon Kaen -Thailand*¹ *UCSD Medical Center Radiology -United States*²

PURPOSE: To review the clinical neuroanatomy and imaging of the facial nerve and its pathologies.

METHODS: This exhibit aims to review the essential neuroanatomy of the facial nerve including its origin, intra and extracranial course, and function. It also covers the imaging of the facial nerve in health and disease within numerous beautiful samples from the authors personal case collections.

RESULTS: A wide spectrum of disease processes can involve the facial nerve including lesions of inflammatory, infectious, neoplastic, posttraumatic, vascular etiologies and even congenital entity.

CONCLUSION: Anatomy and imaging of the facial nerve is certainly fascinating due to being one of the most complex area in the human body.A basic understanding of facial nerve anatomy and knowing spectrum of various facial nerve pathology in both CT, MRI can be of great utility to the practicing neuroradiologists.

EP075-Evaluation of Predictive Value of Diffusion Weighted MRI Parameters for Early Response to Chemotherapy of Recurrence Laryngeal Carcinoma

*Jelena Mihailovic*¹, Vesna Vukovic¹

*National cancer research centre Diagnostic radiology Belgrade-Serbia*¹

PURPOSE: Laryngeal cancer represents one of the most common head and neck malignancies [1]. Therefore, chemo/radiotherapy has become an integral part of potentially curative therapy for these types of cancers and



POSTER PRESENTATIONS ABSTRACTS

has been increasingly used to achieve the goals of organ preservation [2]. If the outcome can be predicted before or at an early stage of treatment, the patient could also be spared from ineffective and unnecessary toxicity.

The purpose of this work was to evaluate whether parameters obtained from diffusion-weighted MRI can be used like potential imaging biomarker for early detection of response to cancer therapy. MATERIAL AND METHODS: This study included 10 patients with recurrent laryngeal tumor. MRI examinations were performed using a 1.5 T Siemens Avanto scanner. Diffusion-weighted MRI was done by using a single-shot spin-echo echo-planar sequence with 6 b-values. The apparent diffusion coefficient (ADC) and kurtosis values were calculated before beginning of chemotherapy and two weeks after receiving the first and the second cycle of chemotherapy. Curves were fitted by equation $\ln(S/S_0) = -bADC + b^2ADC^2K$ and values for ADC and kurtosis were obtained. The ROI was determined on image with $b = 1200 \text{ s/mm}^2$. Results were compared with radiological findings. RESULTS: The average ADC values were lower in tumor before, with values $1.28 \pm 0.30 \times 10^{-3} \text{ mm}^2/\text{s}$, than values obtained after two weeks from the first and the second cycle of chemotherapy, $1.69 \pm 0.20 \times 10^{-3} \text{ mm}^2/\text{s}$ and $1.89 \pm 0.30 \times 10^{-3} \text{ mm}^2/\text{s}$, respectively (Figure 1) with statistical significance between these periods ($p < 0.05$) on t-test. Comparing the initial values with the values after the second course of chemotherapy, tumor response was associated with an increase in kurtosis (0.13 vs 0.16, respectively).

CONCLUSIONS: Our results suggested that tumors with better response tended to alter their internal compositions after chemotherapy. Parameters are potentially useful to monitor the response of a tumor throughout the course of chemotherapy and might predict tumor response early in the course. REFERENCES: A. Jemal, R. Siegel, E. Ward, et al., "Cancer Statistics," CA: A Cancer Journal for Clinicians, Vol. 56, No. 2, 2006, pp. 106-130

S. Conticello, A. Fulcheri, S. Aversa, et al., "Larynx organ preservation in patients with hypopharyngeal-laryngeal cancer," IJOHNS, Vol.2, No. 1, 2013, pp. 27-33

Head and Neck 2

EP076-A Case Report of Congenital Dacryocystocele in Neonate MR Findings

*Kenichi Suzuki*¹, Masaaki Hori², Eiichi Kohta¹, Hideaki Suzuki¹, Masahiro Kobayashi¹, Junichi Kodera¹, Keiko Matsumoto¹, Sunao Mizumura¹, Nobuyuki Shiraga¹

*Toho University Department Of Radiology Tokyo-Japan*¹ *Juntendo University Department Of Radiology -Japan*²

We report a case of congenital dacryocystocele with magnetic resonance imaging (MRI) findings.

Congenital dacryocystocele is an uncommon type of nasolacrimal duct obstruction.

It is caused by obstruction of two valves. Initially, valve of Hasner which is distal valve is obstructed anatomically, causing lacrimal sac distension. Then, valve of Rosenmuller which is proximal valve is obstructed with distended sac and works as a check valve.

As it grows rapidly and may cause respiratory distress with nasal cavity obstruction, it is important to diagnose this disease with MRI. It is also essential to evaluate various complications, such as epiphora, dacryocystitis, periorbital cellulitis, sepsis, etc.

Case report: A 7-day-old female infant presented as a bluish medial canthal mass. She had no problems about pregnancy or birth.

She was diagnosed as congenital dacryocystocele by MRI.

MRI demonstrated cystic lesion in the left medial canthal area extending to the nasal cavity. This finding was considered cylindrically expanded lacrimal sac and expanded lacrimal duct. Partial maximum intensity projection (MIP) images revealed the details of the cystic lesion more precisely than conventional MR image. Axial T2-weighted image (T2WI) showed niveau in the lacrimal sac suggesting associated infection.

She was planned for surgery, but not available, because of dacryocystitis as a complication. Follow up study showed spontaneous drainage due to the destruction of the Hasner valve by abscess.



POSTER PRESENTATIONS ABSTRACTS

The mass reduced the size, and there was not the re-increase afterwards.

CONCLUSION: We report a case of congenital dacryocystocele. MIP image reconstructed with MRI is useful for diagnosis, especially with understanding the location of the expanded nasolacrimal canal and lacrymal duct. And MRI can also exclude tumorous condition and evaluate complications, which decide the indication of operation.

EP077-Diffusion Tensor and Resting State Connectivity Mapping in Deep Brain Stimulation Patients at Very Low RF Power A Feasibility Study

Subhendra N Sarkar ¹, Michael D Fox ², David B Hackney ¹, Ludy C Shih ³, Fernando A Barrios ⁴, Ron L Alterman ⁵, Efstathios Papavassiliou ⁶, *Rafael R Rojas* ¹

Beth Israel Deaconess Medical Center, Harvard Medical School Radiology -United States ¹ *Beth Israel Deaconess Medical Center and Massachusetts General Hospital, Harvard Medical School Neurology -United States* ² *Beth Israel Deaconess Medical Center, Harvard Medical School Neurology -United States* ³ *National Autonomous University of Mexico, Queretaro, Mexico -United States* ⁴ *Beth Israel Deaconess Medical Center, Harvard Medical School Neurosurgery -United States* ⁵ *Beth Israel Deaconess Medical Center, Harvard Medical School Neurosurgery -United States* ⁶

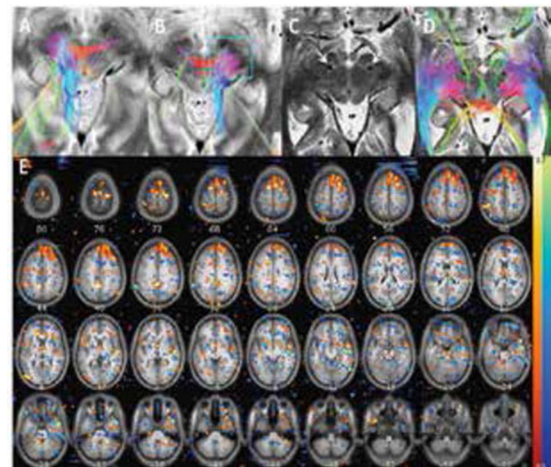
PURPOSE: Patients with deep brain stimulators (DBS) are unable to undergo most MRI sequences due to RF heating concerns. This affects clinical MRI quality as well as potential MR research using diffusion tensor imaging (DTI) and resting state functional MRI (rs-fcMRI) offering structural and functional connectivity. This information could improve DBS placement (1) and understanding of stimulation effects on brain connectivity (2). Building on prior low RF power (low-SAR) anatomical imaging work (3), we developed and tested very low SAR MRI sequences for DTI and rs-fcMRI within the SAR regulatory guidelines of <0.1W/kg.

METHOD AND MATERIALS: Using stretched RF pulses and modified RF flip angles (3) nine Parkinson's disease patients with DBS electrodes in place were imaged at 1.5T using low-power MPRAGE, FSE-STIR and high resolution DTI (2x2x3 mm³ voxel) in less than 30 min. White matter fiber tracts and fractional anisotropy (FA) values were computed using NordicBrainEX DTI Module and compared with pre-implantation high-SAR sequences. Additionally 3 Parkinson's patients with DBS electrodes in place were imaged by a single-shot EPI sequence (TR/TE/Voxel=2s/50ms/4x4x5mm³/interleaved). Motion corrected, normalized images were co-registered with 3D MPRAGE and the resting state default mode network was computed using posterior cingulate as a seed region (4).

RESULTS: The basic arrangement and topography of WM fiber tracts were similar in thalamic and subthalamic regions using conventional high-SAR sequences pre-implantation (panels A,B) and with our novel low-SAR DTI post DBS (panels C,D). FA values were within 10% for pre-and- post DBS (mean FA, 0.41 pre, and 0.38, post-DBS within substantia nigra, P<0.05). Resting state EPI images were somewhat noisy and showed susceptibility artifact from the subcutaneous DBS connecting wires in the temporal lobes, however distributed correlation patterns reminiscent of the default mode network were apparent (panel E).

CONCLUSION: Low-power MRI images were adequate for assessing targeting accuracy and allowed reproducible FA computation. Functional connectivity may be extracted by low-SAR EPI for safe MR monitoring of functional network changes caused by DBS therapy.

REFERENCES: (1) Henderson: *Front. Integr. Neurosci* 24 April 2012. (2) Kahan et al: *Brain* Feb 2014;1-15. (3) Sarkar et al: *Radiology* 2011;259:550. (4) Fox et al: *Nat Rev Neurosci* 2007;700-711.





POSTER PRESENTATIONS ABSTRACTS

EP078-Diagnosis and Treatment Outcome in Orbital Extra Ocular Muscle and Retro Bulbar Optic Nerve Cysticercosis

*Raj Kumar Rauniyar*¹, Mukesh Kumar Gupta², Kalim Ahmed², AK Pant²

*B.P.Koirala Institute of Health Sciences Radio-diagnosis and Imaging Dharan-Nepal*¹ *B P Koirala Institute of Health Sciences Dept. of Radio-diagnosis and Imaging, -Nepal*²

INTRODUCTION: In the orbit the lesions of cysticercosis are usually seen adjacent to the layers of eyeball involving vitreoretinal and sub-conjunctival spaces. Extra ocular cysticercosis can involve orbital muscle (myocysticercosis) but involvement of the optic nerve is extremely rare.

AIM: To evaluate the role of imaging in orbital cysticercosis and to follow the cases for treatment outcome. The secondary aim is to describe the imaging features of orbital cysticercosis.

METHOD: Ultrasonography (USG) and Computed Tomography (CT) were used to evaluate patients with proptosis. Six patients were diagnosed as having orbital myocysticercosis and two patients having optic nerve cysticercosis. These all cases were treated with oral albendazole and corticosteroid. Follow up was undertaken with USG and CT.

RESULT: USG features were confirmatory of myocysticercosis in five eyes where as CT was effective in diagnosing the condition in all eight cases. In three patients the medial rectus was involved, in two the superior rectus and, in the other, the inferior rectus muscles. Serial USG and CT revealed complete resolution of the lesions in 3 months.

CONCLUSION: CT is useful method in diagnosing isolated orbital myocysticercosis and optic nerve cysticercosis. Our report demonstrated that ophthalmic signs and symptoms in the presence of proptosis, especially in an endemic region, should alert the clinician to the possibility of the condition. Though CT is superior, USG can be used as an economical follow up investigation. The response to treatment with oral Albendazole and corticosteroid is very effective in curing the condition.

EP079-Histogram Analysis of Dynamic Contrast Enhanced MR Imaging for Distinguishing between Squamous Cell Carcinomas and Malignant Lymphoma of the Oropharynx

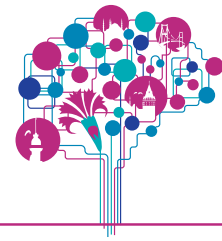
*Jinna Kim*¹, Mina Park¹, Yoon Seong Choi¹, Sung Jun Ahn¹, Seung-Koo Lee¹

*Yonsei University College of Medicine Radiology Seoul-Republic of Korea*¹

PURPOSE: The purpose of this study was to investigate the usefulness of histogram analysis of dynamic contrast-enhanced MR imaging (DCE-MRI) parameters for distinguishing between squamous cell carcinoma (SCC) and malignant lymphoma of the oropharynx.

METHODS: DCE-MRI was prospectively performed in 21 patients with oropharyngeal SCC and 5 patients with oropharyngeal lymphoma, and parameter maps including K_{trans} (microvascular permeability), V_e (extravascular-extracellular space volume), and V_p (plasma volume) were obtained. Enhancing tumors were manually segmented on each slice of parameter maps and data were collected to obtain a histogram for the entire tumor volume. Mean, median, skewness, and kurtosis of the parameters were calculated and compared between the oropharyngeal SCC and lymphoma.

RESULTS: From the histogram analysis of K_{trans} maps, mean, minimum, maximum, 25th percentiles, and 75th percentiles value of the oropharyngeal SCC were higher than those of oropharyngeal lymphoma but no significant difference was observed among them. Only the kurtosis of K_{trans} value was significantly different between the oropharyngeal SCC and lymphoma (P = 0.041). Other DCE parameters including V_e and V_p, did not significantly differ between the two types of tumor.



POSTER PRESENTATIONS ABSTRACTS

CONCLUSIONS: Our preliminary evidence using histogram analysis of DCE-MRI parameters (Ktrans) based on whole tumor volume suggests that it may be useful to differentiate SCC from malignant lymphoma of the oropharynx.

EP080-Application of Dynamic Contrast Enhanced MR Imaging in Head and Neck Squamous Cell Carcinoma A Correlation study of DCE Parameters with Clinicopathologic Characteristics by Histogram Analysis

*Jinna Kim*¹, Mina Park¹, Seung-Koo Lee¹, Meng Law², Mark Shiroishi²

Yonsei University College of Medicine Radiology Seoul-Republic of Korea *1 University of Southern California Radiology -United States*²

PURPOSE: The purpose of this study was to investigate the usefulness of histogram analysis of dynamic contrast-enhanced MR imaging (DCE-MRI) parameters for assessing the clinicopathologic characteristics in the patients with head and neck squamous cell carcinoma (HNSCC).

METHODS: DCE-MRI was performed in a total of 18 consecutive patients with pathologically-confirmed head and neck SCC, and DCE-MRI parameter maps including Ktrans (microvascular permeability), Ve (extravascular-extracellular space volume), and Vp (plasma volume) were obtained. Enhancing tumors were manually segmented on each slice of parameter maps and data were collected to obtain a histogram for the entire tumor volume. Mean, median, skewness, and kurtosis of the parameters were calculated and they were correlated with the clinicopathologic characteristics including tumor differentiation, T stage, N stage, TNM stage, presence of lymphovascular and perineural invasion.

RESULTS: From the histogram analysis of Ktrans maps, mean, median, and kurtosis of the tumors with poor or moderate differentiation, higher stage, presence of lymphovascular and perineural invasion were lower than those of the tumors with well differentiation, lower stage, absence of lymphovascular and perineural invasion, but no significant difference was observed among them. Only the skewness of Ktrans value was significantly different between the tumors according to tumor differentiation (P = 0.005), tumor stage (P = 0.018), and presence of perineural invasion (P = 0.046).

Other DCE parameters including Ve and Vp, did not significantly differ between the groups. CONCLUSIONS: Our preliminary evidence using histogram analysis of DCE-MRI parameters (Ktrans) based on whole tumor volume suggests that it may be useful to predict clinicopathologic characteristics of HNSCC.

EP081-Comparisons of Contrast Enhancement on Inner Ear among Patients with Unilateral Otologic Symptoms in 3D FLAIR MR Images at 10 minutes and 4 Hour after Gadolinium Injection

*Dong Woo Park*¹, Tae Yoon Kim¹, Chung Ki Park¹, Young Jun Lee¹, Ji Young Lee¹

*Hanyang University College of Medicine Radiology Guri-Si-Korea, South*¹

PURPOSE: To compare the signal intensity of the inner ear in patients with unilateral symptomatic ear disease, between 10 minutes and 4 hours delayed intravenous gadolinium enhanced three-dimensional fluid attenuated inversion recovery magnetic resonance images (3D-FLAIR MRI), between affected and unaffected sides, between patients with sudden sensorineural hearing loss (SNHL) and non-sudden SNHL patients, and between patients with viral disease and non-viral disease, based on clinical manifestation.

MATERIALS AND METHODS: Total 50 patients with lateralizing otologic symptom, such as hearing loss, tinnitus, ear fullness, nystagmus, vertigo, facial nerve palsy, who underwent 3D-FLAIR MRI with 10 minutes and 4 hours delayed intravenous gadolinium enhancement, from May 2012 to October 2013, were retrospectively analyzed by 2 neuroradiologists blinded to the clinical



POSTER PRESENTATIONS ABSTRACTS

presentation. The signal intensity (SI) ratio of cochlear, vestibule, vestibulocochlear nerve (VCN), Meckel's cavum and cisternal segment of trigeminal nerve to medulla oblongata is calculated and compared. RESULTS: SI ratio of affected cochlea, vestibule, and VCN is higher than unaffected side in both 10 minutes and 4 hours. SI ratio of VCN in non-sudden SNHL patients is higher than sudden SNHL patients in both 10 minutes and 4 hours. Among sudden SNHL patients, SI ratio of affected cochlea with 10 minutes delayed enhancement is significantly higher than unaffected side. SI ratio of VCN in viral disease group is higher than non-viral disease group, in both 10 minutes and 4 hours.

No statistically linear correlation, but positive correlation between mean of 4 hours delayed SI ratio of Meckel's cavum or cisternal segment of trigeminal nerve and 4 hours delayed SI ratio of unaffected cochlea. CONCLUSION: SI ratio of inner ear in 10 minutes and 4 hours delayed intravenous gadolinium enhancement shows statistically significant increase in many diseases, especially viral origin disease. Anatomic discrimination of IE and VCN is better in 4 hours than 10 minutes. Positive correlation of SI ratios between trigeminal nerve and cochlea may represent the relationship of cranial nerve permeability and blood-labyrinth barrier disturbance, but requires further study.

EP082-CT and MR Imaging in Evaluation of Uncommon Sinonasal Malignancies

*Saida Jerbi Omezzine*¹, Radhouane Hamdi², Nouha Turki³, Maher Dhifallah², Nabil Driss³, Hassine Hamza²
*University Hospital Radiology Mahdia-Tunisia*¹ *University Hospital Radiology -Tunisia*² *University Hospital Otolaryngology -Tunisia*

PURPOSE: The study purpose was to determine the value of magnetic resonance imaging (MRI) and computed tomography (CT) in evaluation of sinonasal neoplasms.

MATERIALS AND METHODS: Twelve patients (8 females and 4 males) were complaining of symptoms related to sinonasal tract. After thorough clinical and local examination, the patients were subjected to the following: CT, MRI, and histopathological examination.

RESULTS: The nasal cavity was the most commonly involved site with sinonasal malignancies followed by the maxillary sinuses.

Malignant sinonasal tumors were present in 12 cases: adenoid cystic carcinoma (n=2), esthesioneuroblastoma (n=3), mucosal melanoma (n=2), sinonasal undifferentiated carcinoma (n=1), sinonasal lymphoma (n=2), chondrosarcoma (n=1) and plasmacytoma (n=1).

CONCLUSION: Primary sinonasal malignancies constitute only 3% of head and neck malignancies and only 0.2% to 0.8% of all malignancy. Exact staging necessitates a clinical and endoscopic examination with biopsy and imaging. Both CT scan and MR imaging are required to accurately determine the extent of local disease. MRI with its superior soft tissue contrast and multiplanar capability is superior to CT in pretreatment evaluation of primary malignant tumors of sinonasal cavity.

EP083-Primary Malignant Mucosal Melanoma of Nasopharynx an Unusual Cause of Unilateral Hearing Loss

Tümay Bekci¹, *Kerim Aslan*¹, Hediye Pınar Günbey¹, Lütfi İncesu¹
*Ondokuz Mayıs University Faculty of Medicine Department of Radiology Samsun-Turkey*¹

There are many causes of unilateral hearing loss. To make a differential diagnosis especially in the elderly patients is difficult. Primary malignant mucosal melanoma of nasopharynx is extremely rare and can cause a variety of symptoms. Hearing loss, as a presenting symptom of mucosal malignant melanoma of nasopharynx, has not been defined in the literature yet. Here in, we report a case of primary mucosal malignant melanoma of nasopharynx presented with unilateral hearing loss in a 75-year-old male. We think it is essential to keep in mind nasopharyngeal tumors as a cause of unilateral hearing loss and also it is important to be familiar with imaging features of nasopharyngeal mucosal malignant melanoma as an extremely rare tumour of this region.



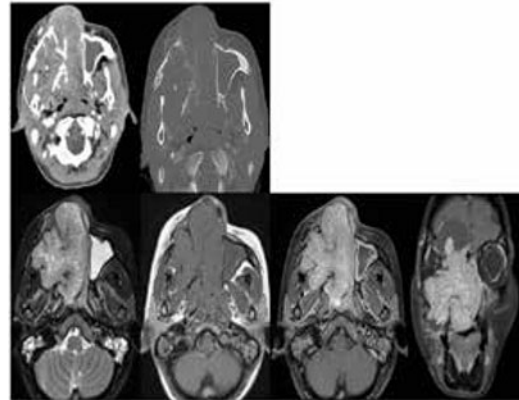
POSTER PRESENTATIONS ABSTRACTS

EP084-Pictorial Review of Sinonasal Malignancies

*Patrick Tze Hern Teo*¹

*National Cancer Centre Singapore Oncologic Imaging
Singapore-Singapore*¹

Sinonasal tumors are rare and account for 3% of head and neck neoplasms. Imaging plays a critical role in the management of sinonasal tumors as they can be intimately related to critical structures of the anterior and central skull base. Mapping the extent of the tumour has important implications for staging, treatment and prognosis. This pictorial essay showcase a series of different histological types of sinonasal tumours (Olfactory neuroblastoma, sarcoma, squamous cell carcinoma, sinonasal undifferentiated carcinoma, adenoid cystic carcinoma, lymphoma as well as recurrent tumour post surgical resection) with emphasis on imaging features which have impact and implications for staging and potential for surgical resection.



Tumor: left Post-contrast CT scan, Right CT Bone window, Axial MRI T1w, Right MRI T2w, Sagittal MRI T1w, Sagittal MRI T2w, Sagittal MRI T1w with contrast, Sagittal MRI T2w with contrast, Sagittal MRI T1w with contrast, Sagittal MRI T2w with contrast.
40-year-old Chinese female with an aggressive nasal cavity mass with bone destruction of the right maxillary sinus and involvement of the sphenoid plate and intracranial extension. First biopsy revealed an inverted papilloma. Repeat biopsies were performed as the imaging appearance suggested a more aggressive pathology. Final pathology was consistent with carcinoma.

EP085-Solitary Fibrous Tumor of the Nasal Cavity a Case Report

*Yukihiro Ogihara*¹, Minoru Morikawa¹, Ninpei Yamaguchi², Haruo Takahashi², Sadanori

Akita³, Akiyoshi Hirano³, Naoe Kinoshita⁴, Junya Fukuoka⁴, Masataka Uetani¹

*Nagasaki University Department of Radiology Nagasaki-Japan*¹ *Nagasaki University Department of Otolaryngology - Head and Neck Surgery -Japan*² *Nagasaki University Department of Plastic and Reconstructive Surgery -Japan*³ *Nagasaki University Department of Pathology -Japan*⁴

PURPOSE: Solitary fibrous tumor (SFT) is an uncommon spindle cell tumor of mesenchymal origin. SFTs usually arise from the visceral or parietal pleura and peritoneum, and found in many areas throughout the body, but SFTs of the nasal cavity and paranasal sinuses are extremely rare. We report a case of SFT of the nasal cavity.

METHODS: A 25-year-old male was admitted to our hospital because of slurred speech with a left nasal mass. We performed physical examination, MRI, CT and digital subtraction angiography (DSA).

RESULTS: MRI showed a nasal cavity tumor consisted of 6 cm in greatest diameter with intermediate signal intensity on T1-weighted images, high signal intensity on T2-weighted images, and inhomogeneous enhancement with gadolinium. CT angiography and digital subtraction angiography revealed the tumor originated from the left lateral nasal wall and supplied by the sphenopalatine artery. Embolization of the feeding artery and transmucosal injection sclerotherapy were performed to reduce arterial flow before tumor resection.

CONCLUSIONS: The tumor was successfully resected and was removed through the oral cavity. The postoperative course has been uneventful without signs of recurrence at 1 year after surgery. Pathological diagnosis was obtained by means of immunohistochemical analysis, which showed vimentin and CD34 cells.

EP086-CT and MR Findings of the Intraosseous Lipoma of the Sphenoid Bone

*Yeliz Pekcevik*¹, Ilker Burak Arslan², Yildiz Arslan³

*Izmir Tepecik Training and Research Hospital Radiology Izmir-Turkey*¹ *Izmir Tepecik Training and Research Hospital Head and Neck Surgery -Turkey*² *Izmir Tepecik Training and Research Hospital Neurology -Turkey*³

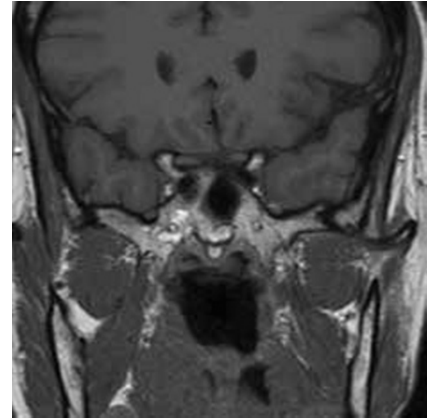
PURPOSE: Intraosseous lipoma is very rare, usually benign tumor of flat bones. Imaging features associated with suspected intraosseous lipoma can mimic more aggressive pathology. The features of this poorly described entity in the skull base were analyzed to aid the radiologist in differentiation from other pathologies.

METHODS: CT and MR imaging findings of the incidentally diagnosed intraosseous lipoma within the sphenoid bone were reviewed.



POSTER PRESENTATIONS ABSTRACTS

RESULTS: Four patients were identified with intraosseous lipoma located in the sphenoid bone. The diagnosis was established due to the characteristic CT and MR imaging features. **CONCLUSION:** Intraosseous lipoma is believed to be a more common benign intraosseous lesion within the skull base than previously reported. Cortical bone thinning and other features normally suggestive of aggressive pathology commonly occur. Radiologists should be aware of these common lesions to avoid unnecessary further investigation.



EP087-False Positivity of Diffusion Weighted Imaging for Revealing Squamous Cell Carcinoma of the Palatine Tonsil

*Yeliz Pekcevik*¹, Ibrahim Cukurova², İlker Burak Arslan²

*Izmir Tepecik Training and Research Hospital Radiology izmir-Turkey*¹ *Izmir Tepecik Training and Research Hospital Head and Neck Surgery -Turkey*²

PURPOSE: Detection of carcinomas in the palatine tonsil can be difficult on conventional imaging using CT or MR imaging because tumors at this site are rarely necrotic and can have a homogeneous appearance similar to that of lymphoid tissue in the tonsil. Apparent diffusion coefficient (ADC) values of normal tonsils and squamous cell carcinoma have been reported to be different earlier. However, the discrimination of acute and chronic tonsillitis from squamous cell carcinoma, that has not been previously reported, is challenging. We aim to show some clinical situations that diffusion weighted imaging give false positive results on diffusion-weighted imaging.

METHODS: Diffusion-weighted images were obtained with a single-shot echo-planar imaging (EPI) sequence using a 1.5 Tesla MR imager. The mean apparent diffusion coefficient (ADC) values of normal tonsil, tonsils with squamous carcinoma and with acute and chronic tonsillitis were retrospectively calculated with ROI measurement.

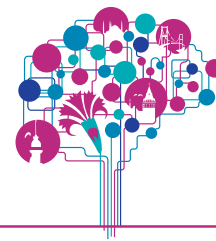
RESULTS: All patients with acute and chronic tonsillitis were previously accepted as tumor due to asymmetric hypertrophy and/or heterogeneous enhancement and low ADC values. ADC measurements of the acute and chronic tonsillitis were found similar with squamous cell carcinoma. **CONCLUSION:** Diffusion weighted imaging has some handicaps in the diagnosis of the squamous cell carcinoma of the palatine tonsil. We should consider conditions that give rise to false positive findings, especially while searching for the site of an unknown primary in head and neck squamous cell carcinoma.

EP088-Two Cases of Clival Chordomas with Atypical Clinical and Radiological Presentation

Ilaria Desideri¹, *Mario Sabato*¹, Ilaria Pesaresi², Roberta Doria³, Michele Puglioli²,

Raffaele Nunziata⁴, Carlo Bartolozzi¹, Mirco Cosottini⁵

*University of Pisa Department of Translational Research and New Technologies in Medicine and Surgery Pisa-Italy*¹ *Unit of Neuroradiology, AOP, Pisa Department of Translational Research and New Technologies in Medicine and Surgery -Italy*² *Unit of Infectious Disease -Italy*³ *Besta Neurologic Institute, Milan -Italy*⁴ *University of Pisa; Unit of Neuroradiology, AOP, Pisa Department of Translational Research and New Technologies in Medicine and Surgery -*⁵



POSTER PRESENTATIONS ABSTRACTS

PURPOSE: We reported two cases of clival chordomas with atypical clinical and radiological presentation.

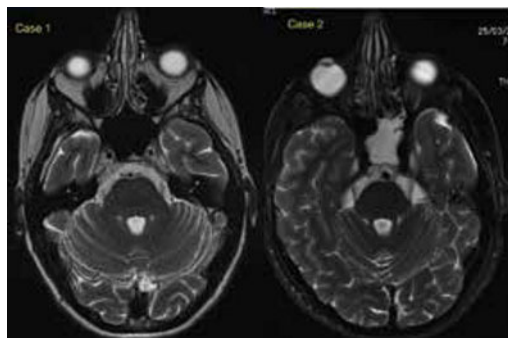
METHODS: Case 1 is a 19 years old woman with progressive appearance of diplopia and bilateral convergent strabismus, ptosis and mydriasis in the left eye.

Case 2 is a 52 years old man with the clinical picture of meningitis secondary to the presence of CSF fistula and pneumocephalus.

Both patients underwent to MRI examination before and after intravenous administration of contrast media, CT examination for the evaluation of bone involvement. Clival lesions were removed with surgical excision and examined at histology.

RESULTS: In our cases chordoma did not manifest as a classic expansile osteolytic clival mass, but in the form of a thin tissutal layer on the surface of the clivus and quadrilateral lamina, that was hyperintense on T2-w images, iso-hypointense on T1-w images and without contrastographic uptake. In case 1 the chordoma extended into the posterior portion of the cavernous sinus enveloping cranial nerves. In case 2 the MR examination shows residual signs of meningitis and the presence of a thin tier of tissue interrupting the clival bone and dura. The communication between the sphenoid sinus and subdural space causes the pneumocephalus.

CONCLUSION: Clival chordoma does not always occur in the typical form of expansive lesion but it can be radiologically subtle manifesting as a thin erosive lamina affecting the sphenoid bone. Accordingly also the clinical manifestation is atypical with oclar nerve palsy, pneumocephalus and meningitis.



EP089-Comparing Radiological Tumor Density and Volume Measurement with Pathological Tumor Stroma Proportion and Volume Measurement; and the Relationship with Prognosis in Patients with Laryngeal Carcinoma

*Eren Özer¹, Emel Ada¹, Mehtat Ünlü², Hasan Oğuz Çetinayak³, Sülen Sarıoğlu², Ahmet Ömer İkiz⁴
Dokuz Eylul University Hospital Department of Radiology Izmir-Turkey¹ Dokuz Eylul University Hospital
Department of Pathology -Turkey² Dokuz Eylul University Hospital Department of Radiation Oncology -Turkey³
Dokuz Eylul University Hospital Department of Otorhinolaryngology -Turkey⁴*

AIM: To compare radiological tumor density and volume measurement with pathological tumor stroma proportion and volume measurement in patients with laryngeal carcinoma treated with surgically. Additional aim of the present study is to investigate if there was any relationship between radiological findings and survival in laryngeal squamous cell carcinoma (LSCCA).

MATERIAL AND METHODS: Thirty patients who underwent total or partial laryngectomy before the date of December 2010, also had record of measurement of the TSP (tumor-stroma proportion) of the tumor in the surgical specimen were enrolled in this study. Patients' preoperative CT studies were reviewed for measurement of tumor density values and primary tumor volume. Tumor characteristics and patients' postsurgical course were recorded retrospectively from the medical archives of the patients.

RESULTS: We could not demonstrate any association between tumor density values and TSP. Median follow up was 51,8 months (range 3 -108). No local disease recurrence was observed among patients. There was no relationship between radiological findings (tumor density values and tumor volume) and overall survival. There was a significant association exists between tumor volume and the pT stage of patient, and also cartilage involvement (respectively p:0,015, p:0,009).



POSTER PRESENTATIONS ABSTRACTS

CONCLUSION: Larger scale prospective studies are needed for investigate the prognostic significance of both tumor density and tumor volume. Although tumour volume is closely associated with T stage and cartilage involvement, it was not identified as prognostic factor for overall survival.

EP090-DCE MRI vs DWI in Nasopharyngeal Carcinoma at 3T Initial Report

*Atilla Kokurcan*¹, Ali Yusuf Öner¹, Ramazan Yildiz², Mustafa Karaca²
*Gazi University Radiology Ankara-Turkey*¹ *Gazi University Oncology -Turkey*²

PURPOSE: To report initial data in the evaluation of quantitative permeability values derived from dynamic contrast-enhanced magnetic resonance imaging (DCE-MRI) together with ADC values of diffusion weighted imaging (DWI) in patients with nasopharyngeal carcinoma

MATERIALS AND METHODS: An institutional review board approval was obtained for this study. A total of 10 patients with NPC were included. Following tumor/node/metastasis (TNM) status and clinical staging conventional, DWI and DCE-MRI following intravenous administration of 0,01mmol/kg of gadoterate meglumine and diffusion sequences were performed for each patient with a 3T scanner. Region of Interests were defined within the nasopharyngeal tumor, masseter muscle and vertebral artery with the help of conventional images. ADC values, Ktrans, Kep and Ve values were then calculated from diffusion weighted and dynamic contrast enhanced images respectively. Quantitative permeability and diffusion data were statistically evaluated.

RESULTS: Both technique together with conventional imaging methods successfully depicted tumor area in all patients. ADC and permeability measurements showed favorable correlation in tumor depiction. This correlation was also found to be present between permeability scores and clinical stage.
CONCLUSION: This initial report indicates that permeability calculation of DCEI is a promising new technique which is expected to help management of treatment and follow up in patients with NPC.

Stroke

EP091-Perfusion CT and Early Thrombolytic Therapy Outcome Our Experiences

*Stipan Jankovic*¹, Ante Buča², Kreimir Kolić², Krešimir Dolić², Sanja Lovrić-Kojundžić²
*¹University Hospital Split Radiology Split-Croatia*¹ *²Universita Hospital Split Radiology -Croatia*²

PURPOSE: The objective of this study was to present our experience with CT perfusion (CTP) compared to noncontrast CT (NCCT) in early diagnosis of acute ischemic stroke at University Hospital Split and to determine the value of these diagnostic procedures in assesment of adequate thrombolytic therapy.

METHODS AND MATERIALS: 87 consecutive patients with acute ischaemic stroke within 3 hours of onset of symptoms underwent Stroke protocol that included NCCT, CTP and MSCTA (MSCT Sensation 16 Siemens). We used 200 ml of nonionic intravenous contrast media iopamidol 370 at an injection rate of 10,0 ml/s. Patients with confirmed presence of an ischemic penumbra recieved thrombolytic therapy (Alteplase).

RESULTS: Ischemic stroke was confirmed in 78,1% patients who were admitted with stroke symptoms to our emergency department. CTP was significantly superior to NCCT in depicting ischemic stroke (41 patients diagnosed with NCCT, in comparison to 68 with CTP, p= 0,008). In 27 cases with negative NCCT there were signs of ischemic stroke on CTP, and 16 of patients with significant penumbra received thrombolytic therapy. NCCT sensitivity (taking CTP as the reference method) was 60,3%. The accuracy of this method was 69%. Negative predictive value of NCCT in comparison to CTP was 41%.

CONCLUSION: CTP is a sensitive tool for identifying early signs of ischemia and it should be done regularly in



POSTER PRESENTATIONS ABSTRACTS

patients presenting with acute ischemic stroke symptoms. It is crucial in determining whether the thrombolysis is appropriate by estimating ischemic penumbra and infarct core.

EP092-Changes in Gray and White Matter Detected on CT Cerebral Perfusion in Patients with Unilateral Cerebral Arterial Stenosis

*Michael Mu Huo Teng Teng*¹, Yi-Hsuan Kao², Chung-Jung Lin³, Feng-Chi Chang³, Wan-Yuo Guo³
 Cheng Hsin General Hospital Medical Imaging Taipei-Taiwan¹ National Yang Min University Biomedical Imaging and Radiological Sciences -Taiwan² Taipei Veterans General Hospital Radiology -Taiwan³

OBJECTIVE: To investigate the perfusion changes in gray matter and white matter in patients with symptomatic unilateral cerebral arterial occlusion or severe stenosis.

MATERIALS AND METHODS: The computed tomography perfusion images of 15 symptomatic patients were retrospectively analyzed. Quantitative measurements of perfusion data were performed after procedures of image registration, removal of bone, vessel, and cerebrospinal fluid voxels, and segmentation of gray and white matter.

RESULTS: According to the measured data on the normal side of the brain, the cerebral volume (CBV) and flow (CBF) for normal gray matter were approximately twice the values of normal white matter. There was CBV increase, CBF decrease, and mean transit time (MTT) prolongation on the symptomatic hemisphere comparing to the contralateral normal brain in both the gray and white matters (white matter CBF: P=0.23, others: P < 0.01). Every patient had an increase in CBV and a decrease in CBF in either or both of the gray and white matters on the symptomatic hemisphere. The percentage changes of CBV, CBF, and MTT on the lesion side from their contralateral normal data were different for gray and white matters: CBV (+13% vs. +20%), CBF (-23% vs. -5%), and MTT (+50% vs. +32%).

CONCLUSION: The absolute values of CBF, CBV, and MTT were different for gray and white matters on the normal hemisphere. In symptomatic hemisphere, there was more decrease in CBF and prolongation of MTT in gray matter than white matter, while more obvious increase in CBV in white matter than gray matter.

Table. Means and standard deviations of CBV, CBF, and MTT measured in gray and white matter region on the normal and lesion sides

	White matter				Gray matter				P value (Normal gray matter vs. normal white matter)
	Normal side	Lesion side	P value	Lesion / Normal ratio	Normal side	Lesion side	P value	Lesion / Normal ratio	
CBV	1.23 ± 0.15	1.47 ± 0.24	*	1.20	2.34 ± 0.26	2.65 ± 0.32	*	1.13	*
CBF	11.1 ± 1.6	10.5 ± 1.3	0.2289	0.95	24.4 ± 3.4	18.7 ± 3.3	*	0.77	*
MTT	6.17 ± 0.69	8.13 ± 1.19	*	1.32	5.80 ± 0.61	8.70 ± 1.27	*	1.50	0.1646

Results of Mann-Whitney U-test: * = P < 0.01. Units: CBV - mL/100 g, CBF- mL/100 g/min, MTT - sec.



POSTER PRESENTATIONS ABSTRACTS

EP093-SWI and DWI Features and Follow Up Imaging Findings of A Case with Cerebral Fat Embolism

*Rahsan Gocmen*¹, Nazire Pinar Acar², Ethem Murat Arsava², Mehmet Akif Topcuoglu²

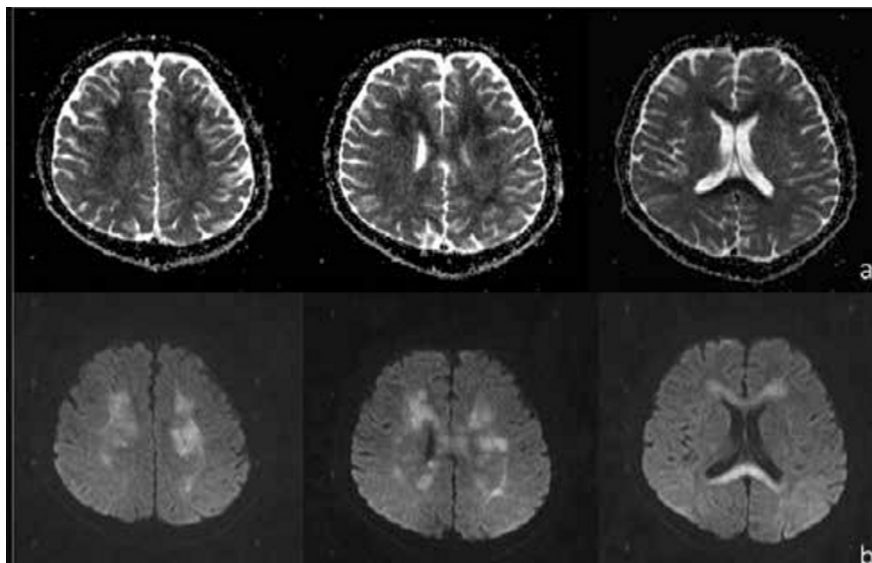
*Hacettepe University Department of Radiology Ankara-Turkey*¹ *Hacettepe University Department of Neurology -Turkey*²

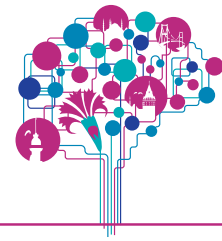
PURPOSE: Cerebral fat embolization (CFE), is a rare and life threatening condition which occurs after long bone fractures. It is characterized by after trauma, following a neurologically silent 12-48 hour occurring period clinic dyspnea, petechial rashes, neurological worsening and coma. We describe a patient with long bone fractures, and demonstrate susceptibility-weighted imaging (SWI) and diffusion-weighted imaging (DWI) findings.

CASE REPORT: After a motorcycle accident 24-year-old male patient was admitted to the hospital with femur and tibia fractures. After several hours from a successful operation cognitive change and extremity weakness. Cranial computed tomography was normal. He had no dyspnea, but had petechial rashes in the nail beds. There wasn't vegetation or patent foramen ovale on transthoracic and transeusophagial echocardiography which were performed to exclude cardiac thromboemboli. A diagnosis of fat embolism syndrome in the imaging and clinical findings context was made. In the follow-up visits his clinic worsened, his Glasgow Coma Score decreased to 3. Haemodialysis was performed because of rhabdomyolysis and he was given under antibiotherapy because of pneumonia, but he died because of septic shock.

IMAGING FINDINGS: Magnetic resonance imaging (MRI) of the brain revealed numerous pinpoint, T2 hyperintense foci in white matter within the internal cerebral artery internal watershed areas, bilaterally. On DWI, there were innumerable punctate foci of restricted diffusion, producing a 'starfield' appearance. The MRI findings with clinical findings were interpreted as the cerebral fat embolism syndrome. Additionally, SWI demonstrated more tiny signal voids consistent with microhemorrhages. Follow-up MRI after 6 days showed confluent lesions which had spreaded throughout the bilateral centrum semiovale and corpus callosum.

SUMMARY&CONCLUSION: Fat embolism syndrome exists as an uncommon but potentially fatal complication of long bone fractures. It is a clinical entity; but characteristic MRI findings are also defined in the literature. Radiologic differential diagnosis should be made with diffuse axonal injury or cardiac thromboembolic events. Treatment remains supportive.





POSTER PRESENTATIONS ABSTRACTS

EP094-The Risk of Aneurysmal Re Bleeding During CT Angiography in Patients with Acute Subarachnoid Hemorrhage

*Naoki Ishige*¹, Hirokazu Tanno¹, Hiroaki Ozaki¹, Yoshihiko Fuse¹, Kobayashi Masayoshi¹
*National Hospital Organization Chiba Medical Center Neurosurgery Chiba-city-Japan*¹

PURPOSE: Computed tomographic angiography (CTA) is becoming accepted as an initial step in detecting a ruptured intracranial aneurysm. It is commonly believed that CTA cannot cause re-bleeding; however we have recently come across four cases in which active bleeding was observed during CTA. We have retrospectively reviewed aneurysmal subarachnoid hemorrhage (SAH) cases in which CTA was carried out within 24 hours after the onset, and evaluate the risk of re-bleeding being caused by the CTA procedure.

METHODS: Between May 2009 and December 2013, 137 SAH patients were transferred to our institute within 24 hours following the initial bleeding. We had employed a strategy in which CTA was carried out soon after admission in all but comatose patients (World Federation of Neurosurgical Societies (WFNS) grade 5). We analysed 109 cases with a ruptured berry aneurysm.

RESULTS: Active contrast extravasation during CTA was visualized in four cases. The intervals between onset and CTA were all within one and a half hours: 35, 50, 55, and 90 minutes, respectively. The pre-CTA neurological status had not been bad, with a WFNS grade of 2 for all four patients. Re bleeding preceded poor outcomes in all cases.

The total number of patients in which CTA was performed within 1.5 hours following the onset of hemorrhage was 41; the incidence of extravasation was 9.7% (4/41) in this group. In the group of 68 cases in which CTA was carried out more than 1.5 hours after the ictus, no extravasation was observed. The incidence of extravasation was significantly different between these two groups.

CONCLUSIONS: There have been occasional reports of contrast extravasation being observed in SAH patients with severely disturbed consciousness. In our series, the incidence of contrast extravasation during CTA within 1.5 hours after the initial hemorrhage was 9.7%. Bearing in mind that comatose cases (WFNS grade 5) were excluded from this study, and that CTA takes only a few minutes to perform, we cannot rule out the possibility that CTA may elevate the risk of aneurysmal re-bleeding in a hyperacute stage. Since January 2014, CTA within 1.5 hours following SAH has been avoided in our institute.

EP095-Blood Brain Barrier Disruption and Related Brain Metabolic Changes after Ischemia Onset in Rats an in vivo CE MRI and 1H MRS study at 7.0 T

Gen Yan¹, Zhuozhi Dai¹, Kuan Geng¹, Yinghua Xuan², *Renhua Wu*¹
*the Second Affiliated Hospital, Shantou University Medical College Department of Radiology -China*¹ *Shantou University Medical College Department of Anatomy -China*²

Blood brain barrier (BBB) damage that occurs within the thrombolytic time window is increasingly appreciated to negatively affect the safety and efficacy of thrombolytic therapy for ischemic stroke. However, the spatiotemporal evolution of BBB damage in this early stroke stage and the related biochemical metabolites changes are not yet clear. We assessed BBB disruption onset time and related neurochemical alteration in MCAO rats using contrast-enhanced magnetic resonance imaging (CE-MRI) and single-voxel localization technique. Proton metabolites were quantified using LCModel software. In 1.5-h MCAO group, after 0.5h reperfusion abnormal hyperintensity signals was seen in the bilateral lateral ventricle and the central canal of CE-T1WI, and expanded to other MCA regions including the ventromedial striatum in 2 h MCAO group, after 0.5 reperfusion. The concentrations of Glu+Gln, Tau and Cr+PCr increased gradually within the first 2 h and then decreased significantly in the following 3 h after ischemia onset evaluated by 1H-MRS. Other metabolites we observed in this study did not show significant changes over the time.



POSTER PRESENTATIONS ABSTRACTS

We identified levels of Glu+Gln, Tau and Cr+PCr may be suitable as new biomarkers to detect BBB damage, and relevant events in the ischemic cascade would be useful to predict the onset time of BBB disruption and improve the accuracy of acute stroke diagnosis in order to predict stroke outcome more reliably.

EP096-Application of Dual energy CT in The Diagnosis of Acute Ischemic Stroke

*Ming-Tsung Chuang*¹, Yi-Sheng Liu¹, Ching-Wen Chen¹, Ming-ching Ou¹, Hong-Ming Tsai¹

National Cheng-Kung Univeristy Hospital Department of Diagnostic Radiology Tainan-Taiwan¹

PURPOSE: The CT perfusion (CTP) and CT angiography (CTA) were clinically useful tools in acute ischemic stroke for determining penumbra area and as a guidance for thrombolytic therapy. This educational exhibit will describe our procedure in clinical practice and introduce some potential pitfalls and technical errors by using DECT (dual energy CT).

APPROACH/METHODS: (a) Technical aspects of CTP/CTA and potential pitfall: introduce our procedures with CTA and CTP using DECT, technical errors in choosing AIF or VOF during CTP. (b)

Pathologic conditions: Infarct (MCA, PCA), vasospasm, subclavian steal syndrome, vertebrobasilar insufficiency, carotid stenosis, postcarotid stenting, postictal change. (c) Mimics of ischemic stroke: hypoglycemia, seizure, old ischemic infarct.

FINDINGS/DISCUSSION: Obtaining an appropriate diagnostic image is very important in dealing with acute ischemic stroke patient for thrombolytic therapy guidance. With the advent of DECT, we can obtain near whole brain perfusion with less contrast amount. CT perfusion can tell us the infarct core and penumbra region while CTA can show us the condition of carotid and vertebrobasilar arteries. We organize a practical way to understand scanning principle and procedure, to interpret various pathologic conditions and to show some stroke mimickers.

SUMMARY/CONCLUSION: With this knowledge, one should be able to understand the role of CTA/CTP in acute ischemic stroke.

EP097-Clinical Outcomes of Manual Aspiration Thrombectomy for Acute Ischemic Stroke Refractory to Stent Based Thrombectomy

*Woong Yoon*¹, Seul Kee Kim¹, Heoung Keun Kang¹

Chonnam National University Hospital Radiology Gwangju-Korea, South¹

BACKGROUND AND PURPOSE: The optimal treatment for acute stroke patients refractory to stent-based thrombectomy (SBT) is unclear. This study aimed to evaluate the efficacy and safety of manual aspiration thrombectomy (MAT) for the treatment of acute ischemic stroke refractory to SBT.

METHODS: From January 2011 to May 2013, a total of 163 consecutive patients with acute ischemic stroke secondary to intracranial large vessel occlusion underwent SBT with a Solitaire stent as first-line endovascular therapy. We retrospectively analyzed clinical and angiographic data of patients who subsequently received MAT with a Penumbra reperfusion catheter because of refractory occlusion after SBT. Refractory occlusion was defined by a lack of successful revascularization (defined as thrombolysis in cerebral infarction (TICI) \geq 2b) after 5 retrieval attempts.

RESULTS: SBT with a Solitaire stent resulted in a primary revascularization rate of 72% (117/163).



POSTER PRESENTATIONS ABSTRACTS

Thirty of 46 patients who failed SBT were subsequently treated with MAT. Successful revascularization was achieved in 83.3% (25/30) of the patients after MAT yielding a final revascularization rate of 87.1% (142/163). Procedure-related complications were found in 6.7% (2/30). No symptomatic hemorrhage occurred. At the 3-month follow-up, 36.7% (11/30) of patients exhibited a good clinical outcome. The mortality rate was 6.7% (2/30) at 3 months.

CONCLUSION: The current study suggests that MAT with the Penumbra reperfusion catheter can significantly further increase the revascularization rate and achieve a low rate of complication in acute stroke patients with refractory occlusions after SBT with a Solitaire stent.

EP098-Emergent Intracranial Angioplasty with or without Stenting for Underlying Atherosclerosis in Patients with Acute Ischemic Stroke

*Woong Yoon*¹, Seoul Kee Kim¹, Heoung Keun Kang¹

*Chonnam National University Hospital Radiology Gwangju-Korea, South*¹

PURPOSE: The goal of our study was to evaluate the outcome of emergent angioplasty with or without stenting for treatment of underlying atherosclerotic stenooclusive lesions in patients with acute ischemic stroke.

MATERIALS AND METHODS: Between January 2011 and March 2013, a total of 175 acute stroke patients presented within 8 hours of stroke onset were treated with endovascular revascularization therapy at a tertiary academic center. Thirty-eight of these 175 patients who underwent emergent angioplasty with (n=24) or without stenting (n=14) for treatment of underlying atherosclerotic lesions were included in this study. Successful recanalization was defined as thrombolysis in cerebral ischemia grades 2b to 3. Outcome measure was the modified Rankin Scale (mRS) score of 0-2 at 3 months. All patients underwent follow-up CT angiography within 1 week after the treatment.

RESULTS: Data from 38 patients were analyzed. Nineteen patients had atherosclerotic lesions in M1 segment of middle cerebral artery (MCA), 12 patients had lesions in basilar artery, and 7 patients had lesions in intracranial internal carotid artery. Fourteen patients were treated with intracranial angioplasty after mechanical thrombectomy with Solitaire stent, and 24 patients were treated with angioplasty alone. Successful recanalization was achieved in 95% (36/38) of patients. Twenty-three patients (61%) had a good clinical outcome at 3 months. Arterial rupture occurred in one patient.

Mortality rate was 18% (7/38). Acute reocclusion of treated vessel occurred in 16% (6/38) of patients on follow-up CT angiography.

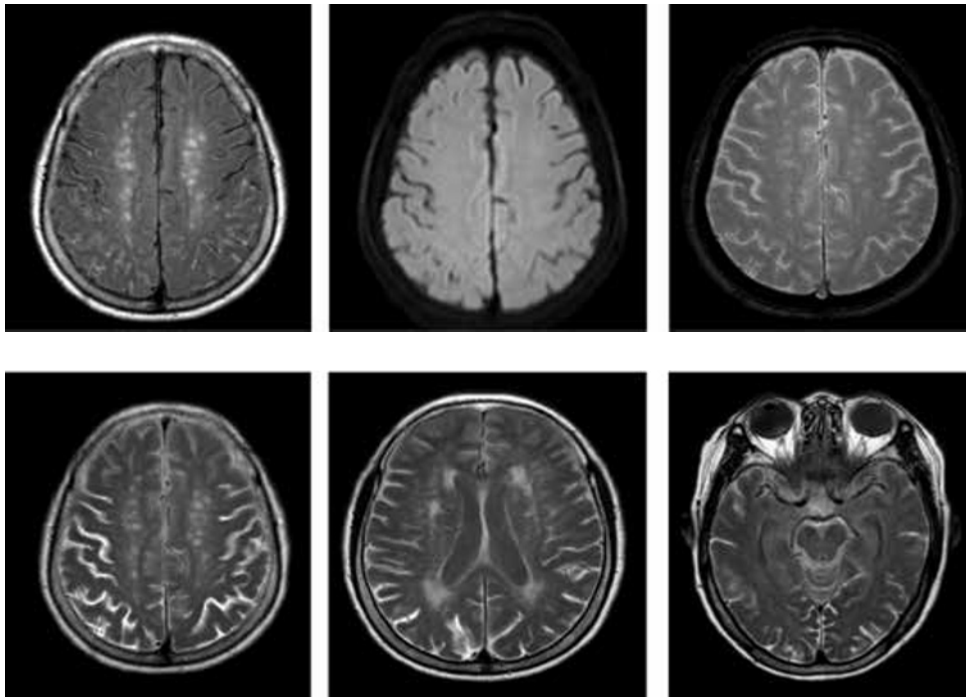
CONCLUSION: This study suggests that emergent intracranial angioplasty is feasible and safe for treatment of underlying atherosclerotic stenooclusive lesions in patients with acute ischemic stroke.

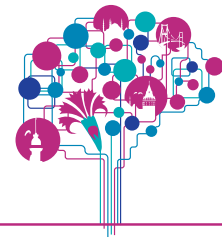
WITHDRAWN



POSTER PRESENTATIONS ABSTRACTS

WITHDRAWN





POSTER PRESENTATIONS ABSTRACTS

EP100-Is Intravenous Thrombolysis an Adequate Choice for Patients with Acute Large Arterial Infarctions with Hyperdense Artery Sign (Red Thrombus)

*Kuei-Hong Kuo*¹, Yi-Ju Pan², Yen-Jun Lai¹

*Far Eastern Memorial Hospital Division of Medical Imaging New Taipei city-Taiwan*¹ *Far Eastern Memorial Hospital Department of Psychiatry -Taiwan*

PURPOSE: Based on histopathological findings, thrombi of large arterial infarctions have been categorized as “red thrombi” - RBC predominant clots presenting with hyperdense artery sign (HAS) and “white thrombi”, formed by fibrin predominant clots. Historically, the presence of HAS was considered to correlate with outcomes of intravenous thrombolysis but findings were inconclusive. The above-mentioned categorization of thrombi (based on both histopathological and radiological findings) may have implications on outcomes because fibrin could be the target of rt-PA (recombinant tissue plasminogen activator) treatment. The current study aims to examine whether the types of thrombi (red vs. white thrombi) could influence outcomes of intravenous thrombolysis in a sample of Asian patients.

METHODS: We enrolled fifty-eight patients who received intravenous thrombolysis following acute stroke with large arterial obstructions between March 2012 and February 2014. All patients had initial CT and post-treatment 24hr follow-up CTA/CTP/MRI. We categorized the subjects into “red thrombi” and “white thrombi” group by correlating the initial CT and follow-up image to identify the presence of HAS. The impacts of thrombi type (HAS) on outcomes (24hr NIHSS, and hemorrhage) were examined taking into considerations patients’ demographic data, risk factors profiles, and rt-PA timing.

RESULTS: Twenty-seven patients had red thrombi (46.6%), and 31 were with white thrombi (53.4%). Patients with red thrombi were more likely to have thrombi of cardiogenic origins and have higher initial NIHSS scores. Overall, 58.4% of patients improved after iv-tPA. In multivariate logistic regressions, types of thrombi did not influence the odds of improvements and bleeding complications. Only the initial NIHSS and timing to receive iv-tPA significantly predicted outcomes of intravenous thrombolysis.

CONCLUSIONS: We found that outcomes of patients with acute large arterial infarctions could be improved by iv-tPA regardless of thrombi types (HAS). Although some previous studies suggested intra-arterial thrombectomy for patients with red thrombi, the current findings supported the effectiveness of iv-tPA for patients with both red thrombi and white thrombi based on a sample of patients in an Asian country.

EP101-Can It Be Detected Lipid Rich Necrotic Core in Carotid Atheroma in vivo By Using Carotid Diffusion Weighted Magnetic Resonance Imaging

*Gyung Ho Chung*¹, Hyo Sung Kwak¹, Seung Bae Hwang¹, Gong Yong Jin¹, Young Min Han¹

*Chonbuk National University Radiology Jeonju-Korea, South*¹

PURPOSE: We evaluate the diagnostic usefulness of the diffusion-weighted MR imaging (DWI) compared with the contrast-enhanced MR imaging for detection of lipid-rich necrotic core of carotid atherosclerotic plaque.

MATERIALS AND METHODS: Twenty-five patients (median age; 66 years, range: 45 – 78 years) with moderate to severe carotid stenosis confirmed using the contrast-enhanced carotid MR angiography were performed the carotid plaque MR imaging. An echo-planner DWI with b0, b200,

b400, b800, b1000, and b2000 was performed along with the carotid plaque MR imaging. Two reviewers analyzed the plaque visualization on DWI by consensus. Contrast-to-noise ratio between lumen and plaque was analyzed between variable b values. Two independent reviewers reported the mean ADC values from regions of interest defining lipid-rich necrotic core on contrast-enhanced MR imaging.



POSTER PRESENTATIONS ABSTRACTS

RESULTS: Only eight patients were identified the carotid atherosclerotic plaque on DWI. One patient with large penetrating ulcer did not show the diffusion restriction. Sixteen patients were not identified on DWI although patients had carotid atherosclerotic plaque. Identified group on DWI had a significantly maximal wall thickness and long segment plaque compared with non-identified group. DWI with b200 was higher contrast-to-noise ratio between lumen and plaque. The mean ADC value from DWI with b200 in lipid-rich necrotic core was $2.51 \pm 1.55 \times 10^{-3} \text{ mm}^2/\text{s}$.

CONCLUSION: DWI for identification of carotid atherosclerotic plaque was relatively lower prevalence compared with contrast-enhanced MR imaging. DWI can be identified the carotid plaque with thick maximal wall thickness and long segment plaque. This study suggests that DWI for detection of carotid plaque including lipid-rich necrotic core cannot replace the contrast-enhanced MR imaging.

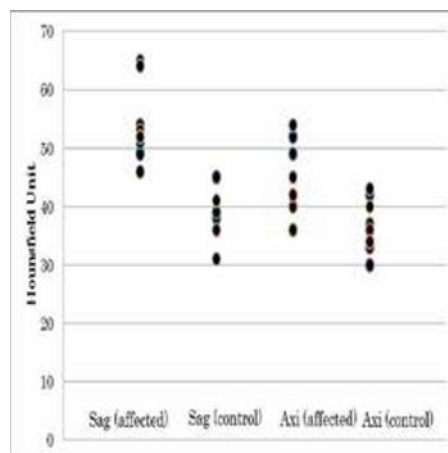
EP102-Improved Detection of Hyperdense MCA Sign by Sagittal Reformations ROI Analysis

Tomoya Nakatsuka ¹, Rumiko Kasai ¹, Shusuke Kasuya ¹, Noriko Kitamura ¹, Masayuki Odashima ¹, Tsutomu Inaoka ¹, Hitoshi Terada ¹
Toho University Sakura Medical Center Department of Radiology -Japan¹

The purpose of this study was to determine whether axial CT images can sufficiently depict the hyperdense middle cerebral artery (MCA) sign in patients with acute brain ischemia. We previously reported higher sensitivity of sagittal images compared to axial images by visual analysis. In this study we performed region of interest analysis to the same group of patients.

MATERIALS AND METHODS: A retrospective review of 92 cases of ischemic brain infarction confirmed nine patients showing hyperdense MCA signs. All of our cases had the hyperdense MCA sign in the M1 segment. CT images were acquired on a 64-slice helical scanner. Images were reconstructed into contiguous 5-mm axial and sagittal images. Round regions of interest (ROI) were placed over the M1 segments of the MCAs and the attenuation values in Hounsfield units (HU) were measured on the sagittal and axial images.

RESULTS: Affected MCAs on axial images had a mean attenuation ranging 36-54 HU versus 30-43 HU for unaffected vessels. Consequently attenuation values for the occluded vessels and those not occluded overlapped significantly (between 36-43 HU). While on sagittal images affected MCAs had a mean attenuation ranging 46-65 HU versus 31-45 HU for unaffected vessels. There was no overlap in attenuation values for occluded vessel and those not occluded (Fig). The mean attenuation of affected MCAs was significantly higher on sagittal images than on axial images ($p < 0.005$). There was no significant difference between the mean attenuation of unaffected MCAs on sagittal images and axial images ($p = 0.36$). **CONCLUSION:** In this study ROI analysis confirmed superiority of sagittal images to distinguish affected MCAs from unaffected MCAs. In patients with acute brain ischemia sagittal images may be superior to axial images for identifying hyperdense MCA sign.





POSTER PRESENTATIONS ABSTRACTS

EP103-Cerebral Venous Thrombosis Presenting As Bilateral Subdural Hematomas

*Biljana Georgievski-Brkic*¹, Magdalena Radovic-Stefanovic², Gordana Milenkovic¹, Tatjana Ducic-Jaramaz³, Petar Nikic³, Svetlana Djokovic³

Stroke hospital "Sveti Sava" Radiology Belgrade-Serbia ¹ *Clinical center Bezanijska kosa Radiology -Serbia* ² *Stroke hospital "Sveti Sava" Neurology -Serbia* ³

PURPOSE: Cerebral venous thrombosis (CVT) is a rare condition that affects fewer than 1 in 10 000 people. CVT is frequently associated with venous infarcts, intraparenchymal or subarachnoid hemorrhage. There are only a few reports in literature of CVT associated with nontraumatic subdural hematoma (SH) as an exclusive manifestation.

METHODS: A 76-year-old man was admitted to the Stroke hospital "Sveti Sava" in Belgrade with symptoms of frontotemporal left-sided headache, pain in both orbits, left-sided hemiparesis and behavior changes. The symptoms started 2 weeks before admittance. No history of trauma, infections, malignancy and surgery. Personal anamnesis data: hypertension and great saphenous vein thrombophlebitis of the right leg, three years ago. We performed brain MSCT, brain MRI, cerebral MR angiography and venography, hematological tests and additional examinations like: CT of the neck, thorax and abdomen, echocardiography and low extremity Doppler.

RESULTS: Brain CT showed bilateral subdural frontoparietal effusions, 7 mm in the right and 4.5 mm on the left side, and hyperdense irregular superior sagittal sinus which was suspicious of venous thrombosis. Brain MRI confirmed subdural hematomas bilaterally, without infarcts and intraparenchymal hemorrhage. DWI showed restricted diffusion in the whole superior sagittal sinus. Hyperintense clots on T1W/T2W/FLAIR and "empty delta" sign on postcontrast study were seen in the superior sagittal sinus, both transverse sinuses predominant in the left, left sigmoid sinus, straight sinus, sinus confluence and left jugular vein. 3D PC MR venography with contrast confirmed absent flow in those vein structures. That suggests subacute dural sinus thrombosis. T2* GRE showed hypointense lesions in cortical bilateral frontal veins in an arborizing fashion and "cord" sign of Torland vein, which represented cortical venous thrombosis. On postcontrast MRI study we noticed the appearance of dilated medullary veins bilaterally. D-dimer was doubled. Other blood non-specific and hematological specific tests, whole body CT, echocardiography and Doppler of leg veins were normal.

CONCLUSION: If a neuroradiologist notices nontraumatic bilateral SH, veno-occlusive disease of the dural, deep and cortical cerebral venous system has to be considered. CVT remains a diagnostic challenge and appropriate imaging study should not be delayed, because adequate therapy should be started immediately.

EP104-The Effect of Cilostazol against the Cerebral Artery Restenosis by Percutaneous Transluminal Cranial Balloon Angioplasty (PTCBA)

*Yoshinori Aoyagi*¹, Takahisa Mori¹, Tomonori Iwata¹, Yuichi Miyazaki¹, Shigen Kasakura¹, Yuhei Tanno¹

Shown at Kamakura General Hospital Stroke Center Stroke Treatment Kamakura-Japan ¹

BACKGROUND: Previous studies have reported that cilostazol may have effects on preventing restenosis following coronary or carotid artery stenting. The purpose of our study was to investigate the effect of cilostazol on reducing restenosis following elective percutaneous transluminal cerebral

balloon angioplasty (PTCBA) for a high-grade symptomatic stenosis of intracranial arteries. **METHODS:** Included were patients 1) who underwent elective PTCBA for a symptomatic stenosis between Feb 2005 and Apr 2013, 2) who started to take dual antiplatelet agents before PTCBA and continued at least for 3 months following PTCBA, 3) who continued to take some antiplatelet agents between 3 and 12 months after PTCBA and 4) who underwent angiographic investigation to assess restenosis at 3 and 12 months after PTCBA.



POSTER PRESENTATIONS ABSTRACTS

Aspirin or cilostazol coupled with thienopyridine agents was used as dual antiplatelet therapy (DAPT). Evaluated were patient's characteristics, antiplatelet agents, binary restenosis at 3 and 12 months after PTCBA and repeat PTCA for restenosis within 12 months. Restenosis was defined as a 50% or more stenosis of the intracranial artery. According to antiplatelet agents, patients were classified into two groups as follows; patients who started to take cilostazol as one of DAPT and continued for 12 months or until restenosis (group CI), and patients who started to take antiplatelet agents except cilostazol as DAPT (group ACr). Binary restenosis was compared between two groups.

RESULTS: During the study period, there were 12 patients in group CI and 18 in group ACr. Overall cumulative restenosis rate was 26.6% (8/30) at 3 months and 50% (15/30) at 12 months. No ischemic strokes occurred with 12 months. In group CI, angiographic restenosis rate was 33.3% (4/12) at 3 months and 41.7% (5/12) at 12 months and 3 patients (25%; 3/12) underwent repeat PTCBA. In group ACr, angiographic restenosis rate was 22.2% (4/18) and 55.6% (10/18) at 12 months and 4 patients (22.2%; 4/18) underwent repeat PTCBA.
CONCLUSION: Cilostazol may have no effects on prevention of restenosis following elective PTCBA.

EP105-Clinical Usefulness of Multishot Diffusion Weighted Sequence (RESOLVE) For the Diagnosis of Acute Infarction at the Brainstem and Posterior Fossa Comparison of Single Shot Echo Planar Diffusion Weighted Sequence

*JeeYoung Kim*¹, *SooAh Im*², *Kook-jin Ahn*², *Yohan Son*³

*Yeouido St. Mary Radiology Seoul-Korea, South*¹ *Seoul St. Mary Radiology -Korea, South*² *Siemens Ltd. Seoul Imaging and Therapy systems Division -Korea, South*³

Single-shot echo-planar imaging (EPI) is well established as the method of choice for clinical, diffusion-weighted imaging with MRI because of its low sensitivity to the motion-induced phase errors that occur during diffusion sensitization of the MR signal. However, the method is prone to artifacts due to susceptibility changes at the tissue interfaces and has a limited spatial resolution. Multishot diffusion-weighted sequence (RESOLVE, readout segmentation of long echo-trains) uses 2D-navigator phase correction to minimize the effect of motion artifact without the requirement for ECG or pulse triggering. Brainstem and posterior fossa are vulnerable to susceptibility artifact. This technique reducing the image distortion.

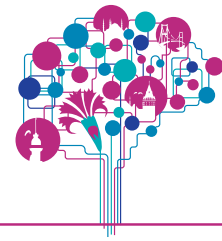
The purpose of this study was to evaluate the clinical usefulness of Multishot diffusion-weighted sequence (RESOLVE) for the diagnosis of acute infarction of brainstem and posterior fossa which, by comparison with single-shot echo-planar diffusion-weighted image at 3T MRI.

EP106-Longitudinal Imaging of [11C] PBR28 Uptake in Neuroinflammation Following Focal Cortical Stroke Model in SD Rat

*Miklós Tóth*¹, *Philip Little*¹, *Fabian Arnberg*¹, *Jan Mulder*², *Haldin Christer*¹, *Balázs Gulyás*¹, *Staffan Holmin*¹

*Karolinska Institutet Department of Clinical Neuroscience -Sweden*¹ *Karolinska Institutet Department of Neuroscience -Sweden*²

PURPOSE: Adequate estimation of neuroinflammatory processes following ischemic stroke is essential for development of novel treatments. With [11C]PBR28, a novel TSPO radioligand showing the activation of microglia, we followed longitudinally the inflammatory response post focal cerebral ischemia in rats. We used a recently developed rat model of focal stroke that produces isolated cortical infarcts with clinical relevance in size and mechanism.



POSTER PRESENTATIONS ABSTRACTS

METHODS: Six Sprague-Dawley rats were included. Occlusion of the M2 segment of the middle cerebral artery (M2o) was performed and animals were imaged at 1, 4, 7 and 14 days after M2o (one animal missing Day 14, scanned on Day 18) with a bolus injection of [11C]PBR28 through tail vein cannulation in nanoScan® PET/MRI and PET/CT scanners (Mediso Ltd, Budapest Hungary). PET scans were co-registered to individual T1-weighted MRI images in PMOD 3.3 (Zurich, Switzerland). Percentage standard uptake values (%SUV) were calculated on a 15-63 minute time period. In an

additional group of animals (n= 26), immunohistochemistry (IHC) was performed with antibodies for microglia (Cd11b), astrocytes (GFAP) and 18 kDa Translocator Protein (TSPO). [B]Results:[/B] [11C]PBR28 showed high uptake in the Infarct region from Day 4 with gradual decrease at later time points. The following average %SUV values were obtained from the Infarct on D1: 67.2 ± 3.7 (n=6),

D4: 151.2 ± 41.6 (n=6), D7: 141.0 ± 51.6 (n=6); D14: 33.3 ± 5.2 (n=5), D18: 93.8 (n=1). At day 4, 7 and 14 we found a significantly increased uptake of [11C]PBR28 uptake compared to the Contralateral Cortex and the Infarct at day 1. No significant increase was detected in the Contralateral Cortex during the 14 days of imaging. Corresponding IHC results also showed TSPO up-regulation in inflammatory cells post injury.

CONCLUSIONS: The longitudinal follow up of inflammatory response with the TSPO radioligand [11C]PBR28 in rats after cerebral ischemia showed significantly up-regulated TSPO related signal in the infarct from day 4, indicating activation of microglia. Activation gradually decreased between day 4 and day 18. The present model appears to be well suited for studies on neuroinflammation.

EP107-The Usefulness of Diffusion Weighted Fluid Attenuated Inversion Recovery Imaging in the Diagnostics And Timing Of Stroke

*Grzegorz Witkowski*¹, *Agnieszka Piliszek*², *Halina Sienkiewicz-Jarosz*¹, *Agnieszka Skierczynska*³, *Renata Poniatowska*³, *Malgorzata Dorobek*⁴, *Anna Filipek-Gliszczyńska*⁴, *Danuta Ryglewicz*¹, *Jerzy Walecki*⁵

*Institute of Psychiatry and Neurology, Sobieskiego*⁹, *02-957, Warsaw, Poland* *I-st Dept of Neurology Warsaw-Poland*¹ *Central Clinical Hospital of the Ministry of Interior, Woloska 137, Warsaw, Poland* *Dept of Radiology -Poland*² *Institute of Psychiatry and Neurology, Sobieskiego*⁹, *02-957, Warsaw, Poland* *Dept of Radiology -Poland*³ *Central Clinical Hospital of the Ministry of Interior, Woloska 137, Warsaw, Poland* *Dept of Neurology -Poland*⁴ *Polish Academy of Science, Pawinskiego*⁵, *Warsaw, Poland* *Mossakowski Medical Research Centre -Poland*⁵

PURPOSE: Patients admitted within 4.5 hours of stroke onset are candidates for reperfusion. However, in wake-up strokes it is impossible to determine the time of onset. It would be useful to find a radiological marker that could be reliable in the timing of stroke onset. One candidate is the Diffusion Weighted Imaging/Fluid

Attenuation Inversion Recovery (DWI/FLAIR) mismatch: the presence of a hyperintensive signal in magnetic resonance (MR) DWI without a relevant change in FLAIR. The goal of the present study was to assess if the DWI/FLAIR mismatch can help to identify patients with both lacunar and nonlacunar acute ischemic stroke within 4.5h of onset.

METHODS: A retrospective study was performed in which the authors analysed data from 864 ischemic stroke patients with a known time of symptom onset. Patients underwent the CT and MR scan. The MR protocol included DWI and FLAIR sequences. The presence of lesions in the applied imaging modalities was assessed in correlation with the duration, type and severity of stroke.

RESULTS: The time from stroke onset to neuroimaging was significantly shorter in patients with an ischemic lesion visible only in the DWI (mean 2.78 hours, range 1.5-7 hours, n=24) as compared to patients with radiological signs of ischemia also in other modalities (mean 8.6 hours, range 2.2-24 hours, n=62) (p=0.0001, Kruskal-Wallis ANOVA). The DWI/FLAIR mismatch was characterised by a global sensitivity of 58%, specificity 94%, PPV 87.5% and NPV 76% in identifying patients in the 4.5h thrombolysis time window.



POSTER PRESENTATIONS ABSTRACTS

For lacunar strokes (n=20) these parameters were as follows: sensitivity 50%, specificity 92.8%, PPV 75% and NPV 81.2%.

CONCLUSIONS: The presence of acute ischemic lesions only in DWI can help identify both lacunar and nonlacunar stroke patients who are in the 4.5h time window for intravenous thrombolysis with high specificity and PPV.

EP108-Imaging the Dynamics of Glucose Metabolism in Experimental Ischemic Stroke

*Fabian Arnberg*¹, Jonas Grafström¹, Johan Lundberg¹, Sahar Nikkhou-Aski¹, Philip Little¹, Li Lu², Michael Söderman¹, Sharon Stone-Elander¹, Staffan Holmin¹

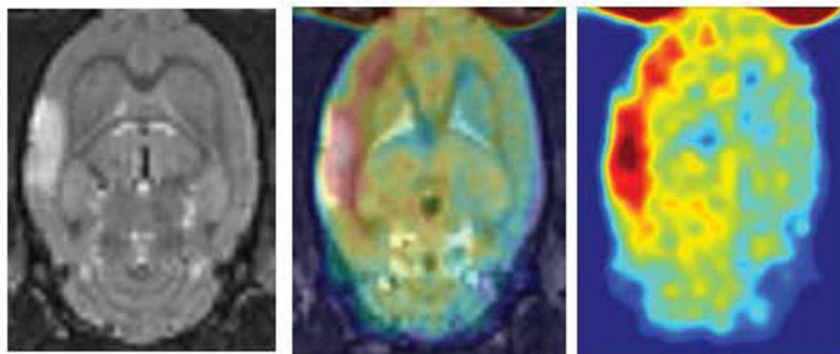
*Karolinska Institutet Department of Clinical Neuroscience Stockholm-Sweden*¹ *Karolinska Experimental Research and Imaging Center (KERIC), Karolinska University Hospital-Solna -Sweden*²

PURPOSE: Following a stroke, hyperglycemia is associated with increased mortality. However, normalization of blood glucose levels by insulin administration in acute stroke does not improve outcomes of neurological deficiency and has been shown to increase infarct size. Thus, we do not know what the optimal level of blood sugar should be after a stroke. An ischemic event in the brain is followed by significant shifts in glucose metabolism in infarct and peri-infarct regions. The

mechanisms and consequences of these changes are fundamentally unclear. By elucidating these mechanisms by multimodal in-vivo imaging of stroke in an experimental setting, we may be able to better predict the consequences of clinical management of stroke-associated hyperglycemia. **METHODS:** Using neurointerventional tools, we have developed a rat model of stroke compatible with experimental imaging systems. With this setup we performed in-bore MRI and in-gantry 18F-FDG PET occlusion and reperfusion of the middle cerebral artery. We used conventional MRI sequences paired with arterial spin labeling (ASL) and MR spectroscopy (MRS). Immunohistological stainings were performed for analysis of cell death and blood-brain barrier (BBB) injury.

RESULTS: Using 18F-FDG PET we detected a significant increase in glucose uptake in the ipsilateral hemisphere during acute ischemic stroke. We found this increase located to both infarct and peri-infarct regions. Further, we found a significant difference in the decrease of cerebral blood flow between the infarct and peri-infarct regions. We detected lactate formation in the infarct whereas no lactate was detected in peri-infarct regions. Apoptosis defined by immunohistochemistry stainings corresponded directly to the MRI lesion. Reactivity for Rat IgG, reflecting BBB disruption, was confined to the MRI lesion.

CONCLUSIONS: In the hyperacute phase of experimental ischemic stroke, glucose uptake in the infarcted hemisphere is increased. Normalization of systemic glucose in this situation could be unfavorable to this pathophysiological response. Our preclinical results may explain the negative outcome in clinical studies applying insulin regimes in the acute phase of ischemic stroke.





POSTER PRESENTATIONS ABSTRACTS

EP109-Bridging Intravenous and Intra Arterial Thrombolysis for Acute Ischemic Stroke Experience in Surabaya Indonesia

*Cindy Sadikin*¹, Hartono Yudi Sarastika², Ardhiana Kasaba³, Agustinus Iskandar⁴, Yanna Saelan⁴
*Siloam Hospital Surabaya Radiology Surabaya-Indonesia*¹ *Dokter Soetomo Hospital Surabaya Radiology -Indonesia*² *Haji Hospital Surabaya Radiology -Indonesia*³ *Siloam Hospital Surabaya Neurology -Indonesia*⁴

PURPOSE: To investigate the feasibility and safety of bridging intravenous (IV) and intra-arterial (IA) thrombolysis in patient with acute ischemic stroke

MATERIAL AND METHODS: Stroke patients age 18 to 80 years old with an National Institutes of Health Stroke Scale (NIHSS) ≥ 10 at baseline and 3 hours of onset were included. IV recombinant tissue plasminogen activator (rt-PA) was administered 0.6mg/kg body weight, 15% bolus IV followed by infusion drip over 30 minutes. Then, IA rt-PA administered via microcatheter at the side of thrombus dose 0.3mg/kg, 10% bolus IA followed by infusion drip over 2 hours or until recanalization achieved. Non contrast head CT scan and restricted diffusion MRI were performed for all cases before the procedure. Non contrast head CT scan was performed immediately after the whole procedure. All patient were send to Intensive Care Unit ward for close observation

RESULTS: From year 2011 until 2013, 23 patients was included. Baseline NIHSS score was 12 – 23. The range of time from door to initiation of IV rt-PA was 45 to 190 minutes and from door to IA rt-PA was 2 hours to 4 hours. Recanalization succesfull rate was 69%. All failure cases was in internal

carotid artery (ICA) and terminal ICA, which we had to performed further percutaneous transluminal angioplasty (PTA) in 7 patients. There were 5 hemmorrhagic infarction (HI) type 1 and 2 in head CT control study.

CONCLUSION: Bridging therapy had the advantages of improving time to initiation of treatment with IV rt-PA, followed by IA rt-PA for more complete recanalization.

EP110-Time of Flight Brain MRA in Predicting Severe Carotid Stenosis

*Hsueh Han Wang*¹, Feng Chi Chang²

*National Yang-Ming University Hospital Department of Radiology Taipei City-Taiwan*¹ *Taipei Veterans General Hospital Department of Radiology -Taiwan*²

PURPOSE: Neck MRA (MR arteriography) is performed as a non-invasive and useful method in evaluating carotid stenosis in embolic stroke patients, but it is time-consuming. We seek to predict severe carotid stenosis using Time-of-Flight (TOF) brain MRA without performing neck MRA.

METHODS: During 2013 to 2014, all patients suspected with middle cerebral artery embolic stroke in our institution underwent brain MRI study, including TOF brain MRA and contrast-enhanced neck MRA. Neck MRA was used as diagnostic reference. Based on neck MRA result, we excluded patients with bilateral carotid stenoses, carotid dissection, or multiple tandem stenotic segments. 57 cases were found to have single ipsilateral significant ($>50\%$) carotid stenosis. 114 carotid arteries were recorded, and we divided the carotid arteries into 5 groups: Group 1: Less than 50% stenosis; Group 2: 50%-69% stenosis; Group 3: 70%-79% stenosis; Group 4: 80%-89% stenosis. Group 5: 90%-99%

stenosis. Three parameters in brain TOF MRA were measured, including: 1. Diameter of distal cervical segment (C1) of bilateral internal carotid arteries (ICAs); 2. Ratio of signal strength of same-side distal C1 segment ICA to ipsilateral external carotid artery (ECA); 3. The visibility of ophthalmic artery in TOF MRA. Statistical analysis between 5 groups of different degree of carotid stenosis and the parameters measured in TOF MRA were calculated.

RESULT: The result was described in the table. Our result showed significant correlation ($p < 0.001$) between the parameters (diameter of ipsilateral distal C1 segment ICA, the ratio of signal strength of same-side ICA to ECA, and visibility of same-side ophthalmic artery) we measured from brain TOF MRA and the degree of upstream carotid artery stenosis.



POSTER PRESENTATIONS ABSTRACTS

CONCLUSION: Carefully chosen parameters measured in brain TOF MRA among embolic stroke patients are useful and reliable in predicting severe carotid stenosis without the extra time needed to perform neck MRA.

	Group 1 (0-50% stenosis) (50 cases)	Group 2 (51-69% stenosis) (10 cases)	Group 3 (70-79% stenosis) (12 cases)	Group 4 (80-89% stenosis) (24 cases)	Group 5 (90-99% stenosis) (18 cases)	p-value
Diameter of distal C1 segment of ICA (mm)	3.91±0.44	3.81±0.51	3.94±0.54	3.52±0.47	3.11±0.66	<0.001
Ratio of signal strength of ipsilateral ICA/ECA	1.66±0.26	1.60±0.18	1.53±0.27	1.35±0.26	1.17±0.25	<0.001
Ipsilateral ophthalmic artery visibility (no. of visible cases/all)	44/50	07.Eki	09.Ara	Tem.24	0/18	<0.001

Adult NR 5

EP111-High Resolution MR Angiography Versus DSA in Diagnosis of Skull Base Meningiomas

Evgeny Shults¹, Igor Pronin¹, Aram Tonoyan¹, Ludmila Fadeeva¹, Valery Kornienko¹

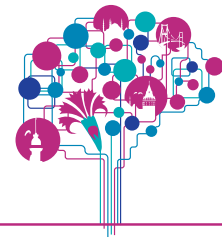
Burdenko Neurosurgery Institute Neuroradiology Moscow-Russia¹

SUMMARY: Meningiomas are the most common type of primary extracranial tumors. Most of meningiomas originate from specialized meningothelial cells in arachnoid granulations. They account for 35.5% of all primary intracranial tumors. Traditionally in clinical practice direct digital angiography (DSA) is used for assessment of vasculature of meningiomas. This method is highly invasive and sometimes causes development of dangerous complications. Nevertheless, by using superselective approach, DSA clearly shows supplying arteries from both external and internal carotid arteries. Development of MRI techniques, application of 3.0T MRI and other methods made it possible to significantly improve capabilities of non-invasive MR-angiography (MRA) in visualization of meningioma blood supply. Use of 3D TOF MRA with a very small pixel size is useful in getting a high quality imaging of small arteries.

MATERIAL AND METHODS: 10 patients with skull base meningiomas were studied on MRI and DSA. 3D TOF MRA has been added to the standard MRI protocol, the technique of which is given below: MRI - 3.0T, Matrix - 640 x 352, TR- 19 ms, TE- 3.4 ms, Thickness - 1.0 mm - 1.2 mm, Slab - 8.0 cm -11.0 cm, Zip - 1024, Pixel size - 0.2 x 0.2 x 1.0. 3 independent neuroradiologists compared MRA and DSA data. Qualitative analysis and anatomical features of cerebral arteries were performed.

RESULTS: Good interobserver reliability was achieved. MRA can compete with DSA in visualization of meningioma blood supply sources. MRA with high special resolution in the majority of cases can visualize not only big sources of blood supply, but in some cases also small arteries even with a tortuous pathway.

CONCLUSIONS: Our investigation demonstrated a good correlation between 3D TOF MRA and DSA. Comparative evaluation of 3D TOF MRA and DSA, obtained during diagnostics of skull base meningiomas blood supply, allowed us to eliminate virtually all invasive technology in favor of non-invasive imaging of cerebral arteries.



POSTER PRESENTATIONS ABSTRACTS

EP112-Magnetic Resonance Appearance of Brain in Snake Bite Patients Resonating The Venomous

Findings

*N Khandelwal*¹, Chirag K Ahuja¹, Vivek Gupta¹, Sameer Vyas¹, Ajay Kumar¹, Ashish Bhalla²
Pgimer Radiodiagnosis Chandigarh-India ¹ *Pgimer Int. Meidcine -India* ²

INTRODUCTION: Snake venoms with neurotoxic activity produce paralysis and respiratory distress by binding the nicotinic acetylcholine receptors, and preventing the depolarizing action of acetylcholine. Hemotoxic effects of the vasculotoxic snakes include hemolysis, fibrinogen proteolysis, and thrombocytopenia, which, along with activation of plasminogen, can lead to a bleeding diathesis in severe envenomation. CNS imaging findings are seen in the form of hypoxic changes, infarcts and hemorrhages.

MATERIAL AND METHODS: All patients with history of snake bite during the last 48 hours presenting to the emergency services of a tertiary care centre over period of 6 months were included in the study. Magnetic Resonance Imaging (MRI) was performed in all patients having neurological symptoms. MRI protocol included T2 weighted axial, 3D-T1 weighted MPRAGE/SPGR, T2 FLAIR weighted axial, diffusion weighted axial, 3D susceptibility weighted sequences, 3D TOF MR angiography (MRA) and 2D TOF MR venography (MRV).

RESULTS: Of the approximately twenty patients who presented to the emergency room during this period, ten patients developed neurological complaints. Of these ten patients who underwent MRI, six claimed to have been bitten by a neurotoxic snake, 1 by a vasculotoxic snake while in the remaining three the snake could not be identified. Four patients showed signs of hypoxic ischemic changes, two in the form of significant global hypoxia secondary to cardiac arrest while remaining two in form of scattered ischemic changes identified as diffusion restricting T2 hyperintense lesions in the white and deep grey matter. Two out of these were secondary to neurotoxin envenomation while the remaining two were in the unidentified group. MRI was normal in 5 patients. MRA showed diffusely attenuated intracranial arterial circulation in those who developed cardiac arrest while it was normal in 8 patients. MRV was normal in all patients.

CONCLUSIONS: This is one of the few small case series highlighting the MRI apparent neurological manifestations of snake bite. The various causes of these hypoxic-ischemic sequelae could be global hypoperfusion/hypoxia secondary to neuroparalysis in neuroparalytic snake bites, thrombotic vascular occlusions in vasculotoxic snake bites and cardiac arrest in either of the varieties.

EP113-Altered Magnetization Transfer Ratio as a Marker of Subclinical Cerebral Oedema in Patients of Minimal Hepatic Encephalopathy

Rahul Rai¹, Rk Dhiman¹, *N Khandelwal*², Chirag K Ahuja², Naveen Kalra², Y Chawla¹,
Ajay Duseja¹

Pgimer Hepatology -India ¹ *Pgimer Radiodiagnosis Chandigarh-India* ²

BACKGROUND: Medical evidence suggests that inflammation modulates cerebral effects of ammonia resulting in low grade cerebral edema causing Minimal hepatic encephalopathy. Decreased magnetization transfer ratio (MTR) in brain has been described to characterize brain edema in cirrhotics, but the data is limited in MHE.

AIMS: To study arterial ammonia, pro-inflammatory interleukins (IL-1, IL-6) and MTR in MHE, before and after treatment.

PATIENTS AND METHODS: Twenty-three cirrhotics (non-MHE, n=9; MHE, n=14) and 6 healthy controls underwent arterial ammonia, IL-1, IL-6, TNF- α and MTR in frontal white matter (FWM), parietal white matter (PWM), internal capsule (IC) and basal ganglia (BG). Seven patients in MHE and non MHE group had similar investigations repeated after 8 weeks; MHE group received rifaximin. **Results:** Arterial ammonia was significantly higher in cirrhotics compared to controls; and in MHE compared



POSTER PRESENTATIONS ABSTRACTS

to non-MHE. IL-1 and IL-6 were significantly elevated in MHE patients when compared with controls. Arterial ammonia correlated positively with IL-1 [$r=0.566$ ($p=0.009$)] and IL-6 [$r=0.566$ ($P=0.008$)]. MTRs in all regions were significantly decreased in MHE compared to controls. After treatment of MHE, MTR increased in all regions; however significant increase was seen only in FWM and IC. IL-6 and ammonia had significantly negative, and psychometric hepatic encephalopathy scores had significantly positive correlations with MTR in various regions.

CONCLUSION: Decreased MTR in MHE patients and improvement after treatment suggests low grade cerebral edema which is reversible. A negative correlation between arterial ammonia, IL-6 levels and MTR; a positive correlation between PHES and MTR in MHE patients suggests, that inflammation has a role to play in ammonia induced low grade cerebral edema in them.

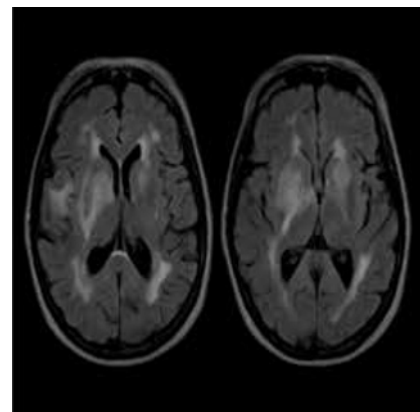
EP114-Diffuse Leucoencephalopathy in a Patient with Rapid Cognitive Decline Consider Lymphomatosis Cerebri

*Luc van den Hauwe*¹, Gunther De Temmerman¹, Stephanie Smet², Stef Meers³, Koen Goedseels⁴, Christine Langenaeken⁵, Joris Beck⁶, Peter Bracke¹

AZ KLINA, Brasschaat, Dept. of Radiology Brasschaat-Belgium¹ AZ KLINA, Brasschaat, Dept. of Neurology -Belgium² AZ KLINA, Brasschaat, Dept. of Hematology -Belgium³ AZ KLINA, Brasschaat, Dept. of Neurosurgery -Belgium⁴ AZ KLINA, Brasschaat, Dept. of Oncology -Belgium⁵ AZ KLINA, Brasschaat, Dept. of Pathology -Belgium⁶

PURPOSE: Lymphomatosis cerebri (LC) is considered a diffuse form of primary central nervous system lymphoma (PCNSL) and is very rare; less than 25 cases have been published. We want to review the imaging findings in a patient with LC who presented with a rapid cognitive decline.

CASE REPORT: A 67-year-old immunocompetent woman was referred to the neurologist because of intermittent facial droopings of changing severity. She complained of dysequilibrium with numerous falls, drowsiness and tendency to fall asleep. According to the son, there was a rapid cognitive decline, including memory and thinking skills. At anamnesis, she presented apathetic. Further clinical examination was quite unremarkable and did not show any focal neurological deficit. Previous medical history included longstanding arterial hypertension and diabetes mellitus, type 2. Initial noncontrast CT showed nonspecific confluent white matter (WM) changes. An additional right frontal mass, isodense with the cortical gray matter was suspected. On MRI, a 2 cm mass lesion implanted in the cortical gray matter was observed. The tumor showed homogeneous contrast enhancement. Since the lesion showed restricted diffusion on diffusion-weighted imaging and low relative cerebral blood volume (rCBV) on perfusion-weighted imaging, a presumable diagnosis of PCNSL was made. Extensive asymmetrical FLAIR/T2 hyperintensities in the subcortical and periventricular WM, right external and internal capsules, right thalamus and basal ganglia, and right cerebral peduncle were also observed. There was no enhancement, and no areas of restricted diffusion could be found. Stereotactic biopsy revealed the diagnosis of diffuse large B-cell lymphoma. Chemotherapy based on high-dose methotrexate, and cytarabine, in combination with rituximab was initiated with a good clinical result. Repeat MRI showed complete remission of the mass and normalization of the signal in the basal ganglia and thalami. The WM signal abnormalities shrank but persisted. Four months later, patient deteriorated (gait disturbances, repetitive falls, progressive cognitive decline). MRI revealed recurrent signal changes in the basal ganglia, thalami, midbrain and brainstem, suggesting LC. She died 6 weeks later.





POSTER PRESENTATIONS ABSTRACTS

SUMMARY: LC is characterized by diffuse infiltration of the cerebral WM by individual lymphoma cells. On MRI, a nonspecific diffuse leucoencephalopathy without contrast enhancement is observed, which may cause diagnostic confusion with other WM diseases (small-vessel disease, infections, ...). Rapidly progressive dementia is typical. A lymphomatous mass lesion may coexist with LC.

EP115-Too Late for a Pilocytic Astrocytoma

João Jacinto ¹, Mariana Diogo ¹, Isabel Fragata ¹, Carla Conceição ¹, Manuela Mafra ², João Reis ¹

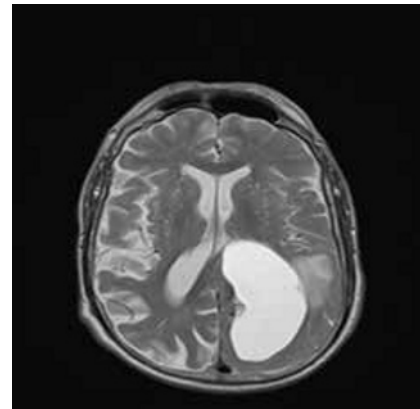
Centro Hospitalar Lisboa Central Neuroradiology -Portugal ¹ *Centro Hospitalar Lisboa Central Pathology -Portugal* ²

INTRODUCTION AND PURPOSE: Astrocytomas are the single largest group of all primary central nervous system (CNS) neoplasms. They are currently classified according to histological features and the subtypes prevalence differs on peak age. The pilocytic subtype occurs almost exclusively in children and frequently in the posterior fossa. In adults, diffuse subtypes are more common and mostly located in the cerebral hemispheres. Our purpose was to review the pilocytic astrocytomas found in older adults in our center.

METHODS: We analyzed our prospective database of CNS neoplasms between January and December 2013. A total of 255 CNS tumors were found, with 10 pilocytic astrocytomas. Of these, 3 were found in adults above 60 years-old (the oldest patient was 80). Clinical data, imagiological findings and pathological features were reviewed.

RESULTS: All three patients were assessed by CT and/or MRI. The 80 year-old patient had acerebellar lesion, while the other two had cerebral hemispheric neoplasms. All lesions were well-circumscribed, cystic, with a mural nodule. One hemispheric tumor had significant adjacent edema. They were submitted to surgery and tumor samples were pathologically analyzed and confirmed the diagnosis of pilocytic astrocytoma.

CONCLUSIONS: Pilocytic astrocytoma is rare in adults and in the cerebral hemispheres in opposite to more malignant astrocytoma subtypes. Nevertheless, it can occur in older adults, infra- or supratentorially, and should be included in the differential diagnosis regardless of age.



EP116-What You See Is Not What You Get...

João Jacinto ¹, Mariana Diogo ¹, Isabel Fragata ¹, Carla Conceição ¹, Manuela Mafra ², João Reis ¹

Centro Hospitalar Lisboa Central Neuroradiology -Portugal ¹ *Centro Hospitalar Lisboa Central Pathology -Portugal* ²

INTRODUCTION AND PURPOSE: Meningiomas are one of the most common Central Nervous System (CNS) tumors. On CT imaging they usually appear mildly to moderately hyperdense compared to brain cortex. MRI often reveals iso to slight hypointensity on T1W1, and iso to mild hyperintensity on T2W1. On both techniques, meningiomas show strong contrast enhancement, and dural tail sign. Many times, hyperostotic changes in adjacent bone can be seen. However, these imaging features are not exclusive as several other neoplasms can mimic this pattern. The purpose of our work was to review some cases of our center of CNS tumors that presented as a common meningioma but had a different final diagnosis.

METHODS: From our prospective database of CNS tumors of 2013 (a total of 255) we searched for patients with neoplasms that were imagiologically (by CT and/or MRI) described as a probable meningioma and compared

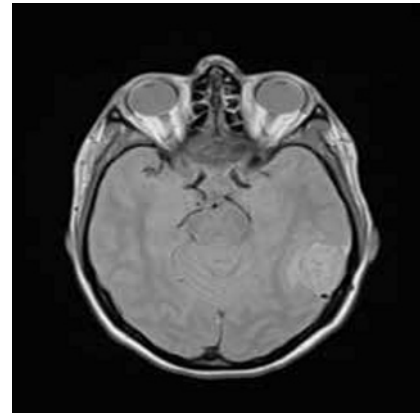


POSTER PRESENTATIONS ABSTRACTS

them with the final diagnosis from pathology. Three cases of “imaging-pathology mismatch” were found. We reviewed the imagiological findings that may have led to a misdiagnosis.

RESULTS: In all three patients, the lesions were extra-axial, well-circumscribed, with a broad dural base. Two were localized at the left ponto-cerebellar angle and the other adjacent to the left temporal lobe. Non-enhanced CT exams were performed in two patients. One lesion was mildly hypodense and the other slightly hyperdense. All patients were submitted to MRI imaging on which the neoplasms presented iso-hypointensity on T1W1, and iso-hyperintensity on T2W1, with strong contrast enhancement. Two of them were surrounded by vasogenic edema and none had adjacent bone changes. On all exams, the described lesions were interpreted as a probable typical meningioma. They were submitted to surgery and the pathology analysis revealed a large B-cell lymphoma, a solitary fibrous tumor and a breast cancer metastasis.

CONCLUSIONS: Despite high prevalence of meningiomas, clinicians should be aware that even typical imagiological features are not pathognomonic, as other primary or secondary neoplasms may have identical presentation. Therefore, differential diagnosis should not be discarded. Advanced MR sequences such as spectroscopy should be performed.



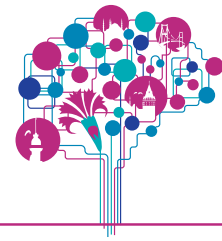
EP117-MR Features of Infections Affecting Basal Ganglia and Thalami

*Ritu Kakkar*¹, Sameer Soneji¹, Shrinivas Desai¹
*Jaslok Hospital CT and MRI Mumbai-India*¹

AIM: To illustrate MRI findings of infections affecting basal ganglia and thalami.

CONTENT ORGANIZATION: Symmetric thalamic hyperintensities was most commonly associated with cerebral malaria in our series with or without associated hemorrhages and cerebellar involvement. Japanese B encephalitis and dengue emerged as viral infections affecting these sites. A child with severe influenza infection of the respiratory tract developed encephalitis showed similar CNS finding. Bilateral strial necrosis was seen in patients with mycoplasma pneumoniae infection. 1 patient with salmonella septicaemia showed basal ganglia involvement, extensive cortical and white matter enhancing lesions. Ring like enhancing lesions with haemorrhages the result of toxoplasmosis and aspergillosis was common in immunocompromised patients. Tuberculous affection was more the result of vasculitic infarcts than granulomas. Chronic infections like HIV encephalopathy and Creutzfeldt Jacob disease also lead to symmetric affection but the clinical presentation and rest of imaging features help distinguish these entities.

SUMMARY: A variety of bacterial, viral, fungal and parasitic agents affect the basal ganglia and thalami. Knowledge of imaging features in conjunction with clinical and laboratory findings aid in appropriate diagnosis and help management.



POSTER PRESENTATIONS ABSTRACTS

EP118-MRI Features of Japanese Encephalitis

*Ritu Kakkar*¹, Sameer Soneji¹, Shrinivas Desai¹
*Jaslok Hospital CT and MRI Mumbai-India*¹

AIM: To highlight spectrum of central nervous system findings in Japanese B encephalitis. We present a series of 22 proved cases.

CONTENT ORGANISATION: Pathology, Japanese encephalitis (JE) is mosquito-borne flaviviral encephalitis predominantly affecting thalami, substantia nigra, corpus striatum, cerebral cortex, brain stem and cerebellum causing glial nodules and circumscribed necrolytic foci.

Imaging, most common finding was bilateral symmetrical thalamic hyperintensities on T2W1 images with or without hemorrhages. Associated lesions in basal ganglia were seen in 3 patients. Symmetrical lesions involving substantia nigra leading to parkinsonism like features was seen in 2 patients. Patchy hyperintensities in brain stem, cerebellum and cerebral cortex were also seen; often in association with thalamic disease. Affection of medial temporal lobe mimicking herpes encephalitis was seen in 2 patients. Japanese B neurocysticercosis (NCC) coinfection with a ring enhancing granuloma in association with basal ganglia and thalamic changes was seen in 2 patients.

SUMMARY: Japanese B encephalitis can have varied imaging findings ranging from bilateral thalamic, basal ganglia and substantia nigra involvement to affection of temporal lobes. Coinfection with NCC is common in endemic areas and highlights the synergistic relationship.

EP119-Assessment of Deep and Cortical Gray Matter Involvement via DTI and Correlation with Volumetric Analysis in MS Patients

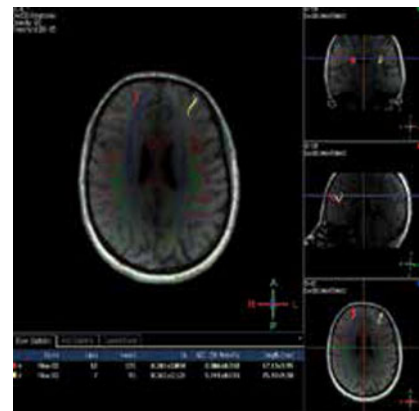
*İsa Çam*¹, Hande Biçkin², Yonca Anik¹, Bahattin Özkul¹, Ali Demirci¹, Serdar Çağlayangil¹
*1Kocaeli Universty Radiology Kocaeli-Turkey*¹ *Kocaeli Universty Neurology -Turkey*²

INTRODUCTION: Multiple Sclerosis (MS) is a chronic inflammatory, demyelinating and neurodegenerative disease characterized with focal demyelinating plaques affecting white and grey matter of brain. In recent years, many researches have been performed in order to detect grey matter lesions and their correlation with clinical findings in MS.

PURPOSE: To determine volume and DTI parameters of deep and cortical gray matter in MS patients To compare them with that of the healthy control group.

MATERIALS AND METHODS: 3T MRI scanner equipment: Philips Achieva Intera Release Einthoven, the Netherlands maximum gradient strength: 139mT/m, slew rate: 346mT/m/msec 8-channel array head coil in supine position 40 MS patients 20 healthy subjects with same demographic characteristics DTI parameters: • sensitivity-encoding single-shot EPI • 2 mm thickness with no gap, • SENSE factor: 2.4 partial Fourier transform, 60%, • b value 0 and 1000 sec/mm², 15 directions • spatial resolution 0.8 x 0.8mm, • matrix 256x256 3D T1 FFE parameters • TR/TE: 5.1/2.3, • matrix: 248 x 232, • slice thickness: 1mm, • gap: 0 MRI data analysis In a separate workstation. (Release 2.5.3.0 2007-12-03, Philips Medical Systems, Netherlands B.V) DTI analysis: Bilateral frontal, temporal, parietal, oksipital region cortical gray matter volumes were measured by manual ROI replacement, MD ve FA values were measured. Total gray matter volumes were assessed by full automated neuroimaging software Statistical analysis: (SPSS 13.0 program) Simple descriptives, Independent t test and Pearson correlation test p<0.05 accepted as significance.

RESULTS: In DTI measurements, FA values of cortical and deep grey matter were lower in all MS patients and MD values were higher in MS patients compared with healthy control group.





POSTER PRESENTATIONS ABSTRACTS

CONCLUSION: Although MS is a demyelinating white matter disease, normal appearing gray matter is also seems to be affected that can be demonstrated by DTI parameters. Besides gray matter volume is significantly decreases in MS patients.

EP120-The Neuroanatomic Knowledge Helping in the Differential

Diagnosis of Lesions of the Brain Stem

*Lázaro Luís Faria do Amaral*¹, Ricardo Tavares Daher¹, Anderson Benine Belizia¹, Victor Hugo Rocha Marussi¹, Saulo Pimenta Lacerda²

*Beneficência Portuguesa Hospital – Medimagem Neuroradiology São Paulo-Brazil*¹ *Delfin Hospital Neuroradiology -Brazil*²

PURPOSE: The outcome of magnetic resonance and their advanced imaging methods have enabled a great knowledge of the anatomy of the brain stem that can be correlated with some specific topographic diagnosis. The purpose of this study is to use these anatomic and topographic information obtained with these studies to narrow the differential diagnosis of each lesion, by using originals examples of some o the more important and common pathologies of the brain stem that we had in our institution in the past few years.

CASE REPORT: We report how the anatomic knowledge and the exactly topographic diagnosis in each structure of the brain stem can help narrow the differential diagnosis in these lesions that involves the medulla for instance, like progressive ataxia and palatal tremor (PAPT) and Wallenberg syndrome.

IMAGE FINDINGS: The work describes the typical anatomic sites involved in each of the main brain stem diseases and how this topographic knowledge helps to narrow differential diagnosis:
MEDULLA: Inferior olivary nucleus - progressive ataxia and palatal tremor (PAPT) (example image 1) and hypertrophic olivary degeneration. Pyramid of the medulla - Motor neuron diseases.

Lateral medulla – Wallenberg syndrome. Floor of fourth ventricle and surround the cerebral aqueduct – Wernicke encephalopathy.

PONS: Trigeminal nerve – Varicela zoster infection. Pontine Transverse Fibers – Pontine myelinolysis

and Multiple System Atrophy type c (MSA-c). Absence of the facial colliculi and hypoplasia of medial lemniscus, associated with the split pons sign – Horizontal gaze palsy with progressive scoliosis.

MIDBRAIN: Hypoplasia of the midbrain tegmentum - Progressive Supranuclear Palsy (PSP)

Cerebral pedunculus sparing substantia nigra and red nucleus, associated with basal ganglia (putamen) impairment – Wilson disease Hypointensity in all sequences involving substantia nigra and red nucleus, with basal ganglia involvement – Aceruloplasminemia.

SUMMARY: This study is a review that shows how the anatomic knowledge and the topographic diagnosis can help narrow differential diagnosis and some times to suggest a specific diagnosis in the different lesions of the brain steam, using original cases that we had in our institution.





POSTER PRESENTATIONS ABSTRACTS

EP121-Isolated Restricted Diffusion of the Splenium Associated with Anorexia Nervosa A Case Report

*Yasemin Kayadibi*¹, Amalya Zeynalova¹, Elmar Bayraktarov¹, Evrim Ozmen¹, Zehra Isik Hasiloglu¹
*Istanbul University Cerrahpasa Medical Faculty Radiology ISTANBUL-Turkey*¹

PURPOSE: To report a rare case of restricted diffusion in splenium of corpus callosum associated with thiamine insufficiency (TI) in a patient with anorexia nervosa (AN).

METHODS: A 20 year-old patient who diagnosed as AN, was under treatment in psychiatry clinic. She had been suffering from headaches for a month. Neurologic examination revealed no abnormality.

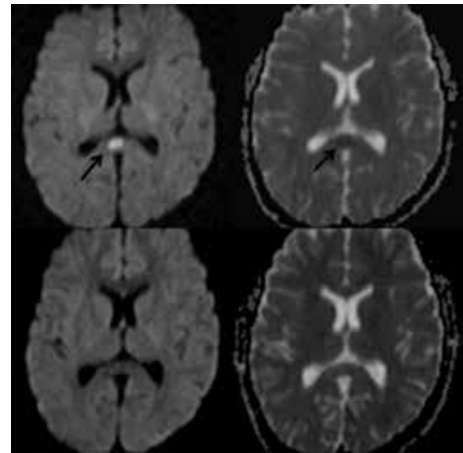
Brain computer tomography (CT) and brain magnetic resonance imaging (MRI) were performed.

RESULTS: CT revealed no abnormality. Diffusion weighted images (DWI) showed isolated high signal intensity and low signal intensity on apparent diffusion coefficient map in splenium of corpus callosum. TI like as early Wernicke encephalopathy (WE) was considered for the probable reason of this atypical finding in this malnourished patient. After psychotherapy and replacement therapy, patient got well and at fourth month control DWI showed no abnormality (Figure1).

DISCUSSION AND CONCLUSIONS: AN is an eating disorder which is associated with underlying mental problems. These patients starve themselves or use laxatives to lose weight. Reversible cerebral atrophy and enlargement of cerebrospinal fluid spaces are typical findings of AN, but there is no study

about DWI in these patients. Restricted diffusion in splenium of corpus callosum and affected areas such as dorsomedial thalamus, periaqueductal gray matter and mamillary bodies in a patient of acute TI in WE had been reported. TI is usually seen in alcoholics but can either be seen in long parenteral

feeding, hyperemesis, after gastrointestinal surgery and prolonged malnutrition. Mental confusion, ataxia and ophthalmoplegia are symptoms of WE and our patient had none of these symptoms. But with a history of prolonged malnutrition and reversible restriction on DWI after replacement therapy, are supporting elements of our diagnosis. In conclusion DWI can be used to show acute TI in suspected patients and used for follow up imaging.



EP122-The Role of Heavily T2 weighted 3D MR Myelography in the Evaluation of CSF Leakage

*Chang June Song*¹, In Ho Lee¹, Da Mi Kim¹, Si Sung Choi², In Kyu Yu³

Chungnam National University Hospital Diagnostic Radiology Daejeon-Korea, South 1 Wonkwang University Hospital Diagnostic Radiology -Korea, South 2 Eulji University Hospital Diagnostic Radiology -Korea, South 3

The Role of Heavily T2-weighted 3D MR Myelography in the Evaluation of CSF Leakage

PURPOSE: It is important to find the exact site of CSF leakage in the patients with spontaneous or iatrogenic intracranial hypotension for therapeutic success. The aim of the study is to evaluate the efficacy of the 3D MR myelography(MRM) using heavily T2-weighted image.

MATERIALS AND METHODS: Symptomatic 31 patients (M:F = 9:22, mean age: 42 years old, age range, 16-57 years) with CSF leakage on heavily T2-weighted MRM between June 2010 and April 2013 were included. 29 of 31 patients underwent both MRM and brain MR imaging (MRI) and 15 of 31 patients underwent follow up MRM. All MR examinations were performed on 3T scanner (Intera Achieva; Philips). The parameters used in MRM were TR= 5883 ms, TE = 650 ms, NEX =1, and matrix size 320x320. The clinical manifestations, the presence, location and morphology of CSF



POSTER PRESENTATIONS ABSTRACTS

leakage, and indirect sign of CSF leakage (presence of diffuse pachymeningeal thickening with enhancement and/or subdural fluid collection) were analyzed. Also the improvement of symptoms or cessation of CSF leakage on FU MRM after the targeted autologous epidural blood patch procedure or the conservative treatment was identified.

RESULTS: CSF leakage was observed in all symptomatic patients. The spontaneous spinal CSF leak was 13 patients and iatrogenic CSF leak such as lumbar puncture or spinal surgery was 9 patients. The other causes of another 9 patients were excessive exercise (n=4), trauma (n=2), and acupuncture history (n=3). The leakage sites were lumbar spine (n=15), thoracic spine (n=11), cervicothoracic junction (n=5), L-S spine (n=1), T-L-S spine (n=1), and C-spine (n=1). Diffuse pachymeningeal thickening with enhancement on brain MRI was detected: definite (n=10), probable (n=10), normal (n=9). Orthostatic headache in all patients was improved after epidural blood patch (n=25) and conservative treatment (n=6). 15 of 31 patients underwent follow up MRM after targeted autologous epidural blood patch (taEBP, n=13) or conservative treatment (n=2): complete recovery: 10, partial recovery: 3, recurrence: 2.

CONCLUSION: It suggests that MRM using heavily T2WI may play a significant role in the detection and localization of the CSF leakage and evaluation of the treatment response.

EP123-Cerebellar Liponeurocytoma Case Report and Literature Review

*Pablo Picasso de Araújo Coimbra*¹, Bruno Braga Penha da Silva², Eduardo Sousa Frota de Almeida², Idalia Luzia Fortaleza Chaves Martins², Cleto Dantas Nogueira³, Paula Galvão de Andrade², Luciana Vieira Farias², Ylana Mayra de Almeida Silveira², Diego Silva Vasconcelos Alves², Kelnner Portela Luz², Walmir Leite Pontes Filho² *Clínica Trajano Almeida Radiology FORTALEZA-Brazil*¹ *Hospital Antonio Prudente Radiology -Brazil*² *Laboratório Argos Pathology -Brazil*³

PURPOSE: To report a case of a 44 year old woman with Cerebellar Liponeurocytoma as well as diagnosis, including medulloblastoma, and treatment are also part of the objectives.

METHODS: Data were obtained through interviews with the patient, the medical records, photographic registration of images of radiological and histopathological studies to which she was review the clinical, radiological and histopathological features of this neoplasm. Discuss the differential submitted and literature.

RESULTS: Female patient, 44 years old, complaining of severe headache sought medical care with a neurosurgeon who requested imaging studies to better review. Magnetic resonance imaging revealed intra-axial solid mass lesion located in the posterior aspect of the right cerebellar hemisphere, with low signal on T1 and hyperintense on T2/FLAIR, restricted diffusion, surrounded by edema and showing areas of enhancement through contrast and images cystic therein. Later, the patient underwent surgical treatment with excision. Histopathology revealed monotonous proliferation of neuroepithelial cells and small round nuclei, scant cytoplasm, rare mitoses and presence of islands of mature adipose tissue. Immunohistochemistry with GFAP, synaptophysin, S100 and Ki67 confirmed the diagnosis of cerebellar liponeurocytoma.

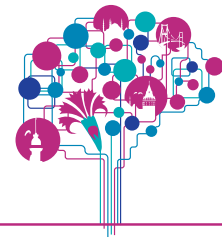
CONCLUSIONS: Cerebellar Liponeurocytoma is a rare disease, with approximately 40 cases reported in the literature, which is mainly manifested in the cerebellum, primarily in adults and is characterized histologically by the presence of mature adipocytes with low mitotic activity, with a good prognosis. Always have to be remember in the differential diagnosis of medulloblastoma, even having prognostic, epidemiological and clinical aspects different.

EP124-Pictorial Review of the Neuroradiology of Thrombotic Thrombocytopenic Purpura

*Fiona Chatterjee*¹, Ayokunle Ogungbemi², Rolf Jager³, Harpreet Hyare⁴

*NHNN Imaging London-United Kingdom*¹ *NHNN imaging -United Kingdom*² *UCLH & NHNN imaging -United Kingdom*³ *UCLH imaging*⁴

BACKGROUND: Thrombotic thrombocytopenic purpura (TTP) is a rare multisystem disorder with an incidence of 3.7 to 17.46 per million which can be idiopathic, acquired or due to congenital ADAMTS13



POSTER PRESENTATIONS ABSTRACTS

deficiency. TTP is a pentad of fever, renal dysfunction, haemolytic anaemia, thrombocytopenia and central nervous system (CNS) involvement.

CONTENT ORGANISATION: We present a multimodality pictorial review of a cohort of 45 patients (mean age 53 years, range 14-83 years) referred to our institution over 4 years. 40 of the cases have MRI with gradient echo sequences (GRE) or susceptibility weighted imaging (SWI). We present the differing neuroradiological presentations of TTP including small and large vessel infarcts, multi territorial infarcts, PRES like syndromes, small vessel disease, haemorrhagic transformation, parenchymal haemorrhage, microhaemorrhages and subdural haemorrhage.

SUMMARY: The spectrum of neuroradiological findings in TTP is broad. SWI or GRE should routinely be included in MRI performed in patients suspected to have TTP.

EP125-Toxoplasmic Myelitis as the Initial Presentation of Aids

Fernando Travassos ¹, Joyce Benevides ¹, Rosivalda Teixeira ¹, Pedro Braga-Neto ¹, Francisco José Mont ¹, Pablo Coimbra ²

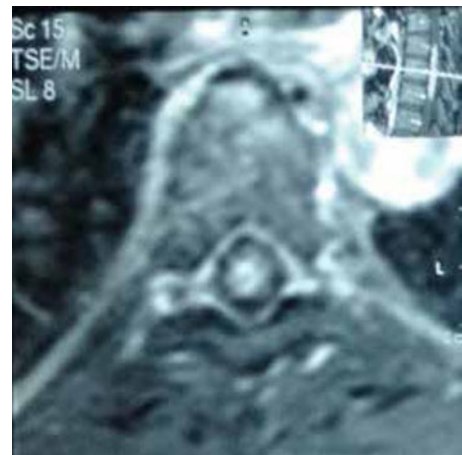
Hospital Geral De Fortaleza Neurology -Brazil ¹ Hospital Geral De Fortaleza Neuroradiology Fortaleza-Brazil ²

PURPOSE: describe a case of medullary neurotoxoplasmosis.

CASE REPORT: Male, 56-years-old, started to have fever, headache and malaise. After one week, he also showed progressive decrease in lower-limb strength associated with disorientation. He had no history of systemic diseases. On admission, physical examination showed the presence of bladder distension, psychomotor agitation, asymmetric espastic paraparesis with hyperreflexy and Babinski present bilaterally. The rapid test for Human immunodeficiency virus was positive. Brain MRI showed disclosing multiple nodular lesions scattered throughout the brain parenchyma, including the lenticular nuclei, right thalamus and frontal lobe, with hyperintense signal on T1 suggestive of hematic

components and intense annular enhancement with nodular uptake of the contrast agent. MRI of the thoracic spine showed extensive signal alteration throughout the spinal cord, including the conus, centrally located, with hyperintense signal in T2/STIR, showing enhancement by the contrast agent from T7 to T9, suggestive of transverse myelitis. The cerebrospinal fluid (CSF) analysis showed mild pleocytosis, increasing protein concentration, normal glucose and IgM on CSF was positive for toxoplasmosis. Treatment for neurotoxoplasmosis was initiated. MRI of the thoracic spine, after 15 days, showed spinal cord with signal alteration, characterized by hyperintense signal on T1 and T2 extending from T7 to T9 without enhancement. **DISCUSSION:** Myelitis is a known complication of AIDS, and is occasionally the initial complaint, of which incidence can reach 20%. Neurotoxoplasmosis usually presents as brain pathology, but there have been reports of myelopathies secondary to toxoplasmosis. The thoracic spine MRI usually shows hypointense signal on T1. The T2 sequence shows hyperintense signal and may contain an area of relative hypointense signal, which corresponds to the granuloma itself. After the gadolinium injection, there is an enhancement similar to those seen in brain injuries.

CONCLUSION: Toxoplasmic myelitis is still a rare entity, with few cases reported in the literature. This diagnosis should be suspected especially in severely immunosuppressed patients with neurological symptoms.





POSTER PRESENTATIONS ABSTRACTS

Wednesday, September 10, 2014

Poster Presentations

10.30-11.30

Vascular Interventional NR 1

EP126-Endovascular Treatment of Carotid Stenosis an Experience in the Single Center Trial

*Daehyun Hwang*¹, Wooyoung You²

*Dongtan Sacred Heart Hospital Radiology Hwaseongsi-Korea, South*¹ *Dongtan Sacred Heart Hospital, Hallym University radiology -Korea, South*²

INTRODUCTION: Ischemic stroke is a major cause of adult disability and the 3rd leading cause of death. Approximately 15-30% of ischemic strokes are caused by obstructive carotid atherosclerosis involving the carotid bifurcation. The purpose of this study is to determine safety, short and mid-term outcomes of CAS (Carotid Artery Stenting) during the last 5 years in a single cerebrovascular disease specialized hospital.

MATERIALS and METHODS: Between January 2006 and December 2010, 101 successful CAS out of 103 attempted procedures in 89 patients were included in this study. The indications for CAS were symptomatic carotid-artery stenosis 60% and asymptomatic stenosis of at least 80%. There were 70 men and 19 women and their age range was 50-79 years (mean 71.1). Self expanding stents with cerebral protection devices were used in all cases. Acetylsalicylic acid (100mg/d) and clopidogrel (75mg/d) were applied for at least 4 to 5 days prior to procedure. Weight-adjusted (70U/kg) heparin was used. Atropine (1mg) was given intravenously, if needed, to reduce bradycardia and hypotension potentially associated with carotid dilation. Acetylsalicylic acid (100mg/d) and clopidogrel (75mg/d) was continued for 3 months after the interventional procedure. Mono antiplatelet therapy (aspirin, clopidogrel, or ticlopidine) was continued indefinitely. One hundred one stents (50 Protégé, 37 Precise stent, 12 Wallstent, and 2 Acculink) and distal filters (89 Spider Rx, 9 Filter-wire, 3 Embo-shield) were used.

RESULTS: There were one death (huge ICH), 4 minor strokes (4.2%), 9 bradycardia (9.4%), and 3 groin hematoma as peri-procedural complications. Follow-up angiography was done in 58 patients (61%) for 6-58 months (mean 17.3), there was only one restenosis (1%). Clinical follow-up was done for 84 patients (88%) for 6-60 months (mean 32), there were two deaths (2.3%, one myocardial infarction, one rectal cancer), one major stroke (basilar artery, 21 months), and one minor stroke (cerebellum, 10 months).

CONCLUSION: CAS is an effective treatment modality and as safe as CEA for carefully selected patients. Judicious selection of the procedure is made on a case-by-case after considering the patient (physiological), lesion, and access (anatomical) factors that increase the risk of CAS and CEA in that particular patient.

EP127-Quantitative Cerebral Angiography Evaluate Cerebral Venous Circulation with Aneurysmal Rupture

*Kwo-Whei Lee*¹, Fong Y Tsai², Wei-Liang Chen¹, Chi-Kuang Liu¹, Chen-Ling Kuo³

*ChangHua Christian Hospital Department of Medical Imaging ChangHua-Taiwan*¹ *Taipei Medical University Imaging Research Center -Taiwan*² *ChangHua Christian Hospital Vascular and Genomic Center -Taiwan*³

PURPOSE: Various spectra of etiology of cerebral aneurysmal rupture and inconsistent factors in clinical practice. Since we encountered one patient with cerebral aneurysmal rupture relating venous circulation and pressure gradient. Retrospectively reviewed 84 patients to evaluate cerebral venous circulation with cerebral aneurysm to validate our previous observation.

MATERIALS and METHODS: Among those 84 patients, 21 patients with dissection and 11 patients with incomplete imaging were excluded. 52 patients with complete data were analyzed.

Male:female=17:35 and age range from 24-85 with average 52.1 years. We compared cerebral venous circulation time among two groups: non-ruptured 13 patients and ruptured 39 patients.



POSTER PRESENTATIONS ABSTRACTS

Quantitative cerebral angiography were performed in all 52 patients by biplane angiographic suite (AXIOM-Artis,Siemens,Erlagen,Germany).The Tmax values of dural sinuses and jugular veins were defined in AP and LAT respectively. Cerebral circulation time(CCT) was measured from distal cervical internal carotid artery to proximal jugular vein junction with sigmoid sinus.Cerebral venous circulation time(Δ CCT)being venous Tmax minus arterial Tmax.

RESULT: Those ruptured group with asymmetrical venous drainage (atresia or aplasia) showed shortening and symmetrical cerebral venous circulation time. Those non-ruptured group showed non statistic difference with asymmetry without shortening of venous circulation time. However, two outlier non-ruptured patients had symmetrical but no shortening of cerebral venous circulation time

CONCLUSION: Certainly,our data do not measure the venous pressure gradients directly.With flow dynamic,smaller diameter vessel requires high pressure to achieve same flow with larger and dominant vessel. Thus pressure gradient which is reflected by shortening and symmetrical cerebral venous circulation may be considered as another potential factor of cerebral aneurysmal rupture.

EP128-Results of Endovascular Treatment for Unruptured Intracranial Aneurysms (UIA) Single Center Experience

*Svetlana Milosevic Medenica*¹

*Center of Radiology and MR, Clinical Center of Serbia Department of Neuroradiology, Belgrade-Serbia*¹

INTRODUCTION: The efficacy of endovascular treatment for unruptured intracranial aneurysms (UIA) has been elaborated in numerous papers and studies, however, there is always some controversy about optimal strategy of their treatment.

PATIENTS and METHODS: We report results of EVT for 33 patients harboring 38 UIA, treated by the author at Neurosurgical Clinic in Belgrade in the period from 2011 to the end of 2013. There were 28 women and 5 men, mean age of 54 years, ranging from 27 to 70 years. In 25 patients the aneurysm was found incidentally, in 3 patients it was found during evaluation for stroke, while 5 patients had an unruptured aneurysm associated with a ruptured one.

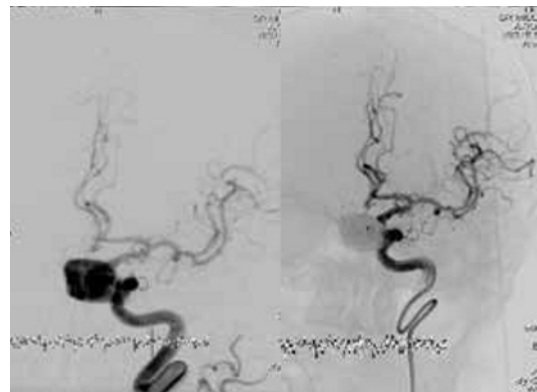
The endovascular treatment was realised by simple coiling in 28 patients and by stent-assisted coil embolization in 5 patients.

RESULTS: Immediate angiographic results demonstrated 17 complete occlusions, 3 neck remnants, and 1 residual dome filling. There were two complications during intervention - one rupture and one occlusion of the parent artery by protrusion of coil packing. Both patients recovered without deficit and in case of occlusion, carotid artery showed spontaneous recanalisation on the first control

angiography. On the 3 months control angiography there were 3 cases of impaction, all in large aneurysms, that were retreated. In one case there was a aneurysmal regrowth, also retreated by stent-assisted coiling. Three cases of residual neck filling were left for further follow up, as well as one case of residual dome filling that was not retreated because of difficult architecture of the MCA aneurysm.

CONCLUSION: Universal approach for patients with UIAs has yet to be established, however, if the treatment is chosen as an option, endovascular treatment has been shown to be a safe and efficient method in prevention of SAH. Our study on small number of patients showed a 0% mortality and immediate morbidity of 6% with an excellent further clinical outcome. Angiographic and clinical follow-up are necessary, especially for large and giant aneurysms where durability of treatment may be under question.

Fig. 1 Large unruptured calcified left cavernous ICA aneurysm treated successfully by coiling. The aneurysm was found incidentally on CT examination done for headache.





POSTER PRESENTATIONS ABSTRACTS

EP129-Covered Stent Placement for Emergency Reconstruction of Ruptured Carotid Artery during or after Transsphenoidal Surgery

*Byung Moon Kim*¹, Pyoung Jeon¹, Dong Joon Kim¹, Dong Ik Kim¹

*Severance Hospital, Yonsei University College of Medicine Radiology Seoul-Korea, South*¹

OBJECT: Internal carotid artery (ICA) rupture during transsphenoidal surgery (TSS) is an extremely difficult complication to treat. This study aimed to evaluate the immediate and long-term outcomes of covered stent placement for emergency reconstruction of ruptured ICAs during or after TSS. **METHODS:** Seven patients underwent covered stent placement for emergency reconstruction of a ruptured ICA during or after TSS. The safety and effectiveness of covered stent placement for emergency reconstruction of ruptured ICAs were retrospectively analyzed.

RESULTS: Pretreatment angiogram showed active bleeding in 6 patients (5 intraoperative and 1 postoperative) and a pseudoaneurysm in 1 patient. Of the 6 patients with active bleeding, 5 were treated with a successive operation to control active bleeding. The other patient was treated just after cardiopulmonary resuscitation due to massive nasal bleeding 20 days after revision of TSS. All active bleeding was controlled immediately after covered stent insertion in these 6 patients. One patient showed a gap between the covered stent and ICA wall without active bleeding 30 minutes after glycoprotein IIb/IIIa inhibitor administration due to in-stent thrombosis. The gap was occluded with coiling after completion of the temporarily held TSS. The 7th patient, whose ICA tear was treated with surgical suture, underwent covered stent placement for a pseudoaneurysm detected on postoperative day 2. During a mean follow-up period of 46 months (range, 12 – 85 months), all patients had excellent outcomes (modified Rankin scale, 0 or 1). All the stented ICAs were patent on vascular imaging follow-up at a mean of 34 months (range, 12 – 85 months).

CONCLUSIONS: Covered stents appear to be a safe and effective option for emergency reconstruction of ruptured ICAs during or after TSS.

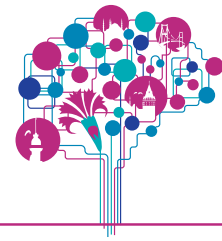
EP130-Retrieval of Dislodged Coil with Stent Retriever

*Mustafa Gok*¹, Celal Cinar², Halil Bozkaya², Ismail Oran²

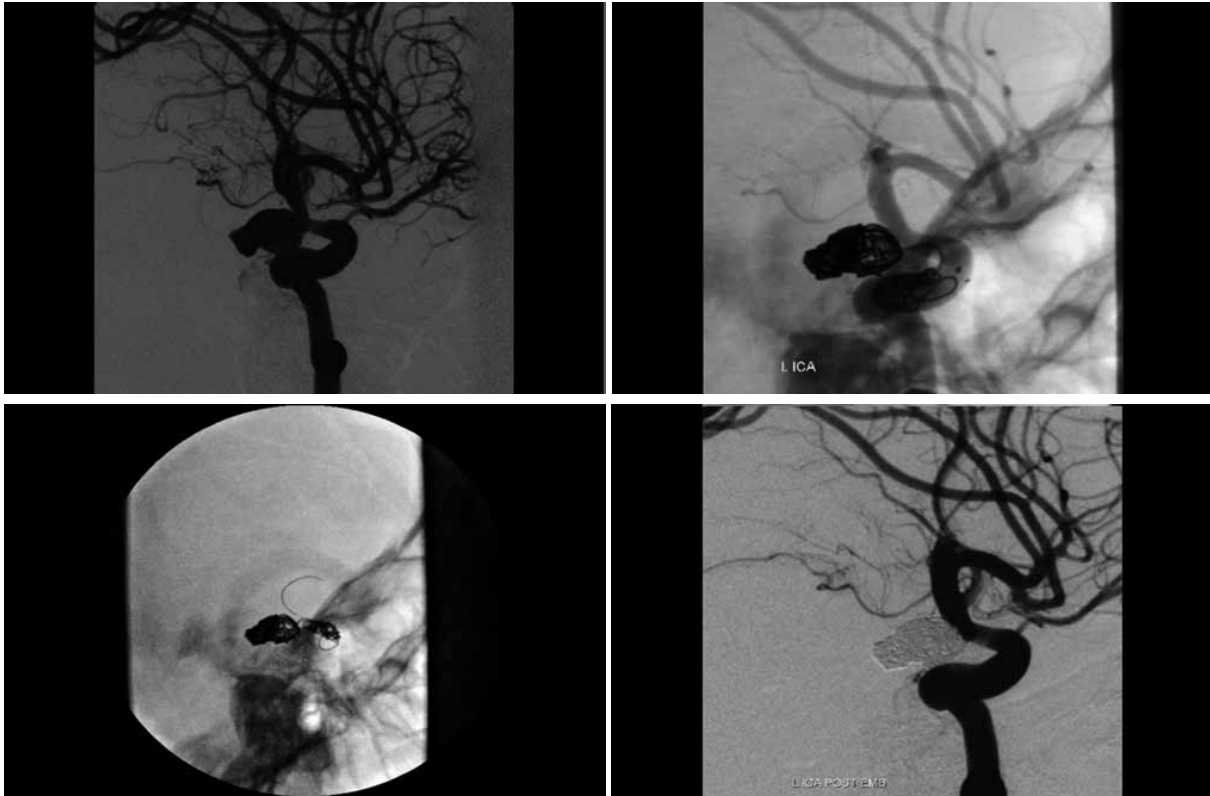
*Kafkas University Hospital, Kars Radiology Izmir-Turkey*¹ *Ege University Hospital, Izmir Interventional Radiology -Turkey*²

Endovascular aneurysm occlusion is proven to be less invasive and safer than open craniotomy and clipping. Although periprocedural complications are unusual during a coiling procedure, they do carry potential devastating consequences. Among the less frequent complications is the complete herniation of a coil from the aneurysm estimated to occur in 2.5–6% of the procedures, requiring either retrieval or fixation. Several commercially available devices are supposed to enable retrieval of a dislodged coil. In our case, 39 y/o female with left internal carotid artery paraclinoid ruptured saccular aneurysm was being treated with endovascular embolization. During embolization detachable coil was uncoiled and then dislodged into the internal carotid artery. We are presenting the retrieval of totally dislodged coil with stent retriever (Solitaire AB).

Solitaire stent, which was originally designed to be a retractable stent for stent-assisted coiling, proved to be effective in the removal of a dislodged coil into parent artery.



POSTER PRESENTATIONS ABSTRACTS



EP131- Onyx in Brain Arteriovenous Malformation Embolisation: Experience in a Malaysian Tertiary Referral Center

Hilwati Hashim¹, A Sobri Muda², Aida Abdul Aziz³, Zuhanis Abdul Hamid³

¹Imaging Unit, Faculty of Medicine, Universiti Teknologi MARA, MALAYSIA

²Department of Radiology, Universiti Kebangsaan Malaysia Medical Centre, MALAYSIA

³Department of Radiology, Hospital Sungai Buloh, MALAYSIA

Purpose: To report our experience in brain arteriovenous malformation (bAVMs) embolisation using Onyx (alone or in combination with histoacryl) in a Malaysian tertiary referral center.

METHODS: A retrospective review was done on all bAVM patients that were embolised at our center. We analyse the bAVM anatomy, technical conditions, complications and clinical outcome.

RESULTS: Between January 2010 to January 2013, 13 patients (6(46.2%) male; 7 (53.8%) female, age 14 – 57 years) were included. A total of 31 procedures were performed (median 2, range 1- 5 procedures). Clinical presentation included haemorrhage (9(69.2%)), seizures and headache (2(15.4%) respectively). Most AVMs were located in the brain hemispheres (12 (92.3%) (12)) and measures <3cm (53.8%(7)).

Complete occlusion of the AVM was obtained in 2(15.4%) patients, as a result of embolisation and natural regression of the nidus following embolisation. 11(84.6%) patients had partial occlusion (6(54.5%) have a <50% nidus occlusion). Of these 11 patients, 6 patients are lost to follow up. 4 patients are currently on expectant management as they are waiting for radiosurgery (3) or refused further intervention (1).

Complications occurred in 4 procedures involving 3(23.1%) patients, related to haemorrhagic complication in 3 procedures and 1 non-haemorrhagic complication (venous thrombosis without infarct which subsequently led to complete occlusion of nidus). This resulted in death in 1 patient (mortality 7.7%) and complete recovery with no disability in 2 patients.



POSTER PRESENTATIONS ABSTRACTS

Conclusions: Onyx is suitable for bAVM embolisation with acceptable morbidity and mortality and good outcome.

EP132-Evaluation of Contrast Enhanced MR Angiography and Time OF Flight MR Angiography at 3Tesla in Previously Coiled Intracranial Aneurysms

Anshu Mahajan ¹, *N Khandelwal*¹, Vivek Gupta ¹, Ajay Kumar ¹, Sk Gupta ²
Pgimer Radiodiagnosis -India 1 Pgimer Neurosurgery -India 2

OBJECTIVE: To determine the usefulness of contrast-enhanced MR angiography for follow up of GDC treated coiled cerebral aneurysms by comparing CE-MRA with 3D time of flight (3D TOF) MRA and DSA.

METHODS: In a prospective comparative study, 23 consecutive patients with 24 saccular aneurysms treated with endovascular coiling underwent simultaneous 3 T TOF-MRA, CE-MRA and DSA at follow-up. Comparison of maximum size of aneurysm remnant using paired t test between all four imaging modalities and Comparison of quality of images between MRA TOF and CE-MRA using Wilcoxon Signed Ranks Test were done.

RESULTS: The mean size of aneurysm remnant on MRA TOF was 4.095+/-4.36mm which was less than that on other modalities with mean size of 4.57+/-4.50mm on CE-MRA, 4.65+/-4.47mm on 2D DSA and with the maximum mean size of 5.78+/-4.53mm on 3D DSA.). Difference between MRA TOF and the other modalities (CE-MRA, 2D DSA and 3D DSA) was found to be highly significant (P<0.001). Difference between the size of remnant on CE-MRA and 2D DSA was not found to be significant (p=0.592). Size of aneurysm remnant on 3D DSA were also compared with size of remnant on MRA TOF, CE-MRA, 2D DSA and 3D DSA and the difference was found to be highly significant (P<0.001). Quality of images on MRA TOF was graded as 1(good) in 12(50%) of the cases, 2(fair) in 7(29.1%) cases and 3(poor) in 5(20.8%) of the cases. Quality of the images were graded as 1(good) in 18(75%) of the cases, 2(fair) in 6(25%) of cases on CE-MRA.

CONCLUSION: CE-MRA was observed as better imaging technique compared to MRA TOF in terms of quality especially in case of stent assisted coiling .CE-MRA is an excellent alternative to 2D DSA in detection of coiled aneurysm remnant and evaluation of parent vessels status aLSO.

EP133-Endovascular Treatment of 88 Anterior Communicating Artery Aneurysms. Overall Perioperative Results

*Yon Kwon Ihn*¹, Won Sang Jung ¹, Yoon Joon Hwang ²

St. Vincent Radiology Suwon-Korea, South 1 Inje University Ilsan Paik Hospital Radiology -Korea, South 2

OBJECT: We present our experience with endovascular treatment of a series of 85 consecutive patients with a anterior communicating artery aneurysm(AcoA).

METHODS: We reviewed database of AcoA management retrospectively. The aneurysms were managed with an endovascular approach in which detachable coils were used. Aneurysm characteristics, endovascular procedures, angiographic outcomes, complications were reviewed.

RESULTS: From May 2002 through March 2013, 88 aneurysms in 85 patients were treated endovascularly. Of the 88 aneurysms, 83 (94 %) were small, 5 (6%) were large. 60 (68%) aneurysms had a small neck, whereas 28(32%) had a wide neck. 62 (70%) aneurysms presented with subarachnoid hemorrhage and 26 (30%) incidentally found. 73 aneurysms were treated with a simple technique while the remaining 15 required adjunctive technique: double microcatheters (n=11), stent assisted coiling (n=3) and balloon assisted technique (n=1). A complete aneurysm occlusion was attained in 74 cases (84%), a neck remnant was detected in 10 cases (11%), and in 4 cases a residual filling of a portion of the aneurysm was observed. No rebleeding occurred. Regarding the neurological outcome at clinical follow up, 73/88 patients (82%) were either intact, improved, or unchanged from their initial clinical results. The procedure-related morbidity-mortality rate were 4.5 % (4



POSTER PRESENTATIONS ABSTRACTS

cases) and 0%, respectively. 5 patients of 88 died for vasospasm after the procedure, both had presented with HH grade IV and Fisher grade III. In patients with incidental aneurysms, the procedure-related morbidity mortality rates were 3% (1case) and 0%, respectively.

CONCLUSIONS: The endovascular treatment of AcoA is feasible, with good overall clinical and anatomical results. Tailored microcatheter shaping and/or adjunctive techniques are necessary for successful aneurysm embolization.

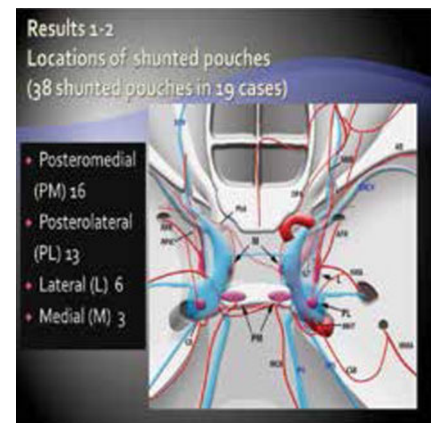
EP134-Shunted Pouches of Cavernous Sinus Dural AVFs Evaluation by 3DRotational Angiography

*Hiro Kiyosue*¹, *Shuichi Tanoue*², *Ryuichi Shimada*¹, *hiromu Mori*¹
*Oita University Radiology Yufu-Japan*¹ *Oita University Radiology -Japan*²

PURPOSE: To evaluate the angioarchitecture of cavernous sinus dural arteriovenous fistulas (CSdAVFs), including the frequency and location of shunted pouches, and their feeding arteries. METHODS: Nineteen consecutive cases of CSdAVFs that underwent 3DDSA/DA and transvenous embolization between 2007 and 2013 were reviewed. MPR images of rotational angiography and selective angiography were reviewed with a particular interest to the shunted pouches.

RESULTS: All cases showed SPs, with numbers ranging from 1 to 4 (mean, 2.2). The location of the SPs was "posteromedial" in 16, "posterolateral" in 13, "lateral" in 6, and "medial" in 3 patients. 6 cases showed posteromedial shunted pouches alone and 3 cases showed posterolateral shunted pouches alone. The other 10 cases showed multiple locations of shunted pouches. All cases were successfully treated by transvenous embolization with sinus packing (n = 11) or selective embolization of the SP (n = 8). Selective embolization is more frequently performed in the cases with posteromedial shunted pouch alone (5 in 6 cases) than others (3 in 13 cases).

CONCLUSION: The SPs are frequently located posteromedial and/or posterolateral to the cavernous sinus. Location and number of SPs are important for the treatment of CSdAVFs.



EP135-Clinical Results of Carotid Artery Revascularization as Carotid Artery Stenting for First Line Treatment Single Center Experience in Japan

*Ichiro Nakahara*¹, *Haruka Miyata*¹, *Tsuyoshi Ohta*¹, *Shoji Matsumoto*¹, *Ryota Ishibashi*¹, *Masanori Gomi*¹, *Masato Saka*¹, *Takuya Okada*¹, *Hidehisa Nishi*¹, *Kazutaka Sonoda*¹, *Junpei Koge*¹, *Sadayoshi Watanabe*¹, *Izumi Nagata*¹

*Kokura Memorial Hospital Department of Neurosurgery, Stroke Center Kitakyushu-shi-Japan*¹

OBJECTIVE: Penetration ratio of carotid artery stenting (CAS) in carotid revascularization exceeds more than 60% in recent years in Japan. CAS has been chosen since more than 10years ago for first-line treatment, while CEA is applied to CAS high-risk patients dependent on factors including plaque characteristics, risk of hyperperfusion, catheter accessibility by multimodality neuroradiological assessment including plaque MRI,SPECT and CT/MRI/DSA. The aim of this study is to evaluate short-term and mid-term results of single center experience of 266 consecutive cases with CAS / CEA for 5 years since January 2009 in our institute.



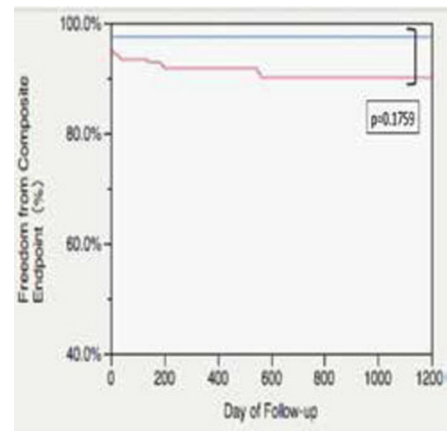
POSTER PRESENTATIONS ABSTRACTS

MATERIALS / METHODS: Consecutive 227 CAS and 39 CEA cases were analyzed retrospectively. The primary outcome measures (short-term results) were any periprocedural (within 30 days after procedure) death, stroke, and acute coronary syndrome, and the rate of postoperative positive lesion in diffusion weighted imaging (DWI) on MRI. The mid-term results include death, stroke, and restenosis requiring retreatment during the follow-up periods.

RESULTS: There were no significant differences in age, underlying disease, and the severity of stenosis in both CEA and CAS group. However, the percentage of symptomatic lesion and the MRI T1WI plaque-sternocleidomastoid muscle ratio (index of the vulnerability of plaque) were higher in CEA than CAS group (69% vs. 48%, $p=0.015$; 1.79 ± 0.46 vs. 1.31 ± 0.37 , $p<0.0001$). Short-term results revealed no mortality in both groups, any stroke 2.6% CEA vs. 4.9% CAS ($p=1$); major stroke 2.6% CEA vs. 0.9% CAS ($p=0.38$); acute coronary syndrome 0% CEA vs. 0.9% CAS ($p=1$); the rate of DWI-positive 24% vs. 39% ($p=0.10$). Mid-term results during the follow-up periods (CEA 18.3 ± 13.5 month, CAS 20.3 ± 14.1 month): death 5.1% CEA vs. 5.7% CAS ($p=1$), stroke 7.7% CEA vs. 11.0%

CAS ($p=0.78$), restenosis requiring retreatment 0% vs. 6.6% ($p=0.14$).

CONCLUSION: The short-term and the mid-term results were excellent and equivalent in CAS and CEA although we apply CEA to high-risk lesions such as fragile plaque or symptomatic lesion. Our protocol, in which most patients undergo less invasive CAS as the first-line while CEA is selected for CAS high-risk patients by multimodality neuroradiological diagnosis, enables to provide high quality treatment for carotid artery revascularization.

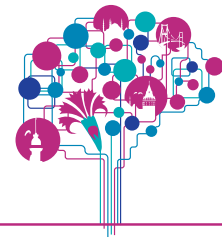


EP136-Endovascular Treatment of Vertebro Vertebral Fistula (VVF) in A Patient with Neurofibromatosis Type 1 (NF1) Present with Right Sided Neck Mass and Pulsatile Tinnitus A Case Experience in Ramathibodi Hospital

*Pakorn Jiarakongmun*¹, Ekkachat Chanthanaphak¹, Thanaboon Worakijthamrongchai¹, Sirintara Pongpech¹
*Ramathibodi Hospital Radiology, INR Bangkok-Thailand*¹

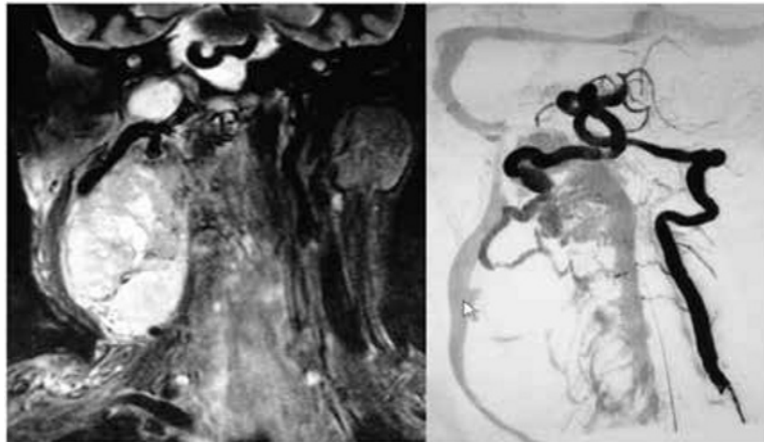
INTRODUCTION: NF1 is a predisposing disease that can lead to direct AVFs in various structures, and rarely to present as VVFs. Clinical presentation, imaging findings and endovascular treatment will be discussed.

METHOD AND RESULT: We retrospectively review a 28-year-old woman, with underlying NF1 with known intra-abdominal nerve sheath tumor, present with progressive enlargement of the right sided neck mass, and right sided pulsatile tinnitus about 5 months. MRI and Contrast MRA of the neck shows large lobulated enhancing mass at right carotid space, representing large neurogenic tumor. There is adjacent multiple vascular flow voids within right sided foramen trans-versarium and asymmetrical dilatation or right sided epidural veins in cervical spinal canal, suggestive of arterio venous fistula or VVF. On 3D cerebral angiogram, the study shows high flow arterio-venous fistula or VVF, at right sided C1-2 level. Proximal right vertebral artery (RVA) shows irregular lobulated appearance, related with high flow arterial wall change or arteropathy in NF1. There is also retrograde flow from LVA and stealing flow of basilar artery to feed the VVF. Further trans-arterial embolization is done successfully, using microcatheter in retrograde fashion from LVA to the VVF, and 9 detachable coils had been applied following by 40% conc. N-butyl cyanoacrylate (NBCA), resulting as total obliteration of the VVF. No neurologic complications is detected.



POSTER PRESENTATIONS ABSTRACTS

CONCLUSION: NF1 is one predisposing disease leading to both neurologic tumor and direct AVFs in various organ, which the artery lying adjacent with vein. VVFs is the most common paraspinous AV shunt in children, with 50% spontaneous evolution and less commonly related with injury or underlying disease. Therefore in spontaneous VVF, the associated or predisposing disease or condition should be aware to avoid periprocedural complication and prognosis. Clinical presentation, imaging findings and endovascular treatment technic and material will be discussed.



EP137-Acute Tonsillar Herniation in Malignant Cranial Dural Arteriovenous Fistula Rapid Recovery Following Transvenous Fiber Coil Embolization A Case Report

*Ekachat Chanthanaphak*¹, Pakorn Jiarakongmun¹, Thanaboon Worakijthamrongchai¹, Sirintara Pongpech¹

*Ramathibodi hospital, Faculty of Medicine, Mahidol University Department of Radiology Bangkok-Thailand*¹

INTRODUCTION: Acute tonsillar herniation is a rare sequelae of cranial dural arteriovenous fistula (AVF) but is an importance for emergency treatment.

METHOD AND RESULT: A 67-year-old female presented with chronic headache for 1 year. In last 1 month, she have had mild impairment of executive function. Neurological examination showed good orientation but slow calculation, symmetrical pupil size and motor power grade V in all extremities. No cranial nerve deficit was found. Immediate CT brain revealed a large venous pouch with a surrounding intraparenchymal hematoma in the right temporal lobe and pressure effect, causing a 3-cm midline shift to the left. In addition, diffuse cerebral swelling and dilated cerebral cortical veins as well as tightness of the basal and prepontine cisterns. No brain herniation was found. Diagnosis is considered as malignant cranial dural AVF. Patient was admitted and closed observation in ICU that had been planned for endovascular treatment in the next day later. During in ICU - 12 hours after admission, patient developed progressive stupor and did not follow to command, GCS = E2V2M5 and asymmetrical pupil size. Immediate CT brain showed progressive diffuse cerebral swelling and new development of acute tonsillar herniation. Emergency cerebral angiography was done demonstrating dural AVF in the middle 1/3 superior sagittal sinus with occlusion of the posterior 1/3 superior sagittal sinus.

It is supplied from dural arteries of bilateral internal and external carotid arteries and bilateral vertebral arteries. Aggressive cortical venous refluxes in bilateral cerebral cortical engorged veins were shown. Subsequently transvenous approach through the occluded posterior 1/3 superior sagittal sinus was done with fiber coils embolization. Post embolized angiogram showed significant reduction of cortical venous reflux. Minimal residual shunt was found. Clinical follow-up in 30-hours after treatment, patient had awaken, GCS = E4V2M6. Additional CT brain was performed showing decrease of cerebral swelling and resolution of tonsillar herniation.



POSTER PRESENTATIONS ABSTRACTS

Patient had gradual clinical improvement and had been discharged in next few days.

CONCLUSION: Acute tonsillar herniation in malignant dural AVF is a rare complication but is an emergency for endovascular treatment. Successful endovascular treatment makes a rapid response and good outcome.

EP138-Treatment of Bizzare Shaped Wide Necked MCA Aneurysms with Penumbra Coils 400 without Supporting Devices Report of 4 Cases and Review of Literature

Svetlana Milosevic Medenica¹

Center of Radiology and MR, Clinical Center of Serbia Department of Neuroradiology, Belgrade-Serbia¹

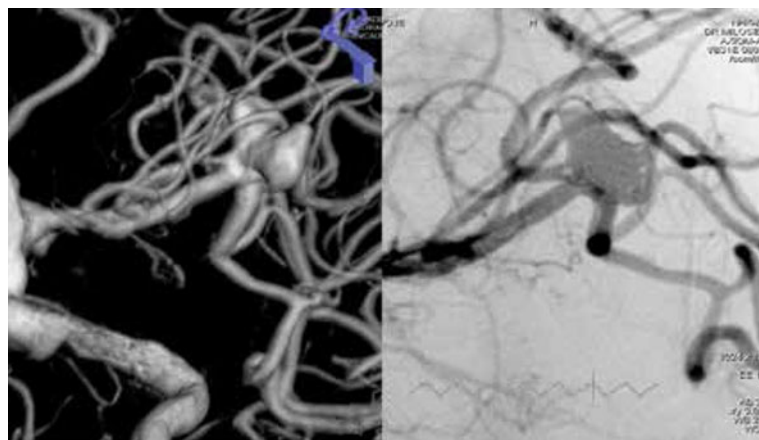
INTRODUCTION: The first experiences with the large diameter Penumbra Coil 400 (PC400) system have shown to be positive in the terms of safety, efficacy and cost effectiveness, because their use enables treatment of cerebral aneurysms with fewer coils, decreased procedure time and increased packing density compared with standard coils.

METHODS: In the period from 2012 up to date, at Neurosurgical Clinic in Belgrade, 14 aneurysms have been treated by the author with Penumbra Coils 400. Four of them were the aneurysms of the MCA bifurcation, of very complex angio-architecture and wide - necked. All 4 aneurysms were unruptured.

RESULTS: With the use of Penumbra coils 400 it was possible to occlude all four, very bizarre shaped, relatively large aneurysms (10 - 15 mm), using fewer coils and without support of stent or balloon. One of them, sized 14 mm, was satisfactorily occluded with the use of only one coil (Fig. 1). There were no complications during, neither after the procedure. Control angiography showed a complete aneurysmal occlusion in two and nearly complete in one patient, while the fourth case was done recently and the control angiography has not yet been done.

CONCLUSION: MCA bifurcation aneurysms may have a very complex angio-architecture and are often difficult to treat by either method. With careful use of appropriately sized Penumbra coils, thanks to their softness and the large diameter, it may be possible to distribute coils inside the sac without protrusion towards parent artery and without occlusion of MCA branches. Properly packed coil loops create some kind of intrasaccular flow diverter that protects the aneurysmal neck. More experience is needed, but the first results are very promising.

Fig.1 Complex shaped aneurysm of the left MCA bifurcation sized 14 mm before and after embolization. This aneurysm was satisfactorily treated by one one Penumbra coil (Complex Standard 14 x 50).





POSTER PRESENTATIONS ABSTRACTS

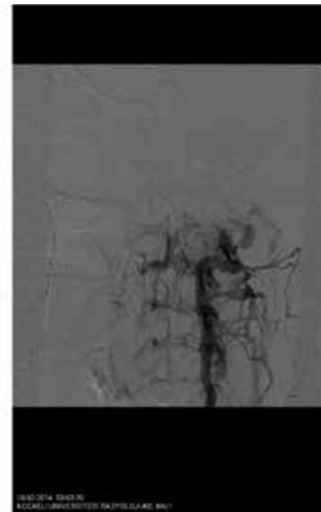
Vascular Interventional NR 2

EP139-Endovascular Treatment of Traumatic Vertebral Artery Arteriovenous Fistula and Pseudoaneurysm

*İsa Çam*¹, Ercüment Çiftçi¹, Sevtap Gümüştaş¹, Halil İbrahim Ada¹, Ahmet Yalınız¹, Bayram Yildirim¹, Tuğçe Ağırlar¹
*Kocaeli University Radiology Kocaeli-Turkey*¹

PURPOSE: The purpose of this study was to describe the clinical and anjiographic findings and present endovascular treatment of vertebral arteriovenous fistula and pseudoaneurysm after vertebral artery injury with gunshot wounds

MATERIAL AN METHODS:53 year old woman was admitted to our hospital with two gunshot wounds to her head and neck . She was eveluated with cranial-cervikal X-ray, computed tomography (CT) (Toshiba aquillion,64 slice), Brain 3T MR (Philips Achievea Intera Release Eindhoven, Netherlands) and angiography. Electrically detachable coils were used for endovascular treatment. **RESULTS:** CT examination revealed multiple fracture of left maxillofacial bones and foramen transversarium on C1 vertebral bone. Postcontrast scan showed pseudoaneurysm of left vertebral artery. Cranial MRI showed no ischemic lesion. After stabilization , selective left vertebral angiography demonstrated pseudoaneurysm and fistula at C1 level between distal segment vertebral artery of PICA with vertebral venous plexus. Therefore a catheter was advanced into the right vertebral artery from right brachial artery. micro catheter (Excelsior SL-10) and microguide (Radiofocus 0.012 90°) was advanced into left vertebral artery via right vertebral artery and basillary artery. Distal part of Arteriovenous fistula and pseudoaneurysm was occluded with electrically detachable coils. Catheter was advanced into the left vertebral artery via right femoral artery. Proximal part of arteriovenous fistula and pseudoaneurysm was occluded with electrically detachable coils. Control anjography showed complete occlusion of the arteriovenous fistula and pseudoaneurysm. **CONCLUSION:** An arteriovenous fistula and psedoaneurysm involving the vertebral artery is rare. These lesions can be of traumatic or spontaneous origin. Traumatic lesions are freuquently associated with penetrating neck injuries. Endovascular techniques are safe and effective method of treatment and is not associated with significant morbidity and mortality.





POSTER PRESENTATIONS ABSTRACTS

EP141-Coil Embolization of Cavernous Sinus Dural Arteriovenous Fistula via Direct Puncture of Superior Ophthalmic Vein after Surgical Exposure of the Vein

*Kostas Lagios*¹, Ioannis Ntountas², Theodoros Bazinas¹, Michalis Mantatzis³

251 Aiforce General Hospital Interventional Neuroradiology Athens-Greece¹ 251 Aiforce General Hospital Ophthalmology -Greece² Democritus University of Thrace, Univ. Hospital of Alexandroupoli Neuroradiology Section, Radiology Department -Greece³

INTRODUCTION: Complicated vessel anatomy may be an impervious obstacle to optimal treatment of challenging dural AV fistulas. We present a case in which we manage to establish a pathway to the cavernous sinus through direct catheterization of the superior ophthalmic vein (SOV) after surgical exposure. **CASE:** A 67-year-old female presented with red eye, high intraocular pressure and blurred vision. Digital subtracted angiography demonstrated a Cavernous Sinus dural AV fistula with feeders arising predominantly from internal carotid artery. After unsuccessful attempt to reach the cavernous sinus by regular routes, the embolisation was attempted by direct surgical exposure of the ipsilateral SOV. The embolisation was uneventful resulted in rapid resolution of her symptoms and signs.

CONCLUSION: Transvenous embolisation via SOV is a good alternative treatment when conventional routes are inaccessible and arterial route considered a high risk procedure. Surgical access to the SOV is direct and can be performed safely in centers where experienced ophthalmic surgeons co-operate with interventional neuro radiologists.

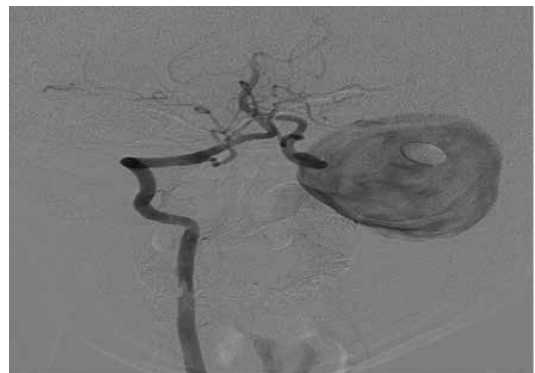
EP142-Endovascular Treatment of Giant Extracranial Vertebral Aneurysms With Neurofibromatosis Type 1 A Report of 3 Cases

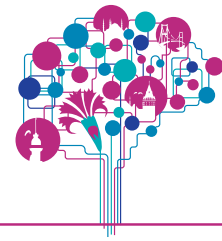
*Pao-Sheng Yen*¹, Chun-Han Liao¹

China Medical University Hospital Dept of Radiology Taichung City-Taiwan¹

PURPOSE: Aneurysms of the extracranial vertebral are uncommon. The majority are caused by major trauma. We present two patients with spontaneous vertebral artery aneurysms associated with neurofibromatosis type1 (NF1) who were successfully managed endovascularly, providing satisfactory mid-term clinical and imaging results. Only 8 cases were identified in the literature we reviewed. **MATERIAL and METHODS:**Case 1. A 44 year old woman of NF1 suffered progressive headache, dizziness, unstable gait and strong pulsatile tinnitus for years. Imaging studies revealed dissecting aneurysm in left distal vertebral artery with high flow vertebro-vertebral fistula(VVF)formation. Endovascular treatment was performed by trapping of the distal vertebral artery with detachable coils. Case 2. A 35 year old woman of NF1 experienced sudden onset severe neck pain with a palpable neck mass on the left side. MRI, CTA and angiography study revealed giant left extracranial vertebral aneurysm. Endovascular treatment was performed by trapping of the vertebral artery with detachable coils. Case 3. A 43 year old woman of NF1, suffered from sudden onset of severe nuchal pain with radiation to left arm due to giant extracranial vertebral aneurysm. The aneurysm was trapped by detachable coils distally and proximal occlusion by graft stent placement in subclavian artery. All patients recovered uneventfully and were discharged.

CONCLUSION: The results suggested that endovascular treatment is a safe and effective technique for the treatment of extracranial vertebral aneurysms with NF1.





POSTER PRESENTATIONS ABSTRACTS

EP143-Intracranial Aneurysms Treated by Flow – Diverting Stents Results of Long – Term Follow – up with Contrast – Enhanced MR – Angiography

*Maximilian Patzig*¹, Lorenz Ertl¹, Robert Forbrig¹, Hartmut Brückmann¹, Gunther Fesl¹
*University of Munich Neuroradiology München-Germany*¹

PURPOSE: Long-term data on aneurysm treatment with flow-diverting stents are still sparse. Recommendations regarding the methods and timing of follow-up are yet to be determined, with protocols differing widely between institutions. We present long-term results, with a focus on the usefulness of 3T-MRI including contrast-enhanced-MR-angiography (ceMRA).

METHODS: Patients with aneurysms treated by flow-diverting stents without additional coiling and follow-up MRI after at least six months were included. Fusiform basilar artery giant aneurysms were excluded, as these data are reported elsewhere. 3T-MRI protocol included dedicated ceMRA in arterial and venous phase. Aneurysm thrombosis, size of the aneurysmal sac and complications were evaluated. Additionally, we graded the ability of MRI with ceMRA to visualize these parameters on a 1–3 scale.

RESULTS: Twenty-one patients were included. Aneurysms were incidental in 15 cases and symptomatic due to cranial nerve compression in six cases. Stenting was performed with “Pipeline” in 17 cases and “Silk” stents in 4 cases. Four technical complications occurred, one of which caused clinically apparent ischaemia. Duration of follow-up was more than two years in 16 patients. Complete occlusion of the aneurysm occurred in 18 cases (86 %). Of 13 cases in which a three-month-follow-up was available, seven were occluded at that time (54 %).

At six months, 18 aneurysms were occluded (86 %). The aneurysmal sac shrank in 16 of the 18 occluded aneurysms, in eleven cases to less than 50% of the original size. On follow-up, one small perianeurysmal haemorrhage and one in-stent stenosis were found on MRI. Three of the symptomatic patients improved clinically. CeMRA assessability of aneurysmal thrombosis and size of the aneurysmal sac was graded as good in all cases. Where available, no discrepancies were found between ceMRA and digital subtraction angiography regarding aneurysm perfusion. Assessability of the stent lumen was reduced in cases treated with “Pipeline” and good in cases treated with “Silk”.

CONCLUSIONS: Flow-diverter treatment can achieve high occlusion rates and cause major aneurysm shrinkage in many cases. The development of aneurysm thrombosis and shrinkage differs between patients, making high-quality follow-up imaging important. MRI with ceMRA proved highly valuable regarding imaging of the aneurysm and late complications. The assessability of the stent lumen on ceMRA depends on the stent type.

EP144-Contrast Enhanced Angiographic Cone Beam CT (CBCT) Practical Usage in Neurointervention Cases

*Ahmad Sobri MUDA*¹, Nik Azuan Nik Ismail¹, Zahiah Mohamed¹, Mohd Redzuan Ismail¹, Rozman Zakaria¹, Yazmin Yaacob¹, Ainul Syahrilfazli Jaafar²
*UKMMC Radiology KUALA LUMPUR-Malaysia*¹ *UKMMC Neurosurgery -Malaysia*²

Angiographic cone beam CT (CBCT) technology improves significantly and now able to provide comparable quality soft tissue images comparable multidetector CT (MDCT).

We have performed over 60 cases of contrast enhanced CBCT in our centre, within a period of one and a half year. The images obtained using a motorized frontal C-arm with soft-tissue-optimized CBCT (VasoCT; Philips Medical System), acquiring 620 projection images over a 200° arc (rotation time, 20.7 seconds) with diluted contrast given direct intrarterially via intrarterial catheters or intravenously via peripheral access, following prescribed injection protocols.

We described pictorial series of the cases illustrating its advantages and issues particularly in correlation to the morphology of the neurovascular lesions and the impact on their treatment.



POSTER PRESENTATIONS ABSTRACTS

EP145-Subacute Recanalization of Parent Artery after Internal Trapping of Ruptured Dissecting Aneurysms Does Not Lead to rebleeding a Report of 3 Cases

*Yasuhiro Takeichi*¹

*Japanese Red Cross Otsu Hospital Neurosurgery Otsu-Japan*¹

PURPOSE: Internal trapping by endovascular surgery has been widely used as a treatment for ruptured dissecting aneurysm, but early recanalization after treatment can lead to rebleeding. We commonly must re-embolize recanalized spaces. However, the natural history of these subacute recanalized cases is unknown.

METHODS: Here we report three cases of subacute recanalization of parent artery after internal trapping of ruptured dissecting aneurysm without re-embolization.

RESULTS: Case 1: A 42-year-old woman with a history of sudden-onset headache (subarachnoid hemorrhage [SAH] of World Federation of Neurological Surgeons [WFNS] grade II) had a right vertebral artery (VA) dissecting aneurysm (posterior inferior cerebellar artery [PICA] distal). Complete internal trapping of the right VA was performed. Anterograde recanalization was confirmed on angiography on day 24. No neurological abnormalities, ischemic complications, or bleeding were seen on angiography two and a half years later.

Case 2: A 44-year-old woman with a history of sudden-onset headache (SAH of WFNS grade II) had a VA dissecting aneurysm (left PICA involve type). Complete internal trapping of the left VA was performed, but angiography on day 28 revealed posterior recanalization of the left VA and left PICA. No neurological abnormalities, ischemic complications, or bleeding were seen on angiography 2 years later.

Case 3: A 43-year-old man with a history of consciousness disturbances (SAH of WFNS grade V) had a left PICA dissecting aneurysm. Complete internal trapping of the left PICA was performed on day 1. Recanalization of the left PICA through the coil mass was realized on day 21. He was discharged alert but with double vision . Follow-up angiography 3 years later revealed no change in the recanalized vessel. All cases had a good prognosis without rebleeding.

CONCLUSIONS: Here, we showed the possibility of successful subacute recanalization in patients who have undergone internal trapping of ruptured dissecting aneurysm.

EP146-Mechanical Coil Insertion System

*Noriaki Matsubara*¹, Shigeru Miyachi¹, Kenichi Haraguchi¹, Yoshitaka Nagano², Hiroyuki

Yamada², N Marui², Akihito Sano³, Hideo Fujimoto³, Takashi Izumi¹, Toshihiko Wakabayashi¹

*Nagoya University Graduate School of Medicine Department of Neurosurgery Nagoya-Japan*¹ *NTN Corporation*

*New Product Development R&D Center -Japan*² *Graduate School of Engineering Nagoya Institute*

*of Technology -Japan*³

BACKGROUND: Like other fields of medicine, robotics and mechanization might be introduced into endovascular coil embolization of intracranial aneurysms for effective treatment. It's been already reported that coil insertion force could be smaller and more stable when the coil delivery wire is driven mechanically at a constant speed. There's the difficulty in synchronizing operators' minds and hands when two operators control the microcatheter and the coil respectively. We have therefore developed a mechanical coil insertion system enabling a single operator to insert coils at a fixed speed while controlling the microcatheter.

METHODS: Using our new system, the operator manipulated the microcatheter with both hands and drove the coil using foot switches simultaneously. A delivery wire force sensor was used concurrently, allowing the operator to detect excessive stress on the wire. In vitro coil embolization was performed using three methods: simple mechanical advance of the coil; simple mechanical advance of the coil with microcatheter control; and driving (forward/backward) of the coil using foot switches in addition to microcatheter control.



POSTER PRESENTATIONS ABSTRACTS

RESULTS: The system worked without any problems, and did not interfere with any procedures. In experimental embolization, delivery wire control using the foot switches and microcatheter manipulation helped to achieve successful insertion of coils. This system could offer the possibility of developing safer and more efficient coil embolization.

CONCLUSIONS: Although we aim at total mechanization and automation of procedures in the future, microcatheter manipulation and synchronized delivery wire control are still indispensable using this system.

EP147-Morbidity Associated with Endovascular Treatment of Complex Intracranial Aneurysms with Self Expanding Stents vs Flow Diverters

Bernardo Lander ¹, García María Berenice ², Alonso Arturo ¹, Alvarado Mariangela ¹, López Stefania ¹, Viso René ¹

Caracas University Hospital Radiology Caracas-Venezuela ¹ *Caracas Medical Center Vascular Explorations Unit -Venezuela* ²

PURPOSE: To assess the morbidity associated with endovascular treatment of complex intracranial aneurysms with self-expanding stents (SES) vs flow diverting devices (FDD).

METHODS: Descriptive, retrospective, multicentric study. 53 patients were included (43 women, mean age 50,25 years old) carriers of 56 aneurysms (2 infundibulum, 12 big, 5 giant, 32 wide neck, 60% from the Internal Carotid Artery) susceptible of endovascular treatment with FDD (Pipeline or Fred) or SES (Enterprise or LVIS) in the Interventional Neuroradiology Unit at Caracas University Hospital (HUC) and Caracas Medical Center (CMC) between April 2010 and April 2014. All patients received oral anti-aggregation therapy with ASA 100mg and Clopidogrel 75mg daily 1 week prior to the procedure and for six months after. Immediate post-embolization changes, morbidity and results of successive angiographic control (1 to 12 months after) were assessed.

RESULTS: 32 patients with 35 aneurysms (60%) were treated with FDD (42 Pipeline, 1 Fred) and 22 patients with 22 aneurysms were treated with SES (11 Enterprise, 11 LVIS). Coils were used in 16 cases and balloon assistance in 3. Immediate post-embolization showed eclipse sign in 23 cases treated with FDD (74%), total aneurysm exclusion in 17 (Raymond 1), partial exclusion in 11 (Raymond 3) and no changes in 3. Neck thrombosis occurred in 1 SES case treated with Tirofiban without additional deficit. Device stenosis happened in 2 cases (FDD) solved mechanically with another FDD or with balloon inflation. 3 deaths associated to the procedure were reported (5,6%): 1 parental vessel rupture (1SES), 1 immediate SAH (FDD) and 1 SAH 13 days post-procedure (FDD). 2 other patients died due to comorbidity: pneumonia (1 SES) and SIADH (1 FDD). Successive angiographic control was performed in 47% of the patients showing total aneurysm exclusion in 15 cases (Raymond 1), partial exclusion in 3 (Raymond 3), sac size reduction in 6 (FDD), parental artery occlusion in 1 (FDD) and displacement of the FDD with sac refill in 1 patient, who underwent a second FDD placement with eclipse sign at immediate angiography.

CONCLUSIONS: Endovascular treatment with FDD and SES was associated to low rate morbidity ($\leq 6,25\%$) with both devices offering a safe and efficient therapeutic alternative for complex intracranial aneurysms.

EP148-Transverse –Sigmoid Sinus Dural Arteriovenous Fistula Presenting With Recurrent Transient Ischaemic Attack a Technical Case Report

Marlina Ramli ¹, Khairul Azmi Abdul Kadir ², *Hilwati Hashim* ³

University Teknologi Mara Medical Imaging Sungai Buloh-Malaysia ¹ *University Malaya Biomedical Imaging Malaysia* ², *University Teknologi Mara Medical Imaging Unit Sungai Buloh-Malaysia* ³

Intracranial dural arteriovenous fistulae (DAVF) are uncommon and account for about 10–15% of all intracranial arteriovenous malformations and approximately 1% of all strokes. All transverse-

POSTER PRESENTATIONS ABSTRACTS

sigmoid sinus DAVFs require treatment because of the low rate of spontaneous regression and the more frequent association with haemorrhagic and non-haemorrhagic aggressive neurologic symptoms. Untreated DAVFs of the anterior cranial fossa or the tentorium have 91% risk of hemorrhage. Endovascular embolization which aims for permanent obliteration of the DAVF is now the primary treatment modality for all DAVFs. Other treatment options available include surgery and radiosurgery. The aim of the treatment is for permanent and complete obliteration of the lesion with resolution of clinical symptoms. We present a 56-year-old patient with long standing history of intermittent TIA-like symptoms. Magnetic resonance (MR) angiography revealed right transverse-sigmoid sinus DAVF and bilateral vertebral arteries occlusion. The patient's intermittent TIA-like symptoms completely resolved upon successful trans-arterial embolization of the DAVF.

DAVF IMAGES

Figure 1- MRI brain images taken 3 days after admission showing:

- 1a and 1b) Axial T2W MRI images showing prominent dilated veins in the right cerebral hemisphere (white arrows).
- 1c and 1d) Axial diffusion weighted MRI images showing multiple hyperintense foci in the occipital lobe and cerebellum (white arrows).
- 1e and 1f) Absence of the distal portion of the vertebral arteries bilaterally in-keeping with occlusion (white arrows).

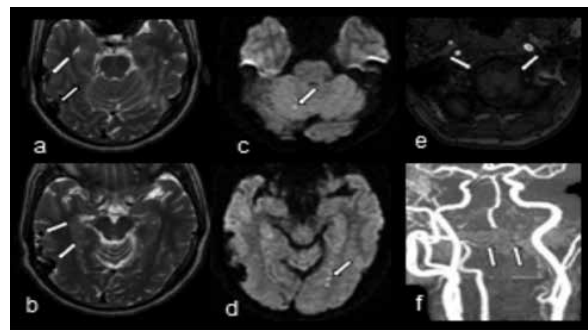


Figure 2:

- a) Lateral projection of the right ECA angiogram reveals a right transverse-sigmoid sinus DAVF (white arrow) fed by the petrosquamous branch of the right middle meningeal artery and trans-osseous branch of the right occipital artery.
- b) There is cortical venous reflux in delayed phase.

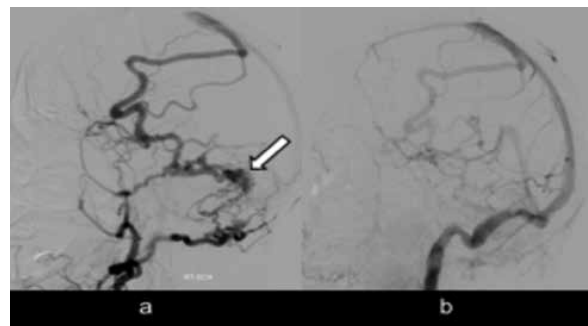
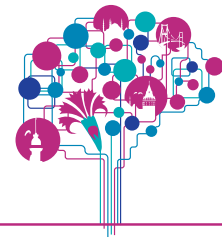


Figure 3:

- a) Microinjection into the petrosquamous segment of the left meningeal artery filling up the fistula and sinus. Onyx cast filled up the fistula (white arrow).
- b) Post-embolization angiogram image showing complete obliteration of the fistula with Onyx (white arrow) with absence of cortical venous reflux.

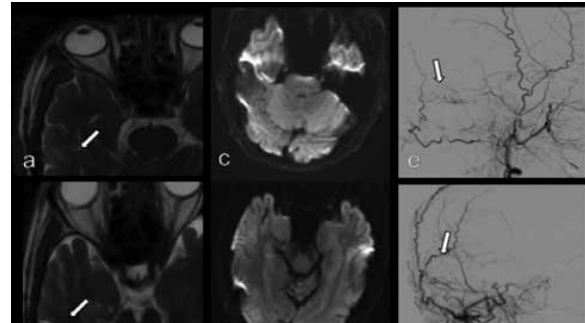




POSTER PRESENTATIONS ABSTRACTS

Figure 4 :

- 4a and 4b) Follow-up axial T2W MRI images showing no recanalization of the DAVF.
- 4b and 4c) Follow-up axial diffusion weighted MRI images showing resolution of the hyperintense areas previously seen in occipital lobe and cerebellum.
- 4d and 4e) Follow-up cerebral angiogram images showing Onyx cast within the fistula (white arrow) with no evidence of recanalization of the DAVF.



EP149-The Rate of Restenosis in Carotid Artery Stents and Late Follow up Results

Rahime Sezer ¹, Ahmet Peker ², Emrah Çağlar ³, Elif Peker ², Umman Sanlıdilek ²

Nigde State Hospital Radiology -Turkey ¹ Ankara University Radiology -Turkey ² Ankara Oncology Research and Training Hospital Radiology -Turkey ³

Stroke remains the leading cause of disability in adults and third leading cause of the death in developed countries. Carotid artery occlusive disease is the primary pathophysiological source of 10 to 20 % of all the strokes. Endovascular treatment of the carotid occlusive disease which is consisting of carotid artery angioplasty and stenting (CAS) currently represents a less invasive percutaneous alternative to conventional carotid endarterectomy(CEA). The availability of cerebral protection systems has expanded the area of application of this procedure. The aim of this study was to report our experience with carotid stenting in our first 191 consecutive patients.

Between June 2002 and November 2011, 191 consecutive patients (142 males, 49 females) with 199 lesions underwent CAS at the our interventional radiology unit. The mean age was 67,6(SD: $\pm 9,5$) years. Comorbid conditions included 87 hypertension, 81 coronary artery disease (21 patients with coronary by-pass, 3 patients with coronary stent) 52 diabetes mellitus. 111 patients was symptomatic while 80 patients were asymptomatic. All procedures were performed through long transfemoral way with using protection device, self-expandible stents and ballon dilatation. Patients were given clopidogrel and aspirin before and after the procedure and heparin during the intervention. All patients underwent routine Doppler ultrasound scanning (CDUS).

The technical success rate was %100. Control angiography showed a minor residual stenosis (<%10) in all patient. 68 patients(18 females, 50 males) of 191 was able to follow up. The mean age was 67,5(40-87)ys. There were 4 patients who had bilaterally carotid artery stenting operation; which means 72 carotid artery stents to follow up. The mean follow up time was 24,5 months(1-106). 59 carotid lesion by CDUS, 12 by Digital subtraction angiography and 1 carotid lesion followed up by computed tomography angiography. As a result 65(%90,3) stents were patent, 4(%5,5) in-stent restenosis, 2(%2,7) stent occlusion, 1(%1,4) restenosis lower than %50 were seen during follow up. As evidenced by the extensive studies endovascular treatment of carotid artery atherosclerotic disease is a safe and effective treatment and an alternative to carotid endarterectomy, especially for patients that are high risk for standart CEA.

EP150-Efficacy and Limitations of Transarterial Acrylic Glue Embolization for Intracranial Dural Arteriovenous Fistulas

Naoko Miyamoto ¹, Isao Naito ¹

Geriatrics Research Institute and Hospital Neurosurgery Maebashi-Japan ¹

The efficacy and limitations of transarterial acrylic glue embolization for the treatment of intracranial dural arteriovenous fistulas (DAVFs) were investigated. Thirty-three DAVFs treated by transarterial embolization



POSTER PRESENTATIONS ABSTRACTS

using n-butyl cyanoacrylate were retrospectively reviewed. The locations of DAVFs were the transverse-sigmoid sinus in 10, tentorium in 10, cranial vault in 9, and superior sagittal sinus, jugular bulb, foramen magnum, and middle cranial fossa in 1 each. Borden classification was type I in 7, type II in 3, and type III in 23. Seven patients had undergone prior transvenous coil embolization.

Complete obliteration rate was 61% immediately after embolization, 76% at follow-up angiography, and 88% after additional treatments (1 transvenous embolization and 3 direct surgery). Perforation of the feeding arteries occurred in 3 patients (1 symptomatic). Transarterial glue embolization is highly effective for Borden type III DAVF with direct cortical venous drainage, but has limitations for Borden type I and II DAVFs in which the affected sinus is part of the normal venous circulation. Onyx is a new liquid embolic material and is becoming the treatment of choice for DAVE. The advantages of glue embolization over Onyx embolization are high thrombogenicity, and relatively low risks of cranial nerve palsies and of excessive migration into the draining veins of high flow fistula. Transarterial glue embolization continues to be useful for selected patients, and complete cure can be expected in most patients with fewer complications if combined with transvenous embolization or direct surgery.

EP151-Transvenous Embolization of Cavernous Sinus Dural Arteriovenous Fistula via Angiographic Occlusive Inferior Petrous Sinus

Chao-Bao Luo ¹, *Michael MH Teng* ², Feng-Chi Chang ¹, Wan-Yuo Guo ¹, Chung-Jung Lin ¹
Taipei Veterans General Hospital and National Yang-Ming University, School of Medicine Department of Radiology -Taiwan ¹ *Cheng Hsin General Hospital and National Yang-Ming University, School of Medicine Department of Medical Imaging Taipei-Taiwan* ²

PURPOSE: Trans-inferior petrous sinus (IPS) coil embolization is an efficient and safe method to manage cavernous sinus dural arteriovenous fistulas (CSDAVFs). However, Some CSDAVFs may associate with occlusive or stenotic IPS leading difficult to access. The purpose of this study is to report our experiences of trans-venous embolization of the CSDAVF via angiographic occlusive IPS. **METHODS:** Over 11-year periods, a total of 57 patients with CSDAVFs underwent trans-IPS detachable coil embolization. From these databases, there were 20 patients attempting to undergo transvenous embolization via angiographic occlusive IPS. There were 7 men, 13 women; age ranged from 41 to 78 years old (mean: 58 yrs). We retrospectively analyses the angioarchitecture of CSDAVFs, procedural time and angiographic as well as clinical outcomes after embolization. **RESULTS:** True occlusive IPS was found in 13, while patent IPS with compartment of the IPS-CS was demonstrated in 7. Successful navigation of microcatheter to fistula site of the CS was achieved in 16 (80%), while 4 failed after many attempts. The mean procedural time in truly occlusive IPS vs compartment of IPS-CS was 111 minutes vs 129 minutes. No recurrent or residual fistula was observed on follow-up neuro-images. Three patients had transient third (n=2) or sixth (n=1) cranial nerve palsy. One patient had perforation of the IPS leading to temporary headache. There was no other significant procedure-related neurological complication. The clinical follow-up period varied from 7 to 34 months (mean: 18 months) **CONCLUSION:** Angiographic occlusive IPS of CSDAVF may relate to true occlusion of IPS or patent IPS with compartment of IPS-CS. There is no statistical significance of procedural times in these two different fistula anatomies. Transvenous embolization of via angiographic occlusive IPS is a feasible and effective method to manage CSDAVF with high successful rate and low peri-procedural risk.



POSTER PRESENTATIONS ABSTRACTS

Adult NR 6

EP152-Visual Deficits and Pituitary Adenomas, the Myth of Bitemporal Hemianopia

In Ho Lee¹, Fabiana Tavares¹, Elcin Zan¹, Ari Blitz¹, Neil Miller², Michael Boland², *David Yousem*¹

The Johns Hopkins Medical Institutions RADIOLOGY Baltimore-United States 1 *The Johns Hopkins Medical Institutions OPHTHALMOLOGY -United States* 2

We sought to test the hypothesis that bitemporal hemianopsia is the most common visual field deficit in patients with pituitary macroadenomas, to assess the degree of optic pathway compression necessary to produce such a deficit, and to determine the frequency by which asymmetric visual deficits are associated with pituitary adenomas that impact the pre-chiasmal optic nerves, optic chiasm or post-chiasmal optic tracts. We retrospectively reviewed the imaging findings and medical records of 186 consecutive patients with pathologically proven pituitary macroadenomas or presumed pituitary macroadenomas between November 2009 and October 2012 who had formal assessment of their visual defects. We evaluated the 1) degree of optic pathway displacement from the unaffected side or expected normal location by the masses, 2) changes in the visual pathway on T2 or FLAIR signal intensity, 3) presence of optic pathway atrophy, 4) enhancement anywhere along the optic pathway,

and 5) presence of hemorrhage in the masses. The degree of optic pathway displacement was classified as no contact, abutting, mild elevation (< 3 mm), and moderate elevation (>3 mm). We correlated the visual deficits with these MR imaging findings.

95 patients presented without visual complaint and the other 91 patients presented with visual disturbances such as blurred vision, diplopia, or visual change. The pituitary macroadenomas abutted but did not displace (n=16), mildly elevated (n=47), moderately elevated (n = 87) or had no contact (n=36) with optic pathway structures. On visual field testing, 120 (65%) patients showed abnormal visual field tests while 66 (35%) patients had unremarkable or mild/nonspecific visual field tests. Of the 120 patients with abnormal tests, bitemporal hemianopsia (n=62) was the most common finding. The displacement of the optic pathway by the mass ranged from 0.3 cm to 2.1 cm. There was atrophy of the optic pathway in 3 cases and hemorrhage in the mass in 26 cases. We found two cases with T2 high signal intensity and no cases with enhancement along the optic pathway compromised by the pituitary adenoma. Bitemporal hemianopsia is the most common visual field deficit (62/186,33%) in patients with pituitary macroadenomas. Bitemporal hemianopsia rarely occurs in the cases of abutting or mild elevation.

EP153-Importance Neuroimaging and Clinical Neurophysiological Methods in Diagnosis and Treatment Vestibulocochlear Syndrome

N.S. Alekseeva¹, M.V. Krotenkova¹, A.A. Baev², *J.V. Bukovskaya*³, T.A. Popova¹, V.V.

Gnezditsky¹, M.S. Semenov¹, O.V. Korepina¹

Scientific Center of Neurology Russian Academy of Medical Sciences Radiology -Russia 1 *Central Clinical*

Hospital № 1 JSC Russian Railways Radiology -Russia 2 *Policlinic #2 Ministry of Economic Development of the*

Russian Federation Radiology Moscow-Russia 3

INTRODUCTION: Repeating attacks of giddiness - frequent symptoms in neurology and the otorhinolaryngologies demanding carrying out exact topical diagnostics of level of a lesion of a vestibular analyzer and pathogenetic therapy. Attacks of giddiness can be implication of a transitional ischemia of a labyrinth or a brain, a brain infarct, a debut of multiple sclerosis, result of an ischemia of a root of the VIII nerve, caused by existence of the neurovascular conflict in the field of a cerebellopontine angle (CPA).



POSTER PRESENTATIONS ABSTRACTS

The purpose of work was studying of a role of neuroimaging and neurophysiological methods in diagnostics the cochleovestibular syndromes (CS).

MATERIAL AND METHODS.: 2 groups of patients with the central and peripheric CS are surveyed. The central CS was studied on the example of 142 MS patients, PCS- at 56 patients with a vertebrobasilar insufficiency. We used MRT (1,5T and 3,0T), and also CT-perfusion.

RESULTS: Comparison of results of otoneurology inspection and MRI, shows their high diagnostic significance. In cases of existence of the single lesion on MRI subtentorial localization at young patients we excluded ischemic nature of focal damage of a brain using CT perfusion. At several patients when carrying out MRT vascular loops, adjacent to the 8th nerve in the field of a CPA were revealed. This pathology was the reason of development in sick typical attacks of dizziness as attacks of Meniere's Disease, or attacks of sudden falling as "dropp-attacks" which stopped after the surgical intervention directed on a separation of a vessel and a nerve. At MR angiography anatom physiological features of vessels vascular loops in the field of a CPA came to light. **CONCLUSION:** The otoneurology symptoms can be objective criterion of defeat of a labyrinth, the 8th nerve, a brainstem and a cerebellum, but these changes have no functional character as was considered earlier. For the purpose of confirmation lesions trunk, both at a demyelination, and at vascular pathology, it is necessary to apply MRT and also CT-perfusion. For PCS diagnostics very important MRA for an exception of the neurovascular conflict.

EP154-CT Angiography after Carotid Artery Stenting Assessment of the Utility of Adaptive Statistical Iterative Reconstruction and Model Based Iterative Reconstruction

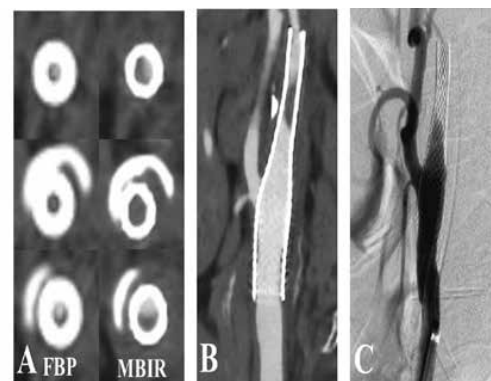
*Keita Kuya*¹, *Yuki Shinohara*¹, *Makoto Sakamoto*², *Shinya Fujii*¹, *Toshio Kaminou*¹, *Takashi Watanabe*², *Toshihide Ogawa*¹

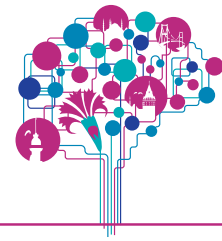
*Tottori University Pathophysiological Therapeutic Science Yonago-Japan*¹ *Tottori University Brain and Neurosciences -Japan*²

PURPOSE: Follow-up CT angiography (CTA) is routinely performed for post-procedure management after carotid artery stenting (CAS). However, the stent lumen tends to be underestimated because of stent artifacts on CTA reconstructed with the filtered back projection (FBP) technique. We assessed the utility of new iterative reconstruction techniques, such as adaptive statistical iterative reconstruction (ASIR) and model-based iterative reconstruction (MBIR), for CTA after CAS in comparison with FBP.

METHODS: In a phantom study, we evaluated the differences among the three reconstruction techniques with regard to the relationship between the stent luminal diameter and the degree of underestimation of stent luminal diameter. In a clinical study, 34 patients who underwent follow-up CTA after CAS were included. We compared the stent luminal diameters among FBP, ASIR and MBIR, and performed visual assessment of plaque in the stent lumen using a three-point scale.

RESULTS: In the phantom study, stent luminal diameter was increasingly underestimated as luminal diameter became smaller in all CTA images. Stent luminal diameter was larger with MBIR than with the other reconstruction techniques. Similarly, in the clinical study, stent luminal diameter was larger with MBIR than with the other reconstruction techniques. Plaque detectability scores of MBIR were greater than or equal to that of FBP and ASIR in all cases. In two cases, both CTA and digital subtraction angiography (DSA) was performed after CAS. The images of one case are shown in figure.





POSTER PRESENTATIONS ABSTRACTS

Cross-sectional CT images with MBIR visualize low attenuation area more clearly than those with FBP (A). Curved multiplanar reconstruction image reconstructed with MBIR (B) correspond well with the DSA image (C). CONCLUSIONS: MBIR improved the accuracy of assessment of stent luminal diameter and plaque detectability in the stent lumen when compared with FBP and ASIR. We conclude that MBIR is a useful reconstruction technique for CTA after CAS.

EP155-Correlation of Volume Transfer Coefficient K Trans and R CBV with High and Low Grade Gliomas

*Laura Barletta*¹, Maurizio Bergamino², Luca Roccatagliata¹, Lucio Castellan¹

*Neuroradiology Services Genoa-Italy*¹ *Laureate Institute for Brain Research (LIBR -United States*²

PURPOSE: Dynamic Contrast Enhanced (DCE) MRI technique is able to evaluate the permeability of brain tumors microcirculation. Our aim is to confirm the correlation between Ktrans (volume transfer constant between blood plasma and extravascular-extracellular space) and ve (Volume of extravascular extracellular space per unit volume of tissue) with tumor grading Worth Health Organization (WHO) classification. We also aim to show that Ktrans, ve and relative Cerebral Blood Volume (r-CBV) values obtained from Dynamic Susceptibility Contrast Enhanced (DSCE) sequence differentiate low grade glioma (WHO II°) from high grade glioma (WHO III°-IV°) while is more difficult to find a cut-off for distinguishing III° from IV° glioma.

METHODS: 26 patients (12F, 14M), mean age 53 years old, 6 low grade (diffuse astrocytoma II°), 7 anaplastic astrocytoma (III°) and 13 glioblastoma (IV°) were studied. MRI examinations were performed using 1.5T Siemens Avanto. 3D Turbo-Flash sequence and a variable flip-angle method, with five separate multi-flip angle (5°,10°,15°, 20°, 30°) were used to assess the pre-contrast T1 mapping in the whole brain. The dynamic DCE sequence was started immediately after contrast bolus injection by using a 3D Turbo-Flash sequence (flip angle 30°); Ktrans and ve were calculated in post-processing by using the extended Toft-Kety algorithm while Arterial Input Function (AIF) was evaluated, for each patient, by using a biexponential input function. DSCE was performed by GE-EPI sequence and r-CBV was calculated by using Siemens software.

RESULTS: The average values of ktrans in low grade glioma were 0.04±0.04 min⁻¹, 0.11±0.10 min⁻¹ in anaplastic astrocytoma and 0.26±0.09 min⁻¹ in glioblastoma; the average values of ve were: 0.05 in low grade, 0.14 in anaplastic astrocytoma and 0.18 in glioblastoma. Finally, r-CBV values were: 1.20±0.14 in low grade, 4.1±1.8 in anaplastic astrocytoma and 6.2±1.9 in glioblastoma. By using Pearson correlation method, significative correlations were obtained between Ktrans and glioma grading (R=0.72; p<0.0001) and between r-CBV and tumor grading (R=0.77; p<0.0001). CONCLUSION: We can confirm that ktrans and r-CBV are two reliable and non invasive parameters useful to distinguish high and low grade gliomas and that they also have strong correlations with the tumor grade.

EP156-The Role Of Diffusion And Perfusion Weighted Magnetic Resonance Imaging In Distinguishing Glioblastoma on The Background Of Multiple Sclerosis Lesions Case Report

*Radoslav Georgiev*¹, Boyan Balev¹, Marianna Novakova¹, Deyan Dzhenkov², Deyan Handzhiev³

*Medical University Varna, St Marina hospital Radiology Varna-Bulgaria*¹ *Medical University Varna, St Marina hospital Pathology -Bulgaria*² *Medical University Varna, St Marina hospital Neurosurgery -Bulgaria*³

INTRODUCTION: We present a case of 38-years-old woman with relapsing-remitting form of multiple sclerosis, since aged 35 years old, who developed multicentric glioblastoma. MR examination on 26.3.2013 with diffusion and perfusion techniques, and seizures raised the possibility of occurring glioma 27/23,5/15,7 millimeters, localized in the right temporal region. The patient refused biopsy. On 6.6.2013 the control MR examination revealed multicentric neoplasm right temoro-parietal, with diffuse edema, contrast enhancement and mass effect. The patient underwent craniotomy and the pathological examination showed



POSTER PRESENTATIONS ABSTRACTS

multicentric glioblastoma IV grade WHO (World Health Organisation). Coincidental MS and primary brain tumors is rare but well known phenomenon, which some scholars explain with chronic gliosis in demyelinating plaques, that may provoke the induction of glial neoplasm. PURPOSE: To show the role of DWI, PWI in discriminating between high-grade glioma and MS tumefactive lesion in this case of coincidental MS and glioblastoma. Contrast and conventional MR imaging sometimes fail to distinguish these entities.

METHODS: Conventional MR images, pre-, and postcontrast, diffusion-weighted imaging, and DSC (dynamic susceptibility contrast) perfusion-weighted Spin-Echo EPI (echo-planar imaging), PET-CT (positron-emission tomography-computed tomography) in patient with long-standing and known MS. Derived ADC (apparent diffusion coefficient) map and CBV (cerebral blood volume) map, and confirmed increased FDG (fluorodeoxyglucose) uptake revealed abnormal intraaxial lesion right temporal on a background of the known MS lesions, which definitely behaved like a high-grade neoplasm, because of high cellularity, high vascularity, and high metabolism, with only discreet contrast-enhancement and slight edema.

RESULTS: ADC in the abnormal lesion right temporal was 0,000617 mm²/sec, relative rADC=0,779 in the corresponding contralateral zone on the left. Relative rCBV was calculated 2,55 between the corresponding symmetrical zones. The FDG uptake was elevated ventromedial to the lesion. There wasn't absolute coincidence of ADC min, rCBV max zones, but they both were included in the FDG elevated zone in the lesion.

CONCLUSIONS: Sometimes contrast-enhancement and conventional MR images are not sufficient in distinguishing HGG, especially on the background of MS lesions. DWI, and PWI are a powerful diagnostic tool in pathophysiological estimate of intraaxial lesions, because we can assume their cellularity, vascularity, which reflects lesion nature, behavior and prognosis.

EP157-MRI Findings in the Diagnosis of Central Nervous System Vasculitis

*Saida Jerbi Omezzine*¹, Radhouane Hamdi², Samia Younes³, Kalthoum Tlili Graeiss², Hassine Hamza²
*University Hospital Radiology Mahdia-Tunisia*¹ *University Hospital Radiology -Tunisia*² *University Hospital Internal medicine -Tunisia*³

PURPOSE: Vasculitis is rare inflammatory diseases resulting in the alteration of the vascular wall in the central nervous system. They may be primary or most often secondary to systemic inflammatory autoimmune, infectious or paraneoplastic diseases. In this review, we discuss and compare their MRI patterns.

MATERIAL AND METHODS: This retrospective study describes a series of 17 patients (11 males and 6 females) with a mean age of 56 years (25-75) explored with a 1.5T MRI in all cases. They presented with an acute infarct (n=6), comitality (n=5), headache (n=4), dementia (n=2), dural venous sinus thrombosis (n=2), pulmonary embolism (n=1), coma (n=1), visual hallucinations (n=1), confusion (n=1) and hearing loss (n=1).

RESULTS: T2 hyperintensity was found in all patients, in the peri-ventricular white matter, basal ganglia, brainstem and cerebellum; MRI also depicted hydrocephaly, cranial nerve and pituitary involvement, leptomeningeal enhancement, dural venous sinus thrombosis, paranasal sinuses abnormalities and at least medullary lesions.

Imaging findings associated with clinicobiological patterns concluded in Behçet disease (n=5), Sjögren's syndrome (n=4), Horton vasculitis (n=3), systemic lupus erythematosus (n=2), antiphospholipid syndrome (n=2) and finally Susac syndrome (n=1).

CONCLUSION: MRI analysis is a key feature in the diagnosis of cerebrospinal vasculitis because of their huge clinicobiological polymorphism and the invasivity and lack of sensibility of cerebral biopsy which remains the unique certainty exam.



POSTER PRESENTATIONS ABSTRACTS

EP158-Extensive Brain Lesions Cystic Necrotic Areas and Poor Outcome in Neuromyelitis Optica

*Gunes Orman*¹, Scott Newsome², Yeliz Pekcevik¹, In Ho Lee¹, Maureen Mealy², Michael

Levy², Izlem Izbudak¹

*Johns Hopkins School of Medicine Radiology/Neuroradiology Baltimore-United States*¹ *Johns Hopkins School of Medicine Neurology -United States*²

PURPOSE: Neuromyelitis optica (NMO) is an autoimmune, inflammatory, demyelinating disease. Diagnosis requires optic neuritis (ON), transverse myelitis (TM), and at least two of the three supportive criteria; 1) longitudinally extensive transverse myelitis (LETM) spanning 3 or more vertebral body levels on sagittal T2 weighted images, 2) onset brain magnetic resonance imaging

(MRI) not meeting diagnostic criteria for multiple sclerosis, or NMO-IgG seropositive status. The presence of extensive brain lesions (EBL) was recently reported as an indicator of higher disease activity and worse prognosis. Thus, we present 5 NMO patients with EBLs; 4/5 was deceased and 1/5 was paraplegic.

MATERIALS AND METHODS: Electronic patient records and brain MRIs of 49 patients were reviewed from September 2001-October 2013. Five patients' brain lesions were distinct compared to the rest of the NMO patients. We defined the brain lesions based on their anatomical locations, T2-FLAIR signal changes and contrast enhancement on T1 weighted images. Clinical features were recorded in details including, gender, age, age at disease onset, relapse times, diagnosis, NMO-IgG status, therapy and outcomes.

RESULTS: All of the patients were African-American. The mean clinical follow-up period was 12.6 (between 2 to 21) years. The mean time interval between the first and last MRIs at our institution was 5.0 (between 1 to 9.3) years. Three of the 5 patients, with highest relapse numbers and younger age at disease onset showed cystic-necrotic cavities within the T2/FLAIR hyperintense signal changes in bilateral periventricular and deep white matter. Four out of 5 patients showed periventricular contrast enhancement. Four out of 5 patients had brain stem involvement and 4/5 patients showed diffuse brain volume loss during the disease course with different degrees of severity. Four out of 5 patients were deceased and 1/5 was paraplegic.

CONCLUSION: EBLs are likely related to poor outcome and neuroimaging might be helpful to predict outcome along with the clinical and laboratory findings.

EP159-Bilateral Hypoplasia of the Internal Carotid Artery a Case Report

*Kaan Esen*¹, Anil Ozgur¹, Hakan Kaleagasi², Engin Kara¹, Arda Yilmaz²

*Mersin University Radiology Mersin-Turkey*¹ *Mersin University Neurology -Turkey*²

PURPOSE: Our aim is to present a patient with bilateral internal carotid artery (ICA) hypoplasia.

METHODS: A 52-year-old male patient referred to our clinic for brain magnetic resonance (MR) imaging with complaint of syncope and urinary incontinence one month ago. The patient didn't have any previous history of syncope and also there was no history of trauma. He had an old polio sequelae in the left lower extremity; his physical examination was otherwise normal. MR imaging, computed tomography (CT), MR angiography (MRA), CT angiography (CTA) and digital subtraction angiography (DSA) were performed.

RESULTS: Bilateral intracranial segments of ICA were not observed on MR examination. CT scan showed bilateral small carotid canals in the petrous bone. At MRA both ICAs were hypoplastic from 0.5 cm above the carotid bifurcation. DSA and CTA were made for a detailed examination. Both of them also revealed hypoplastic ICAs. Vertebral, external and common carotid arteries (CCA) were normal and vertebral arteries were more dominant than the CCA. Anterior circulation was supplied by posterior communicating arteries. There were no aneurysms.

CONCLUSION: Hypoplasia of the ICA is a rare congenital anomaly. To the best of our knowledge about 25 cases of bilateral ICA hypoplasia have been reported in the literature to date. Many patients are asymptomatic because of the developing collateral vasculature. Aneurysmal hemorrhages, infarcts, seizures may occur in these



POSTER PRESENTATIONS ABSTRACTS

patients. Hypoplasia of the carotid canal is an important clue to demonstrate the congenital etiology and to differ from acquired reasons such as chronic dissection. For this reason CT sections from the skull base is needed beside angiographic examinations.

WITHDRAWN

EP161-Multimodal Imaging in Primary Central Nervous System Lymphomas with Typical and Atypical MR Imaging Features

*Youngjin Heo*¹, Sang Joon Kim¹, Ho Sung Kim¹, Choong Gon Choi¹, Seung Chai Jung¹
*Asan medical center Radiology Seoul-Korea, South*¹

PURPOSE: Lymphomas with atypical MR imaging features are not easily differentiated from other brain tumors or nontumorous conditions. In this exhibition, we will present advanced imaging findings of primary central nervous system lymphomas (PCNSL) with typical and atypical imaging features and present useful differentiating points from other tumors or nontumorous conditions.

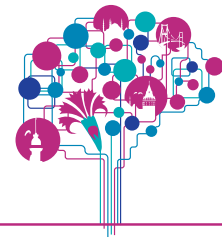
MATERIALS AND METHODS: Multimodal advanced imaging features of PCNSL are reviewed comprehensively based on the data of our own 73 cases and the literature. PCNSL cases are categorized into typical and atypical features based on the conventional imaging findings and advanced imaging findings of each group are analyzed. PCNSL with typical features are defined as solid enhancing mass with discrete or fuzzy margin. All other features including heterogeneous enhancement or nonenhancing lesions are categorized into atypical group. Comparison of advanced imaging findings of PCNSL with those of glioblastoma (GBM) and of tumefactive demyelinating lesions (TDL) will be included. Advanced imaging features will include proton-MR spectroscopy (1H-MRS), diffusion-weighted imaging (DWI), perfusion with dynamic susceptibility contrast (DSC) and dynamic contrast enhancement (DCE) technique, and arterial spin labeling (ASL).

RESULTS: Conventional MR imaging features range from well defined homogeneous enhancing mass in the periventricular area to the patchy or streaky infiltrative, or ring-enhancement pattern and even nonenhancing pattern. Minimum apparent diffusion coefficient (ADC) value is low in PCNSL than in GBM or TDL. Even in

7-12 September 2014
ISTANBUL, TURKEY

LUTFI KIRDAR CONVENTION & EXHIBITION CENTER

XXth
Symposium
Neuroradiologicum



POSTER PRESENTATIONS ABSTRACTS

cases with atypical PCNSL, minimum ADC is lower than in TDL. Relative cerebral blood flow (rCBV) is lower in PCNSL than in GBM and higher than in TDL. On ASL, PCNSL showed lower cerebral blood flow (CBF) than GBM. DCE perfusion showed higher permeability in PCNSL than in TDL. 1H-MRS was also useful to differentiate PCNSL from TDL with higher Cho/Cr ratio and higher Lipid-lactate peak.

CONCLUSION: We present advanced imaging features of PCNSL using DWI, DSC-perfusion, DCE-perfusion, ASL, and 1H-MRS based on the literature and of our own case series. With multimodal MR imaging approach, differentiation of PCNSL from other malignant tumor or from nontumorous conditions such as TDL will be facilitated.

WITHDRAWN

EP163-MRI Aspects in Hyperacute Ischemic Stroke Series of Cases of Peculiar Diffusion Weighted Images (DWI) and Apparent Diffusion Coefficient (ADC) Evolution

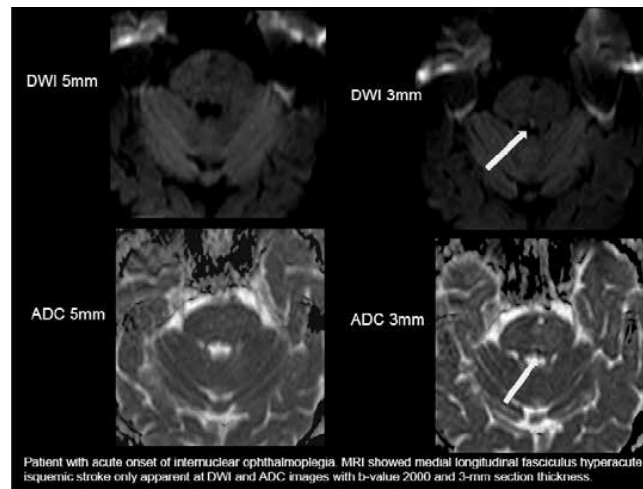
Tatiana Goyanna Lyra ¹, *Daniel de Souza Delgado* ¹, Luis Filipe de Sousa Godoy ¹, Marcos Fernando de Lima Docema ¹, Maria da Graça Martin ¹
Sirio Libanes Hospital neuroradiology -Brazil ¹

DWI allows ready identification of the ischemic lesion with high sensitivity and specificity. The purpose of this exhibit is to present a series of hyper acute stroke MR cases from our digital records emphasizing the ADC map advantages over the DWI images in very early stroke onset and the advantages of DWI with b-value 2000 and 3-mm section thickness to better analyze the ischemic events at posterior fossa. We will also present cases of



POSTER PRESENTATIONS ABSTRACTS

DWI reversibility after thrombolytic therapy, as well as cases of initial false negative DWI. The importance of cerebral perfusion/DWI and FLAIR/DWI mismatch in planning revascularization procedures will be discussed.



EP164-Diabetic Striatopathy in a Patient with Hemiballismus

*Anil Ozgür*¹, Kaan Esen¹, Hakan Kaleagasi², Arda Yilmaz², Engin Kara¹

*Mersin University Radiology Mersin-Turkey*¹ *Mersin University Neurology -Turkey*²

PURPOSE: Our aim is to present neuroimaging findings in a patient with a sudden onset of hemiballismus associated with nonketotic hyperglycemia.

METHODS: A 55-year-old man with known diabetes mellitus presented to the emergency department of our institution with a sudden onset of hemiballismus at the left upper extremity in the last 3 days. Computed tomography (CT), magnetic resonance imaging (MRI), diffusion weighted imaging (DWI) and laboratory tests were performed.

RESULTS: CT revealed mild hyperdensity in the right putamen. MRI demonstrated increased signal in the right putamen on T1-weighted images. No prominent abnormality was detected on DWI. Laboratory tests revealed elevated levels of blood glucose and HbA1c. (fasting blood glucose: 246 mg/dl, HbA1c: 15.4%). Diabetic striatopathy was the final diagnosis based on the imaging findings and laboratory results.

CONCLUSIONS: Chorea-ballismus associated with nonketotic hyperglycemia (diabetic striatopathy) is a rare and life-threatening manifestation of diabetes mellitus. Early recognition with appropriate treatment is in favor of good prognosis. Imaging is relatively helpful in the diagnosis and may demonstrate increased density on CT and increased signal intensity on T1-weighted MR images in the basal ganglia. Diabetic striatopathy should be considered in patients with unilateral movement disorders and contralateral neuroimaging abnormalities of the basal ganglia.

EP165-Intravoxel Incoherent Motion MR Imaging Principles and Clinical Applications

*Hee Mang Yoon*¹, Chong Hyun Suh¹, Jin Seong Lee¹, Young Ah Cho¹, Ah Young Jung¹,
Chong Hyun Yoon¹

*Asan Medical Center Radiology SEOUL -Republic of Korea*¹

PURPOSE:

1. To define basic principles of intravoxel incoherent motion (IVIM) MR imaging.
2. To present the clinical applications of IVIM MR imaging.



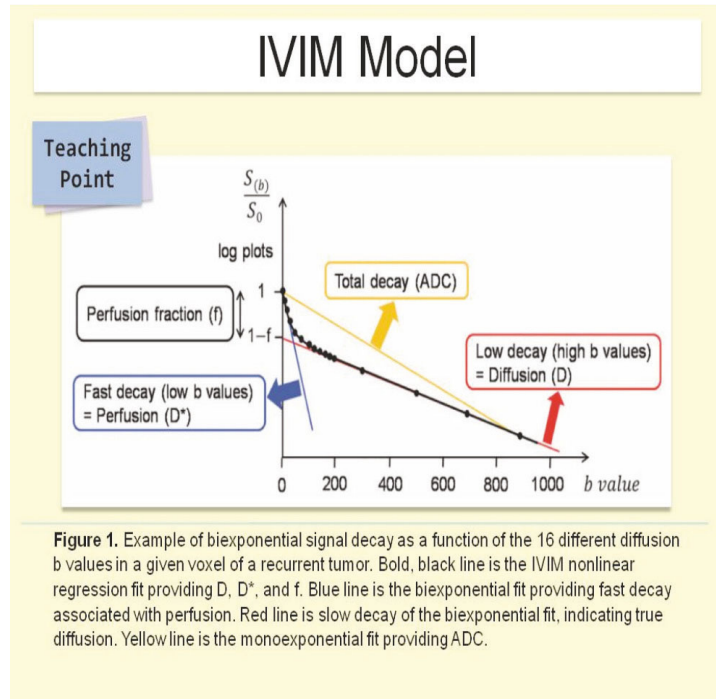
POSTER PRESENTATION ABSTRACTS

CONTENT:

1. IVIM MR basic principles.
 - (1) IVIM model: perfusion fraction (f), diffusion coefficient (D), pseudodiffusion (D^*)
 - (2) Sequence: selection of b values, diffusion gradient polarity, breathing acquisition
 - (3) Simplified biexponential models: Le Bihan's simplified method, Lucaiani method, and Sigmund Method
2. Clinical Applications of IVIM MR imaging. Brain: perfusion measurement, malignant brain tumor, treatment response assessment

CONCLUSION :

1. IVIM MR imaging can simultaneously measure the diffusion and perfusion characteristics of lesions without administration of contrast material.
2. IVIM MR imaging can be a non-contrast, noninvasive imaging method for assessing the diffusion and perfusion characteristics of lesions especially in patients with compromised renal function.



EP166-Evaluation of the Posterior Cingulate Region with FDG PET and Advanced MR Techniques in Patients with Amnesic MCI, Comparison of the Methods

Anna Zimny¹, Joanna Bladowska¹, Adam Macioszek², Elzbieta Trypka³, Renata Wojtynska³, Jerzy Leszek³, Marek Sasiadek¹

Wroclaw Medical University Dep. of General and Interventional Radiology and Neuroradiology Wroclaw-Poland¹ 4th Military Hospital, Wroclaw Dep. of Nuclear Medicine -Poland² Wroclaw Medical University Dep. of Psychiatry -Poland³

PURPOSE: Posterior cingulate region is an area of the earliest pathological changes in amnesic mild cognitive impairment (aMCI). The utility of FDG-PET imaging in dementia is already well established. The aim of the study was to compare FDG-PET with advanced MR measurements: MR spectroscopy (MRS), perfusion weighted imaging (PWI) and diffusion tensor imaging (DTI) within posterior cingulate region in patients with aMCI.

METHODS: Fifty-five patients diagnosed with aMCI (66.5 yrs) and 20 age-matched controls (69 yrs) underwent MR examination including MRS, PWI and DTI followed by FDG-PET scanning. Values of MRS metabolite ratios (NAA/Cr, Cho/Cr, mi/Cr), PWI cerebral blood volume (rCBV) and DTI fractional anisotropy (FA) were compared to the FDG-PET rates of glucose metabolism.

RESULTS: Compared to controls, aMCI patients showed significant ($p < 0.05$) glucose hypometabolism, and lower rCBV and FA values. FDG-PET results correlated significantly with rCBV values. Compared to FDG-PET, PWI showed similar and DTI higher accuracy in distinguishing aMCI from controls. According to FDG-PET findings 2 groups of aMCI patients were established: with lower (PET-positive) and normal (PET-negative) glucose uptake. PET-positive aMCI subjects showed normal MRS findings, lower rCBV and FA values, while PET-negative patients revealed normal MRS and PWI results but significantly lower FA values.

CONCLUSIONS: Advanced MR techniques such as PWI and particularly DTI may be regarded competitive techniques to FDG-PET. DTI was the only method to show alterations in aMCI patients with normal FDG-PET scan, normal PWI and MRS findings. DTI seems to be very sensitive biomarker of early degeneration in aMCI.



POSTER PRESENTATIONS ABSTRACTS

Adult Nr 7

EP167-Sellar Chondrosarcoma without Bone Involvement a Case Report

*Roberto Marileo*¹, Ingeborg Lopez¹, Rodrigo Riveros¹, Cecilia Okuma¹, Aaron Vidal¹,
Rodrigo Rivera¹, J.Gabriel Sordo¹, Lautaro Badilla¹
*Instituto de Neurocirugía Dr. Alfonso Asenjo Neuroradiology Santiago-Chile*¹

SUMMARY: We report a CT and MRI findings in a patient with a heterogeneous intrasellar suprasellar mass, partially calcified, histologically shown to be a chondrosarcoma. The tumor not involved the bone skull base. Our case, therefore, represent a rare presentation form.

CLINICAL HISTORY: 21 years old women who developed four month visual impairment with right eye temporal hemianopia and headache. The CT and MRI demonstrated a heterogeneous intrasellar – suprasellar mass, with thick amorphous calcification, and soft tissue that enhance with contrast material. The tumor not invaded the sellar bone neither the petro occipital fissure. The pathology report a hypocellular chondroid tumor, with mild chondrocytes pleomorphism and mild atypia, without mitosis. Immunohistochemistry stains showed S-100 (+), EMA (-) and pancytokeratin AE1/AE3 (-). This findings are consistent with chondrosarcoma.

EP168-18FDG PET MR Coregistration as a Method for Localization of Epileptogenic Zone in Drug resistant Epilepsy

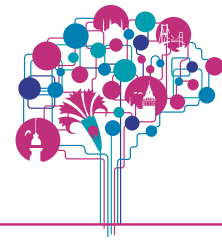
*Dora Zlatareva*¹, Krassimir Minkin², Irena Kostadinova³, Petya Dimova⁴, Marin Penkov⁵
*Medical University, Sofia Department of Diagnostic Imaging Sofia-Bulgaria*¹ *University Hospital "Saint Ivan Rilski" Department of Neurosurgery -Bulgaria*² *Medical University, Sofia Department of Nuclear Medicine -Bulgaria*³ *University Hospital "Saint Naum", Department of Neurology -Bulgaria*⁴ *University Hospital "Saint Ivan Rilski" Department of Radiology -Bulgaria*⁵

PURPOSE: Positron emission tomography with 18Fluor-deoxyglucose (18FDG PET) combined with computed tomography (18FDG PET/CT) is a hybrid method for evaluation of the cerebral metabolism. 18FDG PET/CT has been used as a method for epileptogenic zone localization due to the hypometabolism of epileptogenic zone during the interictal period. In PET/MRI coregistration 18FDG PET images are fused onto the structural MRI and the degree of hypometabolism is color coded. The purpose of this study is to evaluate our initial experience with FDG PET/MR coregistration in patients with drug-resistant epilepsy.

METHODS: Our study has included 21 patients with drug-resistant epilepsy who were evaluated with 18FDG PET from 2010 to 2013. All patients were examined on 1.5T MRI with epilepsy protocol. PET study was fused with 3D SPGR on the Workstation using GE software. Video EEG monitoring was performed in all 21 patients and seizures were recorded in 18 patients.

RESULTS: We found hypometabolic zones in 15 patients. The hypometabolism was focal in 5 patients, multilobar in 9 patients and hemispheric in 1 patient. The MRI was normal in 8 patients. In 3 out of 8 patients with cryptogenic epilepsy we found hypometabolic zones. Epilepsy surgery was performed in 6 cases. All operated patients were with hypometabolic zones. Significant seizure reduction after surgery was observed in 5 of 6 operated patients.

CONCLUSION: 18FDG PET/MR coregistration is a noninvasive method for epileptogenic zone localization which can be added to multimodal presurgical evaluation in patients with drug-resistant epilepsy.



POSTER PRESENTATIONS ABSTRACTS

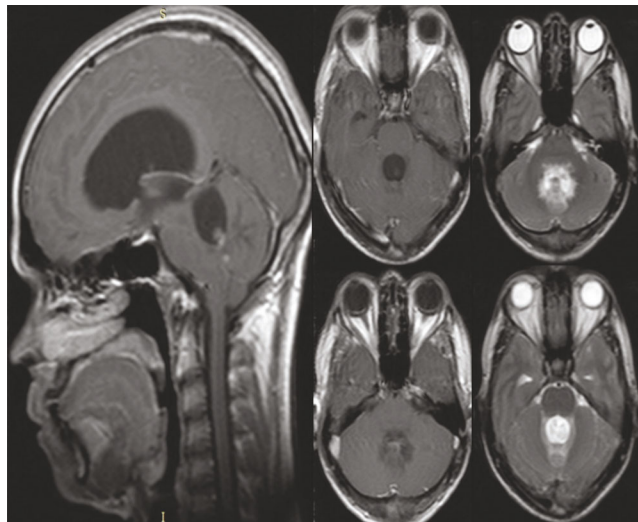
EP169-Neurocysticercosis an Important Differential Diagnosis

*Pablo Picasso de Araújo Coimbra*¹, Rafael Costa Lima Maia², Tiago Silva Holanda Ferreira³, Daniel Gurgel Fernandes Tavora¹, Eliseu Becco Neto², Jackson Augusto Gondim Oliveira², Stelio da Conceição Araújo Filho², Francisco Ramos Júnior², Edson Lopes Júnior²
Hospital Geral de Fortaleza Department of Radiology Fortaleza-Brazil ¹ *Hospital Geral de Fortaleza Department of Neurosurgery* - ² *Universidade de Fortaleza Intern* - ³

PURPOSE: Neurocysticercosis (NCC) is a public health issue in endemic areas and has gaining importance in developed countries. It is considered the most common cause of acquired epilepsy, and the most common parasitic disease of the nervous system by WHO. It is estimated that 50 million people are infected with the parasite and mortality reaches 50 thousand annual deaths worldwide. The case exposed here presents a form that requires attention regarding the differential diagnosis of lesions in the posterior fossa.

CASE REPORT: 23-year-old, male, started gait abnormality and nuchal rigidity three months before admission. Physical examination revealed ataxic gait, without other neurological deficit. MR shows enlargement of the fourth ventricle due to image with heterogeneous signal intensity on T1 and T2 predominantly cystic with mural nodule inside. Neurosurgery to resect the lesion was performed, and histopathology confirmed the clinical suspicion of neurocysticercosis.

CONCLUSIONS: NCC, in its parenchymal disease, should always be considered in the differential diagnosis of cerebral cystic lesions in endemic regions, but is rarely remembered in non-endemic regions. The increased incidence of the disease in other countries can be attributed to the increased mobility of people and migration rates. The knowledge of the various forms of the disease should be so well known and studied.



EP170-Giant Aneurysm of Middle Cerebral Artery with the Size of 6 X 7 cm

*Pablo Picasso de Araújo Coimbra*¹, Rafael Costa Lima Maia², Tiago Silva Holanda Ferreira³, Daniel Gurgel Fernandes Tavora¹, Eliseu Becco Neto², Francisco Ramos Júnior², Stelio da Conceição Araújo Filho², Edson Lopes Júnior²
Hospital Geral de Fortaleza Department of Radiology Fortaleza-Brazil ¹ *Hospital Geral de Fortaleza Department of Neurosurgery -Brazil* ² *Universidade de Fortaleza Intern -Brazil* ³

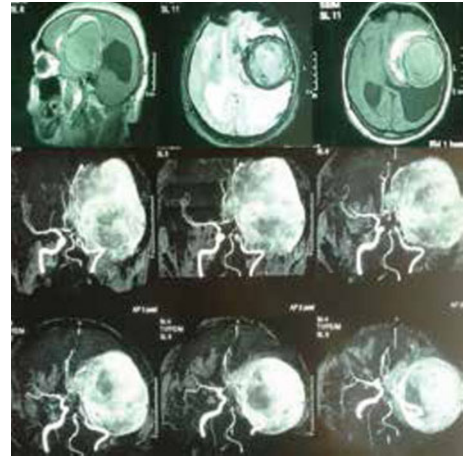
PURPOSE: Cerebral aneurysms account for 80% of cases of spontaneous subarachnoid haemorrhage (SAH), which occur most commonly between 40 and 60 years of age. Most saccular aneurysms, about 85%, occur in the vessels of the Willis polygon or its major branches. Giant intracranial aneurysms (GIA) have been defined as those larger than 25 mm in diameter. An aneurysm of 7x6 cm, as presented here, is a rare form of the disease.

CASE REPORT: 50-year-old man, with previous neurological deficit (cognitive impairment and hemiparesis), without appropriate medical assistance, in use phenobarbital 200 mg and phenytoin 200 mg daily for convulsive seizures, was brought to our service when presented a thunderclap headache associated with worsen hemiparesis and drowsiness. MRI showed extra-axial mass lesion surrounded by edema in the left temporal fossa extending to high convexity, with high attenuation on CT, with high signal intensity on T1, marked low signal intensity on T1, T2, FLAIR, GRE, peripheral enhancement, determining marked compression of the supratentorial ventricular system. Angio-MRI confirmed a Giant Aneurysm of the Middle Cerebral Artery. Neurosurgery was successfully performed to treatment.



POSTER PRESENTATIONS ABSTRACTS

CONCLUSIONS: A determinant of aneurysm rupture is its size. Aneurysms of the internal carotid artery up to 7 mm in diameter have bleeding rate of 0.1% per year, while they can reach 8% per year with greater than 25 mm (GIA) diameter. Previously characterized as physiologically similar to other aneurysms, GIA gained a new connotation about its origin mainly on recurrent bleeding in the Vasa Vasorum subadventitial region. Despite the increased risk of bleeding, the majority of GIA are detected by their mass effect, hemorrhage before itself, which is defined in most cases, a catastrophic event with immediate worsening of clinical symptoms. The average annual rate of bleeding GIA is around 40%.



EP171-Usefulness of MR Spectroscopy with an Elevated Peak at 3.56 PPM in Differentiation between Hemangiopericytoma Solitary Fibrous Tumor and Meningioma

Minoru Morikawa¹, Reiko Ideguchi¹, Hideki Ishimaru¹, Yukihiro Ogihara¹, Takayuki Matsuo², Kensaku Kamata², Naoe Kinoshita³, Mikako Enokizono⁴, Masataka Uetani¹
Nagasaki University Hospital Department of Radiology Nagasaki-Japan *1 Nagasaki University Hospital Department of Neurosurgery -Japan* *2 Nagasaki University Hospital Department of Pathology -Japan*³
*Kanagawa Children's Medical Center Department of Radiology -Japan*⁴

PURPOSE: Intracranial hemangiopericytomas and solitary fibrous tumors (HPC/SFT) are rare tumors and their radiological appearance resembles that of meningiomas. Previous studies of MR spectroscopy (MRS) in an extraaxial tumor, report an elevated peak of myo-inositol can be observed in HPC/SFT and schwannoma. The aim of this retrospective study is to evaluate the usefulness of MRS in differentiation between HPC/SFT and meningioma.

METHODS: We retrospectively evaluated the proton MRS spectra acquired in 24 meningiomas (grade I 18, grade II 6), in 1 HPC and in 1 SFT. Proton MRS was performed using a single-voxel PRESS with short TE (31msec) and long TE (144msec) at 3T system.

RESULTS: The 2 of 24 meningiomas revealed increase metabolite at 3.56 ppm in short and long TE, which may represent glycine. In the remaining 22 of 24 meningiomas, no obvious peak at 3.56 ppm was observed. The 2 of HPC/SFT showed the highest peak in short TE, and no obvious peak in long TE at 3.56 ppm, which may represent myo-inositol.

CONCLUSIONS: The HPC/SFT and meningioma could be distinguished on the basis of their spectral patterns at 3.56 ppm, which showed characteristic changes with echo time.

EP172-Late CO Poisoning

Annapaola Bocchio¹, Davide Machado¹, Alessandra Pozzato², Teodoro Meloni¹, Enrico Visetti²
General Hospital U.Parini Radiology aosta-Italy *1 General Hospital U.Parini Anesthesiology*²

PURPOSE: Carbon monoxide (CO) is a relatively common cause of human injury. It can produce different patterns of brain injury, in the acute and delayed stages. MRI is valuable in the delineation of disease extent and helpful for understanding the pathophysiologic mechanisms.

METHODS: We present the case of a 79 years old woman, brought at emergency by her daughter, for sudden appearance of behavioural changes. She had been previously (20 days) hospitalized for being found unconscious, at home, in the presence of a stove. The patient had promptly recovered and discharged. No specific test had been



POSTER PRESENTATIONS ABSTRACTS

made. At neurological examination she was confused, with poor verbal fluency. CT: non-specific, periventricular white matter hypodensity, consistent with age-related changes. Within 2 days she started with seizures and progressive worsening of consciousness. MR T2-weighted and FLAIR images showed bilateral symmetric hyperintensity in the periventricular white matter and centrum semiovale, more prominent in the frontal lobes. DWI showed bilateral areas of confluent high signal in the same regions, the hyperintensity varying from slight to severe. Mean ADC values in the same areas were lower than those of normal-looking white matter. We suspected a delayed CO poisoning encephalopathy. The patient, due to severe comatose state, died in a few days. RESULTS: Acute and intense CO poisoning can lead to diffuse hypoxic-ischemic encephalopathy, predominantly involving the gray matter. The globus pallidus is the most common site of involvement in CO acute poisoning. The damage usually occurs immediately and may be related to the hypotensive effects of CO in the watershed territory. Delayed effects of CO on the brain, cause demyelination of the white matter. This may be due to lipid peroxidation. The most commonly affected areas are periventricular white matter and centrum semiovale. CONCLUSIONS: Diagnosis of CO poisoning requires a high level of suspicion. Disturbances of brain function predominate in acute CO intoxication, but delayed neurological effects also occur. They are characterized by a recurrence of neurological and psychiatric symptoms, preceded by a temporary asymptomatic period (2-3 weeks). Brain MRI is a useful tool in the diagnosis. DWI and ADC maps of patients with CO poisoning have shown the development of delayed and slowly progressive cytotoxic edema in the cerebral white matter, possibly as the result of delayed cell death and demyelination.

EP173-A Case of Cerebellar Glioblastoma in a Young Adult

*Annapaola Bocchio*¹, Davide Machado¹, Anna Rosano¹, Francesca Nebiolo², Teodoro Meloni¹
*General Hospital U. Parini Radiology Aosta-Italy*¹ *University of Pavia*²

PURPOSE: Glioblastoma multiforme (GBM) is a stage IV tumor and it's the most common primary central nervous tumor in adults. It comprises approximately 50% of all primary intracranial tumors, occurring, generally, in the fifth and sixth decades of life. It's usually located in the deep white matter or in the neighboring deep gray matter, mainly in cerebral hemispheres. Localization in the posterior fossa, in adults, is rare.

METHODS: We present the case of a 40 years-old man, coming with headache, nausea and vomiting. Neurological examination was normal. His past medical history was normal. CT showed large isohypodense mass in the right cerebellum, with intense enhancement and peripheral hypodense areas. MR confirmed the presence of hypointense and hyperintense lesion in the left cerebellum in T1 and in T2-weighted images, respectively. ADC values were high and DWI signal low. The mass had poorly defined borders, mild peritumoral edema and large areas of peripheral necrosis. T1-weighted imaging with Gd-DTPA well defined the 4cm sized lesion, the necrotic areas and the enhancement of the adjacent tentorium.

RESULTS: The patient underwent radical surgical resection. The intraoperative histologic sample was "mesenchymal cells", consistent with meningeal tumor. The definitive histology, reported in two different laboratories, was typical for GBM. The patient underwent RT and CT. MR follow-up, performed every 4 months, never showed evidence of recurrence, during postoperative 26 months (April 2014).

CONCLUSIONS: Cerebellar GBM occurs rarely in adults, accounting for 0.4-3.4% of all GBMs. However, it must be considered in the differential diagnosis of aggressive mass lesions of the cerebellum. Cerebellar metastasis and anaplastic astrocytoma are the common differential diagnosis in an adult. Due to its rarity, cerebellar GBM is not yet completely understood about the pathogenesis and the prognosis. While few studies have compared cerebellar GBMs to their supratentorial counterparts, there is conflicting data regarding their relative prognosis. As with supratentorial GBM, older age is a poor prognostic factor. An explanation for the lesser tendency of cerebellar astrocytes to become malignant has been proposed. It is possible that cerebellar GBM found in young aged patients has a better prognosis, as in anaplastic astrocytomas (AAs), which have a longer survival time than supratentorial GBM.



POSTER PRESENTATIONS ABSTRACTS

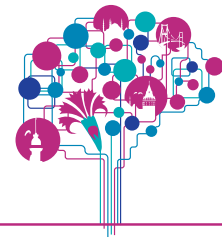
WITHDRAWN

EP175-Role of MRI in Diagnostic Long Standing Overt Ventriculomegaly as a Cause Of Secundar Amenorrhea

Vesna Vukovic 1, Jelena Mihailovic 1

Institute of oncology and radiology of Serbia neuroradiology Belgrade-Serbia 1

PURPOSE: Long-standing overt ventriculomegaly in adults (“LOVA” Sy) is recently defined clinical entity characterized by chronic hydrocephalus probably with infant onset, slow evolution and clinical disturbances during adulthood. The most patients have headache like main symptom, but secondary amenorrhea like clinical manifestation of LOVA Syndrome is so rare. Complete agreement in terms of the need for intervention, timing of intervention, and ideal treatment are not defined. **METHODES:** Patient was diagnosed and followed by MRI of head and pituitary region used MRI strength 1,5T. **RESULTS:** We are presented twenty seven years female who is evaluated by endocrinologist due to absence of menstruation last two years. Occasional headaches and amenorrhea are the main symptoms. The patient was undertaken hormonal analysis. Normal functions of thyroid and adrenal glands were obtained. Value of prolactin and IGF-1 were preserved. ITT (Insulin Tolerance Test), LHRH, Clomiphene tests indicate isolated



POSTER PRESENTATIONS ABSTRACTS

hypogonadotropic hypogonadism without deficiency of other pituitary hormones. MRI of head and pituitary gland are pointed on shallow remodeling sellar pit, enlarged AP diameter, with intrasellar herniation the third ventricle, and considerable distension of pituitary stalk which is moved forward and thinned. MRI of head described enlarge of the third and lateral ventricles with obliterated giral sulci. Worsening of headache and persistent amenorrhea are demanded neuroendoscopic third ventriculostomy twelve months later. Six months after surgical treatment control MRI indicates decreased LL diameter of the third ventricle, low level of compressed pituitary gland and reposition of pituitary stalk in normal position, and finally spontaneous menstruation.

CONCLUSION: MRI imaging has significant role in diagnosis clinical entity "LOVA" and correlated with clinical findings can be useful for choice of treatment options.

EP176-Intraventricular Tumors Typical Imaging Findings on CT and MRI

*Kevin Van Looveren*¹, Luc van den Hauwe², Maxim R. Parizel³, Thomas Van Thielen¹, Frank De Belder¹, Caroline Venstermans¹, Johan W. Van Goethem⁴, Martin Lammens³, Paul M. Parizel¹

*Antwerp University Hospital Radiology Antwerp-Belgium*¹ *Antwerp University Hospital, AZ Klina Brasschaat Radiology -Belgium*² *Antwerp University Hospital Anatomical Pathology -Belgium*³ *Antwerp University Hospital, AZ Nikolaas Sint-Niklaas Radiology -Belgium*⁴

PURPOSE: To present a pictorial essay of intraventricular tumors, and to report the typical anatomic location and imaging findings associated with these lesions.

METHODS: In this retrospective study, we reviewed patient records in the division of neuropathology between January 1st 2004 and December 31st 2013 for histologically proven intraventricular tumors. We used the following search terms: ependymoma, subependymoma, subependymal giant cell astrocytoma (SEGA), central neurocytoma, choroid plexus papilloma, choroid plexus carcinoma, choroid plexus metastasis, xanthogranuloma, intraventricular lymphoma, intraventricular meningioma and medulloblastoma. For each patient, multiple variables were recorded, including tumor location, specific imaging characteristics on CT and MRI, patient gender and age, and follow-up. We reviewed imaging findings on CT (enhancement, hemorrhage, calcifications) and signal characteristics (T1- and T2- signal intensity, presence of diffusion restriction, pattern of enhancement, hemorrhage and calcifications) on MRI for each tumor type.

RESULTS: During the reference period, neuropathological records of eighteen patients with intraventricular tumors were identified. The following list indicates histological diagnosis with number of cases and location: medulloblastoma (n=2, fourth ventricle), central neurocytoma (n=2, lateral ventricles and septum pellucidum), choroid plexus carcinoma (n=1, left lateral ventricle), choroid plexus papilloma (n=2, both in the left lateral ventricle), subependymoma (n=3, all located in the fourth ventricle), ependymoma (n=7, five in the fourth ventricle and two in the lateral ventricles) and SEGA (n=1, left lateral ventricle). No records were available of choroid plexus metastasis, intraventricular lymphoma or intraventricular meningioma. It is important to note that many benign lesions were not operated and thus do not appear in this list which is based on neuropathology records.

CONCLUSIONS: Intraventricular tumors are uncommon lesions, with a broad spectrum of histological diagnoses and imaging findings on CT and MRI. Although our number of patients is rather small, results correspond with larger series published in the literature.



POSTER PRESENTATIONS ABSTRACTS

EP177-Neuroimaging of Intracranial Extra Axial Non Meningiomas Tumors Multimodal MRI Findings

*Ben Abdallah Amel*¹, Mama Nadia¹, Berrich Amira¹, Arifa Nadia¹, Iyadh Ksira², Yacoubi Mohamed Taher³, Tlili Kalthoum¹

*Sahloul Hospital Sousse Radiology Sousse-Tunisia*¹ *Sahloul Hospital Sousse Neurosurgery -Tunisia*² *Hached Hospital Sousse -Tunisia*³

OBJECTIVES: To describe the MR features of intracranial extra-axial non meningiomas on conventional imaging, diffusion weighted imaging (DWI) and MR spectroscopy (MRS) with the aim to determine distinguishing features from meningiomas.

MATERIALS AND METHODS: From 2006 to 2012, we retrospectively reviewed 36 patients with histopathologically confirmed extra-axial non meningiomas. Imaging includes an MR examination on a 1.5 Tesla system. The conventional MR findings (n= 36), DWI features (n=24) and MRS (n=13) were respectively analyzed.

RESULTS: On the basis of histological diagnosis, 13 neurinomas, 7 hemangiopericytomas (HPCs), 9 cystic tumors (3 arachnoid cysts and 6 epidermoid cysts), 3 dural metastases, 1 dural lymphoma, and 1 falx primitive neuroectodermal tumor (PNET) were reviewed. Conventional MR imaging sequences provided sufficient information to establish the extra-axial location. Three Grade II HPCs showed higher values of ADC, whereas Grade III HPCs showed either equal (3 cases) or decreased ADC values (1 case). The ADC values of the epidermoid cysts (n=6) were lower than the arachnoid cysts. DWI demonstrated variable ADC in neurinomas: elevated ADC (n=3) and decreased ADC (n=2). MRS showed in all cases of HPC (n= 5) markedly increased lip/lac and glutamate-glutamine peaks (Glx), decrease of N-acetyl-aspartate (NAA) level with increased choline (Cho)/Creatine (Cr) ratio (n= 3) and prominent myoinositol (mI) peak on short TE (n= 2). Dominant lipids signals were detected in 2 cases of metastasis in conjunction with mildly elevated Cho. Predominant mI peaks with increased Cho and almost absent Cr were observed in the 2 neurinoma MRS cases. Regarding the PNET, MRS showed increased Glx, mI and lipid peaks with presence of Taurine and decreased peak of NAA and Cr.

CONCLUSION: MRI is the modality of choice for imaging of extra-axial tumors. It allows through conventional sequences a definitive radiological diagnosis. Combination of calculated ADC values and MR spectroscopy findings added more information to MR imaging in the differentiation of these tumors.

EP178-MR Findings of Limbic Encephalitis Herpes Simplex Virus versus Autoimmune Encephalitis

*Li Li*¹, Shunji Mugikura¹, Takaki Murata¹, Yumiko Kato¹, Yasuko Tatewaki¹, Daddy Mata Mbemba¹, Keiichi Jingu², Shoki Takahashi¹

*Tohoku University, Graduate School of Medicine Diagnostic Radiology Sendai-Japan*¹ *Tohoku University, Graduate School of Medicine Radiation Oncology -Japan*²

PURPOSE: To review MR imaging findings of limbic encephalitis and what neuroradiologists need to know: Herpes simplex (HSV) versus Autoimmune encephalitis

METHODS: We reviewed for 1. Anatomy of the limbic systems, 2. Classification of limbic encephalitis, 3. Differences in the imaging and clinical findings of HSV and Autoimmune encephalitis, 4. Differences in the HSV and HHV6, 5. Differential diagnosis of limbic encephalitis and 6. Clinical and imaging findings after limbic encephalitis

RESULTS: 1. Anatomy of the limbic systems: Introducing the theory of Triune Brain by Paul D. MacLean, 1960s and MR imaging anatomy of limbic systems and Papez circuit, 2. Classification of limbic encephalitis, 3. Differences in the imaging and clinical findings of HSV versus Autoimmune encephalitis, 4.

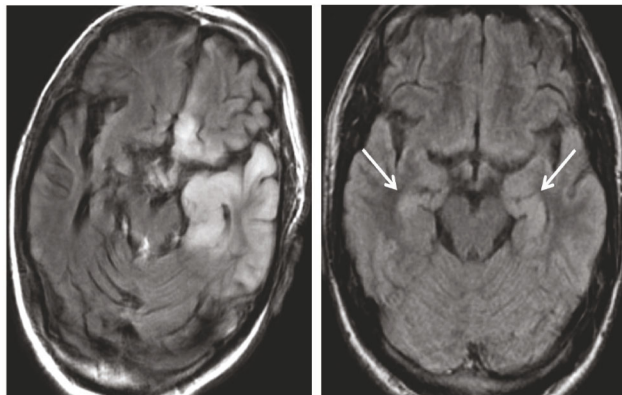


POSTER PRESENTATIONS ABSTRACTS

Differences in the HSV and human herpes virus 6 (HHV6) encephalitis: imaging and clinical findings, 5. Differential diagnosis of limbic encephalitis: cerebral infarction, low grade glioma and postictal encephalopathy, etc. 6. Clinical and imaging findings after limbic encephalitis including epilepsy and memory disturbance.

CONCLUSION: We reviewed MR findings of limbic encephalitis including HSV and Autoimmune encephalitis. Such information may help to differential diagnosis of the limbic encephalitis.

HSV encephalitis versus Autoimmune encephalitis



EP179-Diffusion Weighted Imaging with a b=3000 Improves the Detection of the Lesion Edge and Core in Progressive Multifocal Leucoencephalopathy (PML)

*Claudia Godi*¹, Enrico De Vita², Lewis Haddow³, Indran Davagnanam⁴, Hans Rolf Jäger⁴

UCL Institute of Neurology, Brain repair and rehabilitation Department London-United Kingdom ¹ *UCL Institute of Neurology, Neuroradiological Academic Unit, Department of Brain Repair and Rehabilitation -United Kingdom* ² *University College London, Centre for Sexual Health & HIV Research -United Kingdom* ³ *UCL institute of neurology, Brain repair and rehabilitation -United Kingdom* ⁴

PURPOSE: Progressive Multifocal Encephalopathy (PML) lesions often have a hyperintense rim on trace Diffusion Weighted Imaging (DWI). We found that imaging with b value=3000s/mm²[SUP]2[/SUP](b=3000) improve the depiction of rim in PML lesions. Our aim was to quantitatively assess this phenomenon by 1) measuring the signal intensity and Apparent Diffusion Coefficient (ADC) of rim and core of PML lesions on b=1000 and b=3000; 2) comparing b=3000 with b=1000 trace signal intensities, ADC values and volumes of rim and core.

METHODS: We retrospectively selected all the patients scanned with our routine HIV clinical protocol (including both b=1000 and b=3000 DWI), and diagnosed with PML in the past 10 years. Seven patients (4 males, 3 females, age range:19-66 years) fulfilled the criteria, showing a total of nine lesions with a rim-core pattern typical of PML. Rim and core, and normally appearing white matter (NAWM) were outlined on b=1000 and b=3000 DWI trace using FSL software. Regions of interest were superimposed on ADC maps, and their signal intensities, ADC and volumes were measured. Wilcoxon-Signed Rank Test was applied. P-values<0.05 were considered significant.

RESULTS: The signal intensity ratio of rim:NAWM was 2.06 on b=3000, and 1.6 on b=1000 DWI trace (p-value=0.008). The signal intensity ratio of rim:core on b=3000 DWI trace was significantly higher than on b=1000 (ratio 3.07 vs 1.70). On b=3000, the ADC of the NAWM, rim and core were significantly and consistently inferior compared to b=1000. The ADC ratio of rim:NAWM was 1.03 on b=3000 and 1.21 on b=1000 (p-value=0.002) but there was no significant difference in the rim:core ratios. The average total rim volume on b=1000 was inferior than on b=3000, but the difference was not significant. Conversely, the average core volume on b=3000 was significantly and consistently higher compared to b=1000. **CONCLUSION:** DWI using b=3000 improves the visualisation of the edge of PML lesions based on both diffusion and T2 effects. It can be hypothesised that the core reflects irreversible tissue destruction whereas the edge represents active inflammation. B=3000 DWI not only increase the conspicuity of the rim, but also show consistently larger cores, which could possibly be used as a biomarker for outcome and treatment response.



POSTER PRESENTATIONS ABSTRACTS

EP180-Contrast Perfusion Weighted MR Imaging OF Intracranial Tumors

*Kamel Walha*¹, Amir Abdallah², Aymen Arous², Leila Mchirgui², Cyrine Drissi², Rym Sebai², Nadia Hammami², Sonia Nagi², Hafedh Jemel³, Mohamed Ben Hamouda²

*National Institute Mongi Ben Hamida of Neurology Neuroradiology Tunis-Tunisia*¹ *Neuroradiology -Tunisia*² *Neurosurgery -Tunisia*³

PURPOSE: MRI has a prominent role in the diagnostic of cerebral tumors especially with the progress of new imaging technics such as perfusion. Our study illustrates utility of MR perfusion to diagnose and to stage brain tumors.

METHODS: We included in a retrospective study 190 patients who were admitted in our institution for management of brain tumors during a 12 months period (from December 2011 to December 2012).

All our patients underwent a brain MRI using 3T MR system (Siemens® verio). The protocol included conventional sequences (DWI, FLAIR, T2, T2*, T1 before and after gadolinium enhancement) and also mean dynamic contrast enhanced T1 weighted MR perfusion with a post processing which established some parameters such as brain perfusion map, relative cerebral blood volume (rCBV) and dynamic perfusion curve of tumors.

RESULTS: We diagnosed 56 meningiomas (29,5%), 9 schwannomas (4,7%), 6 other extra-axial non meningiomatous tumors (3,1%), 3 pineal tumors (1,6%), 57 glial tumors (30%), 27 metastasis (14,2%), 12 intra-ventricular tumors (6,3%), 6 hemangioblastomas (3,1%), 4 DNET (2,1%), 4 PNET (2,1%), 2 lymphomas (1%) and 4 other tumors (2,1%). For all meningiomas and hemangioblastomas, a significantly increased rCBV was observed in comparison with other tumors. For glial tumors and metastasis, MR perfusion was useful by showing difference of rCBV values in the peritumoral area leading to differentiate single brain metastasis from glioblastoma. According to rCBV value and mean dynamic perfusion curve in tumoral and peritumoral areas a staging was estimated for both glial and intra-ventricular tumors.

CONCLUSION: Perfusion MRI could provide additionnal information to increase the specific tumor diagnosis and to characterize tumor aggressiveness level.

EP181-Trigeminal Neuralgia Associated with Persistente Primitive

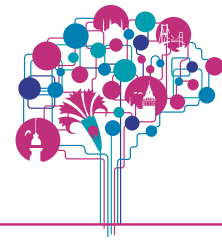
Trigeminal Artery Report of 3 Cases

Marcelo Moraes Valenca¹, *M. de Fatima Vasco Aragao*², Maria Lucia Lima Soares³

Universidade Federal de Pernambuco Pós-Graduação em Neuropsiquiatria e Distúrbio do Comportamento -Brazil

*¹ Multimagem; Universidade Mauricio de Nassau Radiology Recife-Brazil*² *Faculdade de Medicina da Universidade Federal de Alagoas Radiology*³

CASE REPORTS: The trigeminal neuralgia or tic douloureux is a frequent painful condition in which the pathophysiological mechanism is poorly understood. Trigeminal neuralgia is sometimes described as the most excruciating pain known to humanity. It is the most common cause of neuralgic facial pain in the geriatric population. The vast majority of the cases of trigeminal neuralgia are considered idiopathic. In around 1% of the patients with trigeminal neuralgia, a structural lesion is displaced during the neuroimaging evaluation, mainly in the region of the trigeminal nerve path from the brainstem to its entrances in the skull base. In such cases, either a tumor or a vascular compression over the nerve is considered the etiological causal agent. In the literature, a few cases of trigeminal neuralgia have been reported in association with the persistence of the primitive trigeminal artery. Some time the encountered of a persistent trigeminal artery is considered as a incidental finding, since the pain is on the contralateral side. This article intends to present the cases of three patients (2 women) with trigeminal neuralgia that during the investigation the presence of the primitive trigeminal artery (PTA) was disclosed. In two of the patients the trigeminal neuralgia developed in both sides, at different age. In conclusion, unlike to generally accepted in the literature, a persistent trigeminal artery may trigger pain with characteristics of tic douloureux on the contralateral side.



POSTER PRESENTATIONS ABSTRACTS

Thursday, September 11, 2014

13.00-14.00

Spine

EP182-Follow up MR Findings of Spinal Meningioma after Stereotactic Radiotherapy

*Yoon Joon Hwang*¹, Byung Hoon Lee¹, Yon Kwon Ihn²

*Inje University Ilsan Paik Hospital Radiology Goyang-Korea, South*¹ *St. Vincent Radiology -Korea, South*²

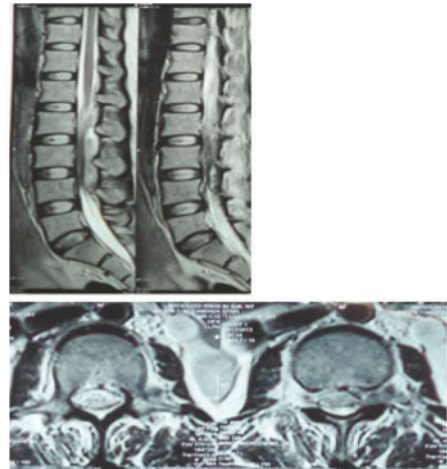
PURPOSE: We retrospectively analyzed pre and post stereotactic radiotherapy MR findings of spinal meningioma. **METHODS:** Eleven spinal meningiomas were treated with Novalis radiotherapy. MR images were reviewed to determine tumor volume, T2 signal intensities and patterns of contrast enhancement. **RESULTS:** Tumor volume was significantly decreased in 10 lesions and unchanged in 1 lesion. T2 signal intensities were persistently decreased in 7 lesions, and in 4 lesions, variable changes were noted. Enhancement pattern was not changed in 10 lesions, but 1 lesion showed central non enhancing focus during the follow up. **CONCLUSION:** Local control of spinal meningioma after stereotactic radiotherapy was successfully done. Main MR features of spinal meningioma after radiotherapy were gradual decrease in T2 signal intensity and no change in contrast enhancement pattern.

EP183-Langerhans Cell Histiocytosis (LCH) of the Lumbar Spine During Pregnancy

*Felicia Pilar Gunadi*¹, Farhan Anwary¹, Rista D Soetikno¹

*RSHS General Hospital Radiology Bandung-Indonesia*¹

Langerhans cell histiocytosis (LCH), previously known as histiocytosis X, a reactive proliferative disease of unknown pathogenesis characterized by proliferation of Langerhans cells is extremely rare (approximately :1,500,000 inhabitants) in the lumbar spine of adults. It often present with pain in calvarium or spine and may cause neuroendocrine symptoms. Characterized by clonal proliferation and excess accumulation of pathologic Langerhans cells, lymphocytes, plasma cells, eosinophils and neutrophils causing local or systemic effects. The gold standard for diagnosing LCH is the detecting of Birbeck Granules by Electron Microscop (EM). LCH is disease of unknown etiology with, a rather unpredictable course since it can spontaneously resolve or progress to a disseminated form, compromising vital functions with occasionally fatal consequences Langerhans cells may cause local or systemic effects. The most frequent sites of these bony lesions are the skull, femur, mandible, pelvis and spine.[SUP]1-6[/SUP] We present an unusual variant of Langerhans cell histiocytosis in a 26-year-old pregnant woman presenting with cauda equina syndrome. MR imaging revealed widespread extradural contrast enhancing mass involvement the lumbar spine. The patient underwent surgical resection of the tumour with three quarter prone position. Diagnosis was confirmed by histological and immunohistochemistry analysis. Langerhans cell histiocytosis should be included in the differential diagnosis of radiolucent lesions of the spine in adults.





POSTER PRESENTATIONS ABSTRACTS

EP184-A Rare Servical Intradural Extramedullary Melanocytoma Case

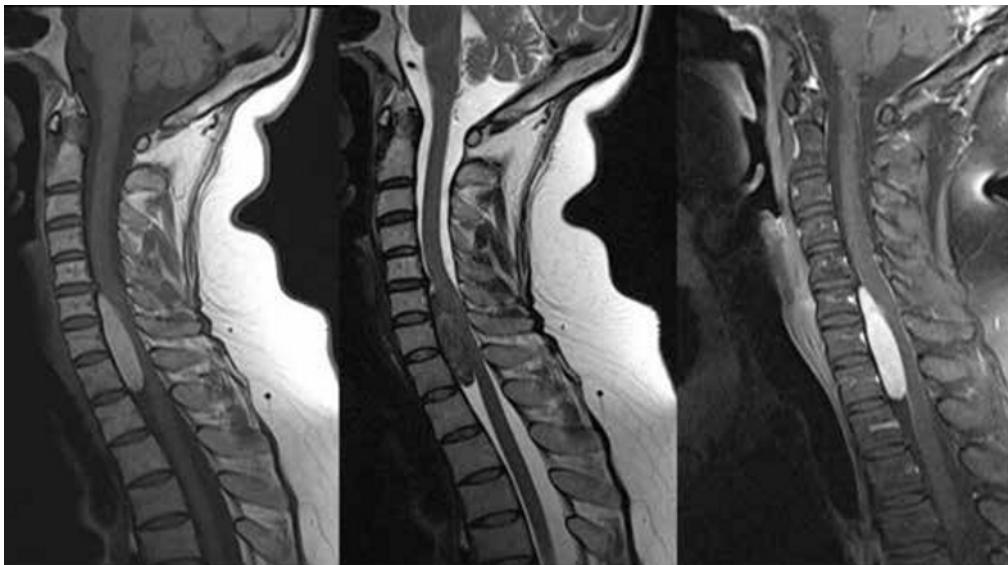
Report

*Amalya Zeynalova*¹, Yasemin Kayadibi¹, Elmar Bayraktarov¹, Evrim Ozmen¹, Zehra Isik Hasiloglu¹

*Istanbul University Cerrahpasa Medical Faculty Radiology Istanbul-Turkey*¹

PURPOSE:To discuss typical radiological findings of a rare servical intradural extrameduller melanocytoma.

METHODS: A 32-year old woman presented with complaints of pain and numbness in left arm for 2 year. Neurological examination showed weakness, numbness and tingling sensation in left arm. Otherwise physical examination was unremarkable. Cervial spinal magnetic resonance imaging (MRI) performed. **RESULTS:** MRI revealed an intradural extramedullary mass which was displacing the spinal cord to posterior. The lesion was hyperintense on T1-weighted images (T1WI) and hypointense on T2-weighted images (T2WI). After intravenous contrast adminstration mild-diffuse echancement of the tumor was revealed. Subtotal resection of the intradural mass was performed under general anesthesia following C6-C7 cervical laminectomy and durotomy. Hystopathological examination was compatible with WHO Grade 1 meningeal melanocytoma. **CONCLUSIONS:** Meningeal melanocytoma is a rare benign intradural extramedullary spinal tumor. It originates from leptomeningeal melanocytes. Although cervical spine is the most common region, symptoms depend on tumor's localization and patients usually present with pain. On CT scans tumor's density could change isodense to hyperdense when compared to medulla spinalis. On MRI it is seen as intradural extramedullary well-circumscribed lesion with iso to high signal intensity on T1W and low signal intensity on T2W and after contrast adminstration it enhances homogeneously. This variable signal intensity is probably associated with melanin content. The differential diagnosis of melanocytic neoplasms includes high cellular tumors, i.e., meningioma, lymphoma, neuroenteric cyst and metastasis. Meningiomas usually show tumor calcification and hyperostosis of adjacent bones. Schwannomas usually heterogenously enhance but small schwannoma could homogeneously enhance after contrast adminstration. Early subacute hematoma also has very similar features with melanocytoma on MRI, but there is no contrast enhancement. Neuroenteric cysts are often associated with vertebral bony abnormalities. Radiologists should be alerted and aware of the findings of these lesions.





POSTER PRESENTATIONS ABSTRACTS

EP185-Vertebrobasilar Territory Stroke Syndromes and Imaging Findings

*Juan Ovalle*¹

*High diagnostic technology - Cedicaf Diagnostic Neuroradiology Ibagué-Colombia*¹

PURPOSE: The purpose of this work is to show from the topographical and radiological and imaging syndromatic different aspects of stroke that compromise the brainstem and cerebellum.

METHODS: Didactic (Schematic) and detailed explanation of the different structures of the posterior fossa and their functional connections that explain the syndromes, brainstem and thalamic region will be used. The diagnostic modality MRI has shown the sensitive and specific in different sequences T2/FLAIR, DWI and ADC map for the detection of acute stroke.

DISCUSSION: The vascularization of the brainstem and cerebellum consists of large, often variable, extrinsic vessels that bring the blood to the surface of the brainstem and small intrinsic vessels that penetrate the stem to supply defined vascular compartments within each part of the stem. The extrinsic vessels include the vertebral artery, anterior spinal artery, posterior spinal artery, basilar artery, posterior inferior cerebellar artery (PICA), anterior inferior cerebellar artery (AICA), and superior cerebellar artery (SCA). The uppermost brainstem also receives supply from the posterior medial choroidal artery, PCA, collicular arterial branches of the PCA, and the anterior choroidal artery. The PICA is more commonly involved (and may produce Wallenberg's syndrome), followed by the superior and anterior inferior cerebellar arteries.

Cerebellar infarctions occur in association with dissection of the vertebral arteries (particularly in younger patients) or with basilar artery disease (in older patients).

In the basilar artery the mortality is 2.5 times higher than with occlusion of one ICA. Common etiologies include embolism, atherosclerosis, vascular malformations of the base of the skull, syphilis, tuberculosis, and fungal meningitis. If only the distal basilar artery is occluded, top-of-the-basilar syndrome is produced (infarctions of thalami, posterior limb of internal capsules, and midbrain). Median thalamic infarctions may result from occlusion of the artery of Percheron (single median thalamoperforator). Patients with distal clots have better prognosis.

We can see different imaging findings in infarctions of the posterior fossa structures and brainstem with different syndromes associate, which ones will be discuss.

SUMMARY: Detailed knowledge of the topography of different neuroanatomical and vascular structures of the vertebrobasilar circulation may imaginological along with demonstrations explain the signs and symptoms of the syndromes associated with stroke in the vertebrobasilar circulation.

EP186-Spinal Cord Glioblastoma Multiforme in a Patient with Down Syndrome

*Pablo Picasso de Araújo Coimbra*¹, Rafael Costa Lima Maia², Tiago Silva Holanda Ferreira³, Daniel Gurgel Fernandes Tavora¹, Wellington Barros Oliveira de Moura⁴, André Soldati Antônio², Stelio da Conceição Araújo Filho², Edson Lopes Júnior²

Hospital Geral de Fortaleza Department of Radiology Fortaleza-Brazil 1 Hospital Geral de Fortaleza Department of Neurosurgery - 2 Universidade de Fortaleza - 3 Centro Integrado de Oncologia - 4

PURPOSE: Glioblastoma multiforme (GBM) is the most common primary brain tumor in adults and one of the most severe cancers across medicine. The spinal extracranial form is rare, representing about 1.5 % of all spine tumors. We present a case of a patient who had this diagnosis after surgery and immunohistochemical study.

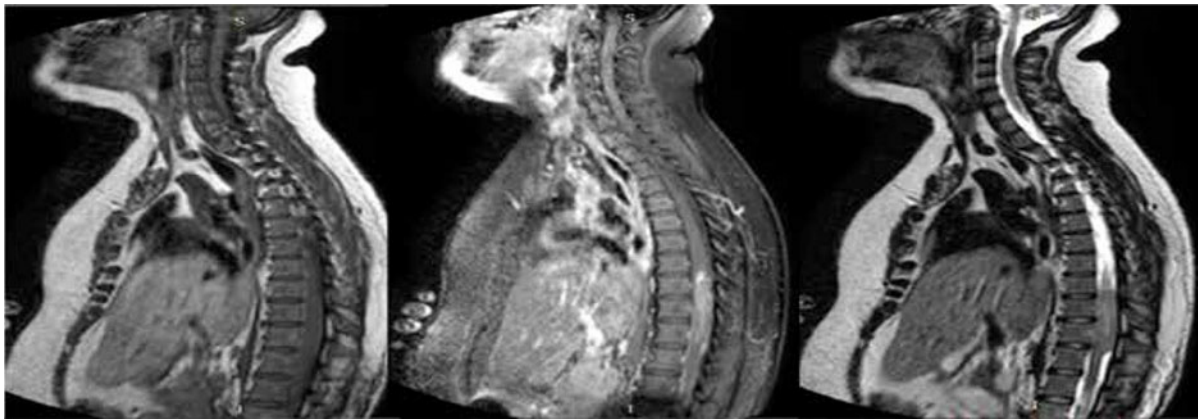
CASE REPORT: 28-years-old, female, with Down syndrome (DS), presented paraparesis two months before hospitalization, being brought by relatives for our service when was already paraplegic. MR showed a exophytic mass lesion with dural intra isosignal T1 and T2 and little enhancement by paramagnetic contrast medium in the thoracic cord in the topography of the vertebral body of T9 spinal cord edema above. Complementary



POSTER PRESENTATIONS ABSTRACTS

study (including cranial CT) showed no other lesions. The patient underwent resection of the tumor, and immunohistochemical study was positive for markers GFAP, AE1-AE3, S-100, A1, Ki-67, and negative for the EMA marker - results suggestive of GBM. Patient was referred for complementary radiotherapy.

CONCLUSIONS: The primary medullary form represents 1-5% of GBM forms and represents 1.5% of all spinal tumors. The rapid progression of the patient's symptoms illustrates the high malignancy of the disease. The supernumerary chromosome 21, found in DS, may be associated with atypical presentations of tumors, when compared with the general population.



EP187-Intraspinal Subdural or Epidural Hygroma in Cases of Intracranial Hypotension. Which One is Correct Diagnosis

Izumi Anno¹

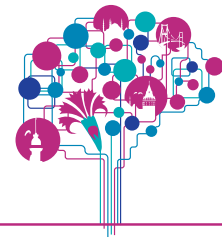
IPU Radiology Ami-Japan¹

PURPOSE: There should be two type of intraspinal fluid collection in cases of spontaneous intracranial hypotension. We shall discuss how to differentiate intracranial subdural hygroma from epidural one.

MATERIALS and METHODS: We have experienced several cases of intracranial hypotension those were concomitant with thoracolumbar spinal subdural hygroma. Etiology of intracranial hypotension is thought to be spontaneous, CSF leakage into epidural space, postoperative iatrogenic causes and so on. However only several reports can be found about the intraspinal subdural hygroma. A report says that the intraspinal subdural hygroma is a consequence of the CSF leakage and consequently results intraspinal hypotension. Some reports says that the iatrogenic reasons such as lumbar puncture and post surgical tear of subarachnoid membrane causes a subdural hygroma.

It is very difficult to find intraspinal subdural hygroma on usual spinal MRI examinations, because the diameter of spinal cord is very small and the arachnoid membrane is much more thinner than intracranial arachnoid membrane. Also, the dynamic range of turbo spine echo pulse sequences which we usually use on the spinal imaging are so narrow to see the intensity differences between intra-arachnoid CSF intensity and subdural CSF one.

It is very sure, there may exist both intraspinal subdural hygroma and epidural hematomas in cases of intracranial hypotension.



POSTER PRESENTATIONS ABSTRACTS

EP188-Interventional Neuroradiology C Spine Procedures

*Francesco Massari*¹, Giuseppe Bonaldi², Alessandro Cianfoni³

*University of Massachusetts Neuroimaging and Intervention Worcester-United States*¹ *Ospedali Riuniti, Bergamo Neuroradiology -Italy*² *Neurocenter of Southern Switzerland, Lugano Neuroradiology -Switzerland*³

PURPOSE: Aim of this presentation is to offer an overview on neuroradiological armamentarium in the minimally invasive percutaneous image-guided procedures on the cervical spine.

MATERIALS and METHODS: Spinal neuro-interventional radiology, through the use of fluoroscopic and/or CT imaging guidance offers a wide variety of percutaneous procedures on the cervical spine, for tissue diagnosis, drainage of fluid collections, pain management, diagnostic and therapeutic blocks, radiofrequency ablations, disc procedures, osteoporotic and neoplastic vertebral fractures treatment. Procedures under fluoroscopy and/or CT guidance, with different approaches (anterior, lateral, posterior, transmaxillary, and trans-oral), are described, and indications, relevant anatomy, procedural techniques, outcomes in three highly specialized medical center in USA and Western Europe, as well as comparison with literature are outlined.

-Anterior approach: Under fluoroscopic or CT guidance, it is used to access: disc spaces, vertebral bodies (from C4 to C7) and Stellate ganglion.

-Lateral approach: Under fluoroscopic or CT guidance, it is used to access: central canal (C1-C2), neuroforamina (C3-C8), zygoapophyseal joints and median branch nerves.

-Posterior approach: Under fluoroscopic or CT guidance, it is used to access: interlaminar space, posterior bony elements (C1 lateral masses), C1 and C2 neuroforamina, C1-C2 joint, zygoapophyseal joints, radiofrequency median branch denervation and radiofrequency transverse occipital nerve denervation.

-Transmaxillary approach: Under CT guidance, it is used to access: C1 and C2 anterior bony elements.

-Transoral approach: Under fluoroscopic guidance, it is used to access: C1-C3 anterior bony elements.

RESULTS: A wide variety of image-guided cervical spine procedures are illustrated, with their different approaches. Fluoroscopic or CT guidance can be chosen on the basis of personal preference, anatomical features, type of approach, and specific procedure to be performed. Percutaneous image-guided procedures on the cervical spine require thorough knowledge of loco-regional anatomy, precise and reliable imaging guidance, and rigorous technique, due to the complex, delicate, and vital anatomical environment, to avoid serious complications. Elements of relevant fluoroscopic and cross sectional anatomy, procedural technique elements, multicentric outcomes as well as comparison with literature, are discussed and displayed.

CONCLUSION: This multicentric analysis illustrates a wide variety of percutaneous image-guided accesses to the cervical spine, utilized for diagnostic and therapeutic purposes, their indications, the anatomy, techniques, outcomes and comparison with literature.

Pediatric NR 1

EP189-Factors Correlating Outcome in Congenital Muscular Torticollis a Single Center Study

*JiHwa Ryu*¹, Choongki Eun¹, KwangHwi Lee¹, HongDae Kim¹

*Haeundae Paik Hospital radiology Busan-Korea, South*¹

PURPOSE: This study aimed to assess clinical factors and sonographic features potentially influencing complete regression in patients with congenital muscular torticollis (CMT).

METHODS: From January 2010 to December 2012, 80 infants underwent neck ultrasound (US) because of clinical suspicion of CMT. We statistically analyzed the correlation between complete regression and clinico-sonographic findings when complete regression was defined as no visible lesion on follow-up US.



POSTER PRESENTATIONS ABSTRACTS

RESULTS: Of the 80 infants, 61 were sonographically diagnosed with CMT; 12, with benign lymph nodes; 6, with no sonographic abnormalities; and 1, with a congenital cystic neck lesion. All 61 patients with CMT were sonographically followed up: (1) 34 underwent physiotherapy, and 27 of them (79.4%) revealed complete regression in follow-up. (2) 27 did not undergo physiotherapy, and 15 of them (55.6%) showed complete regression. Thus, a total of 42 patients showed complete regression. A statistically significant correlation was found between physiotherapy and complete regression ($p < 0.05$), but not between complete regression and the patient sex; the size, volume, and echogenicity of the lesion; and thickness ratio ($p > 0.05$).

CONCLUSION: Physiotherapy was the only factor influencing complete regression in CMT, whereas the patient age was associated with non-regression in CMT.

EP190-Neuroimaging Findings of Twin Sisters with Incontinentia Pigmenti Who Presented With Recurrent Encephalopathy Attacks

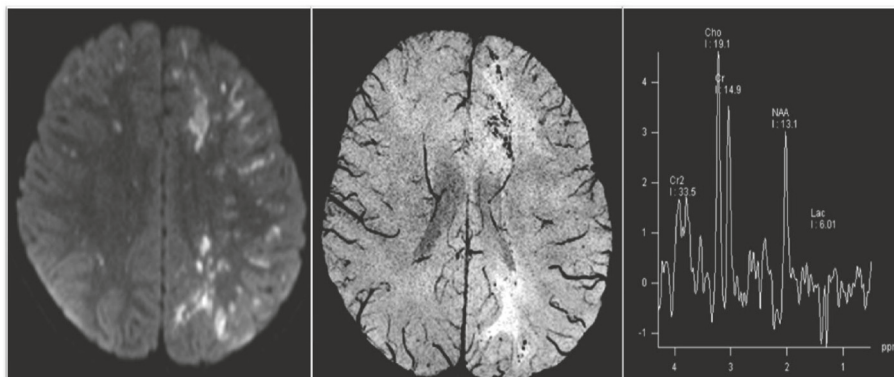
*Rahsan Gocmen*¹, Bahadir Konuskan², Dilek Yalnizoglu², Kader Karli Oguz¹

Hacettepe University Department of Radiology Ankara-Turkey 1 Hacettepe University Department of Pediatric Neurology -Turkey 2

PURPOSE: Incontinentia pigmenti (IP), is a rare, X-linked dominant neuroectodermal disorder that may present with abnormal skin, ocular, hair, tooth, and central nervous system findings. Neurologic symptoms include seizure, growth retardation, microcephaly, hemiparesis, ataxia, and cerebral palsy. Our aim is to present brain magnetic resonance (MR) imaging, diffusion-weighted imaging (DWI), susceptibility-weighted imaging (SWI), and MR spectroscopy, findings with 5-year follow-up of twin sisters, who were diagnosed with IP. To the best of our knowledge, this is the first reported case in which IP was the presenting as recurrent encephalopathy attacks and studying SWI, MR spectroscopy.

CASE REPORT: 5-year-old girl who had 2 encephalopathy attacks in a few years presented with seizure and tendency to sleep. MR imaging that were obtained during the previous encephalopathy attacks, was interpreted in favor of encephalitis/cerebellitis. In her last attack, detailed physical examination revealed linear hyperpigmented skin rashes which were typical for IP. Subsequently, it was found out that her twin sister and mother had similar skin rashes. Her twin sister had an encephalopathy attack when she was 4-month old. Brain MR imaging that was performed during her last attack demonstrated bilateral cerebellar and cerebral cortical-subcortical, millimetric T2 hyperintense lesions with edema. Lesions showed diffusion restriction. SWI demonstrated that some lesions had microhemorrhages. MR spectroscopy showed increased choline, decreased NAA levels, and abnormal lactate peak. Brain lesions which were detected during the previous attacks had been resolved without sequelae. Neurologic symptoms and imaging findings due to last attacks were significantly resolved at the 10-month follow-up.

SUMMARY&CONCLUSION: Although brain MR imaging findings of IP are characteristic, it may not be considered in the first place when making the diagnosis because it is a very rare disorder. Unfortunately, it may be misdiagnosed as encephalitis, ischemic stroke, or acute disseminated encephalomyelitis. Brain lesions presenting with encephalopathy attacks occur simultaneously with edema and inflammation attacks in skin lesions. Imaging findings of IP may represent foci of cytotoxic edema due to acute cerebral microinfarcts and/or underlying probable inflammatory vasculitic pathogenesis.





POSTER PRESENTATIONS ABSTRACTS

EP191-Imaging of Intracranial Lipomas

Jeong Hyun Yoo ¹

Mokdong Hospital, Ewha Womans Univ. Hospital Radiology Seoul-Korea, South 1

PURPOSE: The intracranial lipomas are rare brain lesion and the incidence is variable from 0.06 to 0.46% among intracranial tumors. It is thought to be congenital malformation resulting from persistence and maldifferentiation of meninx primitiva. Lipomas show variable locations, but most commonly located at subarachnoid space because of meninx primitive origin, and tendency to locate at the midlines such as pericallosal, quadrigeminal, suprasellar areas. Purpose of study is to understand the embryologic pathogenesis of the intracranial development and to illustrate the typical intracranial lipomas located in the various typical sites, and to illustrate the associated with various congenital anomalies. **METHODS:** We retrospectively reviewed CT or MR images of 48 intracranial lipomas 45 patients, who showed typical feature of intracranial lipomas. We classified according to their location and their shapes. We also noted flow voids in the lesion representing intra-lesional vessels. And we also recorded about accompanied intracranial anomalies.

RESULTS: There were 48 intracranial lipomas at 45 patients. Thirty one lipomas showed tubulonodular shapes while seventeen showed curvilinear shapes (35.4 %). All of those showed high SI on T1WI, low SI on T2WI.. They noted as hypodensity on CT. And they didn't show enhancement.. Among them, 8 lesions showed flow voids in them. And in 1 lesion showed dark SI foci meant calcification existed.

The most common site was pericallosal (18cases, 37.5%). And most of pericallosal lipomas (n=16) were found at posterior aspect, but only 2 were found at anterior aspect. Next most common location was quadrigeminal area (16cases, 33.3%). Third most common site was suprasellar area (n=9, 18.7%)..

We found 23 associated other intracranial anomalies (47.9%). Corpus callosal anomalies were most common abnormalities which were at 13 cases with variable from agenesis to hypogenesis. Seven of them were associated with pericallosal lipomas, and 4 of them with quadrigeminal lipomas, and last 2 of them with suprasellar lipomas. Associated posterior fossa anomalies included Chiari I malformation and hypoplasia of vermis or midbrain.

CONCLUSIONS: Intracranial lipomas are rare and they most frequently located in the midlines such as pericallosal, and quadrigeminal and suprasellar area. They showed tubulonodular or curvilinear shapes. They show high frequency of accompanied other brain malformations.

EP192-Foetal MRI Correlation between Antenatal Ultrasound Antenatal MRI and Post natal Imaging the Cape Town Experience

Arthur Daire ¹, Savvas Andronikou ², *Sally Candy* ³

University of Malawi Radiology -Malawi 1 Groote Schuur Hospital and University of Cape Town Radiology South Africa 2 GSH Radiology cape town-South Africa 3

OBJECTIVES: To determine the most common indication for foetal MRI, and to correlate ante-natal MRI with ante-natal ultrasound, post-natal imaging and post mortem findings in a high HIV prevalence population.

METHODS: This was a retrospective study of imaging between January 2006 and December 2011. Seventy foetal MRI cases with complete medical records (antenatal and postnatal) were included in the study. Antenatal ultrasound and antenatal MR imaging was compared and also compared with the postnatal imaging findings. Stata 12 was used to analyse the Data. Spearman's test was used to test the agreement between the results.

RESULTS: 20% of cases were HIV positive. There was no significant difference in documented infectious causes between the HIV positive and negative groups.

Intracranial pathology was the most common indication for foetal MRI, with ventriculomegaly being the commonest indication determined from prenatal ultrasound. There was 72% agreement between



POSTER PRESENTATIONS ABSTRACTS

antenatal ultrasound and foetal MRI. In 7 cases (10%) additional findings on MRI such as corpus callosum agenesis,undiagnosed sacral meningocele or holoprosencephaly had a significant prognostic impact on management. There was a strong association between the degree of ventricular enlargement and the presence on MRI of other congenital CNS abnormalities. Mild dilatation was more likely to have resolved on post natal imaging. There was generally poor agreement between postnatal imaging and antenatal imaging though MRI fared better than ultrasound (39 vs 28%). Diaphragmatic hernias, Congenital cystic adenomatous malformations (CCAM)and neck masses were the most common non-CNS indications.

CONCLUSION: In our setting intracranial pathology was the major indication for foetal MRI. HIV positive mothers were not over represented in this group compared with the general Maternity population in Cape Town. The study found good agreement between prenatal ultrasound and foetal MRI but poor agreement between antenatal and postnatal findings, largely due to resolution of ventriculomegaly.

EP193- Value of Diffusion Weighted Imaging in Neonatal Hypoglycemia

*Fuldem Donmez*¹, Muhtesem Agildere¹

*Baskent U Radiology Ankara-Turkey*¹

Value of Diffusion Weighted Imaging in Neonatal Hypoglycemia

PURPOSE: To emphasize the value of DWI in imaging of neonatal brain.

METHODS: A 2-day old baby was admitted to the emergency room with the complaint of poor feeding and cyanosis. There was no problem perinatally. The physical examination was normal except for the cyanosis. At the time of admission, he had generalized seizures. The laboratory tests showed deep hypoglycemia (blood glucose level was 21). He was given 2cc/kg 10% dextrose, control blood glucose was 78 and saturation was 95%. 15 minutes later, the blood glucose decreased again (32) and 100 cc/kg 10% dextrose was injected. Despite these injections, control glucose levels were 42,47 and 57, and during the acute treatment, seizures repeated. Antiepileptic drugs and dextrose were continued. An MRI of the brain was performed.

RESULTS: The MRI was normal except for suspicious faint signal increase on the left occipital lobe. However diffusion MRI (DWI) showed significant periorlandic and right occipital diffusion restriction. Left occipital lobe was normal.MR angiography was also normal ruling out any vascular occlusion.

CONCLUSION: Various injury patterns in hypoglycemia are described based on MRI findings, all showing increased signal on FLAIR or T2-weighted imaging. However, DWI is also important as well as conventional techniques. DWI is not only necessary to distinguish vasogenic edema versus cytotoxic edema, but also leads the diagnosis itself in case of normal conventional MRI findings. In case of poor sedation in neonates, priority should be given to DWI before other sequences

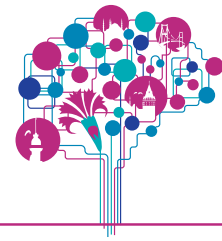
EP194-Traumatic Craniocervical Junction Ligamentous Injuries and Epidural Retroclival Hematoma

Bilal Egemen Çifçi¹, *Gökçen Çoban*¹, Mahmut Gökdemir², Enes Duman¹

*Baskent University Medical School Radiology Department -Turkey*¹ *Baskent University Medical School Pediatrics Department -Turkey*²

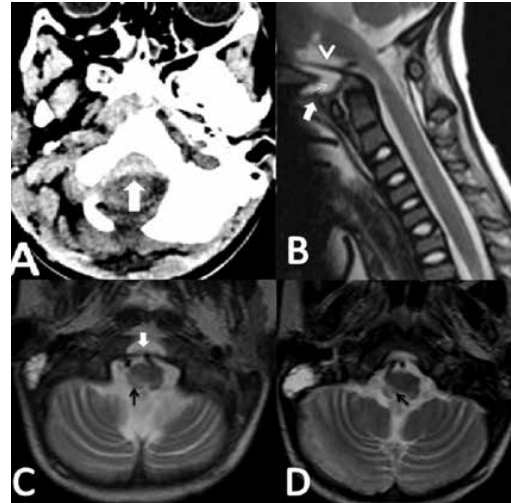
Cervical spine injuries are common in pediatric population and usually seen in craniocervical junction due to the anatomical and physiological differences. Combination of rapid hyperextension/hyperflexion traumas due to high-speed motor vehicle accident are known to be the reason of ligamentous injury and retroclival epidural hematoma.

Our aim is to describe a rare combination injury of the the apical ligament, retroclival epidural hematoma and the suspicion of brain stem slits, due to rapid hyperextension/hyperflexion trauma with high-speed motor vehicle accident in a 3 year 8 month old girl. On head CT there was 10 mm thick retroclival epidural hematoma (Fig. 1a), scattered subarachnoid, quadrigeminal cistern, and left intraventricular hemorrhage, but no bone fracture. There was no bone fracture on cervical spine CT imaging, the dens-basion (DB) and basion-axial



POSTER PRESENTATIONS ABSTRACTS

interval (BAI) were in normal limits. The occipital condyle and the atlas joint was asymmetric and greater than 4 mm, and also C1–C2 inter-laminar space ratio (C1–C2:C2–C3) was greater than 2.5. On the 5th day of admission CT was repeated and there was a significant increase of ventricular sizes. An external ventricular drainage was placed to control hydrocephalus. To evaluate the craniocervical junction, cervical and brain magnetic resonance imaging were performed on the 15th day of admission, after providing hemodynamic stabilization. On MR imaging, there was prominent cerebrospinal fluid between the anterior atlantooccipital and tectorial membrane and C0-1 and C1-2 interlaminar space and tectorial membrane stretching (Fig. 1b-c). The apical ligament was disrupted (Fig. 1b). The anterior and posterior longitudinal ligaments were adjective and in normal shape. Diffusion imaging revealed the diffusion restriction in bilateral perirolandic cortex, posterior parietal-occipital cortex and basal ganglia due to hypoperfusion. There were focal hyperintensities on the ventral ponto-medullary junction and the right caudal cerebellar peduncle suspicion of focal slits (Fig. 1c-d) due to combination of rapid hyperextension/hyperflexion trauma. The cervical spine was immobilized with a Philadelphia collar. She is stil under treatment in the pediatric intensive care unit with a GSC of 8 for six months.



EP195-Metabolic Disorders Presenting in Neonatal Period

*Ritu Kakkar*¹, Sameer Soneji¹, Shrinivas Desai¹
*Jaslok Hospital CT And MRI Mumbai-India*¹

AIM: Emphasize characteristic features of metabolic disorders encountered in neonatal period, a series of 21 cases.

CONTENT ORGANIZATION: Maple syrup urine disease was the most common disorder in our series, showing bilaterally symmetric restricted diffusion and hyperintensities in deep cerebellar white matter, dorsal brainstem, cerebral peduncles, posterior limbs of internal capsule (PLIC) and perirolandic white matter with a peak at 0.9 ppm on MR Spectroscopy (MRS) of branch chain amino acids. Propionic academia presented with similar imaging findings and a glutamine/glutamate peak. Findings in non ketotic hyperglycinemia were hyperintensity in PLIC, midbrain and pons on both sides with glycine peak on MRS. Urea cycle defects showed diffuse cerebral edema with involvement of basal ganglia and glutamine peak. Patient with Zellwegers syndrome showed germinolytic cysts with polymicrogyria. Walker Warburg syndrome presented as gross hydrocephalus with polymicrogyria and cerebellar cysts. 1 patient with molybdenum cofactor A deficiency showed restricted diffusion in deep grey matter and midbrain.

SUMMARY: MR with MRS plays crucial role in early diagnosis of neonatal metabolic disorders, facilitating early treatment which often improves long term prognosis.



POSTER PRESENTATIONS ABSTRACTS

EP196-Magnetic Resonance Fiber Tracking In a Neonate with Hemimegalencephaly

*Laura Scarciolla*¹, Thomas Re², Emi Takahashi², Stefania Galassi³, Lorenzo Figà Talamanca³, Carlo Cosimo Quattrocchi¹, Bruno Bernardi³, Daniela Longo³

University Campus Bio-Medico of Rome Radiology rome-Italy 1 Boston Children Division of Newborn Medicine, Department of Medicine, Fetal and Neonatal Imaging Science -United States 2 Bambino Gesù-Rome Radiology -Italy³

A magnetic resonance (MR) diffusion fiber tracking study in a preterm(male; 37 weeks +5 days) neonate diagnosed with left hemisphere hemimegalencephaly is presented. The patient was admitted to the Neonatal Intensive Care Unit (NICU) of Bambino Gesù' Pediatric Hospital in Rome for seizures appearing the first day of life. Clinical exam was unremarkable except for mild facial asymmetry. Electroencephalogram (EEG) showed abnormal activity in the left temporal, parietal and occipital lobes. Brain ultrasound imaging showed left-dominant volumetric asymmetry of the cerebral cortex. Despite diffuse morphologic deformities identified in conventional imaging, all major pathways were identifiable bilaterally with minor aberrations in vicinity of morphologic lesions. Remarkably, the quantitative value of FA showed great left-right variation in structures which showed no apparent alteration in conventional imaging or tractography.

EP197-"Papillary Glandular Sign" in Large Suprasellar Pilocytic Astrocytomas

*Manzoor Ahmed*¹, Anwar Ul Haq², Essam Alshail², Mohammad Dogar¹, Joyce Mbekeani³

King Faisal Hospital & Research Center Radiology Riyadh-Saudi Arabia 1 King Faisal Hospital & Research Center Neurosurgery -Saudi Arabia 2 King Faisal Hospital & Research Center Ophthalmology -Saudi Arabia 3

PURPOSE/BACKGROUND: Pilocytic astrocytomas(PMA) is now a well established clinical & histologic entity, different than Pilocytic astrocytomas(PA). The MR imaging features in the literature have been essentially non-specific.

Based on our observations, the purpose of the study was to identify specific enhancement pattern in PMAs.

MATERIAL & METHODS: Retrospective MRI review of all the available pathology proven cases of PMAs. The target of the review was an imaging feature ,which we named as "Papillary Glandular Sign"- enhancing gland-like lobule on post contrast T1 imaging with its wall studded with small papillary or bead-like projections. One index case was chosen as a proto-type for comparison.

RESULTS: Out of 18 total cases of PMAs from the data-base, 16 were supra-sellar, 1 optic nerve & 1 in the thalamus. Six supra-sellar cases met the criteria for the target sign. The mean age & tumor size of these cases were 24 months & 7cm, respectively.

CONCLUSION: "Papillary Glandular Sign" can be helpful in the pre-operative diagnosis of PMAs.

EP198-Congenital Adrenal Hyperplasia and Brain Magnetic Resonance Imaging Abnormalities

*Saida Jerbi Omezzine*¹, Radhouane Hamdi², Samia Younes³, Maher Dhifallah², Hassine Hamza²

University Hospital Radiology Mahdia-Tunisia 1 University Hospital Radiology -Tunisia 2 University Hospital Internal Medicine -Tunisia 3

OBJECTIVE: To describe brain magnetic resonance imaging (MRI) abnormalities in a patient with congenital adrenal hyperplasia (CAH).

RESULTS: A 15 year-old- male with CAH was referred to our department with one year history of gradual worsening of tremor. He was diagnosed with salt-wasting 21-hydroxylase deficiency CAH at 40 days old and



POSTER PRESENTATIONS ABSTRACTS

was started on hydrocortisone, fludrocortisone and salt. He was detected to have hypertension at 8 years of age. Detailed investigations failed to detect any cause for secondary hypertension. Physical findings on the current hospitalization objectified obesity, blood pressure 150/80 mmHg, postural and action tremor, a static and kinetic cerebellar syndrome predominant at left, reflex tetra pyramidal syndrome and mental decline. Brain MRI showed bilateral periventricular white matter hyperintensity, more pronounced in the posterior regions and associated with cortico-subcortical atrophy and complete agenesis of the corpus callosum. All investigations for leukoencephalopathy were negatives. Thus, diagnosis of brain MRI abnormalities related to CAH was made and the patient received symptomatic treatment of tremor.

CONCLUSION: Our case reported provides evidence of an increased frequency of brain MRI in CAH. The literature suggests hormonal imbalance and exposure to excess exogenous glucocorticoids as main probable mechanisms. Thus, in clinical practice, CAH should be considered as one of the possible causes of brain MRI abnormalities.

EP199-Dynamic Susceptibility Weighted Contrast Enhanced Perfusion MRI Analysis of Pediatric Intracranial Tumors in the Posterior Foss

*Augusto Elias Mamere¹, Leonir Terezinha Feltrin¹, Renata Mendes Lacerda Fava¹
Barretos Cancer Hospital Radiology Barretos-Brazil¹*

PURPOSE: To assess if relative tumor blood volume (rTBV) measurement, in Dynamic Susceptibility-weighted Contrast-enhanced (DSC) Perfusion Magnetic Resonance Imaging (MRI), would help to predict the grade of pediatric intracranial tumors in the posterior fossa.

METHODS: 19 patients (15 male and 4 female; mean age: 8.9 yo; range: 2 - 17 yo) were included.

The MR images of 9 medulloblastomas, 8 pilocytic astrocytomas, 1 ependymoma and 1 anaplastic ependymoma were retrospectively evaluated. rTBV values were calculated using the colored negative integral DSC Perfusion map. The subjects were separated in two groups: high grade tumor (medulloblastoma and anaplastic ependymoma) and low grade tumor (pilocytic astrocytoma and ependymoma). Apparent diffusion coefficient (ADC) values of the tumors were also analyzed. P value < .05 was considered statistically significant.

RESULTS: Seven tumors (70.0%) in the high grade group showed hypervascularization (rTBV higher than 1.75) and only 2 (22.2%) in the low grade group were hypervascularized. rTBV mean value in the high grade tumor group was 3.24 (SD: 2.84) and in the low grade group was 1.45 (SD: 1.08), with a statistically significant difference (p=.038). Medulloblastomas showed lower ADC mean value (73.3×10^{-5} mm²/s; SD: 17.3) than the other tumors (156.5×10^{-5} mm²/s; SD: 38.9). This difference was also statistically significant (p<.001).

CONCLUSION: Our results provide evidence that DSC Perfusion MRI, using rTBV measurement, may potentially predict the grade of pediatric intracranial tumors in the posterior fossa.

EP200-A Unique Combination of Dyke Davidoff Masson Syndrome and Down Syndrome Diffusion Tensor Tractography Findings

Kerim Aslan¹, Tumay Bekci², Hediye Pinar Gunbey², Lutfi Incesu², Meltem Ceyhan Bilgici¹

Ondokuz Mayıs University Faculty of Medicine Assistance Professor of Radiology SAMSUN-Turkey¹ Ondokuz Mayıs University Faculty of Medicine Radiology -Turkey²

Dyke-Davidoff-Masson syndrome (DDMS) is a rare disease characterized by cerebral hemiatrophy accompanied by ipsilateral compensatory sinus and skull changes. Diffusion tensor tractography (DTT) is a new imaging tool used to evaluate the fibers and other affected sites in the brain. We report a unique combination of DDMS, Down Syndrome, and DTT findings of DDMS in a 15-year-old male patient who having complex partial seizures for nine years. On FLAIR MRI sequences, in the right



POSTER PRESENTATIONS ABSTRACTS

side, cerebral hemiatrophy, periventricular leukomalacia, enlargement in right lateral ventricle and increase in calvarial bone thickness, and a significant expansion in sphenoid sinuses were observed.

The findings were consistent with DDMS. On DTT, in the right side, a reduction in the density of the projection, association fibers, and corticospinal tracts were observed (Fig. 1). In T2-weighted images, white matter areas adjacent to the right lateral ventricular temporal horn were found to be normal. However, DTT was shown that the density and number of inferior longitudinal fasciculus and uncinate fasciculus were less in these areas (Fig. 2). Thus, we were able to show the real resection limits better through DTT when compared with conventional sequences. DTT could be used in virtual surgical planning and incorporated into the routine procedures of the patients with DDMS. DTT can be included among the routine procedures performed in the diagnosis and management of Dyke-Davidoff-Masson Syndrome.

Figure 1

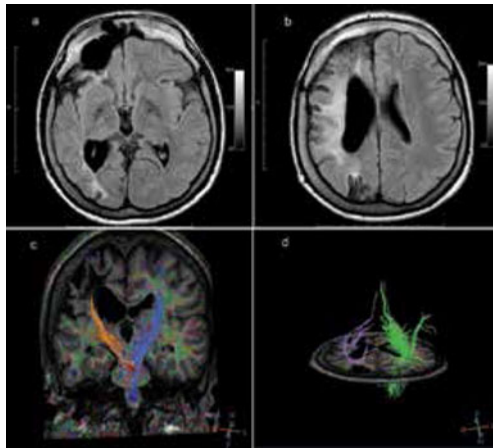
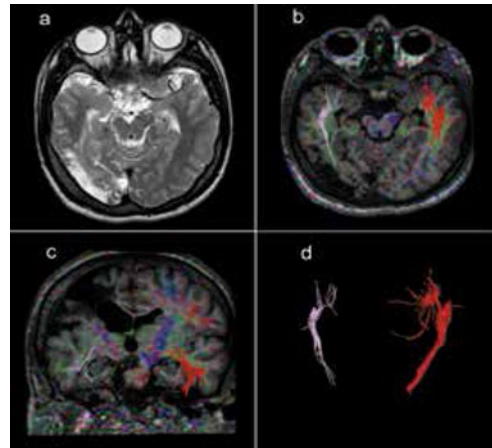


Figure 2

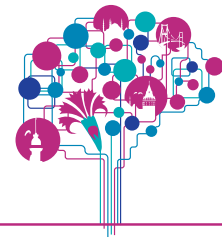


EP201-A Missed Diagnosis Acute Encephalopathy with Biphasic Seizures and Late Reduced Diffusion

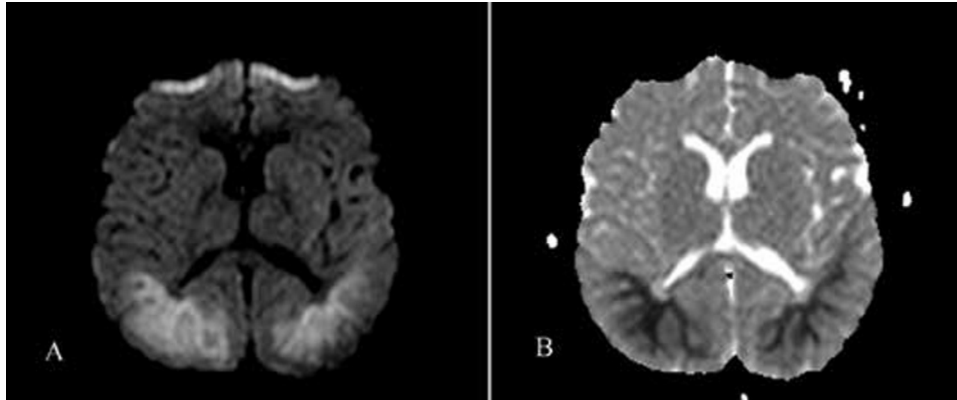
Tümay Bekci ¹, *Kerim Aslan* ¹, Cenk Şecaattin Onaral ², Engin Yosma ³

Ondokuz Mayıs University Faculty of Medicine Department of Radiology Samsun-Turkey ¹ *Ankara Numune Education and Research Hospital Department of Ophthalmology -Turkey* ² *Ondokuz Mayıs University Faculty of Medicine Department of Plastic and Reconstructive surgery -Turkey* ³

Acute encephalopathy with biphasic seizures and late reduced diffusion (AESD) is a very rare encephalopathy subtype which is characterized by biphasic seizures and disturbance of consciousness in the acute stage followed in the subacute stage by restricted diffusion in the subcortical white matter and finally resulting in cerebral atrophy on magnetic resonance imaging. Although exact pathogenesis of AESD is uncertain, the etiology of AESD has been attributed to viral and bacterial infection. Neurological outcome is poor in AESD with reported neurological sequelae such as mental retardation, hemiparesis, spastic quadriplegia and epilepsy. This highlights the importance of early diagnosis and timely treatment. Here we report a case of AESD in a 15-year-old mentally and motor retarded patient, diagnosed based on clinicoradiological correlation. To our knowledge, many patients with AESD are misdiagnosed. Therefore, all physicians should be familiar with this syndrome, its clinical and imaging spectrum and its associated neurological morbidity.



POSTER PRESENTATIONS ABSTRACTS



Pediatric NR 2

EP202-Paraneoplastic Disease. Tumor Ovaries Manifesting As Encephalomyelitis

*Jurkiewicz Elzbieta*¹, Nowak Katarzyna¹, Malczyk Katarzyna¹, Kotulska Katarzyna², Borkowska Julita²

*The Children Department od Diagnostic Imaging Warsaw-Poland*¹ *The Children Department of Neurology Poland*²

PURPOSE: To present the brain and spinal cord MR examinations performed in girls with acute severe neurological presentation of paraneoplastic syndrome associated with ovarian teratomas.

Paraneoplastic disease (PD) is a rare disorder caused by remote effects of malignancy. PD have an immunological basis and specific antibodies were identified. It can be seen as encephalomyelitis, limbic encephalitis, progressive multifocal leukoencephalopathy, cerebellar ataxia, brainstem encephalitis, paraneoplastic cerebellar degeneration. These symptoms are potentially reversible. **METHODS:** We present three girls, aged 13, 17, and 18 years. They all were referred to hospital because of an acute onset severe disseminated encephalomyelitis.

All MR exams were performed on 1.5T scanner with routine brain and spinal cord protocol, including SWI, DWI and DTI sequences. In all cases contrast agent was injected in the standard dose. **RESULTS:** Neurological examination performed at the onset of the disease revealed hemiparesis, seizures, and consciousness disturbances. In one girl visual field loss was also disclosed. They all were healthy before the onset of the disease.

Brain and spinal cord MR imaging revealed multiple hyperintense lesions localised supratentorially in the white matter of the both of hemispheres, in the pons and in the spinal cord. Patients were treated with methylprednisolon IV and IVIG. They all improved, but significant sequelae were present. In two of them, two weeks after the onset of encephalomyelitis, symptoms of acute polyradiculoneuritis appeared. Brain MRI showed progression of the lesions. In 2 patients, anti-Yo antibodies were present in the blood. Extensive examinations revealed bilateral ovarian teratomas in all patients. Surgical resection of teratomas resulted in rapid clinical improvement.

CONCLUSIONS: It is extremely important to remember that paraneoplastic disease can be the first manifestation of malignancy and should be considered in the differential diagnosis of encephalomyelitis. In children and adolescent the ovarian tumor is one of the most commonly associated neoplasm, followed by Hodgkin lymphoma and testicular cancer.



POSTER PRESENTATIONS ABSTRACTS

EP203-Pineal Region Germinal Neoplasia with Adenocarcinoma Transformation

*Roberto Marileo*¹, Ingeborg Lopez¹, Rodrigo Riveros¹, Cecilia Okuma¹, Aaron Vidal¹, Rodrigo Rivera¹, J. Gabriel Sordo¹, Claudia Tissera², Lautaro Badilla¹

Instituto de neurocirugía Dr. Alfonso Asenjo Neuroradiology Santiago-Chile ¹ *Instituto de neurocirugía Dr. Alfonso Asenjo Pathology -Chile* ²

We report a ten years old boy with a pineal region tumor, who presented one month tremors, general weakness, feeding troubles with 16 kg weight loss, blurred vision and intermittent headache. Clinical examination described right hemiparesis, upward gaze paralysis, and papilledema. CT and MRI showed a heterogeneous pineal region mass, with multilocular haemorrhagic cyst and chalky calcifications, that involved the mesencephalon and expanded to the left ventricle. Surgery tumor removal was performed. The pathology report a mixed germinal neoplasia: mature teratoma (75%), immature teratoma (5%) and germinoma (20%), with malignant transformation: adenocarcinoma in situ with suspicious focus of stromal infiltration.

EP204-MRI Findings in Children with Open Spinal Dysraphism Don't Forget to Look at the Brain

*Dora Zlatareva*¹, Assen Tzekov², Arash Rastgou¹

Medical University, Sofia Department of Diagnostic Imaging Sofia-Bulgaria ¹ *Tokuda Hospital Department of Neurosurgery -Bulgaria* ²

PURPOSE: Open spinal dysraphisms (OSD) are anomalies of primary neurulation. Due to defect closure of primary neural tube, defect in the overlying skin, neural tissue exposed to environment. Myelomeningoceles accounts for more than 98% of open spinal dysraphisms. OSD are diagnosed clinically and imaging is not always performed. We present three cases with myelomeningoceles and discuss spine and brain imaging findings in these children

METHODS: Three children aged 3 weeks, 5 months and 7 years were examined. All have clinically diagnosed OSD. Spine and brain MRI were performed on 1.5T MR unit during sedation. Spine imaging protocol consist of sagittal T1W, T2W, axial T1W, T2W. Brain imaging protocol with sagittal T1W, axial T1W, T2W, coronal 3D SPGR, coronal FLAIR was performed.

RESULTS: In two there was a large thoracolumbar mass, and in one – lumbosacral mass. All patients have typical findings for myelomeningocele. Caudal regression syndrome and syrinx was detected in two children. Brain MRI reveals small posterior cranial fossa and hydrocephalus in all children and typical findings for Chiari II malformation in two. One child hasn't got typical vermian downward herniation but only mild cervicomedullary kink and towering cerebellum. In this child we detect supratentorial findings as tectal beaking, enlarged massa intermedia, partial agenesis of corpus callosum, periventricular heterotopia. All children were surgically corrected.

CONCLUSIONS: Although OSD can be diagnosed clinically MRI of the spine and brain can assist in diagnosis. The subtentorial and supratentorial imaging findings can be typical or subtle. Knowledge and systematic approach in reporting can reveal brain pathology.

EP205-Ruptured Intracranial Mycotic Aneurysm in Young Children a Case Report

Mohd Rizal Abu Bakar¹, Rohsila Mohamad¹, *Rohaizan Yunus*²

USM Radiology -Malaysia ¹ *IMU Radiology Seremban-Malaysia* ²

Intracranial arterial aneurysm in children is rare condition accounting for approximately 1-2% of all cases. We are presenting a case of 4 years old young girl who developed severe headache, seizure and left hemiparesis after history of insignificant trauma. Clinically, she has a small wound lesion in the plantar part of the left big toe. She was febrile during admission. Computed tomography revealed right high parietal intraparenchymal hemorrhage.



POSTER PRESENTATIONS ABSTRACTS

Computed tomography angiography (CTA) shows a small aneurysm arises from a branch of right pericallosal artery. She was treated with intravenous antibiotics and her neurological symptoms improved significantly within 2 weeks of duration. Conventional cerebral angiography performed after antibiotic completion shows regression of the aneurysm. We highlight the imaging findings and the role of CTA in diagnosis and further management of this condition.

EP206-Pediatric Cerebral Arteriovenous Malformations (AVMs)

*Angel Sanchez-Montanez*¹, Alvaro Cortes², Ignacio Delgado¹, Fuat Arıkan³, Elida Vazquez¹
University Hospital Vall d Pediatric Neuroradiology Barcelona-Spain *1 University Hospital Vall d Radiology -Spain* *2 University Hospital Vall d Neurosurgery -Spain* *3*

PURPOSE: Arteriovenous malformations (AVMs) are an uncommon pathology, representing a 0.1% in pediatrics patients.

We review the pediatrics AVMs from Vall d`Hebron hospital (HUVH)

METHODS: We performed a retrospective study of all pediatric patients diagnosed and treated for intracranial AVMs during a period of six years.

We analyzed the clinical and neuroradiological information (CT-angiography, MRI-angiography and arteriography (DSA).

RESULTS: We diagnosed 11 patients (9 males and 2 females). The mean age at diagnosis was 11 years (range 5-17 years). The most common clinical presentation was loss of consciousness, followed by seizures and headache. The main locations were fronto-parietal and thalamic, observed in a single patient involvement infratentorial, cerebellar.

According to the classification of Spetzler 54.5% of patients were classified as grade 3. 36.4% met criteria for grade 2 and only one patient (9.1%) corresponded to grade 1. There were no grade 4 or MAV's 5.

The venous drainage of the AVM was superficial in 45'46%, and only one patient had mixed drainage. The size varied from millimeters to 5 cm. 6 patients had involvement of eloquent areas.

Diagnosis was made by arteriography in almost all, except in one patient whose diagnosis was histological. The treatment was surgical in 9 cases (81.8%). One patient was treated by radiosurgery and one was not treated for spontaneous resolution.

CONCLUSIONS: Pediatric AVMs differ from those described in the adult population as a angioarchitecture, clinical presentation, hemodynamic and prognosis. Its diagnostic approach usually starts with CT, followed by advanced MRI allowing greater detail of vascular anatomy and functionality in complex lesions. However, angiography remains the gold standard for the accurate diagnosis and treatment.

EP207-Morphologic Change of the Pituitary Gland on MR in Children with Idiopathic Central Precocious Puberty

*Hee Mang Yoon*¹, Jae-Yeon Hwang², Hye-Kyung Yoon¹, Sae Rom Chung¹, Young Ah Cho¹, Jin Seong Lee¹, Ah Young Jung¹, Chong Hyun Yoon¹
Asan Medical Center Radiology SEOUL -Republic of Korea *1 Pusan National University Children's Hospital Radiology -Republic of Korea* *2*

PURPOSE: The purpose of this study was to evaluate size and shape of the pituitary gland on brain MRI in patients with idiopathic central precocious puberty (ICPP).

METHOD AND MATERIALS: One hundred eleven ICPP patients (11 boys and 100 girls, mean age; 6.3 ± 1.1 years, range; 2–8 years old) who underwent brain MRI for screening of brain abnormality were enrolled. Control group consisted of normal age- and sex-matched 111 children.



POSTER PRESENTATIONS ABSTRACTS

Height, anteroposterior (AP) dimension, right-left dimension, cross-sectional area in mid-sagittal plane, and calculated volume of the pituitary gland were analyzed. Pituitary shape was assessed by using height-to-AP ratio and configuration of the upper border of the gland which was subjectively graded in five categories (marked concavity = 1, mild concavity = 2, flat = 3, mild convexity = 4, and marked convexity = 5). Correlation analysis was performed to evaluate relationship between the pituitary dimensions and the shape of the pituitary gland. Logistic regression analysis was performed to determine significant variables for classifying subjects into the patient and control groups. Statistical significance was considered for P values less than 0.05.

RESULTS: Mean height and area were significantly greater in the patient group ($P = 0.02$ and <0.01 , respectively) whereas other parameters were not. Height-to-AP ratio and pituitary grade were significantly higher in the patient group ($P < 0.01$). Forty three (38.7%) patients showed convex upper border of the pituitary gland in the patient group while 17 (15.3%) patients revealed convex upper border in the control group. Pituitary grade was correlated with height and height-to-AP ratio (correlation coefficients = 0.6 and 0.5, respectively; $P < 0.01$). Area and convex upper border were significant predictors for classifying the patients into ICPP with a 68.0% correct classification rate (Odd ratio = 1.1 and 3.4, respectively, $P < 0.01$).

CONCLUSION: ICPP is associated with significant changes in the size and shape of the pituitary gland; height and area in mid-sagittal plane are increased and the pituitary gland is more spherical in mid-sagittal plane.

EP208-Posterior Fossa Tumors in Childhood Radiologic Findings and Pathologic Correlation

Faten Bouzayen¹, Nadia Mama¹, Mehdi Gaha¹, Aymen Ben Tebra², Hedi Krifa², Med Tahar Yacoubi³,
*Kalthoum Tlili*¹

*Sahloul Hospital Radiology Department - Tunisia*¹ *Sahloul Hospital Neurosurgery Department - Tunisia*² *Farhat Hached Hospital Pathology Department - Tunisia*³

PURPOSE: To assess the correlation between MRI findings especially diffusion weighted imaging (DWI) and proton magnetic resonance spectroscopy and histopathology in posterior fossa tumors of pediatric population.
MATERIALS AND METHODS: Retrospective study of 56 children with posterior fossa tumors collected over a period from 2001 to 2012 (13 medulloblastomas, 20 pilocytic astrocytomas, 11 ependymomas, 5 gangliogliomas, 3 infiltrating gliomas, and 4 other rare tumors), cases were investigated with conventional MRI for all patients, DWI for 30 patients, and spectroscopy using a single-voxel technique for 11 patients.

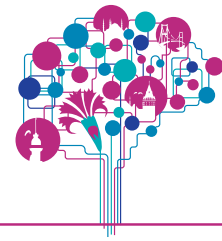
All histological slides were retrospectively studied.

RESULTS: Ependymomas were commonly intraventricular with extension through the foramen of Luschka and/or Magendi in all cases, calcifications were observed in 3 cases, all tumors had a heterogeneous enhancement.

The vermis is the most common location for medulloblastomas; the tumor was exclusively intraventricular in 2 cases.

Pilocytic astrocytomas were frequently localized in the cerebellar hemisphere; solid mural nodule was commonly observed. In 5 cases, it was a heterogeneous soft-tissue mass. Tumor cellularity and tumor grade were correlated to ADC values. Low values were found in all medulloblastomas even in unusual locations and in anaplastic ependymomas too. ADC values were the highest in pilocytic astrocytomas. Taurine, and Choline peaks were biomarkers of medulloblastomas. Elevated levels of myoinositol and glutamine/glutamate were observed in ependymomas. High choline and lactate peak were observed in pilocytic astrocytomas.

CONCLUSION: MRI is the imaging modality of choice in evaluating lesions arising in the posterior fossa. Analysis of the signal characteristics on multiple different imaging sequences may provide information about tissue components and the tumor grade. Advanced techniques are helpful to make correct preoperative diagnosis even in unusual location or morphological pattern.



POSTER PRESENTATIONS ABSTRACTS

EP209-Imaging of Neuronal Tumors of the Central Nervous System

Radiologic Pathologic Correlations

Mouna Laadhari ¹, Nadia Mama ¹, Amel Ben Abdallah ¹, Khaled Kadri ¹, Nadia Arifa ¹, Iadh Ksira ², Med Taher Yacoubi ³, *Kalthoum Tlili* ¹

Sahloul University Hospital Radiology Department -Tunisia ¹ *Sahloul University Hospital Neurosurgery Department -Tunisia* ² *Farhat Hached University Hospital Pathology Department -Tunisia* ³

PURPOSE: Illustrate imaging findings of different neuronal tumors of the central nervous system and correlate to histopathologic patterns.

METHODS: Retrospective study of 11 cases pure neuronal and mixed neuronal-glial tumors which were surgically treated since 2000 at Sahloul hospital. All patients had CT scan. MRI was performed in 10 patients with T1 SE, T2 SE, and, FLAIR, gradient echo T2 * sequences. Diffusion weighted imaging was performed in 5 cases and spectroscopic study in 3 cases.

RESULTS: The average age was 21.6 years. ¾ of patients were older than 20 years. The sex ratio was 1.7. Tumor was supratentorial in 8 cases and located in the posterior fossa in 3 cases. The most common initial symptoms were seizures (5 patients), which had sometimes persisted over long periods of time and, increased intracranial pressure (4 patients). The lesions had variable aspects. The tumors were atypical or by the location or by the imaging pattern in almost all cases. On imaging, the tumor presented a double component in 7 cases, calcification (n = 3), hemorrhage (n = 3), peri-lesional edema (n = 3), mass effect (n = 3) and hydrocephalus (n = 9). Histopathology made the diagnosis in all cases: ganglioglioma (2 cases), desmoplastic infantile ganglioglioma (1 case), dysembryoplastic neuroepithelial tumor (1 case), Lhermitte-Duclos disease (1 case), central neurocytoma (1 case), liponeurocytoma (1 case), glioneuronal malignant tumor (3 cases), glioneuronal papillary tumor (1 case).

CONCLUSIONS: Pure neuronal (NT) and neuroglial (NGT) tumors are rare, they represent about 1% of all brain tumors. Neuro-glial tumors are more common than neural tumors. The most common neuro-glial tumors are gangliogliomas (71%) and dysembryoplastic neuroepithelial tumors (DNET) (20%). The most common neuronal tumor is central neurocytoma (15%). They are distinguished from pure glial tumors by less aggressiveness and better prognosis. Their radiological aspects particularly MRI (cortical and subcortical frequent location, double cystic and solid components, variable enhancement, calcifications, mass effect and mild peri-lesional edema) may suggest the diagnosis. It is important to understand the radiologic findings as well as the pathologic background and classification of neuronal tumors because they are generally benign and their prognosis is generally favorable if appropriate treatment, such as resection, is not delayed.

EP210-Diencephalic–Mesencephalic Junction Dysplasia on Fetal MRI

Mariasavina Severino ¹, Domenico Tortora ², Mariya Malova ³, Rodica Mardari ⁴, Alessandro Parodi ⁵, Dario Paladini ⁶, Luca Ramenghi ⁵, Andrea Rossi ⁷

Istituto Giannina Gaslini Neuroradiology Genoa-Italy ¹ *University of Chieti Radiology -Italy* ² *University of Genoa Pediatric -Italy* ³ *University of Padua Neuroradiology -Italy* ⁴ *Istituto Giannina Gaslini Neonatology -Italy* ⁵ *Istituto Giannina Gaslini Obstetrics and Gynecology -Italy* ⁶ *Istituto Giannina Gaslini Neuroradiology -Italy* ⁷

PURPOSE: Diencephalic–mesencephalic junction (DMJ) dysplasia is a novel autosomal recessive malformation characterized by a poorly defined junction between diencephalon and mesencephalon with characteristic butterfly-like contour of the midbrain on axial sections, variable degrees of supratentorial ventricular dilatation and hypoplasia to complete agenesis of the corpus callosum. Ventriculomegaly (VM) and callosal abnormalities (CA) are the most common brain anomaly in prenatal diagnosis observed with ultrasound (US) and they are usually referred for fetal MRI. We aimed to determine the role of fetal MRI in identifying the midbrain “butterfly sign”, and to describe the fetal and postnatal imaging features of DMJ dysplasia.



POSTER PRESENTATIONS ABSTRACTS

METHODS: We reviewed 250 fetal MRI exams (mean gestational age: 24 weeks) performed between January 2005 and March 2014 for VM and/or CA detected on US at 19 gestational weeks. We evaluated the morphology of diencephalic–mesencephalic junction on single-shot fast spin-echo T2-weighted imaging on three planes, particularly focusing on the following features: the butterfly sign on axial images, poorly defined DMJ on sagittal images, and merger between midbrain and thalami on coronal images. Additional postnatal MRI were evaluated when available.

RESULTS: Two fetuses with DMJ abnormalities were identified out of 250 fetal MRI. Patient 1 underwent MRI at 20 and 30 gestational weeks whereas patient 2 at 21 and 23 gestational weeks. The butterfly sign was clearly visible on axial images as well as poorly DMJ on sagittal images in all fetal MRI studies. Additional findings in both patients were partial agenesis of corpus callosum and progressive supratentorial ventricular dilatation. Postnatal MRI was available for review only in patient 1 and confirmed the prenatal findings. In this patient diffusion tensor imaging (DTI) showed interruption of corticospinal tracts at the level of internal capsule.

CONCLUSION: The butterfly sign can be clearly detected on axial images on fetal MRI thus allowing prenatal diagnosis of DMJ dysplasia. Postnatal MRI with DTI confirms the diagnosis and reveals corticospinal tracts abnormalities underlying the butterfly sign.

EP211-Bandlike Calcification with Simplified Gyration and Polymicrogyria – A Rare Disease with Typical Imaging Findings

*Tiago Rodrigues*¹, *Catarina Magalhães*², *Gabriela Soares*³, *Inês Carilho*², *Luís Botelho*¹, *Pedro Pinto*¹

*Centro Hospitalar do Porto Neuroradiology Porto-Portugal*¹ *Centro Hospitalar do Porto Neuropediatrics - Portugal*² *Centro Hospitalar do Porto Centro de Genética Médica Jacinto Magalhães -Portugal*³

PURPOSE: We aim to draw attention to the imaging findings of “band-like calcification with simplified gyration and polymicrogyria”, a rare autosomal-recessive neurological disease with highly characteristic neuroradiological features.

METHODS: Retrospective review of the patient’s clinical records and imaging studies. **RESULTS:** Female patient, daughter of unrelated parents and with no family history of note. She was born at term by spontaneous vaginal delivery after an uneventful pregnancy. Clinically the patient had microcephaly and dysmorphic facies noted at birth, onset of epilepsy at 3 months of age with bilateral focal motor seizures, a severe psychomotor development delay and a spastic tetraparesis. The

magnetic resonance imaging (MRI) of the brain, performed at the age of 5 years-old, revealed a continuous ribbon of symmetrical cortical calcification in the frontoparietal regions, symmetrical thalamic calcification and focal calcification on the pons; extensive bilateral cortical malformation with a simplified gyral pattern in some areas and polymicrogyria in others; and a reduced white matter volume and abnormal myelination. Intra-uterine infection by toxoplasmosis, rubella and

cytomegalovirus were excluded through serologic tests. The genetic analysis showed bi-allelic deletion in the OCLN gene, establishing the diagnosis of band-like calcification with simplified gyration and polymicrogyria. **CONCLUSION:** Band-like calcification with simplified gyration and polymicrogyria is a rare neurological disease with typical neuroradiological features, namely extensive bilateral cortical malformation with simplified gyration and polymicrogyria, cortical ribbon-like calcification and symmetrical thalamic calcification. Knowledge of these typical imaging findings is essential since it helps in the exclusion of others conditions that also present with intracranial calcifications and allows guiding the genetic testing.



POSTER PRESENTATIONS ABSTRACTS

EP212-Gobbi 's Syndrome

Ariana Jacinto ¹, Pablo Picasso ¹, Carlos Macedo ¹, Alvaro Menezes ¹
Hospital Geral De Fortaleza Centro De Imagem -Brazil ¹

Gobbi 's Syndrome was first described by Giuseppe Gobbi, Uruguay, in 1991, as an association between epilepsy, parietal calcifications and celiac disease. Initially, it was thought this is part of the atypical Sturge-Weber Syndrome. Recently, it was seen that these are two distinct syndromes. The syndrome occurs mainly in people of Italian origin and the seizures originate in the occipital lobes. Its etiology remains uncertain. Among the causes proposals would:

- to chronic deficiency of folic acid ;
- Relationship with the HLA histocompatibility complex;
- DQ2 gene is related to predisposition for celiac disease;
- Autoimmune theory, where calcifications would be consequent to an inflammatory endothelial changes, determined by the formation of immune complexes.

The presence of anti - gliadin antibody in CSF in conjunction with HLA class II genes could generate an immune reaction in people with gluten intolerance. The diagnosis is through the presence of bilateral occipital calcifications on tomography computerized (CT), epilepsy and bilateral occipital calcifications. Typical imaging features on CT are the absence of brain atrophy, absence of contrast enhancement, occipital subcortical calcifications bilateral, symmetrical or not, with varying sizes. Punctate calcifications may be associated with frequent seizures are difficult to control. According to most authors, the presence of calcifications would be related to low efficacy of anticonvulsants and diet low in gluten reduces seizure frequency and improves the cognitive deficit. Therefore the importance of early diagnosis and treatment. The treatment requires an early start of a gluten free diet and anticonvulsants.

EP213-Pediatric Small Bowel Transplant Brain Imaging Findings

Matthew Folorunso Omojola ¹, Diana Florescu ², Steven Johnson ¹, Fang Qiu ³, Matthew L White ¹

UNMC Radiology Omaha-United States ¹ *UNMC Internal Medicine -United States* ² *UNMC Biostatistics United States* ³

PURPOSE: The purpose of our study was to review brain imaging findings in pediatric small bowel and combined liver/small bowel transplant recipients at our Center for patterns of findings. **MATERIALS and METHODS:** We retrospectively reviewed the brain imaging and pertinent clinical records of 97 pediatric patients (< 18 years of age) who underwent isolated small bowel transplant (SBT) or liver-small bowel-pancreas (LSBT) transplantation at our institution over a 5 year period. The study was approved by our Institutional Review Board. Data collected included patient demographics, type of organs transplanted, date of transplantation, brain imaging modalities and findings and time of death. The patients were divided into two groups; imaging group and non-imaging group. The brain images including CT and MRI post- transplant were then individually reviewed for confirmation of the abnormalities.

RESULTS: Of the 38 (39.2%) patients who had brain imaging, 44.7% were males and 56.3% were females. Indications for imaging included seizures 13.4%, mental status changes 11.7%, PTLD 11.7%, fever 7.8%, hemorrhage 4.4%, headache 3.9% and stroke 3.9%. Patients were more likely to be investigated with CT without contrast 47.6% compared to CT without and with contrast 17%. On the other hand when MRI was the method of investigation, MRI was more likely to be contrast enhanced, 23.6% compared to MRI without contrast 11.8%. In the imaging group, 26.3% had one brain imaging and 73.7% had more than one brain imaging. 47.4% had CT scan of the head alone. 10.5% had MRI of the head alone. 42.1% had both CT and MRI. 31.6% of the imaging group had no abnormal findings.



POSTER PRESENTATIONS ABSTRACTS

Clinical findings include volume loss in 37.8%, brain infarcts 27.8%, white matter changes 15.25%. PRES 10.5% with 2 episodes of recurrent PRES. Complications of PRES recorded included hydrocephalus, IVH, infarcts and cortical laminar necrosis.

CONCLUSIONS: 39.2% of our pediatric small bowel transplant population was investigated for neurological disorders. Pediatric small bowel transplant patients were more likely to be investigated by non-contrast CT rather than MRI. Reasons for imaging included seizures, mental status changes, stroke, PTLD and fever. The commonest abnormalities were brain volume loss, ischemic infarcts, PRES and hemorrhages.

EP214-Carotid Blowout Syndrome Endovascular Management by Stenting & Embolization

*Jaime Tisnado*¹

*VCU Health System Interventional Radiology Henrico-United States*¹

Carotid blow out syndrome (CBOS): catastrophic emergency associated with high M&M, caused by head & neck malignant tumor invasion, post operative, inflammatory & trauma. Conventional surgical management, include carotid artery, branch ligation, carotid artery bypass, fraught with high M&M. With the advent of covered & uncovered, balloon-expandable or self-expandable metallic stents, emergent management of CBOS has improved & currently a permanent or temporary success is expected. We have studied 12 patients with CBOS of different etiologies. Insertion of different types of stents, covered/uncovered, self-expanding/balloon-expandable, were successful, using Gore Viabahn® Endoprosthesis, iCast™ (Atrium), Fluency® Plus Stent-Graft (Bard), Wallstent & Wallgraft (Boston Scientific), Protégé (Bard). All procedures done in the IR suite successfully. No major stenting or embolization complications found. Patients had long or temporary survival. Emergent insertion is a safe, effective & easy procedure to permanently or temporarily manage CBOS. Longer follow-up & more treated patients are necessary to determine long-term role of stenting in CBOS. Placement of stents, with or without adjuvant embolization, must be considered the first choice in desperate situations.

EP260-Susceptibility Weighted MR Sequences Technical Insights and Clinical Applications Focusing on Inflammatory and Infectious Diseases of the CNS

*Leandro Tavares Lucato*¹, Livia M. T. Scianni Moraes¹, Jeanette Janaina Jaber Lucato²,

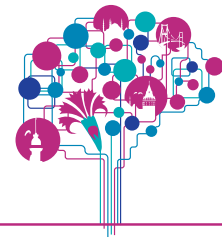
*Germana Titoneli Vieira*¹, *Claudia Costa Leite*¹

*Hospital das Clínicas, Faculdade de Medicina, Universidade de São Paulo Radiology São Paulo-Brazil*¹ *Centro Universitário São Camilo Physical Therapy -Brazil*²

PURPOSE: To cover the major technical concepts related to acquisition of susceptibility-weighted (SW) sequences, with an emphasis in the differences among major vendors; and to describe and illustrate the role of SW sequences in the evaluation of various inflammatory and infectious diseases of the CNS.

MATERIALS AND METHODS: Patients presenting inflammatory or infectious conditions were retrospectively identified in the teaching file database of our institution. CT and MR exams were analyzed, together with medical records; CT images were carefully scrutinized in order to depict calcifications. This database also provided SW images from selected cases in order to demonstrate concepts related to their acquisition, including vendor-related differences

DISCUSSION: A brief background of the physics behind SW techniques will be presented. SW techniques usually employ 3D gradient echo sequences, and especially echo-time related singularities yield slight differences among them, which can potentially impact the way they explore the magnetic susceptibility differences of tissues. SW sequences are a novel and promising neuroimaging tool. They present superb detection capacity of the well-known susceptibility differences present in various tissues (such as blood, iron and calcification); creating a unique contrast, different from that of conventional sequences.



POSTER PRESENTATIONS ABSTRACTS

The technique superiority is based in some features: as it is a 3D sequence, the slice thickness is intrinsically thin; the images are postprocessed using minimal intensity projection (minIP), which enhances hypointense lesions; all choice of parameters are directed to increase the conspicuity of the smaller veins and other sources of susceptibility effects. Besides, the phase images, when available, have potential in differentiating between diamagnetic and paramagnetic susceptibility effects of calcium and blood, respectively. Another aim of this study is to discuss and illustrate the usefulness of this relatively new approach in the evaluation of various inflammatory and infectious diseases of the CNS, including pyogenic abscesses, fungal and other granulomatous infections, and cysticercosis. This unique MR sequence is capable of improving detection of calcification and hemorrhage in this scenario, frequently adding clinically relevant information.

CONCLUSION: SW sequences have taken the detection of calcified and hemorrhagic lesions to a new level. They appear as a valuable tool in differentiating and characterizing diverse inflammatory and infectious conditions.

Adult NR 8

EP215-Time Domain Frequency Decomposition and Filtering of Multiphase Low Dose CT Perfusion Datasets for High Quality Structural Image Reconstruction

Luke Gerke¹

Mount Sinai School of Medicine Radiology New York-United States¹

PURPOSE: Time-resolved CT data are routinely acquired for CT perfusion (CTP) map calculation. As typically presented, these are complementary to structural CT angiography (CTA) which is usually acquired separately as a single higher dose sequence. Efforts to reconstruct multi-phase CTP datasets into images with higher apparent signal to noise (SNR) have had success. Most published algorithms

apply spatial-domain smoothing, which diminishes spatial resolution. A recently published technique applies smoothing only in the time domain, preserving spatial resolution but discarding interesting temporal data. I know of no published technique that uses time-domain Fourier decomposition to segregate contributions from static structures (i.e. noncontrast structures) from dynamic structures (i.e. contrast) from noise. Here, I present a simple technique for performing this process. Reconstruction of images using data from different frequency domains gives images with low noise and high spatial resolution.

METHOD: Ten CTP exams were acquired during the course of clinical work. Each contained a 3D dataset acquired at each of 20 timepoints (by clinical protocol). For each voxel in space, attenuation data were compiled over those 20 timepoints, creating a per-voxel time series. For each time series, zero-padding and Discrete Fourier Transform were performed to decompose the signal into its frequency amplitude and phase components. Frequency thresholds were determined to partition the signal into "low," "medium," and "high" frequency domains. Using one domain at a time, spectral power was measured, yielding a 3D voxel dataset. These were written into the DICOM files as a new sequence and reviewed qualitatively.

RESULTS: Frequency-dependent power maps were created based on time-domain frequency decomposition of low-dose, time-resolved CT acquired for CTP. Each map had higher signal to noise ratio than single source images. Low-frequency power maps were found to correlate well with the expected appearance of non-contrast CT. Mid-frequency power maps had an appearance similar to high-dose subtraction CTA images. High-frequency power maps had little clinical value, primarily reflecting quantum noise.

CONCLUSIONS: I describe a new method for construction of high SNR 3D datasets from time resolved CTP studies. Images created using this technique have direct clinical application for structural evaluation of the vasculature. Frequency-based analysis could reveal information about velocity and direction of flow and is a subject of planned future work.



POSTER PRESENTATIONS ABSTRACTS

EP216-3D Surface Rendered PET CT in Suspected Osteomyelitis Post Cranioplasty and Infected Myocutaneous Flaps Post Craniofacial Reconstructive Surgery

*Shanker Raja*¹, Yasser Orz², Yaser AlJadhai³, Sharad George¹, Sven Larsson³

*Baylor College of Medicine Radiology Bellaire -United States*¹ *KFMC Neurosurgery -Saudi Arabia*² *KFMC Radiology -Saudi Arabia*³

Infections are a common occurrence, following cranial surgery (cranSURG). Uncommonly underlying osteomyelitis (Uosteo) may complicate myocutaneous flaps, craniotomies, and skull base surgeries, leading to persistent/recurrent infected grafts or delayed healing of postsurgical bed. It is essential to determine Uosteo complicating infected grafts, since management significantly differs in complicated vs. uncomplicated grafts. Traditionally Tc-99m bone scan, In-111 labeled WBC/Ga-67 and MRI have been used in evaluating osteomyelitis, however, the traditional modalities are limited in the surgically traumatized bone. PET-CT has been increasingly utilized to evaluate osteomyelitis of the diabetic foot and infected prosthesis. We have explored the use of PET-CT in Uosteo complicating post cranSURG. From Oct 2012 to date we have performed 9 PET-CTs in 7 patients for suspected Uosteo complicating cranSURG with/without grafts. When available, concurrent CT and/or MRI and PET were all coregistered and merged into one single common 3D space, the merged data were surface rendered and fused (gray scale –diag CT/MRI, pseudo-color scale -PET). 4/7 pts were neg for Uosteo by PET and clinical f/u, 2/7 pts had proven Uosteo, while 1 pt. had an infected titanium mesh. Of 2 pts pos for Uosteo, f/u PET-CT showed complete resolution in 1 pt, while the other pt had partial resolution on PET and is on continued treatment.

We will demonstrate in an atlas format the correlative findings on multimodality imaging, emphasizing 3D surface rendered images as a tool for tracking the sinuous sinus tracts in 3D space, as well as pre-procedural guidance for planned surgical interventions.

EP217-MR ADC Histogram Moments Percentiles and Distances in Management of Choroid Plexus Tumors and Correlation with Histopathology and Ki 67

*Shanker Raja*¹, Sharad George¹, Sadeq AlDandan², Abdullah AlRashed³, Sven Larsson³, Ahmed Lary⁴

*Baylor College of Medicine Radiology Bellaire -United States*¹ *KFMC - Riyadh Pathology -Saudi Arabia*² *KFMC - Riyadh Radiology -Saudi Arabia*³ *KFMC - Riyadh Neurosurgery -Saudi Arabia*⁴

PURPOSE: Choroid plexus tumors (CPT) are rare pediatric tumors, histologically classified as papilloma (CPP), atypical (atCP), and Ca (CPCa). We explored if ADC histogram moments, percentiles and distances would be helpful for further management of pts. with CPT.

METHOD AND MATERIALS: Normalized Voxel ADC ratios (tumor/normal tissue) in 11 pts (male=6, female=5; mean age=7 yrs (range=3-516 months), were obtained by co-flagging CPT on coregistered T1W-C+ images and ADC maps (MIMvista workstation, Cleveland, USA). The VOI data were exported to EXCEL for histogram generation, computation of histogram moments (mean, median, SD, kurtosis, skewness), percentiles/ IQR (interquartile range); in addition intra and inter-group histogram distances (Bhattacharyya distance and Chi-square distance) were estimated. Multiple estimates including SD, 95th percentile, and IQR were correlated with Ki-67 index.



POSTER PRESENTATIONS ABSTRACTS

RESULTS: Subtype group means were as follows: SD (0.18, 0.28, 0.36), 95th percentile (1.47, 1.82, 2.40), and IQR (0.18, 0.25, 0.43) in CPCa, CPP and atCP respectively. SD and 95th percentile were good differentiators between CPP and CPCa. Histogram estimates for individual atCP overlapped with those of CPCa and CPP. Subtype group means for the histogram distances were as follows: Bhattacharyya distance (0.73, 0.61, 0.75) and Chi-square distance (1.36, 1.07, 1.38) in CPP, atCP, and CPCa respectively. Histogram distances were not helpful in classifying individual CPT (CPCa vs CPP). Good correlation with Ki-67 and 95th percentile ($r = -0.7$), and SD ($r = -0.66$) were noted.

CONCLUSION: Detailed analysis of ADC histogram metrics, especially histogram moments and percentiles appears promising for the management of CPT. Our findings need to be confirmed in a larger series.

CLINICAL RELEVANCE/APPLICATION: MR-ADC SD and 95th percentile were notable differentiators between CPP and CPCa; while the observed overlap of histogram metrics in individual atCP lesions with those of CPP and CPCa may have management implications.

EP218-Can Multiparametric MRI Reliably Differentiate Choroid Plexus Tumors?

*Abdullah AlRashed*¹, Larrson Sven¹, Sadeq Al-Dandan², Abdulazeez Akintokun³, Amhed Larry⁴, Shanker Raja⁵

*KFMC - Riyadh Radiology Riyadh-Saudi Arabia*¹ *KFMC - Riyadh Pathology -Saudi Arabia*² *KFMC - Riyadh Radio-Therapy -Saudi Arabia*³ *KFMC - Riyadh NeuroSurgery -Saudi Arabia*⁴ *Baylor College of Medicine Radiology -United States*⁵

INTRODUCTION: Though choroid plexus tumors (CPT) are relatively rare, they are histologically classified into 3 subtypes (choroid plexus papilloma (CPP), atypical choroid plexus papilloma (aCPP) choroid plexus carcinoma (CPC)). Whereas CPP are benign and can be curatively resected, CPC warrants a more aggressive approach. It is beneficial to pre-operatively differentiate between the 3 subtypes. Though conventional MR (cMR) sequences (T1WI, T2WI, FLAIR, etc) are unable to reliably differentiate the entities, recently advanced MR (aMR) techniques such as (DWI, PWI MRS) have been found to be helpful in preoperatively differentiating and grading other intracranial malignancies, such as GBM. We explored the role of aMR in differentiating the subtypes of CPT as compared to cMR.

MATERIAL AND METHODS: We retrospectively analyzed a total of 11 CPT (Male=6, female=5; Pediatric age group=9 adults=2) of which CPP=4, aCPP=4 and CPC=3). All patient's MRI were acquired on 3 different scanners with accepted protocols. Considering differences in scanners and the acquisition technical parameters for DWI, we normalized the lesion ADC values by normal contralateral (brain parenchymal) estimates, to obtain ADC/normal ratios. The ADC/normal ratios were statistically analyzed on Excel. The standard deviation for all lesions was computed from non-normalized raw pixel data, and subsequently the pooled variances were separately calculated for CPP, aCPP, CPC respectively. All MRS (no=5) were multivoxel acquisitions (CPP=2, aCPP=2, CPC=1) per accepted protocols.

RESULTS: The mean of ADC/normal ratios and the pooled SD of CPP, aCPP, CPC, were 1.32, 1.39, and 0.9; and 0.55, 0.52 and 0.18 respectively. Multivoxel MRS showed elevated myoinositol in 2/2 CPP, while it was low in each of CPC and aCPPs that were evaluated by MRS. The variance as estimated by SD appears to be a strong differentiator of CPP (higher variance) versus CPC (relatively lower variance).

CONCLUSION: In our small series we found that aMR is able to reliably differentiate CPT. Specifically, unrestricted diffusivity on ADC mapping along with elevated myoinositol on MRS appears to be strong diagnostic signatures for CPP, whereas relatively restricted diffusion on ADC along with lack of myoinositol strongly favors CPC. Our findings need to be confirmed in a larger series.



POSTER PRESENTATIONS ABSTRACTS

EP219-Cases of PML in Natalizumab after 10 Treatments CHU Tlemcen Algeria

*Djaouad Bouchenak Khelladi*¹, Salim Allal²

CHU Tlemcen Algeria Medecine Tlemcen-Algeria¹ CHU Tlemcen Algéria Medecine -Algeria²

PURPOSE: Natalizumab (NTZ) is a monoclonal antibody indicated for the treatment of multiple sclerosis (MS) severe relapsing. It puts them at risk of progressive multifocal leukoencephalopathy (PML). While in the literature, that risk is estimated at 1 in 1000 after 24 months of treatment, we report a case of PML occurring in one of 06 patients treated with natalizumab for a period much less than 24 months.

METHODS: Patient aged 27 followed since 2007 for multiple sclerosis in its relapsing "RR" treated with interferon beta -1a , progressive worsening with continuing relapses as well as EDSS worsening, leading to the RPMS form, has justified the treatment by NTZ. The outcome was favorable until his readmission for total left hemiplegia. Physical examination showed recent pyramidal syndrome and cerebellar syndrome with behavioral troubles. MRI had revealed extensive

T2 hyperintensities and Flair highly suggests PML. Natalizumab was stopped and the patient received 05 plasma exchanges. An initial search of JC virus made after the 4th EP was negative. The short-term outlook was favorable.

RESULTS: PML, a major complication of NTZ is a rare demyelinating disease of the central nervous System subsequent to the infection of oligodendrocytes by the JC virus, which reactivation occurs during severe immunodeficiency.

The effectiveness of NTZ in relapsing forms of MS is currently accepted, however, the profile of patients at risk for developing PML with the waning of NTZ treatment remains hard to determine. The risk factors identified to date are few:

- Prior treatment with immunosuppressive,
- Presence in the blood of anti-JC virus,
- Duration of treatment with NTZ, with an increased risk beyond 24 months of treatment.

CONCLUSIONS: The risk of PML in NTZ can be accurately assessed. This case illustrates that this serious and potentially lethal event occurred to one of our patients who has no potential risk factor for a period much less than that described in the literature. It may justify to review the risk / benefit of treatment and the establishment of a monitoring protocol well codified whose fundamental element is the MRI every two months without waiting for clinical signs.

EP220-Eccentric Target Signs in Cerebral Toxoplasmosis, the Use of 3D

MPRAGE for Lesion Characterization

Zaharuddin Haron¹, *Norzaini Rose Mohd Zain*², Ahmad Sobri Muda¹, Syazarina Syaris

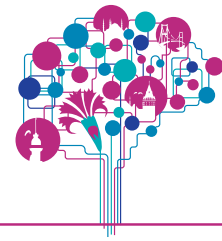
Osman¹, Shahizon Azura Mohamed Mukari¹

UKMMC Department of Radiology -Malaysia¹ Hospital Kuala Lumpur Department of Diagnostic Imaging -Malaysia²

OBJECTIVE: To determine the value of 3D MP-RAGE compared to the 2D sequences in the assessment of cerebral toxoplasmosis and the characteristic of 'eccentric target signs' in cerebral toxoplasmosis.

MATERIAL AND METHODS: All cases of cerebral toxoplasmosis with positive retroviral and IgG for toxoplasmosis, that showed clinical improvement following treatment of anti-toxoplasmosis in UKMMC over 3-year period from 1st Dec 2010 until 1st Dec 2013 were reviewed.

RESULTS: Six patients with a total of 64 lesions were identified. Four patients have both supra and infra-tentorial lesions (66.7%) while one patient each have supra or infra-tentorial lesion only (16.7% respectively). Four patients have more than 3 lesions (66.7%), one patient with 2 lesions and one patient with 1 lesion (16.7% each).



POSTER PRESENTATIONS ABSTRACTS

35.9% of the lesions were located within the frontal lobes. 65.6% of the lesion were identified at the grey white matter junction, 10.9% at the white matter and 23.4% at the deep grey matter. 50.0% of the lesions measured in between 6 to 10 mm with the largest lesion

measuring 31 to 35 mm (1.6%). 81.3% 'eccentric target signs' were demonstrated by 3D MPRAGE post gadolinium as compared to 50% by 2D T1W post gadolinium. 48.4% 'target sign' was seen on T2W/FLAIR sequences. One lesion showed restricted diffusion on DWI (1.6%) while six lesions showed blooming artifacts (hemosiderin) on GRE/SWI (9.4%).

CONCLUSION: 3D MPRAGE is superior to 2D sequences in detecting the 'eccentric target sign'. Cerebral toxoplasmosis are mostly multiple with more than 3 lesions detected mostly involving both the supra and infra-tentorial regions, predominantly at the frontal lobe. The 'target signs' can be demonstrated on T2W sequences with inverse appearance.

EP221-Gemistocystic Astrocytoma with Anaplastic Transformation, the Use of MR Perfusion in Disease Monitoring

Shahizon Azura Mohamed Mukari¹, Zaharuddin Haron², Ahmad Sobri Muda², Syazarina Syaris Osman²,
*Norzaini Rose Mohd Zain*³

*UKMMC Department of Radiology Kuala Lumpur-Malaysia*¹ *UKMMC Department of Radiology -Malaysia*²
*Hospital Kuala Lumpur Department of Diagnostic Imaging -Malaysia*³

Gemistocytic astrocytoma (GA) is a low grade glioma that has variable appearance on conventional MRI, at times mimicking high grade tumour with contrast enhancement. MR Perfusion (MRP) is proven reliable in detecting neovascularisation in a higher grade tumour reflected by high relative cerebral blood volume (rCBV). MRP gives advantages in monitoring cases of a diffuse low grade astrocytoma to look for anaplastic transformation by looking at the rCBV. We reported a case of GA with variable pattern of enhancement in the lesion, one focal area demonstrated intense enhancement post gadolinium that showed increased rCBV on MRP. This area was confirmed to be anaplastic on histology. MRP gives an additional information for proper diagnosis as it will determine management and overall prognosis of the disease.

EP222-Secondary Neuronal Degeneration Caused by Remote Intracranial Lesions MR Imaging Findings

*Ha Hun Song*¹, Young-Joo Kim²

*Cheju Halla Hospital Radiology -Korea, South*¹ *Uijongbu St. Mary's Hospital Radiology Uijongbu-Korea, South*²

PURPOSE: Intracranial lesions often lead to changes in neurons remote from the site of the primary abnormality. The aim of this review is to illustrate and describe the characteristic MR imaging findings in secondary neuronal degeneration to prevent misdiagnosing them as separate primary ischemic, traumatic, or neoplastic process.

METHOD: We retrospectively reviewed various MR imaging features and their implications of secondary neuronal degeneration.

RESULTS: We illustrated Wallerian degeneration, hypertrophic olivary degeneration, crossed cerebellar diaschisis, and mamillary body or fornix atrophy in various intracranial lesions.

CONCLUSION: Knowledge of cranial pathways and imaging findings of secondary neuronal degeneration can prevent misdiagnosing them as separate primary abnormalities.



POSTER PRESENTATIONS ABSTRACTS

EP223-Neurological Manifestations of End Stage Renal Disease MRI

Findings

*Young-Joo Kim*¹, Ha Hun Song²

*Uijongbu St. Mary Radiology Uijongbu-Korea, South*¹ *Cheju Halla Hospital Radiology -Korea, South*²

PURPOSE: End-stage renal disease (ESRD) results in excessive accumulation of urea and toxic metabolites. Hemodialysis is the most frequently administered therapy for ESRD patients. ESRD can have profound and devastating neurologic consequences. The purpose of this study is to discuss acute neurological manifestation in symptomatic patients based on brain MRI findings. **METHODS:** We retrospectively reviewed MR findings of intracranial abnormalities with neurological complications in patients with ESRD.

RESULTS: The MRI findings associated with ESRD are wide-ranging: cerebral infarction, intracerebral hemorrhage, posterior reversible encephalopathy syndrome, osmotic demyelination syndrome, uremic encephalopathy, cerebral infection, and venous sinus thrombosis.

CONCLUSION: Acute cerebrovascular events, which are the most frequent cause of morbidity and mortality in ESRD patients, have various clinical manifestations. In ESRD patients, MRI is a valuable assessment method than aids in the early diagnosis of acute cerebrovascular events.

EP224-Multimodal Imaging in Brain Death Assessment

*Roberto Marileo*¹, Ingeborg Lopez¹, Rodrigo Riveros¹, Cecilia Okuma¹, Rodrigo Rivera¹, Aaron Vidal¹, Juan Sordo¹, Lautaro Badilla¹

*Instituto de neurocirugía Dr. Alfonso Asenjo Neuroradiology Santiago-Chile*¹

By definition, brain death is the complete and irreversible cessation of brain and midbrain functions. Brain death usually is assessed clinically and the criteria may vary in different countries. Nevertheless imaging modalities can be used as ancillary test when clinic criterions cannot be evaluated. We present three cases of areflexic coma patients who were studied with trans cranial Doppler, Computed tomography angiography and Magnetic resonance imaging angiography by brain death suspicion. The imaging assessment can help to establish the early diagnosis of brain death.

EP225-Brain MRI Follow Up After Twenty Years in a Series of Systemic Lupus Erythematosus (SLE) Patients

Maria Teresa Peltz I, Simona Secci¹

*AOBBrotzu Radiology Cagliari-Italy*¹

PURPOSE: To evaluate the long term evolution of brain abnormalities on conventional magnetic resonance imaging of SLE patients(pts)cohort.

METHOD AND MATERIALS: 30pts.(29F, age 53.5+/-11.3 yrs, disease duration 24.9+/-6.7 yrs) with SLE were prospectively observed and brain MRI studies (FSE T1, T2, GRE*T2 and FLAIR sequences) were obtained at baseline (GE MR 1.0 T and 0.5 T) and repeated after 19.4+/- 3.7 yrs of follow up (GE 1.5 T). An experienced neuroradiologist analyzed both MRI studies comparing the following outcomes: 1. Number of sub cortical white matter hyperintensities (WMHI) lesions,

2. Presence of brain damage due to large vessel ischemic insult.
3. Cerebral atrophy assessed and quantified using Evans' index.



POSTER PRESENTATIONS ABSTRACTS

Cumulative MRI brain damage was calculated according to a modified scoring system proposed by Petri et al(1). Pts. were also assessed for neuropsychiatric (NP) manifestation SLE- related or unrelated (NP- nonSLE) according to criteria proposed by the Italian Study Group on NP-SLE. Demographic, clinical and serological data were also recorded in order to identify any risk factors associated with worsening of brain abnormalities. Multiple stepwise regression analysis were applied. P-values <0.05 were considered significant.

RESULTS: 20 pts (66.6%) had an increased number of focal WMHI lesions whilst 8 pts (26.7%) showed a significant increase of Evans' index, defined as an increased greater than the sample mean + standard deviation. Modified Petri's score worsened in 23 pts (76.7%) and when the entire cohort was considered the difference between baseline and follow up was statistically significant (MR-1: 1.3+/-1.5 vs. MR-2: 2.9+/-2.1; p<0.0001). MRI showed brain lesions secondary to large vessels ischemia in 6 pts(20%), 4 not present at baseline. Previous WMHI lesions on MRI (p=0.044; and 95% CI : 1.1-97.0), resulted independent risk factor for development of new WMHI lesions, whilst antimalarials medication (p<0.004, OR 0.01 and 95% CI 0.0-0.25), was independently associated with a reduced risk. Hyperlipidemia (p=0.044, OR 10.1 and 95% CI 1.1-97.0), resulted independently associated with an increased risk for cortical atrophy. A steroid dose higher than 50 gr. (p=0.026; OR 8.8 and 95% CI 1.2-61.0) was the only independent risk factor for increase of cumulative brain MRI damage. 29 pts reported at least one NP event.

CONCLUSION: Brain MRI is a first level diagnostic tool in work-up of SLE patients with NP manifestations and their followup.

EP226-High Resolution Diffusion Weighted Imaging and MR Perfusion with Arterial Spin Labeling (ASL) in Patient with Transient Global

Amnesia (TGA) Another Brick Supporting Vasculopathic Pathogenesis.

*Maria Teresa Peltz*¹, *Simona Secci*¹, *Grazia Bitti*¹, *Maurizio Melis*²

*AOBBrotzu Radiology Cagliari-Italy*¹ *AOBBrotzu Neurology -Italy*²

PURPOSE: To evaluate with DWI small punctate hyperintense lesions of the hippocampus in patients with TGA and their relationship with focal increase of rCBFlow using ASL sequences. **METHOD and MATERIALS:** Twenty-one patients (pts.) with clinical diagnosis of TGA were studied with brain MR, including DWI at B0 values increased from 1000 to 3000 and slice thickness decreased from 5 to 3 mm., brain perfusion with ASL, EEG, DopplerUS of epiaortic vessels and neuropsychologic tests.

RESULTS: Twenty-one pts (12M and 9F, mean age 62, 52-81) were studied with MRI DWI and ASL between 24-72 hours from clinical presentation. 62%(13/21) showed a bright spot of diffusion restriction in the hippocampus (b0 values 1000-3000 3mm): 19% (4/21) on the left, 19% (4/21) on the right, and 19% (4/21) in both hippocampus. ASL showed visual significant focal increase of rCBF in hippocampus and parahippocampal region. In 5 of 8 pts with negative DWI , CBFlow were positive in 4 pts temporally studied proximally to 72 hours. EEGs were normal in 71,4% of cases wether were abnormal in 28.6% with slow aspecific activity. DopplerUs were normal in only 14,2% but abnormal in 85% for parietal atherosclerotic disease. 50% of pts present symptoms after emotional (14,2%) or phisical (23%) stress or both(4.7%) as well as after a cold/hot shower (19%). Increased of at least one of risk factors for cerebrovascular disease were present in 76% of pts such hypertension(52%), hypercholesterolemia (43%),diabetes (4.7%) .Neuropsychologic tests performed shortly after 48 huors from acute event were normal in all pts.

CONCLUSION: Higher DWI resolution increased lesion detectability in clinical TGA pts, studied in the right time window, considering the small size of hippocampal lesions. Significant diagnostic contribution can be obtain integrating ASL in the MRI study even performed later in the time range.Diagnostic added value can be obtained integrating ASL in the MRI-high resolution DWI study as well as a robust contribute to the vascular hypothesis for this acute event .



POSTER PRESENTATIONS ABSTRACTS

EP227-Emergency Magnetic Resonance Imaging (MRI) in Neurological Diseases

*Melda Apaydm*¹, Ö. Tuğçe Kalaycı¹, Fazil Gelal¹
*KÇÜ İAFAH Radiology izmir-Turkey*¹

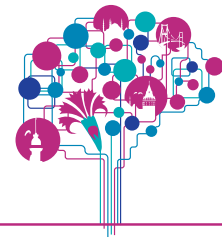
MRI which is an gold standart in neuroimaging studies, is an important tool for the management and treatment of the neurological compromised patients in emergency departments. The indications of urgent MRI, includes neoplastic, traumatic, vascular, infection, inflammatory related pathologies. We will discuss and present some of the pathologies of urgent MRI studies. MRI studies can be categorized like, a) urgent as soon as possible, b) within 12 hours, c) not really an urgent condition, it can be useful for an alternative for computed tomography (CT) or elective MRI. The cerebral neurovascular emergencies, acute paraplegia (cauda equina syndrome) are in the 'A' category. Spinal emergencies with no evidence of neurological compromise and suspicious findings of conventional imaging ; are in the 'B' category. Mangetic resonance angiography for occlusion or atherosclerosis, intracranial hemorrhage follow up, cerebral metastatis suspicion, patient's or clinician's wish are in the 'C' category. Urgent MRI indications are many, but categorization for the MRI is an important tool for the right approach and treatment of these patients.

EP228-Significance of Prominent Hypointense Signals in Draining Veins Adjacent To Areas of Cerebral Infarction on Susceptibility Weighted

Imaging

*Kookjin Ahn*¹, Jinhee Jang¹, Hyunseok Choi¹, Solyung Jung¹, Bumsoo Kim¹
*Seoul St. Mary's Hospital Radiology Seoul-Korea, South*¹

OBJECTIVE: A relative increase in deoxyhemoglobin levels in hypoperfused tissue can cause prominent hypointense signals in the draining veins (PHSV) within areas of impaired perfusion in susceptibility-weighted imaging (SWI). The purpose of this study was to evaluate the usefulness of SWI in patients with acute cerebral infarction by evaluating PHSV within areas of impaired perfusion. **MATERIALS AND METHODS:** In 18 patients with acute cerebral infarction who underwent brain MRI with diffusion-weighted imaging (DWI) and SWI and follow-up brain MRI or CT, we qualitatively reviewed the presence and location of PHSV within and adjacent to areas of cerebral infarction and quantitatively measured the phase value difference ratio (indirect oxygen extraction fraction, OEF) of PHSVs and normal appearing cortical veins on SWI. The relationship between the findings of PHSV and the change in the extent of infarction in follow-up images was analyzed. **RESULTS:** Of the 18 patients, ten showed progression of the infarction, and eight showed little change on follow-up imaging. On SWI, of the ten patients with progression, nine showed peripheral PHSV, and the newly developed infarctions corresponded well to the area with peripheral PHSV on initial SWI. Only one patient without peripheral PHSV showed progression of the infarct. None of the eight patients with little interval change showed peripheral PHSV ($p < 0.01$). The mean phase value difference ratio of the progression group was 2.4, and that of the group with little change was 0.86 ($p < 0.01$). **CONCLUSION:** SWI can reveal peripheral PHSV as a marker of penumbra; this finding can predict the prognosis of acute infarction. The phase value difference of PHSV to brain tissue on SWI can be used in calculating indirect OEF change and predicting the prognosis of acute cerebral infarction.



POSTER PRESENTATIONS ABSTRACTS

EP229-Hematoma Shape Hematoma Size GCS Score and ICH Score which Predict the 30 Day Mortality Better for ICH

*Chun-Jung Juan*¹, Chih-Wei Wang¹, Yi-Jui Liu², Hsian-He Hsu¹

*National Defense Medical Center Radiology Taipei-Taiwan*¹ *Feng Chia University Automatic Control Engineering -Taiwan*²

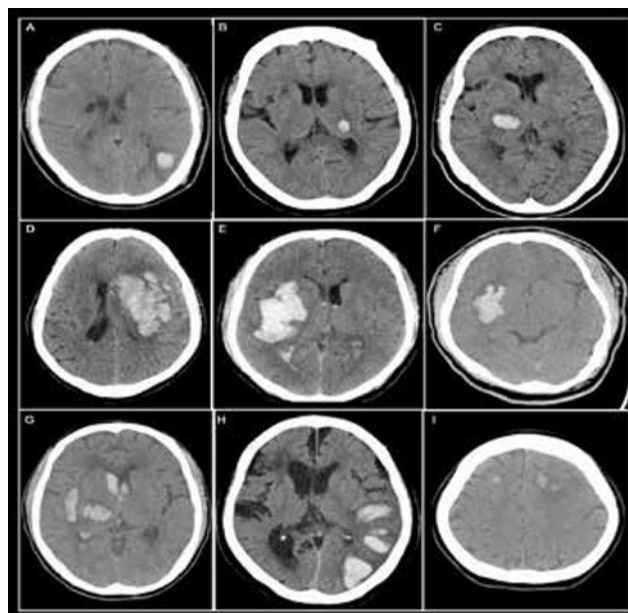
PURPOSE: To investigate the performance of hematoma shape, hematoma size, GCS score, and intracerebral hematoma (ICH) score in predicting the 30-day mortality for ICH patients. To examine the influence of the estimation error of hematoma size on the prediction of 30-day mortality. **MATERIALS AND METHODS:** This retrospective study, approved by a local institutional review board with written informed consent waived, recruited 106 patients diagnosed as ICH by non-enhanced computed tomography study. The hemorrhagic shape, hematoma size, ICH score and GCS score was examined. The predicting performance of 30-day mortality of the aforementioned variables was evaluated. Statistical analysis was performed using Kolmogorov-Smirnov tests, paired t test, nonparametric test, linear regression analysis, and binary logistic regression. The receiver operating characteristics (ROC) curves were plotted and areas under curve (AUC) were calculated for 30-day mortality. A P value less than 0.05 was considered as statistically significant.

RESULTS: The overall 30-day mortality rate was 15.1% of ICH patients. The hematoma shape, hematoma size, ICH score, and GCS score all significantly predict the 30-day mortality for ICH patients, with an AUC of 0.692 ($P = 0.0008$), 0.715 (by ABC/2) to 0.738 (by CAVA), 0.877 (by ABC/2) to 0.882 (by CAVA), and 0.912.

CONCLUSION: Our study shows that hematoma shape, hematoma size, ICH scores and GCS score all significantly predict the 30-day mortality in an increasing order of AUC. The effect of overestimation of hematoma size by ABC/2 formula in predicting the 30-day mortality could be remedied by using ICH score and GCS score.

Abbreviation:

CAVA: computer-assisted volumetric analysis





POSTER PRESENTATIONS ABSTRACTS

EP230-A Case of Thrombosed Vertebral Artery Aneurysm with Brain Stem Compression and Infarction

*Atilla Kokurcan*¹, Emrah Yilmaz¹, Suna Örs², M.Koray Akkan¹, Serap Gültekin¹

*Gazi UNIVERSITY Radiology Ankara-Turkey*¹ *Istanbul Bakırköy Dr.Sadi Konuk Training and Research Hospital Radiology -Turkey*²

INTRODUCTION: Vertebral artery (VA) aneurysms are rare and constitute 0.5 to 3% of intracranial and 20% of posterior circulation aneurysms. We present a case of thrombosed vertebral artery aneurysm which presented with ischemic symptoms due to brain stem compression.

CASE: 50- years-old male patient was admitted to the emergency department with respiratory arrest and low Glasgow coma score. CT examination showed an enlarged fusiform thrombosed aneurysm of the left vertebral artery compressing the pons. Aneurysm was found to be extending to the basilar artery from V4 distal segment of left vertebral artery in CT angiography. Diffusion weighted imaging revealed acute infarction over the pontomedullary junction. Diagnostic angiography confirmed a fusiform left vertebral artery aneurysm extending to the basilar artery, measuring 15 mm in diameter. Subsequently the aneurysm was treated with stent-assisted coil embolization. After treatment the patient was taken to the intensive care unit, with gradual recovery of symptoms.

DISCUSSION: Vertebrobasilar stroke carries a mortality rate of more than 85% because of involvement of the brainstem and it is usually occurs due to atherosclerotic diseases. A pons infarction resulting from the mass effect of a vertebral artery aneurysm as the above presented case is extremely rare. Therefore ischemic lesions should also be kept in mind in addition to other more common life threatening complications of large vertebrobasillary aneurysm.

EP261-Double Inversion Recovery Cervical Cord Imaging at 3T: Is It Better For Multiple Sclerosis Lesion Detection?

*Chian Aun Chang*¹, Abigail Chong¹, Ronil Chandra¹, Kenneth Chuah¹, Cathy Soufan¹, Deepa Rajendran², Ernie Butler², Stephen Stuckey¹

*Monash Health Diagnostic Imaging Clayton-Australia*¹ *Monash Health Monash Neurology, Australia*²

PURPOSE: Double inversion recovery (DIR) brain imaging at 3T has greater diagnostic value in detection of multiple sclerosis (MS) lesions compared to T2-weighted turbo spin-echo (T2-TSE) imaging. Our aim was to compare cervical cord MS lesion detection using 3T sagittal DIR imaging to the sagittal T2-TSE, proton density (PD) and short-tau inversion recovery (STIR) magnetic resonance (MR) sequences recommended by the Consortium of MS Centers.

MATERIALS AND METHODS: We prospectively enrolled patients with MS and imaged the cervical cord with 3T sagittal DIR, sagittal and axial T2-TSE, sagittal PD, sagittal STIR and axial multi-echo recombined gradient echo (MERGE) MRI sequences. Two neuroradiologists blinded to clinical and demographic data reviewed the MR images. A definite MS lesion was defined by either detection on 2 sagittal sequences, or if seen on 1 sagittal sequence alone, then by detection of the same lesion by axial T2-TSE or axial MERGE MR imaging. The cervical cord was divided into 13 segments — C1, C1/2, C2, C2/3, C3, C3/4, C4, C4/5, C5, C5/6, C6, C6/7, and C7. For each MR sequence, we analysed the total number of involved cord segments and compared the normalised lesion-to-cord contrast ratio (LCCR) and the contrast-to-noise ratio (CNR). The Wilcoxon signed-rank test was used for statistical correlation.

RESULTS: Nineteen patients (13 females) with mean age of 47 years (range 23–74 years) were included. Eighty percent had definite cervical cord MS lesions. DIR cervical cord imaging detected definite MS lesions in 48 cervical cord segments. PD detected the greatest number of involved cord segments (n=75), significantly greater than DIR (p=0.0005) and T2-TSE (p=0.01), but similar to STIR (p=0.17). STIR and T2-TSE also detected a significantly greater number of involved cord segments than DIR (STIR, n=67;p=0.01 and T2, n=61;p=0.01). The LCCR was highest for STIR; significantly greater than DIR (p=0.0009). The CNR was highest for PD; significantly greater than DIR (p<0.01).

CONCLUSIONS: Sagittal DIR cervical cord imaging at 3T is inferior to the T2-TSE, PD, and STIR MR sequences recommended by the Consortium of MS Centers for spinal MS lesion detection. Sagittal T2-TSE alone is superior to DIR for cervical cord MS lesion detection at 3T, and performing additional PD or STIR imaging further improves MS lesion detection.



POSTER PRESENTATIONS ABSTRACTS

Friday, September 12, 2014

Poster Presentations

13.00-14.00

Neurological Sciences

EP231-Default Mode Network Functional Connectivity in Middle Age Cognitively Intact APOE ϵ 4 Carriers

*Chi Tseng*¹, David Yen-Ting Chen¹, Chi-Jen Chen¹

*Shuang-Ho Hospital/Taipei Medical University Department of Medical Imaging New Taipei-Taiwan*¹

PURPOSE: Resting-state functional MRI (RS-fMRI) has been widely applied to analyze the functional connectivity (FC) between brain regions. Based on previous studies, diminished default mode network (DMN) FC in elderly apolipoprotein E (APOE) ϵ 4 carriers was found using seed-based correlation analysis. Also, increased DMN in young healthy ϵ 4 carriers was found using dual regression technique. However, there are few studies that have investigated the intrinsic FC of DMN in middle-aged, cognitively intact APOE ϵ 4 carriers. This study aimed to investigate the DMN connectivity derived from independent component analysis (ICA) in middle-aged, cognitively intact APOE ϵ 4 carriers and age- and gender-matched noncarriers.

METHODS: Night APOE ϵ 4 carriers (5 females, age: 52.4 \pm 11.1y) and ten age- and gender-matched noncarriers (5 females, age: 53.9 \pm 6.2y) participated in this study. RS functional images were acquired at a 3T clinical MRI scanner using a T2*-weighted single-shot gradient-echo echo-planar imaging (EPI) sequence (TR/TE/FA=2000ms/30ms/90°, in-plane matrix = 64 x 64, slice thickness = 4mm). Group ICA was performed using GIFT. A set of average group components were created and back-reconstructed into single-subject space. The individual subjects' components were scaled to spatial z-score maps by subtracting the global mean from each voxel and dividing by the global standard deviation and then entered into a one-sample t test ($p < 0.01$, corrected; cluster threshold = 10 voxels). Two-sample t test were performed to assess group differences between carriers and noncarriers results ($p < 0.001$ uncorrected; cluster threshold = 10 voxels).

RESULTS: In the APOE ϵ 4 carriers group, increased DMN connectivity was found in the precuneus and superior frontal gyrus, and decreased DMN connectivity was found in the superior, medial, and inferior frontal gyri, insula and thalamus relative to noncarriers.

CONCLUSION: This study found decreased and increased DMN connectivity in middle-aged, cognitively intact APOE ϵ 4 carriers. Combining with previous studies, these results may indicate progressively decreased FC in cognitively intact APOE ϵ 4 carriers as they become older.

EP232-Neurochemistry in Hypomyelination Model Mouse Depicted on MR Spectroscopy

*Jun-ichi Takanashi*¹, Nobuhiro Nitta², Hitoshi Terada³, A. James Barkovich⁴, Hiroko Tada⁵, Ichio Aoki²

*Tokyo Women's Medical University, Yachiyo Medical Center Pediatrics Yachiyo-shi-Japan*¹ *National Institute of Radiological Sciences Molecular Imaging Center -Japan*² *Toho University, Sakura Medical Center*

*Radiology -Japan*³ *University of California San Francisco Radiology and Biomedical Imaging -United States*⁴

*Saiseikai Narashino Hospital Pediatrics -Japan*⁵

PURPOSE: Hypomyelination describes a permanent, substantial deficit of myelin deposition in the brain. The two major components of myelin are proteolipid protein (PLP) and myelin basic protein (MBP). The purpose of this study is to evaluate the neurochemical changes associated with hypomyelination, in msd mouse with the plp1 mutation, and shiverer mouse with mutation of the mbp gene. **METHODS:** The animals included msd mice with a spontaneous mutation (A242V) in the plp1 gene and wild-type mice at P21; and shiverer mice (shi/shi), heterozygous and wild-type mice at 12 weeks.

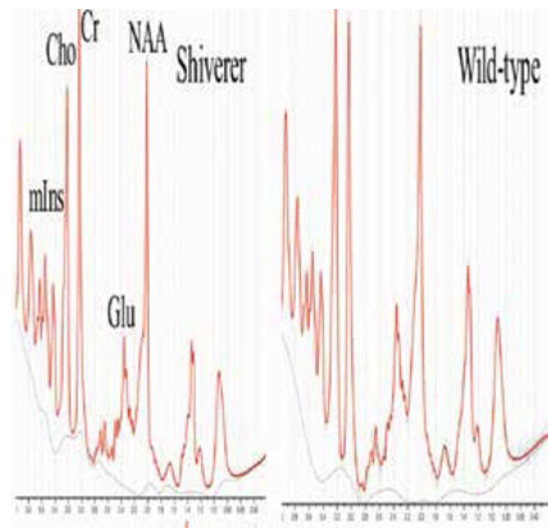


POSTER PRESENTATIONS ABSTRACTS

All MRI experiments were performed on a 7.0 tesla MRI scanner. Single voxel ¹H-MRS (PRESS, TR/TE=4000/20msec) of the thalamus was performed with a VOI of 3x3x3mm, and quantitatively analyzed using the modified water scaling method of LCModel. Immunohistochemical analysis using anti-Mbp, marker for mature myelin sheath, and Gfap, that for astrocytes were performed. RESULTS: In the thalamus, ¹H-MRS in msd mice revealed increased total N-acetylaspartate (tNAA) and decreased choline (Cho), compared with wild-type mice. In shiverer mice, decreased Cho and normal tNAA were observed (Fig), compared with heterozygous and wild-type mice.

Immunohistochemical analysis of msd and shiverer mice revealed hypomyelination. DISCUSSION: NAA is transported to oligodendrocytes, where it is catabolized by aspartoacylase into acetate and aspartate. In msd mice, the absence or dysfunction of mature myelinating oligodendrocytes may either disable the neuron-to-oligodendrocyte NAA transport or affect NAA catabolism in oligodendrocytes, leading to increased tNAA. Unlike in msd mice, oligodendrocyte progenitor cells in shiverer mice can differentiate into mature oligodendrocytes, where NAA may be normally transported from neurons to oligodendrocytes, leading to normal tNAA.

CONCLUSION: The reduction of Cho on ¹H-MRS might be a common marker for hypomyelinating disorders. A normal tNAA level in the thalamus of shiverer mice might be explained by the presence of mature oligodendrocytes.

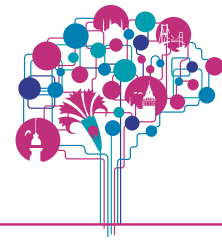


EP233-Clinical of Study of Chemical Exchange Saturation Transfer MRI on Brain Metastases at 1.5 Tesla

Yonggui Yang ¹, Zhiwei Shen ², Zhongping Zhang ³, Fang Chen ⁴, Gang Guo ⁴, Renhua Wu ⁵
The 2nd Hospital of Xiamen Radiology -China ¹ *The 2nd Affiliated Hospital, Shantou University Medical College Radiology* - ² *GE healthcare* - ³ *The 2nd Hospital of Xiamen* - ⁴ *The 2nd Affiliated Hospital, Shantou University Medical College* ⁵

PURPOSE: To investigate the feasibility of CEST in characterizing human brain metastases on a clinical 1.5T MRI scanner.

METHODS: Five patients diagnosed with brain metastases were recruited in this study with approval of the local ethics committee. All patients signed on an informed consent form before the exam. Whole brain underwent CEST scan, and were also imaged with conventional fluid-attenuated inversion recovery (FLAIR), diffusion-weighted imaging (DWI) and perfusion-weighted imaging (PWI) for comparisons. All MR studies were performed on a clinical 1.5T scanner, the amide protons were selectively saturated at radio frequency (RF) offsets of -224Hz (-3.5ppm) and 224Hz (3.5ppm), respectively. APT images were obtained using the magnetization transfer ratio (MTR) asymmetry at 3.5ppm with respect to the water resonance in order to reduce the interference of other saturation effects. The z-spectrum (normalized signal intensities with respect to unsaturated) was acquired over an offset range of ± 255 Hz with a resolution of 10 Hz, which were then fitted through all offsets using a 12th-order polynomial on a pixel-by-pixel basis. For reference, the DW and PW images were also acquired. RESULTS: The brain metastases demonstrated hyperintense on the FLAIR and DWI images, and hypoperfusion on the PW image, as shown in Fig. 1. The APT images had hyperintense at the metastases lesions as shown in Figure 1c. From Fig. 1a and 1b, it can be observed that the signal intensities of the viable tumor cores were significantly higher than both peritumoral edema and the necrotic regions, in agreement of Wen et al 3. The z-spectrum showed the significant differences between tumor tissue, perilesional oedema and normal brain



POSTER PRESENTATIONS ABSTRACTS

parenchyma in the -230~-200 Hz offset range and -224 Hz from water. At the offset of -224 Hz, the mean signal of the tumor tissue, perilesional oedema and normal brain parenchyma were 197 ± 10 , 137 ± 14 , 158 ± 12 , respectively. CONCLUSION: CEST MRI may provide a promising tool used in clinical for specially and sensitively monitoring metastases, predicting response to treatment and thus guiding patient management.

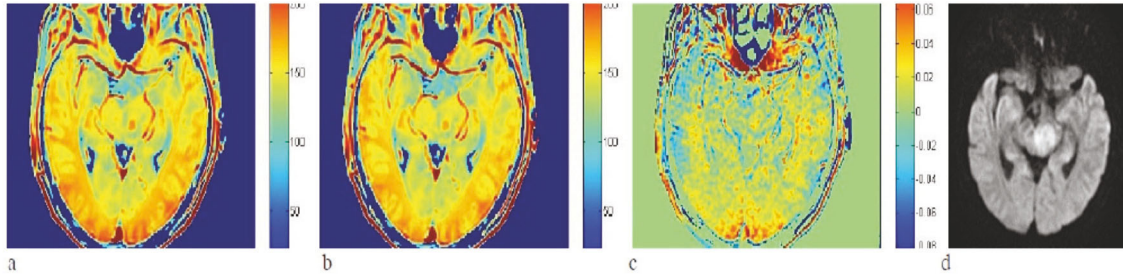


Figure 1. Example of human brain metastases images at 1.5T; a: saturated CEST image at -224Hz (-3.5ppm), b: saturated CEST image at 224Hz (3.5ppm), c: the APT image, d: the DW image.

EP234-Brain Metabolic Alterations of Patients with Diabetic Hypertension A 2D 1H Proton Magnetic Resonance Spectroscopic Imaging Study

Zhen Cao ¹, Bi Di Ye ¹, Zhi Wei Shen ¹, Ren Hua Wu ¹, Ye Yu Xiao ¹

The Second Affiliated Hospital, Shantou University Medical College Department Of Radiology -China ¹

OBJECTIVE: To study the possible metabolic alterations of frontal cortex and parietal white on patients with diabetic hypertension (DHT) by using 2D-1H proton magnetic resonance spectroscopic imaging (2D-1HMRS). **METHODS:** 33 DHT patients and 30 healthy control subjects aged from 45-75 were included in this study. All the subjects were dextrorhous. The spectroscopy data were collected by GE 1.5-T MR scanner. The multi-voxels were located in the semiovale center (TR/TE=1500ms/35ms). The volume of interest was 8 cm×10 cm×2 cm, contained both sides of frontal cortex and parietal white matter.

The spectra data were measured by the SAGE software. The ratios of N-acetylaspartate (NAA)/creatine (Cr) and Choline (Cho)/creatine (Cr) were separately calculated. Statistical analysis was performed with SPSS 17.0. **RESULTS:** NAA/Cr ratio of bilateral prefrontal cortex of DHT group were significantly lower than that of the control group (left $t=-7.854$, $P=0.000$ and right $t=-5.787$, $P=0.000$), Cho/Cr ratio were significantly lower than the control group (left $t=2.422$, $P=0.024$ and right $t=2.920$, $P=0.007$). NAA/Cr ratio of the left parietal white matter of DHT group was significantly lower than that of the control group ($t=-4.199$, $P=0.000$).

CONCLUSIONS: DHT group can result in metabolic disorders in the frontal cortex and parietal white matter but the metabolic alterations are distinct in these regions of brain. The alteration of cerebral metabolism is related to diabetes and hypertension. The ratios of NAA/Cr and Cho/Cr are potential metabolic markers for the brain damage by DHT.



POSTER PRESENTATIONS ABSTRACTS

EP235-A Potential Method for Imaging GABA in vivo Using Chemical Exchange Saturation Transfer

*Tao Zhang*¹, Zhuozhi Dai¹, Yanlong Jia¹, Renhua Wu¹

*The Second Affiliated Hospital, Shantou University Medical College Department Of Radiology Shantou-China*¹

PURPOSE: GABA is an important inhibitory neurotransmitter in the brain. In this study, we develop a novel MRI technique to measure GABA based on chemical exchange saturation transfer (CEST). In addition, we further investigate the concentration dependent CEST effect of GABA in rat brain tumor model with blood brain barrier (BBB) disruption.

METHODS: Z-spectra of GABA and other metabolites (glutamine, myo-inositol, creatine and choline) were acquired at 7T, 37° and pH7.0, respectively. CEST images of phantoms with different concentrations of GABA solutions (pH7.0) and other metabolites were collected to investigate the concentration dependent CEST effect and the potential contributions from other brain metabolites. CEST and 1HMRS data of rat brain with tumor were gathered at baseline and 0.5, 1.0, 1.5 and 2.0h after injection of GABA solution. MRS data were analyzed using LCModel.

RESULTS: CEST effect of GABA was observed at ~2.75 parts per million downfield from bulk water. The CEST effect of GABA increased with B1 amplitude and kept steady after the B1 reached 255 Hz. The CEST effect of GABA was proportional to the GABA concentration in vitro. CEST Imaging of GABA from a rat brain with tumor whose BBB was compromised showed a significant gradual increase in CEST effect after GABA injection, which was consistent with the 1HMRS data. **DISCUSSION:** These findings demonstrate the feasibility and potential to map changes in GABA using CEST, which has excellent spatial and temporal resolution.

EP236-Brain Metabolism in HIV infection a 7T Proton Magnetic Resonance Spectroscopy Study

*Mona Mohamed*¹, Peter Barker¹, Richard Skolasky², Ned Sacktor³

*Johns Hopkins Medical Institutions Radiology Baltimore-United States*¹ *Johns Hopkins Medical Institutions Orthopedic -United States*² *Johns Hopkins Medical Institutions Neurology -United States*³

INTRODUCTION: Using 7T MRS, more reliable in vivo determination of brain metabolites concentrations can be achieved than at lower field strengths. In this on-going study, the feasibility of measuring multiple brain metabolites in 5 different brain regions in patients with HIV infection is demonstrated.

MATERIAL and METHODS: 12 HIV+ subjects were stratified into 3 groups according to their cognitive status using the Frascati dementia severity score. Five (3 males) were asymptomatic neurocognitive impairment (ANI) with age range of 58-71 years, 5 (3 males) had mild neurocognitive disorder (MND) with age range of 50-66 years and 2 (males) had dementia (HAD) with age range of 53-54 years. The HIV+ subjects were under a combination of antiretroviral therapy Three HIV- subjects were also included in the study. Using a 7.0T Philips scanner and 32-channel head coil, brain MRI and single voxel STEAM spectra (TR/TE=3000/14 msec) were acquired from the left frontal white matter (FWM), basal ganglia (BG), Precuneus (PC), Posterior cingulate (PCC) and Hippocampus (Hippo) with and without water suppression. The voxel sizes ranged from 8 to 15 cc. Spectra were analyzed using LCModel (4) and quantified (in mM concentrations, i.u.) relative to the unsuppressed water signal. Metabolite concentrations and ratios relative to creatine (Cr) were calculated for the 3 groups. The data was not normally distributed; therefore, comparisons of the groups' medians (and interquartile ranges) were evaluated for significant differences using non-parametric median test. P < 0.05 was considered significant.

RESULTS: PC and PCC NAA/Cr, and PC and Hippo Glu/Cr, were lower in HIV+ as compared to HIV- (P=0.046). Among those with HIV+, when stratified by cognitive impairment, there were significant decrease in FWM NAA/Cr and Glu/Cr in HAD compared to ANI (P=0.03). BG mI concentrations and mI/Cr ratio were higher in HAD HIV+ as compared to ANI (trend toward significance, P=0.07). NAA and Glu were significantly



POSTER PRESENTATIONS ABSTRACTS

correlated in the FWM ($P=0.03$), but not in the other 4 brain regions.

CONCLUSION: 7T MRS measurement of Glu/Cr, NAA/Cr and mI/Cr can be reliable indicators of neurocognitive dysfunction in patients with HIV.

EP237-Acute Effect of Methadone Maintenance Dose on Cerebral Blood

Flow in Heroin Users under Methadone Maintenance Treatment

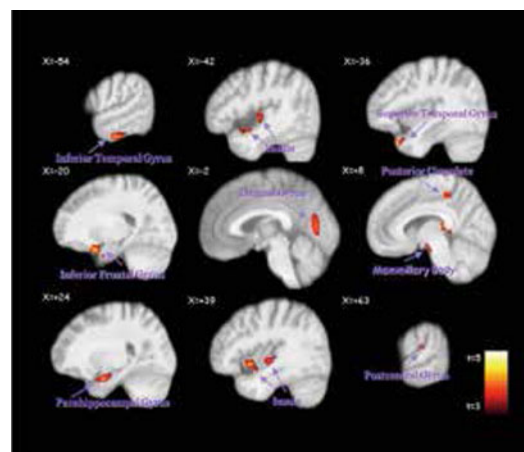
*Hsiu-Ling Chen*¹, *Pei-Chin Chen*¹, *Chien-Chih Chen*², *Meng-Chang Tsai*², *Wei-Che Lin*¹
*Kaohsiung Chang Gung Memorial Hospital, and Chang Gung University College of Medicine Department of Diagnostic Radiology Kaohsiung-Taiwan*¹ *Kaohsiung Chang Gung Memorial Hospital, and Chang Gung University College of Medicine Department of Psychiatry -Taiwan*²

BACKGROUND: Alteration of cerebral blood flow (CBF) in heroin users under Methadone maintenance treatment (MMT) had been reported but the acute impact before and after methadone administration is less known. The purpose of this study is to investigate the acute changes in cerebral blood flow (CBF) of MMT subjects before and after methadone administration using arterial spin labeling (ASL) perfusion MRI, and the relationship with history of heroin and methadone usage. METHOD: Twenty-five MMT patients receiving history taking and neuroimaging were enrolled in this study. Patients were studied before and after administration of their regular daily methadone dose. Perfusion MRI data were acquired with a pulsed continuous ASL technique. CBF maps were calculated from the labeled and unlabeled ASL images. The CBF maps were compared using voxel-based statistics to determine acute differences in MMT subjects before and after methadone administration, with age and sex as covariates.

Correlations between the difference of CBF and other clinical variables, including duration or dose of heroin use and MMT, were assessed by multiple regression analysis. The relationship between acute changes of CBF and craving score value were assessed by partial correlation.

RESULT: Exploratory comparison in MMT subjects revealed decreased CBF after administration of the daily methadone dose in several brain locations, including superior and inferior temporal gyrus, inferior frontal gyrus, postcentral gyrus, thalamus, caudate, insula, posterior cingulate, parahippocampus, amygdala, culmen, lingual gyrus, precuneus and midbrain mammillary body. The time interval since last heroin administration correlated negatively with differences of CBF in left lingual gyrus and right precuneus. The acute changes of craving score and CBF in right culmen revealed positively correlation.

CONCLUSION: The CBF dramatically dropped after administration of the daily methadone dose, especially in patients with recent heroin usage. The decreased value of CBF was also correlated with decreased craving score for heroin. ASL was able to reveal the dynamic fluctuation of cerebral perfusion non-invasively and reflect the acute response of methadone maintenance dose in heroin users.





POSTER PRESENTATIONS ABSTRACTS

P238- Investigating Neuronal Metabolic Characterization in Peritumoral Area of Brain Glioma using 1H MRS at 7T

Meizhi Yi¹, Yan Gen¹, Guishan Zhang¹, Tao Zhang¹, Renhua Wu¹

the Second Affiliated Hospital, Shantou University Medical College Department of Radiology Shantou-China¹

BACKGROUND: Glioma has a tendency to infiltrate the surrounding brain tissue for several centimeters from the core of tumor. The structural MR sequences are insensitive to detect the invaded scope outside the visible tumor border.

OBJECTIVE: This study aimed to establish a repeatable rat glioma model to investigate the metabolic characteristics in different area of brain glioma and assess the peritumoral area of glioma using high field proton magnetic resonance spectroscopy 1H-MRS at 7T.

Methods: The C6 glioma cells were stereotactically implanted into the right basal ganglia region of SD rats. The SD rats were sequentially underwent 1H-MRS at an animal dedicated 7T MR scanner 7days after operation. Neuronal metabolites were measured from the tumor center, tumor solid parts, peritumoral normal-appearing tissue, as well as contralateral white-matter. All spectra were then quantified by LCModel.

RESULTS: This C6 rat glioma model was stable and repeatable. A gradual increase in NAA, tCr, and a decrease in Ala from the tumor center to the contralateral normal white matter were observed. Moreover, the lowest level of Ins and Tau were found in the tumor peripheral area. Significant differences in Ins and Tau can be evidenced between the tumor peripheral area and the other three areas. The highest Glx peaks appeared in the tumor peripheral part. The statistically significant differences in Glx among each region were also found.

CONCLUSION: Our study demonstrated a repeatable animal model for investigating biochemical specificity of glioma. The acquired MRS data supply additional information about the location of glioma potential border.

EP239-Fetal Magnetic Resonance Imaging in the Pathology of the Central Nervous System

Mercedes Serra¹, Maria Sol Toronchik¹, Cecilia Rollan¹, Hernan Chaves¹, Gabriela De Pino

¹, Adolfo Etchegaray², Claudia Cejas¹, *Carlos Romero*¹

Instituto de Investigaciones Neurológicas Raul Carrea, FLENI Radiology -Argentina¹ Hospital Universitario Austral Ultrasonography -Argentina²

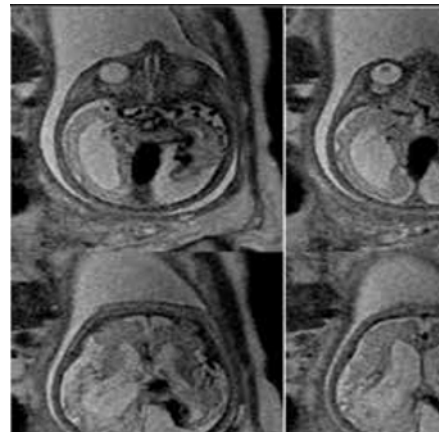
PURPOSE: - To analyze the utility of Fetal Magnetic Resonance Imaging (FMRI) in Central Nervous System (CNS) pathology.

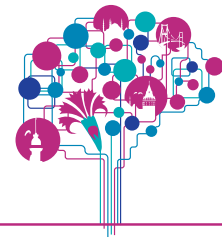
- To compare this novel technique with Fetal Ultrasonography (FUS).
- To exemplify with cases from our institution.

METHODS: US is the gold standard technique for the evaluation of CNS pathology in fetuses. Nonetheless, FMRI has evolved since the first publication of this method by Smith et al. 20 years ago. There are precise indications for the need to evaluate a CNS pathology diagnosed by US with MRI. FMRI can be acquired from the beginning of the second trimester of gestation, being the optimal moment, between weeks 28 and 32.

We reviewed our institutional database selecting CNS pathologic studies of the fetal population evaluated with MRI. All studies were acquired on a 1.5 Tesla MRI Scanner (Signa HDx, GE, Milwaukee, Wis.)

RESULTS: We found 34 patients with CNS pathology evaluated with FMRI at our institution. Pathologies included: cerebellum hypoplasia (2), corpus callosum agenesis (5), mega cisterna magna (4), ventriculomegaly (6), hydrocephalus (2), cerebral ischemia (1), Arnold-Chiari II (4), midline cystic lesion (1), vein of Galen aneurysm (2), lobar holoprosencephaly (1), myelomeningocele (6), sacrococcygeal teratoma (1), intraventricular hemorrhage (1).





POSTER PRESENTATIONS ABSTRACTS

CONCLUSIONS: fMRI is a complimentary technique to FUS. Its utility should be evaluated in each case. MRI availability is increasing, and has low risk for both the mother and the fetus. Prenatal diagnosis of CNS pathology is of core importance for an adequate prenatal counseling.

EP240-Posterior Fossa Malformations Characteristic Findings on MRI

Gabriela Michelin ¹, M. Sol Toronchik ¹, M. Mercedes Serra ¹, Carlos Romero ¹
F.L.E.N.I. Radiology -Argentina ¹

PURPOSE: To review the classification and characteristic findings of the most frequent posterior fossa malformations.

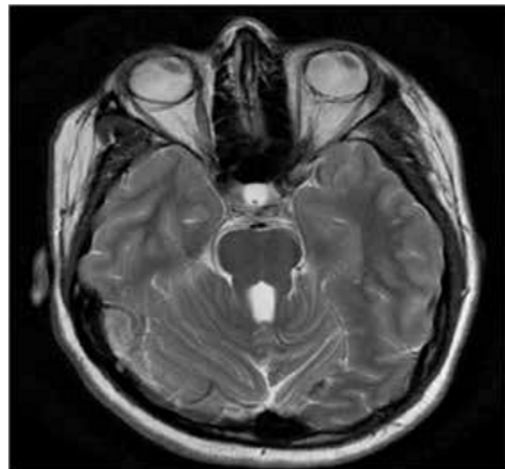
To raise awareness of the differential diagnosis regarding posterior fossa malformations and help the physician make a diagnostic approach in these cases. To illustrate characteristic MRI findings in posterior fossa malformations with cases from our institution.

METHODS: We searched our institutional database for posterior fossa malformations with the keywords Megacisterna Magna, Chiari, Dandy Walker, Joubert and Rombencephalosynapsis.

We retrieved the more representative cases, aiming to illustrate characteristic findings on MRI.

RESULTS: We selected 23 patients from our institutional database with posterior fossa malformations. We included 17 brain MR and 6 fetal MR studies. We selected 5 patients with Dandy Walker malformation, 3 with Dandy Walker variant, 4 with Chiari malformation type I, 5 with Chiari malformation type II, 1 patient with Joubert syndrome and 5 patients with Megacisterna Magna.

CONCLUSION: Knowledge of classification and characteristic findings of posterior fossa malformation on MRI should enable the radiologist to make a more accurate imaging diagnosis and help the physician make a logical approach.



Head tilt syndrome. Axial T2 shows small superior cerebellar peduncles in at course perpendicular to the brainstem (nasal to the right), abnormal rotation and elongation of the 4th ventricle.

EP241-Brain Intrinsic Resting State Functional Connectivity Modulation

Induced by Mental Effort in Multiple Sclerosis Patients with Fatigue

Emanuele Pravata ¹, Carlo Sestieri ², Massimo Caulo ², Chiara Zecca ³, Alessandro Cianfoni ¹, Claudio Gobbi ³
Neurocenter of Italian Switzerland Neuroradiology Lugano-Switzerland ¹ *ITAB Neurosciences -Italy* ²
Neurocenter of Italian Switzerland Neurology -Switzerland ³

PURPOSE: To investigate changes of the resting-state functional connectivity (RS-FC) MRI associated with cognitive fatigue (CF), induced by the execution of a cognitively effortful task, in patients with relapsing-remitting multiple sclerosis (RRMS).

MATERIALS AND METHODS: 22 clinically stable RRMS patients, 11 with CF (F) and 11 without CF (nF) according to the Fatigue Scale for Motor and Cognitive Functions (FSMC) and 12 age- and gender-matched healthy control subjects (HS). RS-FC scans were acquired on a 3T MR scanner immediately before (t0), immediately after (t1) and 20 minutes after (t2) execution of the Paced Auditory Serial Addition Test (PASAT). Differences in the RS-FC strength between each brain voxel and the rest of the gray matter between F, nF and HS were investigated at each time point using a data-driven intrinsic connectivity contrast technique [Martuzzi et



POSTER PRESENTATIONS ABSTRACTS

al, Neuroimage 2011] and 1-way between-subjects ANOVAs. The presence of a correlation between significant t2-t0 RS-FC differences and neuropsychological measures across patients was investigated. Structural and diffusion-tensor (20

gradient directions) data were acquired to evaluate atrophy, lesion load and white matter microstructure.

RESULTS: T2-hyperintense lesion load and brain atrophy did not differ between F and nF. Self-reported CF after PASAT (PASAT-F) was significantly higher in F than nF patients and HS ($p=0.016$, Mann-Whitney U test). Compared to nF and HS, F patients presented stronger RS-FC at t2 between the left dorsolateral prefrontal cortex (L-DLPFC) and pre-motor (Figure), secondary visual, left frontal and temporal areas ($p=0.01$, FDR-corrected). The RS-FC strength of these links at t2 and t0-t2 difference positively correlated with FSMC ($\rho=0.65-0.73$, $p=0.001$) and PASAT-F ($\rho=0.4-0.59$, $p=0.044-0.02$). Tractographic reconstructions of cortico-thalamic projection fibers using L-DLPFC as a seed region, showed reduced fractional anisotropy in F compared to nF patients (0.39 vs. 0.43, $p=0.047$).

CONCLUSIONS: In RRMS patients, the degree of CF is correlated to the persistence of hyperconnectivity within fronto-temporo-occipital networks despite relax after mental effort, and to disconnection of thalamo-cortical projection links. Identification of functional imaging biomarkers of CF explaining RRMS patients reduced resilience may help clinical diagnosis and response assessment to specific medical and rehabilitative treatments.

EP242-Resting State fMRI in Assessing Changes of DMN Activation

Pattern in Neurodegenerative Diseases

*Evgeniia Seliverstova*¹, Yury Seliverstov², Rodion Konovalov³, Marina Krotenkova³,

Sergey Illarioshkin²

*Research Center of Neurology RAMS Department of Radiology Moscow-Russia*¹ *Research Center of Neurology Department of Neurogenetics -Russia*² *Research Center of Neurology Department of Radiology -Russia*³

OBJECTIVE: To assess pattern of activation within default mode network (DMN) in healthy controls and patients with such neurodegenerative diseases like Parkinson's disease (PD) and Huntington's disease (HD).

METHODS: Sixteen healthy volunteers (including 9 females; mean age 41.4 years; right-handed, with no central nervous system diseases), 10 early manifest HD mutation carriers (including 4 females; mean age 32 years; right-handed) of stages 1 and 2 (Shoulson and Fahn, 1979), and 14 patients with PD (including 9 females; Hoehn-Yahr stage 2.5; mean age 63.5 years; right-handed) underwent 1.5 T MRI scanning. Participants were instructed to lie still and relaxed with closed eyes, not to think about anything in particular, and not to fall asleep. Obtained data was processed using software GIFT 2.0, SPM5, and SPM8 (Matlab 2011 and 2013). Gender and age have been taken as covariates in data analysis. A group independent component analysis was used to identify pattern of DMN.

RESULTS: We have identified DMN activation pattern in subjects of all studied groups. However we've found certain differences in DMN activation pattern. In HD patients, we've observed significantly reduced activation ($p<0.05$; $T = 4.07$) in precuneus and posterior cingulate gyrus and significantly higher activation ($p<0.05$; $T = 4.07$) in right parietal lobe (Brodmann area 39). In PD patients, we've found a significant reduction of the activation in inferior parietal lobule of the right hemisphere (which is involved into visual-spatial perception) and significantly greater activation in supramarginal gyrus and precuneus of the left hemisphere; in PD patients, we have also found significantly greater areas of activation in middle temporal gyrus and superior frontal gyrus (supplemental motor area) (both are not parts of DMN) of the right hemisphere [$pFWE_{corr} < 0.05$; $T = 2.82$].

CONCLUSIONS: Our findings may indicate the ongoing neurodegenerative process and reflect neuroplasticity phenomena.



POSTER PRESENTATIONS ABSTRACTS

EP243-FLT PET CT in Restaging Primary AND Metastatic Brain Lesions

*Alexandra Nikaki*¹, Panagiotis Georgoulas², Vassiliki Filippi¹, Ioannis Tsougos³, Fani Vlachou¹, Dimitrios Kechagias¹, Theodoros Pipikos¹, Roxani Efthymiadou¹, Vassilios Prassopoulos¹, Ioannis Andreou¹

*Sa Hygeia Pet/Ct Athens-Greece*¹ *University Of Thessaly Nuclear Medicine -Greece*² *University Of Thessaly Medical Physics -Greece*³

PURPOSE: Fluorothymidine (18F-FLT) is a new PET radiopharmaceutical, suggested to provide functional information and represent tumor cell proliferation. Its utilization is currently tested in Non-Hodgkin Lymphomas (NHL) and multiple solid tumors, among which brain tumors. The purpose of this study is to evaluate FLT-PET/CT in restaging brain lesions.

METHODS: 19 patients underwent 24 FLT-PET/CT in a Biograph Siemens LSO PET scanner 55±5 minutes after the intravenous administration of the radiopharmaceutical, for evaluation of residual disease/recurrence. 12 PET/CT examinations were performed for metastatic lesions, 8 for primary brain tumor and 4 for NHL. PET/CT examinations were recorded as positive or negative based on visual assessment of the images. In particular, any focal uptake of the radiopharmaceutical clearly above background activity was characterized as positive, while mild, diffuse uptake or no uptake was characterized as negative. Semiquantitative analysis was performed for all focal uptake lesions using SUVmax and tumor-to-background (T/B: SUVmax of the lesion/ SUVmax of background) measurements.

RESULTS: 15/24 FLT-PET/CT examinations were characterized as positive and 9 as negative. In total 18 lesions were considered positive, all of which exhibiting SUVmax and T/B >1.5. Mean SUVmax±SD (standard deviation) and T/B±SD of the positive lesions were 3,1±2,7 and 6,5±5,7 respectively. Table below shows mean SUVmax±SD, T/B±SD and the number of PET examinations included for metastatic, primary brain lesions and NHL. Using paired t-test statistically significant differences were recorded between SUVmax and T/B values for primary and metastatic lesions (p <0.05), but not for NHL (p=0.0846). Using unpaired t-test, no statistically significant difference of SUVmax and T/B was recorded between primary and metastatic lesions (p=0.8345 for SUVmax, p=0.8565 for T/B, > 0.05). In 17 cases, patients received treatment after PET examination, 16 of which had a positive PET.

CONCLUSION: With respect to our small and inhomogeneous sample, our preliminary results indicate that 18F-FLT- PET may be a useful tool in brain tumor imaging by offering additional functional information. Semiquantitative measurements may further be utilized. NHL lesions exhibited high SUVmax and T/B values. Mean SUVmax between primary and metastatic lesions did not substantially differ. Variability in T/B values were noted in metastatic lesions partially attributed to differences in primary site and treatment response.

	METASTATIC		PRIMARY		NHL	
	SUVmax	T/B	SUVmax	T/B	SUVmax	T/B
Mean	2.3967	4.7833	2.2786	5.0529	8.8650	19.4500
SD	1.1071	3.4702	1.0919	1.9008	5.8478	7.8489
Number	9	9	7	7	2	2

EP244-Volumetric Analysis of Atrophy in Alzheimer's Disease and Mild Cognitive Impairment

Berrin Cavusoglu¹, *Emel Ada*², Derya Durusu Emek Savas¹, Gorsev Yener³

*Dokuz Eylul University Neuroscience -Turkey*¹ *Dokuz Eylul University Radiology Izmir-Turkey*² *Dokuz Eylul University Neurology -Turkey*³

PURPOSE: To compare the atrophy of whole brain and brain structures volumes in patients who were clinically diagnosed as Alzheimer's disease (AD) and mild cognitive impairment (MCI) patients with a healthy control group (HC).



POSTER PRESENTATIONS ABSTRACTS

SUBJECTS and METHODS: AD (17), MCI (17) and HC (17) subjects were assessed. Left and right hippocampus, cingulate gyrus, corpus callosum, frontal, parietal and temporal lobes and whole brain were annotated on 3D T1W coronal images with a semi automated annotation and volume assessment software package. Mann-Whitney U test was used for statistical assessment and $p < 0,05$ was considered to be significant.

RESULTS: Total brain volumes of AD and MCI were found to be decreased compared to the healthy control (HC) group, but the difference between AD and MCI was not significant. Left hippocampus and cingulate gyrus measurements differed between AD and MCI groups. Right and left hippocampus, frontal and temporal lobe volumes of Alzheimer and MCI patients were significantly decreased according to the HC. Cingulate gyrus and parietal lobe was found to be significantly different between AD and HC.

CONCLUSION: Volumetric MRI can contribute to differentiate AD and MC and useful for validation of biomarkers for diagnosing AD in mild cognitive impairment.

Research

EP245-Vascular Occlusion Effects of Endovascular Radiofrequency Wire Electrode on Rabbit Renal Artery Comparison with PVA Embolization

*Daehyun Hwang*¹, wooyoung You¹

*Dongtan Sacred Heart Hospital Radiology hwaseongsi-Korea, South*¹

BACKGROUND: We are increasing cases in intracranial stenosing and some increasing wire perforation in small arteries. How to solve this problem? We embolized rabbit renal artery by microwire and RF generator. To prospectively evaluate the tissue reaction, the embolic effects and absorption of embolization effects of radiofrequency wire electrode method to comparing with PVA particles.

MATERIALS AND METHODS: This experiment was performed in accordance with regulations on the animal care and experiments. New Zealand white rabbits were divided into two groups according to the materials (PVA, diameter 150-250µm, 4 rabbits) and RF ablation (8 rabbits) by 0.018 inch Teflon coated platinum Mandril guide Wire, Cook, Bjæverskov, Denmark) used for embolization of right renal artery. A rabbit from each group was sacrificed 3 days, 1 week, 2 weeks, 4 weeks after embolization.

Gross and microscopic pathologic findings were examined with Hematoxylin and Eosin staining. RF generator (RF 3000, Boston Scientific Corporation, Boston, USA)

RESULTS: Gross pathologic findings were examined and swelling of embolized kidney was observed 3 days after embolization, whereas shrinkage of the kidney was consistently seen after 2 weeks, with hard consistency and nodular spaces being noted. At the histologic analysis the PVA particles make incomplete obstruction of the arterial lumen and no vasculitis is noted at 3 days later.

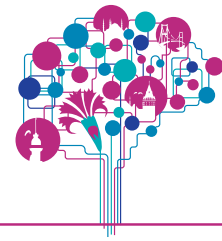
EP246-Preliminary Analysis of Chemical Exchange Saturation Transfer (CEST) Images and Z Spectrum of Different Metabolism Models

Yonggui Yang¹, Zhiwei Shen², Fang Chen³, Zhongping Zhang⁴, Xiaojin Xu³, *Gang Guo*³, Renhua Wu⁵

*The 2nd Hospital of Xiamen Radiology - China*¹ *The 2nd Affiliated Hospital, Shantou University Medical College Radiology* - ² *The 2nd Hospital of Xiamen* - ³ *GE healthcare* - ⁴ *The 2nd Affiliated Hospital, Shantou University* - ⁵

AIM: Our study is to investigate the feasibility of CEST data acquisition and analysis at 1.5T MR scanner under different metabolism models.

METHODS AND MATERIALS: We prepared four phantoms consisted of 50%, 30%, 10% creatine and 50% glutamate, respectively. All imaging experiments were performed on a clinical 1.5T scanner (Signa HDc,



POSTER PRESENTATIONS ABSTRACTS

General Electric Medical Systems). CEST images were acquired by a modified GRE sequence. To investigate the influence of image parameters on the CEST contrast, we repeated the experiments with image matrix and NEX changed to 256×256 and 2, respectively. Afterwards, the corresponding APT images were obtained by calculating the magnetization transfer ratio (MTR) difference between creatine and glutamate.

RESULTS and DISCUSSION: The signal intensity of creatine is slightly higher than that of glutamate in both CEST and APT images. It demonstrated that the CEST imaging can differentiate different types of metabolism and the concentrations. According to difference acquisition parameters, it was shown that the SNR could be improved with the decrease of matrix size and the increase of NEX and flip angle. Note that this experiment may be impacted by pH value. Though we had not test the influence of pH value, some researchers found that as the signal intensities of free water decreased more obviously with the elevated pH3.

CONCLUSION: Experiments show that it can distinguished different metabolisms and their concentrations using CEST image, APT image and Z spectrum. Furthermore, the SNR of CEST images could be improved by reducing the matrix size and increasing the NEX and flip angle.

Figure . Experiment results. (A)~(C) are T1WI, T2WI, T2 FLAIR image; (D)~(F) are saturated CEST image at -224Hz (-3.5ppm), 224Hz (3.5ppm) and the APT image; (G)~(J) are the Z spectrum images. Notes: At 1.5 T, the Larmor frequency of 1H proton is 63.75 MHz. For APT, the resonant frequencies of two protons are separated by approximately 3.5ppm, i.e. 224±5Hz at 1.5 T. For creatine, the difference is about 3.05ppm, i.e. 194.4±5Hz. For glutamate, the difference is about 2.1~2.4ppm and 3.6~3.8ppm, which means 133.8~153Hz and 232.7~242.25Hz respectively.

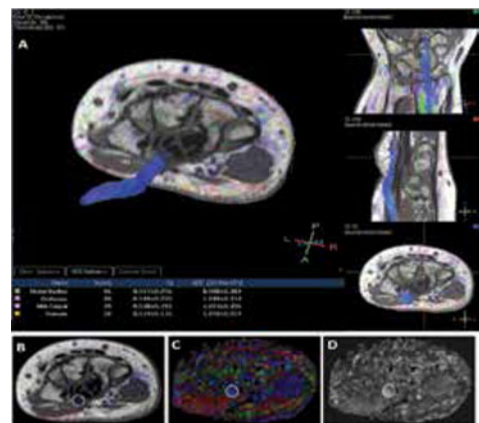


Figure 8. Frequency of the proton resonance shift is well correlated to the chemical shift of the proton resonance shift. (A) T1WI, (B) T2WI, (C) T2 FLAIR, (D) CEST image, (E) CEST image, (F) APT image, (G) Z spectrum, (H) Z spectrum, (I) Z spectrum, (J) Z spectrum.

EP247-Non Invasive Detection of 2 Hydroxyglutarat in Patients with IDH Mutated Glioma via MR Spectroscopy in a Clinical Setting

*Thomas Huber*¹, Christine Preibisch¹, Jan Bauer¹, Tobias Boeck-Behrens¹, Changho Choi², Claus Zimmer¹

*Klinikum rechts der Isar, Munich, Germany Department of Neuroradiology Munich-Germany*¹ *University of Texas Southwestern Medical Center Advanced Imaging Research Center / Radiology -United States*²

PURPOSE: The majority of WHO grade 2 and 3 gliomas shows mutations in isocitrate dehydrogenase (IDH) 1 and 2 leading to impaired enzyme function and the production of the oncometabolite 2-Hydroxyglutarate (2HG) (Yan et al., 2009). Ex vivo detection of IDH mutation is a well established method in the pathological analysis of glioma tissue and correlates with an improved overall survival in patients with IDH-mutated glioma (Andronesi et al., 2013; Yan et al., 2009). 2HG can be used as an indirect marker of IDH mutation proving an impaired enzyme function. Choi et al. were able to detect 2HG in patients with low grade gliomas using in vivo MR-spectroscopy (MRS) (Choi et al., 2012). Non invasive detection of 2HG via MRS could lead to an improved diagnosis of low grade glioma providing a novel, non-invasive tool to detect IDH mutation prior to surgery or biopsy.

Knowing the IDH status could be a helpful information in the decision making process during interdisciplinary tumor boards or for neurosurgery planning.



POSTER PRESENTATIONS ABSTRACTS

METHODS: In a prospective study we acquired 3T-MRS data with a modified PRESS-Sequence (TE=97ms) in patients with a new detected intra-axial cerebral mass. MRS data of the mass and healthy brain tissue were acquired using a single voxel technique. MR-spectra were analyzed for 2HG with LC Model using a customized basis set. After surgery, tumor tissue was analyzed ex vivo for IDH-mutation and clinical information was collected.

RESULTS: Pathological confirmation of IDH mutation after surgery showed a strong correlation between IDH mutation and the 2HG peak in the MR-spectrum. This 2HG peak was never found in healthy brain tissue. In summary, our first results proof that 2HG can be detected in glioma tissue in vivo at our site in patients with IDH-mutated gliomas.

CONCLUSION: Adaption of MRS in our clinical routine reveals metabolic information of tumor tissue beyond the morphologic characteristics obtained from standard MR-sequences like FLAIR or Gd-MPR. Detection of 2HG in vivo with a modified PRESS sequence via MRS is an indirect hint for IDH mutation and can be a novel diagnostic tool for an improved preoperative diagnosis and neurosurgery planning.

EP248-MR Morphometry of Hippocampus in MDD Patients and Healthy Volunteers

MR-morphometry of hippocampus in MDD patients and Ananyeva N. ¹

Bekhterev research Institute diagnostic radiology Saint-Petersburg-Russia ¹

MR-morphometry of hippocampus in MDD patients and healthy volunteers

N.Ananyeva, R.Ezhova, I. Galsman, M.Davlethanova, T. Rostovtseva, A.Sorokina

Saint-Petersburg V.M. Bekhterev Psychoneurological Research Institute, Saint-Petersburg, Russia

BACKGROUND: Affective disorders are one of the most common types of mental pathology. This defines importance of researching structures of the limbic complex that is the main morphological substrate of emotions. Most of the investigators found that hippocampal volume is decreased in patients with major depression disorder (MDD). But the role of the different structural hippocampal variants is still unknown

PURPOSE: Investigation of the hippocampal structural variants in patients with MDD compared to healthy volunteers.

METHODS AND MATERIALS: 148 patients (mean age 36 years) were examined. The first group of patients consisted of 101 healthy volunteers (mean age was 31 year). The second group included 47 patients with MDD according to Montgomery-Asberg depression rating scale, Hospital Anxiety and Depression Scale (HADS) and Beck Depression Inventory (BDI).

MRI was performed on 1,5T Toshiba Vantage scanner using standard brain protocol (T2 WI, T1 WI, FLAIR, DWI, T2* GRE) + 3D MPRAGE sequence (isotropic 1.0 mm) and following voxel

morphometry (VM) using automatic and manual segmentation (FreeSurfer and DISPLAY Software). In the following we performed statistical analysis using IBM SPSS Statistics software package:

correlational analysis (Pearson correlation coefficient, dispersion analysis, Bonferroni method).

RESULTS: • Different structural variants of hippocampal formation were found either in group of healthy volunteers or in group of patients with MDD

• We haven't found significant age correlation of the hippocampal volume in healthy volunteers in the age before 50 years.

• Hippocampal volume was certainly bigger in men than in women.

• Right hippocampal head was certainly smaller in patients with depression disorders compared to healthy control group (after manual segmentation).

• Structural variants of hippocampus were indicated more often in patients with early manifestation of major depression disorder and in patients with severe depression (according to Montgomery-Asberg depression rating scale).



POSTER PRESENTATIONS ABSTRACTS

CONCLUSION: Morphological variants of the mediobasal parts of temporal lobes couldn't be, as we consider, the direct aetiological factor of the MDDr, but it could possibly be the sign of development failure of the brain, and in particular of the brain structures involved in the formation of emotions.

EP249-The Diagnostic and Grading Value of Diffusion Tensor Imaging in Patients with Carpal Tunnel Syndrome

*Haci Taner Bulut*¹, Adem Yildirim², Burcu Ekmekci³, H. Pınar Gunbey⁴

*Medical Faculty of Adiyaman University Radiology Adiyaman -Turkey*¹ *Medical Faculty of Adiyaman University Physical Medicine And Rehabilitation -Turkey*² *Medical Faculty of Adiyaman University Neurology Turkey*³ *Samsun Education and Research hospital Radiology -Turkey*⁴

PURPOSE: In this study we investigated the diagnostic and grading value of diffusion tensor imaging (DTI) in patients with carpal tunnel syndrome (CTS).

MATERIALS AND METHODS: Among the 120 subjects included in the present study, 72 were in the CTS group and 48 were in the healthy control group. Additionally, the CTS patients were further divided into three subgroups based on severity (mild, moderate and severe) according to electrophysiological studies (EPS). DTI-derived parameters (fractional anisotropy; FA, apparent diffusion coefficient; ADC) were evaluated at four median nerve levels. (Figure 1) The mean FA and ADC values of the CTS groups and healthy controls were compared separately. Correlations and possible relationships between DTI parameters and EPS results were analyzed. Receiver operating characteristics (ROC) analysis was used to calculate the FA and ADC cut-off values for CTS diagnosis and grading.

RESULTS: Statistically significant differences were observed in mean FA and ADC between the normal and mild, mild and moderate, and moderate and severe subgroups. Significant correlations were found between DTI parameters and EPS measurements based on severity. FA and ADC threshold values for diagnosing and grading CTS were determined, as well as the sensitivity and specificity levels.

CONCLUSION: DTI parameters can provide helpful information for CTS. The correlations of FA and ADC measurements versus EPS measurements based on severity were significant. Moreover, FA and ADC threshold values were sufficient for the diagnosis and grading of CTS.

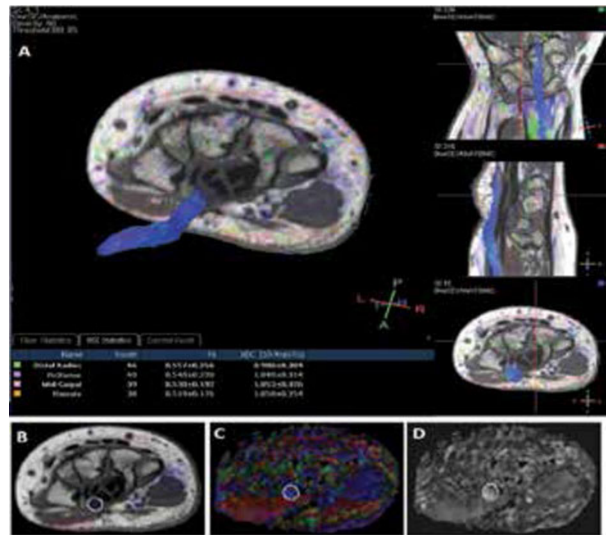


Figure 3. Topography of the median nerve, coded in blue, with superimposed on the coronal reference 3D-T2 weighted image (A) diffusion tensor imaging with superimposed on the posterior reference axial T2-weighted image (B) color coded FA map image (C) FA map image (D). Regions of interests were placed manually, surrounding the median nerve. (SLC2)

EP250-Tracking of Gd DTPA Labeled Mesenchymal Stem Cells by 7T MRI

Kuan Geng¹, Yanlong Jia¹, Tingting Nie², *Renhua Wu*¹

*2nd Affiliated Hospital, Shantou University Medical Department of Medical Imaging -China*¹ *2nd Affiliated Hospital, Shantou University Medical Department of Medical Imaging -China*²

OBJECTIVE: Recent developments in stem cell and gene therapy will require methods to monitor stem cell survival and integration repeatedly and non-invasively with a high temporal and spatial resolution in vivo. The aim of the study was to explore the possibility of the rat mesenchymal stem cells (MSCs) labeled with standard contrast agents (Gd-DTPA) for stem cell tracking.



POSTER PRESENTATIONS ABSTRACTS

METHODS: MSCs from bilateral femur of rats were cultured and propagated. Intracellular uptake of Gd-DTPA was achieved by using a non-liposomal lipid transfection reagent (Effectene) as the transfection agent. Electron microscopy was performed to detect the distribution of Gd-DTPA particles in MSCs, and labeling efficiency of Gd-DTPA particles on MSCs was evaluated using spectrophotometric. Viability and proliferation of labeled MSCs were evaluated using MTT assay. Labeled MSCs were detected with T1-weighted MR imaging in vitro and in rat brain.

RESULTS: The presence of Gd-DTPA particles inside the MSCs was definitely detected by transmission electron microscopy. Labeling efficiency was highly. There was no difference in viability and proliferation between the labeled and unlabeled confirmed by MTT values of light absorption. The labeled MSCs demonstrated the high signal intensity on T1-weighted MRI in vitro and in rat brain.

CONCLUSION: Rat MSCs can be labeled with Gd-DTPA particles without changing the cell viability and proliferation. Obviously labeled MSCs can be imaged in vitro and vivo. Gd-DTPA shows no evident adverse effect on the function of labeled MSCs. Gd-DTPA can be used for the MR imaging tracking of labeled MSCs

EP251-Quantitative MRI for the Evaluation of Active MS Lesions without Gadolinium Based Contrast Agent

*Ida Blystad*¹, Irene Håkansson², Anders Tisell³, Jan Ernerudh², Örjan Smedby⁴, Peter Lundberg³, Elna-Marie Larsson⁵

*Radiology, Department of Medicine and Health sciences, Centre for Medical Image Science and Visualization (CMIV) Linköping University, Sweden Radiology Linköping-Sweden*¹ *Department of Clinical and Experimental Medicine, Linköping University, Department of Neurology, County Council of Östergötland, Linköping, Sweden Neurology -Sweden*² *Radiation Physics, Department of Medicine and Health Sciences, Linköping University Radiationphysics -Sweden*³ *Radiology, Department of Medicine and Health sciences, Linköping University, Department of Radiology Radiology -Sweden*⁴ *Department of Radiology, Oncology and Radiation Science/Radiology, Uppsala University, Uppsala, Sweden Radiology*⁵

PURPOSE: Routine MRI-protocol for multiple sclerosis (MS) patients include intravenous administration of gadolinium based contrast agent (CA) for the detection of active MS-lesions. MS-patients have repeated MRI scans for treatment monitoring, and since there is a small but potential risk for harmful side effects of CA; it would be of great value to use a method without CA to detect active MS-lesions. This study was conducted to evaluate a new quantitative MRI-sequence to perform measurements of T1- and T2-relaxation times and proton density (PD) to assess the possibility of identification of active MS-lesions without CA.

METHOD: 44 patients with early MS were included in a longitudinal cohort study at the Department of Neurology, University Hospital Linköping, Sweden. Patients were examined with MRI at baseline, at relapse and after 1 year, a total of 92 examinations were obtained, 14 examinations had contrast enhancing lesions. The new MRI-sequence, with a 6 minutes scan time, was added to the clinical MRI-protocol. Lesions were classified as enhancing or non-enhancing by a neuroradiologist. 43 regions of interest (ROIs) were drawn in enhancing lesions and 622 ROIs in non-enhancing lesions. Lesional T1- and T2-relaxation times and PD-values were measured before CA-administration.

For comparison of relaxation times and PD-values a voxel based statistical analysis with a mixed linear model with patient and ROI identity as random effects, and Tukey t-test were used. In addition, Receiver Operating Characteristic (ROC) analysis was performed after aggregating data to the ROI level.

RESULTS: There was a significant difference ($p < 0.0001$) in relaxation times and PD-values between enhancing- and non-enhancing MS-lesions, see Table 1, where $R = T/1$. Enhancing lesions had shorter relaxations times than non-enhancing lesions. Receiver operating characteristics (ROC) analysis showed that with the combination of R1, R2 and PD an AUROC value of 0.799 was obtained. The ROC curve gave a sensitivity of 72% in combination with a 69% specificity.

CONCLUSION: Enhancing MS-lesions differs significantly from non-enhancing lesions with shorter



POSTER PRESENTATIONS ABSTRACTS

Seven patients were excluded due to dialysis. Of the 79 remaining patients, 16 were children mean age 11.8 range 10 to 17 years old. Among the remaining group (63 patients), 27 were males (mean age 33.4 years range 20 to 60) and 36 females (mean age 40 years range 18 to 78).

RESULTS: Thirty-two adults (50.8%) and 4 children (25%) had brain MRI evidence of small vessel disease in the basal ganglia, corona radiata, thalamus or brainstem, as well as in the periventricular white matter. Adults with MRI abnormalities were older (51.3 vs 30.6 years old $p < 0.01$).

Three women and one man (7% mean age 61 years) presented chronic microbleeds identified by GRE, in the pallidum and thalamus. Moreover, Flair and T2-weighted images showed evidence of white matter disease and deep grey matter involvement.

Only one patient presented the thalamic abnormality known as pulvinar sign.

CONCLUSION: In our group of adults with FD, without clinical history of CVA or prior dialysis, 50.8% showed evidence of small vessel disease on MRI, and 7%, presented cerebral microbleeds. FD is a treatable disorder that should be included routinely in the differential diagnosis of symptomatic and asymptomatic ischemic and microhemorrhagic lesions in young adults.

EP254-Highly Reconstructed MRI T2 Map by Optimized Principal Component Coefficient Algorithm Based on Compressed Sensing at 7.0 Tesla

*Guishan Zhang*¹, Gang Xiao², Zhiwei Shen¹, Renhua Wu¹

The Second Affiliated Hospital Shantou University Medical College Shantou-China¹ Math and Applied Mathematical Hanshan Normal University -China²

INTRODUCTION: Compressed sensing MRI (CS-MRI) is a burgeoning area of signal acquisition and processing based on the theories of applied mathematics. In this work, we exploit an optimized Principal Component Analysis (PCA) algorithm based on CS aiming to increase peak signal to noise ratio (PSNR) of sub-sampled MRI T2 map.

MATERIALS AND METHODS: The in-vivo SD mice brain experiments were conducted under an Agilent 7.0T animal MRI system, RE Coil =95/63. Routine fast spin echo sequence MRI parameters were used: TR=2500 ms, slice thickness=1mm, field of view (FOV) =60×60 mm², number of average (NSA) =1, bandwidth=50 kHz, frequency code = 256 and the phase encoding of the based image was 256, we sub-sampled the k-space data by altering phase encoding from 32 to 192 with 32 interval. And made the complex dual-tree DWT for the original images by the software of Matlab. The transverse magnetization as a function of time is sparse after combining with the optimized PCA algorithm by selecting principal component coefficients from highly under-sampled MRI data. We reconstructed the MRI T2 map by L2 norm regularization approach.

RESULTS: After being compressed, the number of zeros is 93.73% and the retained energy of the scanned T2 map is 99.29%. Most coefficients are small though nearly all the image pixels have nonzero values. T2 map obtained from a reduced data set can be reconstructed precisely by DWT-PCA algorithm. We closely analyzed the PSNR by comparing with the original one and find that the spatial resolution of the reconstructed T2 map is fine when the acquisition speedup factor is 4.

DISCUSSION: In this work, we proposed an optimized DWT-PCA algorithm based on CS to accelerate MRI T2 map with relatively high spatial resolution when reducing the acquired k-space data at 7.0 Tesla. This was an interesting initial finding. Further investigation of optimizing sequence for sub-sampling of k-space data is being explored. The results obtained are a further step towards the practical value in clinical application.



POSTER PRESENTATIONS ABSTRACTS

EP255-Hippocampal Disease Most Prevalent Pathological Conditions at Our Institution

Estefania Triñanes ¹, Pablo Martin Pfister ¹, Cecilia Rollan ¹, Hernan Chaves ¹, Paulina Yañez ¹, Carlos Romero ¹
*Instituto de Investigaciones Neurológicas Raul Carrea, FLENI Radiology -Argentina*¹

PURPOSE :- To report the most frequent hippocampal alterations found in our institution.

- To exemplify hippocampal formation pathology with cases from our institution.

METHODS: We searched our institutional database with the keyword hippocampal, hippocampus,

dentate, subiculum and fornix. We reviewed all the

MRI studies between June 2012 and June 2013, and

RESULTS: We found 994 patients that met the criteria, from

2-months-old to 93-years-old (mean age: 40-years-old). Pathologic

and malformative conditions were founded in 274 MRI studies,

including: malrotation (29,9%), atrophy (25,9%), mesial temporal

sclerosis (8,39%), tumors (6,57%), cysts (3,32%), transient global

amnesia findings (2,91%), encephalitis (2,19%), ischemia/infarct

(2,19%), and others unspecific conditions (18,61%).

CONCLUSIONS: A wide spectrum of pathological and

malformative conditions may involve de hippocampus.

All of these pathologies should be put into consideration to reach

a correct diagnosis. MRI studies focused on the hippocampal

formation should be tailored.

Quantitative measurements of normal appearing white matter (NAWM), enhancing and non-enhancing MS lesions (Least Square Mean ± Standard Error)			
	R1	R2	PD
NAWM	1.75 ±0.03	13.2 ±0.26	61 ±12
Enhancing lesions	1.11 ±0.03	8.9 ±0.26	80 ±1.22
Non-enhancing lesions	0.89 ±0.03	7.5 ±0.25	90 ±1.18
Difference between lesions	0.23 ***	1.4 ***	10 ***

R1 and R2 presented in [14], PD in %
***p < 0.0001

EP256-Diagnostic Value of Magnetic Resonance Imaging (MRI) and Apparent Diffusion Coefficient (ADC) in Determination of Grading of Astrocytomas

Reyhan Eddy ¹, Rahmad Mulyadi ¹, Tiara Anindhita ², Hartono Tjahjadi ³, Trevino Pakasi ⁴

*Faculty of Medicine University of Indonesia Radiology Jakarta Pusat-Indonesia*¹ *Faculty of Medicine University*

*of Indonesia Neurology -Indonesia*² *Faculty of Medicine University of Indonesia Anatomic Pathology -Indonesia*³

*Faculty of Medicine University of Indonesia Community Medicine*⁴

PURPOSE: Astrocytoma is one of the primary brain tumor with overall high mortality. MRI and ADC could determine astrocytoma grading before histopathological biopsy performed, hence patient education for treatment and prognosis could be established more early.

METHOD: A cross-sectional research is performed using brain MRI of patients with astrocytoma as histopathological diagnosis. Astrocytoma evaluation using MRI image with Dean et al criteria and ADC measurement for all part of tumor (Ab), single (Ap) and multiple (Ar) solid part of tumor in one axial section in ADC map. Data analysis is done to obtain diagnostic value of MRI image using Dean et al parameters and image scoring and ADC value to determine grading of astrocytoma based on sensitivity, specificity, and receiver operating characteristic (ROC) curve.

RESULT: MRI image parameters that is significant to determine low and high grade astrocytomas are border, hemorrhage, and heterogeneity. The sum of astrocytoma image scoring of Dean et al criteria with cut-off value of 7 and the evaluation of astrocytoma image in MRI to determine low and high grade astrocytoma has 90,9% sensitivity and 87,5% specificity. ADC, for Ap and Ar, is significant to determine low and high grade astrocytoma with sensitivity up to 90,9% and specificity up to 87,5%.

CONCLUSION: MRI and ADC has high sensitivity and specificity to determine low and high grade astrocytoma.



POSTER PRESENTATIONS ABSTRACTS

EP257-Effect of a Mediterranean Diet Intervention on 3T MRI Monitored Carotid Plaque Progression and Vulnerability. A Sub Study of the PREDIMED Trial

*Núria Bargalló-Alabart*¹, Aleix Sala-Vila², Rosa Gilabert³, Edwin-Saúl Romero-Mamani⁴, Ramón Estruch⁵, Emilio Ros²

*IDIBAPS, Hospital Clinic de Barcelona MRI Core Facility; Diagnostic Imaging Centre Barcelona-Spain*¹ *IDIBAPS, Hospital Clinic de Barcelona; CIBERobn Lipit Clinic Unit, Endocrinology and Nutrition Service -Spain*² *IDIBAPS, Hospital Clinic de Barcelona Diagnostic Imaging Centre -Spain*³ *IDIBAPS, Hospital Clinic de Barcelona Department of Internal Medicine -Spain*⁴ *IDIBAPS, Hospital Clinic de Barcelona; CIBERobn Department of Internal Medicine -Spain*⁵

AIM: The North-to-South gradient in coronary heart disease mortality could be explained in part by local dietary habits, such as adherence to the Mediterranean diet (MedDiet). We hypothesized that in older individual at high cardiovascular risk with carotid plaque, a MedDiet supplemented with either extra-virgin olive oil (MedDiet+EVOO) or mixed nuts (MedDiet+nuts) would induce changes on vessel wall volume and plaque composition (assessed by 3T magnetic resonance image [MRI]), toward less vulnerability compared to a control (low-fat) diet.

METHODS: Carotid ultrasound was performed in 245 participants in the PREDIMED trial of primary cardiovascular prevention with MedDiets (50% women, mean age 69 y). Subjects with plaques ≥ 2 mm thick (n=92, 38%) were invited to undergo MRI at baseline and after intervention for a mean of 1.8 years. Black-blood T1-weighted, T2-weighted, proton density-weighted images with fat and flow suppression and post gadolinium sagittal 3D MPRAGE and 2DT1 weighted images were obtained to evaluate vessel wall and plaque composition. Carotid bifurcation was covered by 9 slices with 2D sequences. Main outcomes were vessel wall volume, plaque components, total plaque volume and plaque index.

RESULTS: We evaluated 60 subjects with complete data (19 control diet; 20 MedDiet+EVOO; 21 MedDiet+nuts). In a multivariate model, after adjusting for sex, follow-up time and in-trial changes in statin treatment, changes in vessel wall volume (mm³) were (mean [95% CI]): 0 (-51 to 50) for the control group; -29 (-75 to 18) for the MedDiet+Nuts group; and -98 [-145 to -51] for the MedDiet+EVOO group (p=0.024 versus control). No significant changes were observed in other outcomes.

CONCLUSION: Compared to a control diet, consumption of a MedDiet supplemented with EVOO is associated with regression of carotid wall volume. The results contribute mechanistic evidence for the reduction of cardiovascular events observed in the arm supplemented with EVOO in the PREDIMED trial.

EP258-Effects of Selegiline on Lesion Size and Rat Endothelial Cell Adhesion Molecule (RECA) Expression in a Rat Stroke Model

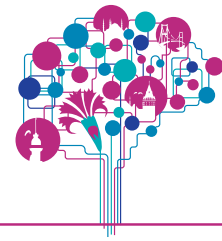
*Nandor Pinter*¹, Sandor Nardai², Zoltan Nagy³

*National Institute of Clinical Neurosciences Department of Neuroradiology Budapest-Hungary*¹ *Semmelweis University Heart and Vascular Center -Hungary*² *National Institute of Clinical Neurosciences -Hungary*³

PURPOSE: Previous studies have shown that acute treatment by selegiline decreases infarct size after occlusion of the middle cerebral artery (MCA) in rodents. Our study focuses on the potential effect of the selegiline on blood-brain barrier (BBB) integrity and post-stroke angiogenesis after transient middle cerebral artery occlusion (tMCAO) by measuring lesion size and rat endothelial cell adhesion molecule (RECA) expression.

METHODS: Brain ischemia was induced in adult male CD rats using MCA filament occlusion model. Treatment started 48 hours after 60 minutes of tMCAO. In Group I and II (n=6+6) animals were infused with 0.2 mg/kg/day of selegiline in a vehicle of 0.9% physiological saline for seven days. In Group III and IV (n=6+6) rats were infused with the vehicle only.

Six days after the initiation of treatment magnetic resonance imaging (MRI) was performed on a 1.5T Philips



POSTER PRESENTATIONS ABSTRACTS

Achieva scanner with 3D T1 FFE (WATSc) and T2 weighted 3D VISTA scan. Planimetric measurement was performed for lesion segmentation.

Nine days after the MCAO procedure tissue was sampled for RNA arrays in Groups I and II and immunostaining for RECA in Groups II and IV. Total number of RECA cells with an identifiable cell nucleus was counted on confocal images.

Planimetry data and immunoreactivity values of the treatment and control animals were compared applying Mann-Whitney tests.

RESULTS: 3D VISTA scan 8 days following tMCAO showed significantly decreased lesion size in selegiline treatment compared to controls ($p=0,047$). 3D T1 FFE did not show significant change in the size of lesions. Our c-DNA study has revealed increased mRNA expression of RECA ($p=0,016$). We have observed an increased density of RECA positive microvascular structures ($p=0,037$) in the selegiline treated animals 9 days after tMCAO.

CONCLUSION: Selegiline treatment significantly elevated the mRNA expression of RECA in the territory surrounding the ischemic lesion, with an associated increase in microvascular density and an increased resorption of edema on MRI.

As the restoration of BBB integrity is crucial for functional recovery of brain tissue following ischemia, and the increased microvascular density in stroke patients is associated with improved prognosis, these effects of selegiline may have clinical significance.

EP259-Lexicographic Analysis of Neuroradiologic Reports for Identification of Key Concepts and Relationships between Them

*Luke Gerke*¹, Bradley Delman¹

*Mount Sinai School of Medicine Neuroradiology New York-United States*¹

PURPOSE: The radiologist's fundamental job is the conversion of images to text reports. This task might be modeled as

-making/interpreting the findings

-composing a textual report that conveys findings as well as elaborations on the findings' import and pertinent negatives.

So, in addition to facts regarding the images, reports give insight into the thought-process of the radiologist. Numerous studies address the identification/interpretation of findings, but we know of no systematic evaluation of reports to discover the radiologist's thought process as conveyed in the report's lexicographic structure.

METHODS: In the course of a quality assurance assessment, we performed basic lexicographic analysis (using well-established linguistics techniques) of a bulk of reports. Statistical analysis of the bodies of reports compared to a large volume of non-medical text identified a library of words and phrases (tokens) that are significantly more commonly used in radiology than elsewhere (eg "subdural hematoma"). Statistical analysis of tokens that commonly were seen to be located "near" each other in radiology prose identified concepts that were closely related (eg "subdural hematoma" and "midline shift"). Subgroup analysis of reports generated by radiologists early in training compared to seasoned radiologists identified tokens and relationships between concepts that are less commonly described by radiologists in training.

RESULTS: Statistical analysis of a large body of reports yields a putative dictionary of tokens important to the practice of neuroradiology. Subsequent analysis of other tokens that were located "near" radiologically-important tokens provided significant relationships between reported concepts. Comparison of reports generated by seasoned neuroradiologists to those of trainees have significant differences in the relationships between tokens. For instance, related to "subdural," attending radiologists are more likely than trainees to use the words "transtentorial," "exert," "hygroma," "sagging," "growing," "empyema," and "onionskin." A subset of relationships is presented graphically, and the entire dataset is made available online with an easily explored web graphical user interface.



POSTER PRESENTATIONS ABSTRACTS

CONCLUSIONS: Prose radiology reports contain more information than just their positive findings. Here, we find that they contain easily-extracted lexicographic structure, which reflects the thinking of their authors. There exist diverse applications for this information, from tailoring of training given to residents and fellows to realtime quality tools that suggest additional topics that a radiologist might address as he dictates.

EP262-Evaluation of Corticospinal Tract Radiation Exposure by Implementation of Tractography in Gamma Knife Treatment Planning of Cerebral AVMs

*Giuseppe Kenneth Ricciardi*¹, Roberto Foroni², Antonio Nicolato², Michele Longhi²,

Pasquale Mirtuono², Francesca Benedetta Pizzini², Alberto Beltramello¹

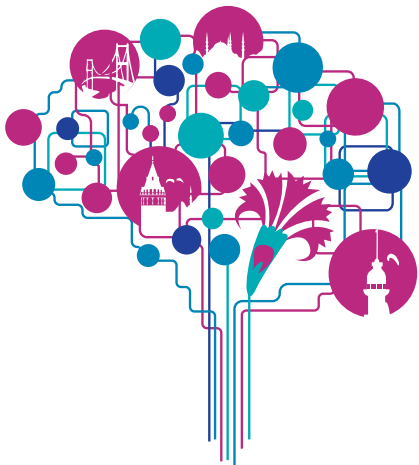
*Azienda Ospedaliera-Universitaria Verona Neuroradiology Verona-Italy*¹ *Azienda Ospedaliera-Universitaria Verona Stereotactic Neurosurgery -Italy*²

PURPOSE: Radiosurgery (RS) is a highly effective procedure. The rate of complications is low but not negligible, especially for AVMs located in critical sites such as cortical areas and white matter tracts. These structures can only be guessed on the basis of knowledge of normal anatomy. We have implemented corticospinal tract (CST) representation, obtained by diffusion tensor imaging (DTI) tractography, into γ -knife treatment planning, to evaluate its exposure in patients with deep cerebral AVMs.

MATERIALS AND METHODS: 34 patients harbouring a cerebral AVM located in close proximity to the CST were studied at 3.0 T with DTI acquired in non-stereotactic conditions. CST tractography was then registered and embedded within the stereotactically acquired treatment planning images obtained at 1.0 T. Measurement of CST spatial separation from AVM margins, evaluation of the maximum dose and integral dose and of the volumes of the tract receiving ≥ 25 -20-15-12 Gy were performed. Patients underwent a median follow-up of 3 years. Results from the retrospective group, 14 pts in which only CST exposure evaluation was performed, were compared with the prospective group, 20 pts in which CST exposure evaluation led to treatment plan modification.

RESULTS: The distance between AVM margins and reconstructed CST varied from 0 (CST inside the target volume) to 17 mm. The volume of the CST receiving ≥ 20 Gy and ≥ 15 Gy and the integral dose were higher in the retrospective group. AVM obliteration rate was 70% in the retrospective group and 72% in the prospective group. Morbidity was 14.3% in the retrospective group, and 5% in the prospective group. Complications occurrence correlated significantly with: volume of the CST receiving ≥ 12 Gy (310 cc for a complication rate of 5%) and integral dose of the CST (10.7 mJ for a complication rate of 5%).

CONCLUSIONS: CST tractography integrated in γ -knife RS of deep-seated brain AVMs can be useful in decreasing post-treatment morbidity rates.



XXth
Symposium
Neuroradiologicum

AUTHORS INDEX



AUTHORS INDEX

AUTHORS INDEX

- A Abdelrahman, O165
Abdallah Amir, EP180
Abdul Hamid Zuhanis, EP131
Abdul Kadir Khairul Azmi, EP148
Abe Kayoko, EP038
Abe Toshi, EP022, EP069
Abela Eugenio, O234
Abo-shaer Hussam, O175
Absil Julie, O134
Acar Nazire Pinar, EP093, EP004
Ada Emel, EP089, EP244
Ada Halil Ibrahim, EP139
Adachi Yuko, O090
Adaletli Ibrahim, O081
Adin Mehmet Emin, O152
Afandiyev Yunus, O079
Aghakhanyan G., O012
Aguilar-pérez Marta, O189, O168
Ağildere Ahmet Muhteşem, EP058
Ağirlar Tuğçe, EP139
Ahmed Dr Kalim, O055, EP078
Ahmed Manzoor, EP197
Ahn Kookjin, EP228, EP105
Ahn Sung Jun, EP079
Ahuja Chirag K, EP112, EP113
Aida Noriko, O078
Aihara Yasuo, EP038
Ajmi Houda, O018
Akashi Toshiaki, O053
Akbari Kaveh, O041
Akbiyik Filiz, O230
Akgul Erol, O178
Akhtar Naveed, O054, O042
Akintokun Abdulazeez, EP218
Akita Sadanori, EP085
Akkon M.koray, EP230
Akmaz Unlu Havva, O081
Aksungur Erol, O178
Akyol Beyoglu Cigdem, O024
Al Rukun Sohail, O054
Alattas, fatima Dr, O205
Alazzaz,abdulkader Prof, O205
Alberawi Mohamed, O006
Aldandan Sadeq, EP217, EP218
Aljadhai Yaser, EP216
Alkan Ozlem, O091
Alkaphoury Mohamed, O042
Alqahtani Sultan, O175
Alrashed Abdullah, EP217, EP218
Alrayahi Jehan, O006
Alsenani Fahmi, O175
Alshail Essam, EP197
Alterman Ron L, EP077
Amel Ben Abdallah, EP177
Amira Berrich, EP177
Anagnostakou Vania, O179
Ananyeva N. Mr-morphometry Of Hippocampus In Mdd Patients And, EP248
Andersson Tommy, O043
Andreou Ioannis, EP243
Andreu Arasa Carlota, EP009
Andronikou Savvas, EP192
Anik Yonca, EP119
Anindhita Tiara, EP256
Ankenbrank Monika, O003
Anno Izumi, EP187
Anwary Farhan, EP183
Aoki Ichio, EP232
Aoki Shigeki, EP053, O090
Aoyagi Yoshinori, O217, EP104, O026
Apaydin Melda, O121
Apaydin Demir, O068
Aprile Italo, EP012
Aquilina Kristian, O034
Arculeo Paolo, EP021
Arculeo Simona, EP021
Arifa Nadia, O018
Arikan Fuat, EP206
Arnberg Fabian, EP106, EP108
Arous Aymen, EP180
Arpaci Rabia, O068
Arrighi R., O012
Arsava Ethem Murat, EP093
Arslan Ilker Burak, O070, EP087
Arturo Alonso, EP147
Arya Monika, O095, O196
Aslan Kerim, EP201
Aşık Murat, EP013
Azizi Amel, O064, O186
Azuma Minako, O135, EP010
Babbel Robert, O141
Babiarz Lukasz S., O002
Bachhav Vrushali, EP017
Bader Ana, O140
Badilla Lautaro, EP047, EP048, EP046
Baek Hye Jin, EP001
Baek Seung Hwan, EP029
Baima Joseph, O141
Balavenkatesh Kanna, O215
Balazs Gyorgy, O016
Balli Tugshan, O178
Bally Julien, O210
Barbour Randall, O225
Barcelo Ines, EP059
Bargalló-alabart Núria, EP257
Barker Peter, EP236
Barkovich A. James, EP232
Barletta Laura, EP155
Barnaure Isabelle, O210
Barone Frank, O225
Barreau Xavier, O159
Barrios Fernando A, EP077
Barros Oliveira De Moura Wellington, EP186
Barsi Peter, O016
Barthol Alexandra, O041
Bartolini Bruno, O171
Bartolozzi Carlo, EP088, O203
Basak Muzaffer, O190
Bashir Mariah H., O005, O060
Bastianello Sefano, O141
Bateman Kathleen, EP025
Battapady Harsha, O004
Bauer Jan, EP247
Baykan Ali Haydar, EP039
Bayraktarov Elmar, EP184
Bazinas Theodoros, EP141
Bäzner Hansjörg, O168, O189
Becco Neto Eliseu, EP170
Beck Joris, EP114
Becker Albert, O209
Bekci Tümay, EP201
Belardinelli Giulia, EP012
Beltramello Alberto, EP262
Ben Hamouda Mohamed, EP180
Ben Tebra Aymen, EP208
Bender Benjamin, O227
Bendszus Martin, O107
Bengtsson Anders, O114
Benine Belizia Anderson, EP120
Beomonte Zobel Bruno, O206
Berestov Vadim, O182



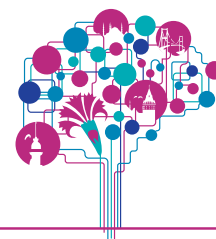
AUTHORS INDEX

- Bergamino Maurizio, EP155
Berge Jerome, O159
Berlis Ansgar, O159
Bernardi Bruno, O086
Berriche Amira, O018
Berroir Pierre, O132
Bert Robert, O038, O060, O005
Bertsias Georgios, O149
Beuing Oliver, O181
Beyaz Pinar, EP013
Beydoun Ahmad, O009
Bhalla Ashish, EP112, O153
Bhanu Kovilapu Uday, O153
Bhate Sanjay, O034
Bhatti Shahzad Karim, O220
Bhuta Sandeep, O146, O073
Biçkin Hande, EP119
Bido José, O111
Bienert Thomas, O021
Bieri Oliver, O098
Bilginer Burcak, EP006
Bilska Margaret, O146
Biondi Alessandra, O064, O187, O188, O186, O181, O159
Bisdas Sotirios, O030, O116, O118, O227, O119, O117
Bitti Grazia, EP226
Bladowska Joanna, EP166, O025
Blanc Rafael, O159
Blanc Raphael, O171
Blitz Ari, EP152, O067, O069
Bloem Bastiaan, EP056
Blystad Ida, EP251
Boccardi Edoardo, O181
Boeck-behrens Tobias, EP247
Boex Colette, O210
Boland Michael, EP152
Bona Francesco, O113
Bonaccorsi Raphaël, O015
Bonafé Alain, O181, O159
Bonaldi Giuseppe, EP188, O013
Bonanni G, O126
Boos Lynn, O216
Boronat Susana, O084
Botelho Luís, EP211
Boumpas Dimitrios, O149
Bouzayen Faten, EP208
Bozkaya Halil, EP130, O156, O212
Bracco Sandra, O043
Bracke Peter, EP114
Braun Christian, O030
Braun Christian Braun, O227
Brem Christian, O164
Brew Stefan, O034
Brouwer Patrick, O181
Brunel Hervé, O159
Brückmann Hartmut, O164, EP143
Bryan Nick, O004, O231, O044
Bryukhov Vasilii, O229
Buča Ante, EP091
Buchory Eppy, O222
Bueltmann Eva, O141
Bulut Haci Taner, EP039, EP249
Burkhard Pierre, O210
Butler Ernie, EP261
Byrd Sharon, EP017
Byun Jun Soo, O133
Callı Cem, O121
Calvo-rado Nestor, EP059
Cambiaso Paola, O086
Canapicchi R., O012
Candy Sally, EP192, EP025
Cano Paola, O084
Cantone E, O126
Cao Zhen, EP234
Caputo Nevia, EP012
Carducci Chiara, O086, O056, O019, O198
Carey John P, O067, O069
Carilho Inês, EP211
Carlos Romero, EP253
Castellan Lucio, EP155
Cattaneo Giorgio, O216
Cattin Françoise, O187, O188
Caulo Massimo, EP241
Cavusoglu Berrin, EP244
Cecilia Rollan, EP253
Cejas Claudia, EP239
Celebi Ozlem, O230
Cerase Alfonso, O043
Ceratto Rosana, EP050
Cerqueira Luís, EP042
Cha Jihoon, O066, O076, O077
Cha Sang-hoon, O226
Chan Cm, O173
Chandra Ronil, EP261
Chang Chian Aun, EP261
Chang Feng Chi, EP110, EP151, O169, O074, EP092, O052, O174, EP055, EP007
Chanthanaphak Ekachat, EP137, EP136
Chapot René, O159
Charchafliéh Jean, O225
Charvat Frantisek, O197
Charyasz Edyta, O118
Chatterjee Fiona, EP124
Chaudhary Umair Javaid, O228
Chaves Hernan, EP255, EP239
Chawla Y, EP113
Chen Cheng-yu, EP011
Chen Chien-chih, EP237
Chen Chih-feng, O233
Chen Chi-jen, EP008, O088, EP231, O046
Chen Ching-wen, EP096
Chen Clayton Chi-chang, EP008
Chen David Yen-ting, O088, EP231, O046
Chen Fang, EP246, O191, O036, EP233
Chen Hsiu-ling, EP237, O115
Chen Pei-chin, EP237
Chen Ty, O109
Chen Wei-liang, EP127
Chen Yao-liang, O059
Cheung YI, O173
Chiang Shih-wei, EP011
Chiras Jacques, O087, O015, O171, O031
Cho Young Ah, EP165, EP207
Choi Changho, EP247
Choi Chi-hoon, O226
Choi Choong Gon, O104, O105, EP161, O103, O108, O232, O106
Choi Choong Gon, O137, O102, O138
Choi Hyunseok, EP228
Choi Jin Wook, O072,
Choi See-sung, EP071
Choi Seung Hong, O139
Choi Si Sung, EP122
Choi Woo Suk, EP052, O033
Choi Yoon Seong, EP079
Choi Young Jun, O232
Chong Abigail, EP261



AUTHORS INDEX

- Chou Kun-hsien, O115
Chou Ming-chung, EP011
Chowchun Prathana, O202
Christer Halldin, EP106
Chuah Kenneth, EP261
Chuang Ming-tsung, EP096
Chuang Tzu-chao, EP007
Chudyk Jorge, O195
Chung Gyung Ho, EP101
Chung Hsiao-wen, EP011, EP007
Chung Sae Rom, EP207
Chung Won Jung, O137
Cianfoni Alessandro, EP241, O013, EP188
Cinar Celal, EP130, O156, O212
Citton V, O126
Citton Valentina, O113
Clarençon Frédéric, O015, O087, O031, O171
Colosimo Cesare, O141
Conceição Carla, EP115, EP042, EP116
Consoli Arturo, O043, O028, O184
Coppola G, O126
Cordier Dominik, O098
Cormier Evelyne, O015, O087
Cortes Alvaro, EP206
Cosottini Mirco, EP088, O203
Costa Lima Maia Rafael, EP170, EP186
Costalat Vincent, O159
Courtheoux Patrick, O159
Craparo Giuseppe, EP021
Cubbison Caroline, O154
Cukurova Ibrahim, O070, EP087
Çağlar Emrah, EP149
Çağlayangil Serdar, EP119
Çam Isa, EP119, EP139
Çetinayak Hasan Oğuz, EP089
Çifçi Bilal Egemen, EP194, EP058
Çiftçi Ercüment, EP139
Çoban Gökçen, EP058, EP194, O022
D Orazio Federico, O198, O019, O056
Da Conceição Araújo Filho Stelio, EP170, EP186
Daga Pankaj, O110
Dahlmann-noor Annegret, O129
Dai Zhuozhi, O125, EP235, EP095
Daire Arthur, EP192
Davagnanam Indran, O200, EP179, O129, O130
Davatzikos Christos, O044, O004
De Belder Frank, EP176
De Carlo E, O126
De La Calle María, O082
De Lima Docema Marcos Fernando, EP163
De Pino Gabriela, EP239
De Sousa Godoy Luis Filipe, EP163
De Souza Delgado Daniel, EP163
De Temmerman Gunther, EP114
De Vita Enrico, EP179
De Vries Joost, O181
Debare Mathieu, O031
Degos Vincent, O031
Deike Katerina, O107
Delgado Ignacio, O084, EP206, O083
Delman Bradley, EP259, O140
Del-valle Mariano, EP059
Demerath Theo, O218
Demir Senay, O091
Demirci Ali, EP119
Derakhshani Shahram, O181
Derinkuyu Betül, O081
D'errico A, O126
Desai Shrinivas, EP117, EP195, O193, EP118
Desal Hubert, O159
Descourvierer Florence, O187
Desideri Iliaria, EP088, O203
Dhifallah Maher, EP082
Dhiman Rk, EP113
Di Maria Federico, O171, O031
Di Renzo Antonio, EP012
Di Rocco Federico, O224
Di Salle F, O126
Dikici Suleyman, EP013
Dimova Petya, EP168
Diogo Mariana, EP116, EP042, EP115
Divano Luisa, O061
Djokovic Svetlana, EP103
Doebroessy Mate, O021
Dogar Mohammad, EP197
Dolić Krešimir, EP091
Doria Roberta, EP088
Dorobek Malgorzata, EP107
Dowlut Sharoona, O010
Driss Nabil, EP082
Drissi Cyrine, EP180
Drózdź Tomasz, O141
Drummond Katharine, O101, O100
Duarte Nancy, O109
Ducic-jaramaz Tatjana, EP103
Duman Enes, EP194
Duncan John S., O110
Duseja Ajay, EP113
Dyawarkonda Kirankumar, O161
Eckstein H.-h., O040
Eddy Reyhan, EP256
Efthymiadou Roxani, EP243
Egger Karl, O021
Ekmekci Burcu, EP249
El Shikh Samer, O159
El Sotouhy Ahmed, O054
Eldib Ahmed, O160
Elefante E, O126
Elibol Bulent, O230
Elshikh Samer, O218
Elsotouhy Ahmed, O006, O042
Emek Savas Derya Durusu, EP244
Enokizono Mikako, O078
Erbaş Oytun, O121
Erbay Ayse, O091
Ernemann Ulrike, O116
Ernerudh Jan, EP251
Ersek-rakic Vera, O017
Ertem Furkan, EP013
Ertl Lorenz, EP143, O164
Erus Guray, O004, O044
Estruch Ramón, EP257
Etchegaray Adolfo, EP239
Eun Choong Ki, EP001, EP063, EP062
Evans Abigail, O211
Evans Matthew Rb, O096, O097
Evren Vedat, O121
Ezura Masayuki, O150
Fadeeva Ludmila, EP111
Fadili Sarah, O087
Fainardi Enrico, O043



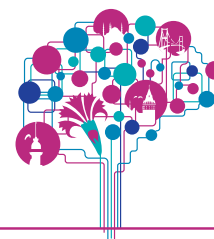
AUTHORS INDEX

- Fanouriakis Antonios, O149
Farah Eviane, O187, O188, O186
Faria Do Amaral Lázaro Luís, EP120
Farrher Ezequiel, O020
Fasen Bram, EP056
Fatterpekar Girish, O140
Fava Renata Mendes Lacerda, EP199
Favaro A, O126
Favaro Angela, O113
Federspiel Andrea, O234
Fellner Christine, O041, O001
Fellner Franz, O001, O041
Feltrin Leonir Terezinha, EP199
Fermin-delgado Rafael, O124
Fernández-zubillaga Amelia, O082
Ferrario Angel, EP050
Fesl Gunther, EP143, O164
Fiaschini Paola, EP012
Fiehler Jens, O159
Figà Talamanca Lorenzo, O086
Filipek-gliszczynska Anna, EP107
Filippi Vassiliki, EP243
Finnsson Johannes, O151
Fischer Sebastian, O168
Fjetland Lars, O049
Flores Arnaud, O188, O187
Florescu Diana, EP213
Flöry Daniel, O041
Foerster Bernd, O154, O111
Forbrig Robert, O164, EP143
Foron Roberto, EP262
Fowkes Mary, O140
Fox Michael D, EP077
Fragata Isabel, EP042, EP115, EP116
Fraser Clare, O200
Frattoni Tiziano, O141
Frijia F., O012
Fritz Joseph, O128
Fu Jui-hsun, EP007, EP044, EP154
Fujii Yuta, O078
Fujimoto Hideo, EP146
Fukami Tadateru, O223
Fukuoka Junya, EP085
Furdal Michal, O025
Furtner Julia, O227
Fuse Yoshihiko, EP094
Futatsuya Koichiro, O023F, O147
Gabrillargues Jean, O159
Gadde Judith, EP037
Gagliardo Cesare, EP021
Gaha Mehdi, EP208
Gaikwad S B, O163
Gaillard Francesco, O100, EP026, O101
Gailloud Philippe, O067
Galassi Stefania, O086
Gallas Sophie, O159
Gallucci Massimo, O056G, O019, O198
Ganesan Vijeya, O034
Gangatharan Shane, EP026
Ganslandt Oliver, O189
Garcia Meritxell, O098
Garzón Gonzalo, O082
Gasiorowski Jacek, O025
Gassent-balaguer Carmen, EP059
Gen Yan, EP238
Geng Kuan, EP095, EP250
George Sharad, EP216, EP217
Georgievski-brkic Biljana, O037, EP103
Georgoulas Panagiotis, EP243
Georgy Bassem, O008
Georgy Mark, O008
Gerke Luke, EP259, EP215
Gersing Alexandra Sophia., O003, O027
Gete Katia, O064, O186, O188
Gevorgyan Tigran, O225
Gilabert Rosa, EP257
Giordano Aldo Victor, O019, O056, O198
Glikstein Raphael, O145
Gloor Monika, O098
Gobbi Claudio, EP241
Gocmen Rahsan, EP006, EP093, EP003, EP004, EP190
Godi Claudia, EP179
Goedseels Koen, EP114
Goh Myeong Ju, O102, EP019
Gok Mustafa, EP130, O156, O212
Goldman Serge, O134
Gomi Masanori, EP135
Gomyo Miho, EP034, EP035
Gonzalez-reinoso Massiel, O154
Goora Tejas, O010
Goraj Bozena, EP056
Gorbatikh Anton, O182
Gounis Mathew, O181
Gowland Penny, O130
Goyal Mayank, O141
Goyanna Lyra Tatiana, EP163
Gökdemir Mahmut, EP194
Graber Harry, O225
Graf Markus, O107
Graff Björn A., O136
Grafström Jonas, EP108
Grant Michael P., O002
Greco V., O012
Greggio Na, O126
Gregori Lorenzo, O019
Grimm Jane, O143
Grinberg Farida, O020
Guida Melania, O203
Guler Ezgi, EP003
Gulyás Balázs, EP106
Gunadi Felicia Pilar, EP183
Gunbey H. Pınar, EP249
Guo Gang, O191, O036, EP233, EP246
Guo Wang-yuo, O074, O052, EP055, O174, O169, EP151, EP092
Gupta Mukesh Kumar, EP078, O055
Gupta Sk, EP132
Gupta Vivek, O213, EP132, EP112
Gurgel Fernandes Tavora Daniel, EP170, EP186
Gursoy Merve, O069, O002, O067
Guryıldırım Melike, O208
Gültekin Serap, EP230
Gümüştaş Sevtap, EP139
Ha Bon Chul, O133
Haas Carola, O021
Hackney David B, EP077
Haddow Lewis, EP179
Haitchi Gerhard, O001
Hakan Demirkan Tulin, O081
Håkansson Irene, EP251
Hamad Ayman, O175
Hamdi Radhouane, EP082, EP157
Hammami Nadia, EP180
Hamza Hassine, EP157, EP082



AUTHORS INDEX

- Han Miran, O072
Han Young Min, EP101
Hanna Michael, O096, O097
Haraguchi Kenichi, EP146
Harkanyi Zoltan, O016
Harrison Simon, EP026
Harsan Laura, O021
Hartmann Marius, O181
Has Arzu Ceylan, O230
Hashim Hilwati, EP131, O051
Hashimoto Takao, EP252
Hasiloglu Zehra Isik, EP013
Hayashida Eri, O135
Haznedari Nicolò, EP012
Heiko Körner, O158
Helle M., O040
Henkes Hans, O189, O168
Heo Youngjin, EP161
Hermoye Laurent, O117
Hernan Chaves, EP253
Hernandez Giancarlo, O111
Herskovits Edward, O231
Hesselink John, EP074
Hirohata Masaru, O180
Hiari Yasuhiro, O147
Hioki Miki, EP252
Hirai Toshinori, O135, EP010, O141
Hirano Akiyoshi, EP085
Hiratsuka Yoshiyasu, EP018, EP020
Hirotoshi Imamura, O181
Hiwatashi Akio, O065
Holmin Staffan, O162, EP106, EP108
Honda Hiroshi, O065
Hong Doran, O035
Hong Gil-sun, O104
Hori Masaaki, EP076, O090
Hosoya Takaaki, EP066
Hourani Roula, O009
Hsiao Yi-hsiu, EP011
Hsu Charlie, O146
Hsu Hsian-he, EP229
Hsu Hui-ling, O088
Hsu Shuo-hsiu, EP007
Huber Thomas, EP247
Huisman Thierry A. G. M., O014
Hung Alex S. C., EP055
Hung Sheng-che, O174
Huppertz Hans-jürgen, O209
Hwang Daehyun, EP126, EP245
Hwang Jae-yeon, EP207
Hwang Jinwoo, O226
Hwang Seung Bae, EP101
Hwang Yoon Joon, EP182, EP133
Hyare Harpreet, EP124
Iaia Alberto, EP037
Iancu Daniela, O145
Ide Satoru, O023
Ide Satoru, O147
Ihn Yon Kwon, EP182I, EP133
Iizuka Yuo, O177
Illarioshkin Sergey, EP242
Im Sooah, EP070I, EP105
Inaoka Tsutomu, EP102
Inkaya Ahmet Cagkan, EP004
Ireland Tim, O073
Irie Ryusuke, O090
Iryo Yasuhiko, O135, EP010
Ishibashi Ryota, EP135
Ishige Naoki, EP094
Isik Hasiloglu Zehra, EP184, O081
Iskandar Agustinus, EP109
Islak Civan, O179, O024
Ismail Mohd Redzuan, O051, EP144
Iwata Tomonori, O026
Iwata Tomonori, O217, EP104
Izbudak Izlem, O032I, EP158, O014
Izumi Takashi, EP146
Ibrahim Tamer, O050
Ikiz Ahmet Ömer, EP089
Jaafar Ainul Syahrilfazli, EP144
Jacinto Ariana, EP212
Jacinto João, EP116, EP115, EP042
Jacobs David, O004
Jager Rolf, EP124
Jäger Hans Rolf, EP179
Jahng Geon-ho, O232, O033, EP052
Jang Ji Hye, EP052, O033
Jang Jinhee, EP228
Janković Stipan, EP091
Janz Philipp, O021
Jasovic Andja, O010
Jean Betty, O159
Jeelani Owase, O034
Jemel Hafedh, EP180
Jeon Pyoung, O155, EP129
Jeon Se-jeong, EP071
Jerbi Omezzine Saida, EP082
Jerbi Omezzine Saida, EP157
Jia Yanlong, EP067J, EP235, EP250, O089
Jiarakongmun Pakorn, EP137, EP136
Jin Gong Yong, EP101
Jin Kwang Nam, O057
Jingu Keiichi, EP178
Jito Junya, O223
Johannessen Frode, O049
Johnson Steven, EP213
Jones Rhondda, O146
Jonsson Stefan, O162
Josefsen Roger, O136
Joseph L, O163
Jönsen Andreas, O114
Juan Chun-jung, EP229
Jung Ah Young, EP165, EP207
Jung Hye Na, O066
Jung Kwan-jin, O005, O060
Jung Seung Chai, O138, O137, EP161, EP019
Jung Solyung, EP228
Jung Won Sang, EP133
Jüni Peter, O234
K Ahuja Chirag, O213
Kadziolka Krzysztof, O159
Kakeda Shingo, O147, O023
Kakehata Seiji, EP066
Kakkar Ritu, EP195, EP117, EP118, O193
Kalra Naveen, EP113
Kalthoum Tlili, EP177
Kamagata Koji, O090Kamagata Koji, EP053
Kamel Hussain, O054, O042, O006
Kaminou Toshio, EP154
Kamiya Kouhei, O090
Kamran Saadat, O054, O042
Kanasaki Yoshiko, EP044
Kang Heoung Keun, EP098K, EP097



AUTHORS INDEX

- Kang Hyun Koo, EP061, EP016
Kang Koungh Mi, O057
Kanoto Masafumi, EP066
Kao Hung-wen, EP011
Kao Yi-hsuan, EP092
Karaca Mustafa, EP090
Karaman Yasemin, O068
Karantanas Apostolos, O149
Karim Yaseen, O160
Karli Oguz Kader, O230
Kasaba Ardhiana, EP109
Kasai Rumiko, EP102
Kasakura Shigen, O026, EP104, O217
Kasuya Shusuke, EP102
Katharina Förster, O216
Kato Yumiko, EP178, O053
Katsaros Vasileios K., O227, O119K, O117, O116., O030, O118
Katsarou Agapi-alexandra, O117
Kavroulakis Eleytherios, O149
Kayadibi Yasemin, O081
Kayadibi Yasemin, EP184
Kechagias Dimitrios, EP243
Kessler Thomas M, O234
Keuler Andreas, O216, O218
Khandelwal N, O153, O213, EP132, EP112, EP113
Kikuchi Kazufumi, O065
Kikuchi Keiichi, EP020, EP018
Kim Bumsoo, EP228
Kim Byung Moon, EP129, O155
Kim Da Mi, EP122
Kim Dae Yoon, EP019, O105
Kim Dong Ik, O155, EP129
Kim Dong Joon, EP129, O155
Kim Eui Jong, O033, EP052
Kim Eunhee, EP023
Kim Hee Kyung, EP030
Kim Ho Sung, EP019, O104, O102, O105, O138, O108, O103, O137, O106, EP161
Kim Hong Dae, EP001
Kim Hongdae, EP063, EP062
Kim Hyung-jin, O066, O076, O077
Kim Jae Kyun, O133
Kim Jeeyoung, EP070, EP105
Kim Ji-hoon, O057, O058
Kim Jin Young, EP028
Kim Jinna, EP080, EP079
Kim Kyung Won, O058
Kim Mi Mi, EP061
Kim Sang Joon, EP019K, O108, O103, O137, O106, O232, EP161, O105, O102
Kim Sang Jun, O138
Kim Seul Kee, EP098, EP097
Kim Sun Yong, O072
Kim Sung Tae, O077, O076K, O066, EP081
Kim Yi-kyung, O077, O066, O076
Kim Yoo-jin, O158
Kim Young-joo, EP222
Kinoshita Naoe, EP085
Kislitsin Dmitry, O182
Kitajima Mika, EP010, O135
Kitamura Noriko, EP102
Kitkhuamdee Amnat, O202
Kiyosue Hiro, EP134
Kizilkilic Osman, O024, O179
Kleinberg Lawrence, O152
Klisch Joachim, O214
Klose Uwe, O118
Knysz Brygida, O025
Kobayashi Masahiro, EP076
Kober Fabian, O027
Koc Ali Murat, O208
Kocak Burak, O024
Kocak Mehmet, EP017
Kocer Naci, O024, O179
Kodera Junichi, EP076
Koechl Arnold, O039
Koerner Heiko, O176
Koge Junpei, EP135
Koh Tong San, O030
Kohno Michihiro, EP252
Kohta Eiichi, EP076
Kokurcan Atilla, EP090, EP230
Kolić Krešimir, EP091
Kollar Katalin, O016
Koltowska Anna, O025
Konishi Yoshifumi, O177
Konno Yoshihiro, EP066
Kononov Rodion, EP242
Konuskan Bahadir, EP190
Koo Hye Soo, O033
Kornienko Valeriy, O020, EP111
Korogi Yukunori, O023, O147
Kostadinova Irena, EP168
Kovacs Eva, O016
Kozák Lajos Rudolf, O228
Kozic Dusko, O037
Körner Heiko, O047
Körner Heiko, O045
Kral John, O225
Kralova Ivana, O197
Kreiser Kornelia, O219
Kremneva Elena, O229
Krifa Hedi, EP208
Krivoshapkin Alex, O182
Krotenkova Marina, O229, EP242
Ksira Iyadh, EP177
Kulikova Sofya, O229
Kumar Ajay, O213, EP132, EP112
Kundel Harold, O231
Kuo Chen-ling, EP127
Kuo Kuei-hong, EP100
Kural Feride, O022
Kurihara Noriko, O150
Kurne Asli, EP004
Kurre Wiebke, O189, O168
Kurugoglu Sebu, O081
Kurz Kathinka D., O049
Kurz Martin W., O049
Kuya Keita, EP154
Kwak Hyo Sung, EP101
Laadhari Mouna, O018
Lagios Kostas, EP141
Lai Ping-hong, EP007
Lai Yen-jun, EP100
Lambre Hector, O195, EP050
Lammens Martin, EP176
Lan Hailong, O122, O123
Lander Bernardo, EP147
Langenaeken Christine, EP114
Laopaiboon Vallop, EP072
Larry Amhed, EP218
Larsson Elna-marie, EP251
Larsson Sven, EP216, EP217
Lary Ahmed, EP217
Lasocki Arian, O101, O100, EP026
Launer Lenore, O004, O044
Law Meng, EP080, O140
Law-ye Bruno, O132



AUTHORS INDEX

- Le Jean Lise, O087
Lebrun Jean Christophe, O134
Lee Aleum, O062, O071
Lee Byung Hoon, EP182
Lee Daniel, O225
Lee Dong Hoon, EP023
Lee Eun Kyung, O057
Lee Han-jui, EP055
Lee Hong Jun, O226
Lee Hwei-ye, EP027
Lee In Ho, EP152, O032, EP158, EP122
Lee Ji Young, O076, O077, EP081
Lee Jiann-der, O233
Lee Jin Seong, EP207, EP165
Lee Ji-ye, EP014
Lee Kwanghwi, EP063, EP062
Lee Kwo-whei, EP008, EP127
Lee Pei-lin, O115
Lee Sang-rae, O226
Lee Seung-koo, EP080, EP079
Lee Woong Jae, O133
Lee Youn Joo, EP029
Lee Youn Joo, EP030, EP028
Lee Young Hen, O035
Lee Young Jun, EP081, EP061
Lee Youngjeon, O226
Lehericy Stéphane, O132
Lemieux Louis, O228
Leszek Jerzy, EP166
Levy Michael, EP158, O032
Lewin Jonathan, O142
Lewis Beth, O004
Ley Desiree, O158
Liauw Lishya, EP027
Lin Xuling, EP027
Li Li, EP178
Li Ximin, O014
Liao Chun-han, EP142
Libien Jenny, O225
Lieb Johanna M., O098
Lilja Åsa, O114
Limbucci Nicola, O184
Limbucci Nicola, O028
Lin Chien-jen, O167
Lin Ching-po, O115
Lin Chung-jung, O174, EP092, EP151, O169
Lin Huey-shyan, EP007
Lin Wei-che, EP237, O115
Liouta Evangelia, O118, O117
Lirng Jiing-feng, O169, O074
Little Philip, EP106, EP108
Litzenberg Marc, O181
Liu Chi-kuang, EP127
Liu Hua-shan, EP011
Liu K.-c., EP064
Liu Kiang, O004
Liu Yi-jui, EP229
Liu Yi-sheng, EP096
Lo Sherman, O173
Lo Bello A, EP021
Loganathan Raghu, O215
Longhi Michele, EP262
Lopes Júnior Edson, EP170, EP186
Lopez Ingeborg, EP047, EP048, EP046
Lorenzano Svetlana, O043
Lovblad Karl-olof, O210
Lovrić-kojundžić Sanja, EP091
Lu C.-r., EP064
Lu Cheng-hsien, O115
Lu Li, EP108
Lu Yueh-hsun, O074, O052
Luanratanakorn Patanaree, EP072, EP073
Luetic-cavor Ljubica, O017
Lundberg Johan, O162, EP108
Lundberg Peter, EP251
Lundquist Javier, O181
Lunn Michael P, O097
Luo Chao-bao, O169, EP151, O174
Lylyk Pedro, O195
Lylyk Pedro, EP050, O181
Mabiglia Chiara, O061
Macedo Carlos, EP212
Macioszek Adam, EP166
Maeda Masayuki, O144
Maffei Pietro, O113
Mafra Manuela, EP116, EP042, EP115
Magalhães Catarina, EP211
Mahajan Anshu, EP132
Malova Mariya, EP210
Malyszczak Krzysztof, O025
Mama Nadia, EP208, O018
Mamere Augusto Elias, EP199
Manara R, O126
Manara Renzo, O113
Mancini Laura, O110
Mandel Catherine, O143
Mangiafico Salvatore, O028, O184, O043
Mangla Sundeep, O225, O215, O160
Mankad Kshitij, O224
Mannfolk Peter, O114
Mansour Ossama, O165, O050, O172
Mantatzis Michalis, EP141
Maravilla Ken, O141
Marchese Paola, EP021
Marcia Stefano, O011
Mardari Rodica, EP210
Margetic Petra, O017
María Berenice García, EP147
Maria Sol Toronchik, EP253
Mariangela Alvarado, EP147
Marileo Roberto, EP048, EP046, EP047
Marini Stefano, O011
Marshall Jan, O113
Martin Maria Da Graça, EP163
Marui N, EP146
Masayoshi Kobayashi, EP094
Mas-bonet Antonio, EP059
Massari Francesco, EP188
Mata Mbemba Daddy, EP178
Mathuria Sn, O213
Matsubara Noriaki, EP146
Matsumoto Keiko, EP076
Matsumoto Shoji, EP135
Matsumoto Yasushi, O150
Matsushima Nobuyoshi, O144
Matsuura Keita, O144
Maximov Ivan, O020
Mbekeani Joyce, EP197
Mcevoy Andrew, O110
Mchirgui Leila, EP180
Mealy Maureen, EP158, O032
Mechtler Laszlo, O128
Meckel Stephan, O214, O216, O218
Meers Stef, EP114
Megahed Mohamed, O172



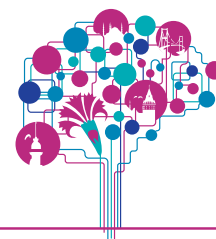
AUTHORS INDEX

- Meijer Frederick, EP056
Melberg Atle, O151
Melis Maurizio, EP226
Melissa Schori, O215
Meneguzzo Paolo, O113
Menezes Alvaro, EP212
Mercedes Serra, EP253
Mery Francisco, O181
Metens Thierry, O134
Metoki Takahiro, O150
Meuli Martin, O007
Meyer Monique, O038
Mishra N K, O163
Mittal Br, O153
Mizumura Sunao, EP076
Michelin Gabriela, EP240
Midiri Massimo, EP021
Mihailovic Jelena, EP075
Mikellidou K., O012
Miklic Dina, O017
Milenkovic Gordana, EP103, O037
Miller Neil, EP152
Milosevic Medenica Svetlana, EP138, EP128
Minkin Krassimir, EP168
Miralbes-celma Salvador, EP059
Mironov Angel, O148
Mirtuono Pasquale, EP262
Miserocchi Anna, O110
Miyachi Shigeru, EP146
Miyamoto Naoko, EP150
Miyata Haruka, EP135
Miyata Mari, O147
Miyazaki Isao, EP035
Miyazaki Yuichi, EP104
Miyoshi Fuminori, EP044
Mochizuki Teruhito, EP018, EP020
Moehrlen Ueli, O007
Mohamed Mona, EP236
Mohamed Zahiah, EP144
Mohamed Mukari Shahizon Azura, O204
Mohamed Taher Yacoubi, EP177
Mohammad Hanafiah, O204
Mohan Suyash, O022, O231
Mohd Zain Norzaini Rose, O204
Moll-servera Apolonia, EP059
Momjian Shahan, O210
Montanaro D., O012
Moraes Valenca Marcelo, O140
Mordasini Livio, O234
Morgan Benjamin, O080
Morioka Motohiro, O180
Mori Hiromu, EP134
Mori Takahisa, O217, EP104, O026
Morikawa Minoru, EP085
Moriya Junji, O023, O147
Morrone M.c., O012
Morrow Jasper M, O096
Morrow Jasper M, O097
Moser Judit, O016
Mothila Shikar, EP025
Mubarak Walid, O006
Muda A Sobri, EP131
Muda Ahmad Sobri, O051, O204, EP144
Muehl-benninhaus Ruben, O176
Mugikura Shunji, EP178, O053, O150
Mukari Shahizon Azura, O051
Mulder Jan, EP106
Mulyadi Rahmad, EP256
Munoz Eric, O038
Murakami Yu, O147, O023
Murata Takaki, EP178, O150, O053
Muti Marco, EP012
Mühl-benninghaus Ruben, O158, O047, O045
Müller Andreas, O158
Na Dong Gyu, O058
Nadia Arifa, EP177
Nadia Mama, EP177
Nagano Yoshitaka, EP146
Nagata Izumi, EP135
Nagi Sonia, EP180
Nagy Zoltan, EP258
Naidich Thomas, O140
Naito Isao, EP150
Nakahara Ichiro, EP135
Nakamura Hideo, O135
Nakamura Yukihiko, O180
Nakanishi Atsushi, O090
Nakatsuka Tomoya, EP102
Nakazawa Takuya, O223
Napoli E, O126
Nappini Sergio, O184
Nardai Sandor, EP258
Nasel Christian, O039
Nasiadko Christin, O007
Nasrallah Ilya, O004, O231
Nasreddine Wassim, O009
Nass Duce Meltem, O068
Necioglu Orken Dilek, O190
Nemoto Shigeru, O221
Neuwirth Jiri, O197
Newsome Scott, EP158, O032
Ng Shu-hang, O059
Nicolato Antonio, EP262
Nie Tingting, O089, EP250, EP067
Nik Ismail Nik Azuan, EP144
Nikaki Alexandra, EP243
Nikic Petar, EP103
Nikkhou-aski Sahar, EP108
Nikoubashman Omid, O127, O224
Nilsson Petra, O114
Nishi Hidehisa, EP135
Nishikori Akira, O090
Nitatori Toshiaki, EP034, EP035
Nitta Naoki, O223
Nitta Nobuhiro, EP232
Nobuyuki Sakai, O181
Nouet Aurélien, O031
Nozaki Kazuhiko, O223
Nozawa Kumiko, O078
Ntountas Ioannis, EP141
Nunziata Raffaele, EP088
Nystedt Jessika, O114
Obata Takayuki, O078
Obmann Markus, O021
Ochsenbein Nicole, O007
Oda Seitaro, O135
Odashima Masayuki, EP102
Ogasawara Atsushi, O147, O023
Ogawa Toshihide, EP044, EP154
Ogihara Yukihiko, EP085
Ogungbemi Ayokunle, EP124
Oguz Kader Karli, EP190
Ohara Arisa, EP034, EP035
Ohnari Norihiro, O023
Ohta Tsuyoshi, EP135
Ohue Shiro, EP020
Okada Hirofumi, EP252



AUTHORS INDEX

- Okada Kazumasa, O023
Okada Takuya, EP135
Okada Yoshikazu, EP038
Okuma Cecilia, EP047, EP048, EP046
Olivi Alessandro, O067, O069
Omojola Matthew Folorunso, EP213
Onal Cem, O091
Onaral Cenk Şecaattin, EP201
Oner Ali Yusuf, O208
Ono Yuko, EP038
Ooue Shirou, EP018
Oporto Sabrina, EP047
Oran Ismail, O156, O212, EP130
Orheim Tone E.d., O136
Orito Kimihiko, O180
Orlov Kirill, O182
Orman Gunes, O014, O032, EP158
Orman Mujgan, O179
Oros-peusquens Ann Maria, O127
Orourke Donald M., O022
Orru Emanuele, O067, O069
Orz Yasser, EP216
Osman Syazarina, O204, O051
Ostojic Jelena, O037
Ottaviano G, O126
Ou Ming-ching, EP096
Ovalle Juan, O092, EP185
Oviedo Jairo, O124, O154, O111
Oweidat Adeeb, O009
Owen Ahmed, O054, O042
Ozaki Hiroaki, EP094
Ozaki Yutaka, O090
Ozer Halil, O208
Ozgür Anil, O068
Ozmen Evrim, O081, EP184
Ozretic David, O157
Öner Ali Yusuf, EP090
Örs Suna, EP230
Özcan Cengiz, O068
Özer Eren, EP089
Özkul Bahattin, EP119
Pablo Pfister, EP253
Padwal Jennifer, O008
Pakasi Trevino, EP256
Paladini Dario, EP210
Palumbo V, O126
Pan Huay-ben, EP007
Pan Yi-ju, EP100
Pandelaki Jacub, O170
Pant Dr Ak, EP078
Pant Sr Ashok, O055
Papadaki Efrosin, O149
Papavassiliou Efstathios, EP077
Pappalardo Maria Pia, EP021
Parada Carolina, O195
Parizel Maxim R., EP176
Parizel Paul M., EP176
Park Choong Ki, EP061
Park Chung Ki, EP081
Park Dong Woo, EP081, EP061
Park Ji Eun, O103, O106, O057
Park Mina, EP080, EP079
Parodi Alessandro, EP210
Pascal-mousselard Hugues, O015
Patel Ankush, EP040
Patel Uresh, EP040
Patil Abhijit, EP017
Patro Satya, O145
Patzig Maximilian, O164, EP143
Paul Moh, O215
Paulina Yañez, EP253
Pavaine Julia, O080
Pavlista Goran, O157
Peiffer Ann, O044
Pekcevik Yeliz, EP087, EP158, O032, O070
Peker Ahmet, EP149
Peker Elif, EP149
Peltz Maria Teresa, EP226, EP225
Penkov Marin, EP168
Pereira Nara, O142
Peresedova Anastasiya, O229
Perez-then Eddy, O154, O111, O124
Perkins Thomas, O128
Pesaresi Ilaria, O203, EP088
Pesce Gianfranco, O013
Pfeil Douglas, O225
Pfister Pablo Martin, EP255
Phuttharak Warinthorn, EP074, EP073, EP072
Picasso Pablo, EP212
Picado-valles Maria J, EP059
Picasso De Araújo Coimbra Pablo, EP186, EP170
Pierot Laurent, O159, O181
Piliszek Agnieszka, EP107
Pimenta Lacerda Saulo, EP120
Pinter Nandor, EP258, O128
Pinto Pedro, EP211
Piotin Michel, O171
Pipikos Theodoros, EP243
Piras Emanuele, O011
Pistocchi Silvia, O171
Pitskhelauri David, O020
Pizzini Francesca Benedetta, EP262
Plant Gordon, O200
Pollak Pierre, O210
Pomero Elisa, O188, O186, O187, O064
Pongpech Sirintara, EP137, EP136
Poniatowska Renata, EP107
Poon Wl, O173
Poppert Holger, O027
Poptani Harish, O022
Prassopoulos Vassilios, EP243
Pravata Emanuele, EP241
Preibisch C., O040
Preibisch Christine, O003, EP247
Price Stephen, O211
Promon Kayoon, O202
Pronin Igor, O020, EP111
Prothmann Sascha, O027
Prud'homme Clara, O187, O188, O186
Puglioli Michele, O203, EP088
Pumarola Felix, O083
Qiu Fang, EP213
Quiñones Tapia Diana, EP009
Radbruch Alexander, O107
Rados Marko, O157
Radovic-stefanovic Magdalena, O037, EP103
Radue Ernst-wilhelm, O098
Rai Rahul, EP113
Raininko Raili, O151
Raja Shanker, EP218, EP216, EP217
Rajendran Deepa, EP261
Ramenghi Luca, EP210
Ramli Marlina, EP148
Ramos Júnior Francisco, EP170
Rashid Umair, O093, O220, O183
Rauniyar Dr Raj Kumar, O055,



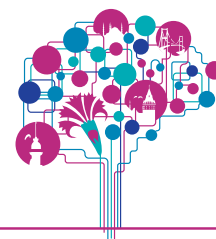
AUTHORS INDEX

- EP078
Ravi Chetan, O163
Rawah Elham, O096
Raybaud Charles, O080
Raz Eytan, O013
Redjem Hocine, O171
Reilly Mary M, O096, O097
Reinert Michael, O013
Reinhard Mathias, O214
Reis João, EP116, EP115, EP042
Reisert Marco, O021
Reiter Gert, O039
Reith Wolfgang, O158, O047, O176, O045
René Viso, EP147
Renieri Leonardo, O184, O028
Rennie Adam, O034
Rennie Ian, O181
Reyes Melinda, O008
Ricardo Reisin, EP253
Ricciardi Giuseppe Kenneth, EP262
Ringel Florian, O219
Rivera Diones, O111
Rivera Rodrigo, EP048, EP046, EP047
Rivera-michlig Roxana, O002
Riveros Rodrigo, EP048, EP046
Rizzati S, O126
Roa Pedro, O154
Roa-sanchez Pedro, O124
Robertson Fergus, O034
Roccatagliata Luca, EP155
Rocha Marussi Victor Hugo, EP120
Roder Constantin, O116, O118
Rodrigues Tiago, EP211
Rodríguez Roberto, O082
Rodríguez-raecke Rea, O124
Rojas Rafael R, EP077
Rollan Cecilia, EP239, EP255
Romano Daniele, O013, O043
Romero Carlos, EP255, EP240, EP239
Romero-mamani Edwin-saúl, EP257
Ros Emilio, EP257
Rosdy Beata, O016
Rosi Andrea, O028, O184
Rosman Azmin Kass, EP131
Rossi Andrea, EP210
Rowley Howard, O120
Royo Aranzazu, O082
Rudas Gabor, O016
Rummel Christian, O234
Runge Michel, O186, O064
Ryglewicz Danuta, EP107
Ryu Chang-woo, EP052, O033
Ryu Jihwa, EP063R, EP062
Sabato Mario, EP088, O203
Sacktor Ned, EP236
Sadeghi Niloufar, O134
Sadikin Cindy, EP109
Saelan Yanna, EP109
Saglam Muzaffer, O179, O024
Saka Esen, O230
Saka Masato, EP135
Sakai Shuji, EP038
Sakakibara Ryuji, EP053
Sakamoto Makoto, EP154
Sakata Kiyohiko, EP022
Sakuma Hajime, O144
Salaj Martina, O017
Sala-vila Aleix, EP257
Salazar Juan Pablo, O083
Saletti Andrea, O043
Salvalaggio Alessandro, O126
Salvatico Rosana, EP050
Samanci Cesur, O081
Sanchez-montanez Angel, EP206, O084, O083
Sanlidilek Umman, EP149
Sano Akihito, EP146
Sarastika Hartono Yudi, EP109
Sarica Mehmet Akif, EP039
Sarioğlu Sülen, EP089
Sarkar Subhendra N, EP077
Sasiadek Marek, EP166, O025
Sato Kanako, EP053, O090
Sawanyawisuth Kittisak, O202
Saygi Serap, EP006
Scheer Ianina, O007
Scheller Bruno, O158
Schittenhelm Jens, O227, O030
Schmid Elisabeth, O168
Schmitt Anne Jutta, O034
Schneider Tanja, O201
Schreiner Pamela, O004
Schultz Tim, O143
Schumacher Martin, O216
Schwaiger Benedikt Jakob, O003, O027
Schwarzwald Ralf, O209
Sebai Rym, EP180
Secci Simona, EP225S, EP226
Seleznev Pavel, O182
Seliverstov Yuri, EP242
Seliverstova Evgeniia, EP242
Seo Hyobin, O058, O057
Seo Hyung Suk, EP023, O035
Seong Su Ok, EP014
Seppala Nicholas, O145
Sergio Nappini, O028
Serra M. Mercedes, EP240, EP239
Server Andres, O136
Sestieri Carlo, EP241
Severino Mariasavina, EP210
Sezer Rahime, EP149
Shadha Abubaker Dr, O205
Shah John, O127
Shah Mukesch, O216
Shah Sachit, O097, O096
Shayakhmetov Timur, O182
Shen Zhi Wei, EP234, O191, EP254, O125, EP233, O089, EP246
Shiraga Nobuyuki, EP076
Shiban Ehab, O219
Shigematsu Yoshinori, O135, EP010
Shih I.-a, EP064
Shih Ludy C, EP077
Shimada Ryuichi, EP134
Shinohara Yuki, EP044, EP154
Shiroishi Mark, EP080
Shishkina Lyudmila, O020
Shotar Eimad, O031, O171
Shroff Manohar, O080
Shuaib Ashfaq, O054
Shults Evgeniy, O020, EP111
Sidiropoulos Prodromos, O149
Singh Paramjeet, O213
Sidipratomo Prijo, O170S, O222
Sienkiewicz-jarosz Halina, EP107
Sigurdsson Sigurdur, O044
Silva Holanda Ferreira Tiago, EP186, EP170



AUTHORS INDEX

- Simgen Andreas, O158, O176, O047, O045
Sinclair Christopher Dj, O096, O097
Sindhvani Vivek, O196, O095
Sinisi Aa, O126
Skalej Martin, O181
Skardelly Marco, O227
Skierczynska Agnieszka, EP107
Skolasky Richard, EP236
Smedby Örjan, EP251
Smet Stephanie, EP114
Smith Alex, O004
Smith Martin, O141
Soares Gabriela, EP211
Soetikno Rista D, EP183
Soldati Antônio André, EP186
Son Yohan, EP105
Soneji Sameer, EP118, O193, EP195, EP117
Song Chang June, EP029S, EP028, EP122
Song Ha Hun, EP222
Song Mina, O076, O066, O077
Song Yunsun, O166
Sonoda Kazutaka, EP135
Soon Weiling E, EP027
Sordo J. Gabriel, EP046, EP048S, EP047
Soufan Cathy, EP261
Souillard Raphaelle, O131
Sourour Nader, O171, O181, O031
Sowden Jane, O129
Söderman Michael, EP108
Spandonis Yiannis, O119
Speckter Herwin, O111
Speckter Herwin, O124
Splendiani Alessandra, O198, O056, O019
Stefanía López, EP147
Steffenhagen Nikolai, O145
Stippich Christoph, O098
Stoeter Peter, O124, O111, O154
Stone-elandar Sharon, EP108
Strandberg Olof, O114
Stranjalis George, O119, O117
Strassila Christoph, O214
Stuckey Stephen, O100, EP261, O101
Suazo Luis, O124, O154, O111
Sugai Yukio, EP066
Sugita Yasuo, EP022
Suh Chong Hyun, EP165
Suh Chong Hyun, O138
Suh Dae Chul, O166
Sundblom Jimmy, O151
Sundgren Pia, O114
Suroyo Indrati, O222
Suzuki Hideaki, EP076
Suzuki Kenichi, EP076
Suzuki Kazufumi, EP038
Suzuki Michimasa, O090
Sven Larrson, EP218
Sychra Vojtech, O214
Szabó Ádám, O228
Szewczyk Pawel, O025
Szikora Istvan, O181
Tabakcı Omer Naci, O190
Taban Hazar, O006
Tacey Mark, O100, O101
Tada Hiroko, EP232
Takagi Kenji, O223
Takahashi Haruo, EP085
Takahashi Shoki, O150, O053, EP178
Takanashi Jun-ichi, EP232
Takayama Miyoko, O090
Takeichi Yasuhiro, EP145
Tali E. Turgut, O208
Tan Kevin, EP027
Tanaka Norimitsu, EP022, EP069
Tanaka Yujirou, EP252
Tang Kw, O173
Tanno Hirokazu, EP094
Tanno Yuhei, EP104, O217, O026
Tanoue Shuichi, EP134
Tanwar Manoj, O231T, O044
Taschner Christian A, O214, O159, O181
Taşkiran Dilek, O121
Tatagiba Marco Soares, O118, O116
Tateishi Hidekatsu, EP035, EP034, EP010
Tatewaki Yasuko, O053, EP178
Tavares Fabiana, EP152
Tavares Daher Ricardo, EP120
Taylor Margot, O080
Teng Michael Mu Huo Teng, O052, EP151, O169, EP092
Teo Patrick Tze Hern, EP084
Teo Tze Hern, O030
Terada Hitoshi, EP102T, EP232, EP053
Teresita Victor, O215
Terzic-beljakovic Aleksandra, O037
Tezer Irsel, EP006
Thalmann George N, O234
Thammaroj Jureerat, O202
Thng Choon Hua, O030
Thompson Carol B., O014
Thornton John, O129, O130, O096, O097
Tin Aung Soe, EP027
Tilouch Samia, O018
Tinelli F, O012
Tisell Anders, EP251
Tisnado Jaime, EP214
Tissera Claudia, EP048
Tjahjadi Hartono, EP256
Tlili Graeiss Kalthoum, EP157, O018, EP208
Toe Boon-ping, EP027
Togao Osamu, O065
Tomiyasu Moyoko, O078
Tonoyan Aram, EP111, O020
Topcuoglu Mehmet Akif, EP006, EP093
Toronchik M. Sol, EP240, EP239
Tortora Domenico, EP210
Toth Vivien, O040, O003
Tóth Miklós, EP106
Triñanes Estefania, EP255
Trypka Elzbieta, EP166
Tsai Fong Y, EP011T, EP127, EP008
Tsai Hong-ming, EP096
Tsai Meng-chang, EP237
Tsai Ping-huei, EP011
Tsai Yuan-hsiung, O233
Tschampa Henriette, O209
Tseng Ying-chi, O088, EP231, O046
Tsougos Ioannis, EP243
Tsuchiya Kazuhiro, EP035, EP034
Tsui Yu-kun, O167



AUTHORS INDEX

- Tsuji Atsusi, O223
 Tsuji Kenichi, O223
 Tsuruta Kouhei, O090
 Tsutsumi Yoshiaki, O177
 Turjman Francis, O181
 Turki Nouha, EP082
 Türkyılmaz Mut Deniz, O190
 Uchiyama Yusuke, EP022, EP069
 Ueda Issei, O023
 Uetani Masataka, EP085
 Ul Haq Anwar, EP197
 Umino Maki, O144
 Urbach Horst, O218, O159, O021,
 O209, O214
 Utrilla Cristina, O082
 Utsunomiya Daisuke, O135
 Uysal Ender, O190
 Uzdogan Andac, O230
 Ünlü Mehtat, EP089
 Valenzuela Santiago, O111
 Vallone Stefano, O043
 Vallop Laopaiboon, EP073
 Valvassori Luca, O181
 Valyi Zsuzsanna, O061
 Van Camp Louise, O073
 Van Den Hauwe Luc, EP114,
 EP176
 Van Goethem Johan W., EP176
 Van Graan Louis André, O228
 Van Looveren Kevin, EP176
 Van Thielen Thomas, EP176
 Vaneckova Manuela, O141
 Varallyay Gyorgy, O016
 Vargas Maria-isabel, O210
 Vasco Aragao M. De Fatima, O140
 Vazquez Elida, O083, O084,
 EP206
 Venneri Annalena, O113
 Venstermans Caroline, EP176
 Verganti Luca, O043
 Verma Rajeev K, O234
 Viaño Juan, EP009
 Vidailhet Marie, O132
 Vidal Aaron, EP048, EP046,
 EP047
 Vignon Clémentine, O132
 Vilchez Carlos, O154
 Vlachou Fani, EP243
 Von Elverfeldt Dominik, O021
 Vosko Milan, O001
 Vukicevic Marjana, O037
 Vukovic Vesna, EP075
 Vyas Sameer, O153, EP112
 Wagner Jan, O209
 Wakabayashi Toshihiko, EP146
 Wakhloo Ajay K, O181
 Waldman Adam, O211
 Walecki Jerzy, EP107
 Walha Kamel, EP180
 Wang Chao-ying, EP011
 Wang Chih-wei, EP229
 Wang Hsueh Han, EP110
 Wang Jiun-jie, O059
 Wang Po-chin, EP007
 Wang Shuu-jiun, O233
 Wang Sumei, O022
 Wang Yi, O033
 Watanabe Daisuke, EP252
 Watanabe Keita, O023, O147
 Watanabe Sadayoshi, EP135
 Watanabe Takashi, EP154
 Watanabe Tomoo, EP066
 Watarai Fumika, EP066
 Wei C.-y, EP064
 Weiß Carolin, O127
 Weisstanner Christian, O234
 Weng Hsu-huei, O233
 White Mark J., O110
 White Matthew L, EP213
 Wies Luca, O113
 Wiesmann Martin, O127, O224
 Wiest Roland, O234
 Wiestler Benedikt, O107
 Winston Gavin P., O110
 Witkowski Grzegorz, EP107
 Wojtynska Renata, EP166
 Wolf-dirk Niesen, O216
 Wong Ho Fai, O109, O059
 Wong Ph, O173
 Woo Seung Tae, O133
 Worakijthamrongchai Thanaboon,
 EP136, EP137
 Wu Chih-chun, EP055
 Wu H.-s, EP064
 Wu Hsiu-mei, EP055
 Wu Mc, O109
 Wu Meilian, O123
 Wu Ren Hua, EP234, O191,
 EP254, O125, O123, EP250,
 EP233, O089, EP246, EP238,
 EP095, EP067, EP235, O122
 Wu Te-chang, O167
 Wunderlich Silke, O219, O003
 Xiao Ye Yu, EP234
 Xiao Gang, EP254
 Xiao Yeyu, O123, O122
 Xu Xiaojin, O191, EP246
 Xu Yong, O225
 Xuan Yinghua, EP095
 Yaacob Yazmin, EP144
 Yacoubi Med Tahar, EP208
 Yahya-cherif Lydia, O132
 Yalniz Ahmet, EP139
 Yalnizoglu Dilek, EP190
 Yamada Hiroyuki, EP146
 Yamaguchi Ninpei, EP085
 Yamamoto A. Kenji, O110
 Yamashita Koji, O065
 Yamashita Sumimasa, O078
 Yamashita Yasuyuki, EP010, O135
 Yan Gen, EP095, EP067
 Yañez Paulina, EP255
 Yang Chan-ming, O074, O052
 Yang Chun-yuh, O233
 Yang Yonggui, O036, EP233,
 O191, EP246
 Yano Shigetoshi, EP010
 Yaziz Sarah, O051
 Yazici Nalan, O091
 Ye Bi Di, EP234
 Yeh Chi-wah, O059
 Yen Pao-sheng, EP142
 Yener Gorsev, EP244
 Yiin Yin Shih Zhu, EP027
 Yildirim Adem, EP249
 Yildirim Bayram, EP139
 Yildirim Erkan, EP058
 Yildiz Ramazan, EP090
 Yilmaz Emrah, EP230
 Yi Kyung Sik, O226
 Yi Meizhi, EP238
 Yilmaz Umut, O158Y, O176,
 O047, O045
 Yokoi Toshihiro, O223
 Yoneda Tetsuya, O147, O023
 Yoo Jeong Hyun, EP065, EP068



AUTHORS INDEX

Yoo Roh-eul, O139
Yoon Chong Hyun, EP207, EP165
Yoon Hee Mang, EP165, EP207
Yoon Hye-kyung, EP207
Yoon Ji Won, O058
Yoon Ra Gyoung, O105, EP019
Yoon Woong, EP097, EP098
Yoshida Ayako, EP022, EP069
Yoshida Mariko, O090
Yoshimura Yayoi, O223
Yoshioka Kazuhiro, O026, O217
Yosma Engin, EP201
You Wooyoung, EP126, EP245
Younes Samia, EP157
Young Julia, O080
Yousem David, O201, O142,
EP152, O067, O002, O069, O152
Yousem Kelly, O142
Yousry Tarek, O130, O129, O096,
O097, O110
Yu Hyungbin, O166
Yu In Kyu, EP030, EP122, EP028,
EP029
Yu Wai-yung, EP027
Zaheer Sohail, O145
Zakaria Rozman, EP144
Zan Elcin, EP152
Zavalishin Igor, O229
Zecca Chiara, EP241
Zeghal Chiheb, O031
Zeleňák Kamil, O185
Zerah Michel, O224
Zeynalova Amalya, EP184
Zhang Guishan, EP254, EP238
Zhang Tao, EP238, EP235, O089
Zhang Zhongping, O036, EP233,
O191, EP246
Ziernhöld Maximilian, O001
Zimmer C., O040
Zimmer Claus, O219, O003,
EP247, O027
Zimny Anna, O025, EP166
Zini Andrea, O043
Zlatareva Dora, EP168
Zupetic Ivana, O017



wfnrs

The World Federation of Neuroradiological Societies

www.wfnrs2014.com